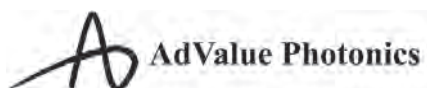


Table of Contents





Schedule-at-a-Glance	2
General Chairs' Welcome Letter	3
Conference Services	5
Sponsoring Societies' Booths	6
Conference Materials	8
Plenary Sessions and Awards Ceremony	9
Workshops	14
Special Symposia	15
Applications & Technology Topical Reviews	19
Short Courses	21
Special Events	26
CLEO:EXPO	
Exhibitors	30
CLEO: Industry Focus	32
CLEO Committees	34
Explanation of Session/Presentation Codes	39
Agenda of Sessions	41
Technical Program	
Abstracts	52
Key to Authors	236

CLEO Management thanks the following corporate sponsors for their generous support:



Conference on Lasers and Electro-Optics®

Schedule-at-a-Glance

	Sunday 5 May	Monday 6 May	Tuesday 7 May	Wednesday 8 May	Thursday 9 May	Friday 10 May
GENERAL						
Registration	07:00–17:30	07:00–18:00	07:00–18:30	07:30–18:30	07:30–18:00	07:30–12:00
Speaker Ready Room	13:00–17:00	07:00–18:00	07:00–18:00	07:00–17:30	07:00–18:00	07:30–15:30
Coffee Breaks Sponsored by  COHERENT. and  THORLABS *on show floor		10:00–10:30 15:30–16:00	10:00–11:30* 15:00–17:00*	10:00–11:30* 15:00–17:00*	10:00–11:30* 16:00–16:30	10:00–10:30
CLEO TECHNICAL PROGRAMMING						
Short Courses	08:30–17:30	08:30–17:30	10:30–14:30			
Technical Sessions		08:00–18:00	13:00–19:00	13:00–19:00	08:00–18:30	08:00–16:00
Special Symposium and A&T Topical Reviews		08:00–16:00	13:00–19:00	13:00–15:00	13:00–18:30	10:30–16:00
CLEO Workshops 		18:30–20:00		10:30–12:00		
Plenary Sessions			08:00–10:00	08:00–10:00		
Posters and Dynamic e-Posters			11:30–13:00	11:30–13:00	11:30–13:00	
Postdeadline Paper Sessions					20:00–22:00	
CLEO:EXPO AND SHOW FLOOR ACTIVITIES						
CLEO:EXPO			10:00–17:00	10:00–17:00	10:00–15:00	
Unopposed EXPO-Only Time			11:30–13:00 15:00–17:00	10:00–13:00 15:00–17:00	10:00–14:00	
Poster Sessions and Free Lunches in Exhibit Hall			11:30–13:00	11:30–13:00	11:30–13:00	
CLEO Theaters I & II			10:00–17:00	10:00–17:00	10:00–14:00	
Meet OSA Publishing Journal Editors Ice Cream Social			15:00–16:30			
Technology Transfer Program					10:15–12:30	
SPECIAL EVENTS						
Pride in Photonics: LGBTQ+ & Ally Workshop	09:00–13:00					
Be Part of the Solution: Pre- venting and Responding to Harassment	14:00–15:30 16:00–17:30					
OSA Presentation Feedback Program		11:00–12:00				
Navigate Your Leadership Trajectory for Senior Leaders		11:00–12:30				
Resumes, LinkedIn, and Networking (with Cheeky Scientist)		13:00–14:00 16:00–17:30				
Social Media in 2019 Panel Discussion		13:00–14:00				
Deliberate Mentoring to Advance Your Career: Special Flash Mentoring		14:30–16:00				
Professional Development for Busy Professionals		16:00–17:30				
Diversity and Inclusion Reception		17:30–18:30				
OSA Technical Group Events		12:30–13:30 18:30–20:00	19:00–20:30		18:30–20:00	
Conference Reception Sponsored by 				19:00–20:30		

Welcome to CLEO!

It is our pleasure to welcome you to CLEO 2019 in San Jose, CA. CLEO continues to be the world's premier international forum for scientific and technical optics, uniting the fields of lasers and electro-optics by bringing together all aspects of laser technology, from basic research to industry applications. Within the scope of a single conference, CLEO provides a forum where attendees can explore new scientific ideas, engineering concepts, and emerging applications in fields such as biophotonics, optical communications, quantum computing, advanced imaging, and novel light sources. While the quality of work presented remains assured by CLEO's world-renowned technical program, the conference continues to evolve with new features to enhance your experience.

CLEO offers high quality content in five core event elements:

Fundamental Science: The premier venue for discussion of basic research in optical and laser physics and related fields. Topics include modern spectroscopy, ultrafast and nonlinear light-matter interactions, quantum optics, low-dimensional optical materials, quantum information science, nanophotonics, plasmonics, and metamaterials.

Science & Innovations: World-leading scientific research and innovation in lasers, optical materials, and photonic devices. Topics include laser processing of materials, terahertz science and technologies, ultrafast optics, biophotonics, nanophotonics, fiber photonics, nonlinear optical and laser technologies, metrology, sensing, and energy-efficient "green" photonics.

Applications & Technology: Exploration of the transition of fundamental research into emerging applications and products. The scope spans innovative laser and EO components and systems and applications. This topic includes biomedical devices for diagnostics and therapeutics, lasers and systems for industrial materials processing, and optical instrumentation and technologies for remote sensing, process monitoring, environmental sensing, and energy generation.

CLEO:EXPO: The exhibition will showcase more than 200 participating companies featuring a wide range of photonics innovations, products and services. It is expected to attract more than 4,000 attendees including researchers, engineers, and leaders from top research institutions and major businesses who represent the fastest growing markets in optics and photonics.

CLEO Theaters: This program focuses on the latest trends in the photonics marketplace and provides a forum to discuss new products and emerging technologies. All presentations and discussions are focused on the latest in photonics products and services that have been playing an important role in the industry and those that potentially hold a future business opportunity.

This year's CLEO features 6 extraordinary plenary speakers. On Tuesday morning, Mial Warren, Naomi Halas, and Chris Xu are our featured speakers. Warren will describe the history, motivation and technologies for LIDAR sensors in automobiles. Halas will discuss metallic nanoparticles and their useful properties for applications ranging from cancer therapy to chemical production. Xu will show how ultrafast lasers enable non-invasive monitoring of brain activity in live animals. On Wednesday morning, the featured speaker is Chris Monroe, who will describe quantum computing with atoms and the critical role for lasers and optics in this field.

The **2018 Nobel Prize in Physics** was awarded to three optics pioneers "for groundbreaking inventions in the field of laser physics." One half of the Prize went to Arthur Ashkin "for the optical tweezers and their application to biological systems." The other half of the Prize went jointly to Gérard Mourou and Donna Strickland "for their method of generating high-intensity, ultra-short optical pulses." CLEO 2019 is the perfect occasion to recognize these breakthroughs with the inclusion of plenary presentations by these Nobel Laureates on Wednesday. We will present a brief video interview with Ashkin. Strickland will highlight the development of chirped pulse amplification (CPA) and its enablement of new types of laser-matter interactions. Mourou will discuss the generation and application of extreme light for investigating fundamental physics at sub-femtosecond time scales and beyond exawatt peak power.

The CLEO Technical Program committee maintains a rigorous peer review system that emphasizes and maintains high technical quality in all presentations. This rigorous process is made possible by the combined efforts of over 300 volunteers in 27 technical committees. In 2019, the conference features an outstanding collection of contributed paper presentations, invited speakers and tutorials. We are excited to offer more than 1145 oral presentations, 182 invited talks by some of the most respected researchers in our international community, and 23 tutorials. This year's poster sessions include an outstanding list of more than 360 posters, including a specially selected subset of posters that are dynamic E-posters. Furthermore, selected topics are highlighted in special symposia and topical reviews that include tutorials and invited talks. Participation from industry is particularly encouraged through these topical reviews. We are pleased to offer a comprehensive short course program featuring 22 courses, including new courses for 2019 in laser radar, quantum optics, and VCSELs.

Finally, CLEO has a new feature in the 2019 program: topical workshops to address timely and important subjects that are not covered by traditional presentations. The workshops are open to all conference registrants and are intended to be more open and interactive discussions between panelists and audience. The workshop topics are

- Beyond Awareness: What Actions Can Be Taken to Improve Diversity in STEM?
- Will Quantum Computing Actually Work?!
- What Will Be the Largest Commercial Application for Optical Frequency Combs in 10 Years?

We extend our sincere thanks to the Technical Program Co-Chairs, Jin Ung Kang and Stephanie Tomasulo in Applications & Technology, Natalia Litchinitser and Sergey Polyakov in Fundamental Science, and Tara Fortier and Christophe Dorrer in Science & Innovations, for coordinating the work of our subcommittees to compile this outstanding CLEO program. We also thank Robert Fisher and Konstantin Vodopyanov, Short Course Co-Chairs, and all of the program committee members whose leadership, dedication, and hard work has been critical to maintaining the high quality of the meeting. Additionally, we would like to thank the APS Division of Laser Science, the IEEE Photonics Society, The Optical Society (OSA), and the exhibitors for their support and contributions to the meeting. Finally, we thank the OSA staff for their professional assistance and dedication in organizing this event.

We welcome you to the conference and thank you for your participation.



Peter Andersen
Technical Univ. of Denmark, Denmark
General Chair



Sterling Backus
Kapteyn-Murnane Laboratories, USA
General Chair



Ben Eggleton
Univ. of Sydney, Australia
General Chair



Michal Lipson
Columbia Univ., USA
General Chair



Michael Mielke
Iradion Laser, USA
General Chair



Irina Novikova
College of William & Mary, USA
General Chair

Conference Services

Registration

Concourse Level

Sunday, 5 May	07:00–17:30
Monday, 6 May	07:00–18:00
Tuesday, 7 May	07:00–18:30
Wednesday, 8 May	07:30–18:30
Thursday, 9 May	07:30–18:00
Friday, 10 May	07:30–12:00

CLEO:EXPO

Exhibit Hall

The CLEO:EXPO is open to all registered attendees. Visit a diverse group of companies representing every facet of the lasers and electro-optics industries. Exhibition information can be found on page 30.

Tuesday, 7 May	10:00–17:00
Wednesday, 8 May	10:00–17:00
Thursday, 9 May	10:00–15:00

Speaker and Presider Ready Room

Room 111

All technical presentation speakers and session presidors are required to check in to the Speaker Ready Room located on the Lower Level in Room 111. Speakers are required to check in 24 hours before their session begins.

Session presidors should check in one to two hours prior to their session for instructions on how to use in-room equipment and check for speaker cancellations and changes. Computers will be available to review uploaded slides.

Sunday, 5 May	13:00–17:00
Monday, 6 May	07:00–18:00
Tuesday, 7 May	07:00–18:00
Wednesday, 8 May	07:00–17:30
Thursday, 9 May	07:00–18:00
Friday, 10 May	07:30–15:30

Coat and Baggage Check

Concourse Level

Coat and baggage check is available to conference attendees for a nominal fee.

Thursday, 9 May	07:30–22:00
Friday, 10 May	07:30–16:30

CLEO Information Center

Concourse Level

For questions about the program, locating sessions or general conference information, visit the Information Center. Lost and Found items will be left at the Information Center for 24 hours. Please put your name on all conference materials (Program Book and Short Course Notes).

Sunday, 5 May	07:00–18:00
Monday, 6 May	07:00–18:00
Tuesday, 7 May	07:00–18:30
Wednesday, 8 May	07:30–18:30
Thursday, 9 May	07:30–18:00
Friday, 10 May	07:30–12:00

First Aid and Emergency Information

The First Aid room, staffed with emergency medical personnel, is located on the Exhibit Level. This room will be open during all conference hours. In the event of an emergency, please contact a security guard or a CLEO staff member.

All accidents, injuries or illnesses in the San Jose McEnergy Convention Center should be reported to the Public Safety Office immediately; call the office at extension 3500 from any white courtesy phone.

Wireless Access

San Jose McEnergy Convention Center offers free Wi-Fi experience. To access the network just connect to the SSID "WickedlyFastWifi".

No personal information or password needed with unlimited Wi-Fi access provided in the Convention Center.

CLEO Announces CLEO KIDS - Child Care Options

CLEO will offer subsidized on-site childcare to attendees who want to bring their kids.

Monday, 6 May	08:00–20:30
Tuesday, 7 May	08:00–19:30
Wednesday, 8 May	08:00–19:30
Thursday, 9 May	08:00–19:00
Friday, 10 May	08:00–16:30

All conference locations are in the San Jose Convention Center unless otherwise noted.

Sponsoring Societies' Booths

APS Booth

Concourse Level

Email: meetings@aps.org

Website: www.aps.org

The American Physical Society (APS) is a non-profit membership organization working to advance and diffuse the knowledge of physics through its outstanding research journals, scientific meetings, education and diversity programs, outreach, advocacy, and international activities. APS represents over 54,000 members, including physicists in academia, national laboratories, and industry in the United States and throughout the world. Please stop by our booth near registration to learn more about APS programs, services, and our new fully open access broad scope journal *Physical Review Research*.

IEEE Photonics Society Booth & Membership Lounge

Concourse Level

Email: photonicsociety@ieee.org

Website: www.PhotonicsSociety.org

The IEEE Photonics Society is the professional home for a global network of scientists and engineers who represent the laser, optoelectronics and photonics community. The Society provides its members with professional growth opportunities, publishes journals, sponsors conferences and supports local chapter and student activities around the world.

Visit the IEEE Photonics Society booth on the Concourse Level, near registration, for more information. When you join or renew an IEEE Membership at the booth, eligible members will receive 50% off membership dues and all benefits through 31 December 2019. An IEEE Photonics Society Membership is as low as US \$10 and only US \$5 for students.

IEEE members are also welcome to visit the IEEE Member Lounge, sponsored by the IEEE Photonics Society. Come to the IEEE members-only lounge to relax, grab a snack and connect to the internet. Meet-ups on Young Professionals, Senior Membership and Women in Photonics will take place throughout the week!

IEEE Lounge Schedule:

Monday, 6 May	10:00–15:00
Tuesday, 7 May	10:00–17:00
Wednesday, 8 May	10:00–17:00
Thursday, 9 May	10:00–15:00

IEEE Photonics Speaker & Volunteer Database

More Diverse Voices Need to Be Heard. To grow our community, the IEEE Photonics Diversity Oversight Committee has created a speaker database where members and volunteers can actively sign up and be called upon to serve within their technical and/or professional subject areas. Chairs and volunteer leaders use this database to recruit for invited talks, keynotes, panels, news stories, and councils.

Visit the IEEE Photonics Society booth on the CLEO Concourse Level, near registration, to sign-up!

IEEE Women in Photonics Travel Grant Program

The IEEE Women in Photonics initiative has established a travel grants program to encourage early career participation and gender inclusivity at its conferences and workshops. The grant funds within this program are intended to be used for travel, lodging expenses and registration to an IEEE Photonics sponsored event. Since gender is not binary, this program is inclusive for people of all genders to apply. However, applicants must be active supporters in the community for gender awareness and/or volunteers of the Women in Photonics program.

Visit the IEEE Photonics Society booth on the CLEO Concourse Level, near registration, to learn more on how to apply!

The IEEE Photonics Society has contributed USD \$100K to The IEEE Photonics Fund. Will you match us with your donation? With the establishment of this fund, you too can play a direct role in this vital work. Visit the IEEE Photonics Society booth or www.PhotonicsSociety.org for more information.

The Optical Society Booth

Exhibit Hall, Booth 1927

Email: info@osa.org

Website: www.osa.org

Founded in 1916, The Optical Society (OSA) is the leading professional association in optics and photonics, home to accomplished science, engineering and business leaders from all over the world.

Through world-renowned publications, meetings, industry resources, membership and professional development programs, OSA provides quality information and inspiring interactions that power achievements in the science of light. 350,000 professionals in over 175 countries and spanning academia, government and industry, call OSA their professional home.

Stop by to meet OSA staff, and learn more about our publications, conferences and meetings and membership for individuals and companies.

All conference locations are in the San Jose Convention Center unless otherwise noted.

The Optical Society Member Lounge

Concourse Level

OSA members are invited to take a brief respite from the conference at the Member Lounge. Whether it's to plan your schedule, meet up with other members or print your boarding pass, the lounge offers comfortable seating, light refreshments, coffee service and a computer/printer. In addition, take advantage of renewing your membership at 50% discount for one year! You can renew at the OSA Member Lounge or the OSA Booth on the Exhibit Floor. This special rate is available whether you're rejoining for the first time or renewing for another year.

OSA Member Lounge Schedule:

Sunday, 5 May	10:00–17:00
Monday, 6 May	10:00–17:00
Tuesday, 7 May	10:00–17:00
Wednesday, 8 May	10:00–17:00
Thursday, 9 May	10:00–17:00

OSA CAM Lounge

Room 213

The Celebrating All Members (CAM) videos are an opportunity for OSA members to share their stories in 3 minutes or less about what/who inspired them to get into their field, what excites them about their current work and what OSA means to them. These short vignettes are shown on our website (osa.org/100), on social media and at some of our conferences. Stop by from Monday to Wednesday between 09:00–17:00 for a quick interview.

Code of Conduct

All CLEO guests, attendees, and exhibitors are subject to the Code of Conduct policy, the full text of which is available at cleoconference.org/codeofconduct. Conference management reserves the right to take any and all appropriate actions to enforce the Code of Conduct, up to and including ejecting from the conference individuals who fail to comply with the policy.

If you wish to report bullying, discrimination, or harassment you have witnessed or experienced, you may do so through the following methods:

- use the online portal osa.org/IncidentReport (or email CodeOfConduct@OSA.org)
- contact any CLEO staff member

All conference locations are in the San Jose Convention Center unless otherwise noted.

Conference Materials

Access to Technical Digest and Postdeadline Papers

Technical attendees have early and continuous access to the CLEO: 2019 Technical Digest, including the Postdeadline Papers. The Technical Digest is comprised of the two-page summaries of tutorial, invited and accepted contributed/post-deadline papers. They can be downloaded individually or by downloading daily .zip files. (.zip files are available for 60 days after the conference).

1. Visit the conference website, www.cleoconference.org.
2. Select the Access Digest Papers link on the right side of the web page.
3. Log in using the same email address and password you used to register for the meeting. You will be directed to the conference page where you will see the .zip file links at the top of the page. Please note: if you are logged in successfully, you will see your name in the upper right-hand corner.

Access is limited to Full Conference attendees only, not Exhibits Pass Plus or One-Day attendees. If you need assistance with your login information, please use the "forgot password" utility or "Contact Help" link.

The available paper summaries will be submitted to the IEEE Xplore Digital Library (www.ieeeexplore.ieee.org), provided that the paper is presented by a co-author during CLEO 2019.

Poster PDFs

Authors presenting posters have the option to submit the PDF of their poster, which will be attached to their papers in OSA Publishing's Digital Library. If submitted, poster PDFs will be available three weeks after the conference. Submit your poster PDF no later than 24 May to cstech@osa.org. Your PDF should be named using your presentation number with "-1" added at the end (JTh2A.24-1.pdf.)

Short Course Notes

Notes typically include a copy of the presentation and any additional materials provided by the instructor. Each course has a unique set of notes, which are distributed on-site to registered course attendees only. Notes are not available for purchase separately from the course.

CLEO App

Manage your conference experience available on your mobile device or in your web browser.

Download the app one of three ways

1. Search for 'CLEO Conference' in the app store.
2. Go to cleoconference.org/app
3. Scan the QR code

Schedule

Search for conference presentations by day, topic, speaker or program type. Plan your schedule by setting bookmarks on programs of interest. Technical attendees can access technical papers within session descriptions.

Exhibit Hall

Search for exhibitors in alphabetical order and set a bookmark reminder to stop by their booth. Tap on the booth number at the top of the description, and you'll find their location on the EXPO floor map. View a daily schedule of all activities occurring on the show floor.

Access Technical Digest Papers

Full technical registrants can navigate directly to the technical papers right from the CLEO mobile app. Locate the session or talk in "Event Schedule" and click on the "Download PDF" link that appears in the expanded description.

IMPORTANT: You will need to log in with your registration email and password to access the technical papers. Access is limited to Full Conference attendees only.



Need assistance?

Contact our support team, available 24 hours a day Monday through Friday, and from 09:00 to 21:00 EDT on weekends, at +1.888.889.3069 option 1.

All conference locations are in the San Jose Convention Center unless otherwise noted.

Plenary Sessions and Awards Ceremony

Plenary Session I

Tuesday, 7 May, 08:00–10:00
Grand Ballroom



Imaging Deeper and Faster: Watching the Brain in Action with Ultrafast Lasers

Chris Xu, Professor, School of Applied and Engineering Physics, The Mong Family Foundation Director, Cornell Neurotech – Engineering, Cornell University, USA

Brain research is a multi-disciplinary endeavor, and inspires the development of innovative measurement tools. By pushing the boundaries of imaging depth and speed, nonlinear optical microscopy enables large-scale, non-invasive monitoring of brain activity in live animals, and is poised to play a major role in understanding how brains work.

Chris Xu is Professor of Applied and Engineering Physics, Cornell University. He is the founding co-director of Cornell Neurotech, and the director of Cornell NeuroNex Hub, an NSF funded center for developing and disseminating neurotechnology. His current research areas are biomedical imaging and fiber optics. Prior to Cornell, he was a member of technical staff at Bell Laboratories, developing fiber optic communication systems. He received his PhD in Applied Physics from Cornell University, and contributed to the early development of multiphoton microscopy. He is a Fellow of The Optical Society, and a fellow of the National Academy of Inventors. He has 32 patents granted or pending.



Plasmonics: Putting Light to Work from the Dipole Up

Naomi J. Halas, Stanley C. Moore Professor of Electrical and Computer Engineering, Professor of Physics, Chemistry, and Bioengineering, Rice University, USA

Metallic nanoparticles, well-known for their vibrant color, have become a central tool in the nanoscale manipulation of light. Their resonant illumination gives rise to intense, local photothermal heating and hot electron generation, properties that are useful in applications ranging from prostate cancer therapy to photocatalysis for producing useful chemicals.

Naomi Halas is the Stanley C. Moore Professor of Electrical and Computer Engineering and Professor of Physics, Chemistry, and Bioengineering at Rice University. She was the first person to demonstrate that the shape of plasmon-supporting metallic nanoparticles determines their color. She pursues studies in nanophotonics with applications in biomedicine, optoelectronics, chemical sensing, solar water treatment and plasmonic photocatalysis. She has more than 300 refereed publications and more than 20 issued patents. She is a member of the National Academy of Engineering, the National Academy of Sciences, the American Academy of Arts and Sciences and fellow of the National Academy of Inventors.



A LIDAR in Every Garage — The Race for Automotive Optical Sensor Supremacy

Mial Warren, Vice President of Technology, TriLumina Corp., USA

Mial Warren will present a review of the history, motivation and technologies for LIDAR sensors in automobiles. There is a multi-billion-dollar race to integrate complex, high-performance optoelectronic systems into the world's largest industry. Warren will explain the unique performance specifications that have been emerging from the automotive industry and how they drive the technology.

Mial Warren is a former DMTS at Sandia National Laboratories, where he did research on vertical-cavity surface-emitting laser (VCSEL) technology, diffractive optical element design and fabrication, micro-optical system integration and nanophotonics. He retired from Sandia in 2012 to join a venture-capital funded start up in Albuquerque, New Mexico. He is currently Vice President of Technology for TriLumina Corporation, where he is leading the development of high-power VCSEL arrays and near-infrared illumination modules for automotive LIDAR and 3D time-of-flight imaging applications.

Plenary Session II and Awards

Wednesday, 8 May, 08:00–10:00
Grand Ballroom



Quantum Computing with Atoms

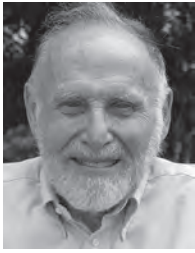
Christopher Monroe, Distinguished University Professor & Bice Sechi-Zorn Professor, University of Maryland, and Chief Scientist, IonQ, Inc., USA

Quantum computers offer hope for attacking problems that are beyond the capability of any possible conventional information processor. Individual atoms are the highest quality components for a scalable quantum computer, with unmatched coherence properties and reconfigurable circuits that are “wired” with laser beams. Monroe will speculate on the future of this field and the critical role lasers and optics will play.

Christopher Monroe is a leading atomic physicist and quantum information scientist. He demonstrated the first quantum gate realized in any system at NIST in the 1990s, and at the University of Michigan and University of Maryland, he discovered new ways to scale trapped ion qubits and simplify their control with semiconductor chip traps, simplified lasers and photonic interfaces for long-distance entanglement. He received the American Physical Society I. I. Rabi Prize and the Arthur Schawlow Laser Science Prize, and has been elected into the National Academy of Sciences. He is Co-founder and Chief Scientist at IonQ in College Park, Maryland.

All conference locations are in the San Jose Convention Center unless otherwise noted.

2018 Nobel Laureates in Physics



Video Presentation: Reflections on Optical Tweezers and the 2018 Nobel Prize in Physics

Nobel Laureate Arthur Ashkin



Passion for Extreme Light

Gérard Mourou, *École Polytechnique, France*

Extreme-light laser is a universal source providing a vast range of high energy radiations and particles along with the highest field, highest pressure, temperature and acceleration. It offers the possibility to shed light on some of the remaining unanswered questions in fundamental

physics like the genesis of cosmic rays with energies in excess of 1020 eV or the loss of information in black-holes. Using wake-field acceleration, some of these fundamental questions can be studied in the laboratory. In addition, extreme-light enables study of the structure of vacuums and particle production in "empty" space, which is one of the field's ultimate goals, reaching into the fundamental QED and possible QCD regimes.

Gérard Mourou is Professor Haut-Collège at the École Polytechnique. He is also the A.D. Moore Distinguished University Emeritus Professor of the University of Michigan. He received his undergraduate education at the University of Grenoble (1967) and his PhD from University Paris VI in 1973. He has made numerous contributions to the field of ultrafast lasers, high-speed electronics and medicine. But his most important invention, demonstrated with his student Donna Strickland while at the University of Rochester is the laser amplification technique known as Chirped Pulse Amplification (CPA). CPA revolutionized the field of optics, opening new branches like attosecond pulse generation, nonlinear QED and compact particle accelerators. It extended the field of optics to nuclear and particle physics. In 2005, Mourou proposed a new infrastructure, the Extreme Light Infrastructure (ELI), which is distributed over three pillars located in the Czech Republic, Romania and Hungary. He also pioneered the field of femtosecond ophthalmology that relies on a CPA femtosecond laser for precise myopia corrections and corneal transplants. Over a million such procedures are now performed annually. Mourou is member of the US National Academy of Engineering, and a foreign member of the Russian Science Academy, the Austrian Sciences Academy and the Lombardy Academy for Sciences and Letters. He is Chevalier de la Légion d'honneur and was awarded the 2018 Nobel Prize in Physics with his former student Donna Strickland.



Generating High-intensity, Ultrashort Optical Pulses

Donna Strickland, *Univ. of Waterloo, Canada*

With the invention of lasers, the intensity of a light wave was increased by orders of magnitude over what had been achieved with a light bulb or sunlight. This much higher intensity led to new phenom-

ena being observed, such as violet light coming out when red light went into the material. After Gérard Mourou and Strickland developed chirped pulse amplification, also known as CPA, the intensity again increased by more than a factor of 1,000 and it once again made new types of interactions possible between light and matter. The two developed a laser that could deliver short pulses of light that knocked electrons off their atoms. This new understanding of laser-matter interactions led to the development of new machining techniques that are used in laser eye surgery and micromachining of glass used in cell phones.

Donna Strickland is one of the recipients of the Nobel Prize in Physics 2018 for co-inventing Chirped Pulse Amplification with Gérard Mourou, her PhD supervisor at the time of the discovery. She earned her PhD in optics from the University of Rochester and her BEng from McMaster University. She was a research associate at the National Research Council Canada, a physicist at Lawrence Livermore National Laboratory and a member of technical staff at Princeton University. In 1997, she joined the technical staff of the University of Waterloo, where her ultrafast laser group develops high-intensity laser systems for nonlinear optics investigations. She is a recipient of a Sloan Research Fellowship, a Premier's Research Excellence Award and a Cottrell Scholar Award. She served as the president of The Optical Society (OSA) in 2013 and is an OSA Fellow.

Awards and Honors

Tuesday, 7 May

Grand Ballroom

OSA Frederic Ives Medal/Jarus W. Quinn Prize

Eli Yablonovitch, *Univ. of California Berkeley, USA*

Recognized for diverse and deep contributions to optical science including photonic crystals, strained semiconductor lasers, and new record-breaking solar cell physics.

The Optical Society's highest honor, this award recognizes overall distinction in optics.

The medal was established in 1928 to honor Frederic Ives for his pioneering contributions to color photography, three-color process printing, and other branches of applied optics. The prize was added in recognition of Jarus W. Quinn's 25 years of service as OSA's first Executive Director.

All conference locations are in the San Jose Convention Center unless otherwise noted.

OSA Charles Hard Townes Medal Recipient

Alexander Gaeta, *Columbia Univ., USA*

Recognized for seminal contributions to chip-based nonlinear photonics, nonlinear optics in photonic crystal fibers, and nonlinear propagation of ultrashort laser pulses.

The Optical Society (OSA) established this medal in 1980 to honor Charles Hard Townes, whose pioneering contributions to masers and lasers led to the development of the field of quantum electronics. It is given to an individual or a group for outstanding experimental or theoretical work, discovery or invention in the field of quantum electronics.

The Optical Society 2019 Fellows

These OSA Fellows are being recognized at CLEO.

Visit osa.org/fellows for a complete list of 2019 Fellows.

Jiming Bao, *Univ. of Houston, USA*

For contributions to semiconductor and metallic nanostructures and their applications in nanophotonics and solar energy harvesting

Pierre Berini, *Univ. of Ottawa, Canada*

For scientific achievements that have led to remarkable new insights in the field of nanophotonics, including pioneering contributions to surface plasmon photonics

Paul Campagnola, *Univ. of Wisconsin-Madison, USA*

For advancing nonlinear optical microscopy for biological applications, focusing on Second Harmonic Generation imaging of diseased states and multiphoton excited polymerization for fabricating tissue engineered scaffolds

Ji-Xin Cheng, *Boston Univ., USA*

For outstanding contributions to invention and development of label-free optical spectroscopic imaging technologies with groundbreaking applications to biology, medicine and materials science

Richard N. Claytor, *Fresnel Technologies Inc, USA*

For entrepreneurial leadership, product innovation, and commercialization of optical products, particularly high-quality Fresnel lenses with wide practical applicability in optical systems such as the passive infrared motion detectors ubiquitous in security and lighting control

Jay W. Dawson, *Lawrence Livermore National Laboratory, USA*

For leadership, innovations, and contributions to the understanding of fiber laser power scaling limits, development of spectrally selective fiber waveguiding structures for Nd³⁺ fibers, and lasers for future accelerators

Shengwang Du, *Hong Kong Univ. of Science and Technology, Hong Kong*

For pioneering contributions in photon-atom quantum interaction, including generation and manipulation of narrowband biphotons, observation of optical precursors, and realization of nontraditional quantum heat engines

Liang Feng, *Univ. of Pennsylvania, USA*

For outstanding pioneering scientific contributions to the field of non-Hermitian photonics and its applications in integrated nanophotonics and optoelectronics

Amr S. Helmy, *Univ. of Toronto, Canada*

For pioneering contributions in utilizing chi² nonlinearities in semiconductors for classical and quantum applications

Ronald Holzwarth, *Menlo Systems GmbH, Germany*

For having a pivotal role in the realisation and commercialisation of optical frequency combs

Sheng-Lung Huang, *National Taiwan Univ., Taiwan*

For contributions to glass-clad crystalline fiber based lasers and broadband light sources for optical coherence tomography

M. Saif Islam, *Univ. of California Davis, USA*

For distinguished contributions to the field of photodetectors, particularly highly sensitive ultra-fast photodetectors enabled by photon-trapping micro and nanostructures for data and telecommunication

Mackillo Kira, *Univ. of Michigan, USA*

For pioneering contributions to the theory of semiconductor quantum optics

Kei May Lau, *Hong Kong Univ. of Science and Technology, Hong Kong*

For exceptional contributions to hetero-epitaxy of III-V on silicon by MOCVD for photonic devices

Anne Matsuura, *Intel Corporation, USA*

For exceptional contributions to the support and advancement of optical sciences and technologies, through the development of national and international activities of government, industry, and academic institutions

Richard Mirin, *National Institute of Standards and Technology, USA*

For outstanding contributions to semiconductor quantum dot devices and quantum optics

Teri W. Odom, *Northwestern Univ., USA*

For pioneering contributions to multi-scale plasmonic nanostructures and nanophotonics

Taiichi Otsuji, *Tohoku Univ., Japan*

For pioneering contributions to terahertz emission and detection exploiting two-dimensional plasmonic and electronic systems with semiconductor nano- and hetero-structures

Geoff Pryde, *Griffith Univ., Australia*

For pioneering developments and advancements in photonic quantum information science, photonic entanglement-enhanced metrology, and the study of quantum measurement

David A. Reis, *Stanford Univ. and SLAC National Accelerator Laboratory, USA*

For pioneering achievements in ultrafast and strong-field phenomena in solids including discovery of solid-state high-harmonic generation, contributions to x-ray nonlinear optics, and invention of a novel femtosecond x-ray scattering method to probe phonon dispersion

Kent Rochford, *SPIE, USA*

For innovative technical leadership in multiple scientific disciplines of highly advanced optical metrology, especially for the US National Institute of Standards and Technology

Shyh-Chiang Shen, *Georgia Institute of Technology, USA*

For the development and advancement of compound semiconductor optoelectronic devices and integrated circuits

All conference locations are in the San Jose Convention Center unless otherwise noted.

Laura Waller, *Univ. of California Berkeley, USA*
For pioneering contributions in computational imaging

Daniel Wasserman, *Univ. of Texas at Austin, USA*
For contributions to the development of novel sources, detectors, and optical materials operating in the mid-infrared wavelength range

Edward A. Whittaker, *Stevens Institute of Technology, USA*
For important contributions to laser spectroscopy for sensitive detection of molecules, and extraordinary editorial service to Optics Letters

IEEE Photonics Society 2018 Fellows

Michael Krames, *Pacific Bell, USA*
For leadership in GaN-based light-emitting device physics and its commercialization

Hong-Bo Sun, *Tsinghua Univ., China*
For contributions to laser nanofabrication and ultrafast spectroscopy

James P. Gordon Memorial Speakership

Established in 2014 with the support of the Gordon family, The James P. Gordon Memorial Endowment funds a speakership on Quantum Information and Quantum Optics to a CLEO invited speaker. This speakership pays tribute to Dr. Gordon for his numerous high-impact contributions to quantum electronics and photonics, including the demonstration of the maser.

The recipient receives a \$1,500 honorarium and their presentation will be recorded and archived in OSA's media library. The contents will serve as an educational resource for the next generation of optics and photonics leaders.

This year's recipient can be viewed at www.osa.org/gordon

Tingye Li Innovation Prize

The Tingye Li Innovation Prize, established in 2013, honors the global impact Dr. Li made to the field of Optics and Photonics. This prize is presented to a young professional with an accepted paper that has demonstrated innovative and significant ideas and/or contributions to the field of optics.

The recipient of this prize receives a \$3,000 stipend, an invitation to the Chairs' Reception, and special recognition at the conference.

Recipients can be viewed at www.osa.org/Tingye

Maiman Student Paper Competition

The Maiman Student Paper Competition honors American physicist Theodore Maiman for his demonstration of the first working laser and his other outstanding contributions to optics and photonics. It recognizes student innovation and research excellence in the areas of laser technology and electro-optics. The competition results will be announced

during the meeting. The prize is endowed by a grant from HRL Laboratories LLC, the IEEE Photonics Society and the APS Division of Laser Science and is administered by the OSA Foundation.

Finalists can be viewed at www.osa.org/maiman

Incubic/Milton Chang Travel Grant

The OSA Foundation is pleased to award 10 recipients this year's Incubic/Milton Chang Student Travel Grant, endowed by Milton and Rosalind Chang. The list of recipients can be viewed at www.osa.org/foundation.

Awards and Honors Presented Elsewhere at CLEO

OSA Esther Hoffman Beller Medal

Rick Trebino, *Georgia Institute of Technology, USA*
For pioneering educational optics practices, including the only textbook on ultrashort-pulse measurement, innovative short courses, and the creation of high-quality graduate and undergraduate optics lectures that are shared freely with students and instructors worldwide.

The medal was established in 1993 by the estate of Esther Hoffman Beller. It is presented for outstanding contributions to education in optical science and engineering. Consideration is given to outstanding teaching and/or original work in optics education that enhances the understanding of optics.

OSA Nick Holonyak Jr. Award

Fumio Koyama, *Tokyo Institute of Technology, Japan*
For seminal contributions to VCSEL photonics and integration.

The award was established in 1997 to honor Nick Holonyak Jr., who has made distinguished contributions to the field of optics through the development of semiconductor based light emitting diodes and semiconductor lasers. It is given to an individual who has made significant contributions to optics based on semiconductor-based optical devices and materials, including basic science and technological applications

The Bernard J. Couillaud Prize

The OSA Foundation (OSAF) and Coherent, Inc. have partnered to create the Bernard J. Couillaud Prize. The Prize provides the opportunity for an early-career professional to pursue a compelling and innovative project that has the potential to make a meaningful and positive impact on the science and applications of ultrafast lasers. One early career professional will receive a merit-based award which includes a \$20,500 USD prize and \$5,000 USD in travel expenses.

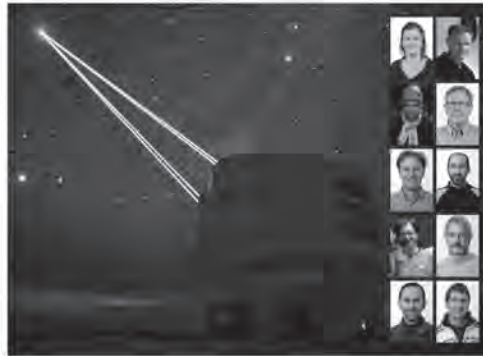
This year's winner can be viewed at osa.org/couillaud.

All conference locations are in the San Jose Convention Center unless otherwise noted.

THE OPTICAL SOCIETY CONGRATULATES

2018 Paul F. Forman Team Engineering Excellence Award Winner Adaptive Optics Facility on the Very Large Telescope (VLT) at European Southern Observatory's Paranal Observatory

The team is recognized for equipping one of the 8-m Unit Telescopes at ESO's Paranal Observatory in Chile with an Adaptive Optics Laser Guide Star Facility, providing exquisite images to the unique 3-D spectrograph MUSE and near-infrared imager HAWK-I.



Congratulations to the team:

Jose Antonio Abad
Matteo Accardo
Emmanuel Aller-Carpentier
Jose-Luis Álvarez
Paola Amico
Javier Argomedo
Robin Arsenault
Pedro Baksai
Juan Beltran
Thomas Bierwirth
Domenico Bonaccini Calia
Pierre Bourget
Stéphane Brillant
Bernard Buzzoni
Giorgio Calderone
Gianluca Chiozzi
Mauro Comin
Ralf Conzelmann
Bernard Delabre
Diego Del Valle
Robert Donaldson
Dario Dorigo
Mark Downing

Michel Duchateau
Philippe Duhoux
Christophe Dupuy
Enrico Fedrigo
Gert Fischer
Christophe Frank
Eloy Fuenteseca
Fernando Gago
Juan Carlos Guerra
Ivan M. Guidolin
Stéphane Guisard
Pablo Gutierrez-Cheetham
Ronald Guzman
Wolfgang Hackenberg
Pierre Haguenaer
Andreas Haimerl
Peter Hammersley
George Hau
Volker Heinz
Pascale Hibon
Ronald Holzloehner
Stefan Huber
Norbert Hubin

Lieselotte Jochum
Paul Jolley
Andreas Jost
Lothar Kern
Mario Kiekebusch
Jean-Paul Kirchbauer
Johann Kolb
Harald Kuntschner
Paolo La Penna
Miska Le Louarn
Samuel Leveque
Steffan Lewis
Jean-Louis Lizon
Pierre-Yves Madec
Antonio Manescau-Hernandez
Steward McClay
Leander Mehrgan
Ivan Munoz
Sylvain Oberti
Juan Carlos Palacio
Jerome Paufique
Lorenzo Pettazzi
Thomas Pfrommer

Jean-Francois Pirard
Dan Popovic
Marco Quattri
Jutta Quentin
Christian Ramirez
Javier Reyes
Rob Ridings
Pierre Sansgasset
Marc Sarazin
Babak Sedghi
Fernando Selman
Christian Soenke
Heiko Sommer
Stefan Stroebele
Marcos Suarez Valles
Mirko Todorovic
Sebastien Tordo
Javier Valenzuela
Ignacio Vera
Elise Vernet
Joël Daniel Roger Vernet
Dominika Wylezalek
Gérard Zins

OSA[®]
The Optical Society

100
Since 1916

Call for 2019 Nominations!
Deadline: 10 July

osa.org/FormanTeamAward

Workshops

New this year are the CLEO Workshops. These sessions provide interactive learning environments and are open to all conference registrants.

The format is intended to be less formal than a technical session or symposium so as to enable open discussion between panelists and the audience to address technical and strategic questions for which there is no clear consensus.

Will Quantum Computing Actually Work?!

Monday, 6 May; 18:30–20:00
Room 210A

The realization of a large-scale quantum computer represents the holy grail for quantum researchers and for those hoping to harness the power of quantum entanglement. Far beyond practical limits of classical computing, quantum computers potentially enable the simulation of all quantum processes in nature, and have profound and immediate practical applications, most famously in cryptography. After decades of painstaking research on small-scale laboratory devices, there has been a recent, dramatic ramping up of commercial interest, spanning boutique companies to tech giants.

This workshop aims to address the question currently on the minds of many — is large-scale, fault-tolerant, universal quantum computing a realistic possibility?

Organizers

Ben Eggleton, *Univ. of Sydney, Australia*
Tara Fortier, *National Institute of Standards & Technology, USA*
Andrew Wilson, *National Institute of Standards & Technology, USA*

Panelists

Jerry Chow, *IBM Corp., USA*
Mikhail Lukin, *Harvard Univ., USA*
Christopher Monroe, *Univ. of Maryland, Joint Quantum Institute & IONQ Inc., USA*
Robert Schoelkopf, *Yale Univ., USA*
Andrew Steane, *Univ. of Oxford, UK*
Jelena Vuckovic, *Stanford Univ., USA*
Birgitta Whaley, *UC Berkeley, USA*

What Will Be the Largest Commercial Application for Optical Frequency Combs in 10 Years?

Monday, 6 May; 18:30–20:00
Room 210B

More than 15 years ago, a committee at CLEO was formed to capture research on precision optical measurement primarily enabled by the development of optical frequency combs. Since their first demonstration in 2000, optical frequency combs have seen rapid changes in laser technology, expansion of applications, and industry interest. This workshop seeks a discussion from experts in government, academia and industry on what the commercial future holds for this versatile technology.

Organizers

Fabrizio Giorgetta, *National Institute of Standards & Technology, USA*
Tara Fortier, *National Institute of Standards & Technology, USA*

Moderator

Fabrizio Giorgetta, *National Institute of Standards & Technology, USA*

Panelists

Ronald Holzwarth, *Menlo Systems GmbH, Germany*
Ursula Keller, *ETH Zürich, Switzerland*
Seung-Woo Kim, *KAIST, South Korea*
Markus Mangold, *IRsweep, Switzerland*
Nate Newbury, *National Institute of Standards & Technology, USA*
Nathalie Picqué, *Max Planck Institute of Quantum Optics, Germany*
Stojan Radic, *University of California San Diego, USA*
Felix Rohde, *TOPTICA Photonics AG, Germany*

Beyond Awareness: What Actions Can Be Taken to Improve Diversity in STEM?

Wednesday, 8 May, 10:30–12:00
Exhibit Hall Theater II

In the hard sciences, women and minorities have seen slower improvements in representation compared to fields such as medicine and law. Information on how to improve this representation in STEM is also difficult to find. This workshop brings together leaders of professional organizations and subject matter experts to discuss policies and actions that can improve gender, racial, LGBTQI and disability diversity within the physics, engineering and optics communities.

Organizers

Arti Agrawal, *University of Technology Sydney, Australia*
Ben Eggleton, *University of Sydney, Australia*
Tara Fortier, *National Institute of Standards & Technology, USA*
Christina Willis, *Consultant, USA*

Panelists

Liz Rogan, *CEO, The Optical Society*
Kent Rochford, *CEO, the International Society for Optics and Photonics*
Kate Kirby, *CEO, American Physical Society*
Doug Razzano, *Executive Director, Institute of Electrical and Electronics Engineers*
Meg Urry, *Yale Univ., USA*

All conference locations are in the San Jose Convention Center unless otherwise noted.

Special Symposia

Symposium on High Average Power Ultrafast Lasers: Trends, Challenges & Applications

Monday, 6 May, Session I: 8:00–10:00; Session II: 10:30–12:30; Session III: 13:30–15:30
Executive Ballroom 210E

Organizers

Thomas Metzger, *Trumpf Scientific Lasers, Germany*
Clara Saraceno, *Ruhr Universität Bochum, Germany*
Thomas Spinka, *Lawrence Livermore National Laboratory, USA*

Ultrafast laser systems combining high peak power and high repetition rate are desired in an extremely large variety of applications, both in scientific and industrial environments. Driven by these applications, the last several years have seen a tremendous increase in research related to high average power ultrafast laser systems and corresponding technologies, which has resulted in exponential progress in achievable performance. Several technologies, mostly based on Yb-doped slabs, fibers and disks, have surpassed the kilowatt average power milestone and continue to push the limits.

This symposium aims to, in a single forum, review the latest progress, trends, and current challenges in the area of high average power ultrafast lasers of all architectures (fiber, disk, and slab lasers), and discuss application needs that will shape the development of these lasers over the next several years.

Invited Speakers

Cristina Hernandez-Gomez, *STFC Rutherford Appleton Laboratory, UK*

High peak power, high average power lasers at the CLF and their potential applications

Norman Hodgson, *Coherent Inc., USA*

Industrial Ultrafast Lasers - Systems, Processing Fundamentals, and Applications

Clemens Hönninger, *Amplitude, France*

Industrial kilowatt femtosecond lasers: potentialities and challenges

Jerome Kasparian, *Univ. of Geneva, Switzerland*

Multi-Wavelength Laser Control of High-Voltage Discharges: From the Laboratory to Säntis Mountain

Ursula Keller, *ETH Zurich, Switzerland*

Recent Advances in SESAM-modelocked High-power Thin Disk Lasers

Andreas Maier, *Univ. of Hamburg, Germany*

Towards Stable Laser-Plasma Electron Acceleration

Dirk Sutter, *TRUMPF Laser GmbH, Germany*

High Power and High Energy Ultrafast Disk Lasers for Industrial Applications

Takunori Taira, *Institute for Molecular Science, Japan*

High Average Power Ultrafast Lasers: Large Aperture Quasi-phase Matched Nonlinear Devices

Johannes Weitenberg, *Max-Planck-Institut für Quantenoptik, Germany*

Nonlinear Pulse Compression at High Average Power Based on Multi-pass Cells

Symposium on Nonreciprocal Photonics

Monday, 6 May, Session I 10:30–12:30;
Session II: 13:30–15:30
Executive Ballroom 210B

Organizers

Pascal Del Hays, *National Physical Laboratory, UK*
Lan Yang, *Washington Univ., USA*
Ewold Verhagen, *AMOLF, Netherlands*

Nonreciprocal photonics has been a rapidly growing research field in recent years. This is motivated by a strong demand for nonreciprocal elements in upcoming generations of integrated optical circuits. In particular, the increasing complexity of photonic circuits and their combination with chip-based laser sources requires new optical elements, e.g. for efficient optical isolators and circulators. On the fundamental physics side, research on optical nonreciprocity has led to many new insights on interaction of light with complex media, optomechanical systems and nonlinear materials. This special symposium aims to provide a forum for discussing the various different means of achieving optical nonreciprocity as well as related applications. This includes nonreciprocity and unidirectional transmission phenomena based on Kerr nonlinearity, optomechanical systems, metamaterials, integrated magneto-optical devices, PT symmetric systems, Brillouin scattering, topological protection, spin-orbit coupling and through other nonlinear optical effects. Beyond the fundamental physics of optical nonreciprocity, this symposium also addresses applications of nonreciprocity e.g. for sensors, integrated photonic circuits and in laser systems.

Invited Speakers

Andrea Alu, *CUNY Advanced Science Research Center, USA*

Nonreciprocal and Topological Photonics

Benjamin Eggleton, *Univ. of Sydney, Australia*

Brillouin Based non-Reciprocal Functions for On-chip Optical Signal Processing

Tsampikos Kottos, *Wesleyan Univ., USA*

Utilizing Floquet Engineering for the Design of Non-reciprocal Transport

Caroline Ross, *Massachusetts Institute of Technology, USA*

Magneto-optical Garnets for Nonreciprocal Integrated Photonics

Edo Waks, *Univ. of Maryland at College Park, USA*

Topological Quantum Photonics

All conference locations are in the San Jose Convention Center unless otherwise noted.

Symposium on Machine Learning Photons: Where Machine Learning and Photonics Intersect I

Monday, 6 May Session I: 13:30–15:30
Salon I & II, Marriott

Organizers

Zongfu Yu, *Univ. of Wisconsin Madison, USA*
Darko Zibar, *Danmarks Tekniske Universitet, Denmark*
Shanhui Fan, *Stanford Univ., USA*
Bahram Jalali, *Univ. of California Los Angeles, USA*
Marin Soljačić, *Massachusetts Institute of Technology, USA*

Over the past 5 years, tremendous progress has been made in machine learning. Its impact has started to emerge across a broad range of fields. Photonics is one of them. This symposium will highlight recent progress at the intersection of photonics and machine learning. Various methods such as deep learning, Bayesian inference, Monte Carlo Markov Chain and Gaussian processes will be addresses on how they can provide new paths for solving the most critical problems in various fields in photonics. For example, deep learning points to new inverse design approach for complex photonic structures while Bayesian inference offers detection methods that can operate at the quantum limit. Combination of deep learning with time stretched measurements has been highly successful in biological cell analysis at extreme throughput. Unlike optimization-driven approaches that require expensive computation, machine learning leverages on learning form the data. Photonics also provides exciting opportunities for all optical implementation of various machine learning techniques. There are also many other exciting developments in microscopy, quantum communication, sensing, bio-medical image recognition, optical communication and opto-mechanics that have benefited from machine learning.

Invited Speakers

Wenshan Cai, *Georgia Institute of Technology, USA*
Generative Model for the Inverse Design of Photonic Nanostructures

Folkert Horst, *International Business Machines Corp., Switzerland*

Integrated Photonics for Neural Network Acceleration

Paul Prucnal, *Princeton Univ., USA*
Multiwavelength Neuromorphic Photonics

Symposium on Intense-field Nonlinear Optics & High Harmonic Generation in Nanoscale Materials I

Tuesday, 7 May; Session I: 13:00–15:00;
Session II: 17:00–19:00
Salon I & II, Marriott

Organizers

Marko Loncar, *Harvard Univ., USA*
Maxim Shcherbakov, *Cornell Univ., USA*
Gennady Shvets, *Cornell Univ., USA*

Nanomaterials are driving many research fields in photonics, from spectroscopy to microscopy, from sensing to telecommunications. Importantly, they can enhance light-matter interactions and funnel optical fields into hot spots, spawning applications in nonlinear optics. They have also shown enormous potential for non-perturbative nonlinear optics

and high-harmonic generation, producing intense extreme-UV pulses on the nanoscale. Several platforms have been suggested, including 2D materials, plasmonic nanostructures, as well as all-dielectric and semiconductor metasurfaces. However, a delicate balance between field localization, losses and dispersion should be kept when designing an efficient material for ultrahigh-power laser applications. This symposium will review and discuss the recent progress in light-matter interactions on an ultra-intense scale, such as nonlinear frequency conversion and generation of high harmonics, assisted by novel nanostructures and metamaterials. We also solicit contributed papers that advance the field of high-intensity light-matter interactions on the nanoscale.

Invited Speakers

Pierre Berini, *Univ. of Ottawa, Canada*
Enhancement of Nonlinear Processes by Surface Plasmons

Igal Brener, *Sandia National Laboratories, USA*
Extreme Nonlinear Optics With Dielectric Metasurfaces

Andrey Fedyanin, *Lomonosov Moscow State Univ., Russia*
Optical Harmonic Generation in Nonlinear All-dielectric Nanoantennas and Metasurfaces

David Reis, *Stanford Univ., USA*
High-harmonic Generation from Bulk to Engineered Solids

Koichiro Tanaka, *Kyoto Univ., Japan*
Extreme nonlinear optics in two dimensional materials

Symposium on Quantum Information in Time-Frequency Domain

Tuesday, 7 May, Session I: 13:00–15:00;
Session II: 17:00–19:00
Executive Ballroom 210A

Symposium Organizers

Pavel Lougovski, *Oak Ridge National Laboratory, USA*
Michael G. Raymer, *Univ. of Oregon, USA*
Brian J. Smith, *Univ. of Oregon, USA*
Andrew M. Weiner, *Purdue Univ., USA*

There has been significant experimental progress in encoding and manipulating quantum information using light's spectral-temporal degrees of freedom. From electro-optics to nonlinear optics — a range of technologies has been utilized to prepare, control and characterize qubits and demonstrate quantum logic. Spectral encoding is naturally compatible with optical fiber networks, amenable to massive parallelization, and valuable for scaling up quantum memories. Spectral beam splitters, based both on optical nonlinearities and electro-optic modulation, have been demonstrated recently. For spectral-temporal encoding, which can be used to store large amounts of information in a single photon, quantum pulse gates based on mixing single photons with shaped control fields have allowed state discrimination of orthogonal time-frequency pulsed modes (temporal modes). Considerable advances have also been made in generating entangled frequency combs from bulk sources and on-chip by using microring resonators, opening new avenues for quantum information processing with qudits. These novel techniques and methods can be combined and readily utilized for applications in quantum networking, computing, key distribution, and classical optical information processing. The aim of this symposium is to bring together researchers from across

All conference locations are in the San Jose Convention Center unless otherwise noted.

these research fields and to expose others to the exciting new opportunities offered by spectral-temporal encoding of light.

Invited Speakers

Benjamin Brecht, *Universität Paderborn, Germany*
Tailored Generation, Manipulation, and Application of Photonic Temporal Modes

Joseph Lukens, *Oak Ridge National Laboratory, USA*
Quantum Information Processing with Frequency-bin Qubits: Progress, Status, and Challenges

Olivier Pfister, *Univ. of Virginia, USA*
Generation of scalable cluster states in the quantum optical frequency comb

Valérian Thiel, *Univ. of Oxford, UK*
Full Single and Two Photon Spectral Mode-function Reconstruction

Nicolas Treps, *Sorbonne Université, France*
Tailored Non-Gaussian Multimode States of Quantum Light

Symposium on Space-borne Quantum Sensors

Tuesday, 7 May, 13:00–15:00
Executive Ballroom 210G

Symposium Organizers

Matthew Hummon, *National Institute of Standards and Technology, USA*
Jeff Sherman, *National Institute of Standards and Technology, USA*

Governments, industry leaders and academic researchers are pursuing and funding the development of quantum technology with renewed intensity. While research into quantum information and exotic quantum states captures headlines, systems which leverage quantum properties of light and matter to enable and enhance measurements of physical quantities are just as likely to broadly alter our technological landscape. Quantum sensors enable measurement of acceleration, rotation, magnetic- and electric-field, temperature, chemical content, low-light intensity, length, time, and frequency — often with high stability and inherent calibration to primary standards. Space missions often impose unique and extreme requirements on sensor technology, and therefore often serve as catalysts for guiding new technologies out of the laboratory and into viable commercial application. Several such missions featuring quantum sensors are scheduled to launch in coming years. This symposium will focus on opportunities and technical challenges related to space-borne quantum sensors, and empirical lessons garnered from recently completed missions.

Invited Speakers

Sergio Mottini, *Thales Alenia Space, Italy*
Atom Interferometry for Space-Borne Sensors

Cheng-Zhi Peng, *Univ. of Science and Technology of China, China*
Quantum Science Experiments with Micius Satellite

Evan Salim, *ColdQuanta Inc., USA*
Enabling Technologies for Space-Based Quantum Systems

Robert James Thompson, *Jet Propulsion Laboratory, USA*
The Coolest Spot in the Universe: Early results from the Cold Atom Laboratory Mission Aboard the International Space Station

Symposium on Coupling Artificial Atoms to Nano- and Opto-mechanical Systems

Wednesday, 8 May, Session I: 13:00–15:00;
Session II: 17:00–19:00
Executive Ballroom 210A

Symposium Organizers

Paul Barclay, *Univ. of Calgary, Canada*
Hailin Wang, *Univ. of Oregon, USA*

This symposium will focus on recent experimental and theoretical advances on coupling artificial atoms, such as defect centers and quantum dots, to nanomechanical or optomechanical resonators. These hybrid quantum systems bring together concepts and techniques from different disciplines — optics and atomic physics, nanophotonics, nanomechanics and quantum information science — and allow spin control of mechanical motion as well as mechanical control of the spin states. Quantum control of both spin and mechanical degrees of freedom in these systems can enable potential applications in quantum information processing such as phononic or phononic-photonic quantum networks, as well as quantum transducers for quantum networking.

Invited Speakers

David Awschalom, *Univ. of Chicago, USA*
Quantum Control of Spins in Silicon Carbide with Photons and Phonons

Yiwen Chu, *Yale Univ., USA*
Creating Quantum States of Sound with Superconducting Qubits

Gregory Fuchs, *Cornell Univ., USA*
Spin and Orbital Resonance Driven by a Mechanical Resonator

Mark Kasperczyk, *Univ. of Basel, Switzerland*
Toward Novel Coherence Protection and Sensing Techniques: Closed Counter Interaction Using a Single Spin

Peter Rabl, *Technische Universität Wien, Austria*
Phonon Networks with SiV Centers in Diamond Waveguides

All conference locations are in the San Jose Convention Center unless otherwise noted.

Symposium on Machine Learning Photons: Where Machine Learning and Photonics Intersect II & III

Friday, 10 May Session II: 10:30–12:30; Session III: 14:00–16:00
Executive Ballroom 210F

Organizers

Zongfu Yu, *University of Wisconsin Madison, USA*

Darko Zibar, *Danmarks Tekniske Universitet, Denmark*

Shanhui Fan, *Stanford University, USA*

Bahram Jalali, *University of California Los Angeles, USA*

Marin Soljačić, *Massachusetts Institute of Technology, USA*

Over the past 5 years, tremendous progress has been made in machine learning. Its impact has started to emerge across a broad range of fields. Photonics is one of them. This symposium will highlight recent progress at the intersection of photonics and machine learning. Various methods such as deep learning, Bayesian inference, Monte Carlo Markov Chain and Gaussian processes will be addresses on how they can provide new paths for solving the most critical problems in various fields in photonics. For example, deep learning points to new inverse design approach for complex photonic structures while Bayesian inference offers detection methods that can operate at the quantum limit. Combination of deep learning with time stretched measurements has been highly successful in biological cell analysis at extreme throughput. Unlike optimization-driven approaches that require expensive computation, machine learning leverages on learning from the data. Photonics also provides exciting opportunities for all optical implementation of various machine learning techniques. There are also many other exciting developments in microscopy, quantum communication, sensing, bio-medical image recognition, optical communication and opto-mechanics that have benefited from machine learning.

Invited Speakers

Hou-Man Chin, *Danmarks Tekniske Universitet, Denmark*

Phase Compensation for Continuous Variable Quantum Key Distribution

Tyler Hughes, *Stanford Univ., USA*

Training of Photonic Neural Networks through In Situ Backpropagation

Bahram Jalali, *Univ. of California Los Angeles, USA*

Deep Imaging Cytometry

Aydogan Ozcan, *Univ. of California Los Angeles, USA*

Deep Learning in Optical Microscopy and Image Reconstruction

Marin Soljačić, *Massachusetts Institute of Technology, USA*

Ken Xingze Wang, *Huazhong Univ. of Science and Technology, China*

Object Recognition with Optical Coherence

Tom Zahavy, *Technion, Israel*

Deep Learning Reconstruction of Ultrashort Laser Pulses and Ptychographic Data from Ambiguous Measurements

All conference locations are in the San Jose Convention Center unless otherwise noted.

Applications & Technology Topical Reviews

A&T Topical Review on Flat Optics

Monday, 6 May: Session I 13:30–15:30;
Session II; 16:00–18:00
Meeting Room 212 A/B

Organizer

Federico Capasso, *Harvard Univ., USA*

Flat Optics I: Physics of metasurfaces and their applications: Metasurfaces enable an unprecedented platform to explore light-matter interaction. This session covers aspects of interesting fundamental topics in metasurfaces, including but not limited to zero index materials, dispersion engineering, ultrafast dynamics, nonreciprocity, nonlinearity and quantum metasurfaces.

Invited Speakers

Mikhail Belkin, *Univ. of Texas at Austin, USA*

Nonlinear metasurfaces for power limiting

Yuri Kivshar, *Australian National Univ., Australia*

Nonlinear and topological dielectric metasurfaces

Vladimir M. Shalaev, *Purdue Univ., USA*

Metasurfaces for Synchrotron radiation generation and ultrafast beam steering

Flat Optics II: Metasurface optical components: Metasurfaces enable the redesign of optical components into thin, planar and multifunctional elements, promising a major reduction in footprint and system complexity as well as the introduction of new optical functions. This session will focus on metasurface-based optical devices and systems for a wide range of applications and will include high-performance components designed by inverse methods.

Invited Speakers

Wei Ting Chen, *Harvard Univ., USA*

Dispersion-engineered and Polarization-insensitive Metasurfaces for Broadband Achromatic Optics

Jonathan Fan, *Stanford Univ., USA*

AI-assisted Design of Topologically Complex Metasurfaces

Byoung-ho Lee, *Seoul National Univ., USA*

Metasurface Devices for AR/VR

A&T Topical Review on Advanced Design, Imaging and Process Technologies for Next Generation Semiconductors

Tuesday, 7 May: 13:00–15:00
Wednesday, 8 May: 13:00–15:00
Theater II

Organizers

Will Conley, *Cymer, USA*

Jae Won Hahn, *Yonsei Univ., South Korea*

The successful integration of design, layout, imaging solutions and advances in process technologies continue to provide viable working solutions to continue the advancement of Logic and Memory technologies. This topical review will highlight recent advances in design layout to on wafer imaging to on wafer final etch of circuitry. Areas of interest include layout ground rules, use of machine learning throughout the design, verification cycle and the application to imaging solutions through pupil and mask optimization (SMO). Insight into metrology issues, Scanner/source (laser) improvements and the integration of etch processes will be reviewed.

Invited Speakers

Will Conley, *Cymer LLC, USA*

Quantifying Improvements in Field to Field and Wafer to Wafer CD Variation from Laser Bandwidth Variation

Yuri Granik, *Mentor Graphics, USA*

Compensation of Optical Distortions in IC Fabrication

Jae W Hahn, *Yonsei University, South Korea*

Nanoscale Three-dimensional Patterning with Plasmonic Lithography

Patrick Naulleau, *Lawrence Berkeley National Labs, USA*

Extending EUV to the High-NA EUV Regime

Robert Socha, *ASML, USA*

Reduction and Control of Edge Placement Error at the 5nm node Through a Holistic Approach

Yoen Sik Jung, *KAIST, South Korea*

Nanopatterning of Things: from Metals, Oxides to Quantum Dots

A&T Topical Review on Progress in the Semiconductor Laser Technology

Tuesday, 7 May: 13:00–15:00;
Wednesday, 8 May: 13:00–15:00
Theater I

Organizer

Edik Rafailov, *Aston Univ., UK*

For over half a century, laser technology has undergone a technological revolution. These technologies, particularly semiconductor lasers have reached mature stage and transformed from a fundamental area of research into emerging applications and products. This topical Review meeting will present recent progress in the development of novel light sources in a broad wavelength range along with their applications (ie lighting, sensing, biophotonics etc).

All conference locations are in the San Jose Convention Center unless otherwise noted.

Invited Speakers

Richard Hogg, *Glasgow Univ., UK*
Photonic Crystal Surface Emitting Lasers

Sven Höfling, *Univ. of Würzburg, Germany*
Interband Cascade Devices for sensing

Takeo Kageyama, *QD Laser Ltd, Japan*
Semiconductor Lasers for Next-generation Applications

Mike Leszczynski, *Institute of High Pressure Physics Warsaw, Poland*

Material issues in GaN-based Laser Diode Manufacturing

A&T Topical Review on Silicon Photonics

Thursday, 9 May; Session I: 14:00-16:00, Session II: 16:30-18:30

Meeting Room 211 A/B

Organizers

Long Chen, *Acacia Communications, USA*

Amy Foster, *Johns Hopkins Univ., USA*

Over the past few decades, silicon photonics technology has matured from one-off demonstrations on optical tables to commercial products in applications generally involving information transfer. The advancement of the field is a result of many fantastic demonstrations by the research community (academic, government, and industry) as well as the establishment of several silicon photonic foundries where researchers can share real estate in multi-project wafers to manufacture

prototype silicon photonic devices up to the sub-system level of integration. The maturity of the field and the increased accessibility of the manufacturing have resulted in a very exciting and application-diverse field of silicon photonics. In this topical review, we will highlight work being done all over the field of silicon photonics with diverse fabrication approaches and application space. We will highlight ongoing efforts at all levels of technology readiness, from basic science to commercial products. Many silicon-based platforms including crystalline, poly-, and amorphous silicon, silicon nitride, silicon germanium, silicon-rich nitride, and silicon oxynitride will be highlighted.

Invited Speakers

Chris Doerr, *Acacia Communications, Inc., USA*

Coherent Silicon Photonic Devices for Communication and Sensing

David Moss, *Swinburne Univ. of Technology, Australia*
RF, Microwave and Communications Applications of Microcombs

Alex Wright, *Ayar Labs, Inc., USA*

Monolithic Silicon optoelectronics with Standard CMOS Processes

Graham Reed, *Univ. of Southampton, UK*

Silicon Photonics

Linjie Zhou, *Shanghai Jiao Tong Univ., China*

Silicon Photonic Phased Arrays

Call for Proposals
Applications & Technology Topical Reviews
Special Symposia
SUBMISSION DEADLINE: 10 JULY 2019

CLEO
Laser Science to Photonic Applications

Technical Conference: 10 – 15 May 2020
CLEO:EXPO: 12 – 14 May 2020
San Jose McEnery Convention Center
San Jose, California, USA

Help Build Next Year's CLEO

These programs respond to the needs and interests of the community by coordinating related presentations to provide in-depth exploration of the most relevant themes. You can help select topics by submitting a proposal.

Applications & Technology Topical Reviews
These sessions emphasize significant recent advances in the application of photonics technologies to address current real-world problems.
cleoconference.org/applications

Special Symposia
Open to any timely, cutting-edge topic and/or new material in a rapidly advancing area, the symposia offer detailed insights from presenters with different perspectives.
cleoconference.org/symposia

APS physics | IEEE Photonics Society | OSA The Optical Society | 100 Since 1976

All conference locations are in the San Jose Convention Center unless otherwise noted.

Short Courses

Short Course Chairs

Robert Fisher, *R. A. Fisher Associates, USA*

Konstantin Vodopyanov; *CREOL, The College of Optics & Photonics, Univ. Central Florida, USA*

The CLEO Short Course Program includes a range of topics at a variety of educational levels. Widely recognized experts in industry and academia lead attendees in building skills and/or achieving new insight, and the small-classroom setting provides a tremendous, interactive learning opportunity. Short Courses are an excellent opportunity to learn about new products, cutting edge technology and vital information at the forefront of the laser science and electro-optics fields.

Certificates of Attendance are available for attendees who register, attend, and complete the course evaluation. If you have any questions about receiving the course evaluation or your Certificate of Attendance upon completion, please email shortcourses@cleoconference.org with your name, Short Course number(s) and inquiry.

Sunday, 5 May 2019

08:30–12:30

SC149: Foundations of Nonlinear Optics
Robert Fisher, *R. A. Fisher Associates, USA*

SC456: How to Start a Company
Jes Broeng, *Danmarks Tekniske Universitet, Denmark*

SC466: Silicon Integrated Nanophotonics
Yurii A. Vlasov, *Univ. of Illinois at Urbana-Champaign, USA*

SC479: Basics of Quantum Optics for Quantum-Enabled Technologies NEW
Bahaa Saleh, *CREOL, Univ. of Central Florida, USA*

13:30–17:30

SC157: Laser Beam Analysis, Propagation, and Shaping Techniques
James Leger, *Univ. of Minnesota, USA*

SC396: Frontiers of Guided Wave Nonlinear Optics
Ben Eggleton, *Univ. of Sydney, Australia*

SC475: Metasurface Flat Optics: A New Paradigm for Optical Components Design and Manufacturing NEW
Federico Capasso, *Harvard Univ., USA*

14:30–17:30

SC478: Microresonator based Optical Frequency Comb and Photonic Waveguide Supercontinuum Sources NEW
Tobias Kippenberg, *École polytechnique fédérale de Lausanne, Switzerland*

Monday, 6 May 2019

08:30–12:30

SC270: High Power Fiber Lasers and Amplifiers
W. Andrew Clarkson, *Univ. of Southampton, UK*

SC352: Introduction to Ultrafast Pulse Shaping--Principles and Applications
Marcos Dantus, *Michigan State Univ., USA*

SC361: Coherent Mid-IR Light: Generation and Applications
Konstantin Vodopyanov, *CREOL, Univ. of Central Florida, USA*

SC477: Laser Radar and Remote Sensing: An Application-oriented Introduction NEW
Fabio Di Teodoro, *Raytheon, USA*

SC481: Fundamentals and Applications of VCSELs NEW
Kent Choquette, *Univ. of Illinois, USA*

13:30–17:30

SC362: Cavity Optomechanics: Fundamentals and Applications of Controlling and Measuring Nano- and Micro-mechanical Oscillators with Laser Light
Tobias Kippenberg, *École polytechnique fédérale de Lausanne, Switzerland*

SC376: Plasmonics
Mark Brongersma, *Stanford Univ., USA*

SC378: Introduction to Ultrafast Optics
Rick Trebino, *Georgia Institute of Technology, USA*

SC476: QCL and QCL Combs NEW
Jérôme Faist, *ETH Zürich, Switzerland*

Tuesday, 15 May 2018

10:30–13:30

SC455: Integrated Photonics for Quantum Information Science and Technology
Dirk Englund, *MIT, USA*

10:30–14:30

SC403: NanoCavity Quantum Electrodynamics and Applications
Jelena Vučković, *Stanford Univ., USA*

SC410: Finite Element Modeling Methods for Photonics and Optics
Arti Agrawal, *Univ. of Technology Sydney, Australia*

SC424: Optical Terahertz Science and Technology
David G. Cooke, *McGill Univ., Canada*

SC438: Photonic Metamaterials
Nader Engheta, *Univ. of Pennsylvania, USA*

All conference locations are in the San Jose Convention Center unless otherwise noted.

Short Course Descriptions

SC149: Foundations of Nonlinear Optics

Robert Fisher, *R. A. Fisher Associates, USA*

Short Course Level: Beginner and Intermediate

This course provides the basic concepts of nonlinear optics. Although some mathematical formulas are provided, the emphasis is on simple explanations. It is recognized that the beginning practitioner in nonlinear optics is overwhelmed by a constellation of complicated nonlinear optical effects, including second-harmonic generation, optical Kerr effect, self-focusing, self-phase modulation, self-steepening, fiber optic solitons, chirping, stimulated Raman and Brillouin scattering and photorefractive phenomena. It is our job in this course to demystify this daunting collection of seemingly unrelated effects by developing simple and clear explanations for how each works, and learning how each effect can be used for the modification, manipulation or conversion of light pulses. Examples will address the nonlinear optical effects that occur inside optical fibers and those that occur in liquids, bulk solids and gases. This course will incorporate the creation of cartoons to lock in the basic concepts.

SC157: Laser Beam Analysis, Propagation and Shaping Techniques

James Leger, *Univ. of Minnesota, USA*

Short Course Level: Advanced Beginner

The propagation and focusing properties of real laser beams are greatly influenced by beam shape, phase distortions, degree of coherence, polarization and aperture truncation effects. The ability to understand, predict and correct these real-world effects is essential to modern optical engineering. Attendees will learn a variety of techniques for measuring and quantifying the important characteristics of real laser beams, be able to calculate the effects of these characteristics on optical system performance and explore a variety of beam shaping techniques to optimize specific optical systems.

SC270: High Power Fiber Lasers and Amplifiers

W. Andrew Clarkson, *Univ. of Southampton, UK*

Short Course Level: Advanced Beginner

Recent advances in cladding-pumped fiber lasers and amplifiers have been dramatic, leading to unprecedented levels of performance in terms of output power, efficiency, beam quality and wavelength coverage. These achievements have attracted growing interest within the community and have fueled thoughts that fiber based sources may one day replace conventional "bulk" solid-state lasers in many application areas. The main attractions of cladding-pumped fiber sources are derived directly from their geometry, which simultaneously allows very efficient generation of coherent light and almost complete immunity from the effects of heat generation — so detrimental to the performance of other types of lasers.

SC352: Introduction to Ultrafast Pulse Shaping — Principles and Applications

Marcos Dantus, *Michigan State Univ., USA*

Short Course Level: Beginner and Advanced Beginner

Pulse shaping is an integral part of every femtosecond laser, and learning about pulse shaping can help us better understand dispersion, pulse characterization and pulse compression. This course begins by describing how the spectral phase

affects the temporal characteristics of a femtosecond pulse with a hands on computer simulation. The essential physics and a brief background of the development of shapers are provided. The course goes over the experimental implementation requirements and then covers some of the most salient applications of pulse shapers, among them: (a) pulse compression, (b) pulse characterization, (c) creation of two or more pulse replicas, (d) control of nonlinear optical processes such as selective two-photon excitation and selective vibrational mode excitation, (e) material processing and (f) microscopy and others. The course provides a good foundation for those wanting to explore the more fundamental aspects of light-matter interactions, and it also provides multiple examples of practical applications that are made possible by pulse shaping.

SC361: Coherent Mid-infrared Sources and Applications

Konstantin Vodopyanov, *CREOL, Univ. of Central Florida, USA*

Short Course Level: Intermediate

This course reviews different techniques to produce coherent light in the important yet challenging mid-IR spectral region (approximately 2–20 μm). It examines, in great detail, a variety of state-of-the-art approaches from diverse areas of photonics: solid-state lasers based on rare-earth and transition metals, fiber lasers, semiconductor lasers (including intra- and intersubband cascade lasers), nonlinear-optical frequency conversion (including difference frequency generators, optical parametric oscillators, and amplifiers), Raman converters and others. The course assesses several emerging technologies such as supercontinuum generation in microresonators, waveguides, and fibers, as well as frequency comb generation. The course examines the most important applications of the mid-IR, such as spectroscopic sensing and imaging, nano-IR imaging, ultrafast interactions, medical and defense applications, plasmonics, extreme nonlinear optics (including attosecond science), particle acceleration and other applications.

SC362: Cavity Optomechanics: Fundamentals and Applications of Controlling and Measuring Nano- and Micro-mechanical Oscillators with Laser Light

Tobias Kippenberg, *École polytechnique fédérale de Lausanne, Switzerland*

Short Course Level: Beginner

Radiation pressure denotes the force that optical fields exert and which have wide-ranging applications in both fundamental science and applications, such as laser cooling or optical tweezers. Radiation pressure can, however, also have a profound influence on micro- and nanophotonic devices, due to the fact that radiation pressure can couple optical and mechanical modes. This optomechanical coupling gives rise to a host of new phenomena and applications in force, displacement and mass sensing. This course is intended to give an introduction of the physics and applications of cavity optomechanics and highlight the rapid developments in this emerging field.

Optomechanical coupling can be used to both cool and amplify mechanical motion and thereby allow new light driven photon clocks. Optomechanical refrigeration of mechanical modes gives insights into the quantum limits of mechanical motion. In addition, radiation pressure coupling enables new way of processing light all optically enabling optical mixers, delay lines or storage elements. Moreover, the basic limita-

All conference locations are in the San Jose Convention Center unless otherwise noted.

tions of optomechanical displacement measurements, due to quantum noise and practical laser phase noise limitations, will be reviewed, relevant across a wide range of sensing experiments.

SC376: Plasmonics

Mark Brongersma, *Stanford Univ., USA*

Short Course Level: Beginner

Plasmonics is an exciting new field of science and technology that aims to exploit the unique optical properties of metallic nanostructures to enable routing and active manipulation of light at the nanoscale. Nanometallic objects derive these properties from their ability to support collective electron excitations, known as surface plasmons (SPs). Presently we are witnessing an explosive growth in both the number and range of plasmonics applications; it is becoming eminently clear that both new fundamental science and device technologies are being enabled by the current plasmonics revolution. The intention of this course is to give the participants a fundamental background and working knowledge of the main physical ideas used in plasmonics, as well as an overview of modern trends in research and applications.

SC378: Introduction to Ultrafast Optics

Rick Trebino, *Georgia Institute of Technology, USA*

Short Course Level: Beginner

Ultrafast Optics, the science and technology of ultrashort laser pulses, is one of the most exciting and dynamic fields of science. While ultrashort laser pulses seem quite exotic, their applications are many — ranging from the study of ultrafast fundamental events to telecommunications to micro-machining to biomedical imaging. The course is a basic introduction to the nature of these lasers and the pulses they generate. It will discuss the principles of their generation and amplification and describe their most common distortions in space and time and how to avoid them — or take advantage of them. In addition, it will cover the nonlinear optics of ultrashort pulses for converting pulses to almost any color, as well as the additional interesting and potentially deleterious effects nonlinear optical processes can cause. Finally, it will cover techniques for ultrashort-pulse measurement.

SC396: Frontiers of Guided Wave Nonlinear Optics

Ben Eggleton, *Univ. of Sydney, Australia*

Short Course Level: Advanced Beginner

This course will review recent research and applications in the field of nonlinear guided wave optics with emphasis on both fundamentals and emerging applications. Starting from a strong foundation in the principles of nonlinear optics, we will review recent progress in emerging nonlinear optical platforms with an emphasis on the different materials, including silicon, chalcogenide, III-V semiconductors, lithium niobate, photonic crystal fibers, nanophotonic circuits and others. We will establish key figures of merit for these different material systems and a general framework for nonlinear guided wave optics with emphasis on the applications in emerging areas of science and technology. We will then review recent progress and breakthroughs in the following areas: all-optical processing, ultra-fast optical communications, slow light, highly nonlinear and emerging waveguides, ultrafast measurement and pulse characterization, frequency combs and optical clock, optical parametric amplifiers and oscillators, generation and

applications of optical supercontinuum, nonlinear localization effects and solitons, nonlinear optics for quantum information.

SC403: NanoCavity Quantum Electrodynamics and Applications

Jelena Vučković, *Stanford Univ., USA*

Short Course Level: Beginner

Strong localization of light in nanophotonic structures leads to enhanced light-matter interaction, which can be employed in a variety of applications, ranging from improved (higher speed, lower threshold) optoelectronic devices, to biophotonics, quantum information and low threshold nonlinear optics.

In particular, quantum dots in optical nanocavities are interesting as a test-bed for fundamental studies of such light-matter interaction (cavity quantum electrodynamics - QED), as well as an integrated platform for information processing. As a result of the strong field localization inside of sub-cubic wavelength volumes, they enable very large emitter-field interaction strengths (vacuum Rabi frequencies in the range of 10's of GHz — a few orders of magnitude larger than in atomic cavity QED). In addition to the study of new regimes of cavity QED, this can also be employed to build devices for quantum information processing. Besides quantum information systems, many classical information processing devices greatly benefit from the enhanced light matter interaction in such structures.

The course will introduce cavity QED (e.g., strong and weak coupling regimes, Purcell effect, etc.), with particular emphasis on semiconductor nanocavities. We will also describe state of the art in solid state cavity QED experiments and applications.

SC410: Finite Element Modeling Methods for Photonics and Optics

Arti Agrawal, *Univ. of Technology Sydney, Australia*

The Finite Element (FE) method is one of the most popular and powerful methods for modeling in photonics. The course starts with Maxwell's equations and explains the basic principles of numerical modeling and the key assumptions involved. This foundation is used to develop the FE method, including a brief tour of the mathematics. How the method can be applied to various optical devices is discussed in detail. How can physical effects be included with the FE method for modeling is considered. The course ends with an explanation of FE based beam propagation methods and how these can be used to find the evolution of the optical fields.

SC424 - Optical Terahertz Science and Technology

David G. Cooke, *McGill Univ., Canada*

Short Course Level: Intermediate

The purpose of this short course is to introduce time-domain optical techniques based on femtosecond lasers for generating, manipulating and detecting light in the 0.1 – 10 THz region, and demonstrate how this interesting part of the spectrum can be used to improve our understanding of materials. I will discuss THz imaging and sensing applications that are driving the development of this technology and discuss new physics that can be probed with short pulses of THz light.

All conference locations are in the San Jose Convention Center unless otherwise noted.

SC438: Photonic MetamaterialsNader Engheta, *Univ. of Pennsylvania, USA***Short Course Level:** Beginner

The course will begin with the basics of electromagnetic wave interaction with material media and structures and discuss some of the specifics of the characteristics of metamaterials and metasurfaces including the dispersion properties, scattering mechanisms, effective-medium phenomena and unconventional features of waves in such environments.

We will then discuss some of the specific topics in photonic metamaterials, such as extreme-parameter metamaterials (i.e., epsilon-near-zero (ENZ), munear-zero (MNZ) and epsilon-and-munear-zero (EMNZ) structures) and their specialized wave-matter interactions, graphene metamaterials as a platform for ideas for one-atom-thick optical device concepts, optical metatronics ("lumped" nanocircuitry) and informatic metastructures for photonic information processing and computing at the nanoscale, scattering engineering using metamaterials (such as cloaking), guided waves in metamaterials and nonreciprocal metastructures.

SC455 - Integrated Photonics for Quantum Information Science and TechnologyDirk Englund; *MIT, USA***Short Course Level:** Advanced Beginner

The rules of quantum mechanics enable applications that are inherently more powerful than their classical counterparts. Quantum key distribution now makes it possible to transmit information with unconditional security; quantum simulation is beginning to address problems that are intractable on classical computers; and quantum metrology techniques push the boundaries of precision measurements. Many of these quantum technologies rely fundamentally on advanced photonics that place extremely demanding requirements on precision, efficiency, and mode complexity. Over the past decade, new generations of photonic integrated circuits have been developed to begin to address these requirements. This course will cover basic concepts and recent progress in photonic integrated circuits technology for quantum information processing, with a focus on two primary application areas: quantum communications -- from quantum cryptography to entanglement distribution over quantum networks -- and quantum computing, including analog and digital approaches. Motivated by these applications, the course will discuss nonclassical light sources, photonic interfaces with atomic memories, high-fidelity mode transformation circuits, nonlinear photonic quantum gates, and waveguide-integrated single photon resolving detectors.

SC456: How to Start a CompanyJes Broeng, *Danmarks Tekniske Universitet, Denmark*

Starting a new business is a rewarding experience. However, the journey from an idea to a successful company is paved with challenges and puts high demands on technology, business and social skills. The upside is tremendous in personal learning and potentially also economically. The course is aimed to help people thinking about starting their own company and provide practice-oriented tools to help aspiring entrepreneurs who have a scientific or engineering background. To commercialize a new technology, the course will help answer questions such as how to know if you have a viable business idea; what to look for in cofounders; and what financing strategy is appropriate for my kind of business.

The course will include a mix of business theory and start-up experience based on a number of successful high-tech companies familiar to the scientists and engineers in attendance. A workshop session will be featured, in which start-up ideas from attendees may be introduced and strengthened under the instructor's guidance.

SC466: Silicon Integrated NanophotonicsYurii A. Vlasov, *Univ. of Illinois at Urbana-Champaign, USA***Short Course Level:** Beginner

Silicon photonics is a rapidly growing industry as well as an active area of advanced research. This course will focus on practical applications of advanced EM concepts to silicon photonics integrated circuits. It combines the rigorous derivation of major physical concepts like matrix optics, waveguiding, coupled mode theory, pin junctions, etc., with the applications of this knowledge toward the design of practical silicon photonic devices like passive wavelength filters, active switches and modulators for optical communications, as well as germanium photodetectors. The emphasis will be given to interaction of guided EM waves with electrical charges in pin junction that would allow participants to understand the operation and design principles of a new class of photonic devices (modulators, switches, photodetectors, etc.) based on carrier-injection/depletion in silicon/germanium integrated optics. Fabrication approaches and CMOS integration challenges will be reviewed. System level analysis of short-reach and long-haul optical links will be analyzed that will drive the design considerations for optical transmitter and receiver subsystems and individual devices.

SC475: Metasurface Flat Optics NEWFederico Capasso, *Harvard Univ., USA***Short Course Level:** Beginner, Advanced Beginner, Intermediate

The course is focused on metasurfaces: sub-wavelength-scale artificially structured metal-dielectric surfaces and upon their applications. Metasurfaces enable the redesign of optical components into thin, planar and multifunctional elements. This leads to a major reduction in thickness, in footprint and in system complexity, simplifying optical alignment and aberration control. As well, this leads to the introduction of new optical functions, thus circumventing the limitations of refractive and conventional diffractive optics. Design, fabrication and measurements of metalenses, holograms, multifunctional metasurfaces and waveplates will be covered with particular emphasis on polarization optics. Applications such as imaging, AR/VR, miniature spectrometers, polarimetry and fiber optics will be discussed.

SC476: QCL and QCL Combs NEWJérôme Faist, *ETH Zürich, Switzerland***Short Course Level:** Intermediate

The first section of this course will discuss the fundamental physical principles behind the operation of a quantum cascade laser. This will entail the models used to describe the electronic states, as well as a discussion of the key scattering mechanism. We will then describe the various active region architectures and their respective advantages. An emphasis will also be given on the fundamental limits of quantum cascade laser structures. The second part of the lecture will discuss the engineering of single mode and broad gain devices. Beside external cavity, multi-wavelength and other Vernier

All conference locations are in the San Jose Convention Center unless otherwise noted.

devices will be discussed as some of the key applications of QCLs. The third and final part of the lecture will address the optical frequency comb quantum cascade laser. It will start by describing the physics behind the comb formation, the Maxwell-Bloch modeling of the QCL combs. The various techniques used to correct the group velocity dispersion of the device will next be discussed. It will then describe the various characterization techniques, as well as some of the emerging applications in broadband time-resolved mid-infrared spectroscopy.

SC477: Laser Radar and Remote Sensing: An Application-oriented Introduction *NEW*

Fabio Di Teodoro, *Raytheon, USA*

Short Course Level: Advanced Beginner and Intermediate

In recent years, LADAR and laser-based remote sensing technologies have advanced and diversified across many disciplines, becoming an irreplaceable resource for mainstream applications such as autonomous navigation and climate studies. This course offers an introduction to state-of-the-art active remote sensing technologies. While covering physical foundations, the course adopts a practical and system-oriented approach. Its main goal is to provide attendees with proper knowledge tools to understand how remote-sensing devices are designed, developed and deployed in real applications spanning the scientific, military and industrial realms. Another goal is to familiarize attendees with the many cutting-edge technologies employed in such applications: from pulsed fiber lasers to optical phase arrays, single-photon detectors, image-extraction algorithms, etc.

SC478: Microresonator-based Optical Frequency Comb and Photonic Waveguide Supercontinuum Sources *NEW*

Tobias Kippenberg, *École polytechnique fédérale de Lausanne, Switzerland*

Short Course Level: Beginner

Optical frequency combs have revolutionized frequency metrology and spectroscopy over the last two decades. Recent advances have allowed generating optical frequency combs in compact optical microresonators using parametric interactions. This course will provide an introduction to the numerical simulation and design, operation principles and measurement techniques of micro-resonator frequency combs. It will cover the formation of dissipative temporal solitons, and discuss how such states can be numerically simulated using the Lugiato Lefever equation. The course will discuss the similarities to soliton-related phenomena known in supercontinuum generation, and will study basics of supercontinuum generation in integrated photonic waveguides, as recently studied. The course will moreover discuss applications of soliton micro-combs in ranging, communications and spectroscopy, and outline the state of the art.

SC479: Basics of Quantum Optics for Quantum-enabled Technologies *NEW*

Bahaa Saleh, *CREOL, Univ. of Central Florida, USA*

Short Course Level: Beginner

This course will begin with a brief overview of the basic quantum principles — superposition, uncertainty, non-clonability and entanglement—highlighting the essence of the “quantum advantage” that has led to the emerging quantum technology leap. The “mixed analog-digital” nature of the quantum bit (qbit) and its role in quantum computing will be introduced, and the distinction between entanglement and ordinary correlation will be clarified. This will be followed by the application of these general quantum principles to light: demonstrating the inherent uncertainty in the optical amplitude, phase, quadrature components and photon number; noting bounds on the uncertainty product dictated by the Heisenberg principle and their manipulation by “squeezing”; and summarizing the photon statistics associated with various quantum states of light.

SC481: Fundamentals and Applications of VCSELs *NEW*

Kent Choquette, *Univ. of Illinois, USA*

Short Course Level: Beginner

This course will review the principles of operation and technological advances of vertical cavity surface emitting lasers (VCSELs). The course will begin with an overview of microcavity laser fundamentals and will include discussions of semiconductor optical gain, Fabry-Perot resonators, electron and photon confinement and the properties of VCSEL emission. The second half of the course will overview the major application areas of VCSELs and will include digital modulation, both incoherent and coherent high power 2-dimensional array performance, and various examples of optical sensing. Specific examples of infrared and visible VCSEL performance will be included as well as the commercial VCSEL manufacturing landscape

Special Events

Pride in Photonics: LGBTQ+ & Ally Workshop

Sunday, 5 May; 9:00–13:00
University Room, Hilton San Jose

The aim for this workshop is to:

- Provide a safe space for LGBTQI+ people, allies and diversity advocates;
- Create a welcoming atmosphere for collaboration and technical dissemination;
- Discuss best practices in LGBTQI+ equality, diversity and inclusion.

The program will consist of technical talks, personal journey stories, best practice take-aways, a panel and open networking time. Again, this is an inclusive event, so all members of the community are encouraged to attend, including LGBTQI+ and diversity allies.

Note that this workshop will be a safe space for collaboration and sharing. The organizers recognize and respect that some individuals may not be “out” in this space, therefore confidentiality is a priority and a code of conduct for the workshop will be made available in advance and addressed at the event.

Sponsored by



Be a Part of the Solution: Preventing and Responding to Harassment

Sunday, 5 May; 14:00–15:30 and 16:00–17:30
University Room, Hilton San Jose

CLEO is committed to providing an environment that is conducive to the free and robust exchange of scientific ideas. This requires that all participants be treated with equal consideration and respect. With this in mind, CLEO is offering this session to help provide members with the skills needed to make this a reality throughout our community. The program will examine different forms of harassment, The Bystander Effect, and Ally Skills. This session is open to all conference attendees, but space is limited.

Sponsored by



OSA Presentation Feedback Program

Monday, 6 May; 11:00–12:00
University Room, Hilton San Jose

Join us for an interactive session focused on providing an effective conference talk or poster. Conference presentations are an important aspect of communicating cutting-edge research. In this workshop we will discuss some key elements of giving an effective conference talk. This will be followed by an interactive session where individual feedback to your slides would be provided by the moderators and by your peers. So, please bring along your laptop with your conference presentation or any other technical talk.

Navigate Your Leadership Trajectory for Senior Leaders

Monday, 6 May; 11:00–12:30
Salon VI, San Jose Marriott

In this interactive session you will:

1. Reflect on both the impact and the opportunity of having both mentors and sponsors in your life
2. Evaluate best practices and internal strategies to elevate others while expanding your personal leadership capabilities and brand
3. Understand and build a business case for mentoring and sponsorship to drive ROI + diversity, retention, knowledge transfer and engagement

What's Next in Integrated Optics – Hot Topics at CLEO: 2019

Monday, 6 May 2019; 12:30–13:30
Room 230A

Join the OSA Integrated Optics Technical Group for a panel discussion during lunch on Monday. Our featured presenters will give their perspective on the exciting research that will be presented at CLEO 2019, followed by a moderated question and answer session. This event is an excellent opportunity to hear from experts in the field on exciting new areas in integrated optics. Panelists include Michal Lipson, *Columbia University*; Marko Loncar, *Harvard University*; and Jelena Vuckovic, *Stanford University*. Please contact TGactivities@osa.org to register, pending availability.

Hosted by 

Resumes, LinkedIn, and Networking (with Cheeky Scientist)

Monday, 6 May; 13:00–14:00 and 16:00–17:00
University Room, Hilton San Jose

Learn more how to select the career path that's right for you and the top 20 industry jobs that PhDs are getting into. Make sure you are prepared to get the salary you deserve as well as making sure you stand out among the sea of candidates. Join Cheeky Scientists as we guide you through the process of getting a job in industry!

Hosted by  OSA
Foundation

Social Media in 2019 Panel Discussion

Monday, 6 May; 13:00–14:00
University, Hilton San Jose

Organizers:

Andrea Armani, *Univ. of Southern California, USA*
Benjamin Eggleton, *Univ. of Sydney, Australia*

Savvy scientists must increasingly engage with social media. It is how and where we share information – with friends, colleagues, acquaintances and any and everyone else. The co-sponsors of CLEO 2019 are hosting a Social Media Career Session to explore the benefits of leveraging social media for advancement. We will explain how anyone at any stage in their career can use social media to influence and grow. You will learn best practices and gain practical takeaways enabling you to optimize your “social” footprint and personal brand.

Please refer to Program Update Sheet for Panelists.

Hosted by



Deliberate Mentoring to Advance Your Career: Special Flash Mentoring Session

Monday, 6 May; 14:30–16:00
Guadalupe Room, San Jose Marriott

Time to Navigate Your Leadership and Career Trajectory FLASH MENTORING @SEA (think ‘speed mentoring’) is a unique and well-respected program that accelerates leaders of all generations to “Come Aboard and Get into the Fast Lane of Your Career Navigation and Leadership”. You will learn the value proposition of mentoring for corporations and organizations; use your storytelling skills and meet, network, mentor, and be mentored by 4–5 other colleagues in this highly dynamic nautical themed session led by Julie Silard Kantor. Kantor is the President & CEO of Twomentor, LLC and passionate about mentor training and strategy to elevate a more diverse, skilled multi-gen workforce.

Professor Daniel Wasserman Meet and Greet

Monday, May 6; 15:30–16:00
SJCC Room 214

Please join us for to meet with Professor Daniel Wasserman and mingle with your colleagues.

All conference locations are in the San Jose Convention Center unless otherwise noted.

Professional Development for Busy Professionals

Monday, 6 May; 16:00–17:30
Salon VI, San Jose Marriott

Developing your professional skill set through continuing education and networking is a career must for the modern day professional. The life of a busy professional does not often allow for many immersive learning experiences but staying up to date on all things work-related is not just something that is good to do—it is now something that is essential for career longevity. Join other aspiring mid-level OSA members and learn how to plan, prioritize and advance your career to the next level.

Diversity and Inclusion Reception

Monday, 6 May; 17:30–18:30
Winchester Room

Join us for a reception to connect with the optics and photonics community to discuss diversity in the field. Come to learn, share and engage with colleagues around this important topic.

Sponsored by



Lasers for Attosecond 2.0

Monday, 6 May; 18:30–20:00
Room 230A

Join the OSA Short Wavelength Sources and Attosecond/High Field Physics Technical Group for a special session on the next generation of laser technology that will support the field of attosecond science in the coming decades. Our featured presenters will be discussing both current and upcoming technology for the next generation of femtosecond lasers. Following the conclusion of these presentations, attendees are invited to join the technical group for a small reception where they can network with colleagues over refreshments. Please contact TGactivities@osa.org to register, pending availability.

Hosted by  OSA Short Wavelength Sources and Attosecond/High Field Physics Technical Group

Meet OSA Publishing Journal Editors Ice Cream Social

Tuesday, 7 May, 15:00–16:30
Exhibit Hall, Networking Zone, Booth 2605

Join OSA Publishing’s Journal Editors for conversation and ice cream. The Editors welcome your questions, concerns, and ideas for any of OSA’s Journals. Topics for discussion can include best practices when submitting a manuscript; elements of a useful manuscript review; criteria editors look for in submitted manuscripts; or the process to propose a Feature Issue topic for publication in an OSA Journal. All are welcome.

OSA Senior Member Reception

Tuesday, 7 May; 17:30–18:30

OSA Member Lounge, Concourse Level

Join us for a reception with other OSA Senior Members, and future OSA Senior Members to learn about this distinction, it's benefits, application process and deadline while networking with colleagues from around the world. Get Involved Today!

OSA Technical Group Poster Session

Tuesday, 7 May; 19:00–20:30

Grand Ballroom 220C

Join the OSA Technical Groups for a series of focused poster sessions, bringing together students and colleagues for an opportunity to share their latest research findings and exchange ideas. After listening to the poster presentations and connecting with fellow attendees over refreshments, you'll have a chance to cast your vote for the best poster from each of the four participating technical groups.

Hosted by 

Conference Reception

Wednesday, 8 May, 19:00–20:30

Grand Ballroom 220B/C

Enjoy a festive evening with your colleagues. The reception is open to all attendees and badges must be worn to enter the reception.

Sponsored by 

Emerging Trends in Nonlinear Optics – A Review of CLEO

Thursday, 9 May; 18:30–20:00

Room 230A

OSA Members are invited to join the OSA Nonlinear Optics Technical Group for a special panel discussion presenting the exciting and hot topics in nonlinear optics that were presented during CLEO. Short presentations from our panelists highlighting important themes from the conference will be followed by moderated question and answer sessions. Following the conclusion of the panel discussion, members are invited to join the technical group for a small reception where they can network with colleagues over refreshments. This technical group event is open to OSA Members only; please contact TGactivities@osa.org to register, pending availability.

Hosted by 

Postdeadline Paper Sessions

Thursday, 9 May, 20:00–22:00

Locations announced on the Update Sheet

The Technical Program Committee has accepted a limited number of postdeadline papers for oral presentation. The purpose of postdeadline papers is to give participants the opportunity to hear new and significant materials in rapidly advancing areas.

Seminar: VirtualLab Fusion Technology and Applications: Interferometry, Microscopy and Fiber Coupling

Friday, 10 May; 09:00–16:00

Room 214

Speaker: Site Zhang, PhD, CTO, LightTrans International UG

Discover the Fast Physical Optics concept with VirtualLab Fusion by means of seminar modules on technology and different applications. You will learn how to use non-sequential field tracing to configure and model various interferometric setups; setting up of modern microscopes and how to perform fully vectorial imaging simulations; using physical optics for fiber coupling efficiency analysis and design of high-NA coupling systems.

Connecting Global Competence



Messe München



THE LEADING LIGHT

BUY TICKET HERE
WORLD-OF-PHOTONICS.COM/TICKETS

JUNE 24–27, 2019, MESSE MÜNCHEN

24th World's Leading Trade Fair with Congress
for Photonics Components, Systems and Applications

world-of-photonics.com

LASER World of **PHOTONICS**



CLEO:EXPO

Exhibit Hall

Make sure to visit the show floor which features a diverse group of companies, representing every facet of the lasers and electro-optics industries. Learn about new products, find technical and business solutions, and gain the most up-to-date perspective of the laser-related business environment. Review the list of exhibitors on the following pages to see the companies you'll meet at CLEO.

CLEO:EXPO is free of charge for all conference registrants.

Exhibit Hall Rules

Children 12 and under must be accompanied by an adult at all times. Strollers are not allowed on the show floor at any time.

Neither photography nor videotaping is permitted in the Exhibit Hall. Exhibitors need to get permission from Show Management to photograph their own booths. Non-compliance may result in the surrendering of film and removal from the hall.

For further questions, visit Registration on the Concourse Level.

Exhibitors (as of 26 March 2019)

3DOptix
 AdValue Photonics, Inc.
 Advanced Research Systems
 AdvR
 AIP Publishing
 Allied Laser Solutions
 Alpine Research Optics
 Altos Photonics, Inc.
 American Physical Society (APS)
 Amplitude Laser Group
 APE - Applied Physics & Electronics Inc.
 asphericon Inc.
 Atseva LLC
 Attocube Systems, Inc.
 AUREA Technology
 Azur Light Systems
 Beam Engineering for Advanced Measurements Co.
 Boston Electronics Corporation
 Bristol Instruments, Inc.
 Calmar Laser, Inc.
 Carmel Instruments
 CASTECH, Inc.
 Changchun BoXin Photoelectric Co., Ltd.
 Changchun New Industries Optoelectronics Tech. Co.
 Chinese Laser Press
 Class 5 Photonics GmbH
 Cobolt by HUBNER Photonics
 Coherent, Inc.
 ColdQuanta, Inc.
 CRC Press – Taylor & Francis Group
 CREOL, University of Central Florida
 CrystaLaser LC
 Crystalline Mirror Solutions
 Cybel, LLC
 Cycle GmbH
 DataRay, Inc.
 Dausinger + Giesen GmbH
 DRS Daylight Solutions, Inc.
 Edmund Optics, Inc.
 EKSMA Optics
 EKSPLA
 Electro-Optics Technology, Inc.
 Energetiq Technology Inc.
 EOSPACE, Inc.
 Epner Technology, Inc.
 Eulitha AG
 EXFO
 FASTLITE
 Femtochrome Research, Inc.

All conference locations are in the San Jose Convention Center unless otherwise noted.

few-cycle
 Gentec Electro-Optics, Inc.
 GTAT Corp.
 Hagitec Co.
 Hamamatsu Corporation
 HILLTOP Technology Lab., Inc.
 Hinds Instruments, Inc.
 Hitronics Technologies, Inc.
 Hiwin Corporation
 HOLOEYE Photonics AG
 Hong Kong University of Science and Technology
 HTA Photomask
 Ibsen Photonics A/S
 IEEE Photonics Society
 IMEC
 IMRA America, Inc.
 INNOLAS
 Inrad Optics
 IPG Photonics Corp.
 IRflex Corporation
 IXBLUE
 Jasper Display Corp.
 KMLabs, Inc.
 Knight Optical
 Kphotonics, LLC
 LaCroix Precision Optics
 Laser Focus World
 Laser Quantum, Inc.
 Lattice Electro Optics, Inc.
 Light Conversion
 Lighthouse Photonics
 LightTrans International UG
 Liquid Instruments
 Luvantix ADM Co., Ltd.
 M Squared Lasers Ltd.
 Menlo Systems
 Mesa Photonics, LLC
 Microphoton Devices
 MKS Instruments
 NKT Photonics
 NM Laser Products
 Northrop Grumman Cutting Edge Optronics, Inc.
 NPI Lasers
 Nuphoton Technologies Inc.
 OEwaves, Inc.
 OPOTEK, Inc.
 Optelligent, LLC
 OptiGrate Corporation
 Optimax Systems, Inc.
 OptoSigma Corporation
 Optronics Co., Ltd., The
 OSA – The Optical Society
 OSA Member Lounge
 Osela, Inc.
 Oxide Corporation
 OZ Optics
 PHASICS Corp.
 Photodigm, Inc.
 Photon Design
 Photon Force Ltd
 Photonics Media/Laurin Publishing
 Photop Technologies, Inc
 PI (Physik Instrumente) LP
 PicoQuant
 Princeton Scientific Corporation
 PriTel, Inc.
 Quantel Laser by Lumibird
 Quantum Design, Inc.
 Quantum Opus
 RAM Photonics, LLC
 Sacher Lasertechnik GmbH
 Sandia National Laboratories
 SaNoor Technologies
 Santec USA Corporation
 Seiwa Optical America, Inc.
 SILIOS Technologies S.A.
 Siskiyou Corporation
 SmarAct, Inc.
 Solid Sealing Technology
 Specialised Imaging
 Spectrolight, Inc.
 SPIE: The Intl Society for Optics and Photonics
 Springer
 Stable Laser Systems
 STANDA
 StellarNet, Inc.
 Swamp Optics, LLC
 Synopsys, Inc.
 Teledyne Judson Technologies
 ThermoTek, Inc.
 Thorlabs
 Tianjin University
 Timbercon, Inc.
 Toptica Photonics, Inc.
 TRUMPF Inc.
 Universal Quantum Devices
 Vescent Photonics, Inc.
 Wuhan National Lab for Optoelectronics
 YSL Photonics Co., Ltd.
 Zaber Technologies
 Zurich Instruments

All conference locations are in the San Jose Convention Center unless otherwise noted.

Beyond Awareness: What Actions Can Be Taken to Improve Diversity in STEM

Wednesday, 8 May, 10:30–12:00
Exhibit Hall Theater II

Organizers

Arti Agrawal, *University of Technology Sydney, Australia*
Ben Eggleton, *University of Sydney, Australia*
Tara Fortier, *National Institute of Standards & Technology, USA*
Christina Willis, *Consultant, USA*
Andrew Wilson, *National Institute of Standards & Technology, USA*

In the physical sciences, women and minorities have seen slower improvements in representation compared to fields such as medicine and law. Information on how to improve this representation in STEM is also difficult to find. This workshop brings together leaders of professional organizations and subject matter experts to discuss policies and actions that can improve gender, racial, LGBTQI and disability diversity within the physics, engineering and optics communities.

Panelists

Kate Kirby, *Chief Executive Officer, American Physical Society*
Doug Razzano, *Executive Director, IEEE Photonics Society*
Kent Rochford, *Chief Executive Officer, SPIE*
Elizabeth A. Rogan, *Chief Executive Officer, The Optical Society*

Please refer to Update Sheet for moderator information.

Exhibit Hall Coffee Breaks

The exhibit floor is the perfect place to build and maintain professional contacts, and these breaks provide ideal networking opportunities. Complimentary coffee will be served at these times:

Tuesday, 7 May	10:00–11:30, 15:00–17:00
Wednesday, 8 May	10:00–11:30, 15:00–17:00
Thursday, 8 May	10:00–11:30

Sponsored by  **COHERENT** 

MKS Student Lounge

Booth 1340

All student attendees are invited to the MKS Student Lounge, co-sponsored by OSA. The lounge provides an opportunity to relax and spend time networking with other students, while enjoying complimentary, wireless internet and refreshments.

Sponsored by  **mks** |  **Newport**

Co-sponsored by  **OSA** |  **100**
The Optical Society | Since 1916

OIDA VIP Industry Leaders Speed Meetings Event

Tuesday, 7 May, 12:00–13:30
Exhibit Hall, Networking Zone, Booth 2605

This session brings together Industry Executives to share their business experience with Young Professionals, Recent Graduates and Students – how they started their careers, lessons learned and using their degree in an executive position.

Informal networking during lunch is followed by a transition to “speed meetings” – brief, small-group visits with each executive to discuss industry trends or career topics.

If you have any questions about this event or are a Student or Recent Graduate and interested in attending, please email trooney@osa.org.

Sponsored by 

Plenary Speaker Meet-n-Greets

Tuesday, 7 May & Wednesday, 8 May, 10:15–10:45
Exhibit Hall, Networking Zone, Booth 2605

Meet CLEO Plenary speakers, ask questions and network with your colleagues.

Quantum Information Science and Technology Initiatives

Tuesday, 7 May, 10:30–12:00
Exhibit Hall Theater I

Organizer

Sergey Polyakov, *National Institute of Standards and Technology, USA*

Nationally-driven research initiatives in quantum information science and technology have grown as quickly as the fields themselves in recent years. This panel will explore the state of the research, the initiatives, and the potential international competitiveness, and cooperation that comes with them.

Panelists:

Marissa Giustina, *Google, USA*

David Lang, *The Optical Society, USA*

Christopher Monroe, *University of Maryland, College Park, USA*

Cheng-Zhi Peng, *University of Science and Technology of China, China*

Michael Raymer, *University of Oregon, USA*

Carl Williams, *National Institute of Standards and Technology, USA*

Free Lunch at the CLEO:EXPO

Tuesday and Wednesday, 7 & 8 May, 11:30–13:00
Thursday, 9 May, 12:30–14:00
Exhibit Hall

Grab some lunch and network with exhibitors to check out their innovative products and services that can help your organization.

All conference locations are in the San Jose Convention Center unless otherwise noted.

Poster Sessions

Exhibit Hall

Poster Sessions are an integral part of the Technical program. Each author is provided with a board with eight-foot-high by four-foot-wide (243cm x121cm) of usable space on which to display the summary and results of his or her paper. Authors should remain in the vicinity of their presentation board for the duration of the sessions to answer questions from attendees. Authors may set up one hour prior to their assigned session and must remove their poster one hour following the session. Authors may submit their poster PDF to cstech@osa.org for publication. The Dynamic e-Posters presentation method combines the richness of multimedia content of oral presentations with the personalized one-on-one interaction of posters.

Tuesday, 7 May	11:30–13:00
Wednesday, 8 May	11:30–13:00
Thursday, 9 May	11:30–13:00

Market Trends: Opportunities in Optics and Photonics

Tuesday, 7 May, 15:30–17:00

Exhibit Hall Theater I

Organizer

Tom Hausken, *OIDA, USA*

This presentation will review the current state and upcoming opportunities for the optics and photonics industry with respect to revenues, product areas, and regions. It will provide a quantitative look at recent performance, and examples of promising markets going forward.

New Commercial Trends in Mid-Infrared Sensing – From Nano-Photonics to Stand-Off Detection

Wednesday, 8 May, 10:30–12:00

Exhibit Hall Theater I

Organizer

Bernadeta A. Wysocka, *Princeton University, USA*

Panelists from industry, government laboratories and academia will discuss novel technologies leveraging infrared sensing for material science, biomedical imaging and chemical detection. The speakers will discuss established technologies and market opportunities in a variety of applications such as industrial process monitoring, bio-medical and pharmaceutical industry, and security. Please consider attending the event, listen and interact with leaders in the mid-infrared sensing community, and share your ideas in an open discussion.

Moderator

Gerard Wysocki, *Associate Professor of Electrical Engineering, Princeton University*

Technology Transfer Program

The Technology Transfer Program includes a Keynote presentation, a Technology Transfer Tutorial and a Pitch Panel. The tutorial speaker provides attendees more information about the licensing process: funding, entrepreneurship, technology transfer and intellectual property. The pitch panel provides entrepreneurs an opportunity to showcase their technology, explain why it's valuable and discuss the next steps to commercialization. In addition, these organizations will feature their license-ready technologies at tabletop displays in the exhibit hall.

Keynote Talk

Thursday, 9 May, 10:15–10:45

Exhibit Hall Theater I

Keynote Speaker

Tim Day, *VP and GM, DRS Daylight Solutions*

Technology Transfer Tutorial

Thursday, 9 May, 10:45–11:15

Exhibit Hall Theater I

Tutorial Speaker

Dr. Eugene R. Cochran III, *PhD, Senior Commercialization Manager, Oak Ridge National Laboratory*

Pitch Panel with Feedback from Panelists

Thursday, 9 May, 11:15–12:30

Exhibit Hall Theater I

Panelists:

Kei May Lau, *PhD, Chair Professor, Hong Kong University of Science and Technology, Hong Kong*

Rachel Grange, *PhD, Leader of the Optical Nanomaterial Group, ETH Zurich, project PolarNon, USA*

Manish D. Kulkarni, *PhD, Chief Executive Officer, Netra Systems, USA*

Max Perez, *Senior Engineer & Business Development, Cold-Quanta Ltd., USA*

Judging Panel:

Robert Mandra, *Managing Director, RSM Advisors, USA*

Sujatha Ramanujan, *PhD, Managing Director, Nextcorp's Luminare, USA*

All conference locations are in the San Jose Convention Center unless otherwise noted.

CLEO Committees

Applications & Technology

Peter Andersen, *Danmarks Tekniske Universitet, Denmark*,
General Chair

Michael M. Mielke, *Iradion Laser, USA*, General Chair
Jin Ung Kang, *Johns Hopkins Univ., USA*, Program Chair
Stephanie Tomasulo, *US Naval Research Laboratory, USA*,
Program Chair

A&T 1: Biomedical Applications

Ilko Ilev, *U.S. Food and Drug Administration, USA*,
Subcommittee Chair
Utkarsh Sharma, *Volk Optical Inc., USA*, Subcommittee Chair
Andrea Armani, *Univ. of Southern California, USA*
Brian Cullum, *Univ. of Maryland Baltimore County, USA*
Qiyin Fang, *McMaster Univ., Canada*
Irene Georgakoudi, *Tufts Univ., USA*
Thomas Huser, *Universität Bielefeld, Germany*
Beop-Min Kim, *Korea Univ., South Korea*
Xingde Li, *Johns Hopkins Univ., USA*
Yuji Matsuura, *Tohoku Univ., Japan*
David Nolte, *Animated Dynamic Inc., USA*
Aydogan Ozcan, *Univ. of California Los Angeles, USA*
Brian Pryor, *LiteCure, USA*
Sean Wang, *B&W Tek Inc, USA*
Yicong Wu, *NIH National Institute of Biomedical Imaging &
Bioengineering, USA*

A&T 2: Industrial Applications

Nicolas Falletto, *Electro Scientific Industries, Inc., USA*,
Subcommittee Chair
Jie Qiao, *Rochester Institute of Technology, USA*,
Subcommittee Chair
David Grojo, *CNRS, France*
Michael Krainak, *NASA Goddard Space Flight Center, USA*
Manyalibo Matthews, *Lawrence Livermore National
Laboratory, USA*
Peter Moselund, *NKT Photonics Inc, Denmark*
Dirk Mueller, *Coherent Inc., USA*
Roberto Osellame, *Istituto di Fotonica e Nanotecnologie,
Italy*
Hong-Bo Sun, *Tsinghua Univ., China*

A&T 3: Laser-Based Instrumentation for Measurements and Monitoring

Gregory Rieker, *Univ. of Colorado at Boulder, USA*,
Subcommittee Chair
Brian Simonds, *National Institute of Standards and
Technology, USA*, Subcommittee Chair
Alexandra Artusio-Glimpse, *National Inst of Standards &
Technology, USA*
Fabio Di Teodoro, *Raytheon SAS, USA*
Christopher Goldenstein, *Purdue Univ., USA*
Peter Fendel, *Thorlabs Inc, USA*
Kara Peters, *North Carolina State Univ., USA*
Steven Wagner, *Technische Universität Darmstadt, Germany*
Azer Yalin, *Colorado State Univ., USA*

A&T 4: Applications in Energy & Environment

Mark Zondlo, *Princeton Univ., USA*, Subcommittee Chair
Daniel Law, *Boeing, USA*, Subcommittee Chair
David Bomse, *Mesa Photonics, LLC, USA*

Mohammad Khan, *Delaware State Univ., USA*
Joel Silver, *Southwest Sciences Inc., USA*

Fundamental Science

Ben Eggleton, *Univ. of Sydney, Australia*, General Chair
Irina Novikova, *College of William & Mary, USA*, General
Chair
Natalia Litchinitser, *Univ. at Buffalo, USA*, Program Chair
Sergey Polyakov, *National Institute of Standards &
Technology, USA*, Program Chair

FS 1: Quantum Optics of Atoms, Molecules and Solids

Tracy Northup, *Universität Innsbruck, Austria*,
Subcommittee Chair
Takao Aoki, *Waseda Univ., Japan*
Adam Black, *US Naval Research Laboratory, USA*
Nathalie de Leon, *Princeton Univ., USA*
Elizabeth Goldschmidt, *US Army Research Laboratory,
USA*
Peter Humphreys, *Technische Universiteit Delft,
Netherlands*
Rudolph Kohn, *Space Dynamics Laboratory, USA*
Lucas Lamata, *Universidad del País Vasco, Spain*
Virginia Lorenz, *Univ. of Illinois at Urbana-Champaign,
USA*
Pavel Lougovski, *Oak Ridge National Laboratory, USA*
Marina Radulaski, *Stanford Univ., USA*
Glenn Solomon, *Joint Quantum Institute, USA*

FS2 Quantum Information and Communication

Joshua Nunn, *Univ. of Oxford, UK*, Subcommittee Chair
Michael Brodsky, *U.S. Army Research Laboratory, USA*
Maria Chekhova, *Max-Planck-Inst Physik des Lichts,
Germany*
Eleni Diamanti, *Universite Pierre et Marie Curie, France*
Thomas Gerrits, *National Inst of Standards & Technology,
USA*
Steve Kolthammer, *Imperial College, UK*
Peter Mosley, *Univ. of Bath, UK*
Valentina Parigi, *Laboratoire Kastler Brossel, France*
Fabrizio Piacentini, *INRIM, Italy*
Polina Sharapova, *Univ. of Paderborn, Germany*
John Sipe, *Univ. of Toronto, Canada*
Philip Walther, *Universitat Wien, Austria*

FS3: Quantum Photonics

Joshua Bienfang, *National Inst of Standards & Technology,
USA*, Subcommittee Chair
Guillaume Bachelier, *Institut NÉEL, CNRS, France*
Sara Ducci, *Université Paris Diderot, France*
John Howell, *Hebrew Univ. of Jerusalem, Israel*
Yuping Huang, *Stevens Institute of Technology, USA*
Jungsang Kim, *Duke Univ., USA*
Marco Liscidini, *Università degli Studi di Pavia, Italy*
Mirko Lobino, *Griffith Univ., Australia*
Raphael Pooser, *Oak Ridge National Laboratory, USA*
Stefan Francis Preble, *Rochester Institute of Technology, USA*
Alexander Sergienko, *Boston Univ., USA*
Martin Stevens, *National Inst of Standards & Technology, USA*
Andrey Sukhorukov, *Australian National Univ., Australia*

All conference locations are in the San Jose Convention Center unless otherwise noted.

FS 4: Optical Excitations and Ultrafast Phenomena in Condensed Matter

Denis Seletskiy, *Polytechnique Montréal, Canada*, Subcommittee Chair
 Elbert Chia, *Nanyang Technological Univ., Singapore*
 Mackillo Kira, *Univ. of Michigan, USA*
 Chih-Wei Lai, *The MITRE Corporation, USA*
 Kaihui Liu, *Peking Univ., China*
 Ilias Perakis, *Univ. of Alabama at Birmingham, USA*
 Mark Sherwin, *Univ. of California Santa Barbara, USA*
 Julia Stähler, *Fritz-Haber-Institut der Max-Planck-Gesellschaft, Germany*
 Diyar Talbayev, *Tulane Univ., USA*
 Vasily Temnov, *IMMM CNRS 6283 Le Mans, France*
 Jerome Tignon, *Ecole Normale Supérieure Paris and Sorbonne Univ., France*
 Lyubov Titova, *Worcester Polytechnic Institute, USA*
 Ulrike Woggon, *Technische Universität Berlin, Germany*
 Luyi Yang, *Univ. of Toronto, Canada*
 Liuyan Zhao, *Univ. of Michigan, USA*

FS 5: Nonlinear Optics and Novel Phenomena

Mercedeh Khajavikhan, *CREOL, Univ. of Central Florida, USA*, Subcommittee Chair
 Andrea Blanco-Redondo, *Univ. of Sydney, Australia*
 Daniel Brunner, *CNRS - FEMTO-ST, France*
 Demetrios Christodoulides, *Univ. of Central Florida, USA*
 Scott Diddams, *National Institute of Standards & Technology, USA*
 Mona Jarrahi, *Univ. of California Los Angeles, USA*
 Arash Mafi, *Univ. of New Mexico, USA*
 Konstantinos Makris, *Univ. of Crete, Greece*
 Alireza Marandi, *California Institute of Technology, USA*
 Sahin Ozdemir, *Pennsylvania State Univ., USA*
 Peter Rakich, *Yale Univ., USA*
 Mikael Rechtsman, *Pennsylvania State Univ., USA*
 Bo Zhen, *Univ. of Pennsylvania, USA*

FS 6: Nano-Optics and Plasmonics

Amit Agrawal, *National Institute of Standards and Technology, USA*, Subcommittee Chair
 Andrea Baldi, *Dutch Institute for Fundamental Energy Research, Netherlands*
 Palash Bharadwaj, *Rice Univ., USA*
 Peter Catrysse, *Stanford Univ., USA*
 Andrea Di Falco, *SUPA, Univ. of St Andrews, UK*
 Hayk Harutyunyan, *Emory Univ., USA*
 Mo Mojahedi, *Univ. of Toronto, Canada*
 Esther Wertz, *Rensselaer Polytechnic Institute, USA*
 Wei Zhou, *Virginia Tech, USA*
 Rashid Zia, *Brown Univ., USA*

FS 7: High-Field Physics and Attoscience

Michael Chini, *Univ. of Central Florida, USA*, Subcommittee Chair
 Luca Argenti, *Univ. of Central Florida, USA*
 Jens Biegert, *ICFO - The Institute of Photonic Sciences, Spain*
 Francesca Calegari, *DESY, Hamburg, Italy*
 Oren Cohen, *Technion Israel Institute of Technology, Israel*
 Shambhu Ghimire, *SLAC/Stanford Univ., USA*
 Nobuhisa Ishii, *Institute for Solid State Physics, Japan*
 Alexandra Landsman, *ETH Zürich, Switzerland*
 Guillaume Laurent, *Auburn Univ., USA*

Julia Mikhailova, *Princeton Univ., USA*
 Arvinder Sandhu, *Univ. of Arizona, USA*
 Emma Springate, *STFC Rutherford Appleton Laboratory, UK*
 Xiaoming Wang, *Washington State Univ., USA*

FS 8: Metamaterials and Complex Media

Zubin Jacob, *Purdue Univ., USA*, Subcommittee Chair
 L. Jay Guo, *Univ. of Michigan, USA*
 Yongmin Liu, *Northeastern Univ., USA*
 Ori Katz, *Hebrew Univ. of Jerusalem, Israel*
 Rajesh Menon, *Univ. of Utah, USA*
 Sushil Mujumdar, *Tata Institute of Fundamental Research, India*
 Ward Newman, *Univ. of Alberta, Canada*
 Junsuk Rho, *POSTECH, South Korea*
 Alessandro Salandrino, *Univ. of Kansas, USA*
 Riccardo Sapienza, *Imperial College London, UK*
 Justin Song, *Nanyang Technological Univ., Singapore*
 Sergei Tretyakov, *Aalto Yliopisto, Finland*
 Martijn Wubs, *Danmarks Teknishe Universitet, Denmark*

Science & Innovations

Sterling Backus, *Kapteyn-Murnane Laboratories, USA*, General Chair
 Michal Lipson, *Columbia Univ., USA*, General Chair
 Tara Fortier, *National Inst of Standards & Technology, USA*, Program Chair
 Christophe Dorrer, *Univ. of Rochester, USA*, Program Chair

S&I 1: Light-Matter Interactions and Materials Processing

Tsing-Hua Her, *Univ. of North Carolina at Charlotte, USA*, Subcommittee Chair
 Nadezhda Bulgakova, *HiLASE, Institute of Physics ASCR, Czech Republic*
 Maria Kandyla, *National Hellenic Research Foundation, Greece*
 Edward Kinzel, *Missouri Univ. of Sci. and Tech., USA*
 Carl Liebig, *Air Force Research Laboratory, USA*
 Chih Wei Luo, *National Chiao Tung Univ., Taiwan*
 Takashige Omatsu, *Chiba Univ., Japan*
 Renee Sher, *Wesleyan Univ., USA*
 Zijie Yan, *Clarkson Univ., USA*

S&I 2: Laser Systems and Facilities

Jake Bromage, *Univ. of Rochester, USA*, Subcommittee Chair
 Lynda Busse, *US Naval Research Laboratory, USA*
 Erhard Gaul, *Univ. of Texas at Austin, USA*
 Aurélie Jullien, *INLN - INPHYNI, CNRS, UNS, France*
 Max Lederer, *European XFEL, Germany*
 Seong Ku Lee, *APRI, GIST, South Korea*
 Xiaoyan Liang, *Shanghai Institute of Optics & Fine Mechanics, China*
 Dimitrios Papadopoulos, *LULI, France*
 Clara Saraceno, *Ruhr Universität Bochum, Germany*
 Emily Sistrunk Link, *Lawrence Livermore National Laboratory, USA*
 David Spence, *Macquarie Univ., Australia*
 Lutz Winkelmann, *DESY, Germany*

All conference locations are in the San Jose Convention Center unless otherwise noted.

S&I 3: Semiconductor Lasers

Mikhail Belkin, *Univ. of Texas at Austin, USA*, **Subcommittee Chair**

Chadwick Canedy, *Naval Research Laboratory, USA*
 Connie Chang-Hasnain, *Univ. of California Berkeley, USA*
 Lan Fu, *Australian National Univ., Australia*
 Nicolas Grandjean, *École polytechnique fédérale de Lausanne, Switzerland*
 Qing Gu, *The Univ. of Texas at Dallas, USA*
 Peter Heim, *Thorlabs Inc., USA*
 Nobu Nishiyama, *Tokyo Institute of Technology, Japan*
 Günther Roelkens, *Universiteit Gent – imec, Belgium*
 Leon Shterengas, *Stony Brook Univ., USA*
 Qijie Wang, *Nanyang Technological Univ., Singapore*

CLEO S&I 4: Nonlinear Optical Technologies

Michelle Y. Sander, *Boston University, USA*, **Subcommittee Chair**

Jaime Cardenas, *Univ. of Rochester, USA*
 Amol Choudhary, *Univ. of Sydney, Australia*
 Kavita Devi, *Indian Institute of Technology (IIT), India*
 Miro Erkintalo, *Univ. of Auckland, New Zealand*
 Katia Gallo, *KTH Royal Institute of Technology, Sweden*
 Shu-Wei Huang, *Univ. of Colorado at Boulder, USA*
 Brandon Shaw, *US Naval Research Laboratory, USA*
 Youjian Song, *Tianjin Univ., China*
 Dawn Tan, *Singapore Univ. of Technology & Design, Singapore*
 Markku Vainio, *Helsingin Yliopisto, Finland*
 Sergey Vasilyev, *IPG Photonics Corp., Mid-IR Lasers, USA*

CLEO S&I 5: Terahertz Science and Technologies

Matthias Hoffmann, *SLAC National Accelerator Laboratory, USA*, **Subcommittee Chair**

Mattias Beck, *ETH Zürich, Switzerland*
 Tyler Cocker, *Michigan State Univ., USA*
 Martin Koch, *Philipps Universität Marburg, Germany*
 Juliette Mangeney, *Laboratoire Pierre Aigrain, France*
 Daniel Mittleman, *Brown Univ., USA*
 Tadao Nagatsuma, *Osaka Univ., Japan*
 Pernille Pedersen, *Aarhus Universitet, Denmark*
 Minah Seo, *Korea Institute of Science & Technology, South Korea*
 Miriam Vitiello, *Scuola Normale Superiore di Pisa, Italy*

CLEO S&I 6: Optical Materials, Fabrication and Characterization

Roberto Paiella, *Boston Univ., USA*, **Subcommittee Chair**
 Jiming Bao, *Univ. of Houston, USA*
 Matthew Escarra, *Tulane Univ., USA*
 Frederic Gardes, *Univ. of Southampton, UK*
 Tingyi Gu, *Univ. of Delaware, USA*
 Eiichi Kuramochi, *NTT Corporation, Japan*
 Lih Lin, *Univ. of Washington, USA*
 Oana Malis, *Purdue Univ., USA*
 Alejandro Manjavacas, *Univ. of New Mexico, USA*
 Richard Osgood, *Columbia Univ., USA*
 Zhipei Sun, *Aalto Yliopisto, Finland*

CLEO S&I 7: Micro- and Nano-Photonic Devices

Takasumi Tanabe, *Keio Univ., Japan*, **Subcommittee Chair**
 Ali Adibi, *Georgia Institute of Technology, USA*
 Vladimir Aksyuk, *National Institute of Standards & Technology, USA*
 Paul Barclay, *Univ. of Calgary, Canada*

Daryl Beggs, *Cardiff Univ., UK*

Alfredo De Rossi, *Thales Research & Technology, France*
 Karen Grutter, *Univ. of Maryland at College Park, USA*
 Tobias Herr, *Swiss Cent for Electronics and Microtech, Switzerland*

Zhihong Huang, *Hewlett Packard laboratories, USA*
 Jin Liu Sun, *Yat-Sen Univ., China*
 Nobuyuki Matsuda, *Tohoku Univ., Japan*
 Yasutomo Ota, *Univ. of Tokyo, Japan*
 Harish Subbaraman, *Boise State Univ., USA*
 Sharon Weiss, *Vanderbilt Univ., USA*
 Lan Yang, *Washington Univ. in St Louis, USA*

CLEO S&I 8: Ultrafast Optics & Applications

Igor Jovanovic, *Univ. of Michigan, USA*, **Subcommittee Chair**

Alan Fry, *SLAC National Accelerator Laboratory, USA*
 Cristina Hernandez-Gomez, *STFC Rutherford Appleton Laboratory, UK*
 Fumihiko Kannari, *Keio Univ., Japan*
 Thomas Planchon, *Delaware State Univ., USA*
 Liejia Qian, *Shanghai Jiao Tong Univ., China*
 Bojan Resan, *Univ. of Applied Sciences FHNW, Switzerland*
 Lucia Saito, *Universidade Presbiteriana Mackenzie, Brazil*
 Lawrence Shah, *Luminar Technologies, Inc., USA*
 Catherine Teisset, *TRUMPF Scientific Lasers, Germany*
 Andreas Vaupel, *IPG Photonics Corp, USA*
 László Veisz, *Max-Planck-Institut für Quantenoptik, Sweden*
 Tobias Witting, *Max-Born-Institute, Germany*

CLEO S&I 9: Photonic Integration

Qiaoqiang Gan, *State Univ. of New York at Buffalo, USA*, **Subcommittee Chair**
 Ozdal Boyraz, *Univ. of California Irvine, USA*
 Jonathan Bradley, *McMaster Univ., Canada*
 Martin Cryan, *Univ. of Bristol, UK*
 Zetian Mi, *Univ. of Michigan, USA*
 Richard Penty, *Univ. of Cambridge, UK*
 Haisheng Rong, *Intel Corporation, USA*
 Laurent Schares, *IBM, USA*
 Jian Wang, *Huazhong Univ. of Science and Technology, China*
 Alan Wang, *Oregon State Univ., USA*
 Shumin Xiao, *Harbin Institute of Technology, China*
 Winnie Ye, *Carleton Univ., Canada*
 Beibei Zeng, *Los Alamos National Laboratory, USA*

CLEO S&I 10: Biophotonics and Optofluidics

Jessica Houston, *New Mexico State Univ., USA*, **Subcommittee Chair**
 Hatice Altug, *École polytechnique fédérale de Lausanne, Switzerland*
 Emily Gibson, *Univ. of Colorado Denver, USA*
 Vernita Gordon, *Univ. of Texas at Austin, USA*
 Aaron Hawkins, *Brigham Young Univ., USA*
 Rainer Leitgeb, *Medical Univ. Vienna, Austria*
 Jakub Nedbal, *King's College London, UK*
 Ute Neugebauer, *Center for Sepsis Control and Care Jena, Germany*
 Raluca Niesner, *Charité-Univ. Medicine Berlin, Germany*
 John Rasmussen, *Univ. of Texas Health Science Center, USA*

All conference locations are in the San Jose Convention Center unless otherwise noted.

CLEO S&I 11: Fiber Photonics: Novel Phenomena, Lasers, Systems and Fabrication

Sze Yun Set, *Univ. of Tokyo, Japan*, Subcommittee Chair
 Kazi Abedin, *OFS Laboratories, USA*
 Rodrigo Amezcua Correa, *Univ. of Central Florida—CREOL, USA*
 Camille-Sophie Brès, *École polytechnique fédérale de Lausanne, Switzerland*
 Neil Broderick, *Univ. of Auckland, New Zealand*
 Guoqing Chang, *Beijing National Laboratory for Condensed Matter Physics, China*
 Maria Chernysheva, *Aston Univ., UK*
 Julien Fatome, *Université de Bourgogne, France*
 Takemi Hasegawa, *Sumitomo Electric Industries Ltd., Japan*
 Stuart Jackson, *Macquarie Univ., Australia*
 Li Qian, *Univ. of Toronto, Canada*
 William Renninger, *Univ. of Rochester, USA*
 Masaki Tokurakawa, *Univ. of Electro-communications, ILS, Japan*
 Kenneth Kin-Yip Wong, *Univ. of Hong Kong, Hong Kong*
 Meng Zhang, *Beihang Univ., China*

CLEO S&I 12: Lightwave Communications and Optical Networks

David Geisler, *Massachusetts Institute of Technology Lincoln Lab, USA*, Subcommittee Chair
 Xi Chen, *Nokia Bell Labs, USA*
 Nan Chi, *Fudan Univ., China*
 Francesco Da Ros, *DTU Fotonik, Denmark*
 Mihaela Dinu, *LGS Innovations LLC, USA*
 Marija Furdek, *KTH Royal Institute of Technology, Sweden*
 Vladimir Grigoryan, *Ciena Corporation, USA*
 Magnus Karlsson, *Chalmers Tekniska Högskola, Sweden*
 Masayuki Matsumoto, *Wakayama Univ., Japan*
 Giovanni Milione, *NEC Laboratories America Inc, USA*
 Ryan Scott, *Keysight Technologies Inc., USA*

CLEO S&I 13: Active Optical Sensing

Todd Stievater, *US Naval Research Laboratory, USA*, Subcommittee Chair
 Brian Brumfield, *Pacific Northwest National Laboratory, USA*
 Denis Donlagic, *Univerza v Mariboru, Slovenia*
 Erik Emmons, *Edgewood Chemical and Biological Center, USA*
 Gamani Karunasiri, *Naval Postgraduate School, USA*
 Waruna Kulatilaka, *Texas A&M Univ., USA*
 Nicolas Le Thomas, *Universiteit Gent, Belgium*
 Andrey Muraviev, *CREOL, Univ. of Central Florida, USA*
 Eric Zhang, *IBM T. J. Watson Research Center, USA*

CLEO S&I 14: Optical Metrology

Laura Sinclair, *National Inst of Standards & Technology, USA*, Subcommittee Chair
 Florian Adler, *Tiger Optics, USA*
 Ladan Arissian, *Univ. of Ottawa, Canada*
 Aurélien Coillet, *Université de Bourgogne, France*
 Flavio Cruz, *Universidade Estadual de Campinas, USA*
 E. Anne Curtis, *National Physical Laboratory, UK*
 Pascal Del'Haye, *National Physical Laboratory, UK*
 Haifeng Jiang, *National Time Service Center, China*
 Nathan Lemke, *Air Force Research Laboratory, USA*
 Takeshi Yasui, *Tokushima Univ., Japan*

CLEO S&I 15: Quantum and Atomic Sensors, and their Applications

Andre Luiten, *Univ. of Adelaide, Australia*, Subcommittee Chair
 Eisuke Abe, *Keio Univ., Japan*
 Warwick Bowen, *Univ. of Queensland, Australia*
 Susannah Jones, *Dstl, UK*
 Shau-Yu Lan, *Nanyang Technology Univ., Singapore*
 Franck Pereira dos Santos, *SYRTE, France*
 Qudsia Quraishi, *US Army Research Laboratory, USA*
 Erling Reis, *Univ. of Strathclyde, Scotland*
 James Schaffer, *Univ. of Oklahoma, USA*
 Susan Schima, *NIST, USA*
 Benjamin Sussman, *National Research Council Canada, Canada*

CLEO Steering Committee

IEEE/Photonics Society

Ann Catrina Coleman, *Univ. of Texas at Dallas, USA*, Chair
 Seth Bank, *Univ. of Texas at Austin, USA*
 Kent Choquette, *Univ. of Illinois at Urbana-Champaign, USA*
 Peter Smowton, *Cardiff Univ., UK*
 Weidong Zhou, *Univ. of Texas at Arlington, USA*

The Optical Society

Craig Arnold, *Princeton Univ., USA*
 Sterling J. Backus, *Kapteyn-Murnane Labs., USA*
 Ingmar Hartl, *DESY, Germany*
 Jessie Rosenberg, *IBM TJ Watson Research Center, USA*
 Yurii Vlasov, *IBM TJ Watson Research Center, USA*

APS/Division of Laser Science

Nicholas Bigelow, *Univ. of Rochester, USA*
 Rohit Prasankumar, *Los Alamos National Laboratory, USA*

Ex-Officio

Peter Andersen, *Danmarks Tekniske Universitet, Denmark*
 Christophe Dorrer, *Univ. of Rochester, USA*
 Ben Eggleton, *Univ. of Sydney, Australia*
 Tara Fortier, *National Institute of Standards & Technology, USA*
 Amr Helmy, *Univ. of Toronto, Canada*
 Jin Kang, *Johns Hopkins Univ., USA*
 Mercedeh Khajavikhan, *CREOL, Univ. of Central Florida, USA*
 Michal Lipson, *Columbia Univ., USA*
 Natalia Litchinitser, *Univ. at Buffalo, USA*
 Michael M. Mielke, *Iradion Laser, USA*
 Tracy Northup, *Universität Innsbruck, Austria*
 Irina Novikova, *College of William & Mary, USA*
 Todd Pittman, *Univ. of Maryland Baltimore County, USA*
 Sergey Polyakov, *National Institute of Standards & Technology, USA*
 Yurii A. Vlasov, *Univ. of Illinois at Urbana-Champaign, USA*
 Shinji Yamashita, *Univ. of Tokyo, Japan*

All conference locations are in the San Jose Convention Center unless otherwise noted.

CLEO Budget Committee

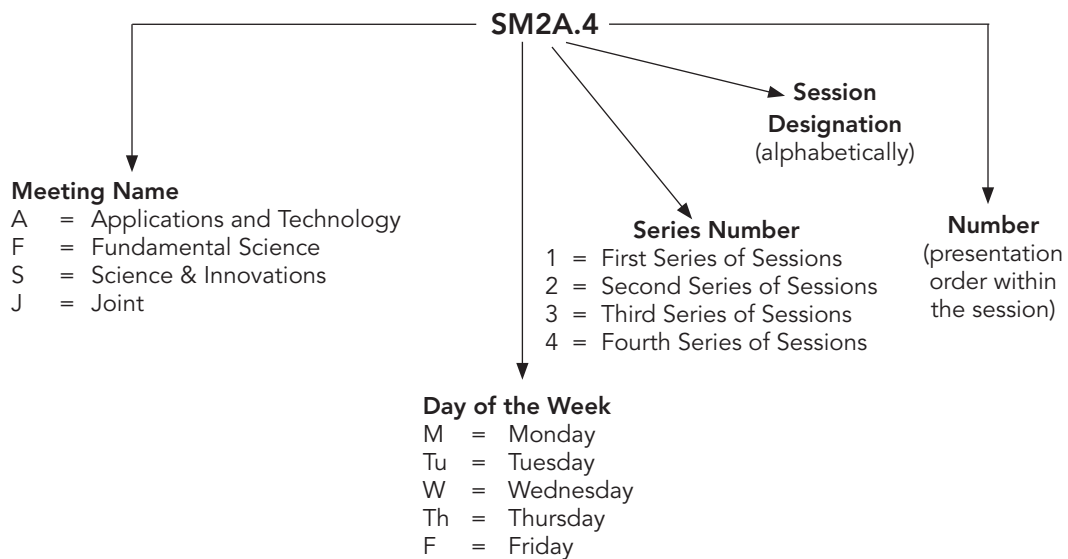
Craig Arnold, *Princeton Univ., USA*
Kent Choquette, *Univ. of Illinois at Urbana-Champaign, USA*
Douglas M. Razzano, *IEEE Photonics Society, USA*
Kristan Corwin, *Kansas State Univ., USA*
Kate Kirby, *American Physical Society, USA*
Rohit Prasankumar, *Los Alamos National Laboratory, USA*
Elizabeth A. Rogan, *The Optical Society, USA*

Joint Council on Applications

Eric Mottay, *Amplitude Systemes, France, Chair*
Wilhelm G. Kaenders, *Toptica Photonics Inc, Germany*
Amy Eskilson, *Inrad Optics, USA*
Peter Fendel, *Thorlabs Inc., USA*
Klausa Klein, *Coherent, Inc., USA*
Tyler Morgus, *Thorlabs Inc., USA*
Rick Plympton, *Optimax Systems, USA*
Carsten Thomsen, *NKT Photonics, Denmark*
Mark Tolbert, *Toptica Photonics, USA*
Chris Wood, *Insight Photonic Solutions, USA*

All conference locations are in the San Jose Convention Center unless otherwise noted.

Explanation of Session/Presentation Codes



The first letter of the code designates the meeting (For instance, A=Applications & Technology, F=Fundamental Science, S=Science and Innovations, J=Joint). The second element denotes the day of the week (Monday=M, Tuesday=Tu, Wednesday=W, Thursday=Th, Friday=F). The third element indicates the session series in that day (for instance, 2 would denote the second parallel sessions in that day). Each series of sessions begins with the letter A in the fourth element and continues alphabetically through a series of parallel sessions. The number on the end of the code (separated from the session code with a period) signals the position of the talk within the session (first, second, third, etc.). For example, a presentation coded SM2A.4 indicates that this paper is part of Science and Innovations (S) and is being presented on Monday (M) in the second series of sessions (2), and is the first parallel session (A) in that series and the fourth paper (4) presented in that session.

Agenda of Sessions — Sunday, 5 May

07:30–17:30	Registration, Concourse Level
08:30–12:30	SC149: Foundations of Nonlinear Optics (Robert Fisher, R. A. Fisher Associates, USA) SC456: How to Start a Company (Jes Broeng, Danmarks Tekniske Universitet, Denmark) SC466: Silicon Integrated Nanophotonics (Yurii A. Vlasov, University of Illinois at Urbana-Champaign, USA) SC479: Basics of Quantum Optics for Quantum-Enabled Technologies (Bahaa Saleh, CREOL, University of Central Florida, USA)
09:00–13:00	Pride in Photonics: LGBTQ+ & Ally Workshop, University Room, Hilton San Jose
13:30–17:30	SC157: Laser Beam Analysis, Propagation, and Shaping Techniques (James Leger, University of Minnesota, USA) SC396: Frontiers of Guided Wave Nonlinear Optics (Ben Eggleton, University of Sydney, Australia) SC475: Metasurface Flat Optics: A New Paradigm for Optical Components Design and Manufacturing (Federico Capasso, Harvard University, USA)
14:00–15:30 16:00–17:30	Be a Part of the Solution: Preventing and Responding to Harassment, University Room, Hilton San Jose
14:30–17:30	SC478: Microresonator based Optical Frequency Comb and Photonic Waveguide Supercontinuum Sources (Tobias Kippenberg, École polytechnique fédérale de Lausanne, Switzerland)

New This Year: Workshops

These sessions provide interactive learning environments and are open to all conference registrants.

Will Quantum Computing Actually Work?!

Monday, 6 May; 18:30–20:00

Room 210A

What Will Be the Largest Commercial Application for Optical Frequency Combs in 10 Years?

Monday, 6 May; 18:30–20:00

Room 210B

Beyond Awareness: What Actions Can Be Taken to Improve Diversity in STEM?

Wednesday, 8 May, 10:30–12:00

Exhibit Hall Theater II



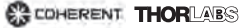
Agenda of Sessions — Monday, 6 May

	Executive Ballroom 210A	Executive Ballroom 210B	Executive Ballroom 210C	Executive Ballroom 210D	Executive Ballroom 210E	Executive Ballroom 210F	Executive Ballroom 210G	Executive Ballroom 210H
07:00–18:00	Registration, <i>Concourse Level</i>							
08:00–10:00	FM1A • Quantum Optomechanics & Transduction	FM1B • Topological Photonics I	FM1C • Novel Phenomena in Classical Nano-Optics	FM1D • Coherent Phenomena in Coupled Resonator Networks	JM1E • Symposium on High Average Power Ultrafast Lasers: Trends, Challenges & Applications I	SM1F • Optical Clocks	SM1G • Ultra-High Capacity Transmission Techniques & SDM	SM1H • Plasmonics for Manipulation & Sensing
08:30–12:30	SC270: High Power Fiber Lasers and Amplifiers (W. Andrew Clarkson, Optoelectronics Research Center, University of Southampton, UK) SC352: Introduction to Ultrafast Pulse Shaping - Principles and Applications (Marcos Dantus, Michigan State University, USA) SC361: Coherent Mid-IR Light: Generation and Applications (Konstantin Vodopyanov, The College of Optics & Photonics, University of Central Florida, USA) SC477: Laser Radar and Remote Sensing: An Application-oriented Introduction (Fabio Di Teodoro, Raytheon, USA) SC481: Fundamentals and Applications of VCSELs (Kent Choquette, University of Illinois, USA)							
10:00–10:30	Coffee Break, <i>Concourse Level</i>							
10:30–12:30	FM2A • Quantum Optics of Atoms and Molecules	JM2B • Symposium on Nonreciprocal Photonics I	FM2C • Nonlinear Nano-Optics	FM2D • Ultrafast Optical Processes in Topological Materials	JM2E • Symposium on High Average Power Ultrafast Lasers: Trends, Challenges & Applications II	SM2F • Quantum Sensing in Solid State Systems	SM2G • Free-Space & Underwater Communication	SM2H • Optical Imaging & Sensing
11:00–12:00	OSA Presentation Feedback Program, <i>University Room, Hilton San Jose</i>							
11:00–12:30	Navigate Your Leadership Trajectory for Senior Leaders, <i>Salon VI, San Jose Marriott</i>							
12:30–13:30	Lunch Break (on your own)							
12:30–13:30	What's Next in Integrated Optics - Hot Topics at CLEO: 2019, <i>Room 230A</i>							
13:00–14:00	Social Media in 2019 Panel Discussion, <i>University Room, Hilton San Jose</i>							
13:00–14:00	Resumes, LinkedIn, and Networking (with Cheeky Scientist), <i>University Room, Hilton San Jose</i>							
13:30–17:30	SC362: Cavity Optomechanics: Fundamentals and Applications (Tobias Kippenberg, Ecole polytechnique federale de Lausanne, Switzerland) SC376: Plasmonics (Mark Brongersma; Stanford University, USA) SC378: Introduction to Ultrafast Optics (Rick Trebino, Georgia Institute of Technology, USA) SC476: QCL and QCL Combs (Jérôme Faist, ETH Zürich, Switzerland)							
13:30–15:30	FM3A • Quantum Nanophotonics I: Plasmonics & Quantum Dots	JM3B • Symposium on Nonreciprocal Photonics II	FM3C • Functional Nanophotonics Using Metasurfaces	FM3D • Ultrafast Coherent Spectroscopy	JM3E • Symposium on High Average Power Ultrafast Lasers: Trends, Challenges & Applications III	SM3F • Hot Topics in Quantum Sensing	SM3G • Data Center Lightwave Communications	SM3H • Fundamentals of Ultrafast Light Matter Interaction
14:30–16:00	Deliberate Mentoring to Advance Your Career: Special Flash Mentoring Session, <i>Guadalupe Room, Marriott</i>							
15:30–16:00	Coffee Break, <i>Concourse Level</i>							
16:00–17:00	Resumes, LinkedIn, and Networking (with Cheeky Scientist), <i>University, Hilton San Jose</i>							
16:00–17:30	Professional Development for Busy Professionals, <i>Salon VI, San Jose Marriott</i>							
16:00–18:00	FM4A • Quantum Nanophotonics II: Diamond & Boron Nitride	FM4B • Topological Photonics II	FM4C • New Systems for Quantum Communications	FM4D • Excitons in Condensed Matter Systems	SM4E • High-Average Power Laser Systems	SM4F • Precision Spectroscopy	SM4G • Access & Radio Over Fiber	SM4H • Advanced Optical Technologies for Cells and Tissues
17:30–18:30	Diversity and Inclusion Reception, <i>Winchester Room, Hilton San Jose</i>							
18:30–20:00	Lasers for Attosecond 2.0, <i>Room 230A</i>							
18:30–20:00	NEW Workshop 2: Will Quantum Computing Actually Work? <i>Room 210 A</i> NEW Workshop 3: What Will be the Largest Commercial Application for Optical Frequency Combs in 10 Years?, <i>Room 210B</i>							

Meeting Room 211 A&B	Meeting Room 211 C&D	Meeting Room 212 A&B	Meeting Room 212 C&D	Marriott Salon I & II	Marriott Salon III	Marriott Salon IV
Registration, <i>Concourse Level</i>						
AM1I • Photobiomodulation Therapeutics	SM1J • Beamforming & Coupling to Free Space	AM1K • Environmental & Atmospheric Sensing I	SM1L • Narrow Linewidth Fiber Lasers	FM1M • Single-Photon Sources	SM1N • Open-path Sensing & Free-electron Lasers	SM1O • Van der Waals Heterostructures
SC270: High Power Fiber Lasers and Amplifiers (W. Andrew Clarkson, Optoelectronics Research Center, University of Southampton, UK) SC352: Introduction to Ultrafast Pulse Shaping - Principles and Applications (Marcos Dantus, Michigan State University, USA) SC361: Coherent Mid-IR Light: Generation and Applications (Konstantin Vodopyanov, The College of Optics & Photonics, University of Central Florida, USA) SC477: Laser Radar and Remote Sensing: An Application-oriented Introduction (Fabio Di Teodoro, Raytheon, USA) SC481: Fundamentals and Applications of VCSELs (Kent Choquette, University of Illinois, USA)						
Coffee Break, <i>Concourse Level</i>						
AM2I • Applied Biophotonic Microscopy & Imaging	SM2J • Optical Computing & Resonator Applications	AM2K • Environmental & Atmospheric Sensing II	SM2L • Fiber Devices	FM2M • Random Numbers & Entanglement	SM2N • Enhanced Cavities for Sensing and Interferometry	SM2O • Micro & Nano Fabrication
OSA Presentation Feedback Program, <i>University Room, Hilton San Jose</i>						
Navigate Your Leadership Trajectory for Senior Leaders, <i>Salon VI, San Jose Marriott</i>						
Lunch Break (on your own)						
What's Next in Integrated Optics - Hot Topics at CLEO: 2019, <i>Room 230A</i>						
Social Media in 2019 Panel Discussion, <i>University Room, Hilton San Jose,</i>						
Resumes, LinkedIn, and Networking (with Cheeky Scientist), <i>University Room, Hilton San Jose</i>						
SC362: Cavity Optomechanics: Fundamentals and Applications (Tobias Kippenberg, Ecole polytechnique federale de Lausanne, Switzerland) SC376: Plasmonics (Mark Brongersma; Stanford University, USA) SC378: Introduction to Ultrafast Optics (Rick Trebino, Georgia Institute of Technology, USA) SC476: QCL and QCL Combs (Jérôme Faist, ETH Zürich, Switzerland)						
AM3I • Biomedical Imaging	SM3J • Silicon Photonics	AM3K • A&T Topical Review on Flat Optics I	SM3L • Fiber Amplifiers	JM3M • Symposium on Machine Learning Photons: Where Machine Learning & Photonics Intersect I	SM3N • Novel Optoelectronic Devices	SM3O • Guided Wave Nonlinear Devices
Deliberate Mentoring to Advance Your Career: Special Flash Mentoring Session, <i>Guadalupe Room, Marriott</i>						
Coffee Break, <i>Concourse Level</i>						
Resumes, LinkedIn, and Networking (with Cheeky Scientist), <i>University, Hilton San Jose</i>						
Professional Development for Busy Professionals, <i>Salon VI, San Jose Marriott</i>						
AM4I • Nanobiophotonics	SM4J • Light Emission & Detection	AM4K • A&T Topical Review on Flat Optics II	SM4L • Specialty Fibers	FM4M • Solid State High Harmonic Generation	SM4N • Surface Emitting Lasers	SM4O • Nonlinear Phonon Interactions
Diversity and Inclusion Reception, <i>Winchester Room, Hilton San Jose</i>						
Lasers for Attosecond 2.0, <i>Room 230A</i>						
NEW Workshop 2: Will Quantum Computing Actually Work? <i>Room 210 A</i> NEW Workshop 3: What Will be the Largest Commercial Application for Optical Frequency Combs in 10 Years?, <i>Room 210B</i>						


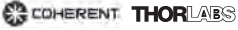

Agenda of Sessions — Tuesday, 7 May

	Executive Ballroom 210A	Executive Ballroom 210B	Executive Ballroom 210C	Executive Ballroom 210D	Executive Ballroom 210E	Executive Ballroom 210F	Executive Ballroom 210G	Executive Ballroom 210H
07:00–18:30	Registration, Concourse Level							
08:00–10:00	Joint Plenary Session, Grand Ballroom 220A							
10:00–17:00	Exhibit Open (10:00–17:00), Coffee Break (10:00–11:30), Exhibit Halls 1-3 Coffee Break Sponsored by 							
10:30–12:00	Quantum Information Science and Technology Initiatives, Exhibit Hall Theater I							
10:30–13:30	SC455: Integrated Photonics for Quantum Information Science and Technology (Dirk Englund, MIT, USA)							
10:30–14:30	SC403: NanoCavity Quantum Electrodynamics and Applications (Jelena Vučković, Stanford University, USA) SC410: Finite Element Modeling Methods for Photonics and Optics (Arti Agrawal, City University, UK) SC424: Optical Terahertz Science and Technology (David G. Cooke, McGill University, Canada) SC438: Photonic Metamaterials (Nader Engheta, University of Pennsylvania, USA)							
11:30–13:00	Poster Session I & Lunch, Exhibit Halls 1-3							
12:00–13:30	OIDA VIP Industry Leaders Speed Meeting Event, Booth 2605 Sponsored by 							
13:00–15:00	JTu3A • Symposium on Quantum Information in Time-Frequency Domain I	FTu3B • PT Symmetry & Exceptional Points	FTu3C • Polaritonic Interactions in Transition Metal Dichalcogenide	FTu3D • Tailored Light-Matter Interactions	STu3E • High Peak-Power Lasers & Technologies I	STu3F • Terahertz Sensing & Devices	JTu3G • Symposium on Space-borne Quantum Sensors	STu3H • Biophotonics & Optofluidics
15:00–17:00	Coffee Break and Exhibit Only Time, Exhibit Halls 1-3 Sponsored by 							
15:00–16:30	Meet the OSA Publishing Journal Editors Ice Cream Social, Networking Zone, Booth 2605							
15:30–17:00	OIDA: Market Trends: Opportunities in Optics and Photonics, Exhibit Hall Theater I							
17:00–19:00	JTu4A • Symposium on Quantum Information in Time-Frequency Domain II	FTu4B • Manipulation of Symmetries in Optics	FTu4C • Nanophotonic Platforms for Optical Computing & Deep Learning	FTu4D • Thermal Photonics	STu4E • High Peak-Power Laser & Technologies II	STu4F • Terahertz Spectroscopy	STu4G • Miniaturizing Quantum Technology	STu4H • Innovations in Machine Learning & Microscopy
17:30–18:30	OSA Senior Member Reception, OSA Member Lounge, Concourse Level							
19:00–20:30	OSA Technical Group Poster Session, Grand Ballroom 220C							

Meeting Room 211 A&B	Meeting Room 211 C&D	Meeting Room 212 A&B	Meeting Room 212 C&D	Marriott Salon I & II	Marriott Salon III	Marriott Salon IV	Theater I	Theater II
Registration, Concourse Level								
Joint Plenary Session, Grand Ballroom 220A								
Exhibit Open (10:00–17:00), Coffee Break (10:00–11:30), Exhibit Halls 1-3 Coffee Break Sponsored by 								
Quantum Information Science and Technology Initiatives, Exhibit Hall Theater I								
SC455: Integrated Photonics for Quantum Information Science and Technology (Dirk Englund, MIT, USA)								
SC403: NanoCavity Quantum Electrodynamics and Applications (Jelena Vučković, Stanford University, USA) SC410: Finite Element Modeling Methods for Photonics and Optics (Arti Agrawal, City University, UK) SC424: Optical Terahertz Science and Technology (David G. Cooke, McGill University, Canada) SC438: Photonic Metamaterials (Nader Engheta, University of Pennsylvania, USA)								
Poster Session I & Lunch, Exhibit Halls 1-3								
OIDA VIP Industry Leaders Speed Meeting Event, Booth 2605 Sponsored by 								
ATu3I • Ultrafast Laser Processing	STu3J • Kerr Frequency Microcombs	ATu3K • Biophotonic Spectroscopy	STu3L • Mode-Locked Fiber Lasers I	JTu3M • Symposium on Intense-field Nonlinear Optics & High Harmonic Generation in Nanoscale Materials I	STu3N • Lasers on Silicon & Nanolasers	STu3O • Emerging Visible Light Communication	ATu3P • A&T Topical Review on Progress in the Semiconductor Laser Technology I	ATu3Q • A&T Topical Review on Advanced Design, Imaging and Process Technologies for Next Generation Semiconductors I
Coffee Break and Exhibit Only Time, Exhibit Halls 1-3 Sponsored by 								
Meet the OSA Publishing Journal Editors Ice Cream Social, Networking Zone, Booth 2605								
OIDA: Market Trends: Opportunities in Optics and Photonics, Exhibit Hall Theater I								
ATu4I • Emerging Lasers for Device Fabrication	STu4J • Quantum Nanostructure	ATu4K • Biosensing Technology	STu4L • Mode-Locked Fiber Lasers II	JTu4M • Symposium on Intense-field Nonlinear Optics & High Harmonic Generation in Nanoscale Materials II	STu4N • Semiconductor-Based Optical Frequency Combs	STu4O • Infrared Photonics & Applications		
OSA Senior Member Reception, OSA Member Lounge, Concourse Level								
OSA Technical Group Poster Session, Grand Ballroom 220C								

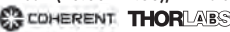
Agenda of Sessions — Wednesday, 8 May

	Executive Ballroom 210A	Executive Ballroom 210B	Executive Ballroom 210C	Executive Ballroom 210D	Executive Ballroom 210E	Executive Ballroom 210F	Executive Ballroom 210G	Executive Ballroom 210H
07:30–18:30	Registration, Concourse Level							
08:00–10:00	Joint Plenary Session, Grand Ballroom 220A							
10:00–17:00	Exhibit Open (10:00–17:00), Coffee Break (10:00–11:30), Exhibit Halls 1-3 Coffee Break Sponsored by 							
10:30–12:00	MIRTHE: New Commercial Trends in Mid-Infrared Sensing – From Nano-Photonics to Stand-Off Detection, Exhibit Hall Theater I							
10:30–12:00	Beyond Awareness: What Actions Can Be Taken to Improve Diversity in STEM, Exhibit Hall Theater II							
11:30–13:00	Poster Session II & Lunch, Exhibit Halls 1-3							
13:00–15:00	JW3A • Sym on Coupling Artificial Atoms to Nano- & Opto-mechanical Systems I	FW3B • Chip-scale Nonlinear Optics	FW3C • Generation & Control of Light Emission at the Nanoscale	FW3D • Topological Photonics III	SW3E • Ultrafast Metrology	SW3F • Terahertz Plasmonics	SW3G • Frequency Combs & Stable Laser Systems	SW3H • Nonlinear Optical Phenomena
15:00–17:00	Coffee Break & Dessert (Exhibit Only Time), Exhibit Halls 1-3 Sponsored by 							
15:30–16:00	Universal Quantum Devices, Product Showcase, Exhibit Hall Theater I							
16:00–16:30	Sandia National Laboratory, Product Showcase, Exhibit Hall Theater I							
16:30–17:00	Class 5, Product Showcase, Exhibit Hall Theater I							
17:00–19:00	JW4A • Sym on Coupling Artificial Atoms to Nano- & Opto-mechanical Systems II	FW4B • Nanoscale Nonlinear Optics	JW4C • Professional Development Session I	FW4D • Chirality, PT Symmetry, & Exceptional Points	SW4E • Ultrafast Pulse Manipulation	SW4F • Terahertz Sources & Communication	SW4G • Optical Frequency Synthesis & Microwave Generation	SW4H • Supercontinuum Generation
19:00–20:30	Conference Reception, Grand Ballroom Sponsored by 							

Meeting Room 211 A&B	Meeting Room 211 C&D	Meeting Room 212 A&B	Meeting Room 212 C&D	Marriott Salon I & II	Marriott Salon III	Marriott Salon IV	Theater I	Theater II
Registration, Concourse Level								
Joint Plenary Session, Grand Ballroom 220A								
Exhibit Open (10:00–17:00), Coffee Break (10:00–11:30), Exhibit Halls 1-3 Coffee Break Sponsored by 								NEW Workshop 1: Beyond Awareness 10:30–12:00
MIRTHE: New Commercial Trends in Mid-Infrared Sensing – From Nano-Photonics to Stand-Off Detection, Exhibit Hall Theater I								
Beyond Awareness: What Actions Can Be Taken to Improve Diversity in STEM, Exhibit Hall Theater II								
Poster Session II & Lunch , Exhibit Halls 1-3								
AW3I • Laser-formed Structures & Additive Manufacturing	SW3J • Photonic Sensing & Mid-infrared Photonics	AW3K • Optical Solutions for Autonomous Driving	SW3L • Ultrasound, Photoacoustic, & Photothermal Sensing	FW3M • Ultrafast Spectroscopy in 2D Materials & Heterostructures	SW3N • Cascade Lasers	SW3O • Long Distance Transmission	AW3P • A&T Topical Review on Progress in the Semiconductor Laser Technology II	AW3Q • A&T Topical Review on Advanced Design, Imaging and Process Technologies for Next Generation Semiconductors II
Coffee Break & Dessert (Exhibit Only Time), Exhibit Halls 1-3 Sponsored by 								
Universal Quantum Devices, Product Showcase, Exhibit Hall Theater I								
Sandia National Laboratory, Product Showcase, Exhibit Hall Theater I								
Class 5, Product Showcase, Exhibit Hall Theater I								
AW4I • Medical Devices & Systems	SW4J • Design & Simulation of Micro- & Nano-photonic Devices	AW4K • Lidar	SW4L • Optical Detection of Vapors or Hazardous Environments	FW4M • Advanced Techniques & Applications in Ultrafast Spectroscopy	SW4N • High Power & Narrow Linewidth Lasers	SW4O • Short-Reach Communication Technologies		
Conference Reception, Grand Ballroom Sponsored by 								

Agenda of Sessions — Thursday, 9 May

	Executive Ballroom 210A	Executive Ballroom 210B	Executive Ballroom 210C	Executive Ballroom 210D	Executive Ballroom 210E	Executive Ballroom 210F	Executive Ballroom 210G	Executive Ballroom 210H
07:30–18:00	Registration, Concourse Level							
08:00–10:00	FTh1A • Exploiting Quantum Degrees of Freedom	FTh1B • Ultrafast Nonlinear Phenomena	FTh1C • Hot-electron Enabled Plasmonics & Optical Vortices	FTh1D • Entanglement Sources	STh1E • Mid-IR Lasers	STh1F • Chip-Scale Trace-Gas Sensing	STh1G • Frequency Comb Spectroscopy	STh1H • Optical Resonance-Based Devices
10:00–11:30	Exhibit Open (10:00–15:00), Coffee Break (10:00–11:30), Exhibit Halls 1–3 Coffee Break Sponsored by 							
10:15–12:30	Technology Transfer Program, Exhibit Hall Theater I							
10:15–10:45	Technology Transfer Program: Keynote, Exhibit Hall Theater I							
10:45–11:15	Technology Transfer Program: Tutorial Talk, Exhibit Hall Theater I							
11:15–12:30	Technology Transfer Program: Pitch Panel, Exhibit Hall Theater I							
11:30–13:00	Poster Session III, Exhibit Halls 1-3							
12:30–14:00	Lunch, Exhibit Halls 1-3							
14:00–16:00	FTh3A • Gateways to Quantum Information Processing	FTh3B • Tailorable Phenomena in Optical Fibers	FTh3C • Emission & Detection of Thermal Radiation	FTh3D • Quantum Photonics: Generation & Manipulation	STh3E • Ultrafast Parametric Sources I	STh3F • Nonlinear THz Phenomena	STh3G • Precision Timing & Optical Time Transfer	STh3H • Modulation & Switching
16:00–16:30	Coffee Break, Concourse Level Sponsored by 							
16:30–18:30	FTh4A • New Protocols in Quantum Communications	FTh4B • Non-Diffractive & Vortex Beams	FTh4C • Advanced Nanophotonic Platforms for Spectroscopy & Sensing	FTh4D • Beyond Photon Pairs	STh4E • Ultrafast Parametric Sources II	JTh4F • Interaction of Strong THz Fields with Condensed Matter Systems	STh4G • Optomechanics	STh4H • Optical Driven Photonics
18:30–20:00	Emerging Trends in Nonlinear Optics - A Review of CLEO: 2019, Room 230A							
18:30–20:00	Dinner Break (on your own)							
20:00–22:00	Postdeadline Paper Sessions, Location Announced in Update Sheet							

Meeting Room 211 A&B	Meeting Room 211 C&D	Meeting Room 212 A&B	Meeting Room 212 C&D	Marriott Salon I & II	Marriott Salon III	Marriott Salon IV
Registration, Concourse Level						
ATh1I • Radiative Cooling & Photovoltaics	STh1J • Nonlinear Photonics	ATh1K • Industrial Metrology & Remote Sensing	STh1L • Hollow Core Fibers	FTh1M • Ultrafast Processes in Gases & Solids	STh1N • Sensing & Switching	STh1O • Metasurfaces & Nanophotonic Materials
Exhibit Open (10:00–15:00), Coffee Break (10:00–11:30), Exhibit Halls 1–3 Coffee Break Sponsored by 						
Technology Transfer Program, Exhibit Hall Theater I						
Technology Transfer Program: Keynote, Exhibit Hall Theater I						
Technology Transfer Program: Tutorial Talk, Exhibit Hall Theater I						
Technology Transfer Program: Pitch Panel, Exhibit Hall Theater I						
Poster Session III, Exhibit Halls 1-3						
Lunch, Exhibit Halls 1-3						
ATh3I • A&T Topical Review on Silicon Photonics I	STh3J • Emerging Nonlinear Platforms	ATh3K • Trace Species Sensing	STh3L • Multi-Mode Fiber Phenomena I	FTh3M • Metasurfaces	STh3N • Hybrid Integration with Si Photonics	STh3O • 2D Materials
Coffee Break, Concourse Level Sponsored by 						
ATh4I • A&T Topical Review on Silicon Photonics II	STh4J • Applications of Lasers & Microcombs	ATh4K • Sources & Techniques for Industrial Monitoring	STh4L • Multi-Mode Fiber Phenomena II	FTh4M • Hyperbolic Photonics Media	STh4N • High-Speed Optical Interconnects	STh4O • Epitaxial Materials & Strain Engineering
Emerging Trends in Nonlinear Optics - A Review of CLEO: 2019, Room 230A						
Dinner Break (on your own)						
Postdeadline Paper Sessions, Location Announced in Update Sheet						

Agenda of Sessions — Friday, 10 May

	Executive Ballroom 210A	Executive Ballroom 210B	Executive Ballroom 210C	Executive Ballroom 210D	Executive Ballroom 210E	Executive Ballroom 210F	Executive Ballroom 210G
07:30–12:00	Registration, <i>Concourse Level</i>						
08:00–10:00	FF1A • Single-Photon Detection	FF1B • Time Varying Metasurfaces	FF1C • Attosecond & High Field Sources	FF1D • Solitons in Microresonators	SF1E • Ultrafast Applications	FF1F • Machine Learning & Quantum Exotica	SF1G • Devices for Communications
10:00–10:30	Coffee Break, <i>Concourse Level</i>						
10:30–12:30	FF2A • Photonic Crystals & Periodic Nano Optics	FF2B • Linear/Non-Linear Metasurfaces	FF2C • Attosecond Pulse Generation & Characterization	FF2D • Frequency Comb & Supercontinuum Generation	SF2E • Ultrafast Phenomena	JF2F • Symposium on Deep-learning Photons: Where Machine Learning & Photonics Intersect II	SF2G • Laser-Based Diagnostics for Material Processing
12:30–14:00	Lunch Break (On your Own)						
14:00–16:00	FF3A • Single-Photon Collection & Characterization	FF3B • Disordered Media	FF3C • Attosecond Dynamic Imaging	FF3D • Nonlinear & Quantum Effects	SF3E • Ultrafast Oscillators	JF3F • Symposium on Deep-learning Photons: Where Machine Learning & Photonics Intersect III	SF3G • Laser-Based 2D/3D Micro- & Nano-fabrication

Executive Ballroom 210H	Meeting Room 211 A&B	Meeting Room 211 C&D	Meeting Room 212 A&B	Meeting Room 212 C&D	Marriott Salon I & II	Marriott Salon III	Marriott Salon IV
Registration, <i>Concourse Level</i>							
SF1H • Phase-matching Techniques	SF1I • Frequency-Comb-Based Sensing	SF1J • Plasmonics, Optomechanics, & Metamaterials	AF1K • Structural Monitoring	SF1L • Fiber Parametric Sources	SF1M • Fiber-Based Information Process	SF1N • AI for Integrated Photonics	SF1O • Perovskites
Coffee Break, <i>Concourse Level</i>							
SF2H • Active & Reconfigurable Devices	SF2I • High Q Cavity, Resonators Application	SF2J • Lithium Niobate & Perovskite Photonic Devices	AF2K • Spectrometers & Wavelength Metrology	SF2L • MID-IR Fiber Sources	JF2M • Professional Development Session II	SF2N • RF Photonics	SF2O • Optoelectronic Materials
Lunch Break (On your Own)							
SF3H • Microresonator Frequency Combs	SF3I • Lasers for Accelerators	SF3J • Metasurface & Plasmonic Structures	AF3K • Imaging, Microscopy, & Specialized Detection	SF3L • Fiber Sensing	FF3M • Quantum Interactions in Nanophotonic Systems	SF3N • Modulators, Phase Arrays & Photodetectors	SF3O • Saturable Absorber Materials & Chalcogenides

Executive Ballroom
210AExecutive Ballroom
210BExecutive Ballroom
210CExecutive Ballroom
210D

CLEO: QELS-Fundamental Science

08:00–10:00

FM1A • Quantum Optomechanics & Transduction
Presider: Gabriel Molina Terriza, Centro de Fisica de Materiales, Spain

FM1A.1 • 08:00

Ultralow Dissipation Mechanical Resonators for Quantum Optomechanics, Nils Johan Engelsen¹, Sergey A. Fedorov¹, Amir H. Ghadimi¹, Mohammad J. Beryhi¹, Alberto Beccari¹, Ryan Schilling¹, Dalziel J. Wilson², Tobias J. Kippenberg³; ¹Ecole Polytechnique Fédérale de Lausanne, Switzerland; ²IBM Research — Zürich, Switzerland. We demonstrate dissipation dilution engineering techniques for ultralow dissipation mechanical resonators. The Si₃N₄ nanobeams show quality factors (Q) as high as 800 million and Q×f exceeding 10¹⁵ Hz—both records at room temperature.

FM1A.2 • 08:15

Dynamical gauge fields for phonons in an optomechanical system, Javier Del Pino¹, John P. Mathew¹, Ewold Verhagen¹; ¹AMOLF, Netherlands. We demonstrate a synthetic gauge field for phonon transport in a nano-optomechanical platform. Employing time-modulated radiation pressure forces, we evidence nonreciprocal nanomechanical phase transfer. We show how this enables new classes of phononic topological insulators.

FM1A.3 • 08:30

Quantum Measurement of a Mechanical Resonator At and Below the Standard Quantum Limit, Massimiliano Rossi^{1,2}, David Mason^{1,2}, Junxin Chen^{1,2}, Yeghishe Tsaturyan¹, Albert Schliesser^{1,2}; ¹Niels Bohr Inst., Denmark; ²Niels Bohr Inst., Center for Hybrid Quantum Networks (Hy-Q), Denmark. We measure mechanical displacements within 35% of the Heisenberg limit. By exploiting quantum correlations in an optomechanical system, we achieve for the first time a total sensitivity below the standard quantum limit by 1.5 dB.

08:00–10:00

FM1B • Topological Photonics I
Presider: To Be Announced

FM1B.1 • 08:00

Spin-Preserving Chiral Photonic Crystal Mirror, Behrooz Semnani^{1,2}, Jeremy Flannery², Zhenghao Ding², Rubayet Al Maruf², Michal Bajcsy^{2,1}; ¹ECE, Univ. of Waterloo, Canada; ²Inst. for Quantum Computing, Canada. We report on experimental realization of a chiral photonic-crystal structure which exhibits extreme intrinsic chira-optical activity. Formation of quasi-bound-states-in-continuum allows selective reflection of the circular polarization states of light and unconventionally preserves the handedness.

FM1B.2 • 08:15

Lossless Zero-Index Guided Modes via Bound States in the Continuum, Momchil Minkov¹, Ian Williamson¹, Meng Xiao¹, Shan-hui Fan¹; ¹Stanford Univ., USA. Zero-index metamaterials are sought for a number of applications, but have thus far always been associated with significant optical loss. We overcome this shortcoming by designing non-radiative zero-index modes in an all-dielectric photonic crystal slab.

FM1B.3 • 08:30

Non-Hermitian-enhanced photonic zero mode, Mingsen Pan^{3,1}, Han Zhao², Pei Miao^{3,1}, Stefano Longhi⁴, Liang Feng³; ¹Dept. of Electrical Engineering, The State Univ. of New York at Buffalo, USA; ²Dept. of Electrical and Systems Engineering, Univ. of Pennsylvania, USA; ³Dept. of Materials Science and Engineering, Univ. of Pennsylvania, USA; ⁴Dipartimento di Fisica, Politecnico di Milano and Istituto di Fotonica e Nanotecnologie del Consiglio Nazionale delle Ricerche, Italy. By ultrafast heterodyne measurements of light transport dynamics in a silicon waveguide lattice, we experimentally demonstrated the existence of a zero-energy mode whose topological characteristics are enhanced by non-Hermitian quantum phase engineering.

08:00–10:00

FM1C • Novel Phenomena in Classical Nano-Optics
Presider: Mo Mojahedi; Univ. of Toronto, USA

FM1C.1 • 08:00

Brightness Theorems for Nanophotonics, Hanwen Zhang¹, Chia Wei Hsu¹, Owen Miller¹; ¹Yale Univ., USA. We present nanophotonic “brightness theorems”, a set of power-concentration bounds that generalize their ray-optical counterparts, and motivate the concept of “wave étendue”. We show their ramifications in the design of metasurfaces and waveguide combiners.

FM1C.2 • 08:15

The Meaning and Use of Phase in Sub-wavelength Scattering, Zhean Shen¹, Aristide Dogariu¹; ¹Univ. of Central Florida, CREOL, USA. We show that the influence of evanescent wave is preserved in the phase of far field as an energetic time delay during scattering. We demonstrate the capability for sub-wavelength sensing by far-field phase measurements.

FM1C.3 • 08:30

Power-Bandwidth Limits in Near-Field Nanophotonics, Owen Miller¹, Hyunki Shim¹; ¹Yale Univ., USA. We find upper bounds to near-field optical response, for any material over any bandwidth. We apply this approach to CDOS, a photon-entanglement measure, and derive the first general bounds to near-field radiative heat transfer.

08:00–10:00

FM1D • Coherent Phenomena in Coupled Resonator Networks
Presider: To Be Announced

FM1D.1 • 08:00 **Invited**

Solving Hard Computational Problems with Coupled Lasers, Nir Davidson¹; ¹Weizmann Inst. of Science, Israel. We present a new system of coupled lasers in a modified degenerate cavity that is used to solve difficult computational tasks.

FM1D.2 • 08:30

Mode-Dependent Coupling and Vectorial Optical Vortices in Metallic Nanolaser Arrays, Midya Parto¹, William Hayenga¹, Demetrios N. Christodoulides¹, Mercedeh Khajavikhan¹; ¹Univ. of Central Florida, CREOL, USA. We demonstrate both theoretically and experimentally that metallic nanolasers display different coupling behaviors depending on the vectorial electromagnetic modes within each nanocavity. Symmetric, antisymmetric, as well as vector-vortex lasing supermodes are observed in such structures.

Executive Ballroom
210E

Joint

08:00–10:00

JM1E • Symposium on High Average Power Ultrafast Lasers: Trends, Challenges & Applications I

JM1E.1 • 08:00 **Invited**

Recent Advances in SESAM-modelocked High-power Thin Disk Lasers, Ursula Keller¹; ¹ETH Zurich, Switzerland. Nonlinear refractive index of the intracavity air is a problem. We review how the negative phase shift achievable from cascaded nonlinearities can cancel the positive phase shift from air to support 210-W average output power.

JM1E.2 • 08:30 **Invited**

High average power ultrafast lasers: large aperture quasi-phase matched nonlinear devices, Takunori Taira^{1,2}, Hideki Ishizuki¹; ¹Inst. for Molecular Science, Japan; ²Laser-Driven Electron-Acceleration Technology Group, Japan. Large aperture (LA) quasi-phase matched (QPM) nonlinear devices have been developed for functional wavelength conversion without catastrophic damages. The LA-QPM Mg-doped LiNbO₃ and Quartz offer the artificial nonlinear short pulse lasers in high power region.

Executive Ballroom
210F

CLEO: Science & Innovations

08:00–10:00

SM1F • Optical Clocks
Presider: Andre Luiten; Univ. of Adelaide, Australia

SM1F.1 • 08:00

Measuring Optical Frequency Ratios with Uncertainties Below 10⁻¹⁷ via the Boulder Atomic Clock Network, Holly F. Leopardi^{1,2}, Kyle Beloy², Martha I. Bodine², Toby Bothwell^{3,1}, Sam Brewer², Sarah Bromley^{3,1}, Jwo-Sy Chen², Jean-Daniel Deschênes⁴, Scott A. Diddams^{2,1}, Robbie Fasano^{1,2}, Tara M. Fortier^{2,1}, David Hume², Dhruv Kedar^{3,1}, Colin Kennedy³, Isaac H. Khader^{2,1}, David Leibbrandt^{2,1}, Andrew Ludlow², Will McGrew^{1,2}, Will Milner^{3,1}, Nathan R. Newbury², Daniele Nicolodi², Eric Oelker^{3,1}, John Robinson^{3,1}, Stephan Schaffer², Jeff A. Sherman², Laura C. Sinclair², Lindsay Sonderhouse^{3,1}, William C. Swann², David Wineland², Jian Yao^{2,1}, Jun Ye^{3,2}, Xiaogang Zhang²; ¹Univ. of Colorado Boulder, USA; ²National Inst. of Standards and Technology, USA; ³JILA, USA; ⁴Octosig Consulting, Canada. We present frequency ratio measurements for ²⁷Al⁺, ¹⁷¹Yb, ⁸⁷Sr with total uncertainties at or below the level of 1x10⁻¹⁷.

SM1F.2 • 08:15

Optical frequency measurements at the 20th decimal digit, Michele Giunta^{1,2}, Wolfgang Hänsel¹, Matthias Lezius¹, Marc Fischer¹, Thomas Udem², Ronald Holzwarth^{1,2}; ¹Menlo Systems GmbH, Germany; ²Max Planck Inst. of Quantum Optics, Germany. We report on a feed-forward method for compensating phase drifts occurring in multi-branch frequency combs. Tracking the optical phase and compensating the drifts, we demonstrate comb accuracy and stability below 10⁻¹⁹ in less than 100s.

SM1F.3 • 08:30 **Invited**

Optical Atomic Clocks: From International Timekeeping to Gravity Potential Measurement, Helen Margolis¹, Heiner Denker², Christian Voigt^{2,4}, Ludger Timmen², Jacopo Grotti³, Silvio Koller³, Stefan Vogt³, Sebastian Haefner³, Uwe Sterr³, Christian Lisdat³, Antoine Rolland¹, Fred Baynes¹, Michel Zamparo⁵, Pierre Thoumany⁶, Marco Pizzocaro⁶, Benjamin Rau^{6,7}, Filippo Bregolin^{6,7}, Anna Tampellini^{6,7}, Piero Barbieri^{6,7}, Massimo Zucco⁶, Giovanni Costanzo^{6,7}, Cecilia Clivati⁶, Filippo Levi⁶, Davide Calonico⁶; ¹National Physical Lab, UK; ²Leibniz Universitaet Hannover, Germany; ³Physikalisch-Technische Bundesanstalt, Germany; ⁴GFZ German Research Centre for Geosciences, Germany; ⁵Laboratoire Souterrain de Modane, France; ⁶Istituto Nazionale di Ricerca Metrologica, Italy; ⁷Politecnico di Torino, Italy. We discuss the relation between atomic clocks and gravity from two perspectives: gravity potential measurements for optical clock comparisons and contributions to international timescales and, conversely, the measurement of gravity potential differences using optical clocks.

Executive Ballroom
210G

08:00–10:00

SM1G • Ultra-High Capacity Transmission Techniques & SDM
Presider: Ryan Scott; Keysight Laboratories, USA

SM1G.1 • 08:00 **Invited**

Recent Advances in Mode-Multiplexed Transmission over Multimode Fibers, Roland Ryf¹, Nicolas K. Fontaine¹, Steffen Wittek^{1,2}, Karthik Choutagunta^{1,3}, Mikael Mazur^{1,4}, haoshuo Chen¹, Juan Carlos Alvarado Zacarias^{1,2}; ¹Nokia Bell Labs, USA; ²CREOL, The Univ. of Central Florida, USA; ³E. L. Ginzton Lab, Stanford Univ., USA; ⁴Photonics Lab, Chalmers Univ. of Technology, Sweden. We present latest advances in multimode fibers and components for mode-multiplexed transmission. In particular we will review large mode count mode-multiplexer and characterization techniques for multimode components and provide a summary of the latest transmission results.

SM1G.2 • 08:30

Mode-Multiplexed Transmission with Crosstalk Mitigation Using Amplified Spontaneous Emission (ASE), Yetian Huang¹, Haoshuo Chen², Hanzhi Huang¹, Yingxiang Song¹, Zhengxuan Li¹, Nicolas K. Fontaine², Roland Ryf², Juan Carlos Alvarado Zacarias³, Rodrigo Amezcua Correa³, Min Wang¹; ¹Shanghai Univ., China; ²Nokia Bell Labs, USA; ³Univ. of Central Florida, USA. We employ the short coherence length property of spectrally filtered amplified spontaneous emission (ASE) noise to mitigate modal crosstalk and demonstrate mode- and wavelength-multiplexed transmission over multimode fiber using a single ASE source.

Executive Ballroom
210H

08:00–10:00

SM1H • Plasmonics for Manipulation & Sensing
Presider: Zijie Yan; Clarkson University, USA

SM1H.1 • 08:00 **Invited**

Optical Manipulation and Heating of Strongly Absorbing and Gate-Keeping Nanoparticles and Their Use in Nanomedicine, Lene Oddershede^{1,2}; ¹The Niels Bohr Inst., Denmark; ²Novo Nordisk Foundation, Denmark. We optically trap individual strongly absorbing metallic nanoparticles. Through direct experimental measurements and modeling we quantify the associated heating and demonstrate bio-medical usage, e.g., for cancer treatment, of these plasmonic and gate-keeping nanoparticles.

SM1H.2 • 08:30

Manipulating Fano coupling in the opto-thermoelectric trap, Linhan Lin¹, Xiaolei Peng¹, Yuebing Zheng¹; ¹Univ. of Texas at Austin, USA. We experimentally demonstrate the on-demand assembly of all-dielectric Fano metamolecules in the opto-thermo-electric trap with both reconfigurability and tunability.

**Meeting Room
211 A/B**
**CLEO: Applications
& Technology**

08:00–10:00

**AM11 • Photobiomodulation
Therapeutics**

Presider: Ilko K. Ilev; *U.S. Food
and Drug Administration, USA*

AM11.1 • 08:00 **Invited**

Non-linearity in Photobiomodulation Therapy Dosing - A Photoceutical Approach to a Quantum Biological Process?, Praveen Arany¹; ¹Univ. at Buffalo, USA. The startling breadth of Photobiomodulation Therapy for human health has been somewhat curbed by the inconsistencies in rigorous clinical protocols. Dose-ranging studies in labs and humans have noted the non-linear nature of its therapeutic responses that will be highlighted in this presentation.

AM11.2 • 08:30 **Invited**

Near Infrared Photoimmunotherapy for Cancer, Hisataka Kobayashi¹; ¹National Inst.s of Health, USA. Near infrared photoimmunotherapy (NIR-PIT) is a newly-developed, molecularly-targeted cancer photo-therapy based on antibody-photosensitizer conjugates. By crashing cancer cells combined with immuno-activation, NIR-PIT activates anti-cancer immunity resulted in curing local and distant metastatic cancers without recurrence.

**Meeting Room
211 C/D**
**CLEO: Science &
Innovations**

08:00–10:00

**SM1J • Beamforming &
Coupling to Free Space**

Presider: Harish Subbaraman;
Boise State Univ., USA

SM1J.1 • 08:00 **Invited**

Optical Phased Array Lidar, Michael R. Watts¹; ¹Analog Photonics, USA. Integrated optical phased arrays provide an attractive solution to LiDAR sensors by enabling solid-state, small-form-factor systems fabricated on 300mm wafers. We present recent results including high-performance beam steering and long-range LiDAR up to almost 200m.

SM1J.2 • 08:30

On-chip Wavefront Shaping with High Contrast Dielectric Metalens, Zi Wang¹, Tiantian Li¹, Anishkumar Soman¹, Tingyi Gu¹; ¹Dept. of Electrical and Computer Engineering, Univ. of Delaware, USA. Compact and lossless on-chip high-contrast transmit-array is experimentally demonstrated on a standard SOI substrate. The integrated metalens has a focal spot size of 0.38λ , transmission of 94% and focusing efficiency of 71%.

**Meeting Room
212 A/B**
**CLEO: Applications
& Technology**

08:00–10:00

**AM1K • Environmental &
Atmospheric Sensing I**

Presider: Mark Zondlo; *Princeton
University, USA*

AM1K.1 • 08:00 **Invited**

Cavity Attenuated Phase Shift (CAPS)-Based Detection of Gas Phase Species and Aerosols, Andrew Freedman¹, Timothy Onasch¹, Paul Kebarian¹, Paola Massoli^{1,2}; ¹Aerodyne Research, Inc., USA; ²MultiSensor Scientific Inc, USA. We describe the use of state-of-the-art monitors that measure both the concentration of nitrogen dioxide and the optical properties of aerosols using Cavity Attenuated Phase Shift (CAPS) techniques. Examples of how they are used in the real world include: measuring soot emissions from jet aircraft engines; determining the atmospheric mixing ratio of NO₂ as a function of altitude; and determining the single scattering albedo of ambient aerosols at both ground level and at altitude.

AM1K.2 • 08:30

Methane Leak Detection Using Chirped Laser Dispersion Spectroscopy, Yifeng Chen¹, Michael Soskind¹, James McSpirtt², Rui Wang², Nathan Li², Mark A. Zondlo², Gerard Wysocki¹; ¹Electrical Engineering, Princeton Univ., USA; ²Civil and Environmental Engineering, Princeton Univ., USA. We present a real-time chirped laser dispersion spectrometer capable of distinguishing path-averaged methane leaks 0 to 8 ppm above the ~2ppm background methane level using low reflectivity (down to 0.01%) surfaces 50 m away.

**Meeting Room
212 C/D**
**CLEO: Science &
Innovations**

08:00–10:00

**SM1L • Narrow Linewidth Fiber
Lasers**

Presider: Sze Y. Set *The University
of Tokyo, Japan*

SM1L.1 • 08:00

High-Order Mode Brillouin Fiber Lasers Based on Intra- and Inter-Modal SBS, Ning Wang¹, Juan Carlos Alvarado Zacarias¹, Md. Selim Habib¹, He Wen¹, Yuanhang Zhang¹, Jose Enrique Antonio-Lopez¹, Pierre Sillard², Adrian Amezcu-Correa², Rodrigo Amezcu-Correa¹, Guifang Li¹; ¹Univ. of Central Florida, CREOL, USA; ²Prismian Group, France. We experimentally demonstrated LP₁₁ mode Brillouin fiber lasers based on both intra- and inter-modal SBS. The OSNRs were over 65 dB, and their mode profiles were clearly observed for both cases.

SM1L.2 • 08:15

Engineering the lasing properties and dynamics of Brillouin Fiber Lasers using pump modulation, Omer Kotlicki¹, Jacob Scheuer¹; ¹Tel-Aviv Univ., Israel. We demonstrate experimentally a self-stable, bi-frequency and switchable, Brillouin fiber laser at telecom wavelengths with engineered spectral properties. The spectral control is obtained by pump modulation while dynamic switching is achieved through the pump level.

SM1L.3 • 08:30

Single-Frequency, Ultra-Narrow Linewidth Hybrid Brillouin-Thulium Fiber Laser based on In-band Pumping, Chaodu Shi¹, Shijie Fu¹, Quan Sheng¹, wei shi¹, Jianquan Yao¹; ¹Tianjin Univ., China. A hybrid Brillouin/thulium fiber laser with an ultra-narrow linewidth of 0.93 kHz was demonstrated, with the output coupling, cavity Q factor and pumping scheme optimized for the narrow linewidth.

Marriott
Salon I & IICLEO: QELS-Fundamental
Science

08:00–10:00

FM1M • Single-Photon Sources

Presider: Mirko Lobino Griffith University,
Australia

FM1M.1 • 08:00

Interfacing solid-state single-photon sources and integrated photonics circuits: high rate three-photon coalescence, Carlos Antón Solanas^{1,2}, Guillaume Coppola^{1,2}, Juan Carlos Loredó^{1,2}, Niko Viggianello³, Helene Ollivier^{1,2}, Abdelmounaim Harouri^{1,2}, Niccolò Somaschi⁴, Andrea Crespi^{5,6}, Isabelle Sagnes^{1,2}, Aristide Lemaitre^{1,2}, Loïc Lanco^{1,7}, Roberto Oselame^{5,6}, Fabio Sciarrino³, Pascale Senellart^{1,2}; ¹CNRS Center of Nanosciences and Nanotechnology, France; ²Universite Paris-Sud, Universite Paris-Saclay, France; ³Dipartimento di Fisica, Sapienza Università di Roma, Italy; ⁴Quandela, SAS, France; ⁵Consiglio Nazionale delle Ricerche Istituto di Fotonica e Nanotecnologie, Italy; ⁶Dipartimento di Fisica, Politecnico di Milano, Italy; ⁷Université Paris Diderot, France. We report the interfacing of an integrated solid-state single-photon source with an integrated, reconfigurable photonic tritter demonstrating a highly efficient quantum interference of three indistinguishable single photons.

FM1M.2 • 08:15

Quantum-dot single-photon source on a CMOS-processed silicon waveguide, Ryota Katsumi¹, Yasutomo Ota², Alto Osada², Takuto Yamaguchi¹, Takeyoshi Tajiri¹, Masahiro Kakuda², Satoshi Iwamoto^{1,2}, Yasuhiko Arakawa²; ¹Inst. of Industrial Science, Japan; ²Inst. for Nano Quantum Information Electronics, Japan. We report a quantum-dot single-photon source integrated onto a CMOS-processed silicon waveguide. The necessary hybrid integration was done in a simple pick-and-place manner with transfer printing, thus fully maintaining the compatibility with CMOS-back-end technology.

FM1M.3 • 08:30

Integration of Quantum Emitters with Lithium Niobate Photonics, Shahriar Aghaeimeibodi¹, Boris Desiatov², Je-Hyung Kim³, Chang-Min Lee¹, Mustafa Buyukkaya¹, Aziz Karasahin¹, Christopher Richardson¹, Richard Leavitt¹, Marko Loncar², Edo Waks¹; ¹Univ. of Maryland, USA; ²Harvard Univ., USA; ³Ulsan National Inst. of Science and Technology, South Korea (the Republic of). We demonstrate integration of telecom quantum dots with lithium niobate photonics using a pick-and-place technique. Second order photon correlation measurement performed with an on-chip beamsplitter confirms the single-photon nature of the emission.

Marriott
Salon III

CLEO: Science & Innovations

08:00–10:00

SM1N • Open-path Sensing & Free-electron Lasers

Presider: Erik Emmons; Edgewood Chemical
Biological Center, USA

SM1N.1 • 08:00

All-Time Single-Photon 3D Imaging Over 21 km, Zheng-Ping Li^{1,2}, Xin Huang^{1,2}, Yuan Cao^{1,2}; ¹Shanghai Branch, Hefei National Lab for Physical Sciences at Microscale and Dept. of Modern Physics, Univ. of Science and Technology of China, China; ²Synergetic Innovation Center of Quantum Information & Quantum Physics, Univ. of Science and Technology of China, China. We experimentally demonstrate active three-dimensional (3D) imaging at a range of up to 21.6 km in daylight by constructing a high-efficiency single-photon LiDAR system and developing a long-range-tailored computational algorithm.

SM1N.2 • 08:15

Sequence-Coded Coherent Laser Range Finder, Keren Shemer¹, Gil Bashan¹, Hilel H. Diamandi¹, Yosef London¹, Arik Bergman¹, Nadav Levanon², Avi Zadok¹; ¹Bar-Ilan Univ., Israel; ²Faculty of Engineering, Tel-Aviv Univ., Israel. A range finder based on an extended sequence of coded pulses is demonstrated. Coherent detection is used to measure the range of weak point reflections, with average energy of only 0.15 photons per code symbol.

SM1N.3 • 08:30

Standoff 250m Open-path Detection of Chemical Plumes Using a Broadband Swept-ECQCL, Mark C. Phillips¹, Bruce E. Bernacki¹, Sivanandan S. Harilal¹, Jeremy Yeak², R. J. Jones³; ¹Pacific Northwest National Lab, USA; ²OpticsLah, LLC, USA; ³College of Optical Sciences, Univ. of Arizona, USA. We measure chemical plumes at a 250 m standoff distance by sweeping an external cavity quantum cascade laser over a broad spectral range of 920-1220 cm⁻¹ at a rate of 200 Hz.

Marriott
Salon IV

08:00–10:00

SM1O • Van der Waals Heterostructures

Presider: Eiichi Kuramochi; NTT, Japan

SM1O.1 • 08:00 **Tutorial**

Plasmonics in Two-dimensional Crystals, Javier García de Abajo^{1,2}; ¹ICFO-The Inst. of Photonic Sciences, Spain; ²ICREA, Spain. We will discuss recent advances in the study of fundamental aspects and applications of plasmons in atomic layers of graphene, noble metals, and their combinations in 2D crystal stacks.



Javier García de Abajo is an ICREA Research Professor at ICFO (Barcelona), where he leads the Nanophotonics Theory group. He is Fellow of APS and OSA and has co-authored 370+ articles with 25,000+ citations (WoK h index 78) in the different aspects of surface science, nanophotonics, and electron microscope spectroscopies.

Executive Ballroom
210AExecutive Ballroom
210BExecutive Ballroom
210CExecutive Ballroom
210D

CLEO: QELS-Fundamental Science

FM1A • Quantum
Optomechanics &
Transduction—ContinuedFM1B • Topological Photonics
I—ContinuedFM1C • Novel Phenomena
in Classical Nano-Optics—
ContinuedFM1D • Coherent Phenomena
in Coupled Resonator
Networks—Continued

FM1A.4 • 09:00

Toward Coherent Control of Single Yb³⁺ Ions in a Nanophotonic Cavity, Jonathan Kindem¹, Andrei Ruskuc¹, John G. Bartholomew¹, Jake Rochman¹, Andrei Faraon¹; ¹California Inst. of Technology, USA. We report on detection and coherent optical driving of single Yb³⁺ ions coupled to a nanophotonic resonator fabricated in the YVO₄ host crystal and outline a path toward control of single ¹⁷¹Yb³⁺ spins.

FM1A.5 • 09:15

Toward Quantum Microwave to Optical Conversion using Rare Earth Ion Containing Crystals, Xavier Fernandez-Gonzalvo¹, Gavin G. King¹, Sebastian Horvath¹, Jonathan Everts¹, Matthew Berrington², Rose Ahlefeldt², Yu-Hui Chen¹, Jevon J. Longdell¹; ¹Dodd Walls Center, Univ. of Otago, New Zealand; ²Australian National Univ., Australia. With an Er:Y₂SiO₅ crystal at 4K we achieve microwave to optical conversion with quantum efficiency 10⁻⁵. Theory and initial results at milli-kelvin temperatures and with fully concentrated rare earth crystals point to significant improvements.

FM1A.6 • 09:30

Coherent Control of Rare-Earth Ions in On-Chip Devices for Microwave-to-Optical Transduction, John G. Bartholomew^{1,2}, Jake Rochman^{1,2}, Jonathan Kindem^{1,2}, Andrei Ruskuc^{1,2}, Ioana Craiciu^{1,2}, Mi Lei^{1,2}, Tian Zhong^{1,2}, Andrei Faraon^{1,2}; ¹Kavli Nanoscience Inst. and Thomas J. Watson, Sr., Lab of Applied Physics, California Inst. of Technology, USA; ²Inst. for Quantum Information and Matter, California Inst. of Technology, USA. Entangling microwave and optical photons is essential to harness disparate technologies for building larger scale quantum networks. We demonstrate coherent microwave-to-optical transduction using a nanobeam waveguide containing rare-earth ions in a dilution refrigerator.

FM1B.4 • 08:45

Nonlinear Imaging of Topological Edge States in Dielectric Metasurfaces, Daria Smirnova¹, Sergey S. Kruk¹, Daniel Leykam², Elizaveta V. Melik-Gaykazyan^{1,3}, Duk-yong Choi¹, Yuri S. Kivshar¹; ¹Australian National Univ., Australia; ²Inst. for Basic Science, South Korea (the Republic of); ³Lomonosov Moscow State Univ., Russia. We fabricate and characterize nonlinear metasurfaces supporting topological edge states at the nanoscale. By employing spectral-selective excitation, we visualize both bulk photonic modes and propagating topological edge states via third-harmonic imaging.

FM1B.5 • 09:00 **Tutorial**

Three-dimensional Topological Metamaterials. Biao Yang¹, Hongwei Jia¹, Qinghua Guo¹, Rui-Xing Zhang², Wenlong Gao¹, Ben Tremain³, Rongjuan Liu⁴, Lauren E Barr³, Qinghui Yan⁴, Hongchao Liu¹, Jing Chen⁵, Jing Hu¹, Yangang Bi¹, Chen Fang¹, Yuanjiang Xiang⁶, Alastair Hibbins³, Ling Lu⁴, Chaoping Liu⁷, Shuang Zhang¹; ¹Univ. of Birmingham, ²University of Maryland, ³University of Exeter, ⁴Chinese Academy of Sciences, ⁵Nankai University, ⁶Shenzhen University, ⁷Pennsylvania State University. I will discuss the realization of 3D topological metamaterials with ideal Weyl points. The photonic 'Fermi arcs' showed Riemann-surface-like helicoid configuration. Artificial magnetic field can be introduced, leading to observation of chiral zero Landau mode.



Professor Shuang Zhang is a professor in the School of Physics & Astronomy, University of Birmingham. He is the recipient of IUPAP Young Scientist Prize in Optics, the Royal Society Wolfson Research Merit Award in 2016. He was elected a Fellow of The Optical Society (OSA) in 2016.

FM1C.4 • 08:45

Experimental Observation of Generalized Snell's Law in an Interface Between Different Photonic Artificial Gauge Fields, Moshe-Ishay Cohen^{1,2}, Christina I. Jörg³, Yaakov Lumer^{1,2}, yonatan plotnik^{1,2}, Georg von Freymann^{3,4}, Mordechai Segev^{1,2}; ¹Physics Dept., Technion - Israel Inst. of Technology, Israel; ²Solid State Inst., Technion - Israel Inst. of Technology, Israel; ³Physics Dept. and Research Center OPTIMAS, TU Kaiserslautern, Germany; ⁴Fraunhofer Inst. for Industrial Mathematics ITWM, Germany. We formulate and experimentally demonstrate generalized laws of refraction and reflection from an interface between two domains with different artificial gauge field.

FM1C.5 • 09:00 **Invited**

Mesoscopic Correlations and Information in Speckles Emerging from Opaque Scattering Media, Remi Carminati¹, Nikos Fayard², Romain Pierrat^{1,3}, Arthur Goetschy¹, Jacopo Bertolotti⁴, Alba Paniagua-Diaz¹, Ilya Starshinov⁴; ¹ESPCI Paris, France; ²ICFO, Spain; ³CNRS, France; ⁴Univ. of Exeter, UK. We demonstrate the existence of mutual information between the speckle patterns generated on both sides of an opaque scattering medium. This opens up new possibilities for the control of light propagation through complex media.

FM1C.6 • 09:30

Experimental study of non-orthogonal modes in tight-binding lattices, Lukas Maczewsky¹, Steffen Weimann¹, Mark Kremer¹, Matthias Heinrich¹, Alexander Szameit¹; ¹Inst. of Physics, Univ. of Rostock, Germany. The non-orthogonality of modes is often neglected yet indispensable for an exact description of the dynamics in tight-binding lattices. We devise a compact arrangement to quantify these additional coupling parameters and observe their influence.

FM1D.3 • 08:45

Self-locked Adiabatic Lasers Solve a Global Optimization Problem, Marco Piccardo¹, Paul Chevalier¹, Benedikt Schwarz², Dmitry Kazakov¹, Yongrui Wang³, Alexey Belyanin³, Federico Capasso¹; ¹Harvard Univ., USA; ²TU Wien, Austria; ³Texas A&M, USA. Laser self-locking is a complex, nonlinear phenomenon. We find that in adiabatic frequency combs this can be simply described as a power optimization problem, which the laser can solve for a large number of modes.

FM1D.4 • 09:00

Sub-Harmonic Synchronization of Kerr Frequency Combs, Jae K. Jang¹, Xingchen Ji^{1,2}, Chaitanya Joshi^{1,2}, Yoshitomo Okawachi¹, Michal Lipson¹, Alexander L. Gaeta¹; ¹Columbia Univ., USA; ²Cornell Univ., USA. We experimentally demonstrate sub-harmonic synchronization of separated soliton-modelocked Kerr frequency combs. Through passive optical coupling between microresonators, we demonstrate entrainments between combs with mode spacings related by integer factors of 2 and 3.

FM1D.5 • 09:30

Nonlinear Interactions in Linearly Uncoupled Resonators, Matteo Menotti², Blair Morrison², Kang Tan², Zachary Vernon², John E. Sipe³, Marco Liscidini¹; ¹Università degli Studi di Pavia, Italy; ²Xanadu Quantum Technologies, Canada; ³Univ. of Toronto, Canada. We demonstrate a system composed of two resonators that are coupled solely through a third-order nonlinear interaction. We show that such a structure has significant advantages in controlling classical and quantum nonlinear interactions in integrated photonics.

Joint

JM1E • Symposium on High Average Power Ultrafast Lasers: Trends, Challenges & Applications I—Continued

JM1E.3 • 09:00

High Average Power 106 W, 1.75 μm , 100 kHz Optical Parametric Chirped Pulse Amplifier, Matthew Windeler^{1,2}, Katalin Mecseki¹, Joseph Robinson¹, James M. Fraser², Alan Fry¹, Franz Tavella¹; ¹SLAC National Accelerator Lab, USA; ²Dept. of Physics, Astronomy and Engineering Physics, Queen's Univ., Canada. We explore average power scaling of OPCPA in KTA at signal center wavelengths spanning 1.5–2.0 μm . At maximum, the OPCPA produced 106 W, centered at 1.75 μm with a repetition rate of 100 kHz.

JM1E.4 • 09:15 **Invited**

Nonlinear pulse compression at high average power based on multi-pass cells, Johannes Weitenberg^{2,1}, Jan Schulte², Thomas Sartorius², Akira Ozawa¹, Thomas Udem¹, Hans-Dieter Hoffmann², Peter Russbuehler², Theodor W. Hänsch¹, Reinhart Poprawe²; ¹Laser Spectroscopy, Max-Planck Inst. of Quantum Optics MPQ, Germany; ²Lasers and Laser Optics, Fraunhofer Inst. for Laser Technology ILT, Germany. We report on the development and recent advances of a nonlinear pulse compression scheme based on multi-pass cells, which is applicable to a large range of pulse energies, highly efficient and power scalable.

SM1F • Optical Clocks—Continued

SM1F.4 • 09:00 **Invited**

Ultra-stable Optical Atomic Clocks for Geodesy, Tanja Mehlstaebler¹; ¹Physikalisch-Tech Bundesanstalt (PTB), Germany. The dependence of atomic frequencies on the gravitational potential makes atomic clocks interesting candidates for new gravity field sensors, delivering long-term height references for geodetic measurements and for the modelling and understanding of our Earth.

SM1F.5 • 09:30

Optical clocks via breather stabilization in chip-scale frequency combs, Abhinav Vinod¹, Shu-Wei Huang², Jinghui Yang¹, Mingbin Yu³, Dim Lee Kwong³, Chee Wei Wong¹; ¹Univ. of California Los Angeles, USA; ²ECE, Univ. Of Colorado, Boulder, USA; ³Inst. of Microelectronics, Singapore. Here we report a novel method to generate low noise microwaves via a chip-scale frequency comb and demonstrate noise suppression of the carrier frequency below the microwaves stabilization limit achieved.

CLEO: Science & Innovations

SM1G • Ultra-High Capacity Transmission Techniques & SDM—Continued

SM1G.3 • 08:45

112 Gb/s CAP-based Data Transmission over 100 m MMF Links using an Artificial Neural Network Equalizer, Xiaohe Dong¹, Nikos Bamiedakis¹, David G. Cunningham¹, Richard V. Penty¹, Ian H. White¹; ¹Univ. of Cambridge, UK. A novel artificial neural network equalizer for use in short-reach optical links is proposed. 112Gb/s and 56Gb/s CAP-16 data transmission are demonstrated by simulation and experiment respectively with receiver sensitivities of -4 and -7 dBm.

SM1G.4 • 09:00 **Invited**

Meeting Capacity Demand in Undersea Fiber Optic Communication Systems., Alexei N. Pilipetskii¹; ¹SubCom, USA. The capacity demand for future undersea cable networks will push the industry to the cable transmission capacity in excess of hundreds of Tb/s. The new technologies and approaches to address capacity demand will be reviewed.

SM1H • Plasmonics for Manipulation & Sensing—Continued

SM1H.3 • 08:45

Surface-enhanced Raman Spectroscopy of Graphene Integrated in Three-dimensional Nanostructured Plasmonic Silicon Platforms, Maria Kandyla¹, Maria Kanidi¹, Alva Dagkli², Nikolaos Kelaidis³, Dimitris Palles¹, Sigjava Ainalragia-Giamini³, Jose Marquez-Velasco³, Allan Colli⁴, Athanasios Dimoulas³, Eleftherios Lidorikis², Efstratios Kamitsos¹; ¹National Hellenic Research Foundation, Greece; ²Univ. of Ioannina, Greece; ³NCSR 'Demokritos', Greece; ⁴Univ. of Cambridge, UK. We integrate graphene with 3D plasmonic laser-nanostructured silicon substrates for SERS and we observe broadband 10^3 Raman enhancement. FDTD numerical simulations elucidate the advantages of the substrate topography and the flexibility of 2D materials.

SM1H.4 • 09:00

Polarization-Dependent Optical Binding of Plasmonic Nanoparticles, Fei Han¹, Fan Nan¹, Zijie Yan¹; ¹Clarkson Univ., USA. Plasmonic metal nanoparticles can self-assemble into anisotropic chains in a linearly polarized optical field and ordered hexagonal arrays in a circularly polarized optical field. Negative optical torque can be observed in the arrays.

SM1H.5 • 09:30

Lithography-free hybrid Ag–Au super absorbing metasurfaces for additive drug sensing, Nan Zhang¹, Dengxin Ji¹, Haomin Song¹, Youhai Liu¹, Lyu Zhou¹, Lorraine Collins¹, Qiaoqiang Gan¹; ¹State Univ. of New York at Buffalo, USA. We demonstrate a lithography-free super absorbing metasurface consisting of hybrid Ag–Au nanoantennas with sub-20-nm nanogaps for surface enhanced Raman spectroscopy sensing to tackle the emerging drug-abuse challenge.

Meeting Room
211 A/BCLEO: Applications
& TechnologyAM11 • Photobiomodulation
Therapeutics—Continued

AM11.3 • 09:00

Label-Free Quantitative Classification of Cancer Cells Measured by Interferometric Phase Microscopy, Natan T. Shaked¹; ¹Tel-Aviv Univ., Israel. I will present our latest advances in label-free quantitative imaging flow cytometry for cancer cell classification using external and portable interferometric modules, where the metastatic potential of the cells is detected.

AM11.4 • 09:15

Cell deformation and assessment with tunable "tug-of-war" optical tweezers, Yi Liang^{1,2}, Yinxiao Xiang^{1,3}, Josh Lasmstein¹, Anna Bezryadina^{1,4}, Zhigang Chen^{1,3}; ¹Dept. of Physics and Astronomy, San Francisco State Univ., USA; ²Guangxi Key Lab for Relativistic Astrophysics, Guangxi Colleges and Universities Key Lab of Novel Energy Materials and Related Technology, School of Physical Science and Technology, Guangxi Univ., China; ³MOE Key Lab of Weak-Light Nonlinear Photonics, TEDA Applied Physics Inst. and School of Physics, Nankai Univ., China; ⁴Dept. of Physics and Astronomy, Dept. of Physics and Astronomy, USA. We assess red-blood-cell (RBC) deformability under different osmotic conditions by employing novel "tug-of-war" optical tweezers. Such a photonic tool enables stable trapping and stretching of single RBCs, attaining over 15% of cell deformation.

AM11.5 • 09:30

Simultaneous Two- and Three-photon Imaging of Multilayer Neural Activities with Remote Focusing, Aaron Mok¹, Tianyu Wang¹, Fei Xia¹, Chunyan Wu¹, Chris Xu¹; ¹Applied Engineering and Physics, Cornell Univ., USA. We present a novel remote focusing and demultiplexing scheme that allows simultaneous two- and three-photon imaging of two-layer neural activities, featuring large axial separation, independent foci tunability and large imaging depth enabled by three-photon microscopy.

Meeting Room
211 C/DCLEO: Science &
InnovationsSM1J • Beamforming &
Coupling to Free Space—
Continued

SM1J.3 • 08:45

Achromatic Subwavelength Grating Lens at Visible Bandwidths, Mao Ye¹, Ray Vishva¹, Ya Sha Yi¹; ¹Univ. of Michigan, USA. The polarization insensitive achromatic micro lens covering the whole visible wavelength is demonstrated that can cover 250 nm of visible bandwidths (from 435 nm to 685 nm) with focal shift less than 5%.

SM1J.4 • 09:00

Optical spatial differentiator based on subwavelength high-contrast gratings, Weiji Yang¹, Zhewei Dong¹, Jiangnan Si¹, Xuanyi Yu¹, Xiaoxu Deng¹; ¹Shanghai Jiaotong Univ., China. Based on subwavelength high-contrast gratings (HCGs), a transmissive optical spatial differentiator without Fourier lens is proposed experimentally, which achieves edge detections of images and provides applications in optical computing systems and parallel data processing.

SM1J.5 • 09:15

Using an Integrated Silicon Emitter to Generate Two Coaxial Orbital-Angular-Momentum Beams with Tunable Mode Orders and Broad Bandwidth, Hao Song¹, Zhe Zhao¹, Runzhou Zhang¹, Jing Du¹, Haoqian Song¹, Long Li¹, Kai Pang¹, Cong Liu¹, Ahmed Almainan¹, Robert Bock², Moshe Tur³, Alan E. Willner¹; ¹Univ. of Southern California, USA; ²R-DEX System, Inc., USA; ³Tel Aviv Univ., Israel. We design and simulate a broadband integrated silicon emitter to generate two coaxial orbital-angular-momentum beams with tunable mode orders ($l = \{-1, 0\}$ or $\{0, +1\}$). Crosstalk < -15 dB is achieved over 1500–1600 nm.

SM1J.6 • 09:30

Achieving Off-Axis Holographic Projections with Uniform Illumination by 3D Printing Blazed Facets on Phase Elements, Hao Wang¹, Yejing Liu¹, Qifeng Ruan¹, Hailong Liu¹, Ray J.H. Ng^{1,2}, You Sin Tan¹, Joel K. W. Yang^{1,2}; ¹EPD, Singapore Univ. of Technology and Design, Singapore; ²Inst. of Materials Research and Engineering, A*STAR (Agency for Science, Technology and Research), Singapore. A new design of diffractive optical elements with blazed facets is fabricated using 3D printing to obtain off-axis holograms with uniform illumination. Experimental holograms without zero order spot are achieved, fit well with diffraction theory.

Meeting Room
212 A/BCLEO: Applications
& TechnologyAM1K • Environmental &
Atmospheric Sensing I—
Continued

AM1K.3 • 08:45

Mid-IR Laser Spectrometer for Balloon-borne Lower Stratospheric Water Vapor Measurements, Manuel Graf^{1,2}, Philipp Scheidegger¹, Herbert Looser¹, Badrudin Stanicki¹, Thomas Peter², Lukas Emmenegger¹, Béla Tuzson¹; ¹Empa, Switzerland; ²IAC, ETH, Switzerland. A lightweight instrument has been developed to measure water vapor up to the lower stratosphere aboard meteorological balloons. The sensor relies on a segmented circular multipass cell which is especially suited for mobile field applications.

AM1K.4 • 09:00

Imaging Technique for In Situ Cloud Characterization, Andrei B. Vakhtin¹, Lev N. Krasnoperov²; ¹Mesa Photonics, LLC, USA; ²New Jersey Inst. of Technology, USA. An imaging technique for in situ characterization of droplets in atmospheric clouds based on analysis of scattered light from droplets illuminated by a pulsed spectrally broadband light source is presented.

AM1K.5 • 09:15 **Invited**

Development of a Compact CO₂ Instrument for Small Aerial Platform, Anthony Gomez¹, Joel A. Silver¹; ¹Southwest Sciences Inc, USA. High accuracy CO₂ instrumentation for airborne platforms would bridge the gap between land and satellite measurements. Here we present ongoing work on a novel temperature and pressure compensated sensor for measuring dry-air corrected CO₂ concentrations.

Meeting Room
212 C/DCLEO: Science &
InnovationsSM1L • Narrow Linewidth Fiber
Lasers—Continued

SM1L.4 • 08:45

Direct Frequency Locking of a Diode Laser to a Meter-Long High-Finesse Fiber Fabry-Perot Cavity, Nabil Md Rakinul Hoque¹, Lingze Duan¹; ¹Univ. of Alabama in Huntsville, USA. We report the demonstration of directly locking the frequency of a diode laser to a meter-long, high-finesse (~1000) fiber Fabry-Perot cavity. This work can serve as a key step toward ultra-sensitive infrasonic strain sensors.

SM1L.5 • 09:00

Rapid and Continuously Tunable Narrow Linewidth Fiber Source Based on a SOA and a Linearly Chirped Fiber Bragg Grating, Xiong Yang^{1,2}, Robert Lindberg³, Walter Margulis^{1,3}, Krister Fröjdh⁴, Fredrik Laurell¹; ¹Applied Physics, Royal Inst. of Technology (KTH), Sweden; ²College of Optical Science and Engineering, Zhejiang Univ., China; ³Fiber Optics, RISE Acreo, Sweden; ⁴Proximion AB, Sweden. We demonstrate a tunable narrow-linewidth laser based on a semiconductor optical amplifier and a linearly chirped FBG. High tuning resolution and small power variation over 40 nm tuning range were achieved by optimizing the drive current.

SM1L.6 • 09:15

Longitudinal Modes in Random Feedback Fiber Lasers, Pedro Tovar¹, Luis Y. Herrera¹, Guilherme P. Temporão¹, Jean Pierre von der Weid¹; ¹PUC-Rio, Brazil. An SOA-based random fiber laser is experimentally demonstrated with multimode operation dominant for high SOA currents. Single mode prevails only near the threshold current. Mode lifetime of ~1 ns and 6 kHz linewidth were measured.

CLEO: QELS-Fundamental
Science

FM1M • Single-Photon Sources—Continued

FM1M.4 • 08:45

Coherent Coupling of Single Molecules to a Chip-Based Optical Circuit, Dominik Rattenbacher¹, Alexey Shkarin¹, Jan Renger¹, Tobias Utikal¹, Stephan Götzinger^{2,1}, Vahid Sandoghdar^{1,2}, ¹Max Planck Inst. for the Science of Light, Germany; ²Friedrich-Alexander Univ. Erlangen-Nürnberg, Germany. We present the coherent coupling of single dye molecules to subwavelength waveguides (nanoguides) and microresonators made of TiO₂ on a chip. Integrated electrodes allow us to tune several molecules into resonance via the Stark effect.

FM1M.5 • 09:00

Controlled Assembly of an Ultrafast Single-Photon Source, Oksana Makarova¹, Simeon Bogdanov¹, xiaohui xu¹, Deesha Shah¹, Alexander Baburin², Ilya Ryzhikov², Soham Saha¹, Ilya Rodionov², Alexander Kildishev¹, Alexandra Boltasseva¹, Vladimir M. Shalaev¹, ¹Purdue Univ., USA; ²FMNS REC, Bauman Moscow State Technical Univ., Russia. We demonstrate a technique for highly controllable assembly of single-photon sources coupled to plasmonic nanoantennas with optimal emitter positioning on the nanoscale, resulting in fluorescence decay rates beyond 10 GHz in single nitrogen-vacancy centers.

FM1M.6 • 09:15

Spin Coherence in Single NV Centers Coupled to Controlably Assembled Nanopatch Antennas, Simeon Bogdanov¹, Oksana Makarova¹, Alexei Lagutchev¹, Deesha Shah¹, Chin-Cheng Chiang¹, Alexander Baburin^{2,3}, Ilya Ryzhikov^{2,4}, Soham Saha¹, Ilya Rodionov^{2,3}, Alexandra Boltasseva¹, Vladimir M. Shalaev¹, ¹Purdue Univ., USA; ²FMNS REC, Bauman Moscow State Technical Univ., Russia; ³Dukhov Research Inst. of Automatics, Russia; ⁴Inst. for Theoretical and Applied Electromagnetics, Russian Academy of Sciences, Russia. We transfer a pre-characterized nanodiamond with a single nitrogen-vacancy (NV) center onto an epitaxial silver substrate and deterministically couple it to a nanopatch antenna. The NV retains its coherent spin dynamics in this process.

FM1M.7 • 09:30

Tailoring nanophotonic frequency converters for quantum dots single-photon sources, Anshuman Singh^{1,2}, Qing Li³, Shunfa Liu⁴, Ying Yu⁴, Christian Schneider⁵, Sven Höfling^{5,6}, John Lawall¹, Varun B. Verma⁷, Richard P. Mirin⁷, Sae Woo Nam⁷, Jin Liu⁴, Kartik Srinivasan¹, ¹Physical Measurement Lab, National Inst. of Standards and Technology, USA; ²Maryland NanoCenter, Univ. of Maryland, College Park, USA; ³Electrical and Computer Engineering, Carnegie Mellon Univ., USA; ⁴School of Electronics and Information Technology, Sun-Yat Sen Univ., China; ⁵Technische Physik, Univ. of Würzburg, Germany; ⁶School of Physics and Astronomy, Univ. of St Andrews, UK; ⁷Physical Measurement Lab, National Inst. of Standards and Technology, USA. We demonstrate the suitability of silicon nanophotonic frequency converters for use with quantum dot single-photon sources. Preservation of photon statistics, operation across an 840-980 nm input wavelength band, and tunable wavelength shifts are shown.

CLEO: Science & Innovations

SM1N • Open-path Sensing & Free-electron
Lasers—Continued

SM1N.4 • 08:45

Nyquist-Limited Efficient Fourier-Transform Spectroscopy, Kazuki Hashimoto^{1,2}, Takuro Ideguchi^{1,3}, ¹Dept. of Physics, The Univ. of Tokyo, Japan; ²Aeronautical Technology Directorate, Japan Aerospace Exploration Agency, Japan; ³PRESTO, Japan Science and Technology Agency, Japan. We demonstrate Nyquist-limited efficient Fourier-transform spectroscopy running at a high-scan rate of over 12 kHz with a spectral resolution of 11.5 GHz and a spectral bandwidth of over 1.5 THz.

SM1N.5 • 09:00

Experimental Demonstration of Enhanced Accuracy of Beam Radial Displacement and Azimuthal Rotation Measurements using Enhanced Gradient of a Beam Composed of Multiple Orbital-Angular-Momentum Modes, Jing Du¹, Zhe Zhao¹, Guodong Xie¹, Runzhou Zhang¹, Long Li¹, Haoqian Song¹, Kai Pang¹, Cong Liu¹, Hao Song¹, Moshe Tur², Shlomo Zach², Nadav Cohen², Alan E. Willner¹, ¹USC, USA; ²Tel Aviv Univ., Israel. We experimentally demonstrate beam radial displacement and azimuthal rotation angle measurements using the intensity gradient of multiple OAM modes. Compared with a Gaussian beam or a beam carrying two opposite OAM modes, using multiple OAM modes can improve the measurement accuracy.

SM1N.6 • 09:15

A Compact, Low Loss Integrated Continuous-Time Electro-Optic-PLL with Maximum Range of >3.3m, Sohail Ahasan¹, Ali Binaie¹, Christopher T. Phare¹, Michal Lipson¹, Harish Krishnaswamy¹, ¹Columbia Univ., USA. We present a Continuous Time ElectroOptic PLL which not only breaks the fundamental trade-off between chirp bandwidth and Mach Zender Interferometer (MZI) delay but also completely eliminates spurs from the PLL and laser output by using IQ single-sideband (SSB) and harmonic reject (HR) mixing.

SM1N.7 • 09:30

Invited

Microscale Magnetic Devices for Ultra-Compact Free Electron Lasers, Robert Candler^{1,2}, ¹Electrical and Computer Engineering, Univ. of California, Los Angeles, USA; ²California NanoSystems Inst., USA. We will discuss efforts toward extreme miniaturization of free electron layers through batch-fabrication of electromagnets that are used to create miniature electron beam optical components, such as quadrupoles and undulators.

SM1O • Van der Waals Heterostructures—
Continued

SM1O.2 • 09:00

Near ultraviolet light emission in hexagonal boron nitride based van der Waals heterostructures, Sanghoon Chae¹, Dongjea Seo², Qingrui Cao¹, Xiang Hua¹, En-Min Shih¹, Takashi Taniguchi³, Kenji Watanabe³, Junyoung Kwon², Gwan-Hyoung Lee², Cory R. Dean¹, David Schimovich¹, Irving P. Herman¹, Heon-jin Choi², Ioannis Kymissis¹, Young Duck Kim⁴, James Hone¹, ¹Columbia Univ., USA; ²Dept. of Materials Science and Engineering, Yonsei Univ., South Korea (the Republic of); ³National Inst. for Materials Science, Japan; ⁴Dept. of Physics, Kyung Hee Univ., South Korea (the Republic of). We demonstrate light emitting devices consisting of graphene layers separated and by thin hexagonal boron nitride (hBN) with additional hBN encapsulation. At high bias through two graphene layer, thin hBN produce near ultraviolet (NUV) light emission at 394 nm.

SM1O.3 • 09:15

A low-power optoelectronic memory device based on MoS₂/BN/graphene heterostructure, Hongzhu Jiang¹, Shuchao Qin¹, Anran Wang¹, Frank (Fengqiu) Wang¹, ¹Nanjing Univ., China. A low-power optoelectronic memory device is demonstrated by charge trapping in a MoS₂/BN/graphene heterostructure. The miniaturized structure, large current switching ratio (~6×10³) and fast read/write speed (50 ms) suggest its potential in integrated non-volatile storage cell.

SM1O.4 • 09:30

Localized Bright Luminescence of Indirect Excitons and Trions in a Type II Van der Waals Heterostructure, Erica Calman¹, Lewis Fowler-Gerace¹, Leonid Butov¹, Dmitri Nikonov², Ian Young², Sheng Hu³, Artem Mishchenko³, Andrei Geim³, ¹Univ. of California, San Diego, USA; ²Intel Corporation, USA; ³Univ. of Manchester, UK. We observe order of magnitude intensity enhancement and narrow, 4 meV, linewidth of luminescence of indirect (interlayer) neutral and charged excitons in localized spot in MoSe₂/WSe₂ heterostructure. The indirect trion binding energy is 26 meV.

Executive Ballroom
210AExecutive Ballroom
210BExecutive Ballroom
210CExecutive Ballroom
210D

CLEO: QELS-Fundamental Science

FM1A • Quantum
Optomechanics &
Transduction—ContinuedFM1B • Topological Photonics
I—ContinuedFM1C • Novel Phenomena
in Classical Nano-Optics—
ContinuedFM1D • Coherent Phenomena
in Coupled Resonator
Networks—Continued

FM1A.7 • 09:45

Toward Microwave-to-Optical Conversion using Erbium Doped Crystals and Integrated Resonators, Jake Rochman¹, John Bartholomew¹, Ioana Craiciu¹, Chuting Wang¹, Tian Xie¹, Jonathan Kindem¹, Keith Schwab¹, Andrei Faraon¹; ¹Caltech, USA. We present progress towards a bidirectional coherent microwave-to-optical photon converter using an ensemble of rare-earth ions coupled to integrated photonic and microwave resonators.

FM1C.7 • 09:45

Absence of frequency ranges of unidirectional propagation in nonreciprocal plasmonics, Siddharth Buddhiraju¹, Yu Shi¹, Alex Song¹, Casey Wojcik¹, Momchil Minkov¹, Ian Williamson¹, Avik Dutt¹, Shanhui Fan¹; ¹Stanford Univ., USA. Surface plasmon-polaritons at a metal-dielectric interface are believed to support a unidirectional frequency range under a magnetic field, where a violation of the time-bandwidth constraint is possible. We show that such unidirectionality is nonphysical.

FM1D.6 • 09:45

Coupled Degenerate Parametric Oscillators Towards Photonic Coherent Ising Machine, Yoshitomo Okawachi¹, Mengjie Yu^{1,2}, Xingchen Ji^{1,2}, Jae K. Jang¹, Michal Lipson¹, Alexander Gaeta¹; ¹Columbia Univ., USA; ²Cornell Univ., USA. We demonstrate on-chip coupling between degenerate parametric oscillators (OPOs) in two different silicon nitride microresonators. The system offers potential towards creating a network of OPOs for the realization of a photonic coherent Ising machine.

08:30–12:30 SC270: High Power Fiber Lasers and Amplifiers (W. Andrew Clarkson, Optoelectronics Research Center, University of Southampton, UK)

SC352: Introduction to Ultrafast Pulse Shaping - Principles and Applications (Marcos Dantus, Michigan State University, USA)

SC361: Coherent Mid-IR Light: Generation and Applications (Konstantin Vodopyanov, The College of Optics & Photonics, University of Central Florida, USA)

SC477: Laser Radar and Remote Sensing: An Application-oriented Introduction (Fabio Di Teodoro, Raytheon, USA)

SC481: Fundamentals and Applications of VCSELs (Kent Choquette, University of Illinois, USA)

10:00–10:30 Coffee Break, Concourse Level

11:00–12:00 OSA Presentation Feedback Program, University Room, Hilton San Jose

11:00–12:00 Navigate Your Leadership Trajectory for Senior Leaders, Salon VI, San Jose Marriott

Executive Ballroom
210E

Executive Ballroom
210F

Executive Ballroom
210G

Executive Ballroom
210H

Joint

CLEO: Science & Innovations

JM1E • Symposium on High Average Power Ultrafast Lasers: Trends, Challenges & Applications I—Continued

JM1E.5 • 09:45

Compact, high-efficiency, ultrafast 2-cycles sources at 1030nm, Florent Guichard¹, Loïc Lavenu¹, Michele Natile¹, Xavier Delen², Yoann Zaouter¹, Marc Hanna², Patrick Georges²; ¹Amplitude Laser Group, France; ²Laboratoire Charles Fabry, France. We present a dual-stage nonlinear compression scheme generating 6.8fs pulses, with a transmission of 61%. The system's compactness, stability, and average power makes it ideally suited to drive high photon flux XUV sources through HHG.

SM1F • Optical Clocks—Continued

SM1F.6 • 09:45

Absolute frequency measurement of molecular iodine hyperfine transition at 534 nm with a femtosecond optical comb, Feihu Cheng¹, Ke Deng¹, Kui Liu¹, Hongli Liu¹, Jie Zhang¹, Zehuang Lu¹; ¹School of Physics, Huazhong Univ. of Science and Technology, China. We report absolute frequency measurements of the a_2 component of the rovibrational transition of molecular iodine R(53) 31-0 transitions at 534 nm by modulation transfer spectroscopy with an optical frequency comb.

SM1G • Ultra-High Capacity Transmission Techniques & SDM—Continued

SM1H • Plasmonics for Manipulation & Sensing—Continued

SM1H.6 • 09:45

High Color Conversion Efficiency for Monolayer WSe₂ Using Plasmonic Metasurface, Cheng-Yuan Chen¹, Chen-An Lin¹, Hsiang-Ting Lin², Chiao-Yun Chang², Hao-Chung Kuo¹, Min-Hsiung Shih^{1,2}; ¹National Chiao Tung Univ., Taiwan; ²Academia Sinica, Taiwan. Color conversion is a potential answer to enhancing the spontaneous emission of transition metal dichalcogenide (TMDC) atomic layer. Therefore, our experiment utilized silver nanodisk to manipulate the color conversion effect between WSe₂ and quantum dots.

08:30–12:30 SC270: High Power Fiber Lasers and Amplifiers (W. Andrew Clarkson, Optoelectronics Research Center, University of Southampton, UK)

SC352: Introduction to UltrafastPulse Shaping - Principles and Applications (Marcos Dantus, Michigan State University, USA)

SC361: Coherent Mid-IR Light: Generation and Applications (Konstantin Vodopyanov, The College of Optics & Photonics, University of Central Florida, USA)

SC477: Laser Radar and Remote Sensing: An Application-oriented Introduction (Fabio Di Teodoro, Raytheon, USA)

SC481: Fundamentals and Applications of VCSELs (Kent Choquette, University of Illinois, USA)

10:00–10:30 Coffee Break, Concourse Level

11:00–12:00 OSA Presentation Feedback Program, University Room, Hilton San Jose

11:00–12:00 Navigate Your Leadership Trajectory for Senior Leaders, Salon VI, San Jose Marriott

**Meeting Room
211 A/B**

**CLEO: Applications
& Technology**

**AM11 • Photobiomodulation
Therapeutics—Continued**

AM11.6 • 09:45

Laser versus radiofrequency catheter ablation of myocardium, Karina S. Litvinova¹, Maria Chernysheva^{5,2}, Igor Kudelin⁵, Sergei Khalimanenko⁴, Francisco Leyva^{1,3}; ¹Aston Medical Research Inst., Aston Univ., UK; ²Leibniz Inst. of Photonic Technology, Germany; ³Queen Elisabeth Hospital, UK; ⁴First Moscow State Medical Univ. (Sechenov Univ.), Russia; ⁵Aston Inst. of Photonic Technologies, Aston Univ., UK. Cardiac ablation is a procedure for heart rhythm problems correction. Laser can create controlled irreversible myocardial lesions without crater formation. We confirmed laser produced similar lesions as RF, without undesirable effects on the ventricular walls.

**Meeting Room
211 C/D**

**CLEO: Science &
Innovations**

**SM1J • Beamforming &
Coupling to Free Space—
Continued**

SM1J.7 • 09:45

One-chip Integrated Near-field Thermophotovoltaic Devices Using Intermediate Transparent Substrates, Takuya Inoue¹, Takaaki Koyama², Dongyeon D. Kang², Takashi Asano², Susumu Noda^{1,2}; ¹Photonics and Electronics Science and Engineering Center, Kyoto Univ., Japan; ²Dept. of Electronic Science and Engineering, Kyoto Univ., Japan. We develop one-chip near-field thermophotovoltaic devices, where thin-film thermal emitters (>1000K) and solar cells are integrated to the top and bottom of intermediate substrates with a sub-wavelength gap (<150nm), realizing 10-fold enhancement in the photocurrent.

**Meeting Room
212 A/B**

**CLEO: Applications
& Technology**

**AM1K • Environmental &
Atmospheric Sensing I—
Continued**

AM1K.6 • 09:45

Multi-Species Environmental Gas Sensing Using Drone-Based Fourier-Transform Infrared Spectroscopy, Marius Rutkauskas¹, Martin Asenov², Subramanian Ramamoorthy², Deryck Reid¹; ¹Heriot-Watt Univ., UK; ²Informatics Forum, Univ. of Edinburgh, UK. We report a broadband FTIR spectrometer integrated with an autonomous UAV enabling quantitative aerial surveys of multiple gas species simultaneously with a demonstrated sensitivity of 37 ppm and an estimated noise-limited performance of 18 ppm.

**Meeting Room
212 C/D**

**CLEO: Science &
Innovations**

**SM1L • Narrow Linewidth Fiber
Lasers—Continued**

08:30–12:30 SC270: High Power Fiber Lasers and Amplifiers (W. Andrew Clarkson, Optoelectronics Research Center, University of Southampton, UK)

SC352: Introduction to Ultrafast Pulse Shaping - Principles and Applications (Marcos Dantus, Michigan State University, USA)

SC361: Coherent Mid-IR Light: Generation and Applications (Konstantin Vodopyanov, The College of Optics & Photonics, University of Central Florida, USA)

SC477: Laser Radar and Remote Sensing: An Application-oriented Introduction (Fabio Di Teodoro, Raytheon, USA)

SC481: Fundamentals and Applications of VCSELs (Kent Choquette, University of Illinois, USA)

10:00–10:30 Coffee Break, Concourse Level

11:00–12:00 OSA Presentation Feedback Program, University Room, Hilton San Jose

11:00–12:00 Navigate Your Leadership Trajectory for Senior Leaders, Salon VI, San Jose Marriott

**CLEO: QELS-Fundamental
Science**

FM1M • Single-Photon Sources—Continued

CLEO: Science & Innovations

SM1N • Open-path Sensing & Free-electron
Lasers—Continued

SM1O • Van der Waals Heterostructures—
Continued

SM1O.5 • 09:45

Deeply-submicron confocal photoluminescence spectroscopy and edge recombination in WS_2 - WSe_2 lateral heterostructure monolayer crystals, Jin ho Kang¹, Abhinav Kumar Vinod¹, Jiahui Huang¹, Zhangji Zhao¹, Peng Chen³, Laurent Bentolila², Xiangfeng Duan⁴, Chee Wei Wong¹; ¹Electrical and Computer Engineering, Univ. of California, Los Angeles, USA; ²California NanoSystems Inst., Univ. of California, Los Angeles, USA; ³Material and Science Engineering, Univ. of California, Los Angeles, USA; ⁴Chemistry and Biochemistry, Univ. of California, Los Angeles, USA. We conducted confocal micro-photoluminescence spectroscopy to scan a WS_2 - WSe_2 lateral heterostructure sample using oil emerged microscopy method. We observed enhanced PL lines at the edges of WSe_2 and spatially enhanced PL at tip of the v-shaped areas.

08:30–12:30 **SC270: High Power Fiber Lasers and Amplifiers** (W. Andrew Clarkson, Optoelectronics Research Center, University of Southampton, UK)

SC352: Introduction to UltrafastPulse Shaping - Principles and Applications (Marcos Dantus, Michigan State University, USA)

SC361: Coherent Mid-IR Light: Generation and Applications (Konstantin Vodopyanov, The College of Optics & Photonics, University of Central Florida, USA)

SC477: Laser Radar and Remote Sensing: An Application-oriented Introduction (Fabio Di Teodoro, Raytheon, USA)

SC481: Fundamentals and Applications of VCSELs (Kent Choquette, University of Illinois, USA)

10:00–10:30 **Coffee Break, Concourse Level**

11:00–12:00 **OSA Presentation Feedback Program, University Room, Hilton San Jose**

11:00–12:00 **Navigate Your Leadership Trajectory for Senior Leaders, Salon VI, San Jose Marriott**

Executive Ballroom
210A

CLEO: QELS-
Fundamental Science

10:30–12:30

FM2A • Quantum Optics of
Atoms and Molecules

Presider: Rudolph Kohn; Space
Dynamics Laboratory, USA

FM2A.1 • 10:30

Entanglement Between a Photonic Time-Bin Qubit and a Collective Atomic Spin Excitation, Pau Farrera¹, Georg Heinze¹, Hugues de Riedmatten^{1,2}; ¹ICFO - The Institute of Photonic Sciences, Spain; ²ICREA-Institució Catalana de Recerca i Estudis Avançats, Spain. Light-matter entanglement combines the long-distance transmission advantage of photonic qubits with the storage and processing capabilities of atomic qubits. In this work we used a laser-cooled atomic cloud to generate entanglement between photonic time-bin qubits and atomic spin excitations.

FM2A.2 • 10:45

Configurable Beam Splitting of Single Photon in Cold Atoms, Yefeng Mei¹, Xianxin Guo¹, Shengwang Du¹; ¹the Hong Kong Univ of Sci & Tech, Hong Kong. We demonstrate a dynamically configurable beam splitter (BS) for single photon wavepacket via electromagnetically-induced-transparency storage in cold atoms. This quantum-memory based controllable BS may have applications in a quantum information processing network.

FM2A.3 • 11:00

Spectral Compression of Narrowband Single Photons with a Near Resonant Cavity, Mathias Seidler², Xi Jie Yeo¹, Alessandro Cere², Christian Kurtsiefer^{2,1}; ¹National Univ. of Singapore, Singapore; ²Centre for Quantum Technologies, NUS, Singapore. We compress the spectrum of narrowband heralded single photons generated by four-wave mixing in cold ⁸⁷Rb atoms using a near-resonant cavity as dispersion medium, without reducing the brightness and almost matching the atomic linewidth.

Executive Ballroom
210B

Joint

10:30–12:30

JM2B • Symposium on
Nonreciprocal Photonics I

JM2B.1 • 10:30 **Invited**

Nonreciprocal and topological photonics, Andrea Alu¹; ¹CUNY Advanced Science Research Center, USA. In this talk, we will overview our recent progress in inducing strong nonreciprocal responses in nanophotonic devices and metasurfaces, and the role of their symmetry breaking features in the realization of topological photonic metamaterials.

JM2B.2 • 11:00

Direct Observation of Topological Edge States in Silicon Photonic Crystals, Nikhil Parappurath¹, Filippo Alpegiani², L. Kuipers², Ewold Verhagen¹; ¹Center for Nanophotonics, AMOLF, Netherlands; ²Dept. of Quantum Nanoscience, Kavli Inst. of Nanoscience, Delft Univ. of Technology, Netherlands. We directly observe the states of topological photonic crystals at telecom wavelengths. Using the states' intrinsic radiation, we measure dispersion, loss, pseudospin, and spin-spin scattering. We image spin-selective unidirectional propagation around sharp corners and junctions.

Executive Ballroom
210C

CLEO: QELS-Fundamental Science

10:30–12:15

FM2C • Nonlinear Nano-Optics

Presider: Thomas A. Searles
Howard; Univ. USA

FM2C.1 • 10:30

Nonlinear Nanoimaging of Ultrafast Coherent Dynamics of Graphene, Tao Jiang^{1,2}, Vasily Kravtsov^{1,2}, Mikhail Tokman³, Alexey Belyanin⁴, Markus B. Raschke^{1,2}; ¹Dept. of Physics, Dept. of Chemistry, and JILA, Univ. of Colorado, USA; ²Center for Experiments on Quantum Materials, Univ. of Colorado, USA; ³Inst. of Applied Physics, Russian Academy of Sciences, Russia; ⁴Dept. of Physics and Astronomy, Texas A&M Univ., USA. Using femtosecond adiabatic plasmonic nanofocusing, we image graphene in broadband four-wave mixing, revealing spatial heterogeneity, 6 fs coherent dynamics, and a long range spatial nonlocality.

FM2C.2 • 10:45

Efficient four wave mixing and low-loss in-coupling in hybrid gap plasmonic waveguides, Nicholas A. Günsken¹, Michael Nielsen¹, Ngoc Nguyen¹, Xingyuan Shi¹, Paul Dichtl¹, Stefan Maier¹, Rupert Oulton¹; ¹Physics, Imperial College London, UK. We show efficient four-wave-mixing over μm length-scales with a signal-to-idler conversion efficiency of 1% enabled by strong non-linearities and highly confined fields. Furthermore, we demonstrate low-loss in-coupling into nanometer gaps with an efficiency of 80%.

FM2C.3 • 11:00

Tailoring Second Harmonic Diffraction in GaAs Metasurfaces via Crystal Orientation, Polina Vabishchevich^{1,2}, Aleksandr Vaskin³, Sadvikas Addamane⁴, Sheng Liu^{1,2}, Andrei P. Sharma⁴, Ganesh Balakrishnan⁴, John Reno^{1,2}, Gordon Keeler¹, Michael B. Sinclair¹, Isabelle Staude³, Igal Brener^{1,2}; ¹Sandia National Labs, USA; ²Center for Integrated Nanotechnologies, USA; ³Inst. of Applied Physics, Abbe Center of Photonics, Friedrich Schiller Univ. Jena, Germany; ⁴Center for High Technology Materials (CHTM), Univ. of New Mexico, Albuquerque, New Mexico USA, USA. We use GaAs metasurfaces with (111) crystal orientation to channel the second harmonic generation (SHG) into the zero-diffraction order that is suppressed for SHG obtained from GaAs metasurfaces with (100) orientation.

Executive Ballroom
210D

10:30–12:30

FM2D • Ultrafast Optical
Processes in Topological
Materials

Presider: Ulrike Woggon
Technische Universitaet Berlin,
Germany

FM2D.1 • 10:30 **Tutorial**

Optical Properties of Topological Materials, Allan H. MacDonald¹; ¹Univ. of Texas at Austin, USA. Topological materials, including Chern (quantum Hall) insulators and quantum spin Hall and quantum valley Hall insulators in two dimensions and topological semimetals in three dimensions have a number of distinct optical properties. My tutorial will discuss how these can be used to identify new topological materials, and how they might be valuable for applications.



Allan H. MacDonald received his B.Sc. degree from St. Francis Xavier University, Antigonish, Nova Scotia, Canada in 1973, and M.Sc. and Ph.D. degrees in physics from the University of Toronto in 1974 and 1978 respectively. He was a member of the research staff of the National Research Council of Canada from 1978 to 1987 and has taught at Indiana University (1987–2000) and the University of Texas at Austin (2000–present).

Executive Ballroom
210E

Executive Ballroom
210F

Executive Ballroom
210G

Executive Ballroom
210H

Joint

CLEO: Science & Innovations

10:30–12:30

JM2E • Symposium on High Average Power Ultrafast Lasers: Trends, Challenges & Applications II

JM2E.1 • 10:30 **Invited**

High Peak Power, High Average Power Lasers at the CLF and Their Potential Applications, Cristina Hernandez-Gomez¹; ¹*STFC Rutherford Appleton Lab, UK*. The continued advancement of short pulse lasers with high average power is crucial for to enable a range of applications. We describe the current performance achieved at the CLF for increasing average power of high power lasers.

JM2E.2 • 11:00

Thermally Induced Spatiotemporal Aberrations in High Average Power Ultra-short Compressors, Zeudi Mazzotta¹, Lucas Ranc^{1,2}, Nathalie Lebas¹, Catherine Le Blanc¹, Ji Ping Zu¹, Luc Martin¹, François Mathieu¹, Frédéric Druon³, Dimitris Papadopoulos¹; ¹*Laboratoire pour l'Utilisation des Lasers Intenses, CNRS, Ecole Polytechnique, CEA, France*; ²*THALES LAS FRANCE SAS, France*; ³*Laboratoire Charles Fabry, Institut d'Optique, CNRS, Univ. Paris Saclay, France*. We study the heating effects of the gratings of an ultrashort pulse compressor using a kW laser diode as thermal source. Based on wavelength-dependent wavefront measurements we evaluate the spatiotemporal impact on the compressed pulses.

10:30–12:30

SM2F • Quantum Sensing in Solid State Systems

Presider: Eisuke Abe; RIKEN, Japan

SM2F.1 • 10:30 **Invited**

Quantum Microscopy for Magnetic and Electrical Nanometrology, Christian Degen¹; ¹*Dept. of Physics, ETH Zurich, Switzerland*. Diamond nanoprobes with single NV centers allow enhancing scanning probe microscopy with quantum metrology. This talk introduces the basic concepts and technology of diamond nanoprobes and provides illustrations of nanoscale imaging of magnetism and currents.

SM2F.2 • 11:00

High-Sensitivity Magnetometry at Room Temperature with Post-Processed Optical Readout of Single NV-Centres, Antonio Gentile¹, Raffaele Santagati¹, Sebastian Knauer², Simon Schmitt³, Stefano Paesani¹, Chris Granade⁴, Nathan Wiebe⁴, Christian Osterkamp³, Liam P. McGuinness³, Jianwei Wang¹, Mark G. Thompson¹, John G. Rarity¹, Fedor Jelezko³, Anthony Laing¹; ¹*Univ. of Bristol, UK*; ²*Univ. of New South Wales, Australia*; ³*Ulm Univ., Germany*; ⁴*Microsoft Research, USA*. Optical readout from nanofabricated single NV centres is enhanced via Bayesian inference techniques, to demonstrate efficient magnetometry at room temperature conditions. We achieve experimentally Heisenberg-limited sensitivities $O(100 \text{ nT s}^{1/2})$, thus competing with state-of-art cryogenic set-ups.

10:30–12:15

SM2G • Free-Space & Underwater Communication

Presider: Mihaela Dinu; LGS Innovations, USA

SM2G.1 • 10:30

An Outdoor Evaluation of 1-Gbps Optical Wireless Communication using AlGaN-based LED in 280-nm Band, Yuki Yoshida¹, Kazunobu Kojima², Masaki Shiraiwa¹, Yoshinari Awaji¹, Atsushi Kanno¹, Naokatsu Yamamoto¹, Shigefusa Chichibu², Akira Hirano³, Masamichi Ippommatsu³; ¹*National Inst of Information & Comm Tech, Japan*; ²*Inst. for Multidisciplinary Research for Advanced Materials, Tohoku Univ., Japan*; ³*UV Craftory Co. Ltd., Japan*. The performance of solar-blind optical wireless communication using AlGaN-based LED at 280 nm-band was evaluated experimentally over a 1.5-m outdoor Line-of-Sight channel. Even under the summer sun, 1.18-Gbps error-free transmission was achieved.

SM2G.2 • 10:45

Modelling of a deep space FSO-link with a SNSPD receiver unit under turbulence-induced fading conditions, Hristo Ivanov¹, Erich Leitgeb¹, Gert Freiberger¹; ¹*Graz Univ. of Technology, Austria*. Performance of a deep space FSO-link incorporating SNSPD parametrized with deadtime, QE and N-array is addressed. Considering atmospheric turbulence fading $\leq 3.5 \text{ dB}$, data rate up to 20 Mbps for -17 (ph/ns)[dB] received signal is reached.

SM2G.3 • 11:00 **Invited**

Progress in Free Space Optical Networks, Linda Thomas¹; ¹*US Naval Research Lab, USA*. Free space optical communication systems can provide high bandwidth data transport over line-of-sight paths. Losses due to atmospheric scintillation and obscurations present challenges to data transport reliability. Progress in networking of free space optical systems will be discussed.

10:30–12:30

SM2H • Optical Imaging & Sensing

Presider: Haifeng Jiang; NTSC, USA

SM2H.1 • 10:30

Absolute distance measurement with a long ambiguity range using a tri-comb mode-locked fiber laser, Ting Li¹, Xin Zhao¹, Jie Chen¹, Jianjun Yang¹, Qian Li¹, Zheng Zheng^{1,2}; ¹*School of Electronic and Information Engineering, Beihang Univ., China*; ²*Beijing Advanced Innovation Center for Big Data-based Precision Medicine, China*. An absolute distance measurement scheme based on a single triple-comb mode-locked fiber laser is demonstrated. It can realize much longer ambiguity range for real-time measurement with a very simple fiber-optic system setup.

SM2H.2 • 10:45

Two-color Dual-comb Ranging Without Precise Environmental Sensing, Zebin Zhu¹, Kai Ni¹, Qian Zhou¹, Guanhao Wu¹; ¹*Dept. of Precision Instrument, Tsinghua Univ., China*. We present a two-color dual-comb ranging (TC-DCR) system without precise environmental sensing. The experimental result demonstrates 46 nm precision with 0.1 s coherent averaging and achieves an accuracy of the order of $\sim 10^{-7}$.

SM2H.3 • 11:00

Fast and Sensitive Quantitative Phase Imaging Using a Frequency Comb, Jeeran Boonruangkan¹, Hamid Ferrokhi^{1,2}, Samuel Kwok¹, Tom Carney¹, Young-Jin Kim¹; ¹*Nanyang Technological Univ., Singapore*; ²*Wellman Center for Photomedicine, Massachusetts General Hospital, and Harvard Medical School, USA*. We report frequency-comb-based quantitative phase imaging (FCR-QPI) providing coherence tunability for better phase sensitivity with suppressed background noise. FCR-QPI can also enable monitoring of fast inter- and intra-cellular dynamic motions.

Monday, 10:30–12:30

Meeting Room
211 A/BCLEO: Applications
& Technology

10:30–12:30

AM2I • Applied Biophotonic
Microscopy & Imaging

Presider: David Nolte; Animated
Dynamic Inc, USA

AM2I.1 • 10:30 **Invited**

Towards Anatomical Profiling of Intact Bones with Tissue Clearing, Custom Microscopy and Algorithms, Alon Greenbaum^{1,2}; ¹Joint Dept. of Biomedical Engineering, North Carolina State Univ., USA; ²Joint Dept. of Biomedical Engineering, UNC Chapel Hill, USA. Bones are complex and vital organs, nevertheless, investigating biological phenomena in the bones is challenging due to their opacity. Bone-CLARITY, a method to render bones transparent allows 3D imaging and analysis of whole mice bone.

AM2I.2 • 11:00 **Invited**

Adding Dimensions to Intravital Imaging, Scott E. Fraser¹; ¹Univ. of Southern California, USA. Intravital imaging provides a key bridge between molecular & cellular data. To address the compromises in live imaging, we are combining 2-photon light-sheet microscopes for 4D imaging with new multispectral analysis tools to permit rapid and unambiguous 5D analyses of multiplex-labeled specimens.

Meeting Room
211 C/DCLEO: Science &
Innovations

10:30–12:30

SM2J • Optical Computing &
Resonator Applications

Presider: Yasutomo Ota;
University of Tokyo, Japan

SM2J.1 • 10:30 **Invited**

Photonic Reservoir Computing in Silicon Photonics, Peter Bienstman¹; ¹Ghent Univ., INTEC, Belgium. Photonic Reservoir Computing is a brain-inspired information processing paradigm that is especially suited for a hardware implementation in photonics. We will present our latest results on a number of applications, ranging from telecom equalization to biological cell sorting.

SM2J.2 • 11:00

All-photonic in-memory computing based on phase-change materials, Carlos Rios^{1,2}, Nathan Youngblood², Zengguang Cheng², Manuel Le Gallo³, Wolfram Pernice³, C. David Wright⁴, Abu Sebastian⁵, Harish Bhaskaran²; ¹MIT (MIT), USA; ²Univ. of Oxford, UK; ³Univ. of Münster, Germany; ⁴Univ. of Exeter, UK; ⁵IBM Zürich, Switzerland. We experimentally demonstrate, for the first time, co-located data storage and processing (i.e. in-memory computing) on an integrated photonic platform based on nonvolatile phase-change materials.

Meeting Room
212 A/BCLEO: Applications
& Technology

10:30–12:30

AM2K • Environmental &
Atmospheric Sensing II

Presider: Mark Zondlo; Princeton
University, USA

AM2K.1 • 10:30 **Invited**

Active and Passive Greenhouse Gas Profiling in the Atmosphere Using Near Infrared Tunable Diode Lasers, Houston Miller¹, D. Michelle Bailey¹, Monica M. Flores¹, David Bomse²; ¹Chemistry, George Washington Univ., USA; ²Mesa Photonics, USA. The development of two laser-based sensors for horizontal and vertical profiling of greenhouse gas levels in the atmosphere including an auto-aligning, open-path instrument and a new variant on laser heterodyne radiometry are presented.

AM2K.2 • 11:00

Simultaneous DIAL, IPDA and point sensor measurements of the greenhouse gases, CO₂ and H₂O, David Plusquellic², Gerd Wagner¹, Kimberly Briggman², Adam Fleisher², David Long³, Joseph Hodges³; ¹DLR, Germany; ²Physical Measurement Lab, NIST, Boulder, USA; ³Material Measurements Lab, NIST, Gaithersburg, USA. Rapid scan IPDA and DIAL systems have been developed based on phase modulators for tuning and hybrid counting systems for detection. The performance of these systems has been evaluated through comparisons with point sensor measurements.

Meeting Room
212 C/DCLEO: Science &
Innovations

10:30–12:30

SM2L • Fiber Devices

Presider: Camille-Sophie Bres;
Ecole Polytechnique Federale de
Lausanne, Switzerland

SM2L.1 • 10:30

Nano-bore fiber focus trap with enhanced performance, Malte Plidschun^{1,2}, Stefan Weidlich^{1,3}, Karina Weber^{1,4}, Martin Šiler⁵, Tomáš Čizmar^{1,5}, Markus Schmidt^{1,2}; ¹Leibniz Inst. of Photonic Technology, Germany; ²Abbe Center of Photonics and Faculty of Physics, FSU Jena, Germany; ³Heraeus Quarzglas GmbH & Co. KG, Germany; ⁴Inst. of Physical Chemistry, FSU Jena, Germany; ⁵Inst. of Scientific Instruments, CAS, Czechia. A novel concept of focus implementation into dual-fiber optical tweezers is presented, enabling a performance increase by >30% for fiber separations <30µm. Simulations are experimentally verified and evaluated using common data processing and fitting routines.

SM2L.2 • 10:45 **Invited**

Temperature Insensitive Fibers, Radan Slavik¹, Eric Numkam Fokoua¹, Wenwu Zhu^{1,2}, Meng Ding¹, Tom Bradley¹, Yong Chen¹, Seyed Reza Sandoghchi¹, Marco N. Petrovich¹, Francesco Poletti¹; ¹Univ. of Southampton, UK; ²Dalian Univ. of Technology, China. Hollow core optical fibers guide light through a hole rather than a silica glass. This strongly reduces the light-glass interaction. This gives these fibers many unique properties like low sensitivity to temperature and low non-linearity.

CLEO: QELS-Fundamental
Science

10:30–12:30

FM2M • Random Numbers & Entanglement

President: Josh Nunn; University of Bath, UK

FM2M.1 • 10:30

Interferometric quantum random number generation on chip, Thomas Roger¹, Innocenzo De Marco^{1,2}, Taofiq Paraiso¹, Davide Marangon¹, Zhiliang Yuan¹, Andrew Shields¹; ¹Toshiba Research Europe Limited, UK; ²School of Electronic and Electrical Engineering, Univ. of Leeds, UK. We demonstrate an on-chip, high-speed quantum random number generator based on the interference of two gain-switched pulsed lasers. FPGA-based electronics allows for real-time processing, providing 8 Gbps random numbers passing all the NIST tests.

FM2M.2 • 10:45

Quantum random number generation (QRNG) by phase diffusion process in a gain-switched semiconductor laser - new insights, Brigitta Septriani¹, Oliver de Vries¹, Markus Graefe¹; ¹Fraunhofer Inst. for Applied Optics and Precision Engineering IOF, Germany. A parametric study of QRNG employing phase diffusion in gain-switched DFB laser diode is presented. New theoretical findings on the maximal raw data rate and explanations on advantage of pulsed regime over cw are given.

FM2M.3 • 11:00 **Invited**

Using Photons to Generate Certified Randomness, Peter Bierhorst¹; ¹Univ. of Colorado at Boulder, USA. A photonic loophole-free Bell experiment is generating random numbers impossible to predict by any agent that cannot send signals faster than the speed of light. This resource has applications in secure communication.

CLEO: Science & Innovations

10:30–12:30

SM2N • Enhanced Cavities for Sensing and Interferometry

President: Denis Donlagic; University of Maribor, Slovenia

SM2N.1 • 10:30 **Tutorial**

Chipscale Soliton Micro-combs, Tobias J. Kippenberg¹; ¹Inst. of Physics, Swiss Federal Inst. of Technology (EPFL), Switzerland. This tutorial will review the fundamental operational principles and latest development in the field of soliton microresonator frequency combs (micro-combs), which utilize spatio-temporal self organization of light in the form of dissipative solitons. Such microcombs provide chipscale and broadband frequency combs, that have been applied to frequency synthesis, LIDAR, astrophysical spectrometer calibration as well as dual comb based ranging and spectroscopy techniques.



Tobias J. Kippenberg is Full Professor of Physics at EPFL. He obtained his PhD at the California Institute of Technology. From 2005-2009 he lead an Independent Research Group at the MPI of Quantum Optics. His research interest encompasses chipscale optical frequency combs and their applications as well as radiation pressure interaction of laser light and mechanical oscillators. He has received the ICO Prize in Optics (2014), the Swiss National Latsis award (2015) and ZEISS Research Award (2018). He is fellow of the APS and OSA, and listed since 2014 in the Clarivate highlycited.com.

10:30–12:30

SM2O • Micro & Nano Fabrication

President: Tingyi Gu; University of Delaware, USA

SM2O.1 • 10:30

Birefringent Photonic Crystal for High Efficiency Polarization Beam Splitting, Ehsan Ordooui¹, Azad Siahmakoun¹, Hossein Alisafaei¹; ¹Physics and Optical Engineering, Rose-Hulman Inst. of Technology, USA. We have modeled and fabricated a birefringent photonic crystal using only TiO₂. The device demonstrates high efficiency for splitting the polarization states of incident light. The fabrication is done using oblique-angle deposition.

SM2O.2 • 10:45

Curvature-controlled Fabrication of Polymer Nanolens Array, Qiang Li¹, Jaeyoun Kim¹; ¹Iowa State Univ., USA. We demonstrate curvature-controlled fabrication of arrayed nanolenses via UV-assisted modification of photopolymer's material characteristics and elastomer-based nanoimprinting. By varying the UV-dose, the *f*# of the 500 nm-diameter nanolens was varied from 1.2 to 10.0.

SM2O.3 • 11:00

High-quality Nanometric Quantum Source: Epitaxially Grown Diamond Nano-pyramids with Silicon-Vacancy Centers, Tzach Jaffe¹, Nina Felgen², Lior Gal¹, Lior Koblum¹, Cyril Popov², Johann Peter Reithmaier², Meir Orenstein¹; ¹Dept. of Electrical Engineering, Technion Israel Inst. of Technology, Israel; ²Inst. of Nanostructure Technologies and Analytics, Univ. of Kassel, Germany. We present a deterministic template-assisted bottom-up process for creating high-quality nanoscale diamond pyramids incorporating optically active silicon vacancy centers (SiV). We achieved deterministic nano-localization and an extraction efficiency enhancement of 4 compared to bulk diamond.

CLEO: QELS-
Fundamental ScienceFM2A • Quantum Optics
of Atoms and Molecules—
Continued

FM2A.4 • 11:15

A Single Shot Measurement of Atomic Coherence in a Thermal Ensemble of Atoms, Arif W. Laskar¹, Niharika Singh¹, Pratik Adhikary¹, Arunabh S. Mukherjee¹, Saikat Ghosh¹; ¹Physics, Indian Inst. of Technology, Kanpur, India. We demonstrate a single shot measurement technique to quantify ground state coherence in atomic system. The quantifier identifies the transition from EIT to Autler-Townes regime. Furthermore, we demonstrate phase coherent control and freezing coherence against decoherence.

FM2A.5 • 11:30

Turning an Organic Molecule into a Coherent Two-Level Quantum System using a Tunable Fabry-Perot Microcavity, Daqing Wang¹, Hrishikesh Kelkar¹, Diego Martin-Cano¹, Dominik Rattenbacher¹, Alexey Shkarin¹, Tobias Utikal¹, Stephan Götzinger^{2,1}, Vahid Sandoghdar^{1,2}; ¹Max Planck Inst. for the Science of Light, Germany; ²Friedrich Alexander Univ. Erlangen-Nuremberg, Germany. By coupling an organic molecule to a Fabry-Perot microcavity, we turn it into a coherent two-level quantum system. We further demonstrate efficient interaction of this system with single photons generated by a second molecule.

FM2A.6 • 11:45

Raman Scattering Beyond the Master Equation: Photon-Matter Correlations and Statistics, Kai B. Shinbrough¹, Yanting Teng¹, Bin Fang¹, Virginia O. Lorenz¹, Offir Cohen¹; ¹Univ of Illinois at Urbana-Champaign, USA. We present 1D and 3D models that take into account Stokes-photon-excitation pair correlations in Raman scattering, revealing non-trivial dependence of the photon statistics on linewidth, dispersion and collection angle.

Joint

JM2B • Symposium on
Nonreciprocal Photonics I—
Continued

JM2B.3 • 11:15

Broadband Pulse Delays in Ultracompact Footprints Enabled through Nonreciprocity, Sander Mann^{1,3}, Dimitrios Sounas^{2,3}, Andrea Alu^{1,3}; ¹Photonics Initiative, Advanced Science Research Center, USA; ²Electrical and Computer Engineering, Wayne State Univ., USA; ³Electrical and Computer Engineering, Univ. of Texas at Austin, USA. We demonstrate large broadband pulse delays in subwavelength structures, enabled through nonreciprocal topologically protected edge states. We develop an equivalent model to study buffer dynamics and accurately predict delays, and demonstrate a new optical resonance.

JM2B.4 • 11:30 **Invited**

Utilizing Floquet Engineering for the Design of Non-reciprocal Transport, Tsampikos Kottos¹; ¹Wesleyan Univ., USA. We present a framework that lays out the rules under which a periodic driving induces nonreciprocal transport. The method unveils the role of an extended Hilbert space where non-reciprocal Floquet networks can be engineered.

CLEO: QELS-Fundamental Science

FM2C • Nonlinear Nano-
Optics—Continued

FM2C.4 • 11:15

Structured Light for Second-Harmonic Spectroscopy in Mie-Resonant AlGaAs Nanoparticles, Elizaveta V. Melik-Gaykazyan^{2,1}, Kirill Koshelev^{1,3}, Jae-Hyuck Choi⁴, Sergey Kruk¹, Hong-Gyu Park⁴, Andrey Fedyanin², Yuri S. Kivshar¹; ¹Nonlinear Physics Centre, Australian National Univ., Australia; ²Faculty of Physics, Lomonosov Moscow State Univ., Russia; ³ITMO Univ., Russia; ⁴Dept. of Physics, South Korea Univ., South Korea (the Republic of). We employ doughnut-shaped cylindrical vector beams to observe the enhanced second-harmonic generation from individual subwavelength AlGaAs nanoparticles which support both electric and magnetic multipolar Mie-type resonances at the fundamental and double frequencies.

FM2C.5 • 11:30

Boosting LSP-enhanced SHG from Au nanoprisms by using NLO polymers, Atsushi Sugita¹, Takumi Makiyama¹, Hikaru Sato¹, Atsushi Ono¹, Wataru Inami¹, Yoshimasa Kawata¹; ¹Shizuoka Univ., Japan. LSP-enhanced SHG from Au nanoprisms surrounded by NLO polymers is presented. Nearly 50-fold increases in LSP-enhanced SHG signals compared to pristine Au nanoprisms are discussed in terms of plasmon-exciton two-photon resonances and molecule-to-metal charge transfer.

FM2C.6 • 11:45

Metal-Dielectric Nanodimers with Hybridized Resonances Probed by Second-Harmonic Polarization, Claude Renault¹, Lang Lukas¹, Frizyuk Kristina², Maria Timofeeva¹, Mihail Petrov², Filipp Komissarenko², Ivan Mukhin², Flavia Timpu¹, Yuri S. Kivshar³, Rachel Grange¹; ¹ETH Zurich, Switzerland; ²ITMO Univ., Russia; ³Australian National Univ., Australia. We fabricate hybrid nanodimers made of gold and barium titanate nanoparticles by a pick-and-place technique. By overlapping their resonances, we achieve 100-times enhancement of the second-harmonic signal at the hybridized mode while reshaping its polarization.

FM2D • Ultrafast Optical
Processes in Topological
Materials—Continued

FM2D.2 • 11:30

Ultrafast Photocurrents in the Weyl Semimetal TaAs, Nicholas Sirica¹, Ra'anan Tobey¹, Dmitry Yarotski¹, Pam Bowlan¹, Stuart Trugman¹, Jian-Xin Zhu¹, Yaomin Dai¹, Abul Azad¹, Ni Ni², Xianggang Qiu³, Antoinette Taylor¹, Rohit Prasankumar¹; ¹Center for Integrated Nanotechnology, USA; ²Physics and Astronomy, Univ. of California Los Angeles, USA; ³Inst. of Physics Chinese Academy of Science, China. Terahertz emission from TaAs reveals highly directional, ultrafast photocurrents whose origin is intrinsically due to crystal structure. This is illustrated by unraveling the polarization dependence, directionality, and intrinsic timescales underlying photocurrent generation and decay.

FM2D.3 • 11:45

Spin and Charge Dynamics Across Topological Heterojunction in Monolayer 1T-WTe₂, Jekwan Lee¹, Wonhyoek Heo¹, Joon Tak¹, Minji Noh¹, Jaeun Eom², Changsoo Lee³, Dohun Kim², Hyunyoung Choi¹; ¹Ultrafast Terahertz Optoelectronics Lab., South Korea (the Republic of); ²Dept. of Physics, Seoul National Univ., South Korea (the Republic of); ³Dept. of Material Science and Engineering, Pohang Univ. of Science and Technology, South Korea (the Republic of). We studied the ultrafast carrier and spin dynamics on the 1T'-WTe₂ monolayer-bilayer interface. Time-resolved optical measurement verified the existence of topological edge state at the continuous interface with weak electron-phonon interaction and long-live electron-electron interaction.

Joint

CLEO: Science & Innovations

JM2E • Symposium on High Average Power Ultrafast Lasers: Trends, Challenges & Applications II—Continued

JM2E.3 • 11:15 **Invited**
Towards Stable Laser-Plasma Electron Acceleration, Andreas R. Maier¹; ¹Univ. of Hamburg, Germany. Driven by a highly stable laser system, the LUX accelerator combines expertise in plasma and conventional accelerator technology. We report on the generation of few-nm undulator radiation and stable operation of the LUX plasma accelerator.

JM2E.4 • 11:45
Supercontinuum-seeded, CEP-stable, high-power 4-micron KTA OPA driven by a 1.4-ps Yb:YAG thin-disk laser and its application to high harmonic generation, Tsuneto Kanai^{1,2}, Yeon Lee^{1,2}, Meenkyo Seo^{1,2}, Dong E. Kim^{1,2}; ¹Max Planck Center for Attosecond Science, South Korea (the Republic of); ²Physics, Postech, South Korea (the Republic of). We demonstrate a supercontinuum-seeded, phase-stable, 17-W mid-IR KTA OPA driven by a 1.4-ps Yb:YAG thin-disk laser. The seeding scheme simplifies the architecture and its performance is demonstrated by sensitive detection of photon signals from ZnSe.

SM2F • Quantum Sensing in Solid State Systems—Continued

SM2F.3 • 11:15
Quantum Sensing in CMOS under Ambient Conditions: On-Chip Detection of Electronic Spin States in Diamond, Christopher Foy¹, Mohamed Ibrahim¹, Donggyu Kim¹, Dirk R. Englund¹, Ruonan Han¹, Matthew Trusheim¹; ¹MIT, USA. We demonstrate the first on-chip NV ODMR for quantum sensing, which combines the compactness of CMOS integrated circuit technologies with nitrogen-vacancy (NV) centers in diamond.

SM2F.4 • 11:30 **Invited**
Creating Highly Coherent NV Centers in Diamond, Ania Bleszynski Jayich¹, Claire McLellan¹, Tim Eichhorn¹, Simon Meynell¹; ¹Univ. of California Santa Barbara, USA. The diamond NV center is a powerful platform for diverse quantum applications. We present novel NV formation techniques, using CVD diamond growth and tunable electron irradiation, that optimize the quantum properties of NV spin ensembles.

SM2G • Free-Space & Underwater Communication—Continued

SM2G.4 • 11:30
Hybrid Femtocell-Attocell Optical Links for High-Speed Indoor Wireless Network, Spencer Liverman¹, Siyuan Chen¹, Arun Natarajan¹, Thinh Nguyen¹, Alan X. Wang¹; ¹Oregon State Univ., USA. A dual channel indoor optical link is presented consisting of a 100Mbps wide-angle femtocell and a 1.5Gbps line-of-sight attocell. Wavelength multiplexing is used to eliminate interference between the two spatially overlapped optical links.

SM2G.5 • 11:45
Optical Broadcasting for Wide Field-of-View Bidirectional Indoor Optical Wireless Communications, Feng Feng¹, Paramin Sangwongngam¹, Hyunchoe Chun¹, Grahame Faulkner¹, Dominic O'Brien¹; ¹Univ. of Oxford, UK. We demonstrate point-to-multipoint optical wireless upstream and downstream data transmission at 12.5Gb/s between a novel holographic beam steering base station with $\pm 30^\circ$ FOV and two nomadic terminals that use mirror-based steering with $\pm 50^\circ$ FOV.

SM2H • Optical Imaging & Sensing—Continued

SM2H.4 • 11:15
All-optical Hilbert transform with optical frequency comb for one-shot three-dimensional imaging, Takashi Kato^{1,2}, Megumi Uchida^{1,2}, Yurina Tanaka^{1,2}, Kaoru Minoshima^{1,2}; ¹The Univ. of Electro-Communications, Japan; ²JST, ERATO MINOSHIMA Intelligent Optical Synthesizer (IOS), Japan. A novel all-optical Hilbert transform with precise relative carrier-phase and envelope control utilizing frequency control of an optical frequency comb is reported. One-shot three-dimensional imaging of a surface profile demonstrated 200-square-pixels resolution and μm -level uncertainty.

SM2H.5 • 11:30
Cascade-Linked Multi-Synthetic-Wavelength Digital Holography Using Line-by-Line Spectral Shaping Optical Frequency Comb, Takeshi Yasui^{1,2}, Masatomo Yamagiwa^{1,2}, Takeo Minamikawa^{1,2}, Isao Morohashi³, Norihiko Sekine³, Iwao Hosako³, Hirotugu Yamamoto⁴; ¹Tokushima Univ., Japan; ²JST, ERATO MINOSHIMA Intelligent Optical Synthesizer, Japan; ³National Inst. of Information and Communications Technology, Japan; ⁴Utsunomiya Univ., Japan. Line-by-line spectral shaping of a 10-GHz optical frequency comb (OFC) is used for cascade-linked multi-synthetic-wavelength digital holography. The proposed method enables the real-time 3D shape measurement with wide axial dynamic range.

SM2H.6 • 11:45
Depth thermography enabled by precise thermal-emission measurements, Yuzhe Xiao¹, Chenghao Wan¹, Alireza Shahsafi¹, Jad Salman¹, Mikhail Kats¹; ¹Univ. of Wisconsin-Madison, USA. We developed and experimentally demonstrated a depth-thermography technique based on infrared thermal emission that enables the extraction of temperatures beneath the surface of an object.

Meeting Room
211 A/BCLEO: Applications
& TechnologyAM2I • Applied Biophotonic
Microscopy & Imaging—
Continued

AM2I.3 • 11:30

Holographic Reconstruction with Bright-field Microscopy Contrast using Cross-Modality Deep Learning, Yilin Luo¹, Yichen Wu¹, Gunvant Chaudhari², Yair Rivenson¹, Ayfer Calis¹, Kevin Haan¹, Aydogan Ozcan^{1,2}; ¹Electrical and Computer Engineering Dept., Univ. of California, Los Angeles, California, USA; ²David Geffen School of Medicine, Univ. of California, Los Angeles, USA. Deep learning-based holographic reconstruction method eliminates twin-image, speckle and other interference artifacts at the output image, matching the contrast of bright-field microscopy, and merges volumetric imaging capability of holography with the contrast of incoherent microscopy.

AM2I.4 • 11:45

Spectral Phase and Amplitude Retrieval and Compensation for Random Access Microscopy, Alyssa M. Allende Motz¹, Charles G. Durfee¹, Jeff Squier¹, Danial Adams¹; ¹Colorado School of Mines, USA. Programmable, two-dimensional, spatial frequency modulation linear and nonlinear imaging combined with a novel and remarkably simple, in-situ quantitative pulse compensation and measurement scheme is demonstrated for the first time.

Meeting Room
211 C/DCLEO: Science &
InnovationsSM2J • Optical Computing
& Resonator Applications—
Continued

SM2J.3 • 11:15

High-resolution Silicon Microring based Architecture for Optical Matrix Multiplier, Natalie Janosik¹, Qixiang Cheng¹, Madeleine Glick¹, Yishen Huang¹, Keren Bergman¹; ¹Columbia Univ., USA. We characterize silicon photonic microring resonators specifically designed with low Quality Factors (Q) to operate with high linearity measured over a range of 1.44 volts suitable for microring-based high resolution optical matrix multiplier architectures.

SM2J.4 • 11:30

Photonic Crystal Design with Mix and Match Unit Cells for Mode Manipulation, Sami I. Halimi¹, Zhongyuan Fu^{1,3}, Francis O. Afzal¹, Joshua Allen², Shuren Hu⁴, Sharon M. Weiss^{1,2}; ¹Dept. of Electrical Engineering and Computer Science, Vanderbilt Univ., USA; ²Interdisciplinary Graduate Program in Materials Science, Vanderbilt Univ., USA; ³State Key Lab of Information Photonics and Optical Communications, Beijing Univ. of Posts and Telecommunications, China; ⁴Dept. of Physics and Astronomy, Vanderbilt Univ., USA. We report simulations and experimental measurement of a photonic crystal designed with mix and match unit cells. Our results enable extreme mode manipulation and potentially also phase and amplitude modification using non-traditional unit cell shapes.

SM2J.5 • 11:45

Directional Asymmetry in Biphoton Correlations, Austin J. Graf¹, Jeremy Staffa¹, Dana Griffith², Steven D. Rogers¹, Usman A. Javid¹, Qiang Lin¹; ¹Univ. of Rochester, USA; ²Wellesley College, USA. We have demonstrated asymmetry in biphoton coherence functions that arises upon reversing the propagation direction of a pump laser coupled into a silicon microdisk. Oscillations in the coherence functions experience an almost total phase shift.

Meeting Room
212 A/BCLEO: Applications
& TechnologyAM2K • Environmental &
Atmospheric Sensing II—
Continued

AM2K.3 • 11:30

Label-free Bio-aerosol Sensing Using On-Chip Holographic Microscopy and Deep Learning, Yichen Wu¹, Ayfer Calis¹, Yi Luo¹, Cheng Chen¹, Maxwell Lutton¹, Yair Rivenson¹, Xing Lin¹, Hatice Ceylan Koydemir¹, Yibo Zhang¹, Hongda Wang¹, Zoltán Göröcs¹, Aydogan Ozcan¹; ¹Univ. of California Los Angeles, USA. We present automated and label-free bio-aerosol sensing using a portable and cost-effective device, enabled by on-chip digital holographic microscopy and deep-learning.

AM2K.4 • 11:45

Open-Path Mid-Infrared Remote Sensing of Atmospheric Gases Using a Broadband Optical Parametric Oscillator, Oguzhan Kara¹, Frazer Sweeney¹, Marius Rutkauskas¹, Carl Farrell², Christopher Leburn², Derryck Reid¹; ¹Heriot Watt Univ., UK; ²Chromacity Ltd., UK. Using active Fourier-transform spectroscopy with a mid-infrared ultrafast optical parametric oscillator we demonstrate quantitative, open-path, simultaneous concentration measurements of water, methane and ethane at over 30-m range with a simple target.

Meeting Room
212 C/DCLEO: Science &
InnovationsSM2L • Fiber Devices—
Continued

SM2L.3 • 11:15

Fabrication of Near-Field Optical Fiber Probes Through Focused Ion Beam, Karen Sloyan¹, Henrik Melkonyan¹, Matteo Chiesa¹, Marcus Dahlem^{2,1}; ¹Khalifa Univ., United Arab Emirates; ²InterUniv. Microelectronics Center (IMEC), Belgium. We describe a procedure to fabricate a near-field optical fiber probe using focused ion beam milling. The method allows to control the fiber taper angle for better throughput, and the taper length for mechanical robustness.

SM2L.4 • 11:30

Low-Loss Ring-Core Fiber Supporting 4 Mode Groups, Heyun Tan², Junwei Zhang¹, Jie Liu¹, Lei Shen³, Guoxuan Zhu¹, Rui Zhang³, Yaping Liu³, Lei Zhang³, Siyuan Yu^{1,4}; ¹School of Electronics and Information Engineering, State Key Lab of Optoelectronic Materials and Technologies, Sun Yat-sen Univ., China; ²School of Physics, State Key Lab of Optoelectronic Materials and Technologies, Sun Yat-sen Univ., China; ³State key Lab of Optical Fiber and Cable Manufacture technology, Yangtze Optical Fiber and Cable Joint Stock Limited Company, China; ⁴Photonics Group, Merchant Venturers School of Engineering, Univ. of Bristol, UK. A ring-core fiber with a novel modulated-refractive-index profile is reported, whose low attenuation (~0.2 dB/km) and low inter-mode-group coupling coefficient (<-36 dB/km for adjacent high-order mode groups), both setting records for a ring-core fiber.

SM2L.5 • 11:45

Poling Optical Fibers with UV Lamp, João Manoel B. Pereira^{1,2}, Alexandre R. Camara^{3,4}, Fredrik Laurell², Oleksandr Tarasenko¹, Walter Margulis²; ¹Fiber Optics, RISE Acreo, Sweden; ²Applied Physics, Royal Inst. of Technology, Sweden; ³Instituto de física, Universidade do Estado do Rio de Janeiro, Brazil; ⁴Programa de Pós-Graduação em Engenharia Eletrônica, Universidade do Estado do Rio de Janeiro, Brazil. Silicate fibers with internal electrodes are optically poled without a laser by side-exposure to radiation from a UV tubular lamp. Electrooptic coefficients $\chi^{(2)} \sim 0.04$ pm/V and $V_{\pi} = 810$ V are obtained.

CLEO: QELS-Fundamental
ScienceFM2M • Random Numbers &
Entanglement—Continued

FM2M.4 • 11:30

Symmetrical Bell state preparation and measurement without a third party, Yong-Su Kim^{1,2}, Tanumoy Pramanik¹, Young-Wook Cho¹, Ming Yang³, Sang-Wook Han¹, Sang-Yun Lee¹, Min-Sung Kang¹, Sung Moon^{1,2}; ¹South Korea Inst. of Science & Technology, South Korea (the Republic of); ²South Korea Univ. of Science and Technology, South Korea (the Republic of); ³Anhui Univ., China. We present a linear optical Bell state preparation and measurement schemes without photon-photon interaction at an optical element. Unlike the standard schemes, it can be symmetrically divided into two parties without a third party.

FM2M.5 • 11:45

Violating Bell inequalities with entangled optical frequency combs and multi-pixel homodyne detection, William N. Plick¹, Francesco Arzani², Nicolas Treps², Damian Markham², Eleni Diamanti²; ¹Univ. of Dayton, USA; ²Sorbonne Universites, France. We theoretically investigated using continuous-variable Bell-type inequalities in a multipartite configuration using an optical parametric oscillator which has been synchronously-pumped with a frequency comb. We find violation is possible.

CLEO: Science & Innovations

SM2N • Enhanced Cavities for Sensing and
Interferometry—Continued

SM2N.2 • 11:30

Frequency Comb phase-locked Cavity Ringdown Spectroscopy, Zachary D. Reed¹, Joseph Hodges¹; ¹NIST, USA. We present a frequency comb phase-locked cavity ringdown spectrometer capable of arbitrary frequency steps with 1 kHz absolute frequency accuracy, and demonstrate determination of molecular line positions with better than 40 kHz accuracy.

SM2N.3 • 11:45

Attenuated Total Reflectance Dual-Comb Spectroscopy of an Organic Liquid-Phase Chemical Reaction, Daniel I. Herman^{1,2}, Eleanor Waxman¹, Gabriel Ycas^{1,2}, Fabrizio R. Giorgetta^{1,2}, Nathan R. Newbury¹, Ian Coddington¹; ¹NIST, USA; ²Physics, Univ. of Colorado Boulder, USA. A mid-infrared dual-comb spectrometer coupled to an attenuated total reflectance cell is used to monitor the hydration of mesityl oxide (MO) into diacetone alcohol (DAA). Our method provides real-time concentrations for MO and DAA.

SM2O • Micro & Nano Fabrication—
Continued

SM2O.4 • 11:30

Light-Directed Nanomanipulation of Colloidal Particles in Ambient Environments, Jingang Li¹, Yaoran Liu¹, Yuebing Zheng¹; ¹The Univ. of Texas at Austin, USA. We report an all-optical technique for the versatile nanomanipulation of various colloidal particles under ambient conditions by harnessing both photothermal effects and optical forces.

SM2O.5 • 11:45

Improvement of lasing threshold of ink-jet printed polymeric microdisk cavity by precise controlled wet etching, Taku Takagishi¹, Hiroaki Yoshioka¹, Yuya Mikami¹, Naoya Nishimura², Yuji Oki¹; ¹Kyushu Univ., Japan; ²Nissan Chemical Corporation, Japan. With well-controlled wet etching process, under-cut structure of ink-jet printed microdisk was successfully formed and we succeeded in lowering the lasing threshold by 10 times, compared with the one on a substrate.

Executive Ballroom
210ACLEO: QELS-
Fundamental ScienceFM2A • Quantum Optics
of Atoms and Molecules—
Continued

FM2A.7 • 12:00

Quantum Few-body Dynamics of Rydberg Atom Clusters, Woojun Lee¹, Minhyuk Kim¹, Hanlae Jo¹, Yunheung Song¹, Jaewook Ahn¹; ¹Dept. of Physics, South Korea Advanced Inst. of Science and Technology, South Korea (the Republic of). We model and experimentally verify the quantum dynamics of small-scale Rydberg-atom quantum simulators, or entangled Rydberg atom clusters, using Lindblad equations with control parameters including spontaneous emission, stochastic atom loss, and laser phase noise.

FM2A.8 • 12:15

Interferometric implementation of Rydberg-atom entanglements, Hanlae Jo¹, Yunheung Song¹, Minhyuk Kim¹, Jaewook Ahn¹; ¹Physics, South Korea Advanced Inst of Science & Tech, South Korea (the Republic of). We propose and experimentally demonstrate interferometrically controlled Rydberg-atom entanglements, for atoms separated farther than their blockade radius, where the interaction phase induced during the time interval between two control pulses implements distance-selective atom-atom entanglement.

Executive Ballroom
210B

Joint

JM2B • Symposium on
Nonreciprocal Photonics I—
ContinuedJM2B.5 • 12:00 **Invited**

Topological Quantum Photonics, Edo Waks¹, Mohammad Hafezi¹, Sabyasachi Barik¹, Shuo Sun², Aziz Karasahin¹, Chris Flower¹; ¹Univ. of Maryland at College Park, USA; ²Stanford Univ., USA. I will describe our work towards developing quantum photonic devices that exhibit strong topological properties such as robust edge states and chiral light-matter interactions.

Executive Ballroom
210C

CLEO: QELS-Fundamental Science

FM2C • Nonlinear Nano-
Optics—Continued

FM2C.7 • 12:00

Tunable Resonator-Upconverted Emission (TRUE) Color Prints for Anti-counterfeiting Applications, Hailong Liu¹, Jiahui Xu², Hao Wang¹, Xiaogang Liu², Joel K. W. Yang¹; ¹Singapore Univ. of Technology & Design, Singapore; ²National Univ. of Singapore, Singapore. We fabricated gap-plasmon resonators with self-assembled upconversion nanoparticles embedded within to simultaneously achieve size-tunable plasmonic and emissive colors and demonstrated tunable resonator-upconverted emission (TRUE) color prints for anti-counterfeiting applications.

Executive Ballroom
210DFM2D • Ultrafast Optical
Processes in Topological
Materials—Continued

FM2D.4 • 12:00

Optoelectronic Valley-locked Spin Photocurrent Generation using WSe₂-Bi₂Se₃ Heterostructure, Minji Noh¹, Soonyoung Cha², Jehyun Kim³, Yoomin Kim¹, Jekwan Lee¹, Hoil Kim², Seunghoon Yang⁴, Sooun Lee¹, Wooyoung Shim¹, Chul-Ho Lee⁴, Jun Sung Kim², Dohun Kim³, Hyunyoung Choi¹; ¹Yonsei Univ., South Korea (the Republic of); ²Pohang Univ. of Science and Technology, South Korea (the Republic of); ³Seoul National Univ., South Korea (the Republic of); ⁴South Korea Univ., South Korea (the Republic of). We demonstrate a new optoelectronic platform using WSe₂-Bi₂Se₃ heterostructures to generate and detect the valley-coupled spin-polarized photocurrents at room temperature. The light polarization and the external electric field can manipulate the magnitude of the current.

FM2D.5 • 12:15

Electric Control over 2D Dirac Plasmon Resonances in Topological Insulator Bi₂Se₃ in Proximity Contact with Graphene, Chihun In¹, Beom Kim¹, Jisoo Moon², Seung Young Seo³, Woosun Jang¹, Hyunseung Jung⁴, Myungwoo Son⁵, Seongshik Oh², Aloysius Soon¹, Hojin Lee⁴, Moon-Ho Ham⁵, Hyunyoung Choi¹; ¹Yonsei Univ., South Korea (the Republic of); ²Rutgers Univ., USA; ³Pohang Univ. of Science and Technology, South Korea (the Republic of); ⁴Soongsil Univ., South Korea (the Republic of); ⁵Gwangju Inst. of Science and Technology, South Korea (the Republic of). Graphene and topological insulator (TI) host two-dimensional (2D) Dirac surface plasmon at the terahertz frequency range. We observed unconventional density-dependence of 2D topological Dirac plasmon upon in proximity to the monolayer graphene.

12:30–13:30 Lunch Break (on your own)

12:30–13:30 What's Next in Integrated Optics – Hot Topics at CLEO: 2019, Room 230A

13:00–14:00 Resumes, LinkedIn, and Networking (with Cheeky Scientist), University Room, Hilton San Jose

13:00–14:00 Social Media in 2019 Panel Discussion, University Room, Hilton San Jose

13:30–17:30 SC362: Cavity Optomechanics: Fundamentals and Applications (Tobias Kippenberg, Ecole Polytechnique Federale de Lausanne, Switzerland)

SC376: Plasmonics (Mark Brongersma; Stanford Univ., USA)

SC378: Introduction to Ultrafast Optics (Rick Trebino, Georgia Institute of Technology, USA)

SC476: QCL and QCL Combs (Jérôme Faist, ETH Zürich, Switzerland)

Joint

CLEO: Science & Innovations

JM2E • Symposium on High Average Power Ultrafast Lasers: Trends, Challenges & Applications II—Continued

JM2E.5 • 12:00 **Invited**
Multi-Wavelength Laser Control of High-Voltage Discharges: From the Lab to Säntis Mountain, Thomas Proruit¹, Guillaume Schimmel¹, Elise Schubert¹, Denis Mongin¹, Ali Rastegari², Chengyong feng², Brian Kamer², Ladan Arissian², Jean-Claude Diels², Pierre Walch², Benoît Mahieu³, Yves-Bernard andre³, Aurelien Houard³, Clemens Herkommer⁴, Robert Jung⁴, Thomas Metzger⁴, Knut Michel⁴, André Mysyrowicz⁵, Jean-Pierre Wolf¹, Jerome Kasparian¹; ¹Univ. of Geneva, Switzerland; ²Univ. of New Mexico, USA; ³LOA, ENSTA ParisTech, France; ⁴TRUMPF Scientific lasers GmbH, Germany; ⁵André Mysyrowicz Consultants, France. We review recent results on multi-wavelength multipulse schemes to control high-voltage discharges with ultrashort pulses, and discuss their implications on lightning control at atmospheric scale.

SM2F • Quantum Sensing in Solid State Systems—Continued

SM2F.5 • 12:00
Anti-Stokes Excitation of Solid-State Quantum Emitters for Nanoscale Thermometry, Trong Toan Tran¹, Blake Regan¹, Evgeny Ekimov², Zhao Mu³, Zhou Yu³, Weibo Gao³, Prineha Narang⁴, Alexander Solntsev¹, Milos Toth¹, Igor Aharonovich¹, Carlo Bradac¹; ¹School of Mathematical and Physical Sciences, Univ. of Technology Sydney, Australia; ²Physics, Inst. for High Pressure Physics, Russia; ³Physics and Applied Physics, Nanyang Technological Univ., Singapore; ⁴John A. Paulson School of Engineering and Applied Sciences, Harvard Univ., USA. We report the first demonstration of Anti-Stokes excitation on a single solid-state quantum emitter—namely the germanium-vacancy center in diamond and its application as a high-sensitive nanoscale thermal sensor.

SM2F.6 • 12:15
4H-SiC-on-Insulator Platform for Quantum Photonics, Daniil Lukin¹, Constantin Dory¹, Marina Radulaski¹, Shuo Sun¹, Sattwik Deb Mishra¹, Melissa Guidry¹, Dries Vercautse¹, Jelena Vuckovic¹; ¹Electrical Engineering, Stanford Univ., USA. We present a 4H-Silicon-Carbide-on-Insulator platform that enables versatile integration of color centers with photonic devices.

SM2G • Free-Space & Underwater Communication—Continued

SM2G.6 • 12:00
60m/2.5Gbps Underwater Optical Wireless Communication with NRZ-OOK Modulation and Digital Nonlinear Equalization, Chunhui Lu¹, Jiemei Wang¹, Shangbin Li¹, Zhengyuan Xu¹; ¹Univ. of Science and Technology, China. We experimentally demonstrate a 2.5Gbps communication system based on a 450nm laser over 60m underwater transmission distance at the BER level of 3.5×10^{-3} by using NRZ-OOK modulation and digital nonlinear equalization technology.

SM2H • Optical Imaging & Sensing—Continued

SM2H.7 • 12:00
All-fiber reflection-based scattering NSOM with low phase drift for guided-wave imaging on a chip, Yizhi Sun^{1,2}, Binbin Wang³, Rafael Salas-Montiel³, Sylvain Blaize³, Renaud Bachelot³, Wei Ding¹; ¹CAS Inst. of Physics, China; ²Beihang Univ., China; ³Université de Technologie de Troyes, France. An all-fiber phase-resolved reflection-based near-field scanning optical microscope with a phase-drift-rate of 0.06°/s is developed. By raster scanning atomic force microscope probe, we measure the complex near-fields and analyze the standing-wave-spectrograms in silicon nano-waveguides.

SM2H.8 • 12:15
Orbital Angular Momentum-resolved Dual-comb Spectroscopy towards Topological Material Studies, Akifumi Asahara^{1,2}, Takuto Adachi¹, Yue Wang^{1,2}, Kaoru Minoshima^{1,2}; ¹Univ. of Electro-Communications, Japan; ²JST, ERATO MINOSHIMA Intelligent Optical Synthesizer, Japan. Orbital angular momentum-resolved dual-comb spectroscopy towards topological material studies is demonstrated. The developed method is a new type of multi-dimensional interferometric comb spectroscopy, generalizing longitudinal and transverse optical modes.

12:30–13:30 Lunch Break (on your own)

12:30–13:30 What's Next in Integrated Optics – Hot Topics at CLEO: 2019, Room 230A

13:00–14:00 Resumes, LinkedIn, and Networking (with Cheeky Scientist), University Room, Hilton San Jose

13:00–14:00 Social Media in 2019 Panel Discussion, University Room, Hilton San Jose

13:30–17:30 **SC362: Cavity Optomechanics: Fundamentals and Applications (Tobias Kippenberg, Ecole Polytechnique Federale de Lausanne, Switzerland)**

SC376: Plasmonics (Mark Brongersma; Stanford Univ., USA)

SC378: Introduction to Ultrafast Optics (Rick Trebino, Georgia Institute of Technology, USA)

SC476: QCL and QCL Combs (Jérôme Faist, ETH Zürich, Switzerland))

Meeting Room
211 A/BCLEO: Applications
& TechnologyAM2I • Applied Biophotonic
Microscopy & Imaging—
Continued

AM2I.5 • 12:00
Computation-enabled Lensless Imaging & Deep-Brain Microscopy, Brian Rodriguez¹, Zhimeng Pan¹, Ruipeng Guo¹, Naveen Nagarajan¹, Kyle Jenks¹, Mario Capecchi¹, Jason Sheperd¹, Rajesh Menon¹; ¹Univ. of Utah, USA. We show imaging using only a CMOS image sensor, and fluorescence microscopy inside the mouse brain using a surgical needle and an image sensor, both enabled by computation including machine learning.

AM2I.6 • 12:15
Enhancing Resolution in Coherent Microscopy Using Deep Learning, Tairan Liu¹, Kevin Haan¹, Yair Rivenson¹, Zhenrong Wei¹, Xin Zeng¹, Yibo Zhang¹, Aydogan Ozcan¹; ¹Univ. of California Los Angeles, USA. A generative adversarial network (GAN) based super-resolution framework is presented. This deep learning-based framework is capable of enhancing the resolution of coherent imaging systems in both pixel size-limited and diffraction-limited microscopy systems.

Meeting Room
211 C/DCLEO: Science &
InnovationsSM2J • Optical Computing
& Resonator Applications—
Continued

SM2J.6 • 12:00
Ultrahigh-Q/V single cell slotted nanocavity operated in water, Eiichi Kuramochi¹, Théo Martel¹, Shota Kita¹, Hideaki Taniyama¹, Akihiko Shinya¹, Masaya Notomi¹; ¹NTT Corporation, Japan. By tuning 30 or more holes, H1 slotted nanocavities with theoretical Q exceeding 10^5 and mode volume smaller than $0.03 (\lambda/n)^3$ in water were designed. A Q factor exceeding 10^4 was measured in ultrapure water.

SM2J.7 • 12:15
Resonant-Cavity Infrared Detector (RCID) with Very Thin Absorber, Chadwick Caneody¹, William W. Bewley¹, Charles Merritt¹, Chul Soo Kim¹, Mijin Kim², Stephanie Tomasulo¹, Michael V. Warren³, Eric M. Jackson¹, Jill A. Nolde¹, Chaffra A. Affouda¹, Edward H. Aifer¹, Igor Vurgaftman¹, Jerry R. Meyer¹; ¹Naval Research Lab, USA; ²KeyW, USA; ³ASEE Postdoctoral Fellow, USA. A resonant-cavity detector with peak sensitivity at $4.0 \mu\text{m}$ reaches 34% external quantum efficiency at room temperature, despite having only five absorbing quantum wells. Multiple passes enhance the peak absorption by nearly 30x.

Meeting Room
212 A/BCLEO: Applications
& TechnologyAM2K • Environmental &
Atmospheric Sensing II—
Continued

AM2K.5 • 12:00 **Invited**
MIRA: A New, Ultrasensitive, Middle Infrared Laser-Based Gas Analyzer for Environmental Monitoring Applications. James J. Scherer¹, Joshua B. Paul¹, Jerome Thiebaud¹, and Stephen So¹. ¹Aeris Technologies, Inc., USA. A new, ultrasensitive lunchbox-sized middle infrared laser-based commercial gas sensor is described, with examples of monitoring key pollutants (CO, HCHO), greenhouse gases (CH₄, N₂O) with 1ppb accuracy levels in a variety of field applications.

Meeting Room
212 C/DCLEO: Science &
InnovationsSM2L • Fiber Devices—
Continued

SM2L.6 • 12:00
The thermal sensitivity of optical path length in standard single mode fibers down to cryogenic temperatures, Wenwu Zhu^{1,2}, Meng Ding², Mingshan Zhao¹, David Richardson², Radan Slavik²; ¹Dalian Univ. of Technology, China; ²Optoelectronics Research Centre, Univ. of Southampton, UK. We measured the thermal sensitivity of SMF-28 fiber in the range -190°C - 25°C and measured a > 3-fold decrease for uncoated fiber towards the lowest measured temperature and far higher sensitivities for coated and jacketed fibers.

12:30–13:30 Lunch Break (on your own)

12:30–13:30 What's Next in Integrated Optics – Hot Topics at CLEO: 2019, Room 230A

13:00–14:00 Resumes, LinkedIn, and Networking (with Cheeky Scientist), University Room, Hilton San Jose

13:00–14:00 Social Media in 2019 Panel Discussion, University Room, Hilton San Jose

13:30–17:30 SC362: Cavity Optomechanics: Fundamentals and Applications (Tobias Kippenberg, Ecole Polytechnique Federale de Lausanne, Switzerland)
SC376: Plasmonics (Mark Brongersma; Stanford Univ., USA)
SC378: Introduction to Ultrafast Optics (Rick Trebino, Georgia Institute of Technology, USA)
SC476: QCL and QCL Combs (Jérôme Faist, ETH Zürich, Switzerland)

**CLEO: QELS-Fundamental
Science**

CLEO: Science & Innovations

**FM2M • Random Numbers &
Entanglement—Continued**

**SM2N • Enhanced Cavities for Sensing and
Interferometry—Continued**

**SM2O • Micro & Nano Fabrication—
Continued**

FM2M.6 • 12:00
Withdrawn

SM2N.4 • 12:00
Trace Gas Sensing through Purcell-Enhanced Raman Scattering in Pressurized Microcavities, Juan S. Gomez Velez¹, Andreas Muller¹; ¹Univ. of South Florida, USA. Minimally long microcavities were constructed for Purcell-enhanced Raman scattering in gases at up to 12 bar pressure. A linear emission rate confirms pressure broadening remains exceeded by the cavity linewidth, making pressurization beneficial.

SM2O.6 • 12:00
High Quality Factor PECVD Si₃N₄ Ring Resonators Compatible with CMOS Process, Xingchen Ji^{1,2}, Samantha Roberts¹, Michal Lipson¹; ¹Columbia Univ., USA; ²Cornell Univ., USA. We demonstrate high-confinement Si₃N₄ resonators with intrinsic quality factor more than 1 million using standard PECVD process. We show that by addressing scattering, the loss at 1.6 μm can be as low as 0.4 dB/cm.

FM2M.7 • 12:15
Verifying Multi-Partite Entanglement with a Few Detection Events, Lee Rozema¹, Valeria Saggio¹, Aleksandra Dimic², Chiara Greganti¹, Philip Walther¹, Borivoje Dakic¹; ¹Univ. of Vienna, Austria; ²Univ. of Belgrade, Serbia. We introduce a new entanglement-verification method and use it to experimentally verify the entanglement in a photonic six-qubit cluster state, created at telecommunication wavelengths, by detecting only 20 copies of the quantum state.

SM2N.5 • 12:15
Near-Infrared Continuous-Filtering Vernier Spectroscopy in a Flame, Chuang Lu¹, Francisco Senna Vieira¹, Florian M. Schmidt², Aleksandra Foltynowicz¹; ¹Dept. of Physics, Umeå Univ., Sweden; ²Dept. of Applied Physics and Electronics, Umeå Univ., Sweden. A continuous-filtering Vernier spectrometer based on an Er:fiber femtosecond laser was developed to acquire broadband H₂O and OH spectra in a premixed CH₄/air flame with 25 ms time resolution and percent precision on concentrations retrieval.

SM2O.7 • 12:15
Fabrication of High-Q, High-Confinement 4H-SiC Microring Resonators by Surface Roughness Reduction, Yi Zheng¹, Minhao Pu¹, Ailun Yi², Ayman N. Kamel¹, Martin R. Henriksen³, Asbjørn A. Jørgensen³, Xin Ou², Haiyan Ou¹; ¹Technical Univ. of Denmark, Denmark; ²Inst. of Microsystem and Information Technology, Chinese Academy of Sciences, China; ³Niels Bohr Inst., Univ. of Copenhagen, Denmark. We improve the Q of SiC microring resonators with a sub-micron cross-sectional dimension by a factor of six by reducing surface roughness. We achieve a high Q (~73,000) for such a device with anomalous dispersion.

12:30–13:30 Lunch Break (on your own)

12:30–13:30 What's Next in Integrated Optics – Hot Topics at CLEO: 2019, Room 230A

13:00–14:00 Resumes, LinkedIn, and Networking (with Cheeky Scientist), University Room, Hilton San Jose

13:00–14:00 Social Media in 2019 Panel Discussion, University Room, Hilton San Jose

13:30–17:30 **SC362: Cavity Optomechanics: Fundamentals and Applications (Tobias Kippenberg, Ecole Polytechnique Federale de Lausanne, Switzerland)**
SC376: Plasmonics (Mark Brongersma; Stanford Univ., USA)
SC378: Introduction to Ultrafast Optics (Rick Trebino, Georgia Institute of Technology, USA)
SC476: QCL and QCL Combs (Jérôme Faist, ETH Zürich, Switzerland)

CLEO: QELS-
Fundamental Science

13:30–15:30

FM3A • Quantum
Nanophotonics I: Plasmonics &
Quantum DotsPresider: Kai-Mei Fu; University of
Washington, USA

FM3A.1 • 13:30

Voltage controlled fine-structure splitting of single photon emitters in a two-dimensional semiconductor, Chitraleema Chakraborty¹, Nicholas Jungwirth², Gregory Fuchs³, Nick Vamivakas⁴; ¹Electrical Engineering and Computer Science, MIT, USA; ²Materials Science, Univ. of Rochester, USA; ³School of Applied and Engineering Physics, Cornell Univ., USA; ⁴The Inst. of Optics, Univ. of Rochester, USA. We report on the modulation of the fine-structure splitting (FSS) of quantum dot-like emitters in a two-dimensional semiconductor. Voltage-controlled suppression of the electron-hole exchange interaction features a 40% increase in circular polarization with decreasing FSS.

FM3A.2 • 13:45

Generation of quantum light in a photon-number superposition, Carlos Antón Solanas^{1,2}, Juan Carlos Loredó^{1,2}, Bogdan Reznichenko^{3,4}, Paul Hilaire^{1,2}, Abdelmounaim Harouri^{1,2}, Clément Millet^{1,2}, Helene Ollivier^{1,2}, Niccolò Somaschi¹, Lorenzo de Santis^{1,2}, Aristide Lemaitre^{1,2}, Isabelle Sagnes^{1,2}, Loïc Lanco^{1,6}, Alexia Auffeves^{3,4}, Olivier Krebs^{1,2}, Pascale Senellart^{1,2}; ¹CNRS Center of Nanosciences and Nanotechnology, France; ²Université Paris-Sud, Université Paris-Saclay, France; ³CNRS Institut Neel, France; ⁴Univ. Grenoble Alpes, France; ⁵Quandela, SAS, France; ⁶Université Paris Diderot, France. We generate highly pure quantum states of light in a coherent superposition of zero, one, and two photons. Such states are generated by coherently driving electrically-controlled QD-microcavity devices with resonant laser pulses.

FM3A.3 • 14:00

A Charge-Tunable Quantum Dot Strongly Coupled to a Nanophotonic Cavity, Zhouchen Luo², Allan S. Bracker¹, Dan Gammon¹, Edo Waks²; ¹Naval Research Lab, USA; ²Inst. for Research in Electronics and Applied Physics, Univ. of Maryland, USA. We report for the first time a strong interface between a charge tunable quantum dot spin and a microcavity embedded in a p-i-n-n structure, which enables control and stabilization of quantum dots charging state.

Joint

13:30–15:30

JM3B • Symposium on
Nonreciprocal Photonics II

Presider: To Be Announced

JM3B.1 • 13:30 **Invited**

Brillouin Based Non-reciprocal Functions for On-chip Optical Signal Processing, Benjamin J. Eggleton¹; ¹Univ. of Sydney, Australia. Stimulated Brillouin Scattering is an efficient opto-mechanical process that generates a sound-wave in an optical waveguide; the direction of the travelling sound wave breaks time-reversal symmetry, enabling non-reciprocity, the basis of isolators and circulators.

JM3B.2 • 14:00

Experimental band structure spectroscopy along the synthetic dimension, Avik Dutt¹, Momchil Minkov¹, Qian Lin¹, Luqi Yuan^{2,1}, David A. Miller¹, Shanhui Fan¹; ¹Stanford Univ., USA; ²Shanghai Jiao Tong Univ., China. We propose the first technique to directly measure the band structures of synthetic lattices, and experimentally demonstrate it in a modulated ring resonator. We also realize long-range couplings, photonic gauge potentials and nonreciprocal bands.

CLEO: QELS-Fundamental Science

13:30–15:30

FM3C • Functional
Nanophotonics Using
MetasurfacesPresider: Wei Ting Chen Harvard
Univ., USA

FM3C.1 • 13:30

A strongly correlated material for tunable metasurfaces, Weijian Li^{1,2}, Gururaj Naik²; ¹Applied Physics Graduate Program, Smalley-Curl Inst., Rice Univ., USA; ²Electrical & Computer Engineering, Rice Univ., USA. We demonstrate intensity dependent optical response in the visible for a strongly correlated material, 1T-TaS₂. Using this tunable material, we show the intensity-dependent diffraction of a meta-grating device useful for imaging, display and sensing technologies.

FM3C.2 • 13:45

Polariton Meta-Optics with Phase-Change Materials, Michele Tamagnone¹, Kundan Chaudhary¹, Xinghui Yin¹, Christina Spagele¹, Jiahua Li², Stefano Oscurato¹, Noah Rubin¹, Luis Jauregui¹, Philip Kim¹, James Edgar², Antonio Ambrosio¹, Federico Capasso¹; ¹Harvard University, USA; ²Kansas State Univ., USA. We created polaritonic metalenses in heterostructures formed by hBN and GeSbTe and characterized them with SNOM. The metalenses are created switching the phase of GeSbTe below hBN from amorphous to crystalline, focusing hBN phonon polaritons.

FM3C.3 • 14:00

All-dielectric Deep Ultraviolet Metasurfaces, Cheng Zhang¹, Shawn Divitt¹, Qingbin Fan², Wenqi Zhu¹, Amit K. Agrawal¹, Ting Xu², Henri Lezec¹; ¹NIST, USA; ²College of Engineering and Applied Science, Nanjing Univ., China. We demonstrate low-loss all-dielectric metasurfaces operating down to a record-short deep-ultraviolet wavelength of 266 nm, with an efficiency of 60%.

13:30–15:30

FM3D • Ultrafast Coherent
SpectroscopyPresider: Keshav Dani Okinawa
Institute of Science and
Technology, Japan

FM3D.1 • 13:30

Revealing the Orientation Dependence of Coherent Coupling in Silicon-Vacancy Centers in Diamond, Matthew W. Day¹, Kelsey Bates¹, Christopher L. Smallwood^{1,2}, Ronald Ulbricht^{4,2}, Travis Autry^{5,2}, Rachel C. Owen¹, Geoffrey M. Diederich⁶, Tim Schröder⁷, Edward S. Bielejec⁸, Mark Siemens⁶, Steven T. Cundiff^{1,2}; ¹Physics, Univ. of Michigan, USA; ²JILA, USA; ³Physics and Astronomy, San Jose State Univ., USA; ⁴Physics and Astronomy, Nanyang Technological Univ., Singapore; ⁵NIST, USA; ⁶Physics and Astronomy, Univ. of Denver, USA; ⁷Physics, Humboldt Univ. of Berlin, Germany; ⁸Sandia National Labs, USA. We investigate the orientation dependence of coherent coupling in the zero phonon line of an ensemble of SIV⁻ centers in diamond. The results indicate that crystal orientation and polarization could be tools for coherent optical control.

FM3D.2 • 13:45

Heterodimensionally confined carriers in III-V semiconductor nanostructures in multidimensional spectroscopy, Mirco Kolarczik¹, Aris Koulas-Simos¹, Bastian Herzog¹, Benjamin Lingnau¹, Sophia Helmrich¹, Kathy Lüdge¹, Nina Owschikow¹, Ulrike K. Woggon¹; ¹Technische Universität Berlin, Germany. Heterodimensional excitonic states are observed in InAs self-assembled quantum dots (QDs). They couple the zero-dimensional QD states to the surrounding continuum, resulting in equal dephasing times for QD ground state and excited state.

FM3D.3 • 14:00

Two-dimensional THz Spectroscopy of Exchange Interactions in Rare-earth Doped Garnets, Shovon Pal¹, Christian Tzschaschel¹, Amadé Bortis¹, Takuya Satoh², Manfred Fiebig¹; ¹Dept. of Materials, ETH Zurich, Switzerland; ²Dept. of Physics, Kyushu Univ., Japan. We study the correlation dynamics of the complex exchange interaction between the rare-earth and the transition metal in a garnet using two-dimensional terahertz spectroscopy. The THz resonance resembles a convolution of the exchange mode with electron transfer between the Kramer's doublet.

Executive Ballroom
210E

Joint

13:30–15:30

JM3E • Symposium on High Average Power Ultrafast Lasers: Trends, Challenges & Applications III

Presider: To Be Announced

JM3E.1 • 13:30 **Invited**

Industrial Ultrafast Lasers - Systems, Processing Fundamentals, and Applications, Norman Hodgson¹, Michael Laha¹, Tony Lee¹, Sebastian Heming^{1,2}, Albrecht Steinkopff^{1,3}; ¹Coherent, Inc., USA; ²Univ. Muenster, Germany; ³Univ. Jena, Germany. The architectures of industrial ultrafast lasers are being reviewed and their performance compared. Ablations rates as a function of pulse duration (0.4 – 19 ps), wavelength and pulse fluence are presented and the main industrial applications are discussed.

JM3E.2 • 14:00 **Invited**

High Power and High Energy Ultrafast Disk Lasers for Industrial Applications, Dirk H. Sutter¹, Thomas Dietz¹, Dominik Bauer¹, Raphael Scelle¹, Aleksander Budnicki¹, Alexander Killi¹, Michael Jenne², Jonas Kleiner², Daniel Flamm², Marc Sailer¹, Malte Kumkar²; ¹R+D, TRUMPF Laser GmbH, Germany; ²Research + Development, TRUMPF Laser- und Systemtechnik GmbH, Germany. Pico- and femtosecond lasers with kilowatt average power levels that are also capable of providing multi-mJ pulse energies will be described. Well established 24/7 industrial ultrafast laser processes allow for an outlook on potential future applications.

Executive Ballroom
210F

13:30–15:30

SM3F • Hot Topics in Quantum Sensing

Presider: Susan Schima; NIST, USA

SM3F.1 • 13:30 **Invited**

Quantum Sensing with Interacting Atoms, Morgan Mitchell^{1,2}; ¹ICFO - The Inst. of Photonic Sciences, Spain; ²ICREA - Catalan Institution for Research and Advanced Studies, Spain. Most quantum sensing literature describes non-interacting particles, or equivalently linear interferometry. Important high performance sensors, in contrast, employ interacting particles. I will discuss the prospects for quantum enhancement of such instruments.

SM3F.2 • 14:00 **Invited**

Tests of Quantum Mechanics and Gravity Using Atom Interferometry, Mark A. Kasevich¹; ¹Stanford Univ., USA. Modern de Broglie wave interferometers separate atomic wavepackets by 0.5 m for times of 2 sec. This talk will discuss the science and technology implications of these results, and describe the techniques employed to realize these instruments.

Executive Ballroom
210G

CLEO: Science & Innovations

13:30–15:30

SM3G • Data Center Lightwave Communications

Presider: Giovanni Milione; NEC Laboratories America Inc., USA

SM3G.1 • 13:30 **Tutorial**

Flexibly Scalable High Performance Architectures with Embedded Photonics, Keren Bergman¹; ¹Columbia Univ., USA. High-performance systems are increasingly bottlenecked by the energy and communications costs of interconnecting numerous compute and memory resources. We will review the opportunities to alleviate these challenges with embedded photonics and deliver flexibly scalable architectures.



Keren Bergman is the Charles Batchelor Professor of Electrical Engineering at Columbia University where she also serves as the Faculty Director of the Columbia Nano Initiative. Prof. Bergman received the B.S. from Bucknell University in 1988, and the M.S. in 1991 and Ph.D. in 1994 from M.I.T. all in Electrical Engineering. At Columbia, Bergman leads the Lightwave Research Laboratory encompassing multiple cross-disciplinary programs at the intersection of computing and photonics. Bergman serves on the Leadership Council of the American Institute of Manufacturing (AIM) Photonics leading projects that support the institute's silicon photonics manufacturing capabilities and Datacom applications. She is a Fellow of the OSA and IEEE.

Executive Ballroom
210H

13:30–15:30

SM3H • Fundamentals of Ultrafast Light Matter Interaction

Presider: Tsing-Hua Her; Univ. of North Carolina at Charlotte, USA

SM3H.1 • 13:30

Multiplicity of Laser-Excited Electromagnetic Modes and their Roles in LIPSS Formation on Thin Metallic Films, Alexandr V. Dostovalov², Thibault Derrien¹, Viktor P. Korolov², Sergey A. Babin², Nadezhda M. Bulgakova¹; ¹HiLASE, Inst. of Physics ASCR, Russia; ²Inst. of Automation and Electrometry SB RAS, Russia. Two types of laser-induced periodic surface structures produced by ultrashort laser pulses on Cr films of different thickness have been created and explained, based on a rigorous model of plasmon polaritons and dynamics of oxidation.

SM3H.2 • 13:45

Single-Shot Few-Cycle Pulse Laser-Induced Damage and Ablation of HfO₂/SiO₂-based Optical Thin Films, Noah Talisa¹, Michael Tripepi^{1,2}, Brandon Harris¹, Abdallah AlShafey¹, Aaron Davenport³, Emmett Randel³, Carmen S. Menoni³, Enam Chowdhury¹; ¹Ohio State Univ., USA; ²Materials and Manufacturing Directorate, Air Force Research Labs, USA; ³Electrical and Computer Engineering Dept., Colorado State Univ., USA. Few-cycle pulse laser damage and ablation of HfO₂/SiO₂-based single-, double-, and quad-layer thin films are studied using time-resolved surface microscopy. Ablation of multilayer samples happens as fast as for the single-layer, indicating a "blow-out" mechanism.

SM3H.3 • 14:00 **Tutorial**

Ultrafast Laser Nanostructuring; Smart Beams for Smart Processes, Razvan Stoian¹; ¹Laboratoire Hubert Curien, CNRS Universite Jean Monnet, France. Nanoscale capability is key to a new generation of precise ultrafast laser material processing tools, relying on smart concepts using designer pulses. We review several mechanisms of laser nanostructuring, with strategies for precise 2D-3D manufacturing.

Monday, 13:30–15:30

continued on page 81

Meeting Room
211 A/B

CLEO: Applications
& Technology

13:30–15:30

AM3I • Biomedical Imaging

President: Ilko K. Ilev U.S. Food and Drug Administration; USA

AM3I.1 • 13:30

Implementation and Characterization of a Compact Multiphoton Endoscope with Large Field of View Working at 1700 nm, Farhad Akhondi¹, Yukun Qin¹, Nasser Peyghambarian¹; ¹Univ. of Arizona, USA. The implementation and characterization of a compact multi-photon endoscope is presented. A miniscule objective lens with a long working distance is used. We utilized a 1700 nm wavelength femtosecond laser to increase penetration depth.

AM3I.2 • 13:45

Reconstruction of Multiple-Scattering Complex Media by Iterative Optical Diffraction Tomography, Shengli Fan¹, Seth D. Smith-Dryden¹, Guifang Li¹, Bahaa Saleh¹; ¹CREOL, The College of Optics & Photonics, USA. We demonstrated the reconstruction of complex media beyond the weakly-scattering regime using iterative diffraction tomography. The accuracy and efficiency of the iterative reconstruction are numerically demonstrated.

AM3I.3 • 14:00 **Invited**

Optoacoustic Imaging Beyond the Diffraction Limit, X Luis Dean-Ben¹, Daniel Razansky¹; ¹Univ. and ETH Zurich, Switzerland. The talk focuses on novel super-resolution optoacoustic approaches enabling imaging beyond the diffraction limit, such as localization tomography of flowing particles, non-linear bleaching effects, dynamic speckle excitation and wavefront shaping.

Meeting Room
211 C/D

CLEO: Science & Innovations

13:30–15:30

SM3J • Silicon Photonics

President: Zhihong Huang; Hewlett Packard laboratories, USA

SM3J.1 • 13:30

Monolithically Integrated InP-on-Si Microdisk Lasers with Room-Temperature Operation, Svenja Mauthe¹, Philipp Staudinger¹, Noelia Vico Trivino¹, Marilyne Sousa¹, Thilo Stöferle¹, Heinz Schmid¹, Kirsten E. Moselund¹; ¹IBM Research Zurich, Switzerland. We present the first monolithic integration of InP microdisk room-temperature lasers on silicon by template-assisted-selective-epitaxy and compare their performance with previously demonstrated GaAs microdisk lasers. InP allows for future integration of QWs for the NIR.

SM3J.2 • 13:45

Waveguide-Integrated Dielectric Laser Particle Accelerators Through the Inverse Design of Photonics, Neil Saprà¹, Kiyoul Yang¹, Dries Verduyck^{1,2}, Logan Su¹, Jelena Vuckovic¹; ¹Ginzton Lab, Stanford Univ., USA; ²Dept. of Physics, KU Leuven, Belgium. We apply the inverse design methodology to waveguide-integrated dielectric laser particle accelerators. These accelerators are optimized to maximize the acceleration gradient. The designs have been fabricated on a silicon-on-insulator platform and experimentally characterized.

SM3J.3 • 14:00 **Invited**

New Concepts in Silicon Photonics: From Optical Communications to the Brain, Joyce K. Poon^{1,2}; ¹Univ. of Toronto, Canada; ²Max Planck Inst. for Microstructure Physics, Germany. I will present monolithically integrated multi-level silicon nitride-on-silicon photonic platforms that support 3D integrated photonic devices and circuits for telecommunications, and our recent efforts to extend this work to realize neurophotonic implants for brain activity mapping.

Meeting Room
212 A/B

CLEO: Applications
& Technology

13:30–15:30

AM3K • A&T Topical Review on Flat Optics I

President: To Be Announced

AM3K.1 • 13:30 **Invited**

New Physics and Applications with Metasurfaces, Vladimir M. Shalaev¹; ¹Purdue Univ./Birck Nanotechnology, USA. Via in-plane optical phase control, metasurfaces serve as an illustration platform for new physical phenomena including ultrafast beam steering, optical switching, synchrotron radiation, and new applications such as multiplexed color display and efficient thermo-photovoltaic generation.

AM3K.2 • 14:00

High NA Free-Space Focusing Using a Metasurface-Integrated Photonic Platform for Atom Trapping, Alexander Yulaev^{1,2}, Wenqi Zhu^{1,2}, Cheng Zhang^{1,2}, Daron Westly², Henri Lezec², Amit K. Agrawal^{1,2}, Vladimir Aksyuk²; ¹IREAP, Univ. of Maryland, USA; ²PML, National Inst. of Standards and Technology, USA. We report a compact, general photonic-to-free-space coupling via integrating metasurfaces with planar photonics. Demonstrated collimated beam projection and high numerical aperture focusing at long distance may enable trapping and interrogating atoms in chip-scale systems.

Meeting Room
212 C/D

CLEO: Science & Innovations

13:30–15:30

SM3L • Fiber Amplifiers

President: Guoqing Chang; Institute of Physics, CAS, China

SM3L.1 • 13:30 **Tutorial**

Coherent Combination of Fiber Amplified Femtosecond Pulses, Jens Limpert¹; ¹Friedrich-Schiller-Universität Jena, Germany. The presentation will review the basics, achievements and newest developments of coherent combination of amplified femtosecond pulses, a concept which has already out-performed single aperture femtosecond laser systems and which allows for a scaling to unprecedented performance levels.



Jens Limpert received his M.S in 1999 and Ph.D. in Physics from the Friedrich Schiller University of Jena in 2003. His research interests include high power fiber lasers in the pulsed and continuous-wave regime, in the near-infrared and visible spectral range. He is author or co-author of more than 350 peer-reviewed journal papers in the field of laser physics. His research activities have been awarded with the WLT-Award in 2006, an ERC starting grant in 2009 and an ERC consolidator grant in 2013. Jens Limpert is founder of the Active Fiber Systems GmbH a spin-off from the University Jena and the Fraunhofer-IOF Jena.

Joint

CLEO: Science & Innovations

13:30–15:30

JM3M • Symposium on Deep-learning Photons: Where Machine Learning & Photonics Intersect I

President: To Be Announced

JM3M.1 • 13:30 **Invited**

Integrated Photonics for Neural Network Acceleration, Folkert Horst¹; ¹IBM Research - Zurich, Switzerland. We will present our work on an analog integrated optical processor for the acceleration of Backpropagation Algorithm based training of Artificial Neural Networks.

JM3M.2 • 14:00 **Invited**

Generative Model for the Inverse Design of Photonic Nanostructures, Wenshan Cai¹; ¹Georgia Inst. of Technology, USA. We present a deep-learning enabled generative framework for the inverse design of photonic structures. When fed with customer-defined optical spectra, the network generates candidate patterns that match the on-demand spectra with high fidelity.

13:30–15:30

SM3N • Novel Optoelectronic Devices

President: Åsa Haglund, Chalmers University of Technology, Sweden

SM3N.1 • 13:30

Self-suspended Single-mode Microdisk Lasers, Wanwoo Noh¹, Matthieu Dupre¹, Abdoulye Ndao¹, Ashok Kodigala¹, Boubacar Kanté¹; ¹Univ. of California San Diego, USA. We report subwavelength microdisk resonators suspended in air by connecting bridges. By optimizing the bridge configuration, we numerically and experimentally demonstrate mode selection and single mode microdisk lasers operating at near-infrared wavelength.

SM3N.2 • 13:45

Bending-induced tunable threshold in random laser, Ya-Ju Lee¹, Ting-Wei Yeh¹, Zu-Po Yang², Yung-Chi Yao¹, Chen-Yu Chang¹, Meng-Tsan Tsai³, Jinn-Kong Sheu⁴; ¹National Taiwan Normal Univ., Taiwan; ²Inst. of Photonic System, National Chiao-Tung Univ., Taiwan; ³Dept. of Electrical Engineering, Chang Gung Univ., Taiwan; ⁴Dept. of Photonics, National Cheng Kung Univ., Taiwan. We investigate the transport mean free path of emitted photons within disordered scatterers istunable by bending substrates, thereby creating a light source able to be operated above and below threshold for desirable spectral emissions.

SM3N.3 • 14:00

Autaptic Circuits of Integrated Laser Neurons, Hsuan-Tung Peng¹, Thomas Ferreira de Lima¹, Mitchell A. Nahmias¹, Alexander N. Tait³, Bhavin J. Shastri², Paul R. Prucnal¹; ¹Princeton Univ., USA; ²Physics, Queen's Univ., Canada; ³National Inst. of Standard Technology, USA. The presence of autapses in neural networks enables complex temporal dynamics and information storage. We experimentally demonstrated feedback dynamics in an integrated laser neuron, which provides a proof-of-principle demonstration of cascability and stable recurrent memory.

13:30–15:15

SM3O • Guided Wave Nonlinear Devices

President: Shu-Wei Huang; University of Colorado, Boulder, USA

SM3O.1 • 13:30 **Invited**

Integrated Lithium Niobate Photonics and Applications, Marko Loncar^{1,2}; ¹Harvard Univ., USA; ²HyperLight Corporation, USA. I will present ultra-low loss thin film lithium niobate photonics platform that enables realization of high-Q optical cavities, efficient electro-optic modulators, and broad frequency combs. Applications in telecommunications, micro-wave-photonics, and quantum photonics will be discussed.

SM3O.2 • 14:00

Ultrabroadband Nonlinear Optics in Dispersion Engineered Periodically Poled Lithium Niobate Waveguides, Marc Jankowski¹, Carsten Langrock¹, Boris Desiatov², Alireza Marandi³, Cheng Wang², Mian Zhang², Christopher Phillips⁴, Marko Loncar², Martin Fejer¹; ¹Stanford Univ., USA; ²John A. Paulson School of Engineering and Applied Sciences, Harvard Univ., USA; ³Caltech, USA; ⁴Dept. of Physics, Inst. of Quantum Electronics, ETH Zurich, Switzerland. We experimentally demonstrate the first generation of dispersion-engineered periodically poled lithium niobate (PPLN) waveguides. These waveguides achieve ultra-broadband second-harmonic generation (SHG) and multi-octave supercontinuum generation (SCG) with record-low pulse energies.

Executive Ballroom
210A

CLEO: QELS-
Fundamental Science

FM3A • Quantum
Nanophotonics I: Plasmonics &
Quantum Dots—Continued

FM3A.4 • 14:15

Spin-Selective AC Stark Shifts in a Charged Quantum Dot, Tristan A. Wilkinson¹, Dillion Cottrill¹, Josh Cramlet¹, Cole Maurer¹, Collin Flood¹, Allan S. Bracker², Dan Gammon², Edward B. Flagg¹; ¹West Virginia Univ., USA; ²Naval Research Lab, USA. We demonstrate a spin-selective modification to the energy structure of a charged quantum dot using the AC Stark effect. This mechanism offers a potentially rapid, reversible, and coherent control of the energy structure.

FM3A.5 • 14:30 **Tutorial**

Quantum Nanophotonics: Manipulating Photons at the Subwavelength Regime, Gabriel Molina-Terriza^{1,2}; ¹IKERBASQUE, Basque Foundation for Science, Spain; ²Materials Physics Center (CSIC-UPV/EHU), Spain. I will give an overview of quantum nanophotonics. I will focus on the control of the quantum correlations of light and its applications to interacting with nanoparticles: single photon, entangled and squeezed states.



I am an Ikerbasque Research Professor leading the Quantum Nanophotonics Laboratory in the Materials Physics Center (Spain). I obtained my Ph.D. in 2002. Since then, my research is focused on the spatial properties of light, such as the angular momentum, and applications to Quantum Information, Nanophotonics and Optical levitation.

Executive Ballroom
210B

Joint

JM3B • Symposium on
Nonreciprocal Photonics II—
Continued

JM3B.3 • 14:15

Spontaneous Symmetry Breaking Based Near-Field Sensing with a Microresonator, Andreas Sveta^{1,2}, Jonathan M. Silver^{1,4}, Leonardo Del Bino^{1,3}, George Ghalanos^{1,2}, Niall Moroney^{1,2}, Michael T. M. Woodley^{1,3}, Shuangyou Zhang¹, Michael Vanner², Pascal DelHaye¹; ¹National Physical Lab, UK; ²Blackett Lab, Imperial College London, UK; ³Heriot-Watt Univ., UK; ⁴City, Univ. of London, UK. The nonlinear Kerr effect causes spontaneous symmetry breaking in bi-directionally pumped whispering gallery mode resonators, providing a system highly sensitive to external perturbations. We demonstrate symmetry-breaking-enhanced near-field sensing within a microresonator's evanescent field.

JM3B.4 • 14:30 **Invited**

Magneto-optical Garnets for Nonreciprocal Integrated Photonics, Caroline Ross¹, Takian Fakhru¹, Yan Zhang², Qungyang Du¹, Lukas Beran³, Stana Tazlaru³, Martin Veis³, Lei Bi², Juejun Hu¹; ¹MIT, USA; ²Univ. of Electronic Science and Technology of China, China; ³Charles Univ., Czechia. The magneto-optical figure of merit of polycrystalline Bi, Ce- and Tb-substituted yttrium iron garnet films on silicon and the performance of integrated TM and TE isolators based on both ring resonators and Mach-Zehnder interferometers with garnet cladding are described.

Executive Ballroom
210C

CLEO: QELS-Fundamental Science

FM3C • Functional
Nanophotonics Using
Metasurfaces—Continued

FM3C.4 • 14:30

High-Q resonance train in a plasmonic metasurface, Md Saad-Bin-Alam¹, Orad Reshef², Mikko J. Huttunen², Graham Carroll³, Brian Sullivan³, Jean-Michel Menard³, Ksenia Dolgaleva^{1,5}, Robert W. Boyd^{1,4}; ¹School of Electrical Engineering and Computer Science, Univ. of Ottawa, Canada; ²Lab of Photonics, Tampere Univ., Finland; ³Iridian Spectral Technologies Inc., Canada; ⁴The Inst. of Optics and Dept. of Physics and Astronomy, Univ. of Rochester, USA; ⁵Dept. of Physics, Univ. of Ottawa, Canada. We experimentally demonstrate a plasmonic surface that supports a series of high-quality-factor (Q~100) surface lattice resonances. These resonances are enabled by tuning the thickness of the top-cladding layer to confine higher order diffraction-orders.

FM3C.5 • 14:45

Nanoplasmonic Metamaterial Devices as Electrically Switchable Perfect Mirrors and Perfect Absorbers, Debabrata Sikdar^{1,2}, Ye Ma¹, Anthony Kucernak¹, Joshua Edel¹, Alexei Kornyshev¹; ¹Imperial College London, UK; ²EEE, Indian Inst. of Technology guwahati, India. We introduce nanoplasmonic metamaterial devices — electrically-switchable between perfect-mirror/absorber states — based on voltage-controlled assembly/disassembly of gold nanoparticles on silver films. These are investigated using effective-medium-theory, verified with simulations and experiments.

Executive Ballroom
210D

FM3D • Ultrafast Coherent
Spectroscopy—Continued

FM3D.4 • 14:15

Ultrafast Analysis and Control of Sub-Nanosecond Intra-band Coherence in Single CdSe/ZnSe Quantum Dots, Christian Traum¹, Philipp Henzler¹, David Nabben¹, Matthias Holtkemper², Doris E. Reiter², Tilmann Kuhn², Denis Seletskiy^{1,3}, Alfred Leitenstorfer¹; ¹Dept. of Physics and Center for Applied Photonics, Univ. of Konstanz, Germany; ²Solid State Theory, Univ. of Münster, Germany; ³Dept. of Engineering Physics, Polytechnique Montréal, Canada. Excited trion triplet states are studied with two-color femtosecond resolution monitoring induced absorption into charged biexciton levels. Quantum beats of single-electron wave packets with sub-nanosecond dephasing are found and controlled by pump and probe polarizations.

FM3D.5 • 14:30

Polarization-Selective Excitation of Triplet State Coherences in CsPbI3 Perovskite Nanocrystals, Albert Liu¹, Diogo B. Almeida², Luiz Bonato³, Gabriel Nagamine², Luiz Zaganel², Ana F. Nogueira³, Lazaro A. Padilha², Steven T. Cundiff¹; ¹Univ. of Michigan, USA; ²Instituto de Física, Universidade Estadual de Campinas, Brazil; ³Instituto de Química, Universidade Estadual de Campinas, Brazil. We study CsPbI3 perovskite nanocrystals using polarization-resolved 2D coherent spectroscopy at cryogenic temperatures. Coherences involving triplet exciton states are revealed and characterized, including inter-triplet coherences with dephasing times on the picosecond timescale.

FM3D.6 • 14:45

Ultrafast Carrier Dynamics in Graphite Studied by Visible/Multi-THz 2D Spectroscopy, Jonas Allerbeck¹, Laurens Spitzner¹, Takayuki Kurihara¹, Alfred Leitenstorfer¹, Daniele Brida^{2,1}; ¹Dept. of Physics and Center for Applied Photonics, Univ. of Konstanz, Germany; ²Physics and Materials Science Research Unit, Université du Luxembourg, Luxembourg. Two-dimensional spectroscopy employing an asymmetric scheme with visible excitation and multi-THz readout is applied to study ultrafast carrier dynamics in graphite, enabling phase sensitive investigation of correlations between high- and low-energy excitations.

Monday, 13:30–15:30

Joint

CLEO: Science & Innovations

JM3E • Symposium on High Average Power Ultrafast Lasers: Trends, Challenges & Applications III—Continued

SM3F • Hot Topics in Quantum Sensing—Continued

SM3G • Data Center Lightwave Communications—Continued

SM3H • Fundamentals of Ultrafast Light Matter Interaction—Continued



Razvan Stoian (MSc Bucharest University, PhD Free University Berlin) is research director at the Centre Nationale de la Recherche Scientifique France. He is leading the Laser-Matter Interaction group at Laboratoire Hubert Curien, St. Etienne. His research interests include laser matter interaction and ultrafast laser micro-nano fabrication for functional surfaces and photonics.

JM3E.3 • 14:30 **Invited**
Industrial kilowatt femtosecond lasers: potentialities and challenges, Clemens Hoenninger¹, Julien Pouysegur¹, Benoit Tropheime¹, Florent Basin¹, Martin Delaigue¹, Jorge Sanabria¹, Guillaume Bonamis¹, Konstantin M. mishchik¹, Eric Audouard¹, Eric Mottay¹; ¹*Amplitude, France*. High throughput micromachining fuels the trend towards kilowatt femtosecond lasers. We present and discuss the potentialities offered as well as challenges to address, including advanced temporal, spectral, and spatial beam shaping.

SM3F.3 • 14:30
Rydberg-Atoms Based Radio-Frequency Electric Field and Power Sensors for Quantum SI-Traceable Measurements, Christopher L. Holloway¹, Matthew Simons¹, Joshua Gordon¹; ¹*NIST, USA*. We discuss a fundamentally new method for electric (E) field strength (V/m) and power (W) metrology based on the interaction of radio-frequency (RF) E-fields with Rydberg atoms (alkali atomic vapor excited optically to Rydberg states).

SM3G.2 • 14:30
FlexLION: A Reconfigurable All-to-All Optical Interconnect Fabric with Bandwidth Steering, Roberto Proietti¹, Gengchen Liu¹, Xian Xiao¹, Sebastian Werner¹, Pouya Fotouhi¹, S.J. Ben Yoo¹; ¹*Univ. of California Davis, USA*. We demonstrate an all-to-all interconnect fabric with bandwidth steering by wavelength routing, wavelength add/drop filtering and spatial switching. We report a proof-of-concept experiment and demonstrate scalability up to 32 ports with aggregated bandwidth of 51.2Tb/s under worst-case crosstalk.

SM3F.4 • 14:45
Atomic cladded waveguide for chip scale stabilization and modulation of telecom wavelengths, Roy T. Zektzer¹, Eliran Talker¹, Yefim Barash¹, Noa Mazurski¹, Uriel Levy¹; ¹*The Hebrew Univ. of Jerusalem, Israel*. We experimentally demonstrate a chip-scale integration of photonic waveguides and alkali vapor for frequency reference and modulation. A telecom signal was stabilized to rubidium ladder transition and was modulated by a 780nm pump laser.

SM3G.3 • 14:45
Demonstration of Kramers-Kronig Detection of Four 20-Gbaud 16-QAM Channels after 50-km Transmission Using Kerr Combs to Perform Shared Phase Estimation, Kaiheng Zou¹, Peicheng Liao¹, Changjing Bao¹, Yinwen Cao¹, Arne Korodts², Ahmed Almainan^{1,3}, Maxim Karpov², Martin Pfeiffer², Fatemeh Alishahi¹, Ahmad Fallahpour¹, Moshe Tur⁴, Tobias J. Kippenberg², Alan E. Willner¹; ¹*Univ. of Southern California, USA*; ²*Ecole Polytechnique Federale de Lausanne, Switzerland*; ³*King Saud Univ., Saudi Arabia*; ⁴*Tel Aviv Univ., Israel*. We experimentally demonstrate KK detection of four 20-Gbaud 16-QAM channels after 50-km transmission using two soliton Kerr combs at transmitter and receiver. The frequency comb coherence enables a shared phase noise estimation among multiple channels.

Meeting Room
211 A/B

CLEO: Applications
& Technology

AM3I • Biomedical Imaging—
Continued

Meeting Room
211 C/D

CLEO: Science &
Innovations

SM3J • Silicon Photonics—
Continued

Meeting Room
212 A/B

CLEO: Applications
& Technology

AM3K • A&T Topical Review on
Flat Optics I—Continued

Meeting Room
212 C/D

CLEO: Science &
Innovations

SM3L • Fiber Amplifiers—
Continued

AM3I.4 • 14:30 **Invited**
Second Harmonic Generation Probes of Human Ovarian Cancer, Paul J. Campagnola¹, Eric Rentchler¹, Manish Patankar¹, Kirby Campbell¹; ¹Univ. of Wisconsin-Madison, USA. We use Second Harmonic Generation microscopy to characterize extracellular matrix changes in human ovarian cancers. Texture analysis and polarization resolved techniques differentiate a spectrum of tumors based on alterations in fibrillar organization and supramolecular structure.

SM3J.4 • 14:30
Efficient Telecom-to-Visible Spectral Translation Using Silicon Nanophotonics, Xiyuan Lu^{1,2}, Gregory Moille^{1,2}, Qing Li^{1,3}, Daron Westly¹, Ashotosh Rao^{1,2}, Su-Peng Yu¹, Travis C. Briles¹, Scott B. Papp¹, Kartik Srinivasan¹; ¹NIST, USA; ²Univ. of Maryland College Park, USA; ³Carnegie Mellon Univ., USA. We demonstrate efficient spectral translation of a continuous-wave optical signal across 250 THz using cavity-enhanced four-wave mixing on a silicon nanophotonics chip, with up to 12.8 % photon number efficiency achieved for sub-mW pump power.

SM3J.5 • 14:45
Experimental demonstration of rapid adiabatic couplers, Josep Fargas Cabanillas¹, Hayk Harutyunyan¹, Anatol Khilo¹, Milos Popovic¹; ¹ECE, Boston Univ., USA. We experimentally demonstrate rapid adiabatic coupling (RAC), a novel design concept that harnesses the benefits and avoids the disadvantages of adiabatic photonic structures. The 31um long 2x2 coupler shows 3±0.3dB splitting over 130nm bandwidth.

AM3K.3 • 14:15
Reconfigurable mid-infrared optical elements using phase change materials, Xinghui Yin¹, Christina Spagele¹, Michele Tamagnone¹, Kundan Chaudhary¹, Stefano Oscurato¹, Jiahan Li², Ruoping Li¹, Noah Rubin¹, Luis Jauregui¹, Philip Kim¹, James Edgar², Antonio Ambrosio¹, Federico Capasso¹; ¹Harvard Univ., USA; ²Chemical Engineering, Kansas State Univ., USA. Reconfigurable optical elements using the phase change material Ge₂Sb₂Te₅ are demonstrated for freely propagating light as well as phonon polaritons in hexagonal boron nitride.

AM3K.4 • 14:30 **Invited**
Nonlinear and topological meta-optics and metasurfaces, Yuri S. Kivshar^{1,2}; ¹Australian National Univ., Australia; ²ITMO Univ., Russia. This talk will summarize the major concepts of all-dielectric Mie-resonant meta-optics, including nanophotonic structures and metasurfaces. It will present also recent advances from my groups in Canberra and St. Petersburg on dielectric nanophotonics as well as nonlinear and topological metasurfaces.

SM3L.2 • 14:30
100-W Average-Power Femtosecond Fiber Laser System with Variable Parameters for Rapid Optimization of Laser Processing, Dai Yoshitomi¹, Hideyuki Takada¹, Kenji Torizuka¹, Yohei Kobayashi²; ¹Natl Inst of Adv Industrial Sci & Tech, Japan; ²Inst. Solid State Physics, Univ. Tokyo, Japan. We developed a femtosecond fiber-laser system delivering an average power up to 100 W with wide variability of parameters: pulse duration, pulse energy, number of pulses, and repetition rate for rapid optimization of laser processing.

SM3L.3 • 14:45
Pre-Chirp Managed Amplification of Circularly Polarized Pulses Using chirped Mirrors for Pulse Compression, Hangdong Huang², Yao Zhang², Hao Teng¹, Shaobo Fang¹, Junli Wang², Jiangfeng Zhu², Guoqing Chang¹, Zhiyi Wei¹; ¹Chinese Academy of Sciences, China; ²Xi dian Univ., China. We demonstrate an Yb-fiber based pre-chirp managed amplification system that amplifies circularly polarized pulses. Using chirped mirrors as the highly efficient (98%) compressor, the system emits 50-MHz, 42-fs pulses with 83-W average power.

JM3M • Symposium on Deep-learning Photons: Where Machine Learning & Photonics Intersect I—Continued

JM3M.3 • 14:30 **Invited**
Multiwavelength Neuromorphic Photonics, Paul R. Prucnal¹, Alexander N. Tait¹, Mitchell A. Nahmias¹, Thomas Ferreira de Lima¹, Hsuan-Tung Peng¹, Bhavin J. Shastri²; ¹Princeton Univ., USA; ²Dept. of Physics, Engineering Physics & Astronomy, Queen's Univ., Canada. Neuromorphic photonics promises orders of magnitude improvements in both speed and energy efficiency over digital electronics. We will give an overview of neuromorphic photonic systems and their application to optimization and machine learning problems.

SM3N • Novel Optoelectronic Devices—Continued

SM3N.4 • 14:15
Blue Superluminescent Diodes with GHz Bandwidth Exciting Perovskite Nanocrystals for High CRI White Lighting and High-Speed VLC, Abdullah Al-atawi^{1,2}, Jorge A. Holguin-Lerma¹, Chun Hong Kang¹, Chao Shen¹, Ibrahim Dursun¹, Lutfan Sinatra³, Abdulrahman albadri², Ahmad Alyamani², Tien Khee Ng¹, Osman Bakr¹, Boon S. Ooi¹; ¹King Abdullah Univ of Sci & Technology, Saudi Arabia; ²National Center for Nanotechnology, King Abdulaziz City for Science and Technology, Saudi Arabia; ³Quantum Solutions LLC, Saudi Arabia. A 442-nm GaN-based superluminescent diode (SLD) is demonstrated with a GHz modulation bandwidth and a linewidth of 7 nm. When use for exciting CsPbBr₃-perovskite nanocrystal-phosphor, warm-white light with a high CRI of 91 was achieved.

SM3N.5 • 14:30
Wideband Self-injection-locked Green Tunable Laser Diode, Md. Hosne Mobarok Shamim¹, Tien Khee Ng², Boon S. Ooi², Mohammed Zahed Mustafa Khan¹; ¹King Fahd Univ. of Petroleum & Mine, Saudi Arabia; ²Computer, Electrical and Mathematical Sciences and Engineering (CEMSE) division, King Abdullah Univ. of Science & Technology (KAUST), Saudi Arabia. A wideband tunability of 6.53 nm with appreciable SMSR (>10 dB) and linewidth (~0.1 nm) is demonstrated from a simple and low-cost tunable self-injection locked InGaN/GaN green laser based external-cavity system, for the first time.

SM3N.6 • 14:45
12.5-GHz InP Quantum Dot Monolithically Mode-Locked Lasers Emitting at 740 nm, Zhibo Li¹, Samuel Shutts¹, Craig Allford¹, Andrey Krysa², Peter Smowton¹; ¹School of Physics and Astronomy, Cardiff Univ., UK; ²Univ. of Sheffield, UK. Monolithic InP/GaN quantum dot passively mode-locked lasers, designed using gain and absorption measurements, are realised for the first time, emitting at 740 nm with 12.5 GHz repetition frequency.

SM3O • Guided Wave Nonlinear Devices—Continued

SM3O.3 • 14:15
Quadratic Cavity Soliton Optical Frequency Combs, Tobias Hansson^{1,2}, P. Parra-Rivas^{3,5}, F. Leo³, M. Bernard², L. Gelens⁵, Stefan Wabnitz^{4,2}; ¹Linköping Univ., Sweden; ²Univ. of Brescia, Italy; ³Free Univ. of Brussels, Belgium; ⁴Sapienza Università di Roma, Italy; ⁵Univ. of Leuven, Belgium. We theoretically demonstrate, in the absence of a temporal walk-off, the existence of both bright and dark coherent cavity soliton optical frequency combs in a dispersive second-harmonic generation cavity system.

SM3O.4 • 14:30
Frequency comb generation in a continuous-wave pumped second-order nonlinear waveguide resonator, Zeina Abdallah¹, Michael Stefszky², Ville Ulvila^{3,4}, Christine Silberhorn², Markku M. Vainio^{3,1}; ¹Lab of Photonics, Tampere Univ. of Technology, Finland; ²Integrated Quantum Optics, Applied Physics, Paderborn Univ., Germany; ³Molecular Science, Dept. of Chemistry, Univ. of Helsinki, Finland; ⁴VTT Technical Research Centre of Finland Ltd, Finland. Optical frequency comb generation has been experimentally studied using an integrated system based on a lithium niobate waveguide resonator featuring a strong quadratic nonlinearity. Our theoretical model shows good agreement with the experimental results.

SM3O.5 • 14:45
Wafer-scale GaAs-on-insulator Waveguide Platform for Diverse Nonlinear Processes, Eric J. Stanton¹, Jeff Chiles¹, Nima Nader¹, Sae Woo Nam¹, Richard P. Mirin¹; ¹Applied Physics Division, National Inst. of Standards and Technology, USA. We detail a 76 mm wafer-bonding process for high-yield GaAs-on-insulator waveguides. Second-harmonic generation waveguides are designed with 120 W⁻¹cm⁻² conversion efficiency, and a microresonator is demonstrated with a 180,000 quality factor.

Executive Ballroom
210A

CLEO: QELS-
Fundamental Science

FM3A • Quantum Nanophotonics I: Plasmonics & Quantum Dots—Continued

Executive Ballroom
210B

Joint

JM3B • Symposium on Nonreciprocal Photonics II—Continued

JM3B.5 • 15:00
Strong-Magneto Optical Response Enabled by Quantum Two-Level Systems, Lei Ying¹, Ming Zhou¹, Zongfu Yu¹; ¹Univ. of Wisconsin-Madison, USA. By tailoring the resonant interplay between quantum two-level systems and classical metallic nanostructures, we theoretically propose a composite material system that exhibits an intrinsic magneto-optical response orders of magnitude stronger than most magneto-optical materials used today.

JM3B.6 • 15:15
Observation of the nonreciprocal adiabatic geometric phase in nonlinear optics, Aviv Karnieli¹, Sivan Trajtenberg-Mills¹, Giuseppe Di Dominico¹, Ady Arie¹; ¹TAU, Israel. We demonstrate both theoretically and experimentally, a robust scheme that generates an adiabatic geometric phase via frequency conversion. By tailoring nonlinear photonic crystals we create nonlinear geometric phase plates which also exhibit optical nonreciprocity.

Executive Ballroom
210C

CLEO: QELS-Fundamental Science

FM3C • Functional Nanophotonics Using Metasurfaces—Continued

FM3C.6 • 15:00
Deep subwavelength plasmonic metamaterial absorbers for infrared detection, Junyu Li¹, Haoran Zhou¹, Fei Yi^{1,2}; ¹Huazhong Univ. of Science and Technology, China; ²Shenzhen Huazhong Univ. of Science and Technology Research Inst., China. Here we report a metal-insulator-metal based infrared plasmonic metamaterial absorber consisting of deep subwavelength meander line nanoantennas. High absorption from 11 μm to 14 μm is experimentally demonstrated with a pixel pitch of 1.47 μm .

FM3C.7 • 15:15
Reconfigurable Dispersion Compensation and Pulse Shaping by Optical Metasurfaces, Wenqi Zhu^{2,1}, Shawn Divitt^{2,1}, Cheng Zhang^{2,1}, Lu Chen², Henri Lezec², Amit K. Agrawal^{2,1}; ¹Univ. of Maryland College Park, USA; ²National Inst. of Standards and Technology, USA. Metasurfaces offer the ability to control optical dispersion with extreme resolution. Here, we demonstrate reconfigurable dispersion control of ultrafast laser pulses through a set of silicon metasurfaces forming a Taylor series expansion in optical phase.

Executive Ballroom
210D

FM3D • Ultrafast Coherent Spectroscopy—Continued

FM3D.7 • 15:00
Terahertz Near-Field Nano-Spectroscopy of Antiferromagnetic Resonance, Richard H. Kim¹, Yilong Luan¹, Zhe Fei¹, Jigang Wang¹; ¹Iowa State Univ., USA. We developed a terahertz scanning near-field nanoscope to visualize the spectral-temporal responses of antiferromagnetic modes in $\text{Sm}_{0.4}\text{Er}_{0.6}\text{FeO}_3$. Our results demonstrate the first detection of collective spin precession at the femtosecond and nanometer scales.

FM3D.8 • 15:15
Strong Coupling of Light with Collective Terahertz Vibrations in Organic Materials, Ran Damari^{1,2}, Omri Weinberg¹, Natalia Demina¹, Katherine Akulov^{1,2}, Daniel Krotkov^{1,2}, Sharly Fleischer^{1,2}, Tal Schwartz^{1,2}; ¹Physical Chemistry Dept., Tel-Aviv Univ., Israel; ²Tel Aviv Center for Light-Matter Interaction, Tel Aviv Univ., Israel. We demonstrate for the first time strong coupling between a terahertz cavity and collective, intermolecular vibrations in organic crystals. Beyond observing the Rabi splitting, we directly measure the vacuum Rabi oscillations using time-domain THz spectroscopy.

14:30–16:00 **Deliberate Mentoring to Advance Your Career: Special Flash Mentoring Session**, *Guadalupe Room, San Jose Marriott*

15:30–16:00 **Coffee Break**, *Concourse Level*

16:00–17:00 **Resumes, LinkedIn, and Networking (with Cheeky Scientist)**, *University Room, Hilton San Jose*

16:00–17:30 **Professional Development for Busy Professionals**, *Salon VI, San Jose Marriott*

Monday, 13:30–15:30

Joint

CLEO: Science & Innovations

JM3E • Symposium on High Average Power Ultrafast Lasers: Trends, Challenges & Applications III—Continued

JM3E.4 • 15:00

1 MHz Ultrafast High Order Cascaded VUV Generation in Negative Curvature Hollow Fibers, Jessica Ramirez¹, David Couch², Daniel Hickstein¹, Mathew Kirchner¹, Henry Kapteyn^{1,2}, Margaret M. Murnane^{2,1}, Sterling J. Backus^{1,2}; ¹KMLabs, USA; ²JILA, Univ. of Colorado, USA. We demonstrate cascaded harmonic generation to 9th harmonic (115nm) of 1040nm by combining the fundamental and SHG in a negative curvature hollow fiber filled with Xenon gas.

SM3F • Hot Topics in Quantum Sensing—Continued

SM3F.5 • 15:00 Invited

Point Source Atom Interferometry for Inertial Navigation and Precision Measurements, Yun-Jih Chen^{1,2}, Azure Hansen¹, John Kitching¹, Elizabeth A. Donley¹; ¹National Inst. of Standards and Technology, USA; ²Univ. of Colorado, USA. We evaluate the technique of point source atom interferometry as a relatively simple approach for building an atom interferometer gyroscope. A sensitivity evaluation for simultaneous measurements of acceleration, rotation, and rotation angle will be presented.

SM3G • Data Center Lightwave Communications—Continued

SM3G.4 • 15:00

8-ary Stokes-Vector Signal Generation and Transmission Employing a Simplified Transmitter, Samir Ghosh², Shota Ishimura^{2,1}, Takahiro Suganuma², Takuo Tanemura², Yoshiaki Nakano²; ¹KDDI Research, Inc., Japan; ²School of Engineering, The Univ. of Tokyo, Japan. We experimentally demonstrate a simple straight-line configuration of Stokes vector modulator with two cascaded phase modulators. Three-dimensional 8-ary Stokesvector-modulated signal is generated at 30 Gb/s and transmitted over a 50-km dispersioncompensated single-mode fiber.

SM3G.5 • 15:15

Iterative Block Decision Feedback Equalization for IM/DD-OCDM System to Mitigate CD-Induced Fading, Xing Ouyang¹, Giuseppe Talli¹, Paul Townsend¹; ¹Photonics Center, Tyndall National Inst., Ireland. We propose an IM/DD-OCDM system with IB-DFE algorithm to mitigate chromatic-dispersion-induced fading and the results confirm that the BER performance can be improved by up to three orders of magnitude by compensating the fading effect.

SM3H • Fundamentals of Ultrafast Light Matter Interaction—Continued

SM3H.4 • 15:00

Femtosecond-laser ablation of monolayer molybdenum disulfide (MoS₂) on sapphire, Joel M. Solomon¹, Hsin-Yu Yao², Li-Syuan Lu³, Wen-Hao Chang³, Tsing-Hua Her¹; ¹Dept. of Physics and Optical Science, The Univ. of North Carolina at Charlotte, USA; ²Dept. of Physics, National Tsing Hua Univ., Taiwan; ³Dept. of Electrophysics, National Chiao Tung Univ., Taiwan. Single-shot femtosecond laser ablation of monolayer molybdenum disulfide is demonstrated. An ablation threshold was found 0.9 nJ/μm², which is too low for two-photon photoionization alone. We show that surface defects and avalanche ionization are important.

SM3H.5 • 15:15

Femtosecond Laser Ablation of Monolayer Graphene with Analysis of the Structural Deformations, Andres Vasquez¹, Mohammad Alaghemandi¹, Junjie Zeng¹, Panagis Samolis¹, Adam Sapp¹, Sahar Sharifzadeh¹, Michelle Y. Sander¹; ¹Boston Univ., USA. Experimental femtosecond laser ablation of graphene at a high repetition rate of 80 MHz with moderate pulse energies up 27.5 nJ is analyzed and structural deformations studied by reactive molecular dynamics simulations.

14:30–16:00 Deliberate Mentoring to Advance Your Career: Special Flash Mentoring Session, Guadalupe Room, San Jose Marriott

15:30–16:00 Coffee Break, Concourse Level

16:00–17:00 Resumes, LinkedIn, and Networking (with Cheeky Scientist), University Room, Hilton San Jose

16:00–17:30 Professional Development for Busy Professionals, Salon VI, San Jose Marriott

Meeting Room
211 A/B

CLEO: Applications
& Technology

AM3I • Biomedical Imaging—
Continued

AM3I.5 • 15:00

Ultra-high-resolution single input state polarization-sensitive OCT with polarization distortion correction, Qiaozhou Xiong¹, Nanshuo Wang¹, Xinyu Liu¹, Si Chen¹, Shufen Chen¹, Haitao Liang¹, Linbo Liu^{1,2}; ¹School of Electrical and Electronic Engineering, Nanyang Technological Univ., Singapore; ²School of Chemical and Biomedical Engineering, Nanyang Technological Univ., Singapore. In an ultra-high-resolution single input PS-OCT, we proposed a method for correcting polarization distortion caused by Quarter-wave plate (QWP) and spectrometers' roll-off mismatch. The method yielded better estimation of polarization properties especially in weakly birefringent samples.

AM3I.6 • 15:15

Fast Two-snapshot Structured Illumination for Wide-field Two-photon Microscopy with Enhanced Axial Resolution and Signal-to-noise Ratio, Yunlong Meng¹, Wei Lin¹, Jialong Chen¹, Chenglin Li¹, Shih-Chi Chen¹; ¹Dept. of Mechanical and Automation Engineering, The Chinese Univ. of Hong Kong, Hong Kong. We have developed a fully adaptive fast two-snapshot structured illumination algorithm for fast data acquisition and image reconstruction, which can be used in wide-field two-photon microscopy with enhanced axial resolution (~1.25x) and signal-to-noise ratio.

Meeting Room
211 C/D

CLEO: Science & Innovations

SM3J • Silicon Photonics—
Continued

SM3J.6 • 15:00

Efficient Conversion to Very High Order Modes in Silicon Waveguides, Utsav D. Dave¹, Michal Lipson¹; ¹Electrical Engineering, Columbia Univ., USA. We demonstrate robust mode conversion up to the 12th higher order mode in silicon waveguides by using an optimized adiabatic directional coupler and using subwavelength waveguides. The conversion efficiency is better than -1.5 dB over a 75 nm bandwidth and tolerating ±30 nm fabrication variations.

SM3J.7 • 15:15

SOI Optical Add-Drop Multiplexers Using Apodized Spiral Contra-Directional Couplers, Mustafa Hammood¹, Stephen Lin¹, Ajay Mistry¹, Minglei Ma¹, Lukas Chrostowski¹, Nicolas Jaeger¹; ¹Univ. of British Columbia, Canada. We use long, spiral contra-directional couplers (contra-DCs) to make optical add-drop filters with 30 dB extinction ratios and 12.2 nm bandwidths, and avoid some of the effects caused by fabrication non-uniformities in long, straight contra-DCs.

Meeting Room
212 A/B

CLEO: Applications
& Technology

AM3K • A&T Topical Review on
Flat Optics I—Continued

AM3K.5 • 15:00 **Invited**

Optical Power Limiters Based on Intersubband Polaritonic Metasurfaces, Nishant Nookala¹, Sander Mann², Ahmed Mekawy², John F. Klem³, Igal Brener³, Andrea Alu², Mikhail A. Belkin¹; ¹Univ. of Texas at Austin, USA; ²Advanced Science Research Center, City Univ. of New York, USA; ³Sandia National Labs, USA. We present a novel class of power limiting polaritonic metasurfaces exploiting saturable intersubband absorption in semiconductor quantum wells coupled to plasmonic resonators. Power limiting is experimentally verified and the metasurface performance limits are theoretically analyzed.

Meeting Room
212 C/D

CLEO: Science & Innovations

SM3L • Fiber Amplifiers—
Continued

SM3L.4 • 15:00

620 nm Source by Second Harmonic Generation of a Phosphosilicate Raman Fiber Amplifier, Anita M. Chandran¹, Timothy H. Runcorn¹, Robert T. Murray¹, James R. Taylor¹; ¹Imperial College London, UK. We demonstrate a nanosecond-pulsed 620 nm source through frequency doubling a 1240 nm phosphosilicate Raman fiber amplifier. The source emits up to 213 mW of average power, and is repetition rate and pulse duration tunable.

SM3L.5 • 15:15

All-fiber polarization maintaining Thulium doped amplifier seeded by coherent polarized supercontinuum, Anupama Rampur^{1,2}, Grzegorz Stepniewski¹, Dominik Dobrakowski^{1,2}, Yuriy Stepanenko³, Alexander Heidt⁴, Thomas Feurer⁴, Mariusz Klimczak^{3,2}; ¹Inst of Electronic Materials Technology, Poland; ²Faculty of Physics, Univ. of Warsaw, Poland; ³Laser Center, Inst. of Physical Chemistry, Polish Academy of Sciences, Poland; ⁴Inst. of Applied Physics, Univ. of Bern, Switzerland. Coherently seeded, broadband ultrafast thulium fiber amplifier is demonstrated. Its architecture comprises only polarization-maintaining fibers. Preliminary results show amplification of 2 nJ, 5.5ps long, 100 nm (3dB) pulses centered at 1900 nm before recompression.

14:30–16:00 Deliberate Mentoring to Advance Your Career: Special Flash Mentoring Session, *Guadalupe Room, San Jose Marriott*

15:30–16:00 Coffee Break, *Concourse Level*

16:00–17:00 Resumes, LinkedIn, and Networking (with Cheeky Scientist), *University Room, Hilton San Jose*

16:00–17:30 Professional Development for Busy Professionals, *Salon VI, San Jose Marriott*

**JM3M • Symposium on Deep-learning
Photons: Where Machine Learning &
Photonics Intersect I—Continued****JM3M.4 • 15:00**

Optimization of Nonlinear Nanophotonic Media for Artificial Neural Inference, Erfan Khoram¹, Ang Chen¹, Dianjing Liu¹, Qiqi Wang², Ming Yuan³, Zongfu Yu¹; ¹Univ. of Wisconsin-Madison, USA; ²MIT, USA; ³Columbia Univ., USA. We show optical waves passing through a nanophotonic medium can perform artificial neural computing. Such a medium exploits linear and nonlinear scatterers to realize complex input-output mapping far beyond the capabilities of traditional nanophotonic devices.

JM3M.5 • 15:15

PhaseStain: Deep Learning-based Histological Staining of Quantitative Phase Images, Yair Rivenson¹, Tairan Liu¹, Zhensong Wei¹, Kevin de Haan¹, Yibo Zhang¹, Aydogan Ozcan¹; ¹Univ. of California Los Angeles, USA. We demonstrate a digital staining framework that transforms quantitative phase images of label-free tissue sections to match the brightfield microscopy images of the same sections, after histological staining. Inference of multiple tissue-stain combinations is demonstrated.

**SM3N • Novel Optoelectronic Devices—
Continued****SM3N.7 • 15:00**

Dual-wavelength operation of the GaSb-based diode lasers with asymmetric coupled quantum wells, Jiang Jiang¹, Leon Shterengas¹, Takashi Hosoda¹, Aaron Stein², Alexey Belyanin³, Gela Kipshidze¹, Gregory Belenky¹; ¹Stony Brook Univ., USA; ²Center for Functional Nanomaterials, Brookhaven National Lab, USA; ³Physics, Texas A&M Univ., USA. The DBR diode lasers with asymmetric tunnel coupled quantum wells having built-in resonant second order nonlinearity were designed and fabricated. The devices can generate comparable power in two bands near 2 μm separated by ~ 13 meV as required for intracavity difference frequency generation.

SM3N.8 • 15:15

Optically-feedbacked mode-locked laser diode for tunable narrow-linewidth photonic millimeter-wave generation, Huan Wang¹, Lu Guo¹, Wu Zhao¹, Guangcan Chen¹, Dan Lu¹, Lingjuan Zhao¹; ¹Inst. of Semiconductors, Chinese Academy of Science, China. A tunable narrow-linewidth photonic millimeter-wave generation scheme is demonstrated by using a mode-locked laser diode with optical feedback. Photonic mode beating signal tunable from 42GHz to 293GHz with a linewidth of several kHz is obtained.

**SM3O • Guided Wave Nonlinear Devices—
Continued****SM3O.6 • 15:00**

Direct Mode-Frequency Control for Nonlinear Optics in Photonic-Crystal Ring Resonators, Su-Peng Yu^{1,2}, Hojoong Jung^{1,2}, Travis C. Briles^{1,2}, David Carlson¹, Gregory Moille³, Xiyuan Lu³, Kartik Srinivasan³, Scott B. Papp^{1,2}; ¹Time and Frequency Division, NIST Boulder, USA; ²Physics, Univ. of Colorado Boulder, USA; ³Center for Nanoscale Science and Technology, NIST Gaithersburg, USA. We demonstrate that photonic-crystal modulation enables individual mode-frequency shifting in ring resonators, and high quality factor. Simulation predicts frequency-comb generation in normal-dispersion resonators and spontaneous pulse formation in both dispersion types.

14:30–16:00 **Deliberate Mentoring to Advance Your Career: Special Flash Mentoring Session**, *Guadalupe Room, San Jose Marriott*

15:30–16:00 **Coffee Break**, *Concourse Level*

16:00–17:00 **Resumes, LinkedIn, and Networking (with Cheeky Scientist)**, *University Room, Hilton San Jose*

16:00–17:30 **Professional Development for Busy Professionals**, *Salon VI, San Jose Marriott*

CLEO: QELS-Fundamental Science

16:00–18:00

FM4A • Quantum Nanophotonics II: Diamond & Boron Nitride

President: Glenn Solomon; Joint Quantum Institute, USA

FM4A.1 • 16:00

Quantum Optics with Tin-Vacancy Emitters in Diamond, Matthew Trusheim¹, Benjamin Pingault², Noel Wan¹, Mustafa Gundogan², Lorenzo de Santis¹, Kevin Chen¹, Mete Atature², Dirk R. Englund¹; ¹MIT, USA; ²Cavendish Lab, Univ. of Cambridge, UK. We investigate the quantum optical properties of single tin-vacancy emitters in diamond through resonant magneto-optical spectroscopy at 4 K. We find radiative lifetime-limited optical transitions associated with long-lived spin states.

FM4A.2 • 16:15

Optical Characterization of Single Tin-Vacancy Centers in Diamond Nanopillars, Alison E. Rugar¹, Constantin Dory¹, Shuo Sun¹, Jelena Vuckovic¹; ¹Stanford Univ., USA. We characterize the optical and spin properties of tin-vacancy centers isolated in diamond nanopillars. We measure spectrometer-limited linewidths <15 GHz, a strong polarization dependence of the emission, and Zeeman splitting behavior consistent with previous theoretical predictions.

FM4A.3 • 16:30 **Invited**

Control and Stabilization of Nitrogen-Vacancy Centers in Photonic Circuits, Kai-Mei Fu¹; ¹Univ. of Washington, USA. We present our results integrating near-surface nitrogen-vacancy (NV) centers into gallium phosphide (GaP) photonic circuits toward photon-mediated spin-spin entanglement.

16:00–18:00

FM4B • Topological Photonics II

President: Zubin Jacob; Purdue University, USA

FM4B.1 • 16:00

Depopulation of Edge States under Local Periodic Driving despite Topological Protection, Christina I. Jörg¹, Zlata Cherpakova², Christoph Dauer¹, Fabian Letscher^{1,3}, Michael Fleischhauer¹, Sebastian Eggert¹, Stefan Linden², Georg von Freymann^{1,4}; ¹Physics, TU Kaiserslautern, Germany; ²Physikalisches Institut, Universität Bonn, Germany; ³Graduate School Materials Science in Mainz, Germany; ⁴Fraunhofer Inst. for Industrial Mathematics ITWM, Germany. We show that edge states can be depopulated despite their topological protection. Local time-periodic driving results in hybridization of edge and bulk states for certain driving frequencies. Experiments are performed using plasmonic and dielectric waveguides.

FM4B.2 • 16:15

Demonstration of a Photonic Topological Z2-Insulator, Lukas Maczewsky¹, Bastian Höckendorf², Mark Kremer¹, Tobias Biesenthal¹, Matthias Heinrich¹, Andreas Alvermann², Holger Fehske², Alexander Szameit¹; ¹Inst. of Physics, Univ. of Rostock, Germany; ²Inst. of Physics, Univ. of Greifswald, Germany. We introduce a photonic topological Floquet Z2-insulator with fermionic time reversal symmetry (TRS). Our experiments demonstrate the characteristic protected counter-propagating edge modes and unequivocally prove the presence of fermionic TRS in this bosonic system.

FM4B.3 • 16:30

Supersymmetric transformations of photonic topological systems, Gerard Queralto Isach¹, Mark Kremer², Matthias Heinrich², Verónica Ahufinger¹, Jordi Mompart¹, Alexander Szameit²; ¹Universitat Autònoma de Barcelona, Spain; ²Universität Rostock, Germany. We explore the interplay between supersymmetry and topology by applying supersymmetric transformations to a photonic lattice supporting topologically protected states. These transformations change the spectrum of the system, leading to topological transitions.

16:00–18:00

FM4C • New Systems for Quantum Communications

President: Thomas Gerrits; NIST, USA

FM4C.1 • 16:00

Satellite based Quantum key distribution using a compact terminal on Tiangong-2 Space lab, Shengkai Liao^{1,2}, Jin Lin^{1,2}, Jigang Ren^{1,2}, Weiyue Liu^{1,2}, Juan Yin^{1,2}, Yang Li^{1,2}, Yuan Cao^{1,2}, Qi Shen^{1,2}, Fengzhi Li^{1,2}, Wenqi Cai^{1,2}, Cheng-Zhi Peng^{1,2}, Jian-Wei Pan^{1,2}; ¹Univ. of Science and Technology of China, Hefei National Lab for Physical Sciences at the Microscale and Dept. of Modern Physics, China; ²Shanghai Branch, CAS Center for Excellence and Synergetic Innovation Center in Quantum Information and Quantum Physics, China. We report a quantum key distribution experiment using a compact terminal on Tiangong-2 spacecraft two years after launch. This robust platform provides an effective solution for realizing a practical satellite-constellation-based global quantum secure network.

FM4C.2 • 16:15

A Daytime Free-Space Quantum-Optical Link using Atomic-Vapor Spectral Filters, Christopher C. Evans¹, David N. Woolf¹, Justin M. Brown¹, Joel M. Hensley¹; ¹Physical Sciences Inc., USA. We establish a free-space quantum-optical link that leverages narrow (~1 GHz) linewidth rubidium-based bandpass filters to drastically reduce solar background. To show its utility, we demonstrate the BB84 quantum key distribution protocol under daytime conditions.

FM4C.3 • 16:30

Measurement-device-independent QKD over asymmetric channels, Hui Liu^{1,2}, Wenyuan Wang³, Kejin Wei^{1,2}, Xiao-Tian Fang^{1,2}, Li Li^{1,2}, Nai-Le Liu^{1,2}, Hao Liang^{1,2}, Si-Jie Zhang^{1,2}, Weijun Zhang⁴, Hao Li⁴, Lixing You¹, Zhen Wang⁴, Hoi-Kwong Lo³, Teng-Yun Chen^{1,2}, Feihu Xu^{1,2}, Jian-Wei Pan^{1,2}; ¹Shanghai Branch, Hefei National Lab for Physical Sciences at Microscale and Dept. of Modern Physics, Univ. of Science and Technology of China, China; ²CAS Center for Excellence and Synergetic Innovation Center in Quantum Information and Quantum Physics, Univ. of Science and Technology of China, China; ³Centre for Quantum Information and Quantum Control (CQIQ), Dept. of Electrical & Computer Engineering and Dept. of Physics, Univ. of Toronto, Canada; ⁴State Key Lab of Functional Materials for Informatics, Shanghai Inst. of Microsystem and Information Technology, Chinese Academy of Sciences, China. We propose and demonstrate an efficient protocol that enables a scalable high-rate measurement-device-independent (MDI) QKD over asymmetric channels. The theoretical and experimental results unleash the full potential of MDI-QKD in practical network settings.

16:00–18:00

FM4D • Excitons in Condensed Matter Systems

President: Denis Seletskiy; Polytechnique Montréal, Canada

FM4D.1 • 16:00

Observation of Narrow-Band Terahertz Gain in Two-Dimensional Magnetoexcitons, Xinwei Li¹, Katsumasa Yoshioka², Qi Zhang³, Fumiya Katsutani¹, Weilu Gao¹, Nicolas Marquez¹, Tim Noe¹, John Watson⁴, Michael Manfra⁴, Ikufumi Katayama², Jun Takeda², Junichiro Kono¹; ¹Rice Univ., USA; ²Yokohama National Univ., Japan; ³Argonne National Labs, USA; ⁴Purdue Univ., USA. We have performed time- and polarization-resolved optical-pump—terahertz-probe magnetospectroscopy measurements on a GaAs quantum well and observed narrow-band, polarization-selective THz gain, whose center frequency shifts with applied magnetic field.

FM4D.2 • 16:30

Optical valley-Hall effect of 2D excitons, Sriram Guddala¹, Mandeep Khatoniar^{1,2}, Nicholas Yama¹, Vinod Menon^{1,2}; ¹City College of New York, USA; ²Physics, 2Graduate Center, City Univ. of New York (CUNY), New York, USA. We demonstrate optical analogue of valley-Hall effect for 2D materials by achieving unidirectional coupling of valley polarized excitonic emission to large wavevector modes in hyperbolic metamaterials.

CLEO: Science & Innovations

16:00–18:00

SM4E • High-Average Power Laser Systems

Presider: Emily Sistrunk Link;
Lawrence Livermore National
Laboratory, USA

SM4E.1 • 16:00

Joule-class 500 Hz Cryogenic Yb:YAG Chirped Pulse Amplifier, Luis E. Zapata¹, Simon Schweistal¹, Jelto Thesinga¹, Collette Zapata¹, Matthias Schust¹, Liu Yizhou¹, Mikhail Pergament¹, Franz Kartner^{1,2}; ¹Center for Free Electron Laser Science, Germany; ²Dept. of Physics & The Hamburg Center for Ultrafast Imaging, Univ. of Hamburg, Germany. A cryogenic Yb:YAG composite-thin-disk laser driver has demonstrated long-term stable operation at 500 Hz with 1-joule 20-ns pulses. Results with chirped pulses will be presented. Joule-level pulses at 500 Hz compressible to 5 ps are expected.

SM4E.2 • 16:30

High Peak and Average Power Yb-doped Tapered Fiber Amplifier, Konstantin K. Bobkov¹, Andrey E. Levchenko¹, Vladimir V. Velmiskin¹, Tatiana A. Kochergina¹, Svetlana Aleshkina¹, Mikhail Bubnov¹, Denis Lipatov², Alexei Guryanov², Mikhail Likhachev¹; ¹Fiber Optics Research Center RAS, Russia; ²Inst. of High Purity Substances of the RAS, Russia. Yb-doped tapered fiber amplifier delivering picosecond pulses with both high peak power (550 kW) and high average power (44 W) is presented.

16:00–18:00

SM4F • Precision Spectroscopy

Presider: Laura Sinclair, NIST, USA

SM4F.1 • 16:00 **Tutorial**

Challenging QED with atomic Hydrogen, Thomas Udem¹, Lothar Maisenbacher¹, Axel Beyer¹, Vitaly Andreev¹, Alexey Grinin¹, Arthur Matveev¹, Ksenia Khabarova¹, Nikolai Kolachevsky¹, Randolph Pohl¹, Dylan Yost¹, Theodor Hänsch¹; ¹Max-Planck-Institut für Quantenoptik, Germany. Testing theories means to compare precise measurements with theoretical predictions. I will describe where we stand with quantum electrodynamics by verifying calculations of energy levels in atomic hydrogen.



Thomas Udem studied physics at the University of Giessen and at the University of Washington. In 1997 he got his PhD from the University of Munich (LMU). After a short post doc at the NIST Boulder he returned Munich where became a research fellow MPQ and since 2016 professor at LMU.

16:00–17:15

SM4G • Access & Radio Over Fiber

Presider: Ryan Scott; Keysight
Laboratories. USA

SM4G.1 • 16:00

SOA-based Metro-Access Coherent Transmission Systems, Giuseppe Talli¹, Cleitus Antony¹, Mark Power¹, Paul Townsend¹; ¹Tyndall National Inst., Ireland. SOAs are demonstrated as in-line amplifiers in a metro-access system with potential for dynamic reconfiguration and traffic convergence with 5 spans of 40km of SMF and up to 7x200Gb/s DP-16QAM channels using 9 concatenated SOAs.

SM4G.2 • 16:15

Bidirectional fiber transmission of mmW signals using remote downconversion and wavelength reuse, Aleksandra Kaszubowska-Anandarajah¹, Amol Delmadede², Eamonn Martin², Prince M. Anandarajah², Liam P. Barry², Colm Browning²; ¹Connect Centre, Trinity College Dublin, Ireland; ²School of Electronic Engineering, Dublin City Univ., Ireland. We demonstrate an RoF system with a simplified RRU, by employing a remote uplink downconversion and downlink wavelength reuse. An error-free transmission of 64-QAM UF-OFDM signals over 12 km of fiber is also shown.

SM4G.3 • 16:30

A Timing-synchronization-free WDM-compatible Colorless DRoF Uplink System for 5G Mobile Fronthaul Employing Gold Sequence Multiplexing, Jhih-Heng Yan¹, Chao-Wei Wang¹, Kai-Hsiang Lin¹, Kai-Ming Feng¹; ¹National Tsing Hua Univ., Taiwan. A Timing-synchronization-free WDM-compatible Colorless DRoF Uplink for 5G Mobile Fronthaul employing Gold sequence multiplexing is experimentally demonstrated. Both signals at different wavelengths with total 6-Gb/s throughput are retrieved without timing synchronization or WDM demultiplexing.

16:00–18:00

SM4H • Advanced Optical Technologies for Cells and Tissues

Presider: Jessica Houston; New
Mexico State Univ., USA

SM4H.1 • 16:00

Intelligent Image-Activated Cell Sorting and Beyond, Yasuyuki Ozeki¹, Nao Nitta^{1,2}, Takeaki Sugimura^{1,2}, Akihiro Isozaki¹, Hideharu Mikami¹, Dino Di Carlo³, Yoichiro Hosokawa⁴, Sotaro Uemura¹, Keisuke Goda¹; ¹Univ. of Tokyo, Japan; ²Japan Science and Technology Agency, Japan; ³Univ. of California, Los Angeles, USA; ⁴Nara Inst. of Science and Technology, Japan. We present a groundbreaking machine intelligence technology called "intelligent image-activated cell sorting" that achieves high-throughput image-triggered sorting of single cells by integrating high-speed fluorescence microscopy, cell focusing, cell sorting, and deep learning.

SM4H.2 • 16:30

Portable Imaging Flow-cytometer Using Deep Learning-based Holographic Image Reconstruction, Zoltán Göröcs¹, Miu Tamamitsu¹, Vittorio Bianco¹, Patrick Wolf¹, Shounak Roy¹, Koyoshi Shindo¹, Kyrolos Yanny¹, Yichen Wu¹, Hatice Ceylan Koydemir¹, Yair Rivenson¹, Aydogan Ozcan¹; ¹Univ. of California Los Angeles, USA. We demonstrate deep learning assisted holographic imaging of waterborne microorganisms in color using a field-portable flow-cytometer capable of high-throughput screening of flowing water samples and report its capabilities using ocean samples containing plankton.

Meeting Room
211 A/B

CLEO: Applications
& Technology

16:00–18:00

AM4I • Nanobiophotonics

President: Andrea Armani;
University of Southern California,
USA

AM4I.1 • 16:00

Wide-field magnetic imaging of sub-50 nm ferromagnetic nanoparticles for time-resolved bio-mechanical orientation measurements, Zeeshawn Kazi¹, Isaac Shelby¹, Nicholas Brunelle¹, Hideyuki Watanabe^{3,6}, Kohei M. Itoh^{5,6}, Paul Wiggins^{1,3}, Kai-Mei Fu^{1,2}; ¹UW Physics Dept., USA; ²Electrical Engineering, Univ. of Washington, USA; ³Bioengineering, Univ. of Washington, USA; ⁴Electronics and Photonics Research Inst., National Inst. of Advanced Industrial Science and Technology (AIST), Japan; ⁵School of Fundamental Science and Technology, School of Fundamental Science and Technology, Japan; ⁶Spintronics Research Center, Keio Univ., Japan. We image the stray magnetic field of commercial chemically functionalized ferromagnetic cobalt nanoparticles using optically detected magnetic resonance of a near-surface ensemble of nitrogen vacancy centers in diamond.

AM4I.2 • 16:15

Nanoplasmonic Interferometric Sensor for Multiplex Detection of MMP-9 and TIMP-1, Yifeng Qian¹, Yu-Han Ho², Sushil Kumar¹, Xuanhong Cheng³, Filbert Bartoli¹; ¹Electrical and Computer Engineering Dept., Lehigh Univ., USA; ²Shanghai Industrial μ Technology Research Inst., China; ³Bioengineering Dept., Lehigh Univ., USA. The secretion of MMP-9 and TIMP-1 was detected simultaneously using a nanoplasmonic interferometric sensor. Dynamic and multiplexed sensing of two secretory proteins suggests the biosensor holds good promise for cell function analysis.

AM4I.3 • 16:30

Holographic Microscopy with Acoustic Modulation for Detection of Nano-sized Particles and Pathogens in Solution, Anirudha Ray¹, Muhammad A. Khalid², Andrijeus Demcenko², Mustafa Daloglu¹, Derek Tseng¹, Julien Reboud², Jonathan Cooper², Aydogan Ozcan¹; ¹Univ. of California, USA; ²Univ. of Glasgow, UK. We present a method for the detection of nanoparticles in solution using an acoustically actuated holographic microscope. This type of microscopy can be used for high-throughput biosensing applications, e.g., detection of viruses in a liquid.

Meeting Room
211 C/D

CLEO: Science & Innovations

16:00–18:00

SM4J • Light Emission & Detection

President: Andrew Young; Bristol Univ., UK

SM4J.1 • 16:00 **Invited**

Single-carbon-nanotube Photonics and Optoelectronics, Yuichiro K. Kato¹; ¹RIKEN, Japan. Single-walled carbon nanotubes exhibit telecom-band emission at room temperature and they can be directly synthesized on silicon substrates. Here we discuss the use of individual carbon nanotubes for generation and manipulation of photons on a chip.

SM4J.2 • 16:30

Graphene-Based Transparent Photodetector Array for Multiplane Imaging, Dehui Zhang¹, Zhen Xu¹, Zhengyu Huang¹, Audrey Rose Gutierrez¹, Il Yong Chun¹, Cameron J. Blocker¹, Gong Cheng¹, Zhe Liu¹, Jeffrey A. Fessler¹, Zhaohui Zhong¹, Theodore B. Norris¹; ¹Univ. of Michigan, USA. We report a transparent photodetector array using graphene as both the active pixel and interconnect material. We demonstrate imaging at multiple focal planes with these arrays. Further applications of position tracing will also be discussed.

Meeting Room
212 A/B

CLEO: Applications
& Technology

16:00–18:00

AM4K • A&T Topical Review on Flat Optics II

President: To Be Announced

AM4K.1 • 16:00 **Invited**

Dispersion-engineered and Polarization-insensitive Metasurfaces for Broadband Achromatic Optics, Wei-Ting Chen¹, Federico Capasso¹; ¹Harvard Univ., USA. Chromatic aberrations are challenging to correct. We show dispersion-tailored and polarization-insensitive metasurfaces comprising anisotropic nanofins that can correct the chromatic aberrations in lens systems (from singlet lenses to sophisticated microscope objectives) with unprecedented compactness.

AM4K.2 • 16:30 **Invited**

Metasurface Devices for AR/VR, Byoungcho Lee¹, Gun-Yeal Lee¹, Jong-Young Hong¹; ¹Electrical and Computer Engineering, Seoul National Univ., South Korea (the Republic of). We introduce recent achievements on metasurface optical applications. In particular, metasurface holography with full complex-amplitude holograms and metals for augmented reality display with large viewing angles are discussed and their outlook is also discussed.

Meeting Room
212 C/D

CLEO: Science & Innovations

16:00–17:30

SM4L • Specialty Fibers

President: Guoqing Chang;
Institute of Physics, CAS, China

SM4L.1 • 16:00 **Invited**

Hybrid Fibers for Dispersion Management at 1 μ m, Svetlana Aleshkina¹, Mikhail Yashkov², Mikhail Salganskii², Denis Lipatov², Liudmila Iskhakova¹, Mikhail Bubnov¹, Alexei Guryanov², Mikhail Likhachev¹; ¹Fiber Optics Res. Ctr the RAS, Russia; ²Inst. of High Purity Substances of the Russian Academy of Sciences, Russia. Hybrid fibers with high (60-400 ps/(nm \times km)) anomalous dispersion at 1.06 μ m were developed. Utilization of such fibers allowed us to fabricate femtosecond all-fiber master oscillator and nonlinear chirped pulses compressor ($P_{\text{peak}} > 3$ kW).

SM4L.2 • 16:30

Efficient High-power Single-mode Yb Three-level Cladding-pumped All-solid Photonic Bandgap Fiber Lasers at ~978nm, Turghun Matniyaz¹, Wensong Li^{1,2}, Monica Kalichevsky-Dong¹, Thomas Hawkins¹, Joshua Parsons¹, Guancheng Gu³, Liang Dong¹; ¹Clemson Univ., USA; ²Dept. of Electronic Engineering, Xiamen Univ., China; ³Coherent/Nufern, USA. We report an efficiency of 62.7% with regard to the launched pump from a Yb cladding-pumped fiber laser at ~978nm. ~84W with an M^2 of 1.11/1.12 was achieved, a significant improvement from a flexible fiber.

CLEO: QELS-Fundamental
Science

16:00–18:00

FM4M • Solid State High Harmonic
Generation

President: Hanieh Fattahi; Max Planck Institute
for Quantum Optics, Germany

FM4M.1 • 16:00

High Harmonic Generation in Reflection and Transmission from Gallium Arsenide, Nobuhisa Ishii¹, Peiyu Xia¹, Changsu Kim¹, Faming Lu¹, Teruto Kanai¹, Hidefumi Akiyama¹, Jiro Itatani¹; ¹Inst. for Solid State Physics, Japan. High harmonic generation in reflection and transmission from gallium arsenide is investigated using femtosecond infrared pulses. Harmonic spectra obtained in both geometries show drastic difference with each other, indicating significant contribution of nonlinear propagation.

FM4M.2 • 16:15

Modeling Harmonic Generation in Polycrystalline ZnSe, Michael G. Hastings¹, Kevin Werner², Aaron Schweinsberg³, Brian L. Wilmer⁴, Drake Austin², Christopher Wolfe⁵, Trenton Ensley⁶, Laura Vanderhoeft⁶, Anthony Valenzuela⁵, Enam Chowdhury², Jerome V. Moloney¹, Miroslav Kolesik¹; ¹College of Optical Sciences, Univ. of Arizona, USA; ²Dept. of Physics, The Ohio State Univ., USA; ³Oak Ridge Inst. for Science and Education, USA; ⁴SURVICE Engineering, USA; ⁵Weapons and Materials Research Directorate, U.S. Army Research Lab, USA; ⁶Sensors and Electron Devices Directorate, U.S. Army Research Lab, USA. High harmonic generation in polycrystalline ZnSe is modeled as an effective medium. The non-perturbative behavior observed experimentally was recreated, showing that an effective model captures the underlying physics.

FM4M.3 • 16:30 **Invited**

Dipole Phase of High-harmonics from Crystals, Yongsing You¹; ¹Stanford Univ., USA. Abstract not available.

CLEO: Science & Innovations

16:00–18:00

SM4N • Surface Emitting Lasers

President: To Be Announced

SM4N.1 • 16:00 **Invited**

Blue and Ultraviolet Vertical-cavity Surface-emitting Lasers, Åsa Haglund¹, Michael Bergmann¹, Filip Hjort¹, Ehsan Hashemi¹, Jörgen Bengtsson¹, Johan Gustavsson¹; ¹Chalmers Univ. of Technology, Sweden. We will summarize state-of-the-art results in III-nitride-based vertical-cavity surface-emitting lasers (VCSELs) for blue and ultraviolet emission, including our schemes for optically guided devices and our approach for UV-VCSELs with double dielectric distributed Bragg reflectors.

SM4N.2 • 16:30

Beam Pattern Projecting On-Chip Lasers at Visible Wavelength, Yoshitaka Kurosaka¹, Kazuyoshi Hirose¹, Akio Ito¹, Masahiro Hitaka¹, Akira Higuchi¹, Takahiro Sugiyama¹, Yu Takiguchi¹, Yoshiro Nomoto¹, Soh Uenoyama¹, Tadadata Edamura¹; ¹Hamamatsu Photonics, Japan. We have successfully demonstrated pattern projecting semiconductor lasers at the red wavelength, for the first time. The two-dimensional pattern was directly emitted on the screen, at the red wavelength, without any lens or scanning system.

16:00–18:00

SM4O • Nonlinear Phonon Interactions

President: Amol Choudhary Indian Institute of
Technology Delhi, India

SM4O.1 • 16:00

Higher Order Cascaded SBS Suppression Using Gratings in a Photonic Integrated Ring Resonator Laser, Matthew Puckett², Debapam Bose¹, Karl Nelson², Daniel Blumenthal¹; ¹Univ. of California, Santa Barbara, USA; ²Honeywell International, USA. An integrated Brillouin laser that maintains lasing in only the first Stokes order with up to 1W input pump power is demonstrated by incorporating Bragg gratings in the resonator waveguide.

SM4O.2 • 16:15

On-Chip Stimulated Brillouin Lasers Based on Chalcogenide Glass Resonators with 10 Million Q-factor, Sangyoon Han¹, Dae-Gon Kim², Joonhyuk Hwang¹, In Hwan Do², Dongin Jeong², Yong-Hee Lee¹, Duk-yong Choi³, Hansuek Lee²; ¹Dept. of Physics, South Korea Advanced Inst. of Science and Technology, South Korea (the Republic of); ²Graduate School of Nanoscience and Technology, South Korea Advanced Inst. of Science and Technology, South Korea (the Republic of); ³Laser Physics Centre, Research School of Physics and Engineering, The Australian National Univ., Australia. On-chip chalcogenide glass resonator with Q-factor of 1.08×10^7 is experimentally demonstrated with a new fabrication approach which avoids direct etch process. Waveguide-coupled stimulated Brillouin laser with 2.5 mW threshold power is implemented by flip-chip coupling.

SM4O.3 • 16:30

Arbitrary Optical Waveform Generation by Nonlinear Frequency-to-Time Conversion, Daniel E. Mittelberger¹, Ryan Muir¹, Mathew Hamamoto¹, Matthew Prantil¹, John Heebner¹; ¹Lawrence Livermore Natl Lab, USA. We propose and demonstrate a novel method of arbitrary optical temporal patterning for generation of long (330 ps) unchirped waveforms with picosecond features. The method is based on frequency-to-time conversion of an imposed spectral pattern.

CLEO: QELS-Fundamental Science

FM4A • Quantum
Nanophotonics II: Diamond &
Boron Nitride—Continued

FM4A.4 • 17:00

Frequency Tunable Single-Photon Emission From a Single Atomic Defect in a Solid, Shuo Sun¹, Linda Jingyuan Zhang¹, Kevin Fischer¹, Michael Burek², Constantin Dory¹, Konstantinos Lagoudakis¹, Yan-Kai Tzeng¹, Marina Radulaski¹, Yousif Kelaita¹, Amir Safavi-Naeini¹, Zhi-Xun Shen¹, Nicholas Melosh¹, Steven Chu¹, Marko Loncar², Jelena Vuckovic¹; ¹Stanford Univ., USA; ²Harvard Univ., USA. We demonstrate generation of frequency tunable single-photon emission based on cavity-enhanced Raman emission from a single silicon-vacancy center in diamond. The demonstrated frequency tuning range (100 GHz) significantly exceeds the spectral inhomogeneity of the emitters.

FM4A.5 • 17:15

Tuning of Quantum Emitters in Hexagonal Boron Nitride, Noah Mendelson¹, Niko Nikolay^{2,3}, Zai-Quan Xu¹, Trong Toan Tran¹, Nikola Sadzak^{2,3}, Florian Bohm^{2,3}, Bernd Sontheimer^{2,3}, Oliver Benson^{2,3}, Milos Toth¹, Igor Aharonovich¹; ¹Univ. of Technology Sydney, Australia; ²AG Nanooptik, Humboldt Universität zu Berlin, Germany; ³IRIS Adlershof, Humboldt Universität zu Berlin, Germany. We demonstrate two different techniques to tune quantum emitters in hBN, achieving record tuning magnitudes for a solid state quantum emitter, as well as dynamic and reversible modulation of the emitters through both methods).

FM4A.6 • 17:30 **Invited**

Probing Spin Transfer Effects with Diamond Defects, Lilian Childress¹, Adrian Solyom¹, Zackary Flansberry¹, Marta Tschudin², Nathaniel Leitao^{1,4}, Michel Pioro-Ladriere^{3,4}, Jack Sankey¹; ¹McGill Univ., Canada; ²Univ. of Basel, Switzerland; ³Univ. of Sherbrooke, Canada; ⁴CIFAR, Canada. A single NV center is used to detect effects of damping and anti-damping spin transfer torques on a proximal magnetic nanowire.

FM4B • Topological Photonics
II—Continued

FM4B.4 • 16:45

Photonic bands in 230 space groups, Ling Lu¹, Haruki Watanabe²; ¹Inst. of Physics, Chinese Academy of Sciences, China; ²Dept. of Applied Physics, Univ. of Tokyo, Japan. We present the symmetry constraints on photonic bands for all 230 space groups with time-reversal symmetry. The results of minimum band connectivities provide useful design insights for photonic crystals, metamaterials, and topological lattices.

FM4B.5 • 17:00

Angular momentum-dependent topological transport, Meng Xiao¹, Tianshu Jiang², Wen-jie Chen³, Yawen Fang², Wing Yim Tam², Che Ting Chan²; ¹School of Physics and Technology, Wuhan Univ., China; ²Dept. of Physics, the Hong Kong Univ. of Science and Technology, Hong Kong; ³School of Physics and Engineering, Sun Yat-Sen Univ., China. Analogs of the quantum spin Hall effect (QSHE) in classical waves are mostly based on the construction of pseudo-spins. Here we demonstrate analogs of QSHE in classical waves by utilizing the orbital angular momentum.

FM4B.6 • 17:15

Non-scattering Systems for Field Localization and Emission Enhancement, Viktor Asadchy¹, Francisco Cuesta¹, Mohammad Mirmoosa¹, Sergei Tretyakov¹; ¹Electronics and Nanoengineering, Aalto Univ., Finland. We propose invisible cavities which do not scatter electromagnetic waves under normal incidence but strongly enhance or suppress the fields inside. They can be used for cloaking sensors and emission enhancement of wave sources.

FM4B.7 • 17:30

Observation of Local Symmetry in a Photonic System, Nora Schmitt¹, Steffen Weimann¹, Christian Morfonios², Malte Roentgen², Matthias Heinrich¹, Peter Schmelcher^{2,3}, Alexander Szameit¹; ¹Inst. of Physics, Univ. of Rostock, Germany; ²Center for Optical Quantum Technologies, Univ. of Hamburg, Germany; ³Hamburg Centre for Ultrafast Imaging, Univ. of Hamburg, Germany. We demonstrate the effect of local symmetries on the dynamics of laser-written photonic waveguide arrays. A non-local continuity equation allows us to distinguish between the three cases of global symmetry, local symmetry and full disorder.

FM4C • New Systems for
Quantum Communications—
Continued

FM4C.4 • 16:45

Integrated photonic devices for measurement-device-independent quantum key distribution, Henry Semenenko^{1,2}, Philip Sibson², Mark G. Thompson², Chris Erven²; ¹H. H. Wills Physics Lab \& Dept. of Electrical and Electronic Engineering, Quantum Engineering Centre for Doctoral Training, UK; ²H. H. Wills Physics Lab \& Dept. of Electrical and Electronic Engineering, Quantum Engineering Technology Labs, UK. We experimentally demonstrate integrated photonic devices for measurement device independent quantum key distribution with state-of-the-art error and clock rates which will lead to more cost effective, practical and secure communication.

FM4C.5 • 17:00

Field Trial of Long Distance Quantum Key Distribution with Polarization Encoding Through Installed Aerial Fibe, Dong-Dong Li^{2,1}, Song Gao¹, Guo-Chun Li³, Lu Xue⁴, Li-Wei Wang¹, Chang-Bin Lu¹, Yao Xiang¹, Zi-Yan Zhao³, Long-Chuan Yan³, Zhi-Yu Chen³, Gang Yu¹, Jianhong Liu^{1,4}; ¹Quantum CTEK, China; ²Univ. of Science and Technology of China, China; ³State Grid Information & Telecommunication Co., Ltd, China; ⁴QuantumCTEK (Beijing), China. We experimentally demonstrate quantum key distribution with polarization encoding through installed aerial fiber link. The fast vibration of polarization is compensated with a homemade feedback module. The key rate reaches 2 kbps over 68-km-long fiber.

FM4C.6 • 17:15

Entangled Photon Transmission from a Quantum Dot over Loop-back Fiber in Cambridge Network, Zi-Heng Xiang^{2,1}, Jan Huwer², R. Mark Stevenson², Joanna Skiba-Szymanska², Martin Ward², Ian Farrer^{3,1}, David Ritchie¹, Andrew Shields²; ¹Univ. of Cambridge, UK; ²Toshiba Research Europe Ltd, UK; ³Univ. of Sheffield, UK. We report the long-term transmission of high-fidelity entangled photons emitted from a telecom wavelength quantum dot device over the Cambridge Fiber Network with a time-multiplexed polarization stabilization system.

FM4C.7 • 17:30

Toward Experimental Implementation of Quantum-Enabled, Bandwidth and Power Efficient Communications, Ivan A. Burenkov^{1,2}, M.V. Jabir², Driss El Idrissi², Abdella Battou², Sergey V. Polyakov²; ¹Joint Quantum Inst., USA; ²NIST, USA. Coherent Frequency Shift Keying (CFSK) protocols paired with a quantum receiver can significantly optimize power and bandwidth efficiency of communication channels. We present our preliminary experimental data obtained with the CFSK quantum communication testbed.

FM4D • Excitons in Condensed
Matter Systems—Continued

FM4D.3 • 16:45

Strong Coupling between Quantum-confined Exciton Polaritons, Eric Martin^{1,2}, Jiaqi Hu¹, Zhaorong Wang¹, Hui Deng¹, Steven T. Cundiff¹; ¹Univ. of Michigan, USA; ²Monstr Sense Technologies, USA. We directly measure coupling between quantum confined exciton-polaritons and the relaxation channels from pumped exciton states into lasing polariton modes. Using double-quantum spectroscopy we demonstrate that interactions dominate the nonlinear signal of quantum confined polaritons.

FM4D.4 • 17:00

Observation of Trionic Optical Gain in Electrically Gated Two-Dimensional Molybdenum Ditelluride, Zhen Wang^{1,2}, Hao Sun^{1,2}, Qiyao Zhang^{1,2}, Jiabin Feng^{1,2}, Jianxing Zhang^{1,2}, Yongzhuo Li^{1,2}, Cun-Zheng Ning^{1,2}; ¹Dept. of Electronic Engineering, Tsinghua Univ., China; ²International Center for Nano-Optoelectronics, Tsinghua Univ., China. We report a new mechanism of optical gain originating from trions at extremely low-density levels in 2D material system by conducting systematic PL and reflectance spectroscopy on electrically-gated MoTe₂ mono- and bi-layer devices.

FM4D.5 • 17:15

Measurement and Reconstruction of the Entire Third-Order Exciton Polarization Using Multidimensional Spectroscopy, Travis Autry¹, Galan Moody¹, Corey McDonald¹, James M. Fraser^{1,2}, Richard P. Mirin¹, Kevin Silverman¹; ¹NIST, USA; ²Physics, Queen's Univ., Canada. We reconstruct the entire third order complex polarization of GaAs excitons using the amplitude and phase of all degenerate third-order wave mixing processes. All first and third order wave mixing processes are measured using multidimensional spectroscopy.

FM4D.6 • 17:30

Flexible Polaritons: Wannier Exciton-Plasmon Coupling in Metal-Semiconductor Structures, Jacob Khurgin¹; ¹Johns Hopkins Univ., USA. When Rabi energy exceeds the exciton binding energy a Wannier Exciton-Plasmon Polariton (WEPP) bound to the metal nanoparticle is formed. It is characterized by small excitonic radius and higher ionization energy that can exceed 100meV

CLEO: Science & Innovations

SM4E • High-Average Power
Laser Systems—Continued

SM4E.3 • 16:45

Towards a Joule-Class Ultrafast Thin-Disk Based Amplifier at Kiloherz Repetition Rate, Clemens Herkommer^{1,2}, Peter Krötzl¹, Sandro Klingebiel¹, Christoph Wandt¹, Dominik Bauer³, Knut Michel¹, Reinhard Kienberger², Thomas Metzger¹; ¹TRUMPF Scientific Lasers GmbH & Co. KG, Germany; ²Physik Dept., Technische Universität München, Germany; ³TRUMPF Laser GmbH, Germany. We report on the development of a thin-disk based multipass amplifier operating at 1 kHz repetition rate. The chirped pulse amplifier delivers 600mJ pulses before compression. A Joule-class laser source with sub-ps pulse durations is currently under construction using further amplifier stages.

SM4E.4 • 17:00 **Invited**

Laser Technologies for PW-Class Peak Power at Multi-kW Average Power, Thomas Spinka¹, David Alessi¹, Andrew J. Bayramian¹, Kyle Chesnut², Alvin Erlandson¹, Thomas Galvin¹, David Gibson¹, Brendan Reagan¹, Craig Siders¹, Emily F. Sistrunk¹, Constantin Haefner¹; ¹Lawrence Livermore National Lab, USA; ²Physics and Astronomy, Univ. of California - Irvine, USA. We will present multi-kW average power, PW-class peak power short pulse (≤ 150 fs) high rep-rate (≥ 10 Hz) laser designs based on Nd:glass and Tm:YLF, and explore progress on technologies that promise to enable or enhance their capabilities.

SM4E.5 • 17:30

Stabilization of Diffractive Beam Combining Using Pattern Recognition, Qiang Du¹, Tong Zhou¹, Lawrence Doolittle¹, Gang Huang¹, Russell Wilcox¹, Wim Leemans¹; ¹Lawrence Berkeley National Lab, USA. A novel method of measuring and controlling phase errors in a 2D diffractive beam combiner is demonstrated. Output power is stabilized to <1% by controlling intensities of uncombined side beams.

SM4F • Precision
Spectroscopy—Continued

SM4F.2 • 17:00

Frequency-comb-referenced phase spectroscopy measures plasmonic dynamics with picometre resolution, Anh D. Nguyen¹, Byung Jae Chun¹, Young-Jin Kim¹; ¹Nanyang Technological Univ. (NTU), Singapore. A 1.94-Å dynamic motion of plasmonic nanohole array was measured with a 1.67 pm resolution using a frequency comb as the light source. This frequency-comb-referenced plasmonic phase spectroscopy could provide high speed, high resolution, and traceability to a time standard.

SM4F.3 • 17:15

Metamaterial infrared refractometer for detecting broadband complex refractive index of liquid material, Hibiki Kagami¹, Tomo Amemiya¹, Makoto Tanaka¹, Keisuke Masuda¹, Nobu Nishiyama¹, Shigehisa Arai¹; ¹Tokyo Inst. of Technology, Japan. We developed a metamaterial refractometer for detecting broadband infrared complex refractive index of liquid materials. Using the device, the complex infrared refractive index of PMMA from 40 to 120 THz was measured for the first time.

SM4F.4 • 17:30

Real-time Reference for Frequency-shifted Fourier-transform Spectrometers using an Arbitrary-wavelength CW Reference Laser, Eric Martin^{2,1}, Christopher L. Smallwood^{3,1}, Torben L. Purz¹, Hanna G. Ruth¹, Steven T. Cundiff^{1,2}; ¹Univ. of Michigan, USA; ²Monstr Sense Technologies, USA; ³Dept. of Physics and Astronomy, San Jose State Univ., USA. Frequency-shifted interferometers enable significant reduction of the measurement noise in Fourier-transform spectrometry and distance metrology. We demonstrate a real-time solution for referencing these interferometers with nanometer precision using an arbitrary-wavelength CW reference laser.

SM4G • Access & Radio Over
Fiber—Continued

SM4G.4 • 16:45

Quasicoherent Receivers for Access Networks Using Fullwave Rectification Based Envelope Detection, Varghese A. Thomas¹, Siddharth Varughese¹, Stephen E. Ralph¹; ¹Georgia Inst. of Technology, USA. We demonstrate a novel quasicoherent receiver architecture based on envelope detection employing fullwave rectification. Signaling rates of up to 18 GBaud (PAM-2) were experimentally achieved using low receiver bandwidths and low received powers.

SM4G.5 • 17:00

Polarization-insensitive Multipoint-to-point (MPTP) RoF Uplink for 5G Mobile Fronthaul, Jih-Heng Yan¹, Sheng-Yang Lin¹, Hsu-Hong Huang¹, Kai-Ming Feng¹; ¹National Tsing Hua Univ., Taiwan. A radio-over-fiber uplink system for 5G mobile fronthaul is experimentally demonstrated with a polarization insensitive optical modulation by reusing the polarization-orthogonal optical carriers from downlink. It's compatible with multipoint-to-point scenario by employing modified-STBC algorithm.

SM4H • Advanced Optical
Technologies for Cells and
Tissues—ContinuedSM4H.3 • 16:45 **Invited**

Deciphering Bioengineered Tissues Functional Properties with Label-free Optical Techniques, Laura Marcu¹; ¹Univ. of California Davis, USA. We present studies demonstrating fluorescence lifetime techniques as a means for monitoring the recellularization processes in vascular constructs grown in bioreactors and for assessing changes in bioengineered cartilage functional properties during matrix maturation.

SM4H.4 • 17:15

Determining Metabolic Changes Associated with Tamoxifen Treatment and Resistance in Breast Cancer, Jessica P. Houston¹, Kevin D. Houston¹, David Rodriguez¹, Yan Zheng¹; ¹New Mexico State Univ., USA. Autofluorescence lifetimes of endogenous NAD(P)H are altered when breast cancer cells are treated with tamoxifen and is distinguishable when comparing tamoxifen sensitive and resistant breast cancer cells.

SM4H.5 • 17:30

Ultrasonically-Assisted In Situ 3D Optical Imaging And Manipulation: Challenges And Opportunities To Access Deep Tissue, Matteo Giuseppe Scopelliti¹, Yasin Karimi¹, Maysamreza Chamanzar¹; ¹Carnegie Mellon Univ., USA. We demonstrate that that non-invasive ultrasound can be used to sculpt reconfigurable 3D optical patterns within tissue for light delivery (optical stimulation) and light collection (imaging) deep into the medium.

Meeting Room
211 A/B

CLEO: Applications
& Technology

AM4I • Nanobiophotonics—
Continued

AM4I.4 • 16:45

Tensorial Shear Stress Sensing Using Elliptically-Shaped Nanopillar Light-Emitting Diodes, Kunook Chung¹, Feng Tian¹, Jingyang Sui¹, Pei-cheng Ku¹; ¹Univ. of Michigan, USA. We experimentally demonstrated a tensorial shear stress sensor capable of detecting both the magnitude and direction of the stress using an array of elliptically-shaped nanopillar GaN light-emitting diodes.

AM4I.5 • 17:00 **Invited**

Mapping Nanoscale Dynamics and Features Throughout Entire Mammalian Cells by 3D Single-Molecule Tracking and 3D Super-Resolution Imaging, Anna-Karin Gustavsson^{1,2}, Petar Petrov¹, Maurice Y. Lee^{1,3}, W. E. Moerner¹; ¹Dept. of Chemistry, Stanford Univ., USA; ²Dept. of Biosciences and Nutrition, Karolinska Inst., Sweden; ³Biophysics Program, Stanford Univ., USA. We demonstrate an approach that combines point-spread function engineering with tilted light sheet illumination for 3D single-molecule tracking and 3D super-resolution imaging throughout entire mammalian cells.

AM4I.6 • 17:30

Comparison of Substrate-dependent SERS Chemical-enhancement Effects in Au and Ag for Compositional Analysis of Single-stranded DNA, Phuong H. Nguyen¹, Brandon Hong¹, Alexei Smolyaninov¹, Yeshaiahu Fainman¹; ¹Univ. of California San Diego, USA. We experimentally observe and isolate chemical-enhancement effects in the Raman spectra of nucleotides on gold nanorod surfaces. We compare the enhanced spectra with similar enhancements observed on silver surfaces, and demonstrate their potential for DNA composition analysis.

Meeting Room
211 C/D

CLEO: Science &
Innovations

SM4J • Light Emission &
Detection—Continued

SM4J.3 • 16:45

A hybrid nanowire photo-detector integrated in a silicon photonic crystal, Masato Takiguchi^{1,2}, Satoshi Sasaki¹, Kouta Tateno^{1,2}, Edward Chen¹, Kengo Nozaki^{1,2}, Sylvain Sergent^{1,2}, Eiichi Kuramochi^{1,2}, Guoqiang Zhang^{1,2}, Akihiko Shinya^{1,2}, Masaya Notomi^{1,2}; ¹NTT Basic Research Labs, Japan; ²NTT Nanophotonics center, Japan. We demonstrate hybridization of silicon photonic crystals with single nanowires to create on-chip photo-detectors. The measured photocurrent is enhanced by the photonic crystal optical antenna.

SM4J.4 • 17:00

Vertically Stacked Silicon Nanowire Photodetectors for Spectral Reconstruction, Jiajun Meng¹, Jasper Cadusch¹, Kenneth Crozier^{1,2}; ¹Dept. of Electrical and Electronic Engineering, Univ. of Melbourne, Australia; ²School of Physics, Univ. of Melbourne, Australia. We experimentally demonstrate the use of vertically stacked silicon nanowire photodetectors for computational spectral reconstruction at visible wavelengths. The method is based on the photodetectors having tailored responsivity spectra, achieved by standard nanofabrication processes.

SM4J.5 • 17:15

Spectrally selective detection with In₂O₃/n-Si radial heterojunction nanowire photodiodes, Han-Don Um¹, Amit Solanki¹, Ashwin Jayaraman², Roy G. Gordon^{1,2}, Fawwaz Habbal¹; ¹John A. Paulson School of Engineering and Applied Sciences, Harvard Univ., USA; ²Dept. of Chemistry and Chemical Biology, Harvard Univ., USA. We demonstrated radial heterojunction nanowire photodiodes consisting of an In₂O₃-shell/Si-core structure using conformal coating of an In₂O₃ layer on n-Si nanowires. We achieve selective spectral response from 400 to 700 nm by tuning the nanowire diameter.

SM4J.6 • 17:30

Tuning Lasing Emission towards Long Wavelengths in GaAs-(In,Al)GaAs Core-Multishell Nanowires, Thomas Stettner¹, Paul J. Schmiedeke¹, Andreas Thurn¹, Markus Döblinger², Jochen Bissinger¹, Sonja Matich¹, Daniel Ruhstorfer¹, Hubert Riedl¹, Jonathan J. Finley¹, Gregor Koblmüller¹; ¹Walter Schottky Institut and Physics Dept., Technical Univ. of Munich, Germany; ²Dept. of Chemistry, Ludwig-Maximilians-Universität München, Germany. We demonstrate lasing from GaAs-InGaAs-based core-multiple quantum well nanowires with lasing emission tunable from ~0.8 to ~1.1 μm. By controlling the shell growth temperature, the quantum well In-molar fraction is increased to 25% without plastic relaxation.

Meeting Room
212 A/B

CLEO: Applications
& Technology

AM4K • A&T Topical Review on
Flat Optics II—Continued

AM4K.3 • 17:00

Inverse-Designed Spectrum Splitters for Color Imaging, Philip Camayd-Muñoz¹, Gregory D. Roberts¹, Max Debbas¹, Conner Ballew¹, Andrei Faraon¹; ¹Caltech, USA. Absorptive filters provide color discrimination in image sensors by eliminating 70% of incident light. Instead, we present a dielectric scatterer that efficiently sorts light based on color. This may improve the sensitivity and functionality of detectors.

AM4K.4 • 17:15 **Invited**

Generating High Performance, Topologically-complex Metasurfaces with Neural Networks, Jonathan A. Fan¹; ¹Electrical Engineering, Stanford Univ., USA. We show that generative neural networks, combined with topology optimization, are a computationally efficient route to producing high efficiency, topologically-complex metasurfaces across a broad operating parameter space.

Meeting Room
212 C/D

CLEO: Science &
Innovations

SM4L • Specialty Fibers—
Continued

SM4L.3 • 16:45

Gain dependent mode analysis of large mode area fiber with confined Ytterbium doping, Stefan Gausmann¹, Jose Enrique Antonio-Lopez¹, James Anderson¹, Stefan Wittek¹, Rodrigo Amezcua Correa¹, Axel Schülzgen¹; ¹Univ. of Central Florida - CREOL, USA. We quantify for the first time higher-order-mode content as a function of gain in large-mode-area fiber with confined Yb-doping using spatially and spectrally resolved imaging. Our results clearly indicate higher-order-mode suppression due to differential gain.

SM4L.4 • 17:00

Influence of sapphire sol-gel cladding on Tm:YAG single crystal fiber laser operation, Ben Eshel^{1,2}, Gisele Maxwell³, Carl Liebig², Kent L. Averett², Sean A. McDaniel², Gary Cook²; ¹Azimuth Corporation, USA; ²Air Force Research Labs, USA; ³Shasta Crystals, USA. A sapphire sol-gel cladding (0–5 deposition cycles) was observed to increase the slope efficiency of a 2% Tm-doped single-crystal YAG fiber laser from 16% to 43.5% with respect to transmitted power and reduce the Rayleigh scattering.

SM4L.5 • 17:15

Precise characterization of rare-earth doped fibers for laser cooling using a non-contact method, Mostafa Peysokhan¹, Esmail Mobini¹, Arman Allahverdi¹, Behnam Abaie¹, Arash Mafi¹; ¹Univ. of New Mexico, USA. A non-contact, non-destructive method is presented for measuring the external quantum efficiency, background absorption, and resonance absorption of a Ytterbium-doped ZBLAN fiber. The precise values of these parameters are essential for optical refrigeration in fibers.

CLEO: QELS-Fundamental
ScienceFM4M • Solid State High Harmonic
Generation—Continued

FM4M.4 • 17:00

Symmetry and Polarization of High-Order Harmonic Generation from Solids, Shima Gholam Mirzaeimoghadar¹, Shicheng Jiang³, Erin Crites¹, John E. Beetar¹, Ruifeng Lu³, Chii-Dong Lin², Michael Chini^{1,4}; ¹Dept. of Physics, Univ. of Central Florida, USA; ²J. R. Macdonald Lab, Dept. of Physics, Kansas State Univ., USA; ³Dept. of Applied Physics, Nanjing Univ. of Science and Technology, China; ⁴College of Optics and Photonics, Univ. of Central Florida, USA. We study the polarization states of high-order harmonics emitted from a-cut ZnO crystals driven by femtosecond mid-infrared laser pulses. The polarization states of even and odd harmonics are sensitive to structural symmetries of the crystal.

FM4M.5 • 17:15

Topological strong field physics on sub-laser cycle timescale, Alvaro Jimenez-Galan¹, Rui Silva^{1,2}, Bruno Amorim³, Olga Smirnova^{1,4}, Misha Ivanov^{1,5}; ¹Max Born Institut, Germany; ²Departamento de Física Teórica de la Materia Condensada, Universidad Autónoma de Madrid, Spain; ³CeFEMA, Instituto Superior Técnico, Universidade de Lisboa, Portugal; ⁴Technische Universität Berlin, Germany; ⁵Blackett Lab, Imperial College London, UK. Topological state is linked with dynamics, as manifested via chiral-edge currents. But is there an inherent timescale, associated with topology? We address this question using unique properties of primary electronic response to strong optical fields.

FM4M.6 • 17:30

High-Harmonic Generation from Topological Insulators, Denitsa Baykusheva¹, Jian Lu¹, Jonathan A. Sobota², Hadas Soifer², Costel R. Rotundu², Patrick S. Kirchmann², David A. Reis¹, Shambhu Ghimire¹; ¹Stanford PULSE Inst., USA; ²Stanford Inst. for Materials and Energy Sciences, USA. We report the observation of efficient high-harmonic generation in the three-dimensional topological insulators Bi₂Se₃ and Bi₂Te₃ driven by mid-infrared laser pulses of peak intensities $\sim 10^{12}$ W/cm².

CLEO: Science & Innovations

SM4N • Surface Emitting Lasers—
Continued

SM4N.3 • 16:45

Lateral Integration of VCSEL and Amplifier with Resonant Wavelength Detuning Design, Shanting Hu¹, Masashi Takanohashi¹, Xiaodong Gu¹, Keisuke Shimura¹, Fumio Koyama¹; ¹Tokyo Inst. of Technology, Japan. We propose and demonstrate the lateral integration of VCSEL and slow-light waveguide amplifier with in-plane resonant wavelength detuning design, enabling the unidirectional coupling. A record quasi-single-mode power (>27 mW) with narrow beam divergence (<0.06°) is presented.

SM4N.4 • 17:00

Compact Dot Projector based on Folded Path VCSEL Amplifier for Structured Light Sensing, Mizuki Morinaga¹, Xiaodong Gu¹, Keisuke Shimura¹, Akihiro Matsutani¹, Fumio Koyama¹; ¹Tokyo Inst. of Technology, Japan. We demonstrate a VCSEL amplifier with folded-path waveguide layout and cylindrical lens array for the dot projection. We obtained >5,000 dots in a viewing angle of 12° x 15° for 0.4 mm² chip size.

SM4N.5 • 17:15

Two-Dimensional Coupling in Tuned Coherent Hexagonal Vertical Cavity Laser Arrays, Bradley J. Thompson¹, Katherine Lakomy¹, Kent D. Choquette¹; ¹Univ. of Illinois, USA. A 6-element hexagonal VCSEL array is resonantly tuned to coherence. The far-field profile is narrowed in two-dimensions, with a FWHM of 2° compared to a single-emitter with 10° FWHM.

SM4N.6 • 17:30

Optimum optical frequency comb generation via externally injection of a gain switched VCSEL, Mohab N. Hammad¹, Eamonn Martin¹, Prajwal Doddaballapura Lakshmiyasimh¹, Aleksandra Kaszubowska-Anandarajah², Pascal Landais¹, Prince M. Anandarajah¹; ¹Dublin City Univ., Ireland; ²Connect, Trinity College Dublin, Ireland. A gain-switched VCSEL is subjected to external optical injection to enable optimized comb generation. The generated comb at 6.25GHz portrays a carrier-to-noise-ratio of 55dB, optical linewidth of 15kHz and a RIN of ~ 130 dB/Hz.

SM4O • Nonlinear Phonon Interactions—
Continued

SM4O.4 • 16:45

Broadband Brillouin-based phase shifter with phase amplification in a silicon waveguide, Luke McKay¹, Moritz Merklein¹, Alvaro Casas-Bedoya¹, Amol Choudhary¹, Yang Liu¹, Micah Jenkins², Charles Middleton², Alex Cramer², Joseph Devenport², Anthony Klee², Richard DeSalvo², Benjamin J. Eggleton¹; ¹The Univ. of Sydney, Australia; ²Harris Corporation, USA. We propose and demonstrate a broadband silicon phase shifter based on Brillouin scattering. We have achieved a 360° phase shift over a 15 GHz bandwidth with a phase amplification factor of 25.7 using only 1.5 dB gain.

SM4O.5 • 17:00

High-resolution RF spectrum analyzer on a chip, Eric Magi¹, Alvaro Casas-Bedoya¹, Moritz Merklein¹, Amol Choudhary¹, Duk-yong Choi², Pan Ma², Khu Vu², Stephen Madden², Robert L. Nelson³, Weimin Zhou⁴, Benjamin J. Eggleton¹; ¹Univ. of Sydney, Australia; ²Australian National Univ., Laser Physics Centre, Australia; ³Air Force Research Lab at Wright Patterson, USA; ⁴US Army Research Lab, USA. We demonstrate a high-resolution microwave spectrum analyzer enabled by an on-chip stimulated Brillouin scattering based tunable bandpass filter configuration. 30 MHz spectral resolution of single and multi-tone RF frequencies up to 12 GHz are demonstrated.

SM4O.6 • 17:15

Suppression of Stimulated Raman Scattering in a Two-Color Three-Beam Setup, Thomas Würthwein¹, Niels Irwin¹, Carsten Fallnich^{1,2}; ¹Inst. of Applied Physics, Germany; ²MESA+ Inst. of Nanotechnology, Netherlands. We present a technique for the suppression of stimulated Raman scattering using probe depletion in a two-color three-beam setup toward label-free sub-diffraction-limited imaging. A Raman suppression up to 79% could be shown.

SM4O.7 • 17:30 **Invited**

Brillouin Microscopy for 3D Biomechanical Imaging, Irina Kabakova¹; ¹Univ. of Technology Sydney, Australia. Brillouin microscopy is a non-contact and marker-free technique for probing viscoelasticity of tissues and cells in 3D. Here I review the principles of Brillouin microscopy, latest breakthroughs and applications to cell mechanobiology and disease diagnostics.

CLEO: QELS-Fundamental Science

FM4A • Quantum Nanophotonics II: Diamond & Boron Nitride—Continued

FM4B • Topological Photonics II—Continued

FM4B.8 • 17:45
Observation of corner states in topological photonic crystal slabs, Xiaodong Chen¹, Wei-Min Deng¹, Fu-Long Shi¹, Jian-Wen Dong¹; ¹*Sun Yat-Sen Univ., China*. With the near-field scanning measurement, we show the observation of in-gap corner states in topological photonic crystal slabs which consist of periodic dielectric rods on a perfect electric conductor.

FM4C • New Systems for Quantum Communications—Continued

FM4C.8 • 17:45
Symmetrical Clock Synchronization with Time-Correlated Photon Pairs, Jianwei Lee¹, Lijiong Shen^{1,2}, Alessandro Cerè¹, James Troupe³, Antia Lamas-Linares⁴, Christian Kurtsiefer^{1,2}; ¹*Centre for Quantum Technologies, Singapore*; ²*Physics, National Univ. of Singapore, Singapore*; ³*Applied Research Labs, USA*; ⁴*Texas Advanced Computing Center, USA*. We demonstrate a distance-independent clock synchronization protocol, using counter-propagating photons from spontaneous parametric down-conversion pair sources, secure against symmetric-delay attacks. With rates of 200 coincidences/s, we record a precision of 51ps over 100s.

FM4D • Excitons in Condensed Matter Systems—Continued

FM4D.7 • 17:45
Gate-tunable terahertz emission at oxide interfaces via ultrafast spin-to-charge current conversion, Qi Zhang¹, Deshun Hong¹, Changjiang Liu¹, Richard Schaller¹, Dillon Fong¹, Anand Bhattacharya¹, Haidan Wen¹; ¹*Argonne National Lab, USA*. We demonstrate gate-tunable spintronic terahertz (THz) emission at the interface of LaAlO₃ / SrTiO₃ due to ultrafast spin-to-charge current conversion. The soft phonon mode of SrTiO₃ is also observed in the emitted THz spectra.

17:30–18:30 Diversity and Inclusion Reception, *Winchester Room, Hilton San Jose*

18:30–20:00 Lasers for Attosecond 2.0, *Room 230A*

18:30–20:00 NEW Workshop 2: Will Quantum Computing Actually Work?, *Room 210A*
 NEW Workshop 3: What Will be the Largest Commercial Application for Optical Frequency Combs in 10 Years?, *Room 210B*

CLEO: Science & Innovations

SM4E • High-Average Power
Laser Systems—Continued

SM4E.6 • 17:45

Deep Learning for Real-Time Modeling of High Repetition Rate, Short Pulse CPA Laser Amplifier, Sandrine I. Herriot¹, Thomas Galvin¹, Brenda Ng¹, Emily Sistrunk Link¹, Shawn Betts³, Craig Siders¹, Thomas Spinka¹, Daniel Smith¹, Sachin Talathi², Wade Williams¹, Constantin Haefner¹; ¹LLNL, USA; ²Unknown, USA; ³UC Irvine, USA. Real-time feedback loop of kHz repetition rate, high intensity laser sets new challenges to the traditional modeling concept. We present a deep learning approach to model amplification and laser-induced damage in CPA laser system enabling high speed analysis above tens of kHz.

SM4F • Precision
Spectroscopy—Continued

SM4F.5 • 17:45

Calibration-free Wavelength Measurement with Sub-femtometer Resolution Based on All-fiber Rayleigh Speckles, Wang Shuai¹, Zhaopeng Zhang¹, Xinyu Fan¹, Bin Wang¹, Zuyuan He¹; ¹Shanghai Jiao Tong Univ., China. We propose an ultra-high resolution wavelength measurement approach with all-fiber based system. By extracting the Rayleigh speckles of a single mode fiber, we achieve a spectral resolution of 0.3 fm in optical frequency measurement.

SM4G • Access & Radio Over
Fiber—ContinuedSM4H • Advanced Optical
Technologies for Cells and
Tissues—Continued

SM4H.6 • 17:45

Nanophotonic Neural Probes for *in vivo* Light Sheet Imaging, Wesley D. Sacher¹, Xinyu Liu¹, Ilan Felts Almog², Anton Fomenko⁴, Thomas Lordello², Fu-Der Chen², Homeira Moradi-Chameh⁴, Azadeh Naderian⁴, Michael Chang⁴, Trevor Fowler¹, Taufik Valiante^{4,5}, Andres M. Lozano^{4,5}, Laurent Moreaux¹, Joyce K. Poon^{2,3}, Michael L. Roukes¹; ¹Division of Physics, Mathematics, and Astronomy, California Inst. of Technology, USA; ²Dept. of Electrical and Computer Engineering, Univ. of Toronto, Canada; ³Max Planck Inst. for Microstructure Physics, Germany; ⁴Krembil Research Inst., Canada; ⁵Division of Neurosurgery, Dept. of Surgery, Toronto Western Hospital, Univ. of Toronto, Canada. We present implantable silicon neural probes with nanophotonic waveguide routing networks and grating emitters for light sheet imaging. Fluorescein beam profiles, fluorescent bead imaging, and fluorescence brain imaging *in vivo* are presented.

17:30–18:30 Diversity and Inclusion Reception, *Winchester Room, Hilton San Jose*

18:30–20:00 Lasers for Attosecond 2.0, *Room 230A*

18:30–20:00 NEW Workshop 2: Will Quantum Computing Actually Work?, *Room 210A*
NEW Workshop 3: What Will be the Largest Commercial Application for Optical Frequency Combs in 10 Years?, *Room 210B*

Meeting Room
211 A/B

**CLEO: Applications
& Technology**

**AM4I • Nanobiophotonics—
Continued**

AM4I.7 • 17:45
Point-of-Care Multiplexing Assay for Dengue Using Barcoded Fluorescent Microspheres, Ryan X. Yuan¹, Srishti Garg¹, Anupriya Gopalsamy², Frederic Fellouse², Sachdev Sidhu², James Dou³, J. Stewart Aitchison¹; ¹Dept. of Electrical & Computer Engineering, Univ. of Toronto, Canada; ²Banting and Best Dept. of Medical Research and Dept. of Medical Genetics, Univ. of Toronto, Canada; ³ChipCare, Canada. Chromatic dispersion is utilized to separate fluorescent signals in different fluorescent dyes. The fluorescence intensity of allophycocyanin is used as the barcode fluorophore for specific biomarkers, enabling a four-plex biomarker detection.

Meeting Room
211 C/D

**CLEO: Science &
Innovations**

**SM4J • Light Emission &
Detection—Continued**

SM4J.7 • 17:45
50 Gb/s PAM4 Low-Voltage Si-Ge Avalanche Photodiode, Binhao Wang¹, Zhihong Huang¹, Xiaoge Zeng¹, Di Liang¹, Marco Fiorentino¹, Wayne Sorin¹, Raymond Beausoleil¹; ¹Hewlett Packard Enterprise, USA. We demonstrate a 50 Gb/s PAM4 operation of an integrated Si-Ge APD with low breakdown voltage of -10 V. The receiver has achieved -17 dBm optical input power at 50 Gb/s PAM4 with a bit error rate of 2.4×10^{-4} .

Meeting Room
212 A/B

**CLEO: Applications
& Technology**

**AM4K • A&T Topical Review on
Flat Optics II—Continued**

AM4K.5 • 17:45
Programmable metamaterials & metasurfaces for ultra-compact multi-functional photonics, Apratim Majumder¹, Sourangsu Banerji¹, Kazumasa Miyagawa¹, Monjurul Meem¹, Mark Mondol², Berardi Sensale-Rodriguez¹, Rajesh Menon¹; ¹Univ. of Utah, USA; ²MIT, USA. We demonstrate the design and experimental verification of several examples of programmable metamaterials and metasurfaces. Such devices offer the advantage of high-density integration and versatility.

Meeting Room
212 C/D

**CLEO: Science &
Innovations**

**SM4L • Specialty Fibers—
Continued**

17:30–18:30 Diversity and Inclusion Reception, Winchester Room, Hilton San Jose

18:30–20:00 Lasers for Attosecond 2.0, Room 230A

18:30–20:00 NEW Workshop 2: Will Quantum Computing Actually Work?, Room 210A
NEW Workshop 3: What Will be the Largest Commercial Application for Optical Frequency Combs in 10 Years?, Room 210B

**CLEO: QELS-Fundamental
Science**

CLEO: Science & Innovations

**FM4M • Solid State High Harmonic
Generation—Continued**

FM4M.7 • 17:45

Enhancement of Harmonic Generation in Gases Using an All-Dielectric Metasurface, Jared S. Ginsberg¹, Adam C. Overvig¹, M. M. Jadidi¹, Stephanie Malek¹, Gauri Patwardhan^{1,2}, Nicolas Swenson², Nanfang Yu¹, Alexander Gaeta¹; ¹*Applied Physics and Applied Mathematics, Columbia Univ., USA*; ²*Applied and Engineering Physics, Cornell Univ., USA*. We design and fabricate a dielectric metasurface for enhancing harmonic generation from gases with mid-infrared pulses. We observe third-harmonic generation in Ar at pump intensities as low as $1.8 \times 10^{12} \text{ W/cm}^2$.

**SM4N • Surface Emitting Lasers—
Continued**

SM4N.7 • 17:45

Energy-Efficient VCSELs for 200+ Gb/s Optical Interconnects, Gunter Larisch¹, Ricardo Rosales², James A. Lott², Dieter Bimberg^{2,1}; ¹*Bimberg Chinese-German Center for Green, China*; ²*Technische Universität Berlin, Germany*. Vertical-cavity surface-emitting lasers for 200+ Gbit/s single fiber data transmission systems emitting at 850 nm, 880 nm, 910 nm, and 940 nm are presented showing a heat-to-bit-rate energy efficiency of 240 fJ/bit.

**SM4O • Nonlinear Phonon Interactions—
Continued**

17:30–18:30 Diversity and Inclusion Reception, Winchester Room, Hilton San Jose

18:30–20:00 Lasers for Attosecond 2.0, Room 230A

18:30–20:00 NEW Workshop 2: Will Quantum Computing Actually Work?, Room 210A
NEW Workshop 3: What Will be the Largest Commercial Application for Optical Frequency Combs in 10 Years?, Room 210B

07:00–18:30 Registration, Concourse Level

08:00–10:00 JTu1A • Joint Plenary Session, Grand Ballroom 220A

10:00–17:00 Exhibit Open (10:00–17:00), Coffee Break (10:00–11:30), Exhibit Halls 1-3
Coffee Break Sponsored by  COHERENT and  THORLABS

10:30–12:00 Quantum Information Science and Technology Initiatives, Exhibit Hall Theater I

10:30–13:30 SC455: Integrated Photonics for Quantum Information Science and Technology (Dirk Englund, MIT, USA)

10:30–14:30 SC403: NanoCavity Quantum Electrodynamics and Applications (Jelena Vuckovic, Stanford University, USA)
SC410: Finite Element Modeling Methods for Photonics and Optics (Arti Agrawal, City University, UK)
SC438: Photonic Metamaterials (Nader Engheta, University of Pennsylvania, USA)
SC424: Optical Terahertz Science and Technology (David G. Cooke, McGill University, Canada)12:00–13:30 OIDA VIP Industry Leaders Speed Meeting Event, Booth 2605, Sponsored by  GoFoton

Exhibit Halls 1-3

11:30–13:00 JTu2A • Poster Session I and Lunch

JTu2A.1

Response of Porcine Articular Cartilage to Irradiation by an Ultrafast, Burst-Mode Laser, Thomas W. Dzelzainis⁶, Sabrina Hammouti⁶, Robin Marjoribanks⁶, Lothar Lilge^{7,2}, Margarete Akens^{1,7}, Omer Ilday³, Hamit Kaylaycioglu³, Seydi Yavas^{4,5}, Sohret Karamuk⁵, Melissa Prickaerts^{1,7}, Kailas Cassidy¹, Ahmad Golaraei^{6,2}, Virginijus Barzda^{6,8}, ¹Techna Inst., Univ. Health Network, Canada; ²Princess Margaret Cancer Centre, Univ. Health Network, Canada; ³Bilkent Univ., Turkey; ⁴Physics, Bogazici Univ., Turkey; ⁵Lumos Laser, Turkey; ⁶Physics, Univ. Of Toronto, Canada; ⁷Medical Biophysics, Univ. of Toronto, Canada; ⁸Chemical and Physical Sciences, Univ. of Toronto Mississauga, Canada. Plasma-mediated ablation by ultrafast pulses is generally considered to be a material-independent process. We show that, in certain circumstances, this assumption may be invalid. Physical processes involved and the impact on applications are discussed.

JTu2A.2

Ultra-short Laser Texturing of Biomimetic Hybrid Thin film Coatings from Natural Polymers and Their Ceramic Composites for Cellular Guidance, Albena Daskalova¹, Irina Bliznakova¹, Anton Trifonov², Liliya Angelova¹, Heidi Deqler-cq³, Ivan Buchvarov²; ¹Inst. of Electronics-BAS, Bulgaria; ²Faculty of Physics, St. Kliment Ohridski Univ. of Sofia, Bulgaria; ³Dept. of Basic Medical Sciences, Ghent Univ., Belgium. The goal of this study was to combine the osteogenic properties of biopolymers with good mechanical properties of ceramics to design improved implant interface and investigate the effect of fs laser texturing on surface characteristics of chitosan (CH) /Hydroxyapatite (HAp)/ ZrO₂ composite biofilms.

JTu2A.3

Multivariate Machine Learning Approaches for Data Fusion: Behavioral and Neuroimaging (Functional Near Infra-Red Spectroscopy) Datasets, Amir H. Gandjbakhche¹, Hadis Dasthestani¹; ¹National Inst.s of Health, USA. Coupling behavioral with neuroimaging datasets promises to provide insight into medical data analyses. Here, we investigate the relation between psychopathic traits and brain activities captured by functional near infra-red spectroscopy during a moral judgment task.

JTu2A.4

Multifocal Compressive Sensing Spectral Domain Optical Coherence Tomography Based on Bessel Beam, Luying Yi¹, Liqun Sun¹; ¹Tsinghua Univ., China. We present a method CS-MB-SDOCT, which combines multifocal Bessel beam spectral-domain optical coherence tomography (MB-SDOCT) and compressive sensing (CS) to increase the imaging depth using a spectrometer with lower spectral resolution.

JTu2A.5

An Absorbance Spectrum Estimation-based Accurate Colorization Method for Holographic Imaging of Pathology Slides, Tairan Liu¹, Yibo Zhang¹, Yujia Huang¹, Da Teng¹, Yinxiu Bian¹, Yichen Wu¹, Yair Rivenson¹, Alborz Feizi¹, Aydogan Ozcan¹; ¹Univ. of California Los Angeles, USA. We present an accurate-color holographic imaging method for pathology slide samples based on absorbance spectrum estimation of histochemical stains, which improves the color accuracy and reduces the required number of illumination wavelengths.

JTu2A.6

Corneal imaging with extended imaging range using dual spectrometer high-resolution SD-OCT, Lulu Wang¹; ¹NTU, Singapore. A dual-spectrometer SD-OCT system with extended imaging range, high spatial resolution was demonstrated for pig corneal imaging ex vivo. Spectra from the two spectrometers are combined to achieve a 3.4 mm maximum depth range with an axial and lateral resolution of 1.86 μm (n=1.38) and 1.96 μm.

JTu2A.7

Generation of surface plasmonic resonance mode on highly ordered diverse conformation of Au nanostructures, Hyerin Song¹, Heesang Ahn¹, Seunghun Lee¹, Tae Young Kang¹, Soojung Kim¹, Taeyeon Kim¹, Kyujung Kim¹; ¹Pusan National Univ., South Korea (the Republic of). Three different shapes of Au nanostructures, which are cone, embossed, and wave-like shapes, were fabricated with a high order based on an anodized aluminum oxide (AAO) template and utilized for surface-enhanced Raman scattering system.

JTu2A.8

Improving the Temporal Resolution of Speckle based Remote Phonocardiogram Sensing via Laser Modulation, Nisan Ozana¹, Zeev Markman², Ran Califa², Zeev Zalevsky¹; ¹Bar Ilan Univ., Israel; ²Continuse Biometrics, Israel. We present a method for remote phonocardiogram sensing which employs temporal modulation of the illumination laser. This method yields a significant enhancement of the temporal bandwidth of the captured speckle image sequence, thus improving performance.

JTu2A.9

Smart Carbon Fiber Sensing Systems Applied to Biomechanics, José R. Galvão¹, Talita Bastos¹, Carlos Zamarreño², John Canning³, Cicero Martelli¹, Jean Carlos Cardozo da Silva¹; ¹Federal Univ. of Technology – Pr, Brazil; ²Univ. of Navarra, Pamplona, Spain; ³Univ. of Technology Sydney, Australia. This paper presents three applications of carbon fiber reinforced polymer with integrated FBG sensor systems in biomechanics. In vivo tests were performed showing that the sensors are robust for the different applications.

JTu2A.10

Color imaging through the scattering media, Lei Zhu¹, Yuxiang Yuxiang¹, Jietao Liu¹, Xiaopeng Shao¹; ¹Xidian Univ., China. We developed a method to realize color imaging through the scattering media based on triple correlation technique. This method enables color imaging through the scattering media without the wavefront shaping technique and deconvolution technique.

JTu2A.11

Flat-top Supercontinuum Generation Based on Electro-optic Optical Frequency Comb, Minje Song^{2,1}, Sang-Pil Han², Sungil Kim², Minhyup Song²; ¹Kyungpook National Univ., South Korea (the Republic of); ²Electronics and Telecommunications Research Inst., South Korea (the Republic of). We demonstrate the optical frequency comb based supercontinuum (OFC-SC) with flatness using the pulse shaping technique and the dispersion compensation. Furthermore, we achieve the short pulse width with electro-optic OFC-SC.

JTu2A.12

In-situ laser fabrication to reduce eccentricity errors in optical encoders, Robin Hahn¹, Christof Pruss¹, Martina Dombrowski¹, Maik Gerngross², Matthias Schirmer², Christian Kreisel³, Bernd Sommer⁴, David Hopp⁵, Christina Schneider⁵, Christian Sellmer⁵, Mathias Wenzler⁵, Wolfgang Osten¹; ¹*Inst. of Applied Optics, Germany*; ²*Allresist GmbH, Germany*; ³*Ac-sys Lasertechnik GmbH, Germany*; ⁴*Stvision GmbH, Germany*; ⁵*Sick Stegmann GmbH, Germany*; Rotational encoders are of high importance of nowadays robotic systems. We present a technique for laser based post assembly fabrication, increasing the accuracy, decreasing the alignment effort and giving the possibility of an increased flexibility.

JTu2A.13

Withdrawn

JTu2A.14

A depth information acquisition method through 3D polarization imaging technology, Xuan Li¹, Fei Liu¹, Fangyi Chen¹, Yudong Cai¹, Xiaopeng Shao¹; ¹*Xidian Univ., China*. We propose a method to get the real depth information of the object based on the spatial coordinate transformation method in 3D polarization imaging. This technique is useful for 3D polarization imaging of single camera.

JTu2A.15

Investigation of Surface Treatment Methods for 3D Printed Optical Components, Joshua Davidson¹, Jianan Zhang¹, Tim Kane¹, Ram Narayanan¹; ¹*Penn State Univ., USA*. This paper proposes a method for preparing 3D printed surfaces as commercial quality optical components. Utilizing Formlabs' dipping method and pulse-reverse electroplating, a surface finish of $\lambda/10$ can be achieved.

JTu2A.16

Well Arranged PDLC Droplets in Grating Structures Inducing the Reduction of Driving Voltage, Chiu-Chang Huang¹, Hsuan-Han Huang¹, Bor-Wei Liang¹, Cheng-Che Lee¹, Bo-Han Kung¹, Chieh-Hsiung Kuan¹; ¹*National Taiwan Univ., Taiwan*. Grating structures were integrated in the polymer dispersed liquid crystal (PDLC) device and induced the arrangement of PDLC droplets which haven't been reported. In addition, the driving voltage was reduced.

JTu2A.17

Optical Engineering of Vector Beams with Parabolic and Elliptic Cross-Sections, Sergejus Orlovas¹, Pavel Gotovski¹, Justas Baltrukonis¹, Vytautas Jukna¹, Titas Gertusis¹; ¹*National Center for Physical Sciences and Technology, Lithuania*. Beam profile engineering is a promising approach in various applications. We introduce vector versions of Mathieu and Weber beams and use those vector beams to engineer controllable spatial phase and amplitude distributions with polarization control.

JTu2A.18

Charging of a Single InAs QD with Electrically-Injected Holes using a Lateral Electric Field, Xiangyu Ma¹, Yuejing Wang¹, Joshua Zide¹, Matthew Doty¹; ¹*Univ. of Delaware, USA*. We design and fabricate a 3-electrode device that applies 2-D electric fields to a single InAs QD. We observe electrical injection of holes into a QD due to the lateral electric field component.

JTu2A.19

Interaction of an Atomic Gas with Light Carrying Orbital Angular Momentum, Guillermo Quinteiro¹, Patricio Grinberg¹, Christian T. Schmiegelow¹; ¹*Universidad de Buenos Aires, Argentina*. The orbital angular momentum of light affects the response of point-like and extended systems. For a gas undergoing S-P transitions we show qualitative differences among collimated and tightly-focused light without and with orbital angular momentum.

JTu2A.20

Highly efficient optical pumping of Rb atoms for evanescent fields at dielectric-vapor interfaces, Eliran Talker³, P. Arora³, Yefim Barash³, David Wilkowski^{1,2}, Uriel Levy³; ¹*School of Physical and Mathematical Sciences, Nanyang Technological Univ., Singapore, Singapore*; ²*MajLab, CNRS-UCASU-NUS-NTU International Joint Research Unit, Singapore, Singapore*; ³*Dept. of Applied Physics, The Hebrew Univ., Givat Ram Campus, Israel*. Optical prism integrated with a vapor cell and excited by evanescent wave under total internal reflection is used to study nanoscale light-atom interactions and to demonstrate efficient optical pumping of rubidium at a dielectric-vapor interface.

JTu2A.21

Single photon spectroscopy of excited state structure in hBN quantum emitters, Matthew Feldman^{1,2}, Claire Marvinney¹, Alex Puretzyk¹, Philip Evans¹, Richard F. Haglund², Benjamin Lawrie¹; ¹*Oak Ridge National Lab, USA*; ²*Vanderbilt Univ., USA*. The electronic structure of hBN defects remains poorly defined despite its importance for room-temperature single-photon sources. We address this deficiency by characterizing shelving dynamics and photon correlations between photochemically modified electronic transitions.

JTu2A.22

Trapped ion slow light: first photonic interaction between a photon from an ion and neutral atoms, John M. Hannegan^{1,2}, James Siverns^{1,2}, Qudsia Quraishi^{3,1}; ¹*Joint Quantum Inst., USA*; ²*Inst. for Research in Electronics and Applied Physics, USA*; ³*US Army Research Lab, USA*. Hybrid quantum systems will enable practical implementation of quantum-memory based photonic networking. Using quantum frequency conversion, we slow photons emitted from $^{138}\text{Ba}^+$ using warm ^{87}Rb vapor, demonstrating the first hybrid interaction between ion-emitted photons and neutral atoms.

JTu2A.23

Measurements of Frequency-Resolved Third-Order Correlations in Quantum Dot Resonance Fluorescence, Yamil A. Nieves¹, Andreas Muller¹; ¹*Univ. of South Florida, USA*. We investigated the three-photon spectrum of quantum dot resonance fluorescence, revealing significantly more pronounced photon antibunching at the Mollow triplet sidebands and more strongly correlated emission through virtual states than at second order.

JTu2A.24

Upper Bound on the Duration of Quantum Jumps, Mathias A. Seidler¹, Alessandro Cere¹, Ricardo Gutierrez-Jauregui², Rocío Jauregui³, Christian Kurtsiefer¹; ¹*National Univ. of Singapore, Singapore*; ²*Instituto de Física, UNAM, Mexico*; ³*Inst. for Quantum Science and Engineering, Texas A&M Univ., USA*. We estimate the time scale of quantum jumps from the time correlation of photon pairs generated from a cascade decay in a cold cloud of ^{87}Rb . We find an upper bound of 21 ± 11 ps.

JTu2A.25

Experimental observation of multi-atom Dicke states in an atomic vapor using optical 2D coherent spectroscopy, Shaogang Yu^{2,1}, Michael Titz², Yifu Zhu², Xiaojun Liu¹, Hebin Li²; ¹*Wuhan Inst. of Physics & Mathematics, China*; ²*Florida International Univ., USA*. We report the first observation of two-, three-, four-, five-, six-, and seven-atom Dicke states in an atomic vapor using optical multi-quantum 2D coherent spectroscopy. This has significant implications in the studies of many-body physics.

JTu2A.26

Characterization of the Superhyperfine Interaction in $^{171}\text{Yb}:\text{YVO}_4$, Yan Qi Huan^{1,2}, Jonathan Kindem^{1,2}, John G. Bartholomew^{1,2}, Andrei Faraon^{1,2}; ¹*Kavli Nanoscience Inst. and Thomas J. Watson, Sr., Lab of Applied Physics, California Inst. of Technology, USA*; ²*Inst. for Quantum Information and Matter, California Inst. of Technology, USA*. We computationally characterize the superhyperfine energy structure of $^{171}\text{Yb}:\text{YVO}_4$ and compare predicted holeburning spectra and coherence times with experimental data. Our simulation can help optimize coherence times for ensemble-based quantum memories and single-ion qubits.

JTu2A.27

Quantum Capacitors for Electronic Read-out in Spin-based Quantum Information Processing, Pouya Dianat¹, Bahram Nabet¹; ¹*Drexel Univ., USA*. Quantum capacitors are demonstrated for gauging of quantum energy states, which provide an unprecedented electronic read-out for spintronic systems applied in quantum information processing.

JTu2A.28

BB84 and DQPS-QKD experiments using one polarization-insensitive measurement setup with a countermeasure against detector blinding and control attacks, Muataz M. Alhussein¹, Kyo Inoue¹, Toshimori Honjo²; ¹*Graduate School of Eng., Osaka Univ., Japan*; ²*NTT Basic Research Labs, NTT Corporation, Japan*. This paper demonstrates phase-encoding BB84-based QKD experiments with active basis selection using one interferometer with no phase and polarization controls, unlike conventional BB84-QKD experiments. A countermeasure against detector blinding attack is also implemented.

JTu2A.29

Withdrawn

JTu2A.30

Solving the Untrusted Source Problem in Measurement-Device-Independent Quantum Key Distribution, Yucheng Qiao¹, Gan Wang¹, Zhengyu Li¹, Bingjie Xu², Bin Luo³, Hong Guo¹; ¹*Peking Univ., China*; ²*Inst. of Southwestern Communication, China*; ³*Beijing Univ. of Posts and Telecommunications, China*. We propose a light source monitoring scheme to solve the untrusted source problem in measurement-device-independent quantum key distribution, and show it performs almost the same as the initial protocol with a trusted source.

JTu2A.31

Generation of Continuous Variable Quantum Entanglement at 1550 nm and Distribution Over Optical Fiber, JinXia Feng^{1,2}, Hao Zhao¹, Dandan Nie¹, Yuanji Li^{1,2}, Kuanshou Zhang^{1,2}; ¹*State Key Lab of Quantum Optics and Quantum Optics Devices, Inst. of Opto-Electronics, Shanxi Univ., China*; ²*Collaborative Innovation Centre of Extreme Optics, Shanxi Univ., China*. Continuous variable quantum entanglement of 8.3 dB are experimentally generated and distributed over 20 km optical fiber. A theoretical prediction considering excess noise in fiber channel is in good agreement with the experimental results.

JTu2A.32

Single Qubit Gates on a Microfabricated Ion Chip Trap with Integrated Diffractive Optics, Erik W. Streed^{1,2}, Jordan Scarbelle¹, Steven Connell¹, Kenji Shimizu¹, Valdis Blums¹, Marcin Piotrowski^{1,3}, Mirko Lobino^{1,4}; ¹*Centre for Quantum Dynamics, Griffith Univ., Australia*; ²*Inst. for Glycomics, Griffith Univ., Australia*; ³*Manufacturing, CSIRO, Australia*; ⁴*Queensland Micro and Nanotechnology Centre, Griffith Univ., Australia*. $^{171}\text{Yb}^+$ was trapped above a Fresnel mirror collimator. Integrated microwave rails provided a 68kHz Rabi rate on the 12.7 GHz transition with a 2.7 ms decoherence time. Doppler recoiling measured a 27 quanta/ms heating rate.

JTu2A.33

Energy-Time Entanglement Based Dispersive Optics Quantum Key Distribution over Optical Fibers of 20 km, Xu Liu^{1,2}, Xin Yao^{1,2}, Heqing Wang³, Hao Li³, Lixing You³, Yidong Huang^{1,2}, Wei Zhang^{1,2}; ¹*Dept. of Electronic Engineering, Beijing National Research Center for Information Science and Technology (BNRIST), Beijing Innovation Center for Future Chips, Electronic Engineering Dept., Tsinghua Univ., China*; ²*Beijing Academy of Quantum Information Sciences, China*; ³*State Key Lab of Functional Materials for Informatics, Shanghai Inst. of Microsystem and Information Technology, Chinese Academy of Sciences, China*. An energy-time entanglement based dispersive-optics quantum key distribution is demonstrated experimentally over 20 km optical fibers, in which photon pairs are generated by spontaneous four wave mixing in a silicon waveguide.

JTu2A.34
Withdrawn**JTu2A.35**

Verifying hidden quantum steering via local filtering operations, Yong-Su Kim¹, Tanumoy Pramanik¹, Young-Wook Cho¹, Sang-Wook Han¹, Sang-Yun Lee¹, Sung Moon¹; ¹South Korea Inst. of Science & Technology, South Korea (the Republic of). We theoretically and experimentally investigate the 'hidden' property of quantum steerability. In particular, we find that there are initially unsteerable states which can reveal the steerability by using local filtering operations on individual quantum systems.

JTu2A.36

Conversion of Position Correlation into Polarization Entanglement, Chithrabhanu Perumangatt¹, Alexander Lohrmann¹, Alexander Ling^{1,2}; ¹Centre for quantum technologies, India; ²Physics, National Univ. of Singapore, Singapore. The photons pairs generated by parametric down conversion of a laser beam have inherent position and momentum correlations. We generate bright, high fidelity polarization entangled photons by manipulating the position correlations using a Mach-Zehnder interferometer.

JTu2A.37

Bright Beams of Intensity Difference Squeezed Light for use in Sub-shot-noise Imaging, Rory W. Speirs¹, Nicholas R. Brewer², Meng-Chang Wu^{1,3}, Paul D. Lett²; ¹Joint Quantum Inst., The Univ. of Maryland, USA; ²Joint Quantum Inst., National Inst. of Standards and Technology, USA; ³Inst. of Physical Science and Technology, The Univ. of Maryland, USA. We present a method for using bright beams of intensity difference squeezed light to perform sub-shot-noise imaging. The intensity correlated twin beams are generated by four wave mixing in rubidium vapour.

JTu2A.38

Detection of 10 dB vacuum noise squeezing at 1064 nm by balanced homodyne detectors with a common mode rejection ratio more than 80 dB, Chien-Ming Wu¹, Shu-Rong Wu¹, Yi-Ru Chen¹, Hsun-Chung Wu¹, Ray-Kuang Lee¹; ¹National Tsing Hua Univ., Taiwan. Quantum noise reduction up to 10 dB is observed, with the help of our home-made balanced homodyne detector (BHD), characterized with a Common Mode Rejection Ratio (CMRR) more than 80 dB.

JTu2A.39

Realization of optical isolator at room temperature in miniaturized vapor cell using light induced atomic desorption, Eiliran Talker¹, P. Arora¹, Mark Dikopoltsev^{1,2}, Uriel Levy¹; ¹Dept. of Applied Physics, The Hebrew Univ. Jerusalem, Israel, Israel; ²RAFAEL, Science Center, Rafael Ltd, Haifa (Israel), Israel. A compact, on-chip atomic optical isolator using light induced atomic desorption technique is demonstrated. A millimeter size fabricated vapor cell integrated with small permanent magnets of ≈ 300 Gauss are used to realize an atomic optical isolator at room temperature.

JTu2A.40

GHz Photon-number-resolving Detection with InGaAs/InP APD, Yan Liang¹, Zhihe Liu¹, Qilai Fei¹, Heping Zeng^{1,2}; ¹USST, China; ²East China Normal Univ., China. Combining ultrashort gates and the robust spike-noise suppression technique, we demonstrate an InGaAs/InP APD based photon-number-resolving detector capable of distinguishing up to 3 photons with the detection efficiency as high as 40% at 1 GHz.

JTu2A.41

Generation and Detection of Down-converted Photon Pairs at 2.080 μm , Shashi Prabhakar¹, Taylor Shields¹, Damian Powell¹, Gregor G. Taylor¹, Dmitry Morozov¹, Mehdi Ebrahim¹, Michael Kues¹, Lucia Caspani², Corin Gawith³, Robert H. Hadfield¹, Matteo Clerici¹; ¹School of Engineering, Univ. of Glasgow, UK; ²Dept. of Physics, Univ. of Strathclyde, UK; ³Covesion Ltd. & Optoelectronics Research Centre, Univ. of Southampton, UK. We report the generation and coincidence-to-accidental ratio characterization of a pulsed spontaneous parametric down-conversion photon pair source at 2.080 μm , as a basis for free-space quantum communication in an atmospheric window with low solar background.

JTu2A.42

Generating polarization-entangled photon pairs in domain-engineered PPLN, Paulina S. Kuo¹, Varun B. Verma², Thomas Gerrits², Sae Woo Nam², Richard P. Mirin²; ¹Information Technology Lab, NIST, USA; ²Physical Measurement Lab, National Inst. of Standards and Technology, USA. Using a periodically poled LiNbO₃ crystal that is domain-engineered for two simultaneous type-II down-conversion processes, we demonstrated polarization-entangled photon-pair generation.

JTu2A.43

Site-controlled InAs quantum dot for hetero-integration of single photon emitter, Young-Ho Ko¹, Won Seok Han¹, Kap-Joong Kim¹, Byung-Seok Choi¹, Kyu Young Kim², Je-Hyung Kim², Heeju Kim³, Yudong Jang³, Donghan Lee³, Chun Ju Youn¹, Jong-Hoi Kim¹, Jung Jin Ju¹; ¹Electronics and Telecom Research Inst, South Korea (the Republic of); ²Ulsan National Inst. of Science and Technology, South Korea (the Republic of); ³Chungnam National Univ., South Korea (the Republic of). For hetero-integration of single photon emitter with silicon photonics, the site-controlled quantum dot was obtained by selective-area growth. The integrated structure was designed as InAs quantum dot on the silicon waveguides with high coupling efficiency and fabricated by micro-transfer technique.

JTu2A.44

Non-phase Matched Spontaneous Parametric Down Conversion in Ultra-thin Lithium Niobate, Cameron S. Okoth^{1,2}, Tomas Santiago^{1,2}, Andrea Cavanna^{1,2}, Maria Chekhova^{1,2}; ¹Max-Planck Inst. for the Science of Light, Germany; ²Physics, Univ. of Erlangen Nuremberg, Germany. We report the generation of entangled photon pairs via type-0 spontaneous parametric down conversion in ultra-thin lithium niobate in which momentum between the pump photon and daughter photons is not conserved.

JTu2A.45

Observing the quantum Cheshire cat with a nondestructive weak measuring device, Yosep Kim², Dong-Gil Im², Yong-Su Kim¹, Sang-Yun Lee¹, Sang-Wook Han¹, Sung Moon¹, Yoon-Ho Kim², Young-Wook Cho¹; ¹South Korea Inst. of Science & Technology, South Korea (the Republic of); ²Pohang Univ. of Science and Technology (POSTECH), South Korea (the Republic of). In this work, we report the experimental observation of the quantum Cheshire cat effect with a nondestructive weak measuring device. A quantum pointer after the weak quantum measurement indicates that the polarization can be found at the path the photon did not take.

JTu2A.46

Design and Production of Femtosecond Laser Writable Borate-based Glasses for Photonic Devices, Antonio Dias¹, Francisco Muñoz², Asier Alvarez², Pedro Moreno-Zarate³, Julia Atienzar¹, Ana Urbiet⁴, Paloma Fernandez², Marina Garcia¹, Rosalia Serna¹, Javier Solis¹; ¹Instituto De Optica 'Daza De Valdes', Spain; ²Ceramics and Glass Inst. (ICV, CSIC), Spain; ³Engineering School, Tepexi Higher Technological Inst., Mexico; ⁴Dept. of Materials Physics, Faculty of Physics, Univ. Complutense, Spain. This work reports the design, synthesis, laser processing and performance of borate glasses that were compositionally designed to be femtosecond laser writable using laser-induced ion migration, leading to the production efficient optical waveguides.

JTu2A.47

Selective Delamination of Thin Films from Ceramic Surfaces upon Femtosecond Laser Ablation, Frederik Kiel¹, Nadezhda M. Bulgakova¹, Andreas Ostendorf², Evgeny Gurevich²; ¹HiLASE, Inst. of Physics ASCR, Russia; ²Applied Laser Technologies, Ruhr-Universität Bochum, Germany. Experimental observation of selective delamination of YSZ ceramics upon femtosecond laser processing of its surface is reported. The delamination mechanism is identified as an interplay between beam defocusing by laser-generated free-electron plasma and Kerr nonlinearity.

JTu2A.48

High-Resolution Mid-Infrared Spectral Reconstruction using a Subwavelength Coaxial Aperture Array, Benjamin J. Craig¹, Jiajun Meng¹, Vivek R. Shrestha¹, Jasper Cadusch¹, Kenneth Crozier¹; ¹Univ. of Melbourne, Australia. We demonstrate mid-infrared computational spectroscopy using an array of coaxial aperture filters. We experimentally determine material transmission spectra using an algorithm whose inputs are the transmission spectra and the power transmitted through each filter.

JTu2A.49

Monolithic integration of an electrically tunable ultrahigh-Q optomechanical device, Zhiwei Fang^{1,4}, Sanaul Haque², Jintian Lin², Rongbo Wu³, Jianhao Zhang², Min Wang^{1,4}, Muniyat Rafa², Ya Cheng^{1,4}, Tao Lu²; ¹State Key Lab of Precision Spectroscopy, East China Normal Univ., China; ²Dept. of Electrical and Computer Engineering, Univ. of Victoria, Canada; ³State Key Lab of High Field Laser Physics, Shanghai Inst. of Optics and Fine Mechanics, China; ⁴XXL—The Extreme Optoelectronics Lab, East China Normal Univ., China. We demonstrate an electrically tunable ultrahigh-Q optomechanical device (mechanical Q $\sim 2.76 \times 10^9$) for the mechanical mode at 100.32 MHz by monolithically integrating an on-chip lithium niobate microresonator (optical Q $\sim 10^7$) with a pair of in-plane microelectrodes.

JTu2A.50

Laser-Induced-Modification Raman Spectroscopy for Probing Microscopic Structural Variation Beyond Conventional Techniques: CZTSe as an Example, Qiong Chen¹, Yong Zhang¹; ¹UNC-Charlotte, USA. Laser-induced-modification Raman spectroscopy coupled with high spatial resolution and high-temperature capability is demonstrated to obtain additional structure information beyond what the conventional techniques offer, revealing microscopic scale variation between nominally similar alloys.

JTu2A.51

Graphene-coated Suspended Metallic Nanostructures for Fast and Sensitive Optomechanical Infrared Detection, Mohammad Wahiduzzaman Khan¹, Parinaz Sadri Moshkenani¹, Md Shafiqul Islam¹, Ozdal Boyraz¹; ¹Univ. of California Irvine, USA. We investigate the effect of incorporating graphene in suspended metallic nanostructures for radiation detection. We have found enhanced absorbance resulting in increased sensitivity and faster operation owing to graphene's extraordinary plasmonic and thermal properties.

JTu2A.52

Room Temperature Control of Valley Coherence in Bilayer WS₂ Exciton Polaritons, Mandeep Khatoniar^{1,4}, Nicholas Yama², Areg Ghazaryan³, Sriram Guddala⁴, Pouyan Ghaemi^{4,1}, Vinod Menon^{4,1}; ¹Physics, Graduate Center, USA; ²Physics, Univ. of Hawaii at Manoa, USA; ³Physics, IST Austria, Austria; ⁴Physics, City College of New York, USA. We demonstrate robust retention of valley coherence and its control via polariton pseudospin precession through the optical TE-TM splitting in bilayer WS₂ microcavity exciton polaritons at room temperature.

JTu2A.53

Laser Interaction in Additive Manufacturing of Optics and Photonics, Nicholas Capps², Jason Johnson¹, Jonathan Goldstein³, Edward Kinzel^{2,1}; ¹Missouri Univ. of Sci. and Tech., USA; ²Aerospace and Mechanical Engineering, Univ. of Notre Dame, USA; ³Air Force Research Laboratory, USA. The laser/glass interaction in Fiber-Fed Laser-Heated Additive Manufacturing is studied. Specifically, the effects of the laser wavelength, power, and interaction time are considered experimentally and using numeric models.

JTu2A.54

Femtosecond Laser- Colored AZO Films on Flexible Mica Substrates, Chih Wei Luo¹, Hung Yang¹, Tien-Tien Yeh¹, Chien-Ming Tu¹; ¹National Chiao Tung Univ., Taiwan. Laser-colored aluminum-doped zinc oxide (AZO) films are fabricated using femtosecond laser annealing. By varying the laser fluences, ripple-like nanostructures are generated on the surface of AZO films, which produces cyan, yellow and orange colors.

JTu2A.55

Phase Retardance and Broadband Spatio-Spectral Overlap of Chiral Hybrid Modes on Large-Area Nanofingernails, Aneek Biswas², Paulina Librizzi³, Ilona Kretschmar³, Luat Vuong¹; ¹Univ. of California at Riverside, USA; ²Physics, City Univ. New York, USA; ³Chemical Engineering, City Univ. New York, USA. Unusually-broadband excitations of chiral hybrid modes on micropore nanofingernails exhibit phase retardation effects, which spatially overlap intensity hotspots across the visible and NIR spectrum. We demonstrate that enhanced chiral scattering occurs without circular dichroism.

JTu2A.56

Optical Detection of Deuterium in Heavy Water: Towards Remote Detection of Tritium, Milos Burger¹, Patrick J. Skrodzki¹, Lauren A. Finney¹, Jörg Hermann², John Nees¹, Igor Jovanovic¹; ¹Univ. of Michigan, USA; ²Aix-Marseille Univ., CNRS, LP3, France. Tritium detection poses a challenge because of the weak beta particle emission and absence of ionizing radiation. We demonstrate the isotopic analysis of deuterated water via laser-induced breakdown spectroscopy as a modality for measuring tritium.

JTu2A.57

Scattered Complex Laguerre-Gaussian Spectrum to Determine the 2-D Transverse Position of a Spherical Silica Particle, Runzhou Zhang¹, Hao Song¹, Zhe Zhao¹, Haoqian Song¹, Jing Du¹, Guodong Xie¹, Long Li¹, Kai Pang¹, Cong Liu¹, Ahmed Almaiman¹, Shlomo Zach², Nadav Cohen², Moshe Tur², Alan E. Willner¹; ¹Univ. of Southern California, USA; ²Tel Aviv Univ., Israel. We study the complex Laguerre-Gaussian (LG) spectrum of single-silica-particle-scattered light by finite-difference-time-domain (FDTD) simulation. We find that complex LG spectrum can be potentially utilized for 2-dimensional localization of a dielectric spherical particle.

JTu2A.58

Multi-shot and Single-shot Time-resolved Visualization of Material Modification During Laser Micromachining With Flexible Glass, Dennis Dempsey¹, Garima C. Nagar¹, James S. Sutherland², Rostislav I. Grynkov¹, Bonggu Shim¹; ¹Binghamton Univ., USA; ²Corning Research & Development Corporation, USA. We visualize material modification during laser micromachining, in particular, laser waveguide fabrication in flexible Corning® Willow® Glass via time-resolved interferometry, and single-shot frequency-domain holography which is a robust technique for studying permanent material change/damage.

JTu2A.59

Joule-level 10 Hz non-collinear multi-pumps SBS amplifier with high combining efficiency used for laser beams combination, Can Cui¹, Yulei Wang¹, Zhiwei Lu¹, Zhenxu Bai¹, Yue Wang¹, Hang Yuan¹; ¹Harbin Inst. of Technology, China. We demonstrated the non-collinear SBS amplifier with the energy extraction efficiency up to 70% and the output of 2.5 J at 10 Hz. Multiple pumps and the increase of optical intensity enhance the performance of the amplifier.

JTu2A.60

A Superluminal Raman Laser with Enhanced Cavity Length Sensitivity, Zifan Zhou¹, Minchuan Zhou¹, Selim M. Shahriar¹; ¹Northwestern Univ., USA. We demonstrate experimentally an optically pumped Raman laser with a self-pumped Raman depletion employing two isotopes of rubidium, achieving an inferred spectral sensitivity to cavity length change by a factor of more than a thousand.

JTu2A.61

Cavity-External Spatial Gain Shaping for Selective Higher-Order Mode Excitation, Florian Schepers¹, Tim Bexter¹, Tim Hellwig¹, Carsten Fallnich^{1,2}; ¹Inst. of Applied Physics, Univ. of Muenster, Germany; ²MESA+ Inst. of Nanotechnology, Univ. of Twente, Netherlands. We present cavity-external spatial gain shaping based on a digital micromirror device for the selective and realignment-free excitation of nearly 1000 different single Hermite-Gaussian modes in an end-pumped Nd:YVO₄.

JTu2A.62

Direct generation of vortex beams from a diode-pumped Pr³⁺:YLF laser, Yuanyuan Ma¹, Jung-Chen Tung², Katsuhiko Miyamoto^{1,3}, Takashige Omatsu^{1,3}; ¹Chiba Univ., Japan; ²National Chiao Tung Univ., Taiwan; ³MCRC Chiba Univ., Japan. We have demonstrated the direct generation of 100 mW level visible scalar and vector vortex modes from a diode-pumped Pr³⁺:YLF laser by employing an off-axis pumping technique.

JTu2A.63

High-order actively mode-locked picosecond fiber laser and Poisson single-photon source, H. Y. Wang¹, Zhengyong Li¹, X. K. Zhan¹, S. C. Wang¹, B. C. Wang¹; ¹Beijing Jiaotong Univ., China. We demonstrate the 200th-order actively mode-locked picosecond fiber laser based on nonlinear polarization rotation in a semiconductor optical amplifier with GHz repetition frequency and 1.63-ps pulse width, which produces a Poisson single-photon source.

JTu2A.64

Pulse compression of multiple plate continuum at 1.55 μm, Chia-Lun Tsai¹, Yi-Hsun Tseng¹, An-Yuan Liang¹, Jhan-You Guo¹, Ming-Wei Lin¹, Shang-Da Yang¹, Ming-Chang Chen¹; ¹Natl Tsing Hua Univ, Taiwan. We experimentally demonstrated nonlinear pulse compression at 1.55 μm from 80 fs to 28 fs by using multiple plate continuum generation and femtosecond pulse shaping.

JTu2A.65

Compensation of Frequency Modulation to Amplitude Modulation Conversion in Regenerative Amplifier, Elodie Boursier¹, Sébastien Montant¹, Jacques Luce¹, Eric Lavastre¹, Denis Penninckx¹; ¹CEA CESTA, France. This work deals with the compensation of FM-to-AM conversion induced by the spectral response of regenerative cavity. We show that it is possible to reduce amplitude modulations from 44% to 9% using an interference filter.

JTu2A.66

Ultraportable laser based on multi-cavity, Lulu Yan^{1,2}, Yanyan Zhang^{1,2}, Pan Zhang¹, Songtao Fan^{1,2}, Xiaofei Zhang^{1,2}, Wenge Guo¹, Shougang Zhang^{1,2}, Haifeng Jiang^{1,2}; ¹National Time Service Center, China; ²Univ. of Chinese Academy of Sciences, China. We report a proposal of developing ultraportable laser referenced to multi-cavity, reducing thermal noise by averaging effect of beam size. We perform an experiment to simulate a two-cavity system and obtained the instability is $5 \times 10^{-16}/1s$, improved by a factor of $\sqrt{2}$ from a single cavity system.

JTu2A.67

Generating a Twisted Spatiotemporal Wave Packet Using Coherent Superposition of Structured Beams with Different Frequencies, Zhe Zhao¹, Runzhou Zhang¹, Hao Song¹, Haoqian Song¹, Long Li¹, Jing Du¹, Cong Liu¹, Kai Pang¹, Ahmed Almaiman¹, Robert Boyd², Moshe Tur³, Alan E. Willner¹; ¹Univ. of Southern California, USA; ²Univ. of Rochester, USA; ³Tel Aviv Univ., Israel. We explore the superposition of different LG modes located on different frequencies to control the wave packet's spatiotemporal structures in simulation. Dependence of its rotating helical envelope on the mode and frequency spectra is analyzed.

JTu2A.68

Development of an Actively Cooled Glass Amplifier at GSI, Marco Patrizio¹, Vincent Bagnoud^{2,3}, Bernhard Zielbauer², Markus Roth^{1,4}; ¹Nuclear Physics, TU Darmstadt, Germany; ²Plasma Physics, GSI Helmholtz Centre for Heavy Ion Research, Germany; ³Helmholtz Inst. Jena, Germany; ⁴Facility for Antiproton and Ion Research (FAIR), Germany. Increasing the repetition rate of a large aperture glass amplifier requires active cooling systems. We present our cooling concept, potential coolants and simulation results achieving an increase in repetition rate by a factor of 10.

JTu2A.69

Beam Pointing Detection by Interference with a Frequency Shifted Higher-Order Mode, Florian Schepers¹, Tim Brüggenkamp¹, Tim Hellwig¹, Carsten Fallnich^{1,2}; ¹Univ. of Muenster, Germany; ²MESA+ Inst. of Nanotechnology, Univ. of Twente, Netherlands. We present the beam pointing detection of a fundamental mode by a superposition with a frequency-shifted higher-order Hermite-Gaussian mode and experimentally demonstrate its applicability for stabilization of beam position.

JTu2A.70

Modulation Bandwidth Enhancement and Chirp Reduction in DFB Lasers with Active Optical Feedback, Yuanfeng Mao¹, Wu Zhao¹, Jiankun Wang¹, Hao Wang¹, Yongguang Huang¹, Dan Lu¹, Chen Ji¹, Qiang Kan¹, Wei Wang¹; ¹Inst. of Semiconductors, CAS, China. 1.55-μm DFB lasers with active optical feedback exhibits high modulation bandwidth and reduced frequency chirp. 25-Gb/s clearly open eyes and 10-km SMF error-free transmission with small power penalty was achieved.

JTu2A.71

Continuous Wave Amplified Spontaneous Emission from Mixed Cation Perovskite devices, Philipp Brenner², Ofer Bar-On¹, Marius Jakob², Isabel Allegro², Bryce Richards², Ulrich Paetzold², Ian Howard², Jacob Scheuer¹, Uli Lemmer²; ¹Tel-Aviv Univ, Israel; ²KIT, Germany. Amplified spontaneous emission from perovskite devices is demonstrated under continuous wave (CW) pumping. The devices are based on mixed cation perovskites, which preserve their phase in temperature, constituting a crucial step towards practical perovskite photonics.

JTu2A.72

High-Power Wide-Bandwidth 1.55-μm Directly Modulated DFB Lasers for Free Space Optical Communications, Hao Wang^{1,2}, Ruikang Zhang¹, Qiang Kan¹, Dan Lu¹, Wei Wang¹, Lingjuan Zhao¹; ¹Inst. of Semiconductors, Chinese Academy of Sciences, China; ²Univ. of Chinese Academy of Sciences, China. Single-mode directly modulated distributed feedback (DFB) lasers working at 1.55-μm with high power of 160 mW output, SMSR beyond 50 dB and large bandwidth of 8.5 GHz are demonstrated.

JTu2A.73

Fast physical random bit generation using broadband chaos generated by self-phase-modulated external-cavity semiconductor laser cascaded with microsphere resonator, Ning Jiang¹, Anke Zhao¹, Yajun Wang¹, Shiqin Liu¹, Chenpeng Xue¹, Kun Qiu¹; ¹Univ of Electronic Science & Tech China, China. We experimentally demonstrate a broadband chaos generation using semiconductor laser subject to self-phase-modulation and microsphere resonator, and a subsequent fast physical random bit generation beyond 300-Gbps by using the broadband chaos as entropy source.

JTu2A.74

All-optical Inhibitory Integrate and Fire Neuron based on a Single-Section Quantum-Dot Semiconductor Laser, Menelaos Skontrakis^{1,2}, George Sarantoglou², Charis Mesaritakis^{1,2}; ¹Information and Communication Systems Engineering, Univ. of the Aegean, Greece; ²Informatics & Telecommunications, National & Kapodistrian Univ. of Athens, Greece. Numerical results concerning all optically triggered inhibitory neurons based on single-section InAs/InGaAs quantum-dot lasers are demonstrated. The devices are isomorphic to biological fire and integrate inhibitory neurons, offering picosecond spikes and wavelength encoding of neural signals.

JTu2A.75

Vertical Metasurface Integrated Cavity Surface-Emitting Lasers (VMCSELS) for collimated lasing emissions, Yiyang Xie², Peinan Ni¹, Qiuhua Wang², Chen Xu², Qiang Kan³, Hongda Chen³, Patrice Genevet¹, ¹CNRS, France; ²BJUT, China; ³Inst. of Semiconductor, China. In this work, vertical metasurface integrated cavity surface-emitting lasers (VMCSELS) have been proposed and designed into back-emitting configuration. We have demonstrated that the integration with metasurface allows the effective control of the lasing emission wavefront.

JTu2A.76

Modelling Directly Reflectivity Modulated Lasers, Guangyao Liu^{2,1}, Argishti Melikyan², S.J. Ben Yoo¹, Po Dong², ¹Univ. of California Davis, USA; ²Nokia Bell Labs, USA. We present the numerical modelling of directly reflectivity modulated laser with high speed modulated mirrors in the time domain for both static and dynamic laser performance.

JTu2A.77

Controlling Light Amplification of Colloidal Quantum Dot in Actively Operating Device, Junhong Yu¹, Sushant Shendre¹, Weon-kyu Koh¹, Baiquan Liu¹, Songyan Hou¹, Chathuranga Hettiarachchi¹, Savas Delikanli¹, Pedro H. Martinez¹, Muhammad D. Birowosuto¹, Hong Wang¹, Hilmi V. Demir^{1,2}, Cuong DANG¹, ¹Nanyang Technological Univ., Singapore; ²Bilkent Univ., Turkey. By applying an external electric field to CQDs, we have demonstrated tunable amplified spontaneous emission (ASE) threshold in a long-sought practical device. Our results open new possibilities for achieving zero-threshold and electrically pumped CQD lasers.

JTu2A.78

A Gain-Embedded Meta-Mirror, Mansoor Sheik-Bahae¹, Zhou Yang¹, Alexander R. Albrecht¹, David Lidsky¹, ¹Univ. of New Mexico, USA. We propose an active mirror structure based on a dielectric high-contrast grating reflector combined with optical gain. This structure is designed to be directly bonded to a thermal substrate for efficient heat removal, thus allowing semiconductor disk lasers with kW output power.

JTu2A.79

Four-Channel Hybrid Silicon Laser Array with low power consumption for on-chip optical interconnects, Hongyan Yu¹, Yajie Li¹, Chaoyang Ge², Xuliang Zhou¹, Guangzhao Ran², Jiaoqing Pan¹, ¹CAS Inst. of Semiconductors, China; ²The State Key Lab for Mesoscopic Physics and School of Physics, Peking Univ., China. A four-wavelength silicon hybrid laser array with a buried ridge stripe (BRS) structure is demonstrated with a threshold current less than 10 mA and a side-mode suppression ratio higher than 40 dB at room temperature.

JTu2A.80

Polarization Stable VCSEL Based on Integration of Sub-wavelength Gratings with Low Refractive Index Medium, Qiuhua Wang¹, Yiyang Xie¹, Chen Xu¹, Guanzhong Pan¹, ¹Beijing Univ. of Technology, China. A polarization stable VCSEL was realized by etching sub-wavelength gratings structure and depositing a low refractive index layer on the surface. The fabricated VCSEL is of low threshold and high polarization power ratio of 123:1.

JTu2A.81

Low Threshold Current Photonic Crystal Surface Emitting Lasers with Beam Modulation Capability, Lih-Ren Chen¹, Han-Lun Chiu¹, Kuo-Bin Hong¹, Tien-Chang Lu¹, ¹Dept. of Photonics, National Chiao Tung Univ., Taiwan. We proposed a GaAs-based photonic crystal surface emitting laser with naturally formed periodic structures on the ITO top cladding layer. Low threshold current density and ability of beam modulation have been demonstrated.

JTu2A.82

Toward All MOCVD Grown InAs/GaAs Quantum Dot Laser on CMOS-compatible (001) Silicon, Lei Wang¹, Bei Shi¹, Hongwei Zhao¹, Simone S. Brunelli¹, Bowen Song¹, Douglas Oakley¹, Jonathan Klamkin¹, ¹Univ. of California, Santa Barbara, USA. Indium arsenide quantum dots (QDs) are demonstrated on gallium arsenide on silicon templates by metalorganic chemical vapor deposition. The template threading dislocation density is only $9.5 \times 10^6 \text{ cm}^{-2}$ and the QDs are of high quality.

JTu2A.83

High-Order Phase-Matching Enabled Octave-Bandwidth Four-Wave Mixing in AlGaAs-On-Insulator Waveguides, Yong Liu¹, Michael Galili¹, Kresten Yvind¹, Leif K. Oxenløwe¹, Hao Hu¹, Minhao Pu¹, ¹Dept. of Photonics Engineering, Tec, Denmark. We show in simulation an ultra-broad continuous four-wave mixing conversion band over an octave span (covering 1.1-2.5 μm wavelength range) by taking advantage of the high-order phase-matching and the ultra-high effective nonlinearity of AlGaAs-on-insulator waveguides.

JTu2A.84

Avoidance of Cross-Phase Modulation in Femtosecond Stimulated Raman Scattering, Thomas Würthwein¹, Niels Irwin¹, Carsten Fallnich^{1,2}, ¹Inst. of Applied Physics, Germany; ²MESA+ Inst. of Nanotechnology, Netherlands. The influence of cross-phase modulation on stimulated Raman scattering in the high peak power regime is investigated, resulting in optimized pulse parameters for reduced cross-phase modulation artefacts.

JTu2A.85

Evolutionary Algorithm Assisted Design of an Elliptical Focusing Build-up Cavity Avoiding the Degradation Problem in BBO, Daniel Preissler¹, Daniel Kiefer¹, Thorsten Führer¹, Thomas Walther¹, ¹Technische Universität Darmstadt, Germany. We report on the design of a novel cavity with cylindrical focusing to overcome crystal degradation effects in the generation of UV radiation using evolutionary algorithms. Experimental results show the advantages of the new set-up.

JTu2A.86

pyLLE: a Fast and User Friendly Lugiato-Lefever Equation Solver, Gregory Moille¹, Qing Li¹, Xiyuan Lu¹, Kartik Srinivasan², ¹NIIST/UMD, USA; ²NIIST, USA. We present the development of pyLLE, a freely accessible Lugiato-Lefever equation solver programmed in Python and Julia and optimized for the simulation of microresonator frequency combs. Examples illustrating its operation and performance are presented.

JTu2A.87

Non-linear Optics and Harmonic Generation in ZnS Using Femtosecond Mid-IR Pulses Near Zero Dispersion Wavelength, Michael Tripepi^{1,2}, Aaron Schweinsberg³, Kevin Werner¹, Noah Talisa¹, Laura Vanderhoef³, Christopher Wolfe³, Trenton Ensley⁴, Anthony Valenzuela³, Enam Chowdhury¹, ¹Dept. of Physics, The Ohio State Univ., USA; ²Materials and Manufacturing Directorate, Air Force Research Labs, USA; ³Weapons and Materials Research Directorate, U.S. Army Research Lab, USA; ⁴Sensors and Electron Devices Directorate, U.S. Army Research Lab, USA. Using intense 3.6 mm, 200 fs, 500 Hz laser pulses, non-linear spectral broadening, filamentation and 2nd-9th harmonic generation in ZnS (Cleartran™) with 3-40 mm propagation distance were observed. Non-linear index of Cleartran was also measured.

JTu2A.88

Above-Octave Supercontinuum Generation in a Hybrid Nonlinear Waveguide for On-Chip Cascaded Third- and Second-Order Nonlinear-Optic Applications, Guillermo Fernando Camacho Gonzalez¹, Marcin Malinowski¹, Amirmahdi Honardoost^{1,2}, Sasan Fathpour^{1,2}, ¹CREOL, Univ. of Central Florida, USA; ²Dept. of Electrical and Computer Engineering, Univ. of Central Florida, USA. It is shown that over 1.25 octaves supercontinuum is attainable in a hybrid chalcogenide-glass/lithium-niobate miniaturized waveguide platform that allows cascaded third- and second-order optical nonlinearities on a monolithic chip, particularly for frequency-stabilized integrated comb sources.

JTu2A.89

1.7- μm high-power laser generation from a thulium-assisted optical parametric oscillator (TAOPO) for bond-selective photoacoustic microscopy, Jiawei Shi¹, Can Li¹, Kenneth Kin-Yip Wong¹, ¹Univ. of Hong Kong, Hong Kong. We present a high-power thulium-assisted optical parametric oscillator (TAOPO), which provides a pulse energy of 146 nJ with a duration of 2 ns at 1.7- μm window. It is a promising exciting source for bond-selective photoacoustic microscopy.

JTu2A.90

Kerr Comb Generation in Raman Effect Dominated Microresonators, Yanzen Zheng¹, Changzheng Sun¹, Bing Xiong¹, Lai Wang¹, Jian Wang¹, Yanjun Han¹, Zhibiao Hao¹, Hongtao Li¹, Yi Luo¹, ¹Dept. of Electronic Engineering, Tsinghua Univ., China. We propose a method to suppress Raman effect in microresonators by incorporating a filter structure. Numerical simulations based on Lugiato-Lefever equation confirm the effectiveness of the design for soliton frequency comb generation at microwave rates.

JTu2A.91

Multi-octave-spanning supercontinuum generation in lead fluoride crystal, Yuxia Yang^{1,2}, Hongbo Cai^{1,2}, Meisong Liao^{1,2}, Yasutake Ohishi³, Wanjun Bi^{1,2}, Xia Li^{1,2}, Takenobu Suzuki³, ¹Key Lab of Materials for High Power Laser, Shanghai Inst. of Optics and Fine Mechanics, Chinese Academy of Sciences, China; ²Univ. of Chinese Academy of Sciences, China; ³Research Center for Advanced Photon Technology, Toyota Technological Inst., Japan. We report the filamentation and supercontinuum generation of femtosecond pulse in a piece of PbF₂ crystal with high bandgap and ultra-broadband frequency window. A broadband supercontinuum spanning from 350 to 9000 nm is demonstrated.

JTu2A.92

High-power High-efficiency Second Harmonic Generation of 1342-nm Laser in LBO and PPKTP, Xingyang Cui^{1,2}, Qi Shen^{1,2}, Mei-Chen Yan^{1,2}, Chao Zeng^{1,2}, Tao Yuan^{1,2}, Wen-Zhuo Zhang^{1,2}, Xing-Can Yao^{1,2}, Cheng-Zhi Peng^{1,2}, Xiao Jiang^{1,2}, Yu-ao Chen^{1,2}, Jian-Wei Pan^{1,2}, ¹Shanghai Branch, National Lab for Physical Sciences at Microscale and Dept. of Modern Physics, Univ. of Science and Technology of China, China; ²Chinese Academy of Sciences (CAS) Center for Excellence and Synergetic Innovation Center in Quantum Information and Quantum Physics, Univ. of Science and Technology of China, China. We present a high-efficiency extra-cavity SHG of high-power CW 1342-nm laser. By employing LBO and PPKTP, we obtained the output power up to 3.3W and 5.2W with the conversion efficiency of 57.9% and 93.8%, respectively.

JTu2A.93

Spectral Modulations in a Picosecond OPO Based on a Chirped Quasi-Phase Matched Crystal, Guillaume Walter¹, Jean-Baptiste Dherbecourt¹, Jean-Michel Melkonian¹, Myriam Raybaut¹, Cyril Drag², Antoine Godard¹, ¹Office Natl d'Etudes Rech Aerospatiales, France; ²Laboratoire de physique des Plasmas, France. We investigate and model spectral modulations that are specific features of OPOs based on chirped quasi-phase matched crystals. Their occurrence is related to cascaded three-wave mixing processes that are quasi-phase matched at different positions.

JTu2A.94

Deterministic Single Soliton Generation without Frequency Tuning in a Graphene-FP Microresonator, Zeyu Xiao¹, Kan Wu¹, Jianping Chen¹, ¹Shanghai Jiao Tong Univ., China. A novel microresonator based on Fabry-Pérot resonator and monolayer graphene has been proposed. This design allows deterministic single soliton generation without frequency tuning and has strong robustness under frequency and timing jitter.

JTu2A.95

Yb-Fiber Laser Pumped Optical Parametric Sources Using LBO Crystals, Pancho Tzankov¹, Jeff Kmetec¹, Igor Samartsev², Valentin P. Gapontsev²; ¹*Silicon Valley Technology Center, IPG Photonics, USA*; ²*IPG Photonics, USA*. Green-pumped OPG/OPAs and OPO using non-critical phase-matching in LBO are investigated at various pulse durations from 1 ps to 13 ns. The OPAs and OPO achieve similar conversion efficiencies of ~50% providing up to 25W output power.

JTu2A.96

Optimization of Si-Photonics Compatible AlN waveguides for Integrated Nonlinear Optics Applications, Aleem M. Siddiqui¹, Daniel Dominguez¹, Christopher Michael¹, Ryan Sims¹, Paul Stanfield¹, Lisa Anne Plucinski Hackett¹, Andrew J. Leenheer¹, Matt Eichenfield¹; ¹*Sandia National Labs, USA*. We explore fabrication-process dependencies on optical losses of AlN films and demonstrate Second Harmonic Generation through modal phase-matching in integrated AlN waveguides. A loss-dependent conversion efficiency model is developed to better design waveguides in lossy AlN media.

JTu2A.97

A Quasi-Autocorrelation System Based on Carbon-Nanotube Saturable Absorber, Pushan Xiao¹, Kan Wu¹, Dong Mao², Jianping Chen¹; ¹*Shanghai Jiao Tong Univ., China*; ²*Northwestern Polytechnical Univ., China*. Quasi-autocorrelation system based on carbon-nanotube saturable absorber is demonstrated at 1550nm with 75fj pulses measured. The nanometer-level thickness and femtosecond-level decay time of nanomaterials allow compact and ultrafast light interaction for future chip-scale pulse characterization.

JTu2A.98

Tunable Parametric Optical Frequency Combs Generation based on an Electroabsorption Modulated Laser, Yumin Cheng¹, Juanjuan Yan¹, Zheng Zheng¹, Siyu Zhao¹; ¹*Beihang Univ., China*. A scheme for parametric optical frequency combs generation with high tunability based on an electroabsorption modulated laser is proposed and experimentally demonstrated. Combs with a tunable spacing and an adjustable center frequency are obtained.

JTu2A.99

Exciton mediated ultrafast feature of hybrid 2D perovskite THz meta-device, Abhishek Kumar¹, Ankur Solanki¹, Manukumar Manjappa¹, Yogesh K. Srivastava¹, Tze C. Sum², Ranjan Singh²; ¹*Division of Physics and Applied Physics, Nanyang Technological Univ. Singapore, Singapore*. We show exciton mediated ultrafast feature in 2D perovskite arises due to quantum confinement of free carriers. Integrating it with metamaterials exhibit 93 % modulation of terahertz field at ultrafast time scales (~ 20 ps).

JTu2A.100

Efficient Graphene Based Ultrafast Field Detector Using Very Slow Electronics, Velat Kilic¹, Jacob Khurgin¹; ¹*Johns Hopkins Univ., USA*. We propose an efficient novel graphene based terahertz field detector architecture which relies on slow electronics to detect the shape of ultrafast pulses. Measurements from an array of slow detectors can be posed as a nonlinear Fredholm integral and the inverse problem can be numerically solved.

JTu2A.101

THz Induced Ultrafast Dynamic in Liquid Jets, Semyon Germansky¹, Peter Zalden^{2,3}, Nilesh Awari^{1,4}, Mohammed Bawata¹, Min Chen¹, Jan-Christoph Deinert¹, Bertram Green¹, Igor Ilyakov¹, Sergey Kovalev¹, Zhe Wang¹, Franz Kärtner^{2,5}, Christian Bressler^{2,3}, Michael Gensch¹; ¹*Helmholtz-Zentrum Dresden-Rossendorf, Germany*; ²*Centre for Ultrafast Imaging CUI, Univ. of Hamburg, Germany*; ³*European XFEL, Germany*; ⁴*Univ. of Groningen, Netherlands*; ⁵*Center for Free-Electron Laser Science CFEL, Deutsches Elektronen-Synchrotron, Germany*. We show measurements of THz induced ultrafast molecular dynamics in various liquids and solutions. Making use of a narrowband high-field high-repetition-rate THz source measurements can be performed in liquid jets with a high signal-to-noise ratio.

JTu2A.102

LT-GaAs-based photomixers with > 2 mW peak output power in the 220-325 GHz frequency band, Fuanki Bave-dila¹, Etienne Okada¹, Jean-François Lampin¹, Guillaume Ducournau¹, Emilien Peytavit¹; ¹*IEMN, France*. It is shown in this communication that a LT-GaAs photomixer based on an optically resonant cavity is able to generate peak output powers above 2 mW in the 220-325 GHz frequency band.

JTu2A.103

Withdrawn

JTu2A.104

Generation of >30 kW radiation at 5.7 THz from seeded KTP off-axis THz parametric oscillator, Ming-Hsiung Wu¹, Wei Che Tsai¹, Yu Chung Chiu¹, Yen Chieh Huang¹; ¹*National Tsing Hua Univ., Taiwan*. We report generation of >30 kW radiation at 5.7 THz from a KTP off-axis THz parametric oscillator, when pumping and seeding it with 13.7-mJ and 7-mJ laser pulses at 1064 and 1085.9 nm, respectively.

JTu2A.105

Efficient multicycle THz generation using a dedicated frequency-comb laser, Halil T. Olgun^{3,1}, Wenlong Tian^{3,2}, Damian Schimpf², Yi Hua^{3,4}, Aram Kalaydzhyan³, Nicholas Matlis³, Franz Kartner^{3,4}; ¹*Helmholtz-Institut Jena, Germany*; ²*School of Physics and Optoelectronic Engineering, China*; ³*Center for Free-Electron Laser Science, DESY, Germany*; ⁴*The Hamburg Centre for Ultrafast Imaging, Germany*. We develop a unique multi-line frequency-comb source designed for multi-millijoule, high-efficiency multicycle THz generation perform first experiments multi-line generation and control.

JTu2A.106

Femtosecond-laser-written circular waveguides in MgO-doped stoichiometric LiTaO₃, Shunsuke Watanabe¹, Junji Hirohashi¹, Koichi Imai¹, Masayuki Hoshi¹, Satoshi Makio¹; ¹*OXIDE Corporation, Japan*. We fabricated depressed cladding circular waveguides by direct femtosecond laser writing with various pulse energies in MgO-doped stoichiometric LiTaO₃. The waveguiding properties were characterized with a CW laser at the wavelength of 1064 nm.

JTu2A.107

Magneto-Optical Faraday Effect of Dy³⁺ Doped Germanate-Phosphate Glasses, Masoud Mollaei¹, Xiushan Zhu¹, David Zelman², Jie Zong¹, Michael Li³, Arturo Chavez³, Nasser Peyghambarian¹; ¹*Univ. of Arizona, USA*; ²*Air Force Research Lab, Wright-Patterson Air Force Base, USA*; ³*NP Photonics Inc., USA*. Highly dysprosium doped germanate-phosphate glasses were fabricated, and their magneto-optical properties were measured. The measurement results show that highly dysprosium doped germanate-phosphate glass is a promising magneto-optical material in the SWIR region.

JTu2A.108

2D crystal MXene Ti₃C₂T_x based all-optical modulator, Qing Wu¹, Meng Zhang¹, Si Chen², Xiantao Jiang², Yunzheng Wang², Zheng Zheng¹, Han Zhang²; ¹*Beihang Univ., China*; ²*Shenzhen Univ., China*. We demonstrate an all-fiber all-optical modulator at 1550 nm using MXene Ti₃C₂T_x (T = F, O, or OH) deposited microfiber. The modulator features a slope efficiency of 0.061 π/mW and a rise time constant of 4.10 ms.

JTu2A.109

Resonant laser printing by Silicon crystallization and oxidation, Joseph A. Staif^{1,2}, Jonathan Bar-David^{1,2}, Jacob Engelberg^{1,2}, Noa Mazurski^{1,2}, Atzmon Vakahi², Sergei Remennik², Inna Popov², Anders Kristensen³, Uriel Levy^{1,2}; ¹*Applied Physics, Hebrew Univ., Israel*; ²*Center for Nanoscience and Nanotechnology, Hebrew Univ., Israel*; ³*Micro- and Nanotechnology, Technical Univ. of Denmark, Denmark*. The absorption in amorphous silicon nano antennas is engineered for the purpose of post process structural change via resonant laser printing by illumination, thus shifting transmission and reflection spectrum in a controlled manner.

JTu2A.110

Material Characterization and Thermal Performance of Au Alloys in a Thin-Film Plasmonic Waveguide, Frank Bello^{1,2}, Okan K. Orhan¹, Nicolas Abadia^{3,4}, David O'Regan¹, John Donegan^{1,2}; ¹*School of Physics, Trinity College Dublin, Ireland*; ²*Centre for Research on Adaptive Nanostructures and Nanodevices (CRANN), Ireland*; ³*School of Physics and Astronomy, Cardiff Univ., UK*; ⁴*Inst. for Compound Semiconductors, UK*. We investigate heatsinking methods and material properties of various Au alloys to be used within thin-film plasmonic resonators to create optimal heating conditions in near-field transducers, with demonstrated application towards heat-assisted magnetic recording devices.

JTu2A.111

Single Nitrogen Vacancy Color Centers Generated by Femtosecond Laser Illumination on Diamond, Youying Rong¹, Zhiping Ju¹, Qiang Ma¹, Shikang Liu¹, Chengda Pan¹, Botao Wu¹, Haifeng Pan¹, E Wu¹; ¹*East China Normal Univ., China*. By focusing high-power femtosecond laser on diamond surface coated with a layer of nano-silicon powder, single nitrogen vacancy centers could be fabricated efficiently around the illuminated craters even without annealing.

JTu2A.112

Enhanced Photoluminescence Intensity and Negative Photoconductivity in Lysine-Doped Graphene Oxide Quantum Dots, Svetta Reina Merden S. Santiago¹, Tzu-Neng Lin¹, Yun-Syuan Chou¹, Ji-Lin Shen¹; ¹*Chung Yuan Christian Univ., Taiwan*. We present a facile synthesis of lysine-doped graphene oxide quantum dots (GOQDs). The proposed doping approach can provide a vehicle to tune the photoluminescence intensity and negative photoconductivity in GOQDs for promising applications in optoelectronics.

JTu2A.113

Grating-patterned Perovskite Light Emitting Diodes for Enhanced Performance, Chen Zou¹, Lih Y. Lin¹; ¹*Univ. of Washington Seattle, USA*. We introduce grating patterns into perovskite films using a simple soft lithography method with common DVD discs as templates. The patterned perovskite films exhibit enhanced photoluminescence and the performance of light emitting diodes is improved.

JTu2A.114

Photothermal Mirror Z-Scan, Aristides Marcano Olaizola¹; ¹*Delaware State Univ., USA*. This work describes a pump-probe photothermal mirror Z-scan experiment aimed at determination of thermal diffusivity, thermoelastic coefficient, and quantum yield of thermal heating of the surface of transparent and non-transparent solid samples including films.

JTu2A.115

Nearly Color-shift Free Full-color Monolithic Hybrid Quantum Dots Semipolar Micro Light-emitting Diodes Display, Sung-Wen Huang Chen¹, Lee-Feng Chen¹, Tingzhu Wu^{2,1}, Chun-Fu Lee¹, Po-Tsung Lee¹, Hao-Chung Kuo¹; ¹*National Chiao Tung Univ., Taiwan*; ²*Xiamen Univ., China*. Full-color displays demonstrate by the semipolar blue micro-light-emitting diodes array and quantum dots color-conversion layer. This display shows a wide color gamut and color stability since reduced quantum confined Stark effect by the semipolar substrate.

JTu2A.116

Energy Transfer in Transition Metal Ions co-Doped Chalcogenide Mid-IR Laser Materials, Vladimir Fedorov^{1,2}, Tristan Carlson¹, Sergey Mirov^{1,2}; ¹*Univ. of Alabama at Birmingham, USA*; ²*IPG Photonics, USA*. We reveal energy transfer between chromium-iron and cobalt-iron ions in co-doped II-VI chalcogenide laser materials with a rate faster than 300 ns, which is attractive for development of effective mid-IR lasers operating over 3.5-6.0 μm.

JTu2A.117

Radical mitigation of photo-darkening effect in Yb-doped fiber through deuterium treatment, Jiaming Li¹, Nan Zhao¹; ¹South China Normal Univ., China. We report radical mitigation of photo-darkening effect in Yb-doped fibers with deuterium. After deuterium loading, the fiber did not exhibit any PD effect. Existed color centers induced by PD could also be eliminated by deuterium.

JTu2A.118

Hydrogen plasma treatment of MoS₂ with graphene protection, Anishkumar Soman¹, Robert A. Burke², Qui Li¹, Michael Valentin², Eugene Zakar³, Ugochukwu Nsofor¹, Steven Hegeudus¹, Ujjwal Das⁴, Jianping Shi⁵, Yanfeng Zhang⁵, Tingyi Gu¹; ¹Univ. of Delaware, USA; ²Univ. of California – Riverside, USA; ³US Army Research Lab, USA; ⁴Inst. of Energy Conversion, USA; ⁵Peking Univ., China. Hydrogen plasma treatment can create defects such as sulfur vacancies in single layer MoS₂. A single layer graphene's protection can effectively reduce the defects formation as confirmed by Raman spectroscopy.

JTu2A.119

Synthesis, Spectroscopy and Efficient Laser Operation of Tm:Lu₃Al₅O₁₂ Transparent Ceramics, Josep Serres², Pavel Loiko³, Venkatesan Jambunathan⁴, Xavier Mateos², Yicheng Wang¹, Jiang Li⁵, Liza Basyrova³, Antonio Lucianetti⁴, Tomas Mocek⁴, Magdalena Aguilo², Francesc Diaz², Uwe Griebner¹, Valentin Petrov¹; ¹Max Born Inst., Germany; ²Universitat Rovira i Virgili, Spain; ³ITMO Univ., Russia; ⁴HiLASE, Czechia; ⁵Shanghai Inst. of Ceramics, China. Tm:Lu₃Al₅O₁₂ ceramics are synthesized by solid-state reactive sintering, and their structure and spectroscopic properties are studied. A Tm:Lu₃Al₅O₁₂ ceramic laser diode-pumped at 793 nm generates 3.12 W at ~2.02 μm with a slope efficiency of 60.2%.

JTu2A.120

Remote Photonic Sensing of Cerebral Hemodynamics via Spatial-Temporal Analysis of Back-Scattered Laser Light, Nisan Ozana¹, Adam Noah², Xian Zhang², Yumie Ono^{2,3}, Joy Hirsch², Zeev Zalevsky¹; ¹Bar Ilan Univ., Israel; ²Yale Univ., USA; ³Meiji Univ., Japan. The ability to remotely extract cerebral hemodynamics from specific locations on the brain using time varied speckle patterns is innovative. The first step towards remote sensing of brain activity and stroke is presented.

JTu2A.121

Effectively enhancing photon-exciton coupling via a gap whispering gallery modes, Qi Zhang¹, Juanjuan Ren¹, Xueke Duan¹, He Hao¹, Qihuang Gong¹, Ying Gu¹; ¹Peking Univ., China. We theoretically demonstrate the coupling coefficient enhancement in cavity quantum electrodynamics system via a nanogap between a dielectric nanotoroid and a dielectric nanowire.

JTu2A.122

Efficiently Loading Cold Atomic Ensemble into an Optical Cavity with High Optical Depth, Yue Jiang¹, Yefeng Mei¹, Yueyang Zou¹, Ying Zuo¹, Shengwang Du¹; ¹The Hong Kong Univ. of Sci&Tech, Hong Kong. We describe a cold atom apparatus for achieving high optical depth (OD) and OD-duty cycle product by loading a dark-line 2D MOT into an optical cavity. Cavity enhanced OD can go up to 7600, with 188 times enhancement of the single-pass OD, and highest OD-duty cycle product is 1697.

JTu2A.123

Quantum-correlated Light Source from Dual-seeded Four-wave Mixing with a Diode Laser System, Meng-Chang Wu³, Nicholas R. Brewer^{3,1}, Rory W. Speirs³, Bonnie L. Schmittberger³, Kevin M. Jones², Paul D. Lett^{3,1}; ¹National Inst. of Standards and Technology, USA; ²Williams College, USA; ³Univ. of Maryland, College Park, USA. We have obtained broadband intensity-difference squeezing from sub 10 Hz to 20 MHz via four-wave mixing (4WM) in a rubidium vapor. This was accomplished by dual-seeding the 4WM process and using semiconductor diode lasers.

JTu2A.124

Machine Learning Applied in Reconstruction of Unitary Matrix for Quantum Computation, Hui Zhang¹, Hong Cai⁴, Stefano Paesani², Raffaele Santagati², Anthony Laing², Leong Chuan Kwek³, Ai Qun Liu¹; ¹Nanyang Technological Univ., Singapore; ²Univ. of Bristol, UK; ³National Univ. of Singapore, Singapore; ⁴Inst. Of Microelectronics, Singapore. Optimal method are applied in characterizing and reconstructing designed unitary matrices on linear optical circuit. The scheme is based on the measurement of single-photon and two-photon statistics using coherent beams.

NOTES

Joint

13:00–15:00

JTu3A • Symposium on Quantum Information in Time-Frequency Domain I

President: To Be Announced

JTu3A.1 • 13:00 **Invited**

Tailored Generation, Manipulation, and Application of Photonic Temporal Modes, Benjamin Brecht¹, Jano G. Lopez¹, Markus Allgaier¹, Vahid Ansari¹, John M. Donohue^{1,2}, Christine Silberhorn¹; ¹Paderborn Univ., Germany; ²Inst. for Quantum Computing, Canada. Pulsed temporal modes form a high-dimensional basis for quantum information applications. By controlling these modes, we can tailor quantum states and measurements for applications such as quantum state tomography or quantum metrology.

JTu3A.2 • 13:30

Spectro-Temporal Asymmetry in Optical Parametric Processes, Usman A. Javid¹, Steven D. Rogers¹, Austin Graf¹, Qiang Lin¹; ¹Univ. of Rochester, USA. We have, for the first time, generated bi-photon quantum states of light with temporal waveforms showing stunning asymmetry and exotic coherence properties using cavity-enhanced four wave mixing in an optical microresonator with selectively split modes.

JTu3A.3 • 13:45

A two-qudit operation on a 256-dimensional Hilbert space, Poolad Imany¹, Mohammed S. Alshaykh¹, Joseph M. Lukens², Jose A. Jaramillo-Villegas³, Daniel E. Leaird¹, Andrew M. Weiner¹; ¹Purdue Univ., USA; ²Oak Ridge National Lab, USA; ³Universidad Tecnológica de Pereira, Colombia. By encoding two 16-dimensional qudits in the time and frequency degrees of freedom of a heralded single photon, we realize a deterministic photonic two-qudit SUM gate operating on a 256-dimensional Hilbert space.

JTu3A.4 • 14:00 **Invited**

Full Single and Two Photon Spectral Mode-function Reconstruction, Valérian Thiel¹, Alex O. Davis^{1,2}, Brian J. Smith^{3,1}; ¹Univ. of Oxford, UK; ²Sorbonne Université, France; ³Univ. of Oregon, USA. We present a novel method to reconstruct the full spectral-temporal mode function of a single photon state. The setup combines spectral sheering interferometry with high resolution spectrometers and is self-referenced. We show that this method can be applied to the full characterization of a photon pair, recovering phase correlations and time/frequency entanglement.

CLEO: QELS-Fundamental Science

13:00–15:00

FTu3B • PT Symmetry & Exceptional Points

President: To Be Announced

FTu3B.1 • 13:00 **Invited**

An On-chip Optical Brillouin Gyroscope with Earth-Rotation-Rate Sensitivity, Kerry J. Vahala¹, Yu-Hung Lai¹, Myoung-Gyun Suh¹; ¹California Inst. of Technology, USA. A chip-based gyroscope is demonstrated that uses counter-propagating Brillouin lasers to measure rotation as a Sagnac-induced frequency shift. Demonstration of rotation measurement below the Earth rotation rate is presented. Prospects for improved performance are discussed.

FTu3B.2 • 13:30

Bimodal Directional Laser via Dynamically Encircling an Exceptional Point, Jason Leshin¹, Yousef Alahmadi¹, Absar U. Hassan¹, Gisela Lopez Galmiche¹, Patrick LiKamWa¹, Demetrios N. Christodoulides¹, Mercedeh Khajavikhan¹; ¹Univ. of Central Florida, USA. We demonstrate dynamical encirclement of an exceptional point in a laser cavity. By continuously varying the detuning and coupling between a pair of PT-symmetric waveguides, the laser simultaneously emits two eigenmodes, one from each facet.

FTu3B.3 • 13:45

Measurement of photon correlations in PT symmetric systems, Friederike Klauck¹, Lucas Teuber¹, Marco Ornigotti¹, Matthias Heinrich¹, Stefan Scheel¹, Alexander Szameit¹; ¹Inst. of Physics, Universität Rostock, Germany. We investigate quantum interference in a PT-symmetric system by measuring a Hong-Ou-Mandel-Dip in waveguide couplers. The nontrivial loss distribution giving rise to PT-symmetry systematically displaces photon bunching with respect to the Hermitian case.

FTu3B.4 • 14:00

Pulse shortening in two coupled rings under amplitude modulations with parity-time symmetry, Luqi Yuan^{1,2}, Qian Lin², Meng Xiao², Avik Dutt², Shanhuai Fan²; ¹Shanghai Jiao Tong Univ., China; ²Stanford Univ., USA. We show pulse shortening in two coupled rings under amplitude modulations, where the modulation phases have a π phase difference. The system exhibits parity-time symmetry, and its importance is highlighted in pulsed laser systems.

13:00–15:00

FTu3C • Polaritonic Interactions in Transition Metal Dichalcogenide

President: Esther Wertz, Rensselaer Polytechnic Institute, USA

FTu3C.1 • 13:00 **Tutorial**

Optical Spectroscopy of Transition Metal Dichalcogenide Monolayers and Heterostructures, Feng Wang^{1,2}; ¹Univ. of California Berkeley, USA; ²Materials Science Division, LBNL, USA. In this tutorial, I will describe a variety of optical techniques that can be used to probe the unique exciton and valley physics and their ultrafast dynamics in transition metal dichalcogenides monolayers and heterostructures.



Feng Wang is an professor of physics at the university of California, Berkeley and faculty scientist at the Lawrence Berkeley National Lab. His research interests have been in ultrafast nano-optics, with special focus on low dimensional materials, including one dimensional carbon nanotubes and two-dimensional graphene and transition metal dichalcogenides.

FTu3C.2 • 14:00

Composite photonic platform based on 2D semiconductor monolayers, Ipsita Datta¹, Sang Hoon Chae¹, Gaurang R. Bhatt¹, Baichang Li¹, Yiling Yu², Chibeom Park³, Jiwoong Park³, Linyou Cao², D. N. Basov¹, James Hone¹, Michal Lipson¹; ¹Columbia Univ., USA; ²Dept. of Material Science and Engineering, North Carolina State Univ., USA; ³Univ. of Chicago, USA. We demonstrate phase modulation in the near infrared (1450 - 1650 nm) by electrostatically doping 2D semiconductor monolayers integrated on SiN waveguides. We show a $V_{\pi}L$ of 1.4 V.cm and 0.8 V.cm for MoS₂ and WS₂, respectively.

CLEO: QELS-Fundamental
Science

13:00–15:00

FTu3D • Tailored Light-Matter Interactions

President: To Be Announced

FTu3D.1 • 13:00

Observation of Branched Flow of light, Anatoly Patsyk¹, Miguel Bandres¹, Mordechai Segev¹, Uri Sivan¹; ¹*Technion-Israel Inst. of Technology, Israel*. We present the first study of optical branched flow. As light propagates in thin dielectric films it experiences scattering from inhomogeneities, forming bundles displaying the features and statistics of the phenomenon known as branched flow.

FTu3D.2 • 13:30

Ballistic Metamaterials., Evgenii E. Narimanov¹; ¹*Purdue Univ., USA*. Ballistic metamaterials, metal-dielectric composites with the unit cell size smaller than electron mean free path, represent a new class of composite media with many unique properties, such as hyperbolic response above the plasma frequency.

FTu3D.3 • 13:45

Fundamental figure of merit for engineering dipole-dipole interactions, Cristian L. Cortes¹, Ward D. Newman¹, Ashwin K. Boddeti¹, Tyler Sents¹, Zubin Jacob¹; ¹*Purdue Univ., USA*. Over the last decade there has been a debate regarding the role of the photonic environment in enhancing, inhibiting and imparting coherence to dipole-dipole interactions. We develop a unified figure of merit to conclusively explain multiple recent experiments.

FTu3D.4 • 14:00

Light-Matter Interaction in Disordered Metal-Dielectric Environments, Sangeeta Rout¹, Monika Biener², Zhen Qi², Carl Bonner¹, T. Shahbazyan³, M. Noginov¹; ¹*Norfolk State Univ., USA*; ²*Lawrence Livermore National Lab, USA*; ³*Dept. of Physics, Atmospheric Sciences & Geoscience, Jackson State Univ., USA*. We studied emission kinetics of HITC dye in disordered metal-dielectric environments and found that the latter, contrary to expectations, can reverse emission kinetics shortening in highly concentrated dyes, caused by a combination of relaxation processes.

CLEO: Science & Innovations

13:00–15:00

STu3E • High Peak-Power Lasers & Technologies I

President: Jake Bromage Univ. of Rochester, USA

STu3E.1 • 13:00

Optimization of wavefront aberration for Shanghai Super-intense Ultrafast Laser Facility by double deformable mirrors, Lianghong Yu¹, Zhen Guo¹, Xiaoyan Liang¹, Ruxin Li¹; ¹*Shanghai Inst Optics & Fine Mech, CAS, China*. A peak intensity of 10^{22} W/cm² was achieved with an f/2.5 off-axis parabolic (OAP) mirror after the wavefront aberration being optimized by double deformable mirrors in the Shanghai super-intense ultrafast laser facility (SULF).

STu3E.2 • 13:15

Generation of the Ultraintense Laser Pulse with an Intensity of 6×10^{22} W/cm², JW Yoon^{2,1}, Seong Ku Lee^{2,1}, Jae Hee Sung^{2,1}, Hwang Woon Lee², Cheonha Jeon², Il Woo Choi^{2,1}, Junghoon Shin², Hyung Taek Kim^{2,1}, Bjorn M. Hegelich^{2,3}, Chang Hee Nam^{2,3}; ¹*Advanced Photonics Research Inst., Gwangju Inst. of Science and Technology, South Korea (the Republic of)*; ²*Center for Relativistic Laser Science, Inst. for Basic Science, South Korea (the Republic of)*; ³*Dept. of Physics and Photon Science, Gwangju Inst. of Science and Technology, South Korea (the Republic of)*. Wavefront correction of the PW laser system at IBS-GIST was performed using deformable mirrors. The PW laser beam was focused by an f/1.6 OAP. The peak intensity is 6×10^{22} W/cm², the highest intensity ever reached.

STu3E.3 • 13:30 **Tutorial**

Optical Interference Coatings for High Performance Lasers, Carmen S. Menoni¹; ¹*Colorado State Univ., USA*. This tutorial will cover the fundamentals of optical interference coatings (IC) design, growth and characterization. It will also review mechanisms of near infrared laser damage and discuss state-of-the-art ICs performance in chirped pulse amplification laser systems.



Carmen S. Menoni is a University Distinguished Professor at Colorado State University in the department of Electrical and Computer Engineering. She directs the Advanced Thin Film Laboratory dedicated to the growth and characterization of thin film oxides for the engineering of interference coatings for high-power lasers and ultrahigh precision optics for gravitational wave interferometers. Her group also specializes in the usage of bright coherent beams of extreme ultraviolet laser light of wavelengths between 10 and 50 nm for optics applications such as nanoscale imaging, ablation and mass spectrometry. Her work is published in over 200 refereed publications and numerous invited and contributed conference presentations. Prof. Menoni was elected Fellow of the IEEE, OSA, APS, AAAS and of SPIE, and received an IEEE Photonics Society Distinguished Lecture Award. Prof. Menoni is President-Elect of the IEEE Photonics Society.

13:00–15:00

STu3F • Terahertz Sensing & Devices

President: James Lloyd-Hughes, Univ. of Warwick, UK

STu3F.1 • 13:00 **Invited**

Recent Advances in THz Scanning Tunneling Microscopy, Vedran Jelic^{1,2}, Yang Luo¹, Jesus Calzada¹, Peter Nguyen¹, Daniel Mildemberger¹, Tianwu Wang¹, Frank Hegmann¹; ¹*Physics, Univ. of Alberta, Canada*; ²*Physics and Astronomy, Michigan State Univ., USA*. Terahertz scanning tunneling microscopy (THz-STM) is a newly developed technique that can probe the ultrafast dynamics of surfaces with single atom resolution. We use THz-STM to explore the subpicosecond tunneling dynamics of a photoexcited semiconductor surface.

STu3F.2 • 13:30

Biomolecule sensing using low energy terahertz photons exploiting nano-slot resonance and two-dimensional materials, Sang-Hun Lee¹, Jong-Ho Choe², Chulki Kim¹, Minah Seo¹; ¹*Sensor system research center, South Korea Inst. of Science and Technology, South Korea (the Republic of)*; ²*Physics Dept., South Korea Univ., South Korea (the Republic of)*. We performed terahertz time-domain spectroscopy for discrimination of biomolecules using absorption enhancement on a graphene-hybridized nano-slot device. The terahertz sensing device shows noticeable signal change with different trends for different nucleotides even in femto-mole level.

STu3F.3 • 13:45

Filling the 5-10 THz Gap Using Ge-based Photoconductive Emitter, Abhishek Singh¹, Alexej Pashkin¹, Stephan Winnerl¹, Manfred Helm^{1,2}, Harald Schneider¹; ¹*Helmholtz Zentrum Dresden-Rossendorf, Germany*; ²*Cfaed and Inst. of Applied Physics, TU Dresden, Germany*. Generating a continuous spectrum covering the 5-10 THz range is difficult due to strong THz absorption in polar materials. We demonstrate that a photoconductive emitter based on non-polar germanium is able to achieve this goal.

STu3F.4 • 14:00

High-Responsivity and Broadband Photoconductive Terahertz Detection via Photon Trapping, Nezhil Yarmici¹, Deniz Turan¹, Semih Cakmakyan¹, Mona Jarrahi¹; ¹*Univ. of California - Los Angeles, USA*. We present a photoconductive terahertz detector, which utilizes photon trapping to offer broadband terahertz detection, over a 0.1-4.5 THz band, with large dynamic ranges, exceeding 100 dB, without using a short-carrier-lifetime semiconductor substrate.

Executive Ballroom
210G

Joint

13:00–15:00

JTu3G • Symposium on Space-borne
Quantum Sensors

JTu3G.1 • 13:00 **Invited**

Atom Interferometry for Space-Borne Sensors, Sergio Mottini¹, Stefano Cesare¹, Alberto Anselmi¹, Linda Mondini², Olivier Carraz², Federica Migliaccio³, Mirko Reguzzoni³, Fiodor Sorrentino³, Khulan Batsukh³, Guglielmo Tino⁴; ¹Thales Alenia Space Italia SpA, Italy; ²European Space Agency, Netherlands; ³Politecnico di Milano, Italy; ⁴INFN-Fi, Italy; ⁵INFN - Ge, Italy. The perspectives for application of atom interferometry in inertial navigation, geophysics, or tests of fundamental physics motivate the interest for the development of space-borne quantum accelerometers and gradiometers. Technical challenges and implementation examples are presented.

JTu3G.2 • 13:30 **Invited**

Enabling Technologies for Space-Based Quantum Systems, Evan A. Salim¹; ¹ColdQuanta, Inc, USA. Quantum technologies have great potential to enable space-based applications of information science, sensing, navigation, and timekeeping. We present enabling technologies to address the technical challenges of preparing cold atom based systems for use in space.

JTu3G.3 • 14:00 **Invited**

The Coolest Spot in the Universe: Early results from the Cold Atom Laboratory Mission Aboard the International Space Station, Robert J. Thompson¹; ¹Jet Propulsion Lab, USA. The Cold Atom Lab launched to the International Space Station in May 2018, and has been operating since then as the world's first multi-user facility for the study of ultra-cold atoms in microgravity. In this talk, I present early results from the Cold Atom Lab (CAL).

Executive Ballroom
210H

CLEO: Science & Innovations

13:00–15:00

STu3H • Biophotonics & Optofluidics
President: Jessica Houston New Mexico State
Univ., USA

STu3H.1 • 13:00

An Optofluidic Tweezer-and-Drag Cell Stretcher in a Microfluidic Channel, Zhanshi Yao¹, Ching Chi Kwan¹, Andrew W. Poon¹; ¹Hong Kong Univ. of Sci. and Tech., Hong Kong. We report an optofluidic tweezer-and-drag cell stretcher in a microfluidic channel. We distinguish healthy and glutaraldehyde-treated rabbit red blood cells based on their different mechanical deformations at a cell-stretching throughput of ~1.2 cells/s.

STu3H.2 • 13:15

Optofluidic Platform with Integrated Optical Waveguides and Sample Preparation for Digitized Detection of Nucleic Acid Targets, Aadhar Jain¹, Gopikrishnan G. Meena¹, Alexandra Stambaugh¹, Jean Patterson³, Aaron Hawkins², Holger Schmidt¹; ¹Univ. of California, Santa Cruz, USA; ²Brigham Young Univ., USA; ³Texas Biomedical Research Inst., USA. An architecture of sensitive solid-core and liquid-core optical waveguides are integrated with a pneumatic valve array on a single optofluidic platform to enable specific capture, labeling and detection of single nucleic acid strands using barcode fluorescence reporters.

STu3H.3 • 13:30

Bend-Insensitive Through-Fiber Stimulated Emission Depletion (STED) Imaging of HeLa Cells, Brendan M. Heffernan¹, Stephanie A. Meyer², Diego Restrepo³, Mark Siemens⁴, Emily A. Gibson², Juliet T. Gopinath¹; ¹Univ. of Colorado, Boulder, USA; ²Bioengineering, Univ. of Colorado Anschutz Medical Campus, USA; ³Cell Biology, Univ. of Colorado Anschutz Medical Campus, USA; ⁴Physics and Astronomy, Univ. of Denver, USA. We demonstrate, for the first time, STED images of biological samples where fluorescence has been collected through the same fiber used to transport excitation and depletion light (through-fiber imaging). We also quantitatively demonstrate fiber-bending-independent resolution.

STu3H.4 • 13:45

Single Particle Detection Enhancement with Wavelet-based Signal Processing Technique, Vahid Ganjalizadeh¹, Gopikrishnan G. Meena¹, Matthew Stott², Holger Schmidt¹, Aaron Hawkins²; ¹ECE, Univ. of California, Santa Cruz, USA; ²Electrical and Computer Engineering, Brigham Young Univ., USA. Chip-based single molecule detection requires ultra-sensitive devices and robust signal processing methods. A new wavelet-based signal processing method is introduced that improves detection and error rates on an optofluidic platform by 2x and 3x, respectively.

STu3H.5 • 14:00 **Tutorial**

Wavefront Shaping – the Threading of Light Through Scattering Media, Changhui Yang¹; ¹California Inst. of Technology, USA. Wavefront shaping has been an active research area over the past decade. Its ability to control light transmission through or into a scattering medium has significant biophotonics, computation, imaging, encryption and other applications. In this tutorial, I will go through the various optical concepts involved in wavefront shaping – feedback iteration, phase conjugation, optical memory effect, guidestar strategies, speckle correlations, etc. I will also survey the use of wavefront shaping in biophotonics. Finally, I will also examine two recent and surprising developments in wavefront shaping. The first is the intentional combination of wavefront shaping and a controlled scattering medium to create novel optical system – in effect, turning scattering from a 'foe' to a 'friend' for wavefront shaping. The second is the complete dropping of phase characterization in a new class of 'wavefront shaping' methods.

Meeting Room
211 A/B

CLEO: Applications
& Technology

13:00–15:00

ATu3I • Ultrafast Laser Processing
President: Dirk Mueller; Coherent Inc., USA

ATu3I.1 • 13:00 **Invited**

Glass Machining and In-situ Metrology: Recovery of Spatio-Temporal Phase Distribution From 2-Dimensional Interference Fringe Movement Caused by Irradiation of Glass with Ultra-Short Laser Pulses at High Pulse Repetition Rates, Kristian Cvecek^{1,2}, Johannes Heberle^{1,2}, Michael Bergler^{1,3}, Isamu Miyamoto^{2,4}, Dominique De Ligny³, Michael Schmidt^{1,2}; ¹Inst. of Photonic Technologies, Friedrich-Alexander-Univ. of Erlangen-Nürnberg, Germany; ²Graduate School in Advanced Optical Technologies, Friedrich-Alexander-Univ. of Erlangen-Nürnberg, Germany; ³Inst. of Glass and Ceramics, Friedrich-Alexander-Univ. of Erlangen-Nürnberg, Germany; ⁴Osaka Univ., Japan. An interferometry-based method for direct observation of phase modifications caused by transient temperature and pressure changes during irradiation of glass using ultra-short laser pulses is shown. The method provides a 3-dimensional time-resolved phase distribution and allows to distinguish between reversible and irreversible laser induced phase changes inside the glass.

ATu3I.2 • 13:30

Femtosecond Laser Polishing of Germanium Towards Fabrication of Freeform Optics, Lauren L. Taylor¹, Jing Xu², Michael Pomerantz², Thomas R. Smith³, John C. Lambropoulos², Jie Qiao¹; ¹Rochester Inst. of Technology, USA; ²Univ. of Rochester, USA; ³Aperture Optical Sciences, USA. A modeling tool and a scanning strategy for polishing germanium using femtosecond lasers are devised. Controllable material removal and sub-nanometer surface roughness are demonstrated, opening the path towards ultrafast laser polishing of freeform optics.

ATu3I.3 • 13:45

A Comparative Study of Surface Modification effects of Femtosecond and Nanosecond Laser on CVD Diamond Tools during Sharpening Processing, Xiaoxu Liu¹, Kohei Natsume¹, Satoru Maegawa¹, Fumihiro Itoigawa¹, Shingo Ono¹; ¹Nagoya Inst. of Technology, Japan. In this study sharpening processing with femtosecond laser was innovatively performed on CVD diamond tools. Furthermore, surface modification effects of femtosecond and nanosecond laser in sharpening processing on CVD diamond were compared with Raman spectroscopy.

ATu3I.4 • 14:00

Surface modification of polycrystalline CVD diamond films with femtosecond laser, Kohei Natsume¹, Xiaoxu Liu¹, Satoru Maegawa¹, Fumihiro Itoigawa¹, Shingo Ono¹, Michiharu Ota²; ¹Nagoya Inst. of Technology, Japan; ²IMRA America, USA. The surface modification of CVD diamond irradiated with femtosecond laser of different fluences has been studied and analyzed with Raman spectroscopy. Through comparing with DLC coating processed equally, this improved crystallinity mechanism has been discussed.

continued on page 116

CLEO: Science & Innovations

13:00–15:00

STu3J • Kerr Frequency Microcombs

President: Brandon Shaw; Naval Research Lab, USA

STu3J.1 • 13:00 **Tutorial**

Novel Material Platforms for Resonator Kerr Combs, Andrea M. Armani¹; ¹Univ. of Southern California, USA. Resonators are an emerging platform for generating Kerr combs. By attaching a range of different nanomaterials to the surface of optical resonators, we demonstrate a new approaches for fabricating high performance frequency combs.



Andrea Armani received her BA in physics from the University of Chicago and her PhD in applied physics from Caltech. She is currently the Ray Irani Chair in Engineering and Materials Science at the University of Southern California. She is also the Director of the W. M. Keck Photonics Cleanroom as well as the soon to open John D. O'Brien Nanofabrication Laboratory, two core nanofabrication cleanrooms at USC.

STu3J.2 • 14:00

Integrated Si₃N₄ Soliton Microcomb Driven by a Compact Ultra-low-noise Laser, Arslan Raja³, Junqiu Liu³, Nicolas Volet¹, Rui Ning Wang³, Jijun He³, Erwan Lucas³, Romain Bouchand³, Paul Morton², John Bowers¹, Tobias J. Kippenberg³; ¹Univ. of California, Santa Barbara (UCSB), USA; ²Morton Photonics, USA; ³École Polytechnique Fédérale de Lausanne, Switzerland. We generate 100-GHz soliton microcombs in a photonic integrated high-Q Si₃N₄ microresonator using an ultra-compact, high-power and low-frequency-noise semiconductor-based laser. The soliton is initiated via direct current tuning of the laser.

CLEO: Applications
& Technology

13:00–15:00

ATu3K • Biophotonic Spectroscopy

President: Ilko K. Ilev; U.S. Food and Drug Administration, USA

ATu3K.1 • 13:00

Femtosecond Laser Micromachining in Ophthalmic Hydrogels: Micro-Raman Spectroscopy of Materials Effects, Dan Yu¹, Ruiting Huang¹, Wayne H. Knox¹; ¹Univ. of Rochester, USA. A one-layer dense line pattern was inscribed into ophthalmic hydrogels using a 405 nm, 8.3 MHz laser. The local microstructural changes, especially the water content, were examined using confocal Raman spectroscopy.

ATu3K.2 • 13:15

Mid-infrared Photothermal Imaging of Fibroblast Cells, Panagis Samolis¹, Michelle Y. Sander¹; ¹Boston Univ., USA. Label-free vibrational mid-infrared photothermal amplitude and phase images of fixed fibroblast cells in a collagen extracellular matrix are presented, providing complementary insights into optical material and thermal diffusion properties.

ATu3K.3 • 13:30

High-speed, high-sensitivity spectroscopic stimulated Raman scattering microscopy by ultrafast delay-line tuning and deep learning, Haonan Lin¹, Fengyuan Deng¹, Kai-Chih Huang¹, Hyeon Jeong Lee¹, Ji-Xin Cheng¹; ¹Boston Univ., USA. We present a stimulated Raman scattering imaging system which acquires a Raman spectrum within 20 μs. A U-Net deep learning network is applied to maintain the sensitivity at high speeds, enabling high-throughput label-free spectroscopic imaging of cells and tissues.

ATu3K.4 • 14:00

Doppler Detection of Pathogenic Activity in Living Tissue by Biodynamic Imaging, Honggu Choi¹, Jessica Zuponic¹, Eduardo Ximenes¹, Michael Ladisch¹, John Turek¹, David D. Nolte¹; ¹Purdue Univ., USA. Bacterial infection of living tissue is monitored by biodynamic imaging based on intracellular Doppler fluctuation spectroscopy. The efficacy of pathogen suppression by antibiotics may enable detection of antibiotic resistant strains *in vitro*.

CLEO: Science & Innovations

13:00–15:00

STu3L • Mode-Locked Fiber Lasers I

President: Camille-Sophie Bres; Ecole Polytechnique Federale de Lausanne, Switzerland

STu3L.1 • 13:00

Generation of 17 fs pulses form a Mamyshev oscillator with intra-cavity photonic crystal fiber, Chunyang Ma^{2,1}, Ankita Khanolkar¹, Yimin Zang¹, Andy Chong¹; ¹Univ. of Dayton, USA; ²Jilin Univ., China. A few cycle pulses (~5 cycles) with broad spectrum (~400 nm) are generated from a Mamyshev oscillator. Such a broad spectrum can be stabilized in the cavity by a self-similar attractor in the gain fiber.

STu3L.2 • 13:30

Femtosecond pulses generated from a compact all-polarization-maintaining (PM) Ytterbium-doped fiber laser, Wu Zhichao^{1,2}, Yujun Feng², SongNian Fu¹, Ming Tang¹, Deming Liu¹, Jonathan Price², Johan Nilsson²; ¹Huazhong Univ of Science and Technology, China; ²Univ. of Southampton, UK. We demonstrate femtosecond dissipative solitons generated from an all-PM Ytterbium-doped fiber laser. The simplified fiber ring cavity has been shown to reliably self-start and provides a route to a robust platform for future development.

STu3L.3 • 13:45

All-Polarization-Maintaining, Polarization-Multiplexed Mode-Locked Er-Fiber Laser with Nonlinear Amplifying Loop Mirror, Yoshiaki Nakajima^{1,2}, Yuya Hata^{1,2}, Yugo Kusumi¹, Kaoru Minoshima^{1,2}; ¹Univ. of Electro-Communications, Japan; ²JST, ERATO MINOSHIMA Intelligent Optical Synthesizer (IOS) Project, Japan. We demonstrate an all-polarization-maintaining, polarization-multiplexed mode-locked Er-fiber laser with nonlinear amplifying loop mirror that generates two mutually coherent frequency combs with slightly different repetition rates at same center wavelength without nonlinear spectral broadening.

STu3L.4 • 14:00

Dispersion Management of Polarization Maintaining Er-doped Figure 9 Ultrashort Pulse Fiber Laser, Hayato Suga¹, Masahito Yamanaka¹, Norihiko Nishizawa¹; ¹Nagoya Univ., Japan. We investigated dispersion management of polarization maintaining Er-doped, figure 9 fiber laser both experimentally and numerically. A 132 fs ultrashort pulse with spectral width of 46 nm was achieved around zero dispersion region.

13:00–15:00

JTu3M • Symposium on Intense-field Nonlinear Optics & High Harmonic Generation in Nanoscale Materials I
Prsident: To Be Announced

JTu3M.1 • 13:00 **Invited**

Extreme Nonlinear Optics With Dielectric Metasurfaces, Igal Brener¹; ¹*Sandia National Labs Livermore, USA*. We have used dielectric metasurfaces made from direct bandgap semiconductors to generate high harmonics and nonlinear mixing simultaneously, without the need of phase matching. Inclusion of broken-symmetry designs and quantum heterostructures can lead to even higher efficiency.

JTu3M.2 • 13:30 **Invited**

Enhancement of Nonlinear Processes by Surface Plasmons, Pierre Berini¹; ¹*Univ. of Ottawa, Canada*. Nonlinear processes using nanoscale metallic structures are of strong interest due to their ability to enhance local fields and engineer the optical density of states. We discuss various nonlinear processes that exploit these effects.

JTu3M.3 • 14:00

Coherent Control of the Non-instantaneous Response of Plasmonic Nanostructures, Eyal Bahar^{3,2}, Uri Arieli^{3,1}, Haim Suchowski^{3,1}; ¹*Condens Matter Physics., Tel Aviv Univ., Faculty of Exact Sciences, Israel*; ²*Condens Matter Physics., Faculty of Exact Sciences, Tel Aviv Univ., Israel*; ³*The Center for Light-Matter Interaction, Faculty of Exact Sciences, Tel Aviv Univ., Israel*. We experimentally demonstrate coherent control of the nonlinear response of resonant nanostructures beyond the weak-field regime. Furthermore, we develop a novel theoretical approach capturing the induced nonlinearities of shaped ultrafast pulses with resonant nanostructured media.

13:00–15:00

STu3N • Lasers on Silicon & Nanolasers
Prsident: Kei May LAU, Hong Kong University of Science and Technology, Hong Kong

STu3N.1 • 13:00

Triple reduction of threshold current for 1.3 μm InAs quantum dot lasers on patterned, on-axis (001) Si, Chen Shang¹, Yating Wan¹, Justin Norman¹, Daehwan Jung¹, Qiang Li², Kei May Lau², Arthur Gossard¹, John Bowers¹; ¹*Univ. of California Santa Barbara, USA*; ²*Hong Kong Univ. of Science and Technology, Hong Kong*. Triple reduction of threshold current was achieved for 1.3 μm InAs quantum dot lasers on patterned, on-axis (001) Si. This was enabled by reducing the threading dislocation density, from 7×10^7 to 3×10^6 cm^{-2} .

STu3N.2 • 13:15

Tunable III-V-on-Si Laser with Resonant Photonic Molecule Mirrors, Guilherme F. de Rezende^{1,2}, Newton Frateschi¹, Gunther Roelkens²; ¹*"Gleb Wataghin" Physics Inst., Universidade Estadual de Campinas, Brazil*; ²*Photonics Research Group, INTEC, Ghent Univ.-imec, Belgium*. We propose, fabricate and characterize a novel III-V-on-Si laser. Resonant mirrors are realized by tailoring supermodes of coupled microrings. A threshold of 40mA, series resistance of 10 Ω and SMSR of 40dB is reported.

STu3N.3 • 13:30

Investigation of SiGeSn/GeSn/SiGeSn Quantum Well Structures and Optically Pumped Lasers on Si, Yiyin Zhou^{1,2}, Joe Margetis⁴, Grey Abernathy^{1,2}, Wei Dou¹, Perry Grant^{1,2}, Bader Alharthi¹, Wei Du², Alicia Wadsworth⁶, Qianying Guo⁶, Huong Tran^{1,3}, Solomon Ojo^{1,2}, Aboozar Mosleh⁷, Seyed Ghetmiri⁷, Gregory Thompson⁶, Jifeng Liu⁸, Greg Sun⁹, Richard Soref⁹, John Tolle⁴, Baohua Li³, Mansour Mortazavi⁷, Shui-Qing Yu¹; ¹*Dept. of Electrical Engineering, Univ. of Arkansas, USA*; ²*Microelectronics-Photonics Program, Univ. of Arkansas, USA*; ³*Arkonics, LLC, USA*; ⁴*ASM, USA*; ⁵*Dept. of Electrical Engineering, Wilkes Univ., USA*; ⁶*Dept. of Metallurgical and Materials Engineering, Univ. of Alabama, USA*; ⁷*Dept. of Chemistry and Physics, Univ. of Arkansas at Pine Bluff, USA*; ⁸*Thayer School of Engineering, Dartmouth College, USA*; ⁹*Dept. of Engineering, Univ. of Massachusetts Boston, USA*. SiGeSn/GeSn/SiGeSn single and multiple quantum well (MQW) structures were characterized. The SiGeSn barriers provide a strong carrier confinement with sufficient barrier height, leading to the lasing with MQW device up to 90 K.

STu3N.4 • 13:45

O-band InAs/GaAs Quantum Dot Micro-disk Lasers on SOI by in-situ hybrid epitaxy, Bin Zhang¹, Wei W. Qi¹, Ting Wang¹, Jianjun Zhang¹; ¹*Inst. of Physics, China*. By implementing III-V/Si hybrid growth technique, we demonstrate the first InAs quantum-dot micro-disk laser on SOI substrates. Threshold pump power as low as 0.39 mW were achieved with the Q factor of 3900.

STu3N.5 • 14:00

Spatially Coherent Interlayer Exciton Lasing in an Atomically-Thin Heterostructure, Eunice Paik¹, Long Zhang¹, William Burg², Rahul Gogna¹, Emanuel Tutuc², Hui Deng¹; ¹*Univ. of Michigan, USA*; ²*Univ. of Texas, USA*. We demonstrate lasing in WSe_2 - MoSe_2 heterostructure integrated in a silicon nitride grating cavity. Signatures of lasing include sharp increase in spatial coherence and super-linear increase in the emission intensity as photon number increases above unity.

13:00–15:00

STu3O • Emerging Visible Light Communication

Prsident: Qiaoqiang Gan, State Univ. of New York at Buffalo, USA

STu3O.1 • 13:00 **Tutorial**

Visible-light Diode-lasers and Integrated Photonics for Lighting and High-bitrate Visible Light Communication, Boon S. Ooi¹; ¹*King Abdullah Univ of Sci & Technology, Saudi Arabia*. The advent of AlInGaN-based devices operating in the violet to green visible-wavelength range has ushered in high performance solid-state lighting and gigahertz visible-light communication (VLC). In this tutorial, we will discuss the recent advances.



Boon S. Ooi (Fellow of OSA, SPIE, and IoP; Ph.D. degree from the University of Glasgow, UK, 1994) joined King Abdullah University of Science and Technology (KAUST) in 2009, from Lehigh University (USA). His group focuses on lasers for solid-state lighting, visible-light and underwater-wireless-optical communication, and nanostructures for energy harvesting.

STu3O.2 • 14:00

Integrated Silicon Photodetector in Thin Film Lithium Niobate Platform for Visible Wavelength Band, Boris Desiatov¹, Marko Loncar¹; ¹*Harvard Univ., USA*. We demonstrate design, fabrication and characterization of amorphous silicon photodetector on lithium niobate photonic platform at visible wavelengths. The device shows the best responsivity of 10mA/W and dark current of less than 0.5nA.

CLEO: Applications & Technology

13:00–15:00

ATu3P • A&T Topical Review on Progress in the Semiconductor Laser Technology I

ATu3P.1 • 13:00

Double-side pumped membrane external-cavity surface-emitting laser (MECSEL) with increased efficiency emitting > 3 W in the 780 nm region, Hermann Kahle¹, Hoy-My Phung¹, Jussi-Pekka Penttinen¹, Patrik Rajala¹, Antti Tukiainen¹, Sanna Ranta¹, Mircea Guina¹; ¹Optoelectronics Research Centre (ORC) - Physics, Tampere Univ., Finland. We demonstrate a double-side pumped MECSEL emitting more than 3 W of output power in the 780 nm wavelength region. The laser exhibits an efficiency as high as 34.4 %.

ATu3P.2 • 13:15

Direct Tunneling Modulation of Semiconductor Lasers, Junyi Qiu¹, Milton Feng¹, Nick Holonyak¹; ¹Univ. of Illinois at Urbana-Champaign, USA. Direct tunneling modulation of semiconductor lasers is realized experimentally in the three-terminal transistor laser through the interaction between the photon absorption by voltage-controlled intra-cavity photon-assisted tunneling and the photon generation by quantum-well recombination.

ATu3P.3 • 13:30 **Invited**

Semiconductor Lasers for Next-generation Applications, Takeo Kageyama¹; ¹QD Laser, Inc., Japan. In this presentation, we will review emerging semiconductor laser applications which have developed remarkably in recent years, such as precision laser machining, variety of sensing, Si-photonics and retinal projection eye wear.

ATu3P.4 • 14:00 **Invited**

Photonic Crystal Surface Emitting Lasers, Richard Hogg¹; ¹Glasgow Univ., UK. Abstract not available.

13:00–15:00

ATu3Q • A&T Topical Review on Advanced Design, Imaging and Process Technologies for Next Generation Semiconductors I

ATu3Q.1 • 13:00

Extending EUV to the High-NA EUV Regime. Patrick Naulleau¹; ¹Lawrence Berkeley National Labs, USA. Abstract not available.

ATu3Q.2 • 13:30

Nanopatterning of Things: from Metals, Oxides to Quantum Dots. Yoen Sik Jung¹; ¹KAIST, South Korea. This talk will introduce deep-nanoscale fabrication technologies based on synergic combinations of self-assembly, photolithography, and transfer-printing applicable to a variety of material systems including polymers, oxides, metals, quantum nanostructures for high-performance sensors, photovoltaics, and displays.

ATu3Q.3 • 14:00

Quantifying Improvements in Field to Field and Wafer to Wafer CD Variation from Laser Bandwidth Variation. Will Conley¹; ¹Cymer LLC, USA. Abstract not available.

Joint

CLEO: QELS-Fundamental Science

JTU3A • Symposium on Quantum Information in Time-Frequency Domain I—Continued

JTU3A.5 • 14:30

Spectral phase coherence in HOM interferometry, Navin B. Lingaraju¹, Hsuan-Hao Lu¹, Suparna Seshadri¹, Poolad Imany¹, Daniel E. Leaird¹, Joseph M. Lukens², Andrew M. Weiner¹; ¹Purdue Univ., USA; ²Quantum Information Science Group, Oak Ridge National Lab, USA. We examine the role of spectral phase in Hong-Ou-Mandel interference by comparing interferograms for pure and mixed states. We find that HOM interference cannot be taken as a signature of coherent frequency superpositions.

JTU3A.6 • 14:45

High-Dimensional Energy-Time Entanglement up to 6 Qubits per Photon through Biphoton Frequency Comb, Kai-chi Chang¹; ¹UCLA, USA. We demonstrate high-dimensional entanglement with ≈ 6 qubits per photon via mode-locked biphoton frequency comb. Hong-Ou-Mandel quantum revival is observed with 61 time-bins and 99.8% visibility.

FTu3B • PT Symmetry & Exceptional Points—Continued

FTu3B.5 • 14:15

Optical amplification at exceptional points, Qi Zhong¹, Sahin K. Ozdemir², Alexander Eisfeld³, A. Metelmann⁴, Ramy El-Ganainy¹; ¹Michigan Technological Univ., USA; ²Pennsylvania State Univ., USA; ³Max Planck Inst. for the Physics of Complex Systems, Germany; ⁴Freie Univ., Germany. We propose a new optical amplifier geometry based on exceptional points. Compared to its standard counterpart device, the proposed structure relaxes the limitation imposed by the gain-bandwidth product.

FTu3B.6 • 14:30

Breakdown of Non-Hermitian Hamiltonian for Correlated Multi-photon Transport Due to Reservoir-induced Correlation Changes, Zihao Chen¹, Yao Zhou¹, Jung-Tsung Shen¹; ¹Washington Univ. in St. Louis, USA. We present a theoretical analysis of multi-photon transport in the presence of reservoir, and unearth the breakdown of widely adopted non-Hermitian Hamiltonian descriptions in the dissipative regime due to reservoir-induced changes of correlations.

FTu3B.7 • 14:45

Non-Hermitian Engineered TCC VCSEL for LIDAR Remote Sensing Technologies, Mohammad H. Teimourpour^{1,2}, Hamed Daliri¹, Elham Heidari³, Volker J. Sorger⁴, Ray T. Chen³; ¹Omega Optics Inc., USA; ²College of Optical Sciences, The Univ. of Arizona, USA; ³ECE Dept., Univ. of Texas at Austin, USA; ⁴The George Washington Univ., USA. We present the main aspects of a new approach to achieve a single mode operation in TCC-VCSEL array based on (1) increasing the spacing of the eigenfrequencies of supermodes, (2) Q-enhancing of the fundamental supermodes.

FTu3C • Polaritonic Interactions in Transition Metal Dichalcogenide—Continued

FTu3C.3 • 14:15

The Ultimate Purcell Factor in Van der Waals Heterostructures, Yaniv Kurman¹, Peter Schmidt², Frank H. Koppens^{2,3}, Ido Kaminer¹; ¹Israel Inst. of technology, Israel; ²ICFO-Institut de Ciències Fotòniques, Spain; ³ICREA – Institució Catalana de Recerca i Estudis Avançats, Spain. We find what mechanisms limit fundamental light-matter interactions of plasmons confined to the atomic scale, when interfacing two-dimensional semiconductor emitters. We show how nonlocality governs the dynamics, limiting the Purcell factor yet reaching ultra-strong coupling.

FTu3C.4 • 14:30

Strong Light-Matter Interaction in Monocrystalline Gold Nanodisks Coupled to Tungsten Disulfide, Nicolas Stenger^{2,3}, Mathias Geisler^{2,3}, Martijn Wubs^{2,3}, Sanshui Xiao^{2,3}, N. Mortensen^{1,4}; ¹Center for Nano Optics, Univ. of Southern Denmark, Denmark; ²Dept. of Photonics Engineering, Technical Univ. of Denmark, Denmark; ³Center for Nanostructured Graphene, Technical Univ. of Denmark, Denmark; ⁴Danish Inst. for Advanced Study, Univ. of Southern Denmark, Denmark. Spectroscopy on plasmonic nanodisks coupled to single and multilayer tungsten disulfide show a Rabi splitting of 108 meV and 180 meV, respectively, the highest splitting reported in transition metal dichalcogenides coupled to plasmonic nanostructures.

FTu3C.5 • 14:45

Controllable coherent plasmon-exciton interaction in MoS₂ monolayer with gold nanorods through photothermal reshaping, Hu Aiqin¹; ¹Peking Univ., China. The plasmon-exciton interactions in an individual gold nanorod with MoS₂ monolayer were investigated with single particle spectroscopy method. Based on photothermal reshaping, we in-situ tuned the surface plasmon resonance of single gold nanorod and investigate at room temperature.

15:00–16:30 Meet the OSA Publishing Journal Editors Ice Cream Social, Networking Zone Booth 2605

15:00–17:00 Coffee Break and Exhibit Only Time, Exhibit Halls 1-3
Coffee Break Sponsored by  COHERENT and  THORLABS

15:30–17:00 OIDA: Market Trends: Opportunities in Optics and Photonics, Exhibit Hall Theater I

**CLEO: QELS-Fundamental
Science**

CLEO: Science & Innovations

**FTu3D • Tailored Light-Matter
Interactions—Continued**

**STu3E • High Peak-Power Lasers &
Technologies I—Continued**

**STu3F • Terahertz Sensing & Devices—
Continued**

FTu3D.5 • 14:15

Optical skyrmions: a new topological state of light, Shai Tseses¹, Evgeny Ostrovsky¹, Kobi Cohen¹, Bergin Gjonaj², Netanel H. Lindner¹, Guy Bartal¹; ¹*Technion-Israeli Inst. of technology, Israel*; ²*Albanian Univ., Albania*. We experimentally demonstrate a new topology for light: optical skyrmions. This discovery may allow a variety of applications, from stimulated creation of skyrmions in matter to new paradigms in optical information processing.

FTu3D.6 • 14:30

Implementing Optimal Field Configurations for Micromanipulation, Michael Horodynski¹, Matthias Kühmayer¹, Andre Brandstätter¹, Kevin Pichler¹, Ulrich Kuhl², Stefan Rotter¹; ¹*Inst. for Theoretical Physics, Vienna Univ. of Technology (TU Wien), Austria*; ²*Institut de Physique de Nice, Université Côte d'Azur, France*. We demonstrate both theoretically and experimentally how to achieve wave states that are optimal for transferring momentum, torque, etc. on a target of arbitrary shape embedded in an arbitrary environment.

FTu3D.7 • 14:45

Quantum State Filtering of Dual-rail Photons with Fiberized Plasmonic Metamaterial, Salih Yanikgonul^{1,2}, Anton N. Vetlugin¹, Ruixiang Guo¹, Angelos Xomalis³, Giorgio Adamo¹, Cesare Soci¹, Nikolay I. Zheludev^{1,3}; ¹*Centre for Disruptive Photonic Technologies, Nanyang Technological Univ., Singapore*; ²*Advanced Concepts and Nanotechnology, Inst. of Materials Research and Engineering, Singapore*; ³*Optoelectronics Research Centre & Centre for Photonic Metamaterials, Univ. of Southampton, UK*. We demonstrate quantum state filtering of dual-rail photons through single-photon interference on a fiberized plasmonic metamaterial, exploiting different optical response of the metamaterial to symmetric and anti-symmetric superpositions of double-path wavefunction of single-photons.

STu3E.4 • 14:30

First commissioning results of the Apollon laser on the 1 PW beam line, Dimitrios N. Papadopoulos¹; ¹*LULI, France*. The Apollon 10 PW laser has recently demonstrated its capacity of generating >1 PW pulses with <22 fs duration. The complete commissioning results of the 1 PW beam line will be presented in this work.

STu3E.5 • 14:45

The 9.2 μm, 2 ps, Multi-Terawatt Laser at the Accelerator Test Facility (ATF) of Brookhaven National Lab, Mikhail N. Polyanskiy¹, Igor V. Pogorelsky¹, Marcus Babzien¹, Mark A. Palmer¹; ¹*Brookhaven National Lab, USA*. A terawatt-class long-wave infrared (LWIR) laser based on chirped-pulse amplification of picosecond pulses in mixed-isotope, high pressure CO₂ amplifiers is in operation at ATF. An overview of the laser system as well as a summary of recent progress and status are presented.

STu3F.5 • 14:15

Non-Scanning THz Spectral Characterization with a Microbolometer Focal Plane Array, Dogeun Jang¹, Yung Jun Yoo¹, Ki-Yong Kim¹; ¹*Univ. of Maryland at College Park, USA*. We demonstrate a single-shot scheme in characterizing terahertz spectrum by using a microbolometer focal plane array. This method measures THz field autocorrelations and can characterize THz radiation up to 30 THz with high temporal resolution.

STu3F.6 • 14:30

A Luneburg Lens for the THz Region, Yasith Amarasinghe¹, Daniel M. Mittleman¹, Rajind Mendis¹; ¹*Brown Univ., USA*. We implement a two-dimensional Luneburg lens for the THz region using a waveguide-based artificial-dielectric technology. The lens can focus an approximately 2-cm diameter input beam at 0.162 THz to a spot size of 3.4 mm.

STu3F.7 • 14:45

Photonics-based multi-spectral THz imaging using a dual-mode laser and a telecentric f-θ lens, Kiwon Moon¹, Il-Min Lee¹, Eui Su Lee¹, Kyung Hyun Park¹; ¹*Electronics and Telecom Research Inst, South Korea (the Republic of)*. We propose a continuous-wave THz imaging system using a semiconductor dual-mode laser, a photomixer and a Schottky barrier diode. Through the broadband frequency tunability of the dual-mode laser, high-resolution multi-spectral THz images were obtained.

15:00–16:30 Meet the OSA Publishing Journal Editors Ice Cream Social, Networking Zone Booth 2605

15:00–17:00 Coffee Break and Exhibit Only Time, Exhibit Halls 1-3
Coffee Break Sponsored by  **COHERENT** and  **THORLABS**

15:30–17:00 OIDA: Market Trends: Opportunities in Optics and Photonics, Exhibit Hall Theater I

Executive Ballroom
210G

Joint

JTu3G • Symposium on Space-borne
Quantum Sensors—Continued

JTu3G.4 • 14:30 **Invited**
Quantum Science Experiments with Micius Satellite,
Cheng-Zhi Peng^{1,2}; ¹Univ of Science and Technology of China,
China; ²Synergetic Innovation Center of Quantum Information
and Quantum Physics, China. The quantum science satellite
have been launched successfully in China. Utilizing this sat-
ellite, we have completed a series of quantum experiments
in space. Here, I will introduce these experiments and our
future plans.

Executive Ballroom
210H

CLEO: Science & Innovations

STu3H • Biophotonics & Optofluidics—
Continued



Professor Yang works on microscopy and wavefront shap-
ing. His group invented the ePetri technology and Fourier
Ptychography for microscopy. His group invented digital
optical phase conjugation technology and was the first to
apply wavefront shaping into biophotonics. He is a fellow of
the Coulter foundation, AIMBE, OSA and SPIE.

Meeting Room
211 A/B

CLEO: Applications
& Technology

ATu3I • Ultrafast Laser Processing—
Continued

ATu3I.5 • 14:15
**Femtosecond + Nanosecond Multiple Pulse Train from a
Thin Disk Regenerative Amplifier**, Atabak Marandi¹, Florian
Fink¹, Joerg Neuhaus¹, Mikhail Larionov¹; ¹Dausinger + Giesen
GmbH, Germany. Demonstration of a regenerative amplifier
with "mixed pulse trains" for micromachining: femtosecond
pulses for effective ablation directly followed by nanosecond
pulses for smoothing of the surface amplified within one
single thin disk resonator.

ATu3I.6 • 14:30
**Thermal damage free materials processing by using ultra-
short pulse laser**, Sungkwon Shin¹, Jungyu Hur¹, Jongkab
Park¹, Dohun Kim¹; ¹AP Systems Corporation, South Korea
(the Republic of). We report thermal damage free processing
in Invar, polyimide, and soda-lime glass by using an ultrashort
pulse laser. Experimental results and a toy model for thermal
accumulation will be discussed.

ATu3I.7 • 14:45
**Efficient ablation of silicon with a high power GHz fem-
tosecond laser source**, Eric Mottay¹, Guillaume Bonamis^{1,2},
Konstantin M. Mishchik¹, John Lopez², Eric Audouard¹,
Clemens Hoenninger¹, Inka Manek-Honninger²; ¹Amplitude,
France; ²Univ. of Bordeaux, France. Ablation of silicon using
high power GHz femtosecond lasers achieves specific removal
rate of 2.5 mm³/min/W. Ablation morphologies are discussed
in terms of thermal and non-thermal mechanisms.

15:00–16:30 Meet the OSA Publishing Journal Editors Ice Cream Social, Networking Zone Booth 2605

15:00–17:00 Coffee Break and Exhibit Only Time, Exhibit Halls 1-3
Coffee Break Sponsored by COHERENT and THORLABS

15:30–17:00 OIDA: Market Trends: Opportunities in Optics and Photonics, Exhibit Hall Theater I

CLEO: Science & Innovations

STu3J • Kerr Frequency Microcombs—
Continued

STu3J.3 • 14:15

Broadband Efficient Soliton Microcombs in Pulse-Driven Photonic Microresonators, Miles H. Anderson¹, Romain Bouchand¹, Ewelina Obrzud^{2,3}, Junqiu Liu¹, Sylvain Karlen², Steve Lecomte², Tobias Herr², Tobias J. Kippenberg¹; ¹Ecole Polytechnique Federale de Lausanne, Switzerland; ²Swiss Center for Electronics and Microtechnology (CSEM), Switzerland; ³Geneva Observatory/PlanetS, Dept. of Astronomy, Univ. of Geneva, Switzerland. Broadband single-soliton based frequency combs, with a detectable repetition rate of 28 GHz, are efficiently generated through pulse-driving of a chip-based Si₃N₄ microresonator. We observe an influence of the pulse-driving rate on the comb mode linewidth.

STu3J.4 • 14:30

Electrically Driven Ultra-compact Photonic Integrated Soliton Microcomb, Arslan Raja¹, Andrey S. Voloshin², Hairun Guo¹, Sofya E. Agafonova², Junqiu Liu¹, Alexander S. Gorodnitskiy², Maxim Karpov¹, Nikolay G. Pavlov², Erwan Lucas¹, Ramzil R. Galiev², Artem E. Shitikov², John D. Jost¹, Michael L. Gorodetsky², Tobias J. Kippenberg¹; ¹Ecole Polytechnique Fédérale de Lausanne, Switzerland; ²Russian Quantum Center, Russia. We demonstrate a current-initiated soliton microcomb by injection-locking a multi-frequency laser diode to a chip-scale high-Q Si₃N₄ microresonator. This approach offers a pathway for integrated and ultra-compact microcomb source for high-volume applications.

STu3J.5 • 14:45

Long-Term Stabilization and Operation of a Soliton Micro-Comb for 9-Days, Tong Lin¹, Avik Dutt¹, Xingchen Ji¹, Christopher T. Phare¹, Chaitanya Joshi¹, Oscar A. Jimenez¹, Min C. Shin¹, Alexander Gaeta¹, Michal Lipson¹; ¹Columbia Univ., USA. We report the long-term stabilization of a soliton micro-comb over 9 days of continuous operation. Using an integrated heater, the original pump-cavity detuning is maintained with a simple active feedback method.

CLEO: Applications
& Technology

ATu3K • Biophotonic Spectroscopy—
Continued

ATu3K.5 • 14:15

High-Sensitivity Coherent Raman Spectroscopy with Doppler Raman, David Smith¹, Jeff Field¹, David Winters¹, Scott Domingue², Jesse Wilson¹, Daniel Kane³, Randy Bartels¹; ¹Colorado State Univ., USA; ²KM Labs, USA; ³Mesa Photonics, USA. Doppler Raman spectroscopy is a novel detection scheme for impulsively stimulated Raman scattering that unlocks high-sensitivity detection of low frequency Raman vibrational modes from 10cm⁻¹ to 1500cm⁻¹ through signal amplification in the external detection system.

ATu3K.6 • 14:30

Shining the Light to Terahertz Spectroscopy of nL-Volume Biological Samples, Sergey Mityukovskiy¹, Mélanie Lavancier¹, Romain Peretti¹, Jean-François Lampin¹, Théo Hannotte¹, Flavie Braud¹, Emmanuel Dubois¹, Goedele Roos²; ¹Inst. of Electronics, Microelectronics and Nanotechnology (IEMN), CNRS/Univ. Lille, France; ²Unit of Structural and Functional Glycobiology (UGSF), CNRS/Univ. Lille, France. We present a technique allowing the confinement of a broadband terahertz pulse to a few-nL volume. The method is approved in terahertz time-domain spectroscopy study of biological samples and further perspectives are discussed.

ATu3K.7 • 14:45

SERS Detection of Trace Level Tetrahydrocannabinol in Body Fluid, Kundan Sivashanmugan¹, Kenneth Squire¹, Yong Zhao^{1,2}, Ailing Tan^{1,2}, Joseph Kraai¹, Gregory Rorrer¹, Alan X. Wang¹; ¹Oregon State Univ., USA; ²Yanshan Univ., China. Silver nanoparticles were grown on a diatom photonic crystal surface to create a hybrid plasmonic-biosilica nanostructure for surface-enhanced Raman scattering. Ultra-sensitive and quantitative detection of Tetrahydrocannabinol in body fluid was achieved to counter measure drug abuse.

CLEO: Science & Innovations

STu3L • Mode-Locked Fiber Lasers I—
Continued

STu3L.5 • 14:15

All-fiber dual-wavelength mode-locked laser by using low-birefringence Lyot-filter and carbon nanotube, Yuanjun Zhu¹, Fulin Xiang¹, Pengtao Yuan¹, Neisei Hayashi¹, Chao Zhang¹, Lei Jin¹, Sze Y. Set¹, Shinji Yamashita¹; ¹Research Center for Advanced Science and Technology, The Univ. of Tokyo, Japan. We firstly demonstrate a dual-wavelength mode-locked EDF laser by utilizing a low-birefringence Lyot-filter and CNT, which delivers dual-wavelength output centers at 1532 nm and 1556 nm corresponds to the difference frequency of 3.02 THz.

STu3L.6 • 14:30

Jitter-Free Multi-Wavelength Fiber Sources using Intermodal Solitons, Lars Rishoj¹, Boyin Tai¹, Fengyuan Deng¹, Ji-Xin Cheng¹, Siddharth Ramachandran¹; ¹Boston Univ., USA. We demonstrate energetic (30nJ) dual-wavelength ultrashort-pulse sources via soliton self-mode conversion in a multimode fiber that are naturally temporally synchronized. Power fluctuations of resultant sum-frequency signals are 11.4dB lower than conventional fiber based dual-wavelength approaches.

STu3L.7 • 14:45

Real-time Observation of Soliton Build-up Dynamics in Bidirectional Mode-Locked Fibre Lasers, Maria Chernysheva^{1,2}, Igor Kudelin¹, Srikanth Sugavanam¹; ¹Aston Univ., UK; ²Leibniz Inst. of Photonic Technology, Germany. By using newly emerged high precision real-time measurement technologies of spatio-temporal intensity reconstruction and dispersive Fourier transformation (DFT), we have experimentally observed the buildup dynamics of solitons in a bidirectional ultrafast fibre laser.

15:00–16:30 Meet the OSA Publishing Journal Editors Ice Cream Social, Networking Zone Booth 2605

15:00–17:00 Coffee Break and Exhibit Only Time, Exhibit Halls 1-3

Coffee Break Sponsored by  COHERENT and  THORLABS

15:30–17:00 OIDA: Market Trends: Opportunities in Optics and Photonics, Exhibit Hall Theater I

Joint

CLEO: Science & Innovations

JTu3M • Symposium on Intense-field Nonlinear Optics & High Harmonic Generation in Nanoscale Materials I—Continued**JTu3M.4 • 14:15**

Unveiling the Mechanism of Highly-efficient Nonlinear Responses from Film-coupled Plasmonic Structures, Qixin Shen¹, Thang B. Hoang¹, Guoce Yang¹, Virginia D. Wheeler², Maiken H. Mikkelsen¹; ¹Duke Univ., USA; ²USA Naval Research Lab, USA. We investigate the mechanism of highly efficient nonlinear responses from dielectric materials in a tiny gap of less than 7 nm between a gold film and metallic nanostructures, which offers potential for on-chip nonlinear devices.

JTu3M.5 • 14:30 **Invited**

Title to be Determined, David A. Reis¹; ¹Stanford Univ., USA. Abstract not available.

STu3N • Lasers on Silicon & Nanolasers—Continued**STu3N.6 • 14:15**

High-temperature Continuous-wave Operation of 1.3- μ m Membrane Distributed Reflector Lasers on SiC, Suguru Yamaoka¹, Ryo Nakao¹, Takuro Fujii¹, Koji Takeda¹, Tatsuro Hiraki¹, Hidetaka Nishi¹, Takaaki Kakitsuka¹, Tai Tsuchizawa¹, Shinji Matsuo¹; ¹NTT Device Technology Labs, Japan. We demonstrate continuous-wave operation of 1.3- μ m membrane distributed reflector lasers on SiC at a 130°C stage temperature. The laser, with its large thermal conductivity and optical confinement, is promising for high-temperature operation.

STu3N.7 • 14:30

Sub-wavelength single-mode all-inorganic perovskite CsPbBr₃ nanolaser, Zhengzheng Liu¹, Jie Yang², Juan Du¹, Xiaosheng Tang², Yuxin Leng¹, Ruxin Li¹; ¹Shanghai Inst. of Optics and Fine Mechanics, Chinese Academy of Sciences, China; ²Chongqing Univ., China. We report the single-mode, high-quality, low-threshold picosecond pulses laser whose physical volume is only $\sim 0.49 \lambda^3$ (where λ is the lasing wavelength in air) from an individual all-inorganic perovskite CsPbBr₃ nanocuboid.

STu3N.8 • 14:45

Measuring the Frequency Response of Metallic Nanolasers, Chi Xu¹, William Hayenga¹, Mercedeh Khajavikhan¹, Patrick LiKamWa¹; ¹Univ. of Central Florida, CREOL, USA. The frequency response of metallic nanolasers are evaluated theoretically and experimentally. The predicted modulation bandwidth is ~ 289 GHz, and the experiments show an effective modulation current efficiency factor (MCEF) of ~ 143.8 GHz/mA^{1/2}.

STu3O • Emerging Visible Light Communication—Continued**STu3O.3 • 14:15**

Liquid-Crystal-Based Visible-Light Integrated Optical Phased Arrays, Jelena Notaros¹, Milica Notaros¹, Manan Raval¹, Michael R. Watts¹; ¹MIT, USA. Liquid-crystal-based integrated optical phased arrays are proposed and experimentally demonstrated for the first time as a method for low-power and compact visible-light beam steering. Beam steering of 10.5° within ± 3.5 V at a 632.8nm wavelength is shown.

STu3O.4 • 14:30

Integrated-Phased-Array-Based Visible-Light Near-Eye Holographic Projector, Jelena Notaros¹, Manan Raval¹, Milica Notaros¹, Michael R. Watts¹; ¹MIT, USA. An integrated-phased-array-based visible-light holographic projector is proposed as a scalable solution towards the next generation of augmented-reality head-mounted displays. A passive pixel-based architecture is developed and projection of a wire-frame cube is experimentally demonstrated.

15:00–16:30 Meet the OSA Publishing Journal Editors Ice Cream Social, Networking Zone Booth 2605

15:00–17:00 Coffee Break and Exhibit Only Time, Exhibit Halls 1-3
Coffee Break Sponsored by  COHERENT and  THORLABS

15:30–17:00 OIDA: Market Trends: Opportunities in Optics and Photonics, Exhibit Hall Theater I

CLEO: Applications & Technology

ATu3P • A&T Topical Review on Progress in the Semiconductor Laser Technology I—Continued

ATu3Q • A&T Topical Review on Advanced Design, Imaging and Process Technologies for Next Generation Semiconductors I—Continued

ATu3P.5 • 14:30

100 GHz colliding pulse mode locked quantum dot lasers directly grown on Si for WDM application, Songtao Liu¹, Xinru Wu^{1,2}, Justin Norman¹, Daehwan Jung¹, MJ Kennedy¹, Hon Ki Tsang², Arthur Gossard¹, John Bowers¹; ¹Univ. of California, Santa Barbara, USA; ²The Chinese Univ. of Hong Kong, China. We demonstrate the first 100 GHz 5th harmonic colliding pulse mode locked quantum dot laser directly grown on CMOS compatible on axis (001) silicon substrate with ~ 0.9 Tb/s PAM-4 transmission capacity.

ATu3P.6 • 14:45

High repetition-rate pulse generation from SESAM-free electrically pumped VECSEL, Nikolai B. Chichkov¹, Amit Yadav¹, Tasnim Munshi², Ksenia Fedorova², Evgeny Viktorov³, Edik U. Rafailov¹; ¹Aston Inst. of Photonic Technologiess, Aston Univ., UK; ²Faculty of Physics and Materials Sciences Center, Philipps-Universität Marburg, Germany; ³ITMO Univ., Russia. High repetition-rate pulse generation in a SESAM-free electrically pumped VECSEL is demonstrated. The laser produces output pulses with a duration of 140 ps, pulse energy of 3.6 pJ, and repetition rate of 1.97 GHz.

15:00–16:30 Meet the OSA Publishing Journal Editors Ice Cream Social, Networking Zone Booth 2605

15:00–17:00 Coffee Break and Exhibit Only Time, Exhibit Halls 1-3
Coffee Break Sponsored by  COHERENT and  THORLABS

15:30–17:00 OIDA: Market Trends: Opportunities in Optics and Photonics, Exhibit Hall Theater I

17:00–19:00

JTu4A • Symposium on Quantum Information in Time-Frequency Domain II

President: To Be Announced

JTu4A.1 • 17:00 **Invited**

Generation of Scalable Cluster States in the Quantum Optical Frequency Comb, Olivier Pfister¹; ¹Univ. of Virginia, USA. Record-level quantum information scalability can be achieved by entangling the multitude of quantum optical resonant fields (qumodes), emitted by a single optical parametric oscillator, into large-scale cluster states suitable for quantum computing and quantum simulation.

JTu4A.2 • 17:30 **Invited**

Tailored Non-Gaussian Multimode States of Quantum Light, Nicolas Treps¹; ¹Laboratoire Kastler Brossel, Sorbonne Université, France. We demonstrate experimentally non-Gaussian states of light from mode-dependant photon subtraction on multimode entangled Gaussian States. We study the propagation properties of non-gaussianity within the graph, and its implications on the nature of entanglement.

JTu4A.3 • 18:00 **Invited**

Quantum Information Processing with Frequency-bin Qubits: Progress, Status, and Challenges, Joseph M. Lukens¹; ¹Oak Ridge National Lab, USA. Frequency-bin encoding has emerged as a promising approach for fiber- and chip-compatible quantum information processing. We overview the basic theory and experiments, as well as offer perspectives on opportunities for continued advances.

17:00–19:00

FTu4B • Manipulation of Symmetries in Optics

President: To Be Announced

FTu4B.1 • 17:00

3D Parity Time symmetry in 2D photonic lattices utilizing artificial gauge fields in synthetic dimensions, Eran Lustig¹, Yonatan Plotnik¹, Zhaoju Yang¹, Moti Segev¹; ¹Technion Israel Inst. of Technology, Israel. We study Parity-Time symmetric lattice models in three dimensions by utilizing a synthetic modal dimension of a 2D lattice of coupled waveguides.

FTu4B.2 • 17:15

A Random Anti-Laser Implemented by Coherent Perfect Absorption in a Disordered Medium, Kevin Pichler¹, Matthias Kühmayer¹, Julian Böhm², Andre Brandstötter¹, Philipp Ambichl¹, Ulrich Kuhl², Stefan Rotter¹; ¹Inst. for Theoretical Physics, Vienna Univ. of Technology, Austria; ²Institut de Physique de Nice, Université Côte d'Azur, France. We report the first experimental implementation of coherent perfect absorption in a disordered medium. We thereby realize a "random anti-laser", which produces the time-reversed process of random lasing at threshold.

FTu4B.3 • 17:30

Experimental Demonstration of 2D PT-Symmetric Graphene: Bulk Properties and Edge States, Mark Kremer¹, Tobias Biesenthal¹, Lukas Maczewsky¹, Matthias Heinrich¹, Ronny Thomale², Alexander Szameit¹; ¹Inst. of Physics, Univ. of Rostock, Germany; ²Dept. of Physics and Astronomy, Univ. of Würzburg, Germany. We report the first realization of a two-dimensional PT-symmetric crystalline structure, based on a novel isotropic loss mechanism. By probing bulk and edge properties, we shed new light on the interplay between PT-symmetry and topology.

FTu4B.4 • 17:45

Bound states in the continuum through environment engineering, Alexander Cerjan¹, Chia Wei Hsu², Mikael C. Rechtsman¹; ¹Pennsylvania State Univ., USA; ²Electrical Engineering, Univ. of Southern California, USA. We propose a new paradigm for realizing bound states in the continuum (BICs): engineering radiating channels in the environment. Examples include points and lines of BICs in a structure embedded in a periodic medium.

FTu4B.5 • 18:00 **Invited**

Irreversible Refractive-Index and Water-Walled Photonics, Tal Carmon¹; ¹Technion Israel Inst. of Technology, Israel. Coupling light from a tapered fiber into a resonator was recently transformed to permit coupling to rapidly-spinning resonators as well as to resonators made strictly of water. I will present recent experiments where light is transmitted in only one direction of the fiber, record finesse is observed, and water-waves exchange energy with light.

17:00–19:00

FTu4C • Nanophotonic Platforms for Optical Computing & Deep Learning

President: Jonathan Fan, Stanford Univ., USA

FTu4C.1 • 17:00 **Invited**

Optical Computing of Spatial Differentiation Without Fourier Optics, Zhichao Ruan¹; ¹Zhejiang Univ., China. We propose optical analog computing of spatial differentiation with two new effects: the surface plasmon excitation and the spin Hall effect of light. Also we experimentally demonstrate their applications on edge-enhanced imaging.

FTu4C.2 • 17:30

Photonic Recurrent Ising Sampler, Charles Roques-Carnes¹, Yichen Shen¹, Cristian Zanoci¹, Mihika Prabhu¹, Fadi Atieh¹, Li Jing¹, Tena Dubcek¹, Vladimir Ceperic¹, John D. Joannopoulos¹, Dirk R. Englund¹, Marin Soljacic¹; ¹MIT, USA. We present the Photonic Recurrent Ising Sampler (PRIS), an algorithm tailored for photonic parallel networks, that can sample distributions of arbitrary Ising problems. The PRIS finds the ground state of general Ising problems and probes critical exponents of universality classes.

FTu4C.3 • 18:00

Deep Learning for Design and Retrieval of Plasmonic Nanostructures, Michael Mrejen², Itzik Malkiel¹, Achiya Nagler², Uri Arieli², Lior Wolf¹, Haim Suchowski²; ¹Computer Science, Tel Aviv Univ., Israel; ²School of Physics and Astronomy, Tel Aviv Univ., Israel. We experimentally demonstrate a novel Deep Learning method capable of retrieving subwavelength dimensions from solely far-field measurements. Moreover, it also directly addresses the inverse problem i.e. obtaining a geometry for a desired electromagnetic response.

CLEO: QELS-Fundamental
Science

17:00–19:00

FTu4D • Thermal Photonics

President: To Be Announced

FTu4D.1 • 17:00

Dual-Band Quasi-Coherent Radiative Thermal Source, Ryan Starko-Bowes², Xueji Wang¹, Jin Dai¹, Ward D. Newman¹, Sean Molesky², Limei Qi³, Aman Satija¹, Ying Tsui², Manisha Gupta², Robert Fedosejevs², Sandipan Pramanik², Yi Xuan¹, Zubin Jacob¹; ¹Birck Nanotechnology Center, Purdue Univ., USA; ²Univ. of Alberta, Canada; ³School of Electronic Engineering, Beijing Univ. of Posts and Telecommunications, China. We design, fabricate and characterize the spectral, polarization, angular and temperature dependence of a microstructured SiC thermal infrared source; achieving independent control of the frequency and polarization of thermal radiation in two spectral bands.

FTu4D.2 • 17:15

High-Temperature Refractory Metasurfaces For Solar Thermophotovoltaic Energy Harvesting, Chun-Chieh Chang^{1,2}, Wilton J. Kort-Kamp^{3,4}, John Nogan⁵, Ting S. Luk⁵, Abul Azad¹, Antoinette Taylor⁶, Diego A. Dalvit⁴, Milan Sykora⁷, Hou-Tong Chen¹; ¹Center for Integrated Nanotechnologies, Los Alamos National Lab, USA; ²Inst. of Electro-Optical Science and Technology, National Taiwan Normal Univ., Taiwan; ³Center for Nonlinear Studies, Los Alamos National Lab, USA; ⁴Theoretical Division, Los Alamos National Lab, USA; ⁵Center for Integrated Nanotechnologies, Sandia National Labs, USA; ⁶Chemistry, Life, and Earth Sciences Directorate, Los Alamos National Lab, USA; ⁷Chemistry Division, Los Alamos National Lab, USA. We experimentally demonstrate refractory metasurfaces for solar thermophotovoltaics (STPV) with tailored absorptance and emittance thermally stable up to at least 1200 C.

FTu4D.3 • 17:30 **Invited**

High Temperature Optical Metamaterials, Alexander Petrov^{1,3}, Manohar Chirumamilla¹, Gnanavel Vaidhyanathan², Tobias Krekeler¹, Matthias Graf², Dirk Jalas¹, Martin Ritter¹, Michael Störmer², Manfred Eich^{1,2}; ¹Hamburg Univ. of Technology, Germany; ²Helmholtz-Zentrum Geesthacht, Germany; ³ITMO Univ., Russia. We investigate spectrally selective high temperature stable metamaterial emitters for thermophotovoltaics. We demonstrate band-edge emitters based on a W-HfO₂ multilayer metamaterial stable up to 1400°C. Conditions for improved selectivity and thermal stability are discussed.

FTu4D.4 • 18:00

Non-Hermitian Selective Thermal Emitters Using Hybrid Plasmonic-Photonic Resonators, Chloe F. Doiron^{1,2}, Gururaj V. Naik¹; ¹Electrical and Computer Engineering, Rice Univ., USA; ²Applied Physics Graduate Program, Smalley-Curl Inst., Rice Univ., USA. We experimentally demonstrate non-Hermitian physics of thermal emitters by coupling a plasmonic resonator with high losses to a bound-state-in-continuum dielectric resonator with low losses. Our thermal emitter exhibits passive PT-symmetry while operating at 700°C.

CLEO: Science & Innovations

17:00–19:00

STu4E • High Peak-Power Laser & Technologies II

President: Dimitris Papadopoulos LULI, France

STu4E.1 • 17:00

Latest developments at Amplitude in the frame of the ELI-HU projects. PW laser at high repetition rate, Franck Falcoz¹; ¹Amplitude, France. We will present in this paper the latest development made in the frame of the ELI projects. We will focus in particular on the development of a 50J @ 532nm, 10Hz pump laser that is compatible with TiSa or OP-CPA pumping. The technology used and the performances obtained will be presented.

STu4E.2 • 17:15

Design study of two-cycle bandwidth, single-color pumped OPCPA chain, Szabolcs Tóth¹, Tomas Stanislaukas², Ignas Balciunas², Rimantas Budriunas², Gediminas Veitas², Janos Csontos¹, Ádám Börzsönyi¹, Károly Osvay¹; ¹ELI-ALPS, ELI-HU Nonprofit Ltd., Hungary; ²Light Conversion Ltd., Lithuania. ELI-ALPS 1kHz SYLOS laser aims to deliver 5.5TW, two-cycle pulses for attosecond pulse and electron beam generation. In this study, broadband NOPCPA schemes were examined based on spectral multiplexing in different BBO and LBO configurations.

STu4E.3 • 17:30 **Invited**

Advanced Laser Technology for Attosecond and Femtosecond Spectroscopy, Hanieh Fattahi¹; ¹Max-Planck-Institut für Quantenoptik, Germany. Molecular fieldoscopy enables the direct measurement of the complex electric field of the emitted free-induction decay of excited molecules with an unparalleled sensitivity and specificity. In this talk, the novel methodology, lasers source, and preliminary results are presented.

STu4E.4 • 18:00

Long-Term Stabilization of Temporal and Spectral Drifts of a Burst-Mode OPCPA System, Nora Schirmel¹, Skirmantas Alisauskas¹, Thomas Hülsenbusch¹, Bastian Manschwetus¹, Christian Mohr¹, Lutz Winkelmann¹, Uwe Große-Wortmann¹, Jiaan Zheng¹, Tino Lang¹, Ingmar Hartl¹; ¹Deutsches Elektronen-Synchrotron, Germany. We demonstrate a stabilization system for temporal and spectral drifts of an OPCPA pump-probe laser at the FLASH soft-X-ray FEL-facility. We achieve drifts of 5.7fs rms and 3.2nm rms, respectively over two days.

17:00–19:00

STu4F • Terahertz Spectroscopy

President: Aydin Babakhani, UCLA, USA

STu4F.1 • 17:00

Ultrafast Time-Domain Spectrometer in the 25 T Split Florida-Helix Magnet, Ashlyn D. Burch¹, Jeremy A. Curtis¹, Biplob Barman¹, A. G. Linn¹, Luke M. McLintock¹, Aidan L. O'Beirne¹, Matthew J. Stiles¹, John Reno², Stephen A. McGill³, Denis Karaiskaj⁴, David J. Hilton¹; ¹Univ. of Alabama at Birmingham, USA; ²Center for Integrated Nanotechnologies, Sandia National Labs, USA; ³National High Magnetic Field Lab, USA; ⁴Physics, Univ. of South Florida, USA. We custom-designed an optical pump-terahertz probe spectrometer to operate under the high external magnetic fields of the 25 T Split Florida-Helix and demonstrated the instrument use by studying a gallium arsenide multiple quantum well sample.

STu4F.2 • 17:15

Pressure- and Temperature-Dependent Terahertz Time-Domain Spectroscopy of Hydroquinone and its Clathrates, Wei Zhang¹, Xuanfu Zhu², Michael T. Ruggiero², Daniel M. Mittleman¹; ¹Brown Univ., USA; ²Dept. of Chemistry, Univ. of Vermont, USA. We study the low-energy dynamics of hydroquinone and its clathrates under pressure using terahertz time-domain spectroscopy. Transitions between different phases are observed. The absorption peaks are assigned to lattice vibrational modes using quantum-mechanical simulations.

STu4F.3 • 17:30

Terahertz Spectroscopy of Metal Halide Perovskites, Michael B. Johnston¹; ¹Univ. of Oxford, UK. Metal halide perovskite semiconductors show great promise as photovoltaic cells. Transient terahertz conductivity spectroscopy on single crystals and vapor co-deposited thin films of these materials reveals the ultrafast charge dynamics in these direct bandgap semiconductors.

STu4F.4 • 17:45

Carrier Mobility and Conduction Anisotropy of Silicon by Sub-Bandgap Time-Resolved Terahertz Spectroscopy, Timothy J. Magnanelli¹, Edwin J. Heilweil¹, Jared K. Wahlstrand¹; ¹NIST, USA. Low density charge mobility from below bandgap, two photon photoexcitation of silicon is interrogated using time resolved terahertz spectroscopy yielding high mobility values and directional conduction anisotropy contrasted with traditional Hall and single photoexcitation metrics.

STu4F.5 • 18:00 **Invited**

Hot Carrier Cooling in Tin- and Lead-based Metal Halide Perovskites, J. Lloyd-Hughes¹, R. Milot¹; ¹University of Warwick, UK. Terahertz photoconductivity spectroscopy and transient optical absorption gave insights into hot carrier cooling rates, charge mobilities and the electron-phonon interaction in Pb- and Sn-based metal halide perovskites.

CLEO: Science & Innovations

CLEO: Applications
& Technology

17:00–19:00

STu4G • Miniaturizing Quantum Technology

President: Max Perez; ColdQuanta, USA

STu4G.1 • 17:00 **Tutorial**

Challenges in Miniaturising Cold Atom Quantum Technology, Matt Himsworth¹; ¹*School of Physics & Astronomy, Univ of Southampton, UK*. I will discuss the current state of the art in integrating a miniaturising magneto optical traps (MOT) for quantum technology. The tutorial will cover on MOT geometries, vacuum systems, lasers, and optical elements.



Matt Himsworth leads the integrated atom-chip group at the University of Southampton. His PhD focused on novel cooling mechanisms using atom interferometry. After a postdoctoral position at the University of Oxford he was awarded a RAEng/ EPSRC fellowship. He is a Co-I in the UK Quantum Hub for Sensors and Metrology.

17:00–19:00

STu4H • Innovations in Machine Learning & Microscopy

President: Jessica Houston; New Mexico State Univ., USA

STu4H.1 • 17:00

Machine Learning Assisted Raman in Optofluidics for User-Independent Biofluid Diagnostics, Emily E. Storey¹, Duxuan Wu¹, Amr S. Helmy¹; ¹*Univ. of Toronto, Canada*. We present a self-contained microfluidic Raman device which achieves signal enhancement of several orders of magnitude and machine-learning-driven analysis which facilitates diagnostically significant biofluid composition analysis, with a physiologically relevant sensitivity below 50 μM .

STu4H.2 • 17:15

Cross-Modality Deep Learning Achieves Super-Resolution in Fluorescence Microscopy, Hongda Wang¹, Yair Rivenson¹, Yiyin Jin¹, Zhensong Wei¹, Ronald Gao¹, Harun Gunaydin¹, Laurent Bentolila¹, Comert Kural², Aydogan Ozcan¹; ¹*Univ. of California Los Angeles, USA*; ²*Ohio State Univ., USA*. Using cross-modality deep learning, we achieved super-resolution in fluorescence microscopy and established image transformations from a lower resolution microscopy modality to a higher resolution modality, without any parameter estimation or assumptions about the imaging system.

STu4H.3 • 17:30 **Invited**

Image-Guided Microfluidic Cell Sorter with Machine Learning, Yi Gu¹, Rui Tang¹, Alex Zhang¹, Yuanyuan Han¹, Yuhwa Lo¹; ¹*Univ. of California San Diego, USA*. We demonstrated an image-guided cell sorter using the techniques of spatial-temporal coding for high throughput cell imaging, real-time image processing and machine learning for cell classification, and microfluidic device in a disposable cartridge for cell sorting.

STu4H.4 • 18:00

Photonic Crystal-Enhanced Fluorescence Imaging of Cardiovascular Biomarker with Machine Learning Analysis, Kenneth Squire¹, Alan X. Wang¹; ¹*Oregon State Univ., USA*. A photonic crystal-enhanced fluorescence imaging immunoassay biosensor is capable of detecting NT-proBNP as a cardiovascular biomarker at various concentrations. Utilizing machine-learning algorithms, we create a predictive model for the analyte quantification.

17:00–19:00

ATu4I • Emerging Lasers for Device Fabrication

President: Manyalibo Matthews; Lawrence Livermore National Laboratory, USA

ATu4I.1 • 17:00 **Invited**

Femtosecond Laser Based Manufacturing of Tailored Flexible Electronics for OLED and OPV Applications, Jiyeon Choi¹, Youngzoo Yoo², Hyo Jung Kim³, Hyun Hwi Lee⁴, Eric Mottay⁵, Rainer Kling⁶; ¹*South Korea Inst. of Machinery & Materials, South Korea*; ²*DUKSAN HI-METAL CO., LTD, South Korea*; ³*Pusan National Univ., South Korea*; ⁴*POSTECH, South Korea (the Republic of)*; ⁵*ALPHANOV, France*; ⁶*Amplitude, France*. This talk presents our approaches for laser based flexible electronics manufacturing. Femtosecond laser processing has been applied to increase the efficiency of organic semiconductors and to form electrodes on flexible substrates possessing novel transparent conductors.

ATu4I.2 • 17:30

Femtosecond Laser decapsulation of micro-electronics Including parameter study and redeposition control, Nicholas May¹, Sina Shahbazmohamadi¹; ¹*REFINE Lab Univ. of CT, USA*. A recipe was constructed resulting in full laser decapsulation of a packaged micro-electronic device. A parametric study on a sub-130 fs laser scanning system considering redeposition control was carried out and quantified with light-confocal microscopy.

ATu4I.3 • 17:45

Single-crystalline Te-hyperdoped silicon via controlling the velocity of ultra-fast cooling during femtosecond-laser irradiation, Zixi Jia¹, Qiang Wu^{1,2}, Ride Wang¹, Xiaorong Jin¹, Song Huang¹, Jianghong Yao^{1,2}, Jingjun Xu^{1,2}; ¹*Key Lab of Weak-Light Nonlinear Photonics, Ministry of Education, TEDA Inst. of Applied Physics and School of Physics, Nankai Univ., China*; ²*Collaborative Innovation Center of Extreme Optics, Shanxi Univ., China*. We implement single-crystalline tellurium (Te)-hyperdoped silicon via controlling the velocity of ultra-fast cooling during femtosecond-laser irradiation, providing a new path of less defective semiconductor hyperdoping, has great potential in applications of low noise semiconductor devices.

ATu4I.4 • 18:00

Low-loss geometrical phase elements by ultrafast laser writing in silica glass, Yuhao Lei¹, Masaaki Sakakura¹, Lei Wang¹, Yanhao Yu¹, Rokas Drevinskis¹, Peter G. Kazansky¹; ¹*Optoelectronics Research Centre, Univ. of Southampton, UK*. Femtosecond laser induced birefringence with negligible transmission loss in silica glass is observed. Ultra-low loss birefringent optical elements including UV retarders and geometric phase optics are demonstrated.

STu4G.2 • 18:00 **Invited**

Integrated Photonic-Atomic Systems for Compact Precision Instrumentation, John Kitching¹; ¹*Time and Frequency Division, NIST, USA*. Lasers are widely used in instrumentation based on atomic spectroscopy. We describe efforts to integrate atomic ensembles with chip-based single-mode photonics to enable a new generation of compact, manufacturable, high-performance devices.

CLEO: Science & Innovations

17:00–19:00

STu4J • Quantum Nanostructure

President: Daryl Beggs, Cardiff Univ., UK

STu4J.1 • 17:00

Enhanced Photo Response at Two-micron-wavelength Using GeSn/Ge Multiple-Quantum-Well Waveguide, Shengqiang Xu¹, Yi-Chiau Huang², Saeid Masudy-Panah¹, Xiao Gong¹, Yee-Chia Yeo¹; ¹National University of Singapore, Singapore; ²Applied Materials Inc., USA. GeSn multiple-quantum-well rib waveguide on Si substrate was fabricated with vertical p-i-n photodiode structure and was characterized at two-micron-wavelength. Enhanced external photo response was achieved as compared to surface-illuminated counterparts, thanks to the waveguide scheme.

STu4J.2 • 17:15

Formation of GeSn Multiple-Quantum-Well Microdisks on Insulating Platform toward Lasing Applications, Shengqiang Xu¹, Yi-Chiau Huang², Kwang Hong Lee³, Kaizhen Han¹, Dian Lei¹, Wei Wang¹, Yuan Dong¹, Chuan Seng Tan^{3,4}, Xiao Gong¹, Yee-Chia Yeo¹; ¹National University of Singapore, Singapore; ²Applied Materials Inc., USA; ³Singapore MIT Alliance for Research and Technology (SMART), Singapore; ⁴Nanyang Technological Univ., Singapore. GeSn multiple-quantum-well microdisks are demonstrated on an 8-inch insulating platform, which was formed using direct wafer bonding technique. Whispering-gallery modes are identified through FDTD simulation, showing potential of such ultra-compact cavities for Group-IV lasing.

STu4J.3 • 17:30

Low threshold 1.55 μm Quantum dash microring lasers, Yating Wan¹, Daehwan Jung¹, Chen Shang¹, Noelle Collins¹, Ian MacFarlane¹, Justin Norman¹, Mario Dumont¹, Art Gossard¹, John Bowers¹; ¹Univ. of California Santa Barbara, USA. We report the first room-temperature-continuous-wave (CW) operation of electrically-injected InAs quantum-dash microring lasers emitting at 1.55 μm telecom window. The microrings sustain CW lasing up to 55°C, while the lowest threshold current density is 528A/cm².

STu4J.4 • 17:45

Deterministic positioning of colloidal quantum dots on silicon nitride nanobeam cavities, Yueyang Chen¹, Albert Ryou¹, Max Friedfeld¹, Taylor Fryett¹, James Whitehead¹, Brandi Cossairt¹, Arka Majumdar¹; ¹Univ. of Washington, USA. We experimentally demonstrated deterministic positioning of solution processed colloidal quantum dots on a silicon nitride nanobeam resonator, with potential applications in nonlinear optics, multi-functional optical devices, and on-chip, solid-state quantum simulators.

STu4J.5 • 18:00 **Invited**

Integrated versatile quantum dot-based photonics on silicon, Di Liang¹, Geza Kurczveil¹, Bassem Tossoun¹, Chong Zhang¹, Antoine Descos¹, Zhihong Huang¹, Xiaoge Zeng¹, Yingtao Hu¹, Marco Fiorentino¹, Raymond Beausoleil¹; ¹Hewlett Packard Labs, Hewlett Packard Enterprise, USA. We review our recent progress to develop multiple robust InAs quantum-dot-based lasers and photodetectors on a heterogeneous silicon substrate. It enables a versatile photonic integration platform to build high-performance photonic chips for communications and computing.

CLEO: Applications & Technology

17:00–19:00

ATu4K • Biosensing Technology

President: Andrea Armani; University of Southern California, USA

ATu4K.1 • 17:00 **Invited**

Dynamic Measurement of Blood Flow Using Laser Speckle Contrast Imaging, Abhishek Rege¹; ¹Vasoptic Medical, Inc., USA. Laser speckle contrast imaging is able to noninvasively obtain blood flow information with high spatio-temporal resolution from optically accessible tissues. Such information has the potential to be useful for diagnostic and other clinical decision making.

ATu4K.2 • 17:30

High-Throughput and Label-Free Detection of Motile Parasites in Bodily Fluids Using Lensless Time-Resolved Speckle Imaging, Yibo Zhang¹, Hatice Ceylan Koydemir¹, Michelle M. Shimogawa¹, Sener Yalcin¹, Alexander Guziak¹, Tairan Liu¹, Ilker Oguz¹, Yujia Huang¹, Bijie Bai¹, Yilin Luo¹, Yi Luo¹, Zhensong Wei¹, Hongda Wang¹, Vittorio Bianco¹, Bohan Zhang¹, Rohan Nadkarni¹, Kent Hill¹, Aydogan Ozcan¹; ¹Univ. of California Los Angeles, USA. We present a lensless time-resolved speckle imaging technique for label-free, sensitive and rapid detection of motile parasites in bodily fluids, by using the locomotion of parasites as a biomarker and contrast mechanism.

ATu4K.3 • 17:45

Particle-Aggregation Based Virus Sensor Using Deep Learning and Lensless Digital Holography, Yichen Wu¹, Aniruddha Ray¹, Qingshan Wei¹, Alborz Feizi¹, Xin Tong¹, Eva Chen¹, Yi Luo¹, Aydogan Ozcan¹; ¹Univ. of California Los Angeles, USA. Deep learning-based lensless holographic microscopy enables a high-throughput and rapid read-out for a particle-aggregation-based virus sensor, achieving a high sensitivity of ~5 viral copies per μL.

ATu4K.4 • 18:00

Time-resolved oxygen monitoring in human breath, Charles L. Patrick¹, Jonas Westberg¹, Gerard Wysocki¹; ¹Princeton University, USA. A small form-factor oxygen sensor is designed for respiratory monitoring to meet specifications: form-factor, sensitivity and real-time (<0.1 % of O₂ at 100Hz). Two designs are demonstrated based on wavelength modulation spectroscopy (WMS) and Faraday rotation spectroscopy (FRS).

CLEO: Science & Innovations

17:00–19:00

STu4L • Mode-Locked Fiber Lasers II

President: Maria Chernysheva Leibniz Institute of Photonic Technology, Germany

STu4L.1 • 17:00

Passive synchronization of Er- and Yb-doped mode-locked fiber lasers based on nonlinear amplifying loop mirror, Jing Zeng¹, Jiwei Gan¹, Qiang Hao¹, Ming Yan², Kun Huang¹, Heping Zeng^{1,2}; ¹Univ of Shanghai Science & Technology, China; ²East China Normal Univ., China. The pulse timing between polarization-maintaining Er- and Yb-doped mode-locked fiber lasers was passively stabilized by an all-optical synchronization scheme based on nonlinear amplifying loop mirror, showing a cavity mismatch tolerance up to 16.2 mm.

STu4L.2 • 17:15

Reduced graphene oxide coated photonic crystal fiber for all-fiber laser mode locking, Rodrigo M. Gerosa¹, Cristiano J. de Matos¹, Pilar G. Vianna¹, Sergio H. Domingues¹; ¹MackGraphe – Graphene and Nanomaterials Research Center, Mackenzie Presbyterian Univ., Brazil. The walls of two holes in a photonic crystal fiber were selectively coated with graphene oxide (GO) using a simple procedure. Thermally reducing GO then yielded 356-fs pulses in an all-fiber passively mode-locked ring laser.

STu4L.3 • 17:30 **Invited**

Functional Pulsed Fiber Lasers for Multicolor Stimulated Raman Scattering Microscopy, Yasuyuki Ozeki¹; ¹Univ. of Tokyo, Japan. I present our development of picosecond pulsed fiber laser sources for realizing high-performance yet practical molecular-vibrational microscopy based on stimulated Raman scattering. Specifically, I introduce a fast wavelength-tunable pulse source and an ultralow-intensity-noise oscillator.

STu4L.4 • 18:00

Characterization of the CEO Phase Noise of an Erbium Fiber Frequency Comb, Christoph Trespl¹, Thomas Puppe¹, Ali Seer¹, Pierre Thoumany¹, Felix Rohde¹, Rafal Wilk¹; ¹TOPTICA Photonics AG, Germany. We measure the carrier-envelope phase noise of our Er: fiber frequency comb based on difference frequency generation. Integrating from 70 mHz to 20 MHz we achieve an excellent RMS phase jitter of only 61 mrad.

17:00–19:00

JTu4M • Symposium on Intense-field Nonlinear Optics & High Harmonic Generation in Nanoscale Materials IIJTu4M.1 • 17:00 **Invited**

Extreme nonlinear optics in two dimensional materials, Koichiro Tanaka¹; ¹Kyoto Univ., Japan. We show recent progress of extreme non-linear optics in two dimensional materials. High-harmonic generation is confirmed not only in semiconductors but also metals under irradiation of mid-infrared femtosecond laser pulses. We found main mechanism changes according to the carrier doping status of the material.

JTu4M.2 • 17:30

Valleytronics on the subcycle timescale, Christoph P. Schmid¹, Stefan Schlauderer¹, Fabian Langer¹, Martin Gmitra¹, Jaroslav Fabian¹, Philipp Nagler¹, Tobias Korn¹, Christian Schüller¹, Peter Hawkins², Johannes T. Steiner², Ulrich Huttner², Markus Borsch³, Benjamin Girodias³, Stephan W. Koch², Mackillo Kira³, Rupert Huber¹; ¹Univ. of Regensburg, Germany; ²Univ. of Marburg, Germany; ³Univ. of Michigan, USA. Intense multi-terahertz waveforms drive electron-hole recollisions in monolayer WSe₂ and enable subcycle switching of the valley pseudospin. This dynamics manifests in high-odd-order sideband generation and opens the door to valleytronic protocols at optical clock rates.

JTu4M.3 • 17:45

Ultrafast laser pulse induced topological resonance in MoS₂ monolayer, Seyyedeh Azar Oliaei Motlagh¹, Jih-Sheng Wu¹, Vadym Apalkov¹, Mark Stockman¹; ¹Georgia State Univ., USA. In MoS₂ monolayer, we predict that a single oscillation femtosecond laser pulse with circular polarization creates a chiral distribution of conduction band electron population. This chirality is an effect of topological resonances in this semiconductor.

JTu4M.4 • 18:00

Carrier-Envelope Phase Detection with Arrays of Electrically Connected Bowtie Nanoantennas, Phillip D. Keathley¹, Yujia Yang¹, William Putnam², Praful Vasireddy¹, Franz Kärtner^{1,3}, Karl Berggren¹; ¹Massachusetts Inst. of Technology, USA; ²NG Next, Northrop Grumman Cooperation, USA; ³Center for Free Electron Laser Science and DESY, Germany. We use arrays of electrically connected bowtie nanoantennas to detect the carrier-envelope phase of few-cycle optical pulses with noise performance close to the shot-noise limit. Our results pave the way towards low-cost, low-profile CEP monitoring and tagging.

17:00–19:00

STu4N • Semiconductor-Based Optical Frequency Combs

President: Ben Williams; UCLA, USA

STu4N.1 • 17:00 **Tutorial**

Quantum Cascade Frequency Combs: Physics and Applications, Jérôme Faist¹; ¹ETH Zurich, Switzerland. Quantum cascade lasers combs have demonstrated watt level emission over 100cm⁻¹ in the mid-infrared, enabling new applications such as spectroscopy protein reaction dynamics. New insight in their physics has recently been gained.



Jérôme Faist has obtained his Ph.D from EPFL, and has worked successively at IBM Rüschlikon, AT&T Bell Laboratories and the University of Neuchatel. He now holds a chair in the physics department of the ETH Zurich.

STu4N.2 • 18:00

Optomechanical Control of the State of Chip-Scale Frequency Combs, David P. Burghoff^{1,2}, Ningren Han^{1,3}, Filippos Kapsalidis⁴, Nathan Henry⁵, Mattias Beck⁴, Jacob Khurgin⁵, Jerome Faist⁴, Qing Hu¹; ¹MIT, USA; ²Univ. of Notre Dame, USA; ³Google, USA; ⁴ETH Zurich, Switzerland; ⁵Johns Hopkins Univ., USA. Quantum cascade laser frequency combs have substantial potential in sensing. We show that by blending them with microelectromechanical comb drives, one can directly manipulate the dynamics of the laser and fully control the comb state.

17:00–19:00

STu4O • Infrared Photonics & Applications

Presiders: Nan Zhang; State University of New York at Buffalo, USA

Haomin Song; State University of New York at Buffalo, USA

STu4O.1 • 17:00

Compact, ultra-tunable InGaSb/AlGaAsSb Si external cavity laser at the Mid-Infrared (MIR), Sia J. Brian¹, Wanjun Wang¹, Zhongliang Qiao¹, Xiang Li¹, Xin Guo¹, Jin Zhou¹, Zecen Zhang¹, Callum Littlejohns^{2,1}, Chongyang Liu¹, Graham T. Reed^{2,1}, Hong Wang¹; ¹Nanyang Technological Univ., Singapore; ²Optoelectronics Reserch Centre, Univ. of Southampton, UK. We present the first MIR hybrid Si external cavity laser with a tunable range below the 2 μm mark. To the best of our knowledge, we have achieved the largest tunable range of 66 nm (1881-1947 nm) near the 2 μm waveband in silicon photonics.

STu4O.2 • 17:15

Withdrawn

STu4O.3 • 17:30

Photonic Integrated Si₃N₄ Ultra-Large-Area Grating Waveguide MOT Interface for 3D Atomic Clock Laser Cooling, Nitesh Chauhan¹, Debapam Bose¹, Matthew Puckett², Renan Moreira¹, Karl Nelson², Daniel Blumenthal¹; ¹Univ. of California, Santa Barbara, USA; ²Honeywell, USA. We describe a silicon nitride (Si₃N₄) photonic integrated circuit (PIC) designed to deliver non-diverging 780nm free-space optical cooling beams to an ⁸⁷Rb atomic magneto optic trap (MOT) via fiber coupled ultra-large-area 3.88mm x 2.08mm gratings.

STu4O.4 • 17:45

2.3 μm Wavelength Range Digital Fourier Transform on-Chip Wavelength Monitor, Anton Vasiliev^{1,2}, Fabio Pavanello^{1,2}, Muhammad Muneeb^{1,2}, Gunther Roelkens^{1,2}; ¹Photonics Research Group, Ghent Univ. - imec, Belgium; ²Center for Nano- and Biophotonics, Belgium. We present a novel approach for on-chip wavelength monitoring based on a digital Fourier Transform spectrometer. We demonstrate 130 nm operational bandwidth and an accuracy of 100 pm in the 2.3 μm wavelength range.

STu4O.5 • 18:00 **Invited**

Ge-rich SiGe Photonic Circuits for Mid IR spectroscopy, Delphine Marris-Morini¹; ¹Universite de Paris-Sud, France. Ge-rich SiGe photonic circuits have been used to demonstrate a whole set of devices in the mid-IR, such as interferometers, spectrometers or cavities. The perspectives towards the realization of optical sources will be also presented.

NOTES

Tuesday, 17:00-19:00

Joint

CLEO: QELS-Fundamental Science

JTu4A • Symposium on Quantum Information in Time-Frequency Domain II—Continued

JTu4A.4 • 18:30

Photonic Controlled-PHASE Gate using Dynamic Cavities and a Kerr Nonlinearity, Mikkel Heuck^{1,2}, Kurt Jacobs^{3,4}, Dirk R. Englund²; ¹Danmarks Tekniske Universitet, Denmark; ²Dept. of Electrical Engineering and Computer Science, MIT, USA; ³Computational and Information Sciences Directorate, U.S. Army Research Lab, USA; ⁴Dept. of Physics, Univ. of Massachusetts at Boston, USA. We propose a photonic CPHASE gate based on Kerr nonlinearities and tunable cavities enabling complete absorption and re-emission of photons. Storing photons about 40 times the width of their wavepackets results in 99% gate fidelity.

JTu4A.5 • 18:45

Exploring Quantum Memory via Optically Induced Bragg Structures, Carlo Page¹, Tom Weaver¹, John Price², Joshua Nunn¹; ¹Univ. of Bath, UK; ²QOLS, Blackett Lab, Imperial College, UK. We investigate short-term light storage for quantum computing by trapping light in an optically induced Bragg grating in warm Rb vapour.

FTu4B • Manipulation of Symmetries in Optics—Continued

FTu4B.6 • 18:30

Controlling Optical Forces between Evanescently Coupled PT-Symmetric Waveguides, Mohammad-Ali Miri^{1,2}, Michele Cotrufo³, Andrea Alu^{3,2}; ¹Queens College of CUNY, USA; ²Physics Program, The Graduate Center of CUNY, USA; ³Advanced Science Research Center of CUNY, USA. We investigate optical forces between evanescently coupled optical waveguides with balanced gain and loss. This system reveals unusual properties, most notably the emergence of a tangential stress component parallel to the direction of wave propagation.

FTu4B.7 • 18:45

Spatially locked mode in defected microring resonators, Hwaseob Lee¹, Tiantian Li¹, Zi Wang¹, Anishkumar Soman¹, Alec Scallo¹, Tingyi Gu¹; ¹Univ. of Delaware, USA. Control of mode-splitting in a microring resonator is achieved by introducing notched scatters on its perimeter. Single step etching on SOI substrate enables the microring resonator to operate at exceptional point.

FTu4C • Nanophotonic Platforms for Optical Computing & Deep Learning—Continued

FTu4C.4 • 18:15

Application of deep learning to direct and inverse problems in plasmonic coloring, Joshua Baxter^{1,2}, Antonino Cala¹, Lesina^{1,2}, Jean-Michel Guay^{1,2}, Arnaud Weck^{2,3}, Pierre Berini^{1,2}, Lora Ramunno^{1,2}; ¹Physics, Univ. of Ottawa, Canada; ²Center for Research in Photonics, Univ. of Ottawa, Canada; ³Mechanical Engineering, Univ. of Ottawa, Canada. Laser pulses can color noble metals by inducing nanoparticles on their surface. We apply deep learning to solve the direct and inverse problems which link nanoparticle distributions and laser parameters to the produced colour.

FTu4C.5 • 18:30

Gb/s physical random bits through mesoscopic chaos in integrated silicon optomechanical cavities, Ciwei Luo¹, Jaime G. Flor Flores², Binglei Shi¹, Mingbin Yu³, Guoqiang Lo³, Jiagui Wu^{1,2}, Chee Wei Wong²; ¹Southwest Univ., China; ²Fang Lu Mesoscopic Optics and Quantum Electronics Lab, Univ. of California, Los Angeles, USA; ³The Inst. of Microelectronics, 11 Science Park Road, Singapore. We present a silicon-based physical random bits (PRBs) generator, where mesoscopic chaos comes from coupled material nonlinearities and optomechanical oscillation have been used to generate fast (1.25Gbit/s) PRBs, which successfully passed NIST-SP800-22 standard randomness tests.

17:30-18:30 OSA Senior Member Reception, OSA Member Lounge, Concourse Level

19:00–20:30 OSA Technical Group Poster Session, Grand Ballroom 220C

CLEO: QELS-Fundamental
Science

FTu4D • Thermal Photonics—Continued

FTu4D.5 • 18:15

Perfect selective emitter with far infrared photonic structure, Se-Yeon Heo¹, Gil Ju Lee¹, Young Min Song¹; ¹*Gwangju Inst. of Science and Technol, South Korea (the Republic of)*. We design and fabricate metasurface radiative cooler, in which high emissivity is achieved over the full range of main transparency window. The results provide one potential route to the absorption tuning at far infrared wavelength.

FTu4D.6 • 18:30

Incoherent Perfect Absorption in Lossy Dielectric Media, Sanjay Debnath¹, Evgenii E. Narimanov¹; ¹*Purdue Univ., USA*. We theoretically demonstrate perfect absorption of incoherent light in lossy anisotropic half-infinite planar dielectric structures, and uncover this effect in existing (meta) materials.

FTu4D.7 • 18:45

All-Dielectric Metalens Integrated with Dispersive Grism for High Spectral Resolution at Mid-Infrared Regime, Semih Cakmakyapan¹, Yi-Chun Ling¹, Mathias Prost¹, S.J. Ben Yoo¹; ¹*UCD, USA*. We present a proof-of-concept beam steering device which resolves the wavelength differences at mid-infrared regime by utilizing an all-dielectric metalens structure integrated with a grism structure.

CLEO: Science & Innovations

STu4E • High Peak-Power Laser &
Technologies II—Continued

STu4E.5 • 18:15

A methodology for designing grism stretchers for idler-based optical parametric chirped-pulse amplification systems, Sara Bucht¹, Dan Haberberger¹, Jake Bromage¹, Dustin Froula¹; ¹*Lab for Laser Energetics, USA*. This paper presents a method for designing grism stretchers and grating compressors that can produce near transform-limited idler pulses from OPCPA systems.

STu4E.6 • 18:30

Pulse Contrast Enhancement via Non-collinear Sum-Frequency Generation of the Signal and Idler of an Optical Parametric Amplifier, Eric Cunningham¹, Eric Galtier¹, Gilliss Dyer¹, Joseph Robinson¹, Alan Fry¹; ¹*SLAC National Accelerator Lab, USA*. We improve the temporal contrast of the front end of a high-intensity laser system to better than twelve orders of magnitude using non-collinear sum-frequency generation of the signal and idler of an optical parametric amplifier.

STu4F • Terahertz Spectroscopy—Continued

STu4F.6 • 18:30

Thickness-Dependent THz Emission From Ultrathin Ferromagnetic Mn₃Ga Films, Igor Ilyakov¹, Nilesh Awari^{1,3}, Sergey Kovalev¹, Ciarán Fowley¹, Karsten Rode², Plamen Stamenov², Yong Chang Lau², Davide Betto², Nivetha Thiyagarajah², Bertram Green¹, Oguz Yildirim¹, Jürgen Lindner¹, Jürgen Fassbender¹, Michael Coey², Alina Deac¹, Michael Gensch¹; ¹*Helmholtz-Zentrum Dresden-Rossendorf, Germany*; ²*Trinity College Dublin, Ireland*; ³*Univ. of Groningen, Netherlands*. An experimental time-domain, room-temperature study of magnetization precession in ultra-thin Mn₃Ga films excited by femtosecond laser pulses is presented. The thickness dependence of the parameters of THz waves emitted from coherently driven magnetic resonances is investigated.

STu4F.7 • 18:45

Monitoring Charge Separation Dynamics Using THz Emission Spectroscopy, Burak Guzelurk^{1,4}, Eric Yue Ma^{2,4}, Guoqing Li³, Linyou Cao³, Zhi-Xun Shen², Tony Heinz^{2,4}, Aaron Lindenberg^{1,4}; ¹*Materials Science and Engineering, Stanford Univ., USA*; ²*Dept. of Applied Physics, Stanford Univ., USA*; ³*Dept. of Materials Science and Engineering, North Carolina State Univ., USA*; ⁴*Stanford Inst. for Materials and Energy Sciences, SLAC, USA*. We present terahertz (THz) emission spectroscopy as a means of monitoring ultrafast charge separation dynamics in layered two-dimensional heterostructures.

17:30-18:30 OSA Senior Member Reception, OSA Member Lounge, Concourse Level

19:00-20:30 OSA Technical Group Poster Session, Grand Ballroom 220C

Executive Ballroom
210G

Joint

STu4G • Miniaturizing Quantum Technology—Continued

STu4G.3 • 18:30

Alkali metal condensation zones in MEMS alkali vapor cells and characterization in CPT clock, Sylvain Karlen¹, Thomas Overstolz¹, Jean Gobet¹, Jacques Haesler¹, Fabien Droz¹, Steve Lecomte¹; ¹CSEM SA, Switzerland. We fabricated MEMS vapor cells gold microdiscs, allowing the condensation of alkali metal on preferred locations without the use of a thermal gradient. Reduction of light-shift induced long-term frequency instability in CPT clock is reported.

STu4G.4 • 18:45

Nanophotonic Integration of Atomic Wavelength References, Douglas Bopp¹, John Kitching¹, Vladimir Aksyuk¹; ¹NIST, USA. Nanophotonic circuitry is interfaced to micro-fabricated alkali vapor cells forming a quantum sensing platform. We operate this device as a wavelength reference using several operation modes and discuss strengths and limitations of such devices.

Executive Ballroom
210H

CLEO: Science & Innovations

STu4H • Innovations in Machine Learning & Microscopy—Continued

STu4H.5 • 18:15

Smartphone-based cancer detection platform based on plasmonic interferometer array biochips, Xie Zeng¹, Yunchen Yang¹, Nan Zhang¹, Dengxin Ji¹, Yun Wu¹, Qiaoqiang Gan¹; ¹State Univ. of New York at Buffalo, USA. We develop a nanoplasmonic interferometer imaging system based on intensity modulation to detect circulating exosomal proteins in real-time with high sensitivity and low cost to enable the early detection of cancer.

STu4H.6 • 18:30

Multicolor Stimulated Raman and Fluorescence Imaging with High-speed Programmable Tunability, Jingwen Shou¹, Robert Oda^{1,2}, Shunji Tanaka¹, Yasuyuki Ozeki¹; ¹Univ. of Tokyo, Japan; ²The Univ. of Hawaii, USA. We demonstrate a multispectral and multimodal microscopy which enables high-speed stimulated Raman and fluorescence imaging. Both the Raman wavenumber and the fluorescence detection wavelength of each frame can be tuned via high-speed galvanometer-driven optical filters.

STu4H.7 • 18:45

Intracellular GaN microrod laser, Minho Song¹, Hyeonjun Baek², Gyu-Chul Yi¹; ¹Seoul National Univ., South Korea (the Republic of); ²Heriot-Watt Univ., UK. We report fabrication of GaN microrods and their intracellular lasing characteristics for individual cell tracking and labeling application.

Meeting Room
211 A/B

CLEO: Applications
& Technology

ATu4I • Emerging Lasers for Device Fabrication—Continued

ATu4I.5 • 18:30

>300-W femtosecond laser with free triggering up to 25 MHz, Florent Basin¹, Julien Pouysegur¹, Martin Delaigue¹, Benoit Tropheme¹, Jorge Sanabria¹, Eric Mottay¹, Clemens Hoenninger¹; ¹Amplitude Laser Group, France. We demonstrate a high power femtosecond laser with up to 500-W and 400-fs pulse width. A unique free-triggering option enables arbitrary pulse train control with unprecedented speed of 25MHz and timing jitter of only 10ns.

ATu4I.6 • 18:45

All-Fiber 2 μm Amplifier Using A Normal Dispersion Thulium Fiber, Yuhao Chen¹, Shaoxiang Chen¹, Kun Liu¹, Qijie Wang¹, Dingyuan Tang¹, Seongwoo Yoo¹; ¹Nanyang Technological Univ., Singapore. Normal dispersion thulium-doped fiber was deployed in all-fiber setup to amplify pulses from a near-2 μm ultrafast fiber ring cavity and demonstrated >27 dB amplification without pulse breaking. Output pulse energy ~525nJ reported at 1852nm.

17:30-18:30 OSA Senior Member Reception, OSA Member Lounge, Concourse Level

19:00-20:30 OSA Technical Group Poster Session, Grand Ballroom 220C

Tuesday, 13:00-15:00

CLEO: Science & Innovations

CLEO: Applications
& Technology

CLEO: Science & Innovations

STu4J • Quantum Nanostructure—
Continued

ATu4K • Biosensing Technology—Continued

STu4L • Mode-Locked Fiber Lasers II—
Continued

STu4J.6 • 18:30

Heterogeneous integrated quantum photonic devices with single, deterministically positioned InAs quantum dots, Peter Schnauber², Anshuman Singh^{1,3}, Johannes Schall², Sven Rodt², Kartik Srinivasan¹, Stephan Reitzenstein², Marcelo I. Davanco¹; ¹NIST, USA; ²Inst. of Solid-State Physics, Technical Univ. of Berlin, Germany; ³Maryland NanoCenter, Univ. of Maryland, USA. We demonstrate integrated Si₃N₄ waveguides containing single-photon emitters based on single InAs quantum dots that were deterministically positioned in a GaAs nanowaveguide via a low-temperature in-situ electron-beam lithography.

ATu4K.6 • 18:30

Deep Learning Enables Virtual Histological Staining of Label-free Tissue Sections Using Auto-fluorescence, Yair Rivenson¹, Hongda Wang¹, Kevin de Haan¹, Zhensong Wei¹, Aydogan Ozcan¹; ¹Univ. of California Los Angeles, USA. We report a data-driven method for label-free virtual histological staining of tissue sections using deep learning. This framework is successfully demonstrated by inferring multiple types of stains on different tissue types using auto-fluorescence signal.

STu4L.6 • 18:30

Resolving the temporal structure of noise-like pulse using a synchronized time magnifier, Bowen Li¹, Jiqiang Kang¹, Sheng Wang¹, Ying Yu¹, Pingping Feng¹, Kenneth Kin-Yip Wong¹; ¹Univ. of Hong Kong, Hong Kong. The detailed temporal structures inside the noise-like pulses have been resolved in real time for the first time using a synchronized parametric time magnifier. Optical rogue waves have been observed under sub-ps temporal resolution.

ATu4K.7 • 18:45

Smart Mattress System Based on Interferometric Fiber Optics for Vital Signs Monitoring, Senmao Wang¹, Lliangye Li¹, Jingyi Wang¹, Zhijun Yan¹, Deming Liu¹, Qizhen Sun¹; ¹Huazhong Univ of Science and Technology, China. A smart mattress system is developed to monitor human vital signs. The heart rate signal and respiration signal are measured simultaneously by the system based on fiber optic Mach-zehnder interferometer.

STu4L.7 • 18:45

Spectrally uniform discrete Fourier domain mode locked fiber laser by time domain modulation, Dongmei Huang¹, Chao Shang², Feng Li¹, Xianting Zhang¹, Zihao Cheng¹, Jinhui Yuan¹, Xinhuan Feng³, P. K. A. Wai¹; ¹The Hong Kong Polytechnic Univ., Hong Kong; ²The Hong Kong Polytechnic Univ. Shenzhen Research Inst., China; ³Jinan Univ., China. We propose and demonstrate a frequency domain linearized discrete Fourier domain mode locked laser with a rate varying pulse modulation in time domain. Discrete swept signal with an identical FSR of 100 GHz is demonstrated.

17:30-18:30 OSA Senior Member Reception, OSA Member Lounge, Concourse Level

19:00-20:30 OSA Technical Group Poster Session, Grand Ballroom 220C

Joint

CLEO: Science & Innovations

JTu4M • Symposium on Intense-field Nonlinear Optics & High Harmonic Generation in Nanoscale Materials II—Continued**JTu4M.5 • 18:15**

Circular dichroism of electrons photoemitted from an emitter array of Au nanospirals, Hong Ye^{1,2}, Anchita Ad-dhya^{1,3}, Sebastian Trippel^{1,4}, Arya Fallahi¹, Subir Ray³, Nirmalya Ghosh³, Oliver D. Mücke^{1,4}, Jochen Küpper^{1,2}, Franz Kärtner^{1,2}; ¹DESY/CFEL, Germany; ²Univ. of Hamburg, Germany; ³Indian Inst. of Science Education and Research Kolkata, India; ⁴The Hamburg Centre for Ultrafast Imaging, Germany. We have investigated photoemission from an emitter array of Au nanospirals on an ultrafast time scale via velocity-map-imaging (VM) spectroscopy. Circular dichroism of the velocity distribution of the emitted electrons is observed.

JTu4M.6 • 18:30 **Invited**

Optical Harmonic Generation in Nonlinear All-Dielectric Nanoantennas and Metasurfaces, Andrey Fedyanin¹; ¹Lomonosov Moscow State Univ., Russia. We present recent experimental results of controllable optical harmonic generation in all-dielectric nanoantennas and metasurfaces fabricated from direct (silicon) and indirect (gallium arsenide) semiconductor nanoparticles possessing low-order Mie-resonances in visible and IR ranges.

STu4N • Semiconductor-Based Optical Frequency Combs—Continued**STu4N.3 • 18:15**

Optical-feedback-stabilized quantum cascade laser frequency combs, Chu Teng¹, Jonas Westberg¹, Gerard Wysocki¹; ¹Princeton Univ., USA. Stabilization of quantum-cascade-laser frequency combs by means of external optical feedback is presented. Experimental results suggest reduced phase-noise in the frequency comb, allowing comb operation in previously unstable regimes.

STu4N.4 • 18:30

Narrow Intrinsic Linewidth Frequency Combs from a Chip-Based Hybrid Integrated InP-Si₃N₄ Diode Laser, Jesse Mak¹, Albert v. Rees¹, Youwen Fan¹, Edwin J. Klein², Dimitri Gekus², Peter van der Slot¹, Klaus J. Boller¹; ¹Univ. of Twente, Netherlands; ²LioniX International BV, Netherlands. We present a hybrid integrated InP-Si₃N₄ laser that generates frequency combs with a record-low intrinsic linewidth of 34 kHz.

STu4N.5 • 18:45

Performance of an injection-locked active demultiplexer for FSR-tunable optical frequency combs, Prajwal Doddaballapura Lakshmiyasimh¹, Eamonn Martin¹, Seán P. Ó Duill¹, Pascal Landais¹, Prince M. Anandarajah¹, Aleksandra Kaszubowska-Anandarajah²; ¹School of Electronics Engineering, Dublin City Univ., Ireland; ²Trinity College Dublin, CON-NECT Research Centre, Ireland. An active injection-locked demultiplexer for optical combs with flexible channel spacing is demonstrated. Relationships between the injected power and frequency detuning of a 6.25GHz comb and the output comb suppression and phase noise are characterized.

STu4O • Infrared Photonics & Applications—Continued**STu4O.6 • 18:30**

Interband cascade laser frequency combs for monolithic and battery driven spectrometers, Benedikt Schwarz², Johannes Hillbrand³, Maximilian Beiser³, Aaron M. Andrews³, Gottfried Strasser³, Hermann Detz^{1,3}, Anne Schade², Robert Weih⁴, Sven Höfling²; ¹CEITEC, Czechia; ²Univ. Würzburg, Germany; ³TU Wien, Austria; ⁴Nanoplus, Germany. We demonstrated a monolithic frequency comb platform based on interband cascade lasers. We show self-starting frequency combs operation utilizing the inherent gain non-linearity and exceptionally fast and sensitive room-temperature photodetection to enable on-chip multi-heterodyne detectors.

STu4O.7 • 18:45

Integrated DFB Lasers on Si₃N₄ Photonic Platform for Chip-Scale Atomic Systems, Kevin F. Gallacher¹, Martin Sinclair¹, Ross Millar¹, Oliver Sharp², Francesco Mirando², Gary Terment², Gordon Mills², Brendan Casey², Douglas J. Paul¹; ¹Univ. of Glasgow, UK; ²Kelvin Nanotechnology, UK. 780 nm wavelength distributed feedback lasers have been integrated onto a Si₃N₄ photonic platform on a Si substrate and coupled into waveguides for laser locking to either a ring resonator or rubidium vacuum cell.

17:30-18:30 OSA Senior Member Reception, OSA Member Lounge, Concourse Level

19:00-20:30 OSA Technical Group Poster Session, Grand Ballroom 220C

NOTES

Tuesday, 17:00-19:00

07:30–18:30 Registration, Concourse Level

08:00–10:00 JW1A • Joint Plenary Session, Grand Ballroom 220A

10:00–17:00 Exhibit Open (10:00–17:00), Coffee Break (10:00–11:30), Exhibit Halls 1-3

Coffee Break Sponsored by  COHERENT and  THORLABS

10:30–12:00 MIRTHE: New Commercial Trends in Mid-Infrared Sensing – From Nano-Photonics to Stand-Off Detection, Exhibit Hall Theater I

10:30–12:00 Beyond Awareness: What Actions Can Be Taken to Improve Diversity in STEM, Exhibit Hall Theater II

Exhibit Halls 1-3

11:30–13:00 JW2A • Poster Session I and Lunch

JW2A.1

Digital Holography for Local Heat Flux Measurement along the Surface of Heated Wire, Varun Kumar¹, Chandra Shakher¹; ¹Indian Inst. of Technology Delhi, India. In this paper, local heat flux $Q(y)$ and convective heat transfer coefficient (h_c) is measured along the surface of electrically heated wire using digital holographic interferometry (DHI). Experiments were performed on tungsten wire of different diameters.

JW2A.2

LMD-ICA Based Intrusion Even Positioning Algorithm for ϕ -OTDR Fiber Optic Perimeter Security System, Yuzhao Ma¹, Wantong Zhang¹, Xinglong Xiong¹; ¹Civil Aviation Univ. of China, China. In the paper we proposed a novel algorithm based on the LMD-ICA method, in order to improve the performance of the intrusion event positioning of the ϕ -OTDR fiber optic perimeter security system.

JW2A.3

Hybrid Square/Rhomb-Rectangular Semiconductor Lasers for Ethylene Detection, Zhengzheng Shen¹, Youzeng Hao¹, Fuli Wang¹, Ke Yang¹, Hongyan Yu¹, Jiaoqing Pan¹, YueDe Yang¹, Jin-Long Xiao¹, YongZhen Huang¹; ¹Inst. of Semiconductors, CAS, China. We present a tunable hybrid square/rhomb-rectangular AlGaInAs/InP semiconductor laser for ethylene detection. Single-mode lasing around 1.626 μm is achieved with a side mode suppression ratio above 30 dB and an output power over 1 mw.

JW2A.4

Testing of an Optomechanical Accelerometer with a High-Finesse On-Chip Microcavity, Feng Zhou¹; ¹NIST, USA. The motion of a microresonator integrated in a silicon hemisphere Fabry-Perot microcavity is used to transduce acceleration. We present the prototype assembly and performance tests of the optomechanical accelerometer.

JW2A.5

Development of Path-integrated Remote Chirped Laser Dispersion Spectrometer with Automatic Target Tracking, Michael G. Soskind¹, Yifeng Chen¹, Gerard Wysocki¹; ¹Princeton Univ., USA. The recent developments in instrumentation for mobile field deployment of a chirped laser dispersion spectroscopy is discussed, including optomechanical considerations, system signal fidelity, and real-time target tracking for chemical plume detection.

JW2A.6

Transparent diffraction gratings using silicon nanowire arrays embedded in flexible polymer, YeongJae Kim¹, Young Jin Yoo¹, Young Min Song¹; ¹Gwangju Inst. of Science and Technol., South Korea (the Republic of). Two dimensional diffraction gratings was demonstrated by using vertical silicon nanowire arrays in transparent and flexible polymer. The high order diffraction was observed by controlling their shapes of the silicon nanowire arrays.

JW2A.7

Experimental demonstration of Vehicle-borne Near Infrared Three-Dimensional Ghost Imaging LiDAR, Xiaodong Mei^{2,1}, Chenglong Wang^{2,1}, Long Pan^{2,1}, Pengwei Wang^{2,1}, Wenlin Gong², Shensheng Han²; ¹Univ. of Chinese Academy of Sciences, China; ²Key Lab for Quantum Optics and Center for Cold Atom Physics of CAS, Shanghai Inst. of Optics and Fine Machines, Chinese Academy of Sciences, China. We propose a Vehicle-borne near infrared 3D ghost imaging LiDAR. The experimental results demonstrate that the image of target at 120m range with 30mm resolution can be obtained when the vehicle's speed is 30km/h.

JW2A.8

Tunable Light Source with LDLS and AOTF, Xiaohua Ye¹, Alex Culter¹, Ron Collins¹, Debbie Gustafson¹, Hailing Zhu¹; ¹Energetiq Inc., USA. Performances of a tunable light source (TLS) using an acousto-optic tunable filter (AOTF) and a Laser-Driven Light Source (LDLSTM) are evaluated. Experimental results of in-band fluxes, FWHM bandwidths between 400nm and 800nm, are presented.

JW2A.9

Dual-parameter sensing based on Fano resonances by a nanobeam cavity side-coupled to a defect waveguide, Zheng Wang¹, Jian Zhou¹, Zhongyuan Fu¹, Fujun Sun¹, Chao Wang¹, Xuepei Li¹, Huiping Tian¹; ¹Beijing Univ of Posts & Telecom, China. We propose a dual-parameter sensor based on multiple Fano resonance modes. Both the sensor matrix and the detection error analysis are investigated. This compact sensor is promising in high-performance lab-on-chip and label-free detection system.

JW2A.10

Stokes polarimeter with polarization-dependent hologram, Hailong Zhou¹, Yanxian Wei¹, Yu Yu¹, Jianji Dong¹, Xinliang Zhang¹; ¹Wuhan National Lab for Optoelectronics, China. A Stokes polarimeter is demonstrated with polarization-dependent hologram. Owing to the low demand on the pattern of hologram, our work offer an easily manufactured scheme to measure the polarization of the light.

JW2A.11

Advanced Spectrometer with Two Spectral Channels Sharing the Same BSI-CMOS Detector, Liang-Yao Chen¹, Kai-Yan Zang¹, Yuan Yao¹, Er-Tao Hu¹, An-Qing Jiang², Yu-Xiang Zheng¹, Song-You Wang¹, Hai-Bin Zhao¹, Yu-Mei Yang¹, Osamu Yoshie², Young-Pak Lee³, David Lynch⁴; ¹Fudan Univ., China; ²Waseda Univ., Japan; ³Hanyang Univ., South Korea (the Republic of); ⁴Iowa State Univ., USA. By consisting of 8 sub-gratings to image two sets of 4-folded spectra on the focal plane of a BSI-CMOS detector, a two-channel spectrometer with a resolution of better than 0.1 nm/pixel in the 200- 950-nm spectral range is studied with the result measured for the Hg-Ar lamp.

JW2A.12

SI-traceable Calibration of Suitcase SOLARIS for CLARREO Pathfinder Mission, Yigit Aytac¹, Kurtis Thome², Brian Wenny¹, Timony M. Shuman³, Julia Barsi¹, Brendan McAndrew⁴, Barbara J. Zukowski⁵, Amit Angal¹, Joel McCorkel⁶; ¹Science Systems and Applications, Inc., USA; ²Biospheric Sciences, NASA Goddard Space Flight Center, USA; ³Fibertek, USA; ⁴NASA Goddard Space Flight Center, USA; ⁵Ball Aerospace, USA. NASA's high accuracy calibration system GLAMR is utilized for testing a portable, visible and near-IR version of an imaging spectrometer that is part of the CLARREO Pathfinder mission to help demonstrate that 0.3% absolute uncertainty in reflectance retrieval is achievable.

JW2A.13

Superluminal Laser Gravitational Wave Detector, Minchuan Zhou¹, Zifan Zhou¹, Selim M. Shahriar¹; ¹Northwestern Univ., USA. We propose a gravitational wave detector that uses two superluminal lasers. Compared to the Advanced LIGO detector, the range for detecting binary neutron star inspirals is enhanced by a factor of 19 using this scheme

JW2A.14

Detection of Rare-Earth Elements Enhanced by Bio-Metal-Organic Frameworks (MOFs) Using UV LED, Hui Lan², Scott Crawford¹, Zach Splain¹, Thomas Boyer¹, Paul Ohodnicki³, Ran Zou¹, Mohan Wang¹, Kevin P. Chen¹; ¹University of Pittsburgh, USA; ²Dept. of Electrical and Computer Engineering, Univ. of Pittsburgh, USA; ³U.S. Dept. of Energy, USA. Spectral characteristics of BioMOF-sensitized trace rare-earth elements dissolved in water are studied at room temperature by laser-induced fluorescence method using a 280-nm LED. This paper presents a low-cost detection scheme toward extraction of rare-earth materials in liquid phase.

JW2A.15

White-Light Photothermal Mirror Spectrophotometer, Aristides Marcano Olaizola¹, May Hlaing¹; ¹Delaware State Univ., USA. We describe an arc-lamp based pump-probe photothermal mirror spectrophotometer to measure the spectrum of the thermal quantum yield of the surface of solid samples. We discuss advantages of the method to characterize solid nontransparent materials.

JW2A.16

Microscale-patterned colored passive radiative cooler, Gil Ju Lee¹, Se-Yeon Heo¹, Young Min Song¹; ¹Gwangju Inst of Science & Technology, South Korea (the Republic of). Thermal management in colored objects has been intensively attractive for a long time. The proposed scheme is based on micro-patterned metal-insulator-metal with thermal emission polymer, which can reduce the temperature of colored objects.

JW2A.17

Double Al nanoparticle array for enhanced absorption in thin film GaAs solar cells, Gurjit Singh¹, S.S. Verma¹; ¹Physics, Sant Longowal Inst. of Engineering and Technology, Longowal, India. The effect of single and double Al nanoparticle array on absorption of thin film GaAs solar cells is investigated by FDTD method. Plasmonic action of double array yields a maximum absorption enhancement factor of 1.74.

JW2A.18

Multispecies Laser Diagnostic System for Vehicle Tailpipe Emission Measurements, Luigi Biondo¹, Oliver Diemel¹, Vadim Doberstein¹, Henrik Gerken¹, Lars Illmann¹, Michael Jonek¹, Marvin Schmidt¹, Tim Steinhaus¹, Steven Wagner¹; ¹Technische Universität Darmstadt, Germany. A multispecies *in situ* TDLAS-system for simultaneous detection of NO, CO, CO₂, H₂O and NH₃ was applied at an engine test rig for exhaust gas measurements and results were compared to commercially available reference systems.

JW2A.19

High Efficiency InP Pillar Array Heterojunction Solar Cells, Lin Gan¹, Seyed Ebrahim Hashemi Amir², Dong-Ying Li², Alan H. Chin³, Yue-Yang Yu², Cun-Zheng Ning^{1,2}; ¹Tsinghua Univ., China; ²Arizona State Univ., USA; ³Light Energy Corporation, USA. Nanopillars can enhance solar cell performance, but the increased surface recombination often cancels performance gains. We demonstrate suppression of surface recombination through passivation of InP-pillar heterojunction solar cells, achieving a very high efficiency of 18.31%.

JW2A.20

Off-Resonant Broadband Photoacoustic Spectroscopy for Online Monitoring of Biogas Concentration with a Wide Dynamic Range, Ramya Selvaraj¹, Nilesh J. Vasa¹, Shiva N. S M¹; ¹Indian Inst. of Technology, Madras, India. Online measurement of CO₂, CH₄ and H₂O in a biogas plant using a Supercontinuum laser based off-resonant broadband photoacoustic spectroscopy is realized. The system exhibits a wide dynamic range from ppbv - 100% concentration.

JW2A.21

Near-infrared broadband cavity-enhanced sensor system for methane detection using a wavelet-denoising assisted Fourier-transform spectrometer, Kaiyuan Zheng¹, Chuan-Tao Zheng¹, Zidi Liu¹, Qixin He¹, Qiaoling Du¹, Yu Zhang¹, Yiding Wang¹, Frank Tittel²; ¹Jilin Univ., China; ²Rice Univ., USA. We demonstrated a broadband cavity-enhanced sensor in the near-infrared range in combination with a wavelet-denoising assisted Fourier-transform spectrometer for high-resolution methane detection. A minimum detectable absorption coefficient of $4.6 \times 10^{-7} \text{ cm}^{-1}$ was achieved.

JW2A.22

Multi-harmonic detection of methane using 3.2 μm mid-IR DFB laser for environmental sensing applications, Caio Azevedo¹, Luil Menberu¹, Devonte Dowdard¹, May Hlaing¹, Mohammad A. Khan¹; ¹Delaware State Univ., USA. We show advantages of higher harmonic 2f and 4f-wavelength modulation spectroscopic detection for improving sensitivity in methane detection. A spectral-line analysis in the wing region is used to achieve 1-sec. precision of 0.3% or 5 ppbv.

JW2A.23

Highly sensitive and robust refractive index sensing using a microfluidic chip with microfiber probe, Fang Fang¹, Junjie Wang¹, Yanpeng Li¹, Yuezhen Sun¹, Liuyang Yang¹, Jie Hu¹, Zhijun Yan¹, Qizhen Sun¹; ¹Huazhong Univ of Science and Technology, China. A microfluidic chip with multimode microfiber probe for refractive index sensing is proposed and experimentally demonstrated. A high RI sensitivity of $\sim 2169.64 \text{ nm/RIU}$ with a good linearity ranging from 1.335 to 1.341 is achieved.

JW2A.24

Role of Mixed-dimensional Excitons in the Phase Dynamics of Semiconductor Optical Lasers and Amplifiers, Bastian Herzog¹, Mirco Kolarczik¹, Sophia Helmrich¹, Kathy Lüdge¹, Ulrike K. Woggon¹, Nina Owschmikow¹; ¹Technische Universität Berlin, Germany. We characterize the dynamic amplitude and phase response of InAs(Sb)/GaAs submonolayer quantum dots as active medium in opto-electronic devices. Mixed-dimensional excitons cause broadband emission and a large alpha parameter, promising for, e.g., chaotic lasing.

JW2A.25

Charge Carrier Dynamics in Conjugated Polymer – MoS₂ Organic-2D Heterojunctions, Christopher Petoukhoff¹, Sofia Kosar¹, Ibrahim Bozkurt², Manish Chhowalla², Keshav M. Dani¹; ¹Okinawa Inst. of Science and Technol., Japan; ²Materials Science and Engineering, Rutgers Univ., USA. We investigate the charge transfer efficiency between 3 different conjugated polymer-MoS₂ heterojunctions using femtosecond transient absorption spectroscopy.

JW2A.26

Carrier Dynamics and Ultrafast Zero-bias Photocurrents in SnS₂ Single Crystals, Erin M. Morissette¹, Kateryna Kushnir¹, Curtis W. Doiron², Ronald L. Grimm², Lyubov V. Titova¹; ¹Physics, Worcester Polytechnic Inst., USA; ²Chemistry and Biochemistry, Worcester Polytechnic Inst., USA. The carrier dynamics of SnS₂ single crystals are investigated via terahertz spectroscopy for photovoltaic applications. Above-bandgap excitation generates long-lived free carriers with high mobility, and three-fold-symmetric THz generation suggests an ultrafast surface shift current.

JW2A.27

Coherent Oscillations in the Vibrational Modes of 1-Aminoanthraquinone and Solvent DMSO Manifest the Ultrafast Intramolecular Charge Transfer, Kooknam Jeon¹, Sebok Lee¹, Myungsam Jen¹, Yoonsoo Pang¹; ¹Gwangju Inst of Science & Technology, South Korea (the Republic of). Ultrafast charge transfer of 1-aminoanthraquinone with the twist of NH₂ group in the excited state is clearly monitored by the coherent oscillations of the coupled vibrational modes of the solute and the surrounding solvent molecules.

JW2A.28

Probing ultrafast, shock-induced chemistry using extremely broadband, ultrashort mid-infrared pulses, Pamela R. Bowlan¹, Michael Powell¹, Romain Perriot¹, Enrique Martinez¹, Edward Kober¹, Marc Cawkwell¹, Shawn McGrane¹; ¹Los Alamos National Lab, USA. Using extremely broad-band mid-infrared pulses (3–14 μm), and a single shot spectrometer, we probe ultrafast chemistry at high pressures (~20 GPa) through changes in the vibrational spectrum. Here we present results on shocked benzene and nitromethane.

JW2A.29

Exciton Diffusion in a Monolayer MoS₂-WS₂ Lateral Heterostructure, Jiahui Huang¹, Monica Lorenzon², Jin Ho Kang¹, Peng Chen³, Xiangfeng Duan³, Ed Barnard², Chee Wei Wong¹, Alexander Weber-Bargioni²; ¹Mesoscopic Optics and Quantum Electronics Lab, Univ. of California, Los Angeles, USA; ²Molecular Foundry, Lawrence Berkeley National Lab, USA; ³Dept. of Chemistry, Univ. of California, Los Angeles, USA. In this paper, we observed preliminary exciton diffusion signature in a WS₂-MoS₂ lateral heterostructure at room temperature. Within center MoS₂, the diffusion appears to be 300 nm, along the WS₂-MoS₂ edge the diffusion appears to be more than 2 μm.

JW2A.30

Population relaxation and coherence times of ¹⁶⁷Er³⁺ diluted to 10 ppm in Y₂SiO₅ at zero magnetic field, Masaya Hirashi^{1,2}, Mark IJspeert¹, Takehiko Tawara^{1,2}, Hiroo Omi¹, Hideki Gotoh¹; ¹NTT Basic Research Labs, Japan; ²Tokyo Univ. of Science, Japan. We investigate population relaxation and optical coherence times in isotopically purified ¹⁶⁷Er³⁺ diluted to 10 ppm in Y₂SiO₅ at zero magnetic-field. It reveals long relaxation time of 130 ms and coherence time of 12 μs.

JW2A.31

Revealing Exciton Dissociation and Inhomogeneity in Metal Halide Perovskite Thin Films, Geoffrey M. Diederich¹, Mark Siemens¹; ¹Univ. of Denver, USA. We present multidimensional spectra of excitons in formamidinium-methylammonium lead triiodide perovskite films at low temperature. The spectra show inhomogeneous broadening and two distinct states, which we assign to free and defect-bound excitonic states.

JW2A.32

Ultrafast Photoluminescence without Phonon Scattering Due to Nonlocal Light-Matter Interaction, Masayoshi Ichimiya^{1,3}, Takuya Matsuda², Hajime Ishihara^{1,2}, Masaaki Ashida¹; ¹Osaka Univ., Japan; ²Osaka Prefecture Univ., Japan; ³The Univ. of Shiga Prefecture, Japan. Ultrafast radiative recombination of confined excitons in a semiconductor mesoscopic thin film has been investigated by temperature dependence of photoluminescence spectra. Sub-100 fs radiative decay competes with phonon scattering even at room temperature.

JW2A.33

Electrical Manipulation of the Valley Polarization and Valley Coherence in a van der Waals Heterostructure, Arunabh S. Mukherjee², Chitrleema Chakraborty^{1,3}, Liangyu Qui², Anthony Vamvakas²; ¹Electrical Engineering and Computer Science, MIT, USA; ²The Inst. of Optics, Univ. of Rochester, USA; ³Material Science, Univ. of Rochester, USA. Valley contrasting polarization selection rules present unique opportunities for optical control in valleytronic devices. In this work, we demonstrate the electric-field control of both valley polarization and valley coherence of excitons in a monolayer semiconductor.

JW2A.34

High-mobility indirect excitons in a wide single quantum well heterostructure, Chelsey Dorow¹, Darius J. Choksy¹, Matt Hasling¹, Jason Leonard¹, Michael Fogler¹, Leonid Butov¹, Kenneth West², Loren Pfeiffer²; ¹Univ. of California San Diego, USA; ²Princeton Univ., USA. We present wide single quantum well (WSQW) heterostructures and the achievement of record-high mobility of indirect excitons (IXs). WSQW heterostructures provide low-disorder platform both for exploring basic IX properties and for developing high-mobility excitonic devices.

JW2A.35

Thermally-induced nonlinear spatial shaping of femtosecond pulses in nematic liquid crystals, Vittorio Maria Di Pietro^{1,2}, Aurelie Jullien², Umberto Bortolozzo², Nicolas Forget¹, Stefania Residori²; ¹Fastlite, France; ²INPHYNI, France. Optically-induced thermal nonlinear effects in a thin nematic liquid-crystal result from light absorption by the ITO coating of an infrared femtosecond laser. Subsequent spatial shaping characterises the thermal gradient, up to the isotropic phase transition

JW2A.36

Orthogonal Four Wave Mixing in AlGaAs Nanowire Waveguides, Kyle A. Johnson¹, J. Stewart Aitchison¹; ¹Univ. of Toronto, Canada. We propose a design and show simulation results for an AlGaAs waveguide device for performing four wave mixing where the pump mode has an orthogonal polarization to the signal and idler modes.

JW2A.37

Four-wave mixing microscopy of resonant silicon-on-insulator two-dimensional zero contrast gratings, Rabintra Biswas¹, Jayanta Deka¹, Keshav K. Jha¹, Vishnu Praveen¹, Lal Krishna A.S¹, Varun Raghunathan¹; ¹Indian Inst. of Science, India. Four-wave mixing microscopy of resonant, silicon-on-insulator, two-dimensional zero-contrast grating is reported for large incident input wavelength separation of $\sim 540 \text{ nm}$. Four-wave mixing signal on-grating is enhanced by 352x when compared to off-grating at resonance.

JW2A.38

Polarization attractors generated from graphene polymer composite mode-locked erbium doped fiber laser, Chang Zhao¹, Qianqian Huang¹, Mohammed AlAraimi³, Zinan Huang¹, Chengbo Mou¹, Aleksey Rozhin², Sergey Sergeev²; ¹Shanghai Univ., China; ²Aston Inst. of Photonic Technologies, Aston Univ., UK; ³Higher College of Technology, Oman. We have experimentally investigated the polarization dynamics of an all-fiber passively mode-locked laser based on graphene using polarimeter for the first time. By carefully adjusting polarization controllers, two types of polarization attractors are obtained.

JW2A.39

Modulation Instability of Discrete Angular Momentum in Fiber Rings, Calum Maitland^{1,2}, Fabio Biancalana¹, Daniele Faccio²; ¹Heriot-Watt Univ., UK; ²School of Physics and Astronomy, Univ. of Glasgow, UK. We present an analysis of modulation instability in a ring of coupled optical fibers. Plane waves are shown to be unstable to perturbations carrying discrete angular momenta, both for normal and anomalous group velocity dispersion.

JW2A.40

High-energy 9 μm LiGaS₂-based Optical Parametric Chirped-Pulse Amplifier, Shizhen Qu¹, Houkun Liang², Xiao Zou¹, Kun Liu¹, Wenkai Li¹, Qijie Wang¹, Ying Zhang²; ¹Nanyang Technological Univ., Singapore; ²Singapore Inst. of Manufacturing Technology, Singapore. We report the first LiGaS₂-based mid-IR OPCPA, pumped by the 1- μm Yb:YAG laser at 10KHz. The idler pulse is centered at 9 μm , covering 7.5-10.2 μm wavelength range, with 13.8 μJ pulse energy.

JW2A.41

Paraxial Accelerating Beams along a Sharply Curved Path, Zekun Pi¹, Yi Hu¹, Zhigang Chen¹, Jingjun Xu¹; ¹Nankai Univ., China. Sharply accelerating beams are commonly believed to exist only under non-paraxial conditions. Here we demonstrate that paraxial accelerating beams can be designed to travel along a steep parabolic path that conventional Airy beams cannot follow.

JW2A.42

Pseudo-Magnetic Monopole and Antimonopole in PT-Symmetric Coupled Waveguides, Rosie S. Hayward¹, Fabio Biancalana¹; ¹Heriot-Watt Univ., UK. PT-symmetric coupled waveguides, for which the Berry curvature corresponds to a hyperbolic pseudo-magnetic monopole or antimonopole, are shown to have a purely imaginary Berry connection, which can induce gain and loss when it is non-periodic.

JW2A.43

Raman Induced Visible Stable Platons and Breather Platons in Microresonator, Shunyu Yao¹, Chengying Bao², Changxi Yang¹; ¹Tsinghua Univ., China; ²California Inst. of Technology, USA. We numerically demonstrate that stable platons and coherent visible Kerr combs can be generated via Raman assisted four wave mixing in a AlN microresonator. Raman induced breather platon dynamics is also observed in our simulations.

JW2A.44

Mid-infrared, Idler-resonant, Picosecond OP-GaAs OPO with Wide Tunability and Good Beam Quality, Qiang Fu¹, Lin Xu¹, Sijing Liang¹, Peter Shardlow¹, David Shepherd¹, Shaif-Ul Alam¹, David Richardson¹; ¹Optoelectronics Research Centre, UK. We report an idler-resonant, watt-level, picosecond OP-GaAs OPO with a tuning range of 4394-6102 nm (idler) and 2997-3661 nm (signal), and diffraction-limited idler beam.

JW2A.45

Guiding and Routing of a Light Pulse via an Airy-like Accelerating Potential, Zhili Li¹, Ping Zhang¹, Xue Mu¹, Yi Hu¹, Zhigang Chen¹, Jingjun Xu¹; ¹Nankai Univ., China. We demonstrate experimentally guiding pulse by pulse in an accelerating potential. Weak signals featured with single/double peaks can be guided to co-accelerate with a self-accelerating Airy pulse in an optical fiber.

JW2A.46

Bright Conical Diffraction at the Exceptional Point of PT and Anti-PT-Symmetric Photonic Lattices, Mojgan Dehghani¹, Hamidreza Ramezani¹; ¹Univ. of Texas Rio Grande Valley, USA. We show that bright conical diffraction occurs at the exceptional points of 1D PT and anti-PT-symmetric photonic lattices.

JW2A.47

Characterization of Kerr Solitons in Microresonators with Parameter Optimization and Nonlinear Fourier Spectrum, Aiguo Sheng¹, Yilong Zhao¹, Guangqiang He¹; ¹Shanghai Jiao Tong Univ., China. We investigate the influence of pump power and the number of driving modes on the soliton step and use nonlinear Fourier transform to characterize the Kerr soliton in the microresonator driven by pulses.

JW2A.48

Nucleation of Optical Vortices in the Wake of a Blockage in Free-Space Propagating Light, William G. Holtzmann², Samuel Alperin^{2,1}, Mark Siemens²; ¹Dept. of Applied Mathematics and Theoretical Physics, Univ. of Cambridge, UK; ²Dept. of Physics & Astronomy, Univ. of Denver, USA. We report experiments observing optical vortex nucleation in light flowing past a blockage in free space. This nucleation in a fully linear system is analogous to fluid flow around different blockages.

JW2A.49

Phase Synchronization of Coupled Optical Oscillator, Mohammad-Ali Miri¹, Jijie Ding¹; ¹Queens College of CUNY, USA. The problem of creating phase synchronization between coupled optical oscillators of different individual frequencies is theoretically investigated. The synchronization coupling threshold is obtained for a dimmer as well as an array of coupled oscillators.

JW2A.50

Measurements of Resonant Kerr Self-focusing and Self-defocusing of Tunable, 4.3 μm Radiation in CO₂ Gas, Jeremy Pigeon², Dana Tovey¹, Sergei Tochitsky¹, Gerhardus Louwrens¹, Ilan Ben-Zvi², Chan Joshi¹, Dmitry Martyshkin³, Vladimir Fedorov³, Krishna Karki³, Sergey Mirov³; ¹Univ of California - Los Angeles, USA; ²Physics and Astronomy, Stony Brook Univ., USA; ³Physics, Univ. of Alabama at Birmingham, USA. We report detailed measurements of resonant self-focusing and self-defocusing of a continuously tunable Fe:ZnSe laser operating within the 4P-branch of the CO₂ molecule. We determine the dispersion of this resonant nonlinearity near a rovibrational transition.

JW2A.51

Enhancement of Third Harmonic Generation in Organically Functionalized Microsphere Cavity, Jinhui Chen¹, Xiaoqin Shen², Qihuang Gong¹, Yun-Feng Xiao¹; ¹Peking Univ., China; ²ShanghaiTech Univ., China. We demonstrate efficient third harmonic generation (THG) in a high quality factor silica microsphere cavity, which is deposited with a layer of high optical nonlinearity molecules. The observed THG conversion efficiency is $\sim 185\%/W^2$.

JW2A.52

Effect of linewidth dispersion in degenerate four wave mixing and Kerr-comb generation, Ali Eshaghian Dorche¹, Ali Eftekhar¹, Ali Adibi¹; ¹Georgia Inst. of Technology, USA. We report the numerical study of linewidth dispersion effect on the degenerate four-wave mixing and the corresponding Kerr comb generation; for asymmetric linewidth difference around pumping wavelength, there is a threshold above which we see non-homogenous response corresponding to Turing roles.

JW2A.53

Sensitivity of Parameter Estimation Near the Exceptional Point of a Non-Hermitian System, Chong Chen¹, Liang Jin², Ren-Bao Liu¹; ¹Dept. of Physics, The Chinese Univ. of Hong Kong, Hong Kong; ²Dept. of Physics, Nankai Univ., China. The eigenvalue susceptibility divergence at the exceptional point (EP) stimulates the idea of high sensitivity metrology. Parameter estimation around the EPs is theoretically studied. We find that the EP bears no enhancement of the sensitivity.

JW2A.54

Large Purcell enhancement with nonreciprocal photon collection in a gap plasmon system, Fan Zhang¹, Lingxiao Shan¹, Xinjie Fang¹, Xueke Duan¹, Qihuang Gong¹, Ying Gu¹; ¹Peking Univ., China. We achieve chiral light-emitter coupling with guided part Purcell enhancement of 1000% γ_{gap} and the directionality of 85% in a designed hybrid gap plasmon system, which provides an efficient way for nonreciprocal quantum photon sources.

JW2A.55

Laser Color Printing on Semicontinuous Silver Films, Sarah N. Chowdhury¹, Piotr Nyga^{1,2}, Zhaxylyk Kudyshev¹, Alexander Kildishev¹, Vladimir M. Shalaev¹, Alexandra Boltasseva¹; ¹Purdue Univ., USA; ²Inst. of Optoelectronics, Military Univ. of Technology, Poland. We demonstrate printing of colors from blue through green, yellow, orange to red using laser photomodification of semicontinuous silver films on mirror with dielectric spacer. The colors are controlled by laser fluence and exposure time.

JW2A.56

Tunable Localized Cosine-Gauss Beam generation through polarization control, Xuesi Zhao¹, Peng Zhao¹, Xue Feng¹, Yidong Huang¹; ¹Tsinghua University, China. A nano-structure on metallic film is designed and fabricated to generate Localized Cosine-Gauss Beam while the propagating direction of generated surface plasmon polariton wave by modulating the polarization of illuminating lightbeam.

JW2A.57

Ultra-compact Polarization Emitter using a Silicon Nanoantenna, Zhongjin Lin¹, Wei Shi¹; ¹Université Laval, Canada. We demonstrate an ultra-compact ($3\lambda \times 3\lambda \times \lambda$) silicon photonic nanoantenna that can generate an arbitrary polarization state through breaking the geometric symmetry. The emitted polarization state shows a weak wavelength dependence over the C-band.

JW2A.58

Using Dynamic Plasmonic Colors for Optical Cryptography, Maowen Song², Di Wang¹, Zhaxylyk Kudyshev¹, Alexandra Boltasseva¹, Honglin Yu², Vladimir M. Shalaev¹, Alexander Kildishev¹; ¹Purdue Univ., USA; ²Chongqing Univ., China. We experimentally demonstrate an all-aluminum metasurface that generates tunable plasmonic colors depending on the polarization states of the incident and reflected light. The metasurface produces high-resolution images and can be used to encrypt arbitrary information.

JW2A.59

Plasmonic System with In-Plane Magnetic Anisotropy for Plasmon Based Magnetic Switching, Mohammad Shahabuddin¹, Natalia Noginova¹; ¹Norfolk State Univ., USA. Profile-modulated permalloy films are promising for magneto-optical applications. We show that such systems demonstrate plasmonic properties and have uniaxial in-plane anisotropy, which may allow sharp magnetization switching using SAM of light.

JW2A.60

Array of Symmetric Nanohole Dimers for STT-RAM Ultrathin Layer Sensing, Parinaz Sadri Moshkenani¹; ¹Univ. of California Irvine, USA. Dimer nanohole array is designed to detect radiation effects in STT-RAM multilayer thin films, showing Fano resonance highly sensitive to dielectric layer changes. Normalized figure of merit is 13.5 times larger than single nanohole array.

JW2A.61

Microcavity-Powered Local Field Enhancement at Plasmonic Nanoantennas, Jui-Nung Liu^{1,2}, Qinglan Huang^{1,2}, Keng-Ku Liu³, Srikanth Singamaneni³, Brian T. Cunningham^{1,2}; ¹Dept. of Electrical and Computer Engineering, Univ. of Illinois at Urbana-Champaign, USA; ²Micro and Nanotechnology Lab, Univ. of Illinois at Urbana-Champaign, USA; ³Dept. of Mechanical Engineering and Materials Science, Washington Univ. in St. Louis, USA. We demonstrate cooperative plasmonic-photonic hybridization with an integration of gold nanorods (as nanoantennas) and an on-resonance dielectric photonic crystal slab (as a microcavity). The cavity-enhanced impedance-matched light-matter interface offers great local field amplifications.

JW2A.62

A Novel Platform for the Detection and Analysis of Plasmonic Nanostructures Based on Nanomechanical Resonator, Miao-Hsuan Chien¹, Mostafa Shawrav¹, Heinz Wanzenboeck², Silvan Schmid¹; ¹Inst. of sensor and actuator system, TU Wien, Austria; ²Inst. of solid state electronics, TU Wien, Austria. A novel platform for the detection of plasmonic resonance is demonstrated with silicon nitride nanomechanical resonator. Absorption cross section could be obtained directly from the detuning of mechanical frequency. This technique provides an alternative for the optimization of plasmonic designs.

JW2A.63

Strontium Niobate for Near Infrared Plasmonics, Aavek Dutta¹, Dongyang Wan², Bixing Yan², Vladimir M. Shalaev¹, Thirumalai Venkatesan², Alexandra Boltasseva¹; ¹Purdue Univ., USA; ²National Univ. of Singapore, Singapore. We study Strontium Niobate (SNO) as an alternate material for plasmonics in the near infrared wavelength range. We demonstrate, experimentally and through numerical simulations, hybrid plasmonic-photonic resonances in a SiO₂-Si nanodisk stack on SNO near technologically important telecom window.

JW2A.64

Near-Ultraviolet Dielectric Metasurfaces for Surface-Enhanced Circular Dichroism Spectroscopy and Handedness-Preserved Reflection, Kan Yao¹, Yuebing Zheng¹; ¹The Univ. of Texas at Austin, USA. We report a design of achiral dielectric metasurfaces that can enhance the circular dichroism of chiral molecules for over 50 times and preserve the spin states of light upon reflection in the near-ultraviolet region.

JW2A.65

A control of localized surface phonon polariton resonance using metal/dielectric multilayer boundary, Satyanarayana R. Kachiraju¹; ¹UTRGV, USA. We fabricated subwavelength grating of a metal/dielectric multilayer on silicon carbide. We experimentally demonstrated a control of localized surface phonon polariton resonance showing near perfect infrared absorption at the optical phonon band of silicon carbide.

JW2A.66

A Comparison of Metal Adhesion Layers for Au Films in Thermo-Plasmonic Applications, William Abbott^{1,2}, Christopher P. Murray^{1,2}, Sorcha NiLochlainn^{1,2}, Frank Bello^{1,2}, Chuan Zhong^{1,2}, Christopher Smith^{1,2}, Amanda Petford-Long³, John Donegan^{1,2}, McCloskey David^{1,2}; ¹School of Physics, Ireland; ²Trinity College, Ireland; ³Material Science Division, Argonne National Lab, USA. The dewetting resistance of Au 50 nm films fabricated atop Ti/Ta/W/Cr/Al adhesion layers (0.5–5 nm) was investigated. Results show sub-nanometer Ta has superior stability under thermal stress, while W & Ti show best plasmonic response.

JW2A.67

Generation of 104 nJ, 100 kHz Pulses directly from all-Normal Dispersion all-PM Yb-fiber Laser with a Nonlinear Amplifying Loop Mirror, Yuhang Shi¹, Zhaochen Cheng¹, Chang Hong¹, ZhiGang Peng¹, Pu Wang¹; ¹Beijing Univ. of Technology, China. We demonstrate a mode-locked all-PM Yb-doped fiber laser using nonlinear amplifying loop mirror, delivering 300 ps pulses with energy of 104 nJ at repetition rate of 100 kHz, which can be compressed to 1.053 ps.

JW2A.68

Generation and Frequency-conversion of Optical Vortex Arrays with Controlled Intensity Distribution, SS Harshith Bachimanchi¹, Goutam Samanta²; ¹IISER Pune, India; ²Atomic, Molecular and Optical Physics, Physical Research Lab(PRL), India. We report on the generation of high power ultrafast optical vortex arrays of controlled intensity distribution. Using microlens array we have generated vortex arrays at 1064 nm and frequency-doubled into vortex arrays at new wavelength.

JW2A.69

Grating-Based Mid-Infrared Long-Pass Filter for High-Power Applications, Wolfgang Schweinberger^{2,3}, Daniel Gerz^{1,2}, Thomas P. Butler¹, Thomas Siefke^{4,6}, Martin Heusinger⁴, Tatiana Amotchkina², Vladimir Pervak², Uwe Zeitner^{4,5}, Joachim Pupeza^{1,2}; ¹Max Planck Institute of Quantum Optics, Germany; ²Dept. of Physics, Ludwig Maximilian Univ. Munich, Germany; ³Dept. of Physics and Astronomy, King Saud Univ., Saudi Arabia; ⁴Inst. of Applied Physics, Abbe Center of Photonics, Friedrich Schiller Univ. Jena, Germany; ⁵Fraunhofer Inst. for Applied Optics and Precision Engineering, Germany; ⁶Physikalisch-Technische Bundesanstalt, Germany. We present a gold-coated silicon grating which provides efficient spatial separation of a broadband mid-infrared (MIR) beam from a collinear, 30W beam of broadband near-infrared (NIR) pulses in a power-scalable and chromatic dispersion-free manner.

JW2A.70

Withdrawn

JW2A.71

Single-shot Subnoise Signal Recovery by Coherent Spectral Energy Redistribution, Benjamin G. Crockett¹, Luis Romero Cortes¹, Saikrishna Reddy K¹, Jose Azana¹; ¹INRS, Canada. We demonstrate single-shot recovery of subnoise signals, completely buried under random in-band noise, through combinations of phase manipulations derived from Talbot effect theory, allowing for reconstruction of signals with a time-bandwidth-product of up to 24.

JW2A.72

Demonstration of Space-Time Wave Packets That Travel in Optical Materials at the Speed of Light in Vacuum, Basanta Bhaduri¹, Murat Yessenov¹, Ayman F. Abouraddy¹; ¹Univ. of Central Florida, CREOL, USA. We synthesize optical wave packets that travel in transparent non-dispersive materials (liquids, glasses, and sapphire) at the speed of light in vacuum, independently of the refractive index, by introducing carefully designed spatio-temporal field spectral correlations.

JW2A.73

High-efficiency nonlinear compression using a gas-filled multipass cell, Florent Guichard¹, Loïc Lavenù¹, Michele Natile¹, Xavier Delen², Yoann Zaouter¹, Marc Hanna², Eric Mottay¹, Patrick Georges²; ¹Amplitude Laser Group, France; ²Laboratoire Charles Fabry, France. We demonstrate nonlinear temporal compression of a Yb-doped fiber amplifier in a multipass-cell filled with argon. The 160μJ 275fs pulses are compressed down to 135μJ and 33fs, corresponding to a transmission of 85%.

JW2A.74

Phase noise performance of filtered optical frequency comb, Lawrence Trask¹, Ricardo Bustos-Ramirez¹, Michael Plascak¹, Peter Delyfett¹; ¹Univ. of Central Florida, USA. We determined the key parameters in low phase noise performance in filtered optical frequency combs. Laser frequency fluctuation and filter passband width as well as spectral phase play a role in obtaining low timing jitter.

JW2A.75

Generation of ultra-stable 50-fs pulses directly from an Er-doped fiber oscillator, Jiaqi Zhou¹, Weiwei Pan¹, Yan Feng¹; ¹Shanghai Inst. of Optics & Fine Mech., China. We report on an Er-doped fiber laser which can generate few-cycle pulses with excellent long-term stability. The all-polarization-maintaining fiber oscillator can produce 50-fs pulses with 13.6-mW average output power at 85.3-MHz repetition rate.

JW2A.76

100% Reliable Frequency-Resolved Optical Gating Pulse-Retrieval Algorithmic Approach, Rana Jafari¹, Travis N. Jones¹, Rick Trebino¹; ¹Georgia Inst. of Technology, USA. We introduce a FROG algorithmic approach that always converges and is faster. It involves retrieving the correct spectrum directly from the trace and implementing a multi-grid scheme with multiple initial guesses.

JW2A.77

Optofluidic SERS Sensing from Photonic Crystal-Plasmonic Mesocapsules, Kundan Sivashanmugan¹, Kenneth Squire¹, Yong Zhao^{1,2}, Ailing Tan², Joseph Kraai¹, Gregory Rorrer¹, Alan X. Wang¹; ¹Oregon State Univ., USA; ²Yanshan Univ., China. We synthesized hybrid photonic crystal-plasmonic mesocapsules using diatom biosilica with in-situ growth silver nanoparticles. The mesocapsules achieved near single-molecule sensitivity for optofluidic SERS sensing with five orders of magnitude higher than colloidal nanoparticles.

JW2A.78

Ring Resonator Based Ultrasound Detection in a Zero-Change Advanced CMOS-SOI Process, Panagiotis Zarkos¹, Olivia Hsu¹, Vladimir Stojanovic¹; ¹UC Berkeley, USA. Optical ultrasound detection using microring resonators (MRRs) in a zero-change 45nm CMOS-SOI electronic-photonic platform with high intrinsic sensitivity of 39.6 fm/kPa and frequency response of 6MHz is reported.

JW2A.79

Ultra-high-speed spatial projection using a nonlinear optical time lens for fast single-pixel imaging, Jasper R. Stroud¹, Mark Foster¹; ¹Johns Hopkins Univ., USA. We present a method for projecting programmable spatial patterns at a rate of 289 Gpixels/s using a nonlinear optical time lens. Using this projector, we demonstrate high-speed single-pixel imaging using compressed sensing.

JW2A.80

Calibration-Free Time-Stretch Optical Coherence Tomography Based on Higher-Order Dispersion Compensation, Lei Zhang¹, Liao Chen¹, Zihui Lei¹, Yuhua Duan¹, Chi Zhang¹, Xinliang Zhang¹; ¹Wuhan National Lab for Optoelectronics, Huazhong Univ. of Science and Technology, China. We demonstrate a calibration-free time-stretch optical coherence tomography, which substitutes the calibration by dispersion compensation. It minimizes the data processing time by 20 times, which is essential for A-scan rate as high as 20 MHz.

JW2A.81

Electronic-Photonic Platform for Label-Free Biophotonic Sensing in Advanced Zero-Change CMOS-SOI Process, Christos G. Adamopoulos¹, Asmaysinh Gharia², Ali Niknejad¹, Mekhail Anwar², Vladimir Stojanovic¹; ¹Dept. of Electrical Engineering and Computer Science, Univ. of California, Berkeley, USA; ²Dept. of Radiation Oncology, Univ. of California, San Francisco, USA. We propose a monolithically integrated platform in a CMOS 45RFSOI process for biophotonic sensing. This platform opens the pathway to the first Lab-on-Chip system with nanophotonic sensing and advanced electronics on a single die.

JW2A.82

Microfluidic Mid-Infrared Spectroscopy via Microresonator-Based Dual-Comb Source, Mengjie Yu^{1,2}, Yoshitomo Okawachi¹, Austin Griffith², Michal Lipson¹, Alexander Gaeta¹; ¹Columbia Univ., USA; ²Cornell Univ., USA. We combine microfluidic technology with microresonator-based mid-infrared dual-comb spectroscopy. We measure flow dynamics of acetone with a spectral acquisition rate of 200-kHz over 90 cm¹ span and <150 fL sample volume over a 100-ms period.

JW2A.83

Beam Shaping with Axicons for Low Loss Microscopy Optics, Natsuha Ochiai¹, Jingwen Shou¹, Yasuyuki Ozeki¹; ¹The Univ. of Tokyo, Japan. We propose a beam shaping method using two axicons for reducing optical loss in broadband microscopy optics. We demonstrate high transmittance and high spatial resolution without sacrificing signal intensity in stimulated Raman scattering microscopy.

JW2A.84
Withdrawn**JW2A.85**

Bound States in a Harmonic Graphene-Mode-Locked Fiber Laser, Bo Fu^{1,2}, Jin Li³, Zhang Cao^{2,1}, Daniel Popa³, ¹Beijing Advanced Innovation Center for Big Data-Based Precision Medicine, Beihang Univ., China; ²School of Instrumentation and Optoelectronic Engineering, Beihang Univ., China; ³Electrical Engineering, Univ. of Cambridge, UK. A solution-processed graphene-film deposited on a fiber-based connector is used for stable bound states of solitons in a harmonic mode-locked all-fiber laser at harmonics up to the 26th.

JW2A.86

104 fs mode-locked fiber laser with a MXene-based saturable absorber, Qing Wu¹, Meng Zhang¹, Xinxin Jin¹, Si Chen², Quanyu Jiang¹, Xiantao Jiang², Zheng Zheng¹, Han Zhang²; ¹Beihang Univ., China; ²Shenzhen Univ., China. We report an all-fiber erbium-doped laser mode-locked by a microfiber-based MXene saturable absorber, generating 104-fs pulses with 42.5-nm spectral width. Our work adds MXene to the growing catalogue of nanomaterials for future nonlinear photonics.

JW2A.87

Spatiotemporal Dynamics of Dual-Soliton States in a Multimode Fiber Laser, Yihang Ding¹, Xiaosheng Xiao¹, Changxi Yang¹; ¹Tsinghua Univ., China. We report on experimental observation of three types of dual-soliton states in a spatiotemporal mode-locked multimode fiber laser. The spatiotemporal dynamics are found different for these states.

JW2A.88

1.94 GHz Passively Harmonic Mode-locked All-fiber Laser Using Polarization-maintaining Helical Long-period Grating, Qianqian Huang¹, Chen Jiang¹, Chuanhang Zou¹, Zinan Huang¹, Chengbo Mou¹, Yunqi Liu¹; ¹Shanghai Univ., China. We have demonstrated an all-fiber passively harmonic mode-locked laser by using helical long-period grating inscribed in polarization-maintaining fiber for the first time. 1.94 GHz pulses at 63rd harmonic with 49.5dB super-mode suppression ratio are obtained.

JW2A.89

High Absorption Low NA Step Index Large-Mode-Area Fiber for High Power Ultrafast Lasers, Raghuraman Sidharthan¹, Kang Jie Lim², Serene Huiting Lim², Huizi Li¹, Yanyan Zhou¹, Junhua Ji¹, Yue Men Seng¹, Song Liang Chua², Seongwoo Yoo¹; ¹Nanyang Technological Univ., Singapore; ²DSO National Labs, Singapore. We report fabrication of >20dB/m cladding absorption step-index LMA fiber with low core NA(<0.07) suitable for ultra-fast fiber lasers. Above 58W output power with a slope efficiency of ~80% was demonstrated in only 0.5m fiber.

JW2A.90

Self-parametric amplification in ultrafast fibre lasers, Heping Zeng¹, Junsong Peng¹; ¹East China Normal Univ., China. Self-parametric amplification is employed as a novel gain mechanism in ultrafast fibre lasers, which transfers energy from the spectral tails to the center within the laser field. The laser outputs three pulses with different spectra.

JW2A.91

Highly Sensitive Liquid Level Sensor Based on Microstructured Optical Fiber, Wei Zhang¹, Fan Ai¹, Zhikun Xing¹, Wei Zhou¹, Zhijun Yan¹, Deming Liu¹, Qizhen Sun¹; ¹Huazhong Univ of Science and Technology, China. A highly sensitive liquid level sensor based on microstructured optical fiber is experimentally demonstrated. The proposed sensor can achieve the fully distributed liquid level monitoring with the resolution of 74 μ m with large detecting range.

JW2A.92

All-Polarization Maintaining, Bi-directional, Er-doped, Dual-comb Fiber Laser with Single Wall Carbon Nanotube, Shuto Saito¹, Masahito Yamanaka¹, Youichi Sakakibara², Emiko Omoda², Hiromichi Kataura², Norihiko Nishizawa¹; ¹Nagoya Univ., Japan; ²AIST, Japan. All polarization maintaining, bi-directional, Er-doped, dual-comb fiber laser using carbon nanotube polyimide film was demonstrated. Optical spectra of output pulses were almost the same, and stable soliton mode-locking operation was achieved for long term.

JW2A.93

Demonstration of the Coherent Mid-IR Supercontinuum Generation in Tapered Tellurite Fiber, Than Singh Saini¹, Hoa P. Nguyen¹, Luo Xing¹, Tong H. Tuan¹, Takenobu Suzuki¹, Yasutake Ohishi¹; ¹Toyota Technological Inst., Japan. Coherent supercontinuum spectrum spanning 1.28 - 3.31 μ m at -40 dB intensity level is obtained using an all-normal dispersion tapered tellurite fiber pumped by 200 fs laser pulse of peak power of 19.8 kW at 2.0 μ m.

JW2A.94

The Impact of Saturable Absorber Recovery Time in Hybrid Mode-Locked Fiber Laser Design, Lei Jin¹, Chao Zhang¹, Neisei Hayashi¹, Sze Y. Set¹, Shinji Yamashita¹; ¹Univ. of Tokyo, Japan. Saturable absorber recovery time plays an important role in a hybrid mode-locked fiber laser. Our investigation reveals that a shorter recovery time is preferred for the hybrid scheme combined with nonlinear polarization rotation.

JW2A.95

Single-aperture passive coherent beam combining of fiber lasers based on diffractive optical element, Gang Bai^{1,2}, Hui Shen¹, Meizhong Liu^{1,2}, Kai Liu¹, Haibo Zhang¹, Xiaxia Niu^{1,2}, Yifeng Yang¹, Bing He^{1,3}, Jun Zhou^{1,3}; ¹Shanghai Key Lab of All Solid-State Laser and Applied Techniques, Shanghai Inst. of Optics and Fine Mechanics, Chinese Academy of Sciences, China; ²Univ. of Chinese Academy of Sciences, China; ³Nanjing Inst. of Advanced Laser Technology, China. We demonstrate a single-aperture coherent beam combination with eight fiber laser beamlets using a one-dimension diffractive optical element in an all-optical feedback loop. The maximum output power is 1.5 W with near diffraction-limited beam quality.

JW2A.96

Light propagation properties of a novel tellurite hollow-core fiber with single hexagonal air-hole layer, Hoang Tuan Tong¹, Nobuhiko Nishiharaguchi¹, Takenobu Suzuki¹, Yasutake Ohishi¹; ¹Toyota Technological Inst., Japan. We experimentally demonstrated the fabrication of a new tellurite hollow core photonic crystal fiber with a single hexagonal air-hole layer and studied its light propagation and transmission properties from 0.4 to 2.4 μ m.

JW2A.97

High Repetition Rate Visible Frequency Comb Generation From Electro-Optic Modulation in the 1550 nm Region, Ken Kashiwagi^{1,2}, Sho Okubo^{1,2}, Hajime Inaba^{1,2}; ¹National Metrology Inst. of Japan, AIST, Japan; ²JST, ERATO, MINOSHIMA Intelligent Optical Synthesizer (IOS), Japan. We generated a 10-GHz spacing visible frequency comb from an EOM-based comb in the 1550 nm region. A waveguide-type periodically-poled lithium niobate produced third and fourth harmonics comb, which ranging in the visible region.

JW2A.98

Dispersion Managed, High Power Tm-doped Ultrashort Pulse Fiber Laser at 1.9 μ m Using Single Wall Carbon Nanotube Polyimide Film, Kenta Watanabe¹, Y. Zhou², Takeshi Saito², Youichi Sakakibara², Norihiko Nishizawa¹; ¹Nagoya Univ., Japan; ²AIST, Japan. High power Tm-doped ultrashort pulse fiber laser operated at 1.9 μ m was demonstrated using single wall carbon nanotube dispersed in polyimide film. A 1.7 nJ, 36 mW high power dissipative soliton pulse was obtained.

JW2A.99

1-MHz, Energetic Ultrafast Source Tunable Between 940-1250 nm for Multi-photon Microscopy, Yang Yu^{1,2}, Shaobo Fang^{2,3}, Hao Teng^{2,3}, Jiangfeng Zhu¹, Junli Wang¹, Guoqing Chang^{2,3}, Zhiyi Wei^{2,3}; ¹Xidian Univ., China; ²Beijing National Lab for Condensed Matter Physics, Inst. of Physics, Chinese Academy of Sciences, China; ³School of Physical Science, Univ. of Chinese Academy of Sciences, China. We demonstrate a 1-MHz ultrafast fiber-optic source that produces ~100-fs pulses tunable from 940 nm to 1250 nm with up to 33-nJ pulse energy. Such a source is ideal for driving multi-photon microscopy.

JW2A.100

Inclinometer Based on Optical Microfiber Probes, Junjie Wang¹, Shijie Tan¹, Wei Zhang¹, Yanpeng Li¹, Qizhen Sun¹, Deming Liu¹; ¹Huazhong Univ of Science and Technology, China. An inclinometer based on optical microfiber probes is proposed and experimentally demonstrated, which is capable of measuring the tilt angle and direction simultaneously with a resolution lower than 0.0004 $^\circ$ within $\pm 5^\circ$.

JW2A.101

High Resolution π -Phase-Shifted Fiber Bragg Grating Demodulator using Frequency Swept DFB Laser, Jiageng Chen¹, Qingwen Liu¹, Zuyuan He¹; ¹Shanghai Jiao Tong Univ., China. A π -phase-shifted fiber Bragg grating demodulator has been proposed based on feed-forward linewidth suppression of frequency swept DFB laser. Wavelength resolution of 3.2 fm in 0.4 nm scan range is achieved in the demonstration.

JW2A.102

Discrete Fourier domain mode locked laser with a microring resonator, Dongmei Huang¹, Feng Li², Huiwen Luo³, Chao Shang¹, Nan Guo¹, Liang Wang³, Sai Chu⁴, Xinhuan Feng⁵, P. K. A. Wai¹; ¹The Hong Kong Polytechnic Univ., Hong Kong; ²The Hong Kong Polytechnic Univ. Shenzhen Research Inst., China; ³Univ. of Science and Technology of China, China; ⁴City Univ. of Hong Kong, Hong Kong; ⁵Jinan Univ., China. We propose and experimentally demonstrate a discrete Fourier domain mode locked (FDML) laser with more than 100 nm bandwidth by utilizing a microring resonator as frequency comb filter.

JW2A.103

Parabolic Pulse Generation in Totally Passive Tapered Multimode Fibers, Helena E. Lopez Aviles², Michael Buttolph¹, Frank W. Wise¹, Rodrigo Amezcua Correa², Demetrios N. Christodoulides¹; ¹School of Applied and Engineering Physics, Cornell Univ., USA; ²CREOL, College of Optics and Photonics, Univ. of Central Florida, USA. We propose a new method to generate self-similar parabolic pulses in exponentially tapered multimode fibers. In such broadband amplification-free settings the input pulse can quickly acquire a parabolic profile with a high quality linear chirp.

JW2A.104

Tri-comb and quad-comb generation from a multi-dimensional-multiplexed fiber laser, Ting Li¹, Xin Zhao¹, Jie Chen¹, Qian Li¹, Zheng Zheng^{1,2}; ¹School of Electronic and Information Engineering, Beihang Univ., China; ²Beijing Advanced Innovation Center for Big Data-based Precision Medicine, China. By tapping into multiple wave-guiding dimensions in optical fiber, it is demonstrated that up to four wavelength/polarization multiplexed, asynchronous ultrashort pulse sequences can be generated with good stability from an all-fiber, ring-cavity, mode-locked fiber laser.

JW2A.105

Surface-enhanced Raman scattering sensor based on soft polymer optical fibers, Jingjing Guo¹, Yuqing Luo¹, Changxi Yang¹, Lingjie Kong¹; ¹Tsinghua Univ., China. We present a novel SERS probes based on soft polymer optical fibers with physio-mechanical properties suitable for implantation, and demonstrate their potential applications for *in-situ* detection of bioanalytes.

JW2A.106

Fast M^2 estimation for fiber beams through deep learning. Liangjin Huang¹, Pu Zhou¹, Yi An¹, Jinyong Leng¹, Lijia Yang¹, Jun Li¹; ¹National Univ of Defense Technology, China. We have firstly utilized deep learning (DL) in M^2 estimation for fiber beams. The simulations have proved our scheme is accurate and M^2 can be determined within ~ 3 ms using a trained DL network.

JW2A.107

Fabrication and Characterization of Birefringent Bismuth and Erbium Co-Doped Photonic Crystal Fiber for Broadband Polarized Near Infrared Emission. Yushi Chu^{1,2}, Yuan Tian², Desheng Fan², Gui Xiao², Shuen Wei², Bowen Zhang², Xinghu Fu², Zhanyu Ma¹, Quan Chai¹, Jing Ren¹, Jianzhong Zhang¹, Yanhua Luo², Gang-Ding Peng²; ¹School of Science, Harbin Engineering Univ., China; ²School of Electrical Engineering & Telecommunications, Univ. of New South Wales, Australia. Birefringent bismuth and erbium co-doped photonic crystal fiber (B-BEPCF) by preform stacking technology has been fabricated and characterized. Results demonstrate broadband and elliptically polarized near infrared (NIR) emission under 532 or 830 nm pumping, respectively.

JW2A.108

Suspended-core fiber based Sagnac interferometer device and sensing applications. Yu Zheng^{1,2}, Perry Ping Shum^{1,2}, Yiyang Luo^{1,2}, Yanan Zhang^{2,3}, Zhifang Wu⁴, Jean-Louis Auguste⁵, Georges Humbert⁵; ¹COFT, School of EEE, Nanyang Technological Univ., Singapore; ²CINTRA, CNRS/NTU/Thales Research Alliance, Singapore; ³College of Information Science and Engineering, Northeastern Univ., China; ⁴College of Information Science and Engineering, Huaqiao Univ., China; ⁵XLIM Research Inst., France. Optical fiber based interferometers have been used for numerous sensing applications. Here, we develop an all-fiber Sagnac interferometer device based on suspended-core fiber, which can be excellent candidates for physical or biochemical sensors.

JW2A.109

Experimental Demonstration of Highly Coherent Near to Mid-Infrared Supercontinuum Generation with All-solid Hybrid Microstructured Tellurite Fiber. Hoa P. Nguyen¹, Tuan H. Tong¹, Luo Xing¹, Thai Singh Saini¹, Takenobu Suzuki¹, Yasutake Ohishi¹; ¹Toyota Technological Inst., Japan. A highly coherent supercontinuum spanning from 1.4 to 3 μm was generated in an all-solid hybrid microstructured tellurite fiber pumped by a laser operating at 2 μm .

JW2A.110

Demonstration of dichroic atomic vapor laser lock in micro fabricated vapor cell using light induced atomic desorption. Eliran Talker¹, P. Arora¹, Roy Zektzer¹, Yefim Barash¹, Noa Mazurski¹, Yoel Sebbag¹, Uriel Levy¹; ¹The Hebrew Univ. of Jerusalem, Israel. We demonstrate Dichroic Atomic Vapor Laser Lock (DAVLL) using light induced atomic desorption in micro fabricated vapor cell. We have stabilized a 780 nm laser with a precision better than 400 kHz without heating.

JW2A.111

A Compact Physics Package of a Chip-scale Atomic Clock with a Built-in Magnetic Shield. Hyun-Gue Hong², Jongcheol Park¹, Tae Hyun Kim¹, Hee Yeoun Kim¹, Sang-Eon Park², Sang-Bum Lee², Myoung-Sun Heo², Taeg Yong Kwon²; ¹National NanoFab Center, South Korea (the Republic of); ²South Korea Research Inst. of Standards and Science, South Korea (the Republic of). We demonstrate a physics package for chip-scale atomic clocks in which the supporting frame itself serves as a primitive magnetic shield ($\sim 20\times$ attenuation). It measures $4.9\times 4.9\times 4.5$ mm³ with its frequency instability $\sim 10^{-10}$ at 1 s.

JW2A.112

Optimizing the dipole trap for loading laser-cooled atoms into hollow-core fibers. Taehyun Yoon¹, Paul Anderson¹, Sheng-Xiang Lin¹, Bryan Duong¹, Michal Bajcsy¹; ¹Univ. of Waterloo, Canada. We study the effects of dipole trap wavelength and power on the number of laser-cooled atoms loaded into a hollow-core optical fiber to optimize the trade-offs between the observed loss mechanisms.

JW2A.113

Coherent atomic microwave sensor. Vladislav Gerginov^{2,1}, Fabio da Silva¹, Craig Nelson¹, Archita Hati¹; ¹Time and Frequency, NIST, USA; ²Physics, Univ. of Colorado Boulder, USA. We developed a room-temperature microwave signal atomic sensor that converts coherently a low-power microwave signal to polarization modulation of a probe light field. The sensitivity rivals that of microwave field probes based on Rydberg atoms.

JW2A.114

Efficient hyperfine optical pumping of Rb atoms in Miniaturized vapor cells. Eliran Talker¹, P. Arora¹, Mark Dikopol-tsev^{1,2}, Uriel Levy¹; ¹Dept. of Applied Physics, The Hebrew Univ. Jerusalem, Israel, Israel; ²RAFAEL, Science Center, Rafael Ltd, Haifa (Israel), Israel. We demonstrate the positive role of buffer gas in achieving highly efficient hyperfine-structure based optical pumping of Rubidium atoms in miniaturized vapor cells. At a pressure of 40 Torr, pumping efficiency of 85% is achieved.

JW2A.115

Sodium Magnetometry. Yan Feng¹, Tingwei Fan¹, Tianhua Zhou¹; ¹Shanghai Inst of Optics & Fine Mechanics, China. Magnetic resonance of sodium fluorescence is investigated and a magnetometer based on sodium vapor is demonstrated. The study is motivated by remote magnetometry with mesospheric sodium. Results of on-sky tests are reviewed.

JW2A.116

Multiparameter Quantum Tracking of Optical Activity. Valeria Cimini¹, Ludovica Ruggiero¹, Ilaria Gianani¹, Marco Sbroscia¹, Tecla Gasperi¹, Emanuele Rocca¹, Luca Mancino¹, Daniela Tofani¹, Fabio Bruni¹, Maria Antonietta Ricci¹, Marco Barbieri¹; ¹Università degli studi Roma Tre, Italy. Quantum sensors can be used to monitor the dynamic of chemical processes. Here we implement a multiparameter protocol, on two different chemical reactions, robust against time-varying noise.

JW2A.117

Truncated nonlinear interferometric cantilever beam-displacement: accessible quantum sensing. Benjamin Lawrie¹, Jacob Beckey¹, Raphael C. Poozer¹; ¹Oak Ridge National Lab, USA. We show that relative beam displacement measurements with two-mode squeezed light sources are identical to truncated SU(1,1) interferometers, enabling a new quantum-enhanced atomic force microscopy suitable for broadband characterization of high-speed dynamics in materials.

JW2A.118

Planar Alignment of Graphene Sheets by a Rotating Magnetic Field for Polarizer and Display Applications. Feng Lin^{2,3}, Guang Yang², Chao Niu¹, Yanan Wang², Zhuan Zhu², Haokun Luo⁴, Chong Dai², Junyi Zhao⁴, Yandi Hu², Xufeng Zhou⁵, Zhaoping Liu⁵, Zhiming Wang³, Jonathan Hu¹, Jiming Bao^{2,3}; ¹Baylor Univ., USA; ²Univ. of Houston, USA; ³Univ. of Electronic Science and Technology of China, China; ⁴Huazhong Univ. of Science and Technology, China; ⁵Chinese Academy of Sciences, China. Rotating magnetic field produced by commercial NdFeB magnet is used for planar alignment of graphene sheets in suspension. We demonstrate high optical anisotropy of aligned graphene sheets for polarizer and display applications.

JW2A.119

Colloidal Self-Assembled Approach Towards Hybrid Waveguide-Plasmon Resonances. Swagato Sarkar¹, Tobias A. König², Joby Joseph¹; ¹Indian Inst. of Technology, Delhi, India; ²Physical Chemistry and Polymer Physics, 1Leibniz-Institut für Polymerforschung Dresden e.V. (IPF), Germany. We demonstrate fabrication of a hybrid opto-plasmonic structure through combination of rapid top-down laser-interference lithography and bottom-up colloidal self-assembly methods. The supported hybridized resonances are compared in depth experimentally along with simulation models.

JW2A.120

Burst-Mode Ultraviolet Laser Pulses at Megawatt Peak Power in a Doubly-Resonant Enhancement Cavity. Abdu-rahim Rakhman¹, Yun Liu¹; ¹Oak Ridge National Lab, USA. We demonstrate power enhancement of burst-mode UV (355 nm) laser with 50 ps pulse width and 402.5 MHz repetition rate. Peak intracavity power of >1.5 MW has been achieved for bunches with 10 μs at 10 Hz rate in a doubly-resonant optical cavity under high vacuum.

JW2A.121

Photonic Crystal Behavior of Nitzschia Filiformis Phytoplankton for Chlorophyll A Photosynthesis. Yannick D'Mello¹, Santiago Bernal¹, James Skoric¹, Dan Petrescu¹, Mark Andrews¹, David V. Plant¹; ¹McGill Univ., Canada. Photonic band structure simulations of Nitzschia Filiformis diatom frustules revealed resonances at wavelengths corresponding to both peaks in the chlorophyll A absorption spectrum. The behavior at 658 nm wavelength was investigated using near-field optical microscopy.

JW2A.122

Optimization of Chalcogenide Negative Curvature Fibers for CO₂ Laser Transmission. Chengli Wei², Curtis R. Menyuk², Jonathan Hu¹; ¹Electrical and Computer Engineering, Baylor Univ., USA; ²Computer Science, Engineering and Physics, Univ. of Mary Hardin-Baylor, USA; ³Computer Science and Electrical Engineering, Univ. of Maryland, Baltimore County, USA. We study the geometry of chalcogenide negative curvature fibers with different numbers of tubes and different core diameters. We optimize the design of chalcogenide negative curvature fibers for CO₂ laser transmission.

Executive Ballroom
210A

Joint

13:00–15:00

JW3A • Sym on Coupling Artificial Atoms to Nano- & Opto-mechanical Systems I

President: To Be Announced

JW3A.1 • 13:00 **Invited**

Toward Novel Coherence Protection and Sensing Techniques: Closed Counter Interaction Using a Single Spin. Mark Kasperczyk¹, Johannes Kolbl¹, Arne Barfuss¹, Patrick Maletinsky¹; *Univ. of Basel, Switzerland*. By studying Nitrogen Vacancy (NV) centers embedded in diamond cantilevers, we show that the coupling between the cantilever and the NV leads to novel coherent population dynamics when combined with two microwave driving fields.

JW3A.2 • 13:30 **Invited**

Spin and Orbital Resonance Driven by a Mechanical Resonator. Gregory Fuchs¹; *Applied and Engineering Physics, Cornell Univ., USA*. I will describe our experiments to drive spin and orbital resonance of single diamond nitrogen-vacancy (NV) centers using the gigahertz-frequency strain oscillations produced within a diamond acoustic resonator.

JW3A.3 • 14:00

Diamond Phononic Crystal Spin-Mechanical Resonators with Spectrally-Stable Nitrogen Vacancy Centers. Ignas Lekavicius¹, Thein Oo¹, Hailin Wang¹; *Univ. of Oregon, USA*. We report the design and fabrication of GHz diamond spin-mechanical resonators embedded in a two-dimensional phononic crystal lattice. Spectrally-stable nitrogen vacancy centers are observed after a soft-etching surface treatment.

Executive Ballroom
210B

CLEO: QELS-Fundamental Science

13:00–15:00

FW3B • Chip-scale Nonlinear Optics

President: To Be Announced

FW3B.1 • 13:00

Second-Harmonic Diffraction from Periodically Structured MoS₂ Monolayer. Franz J. Löchner¹, Rajeshkumar Mupparapu¹, Michael Steinert¹, Antony George², Andrey Turchanin², Thomas Pertsch^{1,3}, Isabelle Staude¹, Frank Setzpfandt¹; *¹Inst. of Applied Physics, Friedrich Schiller Univ. Jena, Germany; ²Inst. of Physical Chemistry, Friedrich Schiller Univ. Jena, Germany; ³Fraunhofer Inst. for Applied Optics and Precision Engineering, Germany*. We investigate second-harmonic generation from one-dimensional gratings in MoS₂ monolayer flakes structured by focused ion beam milling, and observe diffraction orders due to nonlinear diffraction from the periodic structure.

FW3B.2 • 13:15

Non-reciprocal delay based on photon-phonon interactions on a chip. Moritz Merklein¹, Birgit Stiller¹, Khu Vu², Pan Ma², Stephen Madden², Benjamin J. Eggleton¹; *¹The Univ. of Sydney, Australia; ²Australian National Univ., Australia*. We demonstrate a non-reciprocal delay scheme based on stimulated Brillouin scattering in a planar highly nonlinear waveguide. The bandwidth of this scheme approaches a GHz, has wide frequency tunability and scales linearly with data power.

FW3B.3 • 13:30 **Invited**

Heterogeneous Integration of GaAs/AlGaAs Devices for Non-Linear Applications. Marc Sorel¹, Stuart May¹, Matteo Clerici¹, Michael Kues¹, Charalambos Klitis¹, Michael Strain², Benoit Guilhabert², John McPhillimy², Cosimo Lacava³, Periklis Petropoulos³; *¹Univ. of Glasgow, UK; ²Univ. of Strathclyde, UK; ³Univ. of Southampton, UK*. We will review recent progress on the integration of AlGaAs devices for non-linear applications. Second harmonic generation on AlGaAs-on-insulator waveguides and the integration of AlGaAs microdisk resonators on silicon by transfer printing will be discussed.

FW3B.4 • 14:00

Enhanced nonlinearity in lithium niobate on insulator (LNOI) waveguides through engineering of lateral leakage. Andreas Boes^{1,2}, Lin Chang², Thach Nguyen¹, Markus Knoerzer¹, Jon Peters², John Bowers², Arnan Mitchell¹; *¹Royal Melbourne Inst. of Technology, Australia; ²Univ. of California, Santa Barbara, USA*. We present that the nonlinear optical conversion efficiency in LNOI ridge/rib waveguides can be improved by considering the lateral leakage at the second harmonic wavelength, enabling an improved nonlinear optical conversion efficiency of ~780% W⁻¹cm².

Executive Ballroom
210C

13:00–15:00

FW3C • Generation & Control of Light Emission at the Nanoscale

President: Christian Haffner; NIST, USA

FW3C.1 • 13:00

Light Emission from a Waveguide Integrated MOS Tunnel Junction. Michael Doderer¹, Markus Parzefall¹, Andreas Joerg¹, Daniel Chelladurai¹, Nikola Dordevic¹, Yuriy Fedoryshyn¹, Amit K. Agrawal^{2,3}, Henri Lezec², Lukas Novotny¹, Juerg Leuthold¹, Christian Haffner¹; *¹ETH Zurich, Switzerland; ²National Inst. of Standards and Technology, USA; ³Univ. of Maryland, USA*. We report on light generation via inelastic electron tunneling in a metal-oxide-semiconductor (MOS) junction that is directly integrated within a silicon photonic waveguide. We generate an optical power of 6.8 pW.

FW3C.2 • 13:15

Polariton electroluminescence in monolayer WS₂. Biswanath Chakraborty¹, Jie Gu¹, Mandeep Khatoniar¹, Vinod Menon¹; *¹Physics, The City College of New York, CUNY, USA*. We demonstrate a room temperature polariton LED using monolayer WS₂ embedded in a microcavity in the strong coupling regime. Electrical injection is accomplished via graphene contacts and hBN tunnel barriers integrated with the microcavity.

FW3C.3 • 13:30 **Invited**

Spatial and Temporal Coherence of Ultrafast Plasmon Nanolasers. Teri W. Odom¹; *¹Northwestern Univ., USA*. This talk will describe the underlying mechanisms for coherence in two plasmonic nanolasing systems with different cavity structures: nanoparticle arrays and bowtie-shaped particles.

FW3C.4 • 14:00

Probing Electro-Magnetic Local Density of Optical States with Mixed ED-MD Emitters. Dongfang Li^{1,2}, Sinan Karaveli¹, Sebastien Cuffe^{1,3}, Wenhao Li¹, Rashid Zia¹; *¹Brown Univ., USA; ²Center for Integrated Nanotechnologies, Los Alamos National Lab, USA; ³Institut des Nanotechnologies de Lyon, France*. We experimentally demonstrated that the lifetime of quantum emitters with strongly mixed electric dipole (ED) and magnetic dipole (MD) transitions can directly probe the combined electro-magnetic local density of optical states.

CLEO: QELS-Fundamental
Science

13:00–15:00

FW3D • Topological Photonics III

President: To Be Announced

FW3D.1 • 13:00

Towards a Non-magnetic Topological Haldane Laser, Yuzhou Liu¹, Pawel Jung^{1,2}, Midya Parto¹, Jason Leshin¹, Demetrios N. Christodoulides¹, Mercedeh Khajavikhan¹; ¹Univ. of Central Florida, CREOL, USA; ²Faculty of Physics, Warsaw Univ. of Technology, Poland. We introduce a new design for implementing the topological Haldane laser on a non-magnetic platform. Unit cells are provided for detuned nearest neighbor coupling and imaginary next-nearest neighbor coupling based on microring laser networks.

FW3D.2 • 13:15

Mode-locked topological laser in synthetic dimensions, Zhaoju Yang¹, Eran Lustig¹, Gal Harari¹, Yonatan Plotnik¹, Miguel Bandres¹, Mordechai Segev¹; ¹Technion - Israel Inst. of Technolo, Israel. We present topological insulator laser with one spatial and one modal dimensions. The topological lasing state imposes constant phase difference between the multi-frequency modes, forcing the resonators to mode-lock and emit short pulses.

FW3D.3 • 13:30

Observation of Flat-band Line States in Photonic Superhoneycomb Lattices, Wenchao Yan¹, Daohong Song¹, Shiqi Xia¹, Liqin Tang¹, Yiqi Zhang¹, Jingjun Xu¹, Zhigang Chen^{1,2}; ¹The MOE Key Lab of Weak-Light Nonlinear Photonics, TEDA Applied Physics Inst. and School of Physics, Nankai Univ., China; ²San Francisco State Univ., USA. We demonstrate for the first time photonic super-honeycomb lattices established with a cw-laser writing technique, thereby uncovering two different types of flat-band line states that manifest noncontractible-loop-states in infinite flat-band systems arising from real-space topology.

FW3D.4 • 13:45

Fractal Waveguide Arrays Induce Maximal Anderson Localization, Jonathan Guglielmon¹, Mikael C. Rechtsman¹; ¹Pennsylvania State Univ., USA. In recent years, there has been great interest in using Anderson localization or flat-band lattices to eliminate interwaveguide crosstalk for imaging and telecommunications applications. We show that fractal configurations offer strict improvements on these schemes.

FW3D.5 • 14:00

Realization of a Non-Quantized Square-Root Topological Insulator Based on Photonic Aharonov-Bohm Cages, Mark Kremer¹, Ioannis Petrides², Eric Meyer¹, Matthias Heinrich¹, Oded Zilberberg², Alexander Szameit¹; ¹Inst. of Physics, Univ. of Rostock, Germany; ²Inst. for Theoretical Physics, ETH Zürich, Switzerland. We report a new type of insulator that exhibits spectral bands with nonquantized topological properties. Furthermore, a quantisation manifests itself upon squaring the Hamiltonian. We experimentally verify our claims by using photonic Aharonov Bohm cages.

CLEO: Science & Innovations

13:00–15:00

SW3E • Ultrafast Metrology

President: Igor Jovanovic; Univ. of Michigan, USA

SW3E.1 • 13:00

Application of Artificial Neural Networks to Dispersion Scan Retrievals, Sven Kleinert¹, Ayhan Tajalli¹, Tamas Nagy², Uwe Morgner^{1,3}; ¹Leibniz Universität Hannover, Germany; ²Max Born Inst. for Nonlinear Optics and Short Pulse Spectroscopy, Germany; ³Laser Zentrum Hannover e.V., Germany. We present the phase reconstruction of ultrashort pulses from dispersion scan traces using a deep neural network. Compared to conventional algorithms, this reconstruction is more than 3000 times faster, enabling video-rate reconstructions.

SW3E.2 • 13:15

Sensitive Interferometric GRENOUILLE Device, Travis N. Jones¹, Peter Šušnjar², Rok Petkovšek², Rick Trebino¹; ¹Georgia Inst. of Technology, USA; ²Lab for Photonics and Laser Systems, Univ. of Ljubljana, Slovenia. We introduce a practical, sensitive and self-referenced frequency-resolved optical gating technique for measuring picosecond pulses with femtojoule energies. We demonstrate the capability of this technique to measure a pulse with complex temporal and spectral structure.

SW3E.3 • 13:30 **Invited**

Controlling the Velocity of Ultrashort Laser Bursts in Vacuum, Fabien Quéré¹; ¹CEA Saclay, France. This talk will present the intriguing new possibilities offered by spatio-temporal shaping of ultrashort laser beams, and some of the latest developments on the spatio-temporal metrology of femtosecond lasers, up to the PetaWatt power level.

SW3E.4 • 14:00

Coherent Two-Octave-Spanning Supercontinuum Generation in Lithium-Niobate Waveguides, Mengjie Yu¹, Boris Desiatov¹, Yoshitomo Okawachi², Alexander Gaeta², Marko Lončar¹; ¹Harvard Univ., USA; ²Applied Physics and Applied Math, Columbia Univ., USA. We demonstrate a coherent supercontinuum spanning two octaves with 35 pJ pulses in a lithium-niobate waveguide under the presence of second- and third-order nonlinear effects, which allows for detection of the carrier-envelope offset frequency on-chip.

13:00–15:00

SW3F • Terahertz Plasmonics

President: Vedran Jelic; Michigan State Univ., USA

SW3F.1 • 13:00

Tunable magneto-optical polarization device for terahertz waves based on InSb plasmonic structure, Qianyi Mu¹, Fei Fan¹, Jierong Cheng¹, Shengjiang Chang¹; ¹Nankai Univ., China. We demonstrated the InSb magneto-plasmonics for THz polarization conversion. The magneto-optical enhancement mechanisms were found, achieving broadband perfect orthogonal linear polarization conversion modulated by the weak magnetic field in the experiment.

SW3F.2 • 13:15

Magnetoplasmonic Manipulation of THz Transmission and Faraday Rotation Using Graphene Micro-Ribbon Arrays, Prashant Padmanabhan¹, Stéphane Boubanga-Tombet², Taiichi Otsuji³, Rohit Prasankumar¹; ¹Center for Integrated Nanotechnologies, Los Alamos National Lab, USA; ²Telops Inc., Canada; ³Research Inst. of Electrical Communication, Tohoku Univ., Japan. We utilize periodic arrays of graphene micro-ribbons to control the transmission and Faraday rotation spectra of THz pulses by coupling to magnetoplasmon modes whose frequencies are determined by the ribbon width.

SW3F.3 • 13:30 **Invited**

Terahertz Spectroscopy of Dirac Plasmons: Graphene and Topological Insulators, Hyunyong Choi¹; ¹Yonsei Univ., South Korea (the Republic of). Dirac materials like graphene and three-dimensional topological insulators exhibit strong low-energy light-matter interactions. Here I will review recent progresses of terahertz spectroscopy studies of such Dirac materials both in quasi-equilibrium and non-equilibrium limits.

SW3F.4 • 14:00

0.25 mW Pulsed Terahertz Radiation from Bias-Free, Telecommunication-Compatible Plasmonic Nanoantennas, Deniz Turan¹, Nezh Tolga Yardimci¹, Mona Jarrahi¹; ¹Univ. of California, Los Angeles, USA. We present a bias-free, telecommunication-compatible photoconductive terahertz source, which offers radiation powers exceeding 0.25 mW, enabling time-domain terahertz spectroscopy with more than a 90 dB dynamic range over a 0.1-3.5 THz bandwidth.

CLEO: Science & Innovations

CLEO: Applications
& Technology

13:00–15:00

SW3G • Frequency Combs & Stable Laser Systems

President: Ladan Arissian; NRC, USA

SW3G.1 • 13:00

Narrow-linewidth and highly stable optical frequency comb realized with a simple servo control system in a mode-locked Er: fiber laser, Kazumichi Yoshii^{1,4}, Yu Asahina^{1,4}, Yuko Yamada^{1,4}, Yusuke Hisai^{1,4}, Sho Okubo^{2,4}, Masato Wada^{2,4}, Hajime Inaba^{2,4}, Takemi Hasegawa³, Yoshinori Yamamoto³, Feng-Lei Hong^{1,4}, ¹Yokohama National Univ., Japan; ²National Metrology Inst. of Japan, Japan; ³Sumitomo Electric Industries, Japan; ⁴JST, ERATO, MINOSHIMA Intelligent Optical Synthesizer Project, Japan. We developed a mode-locked Er: fiber laser containing a small optical bench with an electro-optic modulator. The bench is used to control the laser repetition frequency at a large servo bandwidth and realize narrow linewidth.

SW3G.2 • 13:15

Stabilized All-Fiber-Based Mode-Filtering Technique for the Generation of a GHz-Repetition-Rate Frequency Comb, Yoshiaki Nakajima^{1,2}, Takuya Hariki^{1,2}, Akiko Nishiyama^{1,2}, Kaoru Minoshima^{1,2}, ¹Univ. of Electro-Communications, Japan; ²JST, ERATO MINOSHIMA Intelligent Optical Synthesizer (IOS) Project, Japan. An all-fiber-based mode-filtering technique is developed for generating a 1 GHz fiber-based frequency comb with a multiplication factor of 21. A high side-mode suppression ratio of approximately of 38 dB is achieved with this comb.

SW3G.3 • 13:30

Broad Visible Frequency Comb with 24-GHz Mode-spacing Based on Mode-Locked Erbium-Fiber Laser, Keisuke Nakamura^{1,2}, Sho Okubo^{1,2}, Ken Kashiwagi^{1,2}, Hajime Inaba^{1,2}, ¹National Metrology Inst. of Japan, Japan; ²JST ERATO, MINOSHIMA Intelligent Optical Synthesizer, Japan. We developed a 24-GHz spacing comb based on a mode-locked Er-fiber laser and mode-filtering technique. The broad comb spectrum in infrared region was converted to visible region by a PPLN waveguide.

SW3G.4 • 13:45

High-Coherence Ultra-Broadband Dual-Comb Fiber Laser with Carrier-Envelope-Offset Frequency, Yoshiaki Nakajima^{1,2}, Yuya Hata^{1,2}, Yugo Kusumi¹, Kaoru Minoshima^{1,2}, ¹Univ. of Electro-Communications, Japan; ²JST, ERATO MINOSHIMA Intelligent Optical Synthesizer (IOS) Project, Japan. A dual-comb fiber laser that generates two high-coherence, ultra-broadband frequency combs with slightly different repetition rates was developed. Carrier-envelope-offset beat signals with a high signal-to-noise-ratio of 30 dB were demonstrated with high controllability.

SW3G.5 • 14:00

Full Stabilization of 1.5-W Kerr-Lens Mode-Locked Yb:CYA Laser Frequency Comb, Ziyue Zhang^{1,2}, Hainian Han^{1,2}, Huibo Wang³, Xiaodong Shao¹, Zhiyi Wei^{1,2}, ¹Inst. of Physics, CAS, China; ²Univ. of Chinese Academy of Science, China; ³School of Physics and Optoelectronics Engineering, Xidian Univ., China. We report a fully stabilized 1.5-W Kerr-lens mode-locked Yb:CYA laser frequency comb. Integrated phase noise of the stabilized carrier-envelope offset frequency is 370 mrad, frequency deviation for more than 3-hours is observed to be 0.8 mHz.

13:00–15:00

SW3H • Nonlinear Optical Phenomena

President: Markku Vainio University of Helsinki, Finland

SW3H.1 • 13:00

Four-wave mixing in orbital angular momentum modes, Xiao Liu¹, Erik N. Christensen^{1,2}, Gautam Prabhakar¹, Karsten Rottwitz², Siddharth Ramachandran¹, ¹Boston Univ., USA; ²DTU fotonik, Technical Univ. of Denmark, Denmark. We report the first, to our knowledge, demonstration of four-wave mixing between fiber modes carrying orbital angular momentum. We show that spin and orbital angular momentum conservation rules lead to diverse phase matching possibilities.

SW3H.2 • 13:15

Fiber event horizon by single color pump, Surajit Bose¹, Oliver Melchert^{1,2}, Ihar Babushkin¹, Mrinmay Pal⁴, Günter Steinmeyer³, Uwe Morgner¹, Ayhan Demircan^{1,2}, ¹Leibniz Univ. Hannover, Germany; ²Hannover Centre for Optical Technologies, Germany; ³Max-Born-Inst., Germany; ⁴CSIR-Central Glass and Ceramic Research Inst., India. We demonstrate both numerically and experimentally the direct creation of an optical event horizon that arises from the interaction of a solitary optical pulse with a group-velocity-matched dispersive wave.

SW3H.3 • 13:30

Temporal Tweezing of Polarization Domain Walls in a Fiber Kerr Resonator, Julien Fatome¹, Nicolas Bertl¹, Bertrand Kibler¹, Bruno Garbin², Stuart Murdoch², Miro J. Erkintalo², Stephane Coen², ¹CNRS - Université Bourgogne Franche Comté, France; ²Univ. of Auckland, New Zealand. We report the experimental demonstration of temporal trapping of polarization domain walls (PDWs) stored in a fiber Kerr resonator. The PDWs are trapped into specific time slots through a phase-modulation scheme of the holding beam.

SW3H.4 • 13:45

Spectral Magnification System for All-Optical WDM Grid Manipulation in Dispersion Un-Compensated Transmission, Frederik Klejs¹, Mads Lilliehölm¹, Michael Galili¹, Leif K. Oxenlöwe¹, ¹FOTONIK, DTU, Denmark. We investigate spectral magnification as a tool for optical spectral grid manipulation in dispersion un-compensated communication systems. The presence of dispersion can be utilized to circumvent the need for temporal synchronization of pumps and signal.

SW3H.5 • 14:00

Measurement of Optical Pulsewidth in the Picosecond Regime Using a Non-linear Fiber and Power Meter, Umair Ahmed Korai Baloch^{1,2}, Zifei Wang³, Cosimo Lacava⁵, Lawrence Chen³, Michael Strain⁴, Ivan Glesk¹, ¹Dept. of Electronic and Electrical, Univ. of Strathclyde, UK; ²Dept. of Telecommunication Engineering, Mehran Univ. of Engineering and Technology, Jamshoro, Pakistan, Pakistan; ³Dept. of Electrical and Computer Engineering, McGill Univ., Canada; ⁴Inst. of Photonics, Dept. of Physics, Univ. of Strathclyde, UK; ⁵Optoelectronics Research Centre, Univ. of Southampton, UK. A technique for the characterization of picosecond pulse widths is presented, based a non-linear optical fiber loop mirror and power meter measurement. Pulse-widths in the 2-10ps range are successfully recovered with a resolution of 0.25ps.

13:00–15:00

AW3I • Laser-formed Structures & Additive Manufacturing

President: Jie Qiao; Rochester Institute of Technology, USA

AW3I.1 • 13:00 **Invited**

A New Dimension in Silicon: "in-chip" Photonic Devices and 3D Micro-structures Enabled with Nonlinear Laser Lithography, Onur Tokel¹, ¹Dept. of Physics, Bilkent Univ., Turkey. I will start by introducing the first buried (in-chip) photonic elements in silicon, followed by 3D laser-sculpting of the chip for industrial applications. I will finish by reviewing potential expansion to other semiconductors.

AW3I.2 • 13:30

Enlarged color gamut by transferring silicon nanowire arrays embedded in flexible polymer on nanoresonator, YeongJae Kim¹, Young Jin Yoo¹, Gil Ju Lee¹, Dong-Wook Lee², Dong Eun Yoo², Vantari Siva¹, Hansung Song¹, Il Suk Kang², Young Min Song¹, ¹Gwangju Inst. of Science and Technol., South Korea (the Republic of); ²South Korea Advanced Inst. of Science and Technology, South Korea (the Republic of). Enlarged color gamut with silicon nanowire arrays is demonstrated both theoretically and experimentally. These structures are comprised of a polymer embedded silicon nanowire arrays (Si NWAs) that are stacked on a metal/insulator/metal (MIM) nanoresonator.

AW3I.3 • 13:45

Additive Fabrication of Multiscale Metasurface by Electrohydrodynamic Nanotexturing of Two-Beam Interference-Patterned Photopolymer Surface, Qiang Li¹, In Ho Cho¹, Rana Biswas¹, Jaeyoun Kim¹, ¹Iowa State Univ., USA. Adding nanotextures to polymer surfaces already corrugated by 2-beam interference lithography is highly challenging. Using softlithography, triboelectricity, and electrohydrodynamic lithography, we fabricate multiscale metasurfaces by adding nanovolcanoes to sinusoidally corrugated NOA73 surfaces.

AW3I.4 • 14:00

Additive Manufacturing of Fused Silica Glass Using Direct Laser Melting, Jincheng Lei¹, Yuzhe Hong², Qi Zhang¹, Fei Peng², Hai Xiao¹, ¹Clemson Univ. COMSET, USA; ²Dept. of Materials Science and Engineering, Clemson Univ., USA. A direct method for additive manufacturing of fused silica glass without any post treatment has been developed. By applying laser to process the fused silica paste, three-dimensional fused silica glass with high transparency was obtained.

CLEO: Science & Innovations

13:00–15:00

SW3J • Photonic Sensing & Mid-infrared Photonics

President: Vladimir Aksyuk; NIST, USA

SW3J.1 • 13:00 **Tutorial**

Photonic Crystal Devices for Sensing, Toshihiko Baba¹; ¹*Yokohama National Univ., Japan*. Two photonic crystal (PC) devices will be presented. The PC nanolaser detects electro-chemical effects, which allows ultrahigh sensitivity or spectral-analysis-free sensing. The PC slow light waveguide is used as a Tx/Rx optical antenna in LiDAR.



Toshihiko Baba received the Ph.D. degree from Yokohama National University in 1990. He became an associate professor and full professor in 1994 and 2005, respectively. He has presented the studies on ARROW waveguides, VCSELs, photonic crystals, Si photonics, micro/nanolasers, slow light, etc. in 200 papers with 12900 citations.

SW3J.2 • 14:00

Mid-Infrared Computational Spectroscopy with an Electrically-Tunable Graphene Metasurface, Vivek R. Shrestha⁴, Benjamin Craig⁴, Matin Amani^{1,3}, James Bullock^{2,1}, Ali Javey^{1,3}, Kenneth Crozier^{4,2}; ¹*Electrical Engineering and Computer Sciences, Univ. of California, Berkeley, Berkeley, USA*; ²*Dept. of Electrical and Electronic Engineering, The Univ. of Melbourne, Australia*; ³*Materials Sciences Division, Lawrence Berkeley National Lab, USA*; ⁴*School of Physics, The Univ. of Melbourne, Australia*. We demonstrate graphene-plasmonic metasurfaces whose mid-infrared reflection spectra are electrically-tunable. Using measurements of the power reflected by the metasurfaces at different drive voltages, the source spectrum is computationally reconstructed by the recursive least squares method.

CLEO: Applications & Technology

13:00–15:00

AW3K • Optical Solutions for Autonomous Driving

President: Fabio Di Teodoro, Raytheon SAS, USA

AW3K.1 • 13:00 **Invited**

Automotive LiDAR: Design Concepts and Challenges, Jake Li¹; ¹*Hamamatsu Corporation, USA*. The presentation will briefly introduce different LiDAR concepts, discusses the techniques of measuring distance with light for the automotive industry based on principles of the direct time of flight (TOF) and indirect TOF – frequency modulated continuous wave (FMCW). The discussion contains the following topics: benefits and challenges of different TOF or FMCW LiDAR concepts in the market today; overview of optical design challenges that's key driver for development of each LiDAR concepts, as well as introducing key optical components (photodetector and light sources) for different LiDAR designs.

AW3K.2 • 13:30

Vernier Si-Photonic Phased Array Transceiver for Grating Lobe Suppression and Extended Field-of-View, Nathan Dostart¹, Michael Brand¹, Bohan Zhang², Daniel Feldkhun¹, Kelvin Wagner¹, Milos Popovic^{2,1}; ¹*Electrical, Computer, and Energy Engineering, Univ. of Colorado at Boulder, USA*; ²*Electrical and Computer Engineering, Boston Univ., USA*. We present a Vernier optical phased array transceiver architecture that suppresses grating lobes and can extend the field-of-view. The first experimental demonstration shows Vernier lobe suppression by transmitting from adjacent TX and RX tiles simultaneously.

AW3K.3 • 13:45

Discrete spectral-temporal encoded LiDAR, Yunshan Jiang¹, Sebastian Karpf¹, Bahram Jalali¹; ¹*Univ. of California Los Angeles, China*. We propose the discrete spectro-temporal LiDAR that realizes non-mechanical scanning in one dimension at 0.342MHz line rate with a single laser and a single-pixel detector. Our implementation is based on an externally modulated FDML MOPA laser.

AW3K.4 • 14:00

Compound period grating coupler for double beams generation and steering, Dachuan Wu¹, Ya Sha Yi¹, Wei Guo¹; ¹*Univ. of Michigan, USA*. We propose a compound period grating coupler by combining two component periods together to generate two outcoupling beams simultaneously. The two beams both response to the wavelength tuning, and thus approximately double the steering range.

CLEO: Science & Innovations

13:00–15:00

SW3L • Ultrasound, Photoacoustic, & Photothermal Sensing

President: Todd Stievater, US Naval Research Laboratory, USA

SW3L.1 • 13:00

Shot-noise-limited optical sensing of ultrasound using pulse interferometry with a free-space Fabry-Pérot, Oleg Volodarsky¹, Yoav Hazan¹, Amir Rosenthal¹; ¹*Technion- Israel Inst. of Technology, Israel*. We demonstrate shot-noise-limited interferometric sensing of ultrasound for optical powers up to 5 mW using an optical scheme based on a pulse laser, fiber stretcher, and free-space Fabry-Pérot.

SW3L.2 • 13:15

Optical phase modulated pulse interferometry for parallel multi-channel ultrasound detection, Yoav Hazan¹, Amir Rosenthal¹; ¹*Technion- Israel Inst. of Technology, Israel*. Optical detection of ultrasound using high Q-factor resonators lack of scalable scheme. In this work, we present phase-modulated pulse interferometry, a scalable scheme, enabling interrogation of multiple resonators simultaneously.

SW3L.3 • 13:30

Sensitivity enhancement of silicon-photonics-based ultrasound sensor via BCB cladding, Resmi R. Kumar¹, Evgeny Hahamovich¹, Shai Tsesses¹, Yoav Hazan¹, Assaf Grinberg¹, Amir Rosenthal¹; ¹*Technion- Israel Inst. of Technology, Israel*. Low photo-elastic response of SOI sensors limits the development of optical detection of ultrasound. We demonstrate ultrasound sensitivity enhancement in silicon waveguides by BCB over-cladding replacing Silica.

SW3L.4 • 13:45

An Integrated Broadband Ultrasound Sensor based on a Photonic Crystal Slab, Eric Y. Zhu¹, Maria C. Charles¹, Cory Rewcastle¹, Raanan Gad¹, Li Qian¹, Ofer Levi¹; ¹*Univ. of Toronto, Canada*. A CMOS-compatible photonic crystal slab (PCS) sensor is used to detect ultrasound signals in water. The range of detection spans 160 kPa down to a noise-equivalent pressure (NEP) of 650 Pa (3.7 Pa/rt Hz). The detection bandwidth spans 1 to 38 MHz, limited only by our measurement apparatus.

SW3L.5 • 14:00

Optical Frequency Comb Photoacoustic Spectroscopy, Ibrahim Sadiq¹, Tommi Mikonnen², Markku M. Vainio^{2,3}, Juha Toivonen², Aleksandra Foltynowicz¹; ¹*Dept. of Physics, Umea Univ., Sweden*; ²*Lab of Photonics, Tampere Univ. of Technology, Finland*; ³*Dept. of Chemistry, Univ. of Helsinki, Finland*. We combine for the first time a mid-infrared optical frequency comb Fourier transform spectrometer with cantilever-enhanced photoacoustic detection and measure high-resolution broadband spectra of the fundamental band of methane in a few milliliter sample volume.

Wednesday, 13:00–15:00

CLEO: QELS-Fundamental
Science

13:00–15:00

FW3M • Ultrafast Spectroscopy in 2D
Materials & Heterostructures

Presider: Mackillo Kira; University of Michigan, USA

FW3M.1 • 13:00

Internal Structure and Ultrafast Dynamics of Tailored Excitons in van der Waals Heterostructures, Philipp Steinleitner¹, Philipp Merkl¹, Philipp Nagler¹, Christian Schüller¹, Tobias Korn¹, Samuel Brem², Malte Selig³, Gunnar Berghäuser³, Ermin Malic², Rupert Huber¹; ¹Physics, Univ. of Regensburg, Germany; ²Physics, Chalmers Univ. of Technology, Sweden; ³Theoretical Physics, Technical Univ. of Berlin, Germany. Phase-locked few-cycle mid-infrared pulses trace how a capping layer of hexagonal boron nitride renormalizes the internal structure of photoexcited excitons in a WSe₂ monolayer and how dark excitons form from initially bright species.

FW3M.2 • 13:15

Direct Measurement of Coherent Coupling in a MoSe₂/WSe₂ Heterostructure, Hanna G. Ruth¹, Eric Martin¹, Torben L. Purz^{1,2}, Pasqual Rivera³, Xiaodong Xu³, Steven T. Cundiff¹; ¹Univ. of Michigan, USA; ²Physics, Univ. of Göttingen, Germany; ³Univ. of Washington, USA. We use multidimensional coherent spectroscopy to identify interlayer coherent coupling between excitons in a MoSe₂/WSe₂ heterostructure, which brings us towards the goal of resolving energy transfer processes in transition metal dichalcogenide heterostructures.

FW3M.3 • 13:30 **Invited**

Evidence for Moiré Excitons in Van der Waals Heterostructures, Xiaoqin Li¹; ¹Univ. of Texas at Austin, USA. Stacking two monolayers of vdW materials, lattice mismatch or rotational misalignment introduces an in-plane moiré superlattice. In this talk, I discuss how a moiré superlattice may influence the optical properties of transition metal dichalcogenide heterostructures.

FW3M.4 • 14:00

Excitonic Effects in Single Layer MoS₂ Probed by Broadband Two-dimensional Electronic Spectroscopy, Margherita Maiuri¹, Stefano dal Conte¹, Mattia Russo¹, Junjia Wang², Giancarlo Soavi², Dumitru Dumcenco³, Andras Kis³, Malte Selig⁴, Sandra Khun⁴, Marten Richter⁴, Andreas Knorr⁴, Andrea C. Ferrari², Giulio Cerullo¹; ¹Politecnico di Milano, Italy; ²Cambridge Graphene Centre, Univ. of Cambridge, UK; ³Electrical Engineering Inst., Ecole Polytechnique Federale de Lausanne, Switzerland; ⁴Technische Universität Berlin, Germany. We exploit two-dimensional electron spectroscopy to coherently excite the A and B excitons in monolayer MoS₂. Combined with simulations, our data distinguish ultrafast bright excitons decoherence and sub-ps scattering decays to dark excitons.

CLEO: Science & Innovations

13:00–15:00

SW3N • Cascade Lasers

Presider: David Burghoff; Univ. Notre Dame, USA

SW3N.1 • 13:00 **Invited**

Novel Interband Cascade Lasers for the Mid-Infrared, James Gupta¹; ¹National Research Council Canada, Canada. We report the latest developments in interband cascade lasers (ICLs) for high-performance, low power-consumption mid-IR sensing applications: type-I ICLs on GaSb for the 3 μ m-range and long-wavelength InAs-based type-II ICLs.

SW3N.2 • 13:30

Square Wave Emission in a Mid-infrared Quantum Cascade Oscillator Under Rotated Polarization, Olivier Spitz^{1,3}, Andreas Herdt², Mathieu Carras³, Wolfgang Elsässer², Frederic Grillot^{1,4}; ¹Télécom ParisTech, France; ²Technische Universität Darmstadt, Germany; ³mirSense, France; ⁴Univ. of New Mexico, USA. Quantum cascade lasers, which are known to only emit a transverse-magnetic wave under free-running operation, can output a square wave with transverse-electric emission under polarization-rotated feedback.

SW3N.3 • 13:45

Catastrophic Degradation in High-Power Buried Heterostructure Quantum Cascade Lasers, Yongkun Sin¹, Zachary Lingley¹, Miles Brodie¹, B Knipfer², C Sigler², C Boyle², J D. Kirch², K Oresick², H Kim², D Botez², L Mawst², D Lindberg³, T Earles³; ¹The Aerospace Corporation, USA; ²Univ. of Wisconsin – Madison, USA; ³Intraband, LLC, USA. Investigation of catastrophic degradation in high-power, buried-heterostructure quantum cascade lasers, using focused ion beam and high-resolution TEM techniques, has revealed dislocations generated, as a result of degradation, mostly in areas away from the active region.

SW3N.4 • 14:00 **Invited**

Terahertz Metasurface Quantum-cascade Lasers: Broadband and High-power Operation, Benjamin S. Williams¹; ¹Univ. of California Los Angeles, USA. Metasurface based external cavity lasers are an attractive approach to the challenge of obtaining simultaneous high-power, tunable single-mode wavelength, and excellent beam pattern from terahertz quantum-cascade lasers.

13:00–15:00

SW3O • Long Distance Transmission

Presider: Xi Chen; Nokia Corporation, USA

SW3O.1 • 13:00

Fiber Nonlinearity Compensation Using Erbium-Doped-Fiber-Assisted Dual-Order Raman Amplification, Mingming Tan¹, Mohammad Al-Khateeb¹, Tingting Zhang¹, Andrew Ellis¹; ¹Aston Univ., UK. We propose a novel dual-order backward-pumped distributed Raman amplification scheme assisted by 25cm erbium-doped-fiber providing nearly perfect multi-span signal power symmetry and 7dB nonlinear threshold improvement for 256Gb/s inline transmission when deploying optical phase conjugation.

SW3O.2 • 13:15

Differential Phase Noise Properties in QD-MLL and its Performance in Coherent Transmission Systems, Mustafa A. Al-Qadi¹, Maurice O'Sullivan², Chongjin Xie³, Rongqing Hui¹; ¹Univ. of Kansas, USA; ²R&D, Ciena Corporation, Canada; ³Alibaba Infrastructure Service, Alibaba Group, Sunnyvale, CA 94085, USA, USA. We show that the differential phase noise between adjacent comb lines in quantum-dot mode-locked lasers may exhibit higher phase noise impacts in coherent transmission systems than their apparent narrow linewidths, due to unique spectral profiles.

SW3O.3 • 13:30

Performance Evaluation of K-Means Clustering Assisted Common Phase Error Estimation, Qiulin Zhang¹, Chester Shu¹; ¹Chinese Univ. of Hong Kong, Hong Kong. We demonstrate that common phase error can be estimated by k-means clustering with just 4 clusters for different modulation formats. Performance comparison between Viterbi-Viterbi algorithm and k-means clustering is conducted in a Kramers-Kronig detection system.

SW3O.4 • 13:45

1,000-km Transmission of 1.5-Gb/s Y-00 Quantum Stream Cipher using 4096-level Intensity Modulation Signal, Fumio Futami¹, Ken Tanizawa¹, Kentaro Kato¹, Osamu Hirota¹; ¹Tamagawa Univ., Japan. A real-time 1.5-Gb/s Y-00 quantum stream cipher transmission for secure optical communication is experimentally demonstrated. An error-free (BER < 10⁻⁹) transmission of 4096-level intensity-modulation cipher signals is achieved in a dispersion-managed link over 1,000 km.

SW3O.5 • 14:00 **Invited**

Modeling and Mitigation of Nonlinear Effects in Uncompensated Coherent Optical Transmission Systems, Gabriella Bosco¹; ¹Politecnico di Torino, Italy. We review recent results on analytical modeling of non-linear interference in multi-span optical systems with high-order modulation and coherent detection, and on performance gains that can be achieved through non-linearity mitigation in digital coherent receivers.

CLEO: Applications & Technology

13:00–15:00

AW3P • A&T Topical Review on Progress in the Semiconductor Laser Technology II

AW3P.1 • 13:00 **Invited**

DFB Interband Cascade Laser Array for Mid Infrared Spectroscopy, Sven Höfling^{1,2}, Julian Scheuermann³, Robert Weih³, Martin Kamp¹, Johannes Koeth³; ¹Universität Würzburg, Germany; ²Univ. of St Andrews, UK; ³nanoplus GmbH, Germany. We demonstrate an interband cascade laser array with multiple spectrally monomode emitters monolithically integrated on a single chip. The targeted emission wavelengths cover the mid infrared regime from around 3.3 to 3.5 microns.

AW3P.2 • 13:30

High Brightness Operation in Broad Area Quantum Cascade Lasers with Reduced Number of Stages, Matthew Suttinger¹, Rowel Go¹, Ahmad Azim¹, Enrique Sanchez¹, Hong Shu¹, Arkadiy Lyakh¹; ¹Univ. of Central Florida, USA. Two 20 μm wide QCL structures demonstrate room temperature watt-level CW power with single lobed behavior. A figure of merit predicts broad area, fundamental mode behavior configurations for QCLs of identical wavelength and stage height.

AW3P.3 • 13:45

Si-based Mid-Infrared GeSn-Edge-Emitting Laser with Operating Temperature up to 260 K, Yiyin Zhou^{1,2}, Wei Dou¹, Wei Du⁴, Solomon Ojo^{1,2}, Huong Tran^{1,3}, Seyed Ghetmiri⁵, Jifeng Liu⁶, Greg Sun⁷, Richard Soref⁷, Joe Margetis⁸, John Tolle⁶, Baohua Li³, Zhong Chen¹, Mansour Mortazavi⁵, Shui-Qing Yu¹; ¹Dept. of Electrical Engineering, Univ. of Arkansas, USA; ²Microelectronics-Photonics Program, Univ. of Arkansas, USA; ³Arktonics, LLC, USA; ⁴Dept. of Electrical Engineering, Wilkes Univ., USA; ⁵Dept. of Chemistry and Physics, Univ. of Arkansas at Pine Bluff, USA; ⁶Thayer School of Engineering, Dartmouth College, USA; ⁷Dept. of Engineering, Univ. of Massachusetts Boston, USA; ⁸ASM, USA. We demonstrated optically pumped GeSn lasers with 20% maximum Sn content based on ridge waveguide with 5 and 20 μm ridge widths. The high operating temperature of 260 K was achieved with wider ridge device.

AW3P.4 • 14:00 **Invited**

Material Issues in GaN-based Laser Diode Manufacturing, Mike Leszczynski^{1,2}; ¹Inst. of High Pressure Physics, Poland; ²TopGaN, Poland. The first part of the talk will be devoted to blue and green laser diode applications: in lighting, RGB projectors, LiFi communication, quantum technologies and others. In the second part, I will present difficulties in growing AlGaInN. In particular, I will focus on point- and extended-defects.

13:00–15:00

AW3Q • A&T Topical Review on Advanced Design, Imaging and Process Technologies for Next Generation Semiconductors II

AW3Q.1 • 13:00

Reduction and Control of Edge Placement Error at the 5nm node Through a Holistic Approach. Robert Socha¹, ¹ASML, USA. Abstract note available.

AW3Q.2 • 13:30

Nanoscale Three-dimensional Patterning with Plasmonic Lithography. Jae W Hahn¹, ¹Yonsei University, South Korea. We fabricated nano-microscale 3D structures, such as a cone, microlens array, a nanoneedle, and a multiscale structure using a plasmonic lithography lithography system. The recent progress of the plasmonic lithography will be discussed.

AW3Q.3 • 14:00

Compensation of Optical Distortions in IC Fabrication. Yuri Granik¹, ¹Mentor Graphics, USA. Abstract not available.

JW3A • Sym on Coupling Artificial Atoms to Nano- & Opto-mechanical Systems I—Continued**JW3A.4 • 14:15**

Strain control of silicon-vacancy centers in diamond nanophotonic devices, Stefan Bogdanovic¹, Bartholomeus Machiels¹, Srujan Meesala¹, Scarlett Gauthier¹, Graham Joe¹, Michelle Chalupnik¹, Jeffrey Holzgrafe¹, Cleaven Chia¹, Mikhail Lukin¹, Marko Loncar¹; ¹Harvard Univ., USA. We present a nano-electromechanical platform for controlling optical transitions from spatially separated color centers in diamond waveguides. We use this technology to greatly suppress spectral diffusion and demonstrate entanglement between separate emitters.

JW3A.5 • 14:30

Dynamic Control of Spontaneous Emission Rate by Optomechanical Cavity QED System, Feng Tian^{2,1}, Hisashi Sumikura², Eiichi Kuramochi², Masato Takiguchi², Masaaki Ono², Akihiko Shinya², Masaya Notomi^{2,1}; ¹Tokyo Inst. of Technology, Japan; ²NTT Basic Research Labs, Japan. We demonstrate all-optical control of the spontaneous-emission rate within the emission lifetime in copper-doped-silicon nanobeam optomechanical cavities via mechanical oscillation driven by repetitive laser pulses, representing the first experimental realization of optomechanical cavity QED systems.

JW3A.6 • 14:45

Phonon-induced multi-color correlations in hBN single-photon emitters, Matthew Feldman^{2,1}, Claire Marvinnay¹, Alex Poretzky¹, Lucas Lindsay¹, Ethan Tucker¹, Dayl Briggs¹, Philip Evans¹, Richard F. Haglund², Benjamin Lawrie¹; ¹Oak Ridge National Lab, USA; ²Vanderbilt Univ., USA. We explore electron-phonon dynamics in hBN defects and observe $g^{(2)}(0)=0.20$ in a phonon replica and $g^{(2)}(0)=0.18$ between a phonon replica and the zero-phonon line, and we examine Purcell enhancement of phonon replicas with phononic cavities.

FW3B • Chip-scale Nonlinear Optics—Continued**FW3B.5 • 14:15**

Record High Squeezing Gain and Sensitivity in $\chi^{(2)}$ -based AlGaAs Parametric Amplifiers, Zhizhong Yan¹, Haoyu He¹, Han Liu¹, Meng Lu¹, Osman Ahmed¹, Eric Chen¹, Youichi Akasaka², Tadashi Ikeuchi², Amr S. Helmy¹; ¹Univ. of Toronto, Canada; ²Fujitsu Labs of America, USA. Record squeezing, with squeezing parameter $r \approx 2.5$ is measured in AlGaAs optical parametric amplifiers using an ultrafast pump centered at 775 nm. Polarization dependent squeezing and parametric gain were obtained with sub-photon per pulse amplifier sensitivity at 1550 nm regime.

FW3B.6 • 14:30

Laser Beat-Wave Induced Enhancement of the Kerr Nonlinearity in Bulk GaAs at 10 μ m, Daniel A. Matteo¹, Jeremy Pigeon¹, Sergei Tochitsky¹, Ulrich Huttner², Mackillo Kira³, Stephan W. Koch^{2,4}, Jerome V. Moloney⁴, Chan Joshi¹; ¹Dept. of Electrical Engineering, Univ. of California Los Angeles, USA; ²Dept. of Physics and Material Sciences Center, Philipps-Universität Marburg, Germany; ³Dept. of Electrical Engineering and Computer Science, Univ. of Michigan, USA; ⁴College of Optical Sciences, Univ. of Arizona, USA. We experimentally and theoretically demonstrate enhancement of the Kerr nonlinearity in semi-insulating GaAs through four-wave mixing of a CO₂ laser beat-wave. Nonlinearity increases with decreasing beat frequency, attributed to nonlinear currents modulated by the beat-wave.

FW3B.7 • 14:45

Wide Bandwidth, Nonmagnetic Linear Optical Isolators based on Frequency Conversion, Tengfei Li¹, Kamal Abdelsalam², Sasan Fathpour², Jacob Khurgin¹; ¹Electrical and Computer Engineering, Johns Hopkins Univ., USA; ²The College of Optics & Photonics, Univ. of Central Florida, USA. We propose a family of nonmagnetic optical isolators based on waveguide frequency conversion and characterized by good isolation properties, high linearity, bandwidth as high as a few THz.

FW3C • Generation & Control of Light Emission at the Nanoscale—Continued**FW3C.5 • 14:15**

Deterministic nanoprinting of single fluorescent molecules, Claudio U. Hail¹, Christian Höller¹, Korenobi Matsuzaki², Rohner Patrik¹, Jan Renger², Vahid Sandoghdar², Dimos Poulikakos¹, Hadi Eghlidi¹; ¹ETH Zürich, Switzerland; ²Max Planck Inst. for the Science of Light, Germany. We report direct non-contact electrohydrodynamic nanodrip printing of a countable number of photostable fluorescent molecules in a host crystal of nanoscopic dimensions with single molecule specificity, high spatial resolution and deterministic dipole orientation.

FW3C.6 • 14:30

nanoLED Wavelength Division Multiplexer Analysis, Sean M. Hooten¹, Nicolas M. Andrade¹, Seth A. Fortuna¹, Kevin Han¹, Ming Wu¹, Eli Yablonovitch¹; ¹Univ. of California Berkeley, USA. Optical antennas can enhance the modulation bandwidth and output power of nanoscale LEDs. Here we analyze a wavelength division multiplexer that uses high Q optical antennas to further increase the total optical power.

FW3C.7 • 14:45

Waveguide Coupling of an Integrated Nanowire Laser on Silicon with Enhanced End-Facet Reflectivity, Jochen Bissinger¹, Daniel Ruhstorfer¹, Thomas Stettner¹, Gregor Koblmüller¹, Jonathan J. Finley¹; ¹Physic Dept., Walter Schottky Institut, Germany. We numerically explored the coupling characteristics and the critical interplay with the end-facet reflectivities of nanowire lasers coupled to proximal silicon-waveguides. A proper waveguide design enables high coupling efficiencies with enhanced end-facet reflectivities of ~83%.

15:00–17:00 Coffee Break & Dessert (Exhibit Only Time), Exhibit Halls 1-3

Coffee Break Sponsored by  COHERENT and  THORLABS

15:30–17:00 Product Showcases, Exhibit Hall Theater I

CLEO: QELS-Fundamental
ScienceFW3D • Topological Photonics III—
Continued

FW3D.6 • 14:15

Wideband Slow Light in a Photonic Topological Insulator, Jonathan Guglielmon¹, Mikael C. Rechtsman¹; ¹*Pennsylvania State Univ., USA*. We demonstrate that chiral edge states can be used to generate wideband slow light. This is achieved by producing an edge state that winds many times around the Brillouin zone as it crosses the bandgap.

FW3D.7 • 14:30

Magnetic Gauge Field for Photons in Synthetic Dimensions by a Propagation-Invariant Photonic Structure, Liat Nemirovsky¹, Moshe-Ishay Cohen¹, Eran Lustig¹, Mordechai Segev¹; ¹*Technion, Israel*. We propose a system that exhibits an effective magnetic field for photons in synthetic - dimensions, implemented by a propagation-invariant (static) potential. The spectrum of this synthetic-space system displays Landau levels.

FW3D.8 • 14:45

Switching light at the interface between anomalous Floquet topological insulators, Francesco Piccioli¹, Lukas Maczewsky¹, Mark Kremer¹, Matthias Heinrich¹, Alexander Szameit¹; ¹*Inst. of Physics, Univ. of Rostock, Germany*. We study interface states at the boundary between two Anomalous Floquet Photonic Topological Insulators and show how their interactions with an chiral edge mode can be used to switch it via the wave number.

CLEO: Science & Innovations

SW3E • Ultrafast Metrology—Continued

SW3E.5 • 14:15

Active f-to-2f interferometer for record-low jitter carrier-envelope phase locking, Ruoyu Liao^{1,2}, Haochen Tian¹, Tianli Feng², Youjian Song¹, Ming-lie Hu¹, Günter Steinmeyer^{2,3}; ¹*Tianjin Univ., China*; ²*Max Born Inst. for Nonlinear Optics and Short Pulse Spectroscopy, Germany*; ³*Humboldt Universität zu Berlin, Germany*. Introduction of optical gain into the infrared arm of f-to-2f interferometers is demonstrated to improve signal-to-noise ratios by > 20 dB. This opens a perspective for CEP stabilization of unstabilizable lasers.

SW3E.6 • 14:30

Single-shot CEP drift measurement at arbitrary repetition rate based on dispersive Fourier transform, Máté Kurucz¹, Szabolcs Tóth¹, Roland Flender¹, Ludovít Haizer¹, Balint Kiss¹, Benjamin Perseille², Eric Cormier²; ¹*ELI-ALPS, Hungary*; ²*Centre Lasers Intenses et Applications, France*. Arbitrary repetition-rate single-shot CEP drift measurement technique is achieved based on dispersive Fourier transform. The technique is validated by comparing the results to an independent measurement. Further improvement is presented allowing jitter-free CEP drift extraction.

SW3E.7 • 14:45

Time-domain vectorial field reconstruction of a circularly polarized harmonic from silicon using 2D spectral shearing interferometry, Fabian Scheiba^{1,2}, Nicolai Klemke^{1,2}, Nicolas Tancogne-Dejean^{1,3}, Giulio Maria Rossi^{1,2}, Angel Rubio^{1,3}, Oliver D. Mücke^{1,4}, Franz Kartner^{1,2}; ¹*Center for Free-Electron Laser Science CFEL, Deutsches Elektronen-Synchrotron DESY, Germany*; ²*Physics Dept., Univ. of Hamburg, Germany*; ³*Max Planck Inst. for the Structure and Dynamics of Matter, Germany*; ⁴*The Hamburg Centre for Ultrafast Imaging, Germany*. A two-dimensional spectral shearing interferometry is demonstrated permitting to reconstruct vectorial optical fields with picojoule energy. As proof of principle, we retrieve the circularly polarized third-harmonic field emitted from 2- μm -thin silicon driven by 2.1- μm pulses.

SW3F • Terahertz Plasmonics—Continued

SW3F.5 • 14:15

Dielectric Membrane Mie-Resonant Metasurfaces, Quanlong Yang^{1,2}, Sergey S. Kruk¹, Yogesh K. Srivastava³, Kirill Koshelev³, Ranjan Singh³, Jiaguang Han², Yuri S. Kivshar¹, Ilya Shadrivov¹; ¹*Australian National Univ., Australia*; ²*Tianjin Univ., China*; ³*Nanyang Technological Univ., Singapore*. We introduce a novel concept of dielectric Mie-resonant membrane metasurfaces for the THz spectral region and fabricated from a free-standing silicon wafer. The metasurfaces support Mie resonances providing a 2π phase coverage and high transmission.

SW3F.6 • 14:30

Reconfigurable MEMS metasurface for active tuning of Fano resonance and logic gate operations at THz frequencies, Manukumara Manjappa^{1,2}, Prakash Pitchappa^{1,2}, Navab Singh³, Nan Wang³, Nikolay I. Zheludev^{2,4}, Chengkuo Lee⁵, Ranjan Singh^{1,2}; ¹*Division of Physics and Applied Physics, School of Physical and Mathematical Sciences, Nanyang Technological Univ., Singapore*; ²*Centre for Disruptive Photonic Technologies, The Photonics Inst., Nanyang Technological Univ., Singapore*; ³*Inst. of Microelectronics, A-star Inst., Singapore*; ⁴*Optoelectronics Research Centre and Centre for Photonic Metamaterials, Univ. of Southampton, UK*; ⁵*Dept. of Electrical & Computer Engineering, National University of Singapore, Singapore*. We experimentally show the excitation of sharp Fano resonances in a MEMS reconfigurable metasurface exhibiting multiple-input-output states in its electro-optical properties. Further, a set of composite logic gates such as exclusive-OR and XNOR are readout using THz pulse.

SW3F.7 • 14:45

500 GHz Plasmonic Mach-Zehnder Modulator, Maurizio Burla¹, Claudia Hoessbacher¹, Wolfgang Heni¹, Christian Haffner¹, Yuriy Fedoryshyn¹, Dominik Werner¹, Tatsuhiko Watanabe¹, Hermann Massler², Delwin L. Elder², Larry R. Dalton³, Juerg Leuthold¹; ¹*ETH Zurich, Switzerland*; ²*Fraunhofer IAF, Germany*; ³*Dept. of Chemistry, Univ. of Washington, USA*. We experimentally demonstrate a plasmonic modulator for sub-THz applications, featuring – at the same time – a short length of 10s of micrometers, high linearity, and a record-high flat frequency response beyond 500 GHz.

15:00–17:00 Coffee Break & Dessert (Exhibit Only Time), Exhibit Halls 1-3

Coffee Break Sponsored by  COHERENT and  THORLABS

15:30–17:00 Product Showcases, Exhibit Hall Theater I

CLEO: Science & Innovations

CLEO: Applications
& TechnologySW3G • Frequency Combs & Stable Laser
Systems—Continued

SW3G.6 • 14:15

Repetition-Rate Multiplication of Mode-locked Lasers Using Harmonic Injection Locking and Gain-Saturated SOA, Chan-Gi Jeon¹, Xiao-Zhou Li¹, Shilong Pan², Jungwon Kim¹; ¹South Korea Advanced Inst of Science & Tech, South Korea (the Republic of); ²Nanjing Univ. of Aeronautics and Astronautics, China. Low-noise repetition-rate multiplication method is proposed by combining harmonic injection locking and gain-saturated SOA. A 1-GHz optical pulse train with 33-dB side-mode-suppression-ratio, 3% modulation depth, and 6.3-fs absolute rms timing jitter [10kHz–1MHz] is demonstrated.

SW3G.7 • 14:30

Laser frequency stabilization at $\leq 10^{-16}$ from a thermal atomic beam, Judith Olson^{1,2}, Richard Fox¹, Tara M. Fortier¹, Chris Oates¹, Andrew Ludlow¹; ¹Optical Frequency Measurements, National Inst. of Standards and Technology, USA; ²Physics, Univ. of Colorado Boulder, USA. We describe a system for ultra-stable laser frequency generation using Ramsey-Borde interferometry with atomic calcium. Unprecedented frequency instabilities from a thermal ensemble are demonstrated.

SW3G.8 • 14:45

An iodine-stabilized laser at the telecom wavelength using a dual-pitch PPLN waveguide, Kohei Ikeda^{1,3}, Chaoyun Chen^{1,3}, Kazumichi Yoshii^{1,3}, Sho Okubo^{2,3}, Ken Kashiwagi^{2,3}, Hajime Inaba^{2,3}, Feng-Lei Hong^{1,3}; ¹Yokohama National Univ., Japan; ²National Metrology Inst. of Japan, AIST, Japan; ³JST, ERATO IOS, Japan. We demonstrate third harmonic generation of a 1542-nm laser using a dual-pitch PPLN waveguide with a chirped polling period. The laser is used for saturation spectroscopy of molecular iodine at 514 nm.

SW3H • Nonlinear Optical Phenomena—
Continued

SW3H.6 • 14:15

Power spectral density analysis of relative phase jitter in a twin-soliton molecule, Haochen Tian¹, Defeng Zhou¹, Yuwei Zhao¹, Youjian Song¹, Ming-lie Hu¹; ¹Tianjin Univ., China. We characterized high-frequency relative phase jitter power spectral density of soliton molecules generated from a passively mode-locked Er:fiber laser based on tracking fast shifts of an spectral interference fringe.

SW3H.7 • 14:30

Enhancing SOI Waveguide Nonlinearities via Microring Resonators, Thomas Ferreira de Lima¹, Hsuan-Tung Peng¹, Mitchell A. Nahmias¹, Chaoran Huang¹, Siamak Abbaslou¹, Alexander N. Tait¹, Bhavin J. Shastri¹, Paul R. Prucnal¹; ¹Princeton Univ., USA. All-optical devices can exploit a suite of nonlinearities in silicon photonics. We study how microring resonators (MRRs) harness these nonlinearities, with theoretical model and experimental validation. Free-carrier effects will practically always dominate Kerr in MRRs.

SW3H.8 • 14:45

Plasmonically Enhanced Nonlinear Generation via a Hybridized Nanopatch Antenna, Andrew J. Traverso¹, Tamra M. Nebabu², Virginia D. Wheeler³, Maiken H. Mikkelsen^{1,2}; ¹Physics, Duke Univ., USA; ²Electrical and Computer Engineering, Duke Univ., USA; ³USA Naval Research Lab, USA. We demonstrate enhanced second harmonic generation by coupling an ultra-thin nonlinear dielectric into the gap-mode of the plasmonic nanopatch antenna. A 10^3 -fold enhancement is achieved relative to the bare dielectric producing up to 3×10^7 photons/s.

AW3I • Laser-formed Structures & Additive
Manufacturing—Continued

AW3I.5 • 14:15

Absorptivity and energy scaling associated with laser powder bed fusion additive manufacturing, Manyalibo J. Matthews¹, Jianchao Ye¹, Leonidas Gargalis², Gabe Guss¹, Saad Khairallah¹, Alexander Rubenchik¹; ¹Lawrence Livermore National Lab, USA; ²Univ. of Nottingham, UK. In situ absorptivity measurements and finite element modeling are used to characterize energy coupling mechanisms and scaling behavior in laser powder bed fusion additive manufacturing. A universal relationship is derived that predicts melt depth and absorptivity.

AW3I.6 • 14:30

On-line Quantitative Analyzing of Molten Alloy Ingredient in Industrial Vacuum Smelting Process Using Laser-Induced Breakdown Spectroscopy, Zhao Tianzhuo^{1,2}, Xin Li^{2,1}, Qixiu Zhong^{2,1}, Hong Xiao¹, Shuzhen Nie¹, Fuqiang Lian¹, Sining Sun³, Zhongwei Fan^{1,2}; ¹Academy of Opto-electronics, Chinese Academy of Sciences, China; ²Academy of Opto-electronics, Univ. of Chinese Academy of Sciences, China; ³Beijing GK Laser Technology Co., Ltd., China. Laser-induced breakdown spectroscopy is used to quantitative analyze molten alloy ingredient in a 2-ton vacuum induction melt furnace. Measurements relative standard deviation of the main elements is 2~10%, trace element (< 0.2%) is lower than 25%.

AW3I.7 • 14:45

Laser Ignition of Cryogenic Propellants in Space Propulsion, Robert G. Stützer¹, Jan Deeken¹, Justin Hardi¹, Dmitry Suslov¹, Michael Börner¹, Michael Oswald¹; ¹German Aerospace Center, Germany. A Q-switched laser system was applied to a research rocket combustor in order to ignite cryogenic propellants by inducing several plasma breakdown events. The optical emission was analyzed using LIBS and other techniques.

15:00–17:00 Coffee Break & Dessert (Exhibit Only Time), Exhibit Halls 1-3

Coffee Break Sponsored by  COHERENT and  THORLABS

15:30–17:00 Product Showcases, Exhibit Hall Theater I

Meeting Room
211 C/D

CLEO: Science & Innovations

SW3J • Photonic Sensing & Mid-infrared Photonics—Continued

SW3J.3 • 14:15

InSb Nanostructures as selective absorbers in the Short and Mid-Wave Infrared, Nicholas Collins¹, Amit Solanki¹, Han-Don Um¹, Ruizhi Huang¹, Fawwaz Habbal¹; ¹Harvard Univ., USA. We demonstrated through a series of electromagnetic simulations and FTIR measurements a proof of concept for using vertically aligned arrays of InSb nanostructures as devices for selective SWIR and MWIR light absorption.

SW3J.4 • 14:30

Suspended group III-V waveguides integrated on silicon substrates for mid-infrared photonics, Jeff Chiles¹, Eric J. Stanton¹, Nima Nader¹, Jeff Shainline¹, Sae Woo Nam¹, Richard P. Mirin¹; ¹NIIST, USA. We demonstrate wafer-scale integration of suspended Al_{0.32}Ga_{0.68}As nanophotonic waveguides on silicon substrates. Micro-ring resonators are fabricated and measured at $\lambda = 1545$ and 2305 nm, showing loaded quality factors of 740,000 and 450,000, respectively.

SW3J.5 • 14:45

Hyperuniform Disordered Polarizers for the Mid-Infrared, Milan Milosevic¹, Wen Zhou², Hon Ki Tsang², Ahmed Osman¹, Stevan Stankovic¹, Yanli Qi¹, Milos Nedeljkovic¹, Zhibo Qu¹, Xingzhao Yan¹, Ali Khokhar¹, Graham T. Reed¹, Goran Mashanovich¹; ¹Zepler Inst. for Photonics and Nanoelectronics, Optoelectronics Research Centre, Univ. of Southampton, UK; ²Dept. of Electronic Engineering, The Chinese Univ. of Hong Kong, Hong Kong. We report on the design, fabrication and characterisation of silicon-on-insulator hyperuniform disordered polarisers at mid-infrared wavelengths. Small device footprint and large operational bandwidth revealed great potential of hyperuniform disordered platform for integrated photonics.

Meeting Room
212 A/B

CLEO: Applications & Technology

AW3K • Optical Solutions for Autonomous Driving—Continued

AW3K.5 • 14:15

Mid-Infrared 2-D Beam Steering, Jason Midkiff¹, Swapnajt Chakravarty², Kyoung Min Yoo¹, Ray T. Chen^{1,2}; ¹Univ. of Texas, USA; ²Omega Optics, USA. We will experimentally demonstrate optical beam steering in the mid-IR spectral region (around $\lambda=4.6\mu\text{m}$) in the InP/InGaAs platform. Both wavelength and phase tuning are utilized for two-dimensional (2D) steering in elevation and azimuthal directions respectively.

AW3K.6 • 14:30

A High-Compactness Electrically Controlled Beam-Steering Chip, Guanzhong Pan¹, Chen Xu¹, Yiyang Xie¹, Yibo Dong¹, Qiuhua Wang¹, Hongda Chen²; ¹Beijing Univ. of Technology, China; ²Inst. of Semiconductor, Chinese Academy of Sciences, China. A novel high-compactness electrically controlled beam-steering chip was achieved via integrating a liquid crystal optical phased array directly on a coherently coupled VCSEL array. One-dimensional beam steering was successfully realized by the chip.

AW3K.7 • 14:45

Multi-order Laser Beam Steering with Digital Micro Mirror Device for High-speed LIDARS, Joshua M. Rodriguez¹, Brandon Hellman¹, Braden Smith¹, Heejoo Choi¹, Dae Wook Kim¹, Yuzuru Takashima¹; ¹Univ. of Arizona, USA. Multi-order DMD based beam steering enables a fast beam steering that scan rate exceeds a frame rate of DMD, over tens of KHz, by redirecting laser pulses to multiple directions within couple of ms timeframe.

Meeting Room
212 C/D

CLEO: Science & Innovations

SW3L • Ultrasound, Photoacoustic, & Photothermal Sensing—Continued

SW3L.6 • 14:30

Photoacoustic spectrometer based on widely tunable mid-infrared pulsed optical parametric, Mikael Lassen¹, Laurent Lamard², David Balslev-Harder¹, Jan Petersen¹, Andre Peremans²; ¹Danish Fundamental Metrology, Denmark; ²Laserspec BVBA, 15 rue Trieux Scieurs, B-5020 Malonne, Belgium, Belgium. We demonstrate the usefulness of a nanosecond pulsed mid-infrared optical parametric oscillator for Photoacoustic spectroscopic measurements. Spectroscopic trace-gas measurements are demonstrated targeting environmental monitoring and breath gas analysis.

SW3L.7 • 14:45

Single-molecule Optical Absorption Imaging by Nanomechanical Photothermal Sensing at Room Temperature, Miao-Hsuan Chien¹, Mario Brameshuber², Benedikt Rosboth², Gerhard Schütz², Silvan Schmid¹; ¹Inst. of sensor and actuator system, TU Wien, Austria; ²Inst. of applied physics, TU Wien, Austria. A novel nanomechanical absorption-based microscopy with unprecedented sensitivity of $16 \text{ fW/Hz}^{1/2}$ is introduced with silicon nitride drum resonator. With 5-order-of-magnitudes higher sensitivity than the state-of-the-art technique, this study provides a sensitive label-free alternative for microscopy.

Wednesday, 13:00–15:00

15:00–17:00 Coffee Break & Dessert (Exhibit Only Time), Exhibit Halls 1-3

Coffee Break Sponsored by  COHERENT and  THORLABS

15:30–17:00 Product Showcases, Exhibit Hall Theater I

CLEO: QELS-Fundamental
ScienceFW3M • Ultrafast Spectroscopy in 2D
Materials & Heterostructures—Continued

FW3M.5 • 14:15

Nonlinear Interaction of Rydberg Exciton-Polaritons in Two-Dimensional WSe₂, Jie Gu^{1,2}, Lutz Waldecker³, Daniel Rhodes⁴, Alexandra Boehmke¹, Archana Raja⁵, Rian Koots¹, James Hone⁴, Tony Heinz², Vinod Menon^{1,2}; ¹Dept. of Physics, City College of New York, USA; ²Dept. of Physics, Graduate Center of the City Univ. of New York (CUNY), USA; ³Dept. of Applied Physics, Stanford Univ., USA; ⁴Dept. of Mechanical Engineering, Columbia Univ., USA; ⁵Kavli Energy NanoScience Inst., Univ. of California, USA. We demonstrate the formation of Rydberg exciton-polaritons in monolayer WSe₂ embedded in a microcavity and their 10X enhanced nonlinear interaction strength compared to the 1S exciton-polaritons owing to their larger size.

FW3M.6 • 14:30

1D and 2D like Exciton-Exciton Interactions in Atomically Thin Black Phosphorus, Vivek Pareek¹, Bala M. Mariserla^{1,2}, Andrew Winchester¹, Julien Madéo¹, Keshav M. Dani¹; ¹OIST Graduate Univ., Japan; ²School of Physical Sciences, Central Univ. of Karnataka, India. We study exciton-exciton annihilation in atomically black phosphorus using micro-transient absorption spectroscopy. Our results show a transition from 1D- to 2D-like interactions as we increase the exciton densities.

FW3M.7 • 14:45

Strong Exciton-Coherent Phonon Coupling In Single-Layer MoS₂, Chiara Trovatello¹, Henrique P. C. Miranda², Alejandro Molina-Sánchez², Rocío Borrego Varillas¹, Luca Moretti¹, Lucia Ganzer¹, Margherita Maiuri¹, Giancarlo Soavi³, Andrea C. Ferrari³, Andrea Marini⁵, Ludger Wirtz⁶, Giulio Cerullo^{1,7}, Davide Sangalli⁵, Stefano Dal Conte¹; ¹Politecnico di Milano, Italy; ²Inst. of Condensed Matter and Nanoscience, Université catholique de Louvain, Belgium; ³Cambridge Graphene Center, Univ. of Cambridge, UK; ⁴Inst. of Materials Science, Univ. of Valencia, Spain; ⁵Division of Ultrafast Process in Materials, Area della Ricerca di Roma 1, Italy; ⁶Université du Luxembourg, Luxembourg; ⁷IFN-CNR, Italy. We use broadband optical pump-probe spectroscopy to study coherent optical phonons in 1L-MoS₂. We detect a strong coupling with the A₁' mode, which is enhanced around the C-exciton peak. Ab-initio calculations of the phonon-induced band structure variation fully confirm this result.

CLEO: Science & Innovations

SW3N • Cascade Lasers—Continued

SW3N.5 • 14:30

High-power edge-emitting terahertz plasmonic quantum-cascade laser, Yuan Jin¹, Liang Gao¹, John Reno², Sushil Kumar¹; ¹Lehigh Univ., USA; ²Sandia National Labs, USA. A scheme to phase-lock multiple terahertz plasmonic microcavities is developed that establishes coherent plasmonic mode traveling in air. Using quantum-cascade gain media, a 3.3THz edge-emitting plasmonic laser with record-high peak output-power of 256mW is demonstrated.

SW3N.6 • 14:45

Controlling the Likelihood of Extreme Pulses in a Quantum Cascade Laser with Optical Feedback and Bias Perturbation, Olivier Spitz^{1,2}, Jia-Gui Wu^{3,4}, Mathieu Carras², Chee Wei Wong³, Frederic Grillot^{1,5}; ¹Télécom ParisTech, France; ²mirSense, France; ³Univ. of California Los Angeles, USA; ⁴Southwest Univ., China; ⁵Univ. of New Mexico, USA. We experimentally generate controllable extreme pulses in a mid-infrared quantum cascade laser with external optical injection and square wave perturbation.

SW3O • Long Distance Transmission—Continued

SW3O.6 • 14:30

Impact of Laser Phase Noise on Nonlinear Frequency Division Multiplexing Systems, Francesco Da Ros¹, Simone Gaiarin¹, Darko Zibar¹; ¹DTU Fotonik, Denmark. The impact of Wiener phase noise on NFDm transmission is experimentally investigated for dual-polarization discrete NFDm systems. The results show minimal OSNR penalty in back-to-back and limited degradation for 2000-km transmission for 750-kHz and 100-kHz linewidth, respectively.

SW3O.7 • 14:45

Frequency Modulation Supported Long-haul Transmission Enabled by Nonlinear Equalization with a Low-cost DML, Shaohua Hu¹, Pingping Lei¹, Jing Zhang¹, Yuzhong Feng¹, Xingwen Yi², Kun Qiu¹; ¹Univ. of Electronic Science & Tech China, China; ²Sun Yat-Sen Univ., China. We experimentally demonstrate an FM-supported 23 Gb/s PAM-4 coherent transmission over 2800 km SSMF utilizing a low-cost DML. The nonlinear equalizers are effective to enable the FM signal recovery.

15:00–17:00 Coffee Break & Dessert (Exhibit Only Time), Exhibit Halls 1-3

Coffee Break Sponsored by  COHERENT and  THORLABS

15:30–17:00 Product Showcases, Exhibit Hall Theater I

CLEO: Applications & Technology

AW3P • A&T Topical Review on Progress in the Semiconductor Laser Technology II—Continued

AW3Q • A&T Topical Review on Advanced Design, Imaging and Process Technologies for Next Generation Semiconductors II—Continued

AW3P.5 • 14:30 **Invited**

Development of Terahertz Quantum-Cascade Lasers for Satellite-Borne Measurement of Key Gas Species. Alexander Valavanis¹, Yingjun Han¹, Eleanor Nuttall¹, Esam Zafar¹, Diego Pardo², Olivier Auriacombe², Thomas Rawlings², Nart Daghestani², Edmund H. Linfield¹, Brian N. Ellison² and A. Giles Davies²; ¹*School of Electronic and Electrical Engineering, University of Leeds, UK*, ²*STFC Rutherford Appleton Laboratory, UK*. We present key developments towards atmospheric chemistry studies using terahertz quantum-cascade lasers (QCLs), including ~1-cm³-scale integration of THz QCLs with waveguides and antennas using precision micromachining, and broadband multimode spectroscopy based on detector-free self-mixing.

15:00–17:00 Coffee Break & Dessert (Exhibit Only Time), Exhibit Halls 1-3

Coffee Break Sponsored by  **COHERENT** and  **THORLABS**

15:30–17:00 Product Showcases, Exhibit Hall Theater I

Executive Ballroom
210A

Joint

17:00–19:00

JW4A • Sym on Coupling Artificial Atoms to Nano- & Opto-mechanical Systems II

President: To Be Announced

JW4A.1 • 17:00 **Invited**

Phonon networks with SiV centers in diamond waveguides, Peter Rabl¹; ¹TU Wien, Austria. In this talk I will discuss recent theoretical ideas for realizing controlled spin-phonon interactions and scalable phononic quantum networks with silicon-vacancy centers coupled to propagating acoustic modes in diamond waveguides.

JW4A.2 • 17:30 **Invited**

Creating Quantum States of Sound with Superconducting Qubits, Yiwen Chu^{2,1}; ¹Yale Univ., USA; ²Physics, ETH Zurich, Switzerland. I will describe our recent experiments involving a high frequency bulk acoustic wave resonator strongly coupled to a superconducting qubit. We use this device to demonstrate quantum operations on the system, including the creation and measurement of quantum mechanical states such as phonon Fock states.

JW4A.3 • 18:00 **Invited**

Quantum Control of Spins in Silicon Carbide with Photons and Phonons, David Awschalom¹; ¹Univ. of Chicago, USA. Isolated spins in silicon carbide are optically probed, revealing long spin coherence times and high-fidelity quantum control. Gaussian surface acoustic wave resonators mechanically drive coherent Rabi oscillations using phonons that are imaged with focused x-rays.

Executive Ballroom
210B

CLEO: QELS-Fundamental
Science

17:00–19:00

FW4B • Nanoscale Nonlinear Optics

President: To Be Announced

FW4B.1 • 17:00

A Hybrid Dielectric-Semiconductor Resonant Nanostructure for Broadband and Efficient Second-Harmonic Generation, Raktim Sarma¹, Domenico de Ceglia², Nishant Nookala³, Maria Antonietta Vincenti⁴, Salvatore Campione¹, Omri Wolf³, Michael Scalora⁵, Mikhail A. Belkin³, Igal Brener¹; ¹Sandia National Labs, USA; ²Univ. of Padova, Italy; ³Univ. of Texas at Austin, USA; ⁴Univ. of Brescia, Italy; ⁵US Army AMRDEC, USA. We experimentally demonstrate a novel approach of coupling leaky-mode resonances in dielectric nanostructures to intersubband transitions in semiconductor quantum wells to realize an ultrathin hybrid device with broadband and high second-harmonic generation efficiency.

FW4B.2 • 17:15

Electrically Tunable Dynamic Phase Modulation Enhanced Second Harmonic Generation of Dielectric Metasurfaces, Xuexue Guo¹, Yimin Ding¹, Xingjie Ni¹; ¹Pennsylvania State Univ., USA. Taking advantage of the dynamic phase modulation arisen from the interaction of dc electrical and optical field, we create super-quadratic field dependent second harmonic generation (SHG) with ultra-high ON/OFF ratio of 15000 on a dielectric metasurface.

FW4B.3 • 17:30

Observation of Extraordinary SHG from All-Dielectric Nanoantennas Governed by Bound States in the Continuum, Kirill Koshelev^{1,2}, Sergey Kruk¹, Jae-Hyuck Choi³, Elizaveta V. Melik-Gaykazyan^{1,4}, Daria Smirnova^{1,5}, Hong-Gyu Park³, Yuri S. Kivshar^{1,2}; ¹Australian National Univ., Australia; ²Dept. of Nanophotonics and Metamaterials, ITMO Univ., Russia; ³Dept. of Physics, South Korea Univ., South Korea (the Republic of); ⁴Faculty of Physics, Lomonosov Moscow State Univ., Russia; ⁵Inst. of Applied Physics, Russia. We observe record-high efficiency of the second-harmonic generation from AlGaAs nanoantennas fabricated on a transparent substrate and pumped with structured light. The engineered nanoantennas exhibit high-quality optical resonances governed by quasi-bound states in the continuum.

FW4B.4 • 18:00

Disorder-Robust Nonlinear Light Generation in Topological Nanostructures, Sergey S. Kruk¹, Alexander Poddubny^{1,2}, Daria Smirnova¹, Ivan Kravchenko³, Barry Luther-Davies¹, Yuri S. Kivshar¹; ¹Australian National Univ., Australia; ²ITMO Univ., Russia; ³Oak Ridge National Lab, USA. We observe topologically nontrivial nonlinear edge states of light in zigzag arrays of silicon nanoparticles. We image the edge states via the third-harmonic generation and demonstrate their robustness against disorder and structural perturbations.

Executive Ballroom
210C

Joint

17:00–19:00

JW4C • Professional Development Session I

President: To Be Announced

New this year are Professional Development sessions organized by the CLEO Committee Chairs. For details please refer to the Program Update Sheet.

CLEO: QELS-Fundamental
Science

17:00–19:00

FW4D • Chirality, PT Symmetry, &
Exceptional Points

President: To Be Announced

FW4D.1 • 17:00

Chiral Metasurface Optomechanics, Simone Zanotto¹, Alessandro Tredicucci^{3,1}, Daniel Navarro-Urrios², Marco Cecchini¹, Giorgio Biasiol⁴, Alessandro Pitanti¹; ¹Istituto di Nanoscienze - CNR, Italy; ²Universitat de Barcelona, Spain; ³Università di Pisa, Italy; ⁴Istituto Officina dei Materiali, Italy. We report on mechanical action on light polarization, and its back-action effect, in a chiral metasurface. Our thin-film nanostructured semiconductor device may prove of relevance for fast polarization state generation and detection.

FW4D.2 • 17:30

Tunable Orbital Angular Momentum Microring Lasers Using Chiral Exceptional Points, William Hayenga¹, Jinhan Ren¹, Midya Parto¹, Fan Wu¹, Mohammad Hokmabadi¹, Christian Wolff², Ramy El-Ganainy³, N. Mortensen^{2,4}, Demetrios N. Christodoulides¹, Mercedeh Khajavikhan¹; ¹Univ. of Central Florida, CREOL, USA; ²Center for Nano Optics, Univ. of Southern Denmark, Denmark; ³Dept. of Physics and Henes Center for Quantum Phenomena, Michigan Technological Univ., USA; ⁴Danish Inst. for Advanced Study, Univ. of Southern Denmark, Denmark. A microring laser generating tunable orbital angular momentum states via chiral exceptional points is demonstrated. An incorporated inner S-bend waveguide construct provides an avenue to enforce unidirectional lasing in a predetermined manner.

FW4D.3 • 17:45

Photonic Spin Polarizer Using Phase-Cancellation Metasurface, Amr Shaltout¹, Jorik van de Groep¹, Yifei Wang¹, Mark Brongersma¹; ¹Stanford Univ., USA. Phase-cancellation metasurfaces are introduced to attenuate the transmission of specific optical mode using destructive interference, and used to implement a broadband circular polarizer with extinction ratio of 20 using silicon based dielectric nanostructures.

FW4D.4 • 18:00

Low Loss Propagation in a Metal-clad Waveguide via PT-Symmetry Breaking, Utsav D. Dave¹, Michal Lipson¹; ¹Electrical Engineering, Columbia Univ., USA. We demonstrate passive PT symmetry breaking between the spatial modes within a single SOI waveguide with metal deposited directly on top. By leveraging this effect, we show low propagation loss of < 1 dB for a 100 μm long, 10 μm wide waveguide partially covered with 100 nm thick metal.

CLEO: Science & Innovations

17:00–19:00

SW4E • Ultrafast Pulse Manipulation

President: Cristina Hernandez-Gomez;
Rutherford Appleton Laboratory, UK

SW4E.1 • 17:00

TW-Peak-Power Post-Compression of 70-mJ pulses from an Yb Amplifier, Guangyu Fan¹, Paolo Carpeggiani¹, Zhen-sheng Tao², Edgar Kaksis¹, Tadas Balciunas³, Gulio Coccia^{1,6}, Vincent Cardin⁴, François Légaré⁵, Bruno E. Schmidt⁶, Andrius Baltuska¹; ¹Inst. of Photonics, TU Wien, Austria; ²Dept. of Physics, Fudan Univ., China; ³Dept. of Applied Physics, Univ. of Geneva, Switzerland; ⁴Institut National de la Recherche Scientifique, Canada; ⁵few-cycle, Inc, Canada; ⁶Dipartimento di Fisica, Politecnico di Milano, Italy. We present the energy record achievement in single stage, stretched hollow core fiber compression. 1 μm , 220fs pulses, are compressed to 25fs, 40mJ with ~60% efficiency.

SW4E.2 • 17:15

Two-Stage Nonlinear Compression of a Yb:KGW Laser Amplifier to Sub-10 fs Duration, John E. Beetar¹, Federico Rivas¹, Shima Gholam Mirzaeimoghaddar¹, Yangyang Liu¹, Michael Chini^{1,2}; ¹Univ. of Central Florida, USA; ²CREOL, The College of Optics and Photonics, USA. We demonstrate the nonlinear compression of pulses from a commercial Yb:KGW laser amplifier using a two-stage hollow-core fiber and multi plate continuum compressor to below 9 fs duration with an overall system transmission of 60%.

SW4E.3 • 17:30

Optical Thin Film Compression for Laser Induced Plasma Diagnostics, Masruri Masruri¹, Jonathan Wheeler^{2,1}, Ioan Dancus¹, Riccardo Fabbri³, Andrei Naziru¹, Radu Secareanu¹, Daniel Ursescu¹, Gabriel Cojocar⁴, Razvan Ungureanu⁴, Deano Farinella⁵, Moana Pittman⁶, Sergey Mironov⁷, Septimiu Balascuta¹, Domenico Doria¹, David Ros⁵, Razvan Dabu¹; ¹ELI-NP, Romania; ²IZEST, France; ³European XFEL GmbH, Germany; ⁴CETAL-PW (INFLPR), Romania; ⁵Univ. of California at Irvine (UCI), USA; ⁶LASERIX (UPSud - LUMAT), France; ⁷Federal Research Center Inst. of Applied Physics of the Russian Academy of Science (IAP RAS), Russia. Zeonor thin film compressor based on self-phase modulation is presented as an ultrashort probe for a plasma diagnostics at ELI-NP. The capability of a compression factor more than two enables a probe of 10 fs.

SW4E.4 • 17:45

Relative-Phase Synchronization in a Sub-Cycle Parametric Waveform Synthesizer, Roland E. Mainz^{1,2}, Giulio Maria Rossi^{1,2}, Fabian Scheiba^{1,2}, Yudong Yang^{1,2}, Giovanni Cirmi^{1,2}, Franz Kärtner^{1,2}; ¹Center for Free-Electron Laser Science, Germany; ²Physics Dept. and the Hamburg Centre for Ultrafast Imaging, Germany. We compare two different methods for relative phase synchronization among two channels of a parallel parametric waveform synthesizer. The achieved stability allows for reproducible high-energy sub-cycle pulses capable to generate isolated attosecond pulses without gating.

SW4E.5 • 18:00

Phase-Locked Programmable Femtosecond Pulse Bursts from a Regenerative Amplifier, Tobias Flöry¹, Edgar Kaksis¹, Andrius Pugzlys^{1,2}, Andrius Baltuska^{1,2}, Gergő Krizsán^{3,4}, Gyula Polónyi^{3,4}, József Fülöp^{3,4}; ¹Photonik Institut, TU Wien, Austria; ²Center for Physical Sciences & Technology, Lithuania; ³Inst. of Physics, Univ. of Pécs, Hungary; ⁴ELI ALPS, Hungary. We demonstrate phase-controlled pulse-burst amplification based on differential pathlength stabilization between the master oscillator and the amplifier cavities. This technique boosts the safe level of extractable burst energy and suppresses fluctuations in various burst-mode applications.

17:00–19:00

SW4F • Terahertz Sources & Communication

President: Dam Mittleman, Brown Univ., USA

SW4F.1 • 17:00

Optimization and fabrication of two-quantum well THz QCLs operating above 200 K, Martin C. Franckie¹, Lorenzo Bosco¹, Mattias Beck¹, Elena Mavrona¹, Jérôme Faist¹; ¹ETH Zürich, Switzerland. We present the first THz quantum cascade laser operating above 200 K. The design is based on two quantum wells per period and was optimized using a non-equilibrium Green's function model.

SW4F.2 • 17:15

Heterogeneous THz quantum cascade lasers: Gain recovery dynamics study, Christian G. Derntl¹, Giacomo Scari², Mattias Beck², Jerome Faist², Karl Unterrainer¹, Juraj Darmo¹; ¹TU Wien, Austria; ²ETH Zürich, Switzerland. We present our investigations of the interactions between the individual stacks of a heterogeneous terahertz quantum cascade laser by measuring their gain recovery time with terahertz pump / terahertz probe time domain spectroscopy.

SW4F.3 • 17:30

20 GHz Continuous Electrical Tuning of a High-power Terahertz Distributed-feedback Laser, Liang Gao¹, Yuan Jin¹, John Reno², Sushil Kumar¹; ¹Lehigh Univ., USA; ²Sandia National Labs, USA. Large electrical tuning of 20GHz is demonstrated for a 3.3THz distributed-feedback quantum-cascade laser at 56K. A new scheme with phase-locked plasmonic microcavities realizes order-of-magnitude greater output-power and significantly improved far-field beam compared to previous results.

SW4F.4 • 17:45

Full W-band Frequency Measurement of THz Waves by Electro-Optic Sampling Using Modulator-Based Optical Comb Source, Isao Morohashi¹, Norihiko Sekine¹, Akifumi Kasamatsu¹, Iwao Hosako¹; ¹National Inst of Information & Comm Tech, Japan. We have demonstrated THz frequency measurement in the full W-band by optical heterodyne using optical combs. Full W-band signals were measured by sweeping the comb spacing on the range from 9 to 10.2 GHz.

SW4F.5 • 18:00 **Invited**

Coherent THz Pulse Generation and Radiation Based on a Fully-Electronic Digital-to-Impulse Technique Implemented in Silicon, Aydin Babakhani¹; ¹ECE, UCLA, USA. In this work, we present the technique of THz pulse generation and radiation based on a laser-free fully-electronic solution implemented in a 130nm SiGe technology. The silicon chip radiates a frequency comb with programmable comb spacing. The chip covers the entire frequency range from 30GHz to 1.1THz with frequency resolution of 2Hz.

CLEO: Science & Innovations

CLEO: Applications
& Technology

17:00–19:00

SW4G • Optical Frequency Synthesis & Microwave Generation

President: Franklyn Quinlan; NIST, USA

SW4G.1 • 17:00

Optically Generated 10-GHz Signal with 10 Microradian Residual Phase Instability, Takuma Nakamura¹, Josue Davila-Rodriguez¹, Holly Leopardi², Jeff A. Sherman¹, Tara M. Fortier^{1,2}, Xiaojun Xie³, Joe C. Campbell³, Scott A. Diddams^{1,2}, Franklyn Quinlan^{1,2}; ¹Time and Frequency Division, National Inst. of Standards and Tech, USA; ²Dept. of Physics, Univ. of Colorado Boulder, USA; ³Dept. of Electrical and Computer Engineering, Univ. of Virginia, USA. We demonstrate ultra-stable 10-GHz generation based on single-fiber-branch Er: fiber combs. Residual rms phase fluctuations were 10 microradians at 10 s, with corresponding fractional frequency instability of 5×10^{-17} at 1 s and 1×10^{-18} at 200 s.

SW4G.2 • 17:30

Ultra-low noise microwave generation using carrier-envelope-offset signal of 25-GHz EOM comb, Atsushi Ishizawa¹, Tadashi Nishikawa², Kenichi Hitachi¹, Kazutaka Hara^{1,2}, Kenya Hitomi^{1,2}, Tomoya Akatsuka¹, Tetsuomi Sogawa¹, Hideki Gotoh¹; ¹NTT Basic Research Labs, Japan; ²Tokyo Denki Univ., Japan. Using carrier-envelope-offset signal of a 25-GHz electro-optics-modulation comb, we demonstrated a record phase-noise reduction of a conventional signal generator and an unprecedented measurement of the absolute optical frequency at 12-order-of-magnitude accuracy without any optical reference.

SW4G.3 • 17:45

Free-running Monolithic Laser-based 8-GHz Photonic Microwave Generation, Manoj P. Kalubovilage², Mamoru Endo², Thomas R. Schibli^{2,1}; ¹JILA, USA; ²Physics, Univ. of Colorado Boulder, USA. An ultra-low noise 8-GHz microwave carrier was generated with a free-running monolithic mode-locked laser. The measured phase noise reached below -163 dBc/Hz at 10 kHz and -178 dBc/Hz at 100 kHz offsets.

SW4G.4 • 18:00

Phase locking of a tunable OEO to an optical frequency comb for microwave synthesis from an optical reference, Antoine Rolland¹, Naoya Kuse¹, Martin E. Fermann¹; ¹IMRA, USA. We phase lock a tunable OEO to an optically referenced stepped precision microwave reference provided with a fiber comb from intermodal beating, overcoming the common stability limits of direct digital synthesis in tunable microwave generation.

17:00–19:00

SW4H • Supercontinuum Generation

President: Jaime Cardenas; Univ. of Rochester, USA

SW4H.1 • 17:00

Polarization effects in silicon-nitride waveguides: Supercontinuum, carrier-envelope offset, and optical beatnotes, Lingfang Wang^{1,2}, Hongquan Li¹, David Carlson³, Scott B. Papp³, Leo Hollberg³; ¹HEPL & Dept. of Physics, Stanford Univ., USA; ²School of Optoelectronic Science and Engineering, Univ. of Electronic Science and Technology of China, China; ³Time and Frequency Division, National Inst. of Standards and Technology, USA. Polarization dependence of second/third-harmonic and supercontinuum generation in silicon-nitride waveguides is mapped from 350-1750 nm. We identify parameters suited for generating coherent signals near 500 and 1000 nm for optical clocks, f_{CEO} and beatnote detection.

SW4H.2 • 17:15

Few-cycle pulses and ultraflat supercontinuum with silicon-nitride waveguides, David R. Carlson¹, Phillips Hutchison¹, Daniel Hickstein¹, Scott B. Papp¹; ¹NIST, USA. We experimentally and numerically demonstrate few-cycle pulse generation in chip-integrated waveguides made from silicon nitride. When these pulses seed supercontinuum generation in two-section waveguides, coherent ultraflat spectra spanning more than an octave can be realized.

SW4H.3 • 17:30 **Invited**

Coherent Supercontinuum Generation in a Silicon Nitride Chip, Yoshitomo Okawachi¹; ¹Columbia Univ., USA. Advances in CMOS-compatible silicon technology offers a path towards chip-scale nonlinear photonic devices. I will discuss our recent work on on-chip supercontinuum generation in silicon-nitride waveguides for applications including spectroscopy, frequency metrology, and optical clocks.

SW4H.4 • 18:00

Lotus-like dual soliton generation and phase shifting in an 88 GHz high-order-mode-suppressed Si₃N₄ microring, Hao Liu¹, Jinghui Yang¹, Shu-Wei Huang², Mingbin Yu³, Dim Lee Kwong³, Chee Wei Wong¹; ¹Univ. of California Los Angeles, USA; ²Dept. of Electrical, Computer, and Energy Engineering, Univ. of Colorado Boulder, USA; ³Inst. of Microelectronics, A*STAR, Singapore. Here we report a unique lotus-like dual dissipative soliton spectrum generated in an 88 GHz tapered Si₃N₄ microring. The mode-locking nature is verified by both amplitude noise and FROG measurement. A continuous phase shifting of such state is successfully observed directly in frequency domain.

17:00–19:00

AW4I • Medical Devices & Systems

President: David Nolte; Animated Dynamic Inc, USA

AW4I.1 • 17:00 **Invited**

OCT with Multi-MHz Swept Lasers, Thomas Klein¹; ¹Optores GmbH, Germany. Recent developments in commercially available wavelength-swept lasers enable optical coherence tomography (OCT) in the multi-MHz range. These unprecedented speeds benefit a wide range of applications, including microangiography, industrial inspection, large-area surveys and OCT-guided surgery.

AW4I.2 • 17:30

Integrated Polyene Photonic Waveguides with Embedded Micromirrors for Light Delivery and Manipulation Deep into Tissue, Jay W. Reddy¹, Maya Lassiter¹, Ramgopal Venkateswaran¹, Maysamreza Chamanzar¹; ¹Electrical and Computer Engineering, Carnegie Mellon Univ., USA. We demonstrate flexible photonic waveguides realized in a biocompatible PDMS/Parylene C platform with broadband out-of-plane input/output coupling. The waveguides are packaged with laser diodes to realize a compact, fully functional photonic device for in-vivo applications.

AW4I.3 • 17:45

Label-free human brain and skin imaging enabled by Er: fiber-laser-based tunable ultrafast sources, Hsiang-Yu Chung^{1,2}, Rüdiger Greinert³, Markus Glatzel⁴, Franz Kärtner^{1,2}, Guoqing Chang⁵; ¹Center for Free-Electron Laser Science, DESY, Germany; ²Physics, Universität Hamburg, Germany; ³Skin Cancer Center Buxtehude, Germany; ⁴Inst. of Neuropathology, Univ. Medical Center Hamburg-Eppendorf, Germany; ⁵Beijing National Lab for Condensed Matter Physics, Inst. of Physics, Chinese Academy of Sciences, China. We demonstrate label-free multiphoton microscopy of human brain and skin tissues with an Er: fiber-laser-based ultrafast source that emits femtosecond pulses at 775 nm and 1250 nm.

CLEO: Science & Innovations

17:00–19:00

SW4J • Design & Simulation of Micro- & Nano-phonic Devices

Presider: Joyce Poon; University of Toronto, Canada

SW4J.1 • 17:00

Nanocavity based on a topological corner state in a two-dimensional photonic crystal, Yasutomo Ota¹, Ryota Katsumi², Katsuyuki Watanabe¹, Feng Liu³, Katsunori Wakabayashi^{3,4}, Satoshi Iwamoto^{1,2}, Yasuhiko Arakawa¹; ¹Nanoquine, The Univ. of Tokyo, Japan; ²ILS, The Univ. of Tokyo, Japan; ³Kwansei Gakuin Univ., Japan; ⁴National Inst. for Material Science, Japan. We demonstrate a photonic crystal nanocavity based on a topological corner state. The design exploits the hierarchical bulk-edge-corner correspondence for the two-dimensional photonic crystal, opening a deterministic route to introduce nanocavities in topological photonics platforms.

SW4J.2 • 17:15

Bloch-Floquet Waves in Optical Ring Resonators, Kathleen McGarvey-Lechable¹, Pablo Bianucci¹; ¹Concordia Univ., Canada. We develop a general theory of the modal coupling of degenerate resonances in optical ring resonators based on Bloch-Floquet theory. This theory can predict the splitting associated with this coupling in all the ring resonances.

SW4J.3 • 17:30

Inverse designed Fano resonance in Silicon microresonators, Kiyoul Yang¹, Jinhie Skarda¹, Michele Cotrufo², Geun Ho Ahn¹, Andrea Alu², Jelena Vuckovic¹; ¹Stanford Univ., USA; ²Univ. of Texas at Austin, USA. We demonstrate, for standard silicon resonators, that a Fano lineshape can be created in the response function by placing an inverse-designed reflector into the side-coupled waveguide. Inverse design allows for control of the Fano spectrum and small device footprint, with applications in photonics.

SW4J.4 • 17:45

An On-chip Full Poincaré Beam Emitter Based on an Optical Micro-ring Cavity, Wenbo Lin¹, Yasutomo Ota², Yasuhiko Arakawa², Satoshi Iwamoto^{1,2}; ¹Inst. of Industrial Science, The Univ. of Tokyo, Japan; ²Inst. of Nano Quantum Information Electronics, The Univ. of Tokyo, Japan. We numerically demonstrate an on-chip full Poincaré beam emitter. We employ a micro-ring resonator augmented with scatterer arrays, which synthesizes the Poincaré beam as a superposition of twisted beams carrying different orbital- and spin-angular momenta.

SW4J.5 • 18:00

Adjoint-based optimization of active nanophotonic devices, Jiahui Wang¹, Yu Shi¹, Tyler Hughes¹, Zhixin Zhao¹, Shanhui Fan¹; ¹Stanford, USA. We combine the adjoint variable method and the multi-frequency finite-difference frequency-domain method for systematic optimization of active nanophotonic devices. As an example, we numerically optimized a dynamic isolator which remains high isolation performance with half the modulation length.

CLEO: Applications & Technology

17:00–19:00

AW4K • Lidar

Presider: Fabio Di Teodoro; Raytheon SAS, USA

AW4K.1 • 17:00 Invited

Imaging through Flames with Coherent Laser Ranging, Esther Baumann¹, Eric W. Mitchell¹, Matthew S. Hoehler¹, Fabrizio R. Giorgetta¹, Torrey Hayden², Gregory B. Rieker², Nathan R. Newbury¹; ¹NIST, USA; ²Univ. of Colorado, USA. We show that coherent laser detection and ranging can see through flames and capture 3D images of a deforming object. A ranging precision of 30 μm through acetylene flame at a 2-meter stand-off is achieved.

AW4K.2 • 17:30

Absolute Distance Measurement with Large Non-ambiguous Range by an Electro-optic Triple-comb, Xianyu Zhao¹, Qu Xinghua¹, Fumin Zhang¹; ¹Tianjin Univ., China. We present a multi-heterodyne interferometry for long distance measurement. The synthetic wavelengths chain can be established through triple-comb with cascaded phase modulators. The experimental results demonstrated a relative ranging precision of about 7×10^{-7} .

AW4K.3 • 17:45

Frequency-modulated continuous-wave lidar using a phase-diversity coherent optical receiver for simultaneous ranging and velocimetry, Hongxiang Zhang¹, Kai Chen¹, Xu Zhongyang¹, Shilong Pan¹, Dan Zhu¹; ¹Nanjing Univ. of Aeronautics and As, China. Conventional FMCW lidar has ambiguous ranging and velocimetry if de-chirped frequency related to distance is close to Doppler frequency shift related to velocity, which is avoided in this work using a phase-diversity coherent optical receiver.

AW4K.4 • 18:00

A Basic Approach for Speed Profiling of Alternating Targets with Photonic Doppler Velocimetry, Mustafa M. Bayer¹, Rasul Torun¹, Imam Uz Zaman¹, Ozdal Boyraz¹; ¹Univ. of California Irvine, USA. Single tone continuous wave lidar system is utilized to construct the speed profile of an oscillating membrane by applying photonic Doppler velocimetry with amplitude-modulated light. Then short-time Fourier Transform is applied to acquire the profile.

CLEO: Science & Innovations

17:00–19:00

SW4L • Optical Detection of Vapors or Hazardous Environments

Presider: Erik Emmons; Edgewood Chemical Biological Center, USA

SW4L.1 • 17:00

Dual-comb laser system for time-resolved studies of fireballs in the MIR, Ryan T. Rhoades¹, Caroline Lecaplain¹, Peter G. Schunemann², R. J. Jones¹; ¹College of Optical Sciences, University of Arizona, USA; ²BAE Systems, USA. We present a high power all-fiber dual-comb system suitable for time-resolved spectroscopy measurements in the mid-infrared to study explosion dynamics and detection of chemical species.

SW4L.2 • 17:15

Broadband Infrared Laser Absorption Spectroscopy of High-explosive Detonations, Mark C. Phillips¹, Brian Brumfield¹, Bruce E. Bernacki¹, Sivanandan S. Harilal¹, Joel M. Schwallier², Nick Glumac²; ¹Pacific Northwest National Lab, USA; ²Mechanical Science & Engineering, Univ. of Illinois at Urbana-Champaign, USA. We measure time-resolved absorption spectra in high-explosive detonations using an external cavity quantum cascade laser swept over the range 2050-2300 cm^{-1} . Absorption from CO, CO₂, H₂O, N₂O, and particulates is characterized.

SW4L.3 • 17:30

Detection of isotopic shifts and hyperfine structures of uranium transitions using LIF of laser ablation plumes, Sivanandan S. Harilal¹, Bruce E. Bernacki¹, Mark C. Phillips¹; ¹Pacific Northwest National Lab, USA. We report isotopic shifts and hyperfine structures of selected U transitions employing tunable laser-induced fluorescence spectroscopy of laser ablation plumes.

SW4L.4 • 17:45

Standoff Detection of Uranyl Fluoride Using Ultrafast Laser Filamentation-induced Fluorescence, Patrick J. Skrodzki¹, Milos Burger¹, Lauren A. Finney¹, Frederic Poineau², Samundeeswari M. Balasekaran², Ken R. Czerwinski², Igor Jovanovic¹; ¹Univ. of Michigan, Ann Arbor, USA; ²Univ. of Nevada Las Vegas, USA. We demonstrate that femtosecond laser filamentation combined with time-resolved laser-induced fluorescence spectroscopy is viable for remote detection of uranyl fluoride, a powerful indicator of uranium enrichment activity.

SW4L.5 • 18:00

Hydrodynamics and Spatio-temporal Mapping of Oxide Formation in Laser-produced U Plasmas, Patrick J. Skrodzki¹, Milos Burger¹, Igor Jovanovic¹, Mark C. Phillips², Sivanandan S. Harilal²; ¹Univ. of Michigan, Ann Arbor, USA; ²Pacific Northwest National Lab, USA. We combine optical emission spectroscopy with hydrodynamic measurements in laser-produced uranium plasma in air to detect formation of higher uranium oxide states. Generation of uranium oxides reduces the excited atomic uranium population.

CLEO: QELS-Fundamental
Science

17:00–19:00

FW4M • Advanced Techniques &
Applications in Ultrafast SpectroscopyPresident: Daniele Brida, University of
Luxembourg, LuxembourgFW4M.1 • 17:00 **Invited**

Imaging the Motion of Charge with Time-Resolved Photoemission Electron Microscopy, Keshav M. Dani¹; ¹Okinawa Inst of Science & Technology, Japan. Combining photoemission electron microscopy with ultrafast pump-probe techniques, we make nanometer/femtosecond scale movies of photocarrier dynamics in semiconductor structures. Our movies capture the evolving, spatially-inhomogeneous photocarrier distribution in van der Waals heterostructures. They reveal new insights into photocarrier trapping at the nanoscale in perovskite photovoltaic films, and in charge-separation processes occurring at the surface of doped semiconductors.

FW4M.2 • 17:30

Time- and Angle-Resolved Photoemission Spectroscopy using an Ultrafast XUV Source at 21.8 eV, Yangyang Liu¹, John E. Beetar¹, Md M. Hosen¹, Gyanendra Dhakal¹, Christopher Sims¹, Marc Etienne¹, Firoza Kabir¹, Klaus Dimitri¹, Sabin Regmi¹, Madhab Neupane¹, Michael Chini¹; ¹Univ. of Central Florida, USA. We demonstrate a novel trARPES setup using high-order harmonic probe pulses produced from a moderately high power Yb: KGW amplifier. The surface band structure of Zr_2Te_2P is measured using a single harmonic at 21.8 eV.

FW4M.3 • 17:45

Laser cooling of semiconductors traced in the time domain, Jan F. Lippmann¹, Alfred Leitenstorfer¹, Denis Seletskiy^{2,1}; ¹Dept. of Physics and Center for Applied Photonics, Univ. of Konstanz, Germany; ²Dept. of Engineering Physics, Polytechnique Montréal, Canada. Despite tremendous progress in optical refrigeration of rare-earth-doped crystals, laser cooling in III-V semiconductors has not been demonstrated to date. Here we report first observation of cooling in GaAs/InGaP double heterostructures on a sub-nanosecond timescale.

FW4M.4 • 18:00

Ultrafast Magnetic Microscopy using High-Harmonic Radiation, Sergey Zayko¹, Ofer Kfir¹, Michael Heigl², Michael Lohmann¹, Murat Sivis¹, Manfred Albrecht², Claus Ropers^{1,3}; ¹Univ. of Göttingen, Germany; ²Experimentalphysik IV, Institut für Physik, Germany; ³International Center for Advanced Studies of Energy Conversion (ICASEC), Univ. of Göttingen, Germany. We report ultrafast nanoscale magnetic microscopy using high-harmonic radiation, reaching 19 nm spatial resolution. The femtosecond-scale demagnetization of worm-like magnetic domains in Co/Pd multilayers is quantitatively mapped with 50-fs temporal resolution.

CLEO: Science & Innovations

17:00–19:00

SW4N • High Power & Narrow Linewidth
LasersPresident: James Gupta, National Research
Council of Canada, Canada

SW4N.1 • 17:00

Supersymmetric Laser Arrays, Mohammad Parvinnezhad Hokmabadi¹, Nicholas Nye¹, Ramy El-Ganainy², Demetrios N. Christodoulides¹, Mercedeh Khajavikhan¹; ¹Univ. of Central Florida, USA; ²Physics, Michigan Technological Univ., USA. By harnessing notions from supersymmetry, we experimentally demonstrate a supersymmetric laser array that is capable of emitting exclusively in its fundamental transverse mode with a large radiance.

SW4N.2 • 17:15

Continuous Wave Green Lasing at Room Temperature in Two-Dimensional Photonic Crystal Perovskite Laser, Jiyoung Moon¹, Masoud Alahbakhshi¹, Abouzar Gharajeh¹, Ross Haroldson¹, Roberta Hawkins¹, Zhitong Li¹, Walter Hu^{1,2}, Anvar Zakhidov^{1,3}, Qing Gu¹; ¹The Univ. of Texas at Dallas, USA; ²Fudan Univ., China; ³ITMO Univ., Russia. Direct patterning of methylammonium lead bromide (MAPbBr₃) perovskite enabled green lasing in two-dimensional photonic crystal on the Si platform, under continuous wave pumping at room temperature for the first time.

SW4N.3 • 17:30 **Invited**

High-Power and High-Beam-Quality Photonic-Crystal Lasers, Susumu Noda¹; ¹Kyoto Univ., Japan. Recent progress in photonic crystal lasers is described. 10W-class high-power and high-beam quality ($M^2=2$) operation is successfully demonstrated using InGaAs/GaAs semiconductor systems. The extension to InGaN/GaN semiconductor systems is also discussed.

SW4N.4 • 18:00

Over 2W Room Temperature Lasing On a Large Area Photonic Crystal Quantum Cascade Laser, Zhixian Wang¹, Yong Liang¹, Bo Meng¹, Yanting Sun², Giriprasanth Omanakuttan², Emilio Gini³, Mattias Beck¹, Iliia Sergachev⁴, Sebastian Lourdos⁴, Jérôme Faist¹, Giacomo Scalari¹; ¹Inst. for Quantum Electronics, ETH Zürich, Switzerland; ²KTH, Sweden; ³FIRST Lab ETH Zürich, Switzerland; ⁴Wysy Zürich, Switzerland. We present a large-area (1.5 mm × 1.5 mm) photonic crystal quantum cascade laser, with over 2 W peak power at room temperature (289 K), and symmetrical, narrow (< 1°), single-lobed surface-emitting beam.

17:00–19:00

SW4O • Short-Reach Communication
TechnologiesPresident: David Geisler, MIT Lincoln
Laboratory, USA

SW4O.1 • 17:00

Experimental Demonstration of a Sparse-FFT Based Quick Synchronization Method for FBMC/OQAM Systems, Yating Xiang¹, Ming Tang¹, Xi Chen¹, Qiong Wu¹, Huibin Zhou¹, Songnian Fu¹, Deming Liu¹; ¹Huazhong Univ. of Sci.&Tech., China. A quick and accurate synchronization algorithm based on the sparse-FFT is proposed for FBMC/OQAM systems with experimental verification of 50km SSMF transmission. The computation complexity is greatly reduced to 6.7% of the conventional correlation-based method.

SW4O.2 • 17:15

50-Gb/s Dispersion-unmanaged DMT Transmission with Injection Locked 10G-class 1.55- μ m DML, Lei Xue^{1,3}, Lilin Yi³, Lu Zhang^{2,3}, Oskars Ozolins^{4,2}, Aleksejs Udalcovs⁴, Xiaodan Pang^{4,5}, Jiajia Chen²; ¹Chalmers Univ. of Technology, Sweden; ²KTH Royal Inst. of Technology, Sweden; ³State Key Lab of Advanced Optical Communication System and Networks, Shanghai Jiao Tong Univ., China; ⁴Networking and Transmission Lab, RISE Acreo AB, Sweden; ⁵Infinera, Sweden. We demonstrate 50-Gb/s DMT signal transmission over 20-km SMF by using a 10G-class 1.55- μ m DML without optical dispersion compensation. Injection locking technique is introduced, which doubles system bandwidth and greatly suppresses DML chirp.

SW4O.3 • 17:30

Variable-step DD-FTN Algorithm for PAM8-based Short-reach Optical Interconnects, Haide Wang¹, Ji Zhou¹, Fan Li², Long Liu¹, Changyuan Yu³, Xingwen Yi², Xincheng Huang¹, Weiping Liu¹, Zhaohui Li²; ¹Dept. of Electronic Engineering, Jinan Univ., China; ²Sun Yat-sen Univ., China; ³The Hong Kong Polytechnic Univ., Hong Kong. We experimentally demonstrate a variable-step DD-FTN algorithm for 129-Gbit/s PAM8-based short-reach optical interconnects. The fast and stable convergence of the proposed algorithm leads to better performance than conventional DD-FTN algorithm.

SW4O.4 • 17:45

Joint Blind Equalization of CD and RSOP Using Kalman Filter in Stokes Vector Direct Detection System, Nan Cui¹, Zibo Zheng¹, Xiaoguang Zhang¹, Wei Yi¹, Ruiyu Guo¹, Wenbo Zhang¹, Lixia Xi¹, Xianfeng Tang¹; ¹Beijing Univ. of Posts and Telecomm, China. We propose a joint blind equalization for CD and RSOP in SV-DD system based on new Kalman structure, which has strong tolerance to CD (more than 2550 ps/nm) combined with ultra-fast RSOP (up to 2Mrad/s).

SW4O.5 • 18:00 **Invited**

Programmable VCSEL-based Transceivers for Multi-terabit Capacity Networking, Michela Svaluto Moreolo¹, Laia Nadal¹, Josep M. Fabrega¹, Ricardo Martínez¹, Ramon Casellas¹; ¹Ctr Tecnològic de Telecom de Catalunya, Spain. Photonic transceivers adopting large-bandwidth vertical cavity surface emitting lasers (VCSELs) at long-wavelength, coherent detection and adaptive digital signal processing are presented as promising programmable architectures to provide multi-terabit capacity in future software-defined optical metro networks.

NOTES

Wednesday, 17:00-19:00

Executive Ballroom
210A

Joint

JW4A • Sym on Coupling Artificial Atoms to Nano- & Opto-mechanical Systems II—Continued

JW4A.4 • 18:30

Quantum Acoustics with Lithium Niobate Nanocavities, Patricio Arrangoiz-Arriola¹, E. Alex Wollack¹, Marek Pechal¹, Wentao Jiang¹, Zhaoyou Wang¹, Timothy McKenna¹, Amir Safavi-Naeini¹; ¹Stanford Univ., USA. We couple a superconducting qubit to a piezoelectric nanomechanical resonator fabricated from thin film lithium niobate (LN). The sizeable piezoelectric coefficient of LN leads to a coupling rate $\frac{\hbar}{2} \pi > 15\hbar$ MHz allowing quantum operations.

JW4A.5 • 18:45

Scalable Phononic Quantum Networks of Spins in Diamond, Mark C. Kuzyk¹; ¹Univ. of Oregon, USA. Phononic quantum networks with alternating phononic crystal waveguides have been developed. This new architecture solves the inherent scalability problem in coupling spins with mechanical vibrations by breaking large networks into small and closed mechanical subsystems.

Executive Ballroom
210B

CLEO: QELS-Fundamental
Science

FW4B • Nanoscale Nonlinear Optics—Continued

FW4B.5 • 18:15

Resonance Splitting and Enhanced Optical Nonlinearities in ITO-based Epsilon-near-zero Metasurface with Cross-shaped Nanoantennas, Cong Liu¹, Kai Pang¹, Karapet Manukyan¹, Orad Reshef², Yiyu Zhou³, Joel Patrow¹, Anuj Pennathur¹, Hao Song¹, Zhe Zhao¹, Runzhou Zhang¹, Fatemeh Alishahi¹, Ahmad Fallahpour¹, Yinwen Cao¹, Ahmed Almaiman¹, Jahan Dawlaty¹, N. Apurv Chaitanya⁵, Israel De Leon⁵, Zahirul Alam², Robert Boyd^{2,3}, Moshe Tur⁴, Alan E. Willner¹; ¹Univ. of Southern California, USA; ²Univ. of Ottawa, Canada; ³Univ. of Rochester, USA; ⁴Tel Aviv Univ., Israel; ⁵Tecnológico de Monterrey, Mexico. We experimentally demonstrate a strong-coupling-induced resonance splitting in indium-tin-oxide (ITO) based epsilon-near-zero (ENZ) metasurface with cross-shaped nanoantennas. An ~11-nm blue shift of the carrier wavelength is observed for this metasurface under ~4-GW/cm² peak-power density.

FW4B.6 • 18:30

Nonlinear and electro-optical properties of epsilon near zero materials: are they all they are believed to be? Jacob Khurgin¹, Hua-Zhou Chen², Ren-Min Ma²; ¹Johns Hopkins Univ., USA; ²School of Physics, Peking Univ., China. Nonlinear and Electro-optical properties of Epsilon-near-zero (ENZ) materials and Epsilon-and-mu-near-zero (EMNZ) materials have been investigated. The ENZ enhancement was shown to be a slow light effect and EMNZ enhancement was found to be nonexistent.

FW4B.7 • 18:45

Vertical emission of second and third harmonic light from GaAs nanowires below the band edge, Michael Scalora¹, Jose Trull², Crina Cojocaru², Maria Antonietta Vincenti³, Luca Carletti⁵, Domenico de Ceglia⁵, Costantino De Angelis^{3,4}; ¹US Army Aviation and Missile Command, USA; ²Physics Dept., Universitat Politècnica de Catalunya, Spain; ³Dept. of Information Engineering, Univ. of Brescia, Italy; ⁴National Inst. of Optics (INO-CNR), Italy; ⁵Dept. of Information Engineering, Univ. of Padova, Italy. Using a hydrodynamic approach we predict bulk- and surface-induced second and third harmonic generation from a GaAs nanowire grating. Absorption is inhibited below the band-edge and conversion efficiencies are predicted to be 0.5% at 333nm.

Executive Ballroom
210C

Joint

JW4C • Professional Development Session I—Continued

New this year are Professional Development sessions organized by the CLEO Committee Chairs. For details please refer to the Program Update Sheet.

Wednesday, 17:00–19:00

19:00–20:30 Conference Reception, Grand Ballroom 220B/C

CLEO: QELS-Fundamental
ScienceFW4D • Chirality, PT Symmetry, &
Exceptional Points—Continued

FW4D.5 • 18:15

Coherent Virtual Absorption and Embedded Eigenstates in non-Hermitian PT-Symmetrical Systems, Aleksandr Krasnok¹, Zarko Sakotic¹, Andrea Alu¹, ¹*CUNY Advanced Science Research Center, USA*. In this work, we demonstrate how the concept of coherent excitation can pave the way to light scattering control in an extreme fashion in non-Hermitian PT-symmetrical systems supporting an embedded eigenstate.

FW4D.6 • 18:30

Robust Exceptional Points, Hamidreza Ramezani¹, Cem Yuce², ¹*Univ. of Texas, Rio Grande Valley, USA*; ²*Dept. of Physics, Eskisehir Technical Univ., Turkey*. We construct a theory to introduce the concept of robust exceptional points against disorder in photonics. Our proposal will advance the concept of topological localized states to an unexplored area of topological extended (bulk) states.

FW4D.7 • 18:45

Extreme All-dielectric Huygens' Metasurfaces based on Quasi-bound States in the Continuum, Mingkai Liu¹, Dukyong Choi^{1,2}, ¹*Australian National Univ., Australia*; ²*Jinan Univ., China*. We introduce and experimentally demonstrate a novel platform to connect the concepts of Huygens' condition and bound states in the continuum, allowing Huygens' metasurfaces with controllable Q-factors over orders of magnitude.

CLEO: Science & Innovations

SW4E • Ultrafast Pulse Manipulation—
Continued

SW4E.6 • 18:15

Programmable Control of Femtosecond Structured Light, Randy A. Lemons^{1,2}, Wei Liu², Charles G. Durfee¹, Josef C. Frisch², Steve Smith², Joseph Robinson², Alan Fry², Sergio Carbajo², ¹*Colorado School of Mines, USA*; ²*SLAC National Accelerator Lab, USA*. We present a laser architecture with programmable control of the polarization vector, transverse and longitudinal intensity, and wavefront in the near and far field as a novel tool to probe and control matter.

SW4E.7 • 18:30

Precision control of intense cycle-sculpted electric fields by fully stabilized three-channel optical waveform synthesizer, Bing Xue¹, Yuuki Tamaru^{1,2}, Yuxi Fu¹, Hua Yuan³, Pengfei Lan³, Oliver D. Mücke^{4,5}, Akira Suda², Katsumi Midorikawa¹, Eiji J. Takahashi¹, ¹*RIKEN Center for Advanced Photonics, RIKEN, Japan*; ²*Tokyo Univ. of Science, Japan*; ³*School of Physics and Wuhan National Lab of Optoelectronics, Huazhong Univ. of Science and Technology, China*; ⁴*Center for Free-Electron Laser Science, DESY, Germany*; ⁵*The Hamburg Centre for Ultrafast Imaging, Germany*. A three-channel optical waveform synthesizer is demonstrated for generating intense continuum soft-x-ray pulses by HHG. With the full stabilization of temporal delays, relative phases, and CEPs, precision control of shot-to-shot reproducible synthesized waveforms is achieved.

SW4E.8 • 18:45

Extended Propagation of Broadband Space-Time Wave Packets for 70 m, Basanta Bhaduri¹, Murat Yessenov¹, Danielle Harper¹, Jessica Pena¹, Monjurul Meem², Shermineh Rostami Fairchild¹, Rajesh Menon², Martin Richardson¹, Ayman F. Abouraddy¹, ¹*Univ. of Central Florida, CREOL, USA*; ²*Electrical Engineering, University of Utah, USA*. We synthesize a femtosecond wave packet of 20-nm bandwidth and spatial beam width of 0.7-mm that propagates diffraction-free for 70-m by virtue of carefully engineered spatio-temporal spectral correlations introduced into the field.

SW4F • Terahertz Sources &
Communication—Continued

SW4F.6 • 18:30

Low-noise THz-wave generation from a dual-wavelength fiber Brillouin cavity coupled to a UTC-photodiode, Yihan Li^{1,2}, Antoine Rolland², Kenta Iwamoto³, Naoya Kuse², Martin E. Fermann¹, Tadao Nagatsuma³, ¹*Beihang Univ., China*; ²*IMRA America, Inc., Boulder Research Lab, USA*; ³*Graduate School of Engineering Science, Osaka Univ., Japan*; ⁴*IMRA America, USA*. A dual-wavelength photonic system for carrier-frequency-stable THz signal generation is demonstrated. An in-loop fractional frequency instability $<10^{-16}$ via synchronization to an external reference while preserving the intrinsic low phase noise of a Brillouin cavity is experimentally demonstrated.

SW4F.7 • 18:45

Spectral-efficient and high-speed THz-wave communication using 40 Gsymbol/s channel-based Nyquist WDM, Koichi Takiguchi¹, ¹*Dept. of Electrical and Electronic Engineering, Ritsumeikan Univ., Japan*. Nyquist WDM was adopted to improve spectral-efficiency and capacity of THz-wave communication. 2 x 40 Gbit/s Nyquist WDM communication in the THz-band was implemented, whose signal generation and reception were both assisted by optical processing.

19:00–20:30 Conference Reception, Grand Ballroom 220B/C

CLEO: Science & Innovations

CLEO: Applications
& Technology

SW4G • Optical Frequency Synthesis & Microwave Generation—Continued

SW4G.5 • 18:15

Kerr Comb-based Transfer Oscillator for Ultralow Noise Photonic Microwave Synthesis, Erwan Lucas¹, Pierre Brochard², Romain Bouchand¹, Stéphane Schiltz², Thomas Südmeyer², Tobias J. Kippenberg¹; ¹EPFL, Switzerland; ²UNINE, Switzerland. We perform optical frequency division of an ultra-stable laser by using a crystalline-based Kerr frequency comb as a transfer oscillator. We demonstrate absolute phase noise levels of -110 dBc/Hz at 200-Hz offset from a 14 GHz carrier.

SW4G.6 • 18:30

An optical frequency synthesizer using an integrated erbium tunable laser, Ming Xin¹, Nanxi Li¹, Neetesh Singh¹, Alfonso Ruocco¹, Zhan Su¹, Emir Salih Magden¹, Jelena Notaros¹, Diedrik Vermeulen¹, Erich Ippen¹, Michael R. Watts¹, Franz Kärtner¹; ¹MIT, USA. We demonstrate a self-calibrated optical frequency synthesizer using a fully-integrated erbium-doped tunable laser. A 20 nm tuning range from 1544 nm to 1564 nm is achieved with $\sim 10^{-13}$ frequency instability at 10s averaging time.

SW4G.7 • 18:45

Comb-rooted synthesis of ultra-narrow multiple optical frequencies of few Hz linewidth, Byung Soo Kim¹, Heesuk Jang¹, Dong-Chel Shin¹, Young-Jin Kim^{2,1}, Seung-Woo Kim¹; ¹South Korea Advanced Inst of Science & Tech, South Korea (the Republic of); ²Nanyang Technological Univ., Singapore. An optical synthesizer is devised to generate ultra-narrow optical frequencies of a 1.0 Hz linewidth directly from a frequency comb stabilized to a high-finesse cavity.

SW4H • Supercontinuum Generation—Continued

SW4H.5 • 18:15

Supercontinuum Generation from Dispersion Engineered AlN Nanophotonic Waveguide Arrays, Hong Chen¹, Jingan Zhou¹, Houqiang Fu¹, Xuanqi Huang¹, Tsung-Han Yang¹, Kai Fu¹, Jossue Montes¹, Chen Yang¹, Yuji Zhao¹; ¹Arizona State Univ., USA. We experimentally study the supercontinuum generation from AlN nanophotonic waveguide arrays. By splitting the fundamental TE mode into TE-odd and TE-even modes, dispersion property of the waveguide is greatly improved.

SW4H.6 • 18:30

Broadband Supercontinuum Generation from a Tm Oscillator in a Highly Nonlinear Silica Fiber, Junjie Zeng¹, Claude-Alban Ranély-Vergé-Dépré¹, Ahmet Akosman¹, Etienne Genier¹, Michelle Y. Sander¹; ¹Boston Univ., USA. A broadband supercontinuum is generated from a thulium ultrafast fiber laser in a highly nonlinear silica fiber with low nJ input pulse energies.

SW4H.7 • 18:45

Observation of broadband frequency down-conversion by adiabatic four-wave mixing in optical fiber, Xiaoyue Ding¹, Kerriane Harrington², Dylan Heberle¹, Noah Flemens¹, Weizung Chang¹, Tim Birks², Jeffrey Moses¹; ¹Cornell University, USA; ²Dept. of Physics, Univ. of Bath, UK. We present the first experimental observation of broadband adiabatic four-wave mixing frequency conversion by using a tapered photonic crystal fiber to generate 2- μ m pulses. This conversion mechanism may prove widely relevant for ultrafast optics applications.

AW4I • Medical Devices & Systems—Continued

AW4I.4 • 18:00 **Invited**

Autonomous Artificial Intelligence Eye Screening: Roles and Challenges in Retinal Imaging, Kaushal Solanki¹, Jisun Moon¹, Malavika Bhaskaranand¹, Chaithanya Ramachandra¹; ¹Eyenuk Inc., USA. Autonomous AI eye screening can provide a highly accurate, accessible and cost-efficient solution for preventable blindness and can potentially do more. Images are one of the critical data. What can be done with autonomous AI image analysis and the roles and challenges in obtaining retinal images will be discussed.

AW4I.5 • 18:30

Femtosecond Micromachining of Ophthalmic Hydrogels: effects of laser repetition rate on the induced phase change in the two photon and four photon absorption limit, Ruiting Huang¹, Wayne H. Knox¹; ¹The Inst. of Optics, USA. We study and model effects of laser wavelength, repetition rate and other parameters on writing refractive index changes with a femtosecond laser in ophthalmic hydrogels.

AW4I.6 • 18:45

In Vivo En Face and Cross-Sectional Imaging with Mirau-Type Optical Coherence Microscopy Based on a Ti:Sapphire Crystal Fiber Light Source, Tuan-Shu Ho¹, Ming-Rung Tsai¹, Chih-Wei Lu¹; ¹Apollo Medical Optics, Taiwan. With a simple optical switch and a low-cost Ti:sapphire crystal fiber light source, a Mirau-type optical coherence microscopy for both high-speed en face and cross-sectional imaging is demonstrated.

19:00–20:30 Conference Reception, Grand Ballroom 220B/C

CLEO: Science & Innovations

SW4J • Design & Simulation of Micro- & Nano-phonic Devices—Continued

SW4J.6 • 18:15

Nanostructured Photonic Power Splitter Design via Convolutional Neural Networks, Keisuke Kojima¹, Mohammad H. Tahersima¹, Toshiaki Koike-Akino¹, Devesh Jha¹, Bingnan Wang¹, Chungwei Lin¹, Kieran Parsons¹; ¹Mitsubishi Electric Research Labs, USA. We train a convolutional neural network (CNN) that can predict the optical response of randomly generated nanopatterned photonic power splitters in a 2⁴⁰⁰ design space with a prediction correlation coefficient of 85%.

SW4J.7 • 18:30

Adjoint-based inverse design of nonlinear nanophotonic devices, Tyler Hughes¹, Momchil Minkov¹, Ian Williamson¹, Shanhui Fan¹; ¹Stanford Univ., USA. We extend the frequency-domain adjoint method to nonlinear optical systems, which enables the gradient-based optimization and inverse design of novel devices. As illustrations, we devise compact photonic switches in a Kerr nonlinear material.

SW4J.8 • 18:45

Topology Optimization of Large-Area Metasurfaces, Zin Lin², Victor Liu³, Raphael Pestourie¹, Steven Johnson²; ¹Harvard Univ., USA; ²Mathematics, MIT, USA; ³—, USA. We demonstrate an inverse design technique for metasurfaces, based on topology optimization, that can take into account electromagnetic interactions over large surface areas. As an example, we present a multi-layered metalens design that can concentrate multiple beams onto a single focus.

CLEO: Applications & Technology

AW4K • Lidar—Continued

AW4K.5 • 18:15

Silicon Nitride Optical Phased Arrays with Cascaded Phase Shifters for Easy and Effective Electronic Control, Shiyang Zhu¹, Yu Li¹, Ting Hu¹, Qize Zhong¹, Yuan Dong¹, Zhengji Xu¹, Navab Singh¹; ¹Inst. of Microelectronics, Singapore. We present integrated optical phased arrays with cascaded phase shifting architectures for easy and effective electronic control. A 32-element SiN OPA was measured to exhibit 16° continuous steering at 13-V bias with 0.7° beam width.

AW4K.6 • 18:30

Efficient Ho:LuLiF MOPA Laser Transmitter with Tailored Pulse Width and Output Energy for Space-Based Coherent Wind Lidar, Jane Lee^{1,2}, Jirong Yu², Teh-Hwa Wong^{1,2}, Larry Petway², Songsheng Chen², Michael J. Kavaya²; ¹Science Systems & Applications, Inc., USA; ²NASA Langley Research Center, USA. A Ho:LuLiF MOPA laser system that generates 75 mJ energy and 200 ns pulse width at 200 Hz PRF was developed for coherent wind lidar measurements, fulfilling the lidar system's figure-of-merit and accuracy requirements.

CLEO: Science & Innovations

SW4L • Optical Detection of Vapors or Hazardous Environments—Continued

SW4L.6 • 18:15

Characterization of a Laser-Induced Plasma Using Time-Resolved Dual-Frequency-Comb Spectroscopy, Yu Zhang^{2,1}, Caroline Lecaplain¹, Reagan R. Weeks¹, Jeremy Yeak⁴, Sivanandan S. Harilal³, Mark C. Phillips³, R. J. Jones¹; ¹College of Optical Sciences, Univ. of Arizona, USA; ²Dept. of Physics, Univ. of Arizona, USA; ³Pacific Northwest National Lab, USA; ⁴Opticslab, USA. We characterize the dynamics of laser-induced plasmas using time-resolved dual-frequency-comb spectroscopy. The temporal evolution of plasma's temperature, population number density are estimated for multiple Fe transitions.

SW4L.7 • 18:30 **Invited**

High-Performance Micro-Gas Chromatography and Optical Sensing, Xudong Fan¹; ¹Univ. of Michigan, USA. Micro-gas chromatography (micro-GC) devices have broad applications in vapor analysis. Here we describe various optical vapor sensors that can be used in micro-GC, including ring resonators, fiber Fabry-Perot cavities, interferometric sensors, and micro-photoionization detectors.

19:00–20:30 Conference Reception, Grand Ballroom 220B/C

CLEO: QELS-Fundamental
Science

CLEO: Science & Innovations

FW4M • Advanced Techniques &
Applications in Ultrafast Spectroscopy—
Continued

SW4N • High Power & Narrow Linewidth
Lasers—Continued

SW4O • Short-Reach Communication
Technologies—Continued

FW4M.5 • 18:30

Ultrafast Spin Dynamics and Phase Competition in a Spin Vortex Crystal Superconductor, Di Cheng^{1,2}, Joongmok Park^{1,2}, Liang Luo^{1,2}, Richard H. Kim^{1,2}, William Meier^{1,2}, Sergey Bud'ko^{1,2}, Paul Canfield^{1,2}, Martin Mootz³, Ilias E. Perakis³, Jigang Wang^{1,2}; ¹Iowa State Univ, USA; ²Ames Lab, USA; ³Physics, Univ. of Alabama at Birmingham, USA. Ultrafast spectroscopy measurements on iron pnictide 1144 superconductor Ca(Fe_{1-x}Ni_x)As₄ revealed, for the first time, spin dynamics of an exotic Spin Vortex Crystal (SVC) phase that competes with superconductivity.

FW4M.6 • 18:45

Carrier Dynamics Between the Ordered and Disordered Orthorhombic Lattice Domains in Methylammonium Lead Iodide Perovskite, Michael Titze¹, Chengbin Fei², Maria Munoz¹, He Wang², Hebin Li¹; ¹Florida International Univ., USA; ²Physics, Univ. of Miami, USA. The carrier dynamics between the ordered and disordered orthorhombic lattice domains in methylammonium lead iodide perovskite are measured. Emission from disordered domain is visible within 250fs, accessing intermediate states inbetween and coupling to coherent phonon.

SW4N.5 • 18:15

Frequency Noise Reduction in a Quantum Cascade Laser Using a Short Free-Space Delay Line, Atif Shehzad¹, Pierre Brochard¹, Renaud Matthey¹, Thomas Südmeyer¹, Stéphane Schilt¹; ¹Univ. of Neuchatel, Switzerland. We present a frequency noise reduction in a mid-infrared quantum cascade laser achieved by stabilization to a short free-space delay line and show a decrease by more than 20 dB at 1-kHz Fourier frequency.

SW4N.6 • 18:30

1550 nm laser with 320 Hz Lorentzian linewidth based on semiconductor gain chip and extended Si₃N₄ Bragg grating, Chao Xiang¹, Paul Morton², John Bowers¹; ¹Dept. of Electrical and Computer Engineering, Univ. of California Santa Barbara, USA; ²Morton Photonics, USA. We demonstrate narrow linewidth lasers based on a semiconductor gain chip coupled to a Si₃N₄ Bragg grating. The laser demonstrates 12 mW fiber coupled output power, > 55 dB SMSR and 320 Hz Lorentzian linewidth.

SW4N.7 • 18:45

Mutually Coupled Distributed Feedback Lasers with 10 Hz Intrinsic Linewidth, Weichao Ma¹, Bing Xiong¹, Changzheng Sun¹, Xu Ke¹, Jian Wang¹, Zhibiao Hao¹, Lai Wang¹, Yanjun Han¹, Hongtao Li¹, Yi Luo¹; ¹Dept. of Electronic Engineering, Tsinghua Univ., China. Pronounced linewidth narrowing in mutually injection locked distributed feedback lasers is confirmed by local oscillator heterodyne and delayed self-heterodyne measurements. White frequency noise of 3 Hz²/Hz is recorded, corresponding to 10 Hz intrinsic linewidth.

SW4O.6 • 18:30

Combined Probabilistic Shaping and Nyquist Pulse Shaping for PAM8 Signal Transmission in WDM Systems, Xiao Han^{1,2}, Mingwei Yang¹, Ivan B. Djordjevic¹, Yang Yue², Qiang Wang², Zhen Qu², Jon Anderson²; ¹Electrical and Computer Engineering, Univ. of Arizona, USA; ²Juniper Networks, USA. We use the LDPC-coded probabilistically shaped PAM8 signaling combined with Nyquist pulse shaping to improve the transmission performance in a WDM system. We find that the combination of these shaping schemes offers great performance improvement.

19:00–20:30 Conference Reception, Grand Ballroom 220B/C

NOTES

Executive Ballroom
210A

Executive Ballroom
210B

Executive Ballroom
210C

Executive Ballroom
210D

CLEO: QELS-Fundamental Science

08:00–10:00
FTh1A • Exploiting Quantum Degrees of Freedom
President: John Sipe, University of Toronto, Canada

FTh1A.1 • 08:00 Tutorial
Quantum Information Science with Integrated Optics and Pulsed Light, Christine Silberhorn¹; ¹Universität Paderborn, Germany. Photonic networks with many modes and quantum input states have been proposed for various quantum applications. Here we present three approaches to overcome current limitations for their implementation: nonlinear integrated quantum optics, temporal modes and time-multiplexing.



Christine Silberhorn is a professor at Paderborn University leading the research group "Integrated Quantum Optics". She received several prizes, most prominently: Gottfried-Wilhelm-Leibniz-prize from the German Science Foundation (2011) and a consolidator ERC-grant (2017). Since 2013 she is member of the Leopoldina, National Academy of Science, and since 2018 OSA Fellow.

08:00–10:00
FTh1B • Ultrafast Nonlinear Phenomena
President: To Be Announced

FTh1B.1 • 08:00 Invited
Optical Picoscopy of Valence Electrons in Solids, Harshit Lakhota^{2,1}, Eleftherios Goulielmakis^{2,1}; ¹Max-Planck-Institut für Quantenoptik, Germany; ²Univ. of Rostock, Germany. We demonstrate that strong field driven high harmonic generation in solids allow acquiring real space pictures of the electronic potential and the electron density. Our approach provides new ways for probing the basic chemical, optical and electronic properties of solids.

FTh1B.2 • 08:30
Subcycle observation of terahertz-driven minimally dissipative spin switching, Stefan Schlauderer¹, Christoph Lange¹, Sebastian Baierl¹, Thomas Ebnet¹, Christoph Schmid¹, Darren C. Valovcin², Anatoly K. Zvezdin^{3,4}, Alexey Kimmel^{5,6}, Rostislav Mikhaylovskiy⁶, Rupert Huber¹; ¹Univ. of Regensburg, Germany; ²Dept. of Physics and the Inst. for Terahertz Science and Technology, Univ. of California at Santa Barbara, USA; ³Prokhorov General Physics Inst. and P.N. Lebedev Physical Inst., Russia; ⁴Moscow Inst. of Physics and Technology (State Univ.), Russia; ⁵Moscow Technological Univ. (MIREA), Russia; ⁶Radboud Univ., Netherlands. Antenna-enhanced single-cycle terahertz pulses ballistically switch the antiferromagnetic spin order in TmFeO₃ between metastable states separated by a potential energy barrier. We directly trace the temporal and spectral fingerprint of this ultrafast minimally dissipative dynamics.

08:00–10:00
FTh1C • Hot-electron Enabled Plasmonics & Optical Vortices
President: Ido Kaminer Technion, Israel

FTh1C.1 • 08:00
Hot carriers generated by plasmons: where they are born, where they are going and how they die, Jacob Khurgin¹; ¹Johns Hopkins Univ., USA. A unified theory of plasmon-induced hot carrier generation in metals is developed with all the relevant mechanisms included. Analytical expressions for carrier generation rates, their locations, energies and directions of motion are obtained.

FTh1C.2 • 08:15
Hot Carrier Induced Plasmon Enhanced Photocatalysis in Hematite Thin Films, Aweek Dutta¹, Alberto Naldoni², Alexander Govorov^{3,4}, Vladimir M. Shalaev¹, Alexandra Boltasseva¹; ¹Purdue Univ., USA; ²Regional Center for Advanced Technologies and Materials, Czechia; ³Ohio Univ., USA; ⁴Univ. of Electronic Science and Technology of China, China. We experimentally demonstrate photocurrent enhancement in thin hematite films due to a combination of enhanced scattering from plasmonic nanodisks and hot carriers generated from plasmon decay.

FTh1C.3 • 08:30
Hot Carrier Photodetection From Fractal Aluminum Films In The Near-IR, Christian Frydendahl¹, Meir Grajower¹, Noa Mazur-ski¹, Joseph Shappir¹, Uriel Levy¹; ¹Dept. of Applied Physics, The Hebrew Univ. of Jerusalem, Israel. Using self-organized random fractal aluminum films, we experimentally observe plasmonically enhanced hot carrier photodetection in p-doped silicon in the short wave infrared wavelength regime, with very high responsivities over a broad range of wavelengths.

08:00–10:00
FTh1D • Entanglement Sources
President: Marco Liscidini; Università degli Studi di Pavia, Italy

FTh1D.1 • 08:00
On-demand photonic entanglement synthesizer, Kan Takase¹, Shuntaro Takeda^{1,2}, Akira Furusawa¹; ¹the Univ. of Tokyo, Japan; ²JST, Japan. We demonstrate on-demand generation of photonic entanglement by dynamically controlling a loop-based circuit at nanosecond timescale. We generate 6 types of entangled states including 1000-mode 1D-cluster states without changing the circuit architecture.

FTh1D.2 • 08:15
Quantum walks and synthetic tight-binding crystals in on-chip electro-optic frequency combs, Christian Reimer¹, Yaowen Hu¹, Mian Zhang^{1,2}, Amirhassan Shams-Ansari¹, Marko Loncar¹; ¹Harvard Univ., USA; ²HyperLight Corporation, USA. We investigate the quantum properties of electro-optic frequency combs and measure quantum walks in the frequency-domain as well as the formation of tight-binding crystals in high-dimensional synthetic space. The frequency combs are achieved using an integrated lithium niobate microring resonator.

FTh1D.3 • 08:30
Scalable feedback control of on-chip entangled photon pair sources, Jacques Carolan¹, Uttara Uttara¹, Nicholas C. Harris², Mihir Pant¹, Tom Baehr-Jones³, Michael Hochberg³, Dirk R. Englund¹; ¹MIT, USA; ²Lightmatter, USA; ³Elenion Technologies, USA. We develop a feedback control technique for single photon sources based on microring resonators. We implement our protocol on a silicon photonic device, and demonstrate feedback controlled quantum state engineering.

Executive Ballroom
210EExecutive Ballroom
210FExecutive Ballroom
210GExecutive Ballroom
210H

CLEO: Science & Innovations

08:00–10:00

STh1E • Mid-IR Lasers

President: Clara Saraceno, Ruhr
Universität Bochum, Germany

STh1E.1 • 08:00

Gain-optimized 2.05 μm pulses at 20 mJ and 1 kHz from multi-pass Ho:YLF amplifier, Krishna Murari^{1,2}, Yanchun Yin^{1,2}, Yi Wu^{1,2}, Xiaoming Ren^{1,2}, Zenghu Chang^{1,2}; ¹College of Optics and Photonics (CREOL), USA; ²Univ. of Central Florida Physics, USA. We present Ho:YLF based multi-pass amplifier emitting pulses at 20 mJ energy and 1 kHz repetition rate seeded by 3-mJ seed pulses from DC-OPA.

STh1E.2 • 08:15

Selective Wavelength KGW/ Tm:YLF Raman Laser, Salman Noach¹, Uzziel Sheintop¹, Daniel Sebbag¹, Pavel Komm², Gilad Marcus²; ¹Jerusalem College of Technology, Israel; ²Applied Physics, Hebrew Univ., Israel. External cavity Raman laser based on KGW crystal emitting at 2197nm and 2263nm is presented. The efficient use of KGW for 2 μm region is demonstrated. Maximum energy of 0.4mJ was achieved, the highest energy reported.

STh1E.3 • 08:30

Robust, high peak power, thulium-doped fiber chirped-pulse amplification system using a dissipative soliton seed laser, Zhengqi Ren¹, Jonathan Price¹, David Richardson¹, Shaif-Ul Alam¹; ¹Univ. of Southampton, UK. We report a dissipative soliton seeded, thulium-doped fiber chirped pulse amplification system at 1950 nm. The amplified pulses are compressed to 545 fs and have an energy of 0.85 μJ corresponding peak power of 1.56 MW.

08:00–10:00

STh1F • Chip-Scale Trace-Gas Sensing

President: Eric Zhang; IBM, USA

STh1F.1 • 08:00 **Invited**

Trace Gas Spectroscopy with Mid-Infrared Nanophotonic Waveguides, Marek Vlček¹, Henock D. Yallew¹, Vinita Mittal², Ganapathy Senthil Murugan², Jana Jagerská¹; ¹UiT The Arctic Univ. of Norway, Norway; ²Optoelectronics Research Centre Southampton, UK. We present a mid-infrared photonic waveguide platform for sensitive and selective detection of trace gases by means of tunable laser absorption spectroscopy.

STh1F.2 • 08:30

Trace-gas Spectroscopy of Methane using a Monolithically Integrated Silicon Photonic Chip Sensor, Eric J. Zhang¹, Yves Martin¹, Jason S. Orcutt¹, Chi Xiong¹, Martin Glodde¹, Tymon Barwicz², Laurent Schares¹, Elizabeth Duch¹, Nathan Marchack¹, Chu C. Teng², Gerard Wysocki², William M. Green¹; ¹IBM T. J. Watson Research Center, USA; ²Electrical Engineering, Princeton Univ., USA. We present a monolithically integrated photonic sensor incorporating an on-chip III-V laser, detector, sealed reference cell, and sensing waveguide capable of near-infrared absorption spectroscopy of methane near $\lambda = 1651$ nm. Sub-100 ppmv Hz^{-1/2} sensitivities are demonstrated.

08:00–10:00

STh1G • Frequency Comb Spectroscopy

STh1G.1 • 08:00

A Compact Mid-infrared Dual-Comb Spectrometer with 1000 nm of Spectral Coverage, Gabriel Ycas^{1,2}, Fabrizio R. Giorgetta^{1,2}, Jacob Friedlein^{1,2}, Daniel Herman^{1,2}, Kevin C. Cossel², Esther Baumann^{1,2}, Nathan R. Newbury², Ian Coddington²; ¹Univ. of Colorado at Boulder, USA; ²Applied Physics Division, National Inst. of Standards and Technology, USA. We present a mid-infrared dual-comb spectrometer employing PPLN waveguides that generates a broad 3-4 μm instantaneous spectrum with 5 mW of power. Outdoor spectroscopy is demonstrated and portable operation should be possible.

STh1G.2 • 08:15

Dual-comb spectroscopy with Si₃N₄ waveguides for gas spectroscopy in the 2 μm – 2.5 μm water window, Esther Baumann^{1,2}, Eli Hoenig¹, Edgar Perez¹, Gabriel Colacion¹, Fabrizio R. Giorgetta^{1,2}, Kevin C. Cossel¹, Gabriel Ycas^{1,2}, David Carlson¹, Daniel Hickstein¹, Kartik Srinivasan¹, Scott B. Papp^{1,2}, Nathan R. Newbury¹, Ian Coddington¹; ¹NIST, USA; ²Physics, Univ. of Colorado Boulder, USA. Dual-comb spectroscopy of CO and CO₂ is reported in the important 2-2.5 μm atmospheric transparency window, using broadening in tailored Si₃N₄ waveguides and extending beyond Si-based fibers' transparency window.

STh1G.3 • 08:30 **Invited**

Precision Fourier Transform Spectroscopy Using Optical Frequency Combs, Aleksandra Foltynowicz¹; ¹Umea Univ., Sweden. We present recent advances in direct and cavity-enhanced optical frequency comb Fourier transform spectroscopy for precision measurements of entire absorption bands in the near- and mid-infrared wavelength range.

08:00–10:00

STh1H • Optical Resonance-Based Devices

President: Lan Yang; Washington
University in St Louis, USA

STh1H.1 • 08:00 **Invited**

Quantum Dot Spins in Micropillar Cavities, Andrew Young¹, Petros Androvitsaneas^{1,2}, Joseph Lennon¹, Christian Schneider³, Sebastian Maier³, Janna Hinchliff¹, George Atkinson¹, Edmund Harbord¹, Martin Kamp³, Sven Höfling³, John G. Rarity¹, Ruth Oulton¹; ¹Bristol Univ., UK; ²Univ. of Exeter, UK; ³Univ. of Würzburg, Germany. We will examine the requirements for generating photonic entanglement using a charged quantum dot in a pillar microcavity. We will discuss how to make an efficient device and parametrise the dynamics of the QD spin.

STh1H.2 • 08:30

Photon Pair Generation and Filtering Using Monolithically Integrated Silicon Micro-disk and Coupled Resonator Optical Waveguide, Rakesh Ranjan Kumar¹, Xinru Wu¹, Hon Ki Tsang¹; ¹Dept. of Electronic Engineering, The Chinese Univ. of Hong Kong, Hong Kong. We demonstrate on-chip pair of photons with spectral brightness of 4.84 $\times 10^7$ pair/s/mW²/GHz in micro-disk resonator integrated with on-chip tunable filter to provide high isolation of the pump.

Meeting Room
211 A/BCLEO: Applications
& Technology

08:00–10:00

ATH11 • Radiative Cooling & Photovoltaics

Presider: Daniel Law; Boeing, USA

ATH11.1 • 08:00

Structured Polymers for High-Performance Passive Daytime Radiative Cooling, Jyotirmoy Mandal¹, Nanfang Yu¹, Yuan Yang¹; ¹Columbia Univ., USA. Structured polymer coatings with exceptional solar reflectance (96–99%) and hemispherical long-wave infrared emittance (~97%) are created using a scalable phase inversion technique. The polymer coatings exhibit excellent passive daytime radiative cooling, with a paint-like convenience.

ATH11.2 • 08:30

All-day Radiative Cooling Using Beam-Controlled Architectures, Lyu Zhou¹, Haomin Song¹, Jian-Wei Liang², Matthew H. Singer¹, Ming Zhou³, Edgars Stegenburgs², Nan Zhang¹, Tien Khee Ng², Zongfu Yu³, Boon S. Ooi², Qiaoqiang Gan¹; ¹State Univ. of New York at Buffalo, USA; ²KAUST Nanophotonics Lab, King Abdullah Univ. of Science and Technology, Saudi Arabia; ³Dept. of Electrical and Computer Engineering, Univ. of Wisconsin, Madison, USA. We report an inexpensive planar polydimethylsiloxane (PDMS)/metal thermal emitter in a beam-controlled architecture for all-day radiative cooling and realized ~11 °C reduction compared with the ambient temperature.

Meeting Room
211 C/D

CLEO: Science & Innovations

08:00–10:00

STh1J • Nonlinear Photonics

Presider: Satoshi Iwamoto; Univ. of Tokyo, Japan

STh1J.1 • 08:00

Third- and Fourth-Harmonic Generation in Cascaded Periodically-Poled Lithium Niobate Ultracompact Waveguides on Silicon, Tracy Sjaardema¹, Ashutosh Rao^{1,2}, Sasan Fathpour¹; ¹The College of Optics and Photonics, CREOL, Univ. of Central Florida, USA; ²NIST, Univ. of Maryland, USA. Cascaded harmonic generation is demonstrated in submicron thin-film periodically poled lithium niobate nonlinear waveguides on a silicon substrate. Harmonics to the third and fourth order are produced through second-harmonic and sum-frequency generation.

STh1J.2 • 08:15

Cavity-enhanced optical parametric generation in a modal-phase-matched lithium niobate microring, Rui Luo¹, Yang He¹, Hanxiao Liang¹, Mingxiao Li¹, Jingwei Ling¹, Qiang Lin¹; ¹Univ. of Rochester, USA. We report cavity-enhanced second-harmonic generation and difference-frequency generation in a high-Q lithium niobate microring resonator with modal phase matching. The second-harmonic generation efficiency is measured to be 1,500% W⁻¹.

STh1J.3 • 08:30 **Invited**

Beyond Metals and Semiconductors: Nano-Oxides for Nonlinear Photonic Devices, Rachel Grange¹; ¹ETH Zurich, Switzerland. I will show several strategies to maximize nonlinear optical signals in oxide-based materials with noncentrosymmetric crystalline structure, because of their wide bandgap, significant second-order optical nonlinearities, strong electro-optic effects, high damage threshold, and biocompatibility.

Meeting Room
212 A/BCLEO: Applications
& Technology

08:00–10:00

ATH1K • Industrial Metrology & Remote Sensing

Presider: Brian Simonds; National Institute of Standards and Technology, USA

ATH1K.1 • 08:00 **Invited**

Optical Systems for Industrial Shop Floor Surface Measurements To Improve Yield, Erik L. Novak¹; ¹Veeco Instruments Inc, USA. Abstract not available.

ATH1K.2 • 08:30

3D surface profile imaging based on time-encoded structured illumination, Teng Jiajie¹, Qiang Guo¹, Yuxi Wang¹, Sigang Yang¹, Minghua Chen¹, Hongwei Chen¹; ¹Tsinghua Univ., China. A novel 3D surface profile imaging method based on time-encoded structured illumination is proposed. With fast and arbitrary illumination pattern generation, low error 3D reconstruction of different objects can be obtained.

Meeting Room
212 C/D

CLEO: Science & Innovations

08:00–10:00

STh1L • Hollow Core Fibers

Presider: Meng Zhang; Beihang Univ., USA

STh1L.1 • 08:00

Highly Efficient Thresholdless Ultraviolet Frequency Conversion in H₂-filled Photonic Crystal Fiber, David Novoa¹, Manoj K. Mridha¹, Pooria Hosseini¹, Philip S. Russell¹; ¹Max-Planck-Inst Physik des Lichts, Germany. Thresholdless ultraviolet frequency conversion with high efficiency is demonstrated in a hydrogen-filled kagome PCF. Raman coherence waves, prepared by a visible pump, up- or down-shift the frequency of an ultraviolet signal upon fulfillment of phase-matching conditions.

STh1L.2 • 08:30

Gas flow within Hollow Core optical fibers, Matthew Partridge¹, Rowan Curtis¹, Kendra Khodabandehloo¹, Yong Chen¹, tom Bradley¹, Natalie V. Wheeler¹, John Hayes¹, Ian Davidson¹, Seyed Reza Sandoghchi¹, Marco N. Petrovich¹, Francesco Poletti¹, David Richardson¹, Radan Slavik¹; ¹Optoelectronics Research Centre, UK. We demonstrate the use of a Mach-Zehnder interferometer to measure gas flow within hollow core fiber during gas pressure changes. These preliminary results demonstrate the method and indicate differences between various hollow core morphologies.

Marriott
Salon I & IICLEO: QELS-Fundamental
Science

08:00–10:00

FTh1M • Ultrafast Processes in Gases &
Solids

Presider: To Be Announced

FTh1M.1 • 08:00

Self-Reinforced Optical Stability Formed by Unseeded Four-Wave Mixing with Two Pump Beams in Atomic Vapor, Erin Knutson¹, Jon D. Swaim¹, Sara Wyllie¹, Ryan T. Glasser¹; ¹Tulane Univ., USA. We demonstrate unseeded multimode four-wave mixing wherein each created photon is correlated to exactly two others, resulting in an “optimal” four-mode output. The generated beams are spatially separated, readily allowing for use in quantum communications.

FTh1M.2 • 08:15

Laser without population inversion of nitrogen ions pumped by femtosecond pulses, Yi Liu^{1,2}, Rostyslav Danylo^{1,2}, Pengji Ding², Aurelien Houard², Vladimir Tikhonchuk³, Xiang Zhang¹, Zhengquan Fan¹, Qingqing Liang¹, Songlin Zhuang¹, Luqi Yuan⁴, Andre Mysyrowicz²; ¹Univ. of Shanghai for Sci. and Tech., China; ²ENSTA Paristech, France; ³Université de Bordeaux, France; ⁴Stanford Univ., USA. We attribute the mechanism of “lasing” action of nitrogen ions pumped by femtosecond IR pulses to a laser without inversion scheme. Numerical simulations reproduce well the temporal dynamics and pressure dependence of the emission.

FTh1M.3 • 08:30

Microwave Radiation from Single and Two Color Mid-Infrared Laser Produced Plasmas in Air, Alexander C. Englesbe^{1,2}, Robert Schwartz³, Anastasia Korolov³, Dogeun Jang³, Daniel Woodbury³, Ki-Yong Kim³, Howard Milchberg³, Remington Reid², Adrian Lucero², Hugh Pohle², Serge Kalmykov², Karl Krushelnick¹, Andreas Schmitt-Sody², Jennifer Elle¹; ¹Univ. of Michigan, USA; ²Directed Energy Directorate, Air Force Research Lab, USA; ³Univ. of Maryland, USA. Plasmas generated by focusing ultrashort laser pulses in air emit broadband microwaves. We present comparisons between the frequency spectrum of radiation from 2-70 GHz due to single and two color mid-infrared laser pulses.

Marriott
Salon III

CLEO: Science & Innovations

08:00–10:00

STh1N • Sensing & Switching

Presider: Ozdal Boyraz; Univ. of California
Irvine, USASTh1N.1 • 08:00 **Invited**

Random Fiber Gratings and Applications, Xiaoyi Bao¹; ¹Physics Dept., Univ. of Ottawa, Canada. Enhancing scattering in optical fibers by random periods can lead to broadband grating, which acts as random distributed feedback in lasers to control the coherence for low noise. It can also create multi-parameters sensors.

STh1N.2 • 08:30

Fingerprint mid-infrared sensing with germanium on silicon waveguides, Ugne Griskeviciute¹, Ross Millar¹, Kevin Gallacher¹, Leonetta Baldassarre², Marc Sorel¹, Michele Ortolani², Douglas J. Paul¹; ¹Univ. of Glasgow, UK; ²Sapienza Univ. of Rome, Italy. Low loss Ge-on-Si waveguides are demonstrated in the 8-14 μ m atmospheric transmission window for the first time, with losses reaching ~1dB/cm. Molecular fingerprint sensing is demonstrated using a polymer with absorption lines in this spectral region.

Marriott
Salon IV

08:00–10:00

STh1O • Metasurfaces & Nanophotonic
Materials

Presider: Roberto Paiella; Boston Univ., USA

STh1O.1 • 08:00 **Invited**

Nonlinear and Tunable Semiconductor Metasurfaces, Isabelle Staude¹; ¹Friedrich-Schiller-Univ. Jena, Germany. Resonant semiconductor metasurfaces were established as a versatile platform for manipulating light fields. This talk reviews our recent advances in the integration of optical nonlinearities into such metasurfaces and on obtaining dynamic control of their optical response.

STh1O.2 • 08:30

Dynamically-tunable Plasmonic Devices Based on Phase Transition of Vanadium Dioxide, Ruwen Peng¹, Fang-Zhou Shu¹, Ren-Hao Fan¹, Mu Wang¹; ¹Nanjing Univ., China. We have experimentally demonstrated several dynamically-tunable plasmonic devices based on phase transition of vanadium dioxide, which include dynamic color generators and dynamically-switchable polarizers. The investigations can be applied in dynamic digital displays and imaging sensors.

Executive Ballroom
210A

Executive Ballroom
210B

Executive Ballroom
210C

Executive Ballroom
210D

CLEO: QELS-Fundamental Science

FTh1A • Exploiting Quantum Degrees of Freedom—Continued

FTh1A.2 • 09:00

Measuring frequency-bin entanglement in depolarized biphoton frequency combs, Oscar Sandoval¹, Navin B. Lingaraju¹, Poolad Imany¹, Daniel E. Leaird¹, Michael Brodsky², Andrew M. Weiner¹; ¹Purdue Univ., USA; ²U.S. Army Research Lab, USA. A polarization diversity phase modulator capable of measuring frequency-bin entanglement, irrespective of polarization fluctuations and the relative orientation between the signal and idler photons, is demonstrated.

FTh1A.3 • 09:15

High Dimensional Quantum Key Distribution with Biphoton Frequency Combs through Energy-Time Entanglement, Murat C. Sarihan¹, Kai-Chi Chang¹, Xiang Cheng^{1,6}, Yoo Seung Lee¹, Tian Zhong², Hongchao Zhou³, Zheshen Zhang⁴, Franco N. Wong⁵, Jeffrey H. Shapiro⁵, Chee Wei Wong¹; ¹Electrical and Computer Engineering, Univ. of California, Los Angeles, USA; ²Inst. for Molecular Engineering, Univ. of Chicago, USA; ³Shandong Univ., China; ⁴College of Optical Sciences, Univ. of Arizona, USA; ⁵Research Lab of Electronics, MIT, USA; ⁶State Key Lab of Information Photonics and Optical Communications, Beijing Univ. of Posts and Telecommunications, China. Biphoton frequency combs offer a photon-efficient way to achieve a very high-rate quantum key distribution by utilizing both time and frequency-bin encoding, while offering theoretically proven unconditional security.

FTh1B • Ultrafast Nonlinear Phenomena—Continued

FTh1B.3 • 08:45

Experimental Nonlinear Observation of TW Laser Propagation Through a 10m Rubidium Vapor Source for Plasma Diagnostics at AWAKE, Valentina Lee¹, Joshua Moody², Gabor Demeter³, Gregory Kriehn¹, Patric Muggli^{2,4}; ¹California State Univ. Fresno, USA; ²Max Planck Inst. for Physics, Germany; ³Wigner Research Center for Physics, Hungary; ⁴CERN, Switzerland. Nonlinear effects from a TW-class laser propagating through a 10m rubidium vapor at AWAKE are experimentally observed. A method of laser field reconstruction via phase retrieval is investigated for the initial conditions of the propagation.

FTh1B.4 • 09:00

Subcycle band structure movie of light-wave-driven Dirac currents, Johannes Reimann², Stefan Schlauderer¹, Christoph P. Schmid¹, Fabian Langer¹, Sebastian Baierl¹, Konstantin A. Kokh³, Oleg E. Tereshchenko⁴, Akio Kimura⁵, Christoph Lange¹, Jens Güdde², Ulrich Höfer², Rupert Huber¹; ¹Univ. of Regensburg, Germany; ²Fachbereich Physik, Philipps-Universität, Germany; ³V.S. Sobolev Inst. of Geology and Mineralogy SB RAS, Russia; ⁴A.V. Rzhanov Inst. of Semiconductor Physics SB RAS, Russia; ⁵Graduate School of Science, Hiroshima Univ., Japan. The first subcycle angle-resolved photoemission study reveals how an intense terahertz field drives topologically protected Dirac currents on the surface of Bi₂Te₃. Spin-momentum locking enables fully ballistic lightwave currents over several 100 nm.

FTh1C • Hot-electron Enabled Plasmonics & Optical Vortices—Continued

FTh1C.4 • 08:45

Enhanced Control of Size and Shape of Gold Nanoparticles Produced by a Simple and Scalable Thermal Process, Nathan Ray¹, Jae Hyuck Yoo¹, Hoang Nguyen¹, Mike Johnson¹, Sal Baxamusa¹, Selim Elhadji¹, Joseph Mckeown¹, Manyalibo J. Matthews¹, Eyal Feigenbaum¹; ¹Lawrence Livermore National Lab, USA. Enhanced control through sub-melting solid state diffusional dewetting is utilized to generate randomly oriented ensembles of nanoparticles on large scales, with controllable regulation over particle size, shape, and separation distance, ideal for large-area plasmonic applications.

FTh1C.5 • 09:00

Full Energy-Momentum Cathodoluminescence Mapping on Circular and Elliptical Plasmonic Bullseye Antennas, Toon Coenen^{2,1}, Albert Polman²; ¹Delmic, Netherlands; ²Center for nanophotonics, AMOLF, Netherlands. We investigate cathodoluminescence emission from circular and elliptical plasmonic bullseye antennas. The emission is mapped both in energy and momentum space, using a novel cathodoluminescence technique in which high-resolution spectroscopy and Fourier imaging are combined.

FTh1C.6 • 09:15

Airy Plasmon Pulses investigated by Multiphoton Photoemission Electron Microscopy (PEEM), Thomas Kaiser¹, Matthias Falkner¹, Amit Singh¹, Matthias Zilk¹, Michael Steinert¹, Thomas Pertsch¹; ¹Inst. of Applied Physics, Germany. We report on multiphoton PEEM measurements of pulsed Airy plasmons generated by a holographic grating. The diffraction-free behavior and high localization are important for generating spatio-temporal electromagnetic hotspots in ultrafast nanophotonics.

FTh1D • Entanglement Sources—Continued

FTh1D.4 • 08:45

Highly Directional Silicon Microring Photon Pair Source, Jeffrey A. Steidle¹, Michael Fanto^{1,2}, Stefan F. Preble¹, Christopher C. Tison², Paul M. Alsing²; ¹Rochester Inst. of Technology, USA; ²Air Force Research Lab, USA. Silicon microrings make for compact, tunable photon-pair sources but typically suffer from an effective 50% loss. Through interferometric coupling, these sources can be highly directional, resulting in a drastically improved performance.

FTh1D.5 • 09:00

Towards a source of entangled photon pairs in gallium phosphide, Paulina S. Kuo¹, Peter G. Schunemann², Mackenzie Van Camp², Varun B. Verma³, Thomas Gerrits³, Sae Woo Nam³, Richard P. Mirin³; ¹Information Technology Lab, NIST, USA; ²BAE Systems, USA; ³Physical Measurement Lab, National Inst. of Standards and Technology, USA. We investigate parametric down-conversion in orientation-patterned GaP. Pumped at 865 nm, the signal and idler are at 1350 nm and 2400 nm, respectively.

FTh1D.6 • 09:15

Spontaneous Parametric Down-Conversion in Integrated Hybrid Si₃N₄-PPLN Waveguides for High-Dimensional Qubit Entanglement, Xiang Cheng^{3,1}, Murat C. Sarihan¹, Kai-Chi Chang¹, Yoo Seung Lee¹, Fabian Laudenbach², Zhongyuan Yu³, Chee Wei Wong¹; ¹Dept. of Electrical Engineering, Univ. of California Los Angeles, USA; ²Security & Communication Technologies, Center for Digital Safety & Security, AIT Austrian Inst. of Technology GmbH, Austria; ³State Key Lab of Information Photonics and Optical Communications, Beijing Univ. of Posts and Telecommunications, China. We design a hybrid Si₃N₄ and PPLN waveguide for high-purity type-II SPDC generation with modeled normalized efficiency of 225% [W⁻¹cm⁻²]. High-dimensional entanglement via this source is predicted by HOM revival with visibility up to 99.79%.

CLEO: Science & Innovations

STh1E • Mid-IR Lasers—
Continued

STh1E.4 • 08:45

CO₂ Laser Optically Pumped by a Tunable 4.3 μm Laser Source, Dana Tovey¹, Jeremy Pigeon², Sergei Tochitsky¹, Gerhard Louwrens¹, Ilan Ben-Zvi², Chan Joshi¹, Dmitry Martyschkin³, Vladimir Fedorov³, Krishna Karki³, Sergey Mirov³; ¹UCLA, USA; ²Stony Brook Univ., USA; ³Univ. of Alabama, Birmingham, USA. A 10 μm CO₂ laser optically pumped by a tunable Fe:ZnSe laser is reported. Gain dynamics, slope efficiency, and self-focusing are studied, demonstrating potential use of an optically pumped CO₂ medium for picosecond pulse amplification.

STh1E.5 • 09:00

Watt-Level fs-Laser-Written Thulium Waveguide Lasers, Esrom Kifle², Pavel Loiko³, Carolina Romero⁴, Javier R. de Aldana⁴, Magdalena Aguiló², Francesc Diaz², Alain Braud³, Patrice Camy³, Uwe Griebner¹, Valentin Petrov¹, Xavier Mateos²; ¹Max Born Inst., Germany; ²Universitat Rovira i Virgili, Spain; ³Université de Caen, France; ⁴Univ. of Salamanca, Spain. A continuous-wave depressed-index channel waveguide laser fabricated by fs direct-laser-writing in monoclinic Tm:KLu(WO₄)₂ generated 1.07 W at 1.84 μm with a slope efficiency of 69.5%. Passive Q-switching by Cr²⁺:ZnS resulted in 2.6 ns/6.9 μJ pulses.

STh1E.6 • 09:15

Single-mode Depressed Cladding Buried Waveguide Laser Based on Single-crystal Cr:ZnS, Nikolai Tolstik^{1,2}, Andrey G. Okhrimchuk^{3,4}, Michail P. Smayev⁴, Vladislav Likhov⁴, Evgeni Sorokin⁵, Irina T. Sorokina^{1,2}; ¹Dept. of Physics, Norwegian Univ. of Science and Technology, Norway; ²ATLA Lasers AS, Norway; ³Fiber Optics Research Center, Russia; ⁴Mendeleyev Univ. of Chemical Technology, Russia; ⁵Photonics Inst., TU Wien, Austria. We report the first single-mode Cr:ZnS depressed cladding buried waveguide laser manufactured by femtosecond laser writing. The laser yields 150 mW average power at 2272 nm wavelength with 11% slope efficiency.

STh1F • Chip-Scale Trace-Gas
Sensing—Continued

STh1F.3 • 08:45

Carbon Dioxide Sensing with Low-confinement High-sensitivity Mid-IR Silicon Waveguides, Flavia Ottonello-Briano¹, Carlos Errando-Herranz¹, Henrik Rödjegård², Hans Martin², Hans Sohlström¹, Kristinn B. Gylfason¹; ¹Micro and Nanosystems, KTH Royal Inst. of Technology, Sweden; ²Senseair AB, Sweden. We present a low-confinement Si waveguide for 4.26 μm wavelength and apply it to sense CO₂ concentrations down to 0.1%. We demonstrate the highest reported waveguide sensitivity to CO₂: 44% of the free-space sensitivity.

STh1F.4 • 09:00

Gas spectroscopy using low threshold mid-infrared radiation generated in Si₃N₄ waveguides, Eirini Tagkoudi¹, Davide Grassani¹, Fan Yang³, Hairun Guo², Tobias J. Kippenberg², Camille-Sophie Bres¹; ¹EPFL STI IEL PHOSL, Switzerland; ²EPFL STI IEL LPQM, Switzerland; ³EPFL SCI STI LT, Switzerland. We report trace-gas absorption spectroscopy based on the efficient generation of a 3.05 μm dispersive wave in a Si₃N₄ waveguide pumped by a 2.09 μm femtosecond mode-locked fiber laser.

STh1F.5 • 09:15

An Affordable, Customizable, and Highly Sensitive Metasurface-Based Refractive Index Sensor, Adam Ollanik¹, Isaac O. Oguntoye¹, George Z. Hartfield¹, Matthew D. Escarra¹; ¹Tulane Univ., USA. We demonstrate a compact, metasurface-based sensor. Techno-economic analysis predicts a ~\$2,400 device capable of detecting changes in the refractive index of a liquid of ~2*10⁻⁸; prototype demonstrates 820% change in transmittance per refractive index unit.

STh1G • Frequency Comb
Spectroscopy—Continued

STh1G.4 • 09:00

Adaptive Sampling Terahertz Dual-Comb Spectroscopy Based on a Free-Running Single-Cavity Dual-Comb Fiber Laser, Jie Chen^{3,1}, Kuzuki Nitta^{1,2}, Xin Zhao³, Takahiko Mizuno^{1,2}, Takeo Minamikawa^{1,2}, Zheng Zheng³, Takeshi Yasui^{1,2}; ¹Tokushima Univ., Japan; ²JST, ERATO MINOSHIMA Intelligent Optical Synthesizer, Japan; ³Beihang Univ., China. Mode-resolved adaptive sampling terahertz dual comb spectroscopy is demonstrated using a free-running wavelength-multiplexed dual-comb fiber laser, which illustrates the capability of such single-cavity dual-comb sources for high-precision THz spectroscopy.

STh1G.5 • 09:15

Time-Resolved Dual Frequency Comb Spectroscopy for Broadband Multi-Species Detection in Laser-Induced Plasmas, Caroline Lecaplain¹, Yu Zhang^{2,1}, Reagan R. Weeks¹, Jeremy Yeak³, Sivanandan S. Harilal⁴, Mark C. Phillips⁴, R. J. Jones¹; ¹College of Optical Sciences, Univ. of Arizona, USA; ²Physics, Univ. of Arizona, USA; ³Opticslab, USA; ⁴Pacific Northwest National Lab, USA. We present the first results using time-resolved broadband dual-comb spectroscopy in a laser-induced plasma. Preliminary results identifying multiple species in a Nd magnet will be shown.

STh1H • Optical Resonance-
Based Devices—Continued

STh1H.3 • 08:45

Thermo-refractive noise in silicon nitride microresonators, Guanhao Huang¹, Erwan Lucas¹, Junqiu Liu¹, Arslan Raja¹, Grigory Lihachev^{2,3}, Michael L. Gorodetsky^{2,3}, Nils Engelsen¹, Tobias J. Kippenberg¹; ¹Inst. of Physics (IPHY), EPFL, Switzerland; ²Faculty of Physics, M.V. Lomonosov Moscow State Univ., Russia; ³Russian Quantum Centre, Russia. Thermodynamic noises limit the frequency stability of resonators. Here, we present the first complete characterization of thermo-refractive noise in Si₃N₄ microresonators. The measurements are in good agreement with theoretical analysis and FEM simulation of the structures.

STh1H.4 • 09:00

All-Optical Control of Pulse Storage Time and Retrieval Phase Using a Diamond Microdisk, Matthew Mitchell¹, David Lake¹, Paul E. Barclay¹; ¹Physics & Astronomy, Univ. of Calgary, Canada. Enhancement of optomechanical pulse storage time is demonstrated, for the first time, in a multimode diamond microdisk cavity. Optical control of the mechanical damping rate and frequency allows > 5× enhancement of the pulse storage time, and a maximum controllable pulse phase shift of ~2π.

STh1H.5 • 09:15

Record-High-Q Microresonators from 650 nm to 1550 nm Wavelengths on a 3C-SiC-on-Insulator Platform, Tianren Fan¹, Xi Wu¹, Ali Eftekhari¹, Ali Adibi¹; ¹Georgia Inst. of Technology, USA. We report record-high-Q SiC microresonators on a 3C-SiC-on-insulator platform with ultra-low (~1.4 Å) roughness after chemical-mechanical polishing. We demonstrate Qs of 242,000 at 1550 nm, 112,000 at 780 nm, and 83,000 at 650 nm.

Meeting Room
211 A/BCLEO: Applications
& TechnologyATH11 • Radiative Cooling &
Photovoltaics—Continued

ATH11.3 • 08:45
Boosted CO₂ Reduction Using Ultra-thin TiO₂ Photocatalyst Films on Nanocavities, Haomin Song¹, Wei Wu², Jian-Wei Liang³, Partha Maity⁴, Omar F. Mohammed⁴, Boon S. Ooi³, Dongxia Liu², Qiaoqiang Gan¹; ¹State Univ. of New York at Buffalo, USA; ²Dept. of Chemical & Biomolecular Engineering, Univ. of Maryland College Park, USA; ³Dept. of Electrical Engineering, King Abdullah Univ. of Science and Technology, Saudi Arabia; ⁴Dept. of Material Science, King Abdullah Univ. of Science and Technology, Saudi Arabia. We created an ultra-thin film photocatalytic light absorber (UFPLA) with 2–22-nm-thick TiO₂ films. The UFPLA structure conquered the intrinsic trade-off between optical absorption and charge carrier extraction efficiency and therefore boosted CO₂ reduction efficiency.

ATH11.4 • 09:00
Silicon Solar Cells Efficiency Enhanced in NIR Band by Coating Plasmonics ITO- and UC Phosphors-particles Layers on Back-side Surface Using Spin-on Film Deposition, Ding-Lun Lin¹, Wen-Jeng Ho¹, Guan-Yu Chen¹, Jheng-Jie Liu¹, Bao-Ying Pan¹, Ying-Lun Haung¹, Po-Yuan Ting¹, Xing-Yu Chen¹; ¹National Taipei Univ. of Technology, Taiwan. We demonstrate efficiency enhanced in NIR-band using plasmonics indium-tin-oxide (ITO) nanoparticles and up-conversion (UC)-phosphors particles on back-side of silicon solar cells. Impressive efficiency enhancement of 17.49% was obtained, compared to the reference-cell without ITO/UC-particles.

ATH11.5 • 09:15
Ultra-Wide Field of View Lens-Let Array for Efficient Solar Collection, Rakan E. Alsaigh¹, Ralf Bauer², Martin P. Lavery¹; ¹Univ. of Glasgow, UK; ²Univ. of Strathclyde, UK. Efficient solar collection over a full-day is a leading challenge for photovoltaic power generation. We present a novel multi-layer lens-let array that increases the daily collection efficiency of standard panels by a factor of 2.32.

Meeting Room
211 C/DCLEO: Science &
InnovationsSTh1J • Nonlinear Photonics—
Continued

STh1J.4 • 09:00
On-Chip Backward Inter-modal Brillouin Scattering, Yang Liu¹, Amol Choudhary¹, Guanghui Ren², Duk-yong Choi³, Alvaro Casas-Bedoya¹, Blair Morrison¹, Pan Ma³, Thach Nguyen², Khu Vu³, Arnan Mitchell², Stephen Madden³, David Marpaung⁴, Benjamin J. Eggleton¹; ¹The Univ. of Sydney, Australia; ²RMIT Univ., Australia; ³Australian National Univ., Australia; ⁴Univ. of Twente, Netherlands. We present the first demonstration of backward stimulated Brillouin scattering between distinct guided optical spatial modes in an integrated multi-modal photonic circuit. This unique opto-acoustic process enables new opportunities for on-chip Brillouin signal processing technology.

STh1J.5 • 09:15
Efficient and Broadband Four-wave Mixing in AlGaAs Microresonator for High-speed Optical Signal Processing, Chanju Kim¹, Erik Stassen¹, Kresten Yvind¹, Minhao Pu¹; ¹DTU Fotonik, Denmark. We demonstrate four-wave mixing in GHz-linewidth AlGaAs microresonators with -10.7-dB conversion efficiency at 4-mW pump power over the telecom S-, C- and L-bands. We achieve 57-dB resonance enhancement for microresonators supporting 10-Gbit/s signal processing.

Meeting Room
212 A/BCLEO: Applications
& TechnologyATH1K • Industrial Metrology &
Remote Sensing—Continued

ATH1K.3 • 08:45
Demonstration of the Hybrid Opto-electronic Correlator for Shift, Scale, and Rotation Invariant Target Recognition, Julian Gamboa¹, Mohamed Fouda¹, Selim M. Shahriar¹; ¹Northwestern Univ., USA. We demonstrate experimentally that our proposed hybrid opto-electronic correlator is capable of detecting objects in a scale, rotation, and shift invariant manner using currently available technologies by incorporating the polar Mellin transform.

ATH1K.4 • 09:00
Ultra-Broadband Photonic Monopulse-Like Radar for Remote Sensing, Bohao Liu¹, Jih-Min Wun², Nathan O'Malley¹, Daniel E. Leaird¹, Nan-Wei Chen³, Jin-Wei Shi², Andrew M. Weiner¹; ¹Purdue Univ., USA; ²National Central Univ., Taiwan; ³Yuan Ze Univ., Taiwan. High depth and transverse resolution remote target sensing using an extremely wide-bandwidth W-band (75 - 110 GHz) photonic monopulse-like radar system is demonstrated, offering prospects for millimeter wave 3-D sensing and imaging.

ATH1K.5 • 09:15
Regularized Phase Reconstruction for Sensing Deep Subwavelength Perturbations on Large-Scale Wafers, Jinlong Zhu¹, Lynford L. Goddard¹; ¹Univ. of Illinois at Urbana-Champaign, USA. We demonstrate that deep subwavelength scale perturbations on large-scale wafers can be inspected using a regularized phase metrology method. This work paves the route to reference-free defect inspection for nanostructures at advanced technology nodes.

Meeting Room
212 C/DCLEO: Science &
InnovationsSTh1L • Hollow Core Fibers—
Continued

STh1L.3 • 08:45
Brillouin Scattering in Anti-Resonant Hollow-Core Fibers, Arjun Iyer¹, Wendao Xu¹, Jose Enrique Antonio-Lopez², Rodrigo Amezcua Correa², William H. Renninger¹; ¹Inst. of Optics, Univ. of Rochester, USA; ²The College of Optics and Photonics, Univ. of Central Florida, USA. We investigate optomechanical interactions in anti-resonant hollow-core fibers, for the first time. Experiments and corresponding theoretical calculations reveal weak optomechanical coupling, which suggests that anti-resonant hollow-core fibers are well-suited for noise-sensitive applications.

STh1L.4 • 09:00 **Invited**
Low Loss Hollow Core Photonic Crystal Fibres: Fabrication to Applications, Natalie V. Wheeler¹, Tom Bradley¹, John Hayes¹, Yong Chen¹, Greg Jason¹, Ian Davidson¹, Hesham Sakr¹, Eric Numkam Fokoua¹, Seyed Reza Sandoghchi¹, Matthew Partridge¹, Shuichiro Rikimi¹, Simon Bawn², Austin Taranta¹, Radan Slavik¹, Marco N. Petrovich^{1,2}, Francesco Poletti¹, David Richardson¹; ¹Univ. of Southampton, UK; ²Lumensity Ltd, UK. We review our latest progress in the fabrication of ultra low loss hollow core photonic crystal fibres for applications including telecommunications, high power laser delivery and gas sensing.

CLEO: QELS-Fundamental
ScienceFTh1M • Ultrafast Processes in Gases &
Solids—Continued

FTh1M.4 • 08:45

Stark shift and gain decay in air lasing of N_2^+ , Ladan Arisian¹, Jean-Claude Diels¹, Brian Kamer¹; ¹*Univ. of New Mexico, Canada*. We present the Stark shift measurement on the individual transition lines of N_2^+ in a pump probe configuration. The time dependence of stark shift of transitions in plasma created by 800 nm filament shows the same time dependence as the gain decay.

FTh1M.5 • 09:00

Electronic quantum coherence in N_2^+ air lasing, Jinming Chen^{1,4}, Jinping Yao¹, Haisu Zhang², Zhaoxiang Liu¹, Bo Xu¹, Wei Chu¹, Lingling Qiao¹, Zhenhua Wang³, Julien Fatome², Olivier Faucher², Chengyin Wu³, Ya Cheng^{1,3}; ¹*State Key Lab of High Field Laser Physics, Shanghai Inst. of Optics and Fine Mechanics, Chinese Academy of Sciences, China*; ²*Universite de Bourgogne, France*; ³*State Key Lab of Precision Spectroscopy, East China Normal Univ., China*; ⁴*School of Physical Science and Technology, Shanghai Tech Univ., China*; ⁵*State Key Lab for Mesoscopic Physics, School of Physics, Peking Univ., China*. We report on the generation of electronic quantum coherence in the ionized nitrogen molecules. The coherence is revealed by observing N_2^+ air lasing with a near-infrared laser and a delayed mid-infrared laser.

FTh1M.6 • 09:15

Energy Transmission Efficiency of Laser-induced Vortical Filaments, Milos Burger¹, Patrick J. Skrodzki¹, John Nees¹, Igor Jovanovic¹; ¹*Univ. of Michigan, USA*. We performed characterization and energy transmission measurements of both ordinary and vortical ultrafast filament structures in air. The results appear to stand in favor of the reduced ionization losses in the case of vortical filaments.

CLEO: Science & Innovations

STh1N • Sensing & Switching—Continued

STh1N.3 • 08:45

A low power superconductor-to-optoelectronic interface, Adam McCaughan¹, Sonia Buckley¹, Varun B. Verma¹, Alexander N. Tait¹, Sae Woo Nam¹, Jeff Shainline¹; ¹*NIST, USA*. We present a ultrahigh-impedance superconducting thermal switch that acts as a superconductor-to-optoelectronic interface. We demonstrated the generation of photons in a cryogenic photonic LED from a low-voltage input, detecting those photons with a waveguide-coupled detector.

STh1N.4 • 09:00

Scalable Space-and-Wavelength Selective Switch Architecture Using Microring Resonators, Qixiang Cheng¹, Meisam Bahadori¹, Madeleine Glick¹, Keren Bergman¹; ¹*Columbia Univ., USA*. A new architecture for space-and-wavelength selective switch fabrics is proposed. This class of designs built with a combination of microring-based channel-selectors and comb-aggregators completely blocks first-order in-band crosstalk enabling highly-scalable and flexible interconnection networks.

STh1N.5 • 09:15

Broadband Low-loss Non-volatile Photonic Switches Using Phase-Change Materials, Jiajiu Zheng¹, Peipeng Xu², Jonathan Doyle³, Arka Majumdar¹; ¹*Univ. of Washington, Seattle, USA*; ²*Key Lab of Photoelectric Materials and Devices of Zhejiang Province, Ningbo Univ., China*; ³*Silicon Photonic Products Division, Intel Corporation, USA*. Based on the non-volatile GST-on-silicon platform, we demonstrate compact (~30 μ m), low-loss (~1 dB), and broadband (over 30 nm with crosstalk < -10 dB) 1 × 2 and 2 × 2 photonic directional coupler switches.

STh1O • Metasurfaces & Nanophotonic
Materials—Continued

STh1O.3 • 08:45

Programmable self-assembled metasurface for strong field enhancement, Tapajyoti Das Gupta¹, Louis Martin-Monier¹, Arthur Lebris¹, Wei Yan¹, Tung Dang Nguyen¹, Alexis Page¹, Fabien Sorin¹; ¹*Material science, Ecole Polytechnique Federale de Lausanne, Switzerland*. Self-assembled chalcogenide metasurfaces is proposed for low-cost manufacturing on large-area unconventional substrates. Programmed control over particle arrangement and periodicity yields strong Fano resonances, highlighting novel applications for bio-detection and second harmonic generation.

STh1O.4 • 09:00

Embedded dielectric metasurface based subtractive color filter on a 300mm glass wafer, Zhengji Xu¹, Yuan Dong¹, Yuan-Hsing Fu¹, Qize Zhong¹, Ting Hu¹, Dongdong Li¹, Yu Li¹, Nanxi Li¹, Ying Lin¹, Qunying Lin¹, Shiyang Zhu¹, Navab Singh¹; ¹*A*STAR, Inst. of Microelectronics, Singapore*. Si metasurface embedded subtractive color filters (SCFs) is firstly demonstrated on a 300mm glass wafer using CMOS-compatible fabrication process. Three transmission dips were observed at 528, 568, and 598 nm wavelengths for different SCF designs.

STh1O.5 • 09:15

Large-area, single material metalens in the visible: An approach for mass-production using conventional semiconductor manufacturing techniques, Joon-Suh Park¹, Shuyan Zhang¹, Alan She¹, Wei-Ting Chen¹, Kerolos M. Yousefi^{1,2}, Federico Capasso¹; ¹*Harvard Univ., USA*; ²*Univ. of Waterloo, Canada*. We present mass-producible, large area, single-material metalens working in the visible wavelength, using conventional deep-ultraviolet (DUV) stepper lithography technique. Having a diameter of 1 cm, our present lens show polarization independent, near-diffraction limited focusing behavior.

**Executive Ballroom
210A**

**Executive Ballroom
210B**

**Executive Ballroom
210C**

**Executive Ballroom
210D**

CLEO: QELS-Fundamental Science

FTh1A • Exploiting Quantum Degrees of Freedom—Continued

FTh1A.4 • 09:30

High-dimensional one-way quantum computation operations with on-chip optical d-level cluster states, Christian Reimer^{1,2}, Michael Kues², Stefania Sciara², Piotr Roztock², Mehedi Islam², Luis Romero Cortes², Yanbing Zhang², Bennet Fischer², Sebastien Loranger³, Raman Kashyap³, Alfonso Cino⁴, Sai Chu⁵, Brent Little⁶, David Moss⁷, Lucia Caspani⁸, William Munro⁹, Jose Azana², Roberto Morandotti², ¹Harvard Univ., USA; ²INRS-EMT, Canada; ³Polytechnique Montreal, Canada; ⁴Univ. of Palermo, Italy; ⁵City Univ. of Hong Kong, China; ⁶Xi'an Inst. of Optics and Precision Mechanics, China; ⁷Swinburne Univ. of Technology, Australia; ⁸Univ. of Strathclyde, UK; ⁹NTT Basic Research Labs, Japan. We implement on-chip generation of hyper-entangled states in the time- and frequency-domain, and transform them into d-level cluster states using a deterministic controlled phase gate. We then demonstrate one-way quantum computing operations and show the state's high tolerance towards noise.

FTh1A.5 • 09:45

Optical Information Processing with Noise-Resistant Entangled Topological States, Alexander V. Sergienko¹, David Simon^{1,2}, Shuto Osawa¹, ¹Boston Univ., USA; ²Stonehill College, USA. Linear-optical photonic quantum walks are used to jointly entangle polarization and winding number. This joint entanglement allows polarization entanglement-based quantum information processing tasks to be performed with high degree of error protection.

FTh1B • Ultrafast Nonlinear Phenomena—Continued

FTh1B.5 • 09:30

Sub-millijoule, 3 μm optical parametric chirped-pulse amplifier at 10 kHz repetition rate, Xiao Zou^{2,1}, Wenkai Li^{2,1}, Houkun Liang², Shizhen Qu^{2,1}, Kun Liu^{2,1}, Qijie Wang¹, Ying Zhang²; ¹Nanyang Technological Univ., Singapore; ²Singapore Inst. of Manufacturing Technology, Singapore. We demonstrate a 3 μm optical parametric chirped pulse amplifier with 802 μJ pulse energy, at 10 kHz repetition rate, and stable carrier-envelope phase. 73 fs pulse width is obtained with an efficient nonlinear compression.

FTh1B.6 • 09:45

Nonlinear Generation of Ultrafast beams with Classical Non-Separable States of Light, Ravi Saripalli¹, Anirban Ghosh¹, Apurv C. Nellikka², Goutam Samanta¹; ¹Atomic, molecular and optical physics division, Physical Research Lab, India; ²Tecnologico de Monterrey, Mexico. We report on non-linear generation of ultrafast optical beams with classical non-separable states in spin and orbital angular momentum degrees-of-freedom with topological order as high as 24 and output power as high as 20 mW.

FTh1C • Hot-electron Enabled Plasmonics & Optical Vortices—Continued

FTh1C.7 • 09:30

Dynamics of Decelerating Plasmonic Vortex Cavities, Grisha Spektor¹, Anna-Katharina Mahro², Eva Prinz^{2,4}, Michael Hartelt², Deirdre Kilbane^{2,3}, Martin Aeschlimann², Meir Orenstein¹; ¹Technion Israel Inst. of Technology, Israel; ²Dept. of Physics, Kaiserslautern Univ., Germany; ³Telecommunications Software & Systems Group, Waterford Inst. of Technology, Ireland; ⁴Graduate School Materials Science in Mainz, Germany. We experimentally demonstrate plasmonic decelerating vortex cavities generating a succession of surface-confined vortex pulses carrying temporally-increasing orbital angular momentum. Using ultra-flat gold surface, we spatiotemporally resolve the evolution within the cavities over 300 femtoseconds.

FTh1C.8 • 09:45

Brownian Dynamics Controlled by Phase Gradients, Cristian Hernando Acevedo¹, Jose Guzman-Sepulveda¹, Aristide Dogariu¹; ¹Univ. of Central Florida, USA. We demonstrate the effect of random forces induced by phase gradients on the dynamics of small particles. We show that subdiffusive regimes could be controlled by the topological charge of an external optical field.

FTh1D • Entanglement Sources—Continued

FTh1D.7 • 09:30

Telecom Narrow Bandwidth Two-photon Source with High Fidelity Polarization Entanglement, Kazuya Niizeki¹, Daisuke Yoshida¹, Mingyang Zheng², Xiuping Xie², Kotaro Okamura³, Nobuyuki Takei⁴, Tomoyuki Horikiri^{1,5}; ¹Yokohama National Univ., Japan; ²Jinan Inst. of Quantum Technology, China; ³Kanagawa Univ., Japan; ⁴Kyoto Univ., Japan; ⁵JST PRESTO, Japan. We demonstrate two-photon sources for long-distance quantum communication. The highest spectral brightness 3.94×10⁵ pairs/(s MHz mW), the narrowest linewidth in telecom of 1.06 MHz and entanglement fidelity of 91.8% are shown.

FTh1D.8 • 09:45

Satellite-Borne High-Brightness Source of Entangled Photons, Yuan Cao¹; ¹Univ. of Science and Technology of China, China. The satellite-borne high-brightness source of polarization-entangled photons was developed and launched with the "Micius" quantum science satellite. With this source we implemented the Bell test between the satellite and the ground stations over 1200 km.

10:00–11:30 Exhibit Open (10:00–15:00), Coffee Break (10:00–11:30), Exhibit Halls 1–3

Coffee Break Sponsored by  COHERENT and  THORLABS

10:15–12:00 Technology Transfer Program, Exhibit Hall Theater I

CLEO: Science & Innovations

STh1E • Mid-IR Lasers—
Continued

STh1E.7 • 09:30

Mid-IR Optical Refrigeration: Optical Cryocoolers and Radiation Balanced Lasers, Saeid Rostami¹, Azzurra Volpi¹, Alexander R. Albrecht¹, Mauro Tonelli², Mansoor Sheikh-Bahae¹; ¹Univ. of New Mexico, USA; ²NEST-CNR, Dipartimento di Fisica, Università di Pisa, Italy. Optical refrigeration in Tm- and Ho-doped crystals is investigated, and their external quantum efficiency, background absorption, and minimum achievable temperatures are reported. Potential of these crystals for mid-IR cryocoolers and radiation balanced lasers are discussed.

STh1F • Chip-Scale Trace-Gas
Sensing—Continued

STh1F.6 • 09:30

Suspended Membrane InGaAs Photonic Crystal Waveguides for ammonia sensing at $\lambda = 6.15 \mu\text{m}$, Kyoung Min Yoo¹, Jason Midkiff¹, Ali Roostamian¹, Swapnajit Chakravarty², Ray T. Chen^{1,2}; ¹Electrical and Computer Engineering, The Univ. of Texas at Austin, USA; ²Omega Optics Inc., USA. Fully suspended InGaAs waveguide devices with holey photonic crystal waveguides (HPCWs) are designed for mid-infrared sensing at $\lambda = 6.15 \mu\text{m}$ in the low index contrast InGaAs-InP platform. We experimentally detect 5ppm ammonia in 1mm long suspended HPCWs.

STh1F.7 • 09:45

Waveguide-Enhanced Raman Spectroscopy Using a Mesoporous Silica Sorbent Layer for Volatile Organic Compound (VOC) Sensing, Haolan Zhao^{1,2}, Ali Raza^{1,2}, Bettina Baumgartner³, Stephane Clemmen^{1,2}, Bernhard Lendl³, Andre Skirtach⁴, Roel Baets^{1,2}; ¹Photonics Research Group, INTEC, Gent Univ., Belgium; ²Center for Nano- and Biophotonics, Ghent Univ., Belgium; ³Inst. of Chemical Technologies and Analytics, Technische Universität Wien, Austria; ⁴Dept. of Molecular Biotechnology, Ghent Univ., Belgium. We report a Raman sensor for broadband vapor-phase volatile organic compounds (VOCs) based on SiN waveguides functionalized with a mesoporous silica top-cladding. A detection limit below 1000ppm is demonstrated and scaling to trace-gas-levels is discussed.

STh1G • Frequency Comb
Spectroscopy—Continued

STh1G.6 • 09:30

Singular spectrum analysis for low SNR signal processing in dual-comb distance measurements, Hui Cao¹, Youjian Song¹, Runmin Li¹, Yuepeng Li¹, Ming-lie Hu¹, Chingyue Wang¹; ¹Tianjin Univ., China. We utilize singular spectrum analysis based post-processing approach to reduce distance measurement uncertainty for moving targets in dual-comb absolute ranging.

STh1G.7 • 09:45

Nanophotonic supercontinuum based mid-infrared dual-comb spectroscopy, Hairun Guo¹, Wenle Weng¹, Junqiu Liu¹, Fan Yang², Wolfgang Hänsel³, Camille-Sophie Bres⁴, Luc Thévenaz², Ronald Holzwarth³, Tobias J. Kippenberg¹; ¹LPQM, École Polytechnique Fédérale de Lausanne, Switzerland; ²GFO, École Polytechnique Fédérale de Lausanne, Switzerland; ³Menlo Systems GmbH, Germany; ⁴PHOSL, École Polytechnique Fédérale de Lausanne, Switzerland. We demonstrate a broadband mid-infrared dual-comb spectroscopy for parallel gas-phase detection in the functional group region from 2800–3600 cm^{-1} , using dispersion engineered silicon nitride dual-core waveguides which produce broadband, intensity-enhanced and coherent mid-infrared frequency combs.

STh1H • Optical Resonance-
Based Devices—Continued

STh1H.6 • 09:30

Fabry-Perot Cavity Using Two Row Photonic Crystal in a Multimode Waveguide, Manuel Mendez-Astudillo¹, Hideaki Okayama², Tomohiro Kita¹; ¹Waseda Univ., Japan; ²Research & Development Center, Oki Electric Industry Co., Ltd, Japan. We experimentally present a Fabry-Perot cavity that uses two-row photonic crystals in a multimode waveguide as the reflecting elements in an add-drop configuration to achieve fine FSR tuning and maximum footprint efficiency.

STh1H.7 • 09:45

New Resonance Behavior based on Bound States in the Continuum in a Silicon Photonic Waveguide Platform, Thach Nguyen¹, Guanghui Ren¹, Steffen Schoenhardt¹, Markus Knoerzer¹, Andreas Boes¹, Arnan Mitchell¹; ¹School of Engineering, RMIT Univ., Australia. A new type of resonance in silicon photonics is demonstrated, achieved by coupling between a continuum of TE slab modes to a discrete TM mode of a silicon ridge to create a single sharp resonance.

10:00–11:30 Exhibit Open (10:00–15:00), Coffee Break (10:00–11:30), Exhibit Halls 1–3

Coffee Break Sponsored by  COHERENT and  THORLABS

10:15–12:00 Technology Transfer Program, Exhibit Hall Theater I

**Meeting Room
211 A/B**

**CLEO: Applications
& Technology**

ATH11 • Radiative Cooling & Photovoltaics—Continued

ATH11.6 • 09:30
Broadband Omni-resonant Enhancement in Near-Infrared Quantum-Efficiency of a Thin Film Amorphous Silicon Solar Cell, Massimo Villinger¹, Abbas Shiri¹, Soroush Shabahang¹, Magued B. Nasr¹, Chris Villinger¹, Ayman F. Abouraddy¹; ¹Univ. of Central Florida, USA. By embedding an amorphous-silicon thin-film solar cell in an omni-resonant micro-cavity, we demonstrate a broadband boost in the near-infrared optical absorption and concomitant enhancement in the quantum efficiency.

ATH11.7 • 09:45
Near Perfect Solar Energy Conversion for Vapor Generation, Youhai Liu¹, Haomin Song¹, Matthew H. Singer¹, Chenyu Li¹, Dengxin Ji¹, Lyu Zhou¹, Nan Zhang¹, Xie Zeng¹, Zongmin Bei¹, Zongfu Yu², Qiaoqiang Gan¹; ¹The State Univ. of New York at Buffalo, USA; ²Univ. of Wisconsin, USA. We demonstrate a strategy to realize ~100% efficiency for solar vapor generation by managing the energy flow, and to further enhance the evaporation by taking energy from the warmer environment.

**Meeting Room
211 C/D**

CLEO: Science & Innovations

STh1J • Nonlinear Photonics—Continued

STh1J.6 • 09:30
Saturable absorption of nonlinear graphene coated waveguides, Pierre Demongodin¹, Houssein El Dirani², Jérémy Lhuillier¹, Malik Kemiche¹, Thomas Wood¹, Ségolène Callard¹, Pedro Rojo-Romeo¹, Corrado Sciancalepore², Christian Grillet¹, Christelle Monati¹; ¹Institut des nanotechnologies de Lyon, France; ²Optics and Photonics Division, CEA-LETI, France. We investigate the saturable absorption of hybrid graphene/silicon-nitride waveguides at telecom wavelengths. By measuring the power dependent transmission of picosecond and sub-picosecond pulses, we clarify the temporal dynamics of photo-excited carriers in graphene.

STh1J.7 • 09:45
Cavity Enhanced Trion Emission from a Bilayer MoTe₂ on Silicon, Jianxing Zhang^{1,2}, Zizhao Zhong^{1,2}, Yongzhuo Li^{1,2}, Jiabin Feng^{1,2}, Lin Gan^{1,2}, Cunzheng Ning^{1,3}; ¹Dept. of Electronic Engineering, Tsinghua Univ., China; ²Beijing National Research Center for Information Science and Technology, China; ³School of Electrical, Computer, and Energy Engineering, Arizona State Univ., USA. We study the coupling of a 2D silicon photonic crystal cavity with the trion emission of a bilayer MoTe₂. Strong cavity enhanced emission of 3.4 times was observed, paving the way for low-energy photonic applications.

**Meeting Room
212 A/B**

**CLEO: Applications
& Technology**

ATH1K • Industrial Metrology & Remote Sensing—Continued

ATH1K.6 • 09:30
Laser-based Frequency Transfer over Underwater Link with Phase Compensation, Dong Hou¹, Guangkun Guo¹, Jiyuan Chen¹, Danian Zhang¹, Ke Liu¹, Fuyu Sun²; ¹Univ. of Elect. Sci. and Tech. of China, China; ²National Time Service Center, Chinese Academy of Science, China. We demonstrate a laser-based transfer of radio-frequency signal with phase compensation over 5 m underwater link. The root-mean-square timing fluctuation of the transferred RF signal is about 2.3 ps within 5000 s.

ATH1K.7 • 09:45
Higher Order Bessel Beams Integrated in Time (HOBBIT) for Underwater Sensing and Metrology, Kaitlyn Morgan¹, Yuan Li¹, Wenzhe Li¹, Keith Miller¹, Joseph Watkins¹, Eric Johnson¹; ¹Clemson Univ., USA. This paper introduces a novel platform for coherently coupled OAM modes that can be dynamically controlled at rates in excess of 100's kHz. Results are provided for a 512-QAM constellation composed of two OAM states.

**Meeting Room
212 C/D**

CLEO: Science & Innovations

STh1L • Hollow Core Fibers—Continued

STh1L.5 • 09:30
Nested-capillary anti-resonant silica fiber with mid-infrared transmission and very low bending sensitivity at 4000 nm, Mariusz Klimczak^{1,2}, Dominik Dobrakowski^{1,2}, Amar Nath Ghosh³, Grzegorz Stepniowski¹, Dariusz Pysz¹, Thibaut Sylvestre³, Ryszard Buczynski^{2,1}; ¹Inst of Electronic Materials Technology, Poland; ²Faculty of Physics, Univ. of Warsaw, Poland; ³Institut FEMTO-ST, CNRS, France. Silica glass nested capillary anti-resonant fiber is reported. Transmission is measured with 150cm long sample over 1700-4200nm wavelengths, revealing a 3500-4200nm window. The fiber is bending insensitive down to 0.5cm radius over a full loop.

STh1L.6 • 09:45
Hollow-Core Conjoined-Tube Negative-Curvature Fiber with Loss approaching Rayleigh Scattering Limit of Silica, Shoufei Gao¹, Yingying Wang¹, Wei Ding², Yifeng Hong¹, Pu Wang¹; ¹Beijing Univ. of Technology, China; ²Inst. of Physics, Chinese Academy of Science, China. We report on a hollow-core conjoined-tube negative-curvature fiber with measured transmission losses of 2.7dB/km at 1150nm and 3.8dB/km at 680nm. The loss from 653 to 706 nm approaches the Rayleigh scattering limit of silica fiber.

10:00–11:30 Exhibit Open (10:00–15:00), Coffee Break (10:00–11:30), Exhibit Halls 1–3
Coffee Break Sponsored by  COHERENT and 

10:15–12:00 Technology Transfer Program, Exhibit Hall Theater I

**CLEO: QELS-Fundamental
Science**

**FTh1M • Ultrafast Processes in Gases &
Solids—Continued**

FTh1M.7 • 09:30

High Intensity 5th Harmonic Generation using CLBO, Sid-dharth Patankar¹, Steven T. Yang¹, Andrew J. Bayramian¹, Mark W. Bowers¹, Phillip S. Datte¹, George F. Swadling¹, Joel Stanley¹, Tracy S. Budge¹, James S. Ross¹; ¹Lawrence Livermore National Lab, USA. We report results from frequency conversion experiments using a 1053 nm Nd:Glass laser system and a CLBO quintupler to generate fifth harmonic (211 nm) output. A peak 211 nm intensity of 0.4 GW/cm² was measured with a fundamental drive intensity of 2.25 GW/cm²

FTh1M.8 • 09:45

Efficient 2-W Average Power 206nm Deep-UV Generation from 100-kHz Picosecond Pulses, Benjamin Willenberg¹, Fabian Brunner¹, Christopher Phillips¹, Ursula Keller¹; ¹ETH Zurich, Switzerland. We present a 100-kHz all-solid-state deep-ultraviolet source delivering 206nm few-picosecond pulses with 2-W average power based on non-collinear sum frequency generation, which features high conversion efficiency by pulse front tilt matching and beam flattening.

CLEO: Science & Innovations

STh1N • Sensing & Switching—Continued

STh1N.6 • 09:30

Low-loss integrated photonic switch using sub-wavelength patterned phase change material, Changming Wu¹, Heshan Yu², Huan Li³, Xiaohang Zhang², Ichiro Takeuchi², Mo Li^{1,3}; ¹Dept. of Electrical and Computer Engineering, Univ. of Washington, USA; ²Dept. of Materials Science and Engineering, Univ. of Maryland, USA; ³Dept. of Electrical and Computer Engineering, Univ. of Minnesota, USA. We demonstrate a 1×2 switch using phase Ge-Sb-Te (GST) integrated micro-ring resonator. The device achieves a low insertion loss of less than 1 dB in both output ports and can be switched photo-thermally and electro-thermally.

STh1N.7 • 09:45

DAC-less PAM4 Transmitter using Electro-optic Polymer Dual-drive Mach-Zehnder Modulator with Imbalanced Binary Driving Electronics, Guo-Wei Lu^{1,2}, Jianxun Hong², Hongbo Zhang^{1,3}, Feng Qiu², Shiyoshi Yokoyama²; ¹Tokai Univ., Japan; ²Kyushu Univ., Japan; ³Chengdu Univ. of Information Technology, China. We experimentally demonstrate a 20-Gb/s PAM4 transmitter using EO polymer dual-drive MZM with imbalanced binary driving electronics, eliminating the need of power-hungry DAC or linear drivers and featuring low power consumption and potentially low cost.

**STh1O • Metasurfaces & Nanophotonic
Materials—Continued**

STh1O.6 • 09:30 **Invited**

Beating the Heat via Radiative Cooling: Tales of the Saharan Silver Ant, Comet Moth Silk Fibers, and Butterfly Wings, Nanfang Yu¹; ¹Columbia Univ., USA. I will present the discovery of radiative cooling in living organisms and the development of bioinspired radiative-cooling technologies.

10:00–11:30 Exhibit Open (10:00–15:00), Coffee Break (10:00–11:30), Exhibit Halls 1–3
Coffee Break Sponsored by  COHERENT and  THORLABS

10:15–12:00 Technology Transfer Program, Exhibit Hall Theater I

JTh2A.1

Controlling Electron Quantum Paths for Generation of Circularly Polarized High-Order Harmonics by H_2^+ Subject to Tailored (ω , 2ω) Counter-Rotating Laser Fields, John T. Heslar¹, Dmitry A. Telnov², Shih-I Chu^{1,3}; ¹Dept. of Physics, National Taiwan Univ., Taiwan; ²Dept. of Physics, St. Petersburg State Univ., Russia; ³Dept. of Chemistry, Univ. of Kansas, USA. We demonstrate the ability to control the electron recollisions giving three returns per one cycle of the fundamental frequency ω using tailored bichromatic (ω , 2ω) counter-rotating circularly polarized laser fields with a molecular target.

JTh2A.2

Low Energy Hollow Core Fiber Pulse Compression Using Molecular Gases, Elissa Haddad¹, Reza Safaei¹, Ojoon Kwon¹, Adrien Leblanc¹, Riccardo Piccoli¹, Young-Gyun Jeong¹, Heide Ibrahim¹, Bruno E. Schmidt², Roberto Morandotti^{1,2}, Luca Razzari¹, François Légaré¹, Philippe Lassonde¹; ¹INRS-EMT, Canada; ²ITMO Univ., Russia; ³Few-cycle Inc., Canada. We show that hydrofluorocarbons can be used for efficient hollow core fiber pulse broadening. Fivefold compression, 45 fs down to ~9 fs, of low-energy titanium-sapphire laser pulses (~16 μ J) is achieved.

JTh2A.3

Phase-matched perturbative wave-mixing in XUV region, Khuong B. Dinh¹, Khoa Anh Tran¹, Peter Hannaford¹, Lap Dao¹; ¹Swinburne Univ. of Technology, Australia. We demonstrate generation of phase-matched four-wave mixing frequencies in XUV region by using a driving field and two control fields. Our findings are promising to produce an XUV quasi-continuum for attosecond pulses synthesis.

JTh2A.4

Brunel harmonics generated from ionizing clusters by few-cycle laser pulses, Xiaohui Gao¹, Bonggu Shim², Michael Downer³; ¹Shaoying Univ., China; ²Binghamton Univ., USA; ³The Univ. of Texas at Austin, USA. We theoretically demonstrate Brunel-type harmonic generation from ionizing nano-clusters irradiated by intense few-cycle laser pulses. Mie oscillations strongly blue-shift and enhance the internal field. The resulting subcycle ionization dynamics efficiently produce broadband VUV radiation.

JTh2A.5

Brunel harmonics in nanostructures, Ihar Babushkin^{2,1}, Liping Shi², Ayhan Demircan^{2,3}, Uwe Morgner^{2,3}, Milutin Kovacev²; ¹Max-Born Inst., Germany; ²Inst. of Quantum Optics, Univ. of Hannover, Germany; ³Hannover Centre for optical Technologies, Germany. Brunel harmonics appear in gases due to tunnel ionization of electrons in strong fields (without recollision with the cores). Here we extend this mechanism to nanostructures. The harmonics are affected by strong field gradients.

JTh2A.6

Optimization of RF Emission from Ultra-short Pulse Laser Filament via Genetic Algorithm and Deformable Mirror, Adrian Lucero¹, Alexander Englesbe¹, Jennifer Elle¹, Jinpu Lin², John Nees², Karl Krushelnick²; ¹AFRL, USA; ²Center for Ultrafast Optical Science, Univ. of Michigan, USA. A genetic algorithm is used to drive a deformable mirror and optimize the RF emission from an ultra-short pulse plasma filament. The optimization process increases the plasma volume, linking plasma conductance to RF emission.

JTh2A.7

Measurements of Plasma Densities in Laser Filamentation in Solids at Various Wavelengths Spanning From Near and Mid Infrared, Garima C. Nagar¹, Dennis Dempsey¹, Bonggu Shim¹; ¹Binghamton Univ., USA. We measure plasma densities in laser filamentation in fused silica using single-shot time-resolved interferometry when the filament driver wavelength is varied between 1.2 and 2.3 μ m. The experimental results are compared with numerical simulations.

JTh2A.8

Towards Precision Measurements of Radiation Reaction, Yarden Sheffer¹, Morgan Lynch¹, Yaron Hadad¹, Ido Kaminker¹; ¹Technion - Israel Inst. of Technology, Israel. We find the long-time dynamics of charges in electromagnetic fields, revealing that charge energy loss to radiation leads to counter-intuitive acceleration. Using this phenomenon, we propose a method to observe radiation reaction with weak fields.

JTh2A.9

Off-focus beam profile optimization for high-order harmonic generation, Jialin Li¹, Tianyi Guo¹, Jonathon White¹, Matthew Weidman², Yi Wu¹, Zenghu Chang¹; ¹Univ. of Central Florida, USA; ²Max-Planck-Institut für Quantenoptik, Germany. Customized wave-front correction was realized by an adaptive optics system in a high-energy femtosecond system to obtain smooth beam profiles far away from focal positions and boost the photon flux of high order harmonic generation.

JTh2A.10

Air-hole-type Valley Photonic Crystal Slab with Simple Triangular Lattice for Valley-contrasting Physics, Taiki Yoda^{1,2}, Masaya Notomi^{1,2}; ¹Tokyo Inst. of Technology, Japan; ²NTT Basic Research Labs, Japan. We theoretically propose a new scheme to realize a valley photonic crystal slab with simple triangular lattice. The eigenstates which are not originated from the Dirac cone can exhibit valley-contrasting physics by breaking inversion symmetry.

JTh2A.11

Control the Wave-front and Polarization of Light Simultaneously with High-efficiency Meta-surfaces, Dongyi Wang¹, Feifei Liu¹, Shulin Sun¹, Qiong He¹, Lei Zhou¹; ¹Fudan Univ., China. We propose a generic approach for designing metasurfaces to efficiently control the wave-front and polarization of light simultaneously, and realized several meta-devices to verify the concept at near-infrared frequencies, which exhibit distinct light-manipulation capabilities.

JTh2A.12

Linking guided waves and surface waves via metasurface on terahertz-integrated platform, Ride Wang¹, Qiang Wu^{1,2}, Zixi Jia¹, Yaqing Zhang¹, Bin Zhang³, Wei Cai^{1,2}, Jingjun Xu^{1,2}; ¹Key Lab of Weak-Light Nonlinear Photonics, Ministry of Education, TEDA Inst. of Applied Physics and School of Physics, Nankai Univ., China; ²Collaborative Innovation Center of Extreme Optics, Shanxi Univ., China; ³College of Science, Civil Aviation Univ. of China, China. We implement the conversion from terahertz guided waves to surface waves via metasurface on lithium niobate subwavelength waveguide, providing a platform for thin-layer effective detection, which provides a more pronounced sensitivity than the normal interaction.

JTh2A.13

Withdrawn

JTh2A.14

Dual-wavelength Terahertz Metalems Based on Geometric Phase Metasurface, Taili Wang¹, Hang Li², Rensheng Xie¹, Sensong An², Shouzheng Zhu¹, Guohua Zhai¹, Wei Guo³, Hualiang Zhang², Jun Ding¹; ¹School of Information and Science Technology, East China Normal Univ., China; ²ECE Dept., Univ. of Massachusetts Lowell, USA; ³Physics and Applied Physics Dept., Univ. of Massachusetts Lowell, USA. We proposed a novel dual-wavelength meta-atom, which could be used to independently modulate the geometric phase of the circularly polarized incident wave at two terahertz frequencies. A prototype dual-wavelength metalems has been designed and verified at the terahertz regime.

JTh2A.15

On-chip plasmon-induced transparency using a metastructure in THz regime, Wenjuan Zhao¹, Yao Lu¹, Qi Zhang¹, Jiwei Qi^{1,2}, Qiang Wu^{1,2}, Jingjun Xu^{1,2}; ¹The Key Lab of Weak-Light Nonlinear Photonics, Ministry of Education, TEDA Inst. of Applied Physics and School of Physics, Nankai Univ., China; ²Collaborative Innovation Center of Extreme Optics, Shanxi Univ., China. We experimentally and numerically demonstrated an investigation of plasmon-induced transparency using a meta-structure on a THz LiNbO₃ chip. A Rabi oscillation-like behavior at the transparency peak was obtained.

JTh2A.16

Control of slow-light effect in metamaterial-loaded Si waveguide, Makoto Tanaka¹, Tomo Amemiya¹, Satoshi Yamasaki¹, Hibiki Kagami¹, Keisuke Masuda¹, Nobu Nishiyama¹, Shigehisa Arai¹; ¹Tokyo Inst. of Technology, Japan. We have demonstrated slow-light effect with the slow-down factor of >10 times in a metamaterial-loaded Si waveguide which can be easily integrated with other Si photonics devices, and proposed optically control method for that effect.

JTh2A.17

Optimal Single Metagrating for Robust Polarization Measurements, Nicolas Pedersen¹, Kai Wang¹, Shaun Lung¹, Andrey A. Sukhorukov¹; ¹Nonlinear Physics Centre, The Australian National Univ., Australia. We formulate a new conceptual approach for full Stokes polarization measurement with a single metagrating, and develop novel design through advanced computational optimization of individual nano-resonator properties delivering robust operation even under strong fabrication inaccuracies.

JTh2A.18

On Speckle Intensity Correlations Over Object Position, Qiaoen Luo¹, Kevin J. Webb¹; ¹Purdue Univ., USA. A general theory for intensity correlations over object position allows an arbitrary object to be imaged through an amount of scatter limited by detector noise. Applications include in vivo imaging, material inspection, and environmental sensing.

JTh2A.19

Spinning Radiation from Topological Insulators, Emroz Khan¹, Evgenii Narimanov¹; ¹Purdue Univ., USA. We show that thermal radiation from a lossy topological insulator carries a nonzero average spin angular momentum.

JTh2A.20

Effect of Fabry-Perot Cavities on Concentration Quenching, Samantha R. Koutsares¹, Srujana Prayakarao¹, Devon Courtwright¹, Carl Bonner¹, M Noginov¹; ¹Norfolk State Univ., USA. We show that concentration quenching of emission of dye molecules – an energy transfer to quenching centers – is inhibited in subwavelength Fabry-Perot cavities (or metal-insulator-metal, MIM, waveguides).

JTh2A.21

High Quality Resonances in Lithium Niobate Metasurfaces and Applications, Bofeng Gao¹, Mengxin Ren¹, Wei Wu¹, Hui Hu², Wei Cai¹, Jingjun Xu¹; ¹School of Physics and TEDA Applied Physics Inst., Nankai Univ., China; ²School of Physics and Microelectronics, Shandong Univ., China. We experimentally demonstrate the lithium niobate metasurfaces. High-quality structural resonances are observed in transmittance spectra. And such lithium niobate metasurfaces are proved to show vivid structural colors.

JTh2A.22

Impact of Surface Recombination and Doping on Optical Gain in Semiconductor Nanostructures, Jinal K. Tapar¹, Saurabh Kishen¹, Kaushik Nayak¹, Naresh K. Emani¹; ¹Indian Institute of Technology, Hyderabad, India. We investigate the impact of surface recombination on optical gain, and show that the lasing threshold can be lowered by introducing strain and p-doping III-V material. This will make lasing in all-dielectric metasurfaces more practical.

JTh2A.23

Non-Paraxial Polarizer Model Based on Optically Anisotropic Media Theory, Site Zhang¹, Christian Hellmann^{1,2}, Frank Wyrowski¹; ¹LightTrans International UG, Germany; ²Wyrowski Photonics UG, Germany; ³Applied Computational Optics Group, Friedrich Schiller Univ. Jena, Germany. We present an idealized polarizer model, based on the fields and modes in optically anisotropic media. The model is derived in the spatial-frequency domain, and the result is presented in a compact 2x2-matrix form.

JTh2A.24

Semi-Analytic Modeling of Chiral Metasurface Stacks, Jan Sperrhake¹, Manuel Decker¹, Matthias Falkner¹, Stefan Fasold¹, Thomas Kaiser¹, Isabelle Stauda¹, Thomas Pertsch^{1,2}; ¹Inst. of Applied Physics, Germany; ²Fraunhofer Institut für Applied Optics and Precision Engineering, Germany. We analyze the polarization response of a fabricated twisted nano-wire metasurface stack using a semi-analytic algorithm. This lifts the requirement for rigorous simulations when designing metasurface stacks with specific target functionalities.

JTh2A.25

Towards High Efficiency Dynamically Tunable Metaholograms, Isaac O. Oguntoye¹, Adam Ollanik¹, Yaping Ji¹, George Z. Hartfield¹, Matthew D. Escarra¹; ¹Physics and Engineering Physics, Tulane Univ., USA. We propose a method for determination of nanoantenna transmitted phase for coupled, resonant nanoantennas in a heterogeneous array, necessary for design of metaholograms with ~90% optical efficiency. Progress toward fabrication of VO₂ nanoantennas is demonstrated.

JTh2A.26

Graphene-based Metamaterial Tunable Phase Modulator for Mid-Infrared Beam Steering, Cheng Shi^{1,2}, Isaac Luxmoore^{1,2}, Geoffrey Nash^{1,2}; ¹College of Engineer, Mathematics and Physics, Univ. of Exeter, UK; ²EPSRC Centre for Doctoral Training in Electromagnetic Metamaterials, Univ. of Exeter, UK. We propose a design for graphene-based metamaterial tunable phase modulator, and investigate its feasibility in steering reflective beams in the mid-infrared regime. Simulations show that up to 45% steering efficiency can be achieved.

JTh2A.27

Light-to-heat conversion by optical absorption in a Si microring resonator, Toshiya Murai¹, Yuya Shoji¹, Tetsuya Mizumoto¹; ¹Tokyo Inst. of Technology, Japan. An efficient light-to-heat conversion by optical absorption in a silicon microring resonator was demonstrated. We measured a wavelength shift due to thermo-optic effect and >300-K raise in temperature with light of 6.8 mW.

JTh2A.28

Design of Nonlinear Optical Ring Resonators, Ming Gong¹, Hui Wu¹; ¹Univ. of Rochester, USA. We present a design methodology of nonlinear microring resonators based on iterations of matrix analysis. This new method is time/memory efficient and scalable, and can be applied to other nonlinear devices.

JTh2A.29

Visualization of a cavity-cavity coupling in a LiNbO₃ subwavelength waveguide at THz frequency, Qi Zhang¹, Deng Zhang¹, Jiwei Qi¹, Qiang Wu¹, Yao Lu¹, Hao Xiong¹, Wenjuan Zhao¹, Ride Wang¹, Jingjun Xu¹; ¹Nankai Univ., China. We achieved a strong cavity-cavity coupling in a LiNbO₃ sub-wavelength waveguide at THz frequency. The wave confinement and radiation in the waveguide-cavity structure were visualized by a phase contrast imaging system.

JTh2A.30

Repair of pseudo time-reversal broken by topological phase transition in a photonic crystal slab, Yao Lu¹, Hao Xiong¹, Qiang Wu^{1,2}, Deng Zhang¹, Qi Zhang¹, Ride Wang¹, Wenjuan Zhao¹, Jingjun Xu^{1,2}; ¹The Key Lab of Weak-Light Nonlinear Photonics, Ministry of Education, TEDA Inst. of Applied Physics and School of Physics, Nankai Univ., China; ²Collaborative Innovation Center of Extreme Optics, Shanxi Univ., China. We demonstrated a repair of pseudo time-reversal broken by topological phase transition in a photonic crystal slab. By changing the spatial structures, the unidirectional topological edge states transit to bidirectional trivial ones.

JTh2A.31

Germanium photodiodes on pyramidal textured surface by Metal-Assisted Chemical Etching, Munho Kim^{2,1}, Soongyu Yi³, Jeong Dong Kim², Xin Yin³, Jun Li³, Jiye Bong³, Dong Liu³, Shih-Chia Liu⁴, Alexander Kvit², Weidong Zhou⁴, Xudong Wang³, Zongfu Yu³, Zhenqiang Ma³, Xiuling Li²; ¹Nanyang Technological Univ., Singapore; ²ECE, Univ. of Illinois Urbana Champaign, USA; ³Univ. of Wisconsin Madison, USA; ⁴Univ. of Texas Arlington, USA. We demonstrate a Ge photodiode on pyramidal textured surface by Metal-Assisted Chemical Etching (MacEtch) technique. This photodiode shows both reduced dark current and enhanced responsivity at near infrared (NIR) wavelength ranges.

JTh2A.32

Narrowband transmission filter based on silicon waveguide gratings, Tzu-Hsiang Yen¹, You-Cheng Lu¹, Yung-Jr Hung¹; ¹National Sun Yat-sen Univ., Taiwan. We demonstrate that employing waveguide gratings in a Michelson interferometer is a much practical approach, as compared to Sagnac counterpart, to realize a narrowband transmission filter due to its shorter and relatively balanced connecting waveguides.

JTh2A.33

Regular-orbit engineered momentum transformation in the mixed phase space of an asymmetric microcavity, Likun Chen¹, Yan-Jun Qian¹, Qihuang Gong¹, Jan Wiersig², Yun-Feng Xiao¹; ¹Peking Univ., China; ²Otto-von-Guericke-Universität, Germany. We demonstrate the momentum transformation engineered by regular orbits in an asymmetric microcavity. It is found that the coupling efficiency from nanowaveguide to whispering gallery modes depends strongly on the initial momentum of light, illustrating localized structures in mixed phase space.

JTh2A.34

A Monolithically Integrated CMOS-MEMS Infrared Emitter with Graphene Oxide for Emission Enhancement, Nanxi Li¹, Hongye Yuan², Jifang Tao¹, Daw Don Cheam¹, Linfang Xu¹, Dan Zhao², Hong Cai¹, Navab Singh¹; ¹Inst. of Microelectronics, A*STAR, Singapore; ²Dept. of Chemical and Biomolecular Engineering, National Univ. of Singapore, Singapore. We demonstrate the emission enhancement of an integrated CMOS-MEMS infrared emitter by using graphene oxide (GO) coating, with an enhancement factor of >2. The characterizations of the GO and the MEMS emitter design are included.

JTh2A.35

Colloidal Quantum Dots for Near-Infrared Phototransistor with CMOS-Compatible Structure, Qi Wei Xu¹, Xihua Wang¹; ¹Univ. of Alberta, Canada. We report a colloidal-quantum-dot photodetector for near-infrared detection. The detector has a CMOS-compatible structure with lower heat generation and interface treatment requirement. The device shows a responsivity of 5.9A/W at 1250 nanometers.

JTh2A.36

Free-Space Layered Sheet-Isolator, Rodion Kononchuk¹, Carl Pfeiffer², Nicholaos Limberopoulos², Igor Anisimov², Ilya Vitebskiy², Andrey Chabanov¹; ¹Physics & Astronomy, Univ. of Texas at San Antonio, USA; ²Sensors Directorate, Air Force Research Lab, USA. We introduce a multilayer acting as a free-space sheet-isolator with unlimited aperture, strong resonant transmission in a forward direction, and a possibility of broadband omnidirectional rejection of light incident on the opposite (back) side of the system.

JTh2A.37

Development of Longwave Infrared Tunable Notch Filters, Neelam Gupta¹, Mark S. Mirotznik²; ¹US Army Research Lab, USA; ²Dept. of Electrical and Computer Engineering, Univ. of Delaware, USA. Spectrally tunable micro-engineered metamaterial notch filters operating from 8 to 12 micron were developed based on the guided mode resonance phenomenon using a subwavelength germanium grating and planar waveguide grown on a zinc selenide substrate.

JTh2A.38

Dynamically-tunable Plasmonic Devices Based on Phase Transition of Vanadium Dioxide, Ruwen Peng¹, Fang-Zhou Shu¹, Ren-Hao Fan¹, Mu Wang¹; ¹Nanjing Univ., China. We have experimentally demonstrated several dynamically-tunable plasmonic devices based on phase transition of vanadium dioxide, which include dynamic color generators and dynamically switchable polarizers. The investigations can be applied in dynamic digital displays and imaging sensors.

JTh2A.39

Phase optimization of a silicon photonic two-dimensional electro-optic phased array, Michael R. Gehl¹, Galen Hoffman¹, Paul Davids¹, Andrew Starbuck¹, Christina Dallo¹, Zeb Barber², Emil Kadlec², R. Krishna Mohan², Stephen Crouch², Christopher Long¹; ¹Sandia National Labs Albuquerque, USA; ²Blackmore Sensors and Analytics, Inc., USA. Phase errors in large optical phased arrays degrade beam quality and must be actively corrected. Using a novel, low-power electro-optic design with matched pathlengths, we demonstrate simplified optimization and reduced sensitivity to wavelength and temperature.

JTh2A.40

Hybrid Photonic-Plasmonic Waveguides with Ultrathin TiN, Soham Saha^{2,1}, Aavek Dutta^{2,1}, Sarah Chowdhury^{2,1}, Alexander Kildishev^{2,1}, Vladimir M. Shalaev^{2,1}, Alexandra Boltasseva^{2,1}; ¹Electrical and Computer Engineering, Purdue Univ., USA; ²Birck Nanotechnology Center, USA. We experimentally demonstrate hybrid photonic-plasmonic waveguides utilizing plasmonic TiN, and index mismatched substrate and superstrate. The design offers lower losses and tighter mode-confinement compared to previously reported long-range surface plasmon polariton waveguides using noble metals.

JTh2A.41

High-Performance Integrated Photonics in Thin Film Lithium Niobate Platform, Meisam Bahadori¹, Arunita Kar¹, Yansong Yang¹, Ali Meygouni Lavasani¹, Lynford L. Goddard¹, Songbin Gong¹; ¹Electrical and Computer Engineering, Univ. of Illinois at Urbana-Champaign, USA. We present integrated photonics devices in thin film LN on insulator. The Q-factor of microrings is currently limited by the cavity loss and must be reduced by two orders of magnitude to hit 1,000,000 target.

JTh2A.42

High-Efficiency Silicon Mach-Zehnder Modulator with U-Shaped PN Junctions, Gangqiang Zhou¹, Linjie Zhou¹, Yuyao Guo¹, Lei Liu², Liangjun Lu¹, Jianping Chen¹; ¹Shanghai Jiaotong Univ., China; ²Huawei Technologies Co. Ltd., China. We demonstrate a silicon Mach-Zehnder modulator with U-shaped PN junctions to achieve a high modulation efficiency of 0.34 V_{cm} at 0 V bias. On-off key modulation is obtained at 32 Gb/s data rate.

JTh2A.43

Largely Tunable Plasmonic Antennas-on-Waveguide Directional Couplers with Deep Subwavelength Volume, Yuan Meng^{1,2}, Futai Hu¹, Yuanmu Yang^{1,3}, Qirong Xiao¹, Zhoutian Liu¹, Mali Gong¹; ¹State Key Lab of Precision Measurement Technology and Instruments, Tsinghua Univ., China; ²Research Lab of Electronics, MIT, USA; ³Sandia National Labs, USA. Ultracompact versatile on-chip couplings are achieved in a largely tunable manner by synergy plasmonic nanoantennas with graphene. The operating wavelength can be tuned over 115 nm around 1.55 μ m in deep-subwavelength volume with high directivity.

JTh2A.44

O-Band Add-Drop Filter in Bragg-Grating-Assisted Mach-Zehnder Interferometers for CWDM, Dominique J. Charron¹, Wei Shi¹, ¹Laval Univ., Canada. We demonstrate a flat-top add-drop filter using silicon photonic Bragg gratings embedded in Mach-Zehnder interferometers. The device implemented using 193-nm lithography shows broad 3-dB bandwidth (>19 nm), low loss (2.3 dB) and high extinction ratio (> 32 dB).

JTh2A.45

ITO Mach-Zehnder Modulator on Si, Rubab Amin¹, Rishi Maiti¹, Caitlin Carfano¹, Zhizhen Ma¹, Mohammad H. Tahersima¹, Yigal Lilach², Dilan Ratnayake², Hamed Dalir², Volker J. Sorger¹; ¹Dept. of Electrical and Computer Engineering, The George Washington Univ., USA; ²Nanofabrication and Imaging Center, George Washington Univ., USA; ³Omega Optics, Inc., USA. We demonstrate a monolithically integrated compact ITO electro-optic modulator in silicon photonics based on a Mach-Zehnder interferometer featuring a high-performance halfwave voltage and active device length product of $V_{\pi}L = 0.59$ V-mm.

JTh2A.46

Adiabatic transitions between supersymmetric structures as a tool to design integrated photonic devices, Gerard Queralt Isach¹, Verónica Ahufinger¹, Jordi Mompart¹; ¹Universitat Autònoma de Barcelona, Spain. We introduce adiabatic transitions between supersymmetric structures as a systematic way to engineer efficient and robust integrated photonic devices by modifying the refractive index profile along the propagation direction.

JTh2A.47

Scaling of Mode Degeneracy and Image Fidelity in a Self-Imaging Optical Resonator, Albert Ryou¹, Shane Colburn¹, Alan Zhan¹, Arka Majumdar¹; ¹Univ. of Washington, USA. Nonlinear optical processing of images in a miniature self-imaging cavity holds enormous potential for optical information processing and artificial neural networks. We analyze the inherent trade-off between the cavity size, image amplification, and image fidelity.

JTh2A.48

Electro-optic polymer surface-normal modulator using silicon high-contrast grating resonator, Makoto Ogasawara¹, Yuji Kosugi¹, Jiaqi Zhang¹, Yuki Okamoto¹, Yoshio Mita¹, Akira Otomo², Yoshiaki Nakano¹, Takuo Tanemura³; ¹The Univ. of Tokyo, Japan; ²National Inst. of Information and Communications Technology, Japan; ³JST PRESTO, Japan. A surface-normal optical modulator using electro-optic polymer embedded inside a 570-nm-thick silicon high-contrast-grating resonator is fabricated. With a voltage applied to silicon grating, we obtain >20% intensity modulation of the transmitted light at 30 MHz.

JTh2A.49

The role of surface passivation in integrated sub-bandgap on-chip silicon photodetectors, Rivka Gherabli¹, Meir Grajower¹, Joseph Shappir¹, Noa Mazurski¹, Uriel Levy¹; ¹Dept. of Applied physics, Hebrew Univ., Israel. We demonstrate the role of passivation in silicon photonics photodetectors based on defect states operating in the sub bandgap regime. Upon passivation removal, higher responsivity is obtained alongside with loss reduction, surprisingly improving over time.

JTh2A.50

Slow cooking of SNAP microresonators, Gabriella Gardosi¹, Yong Yang¹, Misha Sumetsky¹; ¹Aston Univ., UK. We demonstrate a SNAP microresonator permanently introduced at the silica microcapillary by multi-hour heating with hot water from the inside. The discovered effect is presumably caused by water-induced irreversible processes within the micron-scale silica thickness.

JTh2A.51

Producing OAM Information Carriers Using Micro-structured Spiral Phase Plates, Edgars Stegenburgs¹, Andrea Bertoni¹, Abderrahmen Trichili¹, Mohd Sharizal Alias¹, Tien Khee Ng¹, Mohamed-Slim Alouini¹, Carlo Liberale¹, Boon S. Ooi¹; ¹King Abdullah Univ. of Sci & Technology, Saudi Arabia. We report on small foot-print spiral phase plates for orbital angular momentum (OAM) light beam generation used in free space communication. A modal decomposition process confirms high purity of the generated beams at 980-nm wavelength.

JTh2A.52

Extreme Sub-wavelength Optical Confinement in Nanostructured All-dielectric Silicon Waveguides, Nazmus Sakib¹, Judson Ryckman¹; ¹Clemson Univ., USA. Novel approaches for the design of all-dielectric silicon waveguides featuring strong field enhancement and low mode areas are presented. Deeply subwavelength transverse characteristics, previously limited to nanoplasmonic waveguides, are predicted in an all-dielectric platform.

JTh2A.53

Ultrabroadband Integrated Photonic Filters for Waveguide-Based Sensing Systems, Nathan Tyndall¹, Todd H. Stievater¹, Dmitry Kozak¹, Marcel W. Pruessner¹, Scott Holmstrom², William Rabinovich¹; ¹US Naval Research Lab, USA; ²Univ. of Tulsa, USA. We describe the design and characterization of broadband, multi-stage waveguide lattice filters intended for integrated photonic sensing systems. The 8-stage filter provides 20 dB extinction at the filter resonance adjacent to a 190 nm passband.

JTh2A.54

Reconfigurable non-reciprocal acousto-optic modulator, Donggyu B. Sohn¹; ¹Univ. of Illinois, USA. We experimentally demonstrate a reconfigurable non-reciprocal acousto-optic modulator. The directionality of mode conversion is controlled by adjusting the phase of a pair of standing acoustic waves.

JTh2A.55

Near-visible bright-soliton Kerr comb generation in dispersion-engineered lithium niobate coupled optical microresonators, Ali Eshaghian Dorche¹, Ali Eftekhari¹, Ali Adibi¹; ¹Georgia Inst. of Technology, USA. We present an optimized, dispersion-engineered, air-clad, coupled lithium niobate optical-microresonator-based configuration for bright-soliton wideband (40 nm bandwidth at -70 dB window) Kerr-comb generation at the near-visible spectrum.

JTh2A.56

Bridge from Visible Light Communication to Telecommunication via Perovskite-Silicon Photonics, Ziwai Cheng¹, Anyi Mei¹, Zhao Cheng¹, Dingshan Gao¹, Sheng Li¹, Shuang Liu¹, Daiyu Li¹, Yaoguang Rong¹, Yue Hu¹, Hongwei Han¹, Jianji Dong¹, Xinliang Zhang¹; ¹Wuhan National Lab for Optoelectronics, Huazhong Univ. of Science and Technology, China. We propose and fabricate an all-passive, high-efficient, and coin-sized visible-to-telecom converter by hybrid packaging a perovskite detector with an integrated silicon photonic chip. The converter can convert visible light signals into telecommunication band with 200 kHz modulated rate.

JTh2A.57

High-Mobility Transparent Conducting Oxides for Compact Epsilon-Near-Zero Silicon Photonic Phase Modulators, Michael G. Wood¹, Isak Reines¹, Ting S. Luk^{1,2}, Darwin Serkland¹, Salvatore Campione¹; ¹Sandia National Labs, USA; ²Center for Integrated Nanotechnologies, USA. We numerically analyze the role of carrier mobility in transparent conducting oxides in epsilon-near-zero phase modulators. High-mobility materials such as cadmium oxide enable compact photonic phase modulators with a modulation figure of merit of >29 °/dB.

JTh2A.58

High signal-to-noise ratio for high-impedance-loaded nano-photodetector towards attojoule optical reception, Kengo Nozaki¹, Shinji Matsuo¹, Takuro Fujii¹, Koji Takeda¹, Eiichi Kuramochi¹, Akihiko Shinya¹, Masaya Notomi¹; ¹NTT Nanophotonics Center, Japan. We demonstrate a signal-to-noise ratio for a photonic-crystal nano-photodetector loaded with 59-kΩ resistor revealing 30 dB higher than conventional photodetector thanks to thermal-noise suppression. Reception of ultralow optical energy of 74 aJ is theoretically expected.

JTh2A.59

RI sensitivity of Tapered MCF Enhanced by Graphene Coating, HongXing Yu^{2,1}, Donglai Guo², Lijun Wu², Chi Li^{2,1}, Wenbin Hu²; ¹Materials Science and Engineering, Wuhan Univ. of Technology, China; ²National Engineering Lab for Fiber Optic Sensing Technology, Wuhan Univ. of Technology, China. RI-sensitivity of a tapered MCF interferometer is investigated and enhanced by graphene coating. The microstructure with a graphene coating has achieved a RI-sensitivity of 12617.3 nm/RIU within the RI range of 1.4144 to 1.4159.

JTh2A.60

Heterogeneous Integration of Light-Emitting Transistors on Silicon for Hybrid Electronic-Photonic Logic Circuitry, John A. Carlson¹, John M. Dallesasse¹; ¹Electrical and Computer Engineering, Univ. of Illinois, USA. An array of heterogeneously integrated light-emitting transistors is fabricated after an epitaxial transfer process bonds and interconnects active III-V photonic material onto a CMOS-compatible host wafer for the purposes of establishing a photonic logic network.

JTh2A.61

Temperature insensitive Mach-Zehnder interferometer on silicon nitride waveguide platform, Yu Li¹, Jiachen Li¹, Liwei Tang¹, Hongwei Chen¹, Sigang Yang¹, Minghua Chen¹; ¹Tsinghua Univ., China. We demonstrate a temperature insensitive Mach-Zehnder interferometer (MZI) with low thermal sensitivity of 0.5 pm/K at 1560 nm. Across the wavelength range from 1525 nm to 1590 nm, the sensitivity is lower than 2 pm/K.

JTh2A.62

Optical NOR Gate Transistor Laser Integrated Circuit, Ardy Winoto¹, Junyi Qiu¹, Dufei Wu¹, Milton Feng¹; ¹Univ. of Illinois, USA. An optical NOR gate has been demonstrated monolithically in a transistor laser structure using voltage modulation of the light output. The NOR gate can receive multiple optical input signals and produces the corresponding light output.

JTh2A.63

Athermal Operation of Multi-Section PIC, Gaurav Jain^{2,1}, Michael Wallace^{2,1}, M. Deseada Gutierrez Pascual¹, Robert J. McKenna², Frank Smyth¹, Jules Braddell¹, Prince M. Anandarajah¹, John Donegan²; ¹Pilot Photonics, Ireland; ²School of Physics, Trinity College Dublin, Ireland. Energy-efficient athermal bias current procedures based on thermal-tuning is demonstrated for a PIC composed of 2 lasers in a master-slave configuration, achieving mode-hop free wavelength stability of 750 MHz over a temperature range 10-60 °C.

JTh2A.64

Polarization Insensitive Racetrack Ring Resonator Based on Subwavelength Grating Slot Waveguides, Xiaodong Wang¹, Yaqian Li¹, Xueling Quan¹, Xiulan Cheng¹; ¹Shanghai Jiao Tong Univ., China. A polarization-insensitive racetrack ring resonator using subwavelength grating slot waveguides has been demonstrated. The device can realize polarization-insensitive in three free spectral ranges around 1539.345 nm. The extinction ratios are higher than 18 dB.

JTh2A.65

DC Kerr Effect and Limits for Silicon Photonic Modulators, Christian G. Bottenfield¹, Varghese A. Thomas¹, Stephen E. Ralph¹; ¹Georgia Inst. of Technology, USA. We experimentally demonstrate the universal presence of the DC Kerr effect in silicon modulators and report performance trends and theoretical limits for DC Kerr effect optimization with implications for both digital and analog applications.

JTh2A.66

Study of Crystalline Defect Induced Optical Scattering Loss inside AlN Waveguides in UV-Visible Spectral Wavelengths, Hong Chen¹, Jingan Zhou¹, Houqiang Fu¹, Xuanqi Huang¹, Yuji Zhao¹; ¹Arizona State Univ., USA. We study crystalline defect induced scattering loss inside AlN optical waveguides using volume current method. Result indicates that dislocation inside AlN contributes significant scattering loss in UV-visible spectrum wavelengths in certain geometries of waveguides.

JTh2A.67

Inverse Designed Cavity-Waveguide Couplers, Jinhie L. Skarda¹, Kiyoul Yang¹, Dries Vercautere^{1,2}, Neil Sapra¹, Logan Su¹, Jelena Vuckovic¹; ¹Stanford Univ., USA; ²KU Leuven, Belgium. We experimentally demonstrate broadband and multiple wavelength cavity-waveguide coupling by optimizing the coupling region structure to produce a specified coupling spectrum. This work has applications in optical switching and nonlinear optics.

JTh2A.68

Hardware-Based Simulation of Optoelectronic Spiking Neuromorphic Computing Network, Junjie Hu¹, Kaiqi Zhang¹, S.J. Ben Yoo¹; ¹Electrical and Computer Engineering, Univ. of California Davis, USA. We report an optoelectronic spiking neuromorphic computing network and propose a hardware-based simulation method for network design. The simulation result shows that the network can recognize simple patterns and patterns with noise.

JTh2A.69

Manifold-enhanced photon transportation in a chaotic microresonator, Yan-Jun Qian^{1,4}, Qi-Tao Cao^{1,4}, Shuai Wan², Chun-Hua Dong², Qihuang Gong^{1,4}, Qinghai Song³, Yun-Feng Xiao^{1,4}; ¹School of Physics, Peking Univ., China; ²Key Lab of Quantum Information, Univ. of Science and Technology of China, China; ³Shenzhen Graduate School, Harbin Inst. of Technology, China; ⁴Collaborative Innovation Center of Extreme Optics, Shanxi Univ., China. We study the photon transportation from chaotic to regular regions in an on-chip asymmetric microcavity. The manifold-enhanced fiber-cavity coupling is observed by controlling the initial position in phase space, holding potential for integrated photonics.

JTh2A.70

Multi-FSR On-Chip Optical Interconnects Using Silicon Nitride AWGR, Xian Xiao¹, Yu Zhang¹, Kaiqi Zhang¹, Roberto Proietti¹, S.J. Ben Yoo¹; ¹Univ. of California, Davis, USA. We demonstrate multi-FSR 10 Gb/s on-chip optical interconnects using an 8×8 Si-LIONS monolithically integrated with a SiN cyclic AWGR and silicon photonic transceiver arrays.

JTh2A.71

Theoretical and experimental analysis on Ar Implantation-Induced Quantum Dot Intermixing for 1550 nm-Band Photonic Integrated Circuit, Atsushi Matsumoto¹, Yota Akashi², Shohei Isawa², Toshimasa Umezawa¹, Yuichi Matsushima², Katsuyuki Utakak²; ¹National Inst of Information & Comm Tech, Japan; ²Waseda Univ., Japan. In this study, we theoretically and experimentally investigated an Ar ion implantation-induced quantum dot intermixing and its physical mechanism using photoluminescence and numerical simulations for the QD based monolithic PICs.

JTh2A.72

Two-dimensional Large-angle Scanning Optical Phased Array with Single Wavelength Beam, Pengfei Wang¹, Guangzhen Luo¹, Yajie Li¹, Mengqi Wang¹, Fanguan Meng¹, Wenyu Yang¹, Hongyan Yu¹, Xuliang Zhou¹, Yejin Zhang¹, Jiaoqing Pan¹; ¹Inst. of Semiconductors, CAS, China. A two-dimensional scanning optical phased array can easily achieve a circular scanning range of 51.84°, 81.6% emission efficiency and 29.7 dB back suppression ratio at 1550nm by adopting a high contrast grating (HCG) optical antenna.

JTh2A.73

A Switch-based Integrated 2D Beam-steering device for Lidar Application, Chao Li¹, Xianyi Cao¹, Kan Wu¹, Xinwan Li¹, Jianping Chen¹; ¹Shanghai Jiao Tong Univ., China. A switch-based integrated two-dimensional beam-steering device is demonstrated on a silicon nitride platform at 1550nm. The device has O(logN) power consumption for N emitters, allows digital control and achieves 19 dB background suppression.

JTh2A.74

Silicon Grating Coupler for Mode Order Conversion, Iosif Demirtzioglou¹, Cosimo Lacava¹, Abdul Shakoor¹, Ali Khokhar¹, Yongmin Jung¹, David Thomson¹, Periklis Petropoulos¹; ¹Univ. of Southampton, UK. A vertical silicon grating coupler that converts the propagation mode order at the waveguide-fiber interface was fabricated and characterized. Far-field intensity patterns are presented for different device configurations and the coupling efficiency is reported.

JTh2A.75

Broadband On-Chip Adiabatic-Coupling Polarization Mode Splitters in Lithium Niobate Waveguides, Yen-Hung Chen¹, Hung-Pin Chung¹, Chieh-Hsun Lee¹, Kuang-Hsu Huang¹, Song-Lin Yang¹, Kai Wang², Alexander Solntsev³, Andrey A. Sukhorukov², Frank Setzpfandt⁴; ¹National Central Univ., Taiwan; ²The Australian National Univ., Australia; ³Univ. of Technology Sydney, Australia; ⁴Friedrich-Schiller-Universität Jena, Germany. We report the first broadband (>120 nm at >97% splitting efficiency for both polarization modes) polarization mode-splitter in LiNbO₃ adiabatic light-passage configuration. This device can facilitate the on-chip implementation of pump-filtered, broadband tunable Bell-state generators.

JTh2A.76

CMOS Foundry DRC-Conforming Extended Cladding Modulated Integrated Bragg Grating Filters, Gareeyasee Saha¹, Christian G. Bottenfield¹, Patrick S. Goley¹, John D. Cressler¹, Stephen E. Ralph¹; ¹Electrical and Computer Engineering, Georgia Inst. of Technology, USA. We demonstrate a CMOS-compatible extended cladding modulated integrated Bragg Grating filter, while meeting strict DRC requirements of SiPh foundries. A narrow bandwidth of 2.1nm on the phase-shifted portion and 29.2dBm extinction ratio is measured.

JTh2A.77

DPSK-based 65536-ary Ciphering for Secure Optical Communications, Takahiro Kodama¹, Gabriella Cincotti²; ¹Univ. of Yamaguchi, Japan; ²Engineering Dept., Univ. Roma Tre, Italy. We propose and demonstrate a secure DPSK-based multi-dimensional 2¹⁶-ary block ciphering system using a multipoint encoder/decoder for secure optical fiber transmission. The proposed scheme presents a very high physical-level confidentiality.

JTh2A.78

Crosstalk Tracing in Weakly-Coupled Short-Reach Mode-Division Multiplexing Optical Networks with Deep Learning, Ruijie Luo¹, Nan Hua¹, Yanlong Li¹, Zelin Zheng¹, Zhizhen Zhong¹, Xiaoping Zheng¹, Bingkun Zhou¹; ¹Tsinghua Univ., China. We propose a crosstalk tracing method using deep neural networks for weakly-coupled MDM optical networks. Results show that over 95% tracing accuracy is achieved and the impact of time consistency in data collection is revealed.

JTh2A.79

CW-probe-less OOK and BPSK to QPSK optical modulation format conversion and SSMF transmission, Takahiro Kodama¹, Tatsuya Miyazaki¹, Koki Arai¹; ¹Univ. of Yamaguchi, Japan. A pair of OOK and BPSK to QPSK format conversion with XPM and its 50km SSMF transmission of the optically converted QPSK are experimentally demonstrated. A HNL input power tolerance of OOK is also reported.

JTh2A.80

Joint OSNR, Skew, ROF Monitoring of Coherent Channel using Eye Diagram Measurement and Deep Learning, Yiwen Zhang³, Yongxiong Ren¹, Zhi Wang³, Bo Liu³, Hao Zhang³, Si-Ao Li³, Yuxi Fang³, Hao Huang¹, Changjing Bao¹, Zhongqi Pan², Yang Yue³; ¹Dept. of Electrical Engineering, Univ. of Southern California, USA; ²Dept. of Electrical & Computer Engineering, Univ. of Louisiana, USA; ³Inst. of Modern Optics, Nankai Univ., China. CNN-based deep learning is used to monitor coherent channel performance with eye diagram measurement. For 32GBD-QPSK signals, 99.57% prediction accuracy is achieved for 15 to 40dB OSNR, -15 to 15ps skew, 0.05 to 1 ROF.

JTh2A.81

In-band nonlinear distortion measurements for highly linear wideband optical links, Farzad Mokhtari-Koushyar¹, McKay B. Bradford², Thien-An Nguyen², Monireh Moayed Pour Fard², Sriram Vishwanath¹; ¹ECE, Univ. of Texas at Austin, USA; ²Photonics Group, GenXComm Inc, USA. A distortion measurement method is presented for highly-linear wideband optical links. By notching a spur-free region inside signal band before the link and isolating the notch after the link, SFDR of 147.6 dBm/Hz is demonstrated.

JTh2A.82

Demonstration of all-optical clock recovery from NRZ-PM-QPSK and PM-16QAM signals, Manas Srivastava¹, Lakshmi Narayanan Venkatasubramani¹, Balaji Srinivasan¹, Deepa Venkitesh¹; ¹Indian Inst. of Technology, Madras, India. We demonstrate all-optical clock recovery from optical NRZ-PM-QPSK and NRZ-PM-16QAM data at 10 Gbaud after 60 km fiber propagation, through injection-locking of an Erbium-doped fiber laser.

JTh2A.83

Influence of Polarization Transformation in Phase Conjugation of PM-QPSK in Non-linear SOAs, Anesh Sobhanan¹, Lakshmi Narayanan Venkatasubramani¹, R David Koilpillai¹, Deepa Venkitesh¹; ¹Indian Inst. of Technology, Madras, India. Polarization insensitive phase conjugation generation is experimentally demonstrated using a single pump in a nonlinear SOA for 10 Gbaud PM-QPSK data. The influence of polarization transformation properties specific to signal-pump detuning conditions are established.

JTh2A.84

Remote detection of uranium with filament ablation spectroscopy, Lauren A. Finney¹, Patrick J. Skrodzki¹, Milos Burger¹, John Nees¹, Igor Jovanovic¹; ¹Univ. of Michigan, USA. We demonstrate that femtosecond filaments can efficiently excite metallic uranium over distances on the order of 10 meters, and that characteristic uranium atomic and molecular signatures can be simultaneously detected in seconds.

JTh2A.85

Polarization-insensitive amplitude-modulated CW LiDAR, Chao Zhang¹, Neisei Hayashi¹, Sze Y. Set¹, Shinji Yamashita¹; ¹Research Center for Advanced Science and Technology, The Univ. of Tokyo, Japan. We propose a 3D laser scanner having depolarization function which suppresses inherent fading by >20 dB at a maximum. To our knowledge, this is the first report of versatile fading removal for 3D laser scanners.

JTh2A.86

Quantitative TLC-SERS Sensing of Allergen from Seafood, Yong Zhao^{1,2}, Ailing Tan^{1,2}, Alan X. Wang¹; ¹Oregon State Univ., USA; ²Yanshan Univ., China. We report a quantitative analysis method using thin layer chromatograph in tandem with surface-Enhanced Raman scattering sensing to detect seafood allergen, which is enabled by the principal component analysis and partial least squares regression.

JTh2A.87

Integrating Cavity Enhanced Raman Spectroscopy of Trace Gases and Bulk Compounds, Thomas Z. Moore¹, Vladislav Yakovlev^{2,3}, John Mason², Edward Fry², Dawson Nodurft², Vincent Tedford², Kristin Favela¹; ¹Southwest Research Inst., USA; ²Physics, Texas A&M Univ., USA; ³Biomedical Engineering, Texas A&M Univ., USA. The Raman spectra of trace gases and bulk compounds are measured using an integrating cavity enhanced Raman spectroscopy technique. The technique utilizes an integrating cavity formed from fumed silica providing significant Raman signal enhancement.

JTh2A.88

Optoelectronic biosensing in graphene driven fiber resonators with single-molecule sensitivity and selectivity, Baicheng Yao¹, Zhongxu Cao¹, Yu Wu¹, Teng Tan¹, Chenye Qin¹, Yuanfu Chen¹, Yuan Gong¹, Zhenda Xie², Chee Wei Wong³, Yun Jiang Rao¹; ¹Univ. of Electronic Science & Tech China, China; ²Nanjing Univ., China; ³Univ. of California, Los Angeles, USA. By implementing partially-reduced graphene oxide in fiber-calibrated Fabry-Perot resonators, we demonstrate a biosensing platform. By measuring the functionalized FRET and the intermode heterodyne interference, we achieve single-molecule sensitivity and selectivity for multiple target detection.

JTh2A.89

Dual comb-linked cavity ring-down spectroscopy, Weipeng Zhang¹, Xinyi Chen¹, Haoyun Wei¹, Yan Li¹; ¹Tsinghua Univ., China. A dual comb-linked scheme for cavity ring-down is presented, which maintained both an excellent stability of the cavity length and accurate measurement of the probing frequency. Several absorption lines of oxygen were measured.

JTh2A.90

An FBG-based High-resolution Temperature Sensor through Measuring the Beat Frequency of Single-frequency Ring Fiber Laser, Liangcheng Duan¹, Wei Shi¹, Haiwei Zhang^{1,2}, Xianchao Yang¹, Ying Lu¹, Jianquan Yao¹; ¹Tianjin Univ., China; ²Tianjin Univ. of Technology, China. A high-resolution temperature sensor based on narrow-linewidth (<1 kHz) single-frequency ring fiber laser was investigated using optical heterodyne spectroscopy technology. Temperature resolution of $\sim 5 \times 10^{-3}$ °C was achieved in our experiment.

JTh2A.91

Nuclear recoil spectroscopy in an optical trap, Alexander Malychenko^{1,2}; ¹Los Alamos National Lab, USA; ²The Paul Scherrer Inst., Switzerland. We discuss the conditions that allow the observation of nuclear decay recoil for small particles levitated in an optical trap. We report on trapping uranium oxide particles at ambient conditions as a first experimental step.

JTh2A.92

Characterization of small-scale contortions on a physical-surface using a distributed optical-fiber sensor, Raja Ahmad¹, Wing Ko¹, Kenneth S. Feder¹, Paul S. Westbrook¹; ¹OFS Labs, USA. We use spatially continuous measurements of the Bragg-wavelength of a grating in an offset-core fiber to measure continuous, sub-millimeter length-scale variations on the surface of a corrugated metal surface.

JTh2A.93

2.3µm Wavelength Single Photon LIDAR with Superconducting Nanowire Detectors, Gregor G. Taylor¹, Dmitry Morozov¹, Nathan R. Gemmell², Kleanthis Erotokritou¹, Robert H. Hadfield¹; ¹Univ. of Glasgow, UK; ²Univ. of Sussex, UK. A superconducting nanowire single photon detector system designed for 2.3µm wavelength deployed into a single photon light detection and ranging setup. This wavelength takes advantage of lower solar flux and less atmospheric absorption.

JTh2A.94

Plasmonic stripes integrated in a silicon nitride Mach Zehnder Interferometer for high sensitivity refractometric sensors, Athanasios Manolis¹, Evangelia Chatzianagnostou¹, George Dabos¹, Nikos Pleros¹, Bar-tos Chmielak², Anna Lena Giesecke², Caroline Porschatis², Piotr Cegielski², Laurent Markey³, Jean-Claude Weeber³, Alain Dereux³, Dimitris Tsiokos^{1,4}; ¹Dept. of Informatics - Center for Interdisciplinary Research and Innovation, Aristotle Univ. of Thessaloniki, Greece, Greece; ²AMO GmbH, Advanced Microelectronic Center Aachen (AMICA), Otto-Blumen-thal-Strasse, Aachen, Germany, Germany; ³Laboratoire Interdisciplinaire Carnot de Bourgogne (ICB), CNRS UMR 6303, Université de Bourgogne Franche-Comté, 21078, Dijon, France, France; ⁴bialoom Ltd, 72, 28th Octovriou Avenue, Office 301, Engomi, 2414 Nicosia, Cyprus, Cyprus. We demonstrate an interferometric plasmo-photonic sensor based on Si₃N₄ photonic waveguides and gold Surface Plasmon Polariton waveguides. The proposed approach exhibits bulk sensitivity up to 1930 nm²/RIU, holding promise for compact and ultra-sensitive interferometric sensing devices.

JTh2A.95

Hydrostatic Pressure Response of Mo Coated Etched Fiber Bragg Grating Sensor in Side-Hole Packaging, Suneetha Sebastian¹; ¹Instrumentation and Applied Physics, Indian Inst. of Science, India. We demonstrate side-hole packaged; nanolayer Molybdenum (Mo) coated etched Fiber Bragg Grating (eFBG) as hydrostatic pressure sensor. Pressure sensitivity enhancement of nearly 2000 times is observed with such a simple, ruggedized and packaged sensor system.

JTh2A.96

CO₂ Detection with Si Slot Waveguide Ring Resonators toward On-chip Specific Gas Sensing, Yuki Tomono¹, Hayato Hoshi¹, Hiromasa Shimizu¹; ¹Tokyo Univ. of Agri. and Tech., Japan. We fabricated a Si slot waveguide ring resonator detecting CO₂ with RI difference of 1.5×10^{-4} and sensitivity of 3×10^2 nm/RIU. The device satisfies both detecting capability and compatibility with biolayer toward on-chip specific gas sensing.

JTh2A.97

Microring Resonator Biosensor Sensitivity Enhancement through Ring-down Interferograms, Shih-Hsiang Hsu¹, Feng-Chang Chien¹, Chou-Yun Hsu¹; ¹National Taiwan Univ of Science & Tech, Taiwan. The microring resonator biosensor sensitivity is enhanced by round-trip ring-down waveforms interrogated with two-staged Mach-Zehnder interferograms through optical low-coherence interferometry. The sensitivity and resolution on influenza DNA demonstrate 49 µm/µM and 1.53 nM, respectively.

JTh2A.98

Omni-Resonant Micro-Cavity Toggling between Active and Passive Imaging, Soroush Shabahang^{1,2}, Ali K. Jahromi¹, Kenneth L. Schepler¹, Ayman Abouraddy¹; ¹Univ. of Central Florida, USA; ²Harvard Medical School, Massachusetts General Hospital, USA. We have demonstrated an experimental scheme for incorporating two distinct functionalities in the same optical system: narrowband resonant filtering and broadband omni-resonant transmission. Both functionalities are realized in-line in an imaging configuration.

JTh2A.99

A 20-GHz Optoelectronic Oscillator based on an Electroabsorption Modulated Laser, Siyu Zhao¹, Juanjuan Yan¹, Zheng Zheng¹; ¹Beihang Univ., China. An optoelectronic oscillator based on an electroabsorption modulated laser is experimentally demonstrated. The phase noise is measured to be -110.2dBc/Hz at 10kHz offset from the carrier when the oscillation frequency is 20GHz.

JTh2A.100

Single-Mode Fiber Based Pulsed-Optical Timing Link with Few-Femtosecond Precision in SwissFEL, Kemal Shafak¹, Haynes Pak Hay Cheng¹, Anan Dai¹, Maik Kaiser², Vladimir Arsov², Andrej Berlin¹, Erwin Cano¹, Wahid Nasimzada¹, Mathias Neuhaus¹, Philipp Schiepel¹, Stephan Hunziker², Franz Kärtner³; ¹Cycle GmbH, Germany; ²Paul Scherrer Institut, Switzerland; ³Center for Free Electron Laser Science, Deutsches Elektronen Synchrotron, Germany. We present results from a pulsed-optical timing link using single-mode fiber components installed in SwissFEL. The system shows 2.6-fs RMS timing jitter in [1 MHz - 20 µHz] and presents a versatile alternative to polarization-maintaining version.

JTh2A.101

Combination of Lock-in Detection with Dual-Comb Spectroscopy, Hidenori Koresawa^{1,2}, Kyuki Shibuya^{1,2}, Akifumi Asahara^{3,2}, Takeo Minamikawa^{1,2}, Kaoru Minoshima^{3,2}, Takeshi Yasui^{1,2}; ¹Tokushima Univ., Japan; ²JST, ERATO MINOSHIMA Intelligent Optical Synthesizer, Japan; ³The Univ. of Electro-Communications, Japan. We present a method to extract an arbitrary mode in a mode-resolved optical-frequency-comb spectrum by introducing a lock-in detection in dual-comb spectroscopy. The proposed method reduces net measurement time due to no fast-Fourier-transform calculation.

JTh2A.102

Overcoming the Diffraction Limit of Optical Microscopes For Measuring Tapered Optical Fibers, Abderrahim Azzoune¹, Philippe Delaye¹, Sylvie Lebrun¹, Maha Bouhadida¹, Gilles Pauliat¹; ¹Laboratoire Charles Fabry, Institut d'Optique, CNRS, Université Paris-Saclay, France. We describe a technique that allows increasing the resolution of optical microscopes for nanofiber measurements. We demonstrated it by measuring the diameter of tapered fibers for radii ranging from 0.2 to 1.5 µm.

JTh2A.103

Asymmetric fiber delay line interferometer based noise measurement platform for Er: fiber optical frequency combs, Haochen Tian¹, Wenkai Yang¹, Dohyeon Kwon², Runmin Li¹, Youjian Song¹, Jungwon Kim², Minglie Hu¹; ¹Tianjin Univ., China; ²South Korea Advanced Inst. of Science and Technology, South Korea (the Republic of). Frequency noise spectrum for comb-line spacing, carrier envelope offset frequency and optical comb lines are characterized simultaneously in an Er: fiber optical frequency comb, enabling the study of inherent noise correlations.

JTh2A.104

Locking CW Laser to Ultra-stable Optical Frequency Comb by Feed-forward Method, Xiaodong Shao^{1,3}, Hainian Han¹, Yabei Su^{1,2}, Huibo Wang^{1,2}, Ziyue Zhang^{1,3}, Shaobo Fang¹, Guoqing Chang¹, Zhiyi Wei^{1,3}; ¹Beijing National Lab for Condensed Matter Physics, Inst. of Physics, Chinese Academy of Sciences, China; ²School of Physics and Optoelectronics Engineering, Xidian Univ., China; ³Univ. of Chinese Academy of Science, China. We report a precision feed-forward locking between a 1064 nm CW laser and an ultra-stable frequency comb. The relative linewidth of the 1064nm CW laser is 1.14 mHz and the stability reaches 1.5×10^{-17} /s.

JTh2A.105

Polarization and phase shifting interferometry, Sergej Rothau¹, Klaus Mantel^{1,2}, Norbert Lindlein¹; ¹Friedrich-Alexander-Universität, Germany; ²Max Planck Inst. for the Science of Light, Germany. A novel interferometric approach for a full-field and simultaneous measurement of the phase and the polarization state of a light wave is introduced. The same procedure can be used for simultaneous analysis of the phase transmission and the polarization properties of a specimen.

JTh2A.106

Time-Resolved Dual Frequency Comb Phase Spectroscopy of Laser-Induced Plasmas, Reagan R. Weeks¹, Yu Zhang^{2,1}, Caroline Lecaplain¹, Jeremy Yeak³, Sivandan S. Harilal⁴, Mark C. Phillips⁴, R. J. Jones¹; ¹College of Optical Sciences, Univ. of Arizona, USA; ²Physics, Univ. of Arizona, USA; ³Opticslab, USA; ⁴Pacific Northwest National Lab, USA. We present the first results using time-resolved dual-comb phase spectroscopy in a laser-induced plasma. It can allow for simultaneous plasma characterization as well as multi-species detection and plasma characterization.

JTh2A.107

Continuously-chirped guided mode resonance filter for low-cost near-infrared spectroscopic applications, Chuan-Ci Yin¹, Chia-Wei Kao¹, Chia-Wei Huang¹, Yung-Jr Hung¹; ¹National Sun Yat-sen Univ., Taiwan. We demonstrate a continuously period-chirped Ta₂O₅-based guided mode resonance filter to discriminate telecom o-band wavelengths with a filter linewidth of 0.743 nm, thus enables on-chip spectroscopy for near-infrared light in a low-cost manner.

JTh2A.108

Three-Beam Interferometry for Dynamic and Low-Signal Measurements, Adam Ollanik¹, George Z. Hartfield¹, Matthew D. Escarra¹; ¹Tulane Univ., USA. We present an interferometer for the characterization of dynamic optical materials and metasurfaces. A three-beam method provides robust measurements despite unavoidable drift. Measurements are demonstrated with a phase-change material, ultra-thin materials, and a dielectric metasurface.

JTh2A.109

Direct comb multi-heterodyne spectroscopy for rapid detection of trace gases, Jaehyun Lee¹, Keunwoo Lee¹, Jaewon Yang¹, Young-Jin Kim², Seung-Woo Kim¹; ¹KAIST, South Korea (the Republic of); ²School of Mechanical and Aerospace Engineering, NTU, Singapore. We perform high sensitive spectroscopic measurements by combining a single probe comb with multiple cw lasers so as to produce strong RF multi-heterodyne spectra for rapid detection of different trace gases.

JTh2A.110

A nonlinear interferometer using a designable Raman-resonant four-wave-mixing process, Jian Zheng¹, Masayuki Katsuragawa^{1,2}; ¹Graduate School of Informatics and Engineering, Univ. of Electro-Communications, 1-5-1, Chofugaoka, Chofu, Tokyo 182-8585, Japan, Japan; ²JST, ERATO, MINOSHIMA Intelligent Optical Synthesizer Project, 4-1-8, Honcho, Kawaguchi, Saitama 332-0012, Japan, Japan. A new kind of nonlinear interferometer is proposed based on the arbitrary designable Raman-resonant four-wave-mixing process.

JTh2A.111

Cavity-Enhanced Direct Optical Frequency Comb Spectroscopy with Tooth-Width Limited Resolution, Dominik Charczun¹, Grzegorz Kowzan¹, Akiko Nishiyama¹, Przemyslaw Staniszewski¹, Agata Cygan¹, Daniel Lisak¹, Ryszard S. Trawinski¹, Piotr Maslowski¹; ¹Inst. of Physics, Nicolaus Copernicus Univ. in Torun, Poland. We present a multimodal spectroscopic method employing optical frequency combs, optical cavities and Fourier-transform spectrometry. It allows fast and broadband measurements of both absorption and dispersion spectra as well as of dispersion and reflectivity of mirrors.

JTh2A.112

Optical frequency stability transfer using a single-branch Er:fiber frequency comb, Felix Rohde¹, Thomas Puppe¹, Rafal Wilk¹, Burghard Lipphardt², Uwe Sterr², Erik Benkler²; ¹TOPTICA Photonics AG, Germany; ²Physikalisch-Technische Bundesanstalt, Germany. We report on the frequency transfer from an ultrastable laser at 1542 nm to a clock laser at 935 nm using a single-branch commercial Er:fiber optical frequency comb.

JTh2A.113

Cost-efficient thermal tuning and stabilization system for fiber-based optical frequency combs, Aleksander Gluszek¹, Arkadiusz Hudzikowski¹, Jaroslaw Sotor¹, Grzegorz J. Sobon¹; ¹Wroclaw Univ. of Science and Technology, Poland. We present the design of a compact, low-cost thermal stabilization system for mode-locked fiber lasers without using Peltier modules. Repetition rate tuning of 0.85 kHz per 1°C was achieved in a 100 MHz frequency comb.

JTh2A.114

High Brightness Broadband Infrared Light Source, from 0.3 to 20 Microns, Matthew J. Partlow¹, Ron Collins¹, Alex Culter¹, Debbie Gustafson¹, Steve Horne¹, Don McDaniel¹; ¹Energetiq Technology, Inc., USA. Development of broadband, high brightness Laser-Driven Light Sources (LDLS™) covering the infrared spectrum (2 – 20 μm) is described. Radiance performance is compared to that of a ceramic broadband thermal emitter light source.

JTh2A.115

Orbital-Angular-Momentum Azimuthal Phase-Shift-Keying via Digital Holography Through Turbulent Media, Raymond Lopez-Rios¹, Usman A. Javid¹, Qiang Lin¹; ¹Inst. of Optics, Univ. of Rochester, USA. We report a digital holographic technique for retrieving the OAM azimuthal phase difference of coherent beams co-propagating through turbulence. Experimental results suggest that OAM phase-shift keying schemes are feasible for large-bandwidth free-space optical communication.

JTh2A.116

The CLONETS – Clock Network Services Strategy and innovation for clock services over optical-fibre networks, Josef Vojtech¹; ¹CESNET, Czechia. Methods for long-distance time and frequency transfer over optical fibers have demonstrated excellent performances. CLONETS is a EU funded action intended to facilitate the vision of a sustainable, pan-European optical fiber network for precise time and frequency reference dissemination.

JTh2A.117

Boosting Second-Harmonic Generation in Nonlinear Metasurfaces with Bound States in the Continuum, Kirill Koshelev^{1,2}, Andrey Bogdanov², Yuri S. Kivshar^{1,2}; ¹Australian National Univ., Australia; ²Dept. of Nanophotonics and Metamaterials, ITMO Univ., Russia. We apply the concept of bound states in the continuum to nonlinear metasurfaces with a broken in-plane symmetry and realize high-Q resonances boosting dramatically the SHG efficiency via a smart asymmetry engineering.

JTh2A.118

Flat Lenses for Ultra-lightweight Long-wave-Infrared Broadband Imaging, Monjurul Meem¹, Sourangsu Banerji¹, Apratim Majumder¹, Berardi Sensale Rodriguez¹, Rajesh Menon¹; ¹Univ. of Utah, USA. We demonstrate the design and experiments for chromatic aberration rectified, high NA, polarization insensitive, diffractive flat lenses operating in the LWIR (8mm to 12mm) regime.

JTh2A.119

High Q-Factor All-Dielectric Metasurface Based on Bound States in the Continuum, Shaimaa Azzam¹, Krishnakali Chaudhuri¹, Vladimir M. Shalaev¹, Alexandra Boltasseva¹, Alexander Kildishev¹; ¹Purdue Univ., USA. We propose a realization of bound states in the continuum (BICs) with metasurfaces. Resonances with theoretically-infinite quality-factors can be achieved in the BIC regime and with up to a few thousand in the near-BIC.

CLEO: QELS-Fundamental Science

14:00–16:00

FTh3A • Gateways to Quantum Information Processing

Presider: Peter Mosley; Univ. of Bath, UK

FTh3A.1 • 14:00

Repeated Multi-Qubit Readout and Feedback in a Mixed-Species Trapped-Ion Register, Karan Mehta¹, Vlad Negnevitsky¹, Matteo Marinelli¹, Hsiang-Yu Lo¹, Christa Flühmann¹, Jonathan Home¹; ¹ETH Zurich, Switzerland. We measure the parity of two beryllium ion qubits by mapping the relevant operator onto an ancillary calcium qubit, utilizing multi-species entangling gates. Repeated measurement and feedback cycles allow preparation and stabilization of parity subspaces and Bell states.

FTh3A.2 • 14:15

Quantum Computing using MAGIC with Trapped Atomic Ions, Christof Wunderlich¹, Ivan Boldin¹, Hans Briegel^{2,3}, Vedran Dunjko^{2,4}, Elham Esteki¹, Nicolai Friis^{5,2}, Gouri Giri¹, Timm Gloger¹, Michael Johanning¹, Delia Kaufmann¹, Peter Kaufmann¹, Alexander Kraft¹, Bogdan Okhrimenko¹, Moritz Porst¹, Theeraphot Sriarunothai¹, Sabine Wölk^{1,2}; ¹Universität Siegen, Germany; ²Univ. of Innsbruck, Austria; ³Univ. of Konstanz, Germany; ⁴Max Planck Inst. for Quantum Optics, Germany; ⁵Austrian Academy of Sciences, Austria. A programmable quantum computer based on trapped ions interacting via magnetic gradient induced coupling (MAGIC) together with elements for scaling quantum computing – transport of ions and a novel trap for 2D ion arrays – are reported.

FTh3A.3 • 14:30

Variational Quantum Unsampling on a Programmable Nanophotonic Processor, Jacques Carolan¹, Masoud Moshen², Jonathan Olson³, Mihika Prabhu¹, Changchen Chen¹, Darius Bunandar¹, Nicholas C. Harris⁴, Franco N. Wong¹, Michael Hochberg⁵, Seth Lloyd¹, Dirk R. Englund¹; ¹MIT, USA; ²Google Quantum AI Lab, USA; ³Zapata Computing Inc., USA; ⁴Lightmatter, USA; ⁵Elenion Technologies, USA. We introduce the Variational Quantum Unsampling (VQU) protocol, a nonlinear quantum neural network approach for verification and inference of near-term quantum circuits outputs. We experimentally demonstrate this protocol on a quantum photonic processor.

14:00–16:00

FTh3B • Tailorable Phenomena in Optical Fibers

Presider: To Be Announced

FTh3B.1 • 14:00 **Tutorial**

The Curious Properties of Twisted Photonic Crystal Fibres, Philip S. Russell^{1,2}; ¹Max Planck Inst. Science of Light, Germany; ²Dept. of Physics, Univ. of Erlangen-Nuremberg, Germany. Helicallly twisted hollow and solid core photonic crystal fibers display many curious properties: perfect circular birefringence, circular dichroism, birefringence between modes of equal and opposite azimuthal order, and guidance even when there is no core.



Philip Russell is a Director at the Max-Planck Institute for the Science of Light in Erlangen, Germany. A fellow of the Royal Society and The Optical Society (OSA), he specializes in scientific applications of photonic crystal fibre, which he first proposed in 1991. He was the 2015 OSA President.

14:00–16:00

FTh3C • Emission & Detection of Thermal Radiation

Presider: Peter Catrysse, Stanford Univ., USA

FTh3C.1 • 14:00

Near-Field and Far-Field Thermal Emission of individual subwavelength-sized resonators, Yannick De Wilde¹, Claire Li^{1,2}, Joris Doumouro¹, Valentina Krachmalnicoff¹, Patrick Bouchon², Julien Jaecq², Nathalie Bardou³, Karl Joulain⁴, Riad Haidar², Housseem Kallel¹; ¹Institut Langevin, ESPCI Paris, PSL Univ., CNRS, France; ²DOTA, ONERA, Université Paris-Saclay, France; ³Centre de Nanosciences et de Nanotechnologies, CNRS, Université Paris-Sud, Université Paris-Saclay, France; ⁴3 Institut Pprime, CNRS, Université de Poitiers, ISAE-ENSMA, France. We combine spatial modulation FTIR spectroscopy with TRSTM measurements to characterize the thermal emission of plasmonic antennas and silica rods. The fundamental mode of MIM nanoantennas with silica dielectric layer is excited at multiple wavelengths.

FTh3C.2 • 14:15

Machine-learning-assisted topology optimization for highly efficient thermal emitter design, Zhaxylyk A. Kudyshev¹, Alexander Kildishev¹, Vladimir M. Shalaev¹, Alexandra Boltasseva¹; ¹Purdue Univ., USA. We coupled generative adversarial network with topology optimization for efficient thermal emitter design development. The proposed method can generate highly efficient metasurface designs with a non-trivial topology for efficient spectral control of thermal blackbody radiation.

FTh3C.3 • 14:30 **Invited**

Broadband Nanophotonic Control of Low-temperature Thermal Radiation, Aaswath Raman¹; ¹Univ. of Pennsylvania, USA. We highlight new nanophotonic strategies for controlling and tuning the spectral and angular response of broadband, room-temperature thermal radiation in the long-wave infrared. We also introduce novel applications and capabilities enabled by this control, including for energy efficiency.

14:00–16:00

FTh3D • Quantum Photonics: Generation & Manipulation

Presider: Raphaël Pooser; Oak Ridge National Labs, USA

FTh3D.1 • 14:00 **Tutorial**

Quantum Communications, Prem Kumar¹; ¹Northwestern Univ., USA. After comparing and contrasting quantum communications with the traditional classical communications, I will focus on device technologies and review their current state-of-the-art for interconnecting distant quantum data nodes in a quantum network of the future.



Prem Kumar is professor of information technology at Northwestern University. His current research focus is on quantum photonic devices and their applications in quantum communications and networking. During 2013–17, Dr. Kumar was a Program Manager at DARPA. He is a Fellow of the OSA, APS, IEEE, IoP (U.K.), AAAS, and SPIE.

CLEO: Science & Innovations

14:00–16:00
STh3E • Ultrafast Parametric Sources I*Presider: Gabrielle Thomas M Squared Lasers, Scotland*

STh3E.1 • 14:00 **Invited**
High-Average-Power Mid-Infrared Sources for Spectroscopy and Strong-Field Physics at 100 kHz., Nicolas Forget¹, Nicolas Thiré¹, Raman Maksimenka¹, Yoann Pertot¹, Olivier Albert¹, Balint Kiss², Eric Cormier², Károly Osvay²; ¹FASTLITE, France; ²ELI-HU, Hungary. We demonstrate a 100-kHz, 15-W, OPCPA delivering 4-cycle (38 fs) pulses at ~3.2 μm . Over 8h, a pulse-to-pulse energy stability <0.7% rms and a single-shot CEP noise of 65 mrad RMS is reported.

STh3E.2 • 14:30
Sub-Two-Cycle High-Average-Power Pulses at 2.5 μm , Justinas Pupeikis¹, Nicolas Bigler¹, Stefan Hrisafov¹, Lukas Gallmann¹, Christopher Phillips¹, Ursula Keller¹; ¹ETH Zurich, Switzerland. We present a 12.6 W optical parametric chirped-pulse amplifier (OPCPA) generating pulses at 100 kHz centered at 2.5 μm . With a novel pulse shaping scheme, the pulses were compressed to 14.4 fs (1.6 cycles).

14:00–16:00
STh3F • Nonlinear THz Phenomena*Presider: Edbert Sie, Stanford University, USA*

STh3F.1 • 14:00 **Tutorial**
Terahertz photonics of graphene - from nonlinear absorption to high harmonics generation, Dmitry Turchinovich¹; ¹Universität Bielefeld, Germany. Graphene is possibly the most nonlinear electronic material discovered to date. We demonstrate strongly nonlinear THz conductivity of graphene leading to extremely efficient THz high harmonics generation, and explain it using a simple thermodynamic model resting on basic conservation laws.



Dmitry Turchinovich is a full professor of experimental physics at Bielefeld University. His research interests are ultrafast condensed matter physics and general ultrafast science. He received his PhD from the University of Freiburg in 2004. Prior to his current appointment, he held faculty positions at the Technical University of Denmark, MPI for Polymer Research, and the University of Duisburg-Essen. Professor Turchinovich is OSA Senior Member and recipient of EU Career Integration Grant.

14:00–16:00
STh3G • Precision Timing & Optical Time Transfer*Presider: Andrew Metcalf; AFRL, USA*

STh3G.1 • 14:00
Free-Space Optical Time Transfer Between an Atomic Frequency Standard and a Simple Optical Clock, Matthew S. Bigelow¹, Rafe Guidice¹, Kyle Martin¹, Andrew J. Metcalf², Nathan D. Lemke³; ¹Applied Technology Associates, USA; ²Space Vehicles Directorate, Air Force Research Lab, USA; ³Bethel Univ., USA. We present a tabletop demonstration of free-space time-frequency transfer from a compact optical rubidium atomic frequency standard to stabilize a clock based on a fiber laser locked to fiber-delay line compared with a cavity-stabilized laser.

STh3G.2 • 14:15
Optical two-way time transfer with enhanced SNR for longer distance free-space links, Jennifer L. Ellis¹, Isaac H. Khader¹, Martha I. Bodine¹, William C. Swann¹, Sarah A. Stevenson¹, Emily D. Hannah¹, Laura C. Sinclair¹, Nathan R. Newbury¹, Jean-Daniel Deschênes²; ¹NIST, USA; ²Consultation Octo-Sig Inc., Canada. We explore the tradeoffs in signal-to-noise ratio and timing performance for comb-based optical two-way time transfer with a goal of future very long distance free-space links between optical clocks.

STh3G.3 • 14:30
Preliminary Measurements for Three-Node Optical Two-Way Time and Frequency Transfer, Sarah A. Stevenson^{1,2}, Paritosh Manurkar^{1,2}, Martha I. Bodine¹, William C. Swann¹, Jennifer L. Ellis¹, Isaac H. Khader^{1,2}, Emily D. Hannah^{1,2}, Michael Cermak¹, Jean-Daniel Deschênes³, Nathan R. Newbury¹, Laura C. Sinclair¹; ¹National Inst. of Standards and Technology, USA; ²Univ. of Colorado Boulder, USA; ³Octosig Consulting Inc., Canada. Here we present preliminary results for a three-node network using optical two-way time transfer. We discuss the design and initial testing of a fieldable remote node, which shows performance consistent with a previous Lab system.

14:00–16:00
STh3H • Modulation & Switching*Presider: Ali Adibi; Georgia Institute of Technology, USA*

STh3H.1 • 14:00
Efficient Pure Phase Optical Modulator Based on Strongly Over-Coupled Resonators, Guozhen Liang¹, Heqing Huang¹, Sajan Shrestha¹, Ipshita Datta², Michal Lipson², Nanfang Yu¹; ¹Dept. of Applied Physics and Applied Mathematics, Columbia Univ., USA; ²Dept. of Electrical Engineering, Columbia Univ., USA. We demonstrate that large pure optical phase modulation is possible in resonators operated in the strongly over-coupling regime, which suggests efficient phase modulators with high-speed operation, small footprint, low insertion loss, and low power consumption.

STh3H.2 • 14:15
Silicon Photonic Modulator Using Coupled Bragg Grating Resonators in a Mach-Zehnder structure, Omid Jafari¹, Wei Shi¹, Sophie Larochelle¹; ¹Laval Univ., Canada. We demonstrate a silicon modulator enhanced by Bragg-grating resonators. The compact modulator (130- μm phase shifters) with $V\pi \times L = 0.25 \text{ V}\cdot\text{cm}$ has a 32-GHz EO bandwidth consuming only 80 fJ/bit at 10 Gbit/s.

STh3H.3 • 14:30
Low-Voltage-Swing Electro-Absorption Modulator by High Mobility Conductive Oxide on Silicon Waveguide, Qian Gao¹, Erwen Li¹, Alan X. Wang¹; ¹Oregon State Univ., USA. We present a 5 μm length silicon electro-absorption modulator using high mobility indium oxide gate. The device operates at 100 nm optical bandwidth and 2.5 GHz dynamic modulation, which requires only 2V voltage swing.

Meeting Room
211 A/B

CLEO: Applications
& Technology

14:00–16:00
ATH3I • A&T Topical Review on
Silicon Photonics I
President: To Be Announced

ATH3I.1 • 14:00 **Invited**
Monolithic Silicon Optoelectronics with
Standard CMOS Processes, Alex Wright¹;
¹Ayar Labs, USA. Abstract not available.

ATH3I.2 • 14:30
Low loss and robust photonic packaging
using fusion splicing, Juniyali Nauriyal¹, Me-
iting Song¹, Raymond Yu¹, Jaime Cardenas¹;
¹Univ. of Rochester, USA. We show a novel
photonic packaging method for permanent
optical edge coupling between a fiber and
chip using fusion splicing. We demonstrate
minimum loss of 1.0dB per-facet with 0.6dB
penalty over 160nm bandwidth around
1550nm.

Meeting Room
211 C/D

CLEO: Science &
Innovations

14:00–16:00
STh3J • Emerging Nonlinear
Platforms
President: Katia Gallo, KTH,
Sweden

STh3J.1 • 14:00
Near-Visible Microresonator-Based Soliton
Combs, Yun Zhao¹, Xingchen Ji^{1,2}, Bok Young
Kim¹, Prathamesh Donvalkar^{1,2}, Jae K. Jang¹,
Chaitanya Joshi^{1,2}, Mengjie Yu^{1,2}, Renato
Domenegueti³, Felipe A. Barbosa¹, Paulo
Nussenzeveig³, Yoshitomo Okawachi¹, Michal
Lipson¹, Alexander Gaeta¹; ¹Columbia Univ.,
USA; ²Cornell Univ., USA; ³Universidade de
São Paulo, Brazil. We experimentally demon-
strate soliton mode-locked Kerr comb
generation at near-visible wavelengths in a
silicon nitride microresonator. We achieve the
shortest wavelength to-date for mode-locked
Kerr combs through dispersion engineering
of a higher-order mode.

STh3J.2 • 14:15
Chaos-assisted cross-band microcombs,
Hao-Jing Chen¹, Qing-Xin Ji¹, Qihuang
Gong¹, Xu Yi², Yun-Feng Xiao¹; ¹School
of Physics, Peking Univ., China; ²Dept. of
Electrical and Computer Engineering, and
Dept. of Physics, Univ. of Virginia, USA. We
demonstrate microcombs in a deformed
microcavity with emission from 450 nm to
2000 nm. The cross-band intracavity emission
is harnessed to a nanowaveguide through the
chaotic-assisted momentum transformation.

STh3J.3 • 14:30
Thermal Noise and Laser Cooling of Kerr-
Microresonator Frequency Combs, Tara E.
Drake¹, Jordan Stone^{1,2}, Travis C. Briles^{1,2},
Scott B. Papp^{1,2}; ¹NIST, USA; ²Univ. of Colo-
rado, USA. We present measurements and
analysis of the fundamental noise in Kerr-
microresonator frequency combs due to finite
temperature. By exploiting the thermo-optic
locking effect, we reduce the effect of these
thermally-driven fluctuations on the comb
coherence.

Meeting Room
212 A/B

CLEO: Applications
& Technology

14:00–16:00
ATH3K • Trace Species Sensing
President: Brian Simonds, National
Institute of Standards and
Technology, USA

ATH3K.1 • 14:00
The NAOMI GAZL multispecies differential
absorption lidar: realization and testing
on the TADI gas leak simulation facility,
Jean-Baptiste Dherbecourt¹, Jean-Michel
Melkonian¹, Antoine Godard¹, Vincent Lebat¹,
Nicolas Tanguy¹, Cédric Blanchard¹, Xavier
Watremez², Dominique Dubucq², Stéphanie
Doz³, Pierre-Yves Foucher³, Myriam Raybaut¹;
¹DPHY, ONERA, Université Paris Saclay,
France; ²TOTAL, France; ³ONERA/DOTA,
Université de Toulouse, France. We report
on a differential absorption lidar, designed for
remote detection of CH₄ and CO₂, based on
a single-frequency 1.57-1.65 μm parametric
oscillator/amplifier system. The lidar is tested
on a controlled gas release facility.

ATH3K.2 • 14:15
Spectroscopy With Frequency Comb-
Locked Optical Swept Synthesizer, Riccardo
Gotti¹, Thomas Puppe², Yuriy Mayzlin², Julian
Robinson-Tait², Szymon Wojtewicz³, Davide
gatti¹, Bidoor Al Saif⁴, marco lamperti¹, Paolo
Laporta¹, Felix Rohde², Rafal Wilk², Patrick
Leisching², William Kaenders², Marco Maran-
goni¹; ¹Physics, Politecnico di Milano, Italy;
²Toptica Photonics AG, Germany; ³Nicolaus
Copernicus Univ., Poland; ⁴King Abdullah
Univ. for Science and Technology, Saudi
Arabia. A CW-laser phase-locked to an end-
lessly shifting frequency comb enables spectro-
scopic investigations with metrological
quality and high sensitivity at speeds beyond
1 THz/s over frequency ranges that can be
set on demand over 10 THz.

ATH3K.3 • 14:30 **Invited**
Exploiting Coherence for Trace Explosives
Detection, David S. Moore¹, Shawn Mc-
Grane¹, Margo Greenfield¹, Kathryn (Katie)
Brown¹; ¹Los Alamos National Lab, USA. This
talk will present concepts and results applying
coherent control techniques to enhance the
detection capabilities of currently deployed
methods for trace detection of explosives in
the real world.

Meeting Room
212 C/D

CLEO: Science &
Innovations

14:00–16:00
STh3L • Multi-Mode Fiber
Phenomena I
President: To Be Announced

STh3L.1 • 14:00
High-power multi transverse modes
random fiber laser with considerably low
spatial coherence, Rui Ma^{1,2}, Jia Qi Li¹, Jia
Yu Guo¹, Han Wu¹, Hua Hui Zhang¹, Bo
Hu¹, Yun Jiang Rao¹, Wei Li Zhang¹; ¹Univ
of Electronic Science & Tech China, China;
²Aston Inst. of Photonic Technologies, UK. A
high-power multi-transverse modes random
fiber laser is realized with ~56 W output
power and considerably low speckle contrast
~0.01 through the combination of a master
oscillator power-amplifier and a segment of
step-index multimode fiber.

STh3L.2 • 14:15
Robust Cell Imaging through Anderson
Localizing Optical Fiber Based on Deep
Learning, Jian Zhao¹, Yangyang Sun¹, Jose
Enrique Antonio-Lopez¹, Rodrigo Amezcua
Correa¹, Shuo Pang¹, Axel Schülzgen¹;
¹CREOL, The College of Optics & Photonics,
Univ. of Central Florida, USA. Robust artifact-
free cell imaging is demonstrated by comb-
ing a meter-long Anderson localizing optical
fiber with deep learning using incoherent
illumination. The tolerance to fiber bending
can reach ~3 degrees for high-fidelity cell-
image transport.

STh3L.3 • 14:30 **Invited**
Novel Concepts for Sensing, Imaging and
Mode Generation in Fibres Using High-
Index Glass, Heike Ebendorff-Heidepriem¹,
Stephen Warren-Smith¹, Jiawen Li¹, Erik
Schartner¹, Hong Ji¹, Yinlan Ruan¹, Dongbi
Bai², Brant Gibson², Tanya Monro³, Robert
McLaughlin¹; ¹Univ. of Adelaide, Australia;
²RMIT Univ., Australia; ³Univ. of South Aus-
tralia, Australia. The high refractive index of
heavy metal oxide glasses combined with
their low processing temperatures enables
new fiber concepts such as enhanced imag-
ing core density, stable doughnut beam
delivery, miniaturized imaging+sensing and
intrinsic magnetic sensitivity.

CLEO: QELS-Fundamental
Science

14:00–16:00

FTh3M • Metasurfaces

President: Rajesh Menon; Univ. of Utah, USA

FTh3M.1 • 14:00

Computational Holographic Camera with a Dielectric Metasurface Diffuser, Hyoungan Kwon¹, Ehsan Arbabi¹, Seyede M. Kamali¹, MohammadSadeqh Faraji-Dana¹, Andrei Faraon¹; ¹California Inst. of Technology, USA. We experimentally demonstrate computational complex optical field imaging by a metasurface diffuser and the speckle-correlation scattering matrix method. Thus we show that the metasurface diffuser can outperform conventional scattering media in context of computational imaging.

FTh3M.2 • 14:15

Dielectric metasurfaces performing all-analog computing, Concetto Eugenio Andrea Cordaro¹, Hyeon Kwon², Dimitrios Sounas^{2,3}, Femius Koenderink¹, Albert Polman¹, Andrea Alu^{2,4}; ¹AMOLF, Netherlands; ²Dept. of Electrical and Computer Engineering, The Univ. of Texas at Austin, USA; ³Electrical and Computer Engineering, Wayne State Univ., USA; ⁴CUNY Advanced Science Research Center, USA. We present experimental results on metasurfaces capable of performing analog image processing. Specifically, we show designs for 1st and 2nd order spatial differentiation enabling low power and real-time edge detection.

FTh3M.3 • 14:30

Metalens for light field imaging, Cheng Hung Chu², Mu Ku Chen¹, Hsin Yu Kuo¹, Ren Jie Lin¹, Shuming Wang³, Vin-Cent Su⁴, Tsung Lin Chung¹, Jia-Wern Chen¹, Yi-Teng Huang¹, Pin Chieh Wu², Tao Li³, Shining Zhu³, Din Ping Tsai^{2,1}; ¹National Taiwan Univ., Taiwan; ²Academia Sinica, Taiwan; ³College of Engineering and Applied Sciences, School of Physics, China; ⁴National United Univ., Taiwan. We use a 60 × 60 dielectric achromatic metalens array to capture multidimensional optical information including both image and depth. The scene can be reconstructed slice by slice from a series of rendered full-color images.

CLEO: Science & Innovations

14:00–16:00

STh3N • Hybrid Integration with Si
Photonics

President: Beibei Zeng; Corning Inc., USA

STh3N.1 • 14:00

Heterogeneously Integrated Low-power-consumption Semiconductor Optical Amplifier on Si Platform, Tatsuro Hiraki¹, Takuma Aihara¹, Koji Takeda¹, Takuro Fujii¹, Tai Tsuchizawa¹, Takaaki Kakitsuka¹, Shinji Matsuo¹; ¹NTT Device Technology Labs, Japan. A membrane semiconductor optical amplifier heterogeneously integrated with SiN waveguides on SiO₂/Si substrate exhibits 10-dB on-chip gain with 13-mA bias current. Clear eye openings are obtained with 10- and 28-Gbit/s NRZ signals.

STh3N.2 • 14:15

50Gb/s CVD Graphene-Insulator-Graphene Electro-Absorption Modulator on Si waveguide, Vito Soriano¹, Simone Marconi^{2,1}, Marco Angelo Giambra¹, Vaidotas Miseikis^{1,3}, Alberto Montanaro¹, Camilla Coletti^{3,4}, Marco Romagnoli¹; ¹Photonic Networks and Technologies Lab – CNIT, Italy; ²Tecip Inst. - Scuola Superiore Sant'Anna, Italy; ³Graphene Labs, Istituto Italiano di Tecnologia, Italy; ⁴Center for Nanotechnology Innovation @NEST, Istituto Italiano di Tecnologia, Italy. We demonstrate a non-return to zero optical modulation at 50Gb/s with a CVD grown Graphene-Insulator-Graphene electro-absorption modulator integrated on a Si photonic waveguide. The device exhibits a 3dB electro-optical bandwidth of 30GHz.

STh3N.3 • 14:30

Asymmetric graphene-on-silicon nitride waveguide photodetector towards fast speed and high responsivity, Yun Gao¹, Hon Ki Tsang¹, Chester Shu¹; ¹The Chinese Univ. of Hong Kong, Hong Kong. We demonstrate a 6-μm long asymmetric graphene-on-silicon nitride waveguide photodetector with a measured electro-optic bandwidth of 38 GHz and a responsivity of 13 mA/W at 1550 nm. Carrier dynamics in the photodetector are also analyzed.

14:00–16:00

STh3O • 2D Materials

President: Matthew Escarra; Tulane University, USA

STh3O.1 • 14:00

External Quantum Efficiency of Monolayer MoTe₂ based Near-Infrared Light Emitting Diodes, Jiabin Feng¹, Yongzhuo Li¹, Song Fu¹, Jianxing Zhang¹, Zizhao Zhong¹, Hao Sun¹, Lin Gan¹, Cunzheng Ning^{1,2}; ¹Tsinghua Univ., China; ²Arizona State Univ., USA. We demonstrated a monolayer MoTe₂ based near-IR light emitting diode on SiO₂/Si substrate and determined for the first time the external quantum efficiency of the device in the range of 10⁻⁴ ~ 5 × 10⁻³ at 5–300K.

STh3O.2 • 14:15

Birefringence and Dispersion Analysis of Hexagonal Boron Nitride (h-BN), Yoonhyuk Rah¹, Yeonghoon Jin¹, Sejeong Kim², Kyoungsik Yu¹; ¹KAIST, South Korea (the Republic of); ²Univ. of Technology Sydney, Australia. h-BN is a promising material for photonics and electronics applications, but its optical properties are not well known. We observe normal dispersion, near 0 extinction coefficient and birefringence of exfoliated h-BN in the visible wavelengths.

STh3O.3 • 14:30

Direct Growth of Large-area Graphene by Cross-linked Parylene Graphitization toward Photodetection, Yibo Dong¹, Chuantong Cheng², Chen Xu¹, Xurui Mao², Yiyang Xie¹, Guanzhong Pan¹, Qihua Wang¹, Jie Sun³; ¹Beijing Univ. of Technology, China; ²Inst. of Semiconductor, Chinese Academy of Sciences, China; ³Fuzhou Univ., China. Large area uniform graphene was directly grown on insulating substrate by cross-linked Parylene graphitization. The as-grown graphene was used for the fabrication of graphene-Si Schottky junction photodetector with a responsivity of 275.9 mA/W.

CLEO: QELS-Fundamental Science

FTh3A • Gateways to Quantum Information Processing—Continued

FTh3A.4 • 14:45

Deterministic Two-photon Controlled-phase Gate Enabled by Induced pi-phase Shift in Photonic Molecule Generations, Zihao Chen¹, Yao Zhou¹, Jung-Tsung Shen¹; ¹Washington Univ. in St. Louis, USA. We propose a novel deterministic two-photon controlled-phase gate scheme enabled by a nonlinear pi-phase shift imprinted during photonic molecule generations, which serves as a vital building block for scalable photon-based quantum computing network.

FTh3A.5 • 15:00

Error-Disturbance Tradeoff in Sequential Quantum Measurements, Ya-Li Mao¹, Zhi-Hao Ma², Rui-Bo Jin³, Qi-Chao Sun¹, Shao-Ming Fei^{4,5}, Qiang Zhang¹, Jingyun Fan¹, Jian-Wei Pan¹; ¹Univ. of Science and Technology of China, China; ²Shanghai Jiao Tong Univ., China; ³Wuhan Inst. of Technology, China; ⁴Capital Normal Univ., China; ⁵Max-Planck-Inst. for Mathematics in the Sciences, Germany. We derive a state-dependent error-disturbance tradeoff based on statistical distance in the sequential measurements of a pair of noncommutative observables and experimentally verify the relation with a photonic qubit system.

FTh3A.6 • 15:15

Subatomic Many-Body Physics Simulations on a Quantum Frequency Processor, Hsuan-Hao Lu¹, Natalie Klco², Joseph M. Lukens³, Titus D. Morris^{4,5}, Aaina Bansal⁶, Andreas Ekstrom⁶, Gaute Hagen^{4,5}, Thomas Papenbrock^{5,4}, Andrew M. Weiner¹, Martin J. Savage², Pavel Lougovski³; ¹School of Electrical and Computer Engineering, Purdue Univ., USA; ²Inst. for Nuclear Theory, Univ. of Washington, USA; ³Quantum Information Science Group, Oak Ridge National Lab, USA; ⁴Physics Division, Oak Ridge National Lab, USA; ⁵Dept. of Physics and Astronomy, Univ. of Tennessee, USA; ⁶Dept. of Physics, Chalmers Univ. of Technology, Sweden. We demonstrate a photonic quantum simulation on a quantum frequency processor, computing the effective interaction potential between composite particles in the Schwinger model and determining the binding energies of three nuclei (²H, ³He, and ⁴He).

FTh3A.7 • 15:30 **Invited**

Limitations on the Use of the Heisenberg Picture in Quantum Information Applications, James D. Franson¹; ¹Univ. of Maryland Baltimore County, USA. We show that the Heisenberg operator produced by a unitary transformation cannot be used as the input to a second transformation. The experimental implications of this will be illustrated using several examples in quantum optics.

FTh3B • Tailorable Phenomena in Optical Fibers—Continued

FTh3B.2 • 15:00

Entropic Response of Polarization Dynamics in Nonlinear Multimode Optical Systems, Fan Wu¹, Absar U. Hassan¹, Demetrios N. Christodoulides¹; ¹Univ. of Central Florida, USA. We show that the Hamiltonian “energy” of a nonlinear multimode optical system involving two circular polarizations always flows from a hotter to a colder arrangement—as expected from the second law of thermodynamics.

FTh3B.3 • 15:15

Dispersion engineering of Schott-SF6 photonic crystal fibres for nonlinear applications in the infrared, Nicolas Joly^{2,1}, Xin Jiang², Riccardo Pennetta², Jonas Hammer^{1,2}, Fehim Babic², Philip S. Russell^{2,1}; ¹Universität Erlangen-Nürnberg, Germany; ²Max-Planck Inst. for the Science of Light, Germany. An empirical model for estimating the dispersion of solid-core Schott-SF6 photonic crystal fibre is presented. Finite element calculations and experimentally measured power-dependent spectra confirm the accuracy of the model.

FTh3B.4 • 15:30

Beam Self-Cleaning in Multimode Optical Fibers and Hydrodynamic 2D Turbulence, D. S. Kharenko^{1,2}, Oleg Sidelnikov^{1,3}, Vlad A. Gonta¹, M. D. Gervaziev¹, Katarzyna Krupa⁴, Sergei K. Turitsyn^{5,1}, M. P. Fedoruk^{1,3}, E. V. Podivilov^{1,2}, Sergey A. Babin^{1,2}, Stefan Wabnitz^{6,1}; ¹Novosibirsk State Univ., Russia; ²Inst. of Automation and Electrometry, SB RAS, Russia; ³Inst. of Computational Technologies, SB RAS, Russia; ⁴Univ. of Bourgogne, France; ⁵Aston Univ., UK; ⁶Sapienza Università di Roma, Italy. We experimentally demonstrate the conservation of the average mode number in the process of Kerr beam self-cleaning in a graded-index multimode optical fiber, in analogy with wave condensation in hydrodynamic 2D turbulence.

FTh3C • Emission & Detection of Thermal Radiation—Continued

FTh3C.4 • 15:00

Nanoradiator-Mediated Deterministic Opto-Thermoelectric Manipulation, Yaoran Liu¹, Linhan Lin¹, Bharath Bangalore Rajeeva¹, Yuebing Zheng¹; ¹The Univ. of Texas at Austin, USA. We explore the opto-thermoelectric trapping at plasmonic antennas that serve as optothermal nano-radiators to achieve the low-power and deterministic manipulation of nanoparticles.

FTh3C.5 • 15:15

Plasmonic photo-thermo-electric effect in graphene, Viktoryia Shautsova², Nicholas A. Gusken¹, Themistoklis Sidiropoulos⁴, Xiaofei Xiao¹, Nicola Black¹, Adam M. Gilbertson¹, Vincenzo Giannini¹, Stefan Maier^{1,3}, Lesley Cohen¹, Rupert Oulton¹; ¹Physics, Imperial College London, UK; ²Materials Dept., Oxford Univ., UK; ³Physics, LMU Munich, Germany; ⁴ICFO, Spain. We present a novel photo-thermo-electric effect in graphene photo-detectors established by hot electrons concentration gradients at plasmonic contacts. Our description is crucial for an in depth understanding of graphene-based photodetection devices.

FTh3C.6 • 15:30

Field-Resolved Detection of the Temporal Response of a Mid-Infrared Plasmonic Antenna, Marco P. Fischer², Kevin F. Gallacher³, Jacopo Frigerio⁴, Giovanni Pellegrini⁴, Giovanni Isella⁴, Alfred Leitenstorfer², Douglas J. Paul³, Paolo Biagioni¹, Daniele Brida^{2,1}; ¹Univ. of Luxembourg, Luxembourg; ²Univ. of Konstanz, Germany; ³Univ. of Glasgow, UK; ⁴Politecnico di Milano, Italy. We performed electro-optic sampling of the pulses re-emitted by a heavily-doped germanium antenna resonant in the mid-infrared. This field-resolved measurement allows observing the time domain response of a single plasmonic structure in amplitude and phase.

FTh3D • Quantum Photonics: Generation & Manipulation—Continued

FTh3D.2 • 15:00

On-chip nano-electro-mechanical switching of deterministic single photons, Xiaoyan Zhou¹, Camille Papon¹, Henri Thyrestrup¹, Zhe Liu¹, Søren Stobbe^{2,3}, Rüdiger Schott⁴, Andreas Wiek⁴, Arne Ludwig⁴, Peter Lodahl¹, Leonardo Midolo¹; ¹Center for Hybrid Quantum Networks, Niels Bohr Inst., Denmark; ²Niels Bohr Inst., Denmark; ³Dept. of Photonics Engineering, DTU Fotonik, Technical Univ. of Denmark, Denmark; ⁴Ruhr-Universität Bochum, Germany. We demonstrate a nano-electro-mechanical single-photon router integrated with semiconductor quantum emitters, showing an extinction ratio of >20 dB and operation speed of MHz with insertion loss of 0.67 dB and footprint <30 μm².

FTh3D.3 • 15:15

Integrated Quantum Photonics using Site-Controlled Quantum Dots and Tailored-Potential Photonic Crystals, Antoine M. Delgoffe¹, Alessio Miranda¹, Alexey Lyasota¹, Alok Rudra¹, Benjamin Dwir¹, Yi Yu^{1,2}, Eli Kapon¹; ¹Ecole Polytechnique Federale de Lausanne, Switzerland; ²Technical Univ. of Denmark, Denmark. We demonstrate several integrated photonics structures incorporating site-controlled quantum dots and photonic crystal cavities with tailored mode structures. Optimal designs for single photon extraction, routing and switching are presented and discussed.

FTh3D.4 • 15:30

Dual-Pump Design Enables Novel Photon-Pair Characterization and Engineering, Yujie Zhang¹, Ryan Spiniolas¹, Kai B. Shinbrough¹, Bin Fang¹, Offir Cohen¹, Virginia O. Lorenz¹; ¹Univ. of Illinois at Urbana-Champaign, USA. We experimentally demonstrate a dual-pump spontaneous four-wave mixing photon-pair source for which we quantify the noise to determine the generation probability and collection efficiency directly, and that generates photons in pure quantum states.

CLEO: Science & Innovations

STh3E • Ultrafast Parametric
Sources I—Continued

STh3E.3 • 15:00

A high power (11 W), tunable (1.45 – 1.65 μm) OPCPA for THz generation in organic crystals, Ivanka Grguras¹, Torsten Golz¹, Michael Schulz¹, Jan Heye Buß¹, Robert Riedel¹, Mark J. Prandolini¹; ¹Class 5 Photonics GmbH, Germany. For THz generation using organic crystals, a high power, tunable (1.45 – 1.65 μm) OPCPA with pulse duration of < 36 fs at 350 kHz was developed. To enhance the flexibility of this system, a second synchronized probe channel is available, delivering compressed pulses at 850 nm with < 15 fs.

STh3E.4 • 15:15

Optical parametric amplification of short-wave infrared monocycle pulses in BBO crystals pumped by red femtosecond pulses, Y. C. Lin¹, Yasuo Nabekawa¹, Katsumi Midorikawa¹; ¹RIKEN, Japan. We generate infrared pulses with pulse duration of 5.3 fs (0.94 optical cycle) at the center wavelength of 1.7 μm via optical parametric amplification in BBO crystals, pumped by 708-nm femtosecond pulses.

STh3E.5 • 15:30

Compact 1-MHz, 1- μJ , Few-cycle, Passively CEP-stable 2- μm Source, Yizhou Liu^{1,2}, Peter Krogen³, Kyung-Han Hong⁴, Qian Cao^{1,2}, Philip Keathley⁴, Franz Kärtner^{2,1}; ¹Hamburg Univ., Germany; ²DESY, Germany; ³Universität in Santa Barbara, USA; ⁴MIT, USA. We demonstrate a passively CEP-stable, 1-MHz, 2- μm dispersion managed optical parametric amplifier (OPA) with a chirped-pulse DFG front-end, pumped by an all fiber 1- μm source generating compressed μJ -level output pulses with 94.5 fs pulse duration.

STh3F • Nonlinear THz
Phenomena—Continued

STh3F.2 • 15:00

Parallel-Plate THz Waveguides for Relativistic Electron Bunch Compression, Mohamed Othman¹, Matthias C. Hoffmann¹, Renkai Li¹, Emilio Nanni¹, Xijie Wang¹; ¹SLAC National Accelerator Lab, USA. We present results from testing a new dispersion-free THz parallel-plate-based tapered structure optimized for focusing single-cycle THz pulses, producing high fields and with the potential for electron bunch compression to a few femtoseconds.

STh3F.3 • 15:15

Solid-state Biased Coherent Detection of Ultrabroadband Infrared Pulses Using Single Crystal of Diamond, Eiichi Matsumura^{1,2}, Masaya Nagai², Masaaki Ashida²; ¹Osaka Dental Univ., Japan; ²Engineering Science, Osaka Univ., Japan. Using a high-voltage applied single crystal of diamond as a medium, we demonstrated the coherent detection of ultrabroadband infrared pulses generated from two-color pumped air plasma in a spectral range of 1–150 THz.

STh3F.4 • 15:30

Hidden Phase-Matched Narrowband THz Generation via Optical Rectification in Lithium Niobate, Dogeun Jang¹, Yung Jun Yoo¹, Ki-Yong Kim¹; ¹Univ. of Maryland at College Park, USA. We observe efficient narrowband terahertz emission at 15 THz from lithium niobate crystals when irradiated by femtosecond Ti:sapphire laser pulses. This emission arises from phase-matched optical rectification in between resonance frequencies.

STh3G • Precision Timing
& Optical Time Transfer—
Continued

STh3G.4 • 14:45

Long-haul Transfer of Optical Frequencies in Free Space, Hyun Jay Kang¹, Jaewon Yang¹, Young-Jin Kim^{2,1}, Seung-Woo Kim¹; ¹South Korea Advanced Inst of Science & Tech, South Korea (the Republic of); ²Nanyang Technology Univ., Singapore. We report experimental results of concurrent transfer of multiple optical frequencies, coherently generated from an optical frequency comb, over an 18 km free-space link with real-time compensation of atmospheric phase noise.

STh3G.5 • 15:00

Laser Time Transfer Based on Micius Satellite, Hui Dai^{1,2}, Qi Shen^{1,2}, Shuang-Lin Li^{1,2}; ¹Shanghai Branch, National Lab for Physical Sciences at Microscale and Dept. of Modern Physics, Univ. of Science and Technology of China, China; ²Chinese Academy of Sciences (CAS) Center for Excellence and Synergetic Innovation Center in Quantum Information and Quantum Physics, Univ. of Science and Technology of China, China. Based on Micius satellite, we demonstrate two satellite-to-ground laser time transfer experiments with high repetition rate and high precision. It shows the feasibility to combine time transfer network with quantum communication network.

STh3G.6 • 15:15

Attosecond Relative Timing Jitter between Optical Pulses and Rising Edges of Photocurrent Pulses, Minji Hyun¹, Yongjin Na¹, Hayun Chung², Jungwon Kim¹; ¹South Korea Advanced Inst of Science & Tech, South Korea (the Republic of); ²South Korea Univ., South Korea (the Republic of). We characterize relative timing jitter between optical pulses and photocurrent pulses with 300-attosecond resolution. We found that excess timing jitter at the rising edge can show ultra-low ~400-attosecond-level jitter for both p-i-n and MUTC photodiodes.

STh3H • Modulation &
Switching—Continued

STh3H.4 • 15:00

Sub-V Opto-Electro-Mechanical Switch, Christian Haffner¹, Andreas Joerg¹, Felix M. Mayor¹, Michael Doderer¹, Daniel Chelladurai¹, Yuriy Fedoryshyn¹, Maurizio Burla¹, Cosmin Roman¹, Juerg Leuthold¹; ¹ETH Zurich, Switzerland. We demonstrate plasmonic-electro-mechanical-switches that feature a plasmonic resonator ($Q > 1000$). This enables low on/off voltages (875mV) and low insertion losses (~1dB). The performance proofs that plasmonics is competitive with photonics not only at highest speed.

STh3H.5 • 15:15

Surface-Acoustic-Wave-Photonic Devices in Standard Silicon-on-Insulator, Dvir Munk¹, Moshe Katzman¹, Mirit Hen¹, Maayan Priel¹, Avi Zadok¹; ¹Bar-Ilan Univ., Israel. Planar acousto-optic devices are implemented in standard silicon on insulator. Pump light is absorbed in metallic gratings. Stimulated surface waves modulate an optical probe in a ring resonator. Narrowband microwave photonic filtering is demonstrated.

STh3H.6 • 15:30

Resonant, High-frequency Acousto-Optic Modulators (AOM) Fabricated in a MEMS Foundry Platform, Krishna C. Coimbatore Balram¹, Stefano Valle¹; ¹OET Labs & Electrical and Electronic Engineering, Univ. of Bristol, UK. We report the design and characterization of high frequency, resonant acousto-optic modulators in a MEMS foundry process. The doubly resonant cavity design allows us to measure acousto-optic modulation at frequencies upto 4 GHz with high modulation efficiency ($V_{\pi} \sim 350\text{mV}$, $f_{\text{res}} \sim 2\text{GHz}$).

Meeting Room
211 A/B

CLEO: Applications
& Technology

ATH3I • A&T Topical Review on
Silicon Photonics I—Continued

ATH3I.3 • 14:45

Silicon Photonics External Cavity Laser with Misalignment Tolerant Multi-mode RSOA to PIC Interface, Ibrahim Ghannam¹, Manuel Ackermann¹, Sebastian Romero-García¹, Florian Merget¹, Jeremy Witzens¹; ¹Inst. of Integrated Photonics, RWTH Aachen Univ., Germany. We present an external cavity laser with a silicon photonics PIC coupled to an RSOA with a multimode grating coupler. Also acting as a 3-dB splitter inside a Sagnac loop, it relaxes alignment tolerances.

ATH3I.4 • 15:00

Vertically Coupled a-Si:H Multimode Interference Waveguides for Multi-layer Silicon Photonics Platform, Swe Z. Oo¹, Antulio Tarazona¹, Rafidah Petra^{1,2}, Ali Khokhar¹, Graham T. Reed¹, Anna C. Peacock¹, Harold M. Chong¹; ¹Univ. of Southampton, UK; ²Universiti Teknologi Brunei, Brunei Darussalam. We successfully demonstrated low temperature fabrication process of vertical MMI a-Si:H waveguides for multi-layer photonic integrated circuit. Measured MMI loss of 1.97dB/MMI and vertical light coupling of TE polarization at 1550nm wavelength have been achieved.

ATH3I.5 • 15:15 **Invited**

Silicon Photonics, Graham T. Reed¹; ¹Univ. of Southampton, UK. In this paper we will discuss the use of ion implantation of Germanium into Silicon to introduce new functionality to Silicon Photonic circuits, from wafer scale testing, to device trimming and programmable photonic circuits

Meeting Room
211 C/D

CLEO: Science & Innovations

STh3J • Emerging Nonlinear
Platforms—Continued

STh3J.4 • 14:45

Competing Faraday and modulational instabilities in dispersion-managed high-Q microcavities, Wenting Wang¹, Jinghui Yang¹, Abhinav Vinod¹, Hao Liu¹, Mingbin Yu², Dim Lee Kwong², Chee Wei Wong¹; ¹Univ. of California Los Angeles, USA; ²Inst. of Microelectronics, Singapore. We observed the competition between Faraday parametric instability and modulational instability in a dispersion-managed microcavity by changing the effective pump-resonance detuning. The Faraday ripple is triggered by the periodical oscillating group-velocity dispersion along the microcavity.

STh3J.5 • 15:00 **Invited**

Nonlinear Light Propagation in Crystals with Spatially Randomized Domains, Crina Cojocaru¹, Jose Trull¹, Wieslaw Krolikowski²; ¹Dept. of Physics, Universitat Politècnica de Catalunya, Spain; ²Texas A&M Univ. at Qatar, Qatar. A study of the broad band spatial distributed second harmonic generation in a nonlinear crystal having a random size and distribution of nonlinear domains: applications to ultrashort pulse characterization and domain statistic characterization.

STh3J.6 • 15:30

Broadband randomly phase matched OPO using a thin 0.5-mm ZnSe ceramic and a dispersion-free cavity, Qitian Ru¹, Taiki Kawamori¹, Sergey Vasilyev², Sergey Mirov^{2,3}, Konstantin L. Vodopyanov¹; ¹CREOL, College of Optics and Photonics, Univ. of Central Florida, USA; ²IPG Photonics - Mid-infrared Lasers, USA; ³Dept. of Physics, Univ. of Alabama at Birmingham, USA. We used a 0.5-mm randomly-phase-matched ZnSe polycrystal pumped by femtosecond 2.35- μ m pulses and achieved a 3.2–9- μ m-wide spectrum with 53-mW output power in a dispersion-free OPO cavity consisting of gold-coated mirrors and a pump injector.

Meeting Room
212 A/B

CLEO: Applications
& Technology

ATH3K • Trace Species
Sensing—Continued

ATH3K.4 • 15:00

Dual-comb spectroscopy for the emission spectrum analysis, Liao Chen¹, Xi Zhou¹, Xin Dong¹, Yuhua Duan¹, Chi Zhang¹, Xinliang Zhang¹; ¹Wuhan National Lab for Optoelectronics, China. A time-lens based dual-comb spectroscopy for the emission spectrum analysis is demonstrated. As a proof-of-concept, it achieves around 2-pm resolution and 7-nm bandwidth under 4-kHz frame rate, acts as a complementary for absorptive dual-comb spectroscopy.

ATH3K.5 • 15:15

Photoacoustic Pulse Width Measurement using Speckle Contrast Analysis, Matan Benyamin^{1,2}, Hadar Genish², Ran Califa², Nisan Ozana^{1,2}, Ariel Schwarz², Zeev Zalevsky^{1,2}; ¹Faculty of Engineering and the Nanotechnology center, Bar Ilan Univ., Israel; ²ContinUse Biometrics, Israel. A previously demonstrated non-expensive setup for remote photoacoustic signal detection, is extended to overcome its bandwidth limitations and obtain time-domain signal properties.

ATH3K.6 • 15:30

Methane excitation behavior as a comparison of InP, GaSb, IC and QC lasers excitation source by sensor applications, Tobias Milde^{1,2}, Morten Hoppe¹, Herve Tatenguem¹, Christian Assmann¹, Martin Honsberg³, Wolfgang Schade², Joachim R. Sacher¹; ¹Sacher Lasertechnik GmbH, Germany; ²Technische Universität Clausthal, Germany; ³Sensor Photonics GmbH, Germany. The MIR wavelength regime promises better gas detection possibilities than the NIR or the visible region because of the higher absorbencies simulated by HITRAN. These possibilities are tested with different lasers on TDLAS and QEPAS.

Meeting Room
212 C/D

CLEO: Science & Innovations

STh3L • Multi-Mode Fiber
Phenomena I—Continued

STh3L.4 • 15:00

Multi-orthogonal High-order Modes Converter, Linghao Meng¹, Jianfeng Lu¹, Longkun Zhang¹, Fan Shi¹, Xianglong Zeng¹; ¹Shanghai Univ., China. We demonstrate a fiber laser based on a cascaded AIFGs with flexible switching output of multiple modes (LP₀₁, LP₁₁^{a/b}, LP₂₁^{a/b}, LP₀₂). This has potential application in mode division multiplexing, multimode fiber laser.

STh3L.5 • 15:15

Robust compressive imaging through single multimode fiber with millimeter depth of field against bending, Di Guan¹, Li Gao¹, Junhui Li¹, Mingying Lan¹, Yangyang Xiang¹, Guohua Wu¹, Song Yu¹; ¹Beijing Univ. Posts & Telecommunications, China. Single pixel imaging experiment through single multimode fiber demonstrates capability of multi-millimeter depth of field, almost three orders larger than previous work, also robustness against fiber configuration change caused by bending.

STh3L.6 • 15:30

Intracavity cylindrical vector beam generation from an all-PM Er-doped mode-locked fiber laser, Yuwei Zhao¹, Jintao Fan¹, Ruoyu Liao¹, Youjian Song¹, Ming-lie Hu¹; ¹Tianjin Univ., China. We demonstrate a practical method to generate on-demand 1st order and higher order cylindrical vector beams in the 1550 nm band directly from an all-PM mode-locked Er-fiber laser.

CLEO: QELS-Fundamental
Science

FTh3M • Metasurfaces—Continued

FTh3M.4 • 14:45

Metasurface Optics for Ultra-Compact Augmented Reality (AR) Visors, Elyas Bayati¹, Shane Colburn¹, Arka Majumdar¹; ¹Univ. of Washington, USA. We propose to design the next generation of metasurface near-eye visors which will circumvent real-world distortions and provide a large field of view, as needed for an immersive AR experience.

FTh3M.5 • 15:00

Artifact-free Phase-Amplitude Metasurface Holography at up to Three Wavelengths, Adam C. Overvig¹, Sajan Shrestha¹, Stephanie Malek¹, Nanfang Yu¹; ¹Columbia Univ., USA. We report numerical and experimental demonstrations of phase-amplitude metasurface holograms capable of producing 2D holographic images free of “ringing artifacts”. By using a metasurface doublet, this can be extended to three colors simultaneously.

FTh3M.6 • 15:15

Gap-surface Plasmon Metasurfaces for Focused Structured-beams Generation, Fei Ding¹, Sergey I. Bozhevolnyi¹; ¹Univ. of Southern Denmark, Denmark. Capitalizing on gap-surface plasmon metasurfaces (GSPMs), we experimentally generate focused structured-beams in the near-infrared range (750–950 nm) with broadband and highly-efficient performance, including the polarized-converted focused vortex beam (PCFVB) and focused vector-beam (FVB).

FTh3M.7 • 15:30

Semiconductors Meta-Optics: Fabrication and Applications, Gauthier Briere¹, Peinan Ni¹, Sebastien Heron¹, Sebastien Chenot¹, Stephane Veizan¹, Virginie Brandli¹, Benjamin Damilano¹, Jean Yves Duboz¹, Masanobu Iwanaga², Patrice Genevet¹; ¹CNRS, France; ²NIMS, Japan. In this work we present metasurfaces based on Gallium Nitride material. We propose a fabrication method able to preserve the active optical properties of semiconductors, thus paving the way for the realization of tunable metadevices. ©2019 Briere Gauthier, Patrice Genevet.

CLEO: Science & Innovations

STh3N • Hybrid Integration with Si
Photonics—Continued

STh3N.4 • 14:45

Hybrid Silicon-Conductive Oxide Microring Resonators with 261pm/V Tunability, Behzad Ashrafi Nia¹, Erwen Li¹, Alan X. Wang¹; ¹Oregon State Univ., USA. We designed and demonstrated a silicon microring filter with indium-tin oxide gate as the electric-tuning electrode. It achieved ultra-large resonance wavelength tunability of 261pm/V, which is obtained through the high-K HfO₂ insulated capacitor.

STh3N.5 • 15:00 **Invited**

III-V Lasers Emitting at 1.3 to 1.5 mm grown on (001) silicon by MOCVD, Kei May Lau¹; ¹Hong Kong Univ of Science and Technology, USA. We report the growth of quantum-well and quantum-dot lasers on compliant InP/Si substrates by MOCVD. Laser characteristics at 1.3 to 1.5 mm from whispering-gallery-mode (WGM) micro-lasers, nano-ridge lasers and conventional Fabry-Perot lasers will be described.

STh3N.6 • 15:30

Low-Loss TeO₂ Waveguides Integrated on a Si₃N₄ Platform for Active and Nonlinear Optical Devices, Henry Frankis¹, Khadijeh Kiani¹, Dawson Bonneville¹, Chenglin Zhang¹, Samuel Norris², Richard Mateman³, Arne Leinse³, Nabil D. Bassim², Andrew P. Knights¹, Jonathan D. B. Bradley¹; ¹Engineering Physics, Canada; ²Materials Science and Engineering, McMaster Univ., Canada; ³LioniX International, Netherlands. We report on TeO₂-coated Si₃N₄ waveguides with losses down to 0.6 dB/cm at 2 μm. These results are a promising step towards realizing scalable, compact and high-performance tellurite glass devices on a silicon nitride platform.

STh3O • 2D Materials—Continued

STh3O.4 • 14:45

Energy Transport at Hybrid Organic-MoS₂ Interface, Che-Hsuan Cheng¹, Zidong Li¹, Parag Deotare¹; ¹Univ. of Michigan, USA. We report energy transport of charge transfer (CT) excitons at the hybrid interface of low dimensional materials. We find that the transport of hybrid CT excitons is eight times faster than MoS₂ A-excitons.

STh3O.5 • 15:00

Pseudo-van der Waals Epitaxy of MoS₂ on Patterned and Planar GaN Substrates, Xiuling Li¹, Hao-Chung Kuo², Weidong Zhou³, Che-Yu Liu², Wonsik Choi¹, Hsien-Chih Huang¹; ¹Univ. of Illinois, USA; ²National Chiao Tung Univ., Taiwan; ³Univ. of Texas at Arlington, USA. n-MoS₂/p-GaN diodes monolithically formed by pseudo-van der Waals epitaxy show well-defined rectifying behavior. Growth on patterned GaN substrates yields monolayer and few-layer MoS₂ formation on the planar surface and the pyramids, respectively.

STh3O.6 • 15:15

Cryogenic Micro-PL of Monolayer 1T/2H MoS₂ Superlattice, Zhangji Zhao¹, Ibrahim Sarpkaya², Xuejun Xie³, Kaustav Banerjee³, Han Htoon², Chee Wei Wong¹; ¹Univ. of California Los Angeles, USA; ²Center for Integrated Nanotechnologies, Los Alamos National Lab, USA; ³Dept. of Electrical and Computer Engineering, Univ. of California, Santa Barbara, USA. We investigate E-beam irradiated 1T-Phase quantum dots on 2H-MoS₂ by photoluminescence (PL) spectroscopy and mapping. Red-shifted PL spectra from quantum dots under different dose levels are greatly enhanced under 10K than 300K.

STh3O.7 • 15:30 **Invited**

Terahertz and Nonlinear Optics in Graphene, Thomas E. Murphy¹; ¹Univ. of Maryland at College Park, USA. Graphene exhibits unusual optical and thermal properties that allow electrons to be efficiently heated by THz illumination. We discuss the nature, origin, and measurement of the nonlinear response of graphene in the THz regime.

CLEO: QELS-Fundamental Science

FTh3A • Gateways to Quantum
Information Processing—
ContinuedFTh3B • Tailorable Phenomena
in Optical Fibers—Continued

FTh3B.5 • 15:45

Dynamics of photon fluid flows driven by optical pistons, Abdelkrim Bendahmane¹, Gang XU¹, Matteo Conforti¹, Alexandre Kudlinski¹, Arnaud Mussot¹, Stefano Trillo²; ¹CNRS / Lille Univ., France; ²Univ. of Ferrara, Italy. We investigate the optical analogues of the piston shock problem in gas dynamics. Using fast temporal measurements, we recorded dispersive shock waves formed by the propagation of a bi-chromatic photon fluid along an optical fiber.

FTh3C • Emission & Detection
of Thermal Radiation—
Continued

FTh3C.7 • 15:45

Tunable Hyperbolic Plasmons in Self-Assembled Carbon Nanotube Metamaterials, John A. Roberts¹, Shang-Jie Yu², Abram Falk³, Po-Hsun Ho³, Stefan Schoeche⁴, Jonathan A. Fan²; ¹Dept. of Applied Physics, Stanford Univ., USA; ²Dept. of Electrical Engineering, Stanford Univ., USA; ³IBM T.J. Watson Research Center, USA; ⁴J.A. Woollam Co., Inc., USA. We show that self-assembled aligned carbon nanotubes are a tunable hyperbolic metamaterial using spectroscopic ellipsometry. We map the hyperbolic dispersion of plasmonic modes in aligned carbon nanotube films using transmission measurements of nanoribbon resonators.

FTh3D • Quantum Photonics:
Generation & Manipulation—
Continued

FTh3D.5 • 15:45

High visibility Hong-Ou-Mandel interference between independent single photon sources obtained from multi-stage nonlinear interferometers, Jiamin Li¹, Jie Su¹, Liang Cui¹, Xiaoying Li¹, Z. Y. Ou^{1,2}; ¹Tianjin Univ., China; ²Indiana Univ.–Purdue Univ. Indianapolis, USA. Using spontaneous four-wave mixing in a 3-stage nonlinear interferometer for temporal mode shaping, we efficiently generate heralded single photons in single-mode, evidenced by a visibility of 90% in Hong–Ou–Mandel interference between independent sources.

16:00–16:30 Coffee Break, Concourse Level

CLEO: Science & Innovations

STh3E • Ultrafast Parametric
Sources I—ContinuedSTh3F • Nonlinear THz
Phenomena—ContinuedSTh3G • Precision Timing
& Optical Time Transfer—
ContinuedSTh3H • Modulation &
Switching—Continued

STh3F.5 • 15:45

New horizons for high power broadband THz sources driven by ultrafast Yb-based thin disk laser oscillators, Jakub Drs¹, Norbert Modsching¹, Christian Kränkel², Valentin J. Wittwer¹, Olga Razskazovskaya¹, Thomas Südmeyer¹; ¹Universität de Neuchâtel, Switzerland; ²Center for Laser Materials, Leibniz-Institut für Kristallzüchtung, Germany. We confirm the high suitability of ultrafast thin-disk lasers for THz generation, achieving up to 0.33-mW broadband THz radiation in GaP. Moreover, we show 7-THz gapless spectrum by optimization of crystal length and pulse duration.

STh3G.7 • 15:45

Rapid and Precise Displacement Measurement Using Time-of-Flight Detection of Femtosecond Optical Pulses, Yongjin Na¹, Minji Hyun¹, Chan-Gi Jeon¹, Jungwon Kim¹; ¹South Korea Advanced Inst of Science & Tech, South Korea (the Republic of). We demonstrate high-speed and high-resolution displacement measurement method by utilizing electro-optic sampling between electrical pulses from photodetection and femtosecond optical pulses. A 5.8-nm (1.9-nm) resolution is achieved in only 50 μ s (14 ms) update time.

STh3H.7 • 15:45

A Wideband On-Chip Radiator Driven by a Traveling-Wave Photodetector, Craig Ives¹, Behrooz Abiri², Ali Hajimiri¹; ¹California Inst. of Technology, USA; ²Auspion Inc., USA. An integrated broadband Vivaldi antenna driven by an on-chip traveling-wave photodetector is reported. The silicon photonic chip radiates between 21 and 67 GHz with -65 dBm coupled power at 44 GHz.

16:00–16:30 Coffee Break, Concourse Level

Meeting Room
211 A/B

CLEO: Applications
& Technology

ATH3I.6 • 15:45
Electro-Optics with Gigahertz Phonons in Silicon Photonics, Raphaël Van Laer¹, Rishi Patel¹, Jeremy D. Witmer¹, Timothy McKenna¹, Amir Safavi-Naeini¹; ¹Stanford Univ., USA. We demonstrate effective piezoelectricity in silicon nanophotonic structures by breaking silicon's inversion symmetry with an electrical bias field. The devices show promise as low-energy microwave-to-optical interfaces for use in classical and quantum communications.

Meeting Room
211 C/D

CLEO: Science & Innovations

STh3J.7 • 15:45
Logic Gates based on Interaction of Counterpropagating Light in Microresonators, Niall Moroney^{1,2}, Leonardo Del Bino^{1,3}, Michael T. M. Woodley^{1,3}, Jonathan M. Silver^{1,4}, George Ghalanos^{1,2}, Andreas Svela^{1,2}, Shuangyou Zhang¹, Pascal Del'Haye¹; ¹National Physical Lab, UK; ²Physics, Imperial College London, UK; ³Heriot-Watt Univ., UK; ⁴City, Univ. of London, UK. We demonstrate a novel optical logic gate that is mediated by the Kerr effect of counter-propagating beams in a whispering gallery mode microresonator. The universal gate $A \& \neg B$ is presented.

Meeting Room
212 A/B

CLEO: Applications
& Technology

ATH3K.7 • 15:45
High Speed Measurements and Enhancement of QEPAS Sensitivity: Quartz Resonance Frequency Tracking, Herve Taten-guem Fankem¹, Andreas Sacher¹, Morten Hoppe¹, Tobias Milde¹, Joachim R. Sacher¹; ¹Sacher Lasertechnik GmbH, Germany. This study reports on the development of a platform based-on a Field-Programmable Gate Arrays (FPGAs) and suitable for high speed measurements and enhancement of QEPAS sensitivity.

Meeting Room
212 C/D

CLEO: Science & Innovations

16:00–16:30 Coffee Break, Concourse Level

**CLEO: QELS-Fundamental
Science**

CLEO: Science & Innovations

FTh3M.8 • 15:45

Near-IR Wide Field-of-View Huygens Metalens for Outdoor Imaging Applications, Jacob Engelberg¹, Chen Zhou², Noa Mazurski¹, Jonathan Bar-David¹, Uriel Levy¹, Anders Kristensen²; ¹*Applied Physics, Hebrew Univ. Jerusalem Israel, Israel*; ²*Micro- and Nanotechnology, Technical Univ. of Denmark, Denmark*. We present a Huygens nano-antenna based metalens, designed for outdoor photographic applications in the near-infrared. We show that good imaging quality can be obtained over a moderate ± 15 degree field-of-view (FOV).

STh3N.7 • 15:45

Low Loss, Compact Waveguides in GaAs/Oxidized AlGaAs Layers Directly Grown on Silicon, Prashanth Bhasker¹, Chen Shang¹, John Bowers¹, Nadir Dagli¹; ¹*Univ. of California, Santa Barbara, USA*. Waveguides in high index contrast GaAs/Oxidized AlGaAs layers directly grown on silicon are presented. These are very similar to waveguides in Si photonics and can be the basis of very high performance photonic integration platform.

16:00–16:30 Coffee Break, Concourse Level

CLEO: QELS-Fundamental Science

16:30–18:30

FTh4A • New Protocols in Quantum Communications

Presider: Michael Brodsky; *US Army Research Laboratory, USA*

FTh4A.1 • 16:30

Quantum Multiplexing, William Munro^{1,2}, Nicolo Lo Piparo², Kae Nemoto²; ¹*NTT Basic Research Labs, Japan*; ²*National Inst. for Informatics, Japan*. We introduce the concept of quantum-multiplexing for quantum communication systems and repeater networks, which allows us minimize the number of photons needed in entanglement distribution while enhancing the quality of the entangled pairs generated.

16:30–18:30

FTh4B • Non-Diffractive & Vortex Beams

Presider: *To Be Announced*

FTh4B.1 • 16:30

Demonstration of turbulence-resistant propagation of anti-diffracting optical beams beyond kilometer distances, Ze Zhang¹, Xinli Liang¹, Mihalis Goutsoulas², Nikos Efremidis², Zhigang Chen^{3,4}; ¹*Aerospace Information Research Inst., Chinese Academy of Sciences, China*; ²*Dept. of Applied Mathematics, Univ. of Crete, Greece*; ³*The MOE Key Lab of Weak-Light Nonlinear Photonics, TEDA Applied Physics Inst. and School of Physics, Nankai Univ., China*; ⁴*Dept. of Physics and Astronomy, San Francisco State Univ., USA*. We demonstrate robust propagation of anti-diffracting optical beams through atmosphere turbulence beyond kilometer distances. Such Airy-Bessel-like light beams surpass conventional Bessel beams and can, in principle, exhibit “self-focusing” in free space without any optical nonlinearity.

FTh4B.2 • 16:45

Coherent Propulsion with Negative-mass Fields in a Photonic Setting, Yumiao Pei¹, Yi Hu¹, Ping Zhang¹, Chunmei Zhang¹, Cibo Lou², Christian E. Rüter³, Detlef Kip³, Demetrios N. Christodoulides⁴, Zhigang Chen^{1,5}, Jingjun Xu¹; ¹*Nankai Univ., China*; ²*Ningbo Univ., China*; ³*Helmut Schmidt Univ., Germany*; ⁴*Univ. of Central Florida, USA*; ⁵*San Francisco State Univ., USA*. We demonstrate an optical self-accelerating state driven by nonlinear coherent interaction of its constituting components with opposite “mass-sign”. The coherent propulsion, highly immune to initial phase conditions, is surprisingly enhanced comparing to its incoherent counterpart.

FTh4B.3 • 17:00

Engineering the Wavelength and Topological Charge of Non-Diffracting Beams Along Their Axis of Propagation, Ahmed Dorrah¹, Michel Zamboni-Rached², Mo Mojahedi¹; ¹*Dept. of Electrical and Computer Engineering, Univ. of Toronto, Canada*; ²*School of Electrical and Computer Engineering, Univ. of Campinas, Brazil*. We present non-diffracting structured light beams in which their wavelength and local orbital angular momentum can be changed independently and “at will” along the axis of propagation, thus opening new possibilities in laser processing, micro-manipulation, and data communications.

16:30–18:30

FTh4C • Advanced Nanophotonic Platforms for Spectroscopy & Sensing

Presider: Ofer Kfir; *University of Göttingen, Germany*

FTh4C.1 • 16:30 **Invited**

Plasmonic Waveguiding Spectroscopy and Microscop, Hiroshi Ujii^{1,2}, Shuichi Toyouchi², Tomoko Inose¹, Yasuiko Fujita²; ¹*Hokkaido Univ., Japan*; ²*Chemistry, KU Leuven, Belgium*. In this contribution, various applications of plasmonic waveguide will be introduced. Specifically, we will introduce remote excitation of surface enhanced Raman scattering inside a live cell or material surface.

FTh4C.2 • 17:00

Nanospectroscopic Imaging of Vibrational Excitons as a Molecular Ruler, Thomas P. Gray¹, Eric A. Muller¹, Omar Khatib^{1,2}, Hans Bechtel², Markus B. Raschke¹; ¹*Physics, Univ. of Colorado Boulder, USA*; ²*Advanced Light Source Division, Lawrence Berkeley National Lab, USA*. We demonstrate infrared vibrational nano-spectroscopy and -imaging using the evolution of vibrational marker resonances as a molecular ruler to map nanoscale crystallinity in molecular electronic materials.

16:30–18:30

FTh4D • Beyond Photon Pairs

Presider: Marty Stevens; *NIST Boulder Colorado, USA*

FTh4D.1 • 16:30

Repeater-enhanced distributed quantum sensing based on continuous-variable multipartite entanglement, Yi Xia¹, Quntao Zhuang², William Clark³, Zheshen Zhang¹; ¹*Univ. of Arizona, USA*; ²*Univ. of California, Berkeley, USA*; ³*General Dynamics Mission Systems, USA*. We show that noiseless linear amplifiers can serve as quantum relays to overcome entanglement distribution loss for entangled quantum sensors to outperform sensors supplied with the optimum local quantum resources.

FTh4D.2 • 16:45

Plug-and-Play squeezing experiment on chip at telecom wavelength, François Mondain^{2,1}, Tommaso Lunghi^{2,1}, Alessandro Zavatta^{3,4}, Élie Gouzien^{2,1}, Florent Doutre^{2,1}, Marc De Micheli^{2,1}, Sébastien Tanzilli^{2,1}, Virginia D'Auria^{2,1}; ¹*Institut de Physique de Nice (INPHYNI), France*; ²*Université Côte d'Azur (UCA), France*; ³*Istituto Nazionale Di Ottica (INO-CNR), Italy*; ⁴*Lens and Dept. of Physics Università Di Firenze, Italy*. We demonstrate a plug-and-play squeezing experiment entirely based on off-the-shelves guided-wave components and lithium-niobate integrated optics. We achieve -2 dB of squeezing thus validating our original approach as a resource for real-world continuous-variables implementations.

FTh4D.3 • 17:00 **Invited**

Lithium Niobate as a Platform for Continuous Variable Quantum Optics, Mirko Lobino¹, Francesco Lenzi¹, Jiri Janousek², Oliver Thearle², Matteo Villa¹, Ben Haylock¹, Sachin Kature¹, Liang Cui³, Hoang-Phuong Phan¹, Dzung Viet Dao¹, Hidehiro Yonezawa⁴, Ping Koy Lam², Eleanor H. Huntington²; ¹*Griffith Univ., Australia*; ²*Australian National Univ., Australia*; ³*Tianjin Univ., China*; ⁴*The Univ. of New South Wales, Australia*. I will report on the progress towards a fully integrated platform for continuous variable quantum optics in lithium niobate. Our device incorporates generation, manipulation, and detection of nonclassical state of light on a single chip.

FTh4A.2 • 17:00

Quantum Low Probability of Intercept, Jeffrey H. Shapiro¹, Don Boroson², P. Ben Dixon², Matthew Grein², Scott Hamilton²; ¹*MIT, USA*; ²*MIT Lincoln Lab, USA*. Quantum low probability of intercept transmits ciphertext in a way that prevents an eavesdropper possessing the decryption key from recovering the plaintext. It is capable of Gbps communication rates on optical fiber over metropolitan-area distances.

Executive Ballroom
210E

CLEO: Science &
Innovations

16:30–18:30

STh4E • Ultrafast Parametric Sources II

Presider: Jake Bromage; Univ. of Rochester, USA

STh4E.1 • 16:30

High-Power, Widely-Tunable Femtosecond Cylindrical Vector Beam Optical Parametric Oscillator, Jun Zhao¹, Jintao Fan¹, Na Xiao¹, Youjian Song¹, Ming-lie Hu¹; ¹Tianjin Univ., China. We propose a cylindrical vector beam optical parametric oscillator, which is capable of delivering on demand vector beam tunable across 1405–1601 nm directly, with a maximum power of 614 mW at 1505 nm.

STh4E.2 • 16:45

Intracavity enhancement in a doubly resonant OPO, Christian M. Dietrich¹, Ihar Babushkin^{1,2}, José Andrade^{1,3}, Laura Rust¹, Uwe Morgner^{1,3}; ¹Inst. of Quantum Optics and PhoenixD, Germany; ²Max Born Inst., Germany; ³Hannover Centre for optical Technologies, Germany. We show that strong cavity-induced enhancement of signal and idler power with respect to the pump can be achieved intracavity in a doubly resonant optical parametric oscillator pumped by an Yb:YAG thin-disk laser oscillator.

STh4E.3 • 17:00

5-Octave Laser Source Based on Cr:ZnS-GaSe Tandem, Sergey Vasilyev¹, Igor S. Moskalev¹, Viktor O. Smolski¹, Jeremy Peppers¹, Mike Mirov¹, Andrey V. Muraviev³, Konstantin L. Vodopyanov³, Sergey Mirov^{1,4}, Valentin P. Gapontsev²; ¹IPG Photonics - Southeast Technology Center, USA; ²IPG Photonics Corporation, USA; ³CREOL, Univ. of Central Florida, USA; ⁴Dept. of Physics, Univ. of Alabama at Birmingham, USA. We report laser architecture that enables generation of coherent femtosecond continua that span from visible to long-wave IR (0.5–18 μm), and features: high power (4W), high repetition rate (80 MHz), and intrinsic nonlinear interferometry.

Executive Ballroom
210F

Joint

16:30–18:30

JTh4F • Interaction of Strong THz Fields with Condensed Matter Systems

Presider: Dmitry Turchinovich, Universität Bielefeld, Germany

JTh4F.1 • 16:30

THz-Pump UED-Probe on a Topological Weyl Semimetal, Edbert Sie¹, Clara Nyby¹, Das Pemmaraju², Su Ji Park², Xiaozhe Shen², Jie Yang², Matthias C. Hoffmann², Benjamin Ofori-Okai², Renkai Li², Alexander Reid², Stephen Weathersby², Ehren Mannebach¹, Nathan Finney³, Daniel Rhodes³, Daniel Chenet³, Abhinandan Antony³, Luis Balicas⁴, James Hone³, Thomas Devereaux¹, Tony Heinz¹, Xijie Wang², Aaron Lindenberg^{1,2}; ¹Stanford Univ., USA; ²SLAC National Accelerator Lab, USA; ³Columbia Univ., USA; ⁴National High Magnetic Field Lab, USA. We used THz pulses to drive a topological transition in a Weyl semimetal WTe_2 via interlayer shear motion, as crystallographically measured using ultrafast electron diffraction (Sie et al, Nature (2018), in press).

JTh4F.2 • 17:00

Lightwave Driven Valleytronic Qubit Flip, Markus Borsch¹, Benjamin Girodias¹, Johannes T. Steiner², Stephan W. Koch², Christoph P. Schmid³, Stefan Schlauderer³, Fabian Langer³, Rupert Huber³, Mackillo Kira¹; ¹Univ. of Michigan, USA; ²Univ. of Marburg, Germany; ³Univ. of Regensburg, Germany. We demonstrate a flip of the valley pseudo-spin in a tungsten-diselenide monolayer on a sub-5fs timescale using strong terahertz fields. The resulting sideband emission reveals Coulombic many-body effects.

Executive Ballroom
210G

CLEO: Science & Innovations

16:30–18:30

STh4G • Opto-mechanics

Presider: Shau-Yu Lan; Nanyang Technological University, Singapore

STh4G.1 • 16:30

High-Bandwidth Force Sensing with Optical Cavities, Benjamin Reschovsky¹, Akobu Chijioko¹; ¹National Inst. of Standards and Technology, USA. We present a method for measuring dynamic forces by tracking induced frequency shifts of optical cavity resonances with initial tests of a robust laser stabilization scheme featuring large dynamic-range (5 GHz) and high-bandwidth (>1 MHz).

STh4G.2 • 16:45

Optical Loss Uniformity Characterization Using Scanning Cavity Ringdown Measurements, Gar-Wing Truong¹, Tobias Zederbauer², Dominic Bachmann², Paula Heu¹, David Follman¹, Mark E. White¹, Garrett D. Cole¹; ¹Crystalline Mirror Solutions, USA; ²Crystalline Mirror Solutions GmbH, Austria. A cavity ring-down system for probing the spatial variation of optical loss in a high-reflectivity optical interference coating is described. Excellent agreement is observed between the spatial map and differential interference contrast microscopy images of a substrate-transferred crystalline mirror.

STh4G.3 • 17:00

Quasi-2D Optomechanical Crystal Cavity for Quantum Optomechanics, Hengjiang Ren¹, Gregory S. MacCabe¹, Jie Luo¹, Hannes Pfeifer², Andrew Keller¹, Oskar Painter¹; ¹Inst. for Quantum Information and Matter and Thomas J. Watson, Sr., Lab of Applied Physics, California Inst. of Technology, USA; ²Max Planck Inst. for the Science of Light, Germany. We present the design and characterization of a quasi-two-dimensional optomechanical crystal cavity. At refrigerated temperature, an intrinsic mechanical quality factor of 1.2 billion is observed and an effective quantum cooperativity greater than unity is realized under steady-state optical pumping.

Executive Ballroom
210H

16:30–18:30

STh4H • Optical Driven Photonics

Presider: Carl Liebig; AFRL, USA

STh4H.1 • 16:30 Invited

Picosecond Optical Switching in Silicon Photonics Using Phase-Changing Vanadium Dioxide, Richard F. Haglund¹, Kent A. Hallman¹, Kevin J. Miller¹, Sharon M. Weiss¹; ¹Vanderbilt Univ., USA. Experiments in hybrid vanadium dioxide-silicon photonic structures, complemented by finite-difference, time-domain simulations, show how the ultrafast insulator-to-metal transition in VO_2 can be leveraged in nanoscale photonic structures to open new routes to low-loss, high-speed all-optical modulators.

STh4H.2 • 17:00

All-optical synapses based on silicon microring resonators actuated by the phase change material $\text{Ge}_2\text{Sb}_2\text{Te}_5$, Zahng Hanyu¹, Linjie Zhou¹, Xu Jian¹, Liangjun Lu¹, Jianping Chen¹, B. M. A. Rahman²; ¹Shanghai Jiao Tong Univ., China; ²City, Univ. of London, UK. We demonstrate silicon microring resonators integrated with $\text{Ge}_2\text{Sb}_2\text{Te}_5$ material that can be used as all-optical synapses for neuro-morphic computing. Synaptic plasticity is investigated with different resonator coupling conditions.

Meeting Room
211 A/B

CLEO: Applications
& Technology

16:30–18:30
ATH4I • A&T Topical Review on
Silicon Photonics II
Presider: To Be Announced

ATH4I.1 • 16:30 **Invited**
Applications of Integrated Kerr Microcombs to Radio Frequency and Microwave Photonics, Xingyuan Xu,¹ Jiayang Wu,¹ Mengxi Tan,¹ Thach Nguyen², Sai T. Chu,³ Brent E. Little,⁴ Roberto Morandotti,⁵ Arnan Mitchell,² and David J. Moss¹; ¹Centre for Micro-Photonics, Swinburne University of Technology, Hawthorn, VIC 3122 Australia, ²School of Engineering, RMIT University, Melbourne, VIC 3000, Australia, ³Department of Physics and Material Science, City University of Hong Kong, Hong Kong, China, ⁴Xi'an Institute of Optics and Precision Mechanics Precision Mechanics of CAS, Xi'an, China, ⁵INRS –Énergie, Matériaux et Télécommunications, Varennes, Québec, J3X 1S2, Canada. We review our recent work in the use of integrated micro-resonator based optical frequency comb sources as the basis for transversal filtering functions for microwave and radio frequency photonic filtering and advanced functions. We demonstrate a range of novel functions including a Hilbert Transform, first, second and third order RF differentiation, true time delays, an RF channelizer and other functions.

ATH4I.2 • 17:00
Silicon photonics optical frequency synthesizer - SPOFS, Neetesh Singh¹, Ming Xin¹, Nanxi Li¹, Diedrik Vermeulen¹, Alfonso Ruocco¹, Emir Salih Magden¹, Katia Shtyrkova¹, Patrick Callahan¹, Erich Ippen¹, Franz Kartner², Michael R. Watts¹; ¹MIT, USA; ²CFEL, DESY, Germany. We demonstrate a silicon photonics optical frequency synthesizer (SPOFS). The frequency instability obtained in the telecom band is 1×10^{-12} at 1s level, comparable to a bench-top commercial optical frequency synthesizer system.

Meeting Room
211 C/D

CLEO: Science & Innovations

16:30–18:30
STH4J • Applications of Lasers
& Microcombs
Presider: Yoshitomo Okawachi;
Columbia Univ., USA

STH4J.1 • 16:30
Noise Filtering in Synchronously-driven Kerr Frequency Combs, Victor Brasch¹, Ewelina Obrzud^{1,2}, Steve Lecomte¹, Tobias Herr¹; ¹CSEM, Switzerland; ²Dept. of Astronomy, Univ. of Geneva, Switzerland. We demonstrate filtering of an electro-optic modulation frequency comb in a high-Q Fabry-Perot microresonator via different regimes. Using dissipative Kerr solitons the coherence of the electro-optic modulation comb is improved, allowing for more advanced applications.

STH4J.2 • 16:45
Photonic Integrated K-Band Microwave Oscillator Based on Silicon Nitride Soliton Microcomb, Junqiu Liu¹, Arslan Raja¹, Erwan Lucas¹, Jijun He¹, Guan hao Huang¹, Romain Bouchand¹, Rui Ning Wang¹, Maxim Karpov¹, Nils Engelsen¹, Hairun Guo¹, Tobias J. Kippenberg¹; ¹Ecole Polytechnique Fédérale de Lausanne, Switzerland. Using photonic integrated silicon nitride microresonators of quality factor exceeding 15 million, we demonstrate 19-GHz-repetition-rate single soliton with 35 mW optical power, and characterize the phase noise of the repetition rate in the K-band microwave regime.

STH4J.3 • 17:00
Dual-comb imaging using soliton microcombs, Chengying Bao¹, Myoung-Gyun Suh¹, Kerry J. Vahala¹; ¹Caltech, USA. We demonstrate rapid imaging using dual-microcomb interferometry. One of the soliton microcombs is spatially dispersed into two dimensions to record spatial information and the image is read out by multi-heterodyne with the second microcomb.

Meeting Room
212 A/B

CLEO: Applications
& Technology

16:30–18:30
ATH4K • Sources & Techniques
for Industrial Monitoring
Presider: Brian Simonds, National
Institute of Standards and
Technology, USA

ATH4K.1 • 16:30
A Breakthrough Industrial THz Application: Robust In-situ THz-based Paint Layer Monitoring, Deran Maas¹, Andreas Frank¹, Jacobus L. van Mechelen¹; ¹Corporate Research, ABB Switzerland, Switzerland. We present a THz paint analyzer for measuring wet and dry paint multilayers insensitive to surface curvatures and vibrations. The layers can be measured simultaneously with an average error smaller than 1.1 μm .

ATH4K.2 • 16:45
Two-phase flow monitoring with an electrical-optical probe, Rosangela Winter¹, Eduardo Nunes do Santos¹, Rigoberto Eleazar Melgarejo Morales¹, Cicero Martelli¹, Marco José da Silva¹, Jean Carlos Cardozo da Silva¹; ¹Federal Univ. of Technology - Paraná, Brazil. An electrical-optical probe was developed to monitor monophasic and biphasic flow in industrial environments. The probe measures the parameters of electrical conductance and mechanical strain, thereby introducing data redundancy and facilitating auto calibration.

ATH4K.3 • 17:00
Continuous Optical Measurement of Dynamic Colloidal Droplets, Jose Guzman-Sepulveda¹, Ruitao Wu¹, Aristide Dogariu¹; ¹Univ. of Central Florida, USA. We demonstrate the use of spatiotemporal coherence-gated light scattering for measuring the dynamics of colloidal droplets during drying. The measurement is non-contact, non-invasive, and label-free, and permits monitoring the internal structure in optically-isolated, picolitter-sized volumes.

Meeting Room
212 C/D

CLEO: Science & Innovations

16:30–18:30
STH4L • Multi-Mode Fiber
Phenomena II
Presider: Julien Fatome;
Universite de Bourgogne, France

STH4L.1 • 16:30
Self-Cleaning on a Higher Order Mode in Ytterbium-Doped Multimode Fiber with Parabolic Profile, Alioune Niang¹, Vincent Couderc², Alessandro Tonello², Katarzyna Krupa¹, Mesay Addisu¹, Raphael Jauberteau^{1,2}, Marc Fabert², Daniele Modotto¹, Stefan Wabnitz²; ¹Univ. of Brescia, Italy; ²Univ. of Limoges, France; ³Sapienza Università di Roma, Italy. We experimentally demonstrate polarization-dependent Kerr spatial beam self-cleaning into the LP₁₁ mode of an Ytterbium-doped multimode optical fiber with parabolic gain and refractive index profiles.

STH4L.2 • 16:45
Multimode Fiber Beam Self-Cleaning in the Anomalous Dispersion Regime, Yann Leventoux¹, Alexandre Parriaux², Geoffroy Granger¹, M. Jossent³, L. Lavoute³, D. Gaponov², Marc Fabert², Alessandro Tonello¹, Katarzyna Krupa², Agnes Desfarges-Berthelémot¹, Vincent Kermene¹, Oleg Sidelnikov⁴, Guy Millot², Sebastien Fevrier¹, Stefan Wabnitz^{2,4}, Vincent Couderc¹; ¹Univ. of Limoges, France; ²Univ. of Bourgogne Franche-Comte, France; ³Novae Laser, France; ⁴Novosibirsk State Univ., Russia; ⁵Sapienza Università di Roma, Italy. We experimentally demonstrate Kerr beam self-cleaning of picosecond pulses in the anomalous dispersion regime of graded-index multimode optical fibers, with threshold power reduced by two orders of magnitude with respect to the normal dispersion regime.

STH4L.3 • 17:00
Spatiotemporal Mode-Locking as Multi-dimensional Optimization, Logan Wright¹, Pavel Sidorenko¹, Zachary Ziegler¹, Andrei Isichenko¹, Boris Malomed², Curtis R. Menyuk², Demetrios N. Christodoulides⁴, Frank W. Wise¹; ¹Cornell Univ., USA; ²Dept. of Physical Electronics, School of Electrical Engineering, Faculty of Engineering, and the Center for Light-Matter Interaction, Tel-Aviv Univ., Israel; ³Dept. of Computer Science and Electrical Engineering, Univ. of Maryland Baltimore County, USA; ⁴CREOL/College of Optics and Photonics, Univ. of Central Florida, USA. We outline a theoretical framework to understand the multitude of new mode-locked states possible in multi-transverse mode resonators. Full-3D measurements of mode-locked states comprising roughly 30 million modes agree with theoretical expectations.

CLEO: QELS-Fundamental
Science

16:30–18:30

FTh4M • Hyperbolic Photonics Media

President: Moussa N'Gom Rensselaer
Polytechnic Institute, USA

FTh4M.1 • 16:30

Intersubband Plasmons Induced Negative Refraction at mid-IR Frequency in Heterostructured Semiconductor Metamaterials, Mario Ferraro¹, Adrian Hierro², Miguel Montes Bajo², Julien Tamayo-Arriola², Maxime Hugues¹, Jose Ulloa², Massimo Giudici³, Jean Michel Chauveau¹, Patrice Genevet¹; ¹CRHEA-CNRS, France; ²ISOM-Universidad Politécnica de Madrid, Spain; ³InPhyni-CNRS, France. We theoretically and experimentally demonstrate negative refraction in a semiconductor system operating at mid-infrared wavelengths. Such effect is generic and realized by electrons quantum confinement in quantum wells, acting as an adjustable resonance.

FTh4M.2 • 16:45

Enhanced Radiative Emission of MQW by Resonant Modes of Hyperbolic Metamaterial Resonator, Kun-Ching Shen¹, Lung-Hsing Hsu¹, Din Ping Tsai¹, Hao-Chung Kuo², Chien-Chung Lin², Yuh-Jen Cheng¹; ¹Academia Sinica, Taiwan; ²National Chiao Tung Univ., Taiwan. We report the use of resonant modes of a hyperbolic metamaterial cube made of multiple metal/dielectric layer structure to enhance the radiative emission of multiple quantum wells. The mode analysis and photoluminescence will be discussed.

FTh4M.3 • 17:00

Field Enhancement and Ultrafast Plasmonics in Nonlocal Transitional Metamaterials, Brian Wells², Margoth Cordova Castro³, Anatoly Zayats³, Viktor A. Podolskiy¹; ¹Univ. of Massachusetts Lowell, USA; ²Univ. of Hartford, USA; ³King's College London, UK. We analyze spatial and temporal optical response of plasmonic nanocone arrays, relate the strong enhancement of local intensity to excitation of nonlocal plasmonic modes supported by the composites, and discuss potential applications in ultrafast nonlinear optics and plasmonics.

CLEO: Science & Innovations

16:30–18:30

STh4N • High-Speed Optical Interconnects

President: Jonathan Bradley McMaster Univ.,
Canada

STh4N.1 • 16:30

Demonstration of 80 Gbps NRZ-OOK Electro-Absorption Modulation of InP-on-Si DFB Laser Diodes, Mahmoud Shahin¹, Javad Rahimi Vaskasi¹, Joris van Kerrebrouck¹, Amin Abbasi², Kasper Van Gasse¹, Muhammad Muneeb¹, Laurens Breyné¹, Peter Ossieur¹, Xin Yin¹, Johan Bauwelinck¹, Gunther Roelkens¹, Geert Morthier¹; ¹Ghent Univ., Belgium; ²Antwerp space, Belgium. High-speed electro-absorption modulation of a heterogeneously integrated InP-on-Si DFB laser diode is used for the transmission of an 80 Gbps NRZ-OOK signal over 2 km of NZ-DSF fiber below the hard-decision forward-error-correction threshold.

STh4N.2 • 16:45

Waveguide Integrated CVD Graphene Photo-Thermo-Electric Detector With >40GHz Bandwidth, Simone Marconi^{2,1}, Vaidotas Miseikis^{1,3}, Marco Angelo Giambra¹, Alberto Montanaro¹, Vito Sorianello¹, Camilla Coletti^{3,4}, Marco Romagnoli¹; ¹Photonic Networks and Technologies Lab - CNIT, Italy; ²Tecip Inst. - Scuola Superiore Sant'Anna, Italy; ³Graphene Labs, Istituto Italiano di Tecnologia, Italy; ⁴Center for Nanotechnology Innovation @NEST, Istituto Italiano di Tecnologia, Italy. We demonstrated a CVD Graphene near-infrared photodetector based on the photo-thermo-electric effect integrated on a Si₃N₄ waveguide. The device is based on a split-gate induced pn junction working at zero bias and with bandwidth >40GHz.

STh4N.3 • 17:00 **Invited**

Low Power Analog Coherent Links for Next-Generation Datacenters, Clint Schow¹; ¹Univ. of California Santa Barbara, USA. Ever-increasing bandwidth demand in datacenter networks makes a move to coherent links seem inevitable. An "analog coherent" approach using optical phase locked loops can enable low-power consumption, expanded link budgets, low-latency, and future bandwidth scalability.

16:30–18:30

STh4O • Epitaxial Materials & Strain
Engineering

President: Oana Malis; Purdue Univ., USA

STh4O.1 • 16:30

Transparent Displays Using Strain-Engineered Nanopillar Light-Emitting Diodes, Kunook Chung¹, Jingyang Sui¹, Pei-cheng Ku¹; ¹Univ. of Michigan, USA. Using local strain engineering, we fabricated monolithically integrated and individually addressable RGB pixels and showed feasibility for a transparent microdisplay.

STh4O.2 • 16:45

Uniformly Tensile-strained Germanium Enabled by a Recessed Nitride Stressor for Efficient Integrated Photodetectors at Longer Wavelengths, Yiding Lin^{1,2}, Danhao Ma³, Rui-Tao Wen³, Kwang Hong Lee², Xin Guo¹, Jin Zhou¹, Hong Wang¹, Chuan Seng Tan^{1,2}, Jurgen Michel^{2,3}; ¹Nanyang Technological Univ., Singapore; ²Low Energy Electronic Systems (LEES), Singapore-MIT Alliance for Research and Technology, Singapore; ³Materials Science and Engineering, MIT, USA. Germanium photodetector, formed with a self-aligned dry etching method, together with a tensile silicon nitride sidewall stressor, exhibits a strain profile with improved uniformity and a ~2× enhancement on the quantum efficiency at the L-band.

STh4O.3 • 17:00

Ultrawide Strain Tuning of Luminescence from Mechanically Stressed InGaAs Nanomembranes, Xiaowei Wang¹, Xiaorui Cui², Abhishek Bhat², Donald Savage², John Reno³, Max Lagally², Roberto Paiella¹; ¹Boston Univ., USA; ²Univ. of Wisconsin - Madison, USA; ³Sandia National Labs, USA. We investigate the tunability of semiconductor light emission based on the use of nanomembranes under external mechanical stress. Active tuning of the InGaAs emission spectrum over an ultrawide wavelength range (> 250 nm) is demonstrated.

CLEO: QELS-Fundamental Science

FTh4A • New Protocols in Quantum Communications—Continued**FTh4A.3 • 17:15**

Genuine Counterfactual Communication with a Nanophotonic Processor, Irati Alonso Calafell¹, Teodor Strömberg¹, David R. Arvidsson-Shukur^{2,3}, Lee A. Rozema¹, Valeria Saggio¹, Chiara Greganti¹, Nicholas C. Harris³, Mihika Prabhu³, Jacques Carolan³, Michael Hochberg⁴, Tom Baehr-Jones⁴, Dirk R. Englund³, Crispin H. Barnes², Philip Walther¹; ¹Univ. of Vienna, Austria, Austria; ²Univ. of Cambridge, UK; ³MIT, USA; ⁴Elenion Technologies, USA. In counterfactual communication particles and information can travel in opposite directions. With our high-fidelity programmable nanophotonic processor we implement the first trace-free counterfactual protocol without post-selection with a counterfactual violation as low as 2.4%.

FTh4A.4 • 17:30

1 GBaud Heterodyne Continuous Variable Quantum Key Distribution over 26 km Fiber, Max Rückmann¹, Christian G. Schäffer¹; ¹Radio-Frequency Engineering & Photonics, Helmut-Schmidt-Univ., Germany. We experimentally demonstrate a 1 GBaud heterodyne continuous variable quantum key distribution system based on standard telecom components capable to achieve a key rate of 1.71 Mbit/s over 26 km of fiber.

FTh4B • Non-Diffractive & Vortex Beams—Continued**FTh4B.4 • 17:15**

Abruptly Focusing X-waves: Nondiffracting Waves with Localized Disruptions, Liang Jie Wong¹, Ido Kaminer²; ¹SIMTech, Singapore; ²Technion, Israel. We present a family of electromagnetic wavepackets with nondiffracting behavior for most of their propagation, but are capable of extremely strong focusing behavior at specified locations, enhancing their peak intensity by over 200 times.

FTh4B.5 • 17:30

Optimization of Higher-Order Transverse Modes of Cylindrical Vector Beams for Enhanced Spatial Resolution in Image Subtraction, Mio Yoshida¹, Yuichi Kozawa^{1,2}, Shunichi Sato¹; ¹Tohoku Univ., Japan; ²JST PRESTO, Japan. We demonstrate the enhancement of spatial resolution of subtraction imaging in confocal laser scanning microscopy utilizing radially and azimuthally polarized, higher-order mode beams. The spatial resolution close to 100 nm is experimentally achieved.

FTh4C • Advanced Nanophotonic Platforms for Spectroscopy & Sensing—Continued**FTh4C.3 • 17:15**

Near-Field Tomography and Spectroscopy of Surface States on a Three-Dimensional Topological Insulator, Fabian Sandner¹, Fabian Mooshammer¹, Markus A. Huber¹, Martin Zizlsperger¹, Helena Weigand¹, Markus Plankl¹, Christian Weyrich², Martin Lanius², Jörn Kampmeier², Gregor Mussler², Detlev Grützmacher², Jessica L. Boland¹, Tyler L. Cocker³, Rupert Huber¹; ¹Dept. of Physics, Univ. of Regensburg, Germany; ²Peter Grünberg Institut 9, Forschungszentrum Jülich, Germany; ³Dept. of Physics and Astronomy, Michigan State Univ., USA. Beside massless Dirac fermions, topological insulator surfaces can host a massive two-dimensional electron gas. Using near-field spectroscopy, we identify both of these surface states by retrieving the nanoscale dielectric function without any model assumptions.

FTh4C.4 • 17:30

Graphene Modified Plasmonic Guided Mode For CO₂ Detection, Thomas M. Kananen¹, Anishkumar Soman¹, Arnav Malkani¹, Zi Wang¹, Bingjun Xu¹, Tingyi Gu¹; ¹Univ. of Delaware, USA. We observed broadening of the plasmonic guided modes in gold nanorod arrays by a single layer graphene, which can manifest CO₂ detection. The plasmonic modes enhance absorption by over 35% from 729 to 621 cm⁻¹.

FTh4D • Beyond Photon Pairs—Continued**FTh4D.4 • 17:30**

Non-Gaussian Continuous-Variable Graph States, Mattia Walschaers¹, Valentina Parigi¹, Nicolas Treps¹; ¹Laboratoire Kastler Brossel, France. Mode-tunable photon subtraction is a viable method to introduce non-Gaussian features in continuous-variable graph states. Non-Gaussian properties are shown to spread up to next-to-nearest neighbours of the graph's vertex in which the photon was subtracted.

Executive Ballroom
210E

CLEO: Science &
Innovations

STh4E • Ultrafast Parametric
Sources II—Continued

STh4E.4 • 17:30

Broadband, Near Single-Cycle, Waveform-Stable Mid-Infrared Pulses Driven by a 2- μm Femtosecond Source, Thomas P. Butler¹, Daniel Gerz^{1,2}, Christina Hofer^{1,2}, Jia Xu¹, Christian Gaida³, Tobias Heuermann^{3,4}, Martin Gebhardt^{3,4}, Lenard Vamos⁵, Wolfgang Schweinberger^{2,5}, Julia Gessner^{1,2}, Thomas Seifke^{3,6}, Martin Heusinger³, Uwe Zeitner^{3,7}, Alexander Apolonski^{1,2}, Jens Limpert^{3,4}, Ferenc Krausz^{1,2}, Joachim Pupeza^{1,2}, ¹Max Planck Institute of Quantum Optics, Germany; ²Dept. of Physics, Ludwig Maximilian Univ. Munich, Germany; ³Inst. of Applied Physics, Abbe Center of Photonics, Friedrich Schiller Univ. Jena, Germany; ⁴Helmholtz Inst. Jena, Germany; ⁵Dept. of Physics and Astronomy, King Saud Univ., Saudi Arabia; ⁶Physikalisch-Technische Bundesanstalt, Germany; ⁷Fraunhofer Inst. for Applied Optics and Precision Engineering, Germany. We present a novel source of ultrashort, watt-scale, 50-MHz repetition-rate, broadband (6–18 μm , or 555–1666 cm^{-1}) pulses. Generation and electro-optic-sampling of the waveform-stable transients is driven with a femtosecond thulium-based fiber-amplifier.

Executive Ballroom
210F

Joint

JTh4F • Interaction of Strong
THz Fields with Condensed
Matter Systems—Continued

JTh4F.3 • 17:30

Higgs Spectroscopy and Control of Non-Equilibrium Phases in Superconductors by Terahertz Light-Induced Supercurrent Injection, Martin Mootz¹, Ilias E. Perakis¹, Xu Yang², Chirag Vaswani², Liang Luo², Jigang Wang²; ¹Physics, Univ. of Alabama at Birmingham, USA; ²Physics and Astronomy, Iowa State Univ. and Ames Lab, USA. The non-equilibrium dynamics of superconductors after ultrafast terahertz excitation is analyzed. Excitation of selective non-equilibrium phases and detection of Higgs mode in the nonlinear response are demonstrated by inducing supercurrents via terahertz pulse shaping.

Executive Ballroom
210G

CLEO: Science & Innovations

STh4G • Opto-mechanics—
Continued

STh4G.4 • 17:15

Achieving sub-femtometer displacement sensitivity in integrated ultrahigh-Q crystalline microcavities via Pound-Drever-Hall, Yoon-Soo Jang¹, JinKang Lim¹, Seung-Woo Kim², Wei Liang³, Andrey B. Matsko³, Lute Maleki³, Chee Wei Wong¹; ¹UCLA, USA; ²KAIST, South Korea (the Republic of); ³OEwaves, USA. We present real-time and wide dynamic range measurement of sub-femtometer scale displacement of microcavity. We achieve power spectral density of displacement on the MgF_2 whispering gallery mode(WGM) microcavity with sub-femtometer displacement sensitivity.

STh4G.5 • 17:30

All-Fiber Phase-Shifted Demodulation System for Fabry-Perot Interferometric Sensors, Yun Liu¹, Bing Qi¹, Drew Winder¹; ¹Oak Ridge National Lab, USA. A quadrature phase-shifted optical demodulation scheme has been developed for low-coherence fiber-optic Fabry-Perot interferometric sensors. The demodulator shows a great stability of phase shift. Applications to vibration/strain measurements are demonstrated.

Executive Ballroom
210H

STh4H • Optical Driven
Photonics—Continued

STh4H.3 • 17:15

Light and Microwaves in Laser Frequency Combs: An Interplay of Spatio-Temporal Phenomena, Marco Piccardo¹, Dmitry Kazakov¹, Benedikt Schwarz^{2,1}, Paul Chevalier¹, Arman Amirzhan¹, Yongrui Wang³, Feng Xie⁴, Kevin Lascola⁴, Steffen Becker⁵, Lars Hildebrandt⁵, Robert Weh⁵, Alexey Belyanin³, Federico Capasso¹; ¹Harvard Univ., USA; ²TU Wien, Austria; ³Texas A&M, USA; ⁴Thorlabs Quantum Electronics, USA; ⁵Nanoplus Nano-systems and Technologies GmbH, Germany. The study of the interaction between light and microwaves in laser frequency combs reveals novel spatio-temporal dynamic phenomena and allows for new hybrid optical-microwave devices.

STh4H.4 • 17:30

Saturation Effects in Laser Cooling of Crystals, Long Cheng¹, Laura B. Andre¹, Alexander J. Salkeld¹, Stephen C. Rand¹; ¹Univ. of Michigan, USA. Record laser cooling of Yb:YAG and Yb:KYW under ambient conditions is reported and compared quantitatively with analysis indicating that cooling power can theoretically be improved substantially by saturating the impurity absorption.

Meeting Room
211 A/B

CLEO: Applications
& Technology

ATH4I • A&T Topical Review on
Silicon Photonics II—Continued

ATH4I.3 • 17:15 **Invited**
Coherent Silicon Photonic Devices for
Communication and Sensing, Chris Doerr¹;
¹Acacia Communications Inc, USA. Abstract
not available.

Meeting Room
211 C/D

CLEO: Science &
Innovations

STh4J • Applications of Lasers
& Microcombs—Continued

STh4J.4 • 17:30
Dual-polarization frequency combs in a
single Kerr microcavity via single-pumped
mode-crossing, Qingsong Bai¹, Jinghui
Yang¹, Hao Liu¹, Mingbin Yu^{2,3}, Dim Lee
Kwong², Dong Hou⁴, Chee Wei Wong¹;
¹Univ. of California Los Angeles, USA; ²Inst. of
Microelectronics, Singapore; ³Shanghai Inst.
of Microsystem and Information Technology,
China; ⁴School of Automation Engineering,
Univ. of Electronic Science and Technology
of China, China. We report dual-polarization
Kerr frequency combs generated in a single
microcavity by a single pump through mode-
crossing effect engineering. Both of the
combs can be driven to phase-locked state,
with slightly different mode spacing.

Meeting Room
212 A/B

CLEO: Applications
& Technology

ATH4K • Sources & Techniques
for Industrial Monitoring—
Continued

ATH4K.4 • 17:15
Diode Laser-based Film Thickness Measure-
ment of DEF in a generic exhaust gas test
bench for the investigation of SCR-relevant
processes, Anna Schmidt¹, Benjamin Küh-
nreich¹, Matthias Jacob¹, Steven Wagner¹;
¹Technische Universität Darmstadt, Germany.
An absorption based laser sensor for film
thickness measurement of DEF in an exhaust
gas test bench is presented. A wavelength
pre-selection ensures that film-thicknesses
could be measured without cross sensitivity
to temperature or concentration.

ATH4K.5 • 17:30 **Invited**
Diode Laser Spectroscopy for Optimization
of Boilers, Furnaces and Flares, Andrew
D. Sappey^{1,2}; ¹Zolo Technologies, Inc.,
USA; ²John Zink Company, USA. We have
employed tunable diode laser spectroscopy
for nearly 15 years enabling optimization
of large combustion-driven assets ranging
from coal-fired boilers to electric arc furnaces
for steel recycling. Here, we review some
important results.

Meeting Room
212 C/D

CLEO: Science &
Innovations

STh4L • Multi-Mode Fiber
Phenomena II—Continued

STh4L.4 • 17:15
Cascaded Raman lasing in a multimode
diode-pumped graded-index fiber, Ser-
gey A. Babin^{1,2}, Ekaterina A. Evmenova¹,
Alexey G. Kuznetsov¹, Ilya N. Nemov¹, Alexey
Wolf^{1,2}, Alexandr V. Dostovalov^{1,2}, Sergey
I. Kablukov¹, Evgeniy V. Podivilov^{1,2}; ¹Inst.
of Automation and Electrometry, Russia;
²Novosibirsk State Univ., Russia. Multimode
915-nm diode pumped 1.1-km graded-index
fiber is able to generate high-quality ($M^2 \sim 1.6$)
2nd-order Stokes beam at 978-996 nm with
high power/slope efficiency ($\sim 30W/70%$)
provided by combination of FBG cavity and
random distributed feedback.

STh4L.5 • 17:30 **Invited**
Controlling Nonlinearity in Multimode Fi-
bers and Fast Real-Time Wave-Front Shap-
ing, Omer Tzang¹, Eyal Niv¹, Dan Feldkhun¹,
Antonio Caravaca¹, Sakshi Singh¹, Simon
Labouesse¹, Kelvin Wagner¹, Rafael Piestun¹;
¹Univ. of Colorado at Boulder, USA. We show
adaptive computational control of complex
and non-linear interactions in multimode
fibers. We also present novel wave-front
shaping methodologies that are orders of
magnitude faster than other technologies,
and show real-time continues operation.

CLEO: QELS-Fundamental
Science

FTh4M • Hyperbolic Photonics Media—
Continued

FTh4M.4 • 17:15

Nano-scale Hyperbolic Metamaterial cavity system for enhanced Light-Matter interaction at Visible Frequencies, Sita Rama Krishna C. Indukuri¹, Jonathan Bar-David¹, Noa Mazurski¹, Uriel Levy¹; ¹Hebrew Univ. of Jerusalem., Israel. We design and demonstrate experimentally nano-scale hyperbolic metamaterial cavities at the visible frequency to enhance the free space radiation power of quantum dots for applications in solid state light emitting devices.

FTh4M.5 • 17:30

Quantum to Classical Transitions in Multilayer Plasmonic Metamaterials, Evan L. Simmons¹, Kun Li², Andrew Briggs², Seth Bank², Daniel Wasserman², Evgenii Narimanov³, Viktor Podolskiy¹; ¹Physics, Univ. of Massachusetts Lowell, USA; ²Electrical and Computer Engineering, Univ. of Texas at Austin, USA; ³Electrical and Computer Engineering, Purdue Univ., USA. We demonstrate that classical-to-quantum transition of free electron plasma can be used to as a doping-independent parameter controlling optical topology of metamaterials and present a comprehensive description of this phenomenon.

CLEO: Science & Innovations

STh4N • High-Speed Optical
Interconnects—Continued

STh4N.4 • 17:30

All-Plasmonic 100 Gbd Optical Communication Link, Yannick Salamin¹, Ping Ma¹, Benedikt Baeuerle¹, Wolfgang Heni¹, Claudia Hoessbacher¹, Arne Josten¹, Yuriy Fedoryshyn¹, Alexandros Emboras¹, Delwin L. Elder², Larry R. Dalton², Juerg Leuthold¹; ¹ETH Zurich, Switzerland; ²Dept. of Chemistry, Univ. of Washington, USA. We realize an all-plasmonic optical communication link operating at 100 Gbit/s NRZ, in which the optical transmitter and receiver rely on a plasmonic-organic modulator and a plasmonic-graphene photodetector, respectively.

STh4O • Epitaxial Materials & Strain
Engineering—Continued

STh4O.4 • 17:15

RF Read-Out of Minority Carrier Lifetimes in Micro-Scale Infrared Materials, Sukrith Dev¹, Yinan Wang¹, Kyoungwan Kim¹, Marziyeh Zamiri², Clark Kadlec³, Michael Goldflam³, Samuel Hawkins³, Eric Shaner³, Jin Kim³, Sanjay Krishna⁴, Monica Allen⁵, Jeffery Allen⁵, Emanuel Tutuc¹, Daniel Wasserman¹; ¹Univ. of Texas at Austin, USA; ²Univ. of Wisconsin, USA; ³Sandia National Labs, USA; ⁴Ohio State Univ., USA; ⁵Eglin Air Force Base, USA. We present micro-scale time-resolved microwave resonator response (μ -TRMRR), a sensitive technique capable of measuring carrier lifetimes in micron-scale materials, something not typically achievable using common techniques like time-resolved photoluminescence or time-resolved microwave reflectance.

STh4O.5 • 17:30 **Invited**

Germanium-Tin Semiconductors for Silicon-Compatible Mid-Infrared Photonics, Simone Assali¹, Anis Attiaoui¹, Étienne Bouthillier¹, Patrick Del Vecchio¹, Aashish Kumar¹, Samik Mukherjee¹, Jérôme Nicolas¹, Oussama Moutanabir¹; ¹Engineering Physics, Ecole Polytechnique de Montreal, Canada. GeSn alloys have recently been the subject of extensive investigations as a new platform to engineer the band structure in group IV semiconductors thus providing a rich playground to implement silicon-compatible photonics and optoelectronics. Herein, we discuss the growth of these metastable semiconductors and their use in of silicon-compatible devices. We will also discuss the effects of strain and Sn content on the optical, electronic, and structural properties of GeSn semiconductors.

CLEO: QELS-Fundamental Science

FTh4A • New Protocols in
Quantum Communications—
Continued

FTh4A.5 • 17:45

A Continuous-Variable Quantum Repeater based on Quantum Scissors, Kaushik P. Seshadreesan¹, Hari Krovi², Saikat Guha¹; ¹College of Optical Sciences, Univ. of Arizona, USA; ²Quantum Engineering and Computing Physical Sciences and Systems, Raytheon BBN Technologies, USA. Using the quantum scissors operation for entanglement distillation and a single-rail Bell state projection for non-Gaussian entanglement swapping, we show a multiplexed quantum repeater scheme for continuous-variable entanglement distribution over a pure loss communication channel.

FTh4A.6 • 18:00

Experimental demonstration of all-photon quantum repeater, Zheng-Da Li¹, Rui Zhang¹, Xu-Fei Yin¹, Li-Zheng Liu¹, Yi Hu¹, Yu-Qiang Fang¹, Yue-Yang Fei¹, Xiao Jiang¹, Jun Zhang¹, Feihu Xu¹, Yu-ao Chen¹, Jian-Wei Pan¹; ¹Univ. of Science and Technology of China, China. We for the first time demonstrate the all-photon quantum repeater by manipulating a 12-photon interferometry. Our experiment opens a new window of opportunity for a memoryless quantum repeater with efficient photonic graph states.

FTh4B • Non-Diffractive &
Vortex Beams—Continued

FTh4B.6 • 17:45

Ultrafast tunable mid-infrared higher-order optical vortex source, Varun Sharma¹, S Chaitanya Kumar², Goutam Samanta¹, M Ebrahim-Zadeh^{3,4}; ¹PRL Ahmedabad, India; ²Radiantis, Poligon Cami Ral, 08850 Gavà,, Spain; ³ICFO-Institut de Ciències Fotòniques, The Barcelona Inst. of Science and Technology, Spain; ⁴Institucio Catalana de Recerca i Estudis Avancats (ICREA), Spain. We report on the generation of tunable ultrafast, mid-infrared, multi-order, optical vortices from a picosecond singly-resonant optical parametric oscillator in 2493-4035 nm wavelength range with an average output power of up to 800 mW.

FTh4B.7 • 18:00

Optical Clearing and Shielding with Fan-shaped Vortex Beams, Haiping Wang¹, Jina Ma¹, Xiuyan Zheng¹, Liqin Tang^{1,2}, Daohong Song^{1,2}, Yi Hu^{1,2}, Yigang Li^{1,2}, Zhigang Chen^{1,2}; ¹Nankai Univ., China; ²Collaborative Innovation Center of Extreme Optics, Shanxi Univ., China. We propose and demonstrate a new kind of spiral vortex beams by phase engineering. Such fan-shaped optical beams can be effectively controlled and utilized for optical clearing and shielding of target particles in turbulent environments.

FTh4B.8 • 18:15

Evolution and Conservation of Orbital Angular Momentum in Three-Dimensional Structured Light, Ahmed Dorrah¹, Carmelo Rosales-Guzmán², Andrew Forbes², Mo Mojahedi¹; ¹Dept. of Electrical and Computer Engineering, Univ. of Toronto, Canada; ²School of Physics, Univ. of the Witwatersrand, South Africa. We engineer quasi 3D structured light fields in which the orbital angular momentum changes locally in both sign and magnitude along the beam's axis and explain how such transitions occur without violating conservation of angular momentum.

FTh4C • Advanced
Nanophotonic Platforms for
Spectroscopy & Sensing—
Continued

FTh4C.5 • 17:45

2D Perovskite-Based Metasurfaces for Enhanced Plasmonic Sensing, Shuwen Zeng^{1,2}, Guozhen Liang², Alexandre Gheno¹, Sylvain Vedraïne¹, Nanfang Yu²; ¹French National Centre for Scientific Research (CNRS), France; ²Columbia Univ., USA. We demonstrated a surface plasmon resonance sensor based on 2D Perovskite and Goos-Hänchen shift exhibiting sensitivity up to 900,000 um/RIU for refractive index sensing of target analytes.

FTh4C.6 • 18:00

Enhanced Circular Dichroism and Chiral Sensing with Bound States in the Continuum, Kirill Koshelev^{1,2}, Yasaman Jahani³, Andreas Tittl³, Hatice Altug³, Yuri S. Kivshar^{1,2}; ¹Australian National Univ., Australia; ²Dept. of Nanophotonics and Metamaterials, ITMO Univ., Russia; ³Bioengineering Dept., Ecole Polytechnique Federale de Lausanne, Switzerland. We reveal that optical chirality at the nanoscale can be boosted dramatically by bound states in the continuum (BIC). We predict the enhancement of chiroptical signals from nanostructures supporting quasi-BICs in mid-IR with a record-high efficiency.

FTh4C.7 • 18:15

Electrical Detection of Surface Plasmons for Sensing Applications, Tejaswini Ronur Praful¹, David W. Keene¹, Natalia Noginova¹; ¹Norfolk State Univ., USA. Photoinduced voltages in metal films with rectangular profile modulation demonstrate sharp polarity switching at plasmon resonance conditions. We explore this effect for applications for compact plasmonic sensors with electrical detection.

FTh4D • Beyond Photon Pairs—
Continued

FTh4D.5 • 17:45

Experimental preparation of Gottesman-Kitaev-Preskill states by photon-number-resolving detection, Miller Eaton¹, Rajveer Nehra¹, Olivier Pfister¹; ¹Univ. of Virginia, USA. We propose to expand "Fock state filtering" to photon-number-resolving detection and apply it to the generation of displaced single-photon states, cat states, and Gottesman-Kitaev-Preskill ancillas.

FTh4D.6 • 18:00

Beyond Photon Pairs: Nanophotonic Photon Number Difference Squeezing, Reihaneh Shahrokhsahi¹, Blair Morrison¹, Matthew J. Collins¹, Luke G. Helt¹, Nicolas Quesada¹, Dylan H. Mahler¹, Kang Tan¹, Varun D. Vaidya¹, Alain Repingon¹, Jonathan Lavoie¹, Raphael C. Pooser², Adriana Lita³, Sae Woo Nam³, Thomas Gerrits³, Zachary Vernon¹; ¹Xanadu Quantum Technologies Inc, Canada; ²Oak Ridge National Labs, USA; ³National Inst. of Standards and Technology, USA. We demonstrate over 1 dB of photon number difference correlations from two-mode squeezed states having mean photon number above 5, generated with a silicon nitride ring resonator and measured using photon number-resolving transition edge sensors.

18:30–20:00 Emerging Trends in Nonlinear Optics - A Review of CLEO: 2019, Room 230A

18:30–20:00 Dinner Break (on your own)

20:00–22:00 Postdeadline Paper Sessions, Location TBD

Executive Ballroom
210E

CLEO: Science & Innovations

STh4E • Ultrafast Parametric Sources II—Continued

STh4E.5 • 17:45

Near-single-cycle long-wave infrared pulses for coherent linear and nonlinear optics, Abijith Kowligy^{1,3}, Henry Timmers¹, Alexander Lind^{1,3}, Sylvain Karlen^{5,1}, Flavio C. Cruz^{1,3}, Peter G. Schunemann², Jens Biegert⁴, Scott A. Diddams^{1,3}; ¹NIST, USA; ²BAE Systems, USA; ³Physics, Univ. of Colorado, USA; ⁴ICFO, Spain; ⁵CSEM, Switzerland. We generate and detect phase-stable, near-single-cycle long-wave-infrared pulses using intrapulse difference-frequency generation and dual frequency comb electro-optic sampling, respectively. Applications such as high-resolution, super-octave spectroscopy and parametric amplification are described.

STh4E.6 • 18:00

Octave-Spanning Mid-Infrared Intrapulse Difference Frequency Generation With A Few-Cycle Cr:ZnS Laser, Sergey Vasilyev¹, Igor S. Moskalev¹, Viktor O. Smolski¹, Jeremy Peppers¹, Mike Mirov¹, Andrey V. Muraviev², Kevin T. Zawilski³, Peter G. Schunemann³, Sergey Mirov^{1,4}, Konstantin L. Vodopyanov², Valentin P. Gapontsev⁵; ¹IPG Photonics - Southeast Technology Center, USA; ²CREOL, Univ. of Central Florida, USA; ³BAE Systems, USA; ⁴Dept. of Physics, Univ. of Alabama at Birmingham, USA; ⁵IPG Photonics Corporation, USA. We generate longwave mid-IR transients between 4 and 18 μm via optical rectification of 5.9-W 78-MHz 20-fs laser pulses centered at 2.5 μm . We achieve 0.15 W (0.014 W) average power in ZGP (GaSe) crystals.

Executive Ballroom
210F

Joint

JTh4F • Interaction of Strong THZ Fields with Condensed Matter Systems—Continued

JTh4F.4 • 17:45

Terahertz Kerr Effect in β -Alumina Ion Conductors, Andrey D. Poletayev¹, Matthias C. Hoffmann², Samuel Teitelbaum², Mariano Trigo², William Chueh¹, Aaron Lindenberg^{1,2}; ¹Materials Science & Engineering, Stanford Univ., USA; ²Stanford Linear Accelerator Lab, USA. We present THz Kerr effect spectra of Na, K, and Ag β -alumina solid-state ion conductors as model systems for grid-scale battery applications. We show both a field-following response consistent with electronic polarization, and a slower relaxation consistent with translation of mobile ions.

JTh4F.5 • 18:00

Measurement of Quadratic Terahertz Optical Nonlinearities Using Second-Harmonic Lock-in Detection, Shuai Lin¹, Shukai Yu¹, Diyar Talbayev¹; ¹Tulane Univ., USA. We demonstrate a method to measure quadratic terahertz optical nonlinearities in terahertz time-domain spectroscopy by measuring the quadratic terahertz Kerr effect in a (110) GaP crystal in the presence of strong linear electro-optic Pockels effect.

FTh4F.6 • 18:15
Withdrawn

Executive Ballroom
210G

CLEO: Science & Innovations

STh4G • Opto-mechanics—Continued

STh4G.6 • 17:45

Quantum Enhancement of Advanced LIGO Detector Using Squeezed Vacuum States, Maggie Tse¹; ¹LIGO MIT, USA. The Advanced LIGO detector measures the distortion of spacetime from gravitational waves using Michelson interferometers. By injecting a squeezed vacuum state, we have demonstrated shot noise reduction, which enhanced the sensitivity of the LIGO detector.

STh4G.7 • 18:00

Thermo-mechanically Squeezed Graphene Amplifier, Rajan Singh¹, Ryan J. Nicholl², Kirill Bolotin³, Saikat Ghosh¹; ¹Indian Inst. of Technology, Kanpur, India; ²Vanderbilt Univ., USA; ³Freie Universität Berlin, Germany. We demonstrate coupling of mechanical mode of graphene resonator to that of Silicon Nitride resonator, resulting in 38 dB gain. Furthermore, with thermomechanical squeezing of graphene thermal noise, we demonstrate an overall measurement sensitivity of 3.8 fmHz^{-1/2}.

Executive Ballroom
210H

STh4H • Optical Driven Photonics—Continued

STh4H.5 • 17:45

Bright and Ultrafast Photoelectron Emission from Aligned Single-Wall Carbon Nanotubes through Multiphoton Exciton Resonance, Derek A. Bas^{2,1}, Mark E. Green³, Hsin-Yu Yao⁴, Jamie J. Gengler^{2,5}, Robert J. Headrick⁶, Tyson C. Back², Augustine M. Urbas², Matteo Pasquali⁶, Junichiro Kono⁷, Tsing-Hua Her²; ¹Azimuth Corporation, USA; ²Materials and Manufacturing Directorate, Air Force Research Lab, USA; ³Dept. of Physics and Optical Science, UNC Charlotte, USA; ⁴Yonghe Dist., Taiwan; ⁵UES, Inc., USA; ⁶Dept. of Chemical & Biomolecular Engineering, Dept. of Chemistry, Dept. of Materials Science and NanoEngineering, Rice Univ., USA; ⁷Dept. of Materials Science and NanoEngineering, Dept. of Electrical and Computer Engineering, Dept. of Physics and Astronomy, Rice Univ., USA. We report ultrafast photoelectron emission from aligned single-wall carbon nanotubes utilizing strong exciton resonances inherent in this prototypical one-dimensional material. These results establish SWCNT films as novel and promising ultrafast photocathode material.

STh4H.6 • 18:00

Optical Tuning of Graphene Electronics and Plasmonics on Iron Doped Lithium Niobate, Jon Gorecki², Lewis Piper¹, Vasilis Apostolopoulos¹, Sakellaris Mailis², Nikitas Papisimakis²; ¹School of Physics and Astronomy, Univ. of Southampton, UK; ²Optoelectronics Research Centre, Univ. of Southampton, UK. We demonstrate nonvolatile, but reversible, optical control of charge carriers in graphene by virtue of a photorefractive iron doped lithium niobate substrate which leads to tunable electronic and plasmonic devices.

STh4H.7 • 18:15

Strong coupling of Excitons in WS₂ with Fano Resonances in Photonic Crystals, Rezlind Bushati^{1,2}, Sriram Guddala¹, Vinod Menon^{2,1}; ¹Physics, CUNY Graduate Center, USA; ²Physics, CUNY City College, USA. We report strong coupling between excitons in monolayer WS₂ and Fano resonances in a dielectric photonic crystal. This gives rise to a Rabi splitting of ~25 meV at room temperature in an open cavity geometry.

18:30–20:00 Emerging Trends in Nonlinear Optics - A Review of CLEO: 2019, Room 230A

18:30–20:00 Dinner Break (on your own)

20:00–22:00 Postdeadline Paper Sessions, Location TBD

Meeting Room
211 A/B

CLEO: Applications
& Technology

ATH4I • A&T Topical Review on
Silicon Photonics II—Continued

ATH4I.4 • 17:45

Beam-Steering Nanophotonic Phased-Array Neural Probes, Wesley D. Sacher¹, Xinyu Liu¹, Fu-Der Chen², Homeira Moradi-Chameh³, Ilan Felts Almog², Thomas Lordello², Michael Chang³, Azadeh Naderian³, Trevor Fowler¹, Eran Segev¹, Tianyuan Xue², Sara Mahallati³, Taufik Valiante^{3,4}, Laurent Moreaux¹, Joyce K. Poon^{2,5}, Michael L. Roukes¹; ¹Division of Physics, Mathematics, and Astronomy, California Inst. of Technology, USA; ²Dept. of Electrical and Computer Engineering, Univ. of Toronto, Canada; ³Division of Fundamental Neurobiology, Krembil Research Inst., Canada; ⁴Division of Neurosurgery, Univ. of Toronto, Canada; ⁵Max Planck Inst. for Microstructure Physics, Germany. We demonstrate the first implantable nanophotonic neural probes with integrated silicon nitride phased arrays. Coherent beam-steering is achieved in brain tissue by wavelength tuning. Beam profiles, optogenetic stimulation, and functional imaging are validated *in vitro*.

ATH4I.5 • 18:00 **Invited**

Optical Phased Array Beam-steering with a Large Steering Angle and a Tailored Envelope. Linjie Zhou¹, Weihai Xu¹, Liangjun Lu¹, and Jianping Chen¹; ¹Shanghai Jiao Tong University, China. We demonstrate an SOI-based OPA with a curved waveguide array for inter-channel coupling suppression. The far-field diffraction pattern exhibits a plateau envelope, caused by the Fabry-Perot effect from a silica cavity at the emitting end.

Meeting Room
211 C/D

CLEO: Science & Innovations

STh4J • Applications of Lasers
& Microcombs—Continued

STh4J.5 • 17:45

Electrically tunable Kerr combs in graphene-nitride microresonators on-chip, Baicheng Yao^{1,2}, Abhinav Kumar Vinod², Shu-Wei Huang², Yuan Liu², Jaime G. Flores², Chanyeol Choi², Yu Huang², Xiang-feng Duan², Chee Wei Wong²; ¹Univ of Electronic Science & Tech China, China; ²Univ of California, Los Angeles, USA. Dynamic tuning of soliton combs is achieved in graphene actuated SiN microresonators. Driven by single-volt-voltage gating, optical dispersion of the microcavity is controlled, enabling broadband tuning of comb spectrum and diversity of soliton crystal generations.

STh4J.6 • 18:00

Ultrahigh-Q Crystalline Microresonator Fabricated with Computer-controlled Machining without Polishing, Shun Fujii¹, Mika Fuchida¹, Hikaru Amano¹, Ryo Suzuki¹, Yasuhiro Kakinuma¹, Takasumi Tanabe¹; ¹Keio Univ., Japan. We fabricated crystalline whispering gallery mode microresonators with an ultrahigh-Q close to 10⁸ without polishing by employing a computer-controlled ultraprecision machining process.

STh4J.7 • 18:15

High Stability Self-Injection Locked Laser, Anatoliy Savchenkov¹, Skip Williams¹, Andrey B. Matsko¹; ¹OEwaves Inc, USA. We demonstrate a self-injection locked 1550nm laser characterized with Allan deviation of 10⁻¹² at 1s. The stability is achieved using a composite crystalline monolithic optical resonator. The thermal stabilization on the order of 10uK at 1s is achieved using a standard thermo-electric element.

Meeting Room
212 A/B

CLEO: Applications
& Technology

ATH4K • Sources & Techniques
for Industrial Monitoring—
Continued

ATH4K.6 • 18:00

Acousto-Optically Modulated Quantum Cascade Laser (AOM QCL) for Combustion and Detonation Thermometry, Zachary Loparo^{1,2}, Kyle Thurmond¹, Erik Ninnemann¹, Andrew Laich¹, Ahmad Azim^{2,3}, Arkadiy Lyakh^{2,3}, Subith S. Vasu^{1,2}; ¹Mechanical and Aerospace Engineering, Univ. of Central Florida, USA; ²CREOL, College of Optics and Photonics, Univ. of Central Florida, USA; ³NanoScience Technology Center, Univ. of Central Florida, USA. We demonstrate temperature measurements in shock-heated mixtures of carbon monoxide (CO) using an acousto-optically modulated quantum cascade laser. Temperatures between 900 – 1300 K were measured at rates up to 250 kHz.

ATH4K.7 • 18:15

Design of next-generation tunable ECDLs based on MEMS, Morten Hoppe¹, Hanna Rohling¹, Sebastian Schmidtmann², Herve Tatenguem Fankem¹, Tobias Milde¹, Joachim R. Sacher^{1,2}; ¹Sacher Lasertechnik GmbH, Germany; ²Sensor Photonics GmbH, Germany. An External Cavity Diode Laser (ECDL) design of next-generation based on Micro Electro Mechanical System (MEMS) is presented. The excellent results in respect of tuning speed and range as well as repeatability are shown.

Meeting Room
212 C/D

CLEO: Science & Innovations

STh4L • Multi-Mode Fiber
Phenomena II—Continued

STh4L.6 • 18:00

Passive Q-switching Based on Nonlinear Effect of Multimode Interference in Tapered Fiber, Hanieh Afkhamiardakani¹, Jean-Claude Diels¹; ¹CHTM, Univ. of New Mexico, USA. A novel method to passively Q-switch an all-PM fiber laser is presented. A tapered fiber (free standing in air) is used as a saturable absorber based on Kerr effect of multimode interference in tapered section.

18:30–20:00 Emerging Trends in Nonlinear Optics - A Review of CLEO: 2019, Room 230A

18:30–20:00 Dinner Break (on your own)

20:00–22:00 Postdeadline Paper Sessions, Location TBD

**CLEO: QELS-Fundamental
Science**

CLEO: Science & Innovations

**FTh4M • Hyperbolic Photonics Media—
Continued**

**STh4N • High-Speed Optical
Interconnects—Continued**

**STh4O • Epitaxial Materials & Strain
Engineering—Continued**

FTh4M.6 • 17:45

Development of Near-Infrared Rare Earth Doped Organic Materials for Nanophotonics Applications, Joshua K. Asane¹, Alexis Bullock², Marvin Clemmons¹, Natalia Noginova¹, Mikhail Noginov¹; ¹Norfolk State Univ., USA. We have synthesized a series of near-infrared rare-earth doped organic materials for nanophotonics applications and studied their absorption and emission properties. The developed materials show promise as research tools and (meta)device components.

FTh4M.7 • 18:00

Spontaneous emission from a wide quantum electron, Aviv Karnieli¹, Roi Remez¹, Sivan Trajtenberg-Mills¹, Niv Shapira¹, Ido Kaminer², Yossi Lereah¹, Ady Arie¹; ¹Tel Aviv Univ., Israel; ²Technion, Israel. We show that the azimuthal distribution of emitted light in the Smith-Purcell interaction does not depend on the width of the electron wavefunction, thus providing direct evidence for the probabilistic interpretation of the electron wavefunction.

FTh4M.8 • 18:15

Probe the ultimate nonlocal limit of 'threshold-free' Cherenkov radiation, Hao Hu¹, Xiao Lin¹, Dongjue Liu¹, Patrice Genevet², Baile Zhang¹, Yu Luo¹; ¹Nanyang Technological Univ., Singapore; ²CNRS, France. Here we probe the ultimate nonlocal limit of "threshold-free" Cherenkov radiation in hyperbolic metamaterials. The nonlocality, induced by the spatial dispersion from the inhomogeneous structure and the electron screening, determines a nonzero Cherenkov threshold.

STh4N.5 • 18:00

A 10Gb/s Optical Random-Access Memory using a saturated SOA-MZI fast Access Gate and a monolithic InP Flip-Flop, Apostolos Tsakyridis¹, Christos Vagionas¹, Theoni Alexoudi¹, Amalia Miliou¹, Nikos Pleros¹; ¹Aristotle Univ. of Thessaloniki, Greece. We experimentally demonstrate an all-optical static Random-Access Memory (RAM) cell using a monolithic integrated InP Flip-Flop and a fast strongly-saturated push-pull SOA-MZI Access-Gate, reporting 10Gb/s error-free Write/Read operation and the fastest RAM cell to date.

STh4N.6 • 18:15

Silicon Photonic Single-Sideband Generation with Dual-Parallel Mach-Zehnder Modulators, Ashok Kodigala¹, Michael R. Gehl¹, Christopher DeRose¹, Dana Hood¹, Andrew T. Pomerene¹, Christina Dallo¹, Douglas Trotter¹, Penny Moore¹, Andrew Starbuck¹, Jongmin Lee¹, Grant Biedermann¹, Anthony Lentine¹; ¹Sandia National Labs, USA. We demonstrate the first silicon photonic single-sideband (SSB) modulator with dual-parallel Mach-Zehnder modulators (MZMs) operating near 1550 nm with a measured carrier suppression of 27 dB and at least 12 dB sideband suppression at 1 GHz.

STh4O.6 • 18:00

Study of High Performance GeSn Photodetectors with Cutoff Wavelength up to 3.7 μm for Low-Cost Infrared Imaging, Huong Tran¹, Thach Pham¹, Joe Margetis², Yiyin Zhou¹, Wei Dou¹, Perry Grant¹, Joshua Grant¹, Sattar Al-Kabi¹, Wei Du³, Greg Sun⁴, Richard Soref⁴, John Tolle², Baohua Li⁵, Mansour Mortazavi⁶, Shui-Qing Yu¹; ¹Univ. of Arkansas, USA; ²ASM, USA; ³Wilkes Univ., USA; ⁴Univ. of Massachusetts Boston, USA; ⁵Arktonics, LLC, USA; ⁶Univ. of Arkansas at Pine Bluff, USA. The GeSn photodetectors with Sn compositions up to 22.3% were systematically investigated. The maximum cutoff wavelength of 3.7 μm at 300 K and the peak specific detectivity of $9.5 \times 10^9 \text{ cmHz}^{1/2}\text{W}^{-1}$ at 77 K were achieved. Moreover, the infrared images were captured.

STh4O.7 • 18:15

Boron Alloys for GaAs-based 1.3μm Semiconductor Lasers, Rasha H. El-Jaroudi¹, Kyle M. McNicholas¹, Brent A. Bouslog¹, Iram E. Olivares¹, Rachel C. White¹, Joshua McArthur¹, Seth Bank¹; ¹Univ. of Texas at Austin, USA. We present BGalnAs as a potential active region for 1.31μm laser sources on GaAs substrates. We demonstrate high quality BGalnAs films with high indium concentrations and multiple percent boron concentrations that emit at room temperature.

18:30–20:00 Emerging Trends in Nonlinear Optics - A Review of CLEO: 2019, Room 230A

18:30–20:00 Dinner Break (on your own)

20:00–22:00 Postdeadline Paper Sessions, Location TBD

Executive Ballroom
210AExecutive Ballroom
210BExecutive Ballroom
210CExecutive Ballroom
210D

CLEO: QELS-Fundamental Science

08:00–10:00

FF1A • Single-Photon Detection
Presider: Joshua Bienfang; NIST Gaithersburg Maryland, USA

FF1A.1 • 08:00

Invited

Microwave Plasmonic Properties of Superconducting Thin Films May Enable Improved Single-Photon Detection, Karl Berggren¹; ¹MIT, USA. Superconducting thin films have a strong microwave plasmonic characteristic which enables ultra-slow microwave propagation speeds and thus complex on-chip architectures for microwave circuits. We present a novel interferometric scheme for single-photon detection that would use a superconducting-nanowire-based microwave on-chip interferometer.

FF1A.2 • 08:30

Superconducting Nanowire Single Photon Detector with High Efficiency and Time Resolution for Multimode Fiber Coupling, Jin Chang¹, Iman E. Zadeh¹, Johannes W. Los², J Zichi³, Val Zwiller³; ¹Technology Univ. of Delft (TUD), Netherlands; ²Single Quantum B.V., Netherlands; ³Dept. of Applied Physics, Royal Inst. of Technology (KTH), Sweden. In this paper, we report the development of a 50 μm diameter superconducting nanowire single photon detector with sub-19 ps timing jitter and saturated internal efficiency over a broad wavelength range for multimode fiber coupling.

FF1A.3 • 08:45

Exceeding 95% system efficiency within the telecom C-band in superconducting nanowire single photon detectors, Dileep V. Reddy^{1,2}, Robert R. Nerem³, Adriana Lita², Sae Woo Nam², Richard P. Mirin², Varun B. Verma²; ¹Univ. of Colorado Boulder, USA; ²Applied Physics Division, National Inst. of Standards and Technology, USA; ³Montana State Univ.-Bozeman, USA. We present a single-photon detector with system detection efficiencies exceeding 95% over the wavelength range 1520–1550 nm, with polarization sensitivities in the range of 1.02–1.08. The wavelength range is tunable over 200 nm via variation of the top-two dielectric layer thicknesses.

08:00–10:00

FF1B • Time Varying Metasurfaces
Presider: To Be Announced

FF1B.1 • 08:00

Invited

Linear Frequency Conversion in Time-Variant Metasurfaces, Bumki Min¹; ¹South Korea Advanced Inst of Science & Tech, South Korea (the Republic of). The energy of an electromagnetic wave is converted as the wave passes through a temporal boundary. Here, we propose rapidly time-variant metasurfaces as a frequency converting platform and experimentally demonstrate their efficacy at THz frequencies.

FF1B.2 • 08:30

Time-modulated Metasurfaces for Dispersionless Wavefront Engineering of Light, Mohammad Mahdi Salary¹, Hossein Mosalaei¹; ¹Northeastern Univ., USA. We introduce a dispersionless phase gradient for the light undergoing frequency conversion in a time-modulated metasurface and demonstrate its application for dynamic wavefront engineering of generated frequency harmonics in graphene-based and transparent conducting oxide metasurfaces.

FF1B.3 • 08:45

Frequency conversion through time refraction using an epsilon-near-zero material, Yiyu Zhou¹, Mohammad Karimi², Jeremy Upham², Orad Reshef², Cong Liu³, Alan E. Willner³, Zahirul Alam², Robert Boyd^{1,2}; ¹The Inst. of Optics, Univ. of Rochester, USA; ²Dept. of Physics, Univ. of Ottawa, Canada; ³Dept. of Electrical Engineering, Univ. of Southern California, USA. We report a large and tunable frequency shifting over 14.8 THz bandwidth of an infrared probe beam through time refraction in indium tin oxide (ITO) in its epsilon-near-zero region. The sign of the frequency change can be controlled by adjusting the delay between a pump and the probe.

08:00–10:00

FF1C • Attosecond & High Field Sources
Presider: François Légaré; INRS, Canada

FF1C.1 • 08:00

Tutorial

Scaling of Strong-Field Physics into the Long Wavelength Limit, Louis F. DiMauro¹; ¹Physics, The Ohio State Univ., USA. Studies of the wavelength scaling of an intense laser interacting with atoms and molecules is driving a renewed interest in the fundamental physics and a renaissance in potential applications in ultrafast imaging methods.



Louis F. DiMauro is Professor of Physics and Hagenlocker Chair at the Ohio State University. He is the recipient of the 2012 OSU Distinguished Scholar Award, the 2013 OSA Meggers Prize and the 2017 APS Schawlow Prize in Laser Science. He is a Fellow of the APS, OSA and AAAS.

08:00–10:00

FF1D • Solitons in Microresonators
Presider: To Be Announced

FF1D.1 • 08:00

Dual Comb Generation in a Symmetrically Driven Crystalline Microresonator, Romain Bouchand¹, Wenle Weng¹, Erwan Lucas¹, Tobias J. Kippenberg¹; ¹Ecole Polytechnique Fédérale de Lausanne, Switzerland. We develop a dual-comb system based on a single crystalline microresonator by monochromatically pumping counter-propagating solitons in the same spatial mode with equal powers and unveil the role of soliton Cherenkov radiations interference in the process.

FF1D.2 • 08:15

Heteronuclear Soliton Molecules in Optical Microresonators, Wenle Weng¹, Romain Bouchand¹, Erwan Lucas¹, Ewelina Obrzud^{2,3}, Tobias Herr², Tobias J. Kippenberg¹; ¹Ecole Polytechnique Fédérale de Lausanne, Switzerland; ²Swiss Center for Electronics and Microtechnology (CSEM), Switzerland; ³Univ. of Geneva, Switzerland. We enter the multi-stability regime of an optical microresonator to generate heteronuclear soliton molecules. Ultrafast electro-optical sampling reveals the bound structures of such soliton molecules, despite comprising solitons of dissimilar amplitudes, durations and frequencies.

FF1D.3 • 08:30

Measuring the Optical Temperature of a Soliton, Pawel Jung^{1,2}, Fan Wu¹, Absar U. Hassan¹, Demetrios N. Christodoulides¹; ¹The College of Optics and Photonics, Univ. of Central Florida, USA; ²Faculty of Physics, Warsaw Univ. of Technology, Poland. Under thermal equilibrium conditions, we show that the zeroth law of thermodynamics can be used to measure a soliton's optical temperature in a nonlinear multimode system. Here, the modal gain plays the role of an optical thermometer.

FF1D.4 • 08:45

Soliton Elasticity, Oliver Melchert^{1,2}, Stephanie Willms¹, Ihar Babushkin¹, Bernhard Roth², Günter Steinmeyer^{3,4}, Uwe Morgner¹, Ayhan Demircan^{1,2}; ¹Leibniz Univ. Hannover, Germany; ²Hannover Centre for Optical Technologies, Germany; ³Max-Born-Inst., Germany; ⁴Humboldt Univ. Berlin, Germany. We extend the analogy of particle-like behavior of solitons one decisive step further, demonstrating completely Newtonian collisions for unequal solitons, detached from any wave properties. They even act like extended massive objects, exhibiting elastic deformation.

Executive Ballroom
210ECLEO: Science &
Innovations

08:00–10:00

SF1E • Ultrafast Applications

Presider: Alan Fry; SLAC, USA

SF1E.1 • 08:00

Invited

Laser-based 3D Printing for Biomedical Applications, Maria Farsari¹; ¹IESL-FORTH, Greece. We present our most recent results into the 3D laser printing of scaffolds and biomedical implants using a series of novel functional materials.

SF1E.2 • 08:30

Invited

High Performance Nanoscale Imaging with Table-Top XUV Sources, Jan Rothhardt^{1,2}, Wilhelm Eschen^{1,2}, Getnet Tadesse^{1,2}, Robert Klas^{1,2}, Jens Limpert^{1,2}; ¹Helmholtz Inst. Jena, Germany; ²Inst. of Applied Physics, Friedrich-Schiller-Universität, Germany. This talk will present the latest achievements in high performance coherent diffractive imaging at the nanoscale enabled by fiber-laser based high photon flux table-top high harmonic sources.

Executive Ballroom
210FCLEO: QELS-
Fundamental Science

08:00–10:00

FF1F • Machine Learning &
Quantum Exotica

Presider: Peter Mosley; University of Bath, UK

FF1F.1 • 08:00

Entanglement-Enhanced Physical-Layer Classifier Using Supervised Machine Learning, Quntao Zhuang^{1,2}, Zheshe Zhang^{3,4}; ¹Dept. of Physics, Univ. of California, Berkeley, USA; ²Dept. of Electrical and Computer Engineering, Univ. of Arizona, USA; ³Dept. of Materials Science and Engineering, Univ. of Arizona, USA; ⁴College of Optical Sciences, Univ. of Arizona, USA. We introduce physical-layer classifiers enhanced by multipartite entanglement learned through a supervised support-vector machine. The required entangled states are practical and give error probability advantage over classical schemes even in presence of loss.

FF1F.2 • 08:15

Quantum Photonic Neural Networks, Gregory Steinbrecher¹, Jonathan Olson², Dirk R. Englund¹, Jacques Carolan¹; ¹MIT, USA; ²Zapata Computing Inc., USA. We propose an architecture for next generation quantum photonic processors, which maps the features of neural networks into the quantum optical domain. Through numerical simulation we demonstrate a range of new quantum information processing tasks.

FF1F.3 • 08:30

Bayesian machine learning of frequency-bin CNOT, Hsuan-Hao Lu², Joseph M. Lukens¹, Brian P. Williams¹, Poolad Imany², Nicholas A. Peters¹, Andrew M. Weiner², Pavel Lougovski¹; ¹Quantum Information Science Group, Oak Ridge National Lab, USA; ²School of Electrical and Computer Engineering, Purdue Univ., USA. We analyze the first experimental two-photon frequency-bin gate: a coincidence-basis CNOT. A novel characterization approach based on Bayesian machine learning is developed to estimate the gate performance with measurements in the logical basis alone.

Executive Ballroom
210G

CLEO: Science & Innovations

08:00–10:00

SF1G • Devices for
Communications

Presider: Francesco Da Ros; Technical University of Denmark, Denmark

SF1G.1 • 08:00

Invited

Programmable Integrated Photonics: Is it the right time for Field Programmable Arrays?, Jose Capmany¹, Daniel Perez¹, Ivana Gasulla¹, Prometheus Das Mahapatra¹; ¹Universidad Politecnica de Valencia, Spain. Programmable photonics is an emerging paradigm based on using a common integrated optical hardware architecture to implement multiple functions by software programming. Field Programmable Photonic Arrays enable its implementation, but is the technology ready?

SF1G.2 • 08:30

Bit error rate performance of bias-free operational UTC-PD for high baud rate communications up to 100 Gbaud, Toshimasa Umezawa¹, Atsushi Matsumoto¹, Atsushi Kanno¹, Naokatsu Yamamoto¹, Tetsuya Kawamichi^{2,1}; ¹National Inst of Information & Comm Tech, Japan; ²Waseda Univ., Japan. We fabricated a bias free operational high bandwidth photodetector operated over 110-GHz, and characterized the bit error performance at up to 100-Gbaud. At 90-Gbaud, BER < 1 × 10⁻³ was confirmed without a frequency equalizer or a DSP.

Executive Ballroom
210H

08:00–10:00

SF1H • Phase-matching
Techniques

Presider: Sergey Vasilyev; IPG Photonics, USA

SF1H.1 • 08:00

A 2.35- μ m pumped subharmonic OPO reaches the spectral width of two octaves in the mid-IR, Qitian Ru¹, Peter G. Schunemann², Sergey Vasilyev³, Sergey Mirov^{3,4}, Konstantin L. Vodopyanov¹; ¹CREOL, College of Optics and Photonics, Univ. of Central Florida, USA; ²BAE Systems, USA; ³IPG Photonics - Mid-infrared Lasers, USA; ⁴Dept. of Physics, Univ. of Alabama at Birmingham, USA. We used an orientation-patterned gallium phosphide (OP-GaP) crystal combined with an ultrafast 2.35- μ m pump (1.2W, 79 MHz, 62 fs) to demonstrate a subharmonic sync-pumped OPO with an instantaneous output spectrum of 3–12.5 μ m.

SF1H.2 • 08:15

Generation of wavelength- and mode-controllable Poincaré sphere beams from a femtosecond optical parametric oscillator, Jintao Fan¹, Na Xiao¹, Jun Zhao¹, Haosen Shi¹, Ruoyu Liao¹, Chen Xie¹, Youjian Song¹, Minglie Hu¹; ¹Tianjin Univ., China. We report on a femtosecond optical parametric oscillator which is capable of generating on-demand arbitrary higher-order Poincaré (HOP) sphere beams tunable from 1376 to 1626 nm.

SF1H.3 • 08:30

Single-Frequency Operation of a Near-degenerate Optical Parametric Oscillator Using a Transversally Chirped Volume Bragg Grating, Adeline Kabacinski¹, Julie Armougom¹, Jean-Michel Melkonian¹, Myriam Raybaut¹, Jean-Baptiste Dherbecourt¹, Antoine Godard¹, Ruslan Vasilyev², Vadim Smirnov²; ¹ONERA, France; ²Optigrate (IPG), USA. We report on a doubly-resonant optical parametric oscillator emitting single-frequency radiation near 2 μ m using Vernier spectral filtering and a Bragg reflector. The wavelength is tuned over 22 nm using a chirped Bragg grating period.

SF1H.4 • 08:45

Coherent Temporal Phase Transfer in Backward Wave Parametric Oscillator at 1.4 μ m, Anne-Lise Viotti¹, Fredrik Laurell¹, Andrius Zukauskas¹, Carlota Canalias¹, Valdas Pasiskevicius¹; ¹Royal Inst. of Technology, Sweden. The frequency modulation transfer property of a backward wave optical parametric oscillator is employed to generate compressed near-IR pulses at 1.4 μ m with 1.3ps duration. Limitations to the linear frequency modulation transfer in BWPO are investigated.

Meeting Room
211 A/B

CLEO: Science & Innovations

08:00–10:00

SF11 • Frequency-Comb-Based Sensing

Presider: Aleksandra Foltynowicz
Umea University, Sweden

SF11.1 • 08:00

Mid-infrared Dual-comb Spectroscopy of Volatile Organic Compounds Across Long Open-air Paths, Fabrizio R. Giorgetta^{1,2}, Gabriel Ycas^{1,2}, Kevin C. Cossel¹, Eleanor Waxman¹, Esther Baumann^{1,2}, Nathan R. Newbury¹, Ian Coddington¹; ¹NIST, USA; ²Physics, Univ. of Colorado, USA. Volatile organic compounds are probed across up to 1 km-long open-air paths with mid-infrared dual-comb spectroscopy. Quantitative concentrations of released acetone and isopropanol and atmospheric ethane are measured with ppm-level sensitivities.

SF11.2 • 08:30

Background-Free Mid-Infrared Absorption Spectroscopy Based on Interferometric Suppression with a Sign-Inverted Waveform, Teemu Tomberg², Andrey Muraviev¹, Qitian Ru¹, Konstantin L. Vodopyanov¹; ¹Univ. of Central Florida, CREOL, USA; ²Dept. of Chemistry, Univ. of Helsinki, Finland. Using a broadband dual-comb system, we implement a new type of background-free spectroscopy based on a Michelson interferometer operating in a dark fringe. This strongly improves detection sensitivity and reduces requirements for detector dynamic range.

SF11.3 • 08:45

Automatic Interpolation of 25 GHz Mode Spacing in Dual EOM Comb Spectroscopy, Tadashi Nishikawa¹, Akira Oohara¹, Shohei Uda¹, Atsushi Ishizawa², Kenichi Hitachi², Nathalie Picqué^{3,4}, Theodor W. Hänsch^{3,4}; ¹Tokyo Denki Univ., Japan; ²NTT Basic Research Labs, Japan; ³Max-Planck-Institut für Quantenoptik, Germany; ⁴Ludwig-Maximilians-Universität München, Germany. Automatic interpolation of 25GHz mode spacing in dual EOM comb spectroscopy has been demonstrated. By single shot measurement of 9.3ms, H¹³C¹⁴N absorption spectrum spanning more than 0.8THz with 100MHz resolution could be obtained.

Meeting Room
211 C/D

08:00–10:00

SF1J • Plasmonics, Optomechanics, & Metamaterials

Presider: Karen Grutter, Univ. of Maryland at College Park, USA

SF1J.1 • 08:00 **Invited**

A Few Novel Effects in Plasmonics, Marin Soljacic¹; ¹MIT, USA. Some of our recent work in plasmonics will be presented, including novel free-electron light sources, as well as structures for enhanced light emission, and tailoring light-flow.

SF1J.2 • 08:30

Record Purcell Factor in Hybrid Plasmonic Waveguides, Yiwen Su¹, Pohan Chang¹, Charles Lin¹, Amr S. Helmy¹; ¹Univ. of Toronto, Canada. A composite hybrid plasmonic waveguide is demonstrated to exhibit long-range propagation (0.03dB/μm) and subwavelength confinement simultaneously while unrestricted from structural or modal symmetry coupling conditions. Purcell factors of 1.5x10⁴ were measured in traveling-wave ring-resonators.

SF1J.3 • 08:45

Hexagonal boron nitride cavity optomechanics, Praseon Kumar Shandilya¹, Johannes E. Froch², Matthew Mitchell¹, David Lake¹, Sejeong Kim², Milos Toth², Bishnupada Behera¹, Chris Healey¹, Igor Aharonovich², Paul E. Barclay¹; ¹Inst. for Quantum Science and Technology, Univ. of Calgary, Canada; ²Inst. of Biomedical Materials and Devices, Univ. of Technology Sydney, Australia. Hexagonal boron nitride (hBN) is an emerging layered material that plays a key role in a variety of 2D devices. Here, we demonstrate the first hBN cavity optomechanical system by integrating hBN nanobeam with silicon microdisk cavities. The system has 0.29pm/√Hz sensitivity to hBN nanobeam motion.

Meeting Room
212 A/B

CLEO: Applications & Technology

08:00–10:00

AF1K • Structural Monitoring

Presider: Gregory Rieker;
University of Colorado at Boulder, USA

AF1K.1 • 08:00

VCSEL Based FBG Sensor Network Interrogator for Lightning Strike Testing of Airframes, Guodong Guo¹, Brandon Hearley¹, Mark Pankow¹, Kara Peters¹; ¹North Carolina State Univ., USA. We develop a low-power, VCSEL based FBG sensor network interrogator for high-speed measurements of thermal and mechanical induced strains in composite airframes during lightning strikes.

AF1K.2 • 08:30

Sub- μe Static Resolution Fiber Laser Sensor, Shuangxiang Zhao¹, Qingwen Liu¹, Jiageng Chen¹, Zuyuan He¹; ¹Shanghai Jiao Tong Univ., China. A fiber laser sensor system capable of both static and dynamic strain measurement is presented. Using Pound-Drever-Hall and injection-locking techniques, resolution of 276 pε in 1000 s and 450 fε at 1 kHz is demonstrated.

AF1K.3 • 08:45

Strain Sensitivity Enhancement by Polarization-Maintaining Fiber Bragg Gratings, Dipenkumar Barot¹, Lingze Duan¹; ¹Univ. of Alabama in Huntsville, USA. A novel and simple approach for dynamic strain measurement is demonstrated. By using polarization-maintaining fiber Bragg grating and balanced detection, both strain sensitivity and signal-to-noise ratio are enhanced by over an order of magnitude.

Meeting Room
212 C/D

CLEO: Science & Innovations

08:00–10:00

SF1L • Fiber Parametric Sources

Presider: Sze Y. Set The University of Tokyo, Japan

SF1L.1 • 08:00

Femtosecond Optical Parametric Oscillator Based on Vector Four-Wave-Mixing in Step-Index Fiber, Walter P. Fu¹, Frank W. Wise¹; ¹Cornell Univ., USA. We present a fiber optical parametric oscillator based on polarization-maintaining, step-index fiber. Using birefringence-induced phase-matching, we convert chirped pulses at 1 μm to nanjoule-scale, femtosecond pulses at 0.8 μm and 1.3 μm.

SF1L.2 • 08:15

Rapidly and Widely Tunable All-Fiber Optical Parametric Oscillator, Maximilian Brinkmann^{1,2}, Tim Hellwig^{1,2}, Carsten Fallnich^{1,2}; ¹Inst. of Applied Physics, Univ. of Münster, Germany; ²Refined Laser Systems, Univ. of Münster, Germany. We present high-speed tuning in 5 ms per arbitrary wavelength step from 750 to 970 nm of a robust all-fiber optical parametric oscillator without the need for a mechanical delay.

SF1L.3 • 08:30

Stretched-Pulse Solitons in Driven Fiber Resonators, Qian Yang¹, Christopher Spiess¹, Victor G. Bucklew¹, William H. Renninger¹; ¹Univ. of Rochester, USA. Stable broadband solitons are observed in a driven nonlinear resonator consisting of fibers with opposite signs of dispersion. Corresponding numerical simulations reveal periodic temporal stretching of the pulse, characteristic of stretched-pulse solitons in mode-locked lasers.

SF1L.4 • 08:45

Highly-Chirped Solitons in Driven Resonators, Christopher Spiess¹, Qian Yang¹, Victor G. Bucklew¹, William H. Renninger¹; ¹Univ. of Rochester, USA. Here we investigate driven fiber resonators with large net normal dispersion and a narrowband intracavity spectral filter. A range of stable solutions are observed, including the first experimental and numerical observations of highly-chirped solitons.

Marriott
Salon I & IIMarriott
Salon IIIMarriott
Salon IV

CLEO: Science & Innovations

08:00–10:00

SF1M • Fiber-Based Information Process
President: Kazi Abedin, OFS Laboratories, USASF1M.1 • 08:00 **Invited**

Device independent quantum information processing---from Bell inequality to fiber QKD, Qiang Zhang¹; ¹Univ of Science and Technology of China, China. Bell experiment provides not only a way to test quantum nonlocality but also to implement quantum information independent of any device. Here, I shall introduce the recent experimental progress in loophole free Bell test and device independent quantum random number generation.

SF1M.2 • 08:30

Solving large-scale NP-Complete problem with an optical solver driven by a dual-comb 'clock', Yalin Hou¹, Xin Zhao¹, Qian Li¹, Jie Chen¹, Yihong Li¹, Zheng Zheng^{1,2}; ¹School of Electronic and Information Engineering, Beihang Univ., China; ²Beijing Advanced Innovation Center for Big Data-based Precision Medicine, China. A scheme using a simple dual-comb fiber laser to solve large instance NP-C problems is demonstrated based on asynchronous sampling measurement of pulse delays through a fiber network, subpicosecond resolution and nanosecond range are achieved.

SF1M.3 • 08:45

All-optical Ultrafast Switching Based on Plasmon-generated Hot Carriers in Gold-coated Fiber Gratings, Fu Liu¹; ¹Dept. of Electronics, Carleton Univ., Canada. Pump-probe modulation of 4.95% is observed experimentally and by simulations in gold-coated tilted fiber Bragg gratings at power densities of 205 MW/cm² with 25 ps pulses from a tunable laser at wavelengths near 1550 nm.

08:00–10:00

SF1N • AI for Integrated Photonics
President: Alan Wang; Oregon State Univ., USA

SF1N.1 • 08:00

Integrated Nanophotonic Ising Sampler, Mihika Prabhu¹, Charles Roques-Carnes¹, Yichen Shen², Nicholas C. Harris², Li Jing¹, Jacques Carolan¹, Ryan Hamerly¹, Tom Baehr-Jones⁴, Michael Hochberg³, Vladimir Ceperic¹, John D. Joannopoulos¹, Dirk R. Englund¹, Marin Soljacic¹; ¹MIT, USA; ²Lightmatter, USA; ³Lightelligence, USA; ⁴Elenion Technologies, USA. We demonstrate an integrated silicon photonic Markov Chain Monte Carlo sampler capable of high-probability convergence to the ground state of various 4-spin Ising graphs. Robustness to getting trapped in local minima is enhanced by experimental system noise.

SF1N.2 • 08:15

Deep Learning-designed Diffractive Neural Networks, Xing Lin¹, Yair Rivenson¹, Nezhil Yardimci¹, Muhammed Veli¹, Yi Luo¹, Mona Jarrahi¹, Aydogan Ozcan¹; ¹Univ. of California Los Angeles, USA. We report deep learning-based design of diffractive neural networks. Following its fabrication, a diffractive neural network can all-optically perform user-defined tasks through diffraction. We demonstrate the applications of this framework for classification and imaging tasks.

SF1N.3 • 08:30 **Invited**

Programmable Nanophotonics for Machine Learning Acceleration, Nicholas C. Harris¹, Darius Bunandar¹, Carl Ramey¹; ¹Lightmatter, Inc., USA. Recent work has shown compatibility of neural networks with mixed- and low-precision number representations, prompting exploration into analog compute platforms. Here, we will discuss the application of silicon photonics, typically viewed as a communications platform, to the problem of deep learning.

08:00–10:00

SF1O • Perovskites
President: Jiming Bao; Univ. of Houston, USASF1O.1 • 08:00 **Invited**

Efficient, Color Tunable, and Flexible Thin Film Perovskite Light Emitting Devices, Barry P. Rand¹; ¹Princeton Univ., USA. We present a general protocol to prepare light emitting diodes based upon metal halide perovskites exceeding 17% external quantum efficiency, with improved stability, and which are as flexible as organic electronic thin films. Finally, we show stabilized mixed halide (I and Br) and mixed Pb-Sn stoichiometries such that we can tune emission from the green to near infrared.

SF1O.2 • 08:30

High-performance X-ray Detector Based on Solution-synthesized Thin-film Perovskite, Xiangming Liu¹, Zhigang Zang², Ming Wang², Tao Xu¹, Yulong Li¹, Xiaoshi Peng¹, Huiyue Wei¹, Zanyang Guan¹, Yonggang Liu¹, Feng Wang¹; ¹Laser Fusion Research Center, CAEP, China; ²Key Lab of Optoelectronic Technology & Systems, Chongqing Univ., China. We present a high-performance X-ray detector based on a solution-synthesized perovskite film. The sensitivity as high as 30 $\mu\text{C Gy}^{-1}\text{cm}^{-2}$ is realized. More importantly, the as-prepared detectors exhibit a fast photoresponse with a high stability.

SF1O.3 • 08:45

Visualizing the Creation and Healing of Traps in Perovskite Photovoltaic Films by Light Soaking and Passivation treatments, Andrew Winchester¹, Stuart Macpherson², Vivek Pareek¹, Mojtaba Abdi-Jalebi², Zahra Andaji-Garmaroudi², Christopher Petoukhoff¹, E Laine Wong¹, Julien Madéo¹, Michael K. Man¹, Samuel Stranks², Keshav M. Dani¹; ¹Femtosecond Spectroscopy Unit, Okinawa Inst. of Science and Technology, Japan; ²Cavendish Lab, Univ. of Cambridge, UK. Eliminating carrier traps in hybrid organic-inorganic perovskites is crucial for their application. We study the effects of passivation and light soaking treatments on changing surface traps in perovskite films using photoemission electron microscopy.

Executive Ballroom
210AExecutive Ballroom
210BExecutive Ballroom
210CExecutive Ballroom
210D

CLEO: QELS-Fundamental Science

FF1A • Single-Photon
Detection—Continued

FF1A.4 • 09:00

High Efficiency Planar Ge-on-Si Single-Photon Avalanche Diode Detectors, Jaroslav Kirdoda¹, Lourdes Ferre Llin¹, Kateryna Kuzmenko², Peter Vines², Zoe M. Greener², Derek C. Dumas¹, Ross Millar¹, Muhammad M. Mirza¹, Gerald S. Buller², Douglas J. Paul¹; ¹Univ. of Glasgow, UK; ²School of Engineering and Physical Sciences, Heriot-Watt Univ., UK. Planar Ge-on-Si single-photon avalanche diode detectors fabricated using CMOS-compatible processing demonstrate a 38% single photon detection efficiency at 125 K with 1310 nm wavelength illumination, exhibiting 310 ps jitter and 2×10^{-16} WHz^{-1/2} noise equivalent power.

FF1A.5 • 09:15

Single Photon Detectors' Timing-Jitter Quantum Description, Elie Gouzien¹, Bruno Fedrici¹, Alessandro Zavatta^{2,3}, Sébastien Tanzilli¹, Virginia D'Auria¹; ¹Institut de Physique de Nice, Université Côte d'Azur, France; ²Istituto Nazionale di Ottica, Italy; ³LENS and Dept. of Physics, Università di Firenze, Italy. We model single photon detectors by explicitly taking into account their timing-jitter, finite efficiency and dead-time effects. Our model represents the first operational and full description of temporal limitations of those detectors.

FF1A.6 • 09:30

Quantum tomography of a single-photon state by photon-number parity measurements, Rajveer Nehra¹, Aye Win¹, Miller Eaton¹, Niranjan Sridhar^{1,2}, Reihaneh Shah-rokhsheh^{1,3}, Thomas Gerrits⁴, Adriana Lita⁴, Sae Woo Nam⁴, Olivier Pfister¹; ¹Univ. of Virginia, USA; ²Google, Inc., USA; ³Xanadu, Canada; ⁴National Inst. of Standards and Technology, USA. A single-photon state was generated by heralding cavity-enhanced spontaneous parametric downconversion in a PPKTP optical parametric oscillator. The Wigner distribution was reconstructed by quantum state tomography, using photon-number-resolving measurements with a system efficiency of 58 ± 2%.

FF1A.7 • 09:45

Quantum illumination with x-rays, Sason Sofer^{1,2}, Edward Strizhevsky^{1,2}, Aviad Schori^{1,2}, Kenji Tamasaku², Sharon Shwartz^{1,2}; ¹Physics Dept. and Inst. of Nan, Israel; ²RIKEN SPring-8 Center, Japan. We present the experimental realization of quantum illumination with x-rays. By using entangled photons, we detected the presence of an object in a noisy environment and improved the visibility substantially compared to classical methods.

FF1B • Time Varying
Metasurfaces—Continued

FF1B.4 • 09:00

Time-varying Huygens' Metadevices for Parametric Wave Controls, Mingkai Liu¹, David Powell^{2,1}, Yair Zaraté¹, Ilya Shadrivov¹; ¹Australian National Univ., Australia; ²Univ. of New South Wales, Australia. Dynamic and arbitrary control of electromagnetic waves is challenging. We introduce time-varying Huygens' metadevices for efficient parametric conversion and demonstrate experimentally that the amplitude, phase, and scattering of parametric waves can be manipulated almost arbitrarily.

FF1B.5 • 09:15

Broadband Switches Using Photonic Aharonov-Bohm Interferometers and Dynamic Modulation, Ian Williamson¹, Shan-hui Fan¹; ¹Stanford Univ., USA. We introduce an optical switch using an Aharonov-Bohm interferometer constructed from gauge potentials in dynamically modulated waveguides. Our results show that such a switch can have a far broader bandwidth than the conventional Mach-Zehnder interferometer.

FF1B.6 • 09:30

Dynamic Phase Modulation Induced Nonreciprocity of Optical Metasurfaces, Xuexue Guo¹, Yimin Ding¹, Yao Duan¹, Xingjie Ni¹; ¹Pennsylvania State Univ., USA. By exploiting both spatial and temporal phase modulation, we experimentally demonstrate an ultrathin nonlinear metasurface with broken reciprocity at wavelengths around 860 nm. Our approach paves a way for miniaturized on-chip nonreciprocal optical components.

FF1B.7 • 09:45

Noninteracting Multilayer Dielectric Metasurfaces for Multiwavelength Metaoptics, You Zhou¹, Ivan Kravchenko², Hao Wang³, Joshua R. Nolen¹, Gong Gu³, Jason Valentine¹; ¹Vanderbilt Univ., USA; ²Oak Ridge National Lab, USA; ³Univ. of Tennessee, USA. We report a multilayer dielectric metasurface platform that increases the design flexibility of metasurfaces. We numerically and experimentally demonstrate multiwavelength metaoptics using this platform.

FF1C • Attosecond & High Field
Sources—Continued

FF1C.2 • 09:00

Low-Order Harmonic Generation in Mid-Infrared Laser Filaments in Gases, Claudia Gollner², Valentina Shumakova², Audrius Pugzlys², Andrius Baltuska², Pavel G. Polynkin¹; ¹Univ. of Arizona, USA; ²Technical Univ. of Vienna, Austria. We detect up to 11th-order harmonics generated through filamentation of ultrashort laser pulses at 3.9 μm wavelength in air and argon. Harmonic's spectra map the nonlinear evolution of the mid-infrared driver and exhibit CEP-dependent spectral interference.

FF1C.3 • 09:15

Measuring a Few-pulse Attotrain from CEP-dependent Relativistic High Harmonics, Guangjin Ma^{1,2}, Dmitrii Kormin^{3,4}, Antonin Borot³, William Dallari³, Boris Bergues^{3,4}, Mark Aladi⁵, Istvan Foldes⁵, Jin He¹, Laszlo Veisz^{3,6}; ¹Shenzhen SoC Key Lab, Peking Univ. Shenzhen Inst. & PKU-HKUST Shenzhen-Hong Kong Institution, China; ²Center for Free-Electron Laser Science, DESY, Germany; ³Max-Planck-Institut für Quantenoptik, Germany; ⁴Ludwig-Maximilians-Universität München, Germany; ⁵Wigner Research Centre for Physics, Hungarian Academy of Sciences, Hungary; ⁶Dept. of Physics, Umea Univ., Sweden. We present laser-waveform-dependent relativistic high harmonics from plasma surfaces, and use spectral interferometry to understand its generation process. The attotrain structure as well as the field-driven plasma surface motion during the process are revealed.

FF1C.4 • 09:30

First experimental steps toward an in situ gauge for direct measurement of relativistic intensities, Wendell T. Hill¹, Calvin He¹, Luis Roso², José A. Pérez-Hernández², Giancarlo Gatti², Massimo de Marco², Robert Fedosejevs³, Andrew Longman³; ¹Univ. of Maryland at College Park, USA; ²Centro de Láseres Pulsados, Spain; ³Univ. of Alberta, Canada. Nearly 50 years ago Sarachik and Schappert suggested an intensity gauge based on wavelength shifts due to relativistic Thomson scattering. We present the first preliminary experimental results exploiting these shifts to make a direct measurement of peak intensities above 10¹⁸ W/cm².

FF1C.5 • 09:45

Demonstration of Tunable Relativistic, Single-Cycle Infrared Pulses from a Tailored Plasma Structure, Zan Nie¹, Chih-Hao Pai¹, Jie Zhang¹, Xiaonan Ning¹, Jianfei Hua¹, Chaojie Zhang², Yunxiao He¹, Yipeng Wu¹, Qianqian Su¹, Shuang Liu¹, Yue Ma¹, Zhi Cheng¹, Wei Lu¹, Hsu-Hsin Chu³, Jyhpyng Wang^{3,4}, Warren B. Mori², Chan Joshi²; ¹Tsinghua Univ., China; ²Univ. of California Los Angeles, USA; ³National Central Univ., Taiwan; ⁴National Taiwan Univ., Taiwan. We demonstrate that relativistic, single-cycle infrared pulses tunable in the spectral range of 3–19 μm can be generated from a tailored plasma structure using an 810 nm drive laser.

FF1D • Solitons in
Microresonators—Continued

FF1D.5 • 09:00

Perfect soliton crystals in optical microresonators, Maxim Karpov¹, Martin Pfeiffer¹, Hairun Guo¹, Junqiu Liu¹, Wenle Weng¹, Tobias J. Kippenberg¹; ¹Lab. of Photonics and Quantum Measurement, Switzerland. We demonstrate the existence of perfect soliton crystal states and develop the deterministic procedure for their excitation in Si₃N₄ microresonators. We show that despite exceptional symmetrical properties, their behavior is strongly linked to the chaotic regimes of the microresonator.

FF1D.6 • 09:30

Kerr-breather-soliton time crystals, Scott Papp¹, Daniel C. Cole¹; ¹NIST, USA. We describe Kerr-breather-soliton time crystals in which a breathing excitation is sub-harmonically locked to the repetition frequency. Nonlinear modeling explores the behavior of soliton time crystals, and we will report on progress towards their observation.

FF1D.7 • 09:45

Gaussian Pulses in Kerr Nonlinear Microresonators with Pure Quartic Modal Dispersion, Hossein Taheri¹, Andrey B. Matsko², Anatoly Savchenkov²; ¹ECE, Univ. of California, Riverside, USA; ²OEWaves Inc., USA. Gaussian pulses in Kerr-nonlinear microresonators with pure quartic modal dispersion are reported. Using a variational approach, pulse parameters are found in terms of experimentally tunable quantities and verified through numerical simulations and comparison with experiment.

10:00–10:30 Coffee Break, Concourse Level

CLEO: Science & Innovations

SF1E • Ultrafast Applications—Continued

SF1E.3 • 09:00

Ultrafast Infrared Vibrational Nanoscopy: Imaging Structure, Coupling and Dynamics on the Molecular Scale, Jun Nishida¹, Sven A. Dönges¹, Omar Khatib¹, Markus B. Raschke¹; ¹Univ. of Colorado Boulder, USA. We demonstrate spatio-temporal-spectral nano-imaging through vibrational heterodyne pump-probe infrared scattering scanning near-field optical microscopy (HPP IR s-SNOM), revealing the coupled electronic and molecular structural dynamics in a triple cation perovskite film.

SF1E.4 • 09:15

Hyperspectral Microscopy with Broadband Infrared Frequency Combs, Henry Timmers¹, Abijith Kowligy¹, Alexander Lind¹, Nima Nader¹, Jonah Shaw¹, Dobryna Zalvidea², Jens Biegert³, Scott A. Diddams¹; ¹NIST, USA; ²Inst. of Bioengineering of Catalonia, Spain; ³ICFO, Spain. We present a new modality for infrared, hyperspectral microscopy using dual-comb, electro-optic sampling of octave-spanning infrared frequency combs. We obtain hyperspectral images of SU8 test patterns on Si wafers with a spatial resolution of 12 μm .

SF1E.5 • 09:30

Laser Interference Processing of Electron Phase Holograms by Using a Femtosecond Laser, Yuuki Uesugi¹, Ryota Fukushima¹, Shunichi Sato¹, Koh Saitoh²; ¹Tohoku Univ., Japan; ²Nagoya Univ., Japan. Electron phase hologram was fabricated by a single-shot femtosecond laser interference processing. The generation of electron vortices from the fabricated hologram was demonstrated with higher diffraction efficiency than that of amplitude hologram as expected.

SF1E.6 • 09:45

Spatio-temporal Measurement of Ionization-induced Modal Index Evolution in Gas-filled Hollow-core Photonic Crystal Fiber, Mallika I. Suresh¹, Barbara M. Trabold¹, Johannes R. Koehler¹, Michael H. Frosz¹, Francesco Tani¹, Philip S. Russell¹; ¹Max Planck Inst. for the Science of Light, Germany. Using a prism side-coupling technique, we selectively excite four different higher order guided modes in a gas-filled single-ring hollow core photonic crystal fiber and use them to probe transverse photoionization-induced refractive index changes.

CLEO: QELS-Fundamental Science

FF1F • Machine Learning & Quantum Exotica—Continued

FF1F.4 • 09:00

Indistinguishable Photon Source in the 1550-nm Band Optimized by Machine Learning, Chaohan Cui¹, Yi Xia¹, Saikat Guha¹, Nasser Peyghambarian¹, Zheshen Zhang²; ¹College of Optical Sciences, The Univ. of Arizona, USA; ²Dept. of Materials Science and Engineering, The Univ. of Arizona, USA. We report a recipe for optimized poling design to generate spectrally-pure photons around 1550 nm. Our approach hinges on machine-learning techniques without requiring group-velocity matching.

FF1F.5 • 09:15

Non-Abelian Geometric Phases in Photonics and their Optimal Design Strategy Based on Quantum Metric, Mark Kremer¹, Lucas Teuber¹, Alexander Szameit¹, Stefan Scheel¹; ¹Inst. of Physics, Univ. of Rostock, Germany. We experimentally realize non-Abelian geometric phases in photonic structures, hence using an Abelian-gauge field. The process is optimized by the novel concept of utilizing the quantum metric, ensuring the adiabaticity of the underlying process.

FF1F.6 • 09:30

Free Electron Qubits, Ori Reinhardt¹, Chen Mechel¹, Morgan Lynch¹, Ido Kaminer¹; ¹Technion, Israel. We show that a single relativistic free electron can carry one or multiple qubits within its wave-function in Floquet-dressed basis and implement 1-qubit gates based on the electron interaction with designed optical pulses.

FF1F.7 • 09:45

Covert sensing using floodlight illumination, Christos Gagatsos¹, Boulat A. Bash¹, Animesh Datta², Zheshen Zhang¹, Saikat Guha¹; ¹Univ. of Arizona, USA; ²Univ. of Warwick, UK. We present an active covert phase sensing scheme using floodlight illumination from an amplified spontaneous emission (ASE) source. We show that the performance of an ASE source is substantially superior compared to a laser source.

CLEO: Science & Innovations

SF1G • Devices for Communications—Continued

SF1G.3 • 09:00 **Invited**

Coherent Optical Communications with Microresonator Frequency Combs, Victor Torres Company¹; ¹Chalmers Tekniska Högskola, Sweden. In this talk I will describe recent system-level communication experiments based on wavelength division multiplexing using advanced modulation formats and microresonator frequency combs as multi-carrier light sources.

SF1G.4 • 09:30

Theoretical investigation of a Si RRM assisted SSB-OFDM modulator operated with a semiconductor MLL, Jovana Nojic¹, Saeed Sharif Azadeh¹, Juliana Müller¹, Xu Sun², Florian Merget¹, Jeremy Witzens¹; ¹Inst. of Integrated Photonics, RWTH Aachen Univ., Germany; ²Songshanhu Jiawoo Base, Huawei Technologies Co. Ltd, China. Performance of a transmitter with RRM-assisted SSB-OFDM modulator and semiconductor MLL is modeled. Phase noise related penalties arise even in back-to-back configuration and significantly modify the optimum RRM bias point.

SF1H • Phase-matching Techniques—Continued

SF1H.5 • 09:00 **Invited**

Quasi-Phase-matched Semiconductors for Nonlinear Optical Frequency Conversion, Peter G. Schunemann¹; ¹BAE Systems Inc, USA. The orientation-patterned compound semiconductors - OP-GaAs and OP-GaP - exhibit the highest nonlinear coefficients and broadest infrared transparency ranges among all quasi-phase-matched crystals. Processing and device performance are improving, and next-generation materials show great promise.

SF1H.6 • 09:30

Measurement of d-coefficients of CdSiP₂ using Non-phase-matched Second Harmonic Generation of 2700 to 4700 nm Radiation, Shekhar Guha¹, Joel Murray¹, Jean Wei¹, Kevin T. Zawilski², Peter G. Schunemann²; ¹US Air Force Research Lab, USA; ²BAE Systems, USA. A novel experimental approach, based on re-derivation of the Maker-fringe theory, yielded values d_{14} and d_{36} coefficients of CdSiP₂ using a picosecond duration laser tuned between 2700 and 4700 nm.

SF1H.7 • 09:45

High Efficiency Second Harmonic Generation in Gallium Phosphide Ring Resonators on Oxide, Alan Logan¹, Michael Gould¹, Emma Schmidgall¹, Karine Hestroffer³, Zin Lin⁴, Weiliang Jin², Arka Majumdar¹, Fariba Hatami³, Alejandro Rodriguez², Kai-Mei Fu¹; ¹Univ. of Washington, USA; ²Princeton Univ., USA; ³Humboldt-Universität zu Berlin, Germany; ⁴Harvard Univ., USA. Second harmonic conversion from 1550-nm to 775-nm with an efficiency of 400% W^{-1} is demonstrated in quasi-phase matched ring resonators in a gallium phosphide on oxide integrated photonic platform.

2100–10:30 Coffee Break, Concourse Level

Meeting Room
211 A/B

CLEO: Science & Innovations

SF11 • Frequency-Comb-Based Sensing—Continued

SF11.4 • 09:00

High-resolution Dual-comb Spectroscopy with a Free-running All-fiber Laser, Lukasz A. Sterczewski¹, Aleksandra Przewloka², Wawrzyniec Kaszub², Jaroslaw Sotor¹; ¹Faculty of Electronics, Wroclaw Univ. of Science and Technology, Poland; ²Inst. of Electronic Materials Technology, Poland. We use a 1.56 μm computationally-corrected polarization-multiplexed dual-comb laser in free-running mode to measure hydrogen cyanide at 10 Torr. The source with a repetition rate of 142.4 MHz requires only 0.35 W of electrical power.

SF11.5 • 09:15

Quantum Cascade Laser Dual-comb Spectroscopy For Multi-species Detection, Jonas Westberg¹, Lukasz A. Sterczewski^{1,2}, Gerard Wysocki¹; ¹Princeton Univ., USA; ²Faculty of Electronics, Wroclaw Univ. of Science and Technology, Poland. Multi-species detection of analytes in gas-phase by dual-comb spectroscopy using quantum cascade laser frequency combs is demonstrated. These chip-scale, electrically-pumped, semiconductor light sources are highly appealing for portable multi-component chemical spectroscopic sensors.

SF11.6 • 09:30

GHz Dual-comb Spectroscopy with 110-μs Time Resolution, Nazanin Hoghooghi¹, Ryan K. Cole¹, Amanda Makowiecki¹, Gregory B. Rieker¹; ¹Univ. of Colorado Boulder, USA. We demonstrate high-speed dual-comb spectroscopy by spectrally filtering frequency combs using two Fabry-Perot cavities. Using this system, we measured the spectrum of CO with high signal to noise in 110 μs and 1 GHz resolution.

SF11.7 • 09:45

Rapid and high-resolution multidimensional coherent spectroscopy using three frequency combs, Bachana Lomsadze², Brad Smith¹, Steven T. Cundiff¹; ¹Univ. of Michigan, USA; ²Physics, Santa Clara Univ., USA. We present a novel method, tri-comb spectroscopy, which enables the measurement of a high-resolution multidimensional coherent spectrum in 365 ms. This method has the potential to become a field-deployable device for remote-sensing applications.

Meeting Room
211 C/D

SF1J • Plasmonics, Optomechanics, & Metamaterials—Continued

SF1J.4 • 09:00

Dynamical chaos in silicon cavity optomechanics for physically-encrypted secure communications, Jia-Gui Wu^{2,1}, Jaime G. Flor Flores², Qingsong Bai², Jinghui Yang², Xueyan Xiong¹, Mingbin Yu³, Guoqiang Lo³, Shukai Duan¹, Chee Wei Wong²; ¹Southwest Univ., China; ²Fang Lu Mesoscopic Optics and Quantum Electronics Lab, Univ. of California, Los Angeles, USA; ³The Inst. of Microelectronics, 11 Science Park Road, Singapore. We demonstrate pure physical encrypted communication systems using chaos generated on silicon optomechanical nanocavities. Our chaos synchronization correlation coefficient is high at 0.97, and the Mb/s NRZ messages were decoded with a critical 3×10^{-5} BER.

SF1J.5 • 09:15

Ultrasonic acousto-optical receivers based on optomechanical resonance and oscillation, Ke Huang¹, Mani Hossein-Zadeh¹; ¹Univ. of New Mexico, USA. We experimentally demonstrate that radiation pressure based optomechanical interaction in high-Q cavities can be exploited for high sensitivity acousto-optical transduction and direct signal down-conversion in underwater ultrasonic communication links and sensor networks.

SF1J.6 • 09:30

Waveguide-to-waveguide directional coupling beyond a free space wavelength, Orad Reshef¹, Codey Nacker¹, Jeremy Upham¹, Robert Boyd^{1,2}; ¹Univ. of Ottawa, Canada; ²Univ. of Rochester, USA. We investigate the use of integrated zero-index metamaterials in directional coupling. Ring resonators incorporating these materials exhibit critical coupling over larger separations than is possible with evanescent coupling, even exceeding the free space wavelength.

SF1J.7 • 09:45

High Tolerance of Metamaterial Waveguides to Fabrication Variations, Moshe Zadka¹, Utsav D. Dave¹, Michal Lipson¹; ¹Columbia Univ., USA. We demonstrate that silicon metamaterial waveguides have a high tolerance to large fabrication variations. We measured only a 5% drop in the Quality factor of a resonator with a metamaterial segment compared to a 40% drop for a wire waveguide segment, with a 50 nm discontinuity.

Meeting Room
212 A/B

CLEO: Applications & Technology

AF1K • Structural Monitoring—Continued

AF1K.4 • 09:00

Simple High Performance Polarimetric Fiber-Optic Current Sensor Operated with Different Types of Sensing Fiber, Klaus M. Bohnert¹, Andreas Frank¹, Lin Yang¹, Xun Gu³, Georg M. Müller²; ¹Corporate Research, ABB Switzerland Ltd, Switzerland; ²Grid Automation, ABB Switzerland Ltd, Switzerland; ³High Voltage Products, ABB Switzerland Ltd, Switzerland. We investigate a simple polarimetric fiber-optic current sensor with an integrated-optic polarization splitter/combiner for interrogation and coils from spun birefringent fiber and low birefringence fiber. We demonstrate accuracy to within 0.2% between -40 and 85°C.

AF1K.5 • 09:15

Correlation-domain distributed temperature sensing based on enhanced forward Brillouin scattering, Neisei Hayashi¹, Yosuke Mizuno², Kentataro Nakamura², Chao Zhang¹, Lei Jin¹, Sze Y. Set¹, Shinji Yamashita¹; ¹The Univ. of Tokyo, Japan; ²Tokyo Inst. of technology, Japan. We demonstrate distributed temperature sensing based on enhanced forward Brillouin scattering using a correlation-domain technique. A 104-m-long heated section is clearly detected in a 397-m-long highly nonlinear fiber.

AF1K.6 • 09:30

Intrinsic Fabry-Perot Interferometer Fiber Sensor by Femtosecond Laser Induced Rayleigh Backscattering Enhancement, Zhaoqiang Peng¹, Mohan Wang¹, Sheng Huang¹, Ran Zou¹, Jingyu Wu¹, Qirui Wang¹, Kevin P. Chen¹; ¹Univ. of Pittsburgh, USA. This paper reports enhanced Rayleigh backscattering points fabricated in single-mode fiber using a femtosecond laser direct-writing technique for the formation of an intrinsic Fabry-Perot interferometer (FPI) fiber sensor. The temperature sensitivity of the FPI is measured as 7.8 pm/°C.

AF1K.7 • 09:45

94.8 Km-Range Direct Detection Fiber Optic Distributed Acoustic Sensor, Faruk Uyar¹, Talha Onat¹, Canberk Unal¹, Tolga Kartaloglu¹, Ibrahim Ozdur¹, Ekmel Ozbay¹; ¹Bilkent Univ. NANOTAM, Turkey. This work demonstrates an ultra-long range direct detection fiber optic distributed acoustic sensor which can detect vibrations at a distance of 94.8 km with 10 m resolution along the sensing fiber.

Meeting Room
212 C/D

CLEO: Science & Innovations

SF1L • Fiber Parametric Sources—Continued

SF1L.5 • 09:00

Broadband Electro-Optic Dual-Comb Interferometer with High-Resolution, Bingxin Xu¹, Xinyu Fan¹, Shuai Wang¹, Zuyuan He¹; ¹Shanghai Jiao Tong Univ., China. We demonstrate a broadband dual-comb interferometer with high resolution. The combs over 1.5 THz bandwidth with a line spacing of 100 MHz are resolved, and the line spacing can be flexibly adjusted.

SF1L.6 • 09:15

High contrast beating 6 lines to a single branch amplifier-free GHz Yb: fiber laser frequency comb, Yuxuan Ma¹, Fei Meng^{1,2}, Yan Wang¹, Aimin Wang¹, Zhigang Zhang¹; ¹Peking Univ., China; ²National Inst. of Metrology, China. A 0.95 GHz amplifier-free Yb: fiber laser frequency comb was used to generate single branch super-continuum and to beat with 6 visible and near-infrared lasers in 35 dB to 42 dB signal-to-noise-ratio.

SF1L.7 • 09:30

Generation of Raman Dissipative Solitons in an External Phosphosilicate All-Fiber Cavity, Denis S. Kharenko^{1,2}, Vlad D. Efremov^{2,1}, Serge A. Babin^{1,2}; ¹IAE SB RAS, Russia; ²Novosibirsk State Univ., Russia. An external-cavity generation of highly-chirped dissipative solitons near 1.3 μm in all-fiber scheme by using a new type of phosphosilicate polarization maintaining fiber is investigated. The pulses were compressed down to 570 fs.

10:00–10:30 Coffee Break, Concourse Level

CLEO: Science & Innovations

SF1M • Fiber-Based Information Process—
Continued

SF1M.4 • 09:00

Multiple Modal and Wavelength Conversion Process of a 10-Gbit/s Signal in a 6-LP-Mode Fiber, Haisu Zhang¹, Marianne Bigot-Astruc², Laurent Bigot³, Pierre Sillard², Julien Fatome¹; ¹CNRS - Université Bourgogne Franche Comté, France; ²Phymian Group, France; ³IRCIICA - Université de Lille, France. We experimentally demonstrate a simultaneous threefold modal and wavelength conversion process of a 10-Gbit/s NRZ signal in a 1.8-km long 6-LP-mode fiber. The principle of operation is based on a phase-matched inter-modal four-wave mixing phenomenon.

SF1N • AI for Integrated Photonics—
Continued

SF1N.4 • 09:00

Optoelectronic Quantum Capacitors for Configurable Neural Photonic Networks, Pouya Dianat¹, Anna Persano², Fabio Quaranta², Adriano Cola², Bahram Nabet¹; ¹Drexel Univ., USA; ²IMM-CNR, Italy. An optoelectronic quantum capacitor is described as a memristive behaving neuron in a dynamically configurable crossbar network. Activation, weight, and bias for each neuron are dynamically controlled with light, gate voltage, and a sampling frequency, respectively.

SF1N.5 • 09:15

SOA-Based Photonic Integrated Deep Neural Networks for Image Classification, Bin Shi¹, Nicola Calabretta¹, Ripalta Stabile¹; ¹Inst. for Photonic Integration, Eindhoven Univ. of technology, Netherlands. We successfully demonstrate classification of three classes of Iris flowers by implementing a trained neural network on an SOA-based InP cross-connect chip. Classification accuracy of 91.6% is achieved after a fine optimization procedure.

SF1N.6 • 09:30

Towards Optical Neural Networks with Fabrication Noise Immunity, Michael Fang^{1,2}, Sasikanth Manipatruni⁴, Casimir Wierzynski³, Amir Khosrowshahi³, Ian Young⁴; ¹Physics, UC Berkeley, USA; ²Redwood Center for Theoretical Neuroscience, UC Berkeley, USA; ³AI Research, Intel, USA; ⁴Components Research, Intel, USA. Optical neural networks (ONNs) can provide breakthrough energy/op and latency compared to GP-GPUS/ASICs. Here we compare two different architectures of ONNs and explore the effect of the imprecision of constituent photonic components.

SF1O • Perovskites—Continued

SF1O.4 • 09:00

Modulation of CH₃NH₃PbBr₃ perovskite microcrystal morphology for WGM and F-P mode lasers, Bobo Li¹; ¹CUHKSZ, China. We focused on the growth of CH₃NH₃PbBr₃ perovskite crystals with shapes of sub-circular and quasi-cubic under different temperatures for WGM and F-P mode lasers. The lasing emissions exhibit low threshold below 20 μJ/cm².

SF1O.5 • 09:15

Simultaneous Inhibition and Redistribution of Spontaneous Emission from Perovskite Photonic Crystals, Songyan Hou^{1,2}, Teo Hang Tong Edwin^{1,2}, Muhammad Danang Birowosuto², Hong Wang^{1,2}; ¹Nanyang Technological Univ., Singapore; ²CINTRA, Singapore. Here, perovskite PhC exhibits both emission rate inhibition and light energy redistribution simultaneously, as a result of light energy redistribution from 2D guided modes to vertical direction, indicating a high intrinsic light extraction efficiency.

SF1O.6 • 09:30

Quantum-confined Stark effect of lead halide perovskite quantum dots in a mixed dimensional van der Waals heterostructure, Chitrleema Chakraborty¹, Hendrik Utzat², Matthias Ginterseder², Hyowon Moon¹, Cheng Peng¹, Mounji Bawendi², Dirk R. Englund¹; ¹Electrical Engineering and Computer Science, MIT, USA; ²Dept. of Chemistry, MIT, USA. We demonstrate quantum-confined Stark effect in perovskite quantum dots by employing a voltage-tunable vertically stacked van der Waals heterostructure with 2D materials. A spectral shift of 10 meV was observed for the exciton peak.

10:00–10:30 Coffee Break, Concourse Level

CLEO: QELS-Fundamental Science

10:30–12:30

FF2A • Photonic Crystals & Periodic Nano Optics

Presider: Sushil Mujumdar;
Tata Institute of Fundamental
Research, India

FF2A.1 • 10:30

High Reflection from a One-Dimensional Array of Graphene Nanoribbons, Nathan Z. Zhao¹, Zhexin Zhao¹, Ian Williamson¹, Salim Boutami¹, Bo Zhao¹, Shanhui Fan¹; ¹Stanford Univ., USA. We show one-dimensional plasmonic systems such as graphene nanoribbons can be used to engineer extremely large bandwidth, high reflectivity resonances. Further, we prove that the underlying concept relies upon the general observation of the lack of Chu-Harrington limit in one-dimensional systems.

FF2A.2 • 10:45

Photonic Crystal Polaritons in 2D Materials, Rahul Gogna¹, Long Zhang¹, Hui Deng¹; ¹Univ. of Michigan, USA. We demonstrate the important properties of transition-metal dichalcogenides strongly coupled to one-dimensional photonic crystals, including the design considerations and dispersions, as well as the possibility for creating multi-wavelength polariton devices on a single chip.

FF2A.3 • 11:00

Free-Space Modulators Based on Dimerized High Contrast Gratings, Stephanie C. Malek¹, Adam C. Overvig¹, Sajan Shrestha¹, Nanfang Yu¹; ¹Columbia Univ., USA. We investigate periodic symmetry breaking as a method of controlling Fano resonances in high contrast dielectric gratings with small device footprints and report experimental and computational demonstrations of free-space modulators based on these dimerized gratings.

10:30–12:30

FF2B • Linear/Non-Linear Metasurfaces

Presider: To Be Announced

FF2B.1 • 10:30

Non-resonant Enhancement of Second-Harmonic Generation in a Dielectric Particle with a Nanostructured Nonlinear Metamaterial Shell, Joong Hwan Bahng¹, Douglas Montjoy², Saman Jahani¹, Nicholas Kotov², Alireza Marandi¹; ¹California Inst. of Technology, USA; ²Univ. of Michigan, Ann Arbor, USA. We demonstrate a new principle for realizing a miniaturized and scalable platform for nonlinear optics using dielectric particles with nanostructured nonlinear metamaterial shells. We show numerical and experimental results of enhanced second-harmonic generation in them.

FF2B.2 • 10:45

All-Optical Tuning of Fano Resonances in Broken-Symmetry GaAs Metasurfaces, Nicholas Karl^{1,2}, Polina Vabishchevich^{1,2}, Sheng Liu^{1,2}, Michael B. Sinclair¹, Gordon Keeler¹, Gregory Peake¹, Igal Brener^{1,2}; ¹Sandia National Labs, USA; ²Center for Integrated Nanotechnologies, Sandia National Labs, USA. We demonstrate ultrafast tuning of Fano resonances in a broken symmetry III-V metasurface using optical pumping. The resonance is spectrally shifted by 10 nm under low pump fluences of < 100 uJ cm⁻².

FF2B.3 • 11:00

Dielectric nanocavities with enhanced local density of states, Sandro Mignuzzi¹, Javier Cambiasso¹, Stefano Vezzoli¹, Simon A. Horsley², William Barnes², Stefan Maier¹, Riccardo Sapienza¹; ¹Imperial College London, UK; ²Exeter Univ., UK. We demonstrate all-dielectric single photon nanocavities by rational design of the local density of optical states. We unravel an inverse design route to strong emitter's decay rate enhancements, near-unity quantum efficiency, and large bandwidth.

10:30–12:30

FF2C • Attosecond Pulse Generation & Characterization

Presider: Wendell T. Hill, III; Univ. of Maryland, USA

FF2C.1 • 10:30

Reduction of Laser-Intensity-Correlated Noise in High-Harmonic Generation, Mikhail Volkov¹, Justinas Pupeikis¹, Christopher Phillips¹, Fabian Schlaepfer¹, Lukas Gallmann¹, Ursula Keller¹; ¹ETH Zurich, Switzerland. We present a scheme for correcting the spectral fluctuations of high-harmonic radiation by monitoring the generating near-infrared pulse energy. We apply this correction in an attosecond transient absorption experiment yielding an improved confidence interval on the mean.

FF2C.2 • 10:45

Temporal Coherence of Linearly and Circularly Polarized High-Harmonics from Silicon, Nicolai Klemke^{1,2}, Nicolas Tancogne-Dejean^{1,3}, Giulio Maria Rossi^{1,2}, Yudong Yang^{1,4}, Roland E. Mainz^{1,2}, Angel Rubio^{1,3}, Franz Kärtner^{1,2}, Oliver D. Mücke^{1,4}; ¹Center for Free-Electron Laser Science CFEL, Deutsches Elektronen Synchrotron DESY, Germany; ²Physics Dept., Univ. of Hamburg, Germany; ³Max Planck Inst. for the Structure and Dynamics of Matter, Germany; ⁴The Hamburg Centre for Ultrafast Imaging CUI, Germany. Circularly polarized high-harmonics can be generated from solids with elliptical and circular driver polarization. We investigate the temporal coherence properties of both cases and compare them to those of linearly polarized high-harmonics.

FF2C.3 • 11:00

Controlling HHG with a Sub-Cycle mJ-Level Parametric Waveform Synthesizer, Yudong Yang^{1,2}, Giulio Maria Rossi^{1,2}, Roland E. Mainz¹, Fabian Scheiba¹, Giovanni Cirmi^{1,2}, Franz Kärtner^{1,2}; ¹Deutsches Elektronen-Synchrotron DESY, Germany; ²The Hamburg Centre for Ultrafast Imaging CUI, Germany. We present HHG driven with a sub-cycle mJ-level parametric waveform synthesizer. The variation of the HHG spectral shape and yield as a function of the relative phase between the synthesizer channels is shown.

10:30–12:30

FF2D • Frequency Comb & Supercontinuum Generation

Presider: To Be Announced

FF2D.1 • 10:30

Advanced dispersion engineering of dispersive waves in Si3N4 microresonators, Fabien Gremion¹, Anton Lukashchuk¹, Maxim Karpov¹, Junqiu Liu¹, Tobias J. Kippenberg¹; ¹EPFL, LPQM, Switzerland. We experimentally demonstrate the possibility of dispersive wave tuning via advanced dispersion engineering. We utilize hybridized modes of concentric coupled resonators for precise control of the dispersion profile.

FF2D.2 • 10:45

Multi-phase-matched satellite frequency combs, Jinghui Yang¹, Shu-Wei Huang², Zhenda Xie³, Mingbin Yu^{3,4}, Dim Lee Kwong³, Chee Wei Wong¹; ¹Univ. of California Los Angeles, USA; ²Univ. of Colorado Boulder, USA; ³Inst. of Microelectronics, Singapore; ⁴Shanghai Inst. of Microsystem and Information Technology, China; ⁵School of Electronic Science and Engineering, Nanjing Univ., China. We report Kerr frequency combs with satellite clusters spanning beyond conventional phase-matching bandwidth. The evolution of the signal and idler satellites at ≈ 1.3 mm and 1.9 mm regimes are detailed. With proper pump parameters, the satellites can span up to one full octave.

FF2D.3 • 11:00

Microresonator frequency comb generation with simultaneous Kerr and electro-optic nonlinearities, Mian Zhang^{1,2}, Christian Reimer¹, Lingyan He¹, Rebecca H. Cheng¹, Mengjie Yu¹, Rongrong Zhu³, Marko Loncar¹; ¹Harvard Univ., USA; ²HyperLight Corporation, USA; ³Electrical Engineering, Zhejiang Univ., China. We experimentally investigate electro-optic (EO) modulation of a dispersion engineered lithium niobate microring resonator under a strong optical pump. We show that EO modulated Kerr comb spectrum is significantly broader than with either Kerr or EO nonlinearity alone.

Executive Ballroom
210E

CLEO: Science &
Innovations

10:30–12:30
SF2E • Ultrafast Phenomena
President: Guangjin Ma, DESY,
Germany

SF2E.1 • 10:30 **Tutorial**
Harnessing Quantum Light Science for Applications in Materials and Nano Science, Margaret M. Murnane¹; ¹Univ. of Colorado at Boulder, USA. High harmonic generation produces polarization-shaped extreme-ultraviolet and soft X-ray beams that can uncover the fastest charge, spin and lattice dynamics in quantum materials, and enable high-contrast non-destructive imaging of opaque materials at the wavelength limit.



Dr. Margaret Murnane is Director of the US National Science Foundation STROBE Science and Technology Center on functional nanoimaging, a Fellow at JILA and a member of the Departments of Physics and Electrical and Computer Engineering at the University of Colorado. She received her B.S and M.S. degrees from University College Cork, Ireland, and her Ph.D. degree in physics from the University of California at Berkeley in 1989. She runs a joint research group with her husband, Prof. Henry Kapteyn. Margaret's research interests have been in ultrafast laser and x-ray science. She is a Fellow of the American Physical Society, The Optical Society and the AAAS. Her honors include the Maria Goeppert-Mayer Award of the American Physical Society, a John D. and Catherine T. MacArthur Fellowship, and election to the National Academy of Sciences, the American Academy of Arts and Sciences, the American Philosophical Society, and the Royal Irish Academy. She has done extensive service, including serving as Chair of the President's Committee for the (US) National Medals of Science. She is the 2017 recipient of the Ives Medal/ Quinn Prize of The Optical Society—the OSA's highest honor.

Executive Ballroom
210F

Joint

10:30–12:30
JF2F • Symposium on Deep-
learning Photons: Where
Machine Learning & Photonics
Intersect II

JF2F.1 • 10:30 **Invited**
Phase Compensation for Continuous Variable Quantum Key Distribution, Hou-Man Chin¹, Darko Zibar¹, Nitin Jain¹, Tobias Gehring¹, Ulrik Andersen¹; ¹Technical Univ. of Denmark, Denmark. The tracking and compensation of phase noise is critical to reducing excess noise for continuous variable quantum key distribution schemes. This work demonstrates the effectiveness of unscented Kalman filter for phase noise compensation.

JF2F.2 • 11:00 **Invited**
Deep Learning in Optical Microscopy and Image Reconstruction, Aydogan Ozcan¹; ¹Univ. of California Los Angeles, USA. We will discuss recently emerging applications of the state-of-art deep learning methods on optical microscopy and microscopic image reconstruction, which enable new transformations among different modalities of microscopic imaging, driven entirely by image data. We believe that deep learning will fundamentally change both the hardware and image reconstruction methods used in optical microscopy and sensing in a holistic manner.

Executive Ballroom
210G

CLEO: Science & Innovations

10:30–12:30
SF2G • Laser-Based Diagnostics
for Material Processing
President: Ed Kinzel; Uni. of Notre
Dame, USA

SF2G.1 • 10:30
Enantio-enrichment of Racemic Films Using Circularly Polarized Femtosecond Pulses, Katrin E. Oberhofer¹, Farinaz Mortaheb², Johann Riemensberger¹, Florian Ristow¹, Reinhard Kienberger¹, Ulrich K. Heiz², Hristo Iglev¹, Aras Kartouzian²; ¹Physics Dept., Technical Univ. of Munich, Germany; ²Catalysis Research Center, Chair of Physical Chemistry, Technical Univ. of Munich, Germany. Circularly polarized laser pulses are used to desorb chiral molecules enantioselectively from an achiral surface implicating the quantum mechanical nature of this process, moreover demonstrating a new method for enantio-enrichment and enantio-separation.

SF2G.2 • 10:45
Two Dimensional Film Printing by Blister-Based Laser-Induced Forward-Transfer, Nathan T. Goodfriend¹, Oleg Nerushev², Wenshuo Xu³, Mitsuhiro Okada⁴, Ryo Kitaura⁴, Jamie Warner³, Hisanori Shinohara⁴, Alexander Bulgakov¹, Eleanor Campbell^{2,5}, Nadezhda M. Bulgakova¹; ¹HiLASE, Czechia; ²School of Chemistry, EastCHEM, UK; ³Dept. of Materials, Univ. of Oxford, UK; ⁴Dept. of Chemistry, Nagoya Univ., Japan; ⁵Konkuk Univ., South Korea (the Republic of). An investigation into the feasibility of using ultrashort laser pulses to induce deformations on a donor film coated in 2 dimensional materials as a printing technique for the contactless and impurity-free fabrication of devices based on these materials.

SF2G.3 • 11:00 **Invited**
Non-Equilibrium Structural Dynamics in Laser-Driven Materials Studied with Time-Resolved Diffraction, Klaus Sokolowski-Tinten¹; ¹Universität Duisburg-Essen, Germany. This talk will discuss some of our recent results on using time-resolved diffraction with femtosecond X-ray or electron pulses to investigate the non-equilibrium structural response of materials upon intense ultrafast optical excitation.

Executive Ballroom
210H

10:30–12:30
SF2H • Active & Reconfigurable
Devices
President: Vivek Shrestha; Univ. of
Melbourne, Australia

SF2H.1 • 10:30 **Invited**
Topological Phenomena in Active Photonic Platforms, Mercedeh Khajavikhan¹; ¹Univ. of Central Florida, CREOL, USA. Active photonics provides a unique set of opportunities for realizing and harvesting topological phenomena in optics. We will review the recent advances in this field and discuss some of the challenges ahead.

SF2H.2 • 11:00
Photon-level tuning of a high-Q lithium niobate photonic crystal nanocavity, Mingxiao Li¹, Hanxiao Liang¹, Rui Luo¹, Yang He¹, Jingwei Ling¹, Qiang Lin¹; ¹Univ. of Rochester, USA. We report an all-optical approach for extremely efficient tuning of a high-Q lithium niobate photonic crystal nanocavity, with a significant resonance tuning rate of 110-MHz/photon.

Friday, 10:30–12:30

Meeting Room
211 A/B

CLEO: Science & Innovations

10:30–12:30

SF21 • High Q Cavity, Resonators Application

Presider: Haisheng Rong; Intel Corporation, USA

SF21.1 • 10:30

Tunable Optomechanical Cavity Filters, Marcel W. Pruessner¹, Doewon Park¹, Brian Roxworthy¹, Dmitry Kozak¹, Todd Stievater¹, Nathan Tyndall¹, William Rabinovich¹; ¹US Naval Research Lab, USA. Cavity optomechanics enables large-scale index tuning (Δn_{eff}). However, most demonstrations exhibited small Δn_{eff} , or have not considered optical loss at large Δn_{eff} . We demonstrate Δn_{eff} -tuning using gradient electric forces and analyze optomechanically-induced loss and mitigation.

SF21.2 • 10:45

High Q resonators in the GaAs and AlGaAs on insulator platform, Lin Chang¹, Andreas Boes^{1,2}, Paolo Pintus¹, Jon Peters¹, MJ Kennedy¹, Warren Jin¹, Xiaowen Guo¹, Supeng Yu³, Scott B. Papp³, John Bowers¹; ¹Univ. of California Santa Barbara, USA; ²MIT, Austria; ³NIST, USA. We demonstrated a low loss gallium arsenide (GaAs) and aluminum gallium arsenide (AlGaAs) on insulator platform by heterogenous integration. The ring resonators on this platform exhibit record high intrinsic quality factors above 1×10^6 .

SF21.3 • 11:00

Invited

Explore Whispering-gallery Resonators for a Versatile Sensor Platform, Lan Yang¹; ¹Washington Univ. in St Louis, USA. I will talk about opportunities of whispering-gallery-mode resonators tailored in different geometries for various sensing applications. Their potential as a new generation of sensing platform for the Internet of Things applications will be discussed.

Meeting Room
211 C/D

10:30–12:30

SF2J • Lithium Niobate & Perovskite Photonic Devices

Presider: Christian Reimer; HyperLight Corporation, USA

SF2J.1 • 10:30

Ultra-Low Loss Integrated Lithium Niobate Photonics in Visible Wavelengths, Boris Desiatov¹, Amirhassan Shams-Ansari¹, Mian Zhang^{1,2}, Cheng Wang³, Marko Loncar¹; ¹Harvard Univ., USA; ²HyperLight Corporation, USA; ³Dept. of Electronic Engineering, City Univ. of Hong Kong, Hong Kong. We demonstrate a low loss integrated photonic platform in lithium niobate in the visible wavelength range. We show microring resonators with a quality factor of 10^7 and gigahertz intensity modulators.

SF2J.2 • 10:45

Perovskite Micro Laser arrays using Scalable Lithography: Towards Integrated Perovskite Photonics, Ofer Bar-On¹, Philipp Brenner², Uli Lemmer², Jacob Scheuer¹; ¹Tel-Aviv Univ., Israel; ²Karlsruhe Inst. of Technology, Germany. Low threshold Perovskite micro lasers are fabricated and characterized. These devices are realized using the first complete top-down lithography process of metal halide perovskites which presents a crucial step towards integrated perovskite photonics.

SF2J.3 • 11:00

Low-loss waveguides in Y-cut thin film lithium niobate for acousto-optic applications, Lutong Cai¹, Gianluca Piazza¹; ¹Carnegie Mellon Univ., USA. The dependence of waveguide loss on buried oxide thickness in Y-cut lithium niobate on insulator (an ideal platform for acousto-optic devices) was investigated. Waveguide loss of as low as 0.33 dB/cm was measured.

Meeting Room
212 A/B

CLEO: Applications & Technology

10:30–12:30

AF2K • Spectrometers & Wavelength Metrology

Presider: Kara Peters; North Carolina State University, USA

AF2K.1 • 10:30

Microresonator Spectrometer Using Counter-propagating Solitons, Qi-Fan Yang¹, Boqiang Shen¹, Herning Wang¹, Minh Tran², Zhewei Zhang¹, Kiyoul Yang¹, Lue Wu¹, Chengying Bao¹, John Bowers², Amnon Yariv¹, Kerry J. Vahala¹; ¹T. J. Watson Lab of Applied Physics, California Inst. of Technology, USA; ²Dept. of Electrical and Computer Engineering, Univ. of California, Santa Barbara, USA. A spectrometer is demonstrated using self-locked counter-propagating soliton frequency combs in a high-Q silica microresonator. Fast tuning laser waveforms and molecular absorption features are measured with kiloHertz to MegaHertz resolution.

AF2K.2 • 10:45

All-fiber Electro-optic Frequency Comb for Near-Infrared Astronomical Spectrograph Calibration, Ewelina Obrzud^{1,2}, Victor Brasch¹, Steve Lecomte¹, François Wildi², François Bouchy², Francesco Pepe², Tobias Herr¹; ¹Centre Suisse d'Electronique et de Micro, Switzerland; ²Astronomy, Univ. of Geneva, Switzerland. A turn-key, all-fiber 14.5 GHz electro-optic modulation-based near-infrared frequency comb spanning 700 nm for astronomical spectrograph calibration is developed, capable of providing radial velocity calibration with a precision of < 10 cm/s, relevant for exoplanet searches.

AF2K.3 • 11:00

Increasing the Range and Precision of Integrated Wavemeters, Enrique Martin-Lopez¹, David Bitauld¹; ¹Nokia Bell Labs, UK. We demonstrate an integrated wavemeter concept enabling high and wavelength-independent precision over increased spectrum ranges while avoiding ambiguities from the spectrally periodic response. This versatile device can significantly improve the control of integrated tunable lasers.

Meeting Room
212 C/D

CLEO: Science & Innovations

10:30–12:30

SF2L • MID-IR Fiber Sources

Presider: Maria Chernysheva; Leibniz Institute of Photonic Technology, Germany

SF2L.1 • 10:30

Ultrafast mid-infrared fiber lasers beyond 3 μm , Simon Duval^{1,2}, Yuchen Wang^{3,4}, Louis-Rafaël Robichaud^{1,2}, Michel Olivier^{1,5}, Frédéric Jobin¹, Jean-Christophe Gauthier¹, Pascal Paradis¹, Vincent Fortin¹, Paolo Laporta^{3,4}, Martin Bernier¹, Michel Piché¹, Gianluca Galzerano^{3,4}, Réal Vallée¹; ¹Université Laval, Canada; ²Femtum inc., Canada; ³Dipartimento di Fisica, Politecnico di Milano, Italy; ⁴Istituto di Fotonica e Nanotecnologie, Italy; ⁵Département de physique, Cégep Garneau, Canada. We present recent demonstrations of fiber oscillators and amplifiers based on erbium- and dysprosium-doped fluoride fibers that enable the generation of ultrashort pulses above 3 μm .

SF2L.2 • 11:00

~ 3.5 μm self-Q-switched Er³⁺:ZBLAN fiber laser stabilized by an ASE seeded pump source, Jun Liu¹, Jiadong Wu¹, Pinghua Tang¹, Yu Chen¹, Dianyuan Fan¹; ¹Shenzhen Univ., China. We report on a ~ 3.5 μm highly stable self-Q-switched Er³⁺:ZBLAN fiber laser based on a temporally stable ASE seeded pump source. The pulsing dynamics are carefully investigated which can help facilitate their potential applications.

Joint

10:30–12:30

JF2M • Professional Development Session II

Optimizing Career Paths in Optics: the Guide for Young Professionals

Career planning is very important for young professionals in optics. Different career paths are available, each with its own requirements, challenges, and rewards. We invite young professionals to hear firsthand from their more seasoned colleagues about their jobs. Practical questions on how to excel in an optics-related career will be answered. What does it take to get a foot in the door at your target workplace? How to network? Who makes hiring decisions, and how? What qualities are the most sought? What does it get not to get stuck in your career? How could your typical workday look like? What are the most common challenges in maintaining the work-life balance?

Panelists:

J. Stewart Aitchison, *University of Toronto, Canada*
Sterling Backus, *KMLabs, USA*
Ben Eggleton, *University of Sydney, USA*
Tara Fortier, *National Institute of Standards and Technology, USA*
Michael Mielke, *Iradion Laser Inc., USA*
Irina Novikova, *College of William and Mary, USA*
Sergey Polyakov, *National Institute of Standards and Technology, USA*
Stephanie Tomasulo, *U.S. Naval Research Laboratory, USA*

CLEO: Science & Innovations

10:30–12:30

SF2N • RF Photonics

President: Ozdal Boyraz; *Univ. of California Irvine, USA*

SF2N.1 • 10:30

High-Speed Photodetection and Microwave Generation in a Sub-100 mK Environment, Josue Davila-Rodriguez¹, John D. Teufel¹, José A. Aumentado¹, Xiaojun Xie³, Joe C. Campbell³, Scott A. Diddams^{1,2}, Franklyn Quinlan^{1,2}; ¹NIST, USA; ²Dept. of Physics, *Univ. of Colorado, USA*; ³Dept. of Electrical and Computer Engineering, *Univ. of Virginia, USA*. We perform microwave generation via high-speed photodetection at a temperature of 20 mK. Shot noise-limited detection with high linearity was obtained, compatible with continued scaling of the control and readout of superconducting quantum information systems.

SF2N.2 • 10:45

Broadband Local Oscillator Free Photonic Microwave Mixer based on a Coherent Kerr Micro-Comb Source, Jiayang Wu¹, Xingyuan Xu¹, Mengxi Tan¹, Thach Nguyen², Sai Chu³, Brent Little⁴, Roberto Morandotti⁵, Arnan Mitchell², David Moss¹; ¹Swinburne Univ. of Technology, *Australia*; ²MIT Univ., *Australia*; ³City Univ. of Hong Kong, *China*; ⁴Chinese Academy of Science, *China*; ⁵INSR-Énergie, *Matériaux et Télécommunications, Canada*. We demonstrate a photonic microwave mixer based on an integrated micro-comb source. We achieve an operation bandwidth of over 40 GHz with a conversion efficiency of -6.8 dB and a spurious suppression ratio of 43.5 dB.

SF2N.3 • 11:00

Experimental Characterization of Low-Latency Multiple and Tunable Delays of Wideband Analog LFM Signal Using Concatenated Linearly Chirped and Sampled FBGs, Ahmed Almaman¹, Yinwen Cao¹, Fatemeh Alishahi¹, Ahmad Fallahpour¹, Long Li¹, Peicheng Liao¹, Kaiheng Zou¹, Shlomo Zach², Nadav Cohen², Moshe Tur², Alan E. Willner¹; ¹Univ. of Southern California, USA; ²School of Electrical Engineering, *Tel Aviv Univ., Israel*. Concatenated chirped and sampled fiber Bragg gratings are used to simultaneously generate multiple wavelength-tunable delayed versions of a wide bandwidth (10GHz) analog linear-frequency-modulated (LFM) pulse. We measured peak sidelobe level (PSL) > 31 dB.

10:30–12:30

SF2O • Optoelectronic Materials

President: Oana Malis; *Purdue Univ., USA*

SF2O.1 • 10:30

Electrical Characterization of Solar-Blind Deep-Ultraviolet ($\text{Al}_{0.28}\text{Ga}_{0.72}\text{O}_3$) Schottky Photodetectors Grown on Silicon by Pulsed Laser Deposition, Nasir Alfaraj¹, Kuang-Hui Li¹, Chun Hong Kang¹, Davide Priante¹, Laurentiu Braic¹, Zaibing Guo¹, Tien Khee Ng¹, Xiaohang Li¹, Boon S. Ooi¹; ¹King Abdul-lah Univ of Sci & Technology, *Saudi Arabia*. This study reports on $(\text{Al}_{0.28}\text{Ga}_{0.72})_2\text{O}_3$ -based ultraviolet-C Schottky metal-semiconductor-metal and metal-insulator-metal photodetectors with peak responsivities of 1.17 and 0.40 A/W, respectively, for an incident-light wavelength of 230 nm at 2.50 V reverse-bias.

SF2O.2 • 10:45

The Aging Study for Fine Pitch Quantum-Dot Array on LEDs, Yu-Ming Huang¹, Kai-Ling Liang², Yu-Yun Cho¹, Shun-Chieh Hsu¹, Wei-Hung Kuo², Chung-Ping Huang¹, Hao-Chung Kuo³, Yen-Hsiang Fan², Chien-Chung Lin¹; ¹National Chiao-Tung Univ., *Taiwan, Taiwan*; ²Industrial Technology Research Inst. of Taiwan, *Taiwan*; ³National Chiao-Tung Univ., *Taiwan*. In this paper, we fabricated the photoresist mold whose pitch is smaller than 15 mm on light-emitting diode and printed two different cadmium-based quantum dots. Also, we burn-in the LED to compare their lifetime which are pasted barrier film by two different methods.

SF2O.3 • 11:00

Nanoscale inspection of GaN LED devices using $g^{(2)}$ cathodoluminescence imaging, Toon Coenen^{2,1}, Sophie Meuret², Yong-Ho Ra³, Zetian Mi⁴, Albert Polman²; ¹Delmic, *Netherlands*; ²Center for nanophotonics, *AMOLF, Netherlands*; ³Dept. of Electrical and Computer Engineering, *McGill Univ., Canada*; ⁴Dept. of Electrical Engineering and Computer Science, *Univ. of Michigan, USA*. We apply a combination of hyperspectral cathodoluminescence and $g^{(2)}$ imaging to bulk and nanostructured LED materials. From these measurements we extract both excited state lifetimes and the probability of excitation of a single primary electron.

CLEO: QELS-Fundamental Science

FF2A • Photonic Crystals
& Periodic Nano Optics—
Continued

FF2A.4 • 11:15

Beyond the Goos-Hänchen Effect: Resonance-Induced Spatial Reshaping and its Application in Measuring Resonance Linewidth, Wei Zhang¹, Aaron Charous¹, Masaya Nagai², Daniel M. Mittleman¹, Rajind Mendis¹; ¹*School of Engineering, Brown Univ., USA*; ²*Graduate School of Engineering Science, Osaka Univ., Japan*. We study the spatial distribution of a beam as it interacts with a planar resonator. Our result encompasses the familiar Goos-Hänchen effect and more complicated scenarios, and can be used for measuring resonance linewidth.

FF2A.5 • 11:30

Symmetry-Broken High Contrast Gratings, Adam C. Overvig¹, Stephanie Malek¹, Sajan Shrestha¹, Nanfang Yu¹; ¹*Columbia Univ., USA*. We develop an exhaustive catalogue detailing the behavior of normally incident light on symmetry-broken high-contrast gratings. This provides a high-level roadmap for designing compact devices with sharp spectral features within standard nanofabrication constraints.

FF2A.6 • 11:45

Strong Coupling and Bound States in the Continuum in Hybrid Photonic-Plasmonic Structure, Shaimaa Azzam¹, Vladimir M. Shalaev¹, Alexandra Boltasseva¹, Alexander Kildishev¹; ¹*Purdue Univ., USA*. Strong coupling of the photonic and plasmonic modes in a hybrid structure leads to the formation of bound states in the continuum (BICs) with exceptionally high quality factors.

FF2B • Linear/Non-Linear
Metasurfaces—Continued

FF2B.4 • 11:15

Nonlinear Generation of Vacuum Ultraviolet Light with an All-Dielectric Metasurface, Ming Lun Tseng^{2,1}, Michael Semmlinger³, Jian Yang³, Ming Zhang³, Chao Zhang³, Peter Nordlander³, Naomi Halas³, Din Ping Tsai²; ¹*National Taiwan Univ., Taiwan*; ²*Research Center for Applied Science, Academia Sinica, Taiwan*; ³*Dept. of Electrical and Computer Engineering, Rice Univ., USA*. An all-dielectric metasurface device for nonlinear generation of coherent vacuum ultraviolet will be reported. The metasurface made has a resonance at 394 nm and can efficiently generate vacuum ultraviolet under ultrafast laser illumination.

FF2B.5 • 11:30

Optical Needle with Ultra-Small Resolution Enabled by Integrated Metalens, Haowen Liang¹, Qian Sun¹, Yuhao Ren¹, Juntao Li¹; ¹*Sun Yat-sen Univ., China*. We present a metalens composed of integrated metasurfaces to achieve an optical needle with ultra-small optical resolution of $\lambda/5$. This metalens is promising for non-intrusive, fair-field super-resolution optical imaging.

FF2B.6 • 11:45

Terahertz Single-Pixel Imaging System with Electrically Tunable Metamaterial Spatial Light Modulator, Wonwoo Lee¹, Hyunseung Jung², Hyunwoo Jo³, Moon Sung Kang³, Hojin Lee^{1,2}; ¹*Dept. of Information Communication, Materials, and Chemistry Convergence Technology, Soongsil Univ., South Korea (the Republic of)*; ²*School of Electronic Engineering, Soongsil Univ., South Korea (the Republic of)*; ³*Dept. of Chemical Engineering, Soongsil Univ., South Korea (the Republic of)*. We propose a novel terahertz single-pixel imaging system with active metamaterial spatial light modulator using ion-gel gating graphene. From the experimental results, we confirmed the reconstructed image was 93% of agreement with the real image.

FF2C • Attosecond
Pulse Generation &
Characterization—Continued

FF2C.4 • 11:15

Attosecond Phase Retrieval by Deep Neural Network, Jonathon White¹, Zenghu Chang¹; ¹*Univ. of Central Florida, USA*. A deep neural network is used for attosecond pulse phase retrieval. Combination of supervised and unsupervised learning show potential for a fast and accurate phase retrieval method without making the central momentum approximation.

FF2C.5 • 11:30

Generation and Characterization of Attosecond Pulses from an X-ray Free-electron Laser, Siqi Li¹, Philipp Rosenberger², Elio Champenois³, Taran Driver⁴, Phil Bucksbaum³, Ryan Coffee⁵, Averell Gattton⁵, Gregor Hartmann⁶, Wolfram Helm⁷, Zhirong Huang¹, Jonas Knurr³, Matthias Kling^{2,3}, Ming-Fu Lin⁵, James MacArthur¹, Timothy Maxwell¹, Megan Nantel¹, Adi Natan³, Jordan O'Neal³, Niranjana Shivaram⁵, Peter Walter⁵, Thomas Wolf³, James Cryan^{3,5}, Agostino Marinelli¹; ¹*SLAC National Accelerator Lab, USA*; ²*Dept. of Physics, Ludwig-Maximilians-Universität, Germany*; ³*Stanford PULSE Inst., SLAC National Accelerator Lab, USA*; ⁴*Imperial College London, UK*; ⁵*Linac Coherent Light Source, SLAC National Accelerator Lab, USA*; ⁶*Institut für Physik und CINSaT, Universität Kassel, Germany*; ⁷*Max Planck Inst. of Quantum Optics, Germany*. In this report we discuss the generation of attosecond soft-x-ray pulses at Linac Coherent Light Source (LCLS). We measure the attosecond pulses in time domain by the method of angular streaking.

FF2D • Frequency Comb &
Supercontinuum Generation—
Continued

FF2D.4 • 11:15

Experimental evidence of gain-through-loss mechanism in passive fiber ring cavities: toward tunable frequency comb generation, Arnaud Mussot¹, Matteo Conforti¹, Alexandre Kudlinski¹, Florent Bessin¹, Auro Peregro², Sergei K. Turitsyn², Kestutis Staliunas³; ¹*Univ. of Lille Laboratoire PhLAM, France*; ²*Aston Inst. of Photonic Technologies, Aston Univ., UK*; ³*Instituto Catalana de Recerca i Estudis Avançats, Spain*. We experimentally demonstrate a novel method based on the gain-through-losses modulation instability process to generate frequency combs with tunable repetition rate in a normal dispersion externally driven passive fibre resonator.

FF2D.5 • 11:30

Overcoming Spectral Stagnation in Supercontinuum Generation, Haider Zia¹, Niklas M. Lüpken², Tim Hellwig², Carsten Fallnich^{2,1}, Klaus J. Boller^{1,2}; ¹*Universiteit Twente, Netherlands*; ²*Westfälische Wilhelms-Universität Münster, Germany*. We present a new approach that increases bandwidth of supercontinuum generation by alternating the sign of dispersion along the interaction length, bypassing mechanisms that limit bandwidth in typical approaches. The method should be particularly suited for fiber and integrated optical waveguides.

FF2D.6 • 11:45

30 GHz Supercontinuum Generation for Astronomy with Efficient SiN Waveguides, Connor Fredrick^{1,2}, Andrew J. Metcalfe¹, Daniel Hickstein², David R. Carlson², Wesley Brand^{1,2}, Kartik Srinivasan³, Scott Papp^{2,1}, Scott A. Diddams^{2,1}; ¹*Physics, Univ. of Colorado at Boulder, USA*; ²*Time and Frequency, National Inst. of Standards and Technology, USA*; ³*Microsystems and Nanotechnology, National Inst. of Standards and Technology, USA*. Using silicon nitride waveguides we demonstrate octave spanning spectra at a 30 GHz repetition rate with less than 20 pJ of total pulse energy at 1 μ m. This high efficiency supercontinuum enables broadband and robust frequency comb generation for astronomical spectrograph calibration.

Executive Ballroom
210E

CLEO: Science &
Innovations

SF2E • Ultrafast Phenomena—
Continued

SF2E.2 • 11:30

Spectral Correlations of Phase Noise in Ultrabroadband Femtosecond Lasers, Andreas Liehl¹, Philipp Sulzer¹, David Fehrenbacher¹, Denis Seletskiy^{1,2}, Alfred Leitenstorfer¹; ¹Dept. of Physics and Center for Applied Photonics, Univ. of Konstanz, Germany; ²Dept. of Engineering Physics, Polytechnique Montréal, Canada. Phase noise in mode-locked Er:fiber systems shows strong correlations emerging from broadband nonlinear-optical processes. Our fundamental insights are key to maximize the quality of passively phase-stable frequency combs and single-cycle pulse trains.

SF2E.3 • 11:45

Soliton explosions induced by soliton fusion in a mode-locked fibre laser, Heping Zeng¹, Junsong Peng¹; ¹East China Normal Univ., China. We reveal that soliton fusion can induce soliton explosions in a mode-locked fibre laser, using real-time measurement techniques. Two solitons differing in their central wavelengths due to chirp explode as they approach each other.

Executive Ballroom
210F

Joint

JF2F • Symposium on Deep-
learning Photons: Where
Machine Learning & Photonics
Intersect II—Continued

JF2F.3 • 11:30

Deep Learning Reconstruction of Ultrashort Laser Pulses and Ptychographic Data from Ambiguous Measurements, Tom Zahavy¹; ¹EE, Technion, Israel. We propose a deep learning approach to reconstruct ultrashort laser pulses and ptychographic data from optical measurements, based on optimization and calibration of ambiguities in the measurement system. We demonstrate, numerically and experimentally, superior performance and robustness to noise.

Invited

Executive Ballroom
210G

CLEO: Science & Innovations

SF2G • Laser-Based Diagnostics
for Material Processing—
Continued

SF2G.4 • 11:30

Measurements of Optical Nonlinearities at Mid-IR Wavelengths Using a Modified Z-Scan Technique, Manuel R. Ferdinandus^{1,2}, Jamie J. Gengler², Michael Tripepi², Carl Liebig²; ¹Air Force Inst. of Technology, USA; ²Air Force Research Lab, USA. We measure the effective optical nonlinearity of polycrystalline zinc selenide and undoped silicon at mid-IR wavelengths using a variant of Z-scan technique that employs a quadrant photodiode to simplify alignment and enhance sensitivity.

SF2G.5 • 11:45

Optical Diagnostics and Hydrophobicity of Femtosecond Laser-Modified Polymers, Deepak Kallepalli^{1,2}, Alan T. Godfrey^{1,2}, Jesse Ratté^{1,2}, Zygmunt Jakubek², Paul B. Corkum^{1,2}; ¹Univ. of Ottawa, Canada; ²National Research Council, Canada. We report optical diagnostic studies of ultrafast laser-induced changes and hydrophobicity in polyimide films when fs-pulses are focused through glass in backward incident geometry at glass-polymer interface.

Executive Ballroom
210H

SF2H • Active & Reconfigurable
Devices—Continued

SF2H.3 • 11:15

Reducing Actuation Nonlinearity of MEMS Phase Shifters for Reconfigurable Photonic Circuits, Pierre Edinger¹, Carlos Errando-Herranz¹, Kristinn B. Gylfason¹; ¹Micro and Nanosystems, KTH Royal Inst. of Technology, Sweden. The low power consumption of MEMS actuators enables large-scale reconfigurable photonic circuits. However, insertion loss and actuation linearity need improvement. By simulations and experiments, we analyze the dominating design parameters affecting linearity and suggest improvements.

SF2H.4 • 11:30

Reversible Switching of Optical Phase Change Materials Using Graphene Microheaters, Carlos A. Ríos Ocampo¹, Yifei Zhang¹, Tian Gu¹, Juejun Hu¹; ¹MIT, USA. We demonstrate, for the first time, non-volatile tunable photonics that makes use of graphene microheaters to thermally switch large-area, low-loss phase change materials. This framework enables scalable nonvolatile integrated photonics and free-space optics applications.

SF2H.5 • 11:45

High-Q Microresonators Integrated with Microheaters on a 3C-SiC-on-Insulator Platform, XI WU¹, Tianren Fan¹, Ali Eftekhar¹, Ali Adibi¹; ¹Georgia Inst. of Technology, USA. We demonstrate thermally-reconfigurable high-Q microring resonators with integrated microheaters on a 3C-SiC-on-insulator platform. A resonance shift of 30 pm/mW is achieved in 40µm-radius microrings (Q₀~88,000 at λ=1550 nm), corresponding to ~50 mW per π phase shift.

Friday, 10:30–12:30

CLEO: Science & Innovations

CLEO: Applications
& TechnologyCLEO: Science &
Innovations

SF2I • High Q Cavity,
Resonators Application—
Continued

SF2J • Lithium Niobate &
Perovskite Photonic Devices—
Continued

AF2K • Spectrometers &
Wavelength Metrology—
Continued

SF2L • MID-IR Fiber Sources—
Continued

SF2J.4 • 11:15
Integrated Electro-Optic Spectrometers on Thin-Film Lithium Niobate, Marc Reig¹, David Pohl¹, Mohammad Madi², Peter Brotzer¹, Fabian Kaufmann¹, Anton Sergeyev¹, Urs Meier², Edoardo Alberti², Rachel Grange¹; ¹ETH Zürich, Switzerland; ²Micos Engineering GmbH, Switzerland. We demonstrate the concept of an integrated waveguide Fourier transform spectrometer on a thin-film lithium niobate platform. The material's electro-optic properties enable on-chip phase-modulations to overcome undersampling restrictions by shifting the evanescently probed standing wave.

AF2K.4 • 11:15
Dual Comb Assisted Spectrum-to-Time Mapping for Rapid Wavelength-encoded Tomography, Yuhua Duan¹, Lei Zhang¹, Xin Dong¹, Xi Zhou¹, Chi Zhang¹, Xinliang Zhang¹; ¹WNLO, China. Leveraging a stimulated Brillouin scattering filter and the Vernier effect between two optical frequency combs, the wavelength-encoded depth information is time mapped and detected with low bandwidth, with both imaging range and imaging speed enhanced.

SF2L.3 • 11:15
High Power Dy-doped Fluoride Fiber Laser Operating Beyond 3 μm , Vincent Fortin¹, Frédéric Jobin¹, Maxence Larose¹, Martin Bernier¹, Réal Vallée¹; ¹Centre d'optique, photonique et laser (COPL), Université Laval, Canada. We demonstrate an entirely monolithic dysprosium-doped fiber laser system producing a record output power of 10 W at 3.24 μm based on in-band pumping at 2.8 μm .

SF2I.4 • 11:30
Waveguide-Coupled Disk Resonators on a Crack-Free Si_3N_4 Film with a Dense Stress Release Pattern, Kaiyi Wu¹, Andrew W. Poon¹; ¹HKUST, Hong Kong. We deposit a crack-free 780nm-thick Si_3N_4 film on a dense stress release pattern on a 100mm silicon wafer. Our fabricated waveguide-coupled 920 μm -radius Si_3N_4 disk resonator reveals a high loaded quality factor of 1.7×10^6 .

SF2J.5 • 11:30
Self-starting lithium niobate soliton microcombs, Yang He¹, Qi-Fan Yang², Jingwei Ling¹, Rui Luo¹, Hanxiao Liang¹, Mingxiao Li¹, Boqiang Shen², Heming Wang², Kerry J. Vahala², Qiang Lin¹; ¹Univ. of Rochester, USA; ²California Inst. of Technology, USA. We report soliton generation in a high-Q lithium niobate resonator. The photo-refractive effect enables self-starting mode locking and is able to produce stable single solitons on demand that feature reversible switching between soliton states.

AF2K.5 • 11:30
Scalable Bandwidth All-fiber Spectrometer using Spatial Multiplexing, Ziyi Meng¹, Zhenming Yu¹, Jianqiang Li¹, Chunjing Yin¹, Tian Zhang¹, Ming Tang², Weijun Tong³, Kun Xu¹; ¹Beijing Univ of Posts & Telecom, China; ²Huazhong Univ. of Science & Technology, China; ³Yangtze Optical Fibre and Cable Limited Company, China. We propose and experimentally demonstrate a large bandwidth and high-resolution all-fiber speckle-based spectrometer using spatial multiplexing, which is constructed by integrating a multicore fiber (MCF) with a multimode fiber (MMF).

SF2L.4 • 11:30 **Invited**
Breaking Through the Wavelength Barrier: State-of-play on Rare-earth Ion Mid-infrared Fiber Lasers at 4-9 μm , Angela Seddon¹, Zhuoqi Tang¹, David Furniss¹, Emma Barney¹, Lukasz Sojka², Trevor Benson¹, Sławomir Sujecki^{2,1}; ¹Univ. of Nottingham, UK; ²Wroclaw Univ. of Technology, Poland. Fiber lasing at 3.9 μm was reported in 1995, but has not yet been demonstrated at 4 μm or longer wavelengths. Rare-earth-ion behavior in low optical-phonon energy hosts is appraised and host confounding issues explored.

SF2I.5 • 11:45
Continuous scanning of a dissipative Kerr-microresonator soliton comb by Pound-Drever-Hall locking, Naoya Kuse¹, Tomohiro Tetsumoto¹, Yi Xuan^{2,3}, Martin E. Fermann¹; ¹IMRA America Inc, USA; ²School of Electrical and Computer Engineering, Purdue Univ., USA; ³Birk Nanotechnology Center, Purdue Univ., USA. We propose and demonstrate a novel technique for continuous and autonomous scanning of a dissipative Kerr-microresonator soliton comb facilitated by Pound-Drever-Hall locking.

AF2K.6 • 11:45
Super-resolution in a compact Fourier Transform InfraRed (FT-IR) spectrometer, Erga Lifshitz¹, Uri Arieli¹, Shahar Katz¹, Assaf Levanon¹, Michael Mrejen¹, Haim Suchowski¹; ¹Tel Aviv Univ., Israel. We introduce a novel method to achieve a compact, high resolution FT-IR spectrometer. By simulation and experimental results we demonstrate that effectively increasing the size of the FT-IR by stitching different interferograms yields spectral super-resolution.

Joint

CLEO: Science & Innovations

JF2M • Professional Development Session
II—Continued

SF2N • RF Photonics—Continued

SF2O • Optoelectronic Materials—
Continued

SF2N.4 • 11:15

Tunable Photonic RF Bandpass Filters based on an 80 Channel Kerr Micro-Comb Source, Mengxi Tan¹, Xingyuan Xu¹, Jiayang Wu¹, Thach Nguyen², Sai Chu³, Brent Little⁴, Roberto Morandotti⁵, Arnan Mitchell², David Moss¹; ¹Swinburne Univ. of Technology, Australia; ²RMIT Univ., Australia; ³City Univ. of Hong Kong, China; ⁴Chinese Academy of Science, China; ⁵INSR-Energie, Matériaux et Télécommunications, Canada. We demonstrate a tunable photonic RF bandpass filter based on a Kerr micro-comb source providing 80 taps in the C-band. We achieve a widely tunable centre frequency ($0.05FSR_{RF} \sim 0.40FSR_{RF}$) and 3-dB bandwidth (0.5 ~ 4.6 GHz).

SF2N.5 • 11:30

Photonic-chip based RF signal detection system with improved bandwidth and sensitivity, zihang zhu^{1,2}, Moritz Merklein^{1,3}, Duk-yong Choi⁴, Khu Vu⁴, Pan Ma⁴, Stephen Maden⁴, Benjamin J. Eggleton^{5,3}; ¹Inst. of Photonics and Optical Science (IPOS), School of Physics, The Univ. of Sydney, Australia; ²The Faculty of Automation & Information Engineering, Xi'an Univ. of Technology, China; ³Sydney Nano Inst. (Sydney Nano), The Univ. of Sydney, Australia; ⁴Laser Physics Centre, Australian National Univ., Australia. We demonstrate on-chip RF signal detection with high sensitivity and broad bandwidth using a Brillouin opto-electronic oscillator. RF signals with power levels as low as -65dBm and a frequency range of 1.5-40 GHz are detected.

SF2N.6 • 11:45

A Photodetector-Driven Coherent RF Array with Wide Tuning Range, Behrooz Abiri², Craig Ives¹, Ali Hajimiri¹; ¹California Inst. of Technology, USA; ²Auspion Inc., USA. A sixteen-element coherent array of wideband spiral antennas driven by photodetectors is presented. The array radiates between 21 and 65 GHz, with -45 dBm of coupled power at 42 GHz.

SF2O.4 • 11:15

UV Laser Resist-Mask Writing for Low-Cost Prototyping of Integrated Optical Devices, Dawson Bonneville¹, Manuel Arturo Méndez-Rosales¹, Henry Frankis¹, Jonathan D. B. Bradley¹; ¹Engineering Physics, Canada. We report on UV-laser photoresist-mask writing as a tool for fabricating integrated optical waveguides. We investigate feature width and roughness under different write settings and apply the technique to realize integrated Si₃N₄ waveguides and devices.

SF2O.5 • 11:30

Optical and Electrical Properties of Phase Change Materials for High-Speed Optoelectronics, Joshua Burrow¹, Pengfei Guo¹, Gary A. Seivison^{1,2}, Heungdong Kwon³, Christopher Perez³, Mehdi Asheghi³, Joshua R. Hendrickson², Andrew Sarangan¹, Kenneth E. Goodson³, Imad Agha^{4,1}; ¹Electro-Optics, Univ. of Dayton, USA; ²Sensors Directorate, Air Force Research Lab, USA; ³Mechanical Engineering, Stanford Univ., USA; ⁴Physics, Univ. of Dayton, USA. By doping Ge₂Sb₂Te₅ phase change material with tungsten, we produce material with improved electrical properties while simultaneously maintaining the optical contrast necessary for light modulation and switching.

SF2O.6 • 11:45

Optically Re-Writable Dynamic Resistors for Optoelectronic and Reconfigurable Computing Applications, Gary A. Seivison¹, Edward C. Ruff¹, Joshua Burrow¹, Pengfei Guo¹, Joshua R. Hendrickson², Andrew Sarangan¹, Imad Agha^{1,3}; ¹Electro-Optics and Photonics, Univ. of Dayton, USA; ²Sensors Directorate, Wright-Patterson Air Force Research Labs, USA; ³Physics, Univ. of Dayton, USA. By employing the phase transition properties of germanium-antimony-telluride, we demonstrate optically rewritable electronic resistors, which can be used to dynamically reconfigure hardwired electronic circuits for optoelectronic and computing applications.

CLEO: QELS-Fundamental Science

FF2A • Photonic Crystals
& Periodic Nano Optics—
Continued

FF2A.7 • 12:00

Optical Pressure on a Structured Surface, Li-Fan Yang¹, Anurup Datta¹, Yu-Chun Hsueh¹, Xianfan Xu¹, Kevin J. Webb¹; ¹Purdue Univ., USA. We experimentally demonstrate for the first time that the optical pressure on a nanostructured surface can exceed that on a planar mirror by virtue of exploiting the third dimension and an asymmetric plasmon wave resonance.

FF2A.8 • 12:15

Dynamic Control of Plasmonic Beams, Dror weisman¹, Ady Arie¹; ¹Tel Aviv Univ., Israel. We actively control the propagation of plasmonic beams using the thermo-optic effect, by selectively inducing electrical current through specific areas. We demonstrate a dynamic mode converter and a tunable plasmonic lens.

FF2B • Linear/Non-Linear
Metasurfaces—Continued

FF2B.7 • 12:00

Helicity-Multiplexed Hologram via All-dielectric Metasurface in the Visible Domain, Muhammad Afnan Ansari^{1,2}, Muhammad Qasim Mehmood¹, Muhammad Hamza Waseem^{1,3}, Inki Kim⁴, Nasir Mahmood^{5,6}, Tauseef Tauqeer¹, Selcuk Yerci^{2,7}, Junsuk Rho⁴; ¹Information Technology Univ. of the Punjab, Lahore, Pakistan, Pakistan; ²Dept. of Electrical and Electronics Engineering, Middle East Technical Univ., 06800 Çankaya/Ankara, Turkey, Turkey; ³Dept. of Electrical Engineering, Univ. of Engineering and Technology, Lahore 54000, Pakistan, Pakistan; ⁴Dept. of Mechanical Engineering, Pohang Univ. of Science and Technology (POSTECH), Pohang 37673, South Korea, South Korea (the Republic of); ⁵National Univ. of Sciences and Technology (NUST), Islamabad, Pakistan, Pakistan; ⁶Engineering Dept., Univ. of Lahore, Lahore, Pakistan, Pakistan; ⁷Dept. of Micro and Nanotechnology, Middle East Technical Univ., 06800 Çankaya/Ankara, Turkey, Turkey. A transmission type helicity-multiplexed metasurface hologram is demonstrated at wavelength of 633 nm using low loss hydrogenated amorphous silicon to achieve the pragmatic features of metasurfaces in the integrated photonic circuits.

FF2B.8 • 12:15

Multi-Element Meta-lens Systems for Imaging, Sajjan Shrestha¹, Adam C. Overvig¹, Nanfang Yu¹; ¹Columbia Univ., USA. We experimentally demonstrated chromatic and monochromatic aberration correction in a meta-lens triplet system up to a wavelength range of ~300 nm in the near-infrared by utilizing dispersion engineering of meta-atoms.

FF2C • Attosecond
Pulse Generation &
Characterization—Continued

FF2C.6 • 12:00

Helicity in a Twist: Attosecond, Extreme Ultraviolet Vortex Beams with Designer Spin and Orbital Angular Momenta, Kevin Dorney¹, Laura Rego², Nathan Brooks¹, Julio San Román², Chen-Ting Liao¹, Jennifer Ellis¹, Dmitriy Zusin¹, Christian Gentry¹, Quynh L. Nguyen¹, Justin Shaw³, Antonio Picon⁴, Luis Plaja², Henry Kapteyn¹, Margaret Murnane¹, Carlos Hernandez-Garcia²; ¹Physics, JILA - Univ. of Colorado Boulder, USA; ²Departamento de Física Aplicada, Universidad de Salamanca, Spain; ³Quantum Electromagnetics Division, National Inst. of Standards and Technology, USA; ⁴Departamento de Química, Universidad Autónoma de Madrid, Spain. High-harmonics—and attosecond pulses—with controllable spin and orbital angular momenta (SAM and OAM) are generated for the first time. The coupled SAM-OAM conservation laws enable exquisite control over the polarization of attosecond pulse trains.

FF2C.7 • 12:15

An Extreme Ultraviolet Spin Grating for Spatially Resolved, Hyperspectral Magnetic Dichroism Spectroscopies, Nathan J. Brooks⁴, Kevin M. Dorney¹, Jennifer L. Ellis^{4,3}, Daniel Hickstein^{4,3}, Quynh L. Nguyen⁴, Christian Gentry⁴, Carlos Hernandez-Garcia¹, Dmitriy Zusin⁴, Justin Shaw², Matthijs Jansen², Stefan Witte², Henry Kapteyn⁴, Margaret M. Murnane⁴; ¹Departamento de Física Aplicada, Universidad de Salamanca, Spain; ²Advanced Research Center for Nanolithography (ARCNL), Netherlands; ³Time and Frequency Division, National Inst. of Standards and Technology, USA; ⁴Dept. of Physics, JILA, USA; ⁵Quantum Electromagnetics Division, National Inst. of Standards and Technology, USA. Phase-locked, orthogonally polarized high-harmonic sources are employed to produce an extreme ultraviolet optical spin grating. This spin grating is ideal for hyperspectral, dichroic imaging allowing, for example, spatially resolved dichroism measurements at magnetic M edges.

FF2D • Frequency Comb &
Supercontinuum Generation—
Continued

FF2D.7 • 12:00

Supercontinuum Generation in Titanium Dioxide Waveguides, Kamal Hammani¹, Laurent Markey¹, Manon Lamy¹, Bertrand Kibler¹, Juan Arocas¹, Julien Fatome¹, Alain Dereux¹, Jean-Claude Weeber¹, Christophe Finot¹; ¹Laboratoire Interdisciplinaire Carnot de Bourgogne, Université Bourgogne Franche-Comté, France. We report the design and fabrication of titanium dioxide optical waveguides optimized for supercontinuum generation in the mid-infrared. A spectrum spanning from the visible up to 2 μm is experimentally demonstrated.

FF2D.8 • 12:15

Tailoring the Dispersion of a Hybrid Chalcogenide/Silicon-Germanium Waveguide for Mid-Infrared Supercontinuum Generation, Alberto Della Torre¹, Milan Sinobad^{1,4}, Barry Luther-Davis², Pan Ma², Stephen Madden², Sukanta Debbarma², Khu Vu², David Moss³, Arnan Mitchell⁴, Jean-Michel Hartmann⁵, Jean-Marc Fedeli⁵, Christelle Monat¹, Christian Grillet¹; ¹Institut des Nanotechnologies de Lyon, France; ²Australian National Univ., Australia; ³Swinburne Univ. of Technology, Australia; ⁴RMIT Univ., Australia; ⁵CEA-Leti, France. We report mid-infrared supercontinuum generation in a silicon germanium-on-silicon waveguide. We show that the dispersion properties of the waveguide can be precisely tuned by controlling the thickness of a chalcogenide cladding layer.

12:30–14:00 Lunch Break (On your Own)

Executive Ballroom
210E

CLEO: Science &
Innovations

SF2E • Ultrafast Phenomena—
Continued

SF2E.4 • 12:00 **Invited**
Attosecond Tracking of Electron Dynamics in Large Molecules, Francesca Calegari^{1,2}; ¹Deutsches Elektronen Synchrotron, Germany; ²Physics, Hamburg University, Germany. A new attosecond beamline combining 200-as XUV pulses with sub-2 fs UV pulses is presented. The application of attosecond technology for the investigation of electronic processes in bio-relevant molecules is discussed.

Executive Ballroom
210F

Joint

JF2F • Symposium on Deep-
learning Photons: Where
Machine Learning & Photonics
Intersect II—Continued

JF2F.4 • 12:00
Training Deep Neural Networks for the Inverse Design of Nanophotonic Structures, Dianjing Liu¹, Yixuan Tan¹, Erfan Khoram¹, Zongfu Yu¹; ¹Univ. of Wisconsin - Madison, USA. We demonstrate a tandem neural network architecture that tolerates inconsistent training instances in inverse design of nanophotonic devices. It provides a way to train large neural networks for the inverse design of complex photonic structures.

JF2F.5 • 12:15
Large-Scale Optical Neural-Network Accelerators based on Coherent Detection, Ryan Hamerly¹, Alex Sludds¹, Liane Bernstein¹, Marin Soljagic¹, Dirk R. Englund¹; ¹MIT, USA. We present a coherent optical neural-network accelerator based on homodyne detection that is scalable to large ($N > 1000$) networks, and analyze the fundamental quantum limits to its energy efficiency.

Executive Ballroom
210G

CLEO: Science & Innovations

SF2G • Laser-Based Diagnostics
for Material Processing—
Continued

SF2G.6 • 12:00
Atom Probe Tomography with Extreme-Ultraviolet Light, Luis Miaja Avila¹, Ann Chiamonti¹, Paul Blanchard¹, Norman Sanford¹, David Diercks², Brian Gorman²; ¹NIST, USA; ²Colorado School of Mines, USA. We have adapted an atom probe tomograph (APT) with an extreme ultraviolet (EUV) source. The EUV photon energies open a direct photoionization pathway unavailable in conventional near-UV APT.

SF2G.7 • 12:15
Towards Stark Coefficient Determination in Laser-produced Uranium Plasma, Milos Burger¹, Patrick J. Skrodzki¹, Igor Jovanovic¹, Mark C. Phillips², Sivanandan S. Harilal²; ¹Univ. of Michigan, USA; ²Pacific Northwest National Lab, USA. We performed spatiotemporal diagnostics of excitation temperature and electron density of laser-induced uranium plasma. The results are prerequisite for Stark broadening and shift coefficients determination, required for accurate modeling of uranium emission spectra.

Executive Ballroom
210H

SF2H • Active & Reconfigurable
Devices—Continued

SF2H.6 • 12:00
A sub-10 μ K, dual-mode temperature stabilized microresonator, Jinkang Lim^{1,2}, Anatoliy Savchenkov³, Yoon-Soo Jang¹, Andrey B. Matsko³, Chee Wei Wong¹; ¹Univ. of California Los Angeles, USA; ²Photonics Solutions, LGS innovations LLC, USA; ³OEwaves Inc., USA. We show a resonator long-term temperature stability of 8.53 μ K after stabilization and unveil various sources that hinder the stability from reaching sub- μ K in the current system.

SF2H.7 • 12:15
Design of a tapered slot waveguide dielectric laser accelerator for sub-relativistic electrons, Zhixin Zhao¹, Tyler Hughes¹, Si Tan¹, Huiyang Deng¹, Neil Saprà¹, Joel England², Jelena Vuckovic¹, James Harris¹, Robert Byer¹, Shanhui Fan¹; ¹Stanford Univ., USA; ²SLAC National Accelerator Lab, USA. We design and analyze a tapered slot waveguide structure for sub-relativistic electron acceleration. The tapering scheme can be designed, through the eikonal approximation, to achieve phase synchronization with the accelerated electrons.

12:30–14:00 Lunch Break (On your Own)

Friday, 10:30–12:30

Meeting Room
211 A/B

Meeting Room
211 C/D

Meeting Room
212 A/B

Meeting Room
212 C/D

CLEO: Science & Innovations

CLEO: Applications
& Technology

CLEO: Science &
Innovations

SF21 • High Q Cavity,
Resonators Application—
Continued

SF21.6 • 12:00

High-Q Resonators on Single Crystal Aluminum Nitride Grown by Molecular Beam Epitaxy, Yi Sun¹, David Laleyan¹, Eric Reid¹, Ping Wang¹, Xianhe Liu¹, Ayush Pandey¹, Mohammad Soltani², Zetian Mi¹; ¹Dept. of Electrical and Computer Engineering, Univ. of Michigan, USA; ²Raytheon BBN Technologies, USA. We report the demonstration of high-Q (> 70,000) microring resonators at 770 nm wavelength using single crystal aluminum nitride (AlN) grown by molecular-beam-epitaxy (MBE) which is a crucial growth technique enabling electronic/photonics integration with III-Nitrides.

SF21.7 • 12:15

Control of Kerr-microresonator optical frequency comb by a dual-parallel Mach-Zehnder interferometer, Naoya Kuse¹, Travis C. Briles^{2,3}, Scott B. Papp^{2,3}, Martin E. Fermann¹; ¹IMRA America Inc, USA; ²Time and Frequency Division, National Inst. of Standards and Technology, USA; ³Dept. of Physics, Univ. of Colorado, USA. We propose and demonstrate a simple technique to generate a stable dissipative Kerr comb and to control f_{rep} and f_{ceo} of the comb, in which only one device, i.e. dual-parallel Mach-Zehnder interferometer is used.

SF2J • Lithium Niobate &
Perovskite Photonic Devices—
Continued

SF2J.6 • 12:00

High-quality Lithium Niobate Optomechanical Crystal, Wentao Jiang¹, Rishi Patel¹, Felix M. Mayor¹, Timothy McKenna¹, Patricio Arrangoiz-Arriola¹, Christopher J. Sarabalis¹, Raphaël Van Laer¹, Amir Safavi-Naeini¹; ¹Stanford Univ., USA. We demonstrate 1D lithium niobate optomechanical crystal with 1550 nm optical mode with quality factor 300,000 and 1.9 GHz mechanical mode with quality factor 37,000 at 4 Kelvin. The optomechanical coupling rate is measured to be $g/2\pi = 120$ kHz.

SF2J.7 • 12:15

Phase-Shifted Bragg Grating Resonators in Thin-Film Lithium Niobate Waveguides, Mohammad Amin Baghban¹, Katia Gallo¹; ¹KTH Royal Inst. of Technology, Sweden. We demonstrate narrowband integrated filters with 0.23 mm-long phase-shifted Bragg gratings in corrugated single-mode thin-film LiNbO₃ photonic wires, achieving quality factors of 1.24×10^4 and extinction ratios up to 24 dB at telecom wavelengths.

AF2K • Spectrometers &
Wavelength Metrology—
Continued

AF2K.7 • 12:00

Ultrarrow-band metagrating absorbers for sensing and modulation, Aosong Feng¹, Zejie Yu¹, Xiankai Sun¹; ¹Electronics Engineering, The Chinese Univ. of Hong Kong, Hong Kong. An asymmetric metagrating structure with an ultranarrow bandwidth of 0.28 nm at 1.55 μm is proposed. Sensing with figure-of-merit of 1333.33 RIU⁻¹ and electro-optic modulation with dynamic range of 15.52 dB are numerically demonstrated.

AF2K.8 • 12:15

Spherical mirrors based compact multipass cell with dense astigmatic-like spot pattern, Arkadiusz Hudzikowski¹, Aleksander Gluszek¹, Karol Krzempek¹, Jaroslaw Sotor¹; ¹Wroclaw Univ. of Science and Techn., Poland. A multipass trace gas cell with 24 m optical path length and 80 cc volume was developed and built. A direct ray tracing and genetic algorithm was used to determine optimal mirror arrangement.

SF2L • MID-IR Fiber Sources—
Continued

SF2L.5 • 12:00

High Energy Er:ZBLAN LMA Fiber Amplifier Producing ~200 μJ and ~10ns Pulses at 2.72 μm , Weizhi Du¹, Xuan Xiao², Yifan Cui¹, Mingshu Chen¹, Igor Jovanovic², Almantas Galvanauskas¹; ¹Center for Ultrafast Optical Science, Univ. of Michigan, USA; ²Nuclear Engineering and Radiological Sciences, Univ. of Michigan, USA. Pulsed amplification at 2.7 μm in Er:ZBLAN LMA fibers was explored demonstrating up to 194 μJ in 9.7ns, the highest short-pulse energies from these mid-IR fibers. We also measured fiber damage threshold and 650 μJ of stored energy.

SF2L.6 • 12:15

Ultrafast Thulium-Doped Fiber Laser System at 1.8 μm for Multiphoton Microscopy, Yutaka Nomura^{1,2}, Takao Fujii¹; ¹Inst. for Molecular Science, Japan; ²JST, PRESTO, Japan. An ultrafast laser system at 1.8 μm is developed based on thulium-doped ZBLAN fibers. The generated pulses are used in a three-photon microscope to observe the images of fluorescent beads for ~600 nm.

12:30–14:00 Lunch Break (On your Own)

Joint

CLEO: Science & Innovations

JF2M • Professional Development Session
II—Continued

SF2N • RF Photonics—Continued

SF2O • Optoelectronic Materials—
Continued

SF2N.7 • 12:00

Brillouin-loss Enabled Noise Figure Improvement for Chip-based Tunable Microwave Photonic Filters, Yiwei Xie¹, Amol Choudhary¹, Yang Liu¹, David Marpaung², Khu Vu³, Pan Ma³, Duk-yong Choi³, Stephen Madden³, Benjamin J. Eggleton¹; ¹Univ. of Sydney, Australia; ²Univ. of Twente, Netherlands; ³Australian National Univ., Australia. We compare the noise figure (NF) of chip-based tunable microwave photonic band-pass filters using stimulated Brillouin scattering (SBS) gain and loss responses, respectively. The filter using SBS loss scheme exhibits 10-dB lower NF than that using SBS gain scheme.

SF2N.8 • 12:15

Rapid Wideband RF Subsampling and Disambiguation Using Dual Combs, Mohammed S. Al Alshaykh^{1,2}, Daniel E. Leaird^{1,2}, Jason D. McKinney³, Andrew M. Weiner^{1,2}; ¹School of Electrical and Computer Engineering, Purdue Univ., USA; ²Birck Nanotechnology Center, Purdue Univ., USA; ³U.S. Naval Research Lab, USA. Using two electro-optic combs with an offset in the repetition rate, we disambiguate RF signals over 20 Nyquist bands. The setup doesn't require a pulse compression stage and can be readily integrated using existing technology.

SF2O.7 • 12:00

High-Performance Mid-Infrared Crystalline Bragg Mirrors at 4.5 μm , Georg Winkler¹, Lukas Perner¹, Gar-Wing Truong², Dominic Bachmann³, Aline S. Mayer¹, Jakob Fellinger¹, Tobias Zederbauer³, David Follman², Christoph Deutsch³, Garrett D. Cole^{2,3}, Oliver H. Heckl¹; ¹Christian Doppler Lab for Mid-IR Spectroscopy and Semiconductor Optics, Faculty Center for Nano Structure Research, Faculty of Physics, Univ. of Vienna, Austria; ²Crystalline Mirror Solutions LLC, USA; ³Crystalline Mirror Solutions GmbH, Austria. We present state-of-the-art mid-IR high-reflectivity low-loss mirrors at 4.55 μm based on substrate-transferred crystalline coatings. Transmission losses of 150 ppm and excess losses of <50 ppm are demonstrated via cavity-ringdown and direct transmission measurements.

SF2O.8 • 12:15

Nd:Y₂O₃ Transparent Ceramics: Fabrication and Laser Performance, Danlei Yin¹, Jun Wang¹, Zhili Dong¹, Martin Richardson², Dingyuan Tang¹; ¹Nanyang Technological Univ., Singapore; ²Univ. of Central Florida, USA. 0.6 at% Nd:Y₂O₃ transparent ceramics with high optical quality were fabricated by vacuum sintering plus hot isostatic pressing. High efficiency CW laser operation at 1.08 and 1.36 μm were demonstrated.

12:30–14:00 Lunch Break (On your Own)

CLEO: QELS-Fundamental Science

14:00–16:00

FF3A • Single-Photon Collection & Characterization*Presider: Marcelo Davanco; NIST, USA*

FF3A.1 • 14:00

Inverse Designed Diamond Nanophotonics, Constantin Dory¹, Dries Vercautse¹, Kiyoul Yang¹, Neil Saprà¹, Alison E. Rugar¹, Shuo Sun¹, Daniil Lukin¹, Alexander Y. Piggott¹, Linda Jingyuan Zhang¹, Marina Radulaski¹, Konstantinos Lagoudakis¹, Logan Su¹, Jelena Vuckovic¹; ¹Stanford Univ., USA. Combining inverse design optimization methods and quasi-isotropic etching techniques, we develop compact, flexible and efficient photonic components in diamond for applications in quantum technologies.

FF3A.2 • 14:15

Waveguide-coupled Localized Excitons From a WSe₂ monolayer on a Silicon Nitride Photonic Platform, Frédéric Peysskens^{1,2}, Chitrleema Chakraborty¹, Muhammad Muneeb², Dries Van Thourhout², Dirk R. Englund¹; ¹MIT, USA; ²Ghent Univ., Belgium. We demonstrate the coupling of localized excitons from a WSe₂ monolayer into a silicon nitride waveguide by measuring the waveguide-coupled fluorescence, paving the way towards scalable fabrication of on-chip single photon sources.

FF3A.3 • 14:30

Deterministically coupled quantum emitters in a hexagonal Boron Nitride hybrid microcavity system, Nicholas Proscia¹, Harishankar Jayakumar¹, Zav Shotan¹, Gabriel Lopez-Morales¹, Xiaochen Ge², Weidong Zhou², Carlos Meriles¹, Vinod Menon¹; ¹CUNY City College of New York, USA; ²Univ. of Texas at Arlington, USA. We demonstrate a hybrid microphotonic device by integrating a thin film of hexagonal Boron Nitride containing quantum emitters with Si₃N₄ microdisk resonators. We deterministically activate these emitters via strain within a microdisk's evanescent field.

14:00–16:00

FF3B • Disordered Media*Presider: To Be Announced*

FF3B.1 • 14:00

Light Propagation in Temporally Disordered Media, Yonatan Sharabi¹, Eran Lustig¹, Mordechai Segev¹; ¹Technion, Israel. We study light propagation in a medium with a homogeneous refractive index that varies randomly in time. We find that, in stark contrast to spatial disorder, temporal disorder causes exponential increase of the light intensity.

FF3B.2 • 14:15

Spatio-temporal response of random media beyond ensemble averages, Ruitao Wu¹, Aristide Dogariu¹; ¹CREOL, USA. We demonstrate measurements of full spatio-temporal correlations between photon path lengths in highly scattering media. The dependence on the structural characteristics of the medium and the connection to memory-like phenomena are discussed.

FF3B.3 • 14:30

Memory effect of transmission eigenchannels in random media, Hasan Yilmaz¹, Chia Wei Hsu¹, Alexey Yamilov², Hui Cao¹; ¹Yale Univ., USA; ²Dept. of physics, Missouri Univ. of Science & Technology, USA. We have experimentally and numerically studied the angular memory effect of transmission eigenchannels in random media. High-transmission channels have a larger range of memory effect than any input wavefront, thus are robust against sample tilt.

14:00–16:00

FF3C • Attosecond Dynamic Imaging*Presider: Shambhu Ghimire; SLAC National Accelerator Laboratory, USA*FF3C.1 • 14:00 **Invited**

Probing Electronic Binding Potentials with Attosecond Photoelectron Wavepackets, Robert R. Jones¹, Dietrich Kieseewetter², Antoine Camper², Stephen B. Schoun², Pierre Agostini², Louis F. DiMauro²; ¹Univ. of Virginia, USA; ²The Ohio State Univ., USA. We show that energy transfer between a mid-infrared dressing field and low-energy attosecond photoelectron wavepackets provides direct coarse-grained information on the effective binding potential experienced by the electrons during the first femtosecond following their ionization.

FF3C.2 • 14:30

Subcycle dynamics of ionization revealed via polarization of lowest harmonics, Ihar Babushkin^{2,1}, Alvaro G. Galan¹, Virgilijus Vaičaitis³, Anton H. Husakou¹, Felipe Morales¹, Ayhan Demircan^{2,4}, José Andrade^{2,4}, Uwe Morgner^{2,4}, Misha Ivanov¹; ¹Max-Born Inst., Germany; ²Inst. of Quantum Optics, Univ. of Hannover, Germany; ³Laser Research Center, Vilnius Univ., Lithuania; ⁴Hannover Centre for optical Technologies, Germany. We show that by looking at the polarization of lowest (0th and 3d) harmonics of the atomic response it is possible to determine details of attosecond-scale ionization dynamics including ionization time and its temporal asymmetry.

14:00–16:00

FF3D • Nonlinear & Quantum Effects*Presider: To Be Announced*

FF3D.1 • 14:00

Measurement of excitation coherence lengths using multi-spatial-mode four-wave mixing, Torben L. Purz^{1,2}, Eric Martin¹, Zhaorong Wang¹, Hui Deng¹, Steven T. Cundiff¹; ¹Dept. of Physics, Univ. of Michigan, USA; ²Dept. of Physics, Univ. of Goettingen, Germany. We develop a multi-spatial-mode four-wave mixing (FWM) experiment to determine the coherence length of quasiparticles. We present evidence for nonlocal effects in a microcavity polariton system that affect nonlinear optical processes such as FWM.

FF3D.2 • 14:15

Nonlinear Plasmonic Enhancement with Graphene Heterostructures, Irati Alonso Calafell¹, Lee A. Rozema¹, David Alcaraz Iranzo², Alessandro Trenti¹, Hlib Bieliaiev¹, Frank H. Koppens², Philip Walther¹; ¹Univ. of Vienna, Austria, Austria; ²ICFO, Spain. Nonlinear nanoplasmonics provides precise control and manipulation of light. Graphene sustains electrically tunable and long-lived plasmons. By combining these platforms, we observe a 10² enhancement in the third-harmonic generation in graphene heterostructures.

FF3D.3 • 14:30

Spectral and angular dependence of the giant nonlinear refraction of Indium Tin Oxide excited at epsilon-near-zero, Sepehr Benis¹, Natalia Munera¹, David J. Hagan¹, Eric W. Van Stryland¹; ¹Univ. of Central Florida, CREOL, USA. We report beam-deflection measurements of indium tin oxide excited around epsilon-near-zero (ENZ), but probed far from ENZ. Nonlinear refraction is very large even far from ENZ and enhanced as the excitation is tuned through ENZ.

Executive Ballroom
210E

CLEO: Science &
Innovations

14:00–16:00

SF3E • Ultrafast Oscillators

President: Simon Duval; Femtum,
Canada

SF3E.1 • 14:00

20 MW Mamyshev Oscillator featuring LMA-PCF, Wu Liu¹, Ruoyu Liao¹, Jun Zhao¹, Jiahua Cui¹, Youjian Song¹, Chingyue Wang¹, Ming-lie Hu¹; ¹Tianjin Univ., China. We demonstrate a Mamyshev oscillator featuring large-mode-area photonic crystal fibers (LMA-PCF). The laser generates over 1 μ J pulses which can be dechirped down to 41 fs, leading to pulse peak powers of ~20 MW.

SF3E.2 • 14:15

Fiber oscillator mode-locked using a novel scheme for Nonlinear Polarization Evolution in Polarization Maintaining fibers, Jan Szczepanek¹, Tomasz Kardas², Bernard Piechal³, Yuriy Stepanenko³; ¹Inst. of Experimental Physics, Faculty of Physics, Univ. of Warsaw, Poland; ²Fluence sp. z o. o., Poland; ³Inst. of Physical Chemistry PAS, Poland. We present an environmentally stable ultrafast oscillator employing a novel implementation of a multi-segment All Polarization-Maintaining-Fiber Nonlinear Polarization Evolution reflective artificial Saturable Absorber. Oscillator emits 1 nJ pulses with duration of 230 fs after compression.

SF3E.3 • 14:30

Power Scaling of Ultrafast Laser Oscillators: 350-W Output Power Sub-ps SESAM-Modelocked Thin-Disk Laser, Francesco Saltarelli¹, Ivan J. Graumann¹, Lang Lukas¹, Dominik Bauer², Christopher Phillips¹, Ursula Keller¹; ¹ETH Zurich, Switzerland; ²TRUMPF Laser GmbH, Germany. Combining vacuum operation, large pump spot, and multiple passes on the gain medium, we designed a high-power thin-disk oscillator with a record 350-W average power, 40- μ J pulses. We expect 500-W-level modelocking in the near future.

Executive Ballroom
210F

Joint

14:00–16:00

JF3F • Symposium on Deep-

learning Photons: Where
Machine Learning & Photonics
Intersect III

JF3F.1 • 14:30

Object Recognition with Optical Coherence, Ken Xingze Wang¹; ¹Huazhong Univ. of Science and Technology, China. Computer vision systems could be improved by using wave optics instead of geometrical optics. We show that some object recognition tasks are made possible by using optical coherence.

Executive Ballroom
210G

CLEO: Science & Innovations

14:00–16:00

SF3G • Laser-Based 2D/3D

Micro- & Nano-fabrication

President: Takashige Omats; Chiba
University, Japan

SF3G.1 • 14:00

Er and Yb femtosecond laser-induced melting and shaping of indium nanostructures on silicon wafers, Ali Azarm¹, Nasser Peyghambarian¹, Farhad Akhondi¹; ¹Univ. of Arizona, USA. We use erbium and ytterbium femtosecond lasers to melt and shape semi-spherical nanostructure by high spatial frequency laser induced periodic surface structures into linear microstructures of 2 μ m long in the direction of laser polarization.

SF3G.2 • 14:15

Femtosecond-Laser-Induced Blisters in Polymer Thin Films and Application as Microlenses, Alan T. Godfrey^{1,2}, L.N. Deepak Kallepalli^{1,2}, Jesse Ratté^{1,2}, Paul B. Corkum^{1,2}; ¹Uttawa, Canada; ²National Research Council of Canada, Canada. We present the phenomenology of blister formation by nonlinear absorption of femtosecond pulses in polyimide films, characterized by atomic force microscopy. We demonstrate a novel implementation of blisters as microlenses.

SF3G.3 • 14:30

Micron-scale 'ink-jet' created by optical vortex ablation, Ryosuke Nakamura¹, Muneaki Iwata², Akihiro Kaneko², Kohei Toyoda^{1,3}, Katsuhiko Miyamoto^{1,3}, Takashige Omatsu^{1,3}; ¹Chiba Univ., Japan; ²RICOH CT&P Division, Japan; ³MCRC Chiba Univ., Japan. We have demonstrated the creation of a micron-scale 'ink-jet' by employing optical vortex laser ablation. The OAM then provides a spin of the melted ink, thereby stabilizing the formation of the 'ink-jet'.

Executive Ballroom
210H

14:00–16:00

SF3H • Microresonator

Frequency Combs

President: Tara Drake; NIST, USA

SF3H.1 • 14:00 **Invited**

Optical Frequency Measurements with a Silica Disk Microcomb, Erin S. Lamb¹; ¹OFS, USA. Aspects of reliable chip-scale frequency combs are discussed. A silica disk microcomb operating at 15 GHz and broadened in a silicon nitride waveguide is used to measure the frequency drift between two ultrastable reference lasers.

SF3H.2 • 14:30

Generation of Clustered Frequency Comb via Intermodal Four-Wave Mixing in an Integrated Si₃N₄ Microresonator, Ayman N. Kamel¹, Houssein El Dirani², Marco Casale², Sébastien Kerdiles², Carole Socquet-Clerc², Minhao Pu¹, Leif K. Oxenløwe¹, Kresten Yvind¹, Jesper Lægsgaard¹, Corrado Sciancalepore²; ¹DTU, Denmark; ²CEA-LETI, France. We present the generation of a second harmonic wave and a clustered comb at 1 μ m from a telecom wavelength pump in a dispersion engineered Si₃N₄ microresonator.

Friday, 14:00–16:00

CLEO: Science & Innovations

CLEO: Applications
& TechnologyCLEO: Science &
Innovations

14:00–16:00

SF3I • Lasers for Accelerators

President: Lutz Winkelmann; DESY, Germany

SF3I.1 • 14:00

Update on BELLA Center's Free-Electron Laser driven by a Laser-Plasma Accelerator, Fumika Isono^{1,2}, Jeroen Van Tilborg¹, Sam Barber¹, Cameron Geddes¹, Hai-En Tsai¹, Carl Schroeder¹, Wim Leemans^{1,2}; ¹Lawrence Berkeley National Lab, USA; ²Univ. of California, Berkeley, USA. Technology to drive a free-electron laser with a compact laser-plasma accelerator is pursued. Recently we commissioned a new 5-Hz 100 TW laser, produced first electron beams (135 MeV), and built a dedicated FEL beamline, the status of which we report here.

SF3I.2 • 14:15

Laguerre-Gaussian Mode Laser Heater for Microbunching Instability Suppression in Free Electron Lasers, Jingyi Tang¹, Wei Liu¹, Randy Lemons¹, Sharon Vetter¹, Timothy Maxwell¹, Franz-Josef Decker¹, Alberto Lutman¹, Jacek Krzywinski¹, Gabriel Marcus¹, Stefan Moeller¹, Daniel Ratner¹, Zhirong Huang¹, Sergio Carbajo¹; ¹SLAC National Accelerator Lab, USA. We report on the use of a Laguerre-Gaussian transverse mode in the LCLS laser heater resulting in better suppression of microbunching instability. We discuss the impact on FEL performance.

SF3I.3 • 14:30

Ptychographic Characterization of an Intense High-Harmonic-seeded Femto-second Soft X-ray Laser, Michael Zurch^{1,2}, Frederik Tuitje³, Tobias Helk³, Julien Gautier⁴, Fabien Tissandier⁴, Jean-Philippe Goddet⁴, Eduardo Oliva⁵, Alexander Guggenmos², Ulf Kleineberg⁶, Stephane Sebban⁴, Christian Spielmann³; ¹Dept. of Physical Chemistry, Fritz Haber Inst., Germany; ²Chemistry Dept., Univ. of California at Berkeley, USA; ³Friedrich Schiller Univ., Germany; ⁴Laboratoire d'optique appliquée – ENSTA-ParisTech, France; ⁵Departamento de Ingeniería Energética, ETSI Industriales, Universidad Politécnica de Madrid, Spain; ⁶Ludwig-Maximilians-Universität München, Germany. We report the direct wavefront characterization of an intense ultrafast high-harmonic-seeded soft X-ray laser ($\lambda=32.8$ nm) and monitor the laser plasma amplifier depending on the arrival time of the seed pulses by high-resolution ptychographic imaging.

14:00–16:00

SF3J • Metasurface & Plasmonic Structures

President: Takasumi Tanabe; Keio University, Japan

SF3J.1 • 14:00

All-dielectric Metasurfaces for Infrared Absorption Spectroscopy Applications, Aleksandrs Leitis¹, Andreas Tittl¹, Mingkai Liu², Filiz Yesilkoy¹, Duk-yong Choi³, Dragomir Neshev², Yuri S. Kivshar², Hatice Altug¹; ¹Inst. of BioEngineering, Ecole Polytechnique Fédérale de Lausanne (EPFL), Switzerland; ²Nonlinear Physics Centre, Research School of Physics and Engineering, Australian National Univ., Australia; ³Laser Physics Centre, Research School of Physics and Engineering, Australian National Univ., Australia. We present a nanophotonic method capable of detecting mid-infrared molecular fingerprints without the need for spectrometry. We leverage dielectric metasurfaces featuring ultra-sharp resonances at discrete frequencies, enabling us to sample absorption signatures over the mid-IR spectral range.

SF3J.2 • 14:15

Dielectric Metasurface Comprising Color Hologram Encoded into a Color Printing Image, Dandan Wen¹, Jasper Cadusch¹, Jiajun Meng¹, Kenneth Crozier¹; ¹The Univ. of Melbourne, Australia. We experimentally demonstrate a dielectric metasurface that simultaneously provides a color printing image (viewed with a brightfield microscope) and a far-field color hologram (viewed by illuminating the device by red/green/blue lasers).

SF3J.3 • 14:30 **Invited**

Achieving Light-Matter Interaction at Microcavity Q yet Plasmonic Mode Volumes, Femius Koenderink¹; ¹Center for Nanophotonics, AMOLF, Netherlands. We study hybrid plasmonic-photonic resonators that combine subwavelength confinement of nano-antennas with the high Q of silicon nitride microdisk cavities. Fluorescence of quantum dots localized at the antenna hot spots reveals significant hybrid-mode Purcell enhancement.

14:00–16:00

AF3K • Imaging, Microscopy, & Specialized Detection

President: Gregory Rieker; University of Colorado at Boulder, USA

AF3K.1 • 14:00

Full-color, multi-plane image projection with mobile-phone flashlight & a multi-level diffractive hologram, Monjurul Meem¹, Rajesh Menon¹, Apratim Majumder¹; ¹Univ. of Utah, USA. We show the projection of color and covert images in multiple planes using a multi-level diffractive-optical element illuminated by the flashlight of a mobile phone. Such devices could be useful for in secure documents.

AF3K.2 • 14:15

Holographic Speckle-Based Authentication Paradigm, Yoav Blau¹, Ofer Bar-On¹, Yael Hanein¹, Amir Boag¹, Jacob Scheuer¹; ¹Tel Aviv Univ., Israel. An approach for a physical authentication scheme is proposed relying on the irreversible and nonconvex nature of computer-generated holograms. This is demonstrated by proof-of-principle meta-holograms projecting uniquely speckled 2D barcode images.

AF3K.3 • 14:30

Compressive Imaging with a Stochastic Spatial Light Modulator, Jason Schaake^{1,3}, Raphael C. Poeser², Stephen Jesse⁴; ¹Quantum Information Science, Oak Ridge National Lab, USA; ²Oak Ridge Associated Universities, USA; ³Center for Nanophase Materials Science, Oak Ridge National Lab, USA. We present a stochastic analog spatial light modulator designed for non-optical compressive imaging or spectroscopic applications where no spatial modulators exist. This spatial modulator does not require deterministic control.

14:00–16:00

SF3L • Fiber Sensing

President: William Renninger; University of Rochester, USA

SF3L.1 • 14:00

Directional Curvature Sensing Using Multi-core Fiber Bragg Grating and Two-Photon Absorption Process in Si-APD, Yosuke Tanaka¹, Tetsuya Abe¹, Hiromasa Miyazawa¹; ¹Tokyo Univ of Agriculture and Technology, Japan. We demonstrate a directional curvature sensor using a multicore fiber Bragg grating (FBG). The FBGs having almost the same Bragg wavelengths are discriminated by the distance measurement technique using two-photon absorption process in a Si-APD.

SF3L.2 • 14:15

Embedded-core optical fiber for distributed pressure measurement using an autocorrelation OFDR technique, Rodrigo M. Gerosa², Jonas H. Osório¹, Daniel Lopez-Cortez², Cristiano M. Cordeiro¹, Cristiano J. de Matos²; ¹Instituto de Física "Gleb Wataghin", Universidade Estadual de Campinas, Brazil; ²MackGrappe – Graphene and Nanomaterials Research Center, Mackenzie Presbyterian Univ., Brazil. We present a pressure sensor using an optical frequency domain reflectometer and a simplified microstructured fiber. High sensitivity, ease of fabrication and distributed sensing makes the proposed configuration a promising technique for pressure sensing applications.

SF3L.3 • 14:30

Dynamic coherent optical time-domain reflectometry with pulse compression, Ji Xiong¹, Yue Wu¹, Zinan Wang¹, Yun Jiang Rao¹; ¹Univ. Electronic Sci. & Tech. of China, China. We report a novel COTDR using chirped pulse compression. By only adjusting the sweep range of the chirped pulse, the spatial resolution is changed from 5 m to 0.5 m, and dynamic strain sensing is also demonstrated.

CLEO: QELS-Fundamental
Science

14:00–16:00

FF3M • Quantum Interactions in
Nanophotonic Systems

President: Amit Agrawal, NIST, USA

FF3M.1 • 14:00

Coherent Interaction of Light with a Single Molecule and a Plasmonic Nanoparticle, Johannes Zirkelbach^{1,2}, Pierre Türschmann¹, Jan Renger¹, Tobias Utikal¹, Stephan Götzinger^{1,2}, Vahid Sandoghdar^{1,2}; ¹Sandoghdar Division, Max Planck Inst. for the Science of Light, Germany; ²Physics, Friedrich Alexander Univ., Germany. We demonstrate partial cloaking of a gold nanoparticle by a single organic molecule as a result of their coherent interaction with a monochromatic laser beam at cryogenic temperatures. Spectral and fluorescence lifetime analyses are presented.

FF3M.2 • 14:15

Quantum Electron-Photon Entanglement in the Strong-Coupling Regime, Ofer Kfir¹, Claus Ropers¹; ¹Univ. of Göttingen, Germany. We investigate coherent interactions between cavity-photons and electrons at arbitrary coupling strengths, and propose a road-map to approach this regime experimentally. As an example, we explore photon-mediated entanglement of two free electrons.

FF3M.3 • 14:30 **Invited**

Quantum Approaches to Atomic-Scale Plasmon-Enhanced Molecular Spectroscopy, Javier Aizpurua¹; ¹Mat Physics Ctr. CSIC-UPV/ and DIPC, Spain. The interaction between molecular excitations and plasmons can enhance and modify the spectral properties of a molecule. In this context, we address the importance of quantum effects produced by atomic-scale hot spots.

CLEO: Science & Innovations

14:00–16:00

SF3N • Modulators, Phase Arrays &
Photodetectors

President: Jonathan Bradley; McMaster Univ.,
Canada

SF3N.1 • 14:00

MoTe₂ Vertical Heterostructure Waveguide Detector, Ping Ma¹, Nikolaus Flöry¹, Yannick Salamin¹, Alexandros Emboras¹, Takashi Taniguchi², Kenji Watanabe², Lukas Novotny¹, Jürg Leuthold¹; ¹ETH Zurich, Switzerland; ²National Inst. for Material Science, Japan. A high-speed waveguide-integrated photodetector based on MoTe₂ vertical heterostructure is demonstrated. The proposed photodetector features a measured 3 dB bandwidth of 25 GHz around 1310 nm.

SF3N.2 • 14:15

Tiled Silicon-Photonic Phased Array for Large-Area Apertures, Bohan Zhang¹, Nathan Dostart², Michael Brand², Anatol Khilo¹, Daniel Feldkhun², Milos Popovic^{1,2}, Kelvin Wagner²; ¹Electrical and Computer Engineering, Boston Univ., USA; ²Electrical, Computer and Energy Engineering, Univ. of Colorado, Boulder, USA. We present the first demonstration of a tiling scheme to scale silicon photonic optical phased arrays to large-area beam steering apertures. We experimentally demonstrate two co-steering tiles - the first step towards a practical scheme to reach large area apertures.

SF3N.3 • 14:30

Hybrid Integration of Multi-band, Tunable External-Cavity Diode Lasers for Wide-Angle Beam Steering, Yeyu Zhu¹, Siwei Zeng¹, Yunsong Zhao¹, Lin Zhu¹; ¹Clemson Univ., USA. We demonstrate hybrid integration of multi-band tunable external cavity diode lasers with a silicon nitride photonic chip. We realize wide-angle beam steering by using the extremely wide wavelength tuning range provided by multi-band diode lasers.

14:00–16:00

SF3O • Saturable Absorber Materials &
Chalcogenides

President: Tingyi Gu; Univ. of Delaware, USA

SF3O.1 • 14:00

Multiple-wavelength Q-switched Fiber Laser Using Synthetic Single-crystal Diamond Saturable Absorber, Zheyuan Zhang¹, Yuanjun Zhu¹, Pengtao Yuan¹, Hongbo Jiang¹, Zihao Zhao¹, Fulin Xiang¹, Lei Jin¹, Sze Y. Set¹, Shinji Yamashita¹; ¹Univ. of Tokyo, Japan. The saturable absorber properties of synthetic single-crystal diamond is demonstrated, and a Q-switched fiber laser using synthetic diamond as saturable absorber (SA) which could achieve multi-wavelength output is proposed and demonstrated.

SF3O.2 • 14:15

Er- and Tm-doped mode-locked fiber laser with a broadband, microfiber-based MOF saturable absorber, Qian Zhang¹, Meng Zhang¹, Xinxin Jin¹, Quanyu Jiang¹, Xiantao Jiang², Han Zhang², Zheng Zheng¹; ¹Beihang Univ., China; ²Shenzhen Univ., China. We demonstrate mode-locked pulse generation in erbium-doped and thulium-doped fiber lasers by using a microfiber-based metal-organic frameworks saturable absorber. Our results highlight the applicability of such nanomaterial as a broadband SA for ultrafast photonic applications.

SF3O.3 • 14:30

Thulium-doped mode-locked fiber laser with MXene saturable absorber, Quanyu Jiang¹, Meng Zhang¹, Qian Zhang¹, Xinxin Jin¹, Qing Wu¹, Xiantao Jiang², Han Zhang², Zheng Zheng¹; ¹Beihang Univ., China; ²Shenzhen Univ., China. We demonstrate an all-fiber thulium-doped mode-locked laser by using MXene as the saturable absorber, producing 2.11 ps pulses at 13.45 MHz repetition rate. Our work highlights the potential of MXene-based devices for future photonic technologies.

CLEO: QELS-Fundamental Science

FF3A • Single-Photon Collection
& Characterization—Continued

FF3A.4 • 14:45

Emission Statistics and Optical Transition Dipoles of Semiconductor Nanoplatelets, Xuedan Ma¹, Benjamin Diroll¹, Igor Fedin², Wooje Cho², Dmitri Talapin^{2,1}; ¹Argonne National Lab, USA; ²Dept. of Chemistry and James Franck Inst., Univ. of Chicago, USA. We report on the emission statistics and optical transition dipoles of quasi-two-dimensional semiconductor nanoplatelets studied by single particle spectroscopy. We find that the emission properties of the nanoplatelets are strongly dependent on their lateral dimensions.

FF3A.5 • 15:00 **Invited**

Crummy Measurements and Lousy Copies: Methods to Simultaneously Measure X and P in Order to Directly Observe the Quantum Wavefunction, Jeff S. Lundeen¹; ¹Univ. of Ottawa, Canada. We measure position and momentum on a single photon using two methods: weak measurements and optimal quantum-cloning. We demonstrate that either method directly measures the wavefunction so that its real and imaginary components appear straight on our measurement apparatus.

FF3A.6 • 15:30

Quantum, Nonlocal Aberration Cancellation, Andy N. Black¹, Enno A. Giese¹, Boris Braverman², Nicholas Zollo³, Robert Boyd^{1,2}; ¹Dept. of Physics and Astronomy, Univ. of Rochester, USA; ²Dept. of Physics, Univ. of Ottawa, Canada; ³The College of Optics and Photonics, Univ. of Central Florida, USA; ⁴Inst. for Quantum Physics, Ulm Univ., Germany. We demonstrate the effects of aberration and nonlocal aberration cancellation on a photonic transverse entanglement measurement. This technique can be applied to realize nonlocal aberration correction in ghost imaging.

FF3B • Disordered Media—
Continued

FF3B.4 • 14:45

Anderson Localization in Nearly-periodic and Strongly Disordered Finite-supported Systems, Randhir Kumar¹, Sandip Mondal¹, M Balasubrahmaniam¹, Martin Kamp², Sushil A. Mujumdar¹; ¹Tata Inst. of Fundamental Research, India; ²Lehrstuhl fuer Technische Physik, Univ. of Wuerzburg, Germany. We experimentally demonstrate two-dimensional Anderson localization of light in two disorder regimes, namely, in nearly-periodic disorder, and in strong disorder. Measurement of generalized conductance fluctuations demarcates hitherto-unknown differences between the two regimes.

FF3B.5 • 15:00

Transverse localization of transmission eigenchannels in the diffusive regime, Hasan Yilmaz¹, Chia Wei Hsu¹, Alexey Yamilov², Hui Cao¹; ¹Yale Univ., USA; ²Dept. of physics, Missouri Univ. of Science & Technology, USA. We discover transverse localization of transmission eigenchannels in wide diffusive slabs and study the scaling of eigenchannel widths. Such localization enhances energy densities inside turbid media, which are important for light-matter interactions and imaging applications.

FF3B.6 • 15:15

Disorder-Immune Photonics Based on Mie-Resonant Dielectric Metamaterials, Changxu Liu^{1,2}, Mikhail Rybin³, Peng Mao¹, Shuang Zhang¹, Yuri S. Kivshar²; ¹Univ. of Birmingham, UK; ²Australian National Univ., Australia; ³Ioffe Inst., Russia. We study periodic lattices of silicon nanorods and introduce the concept of a phase diagram characterizing the regimes of photonic crystals and metamaterials. We unveil a novel regime with a robust bandgap which can endure disorder beyond 30% of the lattice constant.

FF3B.7 • 15:30

Delay Time inside Disordered 1D Media, Yiming Huang^{1,2}, Azriel Z. Genack^{1,2}; ¹Queens College of CUNY, USA; ²Physics, Graduate Center of CUNY, USA. Microwave measurements and simulations show that the ensemble average of the delay time of waves inside disordered 1D media increases linearly with depth with a slope equal to the inverse of the group velocity.

FF3C • Attosecond Dynamic
Imaging—Continued

FF3C.3 • 14:45

Glory rescattering in strong-field atomic ionization, Qinzi Xia¹, Jianfei Tao², Jun Cai³, Libin Fu⁴, Jie Liu¹; ¹IAPCM, China; ²Beijing Computational Science Research Center, China; ³Jiangsu Normal Univ., China; ⁴Graduate School of China Academy of Engineering Physics, China. Glory rescattering is discovered in strong field atomic ionization. By developing glory rescattering theory, we resolve the discrepancies between theories and experiments on holographic patterns, and shed light on the quantum interference aspects of LES.

FF3C.4 • 15:00

Streaking of Argon L-shell Auger emissions with > 250 eV attosecond X-ray pulses, Seunghwoi Han¹, Peng Xu², Yishan Wang², Kun Zhao³, Zenghu Chang¹; ¹CREOL and Dept. of Physics, Univ. of Central Florida (UCF), USA; ²State Key Lab of Transient Optics and Photonics, Xi'an Inst. of Optics and Precision Mechanics, CAS, China; ³Inst. of Physics, Chinese Academy of Sciences, China. We investigate the Argon Auger decay using isolated attosecond X-ray pulses reach the Carbon K-edge. A home-built electron spectrometer resolves and measures lifetimes of L-shell vacancies of Argon in pump-probe experiment.

FF3C.5 • 15:15

Ultrafast Ring-Opening Dynamics of 1,3-cyclohexadiene Probed via Time-Resolved High-Harmonic Spectroscopy, Keisuke Kaneshima¹, Yuki Ninota¹, Taro Sekikawa¹; ¹Hokkaido Univ., Japan. We demonstrate the simultaneous observation of the electronic and vibrational dynamics of the photo-isomerizing 1,3-cyclohexadiene via high-harmonic spectroscopy. The attosecond high-harmonic interference reveals how the excited-state ionization potential evolves along the reaction coordinate.

FF3C.6 • 15:30

Tracking the Phase Transition in VO₂ using High Harmonic Spectroscopy, Mina Bionta¹, Adrien Leblanc¹, Vincent Gruson^{1,2}, Philippe Lassonde¹, Jérémie Chaillou¹, Nicolas Emond¹, Martin R Otto³, Bradley J Siwick², Mohamed Chaker¹, François Légaré¹; ¹INRS-Energie Mat & Télé Site Varennes, Canada; ²Physics, The Ohio State Univ., USA; ³Physics and Chemistry, McGill, Canada. We investigate the dynamics of the insulator-to-metal phase transition in VO₂ with high temporal resolution using a new method of time-resolved high harmonic spectroscopy in a solid-state system, revealing all electronic states involved.

FF3D • Nonlinear & Quantum
Effects—Continued

FF3D.4 • 14:45

Observing Quantum Turbulent Structure in Laser Speckle, Samuel Alperin^{1,2}, Abigail Grotelueschen¹, Mark Siemens¹; ¹Univ. of Denver, USA; ²Univ. of Cambridge, UK. We demonstrate both experimentally and numerically that vortices in laser speckle obey the same velocity statistics as in turbulent quantum fluids, thus linking the seemingly-disparate fields of classical optics and quantum fluid dynamics.

FF3D.5 • 15:00

Romdom vs. quasi phase matching: frequency conversion in zinc-blende polycrystals, experiment and theory, Taiki Kawamori¹, Qitian Ru¹, Xuan Chen¹, Konstantin L. Vodopyanov¹; ¹Univ. of Central Florida, USA. We develop a model for random-phase matching which takes into account effects of random crystal orientation and grain size fluctuations and show that for ultrafast interactions, random-phase matching can be as efficient as quasi-phase matching.

FF3D.6 • 15:15

Compact quantum imaging based on induced coherence, Marta Gilaberte Basset¹, Josué R. León Torres¹, Markus Graefe¹; ¹Fraunhofer Inst. for Applied Optics and Precision Engineering IOF, Germany. We report on a compact single-crystal setup for quantum imaging based on induced coherence without induced emission. Our first results will pave the way towards extreme light imaging devices for life science.

FF3D.7 • 15:30

Quantum Radiation from Electrons in Strong Fields, Morgan H. Lynch¹, Ori Reinhardt¹, Nicholas Rivera², Ido Kaminer¹; ¹Electrical Engineering, Technion - Israel Inst. of Technology, Israel; ²Physics, Massachusetts Inst. of Technology, USA. We present a mechanism for generating ultrashort high-harmonic radiation pulses in electron microscopes. At the core of this mechanism are transitions between electronic Floquet states formed in the strong nearfield of a nanophotonic structure.

Executive Ballroom
210E

CLEO: Science &
Innovations

SF3E • Ultrafast Oscillators—
Continued

SF3E.4 • 14:45

21 W average power sub-100-fs Yb:Lu₂O₃ thin-disk laser, Norbert Modsching¹, Jakob Drs¹, Julian Fischer¹, Clément Paradis¹, François Labaye¹, Maxim Gaponenko¹, Christian Kränkel², Valentin J. Wittwer¹, Thomas Südmeyer¹; ¹Laboratoire Temps-Fréquence, Université de Neuchâtel, Switzerland; ²Center for Laser Materials, Leibniz-Institut für Kristallzüchtung, Germany. We demonstrate a Kerr lens mode-locked thin-disk laser oscillator operating with 95-fs pulses at 21.1 W of average power. This is the highest average power achieved by any oscillator in the sub-100-fs regime.

SF3E.5 • 15:00

Three-element-cavity enables Kerr-lens mode-locking at 20-GHz repetition rate, Shota Kimura¹, Shuntaro Tani¹, Yohei Kobayashi¹; ¹The Univ. of Tokyo, Japan. We propose a new cavity design for a compact Kerr-lens mode-locked laser using only three optical elements. The repetition rate of 20 GHz was achieved with the pulse duration of 120 fs.

SF3E.6 • 15:15

Graphene mode-locked Tm,Ho:CLNGG laser with 70-fs pulse duration, Yongguang Zhao¹, Weidong Chen¹, Valentin Petrov¹, Li Wang¹, Yicheng Wang¹, Zhongben Pan¹, Xiaojun Dai², Hualei Yuan², Yan Zhang², Huaqiang Cai², Ji Eun Bae³, Sun Young Choi³, Fabian Rotermund³, Pavel Loiko⁴, Josep Serres⁵, Xavier Mateos⁵, Wei Zhou⁶, Deyuan Shen⁶, Uwe Griebner¹; ¹Max-Born Inst., Germany; ²China Academy of Engineering Physics, China; ³Dept. of Physics, South Korea Advanced Inst. of Science and Technology (KAIST), South Korea (the Republic of); ⁴ITMO Univ., Russia; ⁵Universitat Rovira i Virgili, Spain; ⁶Jiangsu Normal Univ., China. We report on a mode-locked Tm,Ho:CLNGG laser employing graphene as a saturable absorber. Pulses as short as 70 fs, i.e., 10 optical cycles, are generated at 2093 nm with a repetition rate of ~89 MHz.

SF3E.7 • 15:30

Sub-10 fs Pulse Generation From a Blue-Diode-Pumped Kerr-Lens Mode-Locked Ti:sapphire Laser, Han Liu¹, Geyang Wang¹, Ke Yang¹, Renzhu Kang¹, Wenlong Tian¹, Dacheng Zhang¹, Liang Guo¹, Jiangfeng Zhu¹, Zhiyi Wei²; ¹Xidian Univ., China; ²Chinese Academy of Sciences, Beijing National Lab for Condensed Matter Physics, Inst. of Physics, China. We demonstrate a blue-diode pumped Kerr-lens mode-locked Ti:sapphire laser generating sub-10 fs pulses for the first time. The laser is centered at 830 nm with 113 nm bandwidth and 22 mW average power.

Executive Ballroom
210F

Joint

JF3F • Symposium on Deep-
learning Photons: Where
Machine Learning & Photonics
Intersect III—Continued

JF3F.2 • 15:00 **Invited**

Training of Photonic Neural Networks through In Situ Backpropagation, Tyler Hughes¹, Momchil Minkov¹, Ian Williamson¹, Yu Shi¹, Shanhui Fan¹; ¹Stanford Univ., USA. We provide a protocol for training photonic neural networks based on adjoint methods. The gradient of the network with respect to its tunable degrees of freedom is computed by physically backpropagating an optical error signal.

JF3F.3 • 15:30 **Invited**

Deep Imaging Cytometry, Yueqin Li¹, Ata Mahjoubfar¹, Bahram Jalali¹, Kayvan Niazi²; ¹UCLA, USA; ²Nantworks, USA. We describe a new implementation of our deep learning time-stretch imaging flow cytometry which avoids data pre-processing and feature extraction. The neural network classifies cancer cells by directly processing the raw serial temporal data.

Executive Ballroom
210G

CLEO: Science & Innovations

SF3G • Laser-Based 2D/3D
Micro- & Nano-fabrication—
Continued

SF3G.4 • 14:45

Two-photon induced chiral mass-transport of azo-polymers as a function of pulse duration, Keigo Masuda¹, Yoshinori Kinezuka¹, Mitsuki Ichijo¹, Ryo Shinozaki¹, Keisaku Yamane², Kohei Toyoda^{1,3}, Katsuhiko Miyamoto^{1,3}, Takashige Omatsu^{1,3}; ¹Chiba Univ., Japan; ²Hokkaido Univ., Japan; ³MCRC Chiba Univ., Japan. We demonstrated two-photon-absorption induced chiral surface relief formation in an azo-polymer film by illumination of picosecond 1- μ m optical vortex pulses. The chiral surface relief formation required at least several times the response-time of trans-cis isomerization.

SF3G.5 • 15:00 **Invited**

Functionalizing Glass by Local Compositional Tuning with Ultrafast Lasers, Javier Solis¹; ¹Instituto De Optica 'Daza De Valdes', Spain. The presentation provides an overview of fs-laser induced ion migration phenomena in glass, with emphasis on recent results of our research group regarding its application for the production of efficient photonic devices.

SF3G.6 • 15:30

Rapid Femtosecond Laser 3D microfabrication using Focal Field Engineering, Yan Li¹, Dong Yang¹, Lipu Liu¹, Hong Yang¹, Qihuang Gong¹; ¹Peking Univ., China. We realize the single-exposure and the single-scan femtosecond laser microfabrication of 3D microstructures by the 3D focal field intensity engineering. The two rapid techniques are further integrated to fabricate a microstructure.

Executive Ballroom
210H

SF3H • Microresonator
Frequency Combs—Continued

SF3H.3 • 14:45

Si-chip frequency combs with 2-octaves bandwidth for longwave-IR gas and liquid dual-comb spectroscopy, Nima Nader¹, Jeff Chiles¹, Henry Timmers¹, Eric J. Stanton¹, Abijith Kowligy¹, Alexander Lind^{1,2}, Sae Woo Nam¹, Scott A. Diddams^{1,2}, Richard P. Mirin¹; ¹National Inst. of Standards and Tech, USA; ²Physics, Univ. Of Colorado, Boulder, USA. We use suspended-silicon waveguides for spectral engineering of mid-infrared frequency combs to achieve spectra spanning 2.0 octaves (2-8.5 μ m). We demonstrate dual-comb spectroscopy of gas and liquid-phase samples with 100 MHz comb-line resolution.

SF3H.4 • 15:00

Silicon-Chip-Based f-2f Interferometer, Yoshitomo Okawachi¹, Mengjie Yu^{1,2}, Jaime Cardenas¹, Xingchen Ji^{1,2}, Michal Lipson¹, Alexander Gaeta¹; ¹Columbia Univ., USA; ²Cornell Univ., USA. Using a single silicon-nitride waveguide, we demonstrate an f-2f interferometer for carrier-envelope-offset frequency (f_{CEO}) detection by simultaneous supercontinuum generation and second-harmonic generation. We measure a f_{CEO} beatnote with a 27-dB SNR with 62-ps pulse energies.

SF3H.5 • 15:30

Microwatt-Level Soliton Frequency Comb Generation in Microresonators Using an Auxiliary Laser, Shuangyou Zhang¹, Jonathan M. Silver¹, Leonardo Del Bino¹, Francois Copie¹, Michael T. M. Woodley¹, George Ghalanos¹, Andreas Svela¹, Niall Moroney¹, Pascal DelHaye¹; ¹National Physical Lab, UK. We report a simple and robust method to generate soliton frequency combs in microresonators assisted by an auxiliary laser. Our method significantly enhances the soliton access range and enables threshold powers down to 780 microwatt.

CLEO: Science & Innovations

CLEO: Applications
& Technology

CLEO: Science & Innovations

SF31 • Lasers for Accelerators—
Continued

SF31.4 • 14:45

Flexible Pulse-Shape Picosecond Front-End for XFEL Photocathode Lasers, Chen Li¹, Lutz Winkelmann¹, Ingmar Hartl¹; ¹Deutsches Elektronen-Synchrotron, Germany. X-ray Free-Electron Lasers rely on low-emittance photo-injectors driven by UV laser pulses. For optimum performance, temporally shaped laser pulses are desired. Here we present a laser front-end which delivers NIR ps-laser pulses of arbitrary pulse-envelope.

SF31.5 • 15:00 **Invited**

Precision Synchronization for large scale Accelerators, Julien Brnard¹, Lukasz Butkowski¹, Marie Kristin Czwilinna¹, Matthias Felber¹, Tomasz Kozak¹, Thorsten Lamb¹, Frank Ludwig¹, Uros Mavric¹, Jost Mueller¹, Sven Pfeiffer¹, Christian Schmidt¹, Sebastian Schulz¹, Cezary Sydlo¹, Mikheil Titberidze¹, Holger Schlarb¹; ¹DESY, Germany. Large scale accelerators such as the European X-ray Free Electron Lasers (XFEL) require femtosecond synchronization over kilometer distance to carry-out complex X-ray photon experiments with high temporal resolution. Recent implementations are summarized in this talk.

SF31.6 • 15:30

Arrival Time Stabilization of the Photocathode Laser at the European XFEL, Jost Mueller¹, Sebastian Schulz¹, Lutz Winkelmann¹, Marie Kristin Czwilinna¹, Ingmar Hartl¹, Holger Schlarb¹; ¹DESY, Germany. Arrival time drifts of the European XFEL photocathode laser pulses were identified using balanced optical cross-correlation and compared to the electron bunch arrival time changes. With a feedback loop this timing error could be compensated to 45 fs.

SF3J • Metasurface & Plasmonic
Structures—Continued

SF3J.4 • 15:00

Optical Chirality Tunable and Reversible Plasmonic Chiral Metasurfaces on Flexible PDMS Substrate, Hsiang-Ting Lin¹, Yao-Yu Hsu^{1,2}, Chiao-Yun Chang¹, Min-Hsiung Shih^{1,2}; ¹Research Center for Applied Sciences, Academia Sinica, Taiwan; ²Dept. of Photonics and Inst. of Electro-Optical Engineering, National Chiao Tung Univ., Taiwan. We demonstrated a flexible plasmonic chiral metasurface which realized optical chirality both tunable and reversible. The controllable circular dichroism from -25% to +30% was achieved in the same metasurface under different stretch situations.

SF3J.5 • 15:15

Dispersion-Engineered Metasurfaces for Aberration-Corrected Spectroscopy, Alexander Y. Zhu¹, Wei-Ting Chen¹, Jared Sisler^{1,2}, Kerolos M. Yousefi^{1,3}, Eric Lee^{1,2}, Yao-Wei Huang^{1,4}, Cheng-wei Qiu⁴, Federico Capasso¹; ¹Harvard Univ., USA; ²Univ. of Waterloo, Canada; ³College of Biotechnology, Misr Univ. of Science and Technology, Egypt; ⁴National Univ. of Singapore, Singapore. We report a miniature aberration-corrected spectrometer comprised of dispersion-engineered off-axis metasurface lenses. It possesses close to diffraction-limited spot sizes across 200 nm in the visible and has nanometer spectral resolution, despite a 4cm beam-propagation distance.

SF3J.6 • 15:30

Metasurface-based Waveplates Demonstrated on 300 mm Si CMOS Platform, Yuan Dong¹, Zhengji Xu¹, Jinchao Tong², Yuan-Hsing Fu¹, Qize Zhong¹, Vladimir Bliznetsov¹, Ting Hu¹, Yu Li¹, Shiyang Zhu¹, Qunying Lin¹, Dao Hua Zhang², Navab Singh¹; ¹Inst. of Microelectronics, Singapore; ²Nanyang Technological Univ., Singapore. Metasurface-based all-Si waveplates are first demonstrated on 300 mm CMOS platform. The cross- and copolarization transmittances are characterized. A polarization conversion efficiency of 87% is achieved near 1.6 μm -wavelength.

AF3K • Imaging, Microscopy,
& Specialized Detection—
Continued

AF3K.4 • 14:45

Improvement of Image Quality in Dual-Comb Microscopy by Post-Amplification of Dual Comb Lights, Takahiko Mizuno^{1,2}, Takuya Tsuda^{1,2}, Eiji Hase^{1,2}, Takeo Minami-kawa^{1,2}, Hirotsugu Yamamoto^{2,3}, Takeshi Yasui^{1,2}; ¹Tokushima Univ., Japan; ²JST, ERATO MINOSHIMA Intelligent Optical Synthesizer (IOS), Japan; ³Utsunomiya Univ., Japan. We combine dual-comb microscopy and post-amplification technique for rapid acquisition of confocal amplitude and phase images. The proposed method significantly improves signal-to-noise ratio in the rapid scan-less imaging.

AF3K.5 • 15:00

Near-Infrared Molecular Fieldoscopy, Ayman Alismail¹, Haochuan Wang¹, Gaia Barbiero¹, Syed Ali Hussain¹, Wolfgang Schweinberger¹, Ferenc Krausz¹, Hanieh Fattahi¹; ¹Max-Planck-Institut für Quantenoptik, Germany. In this work, the concept of near-infrared molecular fieldoscopy is introduced and bench-marking measurements are presented. The new method allows for high-resolution overtone spectroscopy and microscopy with an unparalleled sensitivity and specificity over the entire molecular fingerprint region.

AF3K.6 • 15:15

Time-stretch Network Analyzer for Single-shot Characterization of Electronic Devices, Zhuoya Bai¹, Cejo K. Lonappan¹, Asad M. Madni¹, Bahram Jalali¹; ¹Electrical and Computer Engineering, Univ. of California, Los Angeles, USA. An optically-assisted single-shot instrument with automated Tikhonov calibration for measuring the complex frequency response of electronic devices is presented. High-throughput characterization of microwave amplifiers at 37 million impulse response measurements per second is demonstrated.

AF3K.7 • 15:30

Sub-nanosecond Pulsed Quantum Cascade Laser Driver, Mateusz Zbik¹; ¹VIGO System S.A., Poland. A QCL modulator based on a pair of pulsed HEMT transistors was designed to test the high-speed VIGO System HgCdTe photodetectors response time. A drive current and optical pulse width of approximately 1A and 100ps, respectively, were achieved.

SF3L • Fiber Sensing—
Continued

SF3L.4 • 14:45

Phase Noise Compensation for Ultra-highly Sensitive Fiber-optic Quasi-distributed Acoustic Sensing System, Mengshi Wu¹, Xinyu Fan¹, Zuyuan He¹; ¹Shanghai Jiao Tong Univ., China. An ultra-highly sensitive quasi-distributed acoustic sensing system is proposed with a phase-noise-compensated configuration, which gives a 11.55 dB improvement to the sensitivity. A sensitivity of 92.84 $\text{ft}/\sqrt{\text{Hz}}$ @ 500-2500 Hz is achieved along a 20-km weak reflector array with 20-m spacing.

SF3L.5 • 15:00 **Invited**

Integrated Fibre Detection Architectures for Distributed Quantum Magnetometry, Shai Maayani¹, Christopher Foy¹, Dirk R. Englund¹, Yoel Fink¹; ¹MIT, USA. Here, we constructed a water-immersible 90-meter-long fully-integrated fiber system that allows distributed quantum magnetic sensing over large distances with a sensitivity of 63 nT Hz^{1/2}. Applications include remote detection of ferrous metals, geophysics, and biosensing.

SF3L.6 • 15:30

Twist Sensor Using Chiral Long-Period Grating Written in the Double-Cladding Fiber, Chen Jiang¹, Yunqi Liu¹, Chengbo Mou¹, Tingyun Wang¹; ¹Shanghai Univ., China. We present the fabrication of a chiral long-period grating in twisted double-cladding fiber using CO₂-laser. The near-filled intensity distribution and twist sensing characteristics of the proposed device were investigated experimentally.

CLEO: QELS-Fundamental
ScienceFF3M • Quantum Interactions in
Nanophotonic Systems—Continued

FF3M.4 • 15:00

Tip Enhanced Strong Coupling of a Single Emitter at Room Temperature, Molly A. May¹, Kyoung-Duck Park¹, Haixu Leng², Jaron A. Kropp², Theodosia Gougousi², Matthew Pelton², Markus B. Raschke¹; ¹Dept. of Physics, Dept. of Chemistry, and JILA, Univ. of Colorado Boulder, USA; ²Dept. of Physics, Univ. of Maryland, USA. We use a configurable plasmonic nano-cavity with a nanoscopic mode volume to achieve and control strong coupling to a single quantum dot under ambient conditions using tip-enhanced photoluminescence spectroscopy.

FF3M.5 • 15:15

Tapered atomic cladded nano waveguide for fine control of light-atom interaction, Roy T. Zektzer¹, Noa Mazurski¹, Yefim Barash¹, Uriel Levy¹; ¹The Hebrew Univ. of Jerusalem, Israel. We experimentally demonstrate the chip-scale integration of tapered nano waveguides and rubidium atoms. The optical mode interaction volume with the atoms is controlled by the tapering, giving rise to sub-Doppler atomic features and controlled interactions.

FF3M.6 • 15:30

Imaging the collapse of electron wave-functions: the relation to plasmonic losses, Chen Mechel¹, Yaniv Kurman¹, Aviv Karnieli³, Nicholas Rivera², Ady Arie³, Ido Kaminer¹; ¹Technion, Israel; ²MIT, USA; ³Tel Aviv Univ., Israel. We show how free-electron interaction with plasmons in electron microscopes leads to electron-plasmon entanglement, connecting electron decoherence with plasmonic losses. We utilize this connection to propose a new method to probe plasmonic lifetimes.

CLEO: Science & Innovations

SF3N • Modulators, Phase Arrays &
Photodetectors—Continued

SF3N.4 • 14:45

Acousto-Optic Modulator based on the Integration of Arsenic Trisulfide Photonic Components with Lithium Niobate Surface Acoustic Waves, Mdshofiqulislam Khan¹, Ashraf Mahmoud¹, Lutong Cai¹, Mohamed Mahmoud¹, Tamal Mukherjee¹, James Bain¹, Gianluca Piazza¹; ¹Carnegie Mellon Univ., USA. An acousto-optic modulator formed by an Arsenic Trisulfide (As₂S₃) Mach-Zehnder interferometer placed inside a surface acoustic wave cavity on a Lithium Niobate (LN) wafer is demonstrated for the first time.

SF3N.5 • 15:00

Metalens-enabled Low-power Solid-state 2D Beam Steering, You-Chia Chang^{2,1}, Min Chul Shin², Christopher T. Phare², Steven A. Miller², Euijae Shim², Michal Lipson²; ¹Dept. of Photonics and Inst. of Electro-Optical Engineering, National Chiao Tung Univ., Taiwan; ²Electrical Engineering, Columbia Univ., USA. We demonstrate a platform for low-power solid-state beam steering in 2D using a single wavelength. This platform, based on a metalens and a switchable emitter array, enables steering of 12.4°×26.8° using less than 83 mW.

SF3N.6 • 15:30

True Time Delay Millimeter Wave Beam Steering with Integrated Optical Beamforming Network, Yuan Liu¹, Brandon Isaac¹, Jean Kalkavage², Eric Adles², Thomas Clark², Jonathan Klamkin¹; ¹Univ. of California Santa Barbara, USA; ²The Johns Hopkins Univ. Applied Physics Lab, USA. Abstract A 94 GHz 1x4 phased array antenna with true time delayed integrated optical beamforming network was demonstrated. Steering angles of -51°, +/-32°, +/-15°, and 0° were achieved with excellent beam quality.

SF3O • Saturable Absorber Materials &
Chalcogenides—Continued

SF3O.4 • 14:45

High Power Tolerant SWCNT-BNNT Saturable Absorber for Laser Mode-Lockin, Pengtao Yuan¹, Zheyuan Zhang¹, Shoko Yokokawa¹, Yongjia Zheng², Lei Jin¹, Sze Y. Set¹, Shigeo Maruyama², Shinji Yamashita¹; ¹Research Center for Advanced Science and Technology, Univ. of Tokyo, Japan; ²Department of Mechanical Engineering, The Univ. of Tokyo, Japan. We demonstrate a mode-locked fiber laser using BN-wrapped SWCNT as a high power-tolerant saturable absorber. The new saturable absorber shows a significantly higher optical damage threshold and a great potential for various high-power optical applications.

SF3O.5 • 15:00

Micromachining of chalcogenide waveguides by picosecond laser, Dun Mao¹, Mingkun Chen^{2,1}, Nathan Augenbraun¹, Anishkumar Soman¹, Xiangyu Ma¹, Thomas Kananen¹, Matthew Doty¹, Tingyi Gu¹; ¹Univ. of Delaware, USA; ²Univ. of Rochester, USA. Direct laser inscription creates waveguide structures on chalcogenide thin film. Results of Ge₂Sb₂Te₃ and Ge₂₂Sb₇Se₇₀ are compared by varying laser powers and translation speeds.

SF3O.6 • 15:15

Integration of Nanoimprint and Silver Doping Lithography for Chalcogenide Photonic Crystal Slabs, Le Wei¹, Meng Lu¹, Liang Dong¹; ¹Iowa State Univ., USA. We report a novel nanofabrication approach that combines the imprinting and silver doping lithography processes to pattern chalcogenide materials. The approach can fabricate 3D nanoscale structures in chalcogenide thin film for nanophotonic devices and sensors.

SF3O.7 • 15:30

Complete Photonic Bandgap in Lowest Index Contrast Inverse Rod-Connected Diamond Structured Chalcogenides, Lifeng Chen^{1,2}, Katrina Morgan³, Chung-Che Huang³, Ying-Lung Daniel Ho¹, Mike P. C. Taverne¹, Daniel W. Hewak³, John G. Rarity¹; ¹Univ. of Bristol, UK; ²Sun Yat-Sen Univ., China; ³Univ. of Southampton, UK. We present an inverse rod-connected diamond structure showing a complete bandgap with refractive index contrast down to $n_{\text{high}}/n_{\text{low}} \sim 1.9$. The structures were fabricated using a low-temperature chemical vapor deposition process, via a single-inversion technique.

CLEO: QELS-Fundamental Science

FF3A • Single-Photon Collection
& Characterization—ContinuedFF3B • Disordered Media—
ContinuedFF3C • Attosecond Dynamic
Imaging—ContinuedFF3D • Nonlinear & Quantum
Effects—Continued

FF3A.7 • 15:45

Direct Detection of Quantum Phase Errors in Spatially Multiplexed Transmission Channels, Kai Wang^{1,2}, Falk Eilenberger^{3,4}, Alexander Szameit², Andrey A. Sukhorukov¹; ¹Nonlinear Physics Centre, Research School of Physics and Engineering, Australian National Univ., Australia; ²Inst. for Physics, Rostock Univ., Germany; ³Inst. of Applied Physics, Abbe Center of Photonics, Friedrich Schiller Univ., Germany; ⁴Center for Excellence in Photonics, Fraunhofer Inst. for Applied Optics and Precision Engineering IOF, Germany. We introduce a protocol for direct detection of arbitrary continuous phase errors in transmission of multi-photon spatially entangled quantum states, and present a design and experimental evidence for its realization in an integrated photonic circuit.

FF3B.8 • 15:45

A Novel Phase-Map to Increase the Efficiency of Random Metasurfaces, Hadiseh Nasari¹, Matthieu Dupré¹, Boubacar Kanté¹; ¹Dept. of Electrical and Computer Engineering, Univ. of California San Diego, USA. We report on using a statistical approach to obtain a novel phase-map addressing the near-field coupling between elements and improving the efficiency of random metasurfaces compared to the conventional ones designed by periodic phase-map.

FF3D.8 • 15:45
Withdrawn

Executive Ballroom
210E

CLEO: Science & Innovations

SF3E • Ultrafast Oscillators—Continued

Executive Ballroom
210F

Joint

JF3F • Symposium on Deep-learning Photons: Where Machine Learning & Photonics Intersect III—Continued

Executive Ballroom
210G

CLEO: Science & Innovations

SF3G • Laser-Based 2D/3D Micro- & Nano-fabrication—Continued

SF3G.7 • 15:45
Direct Printing of Gold Nano-Particles by Laser Induced Dewetting, Jae Hyuck Yoo¹, Nathan Ray¹, Hoang Nguyen¹, Mike Johnson¹, Sal Baxamusa¹, Selim Elhadji¹, Joseph Mckeown¹, Manyalibo J. Matthews¹, Eyal Feigenbaum¹; ¹LLNL, USA. Arbitrary patterns, consisting of sub-wavelength sized nano particles, are developed by laser induced dewetting of ultrathin gold films (e.g., 5, 7.5, and 10 nm). We demonstrate that the light induced local temperature determines the resulting dewetting structures.

Executive Ballroom
210H

SF3H • Microresonator Frequency Combs—Continued

SF3H.6 • 15:45
Broadband High-Resolution Scanning of Soliton Micro-Combs, Tong Lin¹, Avik Dutt¹, Xingchen Ji¹, Chaitanya Joshi¹, Alexander Gaeta¹, Michal Lipson¹; ¹Columbia Univ., USA. We demonstrate continuous scanning of a single soliton micro-comb over 88 GHz with an instantaneous linewidth of 60 kHz. We show such a system can acquire spectra of HCN with a high spectral-resolution.

Friday, 14:00–16:00

Meeting Room
211 A/B

Meeting Room
211 C/D

Meeting Room
212 A/B

Meeting Room
212 C/D

CLEO: Science & Innovations

CLEO: Applications
& Technology

CLEO: Science & Innovations

SF3I • Lasers for Accelerators—
Continued

SF3J • Metasurface & Plasmonic
Structures—Continued

AF3K • Imaging, Microscopy,
& Specialized Detection—
Continued

SF3L • Fiber Sensing—
Continued

SF3I.7 • 15:45

High-sensitivity X-ray Optical Cross-Correlator for Next Generation Free-Electron Lasers, Stefan Droste¹, Lingjia Shen¹, Vaughn E. White¹, Elizabeth Diaz-Jacobo¹, Ryan Coffee¹, Sioan Zohar¹, Alexander Reid¹, Franz Tavella¹, Michael P. Minitti¹, Joshua Turner¹, Karl Gumerlock¹, Alan Fry¹, Giacomo Coslovich¹; ¹SLAC / Stanford, USA. We designed a novel X-ray arrival time monitor that cross-correlates X-ray and 1550nm optical pulses. We exploit an interferometric detection scheme and etalon effects in thin-film Germanium to achieve unprecedented high sensitivity to soft X-rays.

SF3J.7 • 15:45

Direct laser writing of optical field concentrators based on chirped three-dimensional photonic crystals, Vyngantas Mizeikis¹, Zeki Hayran², Hamza Kurt², Mirbek Turduev³, Darius Gailevicius⁴, Mangirdas Malinauskas⁴, Saulius Juodkazis⁵, Kestutis Staliunas⁶; ¹Research Inst. of Electronics, Shizuoka Univ., Japan; ²TOBB Univ. of Economics and Technology, Turkey; ³TED Univ., Turkey; ⁴Vilnius Univ., Lithuania; ⁵Swinburne Univ. of Technology, Australia; ⁶Institució Catalana de Recerca i Estudis Avancats, Spain. 3D chirped photonic crystals for applications as electromagnetic field concentrators at optical frequencies were fabricated using Direct Laser Write technique, their optical properties and functionality were characterized experimentally.

AF3K.8 • 15:45

Ultrafast UV Metal–Semiconductor–Metal Photodetector Based on AlGaN with a Response Time Below 20 ps, Yiming Zhao¹; ¹Lab for Laser Energetics, USA. AlGaN UV photodetectors were fabricated with micrometer scale metal–semiconductor–metal structures and tested with an ultrafast 263-nm laser. The best performance devices showed a fast response time of below 20 ps and dark currents below 10 pA.

SF3L.7 • 15:45

Intensity-Interrogated Refractive Index Sensor Based on Exposed-Core Multicore Fiber Mach-Zehnder Interferometer, Shaoxiang Duan¹, Bo Liu¹, Hao Zhang¹, Xu Zhang¹, Haifeng Liu¹, Jixuan Wu², Yuan Yao¹; ¹Inst. of Modern Optics, Nankai Univ., China; ²School of Electronics and Information Engineering, China. A temperature-insensitive intensity-interrogated fiber sensor based on exposed-core multicore fiber for refractive index (RI) measurement is demonstrated by etching a seven-core fiber. The RI sensitivity of -287.252 dB/RIU is experimentally achieved.

CLEO: QELS-Fundamental
Science

FF3M • Quantum Interactions in
Nanophotonic Systems—Continued

FF3M.7 • 15:45

Goos-Hänchen shift in edge-reflections of two-dimensional surface polaritons, Ji-Hun Kang², Sheng Wang¹, Feng Wang¹; ¹Dept. of Physics, Univ. of California Berkeley, USA; ²Dept. of Physics and Astronomy, Seoul National Univ., South Korea (the Republic of). We introduce an analytic model describing the reflection of two-dimensional surface polaritons at an abrupt edge, and reveal that induced evanescent waves during the reflection leads to a Goos-Hänchen phase shift of $\pi/4$ in edge-reflections.

CLEO: Science & Innovations

SF3N • Modulators, Phase Arrays &
Photodetectors—Continued

SF3N.7 • 15:45

Luneburg Lens for Wide-Angle Chip-Scale Optical Beam Steering, Samuel Kim¹, Jamison Sloan¹, Josué López¹, Dave Kharas², Jeffrey Herd², Suraj Bramhavar², Paul Juodawlkis², George Barbastathis¹, Steven Johnson¹, Sorace-Agaskar Cheryl², Marin Soljacic¹; ¹MIT, USA; ²MIT Lincoln Lab, USA. We present a design for a planar generalized Luneburg lens for use in a chip-scale optical beam steering device. The device has a theoretical in-plane field of view of 160° with no off-axis aberrations.

SF3O • Saturable Absorber Materials &
Chalcogenides—Continued

SF3O.8 • 15:45

Growth and Characterization of PbGa₂GeSe₆: A New Quaternary Chalcogenide Nonlinear Crystal for the Mid-IR, Valeriy V. Badikov², Dmitrii Badikov², Li Wang¹, Galina S. Shevyrdyaeva², Vladimir L. Panyutin¹, Anna A. Fintisova², Svetlana G. Sheina², Valentin Petrov¹; ¹Max Born Inst., Germany; ²Kuban State Univ., Russia. Non-centrosymmetric crystals of PbGa₂GeSe₆, grown in large sizes and with good optical quality, are used to characterize its linear (transmission, dispersion, and birefringence) and nonlinear (second order susceptibility) optical properties.

Key to Authors and Presidents

A

A.S, Lal Krishna - JW2A.37
 Abadia, Nicolas - JTu2A.110
 Abaie, Behnam - SM4L.5
 Abbasi, Amin - STh4N.1
 Abbaslou, Siamak - SW3H.7
 Abbott, William - JW2A.66
 Abdallah, Zeina - SM3O.4
 Abdelsalam, Kamal - FW3B.7
 Abdi-Jalebi, Mojtaba - SF1O.3
 Abe, Eisuke - SM2F
 Abe, Tetsuya - SF3L.1
 Abedin, Kazi - SF1M
 Abernathy, Grey - STu3N.3
 Abiri, Behrooz - SF2N.6, STh3H.7
 Abouraddy, Ayman F. - ATH11.6, JTh2A.98, JW2A.72, SW4E.8
 Acevedo, Cristian Hernando - FTh1C.8
 Ackermann, Manuel - Ath3I.3
 Adachi, Takuto - SM2H.8
 Adamo, Giorgio - FTu3D.7
 Adamopoulos, Christos G. - JW2A.81
 Adams, Danial - AM2I.4
 Addamane, Sadhvikas - FM2C.3
 Addhya, Anchita - JTu4M.5
 Addisu, Mesay - STh4L.1
 Adhikary, Pratik - FM2A.4
 Adibi, Ali - JTh2A.55, JW2A.52, SF2H.5, STh1H.5, STh3H
 Adler, Florian - STh1G
 Adles, Eric - SF3N.6
 Aeschlimann, Martin - FTh1C.7
 Affouda, Chaffra A. - SM2J.7
 Afkhamiardakani, Hanieh - STh4L.6
 Afzal, Francis O. - SM2J.4
 Agafonova, Sofya E. - STu3J.4
 Agha, Imad - SF2O.5, SF2O.6
 Aghaeimebodi, Shahriar - FM1M.3
 Agostini, Pierre - FF3C.1
 Agrawal, Amit K. - AM3K.2, FF3M, FM3C.3, FM3C.7, FW3C.1
 Aguilo, Magdalena - JTu2A.119, STh1E.5
 Aharonovich, Igor - FM4A.5, SF1J.3, SM2F.5
 Ahasan, Sohail - SM1N.6
 Ahlefeldt, Rose - FM1A.5
 Ahmad, Raja - JTh2A.92
 Ahmed, Osman - FW3B.5
 Ahn, Geun Ho - SW4J.3
 Ahn, Heesang - JTu2A.7
 Ahn, Jaewook - FM2A.7, FM2A.8
 Ahufinger, Verónica - FM4B.3, JTh2A.46
 Ai, Fan - JW2A.91
 Aifer, Edward H. - SM2J.7
 Aihara, Takuma - STh3N.1
 Aiqa, Hu - FTu3C.5
 Aitchison, J. Stewart - AM4I.7, JW2A.36
 Aizpurua, Javier - FF3M.3
 Akasaka, Youichi - FW3B.5
 Akashi, Yota - JTh2A.71
 Akatsuka, Tomoya - SW4G.2
 Akens, Margaret - JTu2A.1
 Akhoundi, Farhad - AM3I.1, SF3G.1
 Akiyama, Hidefumi - FM4M.1
 Akosman, Ahmet - SW4H.6
 Aksyuk, Vladimir - AM3K.2, STu4G.4, SW3J
 Akulov, Katherine - FM3D.8
 Al Alshaykh, Mohammed S. - SF2N.8
 Al Maruf, Rubayet - FM1B.1
 Al Saif, Bidoor - Ath3K.2
 Aladi, Mark - FF1C.3
 Alaghemandi, Mohammad - SM3H.5
 Alahbakhshi, Masoud - SW4N.2

Alahmadi, Yousef - FTu3B.2
 Alam, Shaif-UI - JW2A.44, STh1E.3
 Alam, Zahirul - FF1B.3, FW4B.5
 AlAraimi, Mohammed - JW2A.38
 Al-atawi, Abdullah - SM3N.4
 Albadi, Abdulrahman - SM3N.4
 Albert, Olivier - STh3E.1
 Alberti, Edoardo - SF2J.4
 Albrecht, Alexander R. - JTu2A.78, STh1E.7
 Albrecht, Manfred - FW4M.4
 Alcaraz Iranzo, David - FF3D.2
 Aleshkina, Svetlana - SM4E.2, SM4L.1
 Alessi, David - SM4E.4
 Alexoudi, Theoni - STh4N.5
 Alfaraj, Nasir - SF2O.1
 Alharthi, Bader - STu3N.3
 Alhoussein, Muataz M. - JTu2A.28
 Alisafae, Hossein - SM2O.1
 Alisauskas, Skirmantas - STu4E.4
 Alishahi, Fatemeh - FW4B.5, SF2N.3, SM3G.3
 Alismail, Ayman - AF3K.5
 Al-Kabi, Sattar - STh4O.6
 Al-Khateeb, Mohammad - SW3O.1
 Allahverdi, Arman - SM4L.5
 Allegro, Isabel - JTu2A.71
 Allen, Jeffery - STh4O.4
 Allen, Joshua - SM2J.4
 Allen, Monica - STh4O.4
 Allende Motz, Alyssa M. - AM2I.4
 Allerbeck, Jonas - FM3D.6
 Allford, Craig - SM3N.6
 Allgaier, Markus - JTu3A.1
 Almaman, Ahmed - FW4B.5, JTu2A.57, JTu2A.67, SF2N.3, SM1J.5, SM3G.3
 Almeida, Diogo B. - FM3D.5
 Alonso Calafell, Irati - FF3D.2, FTh4A.3
 Alouini, Mohamed-Slim - JTh2A.51
 Alpeggiani, Filippo - JM2B.2
 Alperin, Samuel - FF3D.4, JW2A.48
 Al-Qadi, Mustafa A. - SW3O.2
 Alsaigh, Rakan E. - Ath11.5
 AlShafey, Abdallah - SM3H.2
 Alshaykh, Mohammed S. - JTu3A.3
 Alsing, Paul M. - FTh1D.4
 Altug, Hatice - FTh4C.6, SF3J.1
 Alù, Andrea - AM3K.5, FTu4B.6, FW4D.5, JM2B.1, JM2B.3, SW4J.3, FTh3M.2
 Alvarado Zacarias, Juan Carlos - SM1G.1, SM1G.2, SM1L.1
 Alvarez, Asier - JTu2A.46
 Alvermann, Andreas - FM4B.2
 Alyamani, Ahmad - SM3N.4
 Amani, Matin - SW3J.2
 Amano, Hikaru - STh4J.6
 Amarasinghe, Yasith - STu3F.6
 Ambichl, Philipp - FTu4B.2
 Ambrosio, Antonio - AM3K.3, FM3C.2
 Amemiya, Tomo - JTh2A.16, SM4F.3
 Amezcuca Correa, Rodrigo - JW2A.103, SM1G.2, SM1L.1, SM4L.3, STh1L.3, STh3L.2
 Amezcuca-Correa, Adrian - SM1L.1
 Amin, Rubab - JTh2A.45
 Aminimalragia-Giamini, Sigiava - SM1H.3
 Amiri, Seyed Ebrahim Hashemi - JW2A.19
 Amirzhan, Arman - STh4H.3
 Amorim, Bruno - FM4M.5
 Amotchkina, Tatiana - JW2A.69
 An, Sensong - JTh2A.14
 An, Yi - JW2A.106
 Anandarajah, Prince M. - JTh2A.63, SM4G.2, SM4N.6, STu4N.5

Andaji-Garmaroudi, Zahra - SF1O.3
 Andersen, Ulrik - JF2F.1
 Anderson, James - SM4L.3
 Anderson, Jon - SW4O.6
 Anderson, Miles H. - STu3J.3
 Anderson, Paul - JW2A.112
 Andrade, José - FF3C.2, STh4E.2
 Andrade, Nicolas M. - FW3C.6
 Andre, Laura B. - STh4H.4
 Andre, Yves-Bernard - JM2E.5
 Andreev, Vitaly - SM4F.1
 Andrews, Aaron M. - STu4O.6
 Andrews, Mark - JW2A.121
 Androvitsaneas, Petros - STh1H.1
 Angal, Amit - JW2A.12
 Angelova, Liliya - JTu2A.2
 Anisimov, Igor - JTh2A.36
 Anne Plucinski Hackett, Lisa - JTu2A.96
 Ansari, Mohammad Afnan - FF2B.7
 Ansari, Wahid - JTu3A.1
 Anselmi, Alberto - JTu3G.1
 Antón Solanas, Carlos - FM1M.1, FM3A.2
 Antonio-Lopez, Jose Enrique - SM1L.1, SM4L.3, STh1L.3, STh3L.2
 Antony, Abhinandan - JTh4F.1
 Antony, Cleitus - SM4G.1
 Anwar, Mekhal - JW2A.81
 Apalkov, Vadym - JTu4M.3
 Apolonski, Alexander - STh4E.4
 Apostolopoulos, Vasilis - STh4H.6
 Arai, Koki - JTh2A.79
 Arai, Shigehisa - JTh2A.16, SM4F.3
 Arakawa, Yasuhiko - FM1M.2, SW4J.1, SW4J.4
 Arany, Praveen - AM11.1
 Arbabi, Ehsan - FTh3M.1
 Arie, Ady - FF2A.8, FF3M.6, FTh4M.7, JM3B.6
 Arieli, Uri - AF2K.6, FTu4C.3, JTu3M.3
 Arissian, Ladan - FTh1M.4, JM2E.5, SW3G
 Armani, Andrea M. - AM4I, ATu4K, STu3J.1
 Armougom, Julie - SF1H.3
 Arocas, Juan - FF2D.7
 Arora, P. - JTu2A.20, JTu2A.39, JW2A.110, JW2A.114
 Arrangoiz-Arriola, Patricio - JW4A.4, SF2J.6
 Arsov, Vladimir - JTh2A.100
 Arvidsson-Shukur, David R. - FTh4A.3
 Arzani, Franceso - FM2M.5
 Asadchy, Viktor - FM4B.6
 Asahara, Akifumi - JTh2A.101, SM2H.8
 Asahina, Yu - SW3G.1
 Asane, Joshua K. - FTh4M.6
 Asano, Takashi - SM1J.7
 Asenov, Martin - AM1K.6
 Asheghi, Mehdi - SF2O.5
 Ashida, Masaaki - JW2A.32, STh3F.3
 Ashrafi Nia, Behzad - STh3N.4
 Assali, Simone - STh4O.5
 Assmann, Christian - Ath3K.6
 Atature, Mete - FM4A.1
 Atieh, Fadi - FTu4C.2
 Atienzar, Julia - JTu2A.46
 Atkinson, George - STh1H.1
 Attiaoui, Anis - STh4O.5
 Audouard, Eric - ATu3I.7, JM3E.3
 Auffeves, Alexia - FM3A.2
 Augenbraun, Nathan - SF3O.5
 Auguste, Jean-Louis - JW2A.108
 Aumentado, José A. - SF2N.1
 Austin, Drake - FM4M.2
 Auth, Dominik - STu4O.2
 Autry, Travis - FM3D.1, FM4D.5

Averett, Kent L. - SM4L.4
 Awaji, Yoshinari - SM2G.1
 Awari, Nilesh - JTu2A.101, STu4F.6
 Awschalom, David - JW4A.3
 Aytaç, Yigit - JW2A.12
 Azad, Abul - FM2D.2, FTu4D.2
 Azana, Jose - FTh1A.4, JW2A.71
 Azarm, Ali - SF3G.1
 Azevedo, Caio - JW2A.22
 Azim, Ahmad - Ath4K.6, AW3P.2
 Azzam, Shaimaa - FF2A.6, JTh2A.119
 Azzoune, Abderrahim - JTh2A.102

B

B. S., Kavitha - JW2A.84
 B. Nasr, Magued - Ath11.6
 Baba, Toshihiko - SW3J.1
 Babakhani, Aydin - STu4F, SW4F.5
 Babic, Fehim - FTh3B.3
 Babin, Sergey A. - FTh3B.4, SF1L.7, SM3H.1, STh4L.4
 Baburin, Alexander - FM1M.5, FM1M.6
 Babushkin, Ihar - FF1D.4, FF3C.2, JTh2A.5, STh4E.2, SW3H.2
 Babzien, Marcus - STu3E.5
 Bachelot, Renaud - SM2H.7
 Bachmanchi, SS Harshith - JW2A.68
 Bachmann, Dominic - SF2O.7, STh4G.2
 Back, Tyson C. - STh4H.5
 Backus, Sterling J. - JM3E.4
 Badikov, Dmitrii - SF3O.8
 Badikov, Valeriy V. - SF3O.8
 Bae, Ji Eun - SF3E.6
 Baehr-Jones, Tom - FTh1D.3, FTh4A.3, SF1N.1
 Baek, Hyeonjun - STu4H.7
 Baets, Roel - STh1F.7
 Baerle, Benedikt - STh4N.4
 Bagehan, Mohammad Amin - SF2J.7
 Bagnoud, Vincent - JTu2A.68
 Bahadori, Meisam - JTh2A.41, STh1N.4
 Bahar, Eyal - JTu3M.3
 Bahng, Joong Hwan - FF2B.1
 Bai, Bijie - ATu4K.2
 Bai, Dongbi - STh3L.3
 Bai, Gang - JW2A.95
 Bai, Qingsong - SF1J.4, STh4J.4
 Bai, Zhenxu - JTu2A.59
 Bai, Zhuoya - AF3K.6
 Baierl, Sebastian - FTh1B.2, FTh1B.4
 Bailey, D. Michelle - AM2K.1
 Bain, James - SF3N.4
 Bajcsy, Michal - FM1B.1, JW2A.112
 Bakr, Osman - SM3N.4
 Balakrishnan, Ganesh - FM2C.3
 Balascuta, Septimiu - SW4E.3
 Balasekaran, Samundeeswari M. - SW4L.4
 Balasubrahmaniam, M - FF3B.4
 Balciunas, Ignas - STu4E.2
 Balciunas, Tadas - SW4E.1
 Baldassarre, Leonetta - STh1N.2
 Balicas, Luis - JTh4F.1
 Ballew, Conner - AM4K.3
 Balslev-Harder, David - SW3L.6
 Baltrukonis, Justas - JTu2A.17
 Baltuska, Andrius - FF1C.2, SW4E.1, SW4E.5
 Bamiedakis, Nikos - SM1G.3
 Bandres, Miguel - FTu3D.1, FW3D.2
 Banerjeeand, Kaustav - STh3O.6
 Banerji, Sourangsu - AM4K.5, JTh2A.118
 Bangalore Rajeeva, Bharath - FTh3C.4
 Bank, Seth - FTh4M.5, STh4O.7

- Bansal, Aaina - FTh3A.6
 Bao, Changjing - JTh2A.80, SM3G.3
 Bao, Chengying - AF2K.1, JW2A.43, STh4J.3
 Bao, Jiming - JW2A.118, SF10
 Bao, Xiaoyi - STh1N.1
 Barash, Yefim - FF3M.5, JTu2A.20, JW2A.110, SM3F.4
 Barbastathis, George - SF3N.7
 Barber, Sam - SF3I.1
 Barber, Zeb - JTh2A.39
 Barbieri, Marco - JW2A.116
 Barbieri, Piero - SM1F.3
 Barbiero, Gaia - AF3K.5
 Barbosa, Felipe A. - STh3J.1
 Barclay, Paul E. - SF1J.3, STh1H.4
 Bar-David, Jonathan - FTh3M.8, FTh4M.4, JTu2A.109
 Bardou, Nathalie - FTh3C.1
 Barik, Sabyasachi - JM2B.5
 Barman, Biplob - STu4F.1
 Barnard, Ed - JW2A.29
 Barnes, Crispin H. - FTh4A.3
 Barnes, William - FF2B.3
 Barney, Emma - SF2L.4
 Bar-On, Ofer - AF3K.2, JTu2A.71, SF2J.2
 Barot, Dipenkumar - AF1K.3
 Barry, Liam P. - SM4G.2
 Barsi, Julia - JW2A.12
 Bartal, Guy - FTu3D.5
 Bartels, Randy - ATu3K.5
 Bartholomew, John G. - FM1A.4, FM1A.6, FM1A.7, JTu2A.26
 Bartoli, Filbert - AM4I.2
 Barwicz, Tymon - STh1F.2
 Barzda, Virginijus - JTu2A.1
 Bas, Derek A. - STh4H.5
 Bash, Boulat A. - FF1F.7
 Bashan, Gil - SM1N.2
 Basin, Florent - ATu4I.5, JM3E.3
 Basov, D. N. - FTu3C.2
 Bassim, Nabil D. - STh3N.6
 Bastos, Talita - JTu2A.9
 Basyrova, Liza - JTu2A.119
 Bates, Kelsey - FM3D.1
 Batsukh, Khulan - JTu3G.1
 Battou, Abdella - FM4C.7
 Bauer, Dominik - JM3E.2, SF3E.3, SM4E.3
 Bauer, Ralf - Ath1I.5
 Baumann, Esther - AW4K.1, SF1I.1, STh1G.1, STh1G.2
 Baumgartner, Bettina - STh1F.7
 Bauwelinck, Johan - STh4N.1
 Bavedila, Fuanki - JTu2A.102
 Bawatna, Mohammed - JTu2A.101
 Bawendi, Mounji - SF10.6
 Bawn, Simon - STh1L.4
 Baxamusa, Sal - FTh1C.4, SF3G.7
 Baxter, Joshua - FTu4C.4
 Bayati, Elyas - FTh3M.4
 Bayer, Mustafa M. - AW4K.4
 Baykusheva, Denitsa - FM4M.6
 Baynard, Elsa - SW4E.3
 Baynes, Fred - SM1F.3
 Bayramian, Andrew J. - FTh1M.7, SM4E.4
 Beausoleil, Raymond - SM4J.7, STu4J.5
 Beccari, Alberto - FM1A.1
 Bechtel, Hans - FTh4C.2
 Beck, Mattias - STu4N.2, SW4F.1, SW4F.2, SW4N.4
 Becker, Steffen - STh4H.3
 Beckey, Jacob - JW2A.117
 Beckh, Cornelius - STu4L.5
 Beetar, John E. - FM4M.4, FW4M.2, SW4E.2
 Beggs, Daryl - STu4J
 Behera, Bishnupada - SF1J.3
 Bei, Zongmin - Ath1I.7
 Beiser, Maximilian - STu4O.6
 Belenky, Gregory - SM3N.7
 Belkin, Mikhail A. - AM3K.5, FW4B.1
 Bello, Frank - JTu2A.110, JW2A.66
 Beloy, Kyle - SM1F.1
 Belyanin, Alexey - FM1D.3, FM2C.1, SM3N.7, STh4H.3
 Bendahmane, Abdelkrim - FTh3B.5
 Bengtsson, Jörgen - SM4N.1
 Benis, Sepehr - FF3D.3
 Benkler, Erik - JTh2A.112
 Benson, Oliver - FM4A.5
 Benson, Trevor - SF2L.4
 Bentolila, Laurent - SM1O.5, STu4H.2
 Benyamin, Matan - Ath3K.5
 Ben-Zvi, Ilan - JW2A.50, STh1E.4
 Beran, Lukas - JM3B.4
 Bereyhi, Mohammad J. - FM1A.1
 Berggren, Karl - FF1A.1, JTu4M.4
 Berghäuser, Gunnar - FW3M.1
 Bergler, Michael - ATu3I.1
 Bergman, Arik - SM1N.2
 Bergman, Keren - SM2J.3, SM3G.1, STh1N.4
 Bergmann, Michael - SM4N.1
 Bergues, Boris - FF1C.3
 Berini, Pierre - FTu4C.4, JTu3M.2
 Berlin, Andrej - JTh2A.100
 Bernacki, Bruce E. - SM1N.3, SW4L.2, SW4L.3
 Bernal, Santiago - JW2A.121
 Bernard, M. - SM3O.3
 Bernier, Martin - SF2L.1, SF2L.3
 Bernstein, Liane - JF2F.5
 Berrington, Matthew - FM1A.5
 Berti, Nicolas - SW3H.3
 Bertolotti, Jacopo - FM1C.5
 Bertoncini, Andrea - JTh2A.51
 BÉssin, Florent - FF2D.4
 Betto, Davide - STu4F.6
 Betts, Shawn - SM4E.6
 Bewley, William W. - SM2J.7
 Bexter, Tim - JTu2A.61
 Beyer, Axel - SM4F.1
 Bezryadina, Anna - AM1I.4
 Bhaduri, Basanta - JW2A.72, SW4E.8
 Bhaskaran, Harish - SM2J.2
 Bhaskaranand, Malavika - AW4I.4
 Bhasker, Prashanth - STh3N.7
 Bhat, Abhishek - STh4O.3
 Bhatt, Gaurang R. - FTu3C.2
 Bhattacharya, Anand - FM4D.7
 Bi, Lei - JM3B.4
 Bi, Wanjun - JTu2A.91
 Biagioni, Paolo - FTh3C.6
 Bian, Yinxu - JTu2A.5
 Biancalana, Fabio - JW2A.39, JW2A.42
 Bianco, Vittorio - ATu4K.2, SM4H.2
 Bianucci, Pablo - SW4J.2
 Biasiol, Giorgio - FW4D.1
 Biedermann, Grant - STh4N.6
 Biegert, Jens - SF1E.4, STh4E.5
 Bielejec, Edward S. - FM3D.1
 Bieliaiev, Hlib - FF3D.2
 Biener, Monika - FTu3D.4
 Bienfang, Joshua - FF1A
 Bienstman, Peter - SM2J.1
 Bierhorst, Peter - FM2M.3
 Biesenthal, Tobias - FM4B.2, FTu4B.3
 Bigelow, Matthew S. - STh3G.1
 Bigler, Nicolas - STh3E.2
 Bigot, Laurent - SF1M.4
 Bigot-Astruc, Marianne - SF1M.4
 Bimberg, Dieter - SM4N.7
 Binaie, Ali - SM1N.6
 Biondo, Luigi - JW2A.18
 Bionta, Mina - FF3C.6
 Birks, Tim - SW4H.7
 Biriwosuto, Muhammad D. - JTu2A.77
 Bissinger, Jochen - FW3C.7, SM4J.6
 Biswas, Rabintra - JW2A.37
 Biswas, Rana - AW3I.3
 Bitauld, David - AF2K.3
 Black, Andy N. - FF3A.6
 Black, Nicola - FTh3C.5
 Blaize, Sylvain - SM2H.7
 Blanchard, Cédric - Ath3K.1
 Blanchard, Paul - SF2G.6
 Blau, Yoav - AF3K.2
 Bleszynski Jayich, Ania - SM2F.4
 Bliznakova, Irina - JTu2A.2
 Bliznetsov, Vladimir - SF3J.6
 Blocker, Cameron J. - SM4J.2
 Blumenthal, Daniel - SM4O.1, STu4O.3
 Blums, Valdis - JTu2A.32
 Boag, Amir - AF3K.2
 Bobkov, Konstantin K. - SM4E.2
 Bock, Robert - SM1J.5
 Boddeti, Ashwin K. - FTu3D.3
 Bodine, Martha I. - SM1F.1, STh3G.2, STh3G.3
 Boehmke, Alexandra - FW3M.5
 Boes, Andreas - FW3B.4, SF2I.2, STh1H.7
 Bogdanov, Andrey - JTh2A.117
 Bogdanov, Simeon - FM1M.5, FM1M.6
 Bogdanovic, Stefan - JW3A.4
 Bohm, Florian - FM4A.5
 Böhm, Julian - FTu4B.2
 Bohnert, Klaus M. - AF1K.4
 Boland, Jessica L. - FTh4C.3
 Boldin, Ivan - FTh3A.2
 Boller, Klaus J. - FF2D.5, STu4N.4
 Bolotin, Kirill - STh4G.7
 Boltasseva, Alexandra - FF2A.6, FM1M.5, FM1M.6, FTh1C.2, FTh3C.2, JTh2A.119, JTh2A.40, JW2A.55, JW2A.58, JW2A.63
 Bomse, David - AM2K.1
 Bonamis, Guillaume - ATu3I.7, JM3E.3
 Bonato, Luiz - FM3D.5
 Bong, Jihye - JTh2A.31
 Bonner, Carl - FTu3D.4, JTh2A.20
 Bonneville, Dawson - SF2O.4, STh3N.6
 Boonruangkan, Jeeranan - SM2H.3
 Bopp, Douglas - STu4G.4
 Börner, Michael - AW3I.7
 Boroson, Don - FTh4A.2
 Borot, Antonin - FF1C.3
 Borrego Varillas, Rocío - FW3M.7
 Borsch, Markus - JTh4F.2, JTu4M.2
 Bortis, Amadé - FM3D.3
 Bortolozzo, Umberto - JW2A.35
 Börzsönyi, Ádám - STu4E.2
 Bosco, Gabriella - SW3O.5
 Bosco, Lorenzo - SW4F.1
 Bose, Debapam - SM4O.1, STu4O.3
 Bose, Surajit - SW3H.2
 Botez, D. - SW3N.3
 Bothwell, Toby - SM1F.1
 Bottenfield, Christian G. - JTh2A.65, JTh2A.76
 Boubanga-Tombet, Stéphane - SW3F.2
 Bouchand, Romain - FF1D.1, FF1D.2, STh4J.2, STu3J.2, STu3J.3, SW4G.5
 Bouchon, Patrick - FTh3C.1
 Bouchy, François - AF2K.2
 Bouhadida, Maha - JTh2A.102
 Boursier, Elodie - JTu2A.65
 Bouslog, Brent A. - STh4O.7
 Boutami, Salim - FF2A.1
 Bouthillier, Étienne - STh4O.5
 Bowers, John - AF2K.1, ATu3P.5, FW3B.4, SF2I.2, STh3N.7, STu3J.2, STu3N.1, STu4J.3, SW4N.6
 Bowers, Mark W. - FTh1M.7
 Bowlan, Pam - FM2D.2
 Bowlan, Pamela R. - JW2A.28
 Boyd, Robert - FF1B.3, FF3A.6, FW4B.5, JTu2A.67, SF1J.6
 Boyd, Robert W. - FM3C.4
 Boyer, Thomas - JW2A.14
 Boyle, C. - SW3N.3
 Boyraz, Ozdal - AW4K.4, JTu2A.51, SF2N, STh1N
 Bozhvolnyi, Sergey I. - FTh3M.6
 Bozkurt, Ibrahim - JW2A.25
 Bracker, Allan S. - FM3A.3, FM3A.4
 Bradac, Carlo - SM2F.5
 Braddell, Jules - JTh2A.63
 Bradford, McKay B. - JTh2A.81
 Bradley, Jonathan - SF3N, STh4N
 Bradley, Jonathan D. B. - SF2O.4, STh3N.6
 Bradley, Tom - SM2L.2, STh1L.2, STh1L.4
 Braic, Laurentiu - SF2O.1
 Brameshuber, Mario - SW3L.7
 Bramhavar, Suraj - SF3N.7
 Brand, Michael - AW3K.2, SF3N.2
 Brand, Wesley - FF2D.6
 Brandli, Virginie - FTh3M.7
 Brandstötter, Andre - FTu3D.6, FTu4B.2
 Branlard, Julien - SF3I.5
 Brasch, Victor - AF2K.2, STh4J.1
 Braud, Alain - STh1E.5
 Braud, Flavie - ATu3K.6
 Braverman, Boris - FF3A.6
 Brecht, Benjamin - JTu3A.1
 Bregolin, Filippo - SM1F.3
 Brem, Samuel - FW3M.1
 Brener, Igal - AM3K.5, FF2B.2, FM2C.3, FW4B.1, JTu3M.1
 Brenner, Philipp - JTu2A.71, SF2J.2
 Bres, Camille-Sophie - SM2L, STh1F.4, STh1G.7, STu3L
 Bressler, Christian - JTu2A.101
 Breuer, Stefan - STu4O.2
 Brewer, Nicholas R. - JTu2A.123, JTu2A.37
 Brewer, Sam - SM1F.1
 Breyne, Laurens - STh4N.1
 Brian, Sia J. - STu4O.1
 Brida, Daniele - FM3D.6, FTh3C.6, FW4M
 Briegel, Hans - FTh3A.2
 BRIERE, Gauthier - FTh3M.7
 Briggman, Kimberly - AM2K.2
 Briggs, Andrew - FTh4M.5
 Briggs, Daryl - JW3A.6
 Briles, Travis C. - SF2I.7, SM3J.4, SM3O.6, STh3J.3
 Brinkmann, Maximilian - SF1L.2
 Brochard, Pierre - SW4G.5, SW4N.5
 Brodie, Miles - SW3N.3
 Brodsky, Michael - FTh1A.2, FTh4A
 Bromage, Jake - STh4E, STu3E, STu4E.5
 Bromley, Sarah - SM1F.1
 Brongersma, Mark - FW4D.3
 Brooks, Nathan J. - FF2C.6, FF2C.7
 Brotzer, Peter - SF2J.4
 Brown, Justin M. - FM4C.2
 Brown, Kathryn (Katie) - Ath3K.3
 Browning, Colm - SM4G.2
 Brüggenkamp, Tim - JTu2A.69
 Brunfield, Brian - SW4L.2
 Brunelle, Nicholas - AM4I.1
 Brunelli, Simone S. - JTu2A.82
 Bruni, Fabio - JW2A.116
 Brunner, Fabian - FTh1M.8
 Bubnov, Mikhail - SM4E.2, SM4L.1
 Bucht, Sara - STu4E.5
 Buchvarov, Ivan - JTu2A.2

- Bucklew, Victor G. - SF1L.3, SF1L.4
 Buckley, Sonia - STh1N.3
 Bucksbaum, Phil - FF2C.5
 Buczynski, Ryszard - STh1L.5
 Buddhiraju, Siddharth - FM1C.7
 Budge, Tracy S. - FTh1M.7
 Bud'ko, Sergey - FW4M.5
 Budnicki, Aleksander - JM3E.2
 Budriunas, Rimantas - STu4E.2
 Bulgakov, Alexander - SF2G.2
 Bulgakova, Nadezhda M. - JTu2A.47, SF2G.2, SM3H.1
 Buller, Gerald S. - FF1A.4
 Bullock, Alexis - FTh4M.6
 Bullock, James - SW3J.2
 Bunandar, Darius - FTh3A.3, SF1N.3
 Burch, Ashlyn D. - STu4F.1
 Burek, Michael - FM4A.4
 Burenkov, Ivan A. - FM4C.7
 Burg, William - STu3N.5
 Burger, Milos - FTh1M.6, JTh2A.84, JTu2A.56, SF2G.7, SW4L.4, SW4L.5
 Burghoff, David P. - STu4N.2, SW3N
 Burke, Robert A. - JTu2A.118
 Burla, Maurizio - STh3H.4, SW3F.7
 Burrow, Joshua - SF2O.5, SF2O.6
 Bushati, Rezind - STh4H.7
 Buß, Jan Heye - STh3E.3
 Bustos-Ramirez, Ricardo - JW2A.74
 Butkowski, Lukasz - SF3I.5
 Butler, Thomas P. - JW2A.69, STh4E.4
 Butov, Leonid - JW2A.34, SM1O.4
 Buttolph, Michael - JW2A.103
 Buyukkaya, Mustafa - FM1M.3
 Byer, Robert - SF2H.7
- C**
- Cadusch, Jasper - JTu2A.48, SF3J.2, SM4J.4
 Cai, Hong - JTh2A.34, JTu2A.124
 Cai, Huanbo - JTu2A.91
 Cai, Huaqiang - SF3E.6
 Cai, Jun - FF3C.3
 Cai, Lutong - SF2J.3, SF3N.4
 Cai, Wei - JTh2A.12, JTh2A.21
 Cai, Wenqi - FM4C.1
 Cai, Wenshan - JM3M.2
 Cai, Yudong - JTu2A.14
 Cakmaklyapan, Semih - FTu4D.7, STu3F.4
 Cala' Lesina, Antonino - FTu4C.4
 Calabretta, Nicola - SF1N.5
 Calegari, Francesca - SF2E.4
 Califa, Ran - Ath3K.5, JTu2A.8
 Calis, Ayfer - AM2I.3, AM2K.3
 Callahan, Patrick - Ath4I.2
 Callard, Ségolène - STh1J.6
 Calman, Erica - SM1O.4
 Calonico, Davide - SM1F.3
 Calzada, Jesus - STu3F.1
 Camacho Gonzalez, Guillermo Fernando - JTu2A.88
 Camara, Alexandre R. - SM2L.5
 Camayd-Muñoz, Philip - AM4K.3
 Cambiasso, Javier - FF2B.3
 Campagnola, Paul J. - AM3I.4
 Campbell, Eleanor - SF2G.2
 Campbell, Joe C. - SF2N.1, SW4G.1
 Campbell, Kirby - AM3I.4
 Camper, Antoine - FF3C.1
 Campione, Salvatore - FW4B.1, JTh2A.57
 Camy, Patrice - STh1E.5
 Canalias, Carlota - SF1H.4
 Candler, Robert - SM1N.7
 Canedy, Chadwick - SM2J.7
 Canfield, Paul - FW4M.5
 Canning, John - JTu2A.9
 Cano, Erwin - JTh2A.100
- Cao, Hui - FF3B.3, FF3B.5, STh1G.6
 Cao, Linyou - FTu3C.2, STu4F.7
 Cao, Qian - STh3E.5
 Cao, Qingrui - SM1O.2
 Cao, Qi-Tao - JTh2A.69
 Cao, Xianyi - JTh2A.73
 Cao, Yinwen - FW4B.5, SF2N.3, SM3G.3
 Cao, Yuan - FM4C.1, FTh1D.8, SM1N.1
 Cao, Zhang - JW2A.85
 Cao, Zhongxu - JTh2A.88
 Capasso, Federico - AM3K.3, AM4K.1, FM1D.3, FM3C.2, SF3J.5, STh1O.5, STh4H.3
 Capecchi, Mario - AM2I.5
 Capmany, Jose - SF1G.1
 Capps, Nicholas - JTu2A.53
 Caravaca, Antonio - STh4L.5
 Carbajo, Sergio - SF3I.2, SW4E.6
 Cardenas, Jaime - Ath3I.2, SF3H.4, SW4H
 Cardin, Vincent - SW4E.1
 Cardozo da Silva, Jean Carlos - Ath4K.2, JTu2A.9
 Carfano, Caitlin - JTh2A.45
 Carletti, Luca - FW4B.7
 Carlow, Graham - FM3C.4
 Carlson, David R. - FF2D.6, SM3O.6, STh1G.2, SW4H.1, SW4H.2
 Carlson, John A. - JTh2A.60
 Carminati, Remi - FM1C.5
 Carmon, Tal - FTu4B.5
 Carney, Tom - SM2H.3
 Carolan, Jacques - FF1F.2, FTh1D.3, FTh3A.3, FTh4A.3, SF1N.1
 Carpeggiani, Paolo - SW4E.1
 Carpintero, Guillermo - STu4O.2
 Carras, Mathieu - SW3N.2, SW3N.6
 Carraz, Olivier - JTu3G.1
 Casale, Marco - SF3H.2
 Casas-Bedoya, Alvaro - SM4O.4, SM4O.5, STh1J.4
 Casellas, Ramon - SW4O.5
 Casey, Brendan - STu4O.7
 Caspani, Lucia - FTh1A.4, JTu2A.41
 Cassidy, Kailas - JTu2A.1
 Catrysse, Peter - FTh3C
 Cavanna, Andrea - JTu2A.44
 Cawkwell, Marc - JW2A.28
 Cecchini, Marco - FW4D.1
 Cegielski, Pietr - JTh2A.94
 Ceperic, Vladimir - FTu4C.2, SF1N.1
 Cerè, Alessandro - FM2A.3, FM4C.8, JTu2A.24
 Cerjan, Alexander - FTu4B.4
 Cermak, Michael - STh3G.3
 Cerullo, Giulio - FW3M.4, FW3M.7
 Cesare, Stefano - JTu3G.1
 Ceylan Koydemir, Hatice - AM2K.3, ATu4K.2, SM4H.2
 Cha, Soonyoung - FM2D.4
 Chabanov, Andrey - JTh2A.36
 Chae, Sang Hoon - FTu3C.2
 Chae, Sanghoon - SM1O.2
 Chai, Quan - JW2A.107
 Chaillou, Jérémie - FF3C.6
 Chaitanya Kumar, S - FTh4B.6
 Chaitanya, N. Apurv - FW4B.5
 Chaker, Mohamed - FF3C.6
 Chakraborty, Biswanath - FW3C.2
 Chakraborty, Chitraleema - FF3A.2, FM3A.1, JW2A.33, SF1O.6
 Chakraborty, Uttara - FTh1D.3
 Chakravarty, Swapnajat - AW3K.5, STh1F.6
 Chalupnik, Michelle - JW3A.4
 Chamanzar, Maysamreza - AW4I.2, SM4H.5
 Champenois, Elio - FF2C.5
 Chan, Che Ting - FM4B.5
 Chandran, Anita M. - SM3L.4
- Chang, Chen-Yu - SM3N.2
 Chang, Chiao-Yun - SF3J.4, SM1H.6
 Chang, Chun-Chieh - FTu4D.2
 Chang, Guoqing - AW4I.3, JTh2A.104, JW2A.99, SM3L, SM3L.3, SM4L
 Chang, Jin - FF1A.2
 Chang, Kai-Chi - FTh1A.3, FTh1D.6, JTu3A.6
 Chang, Lin - FW3B.4, SF2I.2
 Chang, Michael - Ath4I.4, SM4H.6
 Chang, Pohan - SF1J.2
 Chang, Shengjiang - SW3F.1
 Chang, Wei-Zung - SW4H.7
 Chang, Wen-Hao - SM3H.4
 Chang, You-Chia - SF3N.5
 Chang, Zenghu - FF2C.4, FF3C.4, JTh2A.9, STh1E.1
 Charczun, Dominik - JTh2A.111
 Charles, Maria C. - SW3L.4
 Charous, Aaron - FF2A.4
 Charrou, Dominique J. - JTh2A.44
 Chatzianagnostou, Evangelia - JTh2A.94
 Chaudhari, Gunvant - AM2I.3
 Chaudhary, Kundan - AM3K.3, FM3C.2
 Chaudhuri, Krishnakali - JTh2A.119
 Chauhan, Nitesh - STu4O.3
 Chaveau, Jean Michel - FTh4M.1
 Chavez, Arturo - JTu2A.107
 Cheam, Daw Don - JTh2A.34
 Chekhova, Maria - JTu2A.44
 Chelladurai, Daniel - FW3C.1, STh3H.4
 Chen, Ang - JM3M.4
 Chen, Changchen - FTh3A.3
 Chen, Chaoyun - SW3G.8
 Chen, Cheng - AM2K.3
 Chen, Cheng-Yuan - SM1H.6
 CHEN, Chong - JW2A.53
 Chen, Edward - SM4J.3
 Chen, Eric - FW3B.5
 Chen, Eva - ATu4K.3
 Chen, Fangyi - JTu2A.14
 Chen, Fu-Der - Ath4I.4, SM4H.6
 Chen, Guangcan - SM3N.8
 Chen, Guan-Yu - Ath1I.4
 Chen, Hao-Jing - STh3J.2
 Chen, haoshuo - SM1G.1, SM1G.2
 Chen, Hong - JTh2A.66, SW4H.5
 Chen, Hongda - AW3K.6, JTu2A.75
 Chen, Hongwei - Ath1K.2, JTh2A.61
 Chen, Hou-Tong - FTu4D.2
 Chen, Hua-Zhou - FW4B.6
 Chen, Jiageng - AF1K.2, JW2A.101
 Chen, Jiajia - SW4O.2
 Chen, Jialong - AM3I.6
 Chen, Jianping - JTh2A.42, JTh2A.73, JTu2A.94, JTu2A.97, STh4H.2
 Chen, Jia-Wern - FTh3M.3
 Chen, Jie - JW2A.104, SF1M.2, SM2H.1, STh1G.4
 Chen, Jinhui - JW2A.51
 Chen, Jinming - FTh1M.5
 Chen, Jiyuan - Ath1K.6
 Chen, Junxin - FM1A.3
 Chen, Jwo-Sy - SM1F.1
 Chen, Kai - AW4K.3
 Chen, Kevin P. - AF1K.6, FM4A.1, JW2A.14
 Chen, Lawrence - SW3H.5
 Chen, Lee-Feng - JTu2A.115
 Chen, Liang-Yao - JW2A.11
 Chen, Liao - Ath3K.4, JW2A.80
 Chen, Lifeng - SF3O.7
 Chen, Lih-Ren - JTu2A.81
 Chen, Likun - JTh2A.33
 Chen, Lu - FM3C.7
 Chen, Min - JTu2A.101
 Chen, Ming-Chang - JTu2A.64
 Chen, Minghua - Ath1K.2, JTh2A.61
- Chen, Mingkun - SF3O.5
 Chen, Mingshu - SF2L.5
 Chen, Mu Ku - FTh3M.3
 Chen, Nan-Wei - Ath1K.4
 Chen, Peng - JW2A.29, SM1O.5
 Chen, Qiong - JTu2A.50
 Chen, Ray T. - AW3K.5, FTu3B.7, STh1F.6
 Chen, Shaoxiang - ATu4I.6
 Chen, Shih-Chi - AM3I.6
 Chen, Shufen - AM3I.5
 Chen, Si - AM3I.5, JTu2A.108, JW2A.86
 Chen, Siyuan - SM2G.4
 Chen, Songsheng - AW4K.6
 Chen, Teng-Yun - FM4C.3
 Chen, Weidong - SF3E.6
 Chen, Wei-Ting - AM4K.1, SF3J.5, STh1O.5
 Chen, Wen-jie - FM4B.5
 Chen, Xi - SW3O, SW4O.1
 Chen, Xiaodong - FM4B.8
 Chen, Xing-Yu - Ath1I.4
 Chen, Xinyi - JTh2A.89
 Chen, Xuan - FF3D.5
 Chen, Yen-Hung - JTh2A.75
 Chen, Yifeng - AM1K.2, JW2A.5
 Chen, Yi-Ru - JTu2A.38
 Chen, Yong - SM2L.2, STh1L.2, STh1L.4
 Chen, Yu - SF2L.2
 Chen, Yuanfu - JTh2A.88
 Chen, Yu-ao - FTh4A.6, JTu2A.92
 Chen, Yueyang - STu4J.4
 Chen, Yuhao - ATu4I.6
 Chen, Yu-Hui - FM1A.5
 Chen, Yun-Jih - SM3F.5
 Chen, Zhigang - AM1I.4, FTh4B.1, FTh4B.2, FTh4B.7, FW3D.3, JW2A.41, JW2A.45
 Chen, Zhi-Yu - FM4C.5
 Chen, Zhong - AW3P.3
 Chen, Zihao - FTh3A.4, FTu3B.6
 Chenet, Daniel - JTh4F.1
 CHENG, CHE-HSUAN - STh3O.4
 Cheng, Chuantong - STh3O.3
 Cheng, Di - FW4M.5
 Cheng, Feihu - SM1F.6
 Cheng, Gong - SM4J.2
 Cheng, Haynes Pak Hay - JTh2A.100
 Cheng, Jierong - SW3F.1
 Cheng, Ji-Xin - ATu3K.3, STu3L.6
 Cheng, Long - STh4H.4
 Cheng, Qixiang - SM2J.3, STh1N.4
 Cheng, Rebecca H. - FF2D.3
 Cheng, Xiang - FTh1A.3, FTh1D.6
 Cheng, Xiulan - JTh2A.64
 Cheng, Xuanhong - AM4I.2
 Cheng, Ya - FTh1M.5, JTu2A.49
 Cheng, Yuh-Jen - FTh4M.2
 Cheng, Yumin - JTu2A.98
 Cheng, Zengguang - SM2J.2
 Cheng, Zhao - JTh2A.56
 Cheng, Zhaochen - JW2A.67
 Cheng, Zhi - FF1C.5
 Cheng, Zihao - STu4L.7
 Cheng, Ziwei - JTh2A.56
 Chénot, Sébastien - FTh3M.7
 Chernysheva, Maria - AM1I.6, SF2L, STu3L.7, STu4L
 Cherpakova, Zlata - FM4B.1
 Cheryl, Sorace-Agaskar - SF3N.7
 Chesnut, Kyle - SM4E.4
 Chevalier, Paul - FM1D.3, STh4H.3
 Chhowalla, Manish - JW2A.25
 Chia, Cleaven - JW3A.4
 Chiang, Chin-Cheng - FM1M.6
 Chiaramonti, Ann - SF2G.6
 Chichibu, Shigefusa - SM2G.1
 Chichkov, Nikolai B. - ATu3P.6
 Chien, Feng-Chang - JTh2A.97
 Chien, Miao-Hsuan - JW2A.62, SW3L.7

- Chiesa, Matteo - SM2L.3
 Chijioko, Akobuije - STh4G.1
 Childress, Lilian - FM4A.6
 Chiles, Jeff - SF3H.3, SM3O.5, SW3J.4
 Chin, Alan H. - JW2A.19
 Chin, Hou-Man - JF2F.1
 Chini, Michael - FM4M.4, FW4M.2, SW4E.2
 Chirumamilla, Manohar - FTu4D.3
 Chiu, Han-Lun - JTu2A.81
 Chiu, Yu Chung - JTu2A.104
 Chmielak, Bartos - JTh2A.94
 Cho, In Ho - AW3I.3
 Cho, Wooje - FF3A.4
 Cho, Young-Wook - FM2M.4, JTu2A.35, JTu2A.45
 Cho, Yu-Yun - SF2O.2
 Choe, Jong-Ho - STu3F.2
 Choi, Byung-Seok - JTu2A.43
 Choi, Chanyeol - STh4J.5
 Choi, Duk-yong - FM1B.4, FW4D.7, SF2N.5, SF2N.7, SF3J.1, SM4O.2, SM4O.5, STh1J.4
 Choi, Heejo - AW3K.7
 Choi, Heon-jin - SM1O.2
 Choi, Honggu - ATu3K.4
 Choi, Hyunyoung - FM2D.3, FM2D.4, FM2D.5, SW3F.3
 Choi, Il Woo - STu3E.2
 Choi, Jae-Hyuck - FM2C.4, FW4B.3
 Choi, Jiyeon - ATu4I.1
 Choi, Sun Young - SF3E.6
 Choi, Wonsik - STh3O.5
 Choksy, Darius J. - JW2A.34
 Chong, Andy - STu3L.1
 Chong, Harold M. - ATH3I.4
 Choquette, Kent D. - SM4N.5
 Chou, Yun-Syuan - JTu2A.112
 Choudhary, Amol - SF2N.7, SM4O, SM4O.4, SM4O.5, STh1J.4
 Choutagunta, Karthik - SM1G.1
 Chowdhury, Enam - FM4M.2, JTu2A.87, SM3H.2
 Chowdhury, Sarah N. - JTh2A.40, JW2A.55
 Christensen, Erik N. - SW3H.1
 Christodoulides, Demetrios N. - FF1D.3, FM1D.2, FTh3B.2, FTh4B.2, FTu3B.2, FW3D.1, FW4D.2, JW2A.103, STh4L.3, SW4N.1
 Chrostowski, Lukas - ATu4K.5, SM3J.7
 Chu, Cheng Hung - FTh3M.3
 Chu, Hsu-Hsin - FF1C.5
 Chu, Sai - FTh1A.4, JW2A.102, SF2N.2, SF2N.4
 Chu, Shih-I - JTh2A.1
 Chu, Steven - FM4A.4
 Chu, Wei - FTh1M.5
 Chu, Yiwen - JW4A.2
 Chu, Yushi - JW2A.107
 Chua, Song Liang - JW2A.89
 Chueh, William - JTh4F.4
 Chun, Byung Jae - SM4F.2
 Chun, Hyunchoe - SM2G.5
 Chun, Il Yong - SM4J.2
 Chung, Hayun - STh3G.6
 Chung, Hsiang-Yu - AW4I.3
 Chung, Hung-Pin - JTh2A.75
 Chung, Kunook - AM4I.4, STh4O.1
 Chung, Tsung Lin - FTh3M.3
 Cimini, Valeria - JW2A.116
 Cincotti, Gabriella - JTh2A.77
 Cino, Alfonso - FTh1A.4
 Cirmi, Giovanni - FF2C.3, SW4E.4
 Ćizmar, Tomáš - SM2L.1
 Clark, Thomas - SF3N.6
 Clark, William - FTh4D.1
 Clarison, Tristan - JTu2A.116
 Clemmen, Stephane - STh1F.7
 Clemmons, Marvin - FTh4M.6
 Clerici, Matteo - FW3B.3, JTu2A.41
 Clivati, Cecilia - SM1F.3
 Coccia, Gulio - SW4E.1
 Cocker, Tyler L. - FTh4C.3
 Coddington, Ian - SF1I.1, SM2N.3, STh1G.1, STh1G.2
 Coen, Stephane - SW3H.3
 Coenen, Toon - FTh1C.5, SF2O.3
 Coey, Michael - STu4F.6
 Coffee, Ryan - FF2C.5, SF3I.7
 Cohen, Kobi - FTu3D.5
 Cohen, Lesley - FTh3C.5
 Cohen, Moshe-Ishay - FM1C.4, FW3D.7
 Cohen, Nadav - JTu2A.57, SF2N.3, SM1N.5
 Cohen, Offir - FM2A.6, FTh3D.4
 Coimbatore Balaram, Krishna C. - STh3H.6
 Cojocar, Crina - FW4B.7, STh3J.5
 Cojocar, Gabriel - SW4E.3
 Cola, Adriano - SF1N.4
 Colacion, Gabriel - STh1G.2
 Colburn, Shane - FTh3M.4, JTh2A.47
 Cole, Daniel C. - FF1D.6
 Cole, Garrett D. - SF2O.7, STh4G.2
 Cole, Ryan K. - SF1I.6
 Coletti, Camilla - STh3N.2, STh4N.2
 Colli, Allan - SM1H.3
 Collins, Lorraine - SM1H.5
 Collins, Matthew J. - FTh4D.6
 Collins, Nicholas - SW3J.3
 Collins, Noelle - STu4J.3
 Collins, Ron - JTh2A.114, JW2A.8
 Conforti, Matteo - FF2D.4, FTh3B.5
 Connell, Steven - JTu2A.32
 Cook, Gary - SM4L.4
 Cooper, Jonathan - AM4I.3
 Copie, Francois - SF3H.5
 Coppola, Guillaume - FM1M.1
 Cordaro, Concetto Eugenio Andrea - FTh3M.2
 Cordeiro, Cristiano M. - SF3L.2
 Cordova Castro, Margoth - FTh4M.3
 Corkum, Paul B. - SF2G.5, SF3G.2
 Cormier, Eric - STh3E.1, SW3E.6
 Cortes, Cristian L. - FTu3D.3
 Coslovich, Giacomo - SF3I.7
 Cossairt, Brandi - STu4J.4
 Cossel, Kevin C. - SF1I.1, STh1G.1, STh1G.2
 Costanzo, Giovanni - SM1F.3
 Cotrufo, Michele - FTu4B.6, SW4J.3
 Cottrill, Dillion - FM3A.4
 Couch, David - JM3E.4
 Couderc, Vincent - STh4L.1, STh4L.2
 Courtwright, Devon - JTh2A.20
 Craiciu, Ioana - FM1A.6, FM1A.7
 Craig, Benjamin J. - JTu2A.48, SW3J.2
 Cramer, Alex - SM4O.4
 Cramlet, Josh - FM3A.4
 Crawford, Scott - JW2A.14
 Crespi, Andrea - FM1M.1
 Cressler, John D. - JTh2A.76
 Crites, Erin - FM4M.4
 Crockett, Benjamin G. - JW2A.71
 Crouch, Stephen - JTh2A.39
 Crozier, Kenneth - JTu2A.48, SF3J.2, SM4J.4, SW3J.2
 Cruz, Flavio C. - STh4E.5
 Cryan, James - FF2C.5
 Csontos, Janos - STu4E.2
 Cuff, sebastien - FW3C.4
 Cuesta, Francisco - FM4B.6
 Cui, can - JTu2A.59
 Cui, Chaohan - FF1F.4
 Cui, Jiahua - SF3E.1
 Cui, Liang - FTh3D.5, FTh4D.3
 Cui, Nan - SW4O.4
 Cui, Xiaorui - STh4O.3
 Cui, Xingyang - JTu2A.92
 Cui, Yifan - SF2L.5
 Culter, Alex - JTh2A.114, JW2A.8
 Cundiff, Steven T. - FF3D.1, FM3D.1, FM3D.5, FM4D.3, FW3M.2, SF1I.7, SM4F.4
 Cunningham, Brian T. - JW2A.61
 Cunningham, David G. - SM1G.3
 Cunningham, Eric - STu4E.6
 Curtis, Jeremy A. - STu4F.1
 Curtis, Rowan - STh1L.2
 Cvecek, Kristian - ATu3I.1
 Cygan, Agata - JTh2A.111
 Czerninski, Ken R. - SW4L.4
 Czwalianna, Marie Kristin - SF3I.5, SF3I.6
- D**
- Da Ros, Francesco - SF1G, SW3O.6
 da Silva, Fabio - JW2A.113
 Dabos, George - JTh2A.94
 Dabu, Razvan - SW4E.3
 Dagli, Alva - SM1H.3
 Dagli, Nadir - STh3N.7
 Dahlem, Marcus - SM2L.3
 Dai, Anan - JTh2A.100
 Dai, Chong - JW2A.118
 Dai, Hui - STh3G.5
 Dai, Jin - FTu4D.1
 Dai, Xiaojun - SF3E.6
 Dai, Yaomin - FM2D.2
 Dakic, Borivoje - FM2M.7
 Dal Conte, Stefano - FW3M.4, FW3M.7
 Dalir, Hamed - FTu3B.7, JTh2A.45
 Dallari, William - FF1C.3
 Dallesasse, John M. - JTh2A.60
 Dallo, Christina - JTh2A.39, STh4N.6
 Daloglu, Mustafa - AM4I.3
 Dalton, Larry R. - STh4N.4, SW3F.7
 Dalvit, Diego A. - FTu4D.2
 Damari, Ran - FM3D.8
 Damilano, Benjamin - FTh3M.7
 Danang Birowosuto, Muhammad - SF1O.5
 Dancus, Ioan - SW4E.3
 Dang Nguyen, Tung - STh1O.3
 DANG, Cuong - JTu2A.77
 Dani, Keshav M. - FM3D, FW3M.6, FW4M.1, JW2A.25, SF1O.3
 Danylo, Rostyslav - FTh1M.2
 Dao, Dzung Viet - FTh4D.3
 Dao, Lap - JTh2A.3
 Darmo, Juraj - SW4F.2
 Das Gupta, Tapajyoti - STh1O.3
 Das Mahapatra, Prometheus - SF1G.1
 Das, Ujjwal - JTu2A.118
 Dashtestani, Hadis - JTu2A.3
 Daskalova, Albena - JTu2A.2
 Datta, Animesh - FF1F.7
 Datta, Anurup - FF2A.7
 Datta, Ipshita - FTu3C.2, STh3H.1
 Datte, Phillip S. - FTh1M.7
 Dauer, Christoph - FM4B.1
 D'Auria, Virginia - FF1A.5, FTh4D.2
 Davanco, Marcelo I. - FF3A, STu4J.6
 Dave, Utsav D. - FW4D.4, SF1J.7, SM3J.6
 Davenport, Aaron - SM3H.2
 David, McCloskey - JW2A.66
 Davids, Paul - JTh2A.39
 Davidson, Ian - STh1L.2, STh1L.4
 Davidson, Joshua - JTu2A.15
 Davidson, Nir - FM1D.1
 Davies, Giles - AW3P.5
 Davila-Rodriguez, Josue - SF2N.1, SW4G.1
 Davis, Alex O. - JTu3A.4
 Dawlaty, Jahan - FW4B.5
 Day, Matthew W. - FM3D.1
 de Aldana, Javier R. - STh1E.5
 De Angelis, Costantino - FW4B.7
 de Ceglia, Domenico - FW4B.1, FW4B.7
 de Haan, Kevin - ATu4K.6, JM3M.5
 De Leon, Israel - FW4B.5
 De Ligny, Dominique - ATu3I.1
 De Marco, Innocenzo - FM2M.1
 de Marco, Massimo - FF1C.4
 de Matos, Christiano J. - SF3L.2, STu4L.2
 De Micheli, Marc - FTh4D.2
 de Rezende, Guilherme F. - STu3N.2
 de Riedmatten, Hugues - FM2A.1
 de Santis, Lorenzo - FM3A.2, FM4A.1
 de Vries, Oliver - FM2M.2
 De Wilde, Yannick - FTh3C.1
 Deac, Alina - STu4F.6
 Dean, Cory R. - SM1O.2
 Dean-Ben, X Luis - AM3I.3
 Deb Mishra, Sattwik - SM2F.6
 Debbarma, Sukanta - FF2D.8
 Debbas, Max - AM4K.3
 Debnath, Sanjay - FTu4D.6
 Decker, Franz-Josef - SF3I.2
 Decker, Manuel - JTh2A.24
 Deeken, Jan - AW3I.7
 Degen, Christian - SM2F.1
 Dehghani, Mojgan - JW2A.46
 Deinert, Jan-Christoph - JTu2A.101
 Deka, Jayanta - JW2A.37
 Del Bino, Leonardo - JM3B.3, SF3H.5, STh3J.7
 Del Pino, Javier - FM1A.2
 Del Vecchio, Patrick - STh4O.5
 Delaigue, Martin - ATu4I.5, JM3E.3
 Delaye, Philippe - JTh2A.102
 Delen, Xavier - JM1E.5, JW2A.73
 Delfyett, Peter - JW2A.74
 Delgoffe, Antoine M. - FTh3D.3
 DelHaye, Pascal - JM3B.3, SF3H.5, STh3J.7
 Delikanli, Savas - JTu2A.77
 Della Torre, Alberto - FF2D.8
 Delmado, Amol - SM4G.2
 Demailly, Julien - SW4E.3
 Demcenko, Andriejus - AM4I.3
 Demeter, Gabor - FTh1B.3
 Demina, Natalia - FM3D.8
 Demir, Hilmi V. - JTu2A.77
 Demircan, Ayhan - FF1D.4, FF3C.2, JTh2A.5, SW3H.2
 Demirtzioglou, Iosif - JTh2A.74
 Demongodin, Pierre - STh1J.6
 Dempsey, Dennis - JTh2A.7, JTu2A.58
 Deng, Fengyuan - ATu3K.3, STu3L.6
 Deng, Hui - FF2A.2, FF3D.1, FM4D.3, STu3N.5
 Deng, Huiyang - SF2H.7
 Deng, Ke - SM1F.6
 Deng, Wei-Min - FM4B.8
 Deng, Xiaoxu - SM1J.4
 Denker, Heiner - SM1F.3
 Deotare, Parag - STh3O.4
 Deqlercq, Heidi - JTu2A.2
 Dereux, Alain - FF2D.7, JTh2A.94
 Derntl, Christian G. - SW4F.2
 DeRose, Christopher - STh4N.6
 Derrien, Thibault - SM3H.1
 DeSalvo, Richard - SM4O.4
 Deschênes, Jean-Daniel - SM1F.1, STh3G.2, STh3G.3
 Descos, Antoine - STu4J.5
 Desfarges-Bertheleot, Agnes - STh4L.2
 Desiatov, Boris - FM1M.3, SF2J.1, SM3O.2, STu3O.2, SW3E.4
 Detz, Hermann - STu4O.6
 Deutsch, Christoph - SF2O.7
 Dev, Sukrith - STh4O.4
 Devenport, Joseph - SM4O.4
 Devereaux, Thomas - JTh4F.1

- Dhakal, Gyanendra - FW4M.2
 Dherbecourt, Jean-Baptiste - Ath3K.1, JTu2A.93, SF1H.3
 Di Carlo, Dino - SM4H.1
 Di Domenico, Giuseppe - JM3B.6
 Di Pietro, Vittorio Maria - JW2A.35
 Di Teodoro, Fabio - AW3K, AW4K
 Diamandi, Hilel H. - SM1N.2
 Diamanti, Eleni - FM2M.5
 Dianat, Pouya - JTu2A.27, SF1N.4
 Dias, Antonio - JTu2A.46
 Dias, Leanne - ATu4K.5
 Diaz, Francisc - JTu2A.119, STh1E.5
 Diaz-Jacobo, Elizabeth - SF3I.7
 Dichtl, Paul - FM2C.2
 Diddams, Scott A. - FF2D.6, SF1E.4, SF2N.1, SF3H.3, SM1F.1, STh4E.5, SW4G.1
 Diederich, Geoffrey M. - FM3D.1, JW2A.31
 Diels, Jean-Claude - FTh1M.4, JM2E.5, STh4L.6
 Diemel, Oliver - JW2A.18
 Diercks, David - SF2G.6
 Dietrich, Christian M. - STh4E.2
 Dietz, Thomas - JM3E.2
 Dikopol'tsev, Mark - JTu2A.39, JW2A.114
 DiMauro, Louis F. - FF1C.1, FF3C.1
 Dimic, Aleksandra - FM2M.7
 Dimitri, Klaus - FW4M.2
 Dimoulas, Athanasios - SM1H.3
 Ding, Fei - FTh3M.6
 Ding, Jiajie - JW2A.49
 Ding, Jun - JTh2A.14
 Ding, Meng - SM2L.2, SM2L.6
 Ding, Pengji - FTh1M.2
 Ding, Wei - SM2H.7, STh1L.6
 Ding, Xiaoyue - SW4H.7
 Ding, Yihang - JW2A.87
 Ding, Yimin - FF1B.6, FW4B.2
 Ding, Zhenghao - FM1B.1
 Dinh, Khuong B. - JTh2A.3
 Dinu, Mihaela - SM2G
 Diroll, Benjamin - FF3A.4
 Divitt, Shawn - FM3C.3, FM3C.7
 Dixon, P. Ben - FTh4A.2
 Djordjevic, Ivan B. - SW4O.6
 D'Mello, Yannick - JW2A.121
 Do, In Hwan - SM4O.2
 Doberstein, Vadim - JW2A.18
 Döblinger, Markus - SM4J.6
 Dobrakowski, Dominik - SM3L.5, STh1L.5
 Doddaballapura Lakshmi Jayasimh, Prajwal - SM4N.6, STu4N.5
 Doderer, Michael - FW3C.1, STh3H.4
 Doerer, Chris - Ath4L.3
 Dogariu, Aristide - Ath4K.3, FF3B.2, FM1C.2, FTh1C.8
 Doiron, Chloe F. - FTu4D.4
 Doiron, Curtis W. - JW2A.26
 Dolgaleva, Ksenia - FM3C.4
 Dombrowski, Martina - JTu2A.12
 Domenegueti, Renato - STh3J.1
 Domingue, Scott - ATu3K.5
 Domingues, Sergio H. - STu4L.2
 Dominguez, Daniel - JTu2A.96
 Donegan, John - JTh2A.63, JTu2A.110, JW2A.66
 Dong, Chun-Hua - JTh2A.69
 Dong, Jianji - JTh2A.56, JW2A.10
 Dong, Jian-Wen - FM4B.8
 Dong, Liang - SF3O.6, SM4L.2
 Dong, Po - JTu2A.76
 Dong, Xiaohu - SM1G.3
 Dong, Xin - AF2K.4, Ath3K.4
 Dong, Yibo - AW3K.6, STh3O.3
 Dong, Yuan - AW4K.5, SF3J.6, STh1O.4, STu4J.2
 Dong, Zhewei - SM1J.4
 Dong, Zhili - SF2O.8
 Dönges, Sven A. - SF1E.3
 Donagic, Denis - SM2N
 Donley, Elizabeth A. - SM3F.5
 Donohue, John M. - JTu3A.1
 Donvalkar, Prathamesh - STh3J.1
 Doolittle, Lawrence - SM4E.5
 Dordevic, Nikola - FW3C.1
 Doria, Domenico - SW4E.3
 Dorney, Kevin M. - FF2C.6, FF2C.7
 Dorow, Chelsey - JW2A.34
 Dorrah, Ahmed - FTh4B.3, FTh4B.8
 Dory, Constantin - FF3A.1, FM4A.2, FM4A.4, SM2F.6
 Dostart, Nathan - AW3K.2, SF3N.2
 Dostovalov, Alexandr V. - SM3H.1, STh4L.4
 Doty, Matthew - JTu2A.18, SF3O.5
 Dou, James - AM4I.7
 Dou, Wei - AW3P.3, STh4O.6, STu3N.3
 Doumouro, Joris - FTh3C.1
 Doutré, Florent - FTh4D.2
 Doward, Devonte - JW2A.22
 Downer, Michael - JTh2A.4
 Doyle, Jonathan - STh1N.5
 Doz, Stéphanie - Ath3K.1
 Drag, Cyril - JTu2A.93
 Drake, Tara E. - SF3H, STh3J.3
 Drevinskas, Rokas - ATu4I.4
 Driver, Taran - FF2C.5
 Droste, Stefan - SF3I.7
 Droz, Fabien - STu4G.3
 Drs, Jakob - SF3E.4, STh3F.5
 Druon, Frédéric - JM2E.2
 Du, Jing - JTu2A.57, JTu2A.67, SM1J.5, SM1N.5
 Du, Juan - STu3N.7
 Du, Qiang - SM4E.5
 Du, Qiaoling - JW2A.21
 Du, Qungyang - JM3B.4
 Du, Shengwang - FM2A.2, JTu2A.122
 Du, Wei - AW3P.3, STh4O.6, STu3N.3
 Du, Weizhi - SF2L.5
 Duan, Liangcheng - JTh2A.90
 Duan, Lingze - AF1K.3, SM1L.4
 Duan, Shaoxiang - SF3L.7
 Duan, Shukai - SF1J.4
 Duan, Xiangfeng - JW2A.29, SM1O.5, STh4J.5
 Duan, Xueke - JTu2A.121, JW2A.54
 Duan, Yao - FF1B.6
 Duan, Yuhua - AF2K.4, Ath3K.4, JW2A.80
 Dubcek, Tena - FTu4C.2
 Dubois, Emmanuel - ATu3K.6
 Duboz, Jean Yves - FTh3M.7
 Dubucq, Dominique - Ath3K.1
 Duch, Elizabeth - STh1F.2
 Ducournau, Guillaume - JTu2A.102
 Dumas, Derek C. - FF1A.4
 Dumcenco, Dumitru - FW3M.4
 Dumont, Mario - STu4J.3
 Dunjko, Vedran - FTh3A.2
 Duong, Bryan - JW2A.112
 Dupré, Matthieu - SM3N.1, FF3B.8
 Durfee, Charles G. - AM2I.4, SW4E.6
 Dursun, Ibrahim - SM3N.4
 Dutt, Avik - FM1C.7, FTu3B.4, JM3B.2, SF3H.6, STu3J.5
 Dutta, Aveek - FTh1C.2, JTh2A.40, JW2A.63
 Duval, Simon - SF2L.1, SF3E
 Dwir, Benjamin - FTh3D.3
 Dyer, Gilliss - STu4E.6
 Dzelzainis, Thomas W. - JTu2A.1
 Earles, T. - SW3N.3
 Eaton, Miller - FF1A.6, FTh4D.5
 Ebendorff-Heidepriem, Heike - STh3L.3
 Ebnet, Thomas - FTh1B.2
 Ebrahim, Mehdi - JTu2A.41
 Ebrahim-Zadeh, M. - FTh4B.6
 Edamura, Tadataka - SM4N.2
 Edel, Joshua - FM3C.5
 Edgar, James - AM3K.3, FM3C.2
 Edinger, Pierre - SF2H.3
 Efreimidis, Nikos - FTh4B.1
 Efremov, Vlad D. - SF1L.7
 Eftekhar, Ali - JTh2A.55, JW2A.52, SF2H.5, STh1H.5
 Eggert, Sebastian - FM4B.1
 Eggleton, Benjamin J. - FW3B.2, JM3B.1, SF2N.5, SF2N.7, SM4O.4, SM4O.5, STh1J.4
 Eghlidi, Hadi - FW3C.5
 Eich, Manfred - FTu4D.3
 Eichenfield, Matt - JTu2A.96
 Eichhorn, Tim - SM2F.4
 Eilenberger, Falk - FF3A.7
 Eisefeld, Alexander - FTu3B.5
 Ekimov, Evgeny - SM2F.5
 Ekstrom, Andreas - FTh3A.6
 El Dirani, Houssein - SF3H.2, STh1J.6
 El Idrissi, Driss - FM4C.7
 Elder, Delwin L. - STh4N.4, SW3F.7
 Eleazar Melgarejo Morales, Rigoberto - Ath4K.2
 El-Ganainy, Ramy - FTu3B.5, FW4D.2, SW4N.1
 Elhadji, Selim - FTh1C.4, SF3G.7
 El-Jaroudi, Rasha H. - STh4O.7
 Elle, Jennifer - FTh1M.3, JTh2A.6
 Ellis, Andrew - SW3O.1
 Ellis, Jennifer L. - FF2C.6, FF2C.7, STh3G.2, STh3G.3
 Elsässer, Wolfgang - SW3N.2
 Emani, Naresh K. - JTh2A.22
 Emboras, Alexandros - SF3N.1, STh4N.4
 Emmenegger, Lukas - AM1K.3
 Emmons, Erik - SM1N, SW4L
 Émond, Nicolas - FF3C.6
 Endo, Mamoru - SW4G.3
 Engelberg, Jacob - FTh3M.8, JTu2A.109
 Engelsen, Nils - STh1H.3, STh4J.2
 Engelsen, Nils Johan - FM1A.1
 England, Joel - SF2H.7
 Englesbe, Alexander C. - FTh1M.3, JTh2A.6
 Englund, Dirk R. - FF1F.2, FF3A.2, FM4A.1, FTh1D.3, FTh3A.3, FTh4A.3, FTu4C.2, JF2F.5, JTu4A.4, SF1N.1, SF1O.6, SF3L.5, SM2F.3
 Ensley, Trenton - FM4M.2, JTu2A.87
 Eom, Jaeun - FM2D.3
 Erkintalo, Miro J. - SW3H.3
 Erlanson, Alvin - SM4E.4
 Erotokritou, Kleanthis - JTh2A.93
 Errando-Herranz, Carlos - SF2H.3, STh1F.3
 Erven, Chris - FM4C.4
 Escarra, Matthew D. - JTh2A.108, JTh2A.25, STh1F.5, STh3O
 Eschen, Wilhelm - SF1E.2
 Eshaghian Dorche, Ali - JTh2A.55, JW2A.52
 Eshel, Ben - SM4L.4
 Esteki, Elham - FTh3A.2
 Etienne, Marc - FW4M.2
 Evans, Christopher C. - FM4C.2
 Evans, Philip - JTu2A.21, JW3A.6
 Everts, Jonathan - FM1A.5
 Evmenova, Ekaterina A. - STh4L.4
 Fabbri, Riccardo - SW4E.3
 Fabert, Marc - STh4L.1, STh4L.2
 Fabian, Jaroslav - JTu4M.2
 Fabrega, Josep M. - SW4O.5
 Faccio, Daniele - JW2A.39
 Fainman, Yeshaiah - AM4I.6
 Faist, Jérôme - STu4N.1, STu4N.2, SW4F.1, SW4F.2, SW4N.4
 Fakhru, Takian - JM3B.4
 Falcoz, Franck - STu4E.1
 Falk, Abram - FTh3C.7
 Falkner, Matthias - FTh1C.6, JTh2A.24
 Fallahi, Arya - JTu4M.5
 Fallahpour, Ahmad - FW4B.5, SF2N.3, SM3G.3
 Fallnich, Carsten - FF2D.5, JTu2A.61, JTu2A.69, JTu2A.84, SF1L.2, SM4O.6
 Fan, Sheng - JW2A.107
 Fan, Dianyuan - SF2L.2
 Fan, Fei - SW3F.1
 Fan, Guangyu - SW4E.1
 Fan, Jingyun - FTh3A.5
 Fan, Jintao - SF1H.2, STh3L.6, STh4E.1
 Fan, Jonathan A. - AM4K.4, FTh3C.7, FTu4C
 Fan, Qinguo - FM3C.3
 Fan, Ren-Hao - JTh2A.38, STh1O.2
 Fan, Shanhui - FF1B.5, FF2A.1, FM1B.2, FM1C.7, FTu3B.4, JF3F.2, JM3B.2, SF2H.7, SW4J.5, SW4J.7
 Fan, Shengli - AM3I.2
 Fan, Songtao - JTu2A.66
 Fan, Tianren - SF2H.5, STh1H.5
 Fan, Tingwei - JW2A.115
 Fan, Xinyu - SF1L.5, SF3L.4, SM4F.5
 Fan, Xudong - SW4L.7
 Fan, Yen-Hsiang - SF2O.2
 Fan, Youwen - STu4N.4
 Fan, Zhengquan - FTh1M.2
 Fan, Zhongwei - AW3I.6
 Fang, Bin - FM2A.6, FTh3D.4
 Fang, Fang - JW2A.23
 Fang, Michael - SF1N.6
 Fang, Shaobo - JTh2A.104, JW2A.99, SM3L.3
 Fang, Xiao-Tian - FM4C.3
 Fang, Xinjie - JW2A.54
 Fang, Yawen - FM4B.5
 Fang, Yu-Qiang - FTh4A.6
 Fang, Yuxi - JTh2A.80
 Fang, Zhiwei - JTu2A.49
 Fanto, Michael - FTh1D.4
 Faraji-Dana, MohammadSadeq - FTh3M.1
 Faraon, Andrei - AM4K.3, FM1A.4, FM1A.6, FM1A.7, FTh3M.1, JTu2A.26
 Fargas Cabanillas, Josep - SM3J.5
 Farinella, Deano - SW4E.3
 Farrell, Carl - AM2K.4
 Farrer, Ian - FM4C.6
 Farrera, Pau - FM2A.1
 Farsari, Maria - SF1E.1
 Fasano, Robbie - SM1F.1
 Fasold, Stefan - JTh2A.24
 Fassbender, Jürgen - STu4F.6
 Fathpour, Sasan - FW3B.7, JTu2A.88, STh1J.1
 Fatome, Julien - FF2D.7, FTh1M.5, SF1M.4, STh4L, SW3H.3
 Fattahi, Hanieh - AF3K.5, FM4M, STu4E.3
 Faucher, Olivier - FTh1M.5
 Faulkner, Grahame - SM2G.5
 Favela, Kristin - JTh2A.87
 Fayard, Nikos - FM1C.5
 Fedeli, Jean-Marc - FF2D.8
 Feder, Kenneth S. - JTh2A.92
 Fedin, Igor - FF3A.4

- Fedorov, Sergey A.- FM1A.1
Fedorov, Vladimir - JTu2A.116, JW2A.50, STh1E.4
Fedorova, Ksenia - ATu3P.6
Fedoruk, M. P.- FTh3B.4
Fedoryshyn, Yuriy - FW3C.1, STh3H.4, STh4N.4, SW3F.7
Fedosejevs, Robert - FF1C.4, FTu4D.1
Fedrici, Bruno - FF1A.5
Fedyanin, Andrey - FM2C.4, JTu4M.6
Fehrenbacher, David - SF2E.2
Fehske, Holger - FM4B.2
Fei, Chengbin - FW4M.6
Fei, Qilai - JTu2A.40
Fei, Shao-Ming - FTh3A.5
Fei, Yue-Yang - FTh4A.6
Fei, Zhe - FM3D.7
feigenbaum1, Eyal - FTh1C.4, SF3G.7
Feizi, Alborz - ATu4K.3, JTu2A.5
Fejer, Martin - SM3O.2
Felber, Matthias - SF3I.5
Feldkhun, Daniel - AW3K.2, SF3N.2, STh4L.5
Feldman, Matthew - JTu2A.21, JW3A.6
Felgen, Nina - SM2O.3
Fellinger, Jakob - SF2O.7
Fellouse, Frederic - AM4I.7
Felts Almog, Ilan - Ath4I.4, SM4H.6
Feng, Aosong - AF2K.7
Feng, Chengyong - JM2E.5
Feng, Feng - SM2G.5
Feng, Jiabin - FM4D.4, STh1J.7, STh3O.1
Feng, JinXia - JTu2A.31
Feng, Kai-Ming - SM4G.3, SM4G.5
Feng, Liang - FM1B.3
Feng, Milton - ATu3P.2, JTh2A.62
Feng, Pingping - STu4L.6
Feng, Tianli - SW3E.5
Feng, Xinhuan - JW2A.102, STu4L.7
Feng, Xue - JW2A.56
Feng, Yan - JW2A.115, JW2A.75
Feng, Yujun - STu3L.2
Feng, Yuzhong - SW3O.7
Ferdinandus, Manuel R. - SF2G.4
Fermann, Martin E.- SF2I.5, SF2I.7, SW4F.6, SW4G.4
Fernandez, Paloma - JTu2A.46
Fernandez-Gonzalvo, Xavier - FM1A.5
Ferrari, Andrea C. - FW3M.4, FW3M.7
Ferraro, Mario - FTh4M.1
Ferre Llin, Lourdes - FF1A.4
Ferreira de Lima, Thomas - JM3M.3, SM3N.3, SW3H.7
Ferrokhi, Hamid - SM2H.3
Fessler, Jeffrey A.- SM4J.2
Feurer, Thomas - SM3L.5
Fevrier, Sebastien - STh4L.2
Fiala, Patrick - STu4O.2
Fiebig, Manfred - FM3D.3
Field, Jeff - ATu3K.5
Fink, Florian - ATu3I.5
Fink, Yoel - SF3L.5
Finley, Jonathan J.- FW3C.7, SM4J.6
Finney, Lauren A.- JTh2A.84, JTu2A.56, SW4L.4
Finney, Nathan - JTh4F.1
Finot, Christophe - FF2D.7
Fintisova, Anna A.- SF3O.8
Fiorentino, Marco - SM4J.7, STu4J.5
Fischer, Bennet - FTh1A.4
Fischer, Julian - SF3E.4
Fischer, Kevin - FM4A.4
Fischer, Marc - SM1F.2
Fischer, Marco P.- FTh3C.6
Flagg, Edward B.- FM3A.4
Flamm, Daniel - JM3E.2
Flannery, Jeremy - FM1B.1
Flansberry, Zackary - FM4A.6
Fleischer, Sharly - FM3D.8
Fleischhauer, Michael - FM4B.1
Fleisher, Adam - AM2K.2
Flemens, Noah - SW4H.7
Flender, Roland - SW3E.6
Flood, Collin - FM3A.4
Flor Flores, Jaime G. - FTu4C.5, SF1J.4, STh4J.5
Flores, Monica M.- AM2K.1
Flöry, Nikolaus - SF3N.1
Flöry, Tobias - SW4E.5
Flower, Chris - JM2B.5
Flühmann, Christa - FTh3A.1
Fogler, Michael - JW2A.34
Foldes, Istvan - FF1C.3
Follman, David - SF2O.7, STh4G.2
Foltynowicz, Aleksandra - SF1I, SM2N.5, STh1G.3, SW3L.5
Fomenko, Anton - SM4H.6
Fong, Dillon - FM4D.7
Fontaine, Nicolas K.- SM1G.1, SM1G.2
Forbes, Andrew - FTh4B.8
Forget, Nicolas - JW2A.35, STh3E.1
Fortier, Tara M.- SM1F.1, SW3G.7, SW4G.1
Fortin, Vincent - SF2L.1, SF2L.3
Fortuna, Seth A.- FW3C.6
Foster, Mark - JW2A.79
Fotouhi, Pouya - SM3G.2
Foucher, Pierre-Yves - Ath3K.1
Fouda, Mohamed - Ath1K.3
Fowler, Trevor - Ath4I.4, SM4H.6
Fowler-Gerace, Lewis - SM1O.4
Fowley, Ciarán - STu4F.6
Fox, Richard - SW3G.7
Foy, Christopher - SF3L.5, SM2F.3
Frankie, Martin C.- SW4F.1
Frank, Andreas - AF1K.4, Ath4K.1
Frankis, Henry - SF2O.4, STh3N.6
Franson, James D.- FTh3A.7
Fraser, James M.- FM4D.5, JM1E.3
Fraser, Scott E.- AM2I.2
Frateschi, Newton - STu3N.2
Fredrick, Connor - FF2D.6
Freedman, Andrew - AM1K.1
Freiberger, Gert - SM2G.2
Friedfeld, Max - STu4J.4
Friedlein, Jacob - STh1G.1
Frigerio, Jacopo - FTh3C.6
Friis, Nicolai - FTh3A.2
Frisch, Josef C.- SW4E.6
Froch, Johannes E. - SF1J.3
Fröjd, Krister - SM1L.5
Frosz, Michael H.- SF1E.6
Froula, Dustin - STu4E.5
Fry, Alan - JM1E.3, SF1E, SF3I.7, STu4E.6, SW4E.6
Fry, Edward - JTh2A.87
Frydendahl, Christian - FTh1C.3
Fryett, Taylor - STu4J.4
Fu, Bo - JW2A.85
Fu, Houqiang - JTh2A.66, SW4H.5
Fu, Kai - SW4H.5
Fu, Kai-Mei - AM4I.1, FM3A, FM4A.3, SF1H.7
Fu, Libin - FF3C.3
Fu, Qiang - JW2A.44
Fu, Shijie - SM1L.3
Fu, Song - STh3O.1
Fu, Songnian - STu3L.2, SW4O.1
Fu, Walter P.- SF1L.1
Fu, Xinghu - JW2A.107
Fu, Yuan-Hsing - SF3J.6, STh1O.4
Fu, Yuxi - SW4E.7
Fu, Zhongyuan - JW2A.9, SM2J.4
Fuchida, Mika - STh4J.6
Fuchs, Gregory - FM3A.1, JW3A.2
Führer, Thorsten - JTu2A.85
Fuji, Takao - SF2L.6
Fujii, Shun - STh4J.6
Fujii, Takuro - JTh2A.58, STh3N.1, STu3N.6
Fujita, Yasuiko - FTh4C.1
Fukushima, Ryota - SF1E.5
Fülöp, József - SW4E.5
Furniss, David - SF2L.4
Furusawa, Akira - FTh1D.1
Futami, Fumio - SW3O.4
- G**
Gad, Raanan - SW3L.4
Gaeta, Alexander L.- FM1D.4, FM1D.6, FM4M.7, JW2A.82, SF3H.4, SF3H.6, STh3J.1, STu3J.5, SW3E.4
Gagatsos, Christos - FF1F.7
Gaïarin, Simone - SW3O.6
Gaida, Christian - STh4E.4
Gailevicius, Darius - SF3J.7
Gal, Lior - SM2O.3
Galan, Alvaro G.- FF3C.2
Galiev, Ramzil R.- STu3J.4
Galili, Michael - JTu2A.83, SW3H.4
Gallacher, Kevin F.- FTh3C.6, STh1N.2, STu4O.7
Gallmann, Lukas - FF2C.1, STh3E.2
Gallo, Katia - SF2J.7, STh3J
Galtier, Eric - STu4E.6
Galvanauskas, Almantas - SF2L.5
Galvão, José R.- JTu2A.9
Galvin, Thomas - SM4E.4, SM4E.6
Galzerano, Gianluca - SF2L.1
Gamboa, Julian - Ath1K.3
Gammon, Dan - FM3A.3, FM3A.4
Gan, Jiwei - STu4L.1
Gan, Lin - JW2A.19, STh1J.7, STh3O.1
Gan, Qiaoqiang - Ath1I.2, Ath1I.3, Ath1I.7, SM1H.5, STu3O, STu4H.5
Gandjbakhche, Amir H.- JTu2A.3
Ganjalizadeh, Vahid - STu3H.4
Ganzer, Lucia - FW3M.7
Gao, Bofeng - JTh2A.21
Gao, Dingshan - JTh2A.56
Gao, Li - STh3L.5
Gao, Liang - SW3N.5, SW4F.3
Gao, Qian - STh3H.3
Gao, Ronald - STu4H.2
Gao, Shoufei - STh1L.6
Gao, Song - FM4C.5
Gao, WeiBo - SM2F.5
Gao, Weilu - FM4D.1
Gao, Xiaohui - JTh2A.4
Gao, Yun - STh3N.3
Gaponenko, Maxim - SF3E.4
Gaponov, D. - STh4L.2
Gapontsev, Valentin P. - JTu2A.95, STh4E.3, STh4E.6
Garbin, Bruno - SW3H.3
García de Abajo, Javier - SM1O.1
García, Marina - JTu2A.46
Gardosi, Gabriella - JTh2A.50
Garg, Srishti - AM4I.7
Gargalis, Leonidas - AW3I.5
Gasperi, Tecla - JW2A.116
Gasulla, Ivana - SF1G.1
Gatti, Davide - Ath3K.2
Gatti, Giancarlo - FF1C.4
Gatton, Averell - FF2C.5
Gausmann, Stefan - SM4L.3
Gauthier, Jean-Christophe - SF2L.1
Gauthier, Scarlett - JW3A.4
Gautier, Julien - SF3I.3
Gawith, Corin - JTu2A.41
Ge, Chaoyang - JTu2A.79
Ge, Xiaochen - FF3A.3
Gebhardt, Martin - STh4E.4
Geddes, Cameron - SF3I.1
Gehl, Michael R.- JTh2A.39, STh4N.6
Gehring, Tobias - JF2F.1
Geim, Andrei - SM1O.4
Geisler, David - SW4O
Geisler, Mathias - FTu3C.4
Gelens, L. - SM3O.3
Gemmell, Nathan R. - JTh2A.93
Genack, Azriel Z.- FF3B.7
Genevet, Patrice - FTh3M.7, FTh4M.1, FTh4M.8, JTu2A.75
Gengler, Jamie J.- SF2G.4, STh4H.5
Genier, Etienne - SW4H.6
Gehli, Hadar - Ath3K.5
Gensch, Michael - JTu2A.101, STu4F.6
Gentile, Antonio - SM2F.2
Gentry, Christian - FF2C.6, FF2C.7
George, Antony - JW3L.1
Georges, Patrick - JM1E.5, JW2A.73
Gerginov, Vladislav - JW2A.113
Gerken, Henrik - JW2A.18
Germanskiy, Semyon - JTu2A.101
Gerngross, Maik - JTu2A.12
Gerosa, Rodrigo M. - SF3L.2, STu4L.2
Gerrits, Thomas - FF1A.6, FM4C, FTh1D.5, FTh4D.6, JTu2A.42
Gertus, Titas - JTu2A.17
Gervaziev, M. D.- FTh3B.4
Gerz, Daniel - JW2A.69, STh4E.4
Gesk, Dimitri - STu4N.1
Gessner, Julia - STh4E.4
Gevorgyan, Hayk - SM3J.5
Ghadimi, Amir H.- FM1A.1
Ghaemi, Pouyan - JTu2A.52
Ghalanos, George - JM3B.3, SF3H.5, STh3J.7
Ghannam, Ibrahim - Ath3I.3
Gharajeh, Abouzar - SW4N.2
Gharia, Asmasynh - JW2A.81
Ghazaryan, Areg - JTu2A.52
Gheno, Alexandre - FTh4C.5
Gherabli, Rivka - JTh2A.49
Ghetmiri, Seyed - AW3P.3, STu3N.3
Ghimire, Shambhu - FF3C, FM4M.6
Gholam Mirzaemoghadar, Shima - FM4M.4, SW4E.2
Ghosh, Amar Nath - STh1L.5
Ghosh, Anirban - FTh1B.6
Ghosh, Nirmalya - JTu4M.5
Ghosh, Saikat - FM2A.4, STh4G.7
Ghosh, Samir - SM3G.4
Giambra, Marco Angelo - STh3N.2, STh4N.2
Gianani, Ilaria - JW2A.116
Giannini, Vincenzo - FTh3C.5
Gibson, Brant - STh3L.3
Gibson, David - SM4E.4
Gibson, Emily A.- STu3H.3
Giese, Enno A.- FF3A.6
Giesecke, Anna Lena - JTh2A.94
Gilaberte Basset, Marta - FF3D.6
Gini, Emilio - SW4N.4
Ginsberg, Jared S.- FM4M.7
Ginterseeder, Matthias - SF1O.6
Giorgetta, Fabrizio R.- AW4K.1, SF1I.1, SM2N.3, STh1G.1, STh1G.2
Giri, Gouri - FTh3A.2
Girodias, Benjamin - JTh4F.2, JTu4M.2
Giudici, Massimo - FTh4M.1
Giunta, Michele - SM1F.2
Gjonaj, Bergin - FTu3D.5
Glasser, Ryan T.- FTh1M.1
Glatzel, Markus - AW4I.3
Glesk, Ivan - SW3H.5
Glick, Madeleine - SM2J.3, STh1N.4
Glodde, Martin - STh1F.2

- Gloger, Timm - FTh3A.2
 Glumac, Nick - SW4L.2
 Gluszek, Aleksander - AF2K.8, JTh2A.113
 Gmitra, Martin - JTu4M.2
 Go, Rowel - AW3P.2
 Gobet, Jean - STu4G.3
 Goda, Keisuke - SM4H.1
 Godard, Antoine - Ath3K.1, JTu2A.93, SF1H.3
 Goddard, Lynford L. - Ath1K.5, JTh2A.41
 Goddet, Jean-Philippe - SF3I.3
 Godfrey, Alan T. - SF2G.5, SF3G.2
 Goetschy, Arthur - FM1C.5
 Gogna, Rahul - FF2A.2, STu3N.5
 Golaraei, Ahmad - JTu2A.1
 Goldflam, Michael - STh4O.4
 Goldstein, Jonathan - JTu2A.53
 Goley, Patrick S. - JTh2A.76
 Gollner, Claudia - FF1C.2
 Golz, Torsten - STh3E.3
 Gomez Velez, Juan S. - SM2N.4
 Gomez, Anthony - AM1K.5
 Gong, Mali - JTh2A.43
 Gong, Ming - JTh2A.28
 Gong, Qihuang - JTh2A.33, JTh2A.69, JTu2A.121, JW2A.51, JW2A.54, SF3G.6, STh3J.2
 Gong, Songbin - JTh2A.41
 Gong, Wenlin - JW2A.7
 Gong, Xiao - STu4J.1, STu4J.2
 Gong, Yuan - JTh2A.88
 Gonta, Vlad A. - FTh3B.4
 Goodfriend, Nathan T. - SF2G.2
 Goodson, Kenneth E. - SF2O.5
 Gopalsamy, Anupriya - AM4I.7
 Gopinath, Juliet T. - STu3H.3
 Gordon, Joshua - SM3F.3
 Gordon, Roy G. - SM4J.5
 Gorecki, Jon - STh4H.6
 Gorman, Brian - SF2G.6
 Göröcs, Zoltán - AM2K.3, SM4H.2
 Gorodetsky, Michael L. - STh1H.3, STu3J.4
 Gorodnitskiy, Alexander S. - STu3J.4
 Gorthi, Sai Siva - JW2A.84
 Gossard, Art - STu4J.3
 Gossard, Arthur - ATu3P.5, STu3N.1
 Gotoh, Hideki - JW2A.30, SW4G.2
 Gotovski, Pavel - JTu2A.17
 Gotti, Riccardo - Ath3K.2
 Götzinger, Stephan - FF3M.1, FM1M.4, FM2A.5
 Gougousi, Theodosia - FF3M.4
 Gould, Michael - SF1H.7
 Goulielmakis, Eleftherios - FTh1B.1
 Goutsoulas, Mihalis - FTh4B.1
 Gouzien, Élie - FF1A.5, FTh4D.2
 Govorov, Alexander - FTh1C.2
 Graefe, Markus - FF3D.6, FM2M.2
 Graf, Austin J. - JTu3A.2, SM2J.5
 Graf, Manuel - AM1K.3
 Graf, Matthias - FTu4D.3
 Grajower, Meir - FTh1C.3, JTh2A.49
 Granade, Chris - SM2F.2
 Grange, Rachel - FM2C.6, SF2J.4, STh1J.3
 Granger, Geoffroy - STh4L.2
 Grant, Joshua - STh4O.6
 Grant, Perry - STh4O.6, STu3N.3
 Grassani, Davide - STh1F.4
 Graumann, Ivan J. - SF3E.3
 Gray, Thomas P. - FTh4C.2
 Green, Bertram - JTu2A.101, STu4F.6
 Green, Mark E. - STh4H.5
 Green, William M. - STh1F.2
 Greenbaum, Alon - AM2I.1
 Greener, Zoe M. - FF1A.4
 Greenfield, Margo - Ath3K.3
 Greganti, Chiara - FM2M.7, FTh4A.3
 Grein, Matthew - FTh4A.2
 Greinert, Rüdiger - AW4I.3
 Gremion, Fabien - FF2D.1
 Grguras, Ivanka - STh3E.3
 Griebner, Uwe - JTu2A.119, SF3E.6, STh1E.5
 Griffith, Austin - JW2A.82
 Griffith, Dana - SM2J.5
 Grillet, Christian - FF2D.8, STh1J.6
 Grillot, Frederic - SW3N.2, SW3N.6
 Grimm, Ronald L. - JW2A.26
 Grinberg, Assaf - SW3L.3
 Grinberg, Patricio - JTu2A.19
 Grinin, Alexey - SM4F.1
 Griskeviciute, Ugne - STh1N.2
 Große-Wortmann, Uwe - STu4E.4
 Grotelueschen, Abigail - FF3D.4
 Grotti, Jacopo - SM1F.3
 Gruson, Vincent - FF3C.6
 Grutter, Karen - SF1J
 Grütmacher, Detlev - FTh4C.3
 Grynko, Rostislav I. - JTu2A.58
 Gu, Gong - FF1B.7
 Gu, Guancheng - SM4L.2
 Gu, Jie - FW3C.2, FW3M.5
 Gu, Qing - SW4N.2
 Gu, Tian - SF2H.4
 Gu, Tingyi - FTh4C.4, FTu4B.7, JTu2A.118, SF3O, SF3O.5, SM1J.2, SM2O
 Gu, Xiaodong - SM4N.3, SM4N.4
 Gu, Xun - AF1K.4
 Gu, Yi - STu4H.3
 Gu, Ying - JTu2A.121, JW2A.54
 Guan, Di - STh3L.5
 Guan, Zanyang - SF1O.2
 Guay, Jean-Michel - FTu4C.4
 Guddala, Sriram - FM4D.2, JTu2A.52, STh4H.7
 Güdde, Jens - FTh1B.4
 Guggenmos, Alexander - SF3I.3
 Guglielmon, Jonathan - FW3D.4, FW3D.6
 Guha, Saikat - FF1F.4, FF1F.7, FTh4A.5
 Guha, Shekhar - SF1H.6
 Guichard, Florent - JM1E.5, JW2A.73
 Guidice, Rafe - STh3G.1
 Guidry, Melissa - SM2F.6
 Güllhabert, Benoit - FW3B.3
 Guina, Mircea - ATu3P.1
 Gumerlock, Karl - SF3I.7
 Gunaydin, Harun - STu4H.2
 Gundogan, Mustafa - FM4A.1
 Guo, donglai - JTh2A.59
 Guo, Guangkun - Ath1K.6
 Guo, Guodong - AF1K.1
 Guo, Hairun - FF1D.5, STh1F.4, STh1G.7, STh4J.2, STu3J.4
 Guo, Hong - JTu2A.30
 Guo, Jhan-You - JTu2A.64
 Guo, Jia Yu - STh3L.1
 Guo, Jingjing - JW2A.105
 Guo, Liang - SF3E.7
 Guo, Lu - SM3N.8
 Guo, Nan - JW2A.102
 Guo, Pengfei - SF2O.5, SF2O.6
 Guo, Qiang - Ath1K.2
 Guo, Qianying - STu3N.3
 Guo, Ruipeng - AM2I.5
 Guo, Ruipu - SW4O.4
 Guo, Ruixiang - FTu3D.7
 Guo, Tianyi - JTh2A.9
 Guo, Wei - AW3K.4, JTh2A.14
 Guo, Wenge - JTu2A.66
 Guo, Xianxin - FM2A.2
 guo, xiaowen - SF2I.2
 Guo, Xin - STh4O.2, STu4O.1
 Guo, Xuexue - FF1B.6, FW4B.2
 Guo, Yuyao - JTh2A.42
 Guo, Zaibing - SF2O.1
 Guo, Zhen - STu3E.1
 Gupta, James - SW3N.1, SW4N
 Gupta, Manisha - FTu4D.1
 Gupta, Neelam - JTh2A.37
 Gurevich, Evgeny - JTu2A.47
 Guryanov, Alexei - SM4E.2, SM4L.1
 Güsken, Nicholas A. - FM2C.2, FTh3C.5
 Guss, Gabe - AW3I.5
 Gustafson, Debbie - JTh2A.114, JW2A.8
 Gustavsson, Anna-Karin - AM4I.5
 Gustavsson, Johan - SM4N.1
 Gutierrez Pascual, M. Deseada - JTh2A.63
 Gutierrez, Audrey Rose - SM4J.2
 Gutierrez-Jauregui, Ricardo - JTu2A.24
 Guzelturk, Burak - STu4F.7
 Guziak, Alexander - ATu4K.2
 Guzman-Sepulveda, Jose - Ath4K.3, FTh1C.8
 Gylfason, Kristinn B. - SF2H.3, STh1F.3
 Hang Tong Edwin, Teo - SF1O.5
 Hanna, Marc - JM1E.5, JW2A.73
 Hannaford, Peter - JTh2A.3
 Hannah, Emily D. - STh3G.2, STh3G.3
 Hanmegam, John M. - JTu2A.22
 Hannotte, Théo - ATu3K.6
 Hänsch, Theodor W. - JM1E.4, SF1I.3, SM4F.1
 Hänsel, Wolfgang - SM1F.2, STh1G.7
 Hansen, Azure - SM3F.5
 Hansson, Tobias - SM3O.3
 Hanyu, Zahng - STh4H.2
 Hao, He - JTu2A.121
 Hao, Qiang - STu4L.1
 Hao, Youzeng - JW2A.3
 Hao, Zhibiao - JTu2A.90, SW4N.7
 Haque, Sanaul - JTu2A.49
 Hara, Kazutaka - SW4G.2
 Harari, Gal - FW3D.2
 Harbord, Edmund - STh1H.1
 Hardi, Justin - AW3I.7
 Hariki, Takuya - SW3G.2
 Harilal, Sivanandan S. - JTh2A.106, SF2G.7, SM1N.3, STh1G.5, SW4L.2, SW4L.3, SW4L.5, SW4L.6
 Haroldson, Ross - SW4N.2
 Harouri, Abdelmounaim - FM1M.1, FM3A.2
 Harper, Danielle - SW4E.8
 Harrington, Kerianne - SW4H.7
 Harris, Brandon - SM3H.2
 Harris, James - SF2H.7
 Harris, Nicholas C. - FTh1D.3, FTh3A.3, FTh4A.3, SF1N.1, SF1N.3
 Hartelt, Michael - FTh1C.7
 Hartfield, George Z. - JTh2A.108, JTh2A.25, STh1F.5
 Hartl, Ingmar - SF3I.4, SF3I.6, STu4E.4
 Hartmann, Gregor - FF2C.5
 Hartmann, Jean-Michel - FF2D.8
 Hase, Eiji - AF3K.4
 Hasegawa, Takemi - SW3G.1
 Hashemi, Ehsan - SM4N.1
 Hashimoto, Kazuki - SM1N.4
 Hasling, Matt - JW2A.34
 Hassan, Absar U. - FF1D.3, FTh3B.2, FTu3B.2
 Hastings, Michael G. - FM4M.2
 Hata, Yuya - STu3L.3, SW3G.4
 Hatami, Fariba - SF1H.7
 Hati, Archita - JW2A.113
 Haung, Ying-Lun - Ath11.4
 Hawkins, Aaron - STu3H.2, STu3H.4
 Hawkins, Peter - JTu4M.2
 Hawkins, Roberta - SW4N.2
 Hawkins, Samuel - STh4O.4
 Hawkins, Thomas - SM4L.2
 Hayashi, Neisei - AF1K.5, JTh2A.85, JW2A.94, STu3L.5
 Hayden, Torrey - AW4K.1
 Hayenga, William - FM1D.2, FW4D.2, STu3N.8
 Hayes, John - STh1L.2, STh1L.4
 Haylock, Ben - FTh4D.3
 Hayran, Zeki - SF3J.7
 Hayward, Rosie S. - JW2A.42
 Hazan, Yoav - SW3L.1, SW3L.2, SW3L.3
 He, Bing - JW2A.95
 He, Calvin - FF1C.4
 He, Guangqiang - JW2A.47
 He, Haoyu - FW3B.5
 He, Jijun - STh4J.2, STu3J.2
 He, Jin - FF1C.3
 He, Lingyan - FF2D.3
 He, Qiong - JTh2A.11
 He, Qixin - JW2A.21
 He, Yang - SF2H.2, SF2J.5, STh1J.2
 He, Yunxiao - FF1C.5
 Haan, Kevin - AM2I.3, AM2I.6
 Habbal, Fawwaz - SM4J.5, SW3J.3
 Haberberger, Dan - STu4E.5
 Habib, Md. Selim - SM1L.1
 Hadad, Yaron - JTh2A.8
 Haddad, Elissa - JTh2A.2
 Hadfield, Robert H. - JTh2A.93, JTu2A.41
 Haefner, Constantin - SM4E.4, SM4E.6
 Haefner, Sebastian - SM1F.3
 Haesler, Jacques - STu4G.3
 Hafezi, Mohammad - JM2B.5
 Haffner, Christian - FW3C, FW3C.1, STh3H.4, SW3F.7
 Hagan, David J. - FF3D.3
 Hagen, Gaute - FTh3A.6
 Haglund, Åsa - SM3N, SM4N.1
 Haglund, Richard F. - JTu2A.21, JW3A.6, STh4H.1
 Hahamovich, Evgeny - SW3L.3
 Hahn, Robin - JTu2A.12
 Haidar, Riad - FTh3C.1
 Hail, Claudio U. - FW3C.5
 Haizer, Ludovit - SW3E.6
 Hajimiri, Ali - SF2N.6, STh3H.7
 Halas, Naomi - FF2B.4
 Halimi, Sami I. - SM2J.4
 Hallman, Kent A. - STh4H.1
 Ham, Moon-Ho - FM2D.5
 Hamamoto, Mathew - SM4O.3
 Hamerly, Ryan - JF2F.5, SF1N.1
 Hamilton, Scott - FTh4A.2
 Hammad, Mohab N. - SM4N.6
 Hammani, Kamal - FF2D.7
 Hammer, Jonas - FTh3B.3
 Hammond, Mustafa - SM3J.7
 Hammouti, Sabrina - JTu2A.1
 Han, Fei - SM1H.4
 Han, Hainian - JTh2A.104, SW3G.5
 Han, Hongwei - JTh2A.56
 Han, Jianguang - SW3F.5
 Han, Kaizhen - STu4J.2
 Han, Kevin - FW3C.6
 Han, Ningren - STu4N.2
 Han, Ruonan - SM2F.3
 Han, Sang-Pil - JTu2A.11
 Han, Sang-Wook - FM2M.4, JTu2A.35, JTu2A.45
 Han, Sangyoon - SM4O.2
 Han, Seunghwoi - FF3C.4
 Han, Shensheng - JW2A.7
 Han, Won Seok - JTu2A.43
 Han, Xiao - SW4O.6
 Han, Yanjun - JTu2A.90, SW4N.7
 Han, Yuanyuan - STu4H.3
 Hanein, Yael - AF3K.2

- He, Zuyuan - AF1K.2, JW2A.101, SF1L.5, SF3L.4, SM4F.5
Headrick, Robert J. - STh4H.5
Healey, Chris - SF1J.3
Hearley, Brandon - AF1K.1
Heberle, Dylan - SW4H.7
Heberle, Johannes - ATu3L.1
Heckl, Oliver H. - SF2O.7
Heebner, John - SM4O.3
Heffernan, Brendan M. - STu3H.3
Hegedus, Steven - JTu2A.118
Hegelich, Bjorn M. - STu3E.2
Hegmann, Frank - STu3F.1
Heidari, Elham - FTu3B.7
Heidt, Alexander - SM3L.5
Heigl, Michael - FW4M.4
Heilweil, Edwin J. - STu4F.4
Heinrich, Matthias - FM1C.6, FM4B.2, FM4B.3, FM4B.7, FTu3B.3, FTu4B.3, FW3D.5, FW3D.8
Heinz, Tony - FW3M.5, JTh4F.1, STu4F.7
Heinze, Georg - FM2A.1
Heiz, Ulrich K. - SF2G.1
Helk, Tobias - SF3I.3
Hellman, Brandon - AW3K.7
Hellmann, Christian - JTh2A.23
Hellwig, Tim - FF2D.5, JTu2A.61, JTu2A.69, SF1L.2
Helm, Manfred - STu3F.3
Helml, Wolfram - FF2C.5
Helmrich, Sophia - FM3D.2, JW2A.24
Helmy, Amr S. - FW3B.5, SF1J.2, STu4H.1
Helt, Luke G. - FTh4D.6
Heming, Sebastian - JM3E.1
Hen, Mirit - STh3H.5
Hendrickson, Joshua R. - SF2O.5, SF2O.6
Heni, Wolfgang - STh4N.4, SW3F.7
Henriksen, Martin R. - SM2O.7
Henry, Nathan - STu4N.2
Hensley, Joel M. - FM4C.2
Henzler, Philipp - FM3D.4
Heo, Myoung-Sun - JW2A.111
Heo, Se-Yeon - FTu4D.5, JW2A.16
Heo, Wonhyoek - FM2D.3
Her, Tsing-Hua - SM3H, SM3H.4, STh4H.5
Herd, Jeffrey - SF3N.7
Herd, Andreas - SW3N.2
Herkommer, Clemens - JM2E.5, SM4E.3
Herman, Daniel I. - SM2N.3, STh1G.1
Herman, Irving P. - SM1O.2
Hermann, Jörg - JTu2A.56
Hernandez-Garcia, Carlos - FF2C.6, FF2C.7
Hernandez-Gomez, Cristina - JM2E.1, SW4E
Heron, Sebastian - FTh3M.7
Herr, Tobias - AF2K.2, FF1D.2, STh4J.1, STu3J.3
Herrera, Luis Y. - SM1L.6
Herriot, Sandrine I. - SM4E.6
Herz, Laura - STu4F.5
Herzog, Bastian - FM3D.2, JW2A.24
Heslar, John T. - JTh2A.1
Hestroffer, Karine - SF1H.7
Hettiarachchi, Chathuranga - JTu2A.77
Heu, Paula - STh4G.2
Heuck, Mikkel - JTu4A.4
Heuermann, Tobias - STh4E.4
Heusinger, Martin - JW2A.69, STh4E.4
Hewak, Daniel W. - SF3O.7
Hickstein, Daniel - FF2C.7, FF2D.6, JM3E.4, STh1G.2, SW4H.2
Hiero, Adrian - FTh4M.1
Higuchi, Akira - SM4N.2
Hilaire, Paul - FM3A.2
Hildebrandt, Lars - STh4H.3
Hill, Kent - ATu4K.2
Hill, Wendell T. - FF1C.4, FF2C
- Hillbrand, Johannes - STu4O.6
Hilton, David J. - STu4F.1
Himsworth, Matt - STu4G.1
Hinchliff, Janna - STh1H.1
Hiraishi, Masaya - JW2A.30
Hiraki, Tatsuro - STh3N.1, STu3N.6
Hirano, Akira - SM2G.1
Hirohashi, Junji - JTu2A.106
Hirose, Kazuyoshi - SM4N.2
Hirota, Osamu - SW3O.4
Hirsch, Joy - JTu2A.120
Hisai, Yusuke - SW3G.1
Hitachi, Kenichi - SF1I.3, SW4G.2
Hitaka, Masahiro - SM4N.2
Hitomi, Kenya - SW4G.2
Hjort, Filip - SM4N.1
Hlaing, May - JW2A.15, JW2A.22
Ho, Po-Hsun - FTh3C.7
Ho, Tuan-Shu - AW4I.6
Ho, Wen-Jeng - Ath1I.4
Ho, Ying-Lung Daniel - SF3O.7
Ho, Yu-Han - AM4I.2
Hoang, Thang B. - JTu3M.4
Hochberg, Michael - FTh1D.3, FTh3A.3, FTh4A.3, SF1N.1
Höckendorf, Bastian - FM4B.2
Hodges, Joseph - AM2K.2, SM2N.2
Hodgson, Norman - JM3E.1
Hoehler, Matthew S. - AW4K.1
Hoenig, Eli - STh1G.2
Hoenninger, Clemens - ATu3I.7, ATu4I.5, JM3E.3
Hoessbacher, Claudia - STh4N.4, SW3F.7
Hofer, Christina - STh4E.4
Höfer, Ulrich - FTh1B.4
Hoffman, Galen - JTh2A.39
Hoffmann, Hans-Dieter - JM1E.4
Hoffmann, Matthias C. - JTh4F.1, JTh4F.4, STh3F.2
Höfling, Sven - AW3P.1, FM1M.7, STh1H.1, STu4O.6
Hogg, Richard - ATu3P.4
Hoghooghi, Nazanin - SF1I.6
Hokmabadi, Mohammad - FW4D.2
Holguin-Lerma, Jorge A. - SM3N.4
Hollberg, Leo - SW4H.1
Höller, Christian - FW3C.5
Holloway, Christopher L. - SM3F.3
Holmstrom, Scott - JTh2A.53
Holonyak, Nick - ATu3P.2
Holtkemper, Matthias - FM3D.4
Holtzmann, William G. - JW2A.48
Holzgrafe, Jeffrey - JW3A.4
Holzwarth, Ronald - SM1F.2, STh1G.7
Home, Jonathan - FTh3A.1
Honardoost, Amirmahdi - JTu2A.88
Hone, James - FTu3C.2, FW3M.5, JTh4F.1, SM1O.2
Hong, Brandon - AM4I.6
Hong, Chang - JW2A.67
Hong, Deshun - FM4D.7
Hong, Feng-Lei - SW3G.1, SW3G.8
Hong, Hyun-Gue - JW2A.111
Hong, Jianxun - STh1N.7
Hong, Jong-Young - AM4K.2
Hong, Kuo-Bin - JTu2A.81
Hong, Kyung-Han - STh3E.5
Hong, Yifeng - STh1L.6
Hong, Yuzhe - AW3I.4
Honjo, Toshimori - JTu2A.28
Honsberg, Martin - Ath3K.6
Hood, Dana - STh4N.6
Hooten, Sean M. - FW3C.6
Hopp, David - JTu2A.12
Hoppe, Morten - Ath3K.6, Ath3K.7, Ath4K.7
Hoque, Nabil Md Raknul - SM1L.4
- Horikiri, Tomoyuki - FTh1D.7
Horne, Steve - JTh2A.114
Horodynski, Michael - FTu3D.6
Horsley, Simon A. - FF2B.3
Horst, Folkert - JM3M.1
Horvath, Sebastian - FM1A.5
Hosako, Iwao - SM2H.5, SW4F.4
Hosen, Md M. - FW4M.2
Hoshi, Hayato - JTh2A.96
Hoshi, Masayuki - JTu2A.106
Hosoda, Takashi - SM3N.7
Hosokawa, Yoichiroh - SM4H.1
Hosseini, Pooria - STh1L.1
Hosseini-Zadeh, Mani - SF1J.5
Hou, Dong - Ath1K.6, STh4J.4
Hou, Songyan - JTu2A.77, SF1O.5
Hou, Yalin - SF1M.2
Houard, Aurelien - FTh1M.2, JM2E.5
Houston, Jessica P. - SM4H, SM4H.4, STu3H, STu4H
Houston, Kevin D. - SM4H.4
Howard, Ian - JTu2A.71
Hrisafov, Stefan - STh3E.2
Hsu, Chia Wei - FF3B.3, FF3B.5, FM1C.1, FTu4B.4
Hsu, Chou-Yun - JTh2A.97
Hsu, Lung-Hsing - FTh4M.2
Hsu, Olivia - JW2A.78
Hsu, Shih-Hsiang - JTh2A.97
Hsu, Shun-Chieh - SF2O.2
Hsu, Yao-Yu - SF3J.4
Hsueh, Yu-Chun - FF2A.7
Htoon, Han - STh3O.6
Hu, Bo - STh3L.1
Hu, Er-Tao - JW2A.11
Hu, Futai - JTh2A.43
Hu, Hao - FTh4M.8, JTu2A.83
Hu, Hui - JTh2A.21
Hu, Jiaqi - FM4D.3
Hu, Jie - JW2A.23
Hu, Jonathan - JW2A.118, JW2A.122
Hu, Juejun - JM3B.4, SF2H.4
Hu, Junjie - JTh2A.68
Hu, Ming-lie - JTh2A.103, SF1H.2, SF3E.1, STh1G.6, STh3L.6, STh4E.1, SW3E.5, SW3H.6
Hu, Qing - STu4N.2
Hu, Shanting - SM4N.3
Hu, Shaohua - SW3O.7
Hu, Sheng - SM1O.4
Hu, Shuren - SM2J.4
Hu, Ting - AW4K.5, SF3J.6, STh1O.4
Hu, Walter - SW4N.2
Hu, Wenbin - JTh2A.59
Hu, Yandi - JW2A.118
Hu, Yaowen - FTh1D.2
Hu, Yi - FTh4A.6, FTh4B.2, FTh4B.7, JW2A.41, JW2A.45
Hu, Yingtao - STu4J.5
Hu, Yue - JTh2A.56
Hua, Jianfei - FF1C.5
Hua, Nan - JTh2A.78
Hua, Xiang - SM1O.2
Hua, Yi - JTu2A.105
Huan, Yan Qi - JTu2A.26
Huang Chen, Sung-Wen - JTu2A.115
Huang, Chaoran - SW3H.7
Huang, Chia-Wei - JTh2A.107
Huang, Chiu-Chang - JTu2A.16
Huang, Chung-Che - SF3O.7
Huang, Chung-Ping - SF2O.2
Huang, Dongmei - JW2A.102, STu4L.7
Huang, Gang - SM4E.5
Huang, Guan hao - STh1H.3, STh4J.2
Huang, Hangdong - SM3L.3
Huang, Hanzi - SM1G.2
Huang, Hao - JTh2A.80
- Huang, Heqing - STh3H.1
Huang, Hsien-chih - STh3O.5
Huang, Hsuan-Han - JTu2A.16
Huang, Hsu-Hong - SM4G.5
Huang, Jiahui - JW2A.29, SM1O.5
Huang, Kai-Chih - ATu3K.3
Huang, Ke - SF1J.5
Huang, Kuang-Hsu - JTh2A.75
Huang, Kun - STu4L.1
Huang, Liangjin - JW2A.106
Huang, Qianqian - JW2A.38, JW2A.88
Huang, Qinglan - JW2A.61
Huang, Ruiting - ATu3K.1, AW4I.5
Huang, Ruizhi - SW3J.3
Huang, Sheng - AF1K.6
Huang, Shu-Wei - FF2D.2, SM1F.5, SM3O, STh4J.5, SW4H.4
Huang, Song - ATu4I.3
Huang, Xin - SM1N.1
Huang, Xincheng - SW4O.3
Huang, Xuanqi - JTh2A.66, SW4H.5
Huang, Yao-Wei - SF3J.5
Huang, Yen Chieh - JTu2A.104
Huang, Yetian - SM1G.2
Huang, Yi-Chiau - STu4J.1, STu4J.2
Huang, Yidong - JTu2A.33, JW2A.56
Huang, Yiming - FF3B.7
Huang, Yishen - SM2J.3
Huang, Yi-Teng - FTh3M.3
Huang, Yongguang - JTu2A.70
Huang, Yongzhen - JW2A.3
Huang, Yu - STh4J.5
Huang, Yujia - ATu4K.2, JTu2A.5
Huang, Yu-Ming - SF2O.2
Huang, Zhengyu - SM4J.2
Huang, Zhihong - SM3J, SM4J.7, STu4J.5
Huang, Zhirong - FF2C.5, SF3I.2
Huang, Zinan - JW2A.38, JW2A.88
Huber, Markus A. - FTh4C.3
Huber, Rupert - FTh1B.2, FTh1B.4, FTh4C.3, FW3M.1, JTh4F.2, JTu4M.2
Hudzikowski, Arkadiusz - AF2K.8, JTh2A.113
Hughes, Tyler - JF3F.2, SF2H.7, SW4J.5, SW4J.7
Hughes, Maxime - FTh4M.1
Hui, Rongqing - SW3O.2
Hülsebusch, Thomas - STu4E.4
Humbert, Georges - JW2A.108
Hume, David - SM1F.1
Hung, Yung-Jr - JTh2A.107, JTh2A.32
Huntington, Eleanor H. - FTh4D.3
Hunziker, Stephan - JTh2A.100
Hur, Jungyu - ATu3I.6
Husakou, Anton H. - FF3C.2
Hussain, Syed Ali - AF3K.5
Huster, Jeldrik - STu4L.5
Hutchison, Phillips - SW4H.2
Huttner, Ulrich - FW3B.6, JTu4M.2
Huttunen, Mikko J. - FM3C.4
Huwer, Jan - FM4C.6
Hwang, Joonhyuk - SM4O.2
Hyun, Minji - STh3G.6, STh3G.7
- I
Ibrahim, Heide - JTh2A.2
Ibrahim, Mohamed - SM2F.3
Ichijo, Mitsuki - SF3G.4
Ichimiya, Masayoshi - JW2A.32
Ideguchi, Takuro - SM1N.4
Igliev, Hristo - SF2G.1
IJspeert, Mark - JW2A.30
Ikeda, Kohei - SW3G.8
Ikeuchi, Tadashi - FW3B.5
Ilday, Omer - JTu2A.1
Ilev, Ilko - AM11, AM3I, ATu3K
Illmann, Lars - JW2A.18

- Ilyakov, Igor - JTu2A.101, STu4F.6
 Im, Dong-Gil - JTu2A.45
 Imai, Koichi - JTu2A.106
 Imany, Poolad - FF1F.3, FTh1A.2, JTu3A.3, JTu3A.5
 In, Chihun - FM2D.5
 Inaba, Hajime - JW2A.97, SW3G.1, SW3G.3, SW3G.8
 Inami, Wataru - FM2C.5
 Indukuri, Sita Rama Krishna C.- FTh4M.4
 Inose, Tomoko - FTh4C.1
 Inoue, Kyo - JTu2A.28
 Inoue, Takuya - SM1J.7
 Ippen, Erich - Ath4I.2, SW4G.6
 Ippommatsu, Masamichi - SM2G.1
 Irwin, Niels - JTu2A.84, SM4O.6
 Isaac, Brandon - SF3N.6
 Isawa, Shohei - JTh2A.71
 Isella, Giovanni - FTh3C.6
 Ishihara, Hajime - JW2A.32
 Ishii, Nobuhisa - FM4M.1
 Ishimura, Shota - SM3G.4
 Ishizawa, Atsushi - SF11.3, SW4G.2
 Ishizuki, Hideki - JM1E.2
 Isichenko, Andrei - STh4L.3
 Iskhakova, Liudmila - SM4L.1
 Islam, Md Shafiqul - JTu2A.51
 Islam, Mehedi - FTh1A.4
 Isono, Fumiko - SF3I.1
 Isozaki, Akihiro - SM4H.1
 Itatani, Jiro - FM4M.1
 Ito, Akio - SM4N.2
 Itoh, Kohei M. - AM4I.1
 Itoigawa, Fumihiro - ATu3I.3, ATu3I.4
 Iu, Meng - FW3B.5
 Ivanov, Hristo - SM2G.2
 Ivanov, Misha - FF3C.2, FM4M.5
 Ives, Craig - SF2N.6, STh3H.7
 Iwamoto, Kenta - SW4F.6
 Iwamoto, Satoshi - FM1M.2, STh1J, SW4J.1, SW4J.4
 Iwanaga, Masanobu - FTh3M.7
 Iwata, Muneaki - SF3G.3
 Iyer, Arjun - STh1L.3
- J**
- Jabir, M.V. - FM4C.7
 Jackson, Eric M. - SM2J.7
 Jacob, Matthias - Ath4K.4
 Jacob, Zubin - FM4B, FTu3D.3, FTu4D.1
 Jacobs, Kurt - JTu4A.4
 Jadidi, M. M. - FM4M.7
 Jaecck, Julien - FTh3C.1
 Jaeger, Nicolas - ATu4K.5, SM3J.7
 Jafari, Omid - STh3H.2
 Jafari, Rana - JW2A.76
 Jaffe, Tzach - SM2O.3
 Jagerská, Jana - STh1F.1
 Jahani, Saman - FF2B.1
 Jahani, Yasaman - FTh4C.6
 Jahromi, Ali K. - JTh2A.98
 Jain, Aadhar - STu3H.2
 Jain, Gaurav - JTh2A.63
 Jain, Nitin - JF2F.1
 Jakoby, Marius - JTu2A.71
 Jakubek, Zygmunt - SF2G.5
 Jalali, Bahram - AF3K.6, AW3K.3, JF3F.3
 Jalas, Dirk - FTu4D.3
 Jambunathan, Venkatesan - JTu2A.119
 Jang, Dogeun - FTh1M.3, STh3F.4, STu3F.5
 Jang, Heesuk - SW4G.7
 Jang, Jae K. - FM1D.4, FM1D.6, STh3J.1
 Jang, Woosun - FM2D.5
 Jang, Yoon-Soo - SF2H.6, STh4G.4
 Jang, Yudong - JTu2A.43
 Jankowski, Marc - SM3O.2
 Janosik, Natalie - SM2J.3
- Janousek, Jiri - FTh4D.3
 Jansen, Matthijs - FF2C.7
 Jaramillo-Villegas, Jose A. - JTu3A.3
 Jarrahi, Mona - SF1N.2, STu3F.4, SW3F.4
 Jasion, Greg - STh1L.4
 Jauberteau, Raphael - STh4L.1
 Jauregui, Luis - AM3K.3, FM3C.2
 Jauregui, Roc'io - JTu2A.24
 Javey, Ali - SW3J.2
 Javid, Usman A. - JTh2A.115, JTu3A.2, SM2J.5
 Jayakumar, Harishankar - FF3A.3
 Jayaraman, Ashwin - SM4J.5
 Jayatilleka, Hasitha - ATu4K.5
 Jelezko, Fedor - SM2F.2
 Jelic, Vedran - STu3F.1, SW3F
 Jen, Myungsam - JW2A.27
 Jenkins, Micah - SM4O.4
 Jenks, Kyle - AM2I.5
 Jenne, Michael - JM3E.2
 Jeon, Chan-Gi - STh3G.7, SW3G.6
 Jeon, Cheonha - STu3E.2
 Jeon, Kooknam - JW2A.27
 Jeong, Dongin - SM4O.2
 Jeong, Young-Gyun - JTh2A.2
 Jesse, Stephen - AF3K.3
 Jha, Devesh - SW4J.6
 Jha, Keshav K. - JW2A.37
 Ji, Chen - JTu2A.70
 Ji, Dengxin - Ath1I.7, SM1H.5, STu4H.5
 Ji, Hong - STh3L.3
 Ji, Junhua - JW2A.89
 Ji, Qing-Xin - STh3J.2
 Ji, Xingchen - FM1D.4, FM1D.6, SF3H.4, SF3H.6, SM2O.6, STh3J.1, STu3J.5
 Ji, Yaping - JTh2A.25
 Jia, Zixi - ATu4I.3, JTh2A.12
 Jiajie, Teng - Ath1K.2
 Jian, Xu - STh4H.2
 Jiang, An-Qing - JW2A.11
 Jiang, Chen - JW2A.88, SF3L.6
 Jiang, Haifeng - JTu2A.66, SM2H
 Jiang, Hongbo - SF3O.1
 Jiang, Hongzhu - SM1O.3
 Jiang, Jiang - SM3N.7
 Jiang, Ning - JTu2A.73
 Jiang, Quanyu - JW2A.86, SF3O.2, SF3O.3
 Jiang, Shicheng - FM4M.4
 Jiang, Tao - FM2C.1
 Jiang, Tianshu - FM4B.5
 Jiang, Wentao - JW4A.4, SF2J.6
 Jiang, Xiantao - JTu2A.108, JW2A.86, SF3O.2, SF3O.3
 Jiang, Xiao - FTh4A.6, JTu2A.92
 Jiang, Xin - FTh3B.3
 Jiang, Yue - JTu2A.122
 Jiang, Yunshan - AW3K.3
 Jimenez, Oscar A. - STu3J.5
 Jimenez-Galan, Alvaro - FM4M.5
 Jin, Lei - AF1K.5, JW2A.94, SF3O.1, SF3O.4, STu3L.5
 Jin, Liang - JW2A.53
 Jin, Rui-Bo - FTh3A.5
 Jin, Warren - SF2I.2
 Jin, Weiliang - SF1H.7
 Jin, Xiaorong - ATu4I.3
 Jin, Xinxin - JW2A.86, SF3O.2, SF3O.3
 Jin, Yeonghoon - STh3O.2
 Jin, Yiyin - STu4H.2
 Jin, Yuan - SW3N.5, SW4F.3
 Jing, Li - FTu4C.2, SF1N.1
 Jo, Hanlae - FM2A.7, FM2A.8
 Jo, Hyunwoo - FF2B.6
 Joannopoulos, John D. - FTu4C.2, SF1N.1
 Jobin, Frédéric - SF2L.1, SF2L.3
 Joe, Graham - JW3A.4
 Joerg, Andreas - FW3C.1, STh3H.4
- Johanning, Michael - FTh3A.2
 Johnson, Eric - Ath1K.7
 Johnson, Jason - JTu2A.53
 Johnson, Kyle A. - JW2A.36
 Johnson, Mike - FTh1C.4, SF3G.7
 Johnson, Steven - SF3N.7, SW4J.8
 Johnston, Michael - STu4F.5
 Joly, Nicolas - FTh3B.3
 Jonek, Michael - JW2A.18
 Jones, Kevin M. - JTu2A.123
 Jones, R. J. - JTh2A.106, SM1N.3, STh1G.5, SW4L.1, SW4L.6
 Jones, Robert R. - FF3C.1
 Jones, Travis N. - JW2A.76, SW3E.2
 Jörg, Christina I. - FM1C.4, FM4B.1
 Jørgensen, Asbjørn A. - SM2O.7
 José da Silva, Marco - Ath4K.2
 Joseph, Joby - JW2A.119
 Joshi, Chaitanya - FM1D.4, SF3H.6, STh3J.1, STu3J.5
 Joshi, Chan - FF1C.5, FW3B.6, JW2A.50, STh1E.4
 Jossent, M. - STh4L.2
 Jost, John D. - STu3J.4
 Josten, Arne - STh4N.4
 Joulain, Karl - FTh3C.1
 Jovanovic, Igor - FTh1M.6, JTh2A.84, JTu2A.56, SF2G.7, SF2L.5, SW3E, SW4L.4, SW4L.5
 Ju, Jung Jin - JTu2A.43
 Ju, Zhiping - JTu2A.111
 Jukna, Vytautas - JTu2A.17
 Jullien, Aurelie - JW2A.35
 Jung, Daehwan - ATu3P.5, STu3N.1, STu4J.3
 Jung, Hojoong - SM3O.6
 Jung, Hyunseung - FF2B.6, FM2D.5
 Jung, Pawel - FF1D.3, FW3D.1
 Jung, Robert - JM2E.5
 Jung, Yongmin - JTh2A.74
 Jungwirth, Nicholas - FM3A.1
 Juodawlkis, Paul - SF3N.7
 Juodkazis, Saulius - SF3J.7
- K**
- Kabacinski, Adeline - SF1H.3
 Kabakova, Irina - SM4O.7
 Kabir, Firoza - FW4M.2
 Kablukov, Sergey I. - STh4L.4
 Kachiraju, satyanarayana R. - JW2A.65
 Kadlec, Clark - STh4O.4
 Kadlec, Emil - JTh2A.39
 Kaenders, William - Ath3K.2
 Kagami, Hibiki - JTh2A.16, SM4F.3
 Kageyama, Takeo - ATu3P.3
 Kahle, Hermann - ATu3P.1
 Kaiser, Maik - JTh2A.100
 Kaiser, Thomas - FTh1C.6, JTh2A.24
 Kakinuma, Yasuhiro - STh4J.6
 Kakitsuka, Takaaki - STh3N.1, STu3N.6
 Kaksis, Edgar - SW4E.1, SW4E.5
 Kakuda, Masahiro - FM1M.2
 Kalaydzhyan, Aram - JTu2A.105
 Kalichevsky-Dong, Monica - SM4L.2
 Kalkavage, Jean - SF3N.6
 Kallel, Housseem - FTh3C.1
 Kallepalli, Deepak - SF2G.5
 Kallepalli, L.N. Deepak - SF3G.2
 Kalmykov, Serge - FTh1M.3
 Kalubovilage, Manoj P. - SW4G.3
 Kamali, Seyedeh M. - FTh3M.1
 Kamel, Ayman N. - SF3H.2, SM2O.7
 Kamer, Brian - FTh1M.4, JM2E.5
 Kaminer, Ido - FF1F.6, FF3D.7, FF3M.6, FTh1C, FTh4B.4, FTh4M.7, FTu3C.3, JTh2A.8
 Kamitsos, Efstratios - SM1H.3
- Kamp, Martin - AW3P.1, FF3B.4, STh1H.1
 Kampmeier, Jörn - FTh4C.3
 Kan, Qiang - JTu2A.70, JTu2A.72, JTu2A.75
 Kanai, Teruto - FM4M.1
 Kanai, Tsuneto - JM2E.4
 Kananen, Thomas M. - FTh4C.4, SF3O.5
 Kandyla, Maria - SM1H.3
 Kane, Daniel - ATu3K.5
 Kane, Tim - JTu2A.15
 Kaneko, Akihiro - SF3G.3
 Kaneshima, Keisuke - FF3C.5
 Kang, Chun Hong - SF2O.1, SM3N.4
 Kang, Dongyeon D. - SM1J.7
 Kang, Hyun Jay - STh3G.4
 Kang, Il Suk - AW3I.2
 Kang, Ji-Hun - FF3M.7
 Kang, Jin Ho - JW2A.29, SM1O.5
 Kang, Jiqiang - STu4L.6
 Kang, Min-Sung - FM2M.4
 Kang, Moon Sung - FF2B.6
 Kang, Renzhu - SF3E.7
 Kang, Tae Young - JTu2A.7
 Kanidi, Maria - SM1H.3
 Kanno, Atsushi - SF1G.2, SM2G.1
 Kanté, Boubacar - FF3B.8, SM3N.1
 Kao, Chia-Wei - JTh2A.107
 Kapon, Eli - FTh3D.3
 Kapsalidis, Filippos - STu4N.2
 Kapteyn, Henry - FF2C.6, FF2C.7, JM3E.4
 Kar, Arunita - JTh2A.41
 Kara, Oguzhan - AM2K.4
 Karaiskaj, Denis - STu4F.1
 Karamuk, Sohret - JTu2A.1
 Karasahin, Aziz - FM1M.3, JM2B.5
 Karaveli, Sinan - FW3C.4
 Kardas, Tomasz - SF3E.2
 Karimi, Mohammad - FF1B.3
 Karimi, Yasin - SM4H.5
 Kariki, Krishna - JW2A.50, STh1E.4
 Karl, Nicholas - FF2B.2
 Karlen, Sylvain - STh4E.5, STu3J.3, STu4G.3
 Karnieli, Aviv - FF3M.6, FTh4M.7, JM3B.6
 Karpf, Sebastian - AW3K.3
 Karpov, Maxim - FF1D.5, FF2D.1, SM3G.3, STh4J.2, STu3J.4
 Kartaloglu, Tolga - AF1K.7
 Kartner, Franz - Ath4I.2, JTu2A.105, SM4E.1, SW3E.7, AW4I.3, FF2C.2, FF2C.3, JTh2A.100, JTu2A.101, JTu4M.4, JTu4M.5, STh3E.5, SW4E.4, SW4G.6
 Kartouzian, Aras - SF2G.1
 Kasamatsu, Akifumi - SW4F.4
 Kasevich, Mark A. - SM3F.2
 Kashiwagi, Ken - JW2A.97, SW3G.3, SW3G.8
 Kashyap, Raman - FTh1A.4
 Kasparian, Jerome - JM2E.5
 Kasperczyk, Mark - JW3A.1
 Kasture, Sachin - FTh4D.3
 Kaszub, Wawrzyniec - SF1I.4
 Kaszubowska-Anandarajah, Aleksandra - SM4G.2, SM4N.6, STu4N.5
 Kataura, Hiromichi - JW2A.92
 Katayama, Ikufumi - FM4D.1
 Kato, Kentaro - SW3O.4
 Kato, Takashi - SM2H.4
 Kato, Yuichiro K. - SM4J.1
 Kats, Mikhail - SM2H.6
 Katsumi, Ryota - FM1M.2, SW4J.1
 Katsuragawa, Masayuki - JTh2A.110
 Katsutani, Fumiya - FM4D.1
 Katz, Shahar - AF2K.6
 Katzman, Moshe - STh3H.5
 Kaufmann, Delia - FTh3A.2
 Kaufmann, Fabian - SF2J.4
 Kaufmann, Peter - FTh3A.2

- Kavaya, Michael J. - AW4K.6
 Kawamori, Taiki - FF3D.5, STh3J.6
 Kawanishi, Tetsuya - SF1G.2
 Kawata, Yoshimasa - FM2C.5
 Kaylaycioglu, Hamit - JTu2A.1
 Kazakov, Dmitry - FM1D.3, STh4H.3
 Kazansky, Peter G. - ATu4I.4
 Kazi, Zeeshawn - AM4I.1
 Ke, Xu - SW4N.7
 Keathley, Philip - STh3E.5
 Keathley, Phillip D. - JTu4M.4
 Kebabian, Paul - AM1K.1
 Kedar, Dhruv - SM1F.1
 Keeler, Gordon - FF2B.2, FM2C.3
 Keene, David W. - FTh4C.7
 Kelaidis, Nikolaos - SM1H.3
 Kelaita, Yousef - FM4A.4
 Kelkar, Hrishikesh - FM2A.5
 Keller, Andrew - STh4G.3
 Keller, Kilian R. - STu4L.5
 Keller, Ursula - FF2C.1, FTh1M.8, JM1E.1, SF3E.3, STh3E.2
 Kemiche, Malik - STh1J.6
 Kennedy, Colin - SM1F.1
 Kennedy, MJ - ATu3P.5, SF2I.2
 Kerdiles, Sébastien - SF3H.2
 Kermene, Vincent - STh4L.2
 Kfir, Ofer - FF3M.2, FTh4C, FW4M.4
 Khabarova, Ksenia - SM4F.1
 Khader, Isaac H. - SM1F.1, STh3G.2, STh3G.3
 Khairallah, Saad - AW3I.5
 Khajavikhan, Mercedeh - FM1D.2, FTu3B.2, FW3D.1, FW4D.2, SF2H.1, STu3N.8, SW4N.1
 Khalid, Muhammad A. - AM4I.3
 Khalimananenko, Sergei - AM1I.6
 Khan, Emroz - JTh2A.19
 Khan, Mdshofiqulislam - SF3N.4
 Khan, Mohammad A. - JW2A.22
 Khan, Mohammad Wahiduzzaman - JTu2A.51
 Khan, Mohammed Zahed Mustafa - SM3N.5
 Khanolkar, Ankita - STu3L.1
 Kharas, Dave - SF3N.7
 Kharenko, D. S. - FTh3B.4
 Kharenko, Denis S. - SF1L.7
 Khatib, Omar - FTh4C.2, SF1E.3
 Khatonji, Manddeep - FM4D.2, FW3C.2, JTu2A.52
 Khilo, Anatol - SF3N.2, SM3J.5
 Khodabandehloo, Kendra - STh1L.2
 Khokhar, Ali - Ath3I.4, JTh2A.74, SW3J.5
 Khoram, Erfan - JF2F.4, JM3M.4
 Khosrowshahi, Amir - SF1N.6
 Khun, Sandra - FW3M.4
 Khurgin, Jacob - FM4D.6, FTh1C.1, FW3B.7, FW4B.6, JTu2A.100, STu4N.2
 Kiani, Khadijeh - STh3N.6
 Kibler, Bertrand - FF2D.7, SW3H.3
 Kiefer, Daniel - JTu2A.85
 Kiel, Frederik - JTu2A.47
 Kienberger, Reinhard - SF2G.1, SM4E.3
 Kiesewetter, Dietrich - FF3C.1
 Kifle, Esrom - STh1E.5
 Kilbane, Deirdre - FTh1C.7
 Kildishev, Alexander - FF2A.6, FM1M.5, FTh3C.2, JTh2A.119, JTh2A.40, JW2A.55, JW2A.58
 Kilic, Velat - JTu2A.100
 Killi, Alexander - JM3E.2
 Kim, Beom - FM2D.5
 Kim, Bok Young - STh3J.1
 Kim, Byung Soo - SW4G.7
 Kim, Changsu - FM4M.1
 Kim, Chanju - STh1J.5
 Kim, Chul Soo - SM2J.7
 Kim, Chulki - STu3F.2
 Kim, Dae Wook - AW3K.7
 Kim, Dae-Gon - SM4O.2
 Kim, Dohun - ATu3I.6, FM2D.3, FM2D.4
 Kim, Dong E. - JM2E.4
 Kim, Donggyu - SM2F.3
 Kim, H - SW3N.3
 Kim, Hee Yeoun - JW2A.111
 Kim, Heeju - JTu2A.43
 Kim, Hoil - FM2D.4
 Kim, Hyo Jung - ATu4I.1
 Kim, Hyung Taek - STu3E.2
 Kim, Inki - FF2B.7
 Kim, Jaeyoun - AW3I.3, SM2O.2
 Kim, Jehyun - FM2D.4
 Kim, Je-Hyung - FM1M.3, JTu2A.43
 Kim, Jeong Dong - JTh2A.31
 Kim, Jin - STh4O.4
 Kim, Jong-Hoi - JTu2A.43
 Kim, Jun Sung - FM2D.4
 Kim, Jungwon - JTh2A.103, STh3G.6, STh3G.7, SW3G.6
 Kim, Kap-Joong - JTu2A.43
 Kim, Ki-Yong - FTh1M.3, STh3F.4, STu3F.5
 Kim, Kyoungwan - STh4O.4
 Kim, Kyu Young - JTu2A.43
 Kim, Kyujung - JTu2A.7
 Kim, Mijin - SM2J.7
 Kim, Minhyuk - FM2A.7, FM2A.8
 Kim, Munho - JTh2A.31
 Kim, Philip - AM3K.3, FM3C.2
 Kim, Richard H. - FM3D.7, FW4M.5
 Kim, Samuel - SF3N.7
 Kim, Sejeong - SF1J.3, STh3O.2
 Kim, Seung-Woo - JTh2A.109, STh3G.4, STh4G.4, SW4G.7
 Kim, Soojung - JTu2A.7
 Kim, Sungil - JTu2A.11
 Kim, Tae Hyun - JW2A.111
 Kim, Taeyeon - JTu2A.7
 Kim, YeongJae - AW3I.2, JW2A.6
 Kim, Young-Su - FM2M.4, JTu2A.35, JTu2A.45
 Kim, Yoomin - FM2D.4
 Kim, Yoon-Ho - JTu2A.45
 Kim, Yosep - JTu2A.45
 Kim, Young Duck - SM1O.2
 Kim, Young-Jin - JTh2A.109, SM2H.3, SM4F.2, STh3G.4, SW4G.7
 Kimel, Alexey - FTh1B.2
 Kimura, Akio - FTh1B.4
 Kimura, Shota - SF3E.5
 Kindem, Jonathan - FM1A.4, FM1A.6, FM1A.7, JTu2A.26
 Kinezuka, Yoshinori - SF3G.4
 King, Gavin G. - FM1A.5
 Kinzel, Edward - JTu2A.53, SF2G
 Kip, Detlef - FTh4B.2
 Kippenberg, Tobias J. - FF1D.1, FF1D.2, FF1D.5, FF2D.1, FM1A.1, SM2N.1, SM3G.3, STh1F.4, STh1G.7, STh1H.3, STh4J.2, STu3J.2, STu3J.3, STu3J.4, SW4G.5
 Kipshidze, Gela - SM3N.7
 Kira, Mackillo - FW3B.6, FW3M, JTh4F.2, JTu4M.2
 Kirch, J D. - SW3N.3
 Kirchmann, Patrick S. - FM4M.6
 Kirchner, Mathew - JM3E.4
 Kirdoda, Jaroslav - FF1A.4
 Kis, Andras - FW3M.4
 Kishen, Saurabh - JTh2A.22
 Kiss, Balint - STh3E.1, SW3E.6
 Kita, Shota - SM2J.6
 Kita, Tomohiro - STh1H.6
 Kitaura, Ryo - SF2G.2
 Kitching, John - SM3F.5, STu4G.2, STu4G.4
 Kivshar, Yuri S. - AM3K.4, FF3B.6, FM1B.4, FM2C.4, FM2C.6, FTh4C.6, FW4B.3, FW4B.4, JTh2A.117, SF3J.1, SW3F.5
 Klamkin, Jonathan - JTu2A.82, SF3N.6
 Klas, Robert - SF1E.2
 Klauck, Friederike - FTu3B.3
 Klco, Natalie - FTh3A.6
 Klee, Anthony - SM4O.4
 Klein, Edwin J. - STu4N.4
 Klein, Thomas - AW4I.1
 Kleineberg, Ulf - SF3I.3
 Kleiner, Jonas - JM3E.2
 Kleinert, Sven - SW3E.1
 Klejs, Frederik - SW3H.4
 Klem, John F. - AM3K.5
 Klemke, Nicolai - FF2C.2, SW3E.7
 Klimczak, Mariusz - SM3L.5, STh1L.5
 Kling, Matthias - FF2C.5
 Kling, Rainer - ATu4I.1
 Klingebiel, Sandro - SM4E.3
 klitis, charalambos - FW3B.3
 Kmetec, Jeff - JTu2A.95
 Knauer, Sebastian - SM2F.2
 Knights, Andrew P. - STh3N.6
 Knipfer, B - SW3N.3
 Knoerzer, Markus - FW3B.4, STh1H.7
 Knorr, Andreas - FW3M.4
 Knox, Wayne H. - ATu3K.1, AW4I.5
 Knurr, Jonas - FF2C.5
 Knuthson, Erin - FTh1M.1
 Ko, Wing - JTh2A.92
 Ko, Young-Ho - JTu2A.43
 Kobayashi, Hisataka - AM1I.2
 Kobayashi, Yohei - SF3E.5, SM3L.2
 Kober, Edward - JW2A.28
 Koblmüller, Gregor - FW3C.7, SM4J.6
 Koch, Stephan W. - FW3B.6, JTh4F.2, JTu4M.2
 Kochergina, Tatiana A. - SM4E.2
 Kodama, Takahiro - JTh2A.77, JTh2A.79
 Kodigala, Ashok - SM3N.1, STh4N.6
 Koehler, Johannes R. - SF1E.6
 Koenderink, Femius - FTh3M.2, SF3J.3
 Koeth, Johannes - AW3P.1
 Koh, Weon-kyu - JTu2A.77
 Kohn, Rudolph - FM2A
 Koike-Akino, Toshiaki - SW4J.6
 Koilpillai, R David - JTh2A.83
 Kojima, Kazunobu - SM2G.1
 Kojima, Keisuke - SW4J.6
 Kokh, Konstantin A. - FTh1B.4
 Kolachevsky, Nikolai - SM4F.1
 Kolarczik, Mirco - FM3D.2, JW2A.24
 Kolesik, Miroslav - FM4M.2
 Koller, Silvio - SM1F.3
 Komissarenko, Philipp - FM2C.6
 Komm, Pavel - STh1E.2
 Kong, Lingjie - JW2A.105
 König, Tobias A. - JW2A.119
 Kono, Junichiro - FM4D.1, STh4H.5
 Kononchuk, Rodion - JTh2A.36
 Koots, Rian - FW3M.5
 Koppens, Frank H. - FF3D.2, FTu3C.3
 Korai Baloch, Umair Ahmed - SW3H.5
 Kordts, Arne - SM3G.3
 Koresawa, Hidenori - JTh2A.101
 Kormin, Dmitrii - FF1C.3
 Korn, Tobias - FW3M.1, JTu4M.2
 Kornblum, Lior - SM2O.3
 Kornyshev, Alexei - FM3C.5
 Korolkov, Viktor P. - SM3H.1
 Korolov, Anastasia - FTh1M.3
 Kort-Kamp, Wilton J. - FTu4D.2
 Kosar, Sofia - JW2A.25
 Koshelev, Kirill - FM2C.4, FTh4C.6, FW4B.3, JTh2A.117, SW3F.5
 Kosugi, Yuji - JTh2A.48
 Kotlicki, Omer - SM1L.2
 Kotov, Nicholas - FF2B.1
 Kottos, Tsampikos - JM2B.4
 Koulas-Simos, Aris - FM3D.2
 Koutsares, Samantha R. - JTh2A.20
 Kovacev, Milutin - JTh2A.5
 Kovalev, Sergey - JTu2A.101, STu4F.6
 Kowligy, Abijith - SF1E.4, SF3H.3, STh4E.5
 Kowzan, Grzegorz - JTh2A.111
 Koyama, Fumio - SM4N.3, SM4N.4
 Koyama, Takaaki - SM1J.7
 Kozak, Dmitry - JTh2A.53, SF2I.1
 Kozak, Tomasz - SF3I.5
 Kozawa, Yuichi - FTh4B.5
 Kraai, Joseph - ATu3K.7, JW2A.77
 Krachmalnicoff, Valentina - FTh3C.1
 Kraft, Alexander - FTh3A.2
 Kränkel, Christian - SF3E.4, STh3F.5
 Krasnok, Aleksandr - FW4D.5
 Krasnoperov, Lev N. - AM1K.4
 Krausz, Ferenc - AF3K.5, STh4E.4
 Kravchenko, Ivan - FF1B.7, FW4B.4
 Kravtsov, Vasily - FM2C.1
 Krebs, Olivier - FM3A.2
 Kreisel, Christian - JTu2A.12
 Krekler, Tobias - FTu4D.3
 Kremer, Mark - FF1F.5, FM1C.6, FM4B.2, FM4B.3, FTu4B.3, FW3D.5, FW3D.8
 Kriehn, Gregory - FTh1B.3
 Krishna, Sanjay - STh4O.4
 Krishnaswamy, Harish - SM1N.6
 Kristensen, Anders - FTh3M.8, JTu2A.109
 Kristina, Frizyuk - FM2C.6
 Krizsán, Gergö - SW4E.5
 Krogen, Peter - STh3E.5
 Krolkowski, Wieslaw - STh3J.5
 Kropp, Jaron A. - FF3M.4
 Krotkov, Daniel - FM3D.8
 Krötz, Peter - SM4E.3
 Krovj, Hari - FTh4A.5
 Kruk, Sergey S. - FM1B.4, FM2C.4, FW4B.3, FW4B.4, SW3F.5
 Krupa, Katarzyna - FTh3B.4, STh4L.1, STh4L.2
 Krushelnick, Karl - FTh1M.3, JTh2A.6
 Krysa, Andrey - SM3N.6
 Krzempek, Karol - AF2K.8
 Krzywinski, Jacek - SF3I.2
 Ku, Pei-Cheng - AM4I.4, STh4O.1
 Kuan, Chieh-Hsiung - JTu2A.16
 Kucernak, Anthony - FM3C.5
 Kudelin, Igor - AM1I.6, STu3L.7
 Kudlinski, Alexandre - FF2D.4, FTh3B.5
 Kudyshin, Zhaxylyk A. - FTh3C.2, JW2A.55, JW2A.58
 Kues, Michael - FTh1A.4, FW3B.3, JTu2A.41
 Kuhl, Ulrich - FTu3D.6, FTu4B.2
 Kühmayer, Matthias - FTu3D.6, FTu4B.2
 Kuhn, Tilmann - FM3D.4
 Kühnreich, Benjamin - Ath4K.4
 Kuipers, L. - JM2B.2
 Kumar Vinod, Abhinav - SM1O.5, STh4J.5
 Kumar, Aashish - STh4O.5
 Kumar, Abhishek - JTu2A.99
 Kumar, Prem - FTh3D.1
 Kumar, Rakesh Ranjan - STh1H.2
 Kumar, Randhir - FF3B.4
 Kumar, Resmi R. - SW3L.3
 Kumar, Sushil - AM4I.2, SW3N.5, SW4F.3
 Kumar, varun - JW2A.1
 Kumkar, Malte - JM3E.2
 Kung, Bo-Han - JTu2A.16
 Kuo, Hao-Chung - FTh4M.2, JTu2A.115, SF2O.2, SM1H.6, STh3O.5
 Kuo, Hsin Yu - FTh3M.3

- Kuo, Paulina S.- FTh1D.5, JTu2A.42
 Kuo, Wei-Hung - SF2O.2
 K pper, Jochen - JTu4M.5
 Kural, Comert - STu4H.2
 Kuramochi, Eiichi - JTh2A.58, JW3A.5, SM1O, SM2J.6, SM4J.3
 Kurczveil, Geza - STu4J.5
 Kurihara, Takayuki - FM3D.6
 Kurman, Yaniv - FF3M.6, FTu3C.3
 Kurosaka, Yoshitaka - SM4N.2
 Kurt, Hamza - SF3J.7
 Kurtsiefer, Christian - FM2A.3, FM4C.8, JTu2A.24
 Kurucz, M t  - SW3E.6
 Kuse, Naoya - SF2I.5, SF2I.7, SW4F.6, SW4G.4
 Kushnir, Kateryna - JW2A.26
 Kusumi, Yugo - STu3L.3, SW3G.4
 Kuzmenko, Kateryna - FF1A.4
 Kuznetsov, Alexey G. - STh4L.4
 Kuzyk, Mark C. - JW4A.5
 Kvit, Alexander - JTh2A.31
 Kwan, Ching Chi - STu3H.1
 Kwek, Leong Chuan - JTu2A.124
 Kwok, Samuel - SM2H.3
 Kwon, Dohyeon - JTh2A.103
 Kwon, Heungdong - SF2O.5
 Kwon, Hoyeong - FTh3M.2
 Kwon, Hyoungan - FTh3M.1
 Kwon, Junyoung - SM1O.2
 Kwon, Ojoon - JTh2A.2
 Kwon, Taeg Yong - JW2A.111
 Kwong, Dim Lee - FF2D.2, SM1F.5, STh3J.4, STh4J.4, SW4H.4
 Kymissis, Ioannis - SM1O.2
- L**
 Labaye, Fran ois - SF3E.4
 Labouesse, Simon - STh4L.5
 Lacava, Cosimo - FW3B.3, JTh2A.74, SW3H.5
 Ladisch, Michael - ATu3K.4
 L egsgaard, Jesper - SF3H.2
 Lagally, Max - STh4O.3
 Lagoudakis, Konstantinos - FF3A.1, FM4A.4
 Lagutchev, Alexei - FM1M.6
 Laha, Michael - JM3E.1
 Lai, Yu-Hung - FTu3B.1
 Laich, Andrew - Ath4K.6
 Laing, Anthony - JTu2A.124, SM2F.2
 Lake, David - SF1J.3, STh1H.4
 Lakhotia, Harshit - FTh1B.1
 Lakomy, Katherine - SM4N.5
 Laleyan, David - SF2I.6
 Lam, Ping Koy - FTh4D.3
 Lamard, Laurent - SW3L.6
 Lamas-Linares, Antia - FM4C.8
 Lamb, Erin S. - SF3H.1
 Lamb, Thorsten - SF3I.5
 Lambropoulos, John C. - ATu3I.2
 Lamperti, Marco - Ath3K.2
 Lampin, Jean-Fran ois - ATu3K.6, JTu2A.102
 Lamy, Manon - FF2D.7
 lan, hui - JW2A.14
 Lan, Mingying - STh3L.5
 Lan, Pengfei - SW4E.7
 Lan, Shau-Yu - STh4G
 Lanco, Loic - FM1M.1, FM3A.2
 Landais, Pascal - SM4N.6, STu4N.5
 Lang, Lukas - FM2C.6, SF3E.3
 Lang, Tino - STu4E.4
 Lange, Christoph - FTh1B.2, FTh1B.4
 Langer, Fabian - FTh1B.4, JTh4F.2, JTu4M.2
 Langrock, Carsten - SM3O.2
 Lanius, Martin - FTh4C.3
- Laporta, Paolo - Ath3K.2, SF2L.1
 Larionov, Mikhail - ATu3I.5
 Larisch, Gunter - SM4N.7
 Laroche, Sophie - STh3H.2
 Larose, Maxence - SF2L.3
 Lascola, Kevin - STh4H.3
 Laskar, Arif W. - FM2A.4
 Lasmstein, Josh - AM1I.4
 Lassen, Mikael - SW3L.6
 Lassiter, Maya - AW4I.2
 Lassonde, Philippe - FF3C.6, JTh2A.2
 Lau, Kei May - STh3N.5, STu3N, STu3N.1
 Lau, Yong Chang - STu4F.6
 Laudenbach, Fabian - FTh1D.6
 Laurell, Fredrik - SF1H.4, SM1L.5, SM2L.5
 Lavancier, M lanie - ATu3K.6
 Lavastre, Eric - JTu2A.65
 Lavenu, Loic - JM1E.5, JW2A.73
 Lavery, Martin P. - Ath1I.5
 Lavoie, Jonathan - FTh4D.6
 Lavoute, L. - STh4L.2
 Law, Daniel - Ath1I
 Lawall, John - FM1M.7
 Lawrie, Benjamin - JTu2A.21, JW2A.117, JW3A.6
 Le Blanc, Catherine - JM2E.2
 Le Gallo, Manuel - SM2J.2
 Leaird, Daniel E. - Ath1K.4, FTh1A.2, JTu3A.3, JTu3A.5, SF2N.8
 Leavitt, Richard - FM1M.3
 Lebas, Nathalie - JM2E.2
 Lebat, Vincent - Ath3K.1
 Leblanc, Adrien - FF3C.6, JTh2A.2
 Lebris, Arthur - STh1O.3
 Lebrun, Sylvie - JTh2A.102
 Leburn, Christopher - AM2K.4
 Lecaplain, Caroline - JTh2A.106, STh1G.5, SW4L.1, SW4L.6
 Lecomte, Steve - AF2K.2, STh4J.1, STu3J.3, STu4G.3
 Lee, Byoung-ho - AM4K.2
 Lee, Chang-Min - FM1M.3
 Lee, Changsoo - FM2D.3
 Lee, Cheng-Che - JTu2A.16
 Lee, Chengkuo - SW3F.6
 Lee, Chieh-Hsun - JTh2A.75
 Lee, Chul-Ho - FM2D.4
 Lee, Chun-Fu - JTu2A.115
 Lee, Donghan - JTu2A.43
 Lee, Dong-Wook - AW3I.2
 Lee, Eric - SF3J.5
 Lee, Eui Su - STu3F.7
 Lee, Gil Ju - AW3I.2, FTu4D.5, JW2A.16
 Lee, Gun-Yeal - AM4K.2
 Lee, Gwan-Hyoung - SM1O.2
 Lee, Hansuek - SM4O.2
 Lee, Hojin - FF2B.6, FM2D.5
 Lee, Hwang Woon - STu3E.2
 Lee, Hwaseob - FTu4B.7
 Lee, Hyeon Jeong - ATu3K.3
 Lee, Hyun Hwi - ATu4I.1
 Lee, Il-Min - STu3F.7
 Lee, Jaehyun - JTh2A.109
 Lee, Jane - AW4K.6
 Lee, Jekwan - FM2D.3, FM2D.4
 Lee, Jianwei - FM4C.8
 Lee, Jongmin - STh4N.6
 Lee, Keunwoo - JTh2A.109
 Lee, Kwang Hong - STh4O.2, STu4J.2
 Lee, Maurice Y. - AM4I.5
 Lee, Po-Tsung - JTu2A.115
 Lee, Ray-Kuang - JTu2A.38
 Lee, Sang-Bum - JW2A.111
 Lee, Sang-Hun - STu3F.2
 Lee, Sang-Yun - FM2M.4, JTu2A.35, JTu2A.45
 Lee, Sebok - JW2A.27
- Lee, Seong Ku - STu3E.2
 Lee, Seunghun - JTu2A.7
 Lee, Sooun - FM2D.4
 Lee, Tony - JM3E.1
 Lee, Valentina - FTh1B.3
 Lee, Wonwoo - FF2B.6
 Lee, Woojun - FM2A.7
 Lee, Ya-Ju - SM3N.2
 Lee, Yeon - JM2E.4
 Lee, Yong-Hee - SM4O.2
 Lee, Yoo Seung - FTh1A.3, FTh1D.6
 Lee, Young-Pak - JW2A.11
 Leemans, Wim - SF3I.1, SM4E.5
 Leenheer, Andrew J. - JTu2A.96
 L gar , Fran ois - FF1C, FF3C.6, JTh2A.2, SW4E.1
 Lei, Dian - STu4J.2
 Lei, Jincheng - AW3I.4
 Lei, Mi - FM1A.6
 Lei, Pingping - SW3O.7
 Lei, Yuhao - ATu4I.4
 Lei, Zihui - JW2A.80
 Leibrandt, David - SM1F.1
 Leinse, Arne - STh3N.6
 Leisching, Patrick - Ath3K.2
 Leitao, Nathaniel - FM4A.6
 Leitenstorfer, Alfred - FM3D.4, FM3D.6, FTh3C.6, FW4M.3, SF2E.2, STu4L.5
 Leitgeb, Erich - SM2G.2
 Leitis, Aleksandrs - SF3J.1
 Lekavicius, Ignas - JW3A.3
 Lemaitre, Aristide - FM1M.1, FM3A.2
 Lemke, Nathan D. - STh3G.1
 Lemmer, Uli - JTu2A.71, SF2J.2
 Lemons, Randy A. - SF3I.2, SW4E.6
 Lendl, Bernhard - STh1F.7
 Leng, Haixu - FF3M.4
 Leng, Jinyong - JW2A.106
 Leng, Yuxin - STu3N.7
 Lennon, Joeseeph - STh1H.1
 Lentine, Anthony - STh4N.6
 Lenzini, Francesco - FTh4D.3
 Leo, F. - SM3O.3
 L on Torres, Josu  R. - FF3D.6
 Leonard, Jason - JW2A.34
 Leopardi, Holly F. - SM1F.1, SW4G.1
 Lereah, Yossi - FTh4M.7
 Leshin, Jason - FTu3B.2, FW3D.1
 Leszczynski, Mike - AW3P.4
 Letscher, Fabian - FM4B.1
 Lett, Paul D. - JTu2A.123, JTu2A.37
 Leuthold, Juerg - FW3C.1, STh3H.4, STh4N.4, SW3F.7
 Leuthold, J rg - SF3N.1
 Levanon, Assaf - AF2K.6
 Levanon, Nadav - SM1N.2
 Levchenko, Andrey E. - SM4E.2
 Leventoux, Yann - STh4L.2
 Levi, Filippo - SM1F.3
 Levi, Ofer - SW3L.4
 Levy, Uriel - FF3M.5, FTh1C.3, FTh3M.8, FTh4M.4, JTh2A.49, JTu2A.109, JTu2A.20, JTu2A.39, JW2A.110, JW2A.114, SM3F.4
 Leykam, Daniel - FM1B.4
 Leyva, Francisco - AM1I.6
 Lezec, Henri - AM3K.2, FM3C.3, FM3C.7, FW3C.1
 Lezius, Matthias - SM1F.2
 Lhuillier, J r my - STh1J.6
 Li, Baichang - FTu3C.2
 Li, Baohua - AW3P.3, STh4O.6, STu3N.3
 Li, Bobo - SF1O.4
 Li, Bowen - STu4L.6
 Li, Can - JTu2A.89
 Li, Chao - JTh2A.73
 Li, Chen - SF3I.4
- Li, Chenglin - AM3I.6
 Li, Chenyu - Ath1I.7
 Li, Chi - JTh2A.59
 Li, Claire - FTh3C.1
 Li, Daiyu - JTh2A.56
 Li, Dongdong - STh1O.4
 Li, Dong-Dong - FM4C.5
 Li, Dongfang - FW3C.4
 Li, Dong-Ying - JW2A.19
 Li, Erwen - STh3H.3, STh3N.4
 Li, Fan - SW4O.3
 Li, Feng - JW2A.102, STu4L.7
 Li, Fengzhi - FM4C.1
 Li, Guifang - AM3I.2, SM1L.1
 Li, Guo-Chun - FM4C.5
 Li, Guoqing - STu4F.7
 Li, Hang - JTh2A.14
 Li, Hao - FM4C.3, JTu2A.33
 Li, Hebin - FW4M.6, JTu2A.25
 Li, Hongquan - SW4H.1
 Li, Hongtao - JTu2A.90, SW4N.7
 Li, Huan - STh1N.6
 Li, Huizi - JW2A.89
 Li, Jake - AW3K.1
 Li, Jia Qi - STh3L.1
 Li, Jiachen - JTh2A.61
 Li, Jiahian - FW4M.3, FM3C.2
 Li, Jialin - JTh2A.9
 Li, Jiamin - FTh3D.5
 Li, Jiaming - JTu2A.117
 Li, Junyu - JTu2A.119
 Li, Jianqiang - AF2K.5
 Li, Jiawen - STh3L.3
 Li, Jin - JW2A.85
 Li, Jingsang - SM2O.4
 Li, Jun - JTh2A.31, JW2A.106
 Li, Junhui - STh3L.5
 Li, Juntao - FF2B.5
 Li, Junyu - FM3C.6
 Li, Kuang-Hui - SF2O.1
 Li, Kun - FTh4M.5
 Li, Li - FM4C.3
 Li, Liangye - ATu4K.7
 li, long - JTu2A.57, JTu2A.67, SF2N.3, SM1J.5, SM1N.5
 Li, Michael - JTu2A.107
 Li, Mingxiao - SF2H.2, SF2J.5, STh1J.2
 Li, Mo - STh1N.6
 Li, Nanxi - Ath4I.2, JTh2A.34, STh1O.4, SW4G.6
 Li, Nathan - AM1K.2
 Li, Qian - JW2A.104, SF1M.2, SM2H.1
 Li, Qiang - AW3I.3, SM2O.2, STu3N.1
 Li, Qing - FM1M.7, JTu2A.86, SM3J.4
 Li, Qiu - JTu2A.118
 Li, Renkai - JTh4F.1, STh3F.2
 li, runmin - JTh2A.103, STh1G.6
 Li, Ruoping - AM3K.3
 Li, Ruxin - STu3E.1, STu3N.7
 Li, Shangbin - SM2G.6
 Li, Sheng - JTh2A.56
 Li, Shuang-Lin - STh3G.5
 Li, Si-Ao - JTh2A.80
 Li, Siqi - FF2C.5
 Li, Tao - FTh3M.3
 Li, TENGFEI - FW3B.7
 Li, Tiantian - FTu4B.7, SM1J.2
 Li, Ting - JW2A.104, SM2H.1
 Li, Weijian - FM3C.1
 Li, Wenhao - FW3C.4
 Li, Wenkai - FTh1B.5, JW2A.40
 Li, Wensong - SM4L.2
 Li, Wenzhe - Ath1K.7
 Li, Xia - JTu2A.91
 Li, Xiang - STu4O.1
 Li, Xiaohang - SF2O.1
 Li, Xiaoqin - FW3M.3

- Li, Xiaoying - FTh3D.5
 Li, Xiao-Zhou - SW3G.6
 Li, Xin - AW3I.6
 Li, Xinwan - JTh2A.73
 Li, Xinwei - FM4D.1
 Li, Xiuling - JTh2A.31, STh3O.5
 Li, Xuan - JTu2A.14
 Li, Xuepei - JW2A.9
 Li, Yajie - JTh2A.72, JTu2A.79
 Li, Yan - JTh2A.89, SF3G.6
 Li, Yang - FM4C.1
 Li, Yanlong - JTh2A.78
 Li, Yanpeng - JW2A.100, JW2A.23
 Li, Yaqian - JTh2A.64
 Li, Yigang - FTh4B.7
 Li, Yihan - SW4F.6
 Li, Yihong - SF1M.2
 Li, Yongzhuo - FM4D.4, STh1J.7, STh3O.1
 Li, Yu - AW4K.5, JTh2A.61, SF3J.6, STh1O.4
 Li, Yuan - Ath1K.7
 Li, Yuanji - JTu2A.31
 li, yuepeng - STh1G.6
 Li, Yulong - SF1O.2
 Li, Zhaohui - SW4O.3
 Li, Zheng-Da - FTh4A.6
 Li, Zheng-Ping - SM1N.1
 Li, Zhengxuan - SM1G.2
 Li, Zhengyong - JTu2A.63
 Li, Zhengyu - JTu2A.30
 Li, Zhibo - SM3N.6
 Li, Zhili - JW2A.45
 Li, Zhitong - SW4N.2
 Li, Zidong - STh3O.4
 Lian, Fuqiang - AW3I.6
 Liang, An-Yuan - JTu2A.64
 Liang, Bor-Wei - JTu2A.16
 Liang, Di - SM4J.7, STu4J.5
 Liang, Guozhen - FTh4C.5, STh3H.1
 Liang, Haitao - AM3I.5
 Liang, Hanxiao - SF2H.2, SF2J.5, STh1J.2
 Liang, Hao - FM4C.3
 Liang, Haowen - FF2B.5
 Liang, Houkun - FTh1B.5, JW2A.40
 Liang, Jian-Wei - Ath1I.2, Ath1I.3
 Liang, Kai-Ling - SF2O.2
 Liang, Qingqing - FTh1M.2
 Liang, Sijing - JW2A.44
 Liang, Wei - STh4G.4
 Liang, Xiaoyan - STu3E.1
 Liang, Xinli - FTh4B.1
 Liang, Yan - JTu2A.40
 Liang, Yi - AM1I.4
 Liang, Yong - SW4N.4
 Liao, Chen-Ting - FF2C.6
 Liao, Meisong - JTu2A.91
 Liao, Peicheng - SF2N.3, SM3G.3
 Liao, Ruoyu - SF1H.2, SF3E.1, STh3L.6, SW3E.5
 Liao, Shengkai - FM4C.1
 Liberale, Carlo - JTh2A.51
 Lidorikis, Elefterios - SM1H.3
 Lidsky, David - JTu2A.78
 Liebig, Carl - SF2G.4, SM4L.4, STh4H
 Liehl, Andreas - SF2E.2, STu4L.5
 Lifshitz, Erga - AF2K.6
 Lihachev, Grigory - STh1H.3
 LiKamWa, Patrick - FTu3B.2, STu3N.8
 Likhachev, Mikhail - SM4E.2, SM4L.1
 Likhov, Vladislav - STh1E.6
 Lilach, Yigal - JTh2A.45
 Lilje, Lothar - JTu2A.1
 Lillieholm, Mads - SW3H.4
 Lim, JinKang - SF2H.6, STh4G.4
 Lim, Kang Jie - JW2A.89
 Lim, Serene Huiting - JW2A.89
 Limberopoulos, Nicholaos - JTh2A.36
 Limpert, Jens - SF1E.2, SM3L.1, STh4E.4
 Lin, Charles - SF1J.2
 Lin, Chen-An - SM1H.6
 Lin, Chien-Chung - FTh4M.2, SF2O.2
 Lin, Chii-Dong - FM4M.4
 Lin, Chungwei - SW4J.6
 Lin, Ding-Lun - Ath1I.4
 Lin, Feng - JW2A.118
 Lin, Haonan - ATu3K.3
 Lin, Hsiang-Ting - SF3J.4, SM1H.6
 lin, jin - FM4C.1
 Lin, Jinpu - JTh2A.6
 Lin, Jintian - JTu2A.49
 Lin, Kai-Hsiang - SM4G.3
 Lin, Lih Y.- JTu2A.113
 Lin, Linhan - FTh3C.4, SM1H.2
 Lin, Ming-Fu - FF2C.5
 Lin, Ming-Wei - JTu2A.64
 Lin, Qian - FTu3B.4, JM3B.2
 Lin, Qiang - JTh2A.115, JTu3A.2, SF2H.2, SF2J.5, SM2J.5, STh1J.2
 Lin, Qunying - SF3J.6, STh1O.4
 Lin, Ren Jie - FTh3M.3
 Lin, Sheng-Xiang - JW2A.112
 Lin, Sheng-Yang - SM4G.5
 Lin, Shuai - JTh4F.5
 Lin, Stephen - SM3J.7
 Lin, Tong - SF3H.6, STu3J.5
 Lin, Tzu-Neng - JTu2A.112
 Lin, Wei - AM3I.6
 Lin, Wenbo - SW4J.4
 Lin, Xiao - FTh4M.8
 Lin, Xing - AM2K.3, SF1N.2
 Lin, Y. C. - STh3E.4
 Lin, Yiding - STh4O.2
 Lin, Ying - STh1O.4
 Lin, Zhongjin - JW2A.57
 Lin, Zin - SF1H.7, SW4J.8
 Lind, Alexander - SF1E.4, SF3H.3, STh4E.5
 Lindberg, D - SW3N.3
 Lindberg, Robert - SM1L.5
 Linden, Stefan - FM4B.1
 Lindenberger, Aaron - JTh4F.1, JTh4F.4, STu4F.7
 Lindlein, Norbert - JTh2A.105
 Lindner, Jürgen - STu4F.6
 Lindner, Netanel H.- FTu3D.5
 Lindsay, Lucas - JW3A.6
 Ling, Alexander - JTu2A.36
 Ling, Jingwei - SF2H.2, SF2J.5, STh1J.2
 Ling, Yi-Chun - FTu4D.7
 Lingaraju, Navin B.- FTh1A.2, JTu3A.5
 Lingley, Zachary - SW3N.3
 Lingnau, Benjamin - FM3D.2
 Linn, A. G.- STu4F.1
 Lipatov, Denis - SM4E.2, SM4L.1
 Lipphardt, Burghard - JTh2A.112
 Lippmann, Jan F.- FW4M.3
 Lipson, Michal - FM1D.4, FM1D.6, FTu3C.2, FW4D.4, JW2A.82, SF1J.7, SF3H.4, SF3H.6, SF3N.5, SM1N.6, SM2O.6, SM3J.6, STh3H.1, STh3J.1, STu3J.5
 Lisak, Daniel - JTh2A.111
 Liscidini, Marco - FM1D.5, FTh1D
 Lisdat, Christian - SM1F.3
 Lita, Adriana - FF1A.3, FF1A.6, FTh4D.6
 Little, Brent - FTh1A.4, SF2N.2, SF2N.4
 Littlejohns, Callum - STu4O.1
 Litvinova, Karina S.- AM1I.6
 Liu, Ai Qun - JTu2A.124
 Liu, Albert - FM3D.5
 Liu, Baiquan - JTu2A.77
 Liu, Bo - JTh2A.80, SF3L.7
 Liu, Bohao - Ath1K.4
 Liu, Changjiang - FM4D.7
 Liu, Changxu - FF3B.6
 liu, che-yu - STh3O.5
 Liu, Chongyang - STu4O.1
 Liu, Cong - FF1B.3, FW4B.5, JTu2A.57, JTu2A.67, SM1J.5, SM1N.5
 Liu, Deming - ATu4K.7, JW2A.100, JW2A.91, STu3L.2, SW4O.1
 Liu, Dianjing - JF2F.4, JM3M.4
 Liu, Dong - JTh2A.31
 Liu, Dongjue - FTh4M.8
 Liu, Dongxia - Ath1I.3
 Liu, Fei - JTu2A.14
 Liu, Feifei - JTh2A.11
 Liu, Feng - SW4J.1
 Liu, Fu - SF1M.3
 Liu, Gengchen - SM3G.2
 Liu, Guangyao - JTu2A.76
 Liu, Haifeng - SF3L.7
 Liu, Hailong - FM2C.7, SM1J.6
 Liu, Han - FW3B.5, SF3E.7
 Liu, Hao - STh3J.4, STh4J.4, SW4H.4
 Liu, Hongli - SM1F.6
 Liu, Hui - FM4C.3
 Liu, Jheng-Jie - Ath1I.4
 Liu, Jianhong - FM4C.5
 Liu, Jie - FF3C.3, SM2L.4
 LIU, Jietao - JTu2A.10
 Liu, Jifeng - AW3P.3, STu3N.3
 Liu, Jin - FM1M.7
 Liu, Jui-Nung - JW2A.61
 Liu, Jun - SF2L.2
 Liu, Junqiu - FF1D.5, FF2D.1, STh1G.7, STh1H.3, STh4J.2, STu3J.2, STu3J.3, STu3J.4
 Liu, Kai - JW2A.95
 Liu, Ke - Ath1K.6
 Liu, Keng-Ku - JW2A.61
 Liu, Kui - SM1F.6
 Liu, Kun - ATu4I.6, FTh1B.5, JW2A.40
 Liu, Lei - JTh2A.42
 Liu, Linbo - AM3I.5
 Liu, Lipu - SF3G.6
 Liu, Li-Zheng - FTh4A.6
 Liu, Long - SW4O.3
 Liu, Meizhong - JW2A.95
 Liu, Mingkai - FF1B.4, FW4D.7, SF3J.1
 Liu, Nai-Le - FM4C.3
 Liu, Qingwen - AF1K.2, JW2A.101
 Liu, Ren-Bao - JW2A.53
 Liu, Sheng - FF2B.2, FM2C.3
 Liu, Shih-Chia - JTh2A.31
 Liu, Shikang - JTu2A.111
 Liu, Shiqin - JTu2A.73
 Liu, Shuang - FF1C.5, JTh2A.56
 Liu, Shunfa - FM1M.7
 Liu, Songtao - ATu3P.5
 Liu, Tairan - AM2I.6, ATu4K.2, JM3M.5, JTu2A.5
 Liu, Victor - SW4J.8
 Liu, Wei - SF3I.2, SW4E.6
 Liu, Weiping - SW4O.3
 Liu, Weiyue - FM4C.1
 Liu, Wu - SF3E.1
 Liu, Xiangming - SF1O.2
 Liu, Xianhe - SF2I.6
 Liu, Xiao - SW3H.1
 Liu, Xiaogang - FM2C.7
 Liu, Xiaojun - JTu2A.25
 Liu, Xiaoxu - ATu3I.3, ATu3I.4
 Liu, Xinyu - AM3I.5, Ath4I.4, SM4H.6
 Liu, Xu - JTu2A.33
 Liu, Yang - SF2N.7, SM4O.4, STh1J.4
 Liu, Yangyang - FW4M.2, SW4E.2
 Liu, Yaoran - FTh3C.4, SM2O.4
 Liu, Yaping - SM2L.4
 Liu, Yejing - SM1J.6
 Liu, Yi - FTh1M.2
 Liu, Yizhou - STh3E.5
 Liu, Yong - JTu2A.83
 Liu, Yonggang - SF1O.2
 Liu, Youhai - Ath1I.7, SM1H.5
 Liu, Yuan - SF3N.6, STh4J.5
 Liu, Yun - JW2A.120, STh4G.5
 Liu, Yunqi - JW2A.88, SF3L.6
 Liu, Yuzhou - FW3D.1
 Liu, Zhaoping - JW2A.118
 Liu, Zhaoxiang - FTh1M.5
 Liu, Zhe - FTh3D.2, SM4J.2
 Liu, Zhengzheng - STu3N.7
 Liu, Zhihe - JTu2A.40
 Liu, Zhoutian - JTh2A.43
 Liu, Zidi - JW2A.21
 Liverman, Spencer - SM2G.4
 Lloyd, Seth - FTh3A.3
 Lo Piparo, Nicolo - FTh4A.1
 Lo, Guoqiang - FTu4C.5, SF1J.4
 Lo, Hoi-Kwong - FM4C.3
 Lo, Hsiang-Yu - FTh3A.1
 Lo, Mu-Chieh - STu4O.2
 Lo, Yuhwa - STu4H.3
 Lobino, Mirko - FM1M, FTh4D.3, JTu2A.32
 Löchner, Franz J.- FW3B.1
 Lodahl, Peter - FTh3D.2
 Logan, Alan - SF1H.7
 Lohmann, Michael - FW4M.4
 Lohrmann, Alexander - JTu2A.36
 Loiko, Pavel - JTu2A.119, SF3E.6, STh1E.5
 Lomsadze, Bachana - SF1I.7
 Lonappan, Cejo K.- AF3K.6
 Loncar, Marko - FF2D.3, FM1M.3, FM4A.4, FTh1D.2, JW3A.4, SF2J.1, SM3O.1, SM3O.2, STu3O.2
 Lončar, Marko - SW3E.4
 London, Yosef - SM1N.2
 Long, Christopher - JTh2A.39
 Long, David - AM2K.2
 Longdell, Jevon J.- FM1A.5
 Longhi, Stefano - FM1B.3
 Longman, Andrew - FF1C.4
 Looser, Herbert - AM1K.3
 Loparo, Zachary - Ath4K.6
 Lopez Aviles, Helena E.- JW2A.103
 Lopez Galmiche, Gisela - FTu3B.2
 Lopez, Jano G.- JTu3A.1
 Lopez, John - ATu3I.7
 López, Josué - SF3N.7
 Lopez-Cortes, Daniel - SF3L.2
 Lopez-Morales, Gabriel - FF3A.3
 Lopez-Rios, Raymond - JTh2A.115
 Loranger, Sebastien - FTh1A.4
 Lordello, Thomas - Ath4I.4, SM4H.6
 Loreda, Juan Carlos - FM1M.1, FM3A.2
 Lorenz, Virginia O.- FM2A.6, FTh3D.4
 Lorenzon, Monica - JW2A.29
 Los, Johannes W.- FF1A.2
 Lott, James A.- SM4N.7
 Lou, Cibo - FTh4B.2
 Lougovski, Pavel - FF1F.3, FTh3A.6
 Lourduoss, Sebastian - SW4N.4
 Louwrens, Gerhard - STh1E.4
 Louwrens, Gerhardus - JW2A.50
 Lozano, Andres M.- SM4H.6
 Lu, Chang-Bin - FM4C.5
 Lu, Chih-Wei - AW4I.6
 Lu, Chuang - SM2N.5
 Lu, Chunhui - SM2G.6
 Lu, Dan - JTu2A.70, JTu2A.72, SM3N.8
 Lu, Faming - FM4M.1
 Lu, Guo-Wei - STh1N.7
 Lu, Hsuan-Hao - FF1F.3, FTh3A.6, JTu3A.5
 Lu, Jian - FM4M.6
 Lu, Jianfeng - STh3L.4
 Lu, Liangjun - JTh2A.42, STh4H.2
 Lu, Ling - FM4B.4
 Lu, Li-Syuan - SM3H.4

- Lu, Meng - SF3O.6
 Lu, Ruifeng - FM4M.4
 Lu, Tao - JTu2A.49
 Lu, Tien-Chang - JTu2A.81
 Lu, Wei - FF1C.5
 Lu, Xiyuan - JTu2A.86, SM3J.4, SM3O.6
 Lu, Yao - JTh2A.15, JTh2A.29, JTh2A.30
 Lu, Ying - JTh2A.90
 Lu, You-Cheng - JTh2A.32
 Lu, Zehuang - SM1F.6
 Lu, Zhiwei - JTu2A.59
 Luan, Enxiao - ATu4K.5
 Luan, Yilong - FM3D.7
 Lucas, Erwan - FF1D.1, FF1D.2, STh1H.3,
 STh4J.2, STu3J.2, STu3J.4, SW4G.5
 Luce, Jacques - JTu2A.65
 Lucero, Adrian - FTh1M.3, JTh2A.6
 Lucianetti, Antonio - JTu2A.119
 Lüdge, Kathy - FM3D.2, JW2A.24
 Ludlow, Andrew - SM1F.1, SW3G.7
 Ludwig, Arne - FTh3D.2
 Ludwig, Frank - SF3I.5
 Luiten, Andre - SM1F
 Luk, Ting S.- FTu4D.2, JTh2A.57
 Lukashchuk, Anton - FF2D.1
 Lukens, Joseph M.- FF1F.3, FTh3A.6,
 JTu3A.3, JTu3A.5, JTu4A.3
 Lukin, Daniil - FF3A.1, SM2F.6
 Lukin, Mikhail - JW3A.4
 Lumer, Yaakov - FM1C.4
 Lundeen, Jeff S.- FF3A.5
 Lung, Shaun - JTh2A.17
 Lunghi, Tommaso - FTh4D.2
 Luo, Bin - JTu2A.30
 Luo, Chih Wei - JTu2A.54
 Luo, Ciwei - FTu4C.5
 Luo, Guangzhen - JTh2A.72
 Luo, Haokun - JW2A.118
 Luo, Huiwen - JW2A.102
 Luo, Jie - STh4G.3
 Luo, Liang - FW4M.5, JTh4F.3
 Luo, Qiaoen - JTh2A.18
 Luo, Rui - SF2H.2, SF2J.5, STh1J.2
 Luo, Ruijie - JTh2A.78
 Luo, Yang - STu3F.1
 Luo, Yanhua - JW2A.107
 Luo, Yi - AM2K.3, ATu4K.2, ATu4K.3,
 JTu2A.90, SF1N.2, SW4N.7
 Luo, Yilin - AM2I.3, ATu4K.2
 Luo, Yiyang - JW2A.108
 Luo, Yu - FTh4M.8
 Luo, Yuqing - JW2A.105
 Luo, Zhouchen - FM3A.3
 Lüpken, Niklas - JTu2A.84
 Lüpken, Niklas M.- FF2D.5
 Lustig, Eran - FF3B.1, FTu4B.1, FW3D.2,
 FW3D.7
 Luther-Davies, Barry - FW4B.4, FF2D.8
 Lutman, Alberto - SF3I.2
 Lutton, Maxwell - AM2K.3
 Luxmoore, Isaac - JTh2A.26
 Lyakh, Arkadiy - Ath4K.6, AW3P.2
 Lyasota, Alexey - FTh3D.3
 Lynch, David - JW2A.11
 Lynch, Morgan H.- FF1F.6, FF3D.7,
 JTh2A.8
- M**
- M. Gilbertson, Adam - FTh3C.5
 Ma, Chunyang - STu3L.1
 Ma, Danhao - STh4O.2
 Ma, Eric Yue - STu4F.7
 Ma, Guangjin - FF1C.3, SF2E
 Ma, Jina - FTh4B.7
 Ma, Minglei - SM3J.7
 Ma, Pan - FF2D.8, FW3B.2, SF2N.5,
 SF2N.7, SM4O.5, STh1J.4
 Ma, Ping - SF3N.1, STh4N.4
 Ma, Qiang - JTu2A.111
 Ma, Ren-Min - FW4B.6
 Ma, Rui - STh3L.1
 Ma, Weichao - SW4N.7
 Ma, Xiangyu - JTu2A.18, SF3O.5
 Ma, Xuedan - FF3A.4
 Ma, Ye - FM3C.5
 Ma, Yuanyuan - JTu2A.62
 Ma, Yue - FF1C.5
 Ma, Yuxuan - SF1L.6
 Ma, Yuzhao - JW2A.2
 Ma, Zhanyu - JW2A.107
 Ma, Zhenqiang - JTh2A.31
 Ma, Zhi-Hao - FTh3A.5
 Ma, Zhizhen - JTh2A.45
 Maas, Deran - Ath4K.1
 Maayani, Shai - SF3L.5
 MacArthur, James - FF2C.5
 MacCabe, Gregory S.- STh4G.3
 MacDonald, Allan H.- FM2D.1
 MacFarlane, Ian - STu4J.3
 Machielse, Bartholomeus - JW3A.4
 Macpherson, Stuart - SF1O.3
 Maczewsky, Lukas - FM1C.6, FM4B.2,
 FTu4B.3, FW3D.8
 Madden, Stephen - FF2D.8, FW3B.2,
 SF2N.5, SF2N.7, SM4O.5, STh1J.4
 Madéo, Julien - FW3M.6, SF1O.3
 Madi, Mohammad - SF2J.4
 Madni, Asad M.- AF3K.6
 Maegawa, Satoru - ATu3I.3, ATu3I.4
 Mafi, Arash - SM4L.5
 Magden, Emir Salih - Ath4I.2, SW4G.6
 Magij, Eric - SM4O.5
 Magnanelli, Timothy J.- STu4F.4
 Mahallati, Sara - Ath4I.4
 Mahieu, Benoît - JM2E.5
 Mahler, Dylan H.- FTh4D.6
 Mahmood, Nasir - FF2B.7
 Mahmoud, Ashraf - SF3N.4
 Mahmoud, Mohamed - SF3N.4
 Mahro, Anna-Katharina - FTh1C.7
 Maier, Andreas R.- JM2E.3
 Maier, Sebastian - STh1H.1
 Maier, Stefan - FF2B.3, FM2C.2, FTh3C.5
 Mailis, Sakellaris - STh4H.6
 Mainz, Roland E.- FF2C.2, FF2C.3,
 SW4E.4
 Maisenbacher, Lothar - SM4F.1
 Maiti, Rishi - JTh2A.45
 Maitland, Calum - JW2A.39
 Maity, Partha - Ath1I.3
 Maiuri, Margherita - FW3M.4, FW3M.7
 Majumdar, Arka - FTh3M.4, JTh2A.47,
 SF1H.7, STh1N.5, STu4J.4
 Majumdar, Apratim - AF3K.1, AM4K.5,
 JTh2A.118
 Mak, Jesse - STu4N.4
 Makarova, Oksana - FM1M.5, FM1M.6
 Makio, Satoshi - JTu2A.106
 Makiyama, Takumi - FM2C.5
 Makowiecki, Amanda - SF1I.6
 Maksimenka, Raman - STh3E.1
 Malek, Stephanie C.- FF2A.3, FF2A.5,
 FM4M.7, FTh3M.5
 Maleki, Lute - STh4G.4
 Malic, Ermin - FW3M.1
 Malinauskas, Mangirdas - SF3J.7
 Malinowski, Marcin - JTu2A.88
 Malis, Oana - SF2O, STh4O
 Malkani, Arnav - FTh4C.4
 Malkiel, Itzik - FTu4C.3
 Malomed, Boris - STh4L.3
 Malyzhenkov, Alexander - JTh2A.91
 Man, Michael K.- SF1O.3
 Mancino, Luca - JW2A.116
 Mandal, Jyotirmoy - Ath1I.1
 Manek-Honninger, Inka - ATu3I.7
 Manfra, Michael - FM4D.1
 Manipatruni, Sasikanth - SF1N.6
 Manjappa, Manukumara - JTu2A.99,
 SW3F.6
 Mann, Sander - AM3K.5, JM2B.3
 Mannebach, Ehren - JTh4F.1
 Manolis, Athanasios - JTh2A.94
 Manschwetus, Bastian - STu4E.4
 Mantel, Klaus - JTh2A.105
 Manukyan, Karapet - FW4B.5
 Manurkar, Paritosh - STh3G.3
 Mao, Dong - JTu2A.97
 Mao, Dun - SF3O.5
 Mao, Peng - FF3B.6
 Mao, Xurui - STh3O.3
 Mao, Ya-Li - FTh3A.5
 Mao, Yuanfeng - JTu2A.70
 Marandi, Alireza - FF2B.1, SM3O.2
 Marandi, Atabak - ATu3I.5
 Marangon, Davide - FM2M.1
 Marangoni, Marco - Ath3K.2
 Marcano Olaizola, Aristides - JTu2A.114,
 JW2A.15
 Marchack, Nathan - STh1F.2
 Marconi, Simone - STh3N.2, STh4N.2
 Marcu, Laura - SM4H.3
 Marcus, Gabriel - SF3I.2
 Marcus, Gilad - STh1E.2
 Margetis, Joe - AW3P.3, STh4O.6, STu3N.3
 Margolis, Helen - SM1F.3
 Margulis, Walter - SM1L.5, SM2L.5
 Marinelli, Agostino - FF2C.5
 Marinelli, Matteo - FTh3A.1
 Marini, Andrea - FW3M.7
 Mariserla, Bala M.- FW3M.6
 Marjoribanks, Robin - JTu2A.1
 Markey, Laurent - FF2D.7, JTh2A.94
 Markham, Damian - FM2M.5
 Markman, Zeev - JTu2A.8
 Marpaung, David - SF2N.7, STh1J.4
 Marquez, Nicolas - FM4D.1
 Marquez-Velasco, Jose - SM1H.3
 Marris-Morini, Delphine - STu4O.5
 Martel, Théo - SM2J.6
 Martelli, Cicero - Ath4K.2, JTu2A.9
 Martin, Eamonn - SM4G.2, SM4N.6,
 STu4N.5
 Martin, Eric - FF3D.1, FM4D.3, FW3M.2,
 SM4F.4
 Martin, Hans - STh1F.3
 Martin, Kyle - STh3G.1
 Martin, Luc - JM2E.2
 Martin, Yves - STh1F.2
 Martin-Cano, Diego - FM2A.5
 Martinez, Enrique - JW2A.28
 Martínez, Pedro H.- JTu2A.77
 Martínez, Ricardo - SW4O.5
 Martin-Lopez, Enrique - AF2K.3
 Martin-Monier, Louis - STh1O.3
 Martyshkin, Dmitry - JW2A.50, STh1E.4
 Maruyama, Shigeo - SF3O.4
 Marvinney, Claire - JTu2A.21, JW3A.6
 Mashanovich, Goran - SW3J.5
 Maslowski, Piotr - JTh2A.111
 Mason, David - FM1A.3
 Mason, John - JTh2A.87
 Masruri, Masruri - SW4E.3
 Massler, Hermann - SW3F.7
 Massoli, Paola - AM1K.1
 Masuda, Keigo - SF3G.4
 Masuda, Keisuke - JTh2A.16, SM4F.3
 Masudy-Panah, Saied - STu4J.1
 Mateman, Richard - STh3N.6
 Mateos, Xavier - JTu2A.119, SF3E.6,
 STh1E.5
 Mathew, John P.- FM1A.2
 Mathieu, François - JM2E.2
 Match, Sonja - SM4J.6
 Matlis, Nicholas - JTu2A.105
 Matriyaz, Turghun - SM4L.2
 Matsko, Andrey B.- FF1D.7, SF2H.6,
 STh4G.4, STh4J.7
 Matsubara, Eiichi - STh3F.3
 Matsuda, Takuya - JW2A.32
 Matsumoto, Atsushi - JTh2A.71, SF1G.2
 Matsuo, Shinji - JTh2A.58, STh3N.1,
 STu3N.6
 Matsushima, Yuichi - JTh2A.71
 Matsutani, Akihiro - SM4N.4
 Matsuzaki, Korenobu - FW3C.5
 Matteo, Daniel A.- FW3B.6
 Matthews, Manyalibo J.- ATu4I, AW3I.5,
 FTh1C.4, SF3G.7
 Matthey, Renaud - SW4N.5
 Matveev, Arthur - SM4F.1
 Maurer, Cole - FM3A.4
 Mauthe, Svenja - SM3J.1
 Mavric, Uro - SF3I.5
 Mavrona, Elena - SW4F.1
 Mawst, L - SW3N.3
 Maxwell, Gisele - SM4L.4
 Maxwell, Timothy - FF2C.5, SF3I.2
 May, Molly A.- FF3M.4
 May, Nicholas - ATu4I.2
 May, Stuart - FW3B.3
 Mayer, Aline S.- SF2O.7
 Mayor, Felix M.- SF2J.6, STh3H.4
 Mayzlin, Yurij - Ath3K.2
 Mazur, Mikael - SM1G.1
 Mazurski, Noa - FF3M.5, FTh1C.3,
 FTh3M.8, FTh4M.4, JTh2A.49,
 JTu2A.109, JW2A.110, SM3F.4
 Mazzotta, Zeudi - JM2E.2
 McAndrew, Brendan - JW2A.12
 McArthur, Joshua - STh4O.7
 McCaughan, Adam - STh1N.3
 McCorkel, Joel - JW2A.12
 McDaniel, Don - JTh2A.114
 McDaniel, Sean A.- SM4L.4
 McDonald, Corey - FM4D.5
 McGarvey-Lechable, Kathleen - SW4J.2
 McGilv, Stephen A.- STu4F.1
 McGrane, Shawn - Ath3K.3, JW2A.28
 McGrew, Will - SM1F.1
 McGuinness, Liam P.- SM2F.2
 Mckay, Luke - SM4O.4
 McKenna, Robert J.- JTh2A.63
 McKenna, Timothy - Ath3I.6, JW4A.4,
 SF2J.6
 Mckeown, Joseph - FTh1C.4, SF3G.7
 McKinney, Jason D.- SF2N.8
 McLaughlin, Robert - STh3L.3
 McLellan, Claire - SM2F.4
 McLintock, Luke M.- STu4F.1
 McNicholas, Kyle M.- STh4O.7
 McPhillimy, John - FW3B.3
 McSpirtt, James - AM1K.2
 Mechel, Chen - FF1F.6, FF3M.6
 Mecseki, Katalin - JM1E.3
 Meem, Monjurul - AF3K.1, AM4K.5,
 JTh2A.118, SW4E.8
 Meena, Gopikrishnan G.- STu3H.2,
 STu3H.4
 Meesala, Srujan - JW3A.4
 Mehlstaebler, Tanja - SM1F.4
 Mehmood, Muhammad Qasim - FF2B.7
 Mehta, Karan - FTh3A.1
 Mei, Anyi - JTh2A.56
 Mei, Xiaodong - JW2A.7
 Mei, Yefeng - FM2A.2, JTu2A.122
 Meier, Urs - SF2J.4
 Meier, William - FW4M.5

- Mekkawy, Ahmed - AM3K.5
 Melchert, Oliver - FF1D.4, SW3H.2
 Melik-Gaykazyan, Elizaveta V.- FM1B.4, FM2C.4, FW4B.3
 Melikyan, Argishti - JTu2A.76
 Melkonian, Jean-Michel - ATH3K.1, JTu2A.93, SF1H.3
 Melkonyan, Henrik - SM2L.3
 Melosh, Nicholas - FM4A.4
 Menard, Jean-Michel - FM3C.4
 Menberu, Lul - JW2A.22
 Mendelson, Noah - FM4A.5
 Mendez-Astudillo, Manuel - STh1H.6
 Méndez-Rosales, Manuel Arturo - SF2O.4
 Mendis, Rajind - FF2A.4, STu3F.6
 Meng, Bo - SW4N.4
 Meng, Fangyuan - JTh2A.72
 Meng, Fei - SF1L.6
 Meng, Jiajun - JTu2A.48, SF3J.2, SM4J.4
 Meng, Linghao - STh3L.4
 Meng, Yuan - JTh2A.43
 Meng, Yunlong - AM3I.6
 Meng, Ziyi - AF2K.5
 Menon, Rajesh - AF3K.1, AM2I.5, AM4K.5, FTh3M, JTh2A.118, SW4E.8
 Menon, Vinod - FF3A.3, FM4D.2, FW3C.2, FW3M.5, JTu2A.52, STh4H.7
 Menoni, Carmen S.- SM3H.2, STu3E.3
 Menotti, Matteo - FM1D.5
 Menyuk, Curtis R.- JW2A.122, STh4L.3
 Mergat, Florian - ATH3I.3, SF1G.4
 Meriles, Carlos - FF3A.3
 Merkl, Philipp - FW3M.1
 Merklein, Moritz - FW3B.2, SF2N.5, SM4O.4, SM4O.5
 Merritt, Charles - SM2J.7
 Mesaritakis, Charis - JTu2A.74
 Metcalf, Andrew J.- FF2D.6, STh3G, STh3G.1
 Metelmann, A. - FTu3B.5
 Metzger, Thomas - JM2E.5, SM4E.3
 Meuret, Sophie - SF2O.3
 Meyer, Eric - FW3D.5
 Meyer, Jerry R.- SM2J.7
 Meyer, Stephanie A.- STu3H.3
 Meygoo Lavasani, Ali - JTh2A.41
 Meynell, Simon - SM2F.4
 Mi, Zetian - SF2I.6, SF2O.3
 Miaja Avila, Luis - SF2G.6
 Miao, Pei - FM1B.3
 Michael, Christopher - JTu2A.96
 Michel, Jurgen - STh4O.2
 Michel, Knut - JM2E.5, SM4E.3
 Middleton, Charles - SM4O.4
 Midkiff, Jason - AW3K.5, STh1F.6
 Midolo, Leonardo - FTh3D.2
 Midorikawa, Katsumi - STh3E.4, SW4E.7
 Migliaccio, Federica - JTu3G.1
 Mignuzzi, Sandro - FF2B.3
 Mikami, Hideharu - SM4H.1
 Mikami, Yuya - SM2O.5
 Mikhaylovskiy, Rostislav - FTh1B.2
 Mikkelsen, Maiken H.- JTu3M.4, SW3H.8
 Mikonnen, Tommi - SW3L.5
 Milchberg, Howard - FTh1M.3
 Milde, Tobias - ATH3K.6, ATH3K.7, ATH4K.7
 Mildenberg, Daniel - STu3F.1
 Milione, Giovanni - SM3G
 Miliou, Amalia - STh4N.5
 Millar, Ross - FF1A.4, STh1N.2, STu4O.7
 Miller, David A.- JM3B.2
 Miller, Houston - AM2K.1
 Miller, Keith - ATH1K.7
 Miller, Kevin J.- STh4H.1
 Miller, Owen - FM1C.1, FM1C.3
 Miller, Steven A.- SF3N.5
 Millet, Clement - FM3A.2
 Millot, Guy - STh4L.2
 Mills, Gordon - STu4O.7
 Milner, Will - SM1F.1
 Milosevic, Milan - SW3J.5
 Milot, Rebecca - STu4F.5
 Min, Bumki - FF1B.1
 Minamikawa, Takeo - AF3K.4, JTh2A.101, SM2H.5, STh1G.4
 Minitti, Michael P.- SF3I.7
 Minkov, Momchil - FM1B.2, FM1C.7, JF3F.2, JM3B.2, SW4J.7
 Minoshima, Kaoru - JTh2A.101, SM2H.4, SM2H.8, STu3L.3, SW3G.2, SW3G.4
 Miranda, Alessio - FTh3D.3
 Miranda, Henrique P. C. - FW3M.7
 Mirando, Francesco - STu4O.7
 Miri, Mohammad-Ali - FTu4B.6, JW2A.49
 Mirin, Richard P.- FF1A.3, FM1M.7, FM4D.5, FTh1D.5, JTu2A.42, SF3H.3, SM3O.5, SW3J.4
 Mirmoosa, Mohammad - FM4B.6
 Mironov, Sergey - SW4E.3
 Miroznic, Mark S.- JTh2A.37
 Mirov, Mike - STh4E.3, STh4E.6
 Mirov, Sergey - JTu2A.116, JW2A.50, SF1H.1, STh1E.4, STh3J.6, STh4E.3, STh4E.6
 Mirza, Muhammad M.- FF1A.4
 Miseikis, Vaidotas - STh3N.2, STh4N.2
 Mishchenko, Artem - SM1O.4
 Mishchik, Konstantin M.- ATu3I.7, JM3E.3
 Mistry, Ajay - SM3J.7
 Mita, Yoshio - JTh2A.48
 Mitchell, Arnan - FF2D.8, FW3B.4, SF2N.2, SF2N.4, STh1H.7, STh1J.4
 Mitchell, Eric W.- AW4K.1
 Mitchell, Matthew - SF1J.3, STh1H.4
 Mitchell, Morgan - SM3F.1
 Mityukovskiy, Sergey - ATu3K.6
 Mittal, Vinita - STh1F.1
 Mittelberger, Daniel E.- SM4O.3
 Mittleman, Daniel M.- FF2A.4, STu3F.6, STu4F.2, SW4F
 Miyagawa, Kazumasa - AM4K.5
 Miyamoto, Isamu - ATu3I.1
 Miyamoto, Katsuhiko - JTu2A.62, SF3G.3, SF3G.4
 Miyazaki, Tatsuya - JTh2A.79
 Miyazawa, Hiromasa - SF3L.1
 Mizeikis, Vygtantas - SF3J.7
 Mizumoto, Tetsuya - JTh2A.27
 Mizuno, Takahiko - AF3K.4, STh1G.4
 Mizuno, Yosuke - AF1K.5
 Moayedid Pour Fard, Monireh - JTh2A.81
 Mobini, Esmaeil - SM4L.5
 Mocek, Tomas - JTu2A.119
 Modotto, Daniele - STh4L.1
 Modsching, Norbert - SF3E.4, STh3F.5
 Moeller, Stefan - SF3I.2
 Moerner, W. E. - AM4I.5
 Mohammed, Omar F.- Ath1I.3
 Mohan, R. Krishna - JTh2A.39
 Mohr, Christian - STu4E.4
 Moille, Gregory - JTu2A.86, SM3J.4, SM3O.6
 Mojahedi, Mo - FM1C, FTh4B.3, FTh4B.8
 Mok, Aaron - AM1I.5
 Mokhtari-Koushyar, Farzad - JTh2A.81
 Molesky, Sean - FTu4D.1
 Molina-Sánchez, Alejandro - FW3M.7
 Molina-Terriza, Gabriel - FM1A, FM3A.5
 Mollae, Masoud - JTu2A.107
 Moloney, Jerome V.- FM4M.2, FW3B.6
 Mompert, Jordi - FM4B.3, JTh2A.46
 Monat, Christelle - FF2D.8, STh1J.6
 Mondain, François - FTh4D.2
 Mondal, Sandip - FF3B.4
 Mondin, Linda - JTu3G.1
 Mondol, Mark - AM4K.5
 Mongin, Denis - JM2E.5
 Monro, Tanya - STh3L.3
 Montanaro, Alberto - STh3N.2, STh4N.2
 Montant, Sébastien - JTu2A.65
 Montes Bajo, Miguel - FTh4M.1
 Montes, Jossue - SW4H.5
 Montjoy, Douglas - FF2B.1
 Moody, Galan - FM4D.5
 Moody, Joshua - FTh1B.3
 Moon, Hyowon - SF1O.6
 Moon, Jisoo - FM2D.5
 Moon, Jisun - AW4I.4
 Moon, Jiyoung - SW4N.2
 Moon, Kiwon - STu3F.7
 Moon, Sung - FM2M.4, JTu2A.35, JTu2A.45
 Moore, David S.- Ath3K.3
 Moore, Penny - STh4N.6
 Moore, Thomas Z.- JTh2A.87
 Mooshammer, Fabian - FTh4C.3
 Mootz, Martin - FW4M.5, JTh4F.3
 Moradi-Chameh, Homeira - Ath4I.4, SM4H.6
 Morales, Felipe - FF3C.2
 Morandotti, Roberto - FTh1A.4, JTh2A.2, SF2N.2, SF2N.4
 Moreaux, Laurent - Ath4I.4, SM4H.6
 Moreira, Renan - STu4O.3
 Moreno-Zarate, Pedro - JTu2A.46
 Moretti, Luca - FW3M.7
 Morfonios, Christian - FM4B.7
 Morgan, Kaitlyn - Ath1K.7
 Morgan, Katrina - SF3O.7
 Morgner, Uwe - FF1D.4, FF3C.2, JTh2A.5, STh4E.2, SW3E.1, SW3H.2
 Mori, Warren B. - FF1C.5
 Morinaga, Mizuki - SM4N.4
 Morissette, Erin M.- JW2A.26
 Morohashi, Isao - SM2H.5, SW4F.4
 Moroney, Niall - JM3B.3, SF3H.5, STh3J.7
 Morozov, Dmitry - JTh2A.93, JTu2A.41
 Morris, Titus D.- FTh3A.6
 Morrison, Blair - FM1D.5, FTh4D.6, STh1J.4
 Morteheb, Farinaz - SF2G.1
 Mortazavi, Mansour - AW3P.3, STh4O.6, STu3N.3
 Mortensen, N. - FTu3C.4, FW4D.2
 Morthier, Geert - STh4N.1
 Morton, Paul - STu3J.2, SW4N.6
 Mosallaei, Hossein - FF1B.2
 Moselund, Kirsten E.- SM3J.1
 Moses, Jeffrey - SW4H.7
 Mosheni, Masoud - FTh3A.3
 Moskalev, Igor S.- STh4E.3, STh4E.6
 Mosleh, Aboozar - STu3N.3
 Mosley, Peter - FF1F, FTh3A
 Moss, David - Ath4I.1, FF2D.8, FTh1A.4, SF2N.2, SF2N.4
 Mottay, Eric - ATu3I.7, ATu4I.1, ATu4I.5, JM3E.3, JW2A.73
 Mottini, Sergio - JTu3G.1
 Mou, Chengbo - JW2A.38, JW2A.88, SF3L.6
 Moutanabbir, Oussama - STh4O.5
 Mrejin, Michael - AF2K.6, FTu4C.3
 Mridha, Manoj K.- STh1L.1
 Mu, Qianyi - SW3F.1
 Mu, Xue - JW2A.45
 Mu, Zhao - SM2F.5
 Mücke, Oliver D.- FF2C.2, JTu4M.5, SW3E.7, SW4E.7
 Mueller, Dirk - ATu3I
 Mueller, Jost - SF3I.5, SF3I.6
 Muggli, Patric - FTh1B.3
 Muir, Ryan - SM4O.3
 Mujumdar, Sushil A.- FF2A, FF3B.4
 MUKHERJEE, ARUNABH S.- FM2A.4, JW2A.33
 Mukherjee, Samik - STh4O.5
 Mukherjee, Tamal - SF3N.4
 Mukhin, Ivan - FM2C.6
 Muller, Andreas - JTu2A.23, SM2N.4
 Muller, Eric A.- FTh4C.2
 Müller, Georg M.- AF1K.4
 Müller, Juliana - SF1G.4
 Muneeb, Muhammad - FF3A.2, STh4N.1, STu4O.4
 Munera, Natalia - FF3D.3
 Munk, Dvir - STh3H.5
 Muñoz, Francisco - JTu2A.46
 Munoz, Maria - FW4M.6
 Munro, William - FTh1A.4, FTh4A.1
 Munshi, Tasnim - ATu3P.6
 Mupparapu, Rajeshkumar - FW3B.1
 Murai, Toshiya - JTh2A.27
 Murari, Krishna - STh1E.1
 Muraviev, Andrey V.- SF1I.2, STh4E.3, STh4E.6
 Murdoch, Stuart - SW3H.3
 Murmane, Margaret M.- FF2C.6, FF2C.7, JM3E.4, SF2E.1
 Murphy, Thomas E.- STh3O.7
 Murray, Christopher P.- JW2A.66
 Murray, Joel - SF1H.6
 Murray, Robert T.- SM3L.4
 Murugan, Ganapathy Senthil - STh1F.1
 Mussler, Gregor - FTh4C.3
 Mussot, Arnaud - FF2D.4, FTh3B.5
 Mysyrowicz, Andre - FTh1M.2
 Mysyrowicz, André - JM2E.5
- N**
- N. K., Radhika - JW2A.84
 Na, Yongjin - STh3G.6, STh3G.7
 Nabben, David - FM3D.4
 Nabekawa, Yasuo - STh3E.4
 Nabet, Bahram - JTu2A.27, SF1N.4
 Nacke, Codey - SF1J.6
 Nadal, Laia - SW4O.5
 Nader, Nima - SF1E.4, SF3H.3, SM3O.5, SW3J.4
 Naderian, Azadeh - Ath4I.4, SM4H.6
 Nadkarni, Rohan - ATu4K.2
 Nagai, Masaya - FF2A.4, STh3F.3
 Nagamine, Gabriel - FM3D.5
 Nagar, Garima C.- JTh2A.7, JTu2A.58
 Nagarajan, Naveen - AM2I.5
 Nagatsuma, Tadao - SW4F.6
 Nagler, Achiya - FTu4C.3
 Nagler, Philipp - FW3M.1, JTu4M.2
 Nagy, Tamas - SW3E.1
 Nahmias, Mitchell A.- JM3M.3, SM3N.3, SW3H.7
 Naik, Gururaj V.- FM3C.1, FTu4D.4
 Nakajima, Yoshiaki - STu3L.3, SW3G.2, SW3G.4
 Nakamura, Keisuke - SW3G.3
 Nakamura, Kentataro - AF1K.5
 Nakamura, Ryosuke - SF3G.3
 Nakamura, Takuma - SW4G.1
 Nakano, Yoshiaki - JTh2A.48, SM3G.4
 Nakao, Ryo - STu3N.6
 Naldoni, Alberto - FTh1C.2
 Nam, Chang Hee - STu3E.2
 Nam, Sae Woo - FF1A.3, FF1A.6, FM1M.7, FTh1D.5, FTh4D.6, JTu2A.42, SF3H.3, SM3O.5, STh1N.3, SW3J.4
 Nan, Fan - SM1H.4
 Nanni, Emilio - STh3F.2
 Nantel, Megan - FF2C.5
 Narang, Prineha - SM2F.5
 Narayanan, Ram - JTu2A.15

- Narimanov, Evgenii E.- FTh4M.5, FTu3D.2, FTu4D.6, JTh2A.19
 Nasari, Hadiseh - FF3B.8
 Nash, Geoffrey - JTh2A.26
 Nasimzada, Wahid - JTh2A.100
 Natan, Adi - FF2C.5
 Natarajan, Arun - SM2G.4
 Natile, Michele - JM1E.5, JW2A.73
 Natsume, Kohei - ATu3I.3, ATu3I.4
 Nauriyal, Juniyali - Ath3I.2
 Navarro-Urrios, Daniel - FW4D.1
 Nayak, Kaushik - JTh2A.22
 Naziru, Andrei - SW4E.3
 Ndao, Abdoualye - SM3N.1
 Nebabu, Tamra M. - SW3H.8
 Nedeljkovic, Milos - SW3J.5
 Nees, John - FTh1M.6, JTh2A.6, JTh2A.84, JTu2A.56
 Negnevitsky, Vlad - FTh3A.1
 Nehra, Rajveer - FF1A.6, FTh4D.5
 Nellikka, Apurv C.- FTh1B.6
 Nelson, Craig - JW2A.113
 Nelson, Karl - SM4O.1, STu4O.3
 Nelson, Robert L.- SM4O.5
 Nemirovsky, Liat - FW3D.7
 Nemoto, Kae - FTh4A.1
 Nemov, Ilya N. - STh4L.4
 Nerem, Robert R.- FF1A.3
 Nerushev, Oleg - SF2G.2
 Neshev, Dragomir - SF3J.1
 Neuhaus, Joerg - ATu3I.5
 Neuhaus, Mathias - JTh2A.100
 Neupane, Madhab - FW4M.2
 Newbury, Nathan R.- AW4K.1, SF1I.1, SM1F.1, SM2N.3, STh1G.1, STh1G.2, STh3G.2, STh3G.3
 Newman, Ward D.- FTu3D.3, FTu4D.1
 Ng, Brenda - SM4E.6
 Ng, Ray J.H. - SM1J.6
 Ng, Tien Khee - Ath1I.2, JTh2A.51, SF2O.1, SM3N.4, SM3N.5
 Nguyen, Anh D.- SM4F.2
 Nguyen, Hoa P.- JW2A.109, JW2A.93
 Nguyen, Hoang - FTh1C.4, SF3G.7
 Nguyen, Ngoc - FM2C.2
 Nguyen, Peter - STu3F.1
 Nguyen, Phuong H.- AM4I.6
 Nguyen, Quynh L.- FF2C.6, FF2C.7
 Nguyen, Thach - FW3B.4, SF2N.2, SF2N.4, STh1H.7, STh1J.4
 Nguyen, Thien-An - JTh2A.81
 Nguyen, Thinh - SM2G.4
 Ni, Kai - SM2H.2
 Ni, Ni - FM2D.2
 Ni, Peinan - FTh3M.7, JTu2A.75
 Ni, Xingjie - FF1B.6, FW4B.2
 Niang, Alioune - STh4L.1
 Nicholl, Ryan J.- STh4G.7
 Nicolas, Jérôme - STh4O.5
 Nicolodi, Daniele - SM1F.1
 Nie, Dandan - JTu2A.31
 Nie, Shuzhen - AW3I.6
 Nie, Zan - FF1C.5
 Nielsen, Michael - FM2C.2
 Nieves, Yamil A.- JTu2A.23
 Niizeki, Kazuya - FTh1D.7
 Niknejad, Ali - JW2A.81
 Nikolay, Niko - FM4A.5
 Nikonov, Dmitri - SM1O.4
 NiLochlainn, Sorcha - JW2A.66
 Nilsson, johan - STu3L.2
 Ning, Cunzheng - STh1J.7, STh3O.1
 Ning, Cun-Zheng - FM4D.4, JW2A.19
 Ning, Xiaonan - FF1C.5
 Ninnemann, Erik - Ath4K.6
 Ninota, Yuki - FF3C.5
 Nishi, Hidetaka - STu3N.6
 Nishida, Jun - SF1E.3
 Nishiharaguchi, Nobuhiko - JW2A.96
 Nishikawa, Tadashi - SF1I.3, SW4G.2
 Nishimura, Naoya - SM2O.5
 Nishiyama, Akiko - JTh2A.111, SW3G.2
 Nishiyama, Nobu - JTh2A.16, SM4F.3
 Nishizawa, Norihiko - JW2A.92, JW2A.98, STu3L.4
 Nitta, Kuzuki - STh1G.4
 Nitta, Nao - SM4H.1
 Niu, Chao - JW2A.118
 Niu, Xiaxia - JW2A.95
 Niv, Eyal - STh4L.5
 Noach, Salman - STh1E.2
 Noah, Adam - JTu2A.120
 Noda, Susumu - SM1J.7, SW4N.3
 Nodurft, Dawson - JTh2A.87
 Noe, Tim - FM4D.1
 Nogan, John - FTu4D.2
 Noginov, M - FTu3D.4, JTh2A.20
 Noginov, Mikhail - FTh4M.6
 Noginova, Natalia - FTh4C.7, FTh4M.6, JW2A.59
 Nogueira, Ana F.- FM3D.5
 Noh, Minji - FM2D.3, FM2D.4
 Noh, Wanwoo - SM3N.1
 Nojic, Jovana - SF1G.4
 Nolde, Jill A.- SM2J.7
 Nolen, Joshua R.- FF1B.7
 Nolte, David D.- AM2I, ATu3K.4, AW4I
 Nomoto, Yoshiro - SM4N.2
 Nomura, Yutaka - SF2L.6
 Nookala, Nishant - AM3K.5, FW4B.1
 Nordlander, Peter - FF2B.4
 Norman, Justin - ATu3P.5, STu3N.1, STu4J.3
 Norris, Samuel - STh3N.6
 Norris, Theodore B.- SM4J.2
 Notaras, Jelena - STu3O.3, STu3O.4, SW4G.6
 Notaros, Milica - STu3O.3, STu3O.4
 Notomi, Masaya - JTh2A.10, JTh2A.58, JW3A.5, SM2J.6, SM4J.3
 Novak, Erik L.- Ath1K.1
 Novoa, David - STh1L.1
 Novotny, Lukas - FW3C.1, SF3N.1
 Nozaki, Kengo - JTh2A.58, SM4J.3
 Nsofor, Ugochukwu - JTu2A.118
 Numkam Fokoua, Eric - SM2L.2, STh1L.4
 Nunes do Santos, Eduardo - Ath4K.2
 Nunn, Joshua - FM2M, JTu4A.5
 Nussenzweig, Paulo - STh3J.1
 Nyby, Clara - JTh4F.1
 Nye, Nicholas - SW4N.1
 Nyga, Piotr - JW2A.55
- O**
- Ó Duill, Seán P.- STu4N.5
 O'Brien, Dominic - SM2G.5
 Oakley, Douglas - JTu2A.82
 Oates, Chris - SW3G.7
 O'Beirne, Aidan L.- STu4F.1
 Oberhofer, Katrin E.- SF2G.1
 Obrzud, Ewelina - AF2K.2, FF1D.2, STh4J.1, STu3J.3
 Ochiai, Natsuha - JW2A.83
 Oda, Robert - STu4H.6
 Oddershede, Lene - SM1H.1
 Odom, Teri W.- FW3C.3
 Oelker, Eric - SM1F.1
 Ofori-Okai, Benjamin - JTh4F.1
 Ogasawara, Makoto - JTh2A.48
 Oguntoye, Isaac O.- JTh2A.25, STh1F.5
 Oguz, Ilker - ATu4K.2
 Oh, Seongshik - FM2D.5
 Ohishi, Yasutake - JTu2A.91, JW2A.109, JW2A.93, JW2A.96
 Ohodnicki, Paul - JW2A.14
 Ojo, Solomon - AW3P.3, STu3N.3
 Okada, Etienne - JTu2A.102
 Okada, Mitsuhiro - SF2G.2
 Okamoto, Yuki - JTh2A.48
 Okamura, Kotaro - FTh1D.7
 Okawachi, Yoshitomo - FM1D.4, FM1D.6, JW2A.82, SF3H.4, STh3J.1, STh4J, SW3E.4, SW4H.3
 Okayama, Hideaki - STh1H.6
 Okhrimchuk, Andrey G.- STh1E.6
 Okhrimenko, Bogdan - FTh3A.2
 Oki, Yuji - SM2O.5
 Okoth, Cameron S.- JTu2A.44
 Okubo, Sho - JW2A.97, SW3G.1, SW3G.3, SW3G.8
 Olgun, Halil T.- JTu2A.105
 Oliaei Motlagh, Seyyede Azar - JTu4M.3
 Oliva, Eduardo - SF3I.3
 Olivares, Iram E.- STh4O.7
 Olivier, Michel - SF2L.1
 Ollanik, Adam - JTh2A.108, JTh2A.25, STh1F.5
 Ollivier, Helene - FM1M.1, FM3A.2
 Olson, Jonathan - FF1F.2, FTh3A.3
 Olson, Judith - SW3G.7
 O'Malley, Nathan - Ath1K.4
 Omanakuttan, Giriprasanth - SW4N.4
 Omatsu, Takashige - JTu2A.62, SF3G, SF3G.3, SF3G.4
 Omi, Hiroo - JW2A.30
 Omoda, Emiko - JW2A.92
 Onasch, Timothy - AM1K.1
 Onat, Talha - AF1K.7
 O'Neal, Jordan - FF2C.5
 Ono, Atsushi - FM2C.5
 Ono, Masaaki - JW3A.5
 Ono, Shingo - ATu3I.3, ATu3I.4
 Ono, Yumie - JTu2A.120
 Oo, Swe Z.- Ath3I.4
 Oo, Thein - JW3A.3
 Oohara, Akira - SF1I.3
 Ooi, Boon S.- Ath1I.2, Ath1I.3, JTh2A.51, SF2O.1, SM3N.4, SM3N.5, STu3O.1
 Orcutt, Jason S.- STh1F.2
 Ordouie, Ehsan - SM2O.1
 O'Regan, David - JTu2A.110
 Orenstein, Meir - FTh1C.7, SM2O.3
 Oresick, K - SW3N.3
 Orhan, Okan K.- JTu2A.110
 Orlovas, Sergejus - JTu2A.17
 Orngotti, Marco - FTu3B.3
 Ortolani, Michele - STh1N.2
 Osada, Alto - FM1M.2
 Osawa, Shuto - FTh1A.5
 Oschwald, Michael - AW3I.7
 Oscurato, Stefano - AM3K.3, FM3C.2
 Osellame, Roberto - FM1M.1
 Osman, Ahmed - SW3J.5
 Osório, Jonas H.- SF3L.2
 Ossieur, Peter - STh4N.1
 Osten, Wolfgang - JTu2A.12
 Ostendorf, Andreas - JTu2A.47
 Osterkamp, Christian - SM2F.2
 Ostrovsky, Evgeny - FTu3D.5
 O'Sullivan, Maurice - SW3O.2
 Osvay, Károly - STh3E.1, STu4E.2
 Ota, Michiharu - ATu3I.4
 Ota, Yasutomo - FM1M.2, SM2J, SW4J.1, SW4J.4
 Othman, Mohamed - STh3F.2
 Otomo, Akira - JTh2A.48
 Otsuji, Taiichi - SW3F.2
 Otto, Martin R - FF3C.6
 Ottonello-Briano, Flavia - STh1F.3
 Ou, Haiyan - SM2O.7
 Ou, Xin - SM2O.7
 Ou, Z. Y. - FTh3D.5
 Oulton, Rupert - FM2C.2, FTh3C.5
 Oulton, Ruth - STh1H.1
 Ouyang, Xing - SM3G.5
 Overstolz, Thomas - STu4G.3
 Overvig, Adam C.- FF2A.3, FF2A.5, FF2B.8, FM4M.7, FTh3M.5
 Owen, Rachel C.- FM3G.1
 Owschimikow, Nina - FM3D.2, JW2A.24
 Oxenlewe, Leif K.- JTu2A.83, SF3H.2, SW3H.4
 Ozana, Nisan - Ath3K.5, JTu2A.120, JTu2A.8
 Ozawa, Akira - JM1E.4
 Ozbay, Ekmele - AF1K.7
 Ozcan, Aydogan - AM2I.3, AM2I.6, AM2K.3, AM4I.3, ATu4K.2, ATu4K.3, ATu4K.6, JF2F.2, JM3M.5, JTu2A.5, SF1N.2, SM4H.2, STu4H.2
 Ozdemir, Sahin K.- FTu3B.5
 Ozdur, Ibrahim - AF1K.7
 Ozeki, Yasuyuki - JW2A.83, SM4H.1, STu4H.6, STu4L.3
 Ozolins, Oskars - SW4O.2
- P**
- Padilha, Lazaro A.- FM3D.5
 Padmanabhan, Prashant - SW3F.2
 Paesani, Stefano - JTu2A.124, SM2F.2
 Paetzold, Ulrich - JTu2A.71
 Page, Alexis - STh1O.3
 Page, Carlo - JTu4A.5
 Pai, Chih-Hao - FF1C.5
 Paiella, Roberto - STh1O, STh4O.3
 Paik, Eunice - STu3N.5
 Paik, Oskar - STh4G.3
 Pal, Mrinmay - SW3H.2
 Pal, Shovon - FM3D.3
 Palles, Dimitris - SM1H.3
 Palmer, Mark A.- STu3E.5
 Pan, Bao-Ying - Ath1I.4
 Pan, Chengda - JTu2A.111
 Pan, Guangzhong - AW3K.6, JTu2A.80, STh3O.3
 Pan, Haifeng - JTu2A.111
 Pan, Jian-Wei - FM4C.1, FM4C.3, FTh3A.5, FTh4A.6, JTu2A.92
 Pan, Jiaoqing - JTh2A.72, JTu2A.79, JW2A.3
 Pan, Long - JW2A.7
 Pan, Mingsen - FM1B.3
 Pan, Shilong - AW4K.3, SW3G.6
 Pan, Weiwei - JW2A.75
 Pan, Zhimeng - AM2I.5
 Pan, Zhongben - SF3E.6
 Pan, Zhongqi - JTh2A.80
 Pandey, Ayush - SF2I.6
 Pang, Kai - FW4B.5, JTu2A.57, JTu2A.67, SM1J.5, SM1N.5
 Pang, Shuo - STh3L.2
 Pang, Xiaodan - SW4O.2
 Pang, Yoonsoo - JW2A.27
 Paniagua-Diaz, Alba - FM1C.5
 Pankow, Mark - AF1K.1
 Pant, Mihir - FTh1D.3
 Panyutin, Vladimir L.- SF3O.8
 Papadopoulos, Dimitrios N.- STu3E.4
 Papadopoulos, Dimitris - JM2E.2, STu4E
 Papisimakis, Nikitas - STh4H.6
 Papenbrock, Thomas - FTh3A.6
 Papon, Camille - FTh3D.2
 Papp, Scott B.- FF1D.6, FF2D.6, SF2I.2, SF2I.7, SM3J.4, SM3O.6, STh1G.2, STh3J.3, SW4H.1, SW4H.2
 Paradis, Clément - SF3E.4, STh3F.5
 Paradis, Pascal - SF2L.1
 Paraiso, Taofiq - FM2M.1
 Parappurath, Nikhil - JM2B.2

- Pareek, Vivek - FW3M.6, SF10.3
 Parigi, Valentina - FTh4D.4
 Park, Chibeom - FTu3C.2
 Park, Doewon - SF21.1
 Park, Hong-Gyu - FM2C.4, FW4B.3
 Park, Jiwoong - FTu3C.2
 Park, Jongcheol - JW2A.111
 Park, Jongkab - ATu3L.6
 Park, Joongmok - FW4M.5
 Park, Joon-Suh - STh10.5
 Park, Kyoung-Duck - FF3M.4
 Park, Kyung Hyun - STu3F.7
 Park, Sang-Eon - JW2A.111
 Park, Su Ji - JTh4F.1
 Parra-Rivas, P. - SM30.3
 Parriaux, Alexandre - STh4L.2
 Parsons, Joshua - SM4L.2
 Parsons, Kieran - SW4J.6
 Partlow, Matthew J. - JTh2A.114
 Parto, Midya - FM1D.2, FW3D.1, FW4D.2
 Partridge, Matthew - STh1L.2, STh1L.4
 Parvinnezhad Hokmabadi, Mohammad - SW4N.1
 Parzefall, Markus - FW3C.1
 Pashkin, Alexej - STu3F.3
 Pasiskevicius, Valdas - SF1H.4
 Pasquali, Matteo - STh4H.5
 Patankar, Manish - AM3L.4
 Patankar, Siddharth - FTh1M.7
 Patel, Rishi - Ath3L.6, SF2J.6
 Patrick, Charles L. - ATu4K.4
 Patrik, Rohner - FW3C.5
 Patrizio, Marco - JTu2A.68
 Patrow, Joel - FW4B.5
 Patsyk, Anatoly - FTu3D.1
 Patterson, Jean - STu3H.2
 Patwardhan, Gauri - FM4M.7
 Paul, Douglas J. - FF1A.4, FTh3C.6, STh1N.2, STu4O.7
 Pauliat, Gilles - JTh2A.102
 Pavanello, Fabio - STu4O.4
 Pavlov, Nikolay G. - STu3J.4
 Peacock, Anna C. - Ath3L.4
 Peake, Gregory - FF2B.2
 Pechal, Marek - JW4A.4
 Pedersen, Nicolas - JTh2A.17
 Pei, Yumiao - FTh4B.2
 Pellegrini, Giovanni - FTh3C.6
 Pelton, Matthew - FF3M.4
 Pemmaraju, Das - JTh4F.1
 Pena, Jessica - SW4E.8
 Peng, Cheng - SF10.6
 Peng, Cheng-Zhi - FM4C.1, JTu2A.92, JTu3G.4
 Peng, Fei - AW3L.4
 Peng, Gang-Ding - JW2A.107
 Peng, Hsuan-Tung - JM3M.3, SM3N.3, SW3H.7
 Peng, Junsong - JW2A.90, SF2E.3
 Peng, Ruwen - JTh2A.38, STh1O.2
 Peng, Xiaolei - SM1H.2
 Peng, Xiaoshi - SF10.2
 Peng, Zhaoqiang - AF1K.6
 Peng, ZhiGang - JW2A.67
 Pennathur, Anuj - FW4B.5
 Pennetta, Riccardo - FTh3B.3
 Penninckx, Denis - JTu2A.65
 Penttinen, Jussi-Pekka - ATu3P.1
 Penty, Richard V. - SM1G.3
 Pepe, Francesco - AF2K.2
 Peppers, Jeremy - STh4E.3, STh4E.6
 Perakis, Ilias E. - FW4M.5, JTh4F.3
 Peregro, Auro - FF2D.4
 Pereira, João Manoel B. - SM2L.5
 Peremans, Andre - SW3L.6
 Peretti, Romain - ATu3K.6
 Perez, Christopher - SF2O.5
 Perez, Daniel - SF1G.1
 Perez, Edgar - STh1G.2
 Perez, Max - STu4G
 Pérez-Hernández, José A. - FF1C.4
 Pergament, Mikhail - SM4E.1
 Perner, Lukas - SF2O.7
 Pernice, Wolfram - SM2J.2
 Perriot, Romain - JW2A.28
 Persano, Anna - SF1N.4
 Perseille, Benjamin - SW3E.6
 Pertot, Yoann - STh3E.1
 Pertsch, Thomas - FTh1C.6, FW3B.1, JTh2A.24
 Perumangatt, Chithrabhanu - JTu2A.36
 Pervak, Vladimir - JW2A.69
 Pestourie, Raphael - SW4J.8
 Peter, Thomas - AM1K.3
 Peters, Jon - FW3B.4, SF21.2
 Peters, Kara - AF1K.1, AF2K
 Peters, Nicholas A. - FF1F.3
 Petersen, Jan - SW3L.6
 Petford-Long, Amanda - JW2A.66
 Petkovšek, Rok - SW3E.2
 Petoukhoff, Christopher - JW2A.25, SF1O.3
 Petra, Rafidah - Ath3L.4
 Petrescu, Dan - JW2A.121
 Petrides, Ioannis - FW3D.5
 Petropoulos, Periklis - FW3B.3, JTh2A.74
 Petrov, Alexander - FTu4D.3
 Petrov, Mihail - FM2C.6
 Petrov, Petar - AM4L.5
 Petrov, Valentin - JTu2A.119, SF3E.6, SF3O.8, STh1E.5
 Petrovich, Marco N. - SM2L.2, STh1L.2, STh1L.4
 Petway, Larry - AW4K.6
 Peyghambarian, Nasser - AM3L.1, FF1F.4, JTu2A.107, SF3G.1
 Peyskens, Frédéric - FF3A.2
 Peysokhan, Mostafa - SM4L.5
 Peytavit, Emilien - JTu2A.102
 Pfeiffer, Hannes - STh4G.3
 Pfeiffer, Carl - JTh2A.36
 Pfeiffer, Loren - JW2A.34
 Pfeiffer, Martin - FF1D.5, SM3G.3
 Pfeiffer, Sven - SF3I.5
 Pfister, Olivier - FF1A.6, FTh4D.5, JTu4A.1
 Pham, Thach - STh4O.6
 Phan, Hoang-Phuong - FTh4D.3
 Phare, Christopher T. - SF3N.5, SM1N.6, STu3J.5
 Phillips, Christopher - FF2C.1, FTh1M.8, SF3E.3, SM3O.2, STh3E.2
 Phillips, Mark C. - JTh2A.106, SF2G.7, SM1N.3, STh1G.5, SW4L.2, SW4L.3, SW4L.5, SW4L.6
 Phung, Hoy-My - ATu3P.1
 Pi, Zekun - JW2A.41
 Piazza, Gianluca - SF2J.3, SF3N.4
 Piccardo, Marco - FM1D.3, STh4H.3
 Piccioli, Francesco - FW3D.8
 Piccoli, Riccardo - JTh2A.2
 Piché, Michel - SF2L.1
 Pichler, Kevin - FTu3D.6, FTu4B.2
 Picon, Antonio - FF2C.6
 Picqué, Nathalie - SF1I.3
 Pichal, Bernard - SF3E.2
 Pierrat, Romain - FM1C.5
 Piestun, Rafael - STh4L.5
 Pigeon, Jeremy - FW3B.6, JW2A.50, STh1E.4
 Piggott, Alexander Y. - FF3A.1
 Pilipetskii, Alexei N. - SM1G.4
 Pingault, Benjamin - FM4A.1
 Pintus, paolo - SF21.2
 Pioro-Ladriere, Michel - FM4A.6
 Piotrowski, Marcin - JTu2A.32
 Piper, Lewis - STh4H.6
 Pitanti, Alessandro - FW4D.1
 Pitchappa, Prakash - SW3F.6
 Pittman, Moana - SW4E.3
 Pizzocaro, Marco - SM1F.3
 Plaja, Luis - FF2C.6
 Plankl, Markus - FTh4C.3
 Plant, David V. - JW2A.121
 Plascak, Michael - JW2A.74
 Pleros, Nikos - JTh2A.94, STh4N.5
 Plick, William N. - FM2M.5
 Plidschun, Malte - SM2L.1
 Plotnik, Yonatan - FM1C.4, FTu4B.1, FW3D.2
 Plusquellic, David - AM2K.2
 Poddubny, Alexander - FW4B.4
 Podivilov, E. V. - FTh3B.4
 Podivilov, Evgeniy V. - STh4L.4
 Podolskiy, Viktor A. - FTh4M.3, FTh4M.5
 Pogorelsky, Igor V. - STu3E.5
 Pohl, David - SF2J.4
 Pohl, Randolf - SM4F.1
 Pohle, Hugh - FTh1M.3
 Poineau, Frederic - SW4L.4
 Poletayev, Andrey D. - JTh4F.4
 Poletti, Francesco - SM2L.2, STh1L.2, STh1L.4
 Polman, Albert - FTh1C.5, FTh3M.2, SF2O.3
 Polónyi, Gyula - SW4E.5
 Polyakov, Sergey V. - FM4C.7
 Polyanskiy, Mikhail N. - STu3E.5
 Polynkin, Pavel G. - FF1C.2
 Pomerantz, Michael - ATu3L.2
 Pomerene, Andrew T. - STh4N.6
 Poon, Andrew W. - SF21.4, STu3H.1
 Poon, Joyce K. - Ath4L.4, SM3J.3, SM4H.6
 Pooser, Raphael C. - AF3K.3, FTh3D, FTh4D.6, JW2A.117
 Popa, Daniel - JW2A.85
 Popov, Cyril - SM2O.3
 Popov, Inna - JTu2A.109
 Popovic, Milos - AW3K.2, SF3N.2, SM3J.5
 Poprawe, Reinhart - JM1E.4
 Porschatis, Caroline - JTh2A.94
 Porst, Moritz - FTh3A.2
 Poulidakos, Dimos - FW3C.5
 Pouysegur, Julien - ATu4I.5, JM3E.3
 Powell, Damian - JTu2A.41
 Powell, David - FF1B.4
 Powell, Michael - JW2A.28
 Power, Mark - SM4G.1
 Prabhakar, Gautam - SW3H.1
 Prabhakar, Shashi - JTu2A.41
 Prabhu, Mihika - FTh3A.3, FTh4A.3, FTu4C.2, SF1N.1
 Pramanik, Sandipan - FTu4D.1
 Pramanik, Tanumoy - FM2M.4, JTu2A.35
 Prandolini, Mark J. - STh3E.3
 Prantil, Matthew - SM4O.3
 Prasankumar, Rohit - FM2D.2, SW3F.2
 Praveen, Vishnu - JW2A.37
 Prayakara, Srujana - JTh2A.20
 Preble, Stefan F. - FTh1D.4
 Preissler, Daniel - JTu2A.85
 Priante, Davide - SF2O.1
 Price, John - JTu4A.5
 Price, Jonathan - STh1E.3, STu3L.2
 Prickaerts, Melissa - JTu2A.1
 Priel, Maayan - STh3H.5
 Prinz, Eva - FTh1C.7
 Proietti, Roberto - JTh2A.70, SM3G.2
 Proruit, Thomas - JM2E.5
 Proscia, Nicholas - FF3A.3
 Prost, Mathias - FTu4D.7
 Prucnal, Paul R. - JM3M.3, SM3N.3, SW3H.7
 Pruessner, Marcel W. - JTh2A.53, SF21.1
 Pruss, Christof - JTu2A.12
 Przewloka, Aleksandra - SF1L.4
 Pu, Minhao - JTu2A.83, SF3H.2, SM2O.7, STh1J.5
 Puckett, Matthew - SM4O.1, STu4O.3
 Pugzlys, Audrius - FF1C.2, SW4E.5
 Pupeikis, Justinas - FF2C.1, STh3E.2
 Pupeza, Ioachim - JW2A.69, STh4E.4
 Puppe, Thomas - Ath3K.2, JTh2A.112, STu4L.4
 Puzetky, Alex - JTu2A.21, JW3A.6
 Purz, Torben L. - FF3D.1, FW3M.2, SM4F.4
 Putnam, William - JTu4M.4
 Pysz, Dariusz - STh1L.5

Q

- Qi, Bing - STh4G.5
 Qi, Jiwei - JTh2A.15, JTh2A.29
 Qi, Limei - FTu4D.1
 Qi, Wei W. - STu3N.4
 Qi, Yanli - SW3J.5
 Qi, Zhen - FTu3D.4
 Qian, Li - SW3L.4
 Qian, Yan-Jun - JTh2A.33, JTh2A.69
 Qian, Yifeng - AM4I.2
 Qiao, Jie - ATu3I.2, AW3I
 Qiao, Lingling - FTh1M.5
 Qiao, Yucheng - JTu2A.30
 Qiao, Zhongliang - STu4O.1
 Qin, Chenye - JTh2A.88
 Qin, shuchao - SM1O.3
 Qin, Yukun - AM3L.1
 Qiu, Cheng-wei - SF3J.5
 Qiu, Feng - STh1N.7
 Qiu, Junyi - ATu3P.2, JTh2A.62
 Qiu, Kun - JTu2A.73, SW3O.7
 Qiu, Xianggang - FM2D.2
 Qu, Shizhen - FTh1B.5, JW2A.40
 qu, zhen - SW4O.6
 Qu, Zhibo - SW3J.5
 Quan, Xueling - JTh2A.64
 Quaranta, Fabio - SF1N.4
 Queralto Isach, Gerard - FM4B.3, JTh2A.46
 Quére, Fabien - SW3E.3
 Quesada, Nicolas - FTh4D.6
 Qui, Liangyu - JW2A.33
 Quinlan, Franklyn - SF2N.1, SW4G, SW4G.1
 Quinteiro, Guillermo - JTu2A.19
 Quraishi, Qudsia - JTu2A.22

R

- Ra, Yong-Ho - SF2O.3
 Rabinovich, William - JTh2A.53, SF21.1
 Rabl, Peter - JW4A.1
 Radulaski, Marina - FF3A.1, FM4A.4, SM2F.6
 Rafa, Muniyat - JTu2A.49
 Rafailov, Edik U. - ATu3P.6
 Raghunathan, Varun - JW2A.37
 Rah, Yoonhyuk - STh3O.2
 Rahimi Vaskasi, Javad - STh4N.1
 Rahman, B. M. A. - STh4H.2
 Raja, Archana - FW3M.5
 Raja, Arslan - STh1H.3, STh4J.2, STu3J.2, STu3J.4
 Rajala, Patrik - ATu3P.1
 Rakhman, Abdurahim - JW2A.120
 Ralph, Stephen E. - JTh2A.65, JTh2A.76, SM4G.4
 Ramachandra, Chaithanya - AW4I.4
 Ramachandran, Siddharth - STu3L.6, SW3H.1
 Ramamoorthy, Subramanian - AM1K.6
 Raman, Aaswath - FTh3C.3
 Ramey, Carl - SF1N.3

- Ramezani, Hamidreza - FW4D.6, JW2A.46
Ramirez, Jessica - JM3E.4
Rampur, Anupamaa - SM3L.5
Ramunno, Lora - FTu4C.4
Ran, Guangzhao - JTu2A.79
Ranc, Lucas - JM2E.2
Rand, Barry P.- SF1O.1
Rand, Stephen C.- STh4H.4
Randel, Emmett - SM3H.2
Ranély-Vergé-Dépré, Claude-Alban - SW4H.6
Ranta, Sanna - ATu3P.1
Rao, Ashotosh - SM3J.4
Rao, Ashutosh - STh1J.1
Rao, Yun Jiang - JTh2A.88, SF3L.3, STh3L.1
Rarity, John G.- SF3O.7, SM2F.2, STh1H.1
Raschke, Markus B.- FF3M.4, FM2C.1, FTh4C.2, SF1E.3
Rastegari, Ali - JM2E.5
Ratnayake, Dilan - JTh2A.45
Ratner, Daniel - SF3I.2
Ratté, Jesse - SF2G.5, SF3G.2
Rattenbacher, Dominik - FM1M.4, FM2A.5
Rauf, Benjamin - SM1F.3
Raval, Manan - STu3O.3, STu3O.4
Ray, Aniruddha - AM4I.3, ATu4K.3
Ray, Nathan - FTh1C.4, SF3G.7
Ray, Subir - JTu4M.5
Raybaut, Myriam - Ath3K.1, JTu2A.93, SF1H.3
Raza, Ali - STh1F.7
Razansky, Daniel - AM3I.3
Razskazovskaya, Olga - STh3F.5
Razzari, Luca - JTh2A.2
Reagan, Brendan - SM4E.4
Reboud, Julien - AM4I.3
Rechtsman, Mikael C.- FTu4B.4, FW3D.4, FW3D.6
Reddy K, Saikrishna - JW2A.71
Reddy, Dileep V.- FF1A.3
Reddy, Jay W.- AW4I.2
Reed, Graham T.- Ath3I.4, Ath3I.5, STu4O.1, SW3J.5
Reed, Zachary D.- SM2N.2
Rees, Albert V.- STu4N.4
Regan, Blake - SM2F.5
Rege, Abhishek - ATu4K.1
Regmi, Sabin - FW4M.2
Rego, Laura - FF2C.6
Reguzzoni, Mirko - JTu3G.1
Reid, Alexander - JTh4F.1, SF3I.7
Reid, Derryck - AM1K.6, AM2K.4
Reid, Eric - SF2I.6
Reid, Remington - FTh1M.3
Reig, Marc - SF2J.4
Reimann, Johannes - FTh1B.4
Reimer, Christian - FF2D.3, FTh1A.4, FTh1D.2, SF2J
Reines, Isak - JTh2A.57
Reinhardt, Ori - FF1F.6, FF3D.7
Reis, David A.- FM4M.6, JTu3M.5
Reiter, Doris E.- FM3D.4
Reithmaier, Johann Peter - SM2O.3
Reitzenstein, Stephan - STu4J.6
Remennik, Sergei - JTu2A.109
Remez, Roei - FTh4M.7
Ren, Guanghui - STh1H.7, STh1J.4
Ren, Hengjiang - STh4G.3
Ren, Jigang - FM4C.1
Ren, Jing - JW2A.107
Ren, Jinhua - FW4D.2
Ren, Juanjuan - JTu2A.121
Ren, Mengxin - JTh2A.21
Ren, Xiaoming - STh1E.1
Ren, Yongxiong - JTh2A.80
Ren, Yuhao - FF2B.5
Ren, Zhengqi - STh1E.3
Renaut, Claude - FM2C.6
Renger, Jan - FF3M.1, FM1M.4, FW3C.5
Renninger, William - SF3L, STh3L
Renninger, William H.- SF1L.3, SF1L.4, STh1L.3
Reno, John - FM2C.3, STh4O.3, STu4F.1, SW3N.5, SW4F.3
Rentschler, Eric - AM3I.4
Repington, Alain - FTh4D.6
Reschovsky, Benjamin - STh4G.1
Reshef, Orad - FF1B.3, FM3C.4, FW4B.5, SF1J.6
Residori, Stefania - JW2A.35
Restrepo, Diego - STu3H.3
Rewcastle, Cory - SW3L.4
Reznichenko, Bogdan - FM3A.2
Rho, Junsuk - FF2B.7
Rhoades, Ryan T.- SW4L.1
Rhodes, Daniel - FW3M.5, JTh4F.1
Ricci, Maria Antonietta - JW2A.116
Richards, Bryce - JTu2A.71
Richardson, Christopher - FM1M.3
Richardson, David - JW2A.44, SM2L.6, STh1E.3, STh1L.2, STh1L.4
Richardson, Martin - SF2O.8, SW4E.8
Richter, Marten - FW3M.4
Riedel, Robert - STh3E.3
Riedl, Hubert - SM4J.6
Rieker, Gregory B.- AF1K, AF3K, AW4K.1, SF1I.6
Riemsberger, Johann - SF2G.1
Rikimi, Shuichiro - STh1L.4
Ríos Ocampo, Carlos A.- SF2H.4
Ríos, Carlos - SM2J.2
Rishoj, Lars - STu3L.6
Ristow, Florian - SF2G.1
Ritchie, David - FM4C.6
Ritter, Martin - FTu4D.3
Rivas, Federico - SW4E.2
Rivenson, Yair - AM2I.3, AM2I.6, AM2K.3, ATu4K.6, JM3M.5, JTu2A.5, SF1N.2, SM4H.2, STu4H.2
Rivera, Nicholas - FF3D.7, FF3M.6
Rivera, Pasqual - FW3M.2
Roastamian, Ali - STh1F.6
Roberts, Gregory D.- AM4K.3
Roberts, John A.- FTh3C.7
Roberts, Samantha - SM2O.6
Robichaud, Louis-Rafaël - SF2L.1
Robinson, John - SM1F.1
Robinson, Joseph - JM1E.3, STu4E.6, SW4E.6
Robinson-Tait, Julian - Ath3K.2
Roccia, Emanuele - JW2A.116
Rochman, Jake - FM1A.4, FM1A.6, FM1A.7
Rode, Karsten - STu4F.6
Rodionov, Ilya - FM1M.5, FM1M.6
Rödjegård, Henrik - STh1F.3
Rodríguez, Alejandro - SF1H.7
Rodríguez, Brian - AM2I.5
Rodríguez, David - SM4H.4
Rodríguez, Joshua M.- AW3K.7
Rødt, Sven - STu4J.6
Roelkens, Gunther - STh4N.1, STu3N.2, STu4O.4
Roentgen, Malte - FM4B.7
Roger, Thomas - FM2M.1
Rogers, Steven D.- JTu3A.2, SM2J.5
Rohde, Felix - Ath3K.2, JTh2A.112, STu4L.4
Rohling, Hanna - Ath4K.7
Rojo-Romeo, Pedro - STh1J.6
Rolland, Antoine - SM1F.3, SW4F.6, SW4G.4
Romagnoli, Marco - STh3N.2, STh4N.2
Roman, Cosmin - STh3H.4
Romero Cortes, Luis - FTh1A.4, JW2A.71
Romero, Carolina - STh1E.5
Romero-García, Sebastian - Ath3I.3
Rong, Haisheng - SF2I
Rong, Yaoguang - JTh2A.56
Rong, Youying - JTu2A.111
Ronur Praful, Tejaswini - FTh4C.7
Roos, Goedele - ATu3K.6
Ropers, Claus - FF3M.2, FW4M.4
Roques-Carmes, Charles - FTu4C.2, SF1N.1
Rorrer, Gregory - ATu3K.7, JW2A.77
Ros, David - SW4E.3
Rosales, Ricardo - SM4N.7
Rosales-Guzman, Carmelo - FTh4B.8
Rosenberger, Philipp - FF2C.5
Rosenthal, Amir - SW3L.1, SW3L.2, SW3L.3
Roso, Luis - FF1C.4
Ross, Caroline - JM3B.4
Ross, James S.- FTh1M.7
Rossboth, Benedikt - SW3L.7
Rossi, Giulio Maria - FF2C.2, FF2C.3, SW3E.7, SW4E.4
Rossi, Massimiliano - FM1A.3
Rostami Fairchild, Shermineh - SW4E.8
Rostami, Saeid - STh1E.7
Rotermund, Fabian - SF3E.6
Roth, Bernhard - FF1D.4
Roth, Markus - JTu2A.68
Rothau, Sergej - JTh2A.105
Rothardt, Jan - SF1E.2
Rotter, Stefan - FTu3D.6, FTu4B.2
Rottwitt, Karsten - SW3H.1
Rotundu, Costel R.- FM4M.6
Roukes, Michael L.- Ath4I.4, SM4H.6
Rout, Sangeeta - FTu3D.4
Roxworthy, Brian - SF2I.1
Roy, Shounak - SM4H.2
Rozeza, Lee A.- FF3D.2, FM2M.7, FTh4A.3
Rozhin, Aleksey - JW2A.38
Roztock, Piotr - FTh1A.4
Ru, Qitian - FF3D.5, SF1H.1, SF1I.2, STh3J.6
Ruan, Qifeng - SM1J.6
Ruan, Yinlan - STh3L.3
Ruan, Zhichao - FTu4C.1
Rubenchik, Alexander - AW3I.5
Rubin, Noah - AM3K.3, FM3C.2
Rubio, Angel - FF2C.2, SW3E.7
Rückmann, Max - FTh4A.4
Rudra, Alok - FTh3D.3
Ruff, Edward C.- SF2O.6
Rugar, Alison E.- FF3A.1, FM4A.2
Ruggiero, Ludovica - JW2A.116
Ruggiero, Michael T.- STu4F.2
Rustorfer, Daniel - FW3C.7, SM4J.6
Runcorn, Timothy H.- SM3L.4
Ruocco, Alfonso - Ath4I.2, SW4G.6
Ruskuc, Andrei - FM1A.4, FM1A.6
Russsbueldt, Peter - JM1E.4
Russell, Philip S.- FTh3B.1, FTh3B.3, SF1E.6, STh1L.1
Russo, Mattia - FW3M.4
Rust, Laura - STh4E.2
Rüter, Christian E.- FTh4B.2
Ruth, Hanna G.- FW3M.2, SM4F.4
Rutkauskas, Marius - AM1K.6, AM2K.4
Rybin, Mikhail - FF3B.6
Ryckman, Judson - JTh2A.52
Ryf, Roland - SM1G.1, SM1G.2
Ryou, Albert - JTh2A.47, STu4J.4
Ryzhikov, Ilya - FM1M.5, FM1M.6
- S**
- S M, Shiva N.- JW2A.20
S, Asokan - JW2A.84
Saad-Bin-Alam, Md - FM3C.4
Sacher, Andreas - Ath3K.7
Sacher, Joachim R.- Ath3K.6, Ath3K.7, Ath4K.7
Sacher, Wesley D.- Ath4I.4, SM4H.6
Sadiek, Ibrahim - SW3L.5
Sadri Moshkenani, Parinaz - JTu2A.51, JW2A.60
Sadzak, Nikola - FM4A.5
Safaei, Reza - JTh2A.2
Safavi-Naeini, Amir - Ath3I.6, FM4A.4, JW4A.4, SF2J.6
Saggio, Valeria - FM2M.7, FTh4A.3
Sagnes, Isabelle - FM1M.1, FM3A.2
Saha, Gareeyasee - JTh2A.76
Saha, Soham - FM1M.5, FM1M.6, JTh2A.40
Sakib, Marc - JM3E.2
Saini, Thai Singh - JW2A.109
Saini, Than Singh - JW2A.93
Saito, Shuto - JW2A.92
Saito, Takeshi - JW2A.98
Saitoh, Koh - SF1E.5
Sakakibara, Youichi - JW2A.92, JW2A.98
Sakakura, Masaaki - ATu4I.4
Sakib, Nazmul - JTh2A.52
Sakotic, Zarko - FW4D.5
Sakr, Hesham - STh1L.4
Salamin, Yannick - SF3N.1, STh4N.4
Salary, Mohammad Mahdi - FF1B.2
Salas-Montiel, Rafael - SM2H.7
Saleh, Bahaa - AM3I.2
Salganskii, Mikhail - SM4L.1
Salim, Evan A.- JTu3G.2
Salkeld, Alexander J.- STh4H.4
Salman, Jad - SM2H.6
Saltarelli, Francesco - SF3E.3
Samanta, Goutam - FTh1B.6, FTh4B.6, JW2A.68
Samartsev, Igor - JTu2A.95
Samolis, Panagis - ATu3K.2, SM3H.5
San Román, Julio - FF2C.6
Sanabria, Jorge - ATu4I.5, JM3E.3
Sanchez, Enrique - AW3P.2
Sander, Michelle Y.- ATu3K.2, SM3H.5, SW4H.6
Sandner, Fabian - FTh4C.3
Sandoghchi, Seyed Reza - SM2L.2, STh1L.2, STh1L.4
Sandoghdar, Vahid - FF3M.1, FM1M.4, FM2A.5, FW3C.5
Sandoval, Oscar - FTh1A.2
Sanford, Norman - SF2G.6
Sangalli, Davide - FW3M.7
Sangwongngam, Paramin - SM2G.5
Sankey, Jack - FF4A.6
Santagati, Raffaele - JTu2A.124, SM2F.2
Santiago, Svetta Reina Merden S.- JTu2A.112
Santiago, Tomas - JTu2A.44
Sapienza, Riccardo - FF2B.3
Sapp, Adam - SM3H.5
Sappey, Andrew D.- Ath4K.5
Sapra, Neil - FF3A.1, JTh2A.67, SF2H.7, SM3J.2
Sarabalis, Christopher J.- SF2J.6
Saraceno, Clara - STh1E
Sarangan, Andrew - SF2O.5, SF2O.6
Sarantoglou, George - JTu2A.74
Sarihan, Murat C.- FTh1A.3, FTh1D.6
Saripalli, Ravi - FTh1B.6
Sarkar, Swagato - JW2A.119
Sarma, Raktim - FW4B.1
Sarpkaya, Ibrahim - STh3O.6
Sartorius, Thomas - JM1E.4
Sasaki, Satoshi - SM4J.3
Satija, Aman - FTu4D.1
Sato, Hikaru - FM2C.5
Sato, Shunichi - FTh4B.5, SF1E.5
Satoh, Takuya - FM3D.3

- Savage, Donald - STh4O.3
 Savage, Martin J. - FTh3A.6
 Savchenkov, Anatoliy - FF1D.7, SF2H.6, STh4J.7
 Sbroscia, Marco - JW2A.116
 Scalari, Giacomo - SW4F.2, SW4N.4
 Scallo, Alec - FTu4B.7
 Scalora, Michael - FW4B.1, FW4B.7
 Scarabel, Jordan - JTu2A.32
 Scelle, Raphael - JM3E.2
 Schaake, Jason - AF3K.3
 Schade, Anne - STu4O.6
 Schade, Wolfgang - ATH3K.6
 Schäffer, Christian G. - FTh4A.4
 Schaffer, Stephan - SM1F.1
 Schall, Johannes - STu4J.6
 Schaller, Richard - FM4D.7
 Schares, Laurent - STh1F.2
 Scharner, Erik - STh3L.3
 Scheel, Stefan - FF1F.5, FTu3B.3
 Scheiba, Fabian - FF2C.3, SW3E.7, SW4E.4
 Scheidegger, Philipp - AM1K.3
 Schepers, Florian - JTu2A.61, JTu2A.69
 Schepler, Kenneth L. - JTh2A.98
 Scherer, James - AM2K.5
 Scheuer, Jacob - AF3K.2, JTu2A.71, SF2J.2, SM1L.2
 Scheuermann, Julian - AW3P.1
 Schibli, Thomas R. - SW4G.3
 Schiepel, Philipp - JTh2A.100
 Schilling, Ryan - FM1A.1
 Schilt, Stéphane - SW4G.5, SW4N.5
 Schima, Susan - SM3F
 Schiminovich, David - SM1O.2
 Schimmel, Guillaume - JM2E.5
 Schimpf, Damian - JTu2A.105
 Schirmel, Nora - STu4E.4
 Schirmer, Matthias - JTu2A.12
 Schlaepfer, Florian - FF2C.1
 Schlarb, Holger - SF3I.5, SF3I.6
 Schlauderer, Stefan - FTh1B.2, FTh1B.4, JTh4F.2, JTu4M.2
 Schliesser, Albert - FM1A.3
 Schmelcher, Peter - FM4B.7
 Schmid, Christoph P. - FTh1B.2, FTh1B.4, JTh4F.2, JTu4M.2
 Schmid, Heinz - SM3J.1
 Schmid, Silvan - JW2A.62, SW3L.7
 Schmidgall, Emma - SF1H.7
 Schmidt, Anna - Ath4K.4
 Schmidt, Bruno E. - JTh2A.2, SW4E.1
 Schmidt, Christian - SF3I.5
 Schmidt, Florian M. - SM2N.5
 Schmidt, Holger - STu3H.2, STu3H.4
 Schmidt, Markus - SM2L.1
 Schmidt, Marvin - JW2A.18
 Schmidt, Michael - ATu3I.1
 Schmidt, Peter - FTu3C.3
 Schmidtmann, Sebastian - Ath4K.7
 Schmiedeke, Paul J. - SM4J.6
 Schmiegelow, Christian T. - JTu2A.19
 Schmitt, Nora - FM4B.7
 Schmitt, Simon - SM2F.2
 Schmittberger, Bonnie L. - JTu2A.123
 Schmitt-Sody, Andreas - FTh1M.3
 Schnauber, Peter - STu4J.6
 Schneider, Christian - FM1M.7, STh1H.1
 Schneider, Christina - JTu2A.12
 Schneider, Harald - STu3F.3
 Schoeche, Stefan - FTh3C.7
 Schoenhardt, Steffen - STh1H.7
 Schori, Aviad - FF1A.7
 Schott, Rüdiger - FTh3D.2
 Schoun, Stephen B. - FF3C.1
 Schow, Clint - STh4N.3
 Schroeder, Carl - SF3I.1
 Schröder, Tim - FM3D.1
 Schubert, Elise - JM2E.5
 Schüller, Christian - FW3M.1, JTu4M.2
 Schulte, Jan - JM1E.4
 Schulz, Michael - STh3E.3
 Schulz, Sebastian - SF3I.5, SF3I.6
 Schülzgen, Axel - SM4L.3, STh3L.2
 Schunemann, Peter G. - FTh1D.5, SF1H.1, SF1H.5, SF1H.6, STh4E.5, STh4E.6, SW4L.1
 Schust, Matthias - SM4E.1
 Schütz, Gerhard - SW3L.7
 Schwab, Keith - FM1A.7
 Schwallier, Joel M. - SW4L.2
 Schwartz, Robert - FTh1M.3
 Schwartz, Tal - FM3D.8
 Schwarz, Ariel - Ath3K.5
 Schwarz, Benedikt - FM1D.3, STh4H.3, STu4O.6
 Schweinberger, Wolfgang - AF3K.5, JW2A.69, STh4E.4
 Schweinsberg, Aaron - FM4M.2, JTu2A.87
 Schweistal, Simon - SM4E.1
 Sciancalepore, Corrado - SF3H.2, STh1J.6
 Sciarra, Stefania - FTh1A.4
 Sciarrino, Fabio - FM1M.1
 Scopelliti, Matteo Giuseppe - SM4H.5
 Scott, Ryan - SM1G, SM4G
 Searles, Thomas - FM2C
 Sebastian, Abu - SM2J.2
 Sebastian, Suneetha - JTh2A.95
 Sebbag, Daniel - STh1E.2
 Sebbag, Yoel - JW2A.110
 Sebban, Stephane - SF3I.3
 Secareanu, Radu - SW4E.3
 Seddon, Angela - SF2L.4
 Seer, Ali - STu4L.4
 Segev, Eran - Ath4I.4
 Segev, Mordechai - FF3B.1, FM1C.4, FTu3D.1, FW3D.2, FW3D.7
 Segev, Moti - FTu4B.1
 Seidler, Mathias A. - FM2A.3, JTu2A.24
 Seifke, Thomas - STh4E.4
 Sekikawa, Taro - FF3C.5
 Sekine, Norihiko - SM2H.5, SW4F.4
 Seletskiy, Denis - FM3D.4, FM4D, FW4M.3, SF2E.2
 Selig, Malte - FW3M.1, FW3M.4
 Sellmer, Christian - JTu2A.12
 Selvaraj, Ramya - JW2A.20
 Semenenko, Henry - FM4C.4
 Semmlinger, Michael - FF2B.4
 Semnani, Behrooz - FM1B.1
 Senellart, Pascale - FM1M.1, FM3A.2
 Seng, Yue Men - JW2A.89
 Senna Vieira, Francisco - SM2N.5
 Sensale Rodriguez, Berardi - AM4K.5, JTh2A.118
 Sentz, Tyler - FTu3D.3
 Seo, Dongjea - SM1O.2
 Seo, Meenkyo - JM2E.4
 Seo, Minah - STu3F.2
 Seo, Seung Young - FM2D.5
 Septriani, Brigitta - FM2M.2
 Sergachev, Ilia - SW4N.4
 Sergeant, Sylvain - SM4J.3
 Sergeev, Anton - SF2J.4
 Sergeev, Sergey - JW2A.38
 Sergienko, Alexander V. - FTh1A.5
 Serkland, Darwin - JTh2A.57
 Serna, Rosalia - JTu2A.46
 Serres, Josep - JTu2A.119, SF3E.6
 Seshadreesan, Kaushik P. - FTh4A.5
 Seshadri, Suparna - JTu3A.5
 Set, Sze Y. - AF1K.5, JTh2A.85, JW2A.94, SF1L, SF3O.1, SF3O.4, SM1L, STu3L.5
 Setzpfandt, Frank - FW3B.1, JTh2A.75
 Sevison, Gary A. - SF2O.5, SF2O.6
 Shabahang, Soroush - Ath11.6, JTh2A.98
 Shadrivov, Ilya - FF1B.4, SW3F.5
 Shafak, Kemal - JTh2A.100
 Shah, Deesha - FM1M.5, FM1M.6
 Shahabuddin, Mohammad - JW2A.59
 Shahbazmohamadi, Sina - ATu4I.2
 Shahbazyan, T. - FTu3D.4
 Shahin, Mahmoud - STh4N.1
 Shahriar, Selim M. - Ath1K.3, JTu2A.60, JW2A.13
 Shahrokhshahi, Reihaneh - FF1A.6, FTh4D.6
 Shahsafi, Alireza - SM2H.6
 Shainline, Jeff - STh1N.3, SW3J.4
 Shaked, Natan T. - AM1I.3
 Shaker, Chandra - JW2A.1
 Shakoor, Abdul - JTh2A.74
 Shalaev, Vladimir M. - AM3K.1, FF2A.6, FM1M.5, FM1M.6, FTh1C.2, FTh3C.2, JTh2A.119, JTh2A.40, JW2A.55, JW2A.58, JW2A.63
 Shaltout, Amr - FW4D.3
 Shamim, Md. Hosne Mobarok - SM3N.5
 Shams-Ansari, Amirhassan - FTh1D.2, SF2J.1
 Shan, Lingxiao - JW2A.54
 Shandilya, Prasoon Kumar - SF1J.3
 Shaner, Eric - STh4O.4
 Shang, Chao - JW2A.102, STu4L.7
 Shang, Chen - STh3N.7, STu3N.1, STu4J.3
 Shao, Xiaodong - JTh2A.104, SW3G.5
 Shao, Xiaopeng - JTu2A.10, JTu2A.14
 Shapira, Niv - FTh4M.7
 Shapiro, Jeffrey H. - FTh1A.3, FTh4A.2
 Shappir, Joseph - FTh1C.3, JTh2A.49
 Sharabi, Yonatan - FF3B.1
 Shardlow, Peter - JW2A.44
 Sharif Azadeh, Saeed - SF1G.4
 Sharifzadeh, Sahar - SM3H.5
 Sharizal Alias, Mohd - JTh2A.51
 Sharma, Andrei P. - FM2C.3
 Sharma, Sakshi - FM2M.2
 Sharma, Varun - FTh4B.6
 Sharp, Oliver - STu4O.7
 Shastri, Bhavin J. - JM3M.3, SM3N.3, SW3H.7
 Shautsova, Viktoryia - FTh3C.5
 Shaw, Brandon - STu3J
 Shaw, Jonah - SF1E.4
 Shaw, Justin - FF2C.6, FF2C.7
 Shawrav, Mostafa - JW2A.62
 She, Alan - STh1O.5
 Sheffer, Yarden - JTh2A.8
 Shehzad, Atif - SW4N.5
 Sheik-Bahae, Mansoor - JTu2A.78, STh1E.7
 Sheina, Svetlana G. - SF3O.8
 Sheintop, Uzziel - STh1E.2
 Shekhar, Sudip - ATu4K.5
 Shelby, Isaac - AM4I.1
 Shemer, Keren - SM1N.2
 Shen, Boqiang - AF2K.1, SF2J.5
 Shen, Chao - SM3N.4
 Shen, Deyuan - SF3E.6
 Shen, Hui - JW2A.95
 Shen, Ji-Lin - JTu2A.112
 Shen, Jung-Tsung - FTh3A.4, FTu3B.6
 Shen, Kun-Ching - FTh4M.2
 Shen, Lei - SM2L.4
 Shen, Lijiong - FM4C.8
 Shen, Lingjia - SF3I.7
 Shen, Qi - FM4C.1, JTu2A.92, STh3G.5
 Shen, Qixin - JTu3M.4
 Shen, Xiaoqin - JW2A.51
 Shen, Xiaozhe - JTh4F.1
 Shen, Yichen - FTu4C.2, SF1N.1
 Shen, Zhean - FM1C.2
 Shen, Zhengzheng - JW2A.3
 Shen, Zhi-Xun - FM4A.4, STu4F.7
 Shendre, Sushant - JTu2A.77
 Sheng, Aiguo - JW2A.47
 Sheng, Quan - SM1L.3
 Sheperd, Jason - AM2I.5
 Shepherd, David - JW2A.44
 Sherman, Jeff A. - SM1F.1, SW4G.1
 Sheu, Jinn-Kong - SM3N.2
 Shevrydyayeva, Galina S. - SF3O.8
 Shi, Bei - JTu2A.82
 Shi, Bin - SF1N.5
 Shi, Binglei - FTu4C.5
 Shi, Chaodu - SM1L.3
 Shi, Cheng - JTh2A.26
 Shi, Fan - STh3L.4
 Shi, Fu-Long - FM4B.8
 Shi, Haosen - SF1H.2
 Shi, Jiping - JTu2A.118
 Shi, Jiawei - JTu2A.89
 Shi, Jin-Wei - Ath1K.4
 Shi, Liping - JTh2A.5
 Shi, Wei - JTh2A.44, JTh2A.90, JW2A.57, SM1L.3, STh3H.2
 Shi, Xingyuan - FM2C.2
 Shi, Yu - FM1C.7, JF3F.2, SW4J.5
 Shi, Yuhang - JW2A.67
 Shibuya, Kyuki - JTh2A.101
 Shields, Andrew - FM2M.1, FM4C.6
 Shields, Taylor - JTu2A.41
 Shih, En-Min - SM1O.2
 Shih, Min-Hsiung - SF3J.4, SM1H.6
 Shim, Bonggu - JTh2A.4, JTh2A.7, JTu2A.58
 Shim, Euijae - SF3N.5
 Shim, Hyungki - FM1C.3
 Shim, Wooyoung - FM2D.4
 Shimizu, Hiromasa - JTh2A.96
 Shimizu, Kenji - JTu2A.32
 Shimogawa, Michelle M. - ATu4K.2
 Shimura, Keisuke - SM4N.3, SM4N.4
 Shin, Dong-Chel - SW4G.7
 Shin, Junghoon - STu3E.2
 Shin, Min C. - STu3J.5
 Shin, Min Chul - SF3N.5
 Shin, Sungkwon - ATu3I.6
 Shinbrough, Kai B. - FM2A.6, FTh3D.4
 Shindo, Koyoshi - SM4H.2
 Shinohara, Hisanori - SF2G.2
 Shinozaki, Ryo - SF3G.4
 Shinya, Akihiko - JTh2A.58, JW3A.5, SM2J.6, SM4J.3
 Shiraiwa, Masaki - SM2G.1
 Shiri, Abbas - Ath11.6
 Shitikov, Artem E. - STu3J.4
 Shivaram, Niranjan - FF2C.5
 Shkarin, Alexey - FM1M.4, FM2A.5
 Shoji, Yuya - JTh2A.27
 Shoman, Hossam - ATu4K.5
 Shotan, Zav - FF3A.3
 Shou, Jingwen - JW2A.83, STu4H.6
 Shrestha, Sajjan - FF2A.3, FF2A.5, FF2B.8, FTh3M.5, STh3H.1
 Shrestha, Vivek R. - JTu2A.48, SF2H, SW3J.2
 Shterengas, Leon - SM3N.7
 Shtyrkova, Katia - Ath4I.2
 Shu, Chester - STh3N.3, SW3O.3
 Shu, Fang-Zhou - JTh2A.38, STh1O.2
 Shu, Hong - AW3P.2
 Shuai, Wang - SM4F.5
 Shum, Perry Ping - JW2A.108
 Shumakova, Valentina - FF1C.2
 Shuman, Timony M. - JW2A.12
 Shutts, Samuel - SM3N.6
 Shwartz, Sharon - FF1A.7
 Si, Jiangnan - SM1J.4

- Siahmakoun, Azad - SM2O.1
 Sibson, Philip - FM4C.4
 Siddiqui, Aleem M. - JTu2A.96
 Sidelnikov, Oleg - FTh3B.4, STh4L.2
 Siders, Craig - SM4E.4, SM4E.6
 Sidharthan, Raghuraman - JW2A.89
 Sidhu, Sachdev - AM4I.7
 Sidiropoulos, Themistoklis - FTh3C.5
 Sidorenko, Pavel - STh4L.3
 Sie, Edbert - JTh4F.1, STh3F
 Siefke, Thomas - JW2A.69
 Siemens, Mark - FF3D.4, FM3D.1, JW2A.31, JW2A.48, STu3H.3
 Sigler, C. - SW3N.3
 Sikdar, Debabrata - FM3C.5
 Silberhorn, Christine - FTh1A.1, JTu3A.1, SM3O.4
 Šiler, Martin - SM2L.1
 Sillard, Pierre - SF1M.4, SM1L.1
 Silva, Rui - FM4M.5
 Silver, Joel A. - AM1K.5
 Silver, Jonathan M. - JM3B.3, SF3H.5, STh3J.7
 Silverman, Kevin - FM4D.5
 Simmons, Evan L. - FTh4M.5
 Simon, David - FTh1A.5
 Simonds, Brian - ATH1K, ATH3K, ATH4K
 Simons, Matthew - SM3F.3
 Sims, Christopher - FW4M.2
 Sims, Ryan - JTu2A.96
 Sin, Yongkun - SW3N.3
 Sinatra, Lutfan - SM3N.4
 Sinclair, Laura C. - SM1F.1, SM4F, STh3G.2, STh3G.3
 Sinclair, Martin - STu4O.7
 Sinclair, Michael B. - FF2B.2, FM2C.3
 Singamaneni, Srikanth - JW2A.61
 Singer, Matthew H. - ATH11.2, ATH11.7
 Singh, Abhishek - STu3F.3
 Singh, Amit - FTh1C.6
 Singh, Anshuman - FM1M.7, STu4J.6
 Singh, Gurjit - JW2A.17
 Singh, Navab - AW4K.5, JTh2A.34, SF3J.6, STh1O.4, SW3F.6
 Singh, Neetesh - Ath4I.2, SW4G.6
 Singh, Niharika - FM2A.4
 Singh, Rajan - STh4G.7
 Singh, Ranjan - JTu2A.99, SW3F.5, SW3F.6
 Singh, Sakshi - STh4L.5
 Sinobad, Milan - FF2D.8
 Sipe, John E. - FM1D.5, FTh1A
 Sirica, Nicholas - FM2D.2
 Sisler, Jared - SF3J.5
 Sistrunk Link, Emily - SM4E, SM4E.6
 Sistrunk, Emily F. - SM4E.4
 Siva, Vantari - AW3I.2
 Sivan, Uri - FTu3D.1
 Sivashanmugan, Kundan - ATu3K.7, JW2A.77
 Siverns, James - JTu2A.22
 Sivos, Murat - FW4M.4
 Siwick, Bradley J. - FF3C.6
 Sjaardema, Tracy - STh1J.1
 Skarda, Jinhie L. - JTh2A.67, SW4J.3
 Skiba-Szymanska, Joanna - FM4C.6
 Skirtach, Andre - STh1F.7
 Skontranis, Menelaos - JTu2A.74
 Skoric, James - JW2A.121
 Skrodzki, Patrick J. - FTh1M.6, JTh2A.84, JTu2A.56, SF2G.7, SW4L.4, SW4L.5
 Slavik, Radan - SM2L.2, SM2L.6, STh1L.2, STh1L.4
 Sloan, Jamison - SF3N.7
 Sloyan, Karen - SM2L.3
 Sludds, Alex - JF2F.5
 Smallwood, Christopher L. - FM3D.1, SM4F.4
 Smayev, Michail P. - STh1E.6
 Smirnov, Vadim - SF1H.3
 Smirnova, Daria - FM1B.4, FW4B.3, FW4B.4
 Smirnova, Olga - FM4M.5
 Smith, Brad - SF11.7
 Smith, Braden - AW3K.7
 Smith, Brian J. - JTu3A.4
 Smith, Christopher - JW2A.66
 Smith, Daniel - SM4E.6
 Smith, David - ATu3K.5
 Smith, Steve - SW4E.6
 Smith, Thomas R. - ATu3I.2
 Smith-Dryden, Seth D. - AM3I.2
 Smolski, Viktor O. - STh4E.3, STh4E.6
 Smolyaninov, Alexei - AM4I.6
 Smowton, Peter - SM3N.6
 Smyth, Frank - JTh2A.63
 Soavi, Giancarlo - FW3M.4, FW3M.7
 Sobhanan, Aneesh - JTh2A.83
 Sobon, Grzegorz J. - JTh2A.113
 Sobota, Jonathan A. - FM4M.6
 Soci, Cesare - FTu3D.7
 Socquet-Clerc, Carole - SF3H.2
 Sofer, Sason - FF1A.7
 Sogawa, Tetsuomi - SW4G.2
 Sohlström, Hans - STh1F.3
 Sohn, Donggyu B. - JTh2A.54
 Soifer, Hadas - FM4M.6
 Sojka, Lukasz - SF2L.4
 Sokolowski-Tinten, Klaus - SF2G.3
 Solanki, Amit - SM4J.5, SW3J.3
 Solanki, Ankur - JTu2A.99
 Solanki, Kaushal - AW4I.4
 Solis, Javier - JTu2A.46, SF3G.5
 Soljagic, Marin - FTu4C.2, JF2F.5, SF1J.1, SF1N.1, SF3N.7
 Solntsev, Alexander - JTh2A.75, SM2F.5
 Solomon, Glenn - FM4A
 Solomon, Joel M. - SM3H.4
 Soltani, Mohammad - SF2I.6
 Solyom, Adrian - FM4A.6
 Soman, Anishkumar - FTh4C.4, FTu4B.7, JTu2A.118, SF3O.5, SM1J.2
 Somaschi, Niccolo - FM1M.1, FM3A.2
 Sommer, Bernd - JTu2A.12
 Son, Myungwoo - FM2D.5
 Sonderhouse, Lindsay - SM1F.1
 Song, Alex - FM1C.7
 Song, Bowen - JTu2A.82
 Song, Daohong - FTh4B.7, FW3D.3
 Song, Hansung - AW3I.2
 Song, Hao - FW4B.5, JTu2A.57, JTu2A.67, SM1J.5, SM1N.5
 Song, Haomin - Ath11.2, Ath11.3, Ath11.7, SM1H.5, STu4O
 Song, Haoqian - JTu2A.57, JTu2A.67, SM1J.5, SM1N.5
 Song, Hyerin - JTu2A.7
 Song, Maowen - JW2A.58
 Song, Meiting - Ath3I.2
 Song, Minho - STu4H.7
 Song, Minhyup - JTu2A.11
 Song, Minje - JTu2A.11
 Song, Qinghai - JTh2A.69
 Song, Yingxiong - SM1G.2
 Song, Youjian - JTh2A.103, SF1H.2, SF3E.1, STh1G.6, STh3L.6, STh4E.1, SW3E.5, SW3H.6
 Song, Young Min - AW3I.2, FTu4D.5, JW2A.16, JW2A.6
 Song, Yunheung - FM2A.7, FM2A.8
 Sontheimer, Bernd - FM4A.5
 Soon, Aloysius - FM2D.5
 Soref, Richard - AW3P.3, STh4O.6, STu3N.3
 Sorel, Marc - FW3B.3, STh1N.2
 Sorger, Volker J. - FTu3B.7, JTh2A.45
 Sorianello, Vito - STh3N.2, STh4N.2
 Sorin, Fabien - STh1O.3
 Sorin, Wayne - SM4J.7
 Sorokin, Evgeni - STh1E.6
 Sorokina, Irina T. - STh1E.6
 Sorrentino, Fiodor - JTu3G.1
 Soskind, Michael G. - AM1K.2, JW2A.5
 Sotor, Jaroslav - AF2K.8, JTh2A.113, SF11.4
 Sounas, Dimitrios - FTh3M.2, JM2B.3
 Sousa, Marilyne - SM3J.1
 Spagele, Christina - AM3K.3, FM3C.2
 Speirs, Rory W. - JTu2A.123, JTu2A.37
 Spektor, Grisha - FTh1C.7
 Sperrhake, Jan - JTh2A.24
 Spielmann, Christian - SF3I.3
 Spiess, Christopher - SF1L.3, SF1L.4
 Spiniolas, Ryan - FTh3D.4
 Spinka, Thomas - SM4E.4, SM4E.6
 Spitz, Olivier - SW3N.2, SW3N.6
 Spitzner, Laurens - FM3D.6
 Splain, Zach - JW2A.14
 Squier, Jeff - AM2I.4
 Squire, Kenneth - ATu3K.7, JW2A.77, STu4H.4
 Sriarunothai, Theeraphot - FTh3A.2
 Sridhar, Niranjan - FF1A.6
 Srinivasan, Balaji - JTh2A.82
 Srinivasan, Kartik - FF2D.6, FM1M.7, JTu2A.86, SM3J.4, SM3O.6, STh1G.2, STu4J.6
 Srivastava, Manas - JTh2A.82
 Srivastava, Yogesh K. - JTu2A.99, SW3F.5
 Stabile, Ripalta - SF1N.5
 Staffa, Jeremy - SM2J.5
 Staif, Joseph A. - JTu2A.109
 Staliunas, Kestutis - FF2D.4, SF3J.7
 Stambaugh, Alexandra - STu3H.2
 Stamenov, Plamen - STu4F.6
 Stanfield, Paul - JTu2A.96
 Stanicki, Badrudin - AM1K.3
 Stanislauskas, Tomas - STu4E.2
 Staniszewski, Przemyslaw - JTh2A.111
 Stankovic, Stevan - SW3J.5
 Stanley, Joel - FTh1M.7
 Stanton, Eric J. - SF3H.3, SM3O.5, SW3J.4
 Starbuck, Andrew - JTh2A.39, STh4N.6
 Starke-Bowes, Ryan - FTu4D.1
 Starshinov, Ilya - FM1C.5
 Stassen, Erik - STh1J.5
 Staude, Isabelle - FM2C.3, FW3B.1, JTh2A.24, STu1O.1
 Staudinger, Philipp - SM3J.1
 Stefszky, Michael - SM3O.4
 Stegenburgs, Edgars - Ath11.2, JTh2A.51
 Steidle, Jeffrey A. - FTh1D.4
 Stein, Aaron - SM3N.7
 Steinbrecher, Gregory - FF1F.2
 Steiner, Johannes T. - JTh4F.2, JTu4M.2
 Steinert, Michael - FTh1C.6, FW3B.1
 Steinhaus, Tim - JW2A.18
 Steinkopff, Albrecht - JM3E.1
 Steinleitner, Philipp - FW3M.1
 Steinmeyer, Günter - FF1D.4, SW3E.5, SW3H.2
 Stenger, Nicolas - FTu3C.4
 Stepanenko, Yuriy - SF3E.2, SM3L.5
 Stepniewski, Grzegorz - SM3L.5, STh1L.5
 Sterczewski, Lukasz A. - SF11.4, SF11.5
 Sterr, Uwe - JTh2A.112, SM1F.3
 Stettner, Thomas - FW3C.7, SM4J.6
 Stevens, Martin - FTh4D
 Stevenson, R. Mark - FM4C.6
 Stevenson, Sarah A. - STh3G.2, STh3G.3
 Stievater, Todd H. - JTh2A.53, SF2I.1, SW3L
 Stiles, Matthew J. - STu4F.1
 Stiller, Birgit - FW3B.2
 Stobbe, Søren - FTh3D.2
 Stockman, Mark - JTu4M.3
 Stöferle, Thilo - SM3J.1
 Stoian, Razvan - SM3H.3
 Stojanovic, Vladimir - JW2A.78, JW2A.81
 Stone, Jordan - STh3J.3
 Storey, Emily E. - STu4H.1
 Störmer, Michael - FTu4D.3
 Stott, Matthew - STu3H.4
 Strain, Michael - FW3B.3, SW3H.5
 Stranks, Samuel - SF1O.3
 Strasser, Gottfried - STu4O.6
 Streed, Erik W. - JTu2A.32
 Strizhevsky, Edward - FF1A.7
 Strzembeg, Teodor - FTh4A.3
 Stroud, Jasper R. - JW2A.79
 Stützer, Robert G. - AW3I.7
 Su, Jie - FTh3D.5
 Su, Logan - FF3A.1, JTh2A.67, SM3J.2
 Su, Qianqian - FF1C.5
 Su, Vin-Cent - FTh3M.3
 Su, Yabei - JTh2A.104
 Su, Yiwen - SF1J.2
 Su, Zhan - SW4G.6
 Subbaraman, Harish - SM1J
 Suchowski, Haim - AF2K.6, FTu4C.3, JTu3M.3
 Suda, Akira - SW4E.7
 Südmeyer, Thomas - SF3E.4, STh3F.5, SW4G.5, SW4N.5
 Suga, Hayato - STu3L.4
 Suganuma, Takahiro - SM3G.4
 Sugavanam, Srikanth - STu3L.7
 Sugimura, Takeaki - SM4H.1
 Sugita, Atsushi - FM2C.5
 Sugiyama, Takahiro - SM4N.2
 Suh, Myoung-Gyun - FTu3B.1, STh4J.3
 Sui, Jingyang - AM4I.4, STh4O.1
 Sujeci, Slawomir - SF2L.4
 Sukhorukov, Andrey A. - FF3A.7, JTh2A.17, JTh2A.75
 Sullivan, Brian - FM3C.4
 Sulzer, Philipp - SF2E.2, STu4L.5
 Sum, Tze C. - JTu2A.99
 Sumetsky, Misha - JTh2A.50
 Sumikura, Hisashi - JW3A.5
 Sun, Changzheng - JTu2A.90, SW4N.7
 Sun, Fujun - JW2A.9
 Sun, Fuyu - Ath1K.6
 Sun, Greg - AW3P.3, STh4O.6, STu3N.3
 Sun, Hao - FM4D.4, STh3O.1
 Sun, Jie - STh3O.3
 Sun, Liqun - JTu2A.4
 Sun, Qian - FF2B.5
 Sun, Qi-Chao - FTh3A.5
 Sun, Qizhen - ATu4K.7, JW2A.100, JW2A.23, JW2A.91
 Sun, Shulin - JTh2A.11
 Sun, Shuo - FF3A.1, FM4A.2, FM4A.4, JM2B.5, SM2F.6
 Sun, Sining - AW3I.6
 Sun, Xiankai - AF2K.7
 Sun, Xu - SF1G.4
 Sun, Yangyang - STh3L.2
 Sun, Yanting - SW4N.4
 Sun, Yi - SF2I.6
 Sun, Yizhi - SM2H.7
 Sun, Yuezhen - JW2A.23
 Sung, Jae Hee - STu3E.2
 Suresh, Mallika I. - SF1E.6
 Suslov, Dmitry - AW3I.7
 Šušnjar, Peter - SW3E.2
 Sutherland, James S. - JTu2A.58
 Sutter, Dirk H. - JM3E.2
 Suttinger, Matthew - AW3P.2
 Suzuki, Ryo - STh4J.6

- Suzuki, Takenobu - JTu2A.91, JW2A.109, JW2A.93, JW2A.96
 Svaluto Moreolo, Michela - SW4O.5
 Sveta, Andreas - JM3B.3, SF3H.5, STh3J.7
 Swadling, George F. - FTh1M.7
 Swaim, Jon D. - FTh1M.1
 Swann, William C. - SM1F.1, STh3G.2, STh3G.3
 Sweeney, Frazer - AM2K.4
 Swenson, Nicolas - FM4M.7
 Sydlo, Cezary - SF3I.5
 Sykora, Milan - FTu4D.2
 Sylvestre, Thibaut - STh1L.5
 Szameit, Alexander - FF1F.5, FF3A.7, FM1C.6, FM4B.2, FM4B.3, FM4B.7, FTu3B.3, FTu4B.3, FW3D.5, FW3D.8
 Szczepanek, Jan - SF3E.2
- T**
 Tadesse, Getnet - SF1E.2
 Tagkoudi, Eirini - STh1F.4
 Taheri, Hossein - FF1D.7
 Tahersima, Mohammad H. - JTh2A.45, SW4J.6
 Tai, Boyin - STu3L.6
 Taira, Takunori - JM1E.2
 Tait, Alexander N. - JM3M.3, SM3N.3, STh1N.3, SW3H.7
 Tajalli, Ayhan - SW3E.1
 Tajiri, Takeyoshi - FM1M.2
 Tak, Joon - FM2D.3
 Takada, Hideyuki - SM3L.2
 Takagishi, Taku - SM2O.5
 Takahashi, Eiji J. - SW4E.7
 Takanohashi, Masashi - SM4N.3
 Takase, Kan - FTh1D.1
 Takashima, Yuzuru - AW3K.7
 Takeda, Jun - FM4D.1
 Takeda, Koji - JTh2A.58, STh3N.1, STu3N.6
 Takeda, Shuntaro - FTh1D.1
 Takei, Nobuyuki - FTh1D.7
 Takeuchi, Ichiro - STh1N.6
 Takiguchi, Koichi - SW4F.7
 Takiguchi, Masato - JW3A.5, SM4J.3
 Takiguchi, Yu - SM4N.2
 Talapin, Dmitri - FF3A.4
 Talathi, Sachin - SM4E.6
 Talbayev, Diyar - JTh4F.5
 Talisa, Noah - JTu2A.87, SM3H.2
 Talker, Eliran - JTu2A.20, JTu2A.39, JW2A.110, JW2A.114, SM3F.4
 Talli, Giuseppe - SM3G.5, SM4G.1
 Tam, Wing Yim - FM4B.5
 Tamagnone, Michele - AM3K.3, FM3C.2
 Tamamitsu, Miu - SM4H.2
 Tamaru, Yuuki - SW4E.7
 Tamasaku, Kenji - FF1A.7
 Tamayo-Arriola, Julien - FTh4M.1
 Tampellini, Anna - SM1F.3
 Tan, Ailing - ATu3K.7, JTh2A.86, JW2A.77
 Tan, Chuan Seng - STh4O.2, STu4J.2
 Tan, Heyun - SM2L.4
 Tan, Kang - FM1D.5, FTh4D.6
 Tan, Mengxi - SF2N.2, SF2N.4
 Tan, Mingming - SW3O.1
 Tan, Shijie - JW2A.100
 Tan, Si - SF2H.7
 Tan, Teng - JTh2A.88
 Tan, Yixuan - JF2F.4
 Tan, You Sin - SM1J.6
 Tanabe, Takasumi - STh4J.6
 Tanaka, Koichiro - JTu4M.1
 Tanaka, Makoto - JTh2A.16, SM4F.3
 Tanaka, Shunji - STu4H.6
 Tanaka, Yosuke - SF3L.1
 Tanaka, Yurina - SM2H.4
- Tancogne-Dejean, Nicolas - FF2C.2, SW3E.7
 Tanemura, Takuo - JTh2A.48, SM3G.4
 Tang, Dingyuan - ATu4I.6, SF2O.8
 Tang, Jingyi - SF3I.2
 Tang, Liqin - FTh4B.7, FW3D.3
 Tang, Liwei - JTh2A.61
 Tang, Ming - AF2K.5, STu3L.2, SW4O.1
 Tang, Pinghua - SF2L.2
 Tang, Rui - STu4H.3
 Tang, Xianfeng - SW4O.4
 Tang, Xiaosheng - STu3N.7
 Tang, Zhuoqi - SF2L.4
 Tanguy, Nicolas - Ath3K.1
 Tani, Francesco - SF1E.6
 Tani, Shuntaro - SF3E.5
 Taniguchi, Takashi - SF3N.1, SM1O.2
 Taniyama, Hideaki - SM2J.6
 Tanizawa, Ken - SW3O.4
 Tanzilli, Sébastien - FF1A.5, FTh4D.2
 Tao, Jianfei - FF3C.3
 Tao, Jifang - JTh2A.34
 Tao, Zhensheng - SW4E.1
 Tapar, Jinal K. - JTh2A.22
 Taranta, Austin - STh1L.4
 Tarasenko, Oleksandr - SM2L.5
 Tarazona, Antulio - Ath3L.4
 Tatenguem Fankem, Herve - Ath3K.7, Ath4K.7
 Tatenguem, Herve - Ath3K.6
 Taten, Kouta - SM4J.3
 Tauqeer, Tauseef - FF2B.7
 Tavella, Franz - JM1E.3, SF3I.7
 Taverne, Mike P. C. - SF3O.7
 Tawara, Takehiko - JW2A.30
 Taylor, Antoinette - FM2D.2, FTu4D.2
 Taylor, Gregor G. - JTh2A.93, JTu2A.41
 Taylor, James R. - SM3L.4
 Taylor, Lauren L. - ATu3I.2
 Tazlaru, Stana - JM3B.4
 Tedford, Vincent - JTh2A.87
 Teimourpour, Mohammad H. - FTu3B.7
 Teitelbaum, Samuel - JTh4F.4
 Telnov, Dmitry A. - JTh2A.1
 Temporão, Guilherme P. - SM1L.6
 Teng, Chu C. - STh1F.2, STu4N.3
 Teng, Da - JTu2A.5
 Teng, Hao - JW2A.99, SM3L.3
 Teng, Yanting - FM2A.6
 Tereshchenko, Oleg E. - FTh1B.4
 Ternent, Gary - STu4O.7
 Tetsumoto, Tomohiro - SF2I.5
 Teuber, Lucas - FF1F.5, FTu3B.3
 Teufel, John D. - SF2N.1
 Thearle, Oliver - FTh4D.3
 Thesinga, Jelto - SM4E.1
 Thévenaz, Luc - STh1G.7
 Thiel, Valérian - JTu3A.4
 Thiré, Nicolas - STh3E.1
 Thiyagarajah, Nivetha - STu4F.6
 Thomale, Ronny - FTu4B.3
 Thomas, Linda - SM2G.3
 Thomas, Varghese A. - JTh2A.65, SM4G.4
 Thome, Kurtis - JW2A.12
 Thompson, Bradley J. - SM4N.5
 Thompson, Gregory - STu3N.3
 Thompson, Mark G. - FM4C.4, SM2F.2
 Thompson, Robert J. - JTu3G.3
 Thomson, David - JTh2A.74
 Thoumany, Pierre - SM1F.3, STu4L.4
 Thurmond, Kyle - Ath4K.6
 Thurn, Andreas - SM4J.6
 Thyrestrop, Henri - FTh3D.2
 Tian, Feng - AM4I.4, JW3A.5
 Tian, Haochen - JTh2A.103, SW3E.5, SW3H.6
 Tian, Huiping - JW2A.9
- Tian, Wenlong - JTu2A.105, SF3E.7
 Tian, Yuan - JW2A.107
 Tianzhuo, Zhao - AW3I.6
 Tikhonchuk, Vladimir - FTh1M.2
 Timmen, Ludger - SM1F.3
 Timmers, Henry - SF1E.4, SF3H.3, STh4E.5
 Timofeeva, Maria - FM2C.6
 Timpu, Flavia - FM2C.6
 Ting, Po-Yuan - Ath1I.4
 Tino, Guglielmo - JTu3G.1
 Tison, Christopher C. - FTh1D.4
 Tissandier, Fabien - SF3I.3
 Titberidze, Mikheil - SF3I.5
 Titova, Lyubov V. - JW2A.26
 Tittel, Frank - JW2A.21
 Tittel, Andreas - FTh4C.6, SF3J.1
 Titze, Michael - FW4M.6, JTu2A.25
 Tobey, Ra'an'an - FM2D.2
 Tochitsky, Sergei - FW3B.6, JW2A.50, STh1E.4
 Tofani, Daniela - JW2A.116
 Toivonen, Juha - SW3L.5
 Tokel, Onur - AW3I.1
 Tokman, Mikhail - FM2C.1
 Tolle, John - AW3P.3, STh4O.6, STu3N.3
 Tolstik, Nikolai - STh1E.6
 Tomasulo, Stephanie - SM2J.7
 Tomberg, Teemu - SF1I.2
 Tomono, Yuki - JTh2A.96
 Tonelli, Mauro - STh1E.7
 Tonello, Alessandro - STh4L.1, STh4L.2
 Tong, Hoang Tuan - JW2A.96
 TONG, JINCHAO - SF3J.6
 Tong, Tuan H. - JW2A.109
 Tong, Weijun - AF2K.5
 Tong, Xin - ATu4K.3
 Torizuka, Kenji - SM3L.2
 Torres Company, Victor - SF1G.3
 Torun, Rasul - AW4K.4
 Tossoun, Bassem - STu4J.5
 Toth, Milos - FM4A.5, SF1J.3, SM2F.5
 Tóth, Szabolcs - STu4E.2, SW3E.6
 Tovar, Pedro - SM1L.6
 Tovey, Dana - JW2A.50, STh1E.4
 Townsend, Paul - SM3G.5, SM4G.1
 Toyoda, Kohei - SF3G.3, SF3G.4
 Toyouchi, Shuichi - FTh4C.1
 Trabold, Barbara M. - SF1E.6
 Trajtenberg-Mills, Sivan - FTh4M.7, JM3B.6
 Tran, Huong - AW3P.3, STh4O.6, STu3N.3
 Tran, Khoa Anh - JTh2A.3
 Tran, Minh - AF2K.1
 Tran, Trong Toan - FM4A.5, SM2F.5
 Trask, Lawrence - JW2A.74
 Traum, Christian - FM3D.4
 Traverso, Andrew J. - SW3H.8
 Trawinski, Ryszard S. - JTh2A.111
 Trebino, Rick - JW2A.76, SW3E.2
 Tredicucci, Alessandro - FW4D.1
 Trenti, Alessandro - FF3D.2
 Treps, Nicolas - FM2M.5, FTh4D.4, JTu4A.2
 Tresp, Christoph - STu4L.4
 Tretyakov, Sergei - FM4B.6
 Trichili, Abderrahmen - JTh2A.51
 Trifonov, Anton - JTu2A.2
 Trigo, Mariano - JTh4F.4
 Trilo, Stefano - FTh3B.5
 Tripepi, Michael - JTu2A.87, SF2G.4, SM3H.2
 Trippel, Sebastian - JTu4M.5
 Tropheme, Benoit - ATu4I.5, JM3E.3
 Trotter, Douglas - STh4N.6
 Troupe, James - FM4C.8
 Trovatiello, Chiara - FW3M.7
 Trugman, Stuart - FM2D.2
 Trull, Jose - FW4B.7, STh3J.5
 Truong, Gar-Wing - SF2O.7, STh4G.2
- Trusheim, Matthew - FM4A.1, SM2F.3
 Tsai, Chia-lun - JTu2A.64
 Tsai, Din Ping - FF2B.4, FTh3M.3, FTh4M.2
 Tsai, Hai-En - SF3I.1
 Tsai, Meng-Tsan - SM3N.2
 Tsai, Ming-Rung - AW4I.6
 Tsai, Wei Che - JTu2A.104
 Tsakyridis, Apostolos - STh4N.5
 Tsang, Hon Ki - ATu3P.5, STh1H.2, STh3N.3, SW3J.5
 Tsaturyan, Yeghishe - FM1A.3
 Tschudin, Marta - FM4A.6
 Tse, Maggie - STh4G.6
 Tseng, Derek - AM4I.3
 Tseng, Ming Lun - FF2B.4
 Tseng, Yi-Hsun - JTu2A.64
 Tseses, Shai - FTu3D.5, SW3L.3
 Tsiokos, Dimitris - JTh2A.94
 Tsuchizawa, Tai - STh3N.1, STu3N.6
 Tsuda, Takuya - AF3K.4
 Tsui, Ying - FTu4D.1
 Tu, Chien-Ming - JTu2A.54
 Tuan, Tong H. - JW2A.93
 Tucker, Ethan - JW3A.6
 Tuitje, Frederik - SF3I.3
 Tukiainen, Antti - ATu3P.1
 Tung, Jung-Chen - JTu2A.62
 Tur, Moshe - FW4B.5, JTu2A.57, JTu2A.67, SF2N.3, SM1J.5, SM1N.5, SM3G.3
 Turan, Deniz - STu3F.4, SW3F.4
 Turchanin, Andrey - FW3B.1
 Turchinovich, Dmitry - JTh4F, STh3F.1
 Turdjev, Mirbek - SF3J.7
 Turek, John - ATu3K.4
 Turitsyn, Sergei K. - FF2D.4, FTh3B.4
 Turner, Joshua - SF3I.7
 Türschmann, Pierre - FF3M.1
 Tutuc, Emanuel - STh4O.4, STu3N.5
 Tuzson, Béla - AM1K.3
 Tyndall, Nathan - JTh2A.53, SF2I.1
 Tzang, Omer - STh4L.5
 Tzankov, Pancho - JTu2A.95
 Tzeng, Yan-Kai - FM4A.4
 Tzschaschel, Christian - FM3D.3
- U**
 Uchida, Megumi - SM2H.4
 Uda, Shohei - SF1I.3
 Udalcovs, Aleksejs - SW4O.2
 Udem, Thomas - JM1E.4, SM1F.2, SM4F.1
 Uemura, Sotaro - SM1K.3
 Uenoyama, Soh - SM4N.2
 Uesugi, Yuuki - SF1E.5
 Ujii, Hiroshi - FTh4C.1
 Ulbricht, Ronald - FM3D.1
 Ulloa, Jose - FTh4M.1
 Ulvila, Ville - SM3O.4
 Um, Han-Don - SM4J.5, SW3J.3
 Umezawa, Toshimasa - JTh2A.71, SF1G.2
 Unal, Canberk - AF1K.7
 Ungureanu, Razvan - SW4E.3
 Unterrainer, Karl - SW4F.2
 Upham, Jeremy - FF1B.3, SF1J.6
 Urbas, Augustine M. - STh4H.5
 Urbieta, Ana - JTu2A.46
 Ursescu, Daniel - SW4E.3
 Utakak, Katsuyuki - JTh2A.71
 Utikal, Tobias - FF3M.1, FM1M.4, FM2A.5
 Utzat, Hendrik - SF1O.6
 Uyar, Faruk - AF1K.7
- V**
 Vabishchevich, Polina - FF2B.2, FM2C.3
 Vagionas, Christos - STh4N.5
 Vahala, Kerry J. - AF2K.1, FTu3B.1, SF2J.5, STh4J.3
 Vaiçaitis, Virgilijus - FF3C.2

- Vaidhyanathan, Gnanavel - FTu4D.3
 Vaidya, Varun D. - FTh4D.6
 Vainio, Markku M. - SM3O.4, SW3H, SW3L.5
 Vakahi, Atzmon - JTu2A.109
 Vakhtin, Andrei B. - AM1K.4
 Valentin, Michael - JTu2A.118
 Valentine, Jason - FF1B.7
 Valenzuela, Anthony - FM4M.2, JTu2A.87
 Valiante, Taufik - Ath4I.4, SM4H.6
 Valle, Stefano - STh3H.6
 Vallée, Réal - SF2L.1, SF2L.3
 Valovcin, Darren C. - FTh1B.2
 Vamivakas, Anthony - JW2A.33
 Vamivakas, Nick - FM3A.1
 Vamos, Lenard - STh4E.4
 Van Camp, Mackenzie - FTh1D.5
 van de Groep, Jorik - FW4D.3
 van der Slot, Peter - STu4N.4
 Van Gasse, Kasper - STh4N.1
 van kerrebrouck, joris - STh4N.1
 Van Laer, Raphaël - Ath3I.6, SF2J.6
 van Mechelen, Jacobus L. - Ath4K.1
 Van Stryland, Eric W. - FF3D.3
 Van Thourhout, Dries - FF3A.2
 Van Tilborg, Jeroen - SF3I.1
 Vanderhoef, Laura - FM4M.2, JTu2A.87
 Vanner, Michael - JM3B.3
 Varughese, siddharth - SM4G.4
 Vasa, Nilesh J. - JW2A.20
 Vasilev, Anton - STu4O.4
 Vasilyeu, Ruslan - SF1H.3
 Vasilyev, Sergey - SF1H, SF1H.1, STh3J.6, STh4E.3, STh4E.6
 Vasiredddy, Praful - JTu4M.4
 Vaskin, Aleksandr - FM2C.3
 Vasquez, Andres - SM3H.5
 Vasu, Subith S. - Ath4K.6
 Vaswani, Chirag - JTh4F.3
 Vedraïne, Sylvain - FTh4C.5
 Veis, Martin - JM3B.4
 Veisz, Laszlo - FF1C.3
 Veitas, Gediminas - STu4E.2
 Veli, Muhammed - SF1N.2
 Velmiskat, Vladimir V. - SM4E.2
 VENKATASUBRAMANI, LAKSHMI NARAYANAN - JTh2A.82, JTh2A.83
 Venkatesan, Thirumalai - JW2A.63
 Venkateswaran, Ramgopal - AW4I.2
 Venkitesh, Deepa - JTh2A.82, JTh2A.83
 Verccruyse, Dries - FF3A.1, JTh2A.67, SM2F.6, SM3J.2
 Verhagen, Ewold - FM1A.2, JM2B.2
 Verma, S S. - JW2A.17
 Verma, Varun B. - FF1A.3, FM1M.7, FTh1D.5, JTu2A.42, STh1N.3
 Vermeulen, Diedrik - Ath4I.2, SW4G.6
 Vernon, Zachary - FM1D.5, FTh4D.6
 Vetlugin, Anton N. - FTu3D.7
 Vetter, Sharon - SF3I.2
 Veziari, Stephane - FTh3M.7
 Vezzoli, Stefano - FF2B.3
 Vianna, Pilar G. - STu4L.2
 Vico Trivino, Noelia - SM3J.1
 Viggianello, Niko - FM1M.1
 Viktorov, Evgeny - ATu3P.6
 Villa, Matteo - FTh4D.3
 Villinger, Chris - Ath11.6
 Villinger, Massimo - Ath11.6
 Vincenti, Maria Antonietta - FW4B.1, FW4B.7
 Vines, Peter - FF1A.4
 Vinod, Abhinav - SM1F.5, STh3J.4
 Viotti, Anne-Lise - SF1H.4
 Vishva, Ray - SM1J.3
 Vishwanath, Sriram - JTh2A.81
 Vitebskiy, Ilya - JTh2A.36
 Vlk, Marek - STh1F.1
 Vodopyanov, Konstantin L. - FF3D.5, SF1H.1, SF1L.2, STh3J.6, STh4E.3, STh4E.6
 Vogt, Stefan - SM1F.3
 Voigt, Christian - SM1F.3
 Vojtech, Josef - JTh2A.116
 Volet, Nicolas - STu3J.2
 Volkov, Mikhail - FF2C.1
 Volodarsky, Oleg - SW3L.1
 Voloshin, Andrey S. - STu3J.4
 Volpi, Azzurra - STh1E.7
 von der Weid, Jean Pierre - SM1L.6
 von Freymann, Georg - FM1C.4, FM4B.1
 Vu, Khu - FF2D.8, FW3B.2, SF2N.5, SF2N.7, SM4O.5, STh1J.4
 Vuckovic, Jelena - FF3A.1, FM4A.2, FM4A.4, JTh2A.67, SF2H.7, SM2F.6, SM3J.2, SW4J.3
 Vurgaftman, Igor - SM2J.7
- W**
- Wabnitz, Stefan - FTh3B.4, SM3O.3, STh4L.1, STh4L.2
 Wada, Masato - SW3G.1
 Wadsworth, Alicia - STu3N.3
 Wagner, Gerd - AM2K.2
 Wagner, Kelvin - AW3K.2, SF3N.2, STh4L.5
 Wagner, Steven - Ath4K.4, JW2A.18
 Wahlstrand, Jared K. - STu4F.4
 Wai, P. K. A. - JW2A.102, STu4L.7
 Wakabayashi, Katsunori - SW4J.1
 Waks, Edo - FM1M.3, FM3A.3, JM2B.5
 Walch, Pierre - JM2E.5
 Waldecker, Lutz - FW3M.5
 Wallace, Michael - JTh2A.63
 Walschaers, Mattia - FTh4D.4
 Walter, Guillaume - JTu2A.93
 Walter, Peter - FF2C.5
 Walther, Philip - FF3D.2, FM2M.7, FTh4A.3
 Walther, Thomas - JTu2A.85
 Wan, Chenghao - SM2H.6
 Wan, Dongyang - JW2A.63
 Wan, Noel - FM4A.1
 Wan, Shuai - JTh2A.69
 Wan, Yating - STu3N.1, STu4J.3
 Wandt, Christoph - SM4E.3
 Wang, Aimin - SF1L.6
 Wang, Alan X. - ATu3K.7, JTh2A.86, JW2A.77, SF1N, SM2G.4, STh3H.3, STh3N.4, STu4H.4
 Wang, Anran - SM1O.3
 Wang, B. C. - JTu2A.63
 Wang, Bin - SM4F.5
 Wang, Binbin - SM2H.7
 Wang, Bingnan - SW4J.6
 Wang, Binhao - SM4J.7
 Wang, Chao - JW2A.9
 Wang, Chao-Wei - SM4G.3
 Wang, Cheng - SF2J.1, SM3O.2
 Wang, Chenglong - JW2A.7
 Wang, Chingyue - SF3E.1, STh1G.6
 Wang, Chuting - FM1A.7
 Wang, Daqing - FM2A.5
 Wang, Di - JW2A.58
 Wang, Dongyi - JTh2A.11
 Wang, Feng - FF3M.7, FTu3C.1, SF1O.2
 Wang, Frank (Fengqiu) - SM1O.3
 Wang, Fuli - JW2A.3
 Wang, Gan - JTu2A.30
 Wang, Geyang - SF3E.7
 Wang, H. Y. - JTu2A.63
 Wang, Haide - SW4O.3
 Wang, Hailin - JW3A.3
 Wang, Haiping - FTh4B.7
 Wang, Hao - FF1B.7, FM2C.7, JTu2A.70, JTu2A.72, SM1J.6
 Wang, Haochuan - AF3K.5
 Wang, He - FW4M.6
 Wang, Heming - AF2K.1, SF2J.5
 Wang, Heqing - JTu2A.33
 Wang, Hong - JTu2A.77, SF1O.5, STh4O.2, STu4O.1
 Wang, Hongda - AM2K.3, ATu4K.2, ATu4K.6, STu4H.2
 Wang, Huan - SM3N.8
 Wang, Huibo - JTh2A.104, SW3G.5
 Wang, Jiahui - SW4J.5
 Wang, Jian - JTu2A.90, SW4N.7
 Wang, Jiankun - JTu2A.70
 Wang, Jianwei - SM2F.2
 Wang, Jiemei - SM2G.6
 Wang, Jigang - FM3D.7, FW4M.5, JTh4F.3
 Wang, Jingyi - ATu4K.7
 Wang, Jun - SF2O.8
 Wang, Junjia - FW3M.4
 Wang, Junjie - JW2A.100, JW2A.23
 Wang, Junli - JW2A.99, SM3L.3
 Wang, Jyhpyng - FF1C.5
 Wang, Kai - FF3A.7, JTh2A.17, JTh2A.75, JW2A.70
 Wang, Ken Xingze - JF3F.1
 Wang, Lai - JTu2A.90, SW4N.7
 Wang, Lei - ATu4I.4, JTu2A.82
 Wang, Li - SF3E.6, SF3O.8
 Wang, Liang - JW2A.102
 Wang, Lingfang - SW4H.1
 Wang, Li-Wei - FM4C.5
 Wang, Lulu - JTu2A.6
 Wang, Mengqi - JTh2A.72
 Wang, Min - JTu2A.49, SM1G.2
 Wang, Ming - SF1O.2
 Wang, Mohan - AF1K.6, JW2A.14
 Wang, Mu - JTh2A.38, STh1O.2
 Wang, Nan - SW3F.6
 Wang, Nanshuo - AM3I.5
 Wang, Ning - SM1L.1
 Wang, Pengfei - JTh2A.72
 Wang, Pengwei - JW2A.7
 Wang, Ping - SF2I.6
 Wang, Pu - JW2A.67, STh1L.6
 Wang, Qiang - SW4O.6
 Wang, Qijie - ATu4I.6, FTh1B.5, JW2A.40
 Wang, Qiqi - JM3M.4
 Wang, Qirui - AF1K.6
 Wang, Qiuhua - AW3K.6, JTu2A.75, JTu2A.80, STh3O.3
 Wang, Ride - ATu4I.3, JTh2A.12, JTh2A.29, JTh2A.30
 Wang, Rui - AM1K.2
 Wang, Rui Ning - STh4J.2, STu3J.2
 Wang, S. C. - JTu2A.63
 Wang, Senmao - ATu4K.7
 Wang, Sheng - FF3M.7, STu4L.6
 Wang, Shuai - SF1L.5
 Wang, Shuming - FTh3M.3
 Wang, Song-You - JW2A.11
 Wang, Tailei - JTh2A.14
 Wang, Tianwu - STu3F.1
 Wang, Tianyu - AM1I.5
 Wang, Ting - STu3N.4
 Wang, Tingyun - SF3L.6
 Wang, Wanjun - STu4O.1
 Wang, Wei - JTu2A.70, JTu2A.72, STu4J.2
 Wang, Wenting - STh3J.4
 Wang, Wenyuan - FM4C.3
 Wang, Xiaodong - JTh2A.64
 Wang, Xiaowei - STh4O.3
 Wang, Xihua - JTh2A.35
 Wang, Xijie - JTh4F.1, STh3F.2
 Wang, Xudong - JTh2A.31
 Wang, Xueji - FTu4D.1
 Wang, Yajun - JTu2A.73
 Wang, Yan - SF1L.6
 Wang, Yanan - JW2A.118
 Wang, Yicheng - JTu2A.119, SF3E.6
 Wang, Yiding - JW2A.21
 Wang, Yifei - FW4D.3
 Wang, Yinan - STh4O.4
 Wang, Yingying - STh1L.6
 Wang, Yishan - FF3C.4
 Wang, Yongrui - FM1D.3, STh4H.3
 Wang, Yuchen - SF2L.1
 Wang, Yue - JTu2A.59, SM2H.8
 Wang, Yuejing - JTu2A.18
 Wang, Yulei - JTu2A.59
 Wang, Yunzheng - JTu2A.108
 Wang, Yuxi - Ath1K.2
 Wang, Zhaorong - FF3D.1, FM4D.3
 Wang, Zhaoyou - JW4A.4
 Wang, Jingyi - ATu4K.7
 Wang, Zhen - FM4C.3, FM4D.4
 Wang, Zheng - JW2A.9
 Wang, Zhenhua - FTh1M.5
 Wang, Zhi - JTh2A.80
 Wang, Zhiming - JW2A.118
 Wang, Zhixin - SW4N.4
 Wang, Zi - FTh4C.4, FTu4B.7, SM1J.2
 Wang, Zifei - SW3H.5
 Wang, Zinan - SF3L.3
 Wanzenboeck, Heinz - JW2A.62
 Ward, Martin - FM4C.6
 Warner, Jamie - SF2G.2
 Warren, Michael V. - SM2J.7
 Warren-Smith, Stephen - STh3L.3
 Waseem, Muhammad Hamza - FF2B.7
 Wasserman, Daniel - FTh4M.5, STh4O.4
 Watanabe, Haruki - FM4B.4
 Watanabe, Hideyuki - AM4I.1
 Watanabe, Katsuyuki - SW4J.1
 Watanabe, Kenji - SF3N.1, SM1O.2
 Watanabe, Kenta - JW2A.98
 Watanabe, Shunsuke - JTu2A.106
 Watanabe, Tatsuhiko - SW3F.7
 Watkins, Joseph - Ath1K.7
 Watremez, Xavier - Ath3K.1
 Watson, John - FM4D.1
 Watts, Michael R. - Ath4I.2, SM1J.1, STu3O.3, STu3O.4, SW4G.6
 Waxman, Eleanor - SF11.1, SM2N.3
 Weathersby, Stephen - JTh4F.1
 Weaver, Tom - JTu4A.5
 Webb, Kevin J. - FF2A.7, JTh2A.18
 Weber, Christoph - STu4O.2
 Weber, Karina - SM2L.1
 Weber-Bargioni, Alexander - JW2A.29
 Weck, Arnaud - FTu4C.4
 Weeber, Jean-Claude - FF2D.7, JTh2A.94
 Weeks, Reagan R. - JTh2A.106, STh1G.5, SW4L.6
 Wei, Chengli - JW2A.122
 Wei, Haoyun - JTh2A.89
 Wei, Huiyue - SF1O.2
 Wei, Jean - SF1H.6
 Wei, Kejin - FM4C.3
 Wei, Le - SF3O.6
 Wei, Qingshan - ATu4K.3
 Wei, Shuen - JW2A.107
 Wei, Yanxian - JW2A.10
 Wei, Zhensong - AM2I.6, ATu4K.2, ATu4K.6, JM3M.5, STu4H.2
 Wei, Zhiyi - JTh2A.104, JW2A.99, SF3E.7, SM3L.3, SW3G.5
 Weidlich, Stefan - SM2L.1
 Weidman, Matthew - JTh2A.9
 Weigand, Helena - FTh4C.3
 Weih, Robert - AW3P.1, STh4H.3, STu4O.6
 Weimann, Steffen - FM1C.6, FM4B.7
 Weinberg, Omri - FM3D.8

- Weiner, Andrew M.- Ath1K.4, FF1F.3, FTh1A.2, FTh3A.6, JTu3A.3, JTu3A.5, SF2N.8
- weisman, Dror - FF2A.8
- Weiss, Sharon M.- SM2J.4, STh4H.1
- Weitenberg, Johannes - JM1E.4
- Wells, Brian - FTh4M.3
- Wen, Dandan - SF3J.2
- Wen, Haidan - FM4D.7
- Wen, He - SM1L.1
- Wen, Rui-Tao - STh4O.2
- Weng, Wenle - FF1D.1, FF1D.2, FF1D.5, STh1G.7
- Wenny, Brian - JW2A.12
- Wenzler, Mathias - JTu2A.12
- Werner, Dominik - SW3F.7
- Werner, Kevin - FM4M.2, JTu2A.87
- Werner, Sebastian - SM3G.2
- Wertz, Esther - FTu3C
- West, Kenneth - JW2A.34
- Westberg, Jonas - ATu4K.4, SF11.5, STu4N.3
- Westbrook, Paul S.- JTh2A.92
- Westly, Daron - AM3K.2, SM3J.4
- Weyrich, Christian - FTh4C.3
- Wheeler, Jonathan - SW4E.3
- Wheeler, Natalie V.- STh1L.2, STh1L.4
- Wheeler, Virginia D.- JTu3M.4, SW3H.8
- White, Ian H.- SM1G.3
- white, jonathon - FF2C.4, JTh2A.9
- White, Mark E.- STh4G.2
- White, Rachel C.- STh4O.7
- White, Vaughn E.- SF3I.7
- Whitehead, James - STu4J.4
- Wiebe, Nathan - SM2F.2
- Wieck, Andreas - FTh3D.2
- Wiersig, Jan - JTh2A.33
- Wierzynski, Casimir - SF1N.6
- Wiggins, Paul - AM4I.1
- Wilcox, Russell - SM4E.5
- Wildi, François - AF2K.2
- Wilk, Rafal - Ath3K.2, JTh2A.112, STu4L.4
- Wilkinson, Tristan A.- FM3A.4
- Wilkowski, David - JTu2A.20
- Willenberg, Benjamin - FTh1M.8
- Williams, Benjamin S.- STu4N, SW3N.4
- Williams, Brian P.- FF1F.3
- Williams, Skip - STh4J.7
- Williams, Wade - SM4E.6
- Williamson, Ian - FF1B.5, FF2A.1, FM1B.2, FM1C.7, JF3F.2, SW4J.7
- Willms, Stephanie - FF1D.4
- Willner, Alan E.- FF1B.3, FW4B.5, JTu2A.57, JTu2A.67, SF2N.3, SM1J.5, SM1N.5, SM3G.3
- Wilmer, Brian L.- FM4M.2
- Wilson, Dalziel J.- FM1A.1
- Wilson, Jesse - ATu3K.5
- Win, Aye - FF1A.6
- Winchester, Andrew - FW3M.6, SF1O.3
- Windeler, Matthew - JM1E.3
- Winder, Drew - STh4G.5
- Wineland, David - SM1F.1
- Winkelmann, Lutz - SF3I, SF3I.4, SF3I.6, STu4E.4
- Winkler, Georg - SF2O.7
- Winnerl, Stephan - STu3F.3
- Winoto, Ardy - JTh2A.62
- Winter, Rosangela - Ath4K.2
- Winters, David - ATu3K.5
- Wirtz, Ludger - FW3M.7
- Wise, Frank W.- JW2A.103, SF1L.1, STh4L.3
- Witmer, Jeremy D. - Ath3I.6
- Witte, Stefan - FF2C.7
- Wittek, Steffen - SM1G.1, SM4L.3
- Wittwer, Valentin J.- SF3E.4, STh3F.5
- Witzens, Jeremy - Ath3I.3, SF1G.4
- Woggon, Ulrike K.- FM2D, FM3D.2, JW2A.24
- Wojcik, Casey - FM1C.7
- Wojtewicz, Szymon - Ath3K.2
- Wolf, Alexey - STh4L.4
- Wolf, Jean-Pierre - JM2E.5
- Wolf, Lior - FTu4C.3
- Wolf, Omri - FW4B.1
- Wolf, Patrick - SM4H.2
- Wolf, Thomas - FF2C.5
- Wolfe, Christopher - FM4M.2, JTu2A.87
- Wolff, Christian - FW4D.2
- Wölk, Sabine - FTh3A.2
- Wollock, E. Alex - JW4A.4
- Wong, Chee Wei - FF2D.2, FTh1A.3, FTh1D.6, FTu4C.5, JTh2A.88, JW2A.29, SF1J.4, SF2H.6, SM1F.5, SM1O.5, STh3J.4, STh3O.6, STh4G.4, STh4J.4, STh4J.5, SW3N.6, SW4H.4
- Wong, E Laine - SF1O.3
- Wong, Franco N.- FTh1A.3, FTh3A.3
- Wong, Kenneth Kin-Yip - JTu2A.89, STu4L.6
- Wong, Liang Jie - FTh4B.4
- Wong, Teh-Hwa - AW4K.6
- Wood, Michael G.- JTh2A.57
- Wood, Thomas - STh1J.6
- Woodbury, Daniel - FTh1M.3
- Woodley, Michael T. M. - JM3B.3, SF3H.5, STh3J.7
- Woolf, David N.- FM4C.2
- Wright, Alex - Ath3I.1
- Wright, C. David - SM2J.2
- Wright, Logan - STh4L.3
- Wu, Botao - JTu2A.111
- Wu, Changming - STh1N.6
- Wu, Chengyin - FTh1M.5
- Wu, Chien-Ming - JTu2A.38
- Wu, Chunyan - AM1I.5
- Wu, Dachuan - AW3K.4
- Wu, Dufei - JTh2A.62
- Wu, Duxuan - STu4H.1
- Wu, E - JTu2A.111
- Wu, Fan - FF1D.3, FTh3B.2, FW4D.2
- Wu, Guanhao - SM2H.2
- Wu, Guohua - STh3L.5
- Wu, Han - STh3L.1
- Wu, Hsun-Chung - JTu2A.38
- Wu, Hui - JTh2A.28
- Wu, Jih-Sheng - JTu4M.3
- Wu, Jiadong - SF2L.2
- Wu, Jia-Gui - FTu4C.5, SF1J.4, SW3N.6
- Wu, Jiayang - SF2N.2, SF2N.4
- Wu, Jingyu - AF1K.6
- Wu, Jixuan - SF3L.7
- WU, Kaiyi - SF2I.4
- Wu, Kan - JTh2A.73, JTu2A.94, JTu2A.97
- Wu, LiJun - JTh2A.59
- Wu, Lue - AF2K.1
- Wu, Meng-Chang - JTu2A.123, JTu2A.37
- Wu, Mengshi - SF3L.4
- Wu, Ming - FW3C.6
- Wu, MingHsiung - JTu2A.104
- Wu, Pin Chieh - FTh3M.3
- Wu, Qiang - ATu4I.3, JTh2A.12, JTh2A.15, JTh2A.29, JTh2A.30
- Wu, Qing - JTu2A.108, JW2A.86, SF3O.3
- Wu, Qiong - SW4O.1
- Wu, Rongbo - JTu2A.49
- Wu, Ruitao - Ath4K.3, FF3B.2
- Wu, Shu-Rong - JTu2A.38
- Wu, Tingzhu - JTu2A.115
- Wu, Wei - Ath1I.3, JTh2A.21
- wu, xi - SF2H.5, STh1H.5
- Wu, Xinru - ATu3P.5, STh1H.2
- Wu, Yi - JTh2A.9, STh1E.1
- Wu, Yichen - AM2I.3, AM2K.3, ATu4K.3, JTu2A.5, SM4H.2
- Wu, Yipeng - FF1C.5
- Wu, Yu - JTh2A.88
- Wu, Yue - SF3L.3
- Wu, Yun - STu4H.5
- Wu, Zhifang - JW2A.108
- Wubs, Martijn - FTu3C.4
- Wun, Jih-Min - Ath1K.4
- Wunderlich, Christof - FTh3A.2
- Würthwein, Thomas - JTu2A.84, SM4O.6
- Wyllie, Sara - FTh1M.1
- Wyrowski, Frank - JTh2A.23
- Wysocki, Gerard - AM1K.2, ATu4K.4, JW2A.5, SF1I.5, STh1F.2, STu4N.3
- X**
- Xi, Lixia - SW4O.4
- Xia, Fei - AM1I.5
- Xia, Peiyu - FM4M.1
- Xia, Qinzi - FF3C.3
- Xia, Shiqi - FW3D.3
- Xia, Yi - FF1F.4, FTh4D.1
- Xiang, Chao - SW4N.6
- Xiang, Fulin - SF3O.1, STu3L.5
- Xiang, Yangyang - STh3L.5
- Xiang, Yao - FM4C.5
- Xiang, Yating - SW4O.1
- Xiang, Yinxiao - AM1I.4
- Xiang, Zi-Heng - FM4C.6
- Xiao, Gui - JW2A.107
- xiao, hai - AW3I.4
- Xiao, Hong - AW3I.6
- Xiao, Jin-Long - JW2A.3
- Xiao, Meng - FM1B.2, FM4B.5, FTu3B.4
- Xiao, Na - SF1H.2, STh4E.1
- Xiao, Pushan - JTu2A.97
- Xiao, Qirong - JTh2A.43
- Xiao, Sanshui - FTu3C.4
- Xiao, Xian - JTh2A.70, SM3G.2
- Xiao, Xiaofei - FTh3C.5
- Xiao, Xiaosheng - JW2A.87
- Xiao, Xuan - SF2L.5
- Xiao, Yun-Feng - JTh2A.33, JTh2A.69, JW2A.51, STh3J.2
- Xiao, Yuzhe - SM2H.6
- Xiao, Zeyu - JTu2A.94
- Xie, Chen - SF1H.2
- Xie, Chongjin - SW3O.2
- Xie, Feng - STh4H.3
- xie, guodong - JTu2A.57, SM1N.5
- Xie, Rensheng - JTh2A.14
- Xie, Tian - FM1A.7
- Xie, Xiaojun - SF2N.1, SW4G.1
- Xie, Xiuping - FTh1D.7
- Xie, Xuejun - STh3O.6
- Xie, Yiwei - SF2N.7
- Xie, Yiyang - AW3K.6, JTu2A.75, JTu2A.80, STh3O.3
- Xie, Zhenda - FF2D.2, JTh2A.88
- Ximenes, Eduardo - ATu3K.4
- Xin, Ming - Ath4I.2, SW4G.6
- xing, luo - JW2A.109, JW2A.93
- Xing, Zhikun - JW2A.91
- Xinghua, Qu - AW4K.2
- Xiong, Bing - JTu2A.90, SW4N.7
- Xiong, Chi - STh1F.2
- Xiong, Hao - JTh2A.29, JTh2A.30
- Xiong, Ji - SF3L.3
- Xiong, Qiaozhou - AM3I.5
- Xiong, Xinglong - JW2A.2
- Xiong, Xueyan - SF1J.4
- Xomalis, Angelos - FTu3D.7
- Xu, Bingjie - JTu2A.30
- Xu, Bingjun - FTh4C.4
- Xu, Bingxin - SF1L.5
- Xu, Bo - FTh1M.5
- Xu, Chen - AW3K.6, JTu2A.75, JTu2A.80, STh3O.3
- Xu, Chi - STu3N.8
- Xu, Chris - AM1I.5
- Xu, Feihu - FM4C.3, FTh4A.6
- XU, Gang - FTh3B.5
- Xu, Jia - STh4E.4
- Xu, Jiahui - FM2C.7
- Xu, Jing - ATu3I.2
- Xu, Jingjun - ATu4I.3, FTh4B.2, FW3D.3, JTh2A.12, JTh2A.15, JTh2A.21, JTh2A.29, JTh2A.30, JW2A.41, JW2A.45
- Xu, Kun - AF2K.5
- Xu, Lin - JW2A.44
- Xu, Linfang - JTh2A.34
- Xu, Peipeng - STh1N.5
- Xu, Peng - FF3C.4
- Xu, Qi Wei - JTh2A.35
- Xu, Shengqiang - STu4J.1, STu4J.2
- Xu, Tao - SF1O.2
- Xu, Ting - FM3C.3
- Xu, Wendao - STh1L.3
- Xu, Wenshuo - SF2G.2
- Xu, Xianfan - FF2A.7
- Xu, Xiaodong - FW3M.2
- xu, xiaohui - FM1M.5
- Xu, Xingyuan - SF2N.2, SF2N.4
- Xu, Zai-Quan - FM4A.5
- Xu, Zhen - SM4J.2
- XU, Zhengji - AW4K.5, SF3J.6, STh1O.4
- Xu, Zhengyuan - SM2G.6
- Xuan, Yi - FTu4D.1, SF2I.5
- Xue, Bing - SW4E.7
- Xue, Chenpeng - JTu2A.73
- xue, lei - SW4O.2
- Xue, Lu - FM4C.5
- Xue, Tianyuan - Ath4I.4
- Y**
- Yablonoitch, Eli - FW3C.6
- Yadav, Amit - ATu3P.6
- Yakovlev, Vladislav - JTh2A.87
- Yalcin, Sener - ATu4K.2
- Yallew, Henock D.- STh1F.1
- Yama, Nicholas - FM4D.2, JTu2A.52
- Yamada, Yuko - SW3G.1
- Yamagiwa, Masatomo - SM2H.5
- Yamaguchi, Takuto - FM1M.2
- Yamamoto, Hirotsugu - AF3K.4, SM2H.5
- Yamamoto, Naokatsu - SF1G.2, SM2G.1
- Yamamoto, Yoshinori - SW3G.1
- Yamanaka, Masahito - JW2A.92, STu3L.4
- Yamane, Keisaku - SF3G.4
- Yamaoka, Suguru - STu3N.6
- Yamasaki, Satoshi - JTh2A.16
- Yamashita, Shinji - AF1K.5, JTh2A.85, JW2A.94, SF3O.1, SF3O.4, STu3L.5
- Yamilov, Alexey - FF3B.3, FF3B.5
- Yan, Bixing - JW2A.63
- Yan, Jih-Heng - SM4G.3, SM4G.5
- Yan, Juanjuan - JTh2A.99, JTu2A.98
- Yan, Long-Chuan - FM4C.5
- Yan, Lulu - JTu2A.66
- Yan, Mei-Chen - JTu2A.92
- Yan, Ming - STu4L.1
- Yan, Wei - STh1O.3
- Yan, Wenchao - FW3D.3
- Yan, Xingzhao - SW3J.5
- Yan, Zhijun - ATu4K.7, JW2A.23, JW2A.91
- Yan, Zhizhong - FW3B.5
- Yan, Zijie - SM1H, SM1H.4
- Yang, Changhui - STu3H.5
- Yang, Changxi - JW2A.105, JW2A.43, JW2A.87
- Yang, Chen - SW4H.5

- Yang, Dong - SF3G.6
 Yang, Fan - STh1F.4, STh1G.7
 Yang, Guang - JW2A.118
 Yang, Guoce - JTu3M.4
 Yang, Hong - SF3G.6
 Yang, Hung - JTu2A.54
 Yang, Jaewon - JTh2A.109, STh3G.4
 Yang, Jian - FF2B.4
 Yang, Jianjun - SM2H.1
 Yang, Jie - JTh4F.1, STu3N.7
 Yang, Jinghui - FF2D.2, SF1J.4, SM1F.5, STh3J.4, STh4J.4, SW4H.4
 Yang, Joel K. W. - FM2C.7, SM1J.6
 Yang, Ke - JW2A.3, SF3E.7
 Yang, Kiyoul - AF2K.1, FF3A.1, JTh2A.67, SM3J.2, SW4J.3
 Yang, Lan - SF2I.3, STh1H
 Yang, Li-Fan - FF2A.7
 Yang, Lijia - JW2A.106
 Yang, Lin - AF1K.4
 Yang, Liuyang - JW2A.23
 Yang, Ming - FM2M.4
 Yang, Mingwei - SW4O.6
 Yang, Qian - SF1L.3, SF1L.4
 Yang, Qi-Fan - AF2K.1, SF2J.5
 Yang, Quanlong - SW3F.5
 Yang, Seunghoon - FM2D.4
 Yang, Shang-Da - JTu2A.64
 Yang, Sigang - ATH1K.2, JTh2A.61
 Yang, Song-Lin - JTh2A.75
 Yang, Steven T. - FTh1M.7
 Yang, Tsung-Han - SW4H.5
 Yang, Weiji - SM1J.4
 Yang, wenkai - JTh2A.103
 Yang, Wenyu - JTh2A.72
 Yang, Xianchao - JTh2A.90
 Yang, Xiong - SM1L.5
 Yang, Xu - JTh4F.3
 Yang, Yansong - JTh2A.41
 Yang, Yifeng - JW2A.95
 Yang, Yong - JTh2A.50
 Yang, Yuan - ATH1I.1
 Yang, Yuanmu - JTh2A.43
 Yang, Yudong - FF2C.2, FF2C.3, SW4E.4
 Yang, YueDe - JW2A.3
 Yang, Yujia - JTu4M.4
 Yang, Yu-Mei - JW2A.11
 Yang, Yunchen - STu4H.5
 Yang, Yuxia - JTu2A.91
 Yang, zhaou - FTu4B.1, FW3D.2
 Yang, Zhou - JTu2A.78
 Yang, Zu-Po - SM3N.2
 Yanikgonul, Salih - FTu3D.7
 Yanny, Kyrollos - SM4H.2
 Yao, Baicheng - JTh2A.88, STh4J.5
 Yao, Hsin-Yu - SM3H.4, STh4H.5
 Yao, Jian - SM1F.1
 Yao, Jianghong - ATu4I.3
 Yao, Jianquan - JTh2A.90, SM1L.3
 Yao, Jinping - FTh1M.5
 Yao, Kan - JW2A.64
 Yao, Shunyu - JW2A.43
 Yao, Xin - JTu2A.33
 Yao, Xing-Can - JTu2A.92
 Yao, Yuan - JW2A.11, SF3L.7
 Yao, Yung-Chi - SM3N.2
 Yao, Yung-Shi - STu3H.1
 Yardimci, Nezhir - SF1N.2, STu3F.4
 Yardimci, Nezhir Tolga - SW3F.4
 Yariv, Amnon - AF2K.1
 Yarotski, Dmitry - FM2D.2
 Yashkov, Mikhail - SM4L.1
 Yasui, Takeshi - AF3K.4, JTh2A.101, SM2H.5, STh1G.4
 Yavas, Seydi - JTu2A.1
 Ycas, Gabriel - SF1I.1, SM2N.3, STh1G.1, STh1G.2
 Ye, Hong - JTu4M.5
 Ye, Jianchao - AW3I.5
 Ye, Jun - SM1F.1
 Ye, Mao - SM1J.3
 Ye, Xiaohua - JW2A.8
 Yeak, Jeremy - JTh2A.106, SM1N.3, STh1G.5, SW4L.6
 Yeh, Tien-Tien - JTu2A.54
 Yeh, Ting-Wei - SM3N.2
 Yen, Tzu-Hsiang - JTh2A.32
 Yeo, Xi Jie - FM2A.3
 Yeo, Yee-Chia - STu4J.1, STu4J.2
 Yerci, Selcuk - FF2B.7
 Yesilkoy, Filiz - SF3J.1
 Yessenov, Murat - JW2A.72, SW4E.8
 Yi, Ailun - SM2O.7
 Yi, Fei - FM3C.6
 Yi, Gyu-Chul - STu4H.7
 Yi, lilin - SW4O.2
 Yi, Luying - JTu2A.4
 Yi, Soongyu - JTh2A.31
 Yi, Wei - SW4O.4
 Yi, Xingwen - SW3O.7, SW4O.3
 Yi, Xu - STh3J.2
 Yi, Ya Sha - AW3K.4, SM1J.3
 Yildirim, Oguz - STu4F.6
 Yilmaz, Hasan - FF3B.3, FF3B.5
 Yin, Chuan-Ci - JTh2A.107
 Yin, Chunjing - AF2K.5
 Yin, Danlei - SF2O.8
 Yin, Juan - FM4C.1
 Yin, Xin - JTh2A.31, STh4N.1
 Yin, Xinghui - AM3K.3, FM3C.2
 Yin, Xu-Fei - FTh4A.6
 Yin, Yanchun - STh1E.1
 Ying, Lei - JM3B.5
 Yizhou, Liu - SM4E.1
 Yoda, Taiki - JTh2A.10
 Yokokawa, Shoko - SF3O.4
 Yokoyama, Shiyoshi - STh1N.7
 Yonezawa, Hidehiro - FTh4D.3
 Yoo, Dong Eun - AW3I.2
 Yoo, Jae Hyuck - FTh1C.4, SF3G.7
 Yoo, Kyoung Min - AW3K.5, STh1F.6
 Yoo, S.J.Ben - FTu4D.7, JTh2A.68, JTh2A.70, JTu2A.76, SM3G.2
 Yoo, Seongwoo - ATu4I.6, JW2A.89
 Yoo, Young Jin - AW3I.2, JW2A.6
 Yoo, Youngzoo - ATu4I.1
 Yoo, Yung Jun - STh3F.4, STu3F.5
 Yoon, JW - STu3E.2
 Yoon, Taehyun - JW2A.112
 Yoshida, Daisuke - FTh1D.7
 Yoshida, Mio - FTh4B.5
 Yoshida, Yuki - SM2G.1
 Yoshie, Osamu - JW2A.11
 Yoshii, Kazumichi - SW3G.1, SW3G.8
 Yoshioka, Hiroaki - SM2O.5
 Yoshioka, Katsumasa - FM4D.1
 Yoshitomi, Dai - SM3L.2
 Yost, Dylan - SM4F.1
 You, Lixing - FM4C.3, JTu2A.33
 You, Yongsing - FM4M.3
 Youn, Chun Ju - JTu2A.43
 Young, Andrew - SM4J, STh1H.1
 Young, Ian - SF1N.6, SM1O.4
 Youngblood, Nathan - SM2J.2
 Yousef, Kerolos M. - SF3J.5, STh1O.5
 Yu, Changyuan - SW4O.3
 Yu, Dan - ATu3K.1
 Yu, Gang - FM4C.5
 Yu, Heshan - STh1N.6
 Yu, Honglin - JW2A.58
 Yu, HongXing - JTh2A.59
 Yu, Hongyan - JTh2A.72, JTu2A.79, JW2A.3
 Yu, Jirong - AW4K.6
 YU, JUNHONG - JTu2A.77
 Yu, Kyoungsik - STh3O.2
 Yu, Lianghong - STu3E.1
 Yu, Mengjie - FF2D.3, FM1D.6, JW2A.82, SF3H.4, STh3J.1, SW3E.4
 Yu, Mingbin - FF2D.2, FTu4C.5, SF1J.4, SM1F.5, STh3J.4, STh4J.4, SW4H.4
 Yu, Nanfang - Ath11.1, FF2A.3, FF2A.5, FF2B.8, FM4M.7, FTh3M.5, FTh4C.5, STh1O.6, STh3H.1
 Yu, Raymond - Ath3I.2
 Yu, Shang-Jie - FTh3C.7
 Yu, Shaogang - JTu2A.25
 Yu, Shui-Qing - AW3P.3, STh4O.6, STu3N.3
 Yu, Shukai - JTh4F.5
 Yu, Siyuan - SM2L.4
 Yu, Song - STh3L.5
 Yu, supeng - SF2I.2
 Yu, Su-Peng - SM3J.4, SM3O.6
 Yu, Xuanyi - SM1J.4
 Yu, Yang - JW2A.99
 Yu, Yanhao - ATu4I.4
 Yu, Yi - FTh3D.3
 Yu, Yiling - FTu3C.2
 Yu, Ying - FM1M.7, STu4L.6
 Yu, yu - JW2A.10
 Yu, Yue-Yang - JW2A.19
 Yu, Zejie - AF2K.7
 Yu, Zhenming - AF2K.5
 Yu, Zhongyuan - FTh1D.6
 Yu, Zhou - SM2F.5
 Yu, Zongfu - Ath11.2, Ath11.7, JF2F.4, JM3B.5, JM3M.4, JTh2A.31
 Yuan, Hang - JTu2A.59
 Yuan, Hongye - JTh2A.34
 Yuan, Hua - SW4E.7
 Yuan, Hualei - SF3E.6
 Yuan, Jinhui - STu4L.7
 Yuan, Luqi - FTh1M.2, FTu3B.4, JM3B.2
 Yuan, Ming - JM3M.4
 Yuan, Pengtao - SF3O.1, SF3O.4, STu3L.5
 Yuan, Ryan X. - AM4I.7
 Yuan, Tao - JTu2A.92
 Yuan, Zhiliang - FM2M.1
 Yuce, Cem - FW4D.6
 Yue, yang - JTh2A.80, SW4O.6
 Yulaev, Alexander - AM3K.2
 Yuxiang, Yuxiang - JTu2A.10
 Yvind, Kresten - JTu2A.83, SF3H.2, STh1J.5
 Z
 Zach, Shlomo - JTu2A.57, SF2N.3, SM1N.5
 Zadeh, Iman E. - FF1A.2
 Zadka, Moshe - SF1J.7
 Zadok, Avi - SM1N.2, STh3H.5
 Zagonel, Luiz - FM3D.5
 Zahavy, Tom - JF2F.3
 Zakar, Eugene - JTu2A.118
 Zakhidov, Anvar - SW4N.2
 Zalden, Peter - JTu2A.101
 Zalevsky, Zeev - Ath3K.5, JTu2A.120, JTu2A.8
 Zalvidea, Dobryna - SF1E.4
 Zaman, Imam Uz - AW4K.4
 Zamarreño, Carlos - JTu2A.9
 Zamboni-Rached, Michel - FTh4B.3
 Zamiri, Marziyeh - STh4O.4
 Zampaolo, Michel - SM1F.3
 Zang, Kai-Yan - JW2A.11
 Zang, Yimin - STu3L.1
 Zang, Zhigang - SF1O.2
 Zanoci, Cristian - FTu4C.2
 Zannotto, Simone - FW4D.1
 Zaouter, Yoann - JM1E.5, JW2A.73
 Zapata, Collette - SM4E.1
 Zapata, Luis E. - SM4E.1
 Zarate, Yair - FF1B.4
 Zarkos, Panagiotis - JW2A.78
 Zavatta, Alessandro - FF1A.5, FTh4D.2
 Zawilski, Kevin T. - SF1H.6, STh4E.6
 Zayats, Anatoly - FTh4M.3
 Zayko, Sergey - FW4M.4
 Zbik, Mateusz - AF3K.7
 Zederbauer, Tobias - SF2O.7, STh4G.2
 Zeitner, Uwe - JW2A.69, STh4E.4
 Zektzer, Roy T. - FF3M.5, JW2A.110, SM3F.4
 Zelmon, David - JTu2A.107
 Zeng, Beibei - STh3N
 Zeng, Chao - JTu2A.92
 Zeng, Heping - JTu2A.40, JW2A.90, SF2E.3, STu4L.1
 Zeng, Jing - STu4L.1
 Zeng, Junjie - SM3H.5, SW4H.6
 Zeng, Shuwen - FTh4C.5
 Zeng, Siwei - SF3N.3
 Zeng, Xianglong - STh3L.4
 Zeng, Xiaogeng - SM4J.7, STu4J.5
 Zeng, Xie - Ath11.7, STu4H.5
 Zeng, Xin - AM2I.6
 Zhai, Guohua - JTh2A.14
 Zhan, Alan - JTh2A.47
 Zhan, X. K. - JTu2A.63
 Zhang, Alex - STu4H.3
 Zhang, Baile - FTh4M.8
 Zhang, Bin - JTh2A.12, STu3N.4
 Zhang, Bohan - ATu4K.2, AW3K.2, SF3N.2
 Zhang, Bowen - JW2A.107
 Zhang, Chao - AF1K.5, FF2B.4, JTh2A.85, JW2A.94, STu3L.5
 Zhang, Chaojie - FF1C.5
 Zhang, Cheng - AM3K.2, FM3C.3, FM3C.7
 Zhang, Chenglin - STh3N.6
 Zhang, Chi - AF2K.4, Ath3K.4, JW2A.80
 Zhang, Chong - STu4J.5
 Zhang, Chunmei - FTh4B.2
 Zhang, Dacheng - SF3E.7
 Zhang, Danian - Ath1K.6
 ZHANG, DAO HUA - SF3J.6
 Zhang, Dehui - SM4J.2
 Zhang, Deng - JTh2A.29, JTh2A.30
 Zhang, Eric J. - STh1F, STh1F.2
 Zhang, Fan - JW2A.54
 Zhang, Fumin - AW4K.2
 Zhang, Guoqiang - SM4J.3
 Zhang, Haibo - JW2A.95
 Zhang, Haisu - FTh1M.5, SF1M.4
 Zhang, Haiwei - JTh2A.90
 Zhang, Han - JTu2A.108, JW2A.86, SF3O.2, SF3O.3
 Zhang, Hanwen - FM1C.1
 Zhang, Hao - JTh2A.80, SF3L.7
 zhang, hongbo - STh1N.7
 Zhang, Hongxiang - AW4K.3
 Zhang, Hua Hui - STh3L.1
 Zhang, Hualiang - JTh2A.14
 Zhang, Hui - JTu2A.124
 ZHANG, JIANAN - JTu2A.15
 Zhang, Jianhao - JTu2A.49
 Zhang, Jianjun - STu3N.4
 Zhang, Jianxing - FM4D.4, STh1J.7, STh3O.1
 Zhang, Jianzhong - JW2A.107
 Zhang, Jiaqi - JTh2A.48
 Zhang, Jie - FF1C.5, SM1F.6
 Zhang, Jing - SW3O.7
 Zhang, Jun - FTh4A.6
 Zhang, Junwei - SM2L.4
 Zhang, Kaiqi - JTh2A.68, JTh2A.70
 Zhang, Kanshou - JTu2A.31
 Zhang, Lei - AF2K.4, JW2A.80, SM2L.4
 Zhang, Linda Jingyuan - FF3A.1, FM4A.4

- Zhang, Long - FF2A.2, STu3N.5
 Zhang, Longkun - STh3L.4
 Zhang, Lu - SW4O.2
 Zhang, Meng - JTu2A.108, JW2A.86, SF3O.2, SF3O.3, STh1L
 Zhang, Mian - FF2D.3, FTh1D.2, SF2J.1, SM3O.2
 Zhang, Ming - FF2B.4
 Zhang, Nan - ATH11.2, ATH11.7, SM1H.5, STu4H.5, STu4O
 Zhang, Pan - JTu2A.66
 Zhang, Ping - FTh4B.2, JW2A.45
 Zhang, Qi - AW31.4, FM4D.1, FM4D.7, JTh2A.15, JTh2A.29, JTh2A.30, JTu2A.121
 Zhang, Qian - SF3O.2, SF3O.3
 Zhang, Qiang - FTh3A.5, SF1M.1
 Zhang, Qiulin - SW3O.3
 Zhang, Qiyao - FM4D.4
 Zhang, Rui - FTh4A.6, SM2L.4
 Zhang, Ruikang - JTu2A.72
 Zhang, Runzhou - FW4B.5, JTu2A.57, JTu2A.67, SM1J.5, SM1N.5
 Zhang, Shougang - JTu2A.66
 Zhang, Shuang - FF3B.6, FM1B.5
 zhang, Shuangyou - JM3B.3, SF3H.5, STh3J.7
 Zhang, Shuyan - STh1O.5
 Zhang, Si-Jie - FM4C.3
 zhang, site - JTh2A.23
 Zhang, Tian - AF2K.5
 Zhang, Tingting - SW3O.1
 Zhang, Wantong - JW2A.2
 Zhang, Wei - FF2A.4, JTu2A.33, JW2A.100, JW2A.91, STu4F.2
 Zhang, Wei Li - STh3L.1
 Zhang, Weijun - FM4C.3
 Zhang, Weipeng - JTh2A.89
 Zhang, Wenbo - SW4O.4
 Zhang, Wen-Zhuo - JTu2A.92
 Zhang, Xian - JTu2A.120
 Zhang, Xiang - FTh1M.2
 Zhang, Xianting - STu4L.7
 Zhang, Xiaofei - JTu2A.66
 Zhang, Xiaogang - SM1F.1
 Zhang, Xiaoguang - SW4O.4
 Zhang, Xiaohang - STh1N.6
 Zhang, Xinliang - AF2K.4, Ath3K.4, JTh2A.56, JW2A.10, JW2A.80
 Zhang, Xu - SF3L.7
 Zhang, Yan - JM3B.4, SF3E.6
 Zhang, Yanan - JW2A.108
 Zhang, Yanbing - FTh1A.4
 Zhang, Yanfeng - JTu2A.118
 Zhang, Yanyan - JTu2A.66
 Zhang, Yao - SM3L.3
 Zhang, Yaqing - JTh2A.12
 Zhang, Yejin - JTh2A.72
 Zhang, Yibo - AM21.6, AM2K.3, ATu4K.2, JM3M.5, JTu2A.5
 Zhang, Yifei - SF2H.4
 Zhang, Ying - FTh1B.5, JW2A.40
 Zhang, Yiqi - FW3D.3
 Zhang, Yiwen - JTh2A.80
 Zhang, Yong - JTu2A.50
 Zhang, Yu - JTh2A.106, JTh2A.70, JW2A.21, STh1G.5, SW4L.6
 Zhang, Yuanhang - SM1L.1
 Zhang, Yujie - FTh3D.4
 Zhang, Ze - FTh4B.1
 Zhang, Zecen - STu4O.1
 Zhang, Zhaopeng - SM4F.5
 Zhang, Zheshen - FF1F.1, FF1F.4, FF1F.7, FTh1A.3, FTh4D.1
 Zhang, Zhewei - AF2K.1
 Zhang, Zheyuan - SF3O.1, SF3O.4
 Zhang, Zhigang - SF1L.6
 Zhang, Ziyue - JTh2A.104, SW3G.5
 Zhao, Anke - JTu2A.73
 Zhao, Bo - FF2A.1
 zhao, Chang - JW2A.38
 Zhao, Dan - JTh2A.34
 Zhao, Hai-Bin - JW2A.11
 Zhao, Han - FM1B.3
 Zhao, Hao - JTu2A.31
 Zhao, Haolan - STh1F.7
 Zhao, Hongwei - JTu2A.82
 Zhao, Jian - STh3L.2
 Zhao, Jun - SF1H.2, SF3E.1, STh4E.1
 Zhao, Junyi - JW2A.118
 Zhao, Kun - FF3C.4
 Zhao, Lingjuan - JTu2A.72, SM3N.8
 Zhao, Mingshan - SM2L.6
 Zhao, Nan - JTu2A.117
 Zhao, Nathan Z. - FF2A.1
 Zhao, Peng - JW2A.56
 Zhao, Shuangxiang - AF1K.2
 Zhao, Siyu - JTh2A.99, JTu2A.98
 Zhao, Wenjuan - JTh2A.15, JTh2A.29, JTh2A.30
 Zhao, Wu - JTu2A.70, SM3N.8
 Zhao, Xianyu - AW4K.2
 Zhao, Xin - JW2A.104, SF1M.2, SM2H.1, STh1G.4
 Zhao, Xuesi - JW2A.56
 Zhao, Yilong - JW2A.47
 Zhao, Yiming - AF3K.8
 Zhao, Yong - ATu3K.7, JTh2A.86, JW2A.77
 Zhao, Yongguang - SF3E.6
 Zhao, Yuji - JTh2A.66, SW4H.5
 Zhao, Yun - STh3J.1
 Zhao, Yunsong - SF3N.3
 Zhao, Yuwei - STh3L.6, SW3H.6
 Zhao, Zhangji - SM1O.5, STh3O.6
 Zhao, Zhe - FW4B.5, JTu2A.57, JTu2A.67, SM1J.5, SM1N.5
 Zhao, Zhixin - FF2A.1, SF2H.7, SW4J.5
 Zhao, Zihao - SF3O.1
 Zhao, Zi-Yan - FM4C.5
 Zheludev, Nikolay I. - FTu3D.7, SW3F.6
 Zheng, Chuan-Tao - JW2A.21
 Zheng, Jiaan - STu4E.4
 Zheng, Jiajiu - STh1N.5
 Zheng, Jian - JTh2A.110
 Zheng, Kaiyuan - JW2A.21
 Zheng, Mingyang - FTh1D.7
 Zheng, Xiaoping - JTh2A.78
 Zheng, Xiuyan - FTh4B.7
 Zheng, Yan - SM4H.4
 Zheng, Yanzhen - JTu2A.90
 Zheng, Yi - SM2O.7
 Zheng, Yongjia - SF3O.4
 Zheng, Yu - JW2A.108
 Zheng, Yuebing - FTh3C.4, JW2A.64, SM1H.2, SM2O.4
 Zheng, Yu-Xiang - JW2A.11
 Zheng, Zelin - JTh2A.78
 Zheng, Zheng - JTh2A.99, JTu2A.108, JTu2A.98, JW2A.104, JW2A.86, SF1M.2, SF3O.2, SF3O.3, SM2H.1, STh1G.4
 Zheng, Zibo - SW4O.4
 Zhichao, Wu - STu3L.2
 Zhong, Chuan - JW2A.66
 ZHONG, QI - FTu3B.5
 Zhong, Qixiu - AW3I.6
 Zhong, Qize - AW4K.5, SF3J.6, STh1O.4
 Zhong, Tian - FM1A.6, FTh1A.3
 Zhong, Zhaohui - SM4J.2
 Zhong, Zhizhen - JTh2A.78
 Zhong, Zizhao - STh1J.7, STh3O.1
 Zhongyang, Xu - AW4K.3
 Zhou, Bingkun - JTh2A.78
 Zhou, Chen - FTh3M.8
 Zhou, defeng - SW3H.6
 Zhou, feng - JW2A.4
 Zhou, Gangqiang - JTh2A.42
 Zhou, hailong - JW2A.10
 Zhou, Haoran - FM3C.6
 Zhou, Hongchao - FTh1A.3
 Zhou, Huibin - SW4O.1
 Zhou, Ji - SW4O.3
 Zhou, Jian - JW2A.9
 Zhou, Jiaqi - JW2A.75
 Zhou, Jin - STh4O.2, STu4O.1
 Zhou, Jingan - JTh2A.66, SW4H.5
 Zhou, Jun - JW2A.95
 Zhou, Lei - JTh2A.11
 Zhou, Linjie - Ath4I.5, JTh2A.42, STh4H.2
 Zhou, Lyu - Ath11.2, Ath11.7, SM1H.5
 Zhou, Minchuan - JTu2A.60, JW2A.13
 Zhou, Ming - Ath11.2, JM3B.5
 Zhou, Pu - JW2A.106
 Zhou, Qian - SM2H.2
 Zhou, Tianhua - JW2A.115
 Zhou, Tong - SM4E.5
 Zhou, Wei - JW2A.91, SF3E.6
 Zhou, Weidong - FF3A.3, JTh2A.31, STh3O.5
 Zhou, Weimin - SM4O.5
 Zhou, Wen - SW3J.5
 Zhou, Xi - AF2K.4, Ath3K.4
 Zhou, Xiaoyan - FTh3D.2
 Zhou, Xufeng - JW2A.118
 Zhou, Xuliang - JTh2A.72, JTu2A.79
 Zhou, y - JW2A.98
 Zhou, Yanyan - JW2A.89
 Zhou, Yao - FTh3A.4, FTu3B.6
 Zhou, Yiyin - AW3P.3, STh4O.6, STu3N.3
 Zhou, Yiyu - FF1B.3, FW4B.5
 Zhou, You - FF1B.7
 Zhou, Zifan - JTu2A.60, JW2A.13
 Zhu, Alexander Y. - SF3J.5
 Zhu, Dan - AW4K.3
 Zhu, Eric Y. - SW3L.4
 Zhu, Guoxuan - SM2L.4
 Zhu, Huiling - JW2A.8
 Zhu, Jiangfeng - JW2A.99, SF3E.7, SM3L.3
 Zhu, Jian-Xin - FM2D.2
 Zhu, Jinlong - Ath1K.5
 Zhu, Lei - JTu2A.10
 Zhu, Lin - SF3N.3
 Zhu, Rongrong - FF2D.3
 Zhu, Shining - FTh3M.3
 Zhu, Shiyang - AW4K.5, SF3J.6, STh1O.4
 Zhu, Shouzheng - JTh2A.14
 Zhu, Wenqi - AM3K.2, FM3C.3, FM3C.7
 Zhu, Wenwu - SM2L.2, SM2L.6
 Zhu, Xiushan - JTu2A.107
 Zhu, Xuanfu - STu4F.2
 Zhu, Yeyu - SF3N.3
 Zhu, Yifu - JTu2A.25
 Zhu, Yuanjun - SF3O.1, STu3L.5
 Zhu, Zebin - SM2H.2
 Zhu, Zhuan - JW2A.118
 Zhu, Zihang - SF2N.5
 Zhuang, Quntao - FF1F.1, FTh4D.1
 Zhuang, Songlin - FTh1M.2
 Zia, Haider - FF2D.5
 Zia, Rashid - FW3C.4
 Zibar, Darko - JF2F.1, SW3O.6
 Zichi, J - FF1A.2
 Zide, Joshua - JTu2A.18
 Ziegler, Zachary - STh4L.3
 Zielbauer, Bernhard - JTu2A.68
 Zilberberg, Oded - FW3D.5
 Zilk, Matthias - FTh1C.6
 Zirkelbach, Johannes - FF3M.1
 Zizlsperger, Martin - FTh4C.3
 Zohar, Sioan - SF3I.7
 Zollo, Nicholas - FF3A.6
 Zondlo, Mark A. - AM1K, AM1K.2, AM2K
 Zong, Jie - JTu2A.107
 Zou, Chen - JTu2A.113
 Zou, Chuanhang - JW2A.88
 Zou, Kaiheng - SF2N.3, SM3G.3
 Zou, Ran - AF1K.6, JW2A.14
 Zou, Xiao - FTh1B.5, JW2A.40
 ZOU, Yueyang - JTu2A.122
 Zu, Ji Ping - JM2E.2
 Zuponcic, Jessica - ATu3K.4
 Zurch, Michael - SF3I.3
 Zusin, Dmitry - FF2C.6, FF2C.7
 Zvezdin, Anatoly K. - FTh1B.2
 Zwiller, Val - FF1A.2